N70-21226-247

NASA SP-3051

SPACE MATERIALS HANDBOOK

Third Edition

CASE FILE COPY

NATIONAL AERONAUTICS AND SPACE ADMINISTRATION

NASA SP-3051

SPACE MATERIALS HANDBOOK

Third Edition

BY JOHN B. RITTENHOUSE AND JOHN B. SINGLETARY
Lockheed Palo Alto Research Laboratory

Sponsored by
NATIONAL AERONAUTICS AND SPACE ADMINISTRATION
AND THE UNITED STATES AIR FORCE, and prepared under
Air Force Contract by Lockheed Missiles and Space Company,
Sunnyvale, California. A limited number of copies have
been released by the United States Air Force as
AMFL–TR–68–205

Scientific and Technical Information Division
OFFICE OF TECHNOLOGY UTILIZATION 1969
NATIONAL AERONAUTICS AND SPACE ADMINISTRATION
Washington, D.C.

For sale by the Clearinghouse for Federal Scientific and Technical Information
Springfield, Virginia 22151 – Price $3.00

ABSTRACT

This edition is the result of an extensive revision and reworking of the second edition of the Space Materials Handbook along with the incorporation of entirely new subject matter coverage and new materials data. All of the most significant material, phenomena, properties, and principles covered in the original Handbook are presented and expanded in this revised and updated version. However, treatment of theoretical aspects has been condensed in order that more emphasis could be placed on the extensive new materials knowledge and data obtained from the design and successful launching of a wide variety of space systems. The handbook is organized into four parts, namely: space environment, effect of space environment on materials, materials in space, and biological interaction with spacecraft materials. Information on mechanical, physical, and chemical properties and characteristics is given for a wide variety of metallic and nonmetallic materials. The effects of natural and induced environments on materials are appraised. Materials categories include coverage of thermal control materials, optical materials, adhesives, organic structural materials, inorganic structural materials, electronic components and materials, materials for sealing applications, and lubrication materials. In addition, a comprehensive multiple citation index is incorporated which gives ready access to information on specific subject areas with regard to their locations within the Handbook.

Chapter Page

PART 2: EFFECT OF SPACE ENVIRONMENT ON MATERIALS

7 THERMAL CONTROL MATERIALS – M. E. Sibert 77
7.1 The Thermal Environment in Space 79
7.2 Thermal Control Systems 83
7.3 Selection of Spacecraft Thermal Control Materials 91
7.4 Effects of the Prelaunch Environment 99
7.5 Effects of the Ascent Environment 104
7.6 Effects of the Space Environment 117
7.7 Summary 161
7.8 References 163

8 OPTICAL MATERIALS – J. B. Singletary 173
8.1 Effects of the Vacuum Environment 174
8.2 Surface Degradation in the Space Environment 175
8.3 Radiation Effects on Optical Materials 177
8.4 Effects of High Temperatures on Optical Materials 191
8.5 References 196

9 MATERIALS FOR LUBRICATION APPLICATIONS – H. I. Silversher 199
9.1 Mechanism of Friction and Adhesion 199
9.2 Lubrication 204
9.3 Influence of Total Mission Environment on Lubrication 205
9.4 Requirements of Materials and Mechanisms for Space Lubrication Systems 208
9.5 Space Simulation Testing of Lubricants 227
9.6 Gear Materials and Lubrication 236
9.7 References 238

10 ADHESIVES – R. E. Mauri 241
10.1 Classes of Adhesives 242
10.2 Effects of Temperature 245
10.3 Effects of High-Energy Radiation on Adhesives 275
10.4 References 290

11 MATERIALS FOR SEALING APPLICATIONS – R. F. Betts 293
11.1 Sealing Applications in Aerospace Vehicles 294
11.2 Sealing Materials 296
11.3 Seal Leakage 310
11.4 Environmental Effects on Sealing Materials 311
11.5 References 351

12 ORGANIC MATERIALS FOR STRUCTURAL APPLICATIONS – R. E. Mauri 355
12.1 Penetrating Radiation Effects 355
12.2 Solar Ultraviolet Radiation Effects 363

CONTENTS

Chapter		Page
1	INTRODUCTION – J. B. Rittenhouse and J. B. Singletary	1
	PART 1: THE SPACE ENVIRONMENT	
2	THE ASCENT ENVIRONMENT – J. B. Singletary	3
	2.1 Aerodynamic Heating	3
	2.2 Vibration, Shock, and Random Noise	7
	2.3 Conclusions	10
	2.4 References	10
3	THE UPPER ATMOSPHERE – A. D. Anderson and W. E. Francis	13
	3.1 Atmospheric Variations	14
	3.2 Physics of the Upper Atmosphere	15
	3.3 Atmospheric Composition	18
	3.4 A Model for Atmospheric Properties	19
	3.5 General Effects on Materials	23
	3.6 References	23
4	NONPENETRATING RADIATIONS – A. D. Anderson	25
	4.1 Solar Radiation	25
	4.2 Albedo	26
	4.3 Thermal Radiation of the Earth	32
	4.4 General Effects on Materials	34
	4.5 References	34
5	PENETRATING RADIATIONS – E. E. Gaines and W. L. Imhof	37
	5.1 Natural Radiation Environment	37
	5.2 Man-Made Radiation	55
	5.3 Internal Environments	57
	5.4 References	59
6	METEOROIDS – J. B. Rittenhouse	63
	6.1 Meteoroid Density	64
	6.2 Meteoroid Velocity	64
	6.3 Flux-Mass Relationship	65
	6.4 Meteoroid Impingement	65
	6.5 References	74

Chapter		Page
	12.3 Effects of Temperature Extremes	364
	12.4 Vacuum Effects	370
	12.5 References	381
13	MATERIALS FOR ANTENNA SYSTEMS – A. S. Dunbar	383
	13.1 Antenna Types and Applications	383
	13.2 Space Environment Factors Important to Antenna Design	387
	13.3 General Systems Considerations	392
	13.4 Mechanical Requirements and Mechanisms	393
	13.5 References	399
14	ELECTRONIC MATERIALS AND COMPONENTS – P. S. Castro, R. A. Glass, J. C. Lee, P. V. Phung, and F. F. Stucki	403
	14.1 Radiation Effects	403
	14.2 Other Environmental Effects	426
	14.3 References	430
15	METALLIC AND CERAMIC MATERIALS FOR STRUCTURAL APPLICATIONS – R. W. Parcel	433
	15.1 Temperature Effects	434
	15.2 Vacuum Effects	436
	15.3 Radiation Effects	442
	15.4 Meteoroid Penetration	445
	15.5 References	445
16	MISCELLANEOUS MATERIALS – J. B. Singletary	449
	16.1 Organic Fluids	449
	16.2 Photographic Emulsions	450
	16.3 Explosives and Propellants	450
	16.4 References	456
	PART 3: MATERIALS IN SPACE	
17	SPACECRAFT MATERIALS EXPERIENCE – J. B. Singletary and J. B. Rittenhouse	457
	17.1 Résumé of Successfully Launched Spacecraft	460
	17.2 Materials Used in Successfully Orbited Spacecraft	481
	17.3 References	555
18	SELECTION OF MATERIALS FOR OPTIMUM PERFORMANCE – J. B. Rittenhouse and J. B. Singletary	565
	18.1 Thermal Control Materials	568
	18.2 Optical Materials	574
	18.3 Materials for Lubricated Systems	576
	18.4 Polymeric Materials for Adhesives, Seals, and Structural Applications	590
	18.5 Materials for Spacecraft Antennas	609

Chapter Page

18.6 Electronic and Miscellaneous Components and Materials 615
18.7 Structural Materials – Inorganic 618
18.8 References 630

PART 4: BIOLOGICAL INTERACTION WITH SPACECRAFT MATERIALS

19 MATERIALS FOR MANNED SYSTEMS – M. Honma and G. B. McCauley 633
19.1 Selection of Materials 633
19.2 Acceptability Limits of Materials 636
19.3 Techniques for Evaluation of Nonmetallic Materials 638
19.4 Acceptable Materials for Manned Spacecraft 642
19.5 References 648

20 EFFECTS OF MATERIALS DEGRADATION PRODUCTS ON MAN – J. T. Wilson, Jr., and R. J. Jaffe 651
20.1 Effects of Materials Degradation Products on Man 651
20.2 Derivation of Limits 652
20.3 Provisional Limits for Spacecraft Atmospheres 654
20.4 Control of Spacecraft Atmospheric Contamination 654
20.5 References 654

21 EFFECTS OF MANNED OCCUPANCY ON SPACECRAFT MATERIALS – L. L. Reed 659
21.1 Urine 659
21.2 Feces 663
21.3 Flatus 665
21.4 Sweat 666
21.5 Sebum 667
21.6 Exhaled Air 667
21.7 Vomit 670
21.8 Fungi and Bacteria 670
21.9 References 671

22 EFFECTS OF STERILIZATION PROCEDURES ON SPACECRAFT MATERIALS – J. B. Rittenhouse and W. G. Jurevic 673
22.1 Sterilization and Decontamination 674
22.2 Effects on Metals and Alloys 675
22.3 Effects on Plastics 677
22.4 Effects on Materials Used in Electronic Components 679
22.5 Miscellaneous Materials 680
22.6 References 681

GLOSSARY 683
General Terms 683
Polymer Terms 691
CONVERSION FACTORS 693
INDEX 695

Chapter 1

INTRODUCTION

J. B. Rittenhouse
J. B. Singletary

The scientific and technological investigations carried out as a part of our exploration of near-Earth and interplanetary space during the past eleven years have contributed a wealth of new information about the nature of the space environment and its effects on the materials of construction of spacecraft. The performance of and scientific data gained by lunar-exploring spacecraft have probably been the most striking accomplishments of recent years. At the same time, great advances have been recorded in the scientific and technological exploitation of near-Earth space by Earth satellites. Our progress farther away from Earth has been represented by a relatively few number of solar-orbiting spacecraft. As materials performance information continues to be gathered and compared from all these spacecraft missions, the extent of both our knowledge and what is yet to be learned becomes clearer.

The interplanetary radiation environment has continued to provide surprises since its initial discovery by one of the first man-made satellites. That more is still being learned is borne out by the discoveries recently made by Pioneer spacecraft of the complicated paths taken by solar wind particles in their journey outward from the sun. The radiation environment is continuously changing due to the decay of the artificial component of the trapped radiation belts and their interaction with the solar wind and solar flares.

The space age was ushered in in 1957 during a period of high solar activity and increasing activity in the exploration of interplanetary space has proceeded through the years of the quiet sun into another period of increasing solar activity with much still to be learned regarding the influence of the sun's cycles on the space environment.

During this period experiments on board spacecraft have provided considerable information about the behavior of some spacecraft materials in the space environment. Such experiments have revealed the need for improvements in ground-based space simulation testing techniques. Meteoroid penetration detectors on Explorer and Pegasus spacecraft have helped to resolve the meteoroid flux-mass relationship and the flux-thickness penetrated relationship.

Experiments on the changes in properties of thermal control materials have shown that when absorptance properties are measured in air after exposure to ultraviolet radiation in vacuum, the exposure to air caused a bleaching of the material with respect to its properties in vacuum after irradiation. This partial restoration of absorptance properties of thermal control materials was observed when spacecraft solar absorptance data was compared with the ground based data for the same materials. This insight has led to improvements in laboratory measurement of the change in properties of these materials.

Measurement of the change in output of solar cell modules made of different semiconductor materials protected from the space environment by different cover materials has led to the use of n-on-p semiconductors because of their better resistance to the effect of penetrating radiation. Combining knowledge of the environment, the behavior of cover materials in the space and simulated environments has permitted designers to specify the optimum thickness and materials for solar cell covers.

This Third Edition of the Space Materials Handbook is divided into four parts. In Part I, five chapters give an up-to-date description of the ascent and the space environments. The reentry environment is beyond the scope of this handbook.

In Part II, the effects of the environment on material is discussed for the several functional applications in spacecraft. This Part II consists of ten chapters that deal with thermal control materials, optical materials, materials for lubrication applications, adhesives, materials for sealing application, organic materials for structural applications, materials for antenna systems, electronic materials and components, metallic and ceramic materials for structural applications, and miscellaneous materials.

In Part III a discussion of space materials experience in actual spacecraft applications is given for the materials of the several functional applications treated in Part II. A second chapter in Part III gives recommended materials for the several spacecraft functional applications based upon the space materials experience and ground-based simulation data.

Part IV comprises four chapters that deal with the biological interactions with materials. The presence of man in the spacecraft makes necessary the consideration both of the potential toxicity of offgassing products on man and the flammability of organic construction materials. The effects of manned occupancy on spacecraft materials impose still other constraints on the spacecraft designer. For unmanned spacecraft, which may impact on another celestial body, the possibility of extraterrestrial life requires sterilization of these vehicles. The effects of heat sterilization and ethylene oxide decontamination on spacecraft materials are discussed in the last chapter of the handbook.

PART 1

THE SPACE ENVIRONMENT

Chapter 2

THE ASCENT ENVIRONMENT

J. B. Singletary

The placement into Earth or solar orbit of a spacecraft requires that a considerable amount of energy be expended in removing it from the gravitational field of the Earth. During this removal process or ascent phase, much of the energy is unavoidably wasted, such as that used to heat the atmosphere, and some of the waste energy is transferred to the spacecraft or payload stage of the rocket vehicle. This may take the form either of thermal energy arising from aerodynamic interaction of the vehicle with the atmosphere or of mechanical energy sources such as aerodynamic pressure and shear forces, acceleration loading, and shock and vibration. All of these factors are here collectively termed the ascent environment of the spacecraft.

Since the ascent environment is not a natural one but a consequence of spacecraft launching, it will show considerable variation depending on the booster rocket used as well as the design of the spacecraft, particularly its coupling with the booster upper stage and its nose fairing protective device. Because of this variability in the environment, it must be rather carefully defined in nature and effects for each combination of spacecraft and launch vehicle. Therefore, this chapter will attempt only to discuss the ascent environment in a broad and generalized manner and to illustrate its potential effects through the citing of some specific examples of the environment expected for particular launch combinations where these combinations are considered to be representative.

2.1 AERODYNAMIC HEATING

Aerodynamic heating refers to the thermal energy transfer between air and a body moving through it at high velocity. The sources of the thermal energy are the frictional forces generated by the relative movement of the air and body. This same relative movement imposes aerodynamic shear or frictional forces tangentially along the body surfaces and creates forces normal to them. The energy balance for an element of external vehicle skin of unit area may be expressed as

$$C \frac{dT_w}{dt} = h(T_R - T_w) + q_{rad} \qquad (2.1)$$

where

C = specific heat of skin element
T_w = temperature of skin element
h = convection coefficient
T_R = adiabatic wall temperature
q_{rad} = net thermal radiation to skin element per unit time per unit area
t = time

Here, the skin section, of which this element is a part, is considered to be at a uniform temperature, and the inside face is insulated.

Fundamentally, air particles exchange energy with the skin element upon collision. The mechanisms giving rise to these collisions and influencing the attendant energy interchange may include molecular thermal conduction between the skin surface and the adjacent air layer as well as between layers of air; energy transport by diffusion of turbulent eddies of air from a hot portion to a cooler portion; and the formation of shock waves. Three types of molecular flow may be considered in discussing aerodynamic effects: continuum, transition, and free-molecule flow. Continuum flow is commonly encountered during ascent to altitudes of about 60 sm. In this type of interaction, molecule-molecule and molecule-vehicle collisions are so numerous that the air may be treated as a continuous fluid. When a body moves through this fluid at a high velocity, kinetic energy of motion is converted to thermal energy both by compression, as through shock waves, and by friction between fluid particles. The rate at which this heat is transferred to the body by the fluid is represented by the term $h(T_R - T_W)$ in Eq. (2.1). Here, T_W is the skin temperature and T_R is a temperature corresponding to conditions in the fluid adjacent to the body; T_R is commonly the adiabatic wall temperature, i.e., the temperature that would be assumed by the skin in a given situation if the skin (wall) were formed of a perfect thermal insulator (adiabatic wall) (Ref. 1). The convection coefficient is , in general, a function of the density, viscosity, specific heat, and thermal conductivity of the fluid, the vehicle velocity, the ambient temperature, the position of the skin element on the body, and the shape of that body. The radiant energy interchange between the skin and its surroundings, q_{rad}, will become significant if either the skin itself or the surrounding fluid assumes sufficiently high temperatures.

As higher altitudes are reached, the average distance traveled by molecules between collisions (mean free path) becomes larger as a consequence of the decreasing air density. This causes deviations from continuum flow, at first in the immediate vicinity of the vehicle surface. With further decrease in air density, the mean free path of the gas molecules becomes greater by an order of magnitude than the dimensions of the space vehicle, resulting in free-molecule flow in which individual molecular collisions must be treated by kinetic theory. The parameters governing h in Eq. (2.1) become the temperature, the density and composition of the air, the vehicle velocity, the component of vehicle velocity normal to the skin element of interest, and the accommodation coefficient of the vehicle surface (Ref. 2).

The magnitude of aerodynamic heating on the exterior of the shroud may be quite intense during the launch phase even though it is of short duration. Most of the heat absorbed by the shroud during launch is, however, carried away when the shroud is jettisoned. As representative illustrations of the sort of heating to be expected, idealized launch heating profiles are shown in Figs. 2-1, 2-2, and 2-3 for three typical spacecraft launching rocket combinations (Ref. 3). The curves marked "outside shroud" cannot, of course, represent temperatures of equivalent points on the different launch vehicles due to differences in external configuration. In any case, they are presented only to show representative heating profiles. Heating of these and other launch vehicles will generally be contained in the following profile: nose cone stagnation temperature from ambient to 1600°F in 100 sec and shroud temperature near cylindrical section to 600°F in 100 sec.

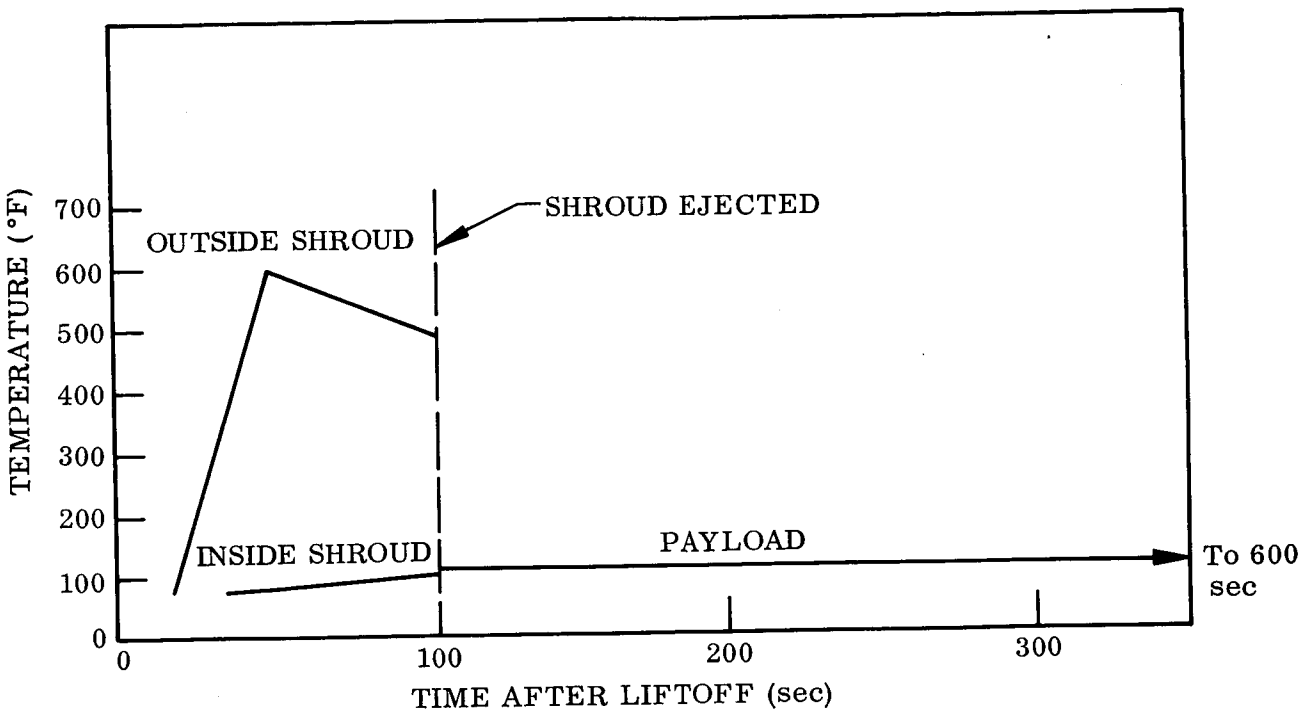

Fig. 2-1 Representative Heating Profile for Scout Launch Vehicle

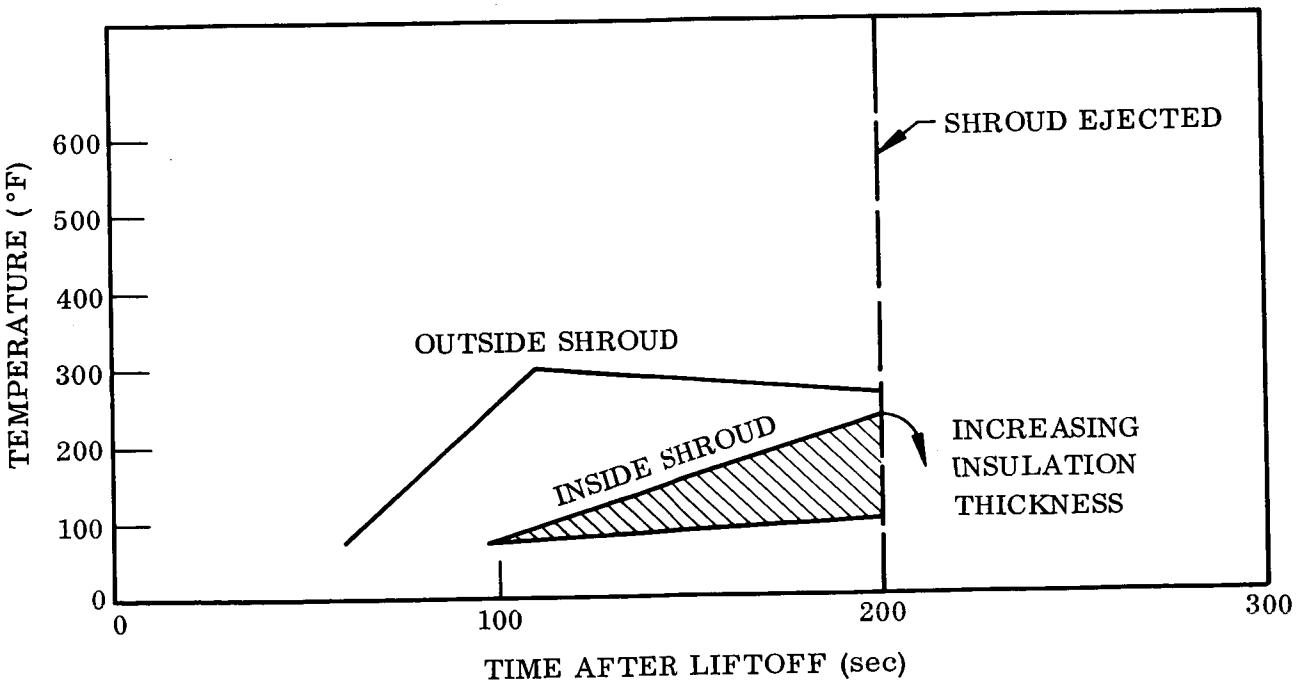

Fig. 2-2 Representative Heating Profile for Thor-Agena B Vehicle

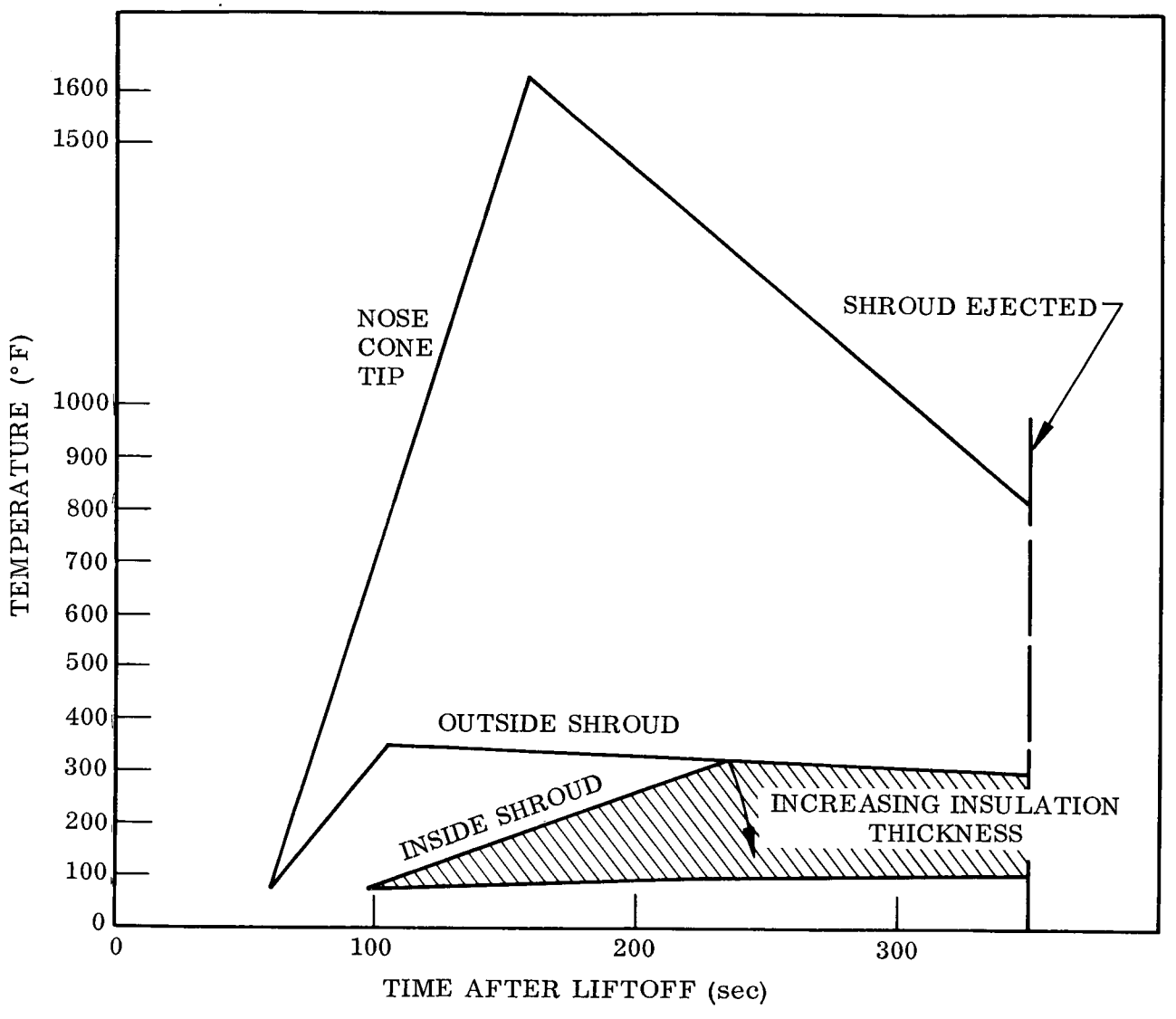

Fig. 2-3 Representative Heating Profile for Atlas-Agena B Vehicle

Peak internal temperatures of the shroud and of the spacecraft payload are much lower than peak external temperatures, as shown in the examples of Figs. 2-1, 2-2, and 2-3. The maximum temperature of the inside of the forward cylindrical section of the shroud is no more than 300 °F, reached in 200 sec (Ref. 3). The ejected shroud carries away with it most of the heat absorbed during launch. After shroud ejection, the spacecraft is subjected to free molecular heating as well as direct solar radiation. For some trajectories, considerable heating may occur in free-molecule flow before the vehicle reaches altitudes at which aerodynamic heating is negligible. The magnitude of this effect must be examined for each spacecraft, trajectory, and launch vehicle combination considered.

In one detailed analytical and experimental study made of the boost phase heating to be expected for a particular satellite vehicle, spacecraft 1963 22A (Ref. 4), it was found for example that the maximum temperature rise possible on any portion of the spacecraft was 38 °F before heat shield ejection and about 240 °F after jettisoning of the heat shield. It was determined that the latter temperature was localized in such a way that the total heat input could be easily accommodated by the spacecraft without a significant overall temperature increase. This analysis considered the heating in two stages: (1) radiative and convective heat transfer between heat shield and spacecraft and (2) direct aerodynamic heating after heat shield ejection.

2.2 VIBRATION, SHOCK, AND RANDOM NOISE

The coupling of mechanical energy into a spacecraft payload from its booster rocket system may occur in a variety of ways. It is termed vibration, shock, random noise, or sometimes aerodynamic or acoustic excitation, depending on the distribution of the excitation with time and with frequency. In a fundamental sense, all these terms refer to the same thing insofar as they are all manifestations of mechanical energy; however, due to their variation in time and frequency distribution as well as their differing sources, it is convenient to give them separate treatment. Shock usually refers to a force or acceleration represented by a discontinuous function of time, or, in a practical sense, a force or acceleration which has a rise time very short compared with other characteristic times of the system under consideration. On the other hand, vibration refers to a force or acceleration which varies continuously with time above and below a mean value. Usually, vibration is restricted to mean a periodic function of time but it may also be used to include random noise or vibration that has no definite period.

The spacecraft vibration environment depends, as does the ascent heating environment, on the spacecraft size and construction as well as the characteristics of the boost rockets and the efficiency of energy coupling between rocket and spacecraft. Vibration and shock inputs may arise from several sources, of which the major ones are probably engine ignition shocks, engine acoustic pressures, aerodynamic forces, and stage separation shocks. Such inputs may contribute the following effects to the satellite vibration environment:

- Fatigue of structural components
- Loss of temperature control surfaces through loosening of the surface from its substrate
- Degradation of shaped optical surfaces

At least three aspects of the vibration environmental problem immediately present themselves: prediction of loads, calculation of response, and design of simulation. Of these, the description of the environment or prediction of loads is probably the least advanced due to both theoretical and experimental difficulties (Ref. 5). The various loads from different sources that are experienced by a spacecraft appear at different places during different periods of its trajectory, and their intensity and excitation characteristics depend on both trajectory and geometric parameters. An estimate of the environment for a particular space vehicle is often a composite of theoretical computation, laboratory studies on models, and flight measurements on vehicles (Ref. 6).

A typical pattern of vibration excitation of a spacecraft mounted on a boost vehicle may consist of several relatively widely separated but related parts. While the vehicle is still on the ground, the intense acoustic field created by the rocket engine exhaust is reverberated from the ground to space vehicle components. This source of excitation diminishes rapidly as the vehicle gains velocity. For a period, the excitation decreases to approximately the preignition hum level, indicating an essentially still condition. When the missile velocity approaches the speed of sound, the excitation increases sharply and attains a maximum level during the transonic period. This source of vibration decays at approximately the same rate as it built up. The vibration level again diminishes to the preignition level and remains very low until separation, at which time shocks are sensed throughout the vehicle when the connecting bolts are exploded and the second-stage engine is ignited. These shocks constitute the last major excitation detected.

This typical pattern may be seen in Fig. 2-4, which traces the vibration history of a spacecraft lifted by a liquid-fueled booster (Ref. 7). The initial contribution of acoustic excitation is seen as the early peak to about 8 g. The transonic vibration maximum is the large peak at about 50 sec after liftoff, while stage separation shock is seen as a narrow peak at about 165 sec. The actual time of the stage separation shock is much smaller than shown in Fig. 2-4, in which the peak is broadened by the characteristics of the measuring instrument. These values were taken from telemetered data on actual flights. The distributions with frequency of the acceleration energy density and the acoustic energy density for the same flight situation are shown in Figs. 2-5 and 2-6.

A considerable amount of protection from the hazards associated with the ascent environment may be afforded by a nose fairing which is jettisoned after ascent through the major part of the atmosphere. However, the process of jettisoning this nose fairing may in itself create new potential problem areas of the ascent environment. For instance, in one study of shock loading due to a pyrotechnic nose fairing separation device (Ref. 7), it was found that shock levels ranged from approximately 5000 peak g's adjacent to the separation charge to less than 100 peak g's at the lowest point observed on the spacecraft. In a similar study of shroud separation shock spectra on the Ranger spacecraft, about 50 g's peak-to-peak amplitude were observed (Ref. 8). Pretesting of spacecraft components and subassemblies to the expected shock loading is thus indicated if pyrotechnic separation devices are used.

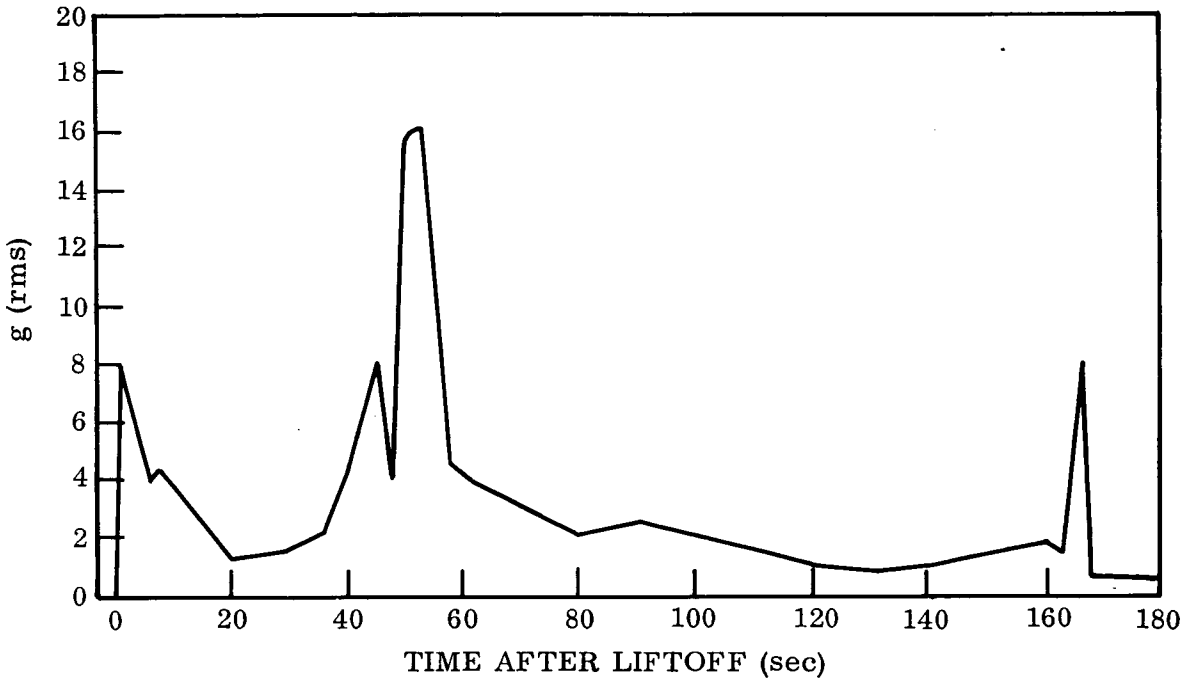

Fig. 2-4 Vibration History of Spacecraft on Liquid-Fueled Booster

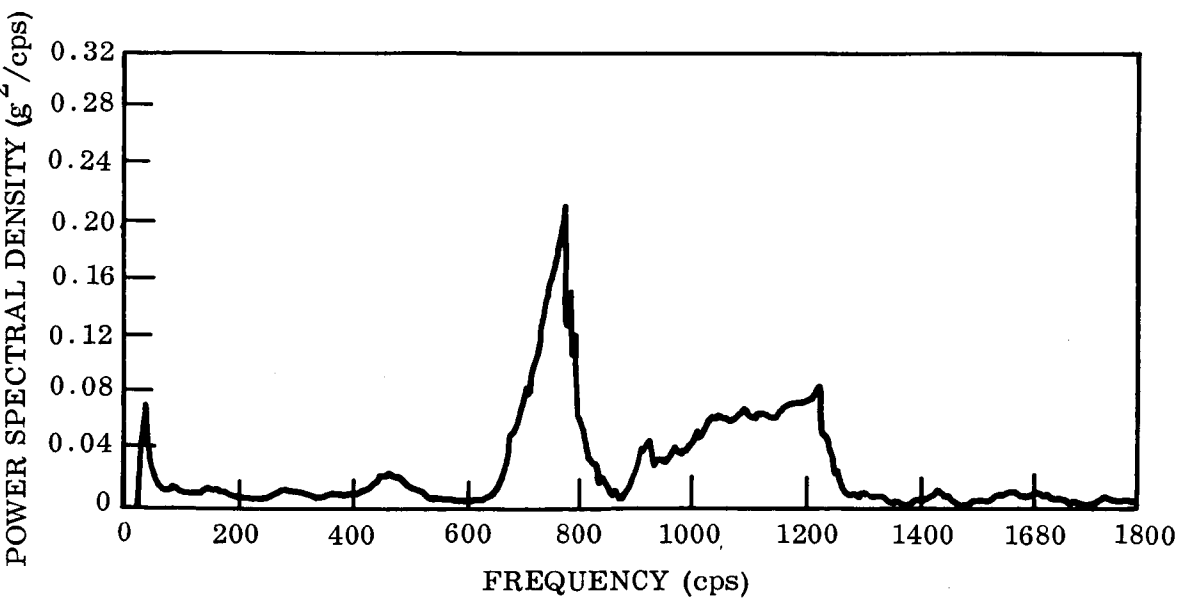

Fig. 2-5 Acceleration Power Spectral Density at Liftoff Versus Frequency, Spacecraft on Liquid-Fueled Booster

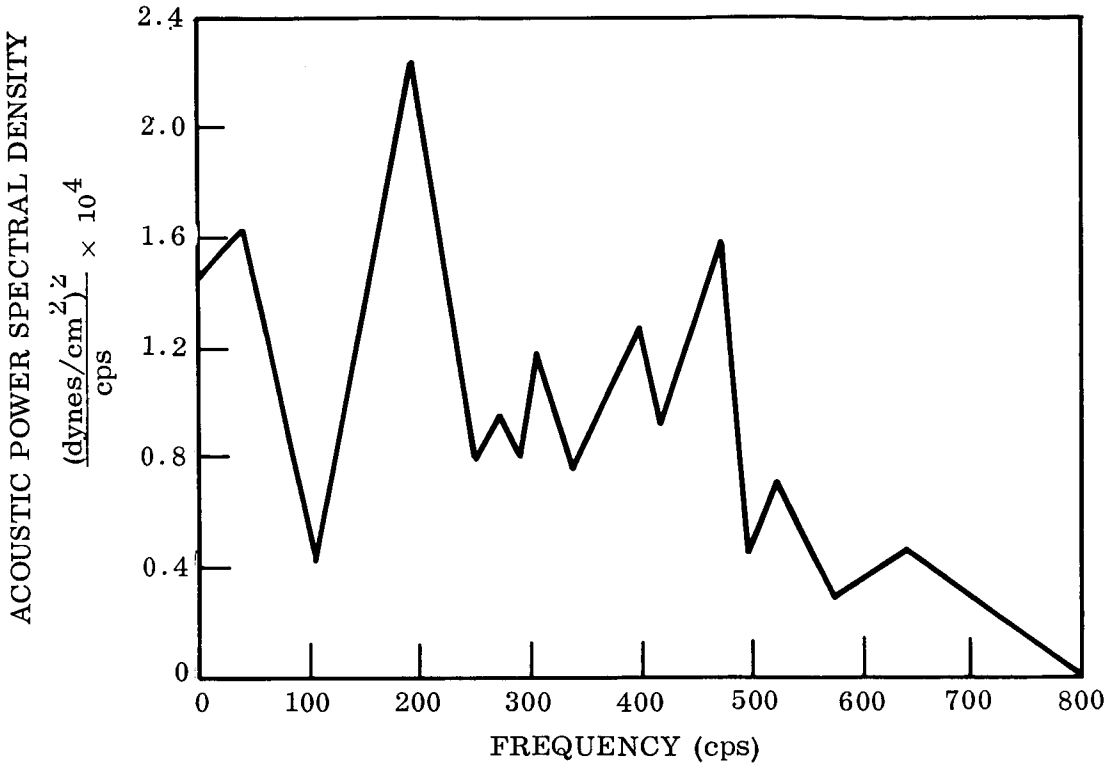

Fig. 2-6 Acoustic Power Spectral Density at Liftoff Versus Frequency, Spacecraft on Liquid-Fueled Booster

2.3 CONCLUSIONS

The typical data presented in this chapter on the ascent environment are intended only to point out some of the general problems involved during the ascent phase. Once the ascent environment has been adequately defined for the particular combination of spacecraft and booster rockets to be used, some estimate of the spacecraft response to this environment must then be made and finally the spacecraft or its component parts or both tested to appropriate levels to inspire a sufficient level of confidence so that the spacecraft will survive the ascent phase and perform its intended mission. A general analysis of the development of test specifications is given in Ref. 10.

2.4 REFERENCES

1. W. H. McAdams, Heat Transmission, 3rd ed., McGraw-Hill, New York, p. 313 1954

2. A. K. Oppenheim, "Generalized Theory of Convective Heat Transfer in Free-Molecule Flow," J. Aeronaut Sci. 20, 49-58, 1953

3. W. J. Neff and R. A. Montes de Oca, Launch Environment Profiles for Sounding Rockets and Spacecraft, NASA-TN-D-1916, January 1964

4. R. M. Vernon, Satellite Boost Phase Heating, CF-3076 (AD 622484), Johns Hopkins University, Applied Physics Laboratory, Silver Spring, Md., March 1964

5. R. H. Lyon, Random Noise and Vibration in Space Vehicles, SVM-1, The Shock and Vibration Information Center, United States Department of Defense, 1967

6. Flight-Loads Measurements During Launch and Exit, NASA SP-8002, National Aeronautics and Space Administration, Washington, D. C., December 1964

7. C. C. Osgood, Spacecraft Structures, Prentice-Hall, Inc., Englewood Cliffs, N. J., 1966

8. J. M. Otera, Spacecraft Shock Environment Induced by Nose Fairing Separation Pyrotechnics, STL 2411-6001-RU-000, Space Technology Laboratories, Redondo Beach, Calif., April 1963

9. D. B. Wiksten, Dynamic Environment of the Ranger Spacecraft: I Through IX (Final Report), TR 32-909, Jet Propulsion Laboratory, Pasadena, Calif., May 1966

10. G. H. Klein and A. G. Piersol, The Development of Vibration Test Specifications for Spacecraft Applications, NASA CR-234, Measurement Analysis Corp., May 1965

Chapter 3

THE UPPER ATMOSPHERE

A. D. Anderson

W. E. Francis

The main regions of the earth's atmosphere are listed in Table 3-1. Since the dominant process in the atmosphere is mixing, up to at least 56 sm* (90 km), the composition of the air and the mean molecular weight remain constant from 0 to 56 sm, defining a region termed the homosphere. Above 56 sm, the molecular weight decreases as the composition changes with altitude, because of molecular dissociation and diffusion. The U.S. Standard Atmosphere (Ref. 1) is the best available reference for atmospheric properties in the homosphere. This atmosphere is a middle-latitude (approximately 45°) year-round mean over the range of solar activity between sunspot minima and maxima. Seasonal and latitudinal variations of properties in the homosphere can be taken into account, if desired, by using values from the supplemental atmospheres derived in Ref. 2.

The principal problem related to atmospheric structure is the calculation of accurate values for all primary properties in the heterosphere (above 56 sm) as a function of time, location, and date by taking into account the relevant processes. The primary atmospheric properties are temperature, pressure, density, and mean molecular mass

Table 3-1

MAIN REGIONS OF THE EARTH'S ATMOSPHERE

Atmospheric Region	Region	Approximate Altitude Range (sm)	Characteristic Features
Homosphere	Troposphere	0–7	Mean molecular weight constant; heat transfer by convection
	Stratosphere	7–30	Constant molecular weight; increasing temperatures; region strongly heated by both earth infrared and solar ultraviolet radiation
	Mesosphere	30–56	Constant molecular weight; decreasing temperature; mixing processes dominant throughout homosphere
Heterosphere	Thermosphere	56–340	Frequent particle collisions; diffusion process dominant
	Exosphere	340–37,000	Collisions rare; temperature constant to about 5,300 sm; diffusion process dominant

*Statute miles.

(or composition). To account for their variations, the following factors must be considered: (1) time (hour, day, sun-rotation period, season, year, sunspot cycle); (2) location (altitude, latitude, longitude); (3) solar activity (ultraviolet radiation, x-rays, solar plasma, and associated magnetic storms); and (4) processes (conduction, diffusion, mass transport, photoionization, dissociation, recombination, particle escape into space). The problem of describing upper atmospheric behavior is difficult because many of these elements are interrelated.

3.1 ATMOSPHERIC VARIATIONS

The magnitudes of the atmospheric properties in the upper atmosphere are derived from measurements made from satellites, rockets, meteor observations, sky emissions, and the propagation of sound and radio waves. The data are sparse and are very uncertain above 125 sm. The density (drag) data resulting from tracking satellites are the most precise and also the most numerous. Study of the orbital decay data has clearly established that two major systematic density variations occur: (1) a solar activity effect in which variations in atmospheric heating and density occur above 56 sm due to variations in solar ultraviolet radiation; and (2) a diurnal (time-of-day) effect, in which the solar heating results in the atmosphere bulging toward the sun, producing relatively large density increases at altitudes above 190 sm in the sunlit region of the earth. At 500 sm, due to effect (1), the density can be 40 times greater during solar maximum conditions than during solar minimum; and due to effect (2), 15 times greater during the day than during the night. The combination of (1) and (2) can result in densities 500 times greater at 500 sm during solar maximum (day) than during solar minimum (night). This extreme variability in density also applies to pressure.

Upper-atmosphere density variations with latitude and season are much smaller than the two preceding primary effects. The diurnal effect is one in which the density varies with local time or the longitude difference between the given location and the subsolar point. From the strong diurnal effect, one would expect latitudinal and seasonal effects, and considerably lower density in the winter polar region. Until recently, it was not possible to prove definitely the existence of any significant latitudinal variation in density. Different investigators have reported slight latitudinal density variations, but the various findings were not in agreement. Now, the existence of an appreciable latitudinal density gradient has been demonstrated by May (Ref. 3), who analyzed data from certain recoverable satellites, the altitudes of which ranged between 118 and 162 sm and inclinations of about 80°. May concluded that the air density at a fixed height is a function of latitude and is about 30% smaller at the poles than at the equator. His conclusion is corroborated by an independent analysis by Anderson (Ref. 4) based on a different method of deriving the behavior of density with latitude. Theoretical support for the stated density variation is given by Lagos and Mahoney (Ref. 5) whose study of solar heating shows that seasonal variability is much more important than the diurnal variability at 45° latitude. Another conclusion from their study is that the meridional

density gradients are significant at all times and are particularly large at solstice. It should be emphasized that circulation effects, neglected by Lagos and Mahoney, may introduce appreciable modifications in the latitudinal density variation. At higher altitudes – above 380 sm – this simple picture may not hold near the polar regions. Keating and Prior (Ref. 6) conclude that there are two diurnal atmospheric density bulges, one due to atomic oxygen and the other due to helium. Thus, as the altitude increases to where helium replaces atomic oxygen as the principal constituent (380–440 sm), there is a shift from the atomic oxygen bulge on the sun side of the equator to a high-latitude "winter" helium bulge on the opposite side of the equator.

A semiannual effect in satellite orbital decay data has been found by Paetzold and Zschörner (Ref. 7). Thus far, no generally acceptable explanation for this effect has been proposed. One hypothesis (Ref. 8) which would explain qualitatively all the observed features of the semiannual effect is based on the existence of an appreciable latitudinal density variation in the winter hemisphere. There is some support for such a density gradient (Refs. 3, 4, and 5). The conclusions of Keating and Prior (Ref. 6), if correct, would place the marked meridional density gradient of the winter hemisphere at low and middle latitudes above 380 sm. Finally, magnetic storms cause a conspicuous drag effect on satellites. At present, it is not possible to make more than a rough estimate of the effect of magnetic heating on density (Ref. 9).

3.2 PHYSICS OF THE UPPER ATMOSPHERE

Assuming that the earth's atmosphere is a continuous medium consisting of a gas in static equilibrium, the equation connecting the pressure P and density ρ at any altitude h is

$$dP = -g\rho\, dh \tag{3.1}$$

where g is the gravitational acceleration. The variation in g with altitude can be taken into account by using the relationship

$$g = \frac{g_o R_o^2}{\left(R_o + h\right)^2} \tag{3.2}$$

where g_o is the acceleration of gravity at the earth's surface and R_o is the earth's radius. Equation (3.1) is the hydrostatic equation in differential form. If m is the mean molecular mass of the gas and n denotes the number density or concentration, the density ρ becomes

$$\rho = nm \tag{3.3}$$

Since the terrestrial atmosphere is almost a perfect gas, the pressure is given by the equation of state

$$P = nkT \tag{3.4}$$

where T is the absolute temperature (°K) and k is the Boltzmann constant (1.38×10^{-16} erg deg^{-1}). Multiplying both sides of Eq. (3.3) by g and dividing the result into Eq. (3.4) gives

$$\frac{P}{\rho g} = \frac{kT}{mg} = H \tag{3.5}$$

where $H = kT/mg$ is known as the pressure scale height, a parameter convenient for atmospheric calculations.

From Eqs. (3.1), (3.3), and (3.4), we may write

$$\frac{dP}{P} = -\frac{mg}{kT}\,dh \tag{3.6}$$

Integrating Eq. (3.6) gives the barometric law

$$\frac{P}{P_o} = \exp\left[-\int_o^h \frac{mg}{kT}\,dh\right] \tag{3.7}$$

From Eqs. (3.4) and (3.7), we get

$$\frac{n}{n_o} = \frac{T_o}{T}\exp\left[-\int_o^h \frac{mg}{kT}\,dh\right] \tag{3.8}$$

and from Eqs. (3.3) and (3.8),

$$\frac{\rho}{\rho_o} = \frac{mT_o}{m_o T}\exp\left[-\int_o^h \frac{mg}{kT}\,dh\right] \tag{3.9}$$

in Eqs. (3.7) to (3.9), P, n, and ρ are the pressure, particle concentration, and density, respectively, at altitude h, and P_o, n_o, and ρ_o are the corresponding values at an arbitrary reference level at which h is assigned the value zero.

Equations (3.1) to (3.9) are applicable in the atmosphere where the escape into space of a constituent is not important. The hydrostatic equation, Eq. (3.1), is based on the concept of local thermodynamic equilibrium in which collisions between particles are frequent enough to cause a complete statistical exchange of particle energy and momentum in the volume under consideration. In the thermosphere (Table 3-1), the particles collide often enough to ensure a Maxwellian velocity distribution and the existence of a meaningful kinetic temperature. In the exosphere, above about 340 sm, collisions are sufficiently reduced so that the existence of a Maxwellian distribution, and consequently

the validity of applying the hydrostatic relationship must be examined anew. Liouville's theorem can be used to show that the Maxwellian velocity distribution below the base of the exosphere applies equally well in the exosphere, provided that the escape of particles to space is negligible. The atmosphere is so rarefied in the exosphere that little solar radiation is absorbed. Also, there are no energy loss mechanisms to disturb the Maxwellian velocity distribution. At the existing temperatures, the distribution is disturbed only by the escape of neutral hydrogen from well above the base of the exosphere. It follows that the maximum altitude in the atmosphere where the hydrostatic equation is applicable can be determined by calculating the altitude in the exosphere where the density of the neutral hydrogen starts to be significantly affected by the escape of hydrogen atoms. Consequently, the greatest error involved in using the hydrostatic assumption will occur during the day near sun-spot maximum conditions, inasmuch as temperatures are highest then. Calculations indicate that the error will start to become significant above about 3,100-sm altitude (Ref. 10). For average sunspot conditions, the altitude is above 5,300 sm. For sunspot minimum conditions, the error will not be significant below 6,200 sm.

Inasmuch as the atmosphere consists of a mixture of gases subject to a force field, the equilibrium distribution of its constituents can be expected to show some degree of diffusive separation. Although turbulent mixing below 60 sm does not allow the development of diffusive equilibrium distributions, there is experimental evidence that diffusive equilibrium does exist above this altitude. In the geopotential field, diffusive equilibrium gives concentration distributions for neutral particles that vary exponentially with the geopotential, with a more rapid decrease in concentration with increasing geopotential for the heavier constituents in the atmosphere than for the lighter. The result is a static distribution of gas constituents under the action of the external force field, expressed by independent application of the barometric law [Eq. (3.7)] for each atmospheric constituent.

The concept that the atmosphere extending above 250 sm over a given location on the earth's surface is isothermal in the sense that the temperature does not vary with altitude is now well established. In the tenuous gas of the upper thermosphere, the thermal conductivity is independent of the pressure whereas the heat capacity varies linearly with density. Consequently, the conductivity is very large compared with the heat capacity. Above 250 sm the absorption of energy is negligible and the relatively high heat conductivity eliminates temperature differences; hence, the kinetic temperature is nearly constant with altitude for many thousands of miles. The kinetic temperature can be determined only for a gas with a Maxwellian velocity distribution. As pointed out under the discussion of the accuracy of the hydrostatic assumption, the Maxwellian velocity distribution applies in the exosphere provided that the escape of particles to space is negligible. For hydrogen, the escape of atoms is comparatively rapid so that the velocity distribution in the upper exosphere is not Maxwellian. Therefore, the hydrogen atoms in the upper exosphere have a non-Maxwellian distribution that becomes more pronounced with altitude (Ref. 4). Under these circumstances, the concept of kinetic temperature is not entirely applicable, although an effective temperature can be defined by considering the average energy of the hydrogen atoms. This

effective temperature is not constant as a function of distance from the earth. The same altitude above which the use of the hydrostatic equation becomes questionable can also be taken to be where the deviation between the kinetic and effective temperature becomes significant. This altitude was at about 5,300 sm for average sunspot conditions.

3.3 ATMOSPHERIC COMPOSITION

The neutral atmosphere above 60 sm consists almost completely of molecular nitrogen and oxygen and atomic argon, oxygen, helium, and hydrogen; the relative concentrations of these constituents depend strongly on altitude and temperature. The composition of the upper atmosphere can be explained, at least in a qualitative sense, by the types of photochemical reactions that can occur. In the following paragraphs, the reactions leading to the neutral constituents only will be discussed.

At about 60 sm, the absorption of solar radiation with wavelengths shorter than 1850 Å down to about 1300 Å leads to the dissociation of oxygen molecules into oxygen atoms. For wavelengths of less than 1026 Å, the oxygen molecule can be ionized; this ionization is normally followed by a dissociative recombination producing atomic oxygen. Although the oxygen atoms can recombine into molecules, photochemical equilibrium does not prevail because of the important role played by vertical transport processes in determining the atomic and molecular concentrations at various levels near 60 sm. More oxygen dissociates than recombines above 60 sm due to the rapid decrease of the recombination processes with altitude. Below 60 sm, collisions occur frequently enough for recombination to prevail, and hence more oxygen recombines than dissociates. Consequently, there is a steady flux of molecular oxygen upward and atomic oxygen downward through the 60-sm level due to the effects of diffusion and mixing. Atomic oxygen is the most important constituent in the upper thermosphere.

The most active process leading to the dissociation of molecular nitrogen is ionization followed by dissociative recombination, producing atomic nitrogen. Atomic nitrogen can react with molecular oxygen to form nitric oxide and atomic oxygen. The nitric oxide in turn reacts with atomic nitrogen to form molecular nitrogen and atomic oxygen. The effectiveness of these reactions, together with the slowness with which molecular nitrogen dissociates, causes atmospheric nitrogen to remain predominantly in molecular form.

Photodissociation of water vapor and methane near 50 sm constitutes the principal source of atomic hydrogen. Owing to the small mass of the hydrogen atom compared with other atmospheric constituents, the hydrogen concentration does not decrease with altitude as rapidly as do the other atmospheric constituents in the altitude region where diffusion proceeds rapidly; hence, atomic hydrogen becomes an increasingly important atmospheric constituent with increasing altitude. However, atomic hydrogen is such a minor constituent in the thermosphere that it does not become the dominant constituent until an altitude of 800 to 1,900 sm, remaining so until about 12,000 sm where the hydrogen ion becomes dominant. The source of atomic hydrogen near 50 sm can be expected to remain essentially constant through the sunspot cycle, but the rate of

escape, depending on the temperature at the base of the exosphere, varies with the sunspot cycle. The escape will be relatively rapid when the temperature is high, and the concentration of hydrogen will be correspondingly low in the exosphere near sunspot maximum. The escape is relatively slow when the temperature is low, so that the concentration must be comparatively high near sunspot minimum.

Nicolet (Ref. 11) showed that helium atoms are an important constitutent in the lower exosphere. He explains the high densities derived from the rate of change of the period of the Echo satellite by the presence of helium. The slow density decrease between 470 and 930 sm cannot be attributed to atomic oxygen, nitrogen, or hydrogen. Although atomic oxygen is the most important constituent in the upper thermosphere, atomic helium dominates over atomic oxygen somewhere above 500 to 620 sm. Atomic hydrogen dominates over helium somewhere above 800 to 1,900 sm.

3.4 A MODEL FOR ATMOSPHERIC PROPERTIES

Upper-atmosphere measurements are not made on a regular enough basis, in kind, time, or space, to allow them to be used without the aid of a model to represent atmospheric conditions. The approach of most models used to derive atmospheric properties is to assume altitude profiles for some of the properties in order to calculate the remainder. Almost all the models deal with data referring only to density, pressure, or temperature. The altitude variation of the mean molecular mass is introduced somewhat arbitrarily and therefore a physically consistent vertical distribution of the composition could not be obtained. To avoid some of the assumptions of the other methods and to attempt to take into account the factors mentioned above under atmospheric physics and composition, a new method was devised for computing atmospheric properties (Ref. 10). In this model, no major assumptions are made regarding the property profiles. Instead, the primary properties are calculated by starting with an empirical density profile from a density model as the chief input, assuming diffusive equilibrium conditions above 68 sm and isothermal conditions with altitude above 250 sm. The density profile used as starting input for this new property model is represented in a previous empirical model as a function of local time and solar activity from 125 to 500 sm (Ref. 12).

This density model can be used, along with some index of the sun's extreme ultraviolet radiation (EUV), to calculate the marked variations in density that occur from day to day. Although the 10.7-cm flux from the sun has generally been used as this index of the EUV responsible for most of the upper-atmosphere heating producing density changes, it is not a precise index of the EUV effect (Ref. 12). A more accurate indicator of the EUV than the 10.7-cm flux has been derived (Ref. 13), and this parameter, designated S', is used in the model to indicate the degree of solar activity. The remaining atmospheric properties are then derived by using the hydrostatic equation and the equation of state that relate density, pressure, temperature, and mean molecular mass as a function of altitude [Eqs. (3.7) and (3.8)], together with boundary values based on measurements.

The model in Ref. 10 describes the atmosphere up to 10,000 km, an appreciable extension beyond the altitude range covered by most models. To do this, it accounts for the

variation in the rate of escape of atomic hydrogen from the exosphere over a solar cycle. In addition, the model represents the diurnal variation of hydrogen in the exosphere, a factor previously neglected. Finally, the diurnal and solar activity effects are enumerated in a consistent way from 100 to 200 km. Most models start at 120 km and do not allow any variation in properties at this altitude. The equations embodying the model are programed for an IBM-7090 computer. The results of the computations made from the model are given in Tables 3-2 and 3-3 and Fig. 3-1. The tables exhibit the neutral atmospheric properties and composition (number densities) versus altitude for both sunspot maximum and sunspot minimum. The differential value of the extreme ultraviolet flux, S', has been taken as 250×10^{-22} W/m^2 Hz for sunspot maximum and 50×10^{-22} W/m^2 Hz for sunspot minimum. Both tables are for t = 2100 hr local time; the density for this time has been found to approximate closely the diurnally averaged density or the sum of the densities for every hour of the day divided by 24. Since secondary effects such as those due to latitude have been neglected, the model is most representative of conditions in the equatorial and mid-latitude regions. The computations of the basic atmospheric properties – pressure, temperature, and mean molecular weight – are in good agreement with published values, the error being less than 5 percent throughout the region specified by the input data (Ref. 14). Also, the basic atmospheric concentrations of N_2, O_2, O, and He agree with published values to within errors of 6, 20, 12, and 6 percent, respectively, at 120 km.

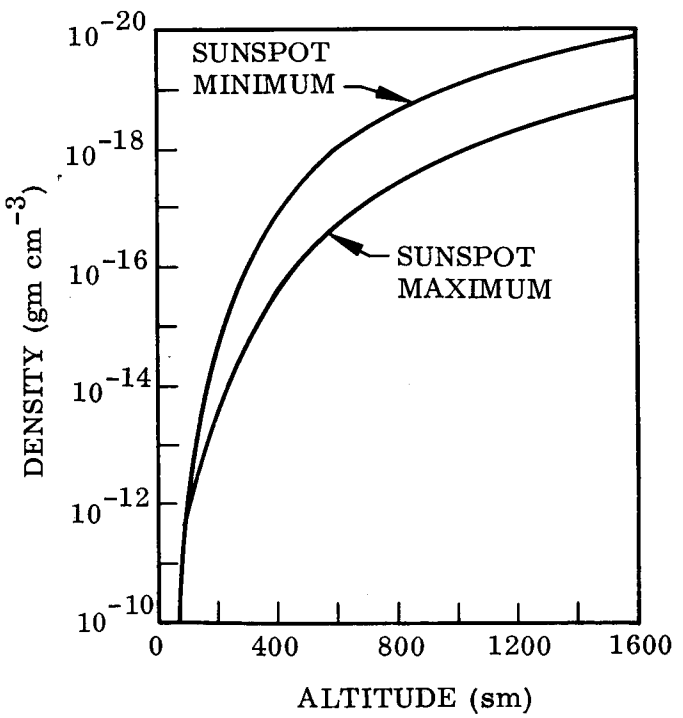

Fig. 3-1 Average Atmospheric Density at Extremes of Sunspot Cycles

Table 3-2

NEUTRAL PROPERTIES OF UPPER ATMOSPHERE AT SUNSPOT MAXIMUM FOR VARIOUS ALTITUDES

Altitude		Pressure[a] (dynes/cm^2)	Pressure[a] (Torr)	Temperature (° K)	Molecular Weight	Scale Height (km)	Density[a] (g/cm^3)	Concentration[a]						
								Total (cm^{-3})	Constituent (cm^{-3})					
(km)	(sm)								n(N_2)	n(O_2)	n(A)	n(O)	n(He)	n(H)
100	62.1	3.3 (-1)	2.48 (-4)	223	27.76	7.0	5.00 (-10)	1.09 (13)	8.15 (12)	1.76 (12)	7.42 (10)	8.81 (11)	4.10 (8)	1.11 (6)
120	74.6	3.8 (-2)	2.85 (-5)	348	24.41	12.6	3.18 (-11)	7.83 (11)	4.54 (11)	6.89 (10)	1.92 (9)	2.59 (11)	1.18 (8)	3.53 (4)
140	87.0	1.1 (-2)	8.25 (-6)	569	22.44	22.5	5.42 (-12)	1.45 (11)	6.68 (10)	8.27 (9)	1.53 (8)	7.01 (10)	5.91 (7)	2.06 (4)
160	99.4	5.5 (-3)	4.13 (-6)	758	21.12	32.0	1.84 (-12)	5.24 (10)	1.95 (10)	2.11 (9)	2.99 (7)	3.07 (10)	3.88 (7)	1.49 (4)
180	111.9	3.1 (-3)	2.33 (-6)	826	20.09	36.9	9.00 (-13)	2.70 (10)	8.15 (9)	7.89 (8)	8.90 (6)	1.80 (10)	3.18 (7)	1.33 (4)
200	124.3	1.8 (-3)	1.35 (-6)	882	19.24	41.4	4.84 (-13)	1.51 (10)	3.68 (9)	3.21 (8)	2.94 (6)	1.11 (10)	2.68 (7)	1.22 (4)
240	149.1	7.7 (-4)	5.78 (-7)	984	18.01	49.9	1.69 (-13)	5.64 (9)	8.81 (8)	6.36 (7)	4.00 (5)	4.68 (9)	1.99 (7)	1.04 (4)
300	186.4	2.6 (-4)	1.95 (-7)	1,085	16.94	59.6	4.83 (-14)	1.72 (9)	1.38 (8)	7.77 (6)	2.96 (4)	1.56 (9)	1.41 (7)	8.85 (3)
340	211.3	1.3 (-4)	9.75 (-8)	1,108	16.50	63.2	2.41 (-14)	8.78 (8)	4.56 (7)	2.19 (6)	6.12 (3)	8.19 (8)	1.18 (7)	8.34 (3)
400	249	5.3 (-5)	3.98 (-8)	1,109	16.01	66.4	9.24 (-15)	3.48 (8)	9.24 (6)	3.54 (5)	6.26 (2)	3.29 (8)	9.38 (6)	7.87 (3)
500	311	1.2 (-5)	9.00 (-9)	1,109	15.15	72.2	2.06 (-15)	8.17 (7)	6.89 (5)	1.82 (4)	1.53 (1)	7.45 (7)	6.47 (6)	7.17 (3)
600	373	3.4 (-6)	2.55 (-9)	1,109	13.59	82.9	5.01 (-16)	2.22 (7)	5.53 (4)	1.02 (3)		1.76 (7)	4.51 (6)	6.51 (3)
700	435	1.2 (-6)	9.00 (-10)	1,109	10.93	106	1.37 (-16)	7.54 (6)	4.77 (3)	6.19 (1)		4.35 (6)	3.18 (6)	5.96 (3)
800	497	5.2 (-7)	3.90 (-10)	1,109	7.95	150	4.46 (-17)	3.38 (6)	4.40 (2)	4.06 (0)		1.11 (6)	2.26 (6)	5.48 (3)
900	559	2.9 (-7)	2.18 (-10)	1,109	5.84	210	1.87 (-17)	1.93 (6)	4.34 (1)			2.96 (5)	1.62 (6)	5.04 (3)
1,000	621	1.9 (-7)	1.42 (-10)	1,109	4.76	264	1.00 (-17)	1.26 (6)	4.55 (0)			8.17 (4)	1.18 (6)	4.64 (3)
1,200	746	9.9 (-8)	7.43 (-11)	1,109	4.11	323	4.40 (-18)	6.45 (5)				6.88 (3)	6.34 (5)	3.97 (3)
1,400	870	5.5 (-8)	4.13 (-11)	1,109	3.99	350	2.37 (-18)	3.57 (5)				6.58 (2)	3.53 (5)	3.43 (3)
1,600	994	3.1 (-8)	2.33 (-11)	1,109	3.96	372	1.35 (-18)	2.05 (5)				7.08 (1)	2.02 (5)	2.98 (3)
1,800	1,119	1.9 (-8)	1.42 (-11)	1,109	3.94	393	7.94 (-19)	1.22 (5)				8.50 (0)	1.19 (5)	2.60 (3)
2,000	1,243	1.1 (-8)	8.25 (-12)	1,109	3.91	416	4.81 (-19)	7.41 (4)				1.13 (0)	7.18 (4)	2.29 (3)
2,500	1,553	3.7 (-9)	2.78 (-12)	1,109	3.79	481	1.52 (-19)	2.42 (4)					2.24 (4)	1.70 (3)
3,000	1,864	1.4 (-9)	1.05 (-12)	1,109	3.58	569	5.49 (-20)	9.26 (3)					7.95 (3)	1.31 (3)
3,500	2,175	6.4 (-10)	4.80 (-13)	1,109	3.26	693	2.25 (-20)	4.15 (3)					3.12 (3)	1.03 (3)
4,000	2,486	3.3 (-10)	2.48 (-13)	1,109	2.86	872	1.03 (-20)	2.17 (3)					1.34 (3)	8.27 (2)
4,500	2,796	2.0 (-10)	1.50 (-13)	1,109	2.44	1,122	5.28 (-21)	1.30 (3)					6.25 (2)	6.78 (2)
5,000	3,107	1.3 (-10)	9.75 (-14)	1,109	2.07	1,450	3.00 (-21)	8.75 (2)					3.11 (2)	5.64 (2)
6,000	3,728	7.6 (-11)	5.70 (-14)	1,109	1.55	2,290	1.28 (-21)	4.99 (2)					9.11 (1)	4.08 (2)
7,000	4,350	5.2 (-11)	3.90 (-14)	1,109	1.28	3,226	7.23 (-22)	3.40 (2)					3.21 (1)	3.08 (2)
8,000	4,971	3.9 (-11)	2.93 (-14)	1,109	1.15	4,142	4.86 (-22)	2.53 (2)					1.30 (1)	2.40 (2)
9.000	5,592	3.0 (-11)	2.25 (-14)	1,109	1.09	5,019	3.60 (-22)	1.99 (2)					5.97 (0)	1.93 (2)
10,000	6,214	2.5 (-11)	1.88 (-14)	1,109	1.06	5,878	2.83 (-22)	1.62 (2)					3.00 (0)	1.59 (2)

(a) Numbers in parentheses denote powers of 10. Thus, 3.3 (-1) means 3.3×10^{-1}.

Table 3-3

NEUTRAL PROPERTIES OF UPPER ATMOSPHERE AT SUNSPOT MINIMUM FOR VARIOUS ALTITUDES

Altitude		Pressure [a] (dynes/cm^2)	Pressure [a] (Torr)	Temperature (° K)	Molecular Weight	Scale Height (km)	Density[a] (g/cm^3)	Concentration[a]						
								Total (cm^{-3})	Constituent (cm^{-3})					
(km)	(sm)								n(N_2)	n(O_2)	n(A)	n(O)	n(He)	n(H)
100	62.1	2.9 (-1)	2.18 (-4)	204	28.11	6.4	4.83 (-10)	1.04 (13)	8.14 (12)	1.74 (12)	6.65 (10)	4.80 (11)	1.44 (8)	1.83 (6)
120	74.6	2.1 (-2)	1.58 (-5)	287	26.77	9.4	2.40 (-11)	5.41 (11)	4.07 (11)	5.86 (10)	1.39 (9)	7.49 (10)	1.57 (7)	1.06 (5)
140	87.0	3.9 (-3)	2.92 (-6)	420	25.08	14.8	2.79 (-12)	6.71 (10)	4.43 (10)	4.90 (9)	6.86 (7)	1.79 (10)	8.28 (6)	6.77 (4)
160	99.4	1.3 (-3)	9.75 (-7)	588	23.53	22.3	6.23 (-13)	1.60 (10)	8.91 (9)	8.23 (8)	7.97 (6)	6.20 (9)	4.93 (6)	4.62 (4)
180	111.9	6.0 (-4)	4.50 (-7)	730	22.24	29.4	2.19 (-13)	5.93 (9)	2.79 (9)	2.25 (8)	1.63 (6)	2.91 (9)	3.47 (6)	3.60 (4)
200	124.3	3.2 (-4)	2.40 (-7)	824	21.15	35.1	9.91 (-14)	2.82 (9)	1.11 (9)	7.98 (7)	4.64 (5)	1.63 (9)	2.74 (6)	3.10 (4)
240	149.1	1.2 (-4)	9.00 (-8)	948	19.44	44.6	2.91 (-14)	9.01 (8)	2.41 (8)	1.43 (7)	6.06 (4)	6.43 (8)	1.95 (6)	2.56 (4)
300	186.4	3.4 (-5)	2.55 (-8)	996	17.75	52.2	7.39 (-15)	2.51 (8)	3.59 (7)	1.62 (6)	4.24 (3)	2.12 (8)	1.43 (6)	2.28 (4)
340	211.3	1.6 (-5)	1.20 (-8)	997	17.02	55.1	3.36 (-15)	1.19 (8)	1.08 (7)	4.12 (5)	7.74 (2)	1.07 (8)	1.20 (6)	2.18 (4)
400	249	5.7 (-6)	4.28 (-9)	997	16.27	58.7	1.12 (-15)	4.15 (7)	1.83 (6)	5.42 (4)	6.30 (1)	3.87 (7)	9.32 (5)	2.05 (4)
500	311	1.1 (-6)	8.25 (-10)	997	15.21	64.7	2.06 (-16)	8.16 (6)	1.02 (5)	1.99 (3)	1.06 (0)	7.42 (6)	6.17 (5)	1.85 (4)
600	373	2.6 (-7)	1.95 (-10)	997	13.34	75.9	4.27 (-17)	1.93 (6)	6.15 (3)	8.07 (1)		1.49 (6)	4.13 (5)	1.67 (4)
700	435	8.4 (-8)	6.30 (-11)	997	10.13	103	1.02 (-17)	6.10 (5)	4.02 (2)	3.58 (0)		3.14 (5)	2.80 (5)	1.51 (4)
800	497	3.8 (-8)	2.85 (-11)	997	6.87	156	3.13 (-18)	2.74 (5)	2.84 (1)			6.91 (4)	1.92 (5)	1.38 (4)
900	559	2.2 (-8)	1.65 (-11)	997	4.95	223	1.32 (-18)	1.61 (5)	2.16 (0)			1.58 (4)	1.33 (5)	1.25 (4)
1,000	621	1.5 (-8)	1.13 (-11)	997	4.10	276	7.35 (-19)	1.08 (5)				3.78 (3)	9.27 (4)	1.15 (4)
1,200	746	7.8 (-9)	5.86 (-12)	997	3.54	337	3.32 (-19)	5.65 (4)				2.41 (2)	4.66 (4)	9.64 (3)
1,400	870	4.5 (-9)	3.38 (-12)	997	3.25	387	1.75 (-19)	3.24 (4)				1.77 (1)	2.42 (4)	8.19 (3)
1,600	994	2.8 (-9)	2.10 (-12)	997	2.95	448	9.83 (-20)	2.00 (4)				1.48 (0)	1.30 (4)	7.00 (3)
1,800	1,119	1.8 (-9)	1.35 (-12)	997	2.64	528	5.80 (-20)	1.33 (4)					7.23 (3)	6.04 (3)
2,000	1,243	1.3 (-9)	9.75 (-13)	997	2.32	629	3.61 (-20)	9.36 (3)					4.12 (3)	5.24 (3)
2,500	1,553	6.8 (-10)	5.10 (-13)	997	1.69	969	1.38 (-20)	4.91 (3)					1.13 (3)	3.78 (3)
3,000	1,864	4.4 (-10)	3.30 (-13)	997	1.34	1,368	7.05 (-21)	3.18 (3)					3.56 (2)	2.82 (3)
3,500	2,175	3.2 (-10)	2.40 (-13)	997	1.17	1,741	4.43 (-21)	2.29 (3)					1.26 (2)	2.17 (3)
4,000	2,486	2.4 (-10)	1.80 (-13)	997	1.08	2,065	3.16 (-21)	1.75 (3)					4.94 (1)	1.70 (3)
4,500	2,796	1.9 (-10)	1.43 (-13)	997	1.05	2,354	2.41 (-21)	1.39 (3)					2.11 (1)	1.37 (3)
5,000	3,107	1.6 (-10)	1.20 (-13)	997	1.03	2,624	1.92 (-21)	1.13 (3)					9.68 (0)	1.12 (3)
6,000	3,728	1.1 (-10)	8.26 (-14)	997	1.01	3,156	1.32 (-21)	7.88 (2)					2.47 (0)	7.85 (2)
7,000	4,350	8.0 (-11)	6.00 (-14)	997	1.00	3,707	9.65 (-22)	5.78 (2)						5.78 (2)
8,000	4,971	6.1 (-11)	4.58 (-14)	997	1.00	4,290	7.36 (-22)	4.42 (2)						4.42 (2)
9,000	5,592	4.8 (-11)	3.60 (-14)	997	1.00	4,912	5.80 (-22)	3.49 (2)						3.49 (2)
10,000	6,214	3.9 (-11)	2.93 (-14)	997	1.00	5,574	4.70 (-22)	2.83 (2)						2.83 (2)

(a) Numbers in parentheses denote powers of 10. Thus, 2.9 (-1) means 2.9×10^{-1}.

3.5 GENERAL EFFECTS ON MATERIALS

The behavior of materials under the lowered pressure effective at the altitude of satellite orbits is marked by two major effects. First, evaporation of the materials, or of a volatile component of the materials, is greatly enhanced by the absence of an atmosphere. Second, the layer of absorbed gas on the surface of the material may be partially removed.

In the case of structural metals, evaporation of material will not be a problem. This matter is discussed in greater detail in Chapter 15. Dushman (Ref. 15) has compiled experimental data on temperature versus vapor pressure correlation for many metals and has calculated the evaporation rates in vacuum conditions as a function of temperature and corresponding vapor pressure. In the case of plastics which contain a plasticizer of high vapor pressure, the loss of this constituent may cause significant changes in properties. Generally, plastics formed entirely from the polymerization of pure materials such as polyethylene have lower vapor pressures.

The possible removal by evaporation of both a film of conventional lubricant and of the layer of physically adsorbed gas which may act as a lubricant can cause an increase in friction of bearings and sliding surfaces unless special precautions are taken. Materials for lubricated systems will be discussed in Chapter 9. The optical properties of mirrors or the radiating characteristics of temperature-control surfaces may be altered when the surface layer of physically adsorbed gases has evaporated. On the other hand, a number of investigators have shown that the fatigue properties of metals in high vacuum are significantly better than they are in 1 atm of air (Refs. 16 and 17), although there is one limited exception to this general trend (Ref. 18).

3.6 REFERENCES

1. U.S. Standard Atmosphere, 1962, U.S. Government Printing Office, Washington, D.C., 1962
2. U.S. Standard Atmosphere Supplements, 1966, U.S. Government Printing Office, Washington, D.C., 1966
3. R. R. May, "Upper Air Density Derived From Orbits of [recoverable] Satellites and Its Variations With Latitude," Planet. Space Sci. 12, 1179–1185, 1964
4. A. D. Anderson, "Existence of a Significant Latitudinal Variation in Density From 200 to 800 Kilometers," Nature 209, 656–661, 1966
5. C. P. Lagos and J. R. Mahoney, "Numerical Studies of Seasonal and Latitudinal Variability in a Model Thermosphere," J. Atmos. Sci. 24, 89–94, 1967
6. G. M. Keating and E. J. Prior, "The Winter Helium Bulge," 1967 IQSY/COSPAR Assembly, London, England, 17–29 July 1967
7. K. K. Paetzold and H. Zschörner, "The Structure of the Upper Atmosphere and Its Variations After Satellite Observations," Space Res. 2, 958–973, 1961

8. A. D. Anderson, "An Hypothesis for the Semi-Annual Effect Appearing in Satellite Orbital Decay Data," Planet. Space Sci. 14, 849–861, 1966

9. L. Jacchia, J. Slowey, and F. Verniani, "Geomagnetic Perturbations and Upper-Atmosphere Heating," J. Geophys. Res. 72, 1423–1434, 1967

10. A. D. Anderson and W. E. Francis, "The Variation of the Neutral Atmospheric Properties With Local Time and Solar Activity From 100 to 10,000 km," J. Atmos. Sci. 23, 110–124, 1966

11. M. Nicolet, "Helium, an Important Constituent in the Lower Thermosphere," J. Geophys. Res. 66, 2263–2264, 1961

12. A. D. Anderson, "On the Inexactness of the 10.7-cm Flux From the Sun as an Index of the Total Extreme Ultraviolet Radiation," J. Atmos. Sci. 21, 1–14, 1964

13. A. D. Anderson, "Long-Term (Solar Cycle) Variation of the Extreme Ultraviolet Radiation and 10.7-Centimeter Flux From the Sun," J. Geophys. Res. 70, 3231–3234, 1965

14. W. E. Francis, "A Least Squares Method of Computing Density-Based Model Atmospheres," J. Atmos. Sci. 23, 431–442, 1966

15. S. Dushman, Scientific Foundations of Vacuum Technique, 2nd ed., John Wiley and Sons, Inc., New York, 1962

16. C. M. Hudson, Problems of Fatigue of Metals in a Vacuum Environment, National Aeronautics and Space Administration, Langley Research Center, Hampton, Va., NASA-TN-D-2563, January 1965

17. H. T. Sumsion, "Effect of High Vacuum on the Fatigue Properties of Magnesium and Two Magnesium Alloys," pp. 91–96 in Proceedings of Second Space Simulation Conference, Philadelphia, Pa., 11–13 September 1967

18. R. H. Christensen, "Fatigue of Metal Accelerated by Prolonged Exposure to High Vacuum," Trans. Am. Soc. Met. 57, 373, June 1964

Chapter 4

NONPENETRATING RADIATIONS

A. D. Anderson

Temperatures of artificial satellites or spacecraft orbiting about a planet (or a moon) in the solar system are determined mainly by (1) the direct solar radiation; (2) the reflected solar radiation, or albedo, of the planet (moon); (3) the emitted radiation of the planet (moon); and (4) the surface radiation characteristics of the artificial satellite or spacecraft, which depend on its composition, shape, and orientation. This radiation can be considered to be nonpenetrating radiation. With regard to the planet earth, its albedo radiation (reflected solar radiation) consists of ultraviolet, visible, and infrared emissions between 0.29 and 4.0 μ (Table 4-1), where $1\mu = 10^{-4}$ cm $= 10^{4}$ Å. The radiation categories cited above will be discussed in turn in this chapter.

4.1 SOLAR RADIATION

The total amount of electromagnetic radiation emitted from the sun is the same as that from a 5800°K blackbody. Solar radiation covers the spectrum from wavelengths shorter than $10^{-4}\mu$ to wavelengths longer than $10^{8}\mu$. (See Table 4-1.)

Table 4-1

CLASSIFICATION OF ELECTROMAGNETIC RADIATION BY WAVELENGTH

Wavelength (μ)	Classification
<0.01	X-Rays and γ-Rays
0.01 – 0.2	Far-Ultraviolet
0.2 – 0.32	Middle-Ultraviolet
0.32 – 0.38	Near-Ultraviolet
0.38 – 0.72	Visible
0.72 – 1.5	Near-Infrared
1.5 – 5.6	Middle-Infrared
5.6 – 1000	Far-Infrared
>1000	Microwaves and Radio Waves

The nonpenetrating portion of the solar spectrum lies between the wavelength limits 0.01 and 15 μ. About 99% of the energy of the solar spectrum lies between 0.3 and 4.0 μ. In the region between wavelengths of 0.085 and 7.0 μ the solar-spectral-irradiance data of Tables 4-1 and 4-2 of Ref. 1 are considered the best available.

These values represent the distribution of energy in the solar radiation incident on the earth's upper atmosphere when the earth is at its mean distance from the sun. The solar constant is the total solar irradiance at the earth's mean distance from the sun; it has the value 0.140 W/cm^2.* Because the orbit of the earth around the sun is slightly elliptical, the distance of the earth from the sun – and therefore the value of the solar constant – changes throughout the year. Use of the solar constant at the mean distance cited above results in a maximum error of ±3.5%.

The sun is a very stable source of radiation in the visible and adjoining spectral regions. The continuum radiation probably does not change noticeably during a solar cycle, which averages 11 years, even in the ultraviolet. However, the line radiations exhibit variations that become more important at the shorter wavelengths. The largest solar cycle variation occurs in the far ultraviolet below 0.1 μ, at wavelengths sometimes designated as the extreme ultraviolet (Table 4-1). The 10.7-cm flux from the sun is an approximate index of this variation (Ref. 2).

The data and observations discussed above have been gathered into a single curve of the solar spectrum in Fig. 4-1 (Ref. 3), which shows the spectral radiance versus wavelength. From 0.14 μ to the middle infrared, the spectrum is a continuum with superimposed absorption (Fraunhofer) lines. This portion of the curve has been smoothed to eliminate the fine detail. The solar spectrum below 0.14 μ consists entirely of sharp emission lines. These have been smoothed to intervals of 0.005 μ in order to make the continuous curve. A list of the stronger lines that show up in the solar ultraviolet spectrum below 0.19 μ is given in Table 4-2. These contribute only a small amount of energy compared with the continuum at all wavelengths longer than 0.085 μ, except in the region of the atomic-hydrogen Lyman-alpha line (0.1216 μ). At shorter wavelengths, it is also likely that the background continuum radiation contains more energy than all but the strongest lines. The intensities of the lines over the spectral region below 0.1 μ must still be regarded as tentative. Below about 0.01 μ, the coronal spectrum consists of x-rays. This penetrating radiation is discussed in Chapter 5.

4.2 ALBEDO

The albedo of an object is the ratio of the emergent light flux scattered and reflected in a given spectral region to the incident light flux in the same spectral region. If the emergent spectral intensity is known, then the albedo a_1 for a source like the sun is

$$a_1(\lambda_1, \lambda_2) = \frac{\int_{\lambda_1}^{\lambda_2} \int_0^{2\pi} \int_0^{\pi/2} I_\lambda(\theta, \varphi) \cos\theta \sin\theta \, d\theta \, d\varphi \, d\lambda}{\int_{\lambda_1}^{\lambda_2} \pi F_\lambda \cos Z \, d\lambda} \qquad (1)$$

where I_λ = emergent spectral intensity
F_λ = incident spectral intensity
Z = solar zenith angle

* On 17 October 1967 the solar constant was measured directly at 82 km; its value was 0.136 W/cm^2 (Nature 218, 259, 1968).

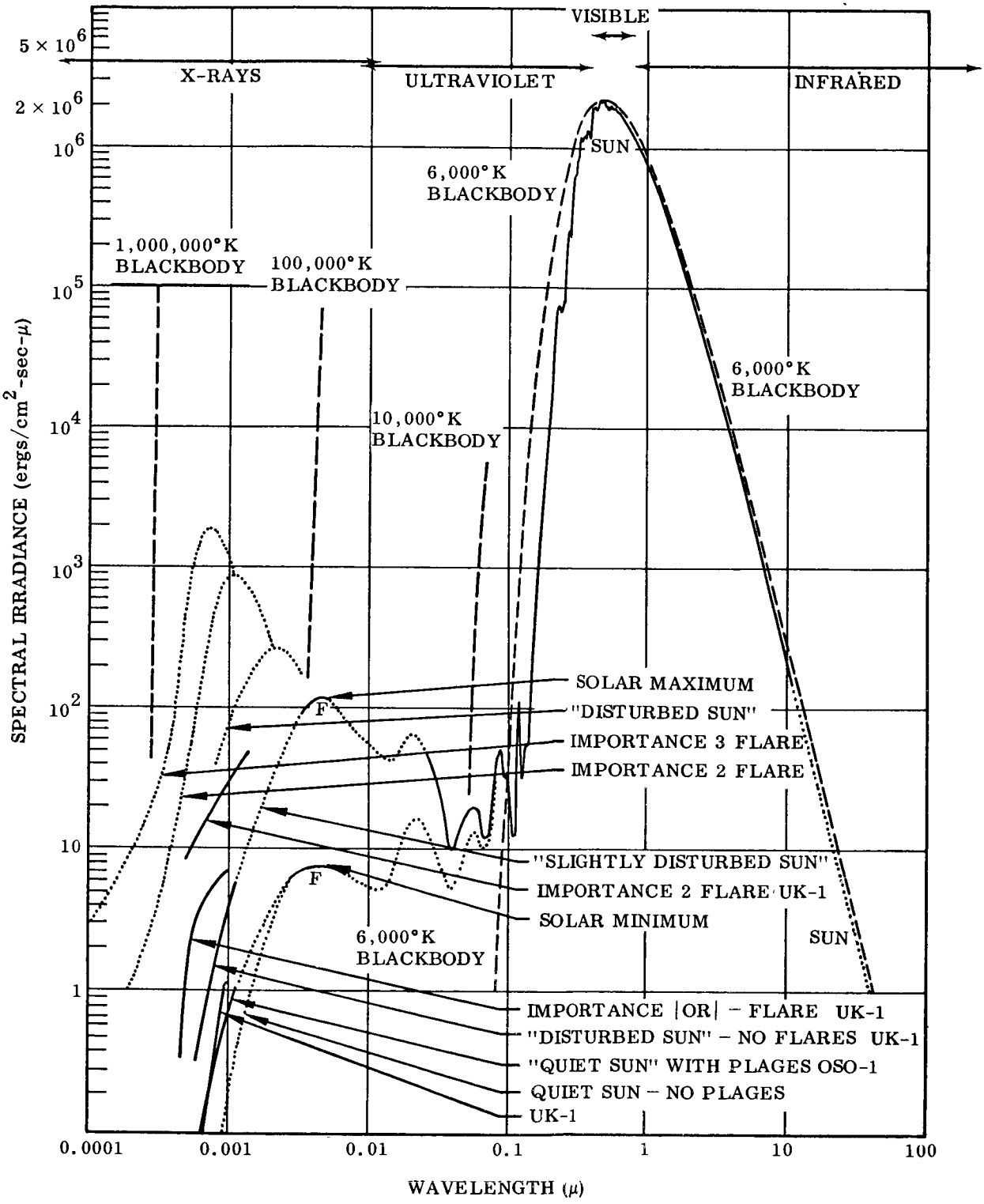

Fig. 4-1 The Solar Electromagnetic Radiation Spectrum. Solid lines represent measurements; dotted lines, estimates

Table 4-2

SOLAR-ULTRAVIOLET-SPECTRAL-LINE INTENSITIES (Ref. 1)

Source	λ (Å)	Intensity (10^{-8} W/cm^2)	Source	λ (Å)	Intensity (10^{-8} W/cm^2)
Si III	1892.03	1.0	N III	991.58	0.10
Si II[a]	1817.42	4.5	N III[a]	989.79	0.06
Si II	1808.01	1.5	C III	977.03	0.50
Al II	1670.81	0.8	H I(δ)	949.74	0.10
C I[a]	1657.00	1.6	H I(ϵ)	937.80	0.05
He II	1640.47	0.7	H I(Cont.)	911−840	2.3
C I	1561.40	0.9	O II, III[a]	835	0.13
C IV	1550.77	0.6	O IV[a]	790.2	0.03
C IV	1548.19	1.1	O IV	787.7	0.08
Si II	1533.44	0.41	Ne VIII	780.3	0.04
Si II	1526.70	0.38	Ne VIII	770.4	0.11
Si IV	1402.73	0.13	N IV	765.1	0.06
Si IV	1393.73	0.30	O III[a]	703	0.07
C II	1335.68	0.50	O V	629.7	0.56
C II	1334.51	0.50	Mg X	625	0.13
O I	1306.02	0.25	Mg X	610	0.26
O I	1304.86	0.20	He I	584.3	0.54
O I	1302.17	0.13	O IV[a]	555−553	0.19
Si II	1265.04	0.20	He I	537	0.05
Si II[a]	1260.66	0.10	Si XII	499	0.17
N V[a]	1242.78	0.03	Ne VII	465.2	0.12
N V	1238.80	0.04	Mg IX	368.1	0.32
H I(α)	1215.67	51.0[b]	He II(α)	303.8	2.5
Si III	1206.52	0.30	Fe XV	283	0.43
C III[a]	1175.70	0.10	He II	256	0.23
C I[a]	1139.89	0.03		<200	10
N II[a]	1085.70	0.06		<20	0.23
O VI	1037.61	0.25		<8	0.02
O VI	1031.91	0.20			
H I(β)	1025.72	0.60			

(a) Blended with additional lines.
(b) Within 1 Å bandwidth centered on line.

The albedo a_1 is the albedo of a point. The albedo of an object would have to be obtained by averaging over the object.

4.2.1 Albedos of the Moon and Planets

The normal albedo of the moon is the value for an object near the center of the full moon (Ref. 4). This concept is widely used in lunar photometry and is quite simple for practical purposes. Lunar photographs show two main types of surface: the dark maria (normal albedo 0.065) and the brighter terrae (normal albedo 0.105). The darkest spot – inside Oceanus Procellarum – has a normal albedo of 0.051, and the brightest spot is the crater Aristarchus with a normal albedo of 0.176.

The Bond albedo, the ratio of the total flux reflected in all directions to the total incident flux, appears to be the most suitable for use in discussion of the planets. The Bond albedo, A, is given in Chapter 8 of Ref. 4 as

$$A = pq \tag{2}$$

where p is the geometric albedo and q is the phase integral. The factor p depends only on observations made at full phase and can be derived for all planets whose diameters are known. The factor q can be computed from the observed variation in brightness with solar phase angle for Mercury, Venus, earth, and the moon but must be estimated from theory for the remaining planets. Table 4-3 presents p, q, and A for the moon and the planets (Chapter 8 of Ref. 4).

Table 4-3

ALBEDOS OF THE MOON AND PLANETS

	p	q	A
Moon	0.115	0.585	0.067
Mercury	0.100	0.563	0.056
Venus	0.586	1.296	0.76
Earth	0.367	1.095	0.40(a)
Mars	0.154	1.04	0.16
Jupiter	0.445	1.65	0.73
Saturn	0.461	1.65	0.76
Uranus	0.565	1.65	0.93
Neptune	0.509	1.65	0.84
Pluto	0.130	1.04	0.14

(a) Based on observations in France only, a mean value for the entire earth is 0.36.

The Bond albedo is only approximate in that it assumes that the brightness of the planet depends only on the phase angle, i.e., that the surface has uniform properties of diffuse reflection. This is not true, for instance, in the case of Mars with regard to its north or south poles. The uncertainty in the values of p in Table 4-3 is nearly 5%, and additional uncertainty is indicated for Mercury and Pluto because their diameters are not well known. The value of q adopted for Pluto is the same as that derived for Mars, although a value nearer to that used for Mercury may be more appropriate.

4.2.2 Albedo of the Earth

The albedo of a point on the earth's surface, a_2, as measured from an orbiting satellite is (Ref. 5)

$$a_2 = \frac{F}{\cos Z \int S_\lambda \Phi(\lambda)\, d\lambda} \tag{3}$$

where

F = flux measured by the sensor
S_λ = incident spectral flux
$\Phi(\lambda)$ = effective spectral response of the sensor

In order to use Eq. (3) to determine the albedo of an area, an assumption has to be made as to the scattering function of the area. One assumption made is that the surface scatters isotropically. The albedo of an area measured in this way is dependent (especially for a portion of the earth where scattering from the atmosphere is the major contributor) on the exact shape of the spectral response of the sensor. Actually, the area neither reflects nor radiates according to Lambert's law (like a perfectly diffuse surface). Assumptions about the nonisotropic nature of the radiation can be made so that calculations of this radiation emerging from the atmosphere can be based on model atmospheres (Ref. 6).

For the earth, the visual albedo will not be observed directly until a lunar observatory is established on the surface of the moon or an orbital observatory is used at a distance comparable to that of the moon. Usually, the albedo of the earth is derived theoretically or inferred from a series of local observations, each of which refers to a limited area. Since the total of these observations covers only a small portion of the surface of the earth in a reasonable period of time, they leave considerable doubt as to the total albedo. The albedo of the earth has been computed from measurements made from artificial satellites. However, there is some uncertainty concerning the satellite data used because of instrumental degradation (Ref. 7).

Another, little-used, method is the computation of the albedo of the entire earth from observations of earth-light reflected from a new moon (Ref. 8). In this type of observation, a comparison is made between the brightness of the portion of the moon illuminated by the sun and the portion illuminated by the earth. A correction is applied for

the geometry, and the brightness of the earth relative to that of the sun is derived. This then leads to the albedo of the earth. To calculate accurately the albedo of the earth by this method, it is necessary to know the phase curve of both the moon and the earth. Because of the long-term nature of these studies, it is important that observations be made continuously, and preferably they should be made from scattered localities over the earth to establish an albedo for the whole earth. Phase curves for the portions of the earth observable from each of these places is necessary. It will be some years before they are available for localities other than Europe (Ref. 9).

The earth's albedo may be regarded as the sum of three components: (1) the albedo of the earth's surface, (2) the albedo associated with the backscattering of the incident radiation by the atmosphere; and (3) the albedo of clouds. The mean albedo is about 50% in the ultraviolet range and 28% in the infrared range. In the visible region, it is 30 to 40%. For a cloud-covered earth, the albedo is 50 to 60%; for a cloudless earth, it is about 16%. Table 4-4 presents a list of the albedo ranges of the earth for various cases.

Table 4-4

EARTH ALBEDO

Source	Albedo Range (%)	Ref.
Clouds	17–81	10
Terrain	7–28	11
Soils	5–43	12
Snow Cover	29–86	12
Ice Surface	12–36	12
Sea Surface	2–70	12
Latitude and Seasonal Averages	28–50	12
Latitude Variation Under Various Sky Conditions	12–92	13
Various Surfaces for Different Wavelengths and Cloudiness	1–37	12

Most of the solar energy reflected to space is reflected from clouds. The albedo of clouds is so variable that it is impossible to specify an average value for the total reflection of clouds. Therefore, it is necessary to measure the albedo of the whole earth first and then subtract the contributions by the atmosphere and the ground. The remainder is the albedo of the clouds. One computation, based on moon measurements, indicates that the average albedo of clouds is about 50 to 55% of the energy incident on the clouds (Ref. 14).

Inasmuch as the data referenced in Table 4-4 represent experimental averages, individual measurements may depart considerably from these data. The values of the

albedo are averages over various kinds of surface cover and also averages with respect to time. The term "soil" must be defined in terms of the amount of moisture, the grain size (roughness of surface), and the color of the surface. The albedo of all kinds of soil decreases with increasing moisture because the albedo of water is lower than that of soil. The albedo of snow depends on the amount of impurity it contains, on its surface roughness, and on the angle of incidence.

The values of the albedo for water surfaces are noticeably different for direct solar radiation and for scattered sky radiation. Robinson (Ref. 12) presents computed and observed values of the albedo for direct radiation at various angles of incidence on a smooth water surface. The experimental values of the albedo are in good agreement with the theoretical calculations made with the Fresnel formula. Robinson also gives theoretical values of the albedo for smooth and rough water surfaces at various zenith distances of the sun. Experimental determinations of the albedo of water surfaces for scattered radiation have led to values between 5 and 8%. This albedo varies considerably with the degree of cloudiness of the sky. However, even during a clear sky, it varies markedly due to the anisotropy of the sky's luminence. Since the albedo varies with the elevation angle of the sun, it exhibits a diurnal and an annual variation, increasing with decreasing elevation of the sun. Also, the albedo depends on the spectral composition of the incident radiation. The incident radiation contains a higher proportion of the short-wave radiation as the elevation of the sun increases. The effect of the wavelength on the albedo is toward an increase in the albedo with decreasing elevation of the sun, contributing toward a diurnal variation.

4.3 THERMAL RADIATION OF THE EARTH

The thermal radiation of the earth and atmosphere is infrared radiation with a wavelength greater than 1.5 μ (Table 4-1). Table 4-5 gives values for the total outgoing radiation as extracted by Johnson (Ref. 1) from Baur and Phillips (Ref. 15). The values have been averaged over a period of a day or longer. Houghton's annual-average values for the long-wave radiation (Ref. 16) are shown in the "Annual" column of Table 4-5. His data are considered to be more accurate than Baur and Phillips' in terms of annual averages, but they do not show the seasonal trend indicated by Baur and Phillips. The quantities of interest for satellite thermal control are the long-term averages. Thermal time constants and the times for material degradation are great enough to mask the effects of short-term, localized variations in earth thermal emission. Only small errors ensue when the annual average emission is used for any season. Also, because of the effect of heat storage, the change in absorbed solar radiation causes only small seasonal variations in the average emission of the whole earth. Therefore, earth emission can be taken to be independent of season without introducing significant error. Houghton's average annual values listed in Table 4-5 are adequate for any time of the year.

Johnson (Ref. 1) has presented curves for the earth and atmospheric emission spectra. These curves are shown in Fig. 4-2, where the solid curve is the approximate radiation from the earth and atmosphere; the 288°K blackbody curve approximates the radiation from the earth's surface; and the 218°K blackbody curve approximates the

Table 4-5

TOTAL LONG-WAVE RADIATION FROM THE EARTH AND ATMOSPHERE

Latitude (deg)	Long-Wave Energy Radiated (W/cm^2)				
	Jan	21 Mar	Jul	23 Sep	Annual
0–10	0.0203	0.0212	0.0209	0.0206	0.0225
10–20	0.0206	0.0210	0.0210	0.0211	0.0230
20–30	0.0203	0.0204	0.0213	0.0213	0.0228
30–40	0.0193	0.0194	0.0216	0.0213	0.0222
40–50	0.0175	0.0175	0.0202	0.0201	0.0210
50–60	0.0164	0.0164	0.0195	0.0185	0.0195
60–90	0.0156	0.0152	0.0189	0.0177	0.0183

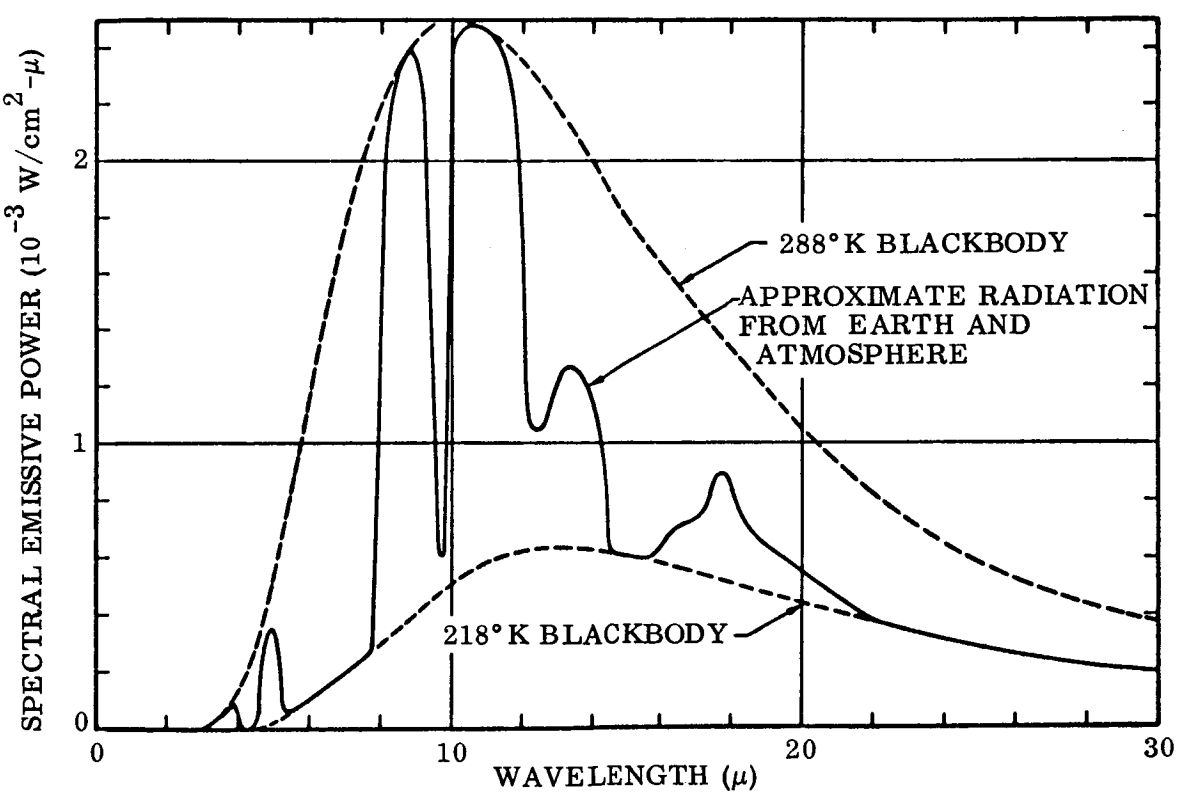

Fig. 4-2 Typical Spectral Emissive Power Curve for the Thermal Radiation Leaving the Earth

radiation from the atmosphere in spectral regions where the atmosphere is opaque. The temperature of a satellite depends on absorbed energy or on the spectral distribution of incident energy and the spectral radiation characteristics of the satellite surface. However, the total earth emissive power and total absorptance for long-wavelength energy can be used to calculate satellite heating. Absorptance for most materials shows only small variations with wavelength beyond 8 μ, and, as illustrated in Fig. 4-2, nearly all the energy emitted by the earth-atmosphere system is beyond 8 μ. Camack (Ref. 13) presents a model that establishes extremes in the variation of earth radiation and albedo and assumes a frequency distribution for occurrences between these extremes.

4.4 GENERAL EFFECTS ON MATERIALS

Solar radiation, mostly visible and infrared, is one of the most important factors in determination of the thermal equilibrium of spacecraft. In addition, temperatures of near-earth artificial satellites are governed by the thermal radiation interchange between the earth and the satellite, consisting of albedo, visible and infrared radiation, and earth infrared emission. Owing to differences in absorption coefficients, the effects in the visible range are somewhat less than those for the thermal range. Nearly all materials display a monochromatic absorptance that is practically independent of wavelength in the spectral region covered by earth radiation.

Prolonged exposure to solar ultraviolet and x-ray radiation can cause serious damage to insulation and optical elements. In plastics there can be embrittlement, softening, changes in electrical properties, and discoloration with changes in optical properties. Degradation of satellite surface materials also occurs because of the earth albedo ultraviolet radiation. The solar and earth albedo ultraviolet radiation possesses enough energy per quantum to induce rupture of many chemical bonds and thus initiate chemical reactions (Refs. 17 and 18). The effect of ultraviolet radiation on structural metals is negligible except for a static charge produced by the removal of electrons by the photoelectric effect. The effects of solar ultraviolet radiation on the properties of materials for spacecraft construction are covered in detail in Chapters 7 through 16.

4.5 REFERENCES

1. F. S. Johnson, "Solar Radiation," Chapter 4 in Satellite Environment Handbook, 2nd ed., ed. F. S. Johnson, Stanford University Press, Stanford, Calif., 1965

2. A. D. Anderson, "Long-Term (Solar Cycle) Variation of the Extreme Ultraviolet Radiation and 10.7-cm Flux From the Sun," J. Geophys. Res. 70, 3231–3234, 1965

3. Solar Electromagnetic Radiation, NASA SP-8005, National Aeronautics and Space Administration, June 1965

4. G. P. Kuiper and B. M. Middlehurst, "Planets and Satellites," Vol. III of The Solar System, University of Chicago Press, Chicago, Ill., 1961

5. L. P. Whitehill, Survey on Earth Albedo, Massachusetts Institute of Technology Tech. Note 1966 – 53, October 1966

6. W. Bandeen et al., "Infrared and Reflected Radiation Measurements From the Tiros II Meteorological Satellite," J. Geophys. Res. 66, 3171, 1961

7. W. Nordberg, "Research With Tiros Radiation Measurements," Astronautics and Aerospace Eng. 1, 82, April 1963

8. A. Danjon, "Albedo, Color, and Polarization of the Earth," pp. 726 – 738 in The Earth as a Planet, ed. G. P. Kuiper, University of Chicago Press, Chicago, Ill., 1954

9. W. B. Murcray, Study of the Albedo of the Earth, Final Report on Contract Nonr 3010(03)(AD 642 356), Geophysical Institute, University of Alaska, September 1966

10. S. Fritz, "Solar Radiant Energy and Its Modification by the Earth and Its Atmosphere," pp. 13 – 33 in Compendium of Meteorology, ed. T. F. Malone, American Meteorological Society, Boston, Mass., 1951

11. R. J. List, Smithsonian Meteorological Tables, Vol. 114, Smithsonian Institution, Washington, D.C., pp. 442 – 444, 1958

12. N. Robinson, Solar Radiation, Elsevier Publishing Company, New York, 1966

13. W. G. Camack, "Albedo and Earth Radiation," Chapter 6 in Space Materials Handbook, eds. C. Goetzel, J. Rittenhouse, and J. Singletary, Addison-Wesley Publishing Company, Palo Alto, Calif., 1965

14. S. Fritz, "The Albedo of the Planet Earth and of Clouds," J. Meteor. 6, 277 – 282, 1949

15. F. Baur and H. Phillips, "Der Wärmenhaushalt der Lufthülle der Nordhalbkugel in Januar und Juli and zur Zeit der Äquinoktien und Solstien," Part 1, Gerlands Beitr. Geophysik 42, 160 – 207, 1934

16. H. G. Houghton, "On the Annual Heat Balance of the Northern Hemisphere," J. Meteor. 11, 1 – 9, 1954

17. F. A. Bovey, Effects of Ionizing Radiation on Natural and Synthetic High Polymers, Interscience Publishers, New York, 1958

18. A. J. Swallow, Radiation Chemistry and Organic Compounds, Pergamon Press, London, 1960

Chapter 5

PENETRATING RADIATIONS

E. E. Gaines
W. L. Imhof

The components of the penetrating radiation environment for a given spacecraft which may arise from various sources are characterized by quite different spatial configurations and time variations. Thus, assessment of the accumulated fluxes of radiation encountered by a space vehicle over any length of time is, in general, a complex problem. These components, from natural and man-made sources, are discussed in the following sections, along with a description of the methods available for calculating the cumulative external radiation environment and the local environment within a spacecraft or other shielded configuration.

5.1 NATURAL RADIATION ENVIRONMENT

The natural radiation environment, as differentiated from the radiations that are present only because of actions taken by man, consists of energetic particles both charged and neutral as well as high-energy electromagnetic radiations. The most important of these from the standpoint of damage to materials in space are the charged particles because of their relatively high intensities and damage coefficients.

5.1.1 Charged Particles

Although most of the known charged particles may be present in space, only electrons, protons, and helium nuclei exist in sufficient numbers to be of interest in their effects on spacecraft materials. These particles display varying energy distributions and temporal fluctuations in different regions of space, so that it is convenient to assess the effects of a single particle type on a given spacecraft separately for the various spatial regions.

5.1.1.1 Geomagnetically Trapped Radiation

For orbits near the earth (up to approximately 20,000-nm or 23,000-sm in altitude), geomagnetically trapped or Van Allen radiation is of great importance. This radiation is confined to the volume occupied by the earth's magnetic field which is bounded by the region of interaction between the magnetosphere and the solar plasma. The earth's magnetic field is very nearly a pure dipole field, so that the magnetic shell described by the set of field lines having the same integral invariant is an approximately toroidal surface. A charged particle trapped on a field line follows a helical path around the field line; this path is determined by the initial conditions at the time the particle is injected, such as the initial energy of the particle and its pitch angle with respect to the field line direction. At some point on the field line, the particle "mirrors" or reverses its motion parallel to the field and bounces back and forth between mirror

points of equal field strength, at the same time drifting in longitude on the shell. If the mirror points are in a low enough atmospheric density so that the probability of scattering is small, the particle will be stably trapped unless the field line on which it is trapped becomes distorted. If one or both of the mirror points are in a part of the atmosphere where the density is sufficiently great, the motion of the particle may be changed by scattering from atoms or electrons; and, as a result of the energy loss or change in direction of the particle, it is eventually lost as a trapped radiation particle.

Since the spatial distribution of trapped particles is a function of the magnetic field, and since a dipole field possesses a high degree of symmetry, a convenient system for mapping the intensities of trapped particles is in terms of two coordinates that describe the magnetic shell upon which a particle remains trapped: the total field strength, B, and the radial distance to the intersection of the field line with the magnetic equatorial plane, L(Ref. 1). This system can be transformed for easier visualization to R , λ coordinates where R is the radial distance from the center of the earth and λ is the geomagnetic latitude. In this system, R and L are approximately equal at the geomagnetic equator and are usually expressed in units of earth radii.

Trapped protons. The trapped proton belt is the most important region of the radiation environment for many spacecraft in low to medium altitude orbits because of the high flux intensities, large damage coefficients, and deep penetration of materials.

A compilation of measurements of the trapped protons made between 1961 and 1965 (Refs. 2 and 3) has resulted in a good model of this portion of the environment including spatial intensity distributions, energy spectra, and some assumptions as to the temporal variations of the first two parameters. The integral flux distributions above 0.4, 4, and 34 MeV energy thresholds are shown in Figs. 5-1, 5-2, and 5-3 in the form of isoflux contours on R , λ maps. It is evident from the difference in spatial extent between the 0.4-MeV map and the two higher energy maps that it is convenient to think of zones in the proton belt, one with virtually no protons with energies greater than 4 MeV. This may be called the "outer" radiation zone, which extends between an L value of about 4 (in units of earth radii) to the outer boundary of particle trapping. This zone is characterized by time variations in flux intensities and corresponding changes in energy spectra with time. Measurements in this region do not have very extensive time coverage, so the intensities and spectra presented here are primarily based on 1962 data (Ref. 4) which were rather complete in spatial coverage and which showed higher intensities than some later measurements. These intensities are probably not upper limits for this zone but are more conservative as far as making predictions of damage to spacecraft.

Energy spectra at the magnetic equator for various L values in the inner and outer proton zones are presented in Figs. 5-4 and 5-5. Variations in the outer zone spectra with time occur because of energy selective changes in proton intensities. The spectra shown can generally be fit rather well by an exponential form: $\Phi(E) = \Phi_1 \exp[-(E - E_1)/Eo]$ where Φ_1 is the integral flux above the reference energy E_1 (0.4 MeV in this case), and Eo is the spectral energy parameter. A power law spectral fit can

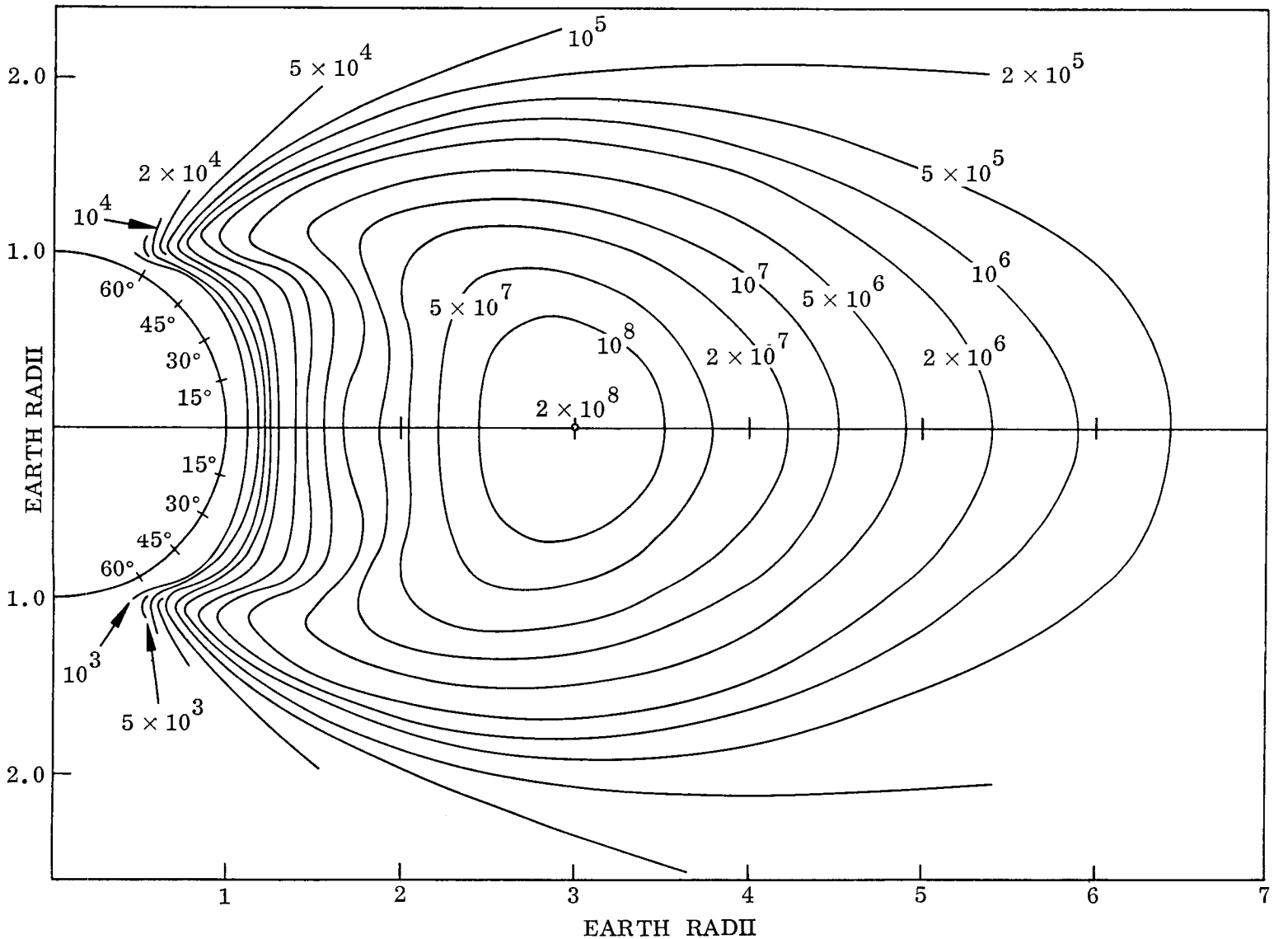

Fig. 5-1 Proton Isoflux Contours (E > 0.4 MeV) (Contours are labeled in units of protons/cm^2-sec.)

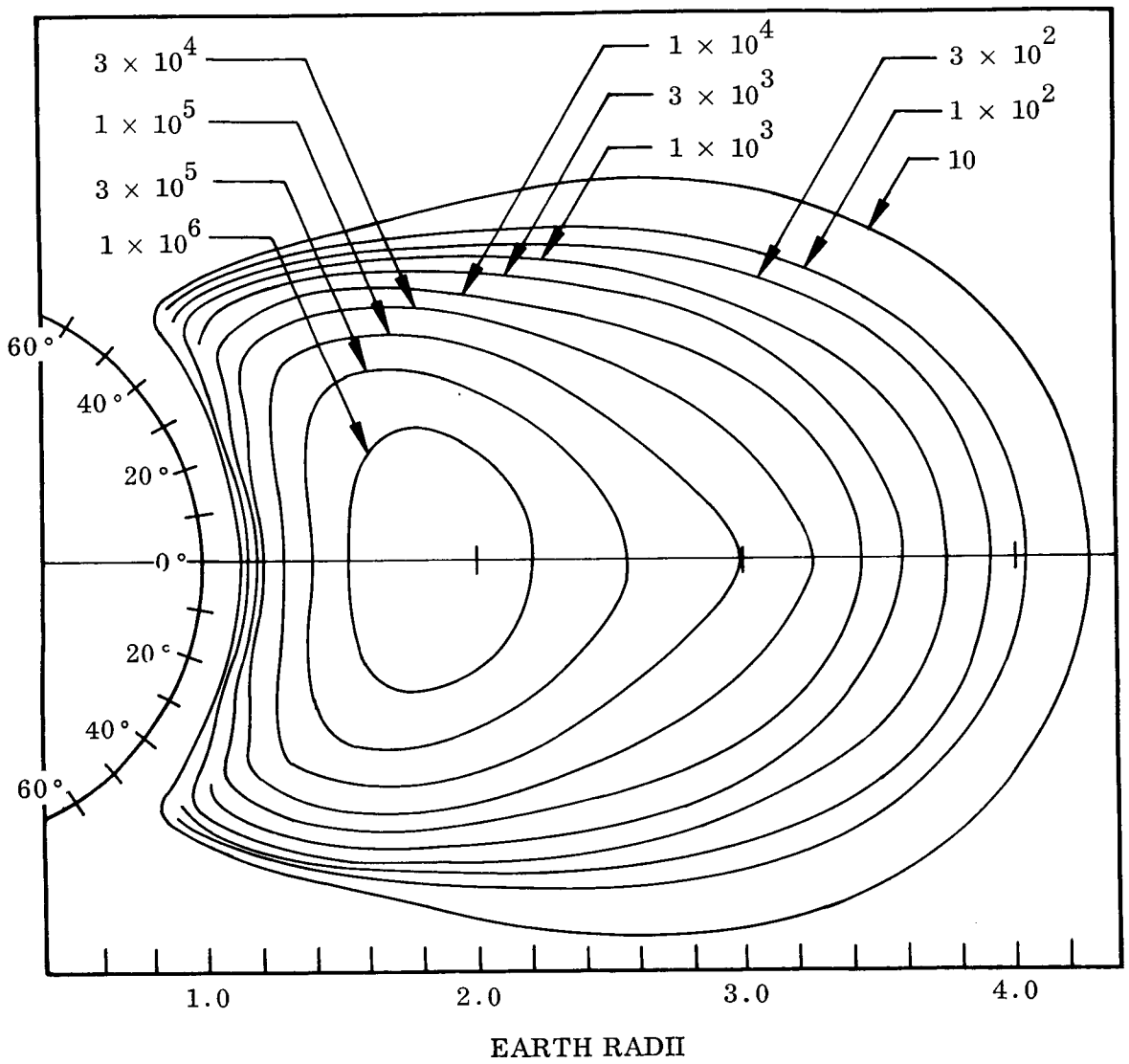

Fig. 5-2 Proton Isoflux Contours (E > 4 MeV). (Contours are labeled in units of protons/cm^2-sec.)

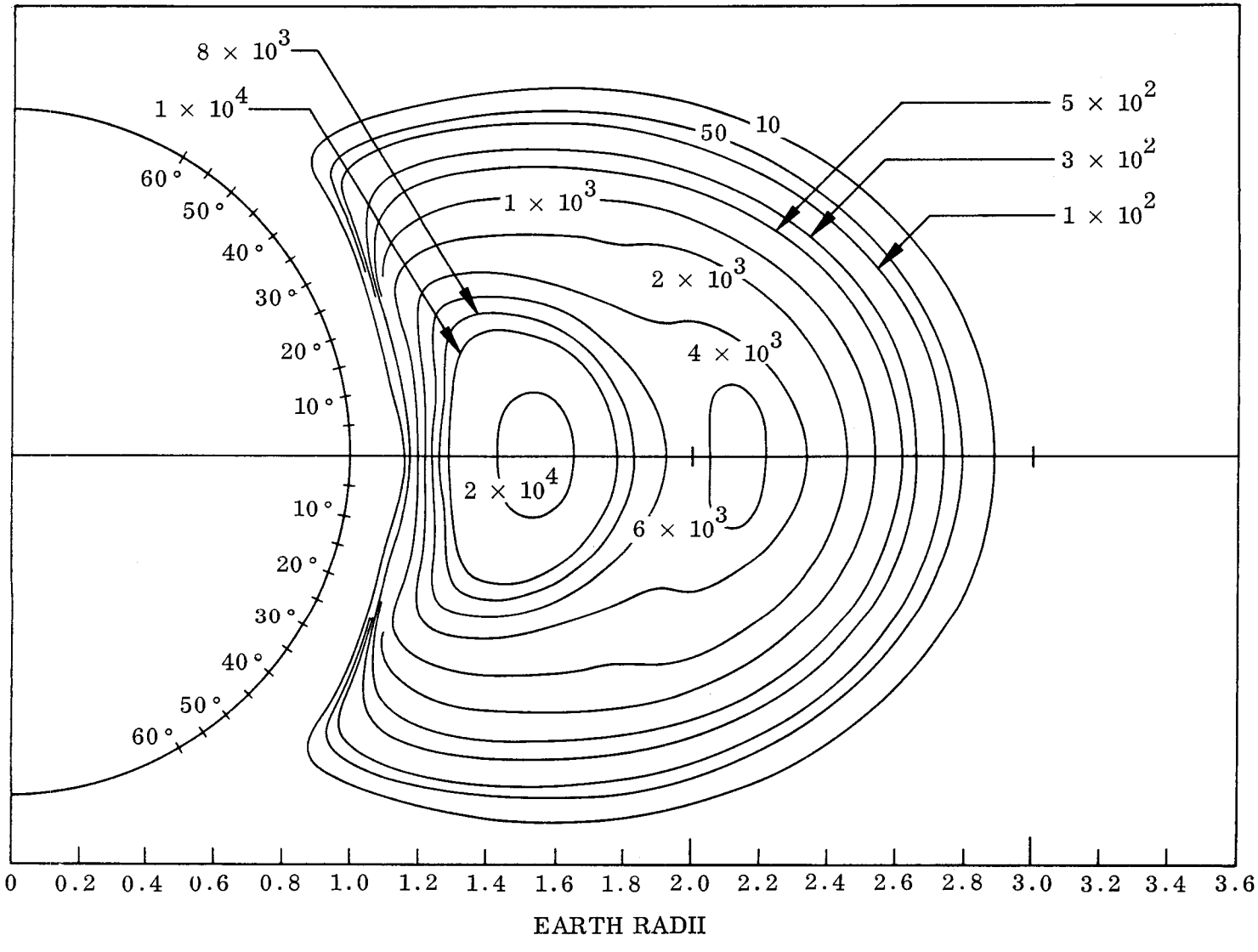

Fig. 5-3 Proton Isoflux Contours (E > 34 MeV). (Contours are labeled in units of protons/cm^2-sec.)

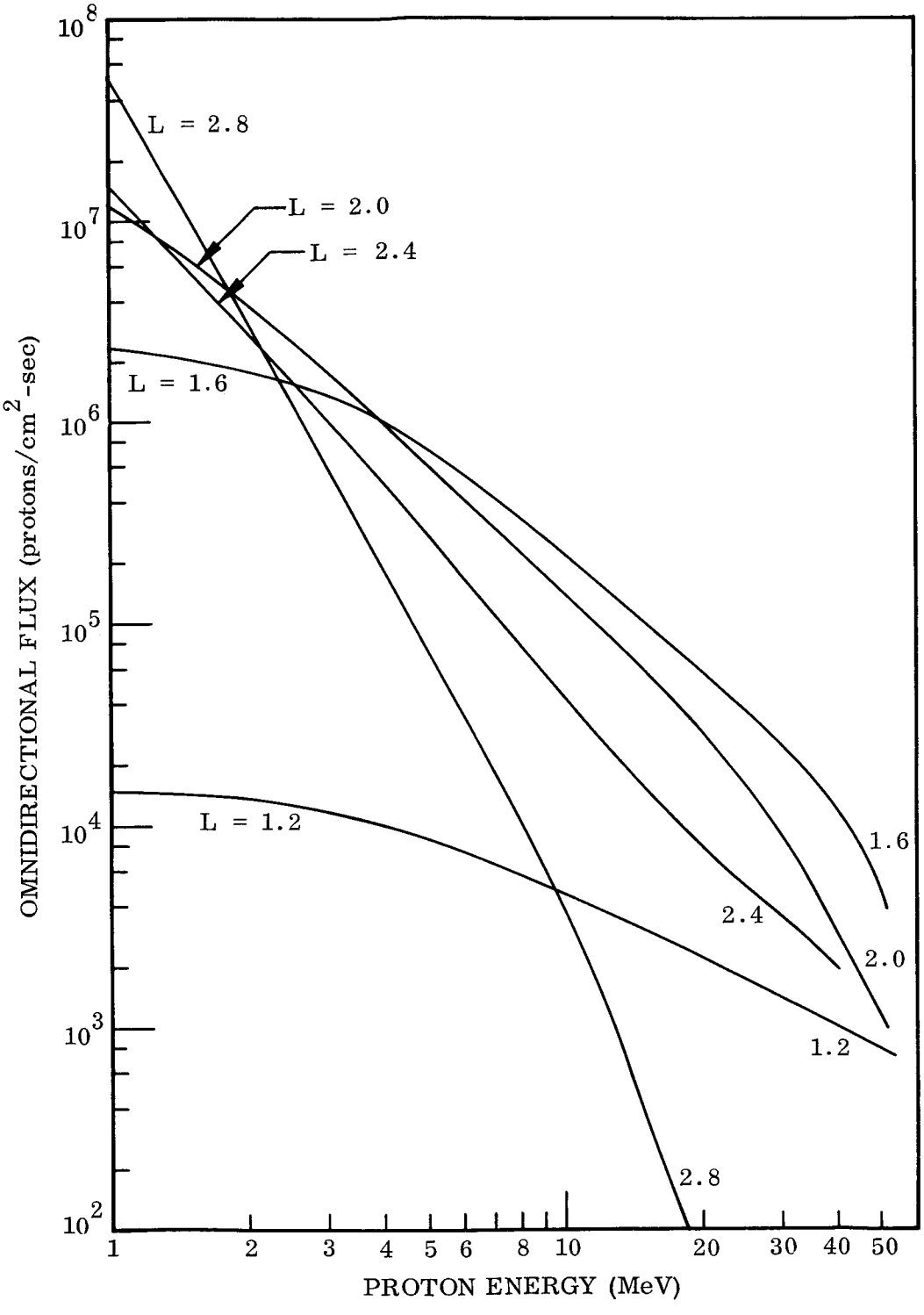

Fig. 5-4 Inner Zone Proton Spectra

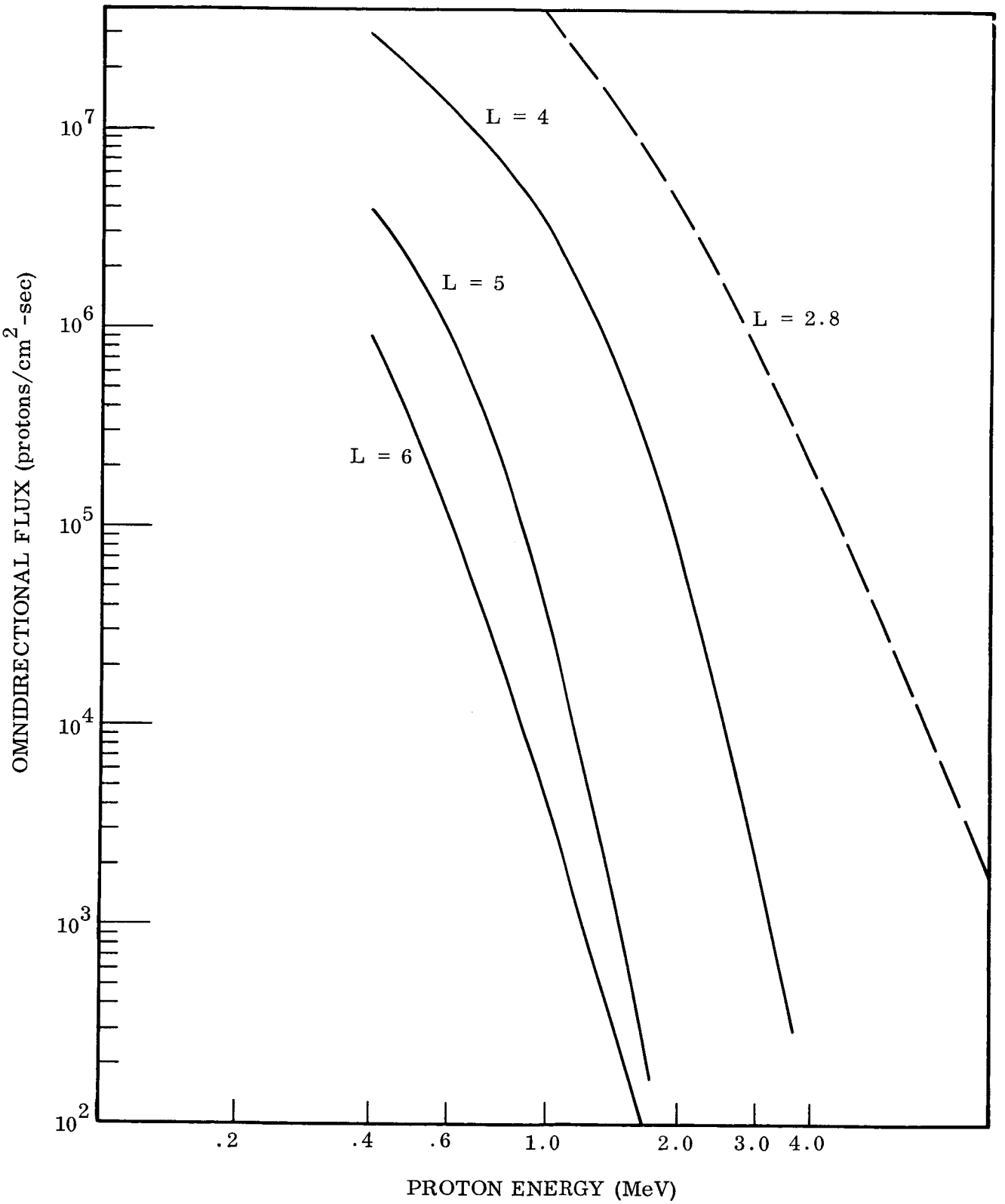

Fig. 5-5 Outer Zone Proton Spectra

also represent the data over a limited energy range, and there are not enough data to indicate clearly that either form is the more representative of the proton fluxes in the outer zone. Fluxes of protons at energies lower than the limits shown in Figs. 5-4 and 5-5 do exist and may be of importance in producing surface damage in materials. However, the data describing these portions of the spectra are rather limited, and large uncertainties would be inherent in trying to extend this portion of the proton model.

The intensities and energy spectra of protons for $L \lesssim 2$ in the inner zone are much more stable in time than those in the outer zone (Refs. 5 and 6). This is due to the fact that the higher rigidity of the magnetic field in this region makes it less susceptible to distortion from magnetic disturbances originating outside the magnetosphere. There is a variation in flux intensities in the lower edge of the inner zone over the 11-year period of the solar cycle (Refs. 7 and 8). This is due to an increase in the effective density in the upper atmosphere during the period of maximum solar activity. The effect of this variation will be a decrease in flux intensities at altitudes up to a few hundred nautical miles during the solar maximum as compared with the solar minimum period. This reduction in fluxes is approximately a factor of 2 between 1966 and November 1967 for altitudes up to about 300 nm (Ref. 8). The energy spectra of protons in this region would be expected to change with the variations in flux since particle loss from atmospheric scattering is an energy dependent process. Few measurements of these spectral changes during solar maximum are available, but more should be forthcoming beginning this year and through the current solar cycle maximum.

Trapped Electrons. The trapped electron belt coincides spatially with the proton belt but has different configurations in its intensity and energy spectrum distributions. A model of these distributions was derived from data accumulated between late 1962 and 1965 (Ref. 9). All of these measurements were made after the creation of the artificial electron belt by beta decay electrons from the Starfish high-altitude nuclear explosion on 9 July 1962. A more detailed discussion of man-made portions of the radiation environment appears in section 5.2, and only the gross characteristics of the artificial electron belt as they pertain to the current environment will be covered here. Since trapped electrons of natural origin were not well measured before 1962, our present knowledge does not permit a clean separation in the inner radiation belt between naturally occurring electrons and those of artificial origin.

The integral flux distribution above 0.5 MeV electron energy as of August 1964 is given in Fig. 5-6. As in the case of trapped protons, the electron belt is divided into an inner and outer zone, with the zone boundary being taken at a minimum in the distribution of high-energy electrons at $L \sim 2.5 - 3$ earth radii. The inner zone in late 1964 was characterized by energy spectra generally similar to a fission beta spectrum (Fig. 5-7) and by monotonic losses in intensity, the loss rate being highest at very low L values and fairly uniform at about a factor of 3 decrease in intensities each year for $L \lesssim 1.3$ (Ref. 10). Thus, for the main portion of the inner zone, the fluxes of artificially injected electrons will be about two orders of magnitude lower in late 1968 than those shown in Fig. 5-6.

The electron flux intensities in the outer zone ($L \gtrsim 2.5$) shown in Fig. 5-6 are approximate mean values from data taken from 1962 to 1964, near a period of minimum solar activity. Intensities throughout this zone show fluctuations of as much as two orders of magnitude over time periods of weeks or a few months. Since changes in spectral shape might be expected to accompany the intensity fluctuations, the spectra shown for L = 3,4, and 5 in Fig. 5-7 are typical only. They may, however, be representative of longer time averaged spectra, since selected data from which they were derived agreed relatively well over the period 1962–1964. For a period of maximum solar activity, it may not be unreasonable to assume that the average electron flux intensities in the outer zone may be closer to the peak fluxes measured in the quiet period 1962–1964, or nearly an order of magnitude higher than those shown in Fig. 5-6. This assumption, although it is not supported by experimental data, will result in more conservative radiation effects predictions for the solar maximum period 1968–1971.

Trapped Alpha Particles. Alpha particles trapped in the geomagnetic field have been observed from the satellite Injun IV (Ref. 11). The peak of the alpha flux intensity occurs at $L \sim 3.1$, and at this position the ratio of the flux of alpha particles with energies greater than 2.09 MeV to that of protons with energies greater than 0.52 MeV is 2.3×10^{-4}. The energy spectrum of the trapped alpha particles through the region of maximum intensity can be represented analytically by an exponential form with a spectral parameter energy Eo = 1.5 MeV. This steep spectrum, with almost no particles above 10 MeV, coupled with the low integral intensities, allows one to ignore trapped alpha particles as compared with protons and electrons in radiation effects calculations.

Calculation of Accumulated Fluxes. It can be seen from the foregoing discussion of trapped radiation that the calculation of the particle fluxes accumulated by a particular spacecraft at a given time involves many variables and is not simple to perform. Computers are quite well suited to this type of calculation. Programs have been in use for some time which compute B and L coordinates from the spacecraft position coordinates, interpolate the flux at that position from an input flux map, and sum the resultant fluxes over the spacecraft orbit for any required period of time. One such program which has been modified for flexibility and convenience at the Lockheed Palo Alto Research Laboratory will either read the spacecraft positions from an ephemeris tape or compute them from input orbital parameters. The program computes the instantanous and summed integral fluxes of protons and electrons above five threshold energies for each type of particle. The electron map is adjusted by the program for losses from the inner zone and solar maximum increases in the outer zone for future proposed vehicles by putting in the elapsed time between the date of the original map and the orbiting date of the vehicle.

Since a large fraction of spacecraft in the past have been in low-altitude circular orbits and it is probable that this type of orbit will continue to be used in the future, calculations have been made for two orbital inclination angles, 30 and 90 deg, at various altitudes. The electron flux per day of particles with energies greater than 0.5 MeV in December 1968 versus orbital altitude is presented in Fig. 5-8. The fluxes shown in this figure can be taken as upper limits for later dates, barring any

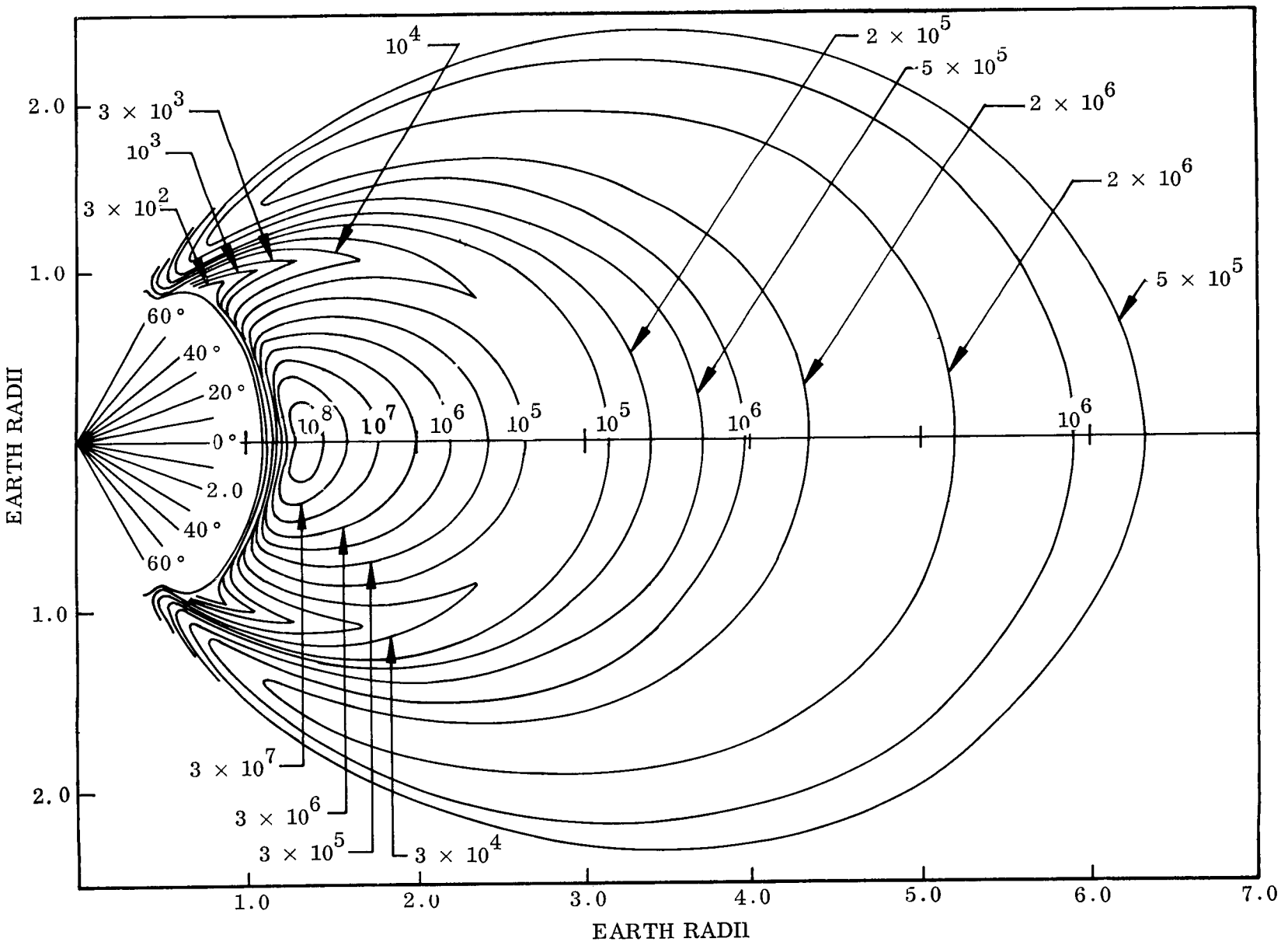

Fig. 5-6 Trapped Electron Isoflux Contours (E > 0.5 MeV) as of August 1964. (Contours are labeled in units of electrons/cm^2-sec.)

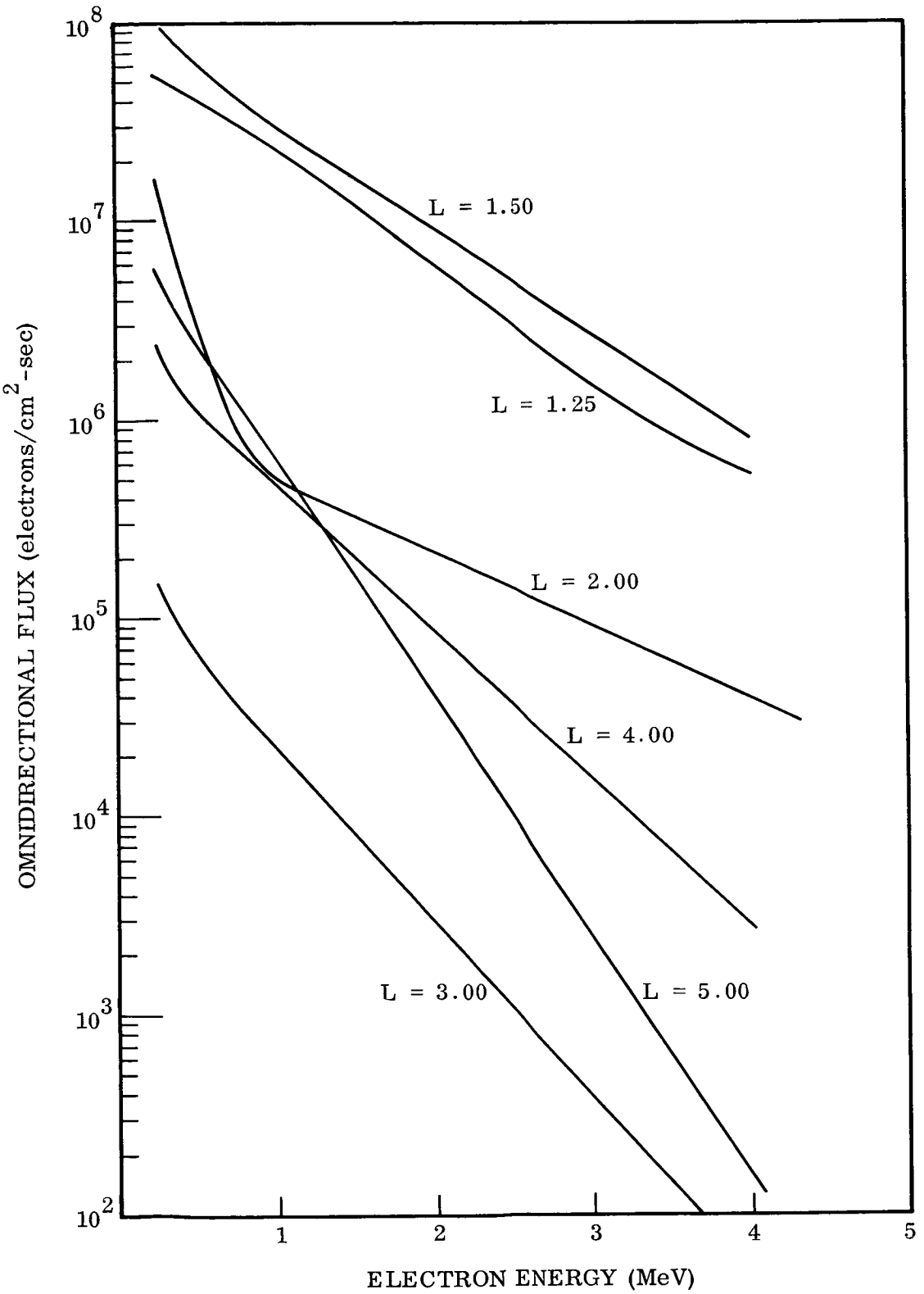

Fig. 5-7 Trapped Electron Spectra

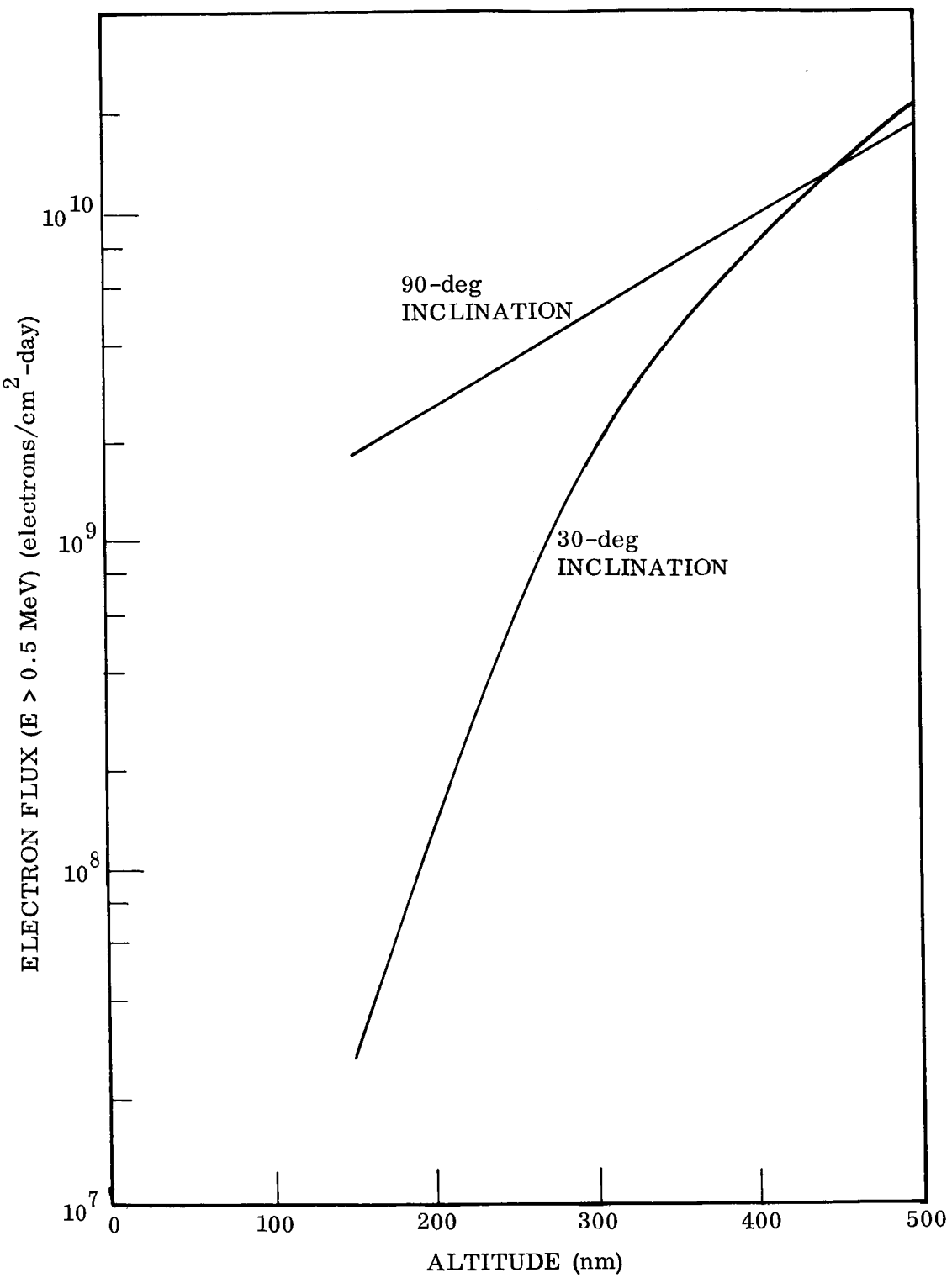

Fig. 5-8 Electron Flux per Day Encountered in Circular Orbits for December 1968

future artificial injections of electrons, since the inner belt intensities are declining and a best estimate of the maximum outer belt fluxes occurring at the solar maximum period has been used. Figure 5-9 shows the corresponding proton fluxes per day with energies greater than 4 MeV. The solar cycle changes in the lower edge of the belt have not been included in these calculations, since the magnitude of the effect has not been well established. For this reason, the figure is not dated for a specific time period, but the fluxes can still be used as conservative upper limits for the solar maximum period. Obviously, spacecraft with highly eccentric or unusual orbital configurations must be treated individually because variables such as the angle of the line of apsides will change the attitude of the orbit with respect to the trapped radiation belts.

5.1.1.2 Solar Particles

The geomagnetic field deflects charged particles incident on it from interplanetary space and thus provides very effective shielding to the region of space between about 60° north and south magnetic latitudes within the magnetosphere. Near the magnetic poles and in interplanetary space outside the boundary of the magnetosphere, the direct charged-particle radiation from the sun can be observed. This radiation consists of two components: high-energy particles that occur sporadically, usually in correlation with visible disturbances on the surface of the sun or solar flares; and low-energy protons and electrons, which are present more continuously.

Solar flare radiation. The charged particles in solar flare radiation events are electrons, protons, alpha particles or helium nuclei, and very small numbers of charged nuclei of mass greater than helium.

Electrons in the energy range 40 to 150 keV have been measured when accompanying a number of small solar flares during solar minimum (Ref. 12). One case of very high energy electrons with energies in the range 100 to 1000 MeV was observed after a succession of three fairly large solar flares within four days during 1961 (Ref. 13). The fluxes of electrons observed in all cases were small from a damage standpoint.

Protons from solar flares present perhaps the most important source of damaging particles for many orbital configurations. Since solar proton events occur sporadically and vary widely in peak proton flux and duration, the total flux of protons expected within a particular time period is treated statistically. Information obtained on proton fluxes during the last solar cycle maximum has been incorporated into a statistical model which gives the probability of encountering a total flux of protons greater than Φ for various time periods (Ref. 14). Plots of this probability versus the total flux Φ of protons with energies greater than 30 MeV for mission durations of 2 weeks and 1 year are shown in Fig. 5-10. The extrapolation of the 52-week curve follows from extending the measured distribution of sizes of individual flares. This allows for the possibility of the occurrence of proton events more intense than any observed during the last solar maximum period. The energy spectra of solar flare protons vary from event to event and also change with time during a single event (Ref. 15). A spectrum

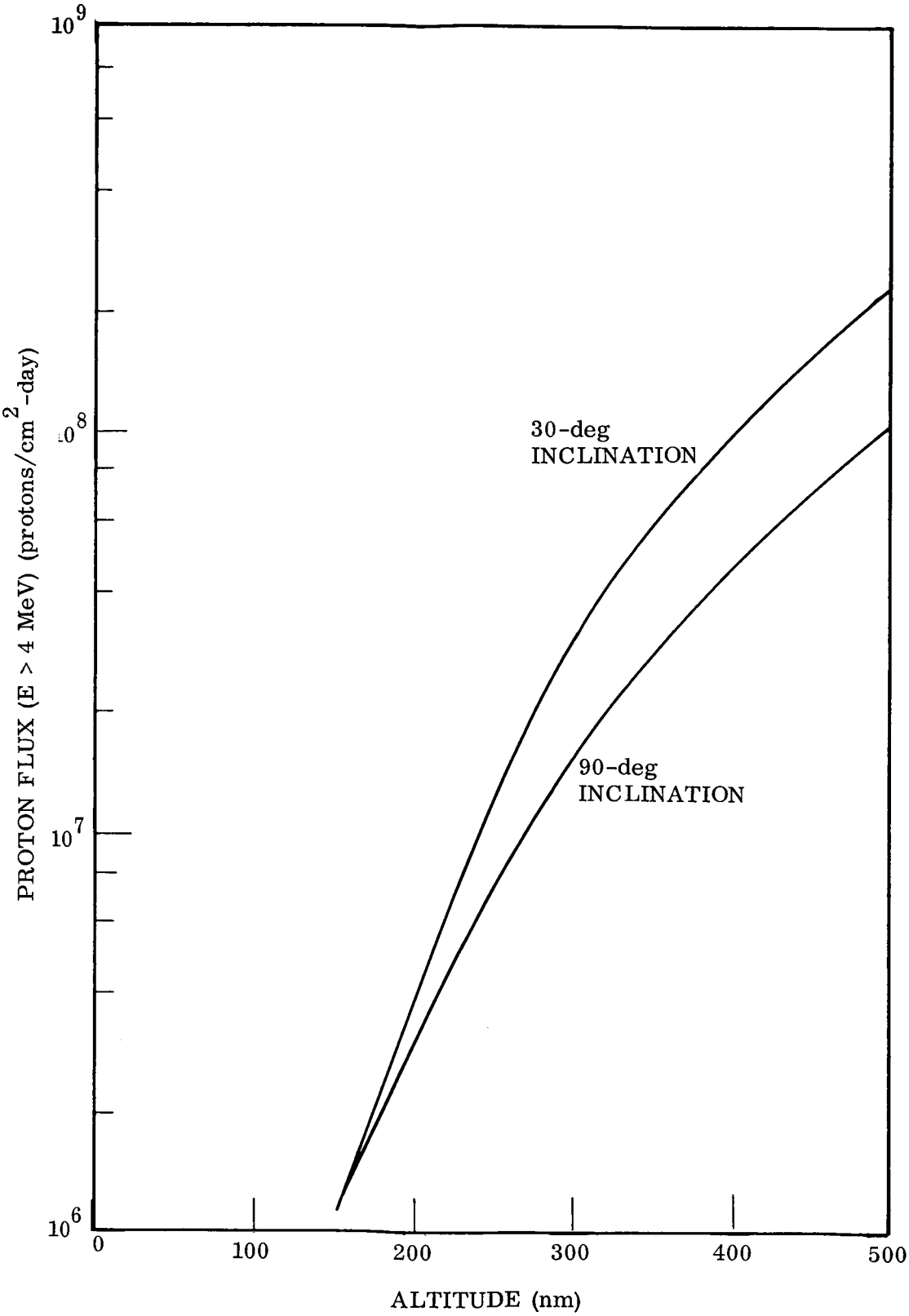

Fig. 5-9 Proton Flux per Day Encountered in Circular Orbits

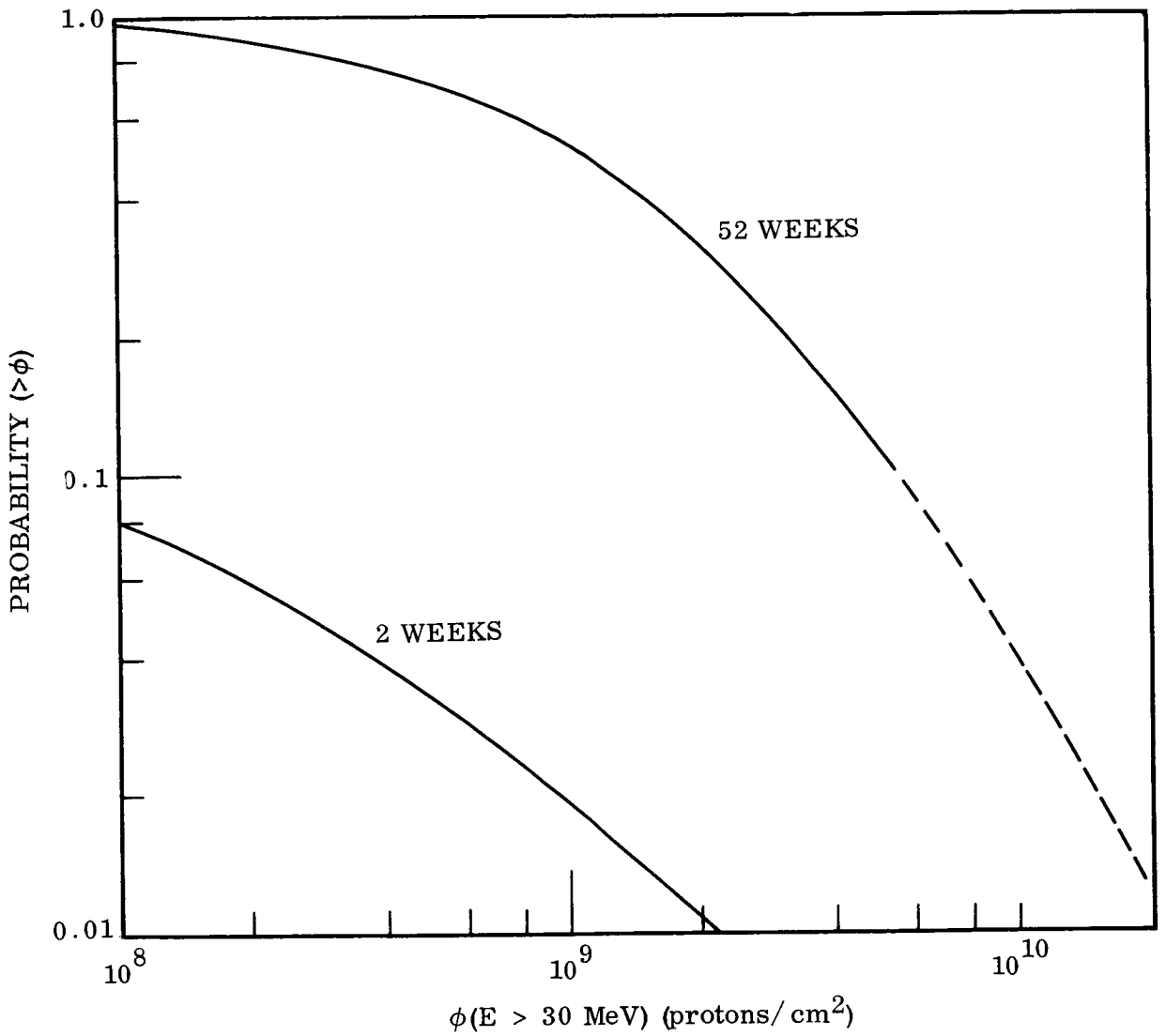

Fig. 5-10 Free-Space Solar Flare Proton Environment for a 2-Week and a 52-Week Mission

taken as most representative of the average of 29 solar flares between 1956 and 1961 (Ref. 14) is shown in Fig. 5-11 as a differential energy spectrum normalized to an integral flux above 30 MeV of 1 proton/cm^2. The proton intensity at any energy is obtained by multiplying the value from Fig. 5-11 by the integral flux above 30 MeV for a selected probability from Fig. 5-10. The curve in Fig. 5-11 follows the same analytic form below 30 MeV proton energy as it does at higher energies but is shown as a dashed line because the direct particle measurements did not extend this low in energy and the uncertainties associated with other types of measurements in the low energy region are much greater. The solar proton model described, while based on solar maximum conditions, can serve as a conservative upper limit for estimates during solar minimum.

Alpha particles and charged nuclei of higher atomic number accompany the fluxes of protons from solar flares. In several cases where both alphas and heavier nuclei have been observed, the ratio between their numbers has been constant at about 60. The ratio of protons to alphas within the same energy range appears to vary considerably, the number ranging from about 10 to several hundred (Refs. 15 and 16).

Solar wind. The solar wind is a plasma consisting of protons, electrons, and alpha particles which continuously streams radially outward from the sun (Ref. 17). The particle velocity in the vicinity of the earth was found to vary with solar modulation between about 350 and 700 km/sec, which corresponds to energies of approximately 0.6 to 2.6 keV for protons. The particle flux intensity varied between about 3×10^7 and 1×10^9 cm^{-2}-sec^{-1}. These are large fluxes of particles, but since the energy per particle is small, the damage to materials from solar wind particles will be confined to surfaces.

Auroral region radiation. Intense fluxes of protons and electrons have been observed in the auroral regions from about 60° to 70° geomagnetic latitude with somewhat lower fluxes at higher latitudes up to the magnetic poles (Refs. 18 and 19). The particle intensities fluctuate over several orders of magnitude but may always be present in these regions at altitudes to at least 500 nm. The exact origin of these fluxes and the mechanisms of their trapping or storage and precipitation into the atmosphere are not well understood. They seem to be correlated with solar activity, however, and the most reasonable source with sufficient total energy to produce the observed fluxes is the solar wind.

The average energies of electrons observed in the auroral regions is of the order of a few kilovolts to tens of kilovolts (Ref. 20). Intensities for these electrons are difficult to estimate for assessing damage to materials because of their large variations, the relatively short time span covered by observations, and the fact that the fluxes may be highly anisotropic at times and nearly isotropic at other times. A rough estimate based on the highest activity data from Ref. 20 and assuming an average energy of 10 keV gives approximately 10^{12} electrons/cm^2-day for a low-altitude polar orbiting satellite.

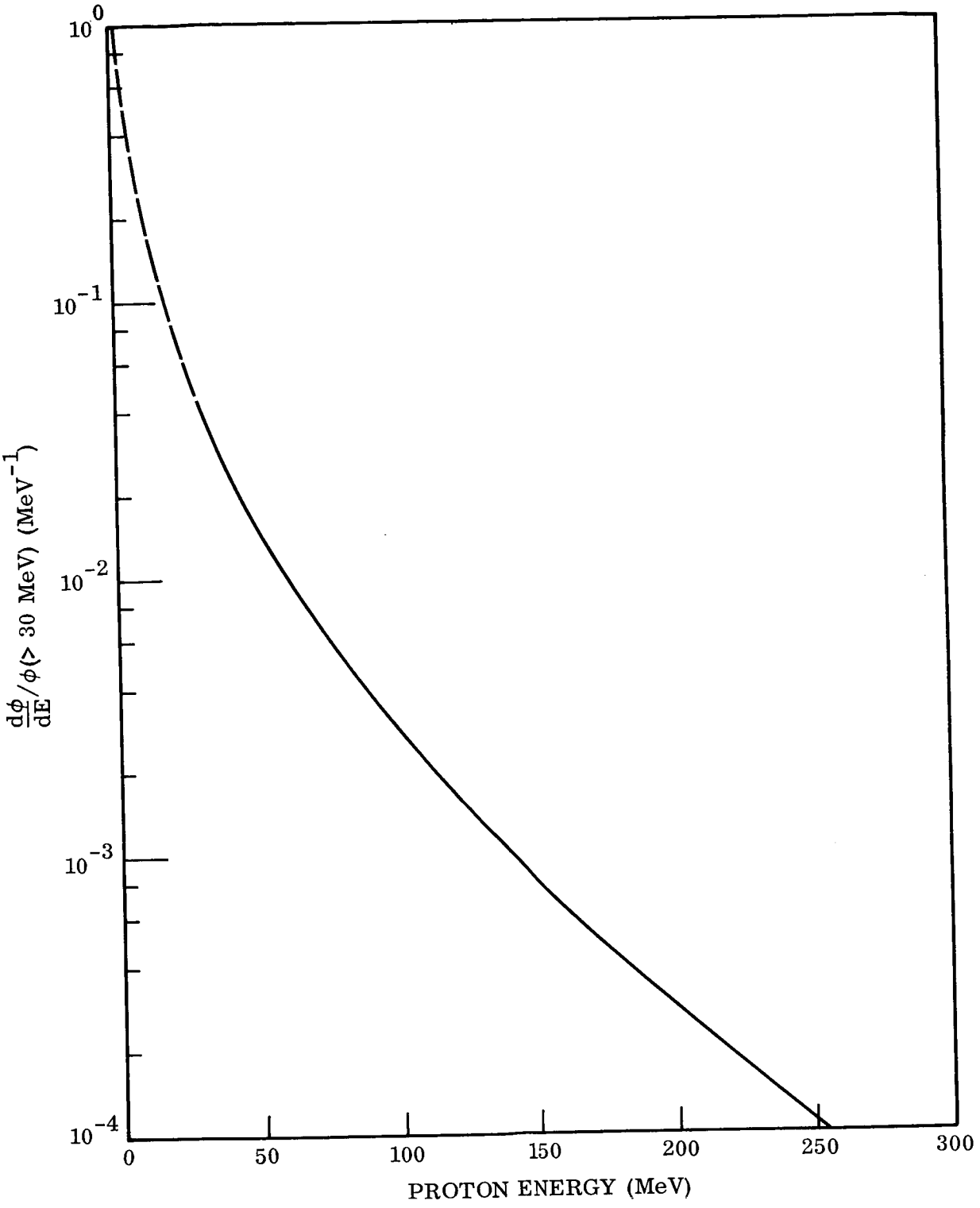

Fig. 5-11 Differential Solar Flare Proton Spectrum in Free Space

Observations of precipitating protons in the auroral regions in 1965 showed average particle energies of 10 to 20 keV and peak fluxes greater than 10^6 protons/cm^2-sec-steradian for energies greater than 20 keV (Ref. 21). A rough estimate similar to that provided above for the electrons gives approximately 10^{10} protons/cm^2-day, with an average energy of 15 keV. It must be borne in mind that these calculations are based on very limited data and are order-of-magnitude estimates for the time period during which the data were obtained.

5.1.1.3 Galactic Cosmic Rays

Galactic cosmic rays have been studied for several decades, but more detailed data are still needed for a complete quantitative understanding of the subject. Within the solar system, cosmic rays consist mostly of protons (about 90%), 10% helium nuclei, and very small percentages of heavier nuclei having atomic numbers up to approximately 30 (Ref. 22). There is also evidence of primary cosmic electrons and positrons (Ref. 23) constituting perhaps less than 1% of the proton flux at a given energy. The energies of cosmic protons may be as high as 10^{10} GeV, although most of the flux is in the energy range from approximately 1 to 10 GeV. The integral flux of protons above 40 MeV is about 2 protons/cm^2-sec during solar maximum and about 5 protons/cm^2-sec during solar minimum. This solar modulation is energy dependent, affecting the fluxes of protons with energies between a few tenths of a giga electron volt to a few giga electron volts strongly.

5.1.2 Neutral Particles and Electromagnetic Radiation

Since uncharged particles and electromagnetic radiation are unaffected by magnetic fields, they will be more uniformly distributed in space near the earth from primary sources than, for instance, the trapped charged particle radiation. The spatial distribution of the radiations arising from the interaction of primary charged particles with matter such as the atmosphere of the earth and the spacecraft itself will be quite localized in nature.

5.1.2.1 Primary Sources

Solar origin. An upper limit of 10^{-2} neutron/cm^2-sec average flux of direct solar neutrons has been estimated as the solar minimum (Ref. 24). Similarly, only upper-limit estimates have been made for direct neutrons accompanying solar flares. In either case, the total flux is negligible compared with other sources.

The sun continuously emits fluxes of x rays in addition to visible and ultraviolet light. The average intensity in the evergy range 1.55 – 12.4 keV during a period of moderate solar activity in 1966 was 2×10^{-4} ergs/cm^2-sec (Ref. 25). The intensity of the x-ray flux in the energy range 1 - 6 keV from a major solar x-ray flare on 7 July 1966 was observed to rise from about 10^{-3} ergs/cm^2-sec before the flare to a peak of 3×10^{-2} ergs/cm^2-sec during the flare (Ref. 26). The time integral for this flare was 97 ergs/cm^2. The observations of solar flare x rays are too limited to try to estimate the magnitude of their effect over a long time period. However, the energies of the x rays are fairly low so that damage from them will generally be confined to surfaces.

An experiment to measure gamma rays with energies greater than 20 MeV did not show a significant increase in flux over background from the direction of the sun, but set an upper limit of 2.8×10^{-2} photons/cm2 - sec for this source during a mildly active period of the sun in 1959 (Ref. 27).

Galactic origin. If neutrons are produced in our galaxy or others, they would not be detectable as such except in areas relatively close to their source since free neutrons decay with a 12-min half-life into protons which would then merely add to the cosmic ray proton flux.

Thermalized neutral atoms, mostly hydrogen, exist in interstellar space at an approximate average density of 1 atom/cm^3, although the regional density may vary by orders of magnitude (Ref. 28). To a space vehicle traveling through this medium, the particles would appear as a bombarding flux with a relative velocity equal to that of the vehicle. A vehicle with a velocity of 10^8 cm/sec would encounter an average flux of 10^8 atoms/cm^2-sec with an apparent energy of about 5 keV.

Fluxes of x rays from stellar sources have been observed to be of the order of 0.1 photons/cm^2-sec in the energy range of about 20 to 40 keV (Refs. 29 and 30). Gamma rays with energies greater than 20 MeV from the directions of several stellar x-ray sources were not detectable above background level, and upper limits of 1×10^{-2} to 2×10^{-2} photons/cm^2-sec were established for the period of observation (Ref. 27).

5.1.2.2 Secondary Sources

Numerous types of particles as well as electromagnetic radiation may arise from the interaction of primary particles from solar and galactic origin when incident on the atmosphere of the earth. The most significant of these secondary radiations are bremsstrahlung x rays produced by trapped electrons stopping in vehicle materials, and to a lesser degree by solar flare electrons stopping in the vehicle and atmosphere and albedo neutrons produced by nuclear reactions between high-energy solar and galactic protons and the vehicle and atmosphere. The bremsstrahlung intensity and energy spectrum is a function of the electron flux intensity and energy spectrum and the material in which the electrons are stopped. In general, the effect of the bremsstrahlung will be much lower in magnitude than effects from the primary radiation. The flux of albedo neutrons from atmospheric reactions is approximately 1 neutron/cm^2-sec at altitudes up to a few thousand nautical miles.

5.2 MAN-MADE RADIATION

The most intense man-made radiations in space have originated from high-altitude nuclear device detonations. In this discussion, these radiations will be divided into two categories: (1) charged and neutral particles and electromagnetic radiations arising from the detonation itself and from the fission debris, and (2) the charged particles injected by the explosion into trapped orbits in the earth's magnetosphere. Other possible sources of direct and trapped radiation such as leakage from satellite-borne reactors and radioactive isotope sources or proposed experimental accelerators could be significant, but to date have not presented appreciable radiation levels in space.

5.2.1 Direct Radiation From Nuclear Devices

A large proportion of the energy of a nuclear detonation is released in the form of thermal radiation (Ref. 31, p. 316). In the exploding device, the temperature is several tens of million degrees Kelvin. Most of the (primary) thermal radiation is then in the wavelength range of about 0.1 to 100Å , i.e., 120 to 0.12 keV energy, corresponding roughly to the soft x-ray region (Ref. 31, p. 351). For altitudes above 70 sm, the air density is less than 10^{-7} of that at sea level. The mean free path of the dominant thermal x rays produced in the nuclear detonation is then several hundred miles (Ref. 31, p. 355).

It is convenient, for practical purposes, to consider the nuclear radiations from an explosion as being divided into two time categories, initial or prompt and residual. Most of the neutrons and some of the gamma rays are emitted in the fission and/or fusion processes simultaneously with the explosion. Residual radiations (gamma rays, electrons, positrons, neutrons, and alpha particles) are liberated over an extended period of time as the fission products undergo radioactive decay. At any point of interest in space, the relative intensities of both the prompt and residual radiations from a nuclear detonation depend on its altitude, the particular characteristics of the nuclear device, and the location of the point of interest relative to the position of the detonation. It is an extremely complex system to assess even when all the parameters for a given case are specified, so that a quantitative treatment of the subject is beyond the scope of this handbook.

5.2.2 Particles Trapped in the Geomagnetic Field

The charged-particle radiations from nuclear devices which may become trapped in the geomagnetic field include electrons and perhaps positrons from beta decay of the fission fragments, protons from the decay of neutrons emitted by the device, and heavier charged particles. In addition, significant perturbations in the trapped populations may also occur at the time of a nuclear detonation. Electrons have been observed to remain trapped in large numbers for various lengths of time after these tests. The trapping of the other kinds of particles in conjunction with nuclear detonations has not been well established. The subject of injection and subsequent trapping of electrons from nuclear devices is complex, and a quantitative understanding is not yet complete. A description of the trapped electron histories of seven high-altitude nuclear tests with particular emphasis on the Starfish event may be instructive.

Three detonations in the Argus series in 1958 were designed to investigate the injection of electrons into the geomagnetic field using nuclear devices as a source (Ref. 32). The devices had nominal yields of 1.4 KT TNT equivalent and were detonated at ~200- to 400-km altitudes on L shells of 1.7 to 2.1 in the Southern Hemisphere. The observed lifetime of electron fluxes was approximately 3 to 4 weeks, with initial maximum fluxes of 10^5 to 10^6 electrons/cm^2-sec (Ref. 33).

Three detonations by the USSR in late 1962 on L shells of 1.8, 1.9, and 2.0 resulted in initial maximum fluxes of about 10^7 electrons/cm^2-sec with lifetimes of approximately 1 month for each injection (Ref. 33). The altitudes of the detonations and exact yields

are not available. However, it was estimated that two of the series were submegaton yield and the third was of the order of a megaton yield (Ref. 33).

The Starfish nuclear burst occurred on 9 July 1962 at an altitude of about 400 km near Johnston Island which corresponds to an L shell of 1.12 (Refs. 33 and 34). The yield was 1.4 MT, which could produce approximately 5×10^{26} fission product decay electrons. The initial electron fluxes were very high – of the order of 10^9 electrons/cm^2-sec in the first day. Many of the particles were in very unstable trapping configurations, as evidenced by the rapid decrease in intensity in the first few weeks following the detonation. At later times, the decrease in intensity appeared to slow to rates that could be described by exponential functions in which the exponential parameter, the mean lifetime, is a function of L. Measurements of mean lifetime made in late 1962 and 1963 showed a peak value of about 1-1/2 years for L = 1.5 earth radii. This corresponds to the slowest decay rate, so that the maximum in flux intensity shown in Fig. 5-6 will shift toward L = 1.5 as the Starfish electron belt decays.

From the foregoing examples, it is evident that the intensities of electron fluxes and the length of time they remain trapped after injection depend on the yield of the device and the altitude and geomagnetic location of the detonation. In particular, as a result of a nuclear detonation, high fluxes of electrons can be injected into low-altitude regions of space where the fluxes of naturally trapped electrons and protons are rather low. Thus, the injection of electrons from nuclear detonations can present a serious hazard for years to many satellite programs designed to take advantage of the normally low radiation levels at altitudes of ~ 150 nm.

5.3 INTERNAL ENVIRONMENTS

Due to the presence of shielding provided by the spacecraft structure and to the possible existence of an on-board nuclear reactor or radioactive isotopes, the internal radiation environment may be quite different from the external environments discussed in the previous section.

Existing procedures for calculating modifications of the intensities and energy spectra by the shielding are rather complex. Accordingly, the subject will be discussed here only in rather general terms. In addition, radiation levels will be given for typical on-board reactors or radioactive sources.

5.3.1 Attenuation by Shielding

As they penetrate matter, radiations lose energy by a variety of interactions, some leading to secondary radiations. Accordingly, calculations of transmissions may involve many complex procedures. In certain special cases, various assumptions that lead to rather simple calculations can be made. For example, with thin, low atomic number shielding, the secondary radiations may not make a significant contribution. Thus, the environment at the center of a uniform thin spherical shell in an omnidirectional flux can be calculated rather well with simple techniques. For thicker, more complex shielding configurations, it may be necessary to employ more sophisticated time-consuming computational procedures. Computer programs have been developed

which take into account complex geometries while using simplified interaction models (Refs. 35, 36, and 37). For a more detailed and realistic treatment of the environment and its interaction with shielding materials, Monte Carlo programs are used. Various computer codes of this type, in which individual particles or photons are followed as they interact with the shielding material, have been developed for electron, nucleon, and electromagnetic radiations (Refs. 38, 39, and 40).

5.3.2 Energy Deposit in Materials

For certain radiation damage assessments, direct correlation of damage coefficients with fluxes and energy spectra of the incident radiations are most satisfactory. This is true of cases such as semiconductor damage, which involves perturbation of atoms in a crystal lattice by particle radiations, particularly protons, neutrons, and heavier particles where the total damage may be more than that produced by ionization energy deposit. For other types of radiation damage, it is convenient to convert the radiation environment incident on material to the energy deposited per unit mass or dose in the material (Refs. 31, 41, and 42). This applies particularly to materials in which the main damage is from breakage of chemical bonds (e.g., organic spacecraft materials and animal tissue). The currently used unit of dose is the rad, defined as 100 ergs of energy absorbed per gram of material on which the radiation is incident.

Particle radiations will produce damage in materials that is disproportionate to the linear energy transfer from the particles through ionization. The damage per unit energy transfer becomes greater as the particle slows down and its ionization rate becomes greater. This excess damage is specified for tissue dose as a relative biological effectiveness (RBE) factor which is a function of particle energy and is used as a multiplier to convert doses from lower energy particles to what would be produced by high-energy particles only. For biological doses, the dose unit is the rem, which is equal to a rad multiplied by the RBE for the radiation.

The charged particle dose in biological tissue thick enough to stop all of the incident radiations is given by

$$D = \int_0^R \frac{dE}{dx}(E) \cdot RBE(E)\ dx$$

where

RBE(E) = relative biological effectiveness

dE/dx = linear energy transfer of the particle or, conversely, the stopping power of the material

R = range or distance the particle travels before it is stopped

The integral is evaluated over the range of the particle, and the quantities dE/dx and RBE will be functions of the remaining particle energy. A simplification of this relationship holds when the thickness of the tissue is such that a small amount of the

particle energy is lost in penetrating the material. Thus, surface dose or skin dose from particles of energy E can be expressed as

$$D_s = \frac{dE}{dx}(E) \cdot RBE(E) \quad \Delta t$$

where Δt is the material or skin thickness.

5.3.3 Environment From On-Board Sources and Nuclear Reactors

The use of nuclear reactors for propulsion or for power generation and the use of radio isotope power sources on board space vehicles can pose radiation damage problems from the leakage fluxes.

Isotope sources have a relatively low potential power output per unit mass. Their use would probably be constrained to modest power requirements from weight considerations such that the radiation escaping the power source and contributing to the vehicle internal environment may not be a serious problem compared with that caused by external radiation. The principal leakage radiation from such sources would be gamma rays and bremsstrahlung, the relative intensities depending upon the choice of isotope.

Nuclear reactors for either power or propulsion have the capability of very high power output, and for efficient utilization would probably range from hundreds of kilowatts to many megawatts. The primary leakage radiations from reactor cores are neutrons and gamma rays from the fission process. Since a significant fraction of the neutrons have energies in excess of 1 MeV and the fission gamma ray spectrum peaks at around 1 MeV, these radiations are difficult to shield against. The unshielded radiation rates 100 ft from a 1000-MW reactor might be as high as 10^{11} neutrons/cm^2-sec and 10^6 rad/hr from gamma rays. Thus, serious damage to many components would occur in a short time in this environment unless very effective shielding were provided.

5.4 REFERENCES

1. C. E. McIlwain, "Coordinates for Mapping the Distribution of Magnetically Trapped Particles," J. Geophys. Res. 66, 3681, 1961

2. J. I. Vette, Models of the Trapped Radiation Environment, Vol.I,"Inner Zone Protons and Electrons," NASA SP-3024, 1966

3. J. H. King, Models of the Trapped Radiation Environment, Vol.IV, "Low Energy Protons," NASA SP-3024, 1967

4. L. R. Davis and J. M. Williamson, "Low Energy Trapped Protons," Space Research III, 365, 1963

5. G. Pizzella, C. E. McIlwain, and J. A. Van Allen, "Time Variations of Intensity in the Earth's Inner Radiation Zone, October 1959 Through December 1960," J. Geophys. Res. 67, 1235, 1962

6. R. W. Fillius, "Trapped Protons of the Inner Radiation Belt," J. Geophys. Res. 71, 97, 1966

7. R. C. Blanchard and W. N. Hess, "Solar Cycle Changes in Inner Zone Protons," J. Geophys. Res. 69, 3927, 1964

8. G. H. Nakano and H. H. Heckman, "Evidence for Solar Cycle Changes in the Inner Belt Protons" (Manuscript)

9. J. I. Vette, A. B. Lucero, and J. A. Wright, Models of the Trapped Radiation Environment, Vol. II, "Inner and Outer Zone Electrons," NASA SP-3024, 1966

10. C. O. Bostrom and D. J. Williams, "Time Decay of the Artificial Radiation Belt," J. Geophys. Res. 70, 240, 1965

11. S. M. Krimigis and J. A. Van Allen, "Geomagnetically Trapped Alpha Particles," J. Geophys. Res. 72, 5779, 1967

12. A. W. Schardt and A. G. Opp, "Particles and Fields: Significant Achievements," Reviews of Geophysics 5, 411, 1967

13. P. Meyer and R. Vogt, "High-Energy Electrons of Solar Origin," Phys. Rev. Letters 8, 387, 1962

14. J. L. Modisette, T. M. Vinson, and A. C. Hardy, Model Solar Proton Environments for Manned Spacecraft Design, NASA TN D-2746, April 1965

15. W. R. Webber, An Evaluation of the Radiation Hazard due to Solar-Particle Events, D2-90469, Boeing Co., Seattle, Wash., December 1963

16. S. Biswas and C. E. Fichtel, "Composition of Solar Cosmic Rays," Space Sci. Rev. 4, 709, 1965

17. C. W. Snyder and M. Neugebauer, "Interplanetrary Solar Wind Measurements by Mariner II," Space Research 4, 89, 1964

18. J. E. Evans et al., "Recent Results From Satellite Measurements of Low Energy Particles Precipitated at High Latitudes," Space Sci. Rev. 7, 263, 1967

19. B. J. O'Brien, "Precipitation of Energetic Particles Into the Atmosphere," Chapter 5 in Auroral Phenomena, ed. Martin Walt, Stanford University Press, Stanford, Calif., 1965

20. R. D. Sharp and R. G. Johnson, "Some Average Properties of Auroral Electron Precipitation as Determined From Satellite Observations," J. Geophys. Res. 73, 969, 1968

21. R. D. Sharp et al., "Satellite Measurements of Precipitating Protons in the Auroral Zone," J. Geophys. Res. 72, 227, 1967

22. S. N. Vernov and A. E. Chudahov, "Terrestrial Corpuscular and Cosmic Rays," Space Research I, 751, 1960

23. P. Meyer, "Primary Electrons and Positrons in the Cosmic Radiation," Proc. Internat. Conf. on Cosmic Rays, London, 1965

24. S. J. Bame and J. R. Asbridge, A Search for Solar Neutrons Near Solar Minimum, LA-DC-7973, Los Alamos Scientific Laboratory, 1965

25. B. N. Gregory and R. W. Kreplin, "Observations of Solar X-Ray Activity Below 20 Angstroms," J. Geophys. Res. 72, 4815, 1967

26. J. A. Van Allen,"Solar X-Ray Flare of July 7, 1966," J. Geophys. Res. 72, 5903, 1967

27. G. M. Frye, Jr., F. Reines, and A. H. Armstrong, "Search for Solar and Cosmic Gamma Rays," J. Geophys. Res. 71, 3119, 1966

28. L. Goldberg and E. R. Dyer, Jr., "Galactic and Extragalactic Astronomy," Chapter 18 in Science in Space, eds. L. V. Berkner and H. Odishaw, McGraw-Hill Book Co., Inc., New York, 1961

29. R. C. Haymes and W. L. Craddock, Jr., "High Energy X-Rays From the Crab Nebula," J. Geophys. Res. 71, 3261, 1966

30. P. J. Edwards and K. G. McCracken, "Upper Limits to the Hard X-Ray Flux From the Quiet Sun and Jupiter," J. Geophys. Res. 72, 1809, 1967

31. S. Glasstone, The Effects of Nuclear Weapons, U. S. Atomic Energy Commission, 1962

32. N. C. Christofilos, "Sources of Artificial Radiation Belts," pp. 565-574 in Radiation Trapped in the Earth's Magnetic Field, ed. B. M. McCormac, D. Reidel Publishing Co., Dordrecht, Holland, 1966

33. J. A. Van Allen, "Spatial Distribution and Time Decay of the Intensities of Geomagnetically Trapped Electrons From the High Altitude Nuclear Burst of July 1962," pp. 575-592 in Radiation Trapped in the Earth's Magnetic Field, ed. B. M. McCormac, D. Reidel Publishing Co., Dordrecht, Holland, 1966

34. W. L. Imhof et al., Analysis and Evaluation of Measurements of Geomagnetically Trapped Electrons From High-Altitude Nuclear Explosions, DASA Report No. 1540, Lockheed Missiles & Space Co., Palo Alto, Calif., 1964

35. D. L. Dye, "Space Proton Doses at Points Within the Human Body," Proc. of Symposium on Protection Against Radiation Hazards in Space, NASA TN D 7652, November 1962

36. B. W. Mar, Electron Shielding Codes for Evaluation of Space Radiation Hazards, Boeing Co., Seattle, Wash., D2-90414, June 1963

37. K. M. Simpson, C. W. Hill, and C. C. Douglass, "A Space Radiation Shielding Code for Realistic Vehicle Geometries," Second Symposium on Protection Against Radiations in Space, NASA SP-71, 1965

38. M. J. Berger, Methods in Computational Physics, Vol. 1., Academic Press, Inc., New York, 1963

39. Computer Codes for Space Radiation Environment and Shielding, Vol. 1, WL TDR-64-71, Vol. 1, Air Force Weapons Laboratory, 1964

40. W. E. Kinney, The Nucleon Transport Code, NTC, ORNL-3610, Oak Ridge National Laboratory, August 1964

41. G. J. Hine and G. L. Brownell, eds., Radiation Dosimetry, Academic Press, New York, 1956

42. Radiation Quantities and Units, International Commission on Radiological Units and Measurements Report 10a, National Bureau of Standards Handbook 84, November 1962

Chapter 6

METEOROIDS

J. B. RITTENHOUSE

One of the environments in which a spacecraft must function successfully is that of the extraterrestrial solid debris or meteoroids. Until the advent of the Space Age in 1957, our understanding of this environment has stemmed from terrestrial observations of the interaction of the debris with the upper atmosphere, studies of the solar corona and zodiacal light, and collection of dust particles at high altitudes or recovered from deep sea or ocean sediments. Starting with Explorer 1 in 1958, several spacecraft have carried some form of meteroid detector, culminating with the penetration devices carried on board Explorers 16 and 23 and Pegasus 1, 2, and 3. Each of the observational techniques—astronomical, photographic, radio, dust collection, and spacecraft impact detectors—has a sensitivity for a particular range of particle mass population. These methods of detection are shown in Table 6-1 (Ref. 1).

Table 6-1

METEOROID SIZES AND METHOD OF DETECTION

Class of Body	Range of Dimension	Range of Mass (gm)	Method of Detection
Micrometeoroid	$< 1\ \mu$	10^{-12} to 10^{-6}	Spacecraft and sounding rockets
Micrometeoroid	1 to 100 μ	–	Light scattering in space (zodiacal light); light scattering in atmosphere, meteoroic dust collection, deep sea sediments, sounding rockets
Faint Meteoroid	100 μ to 0.1 cm	10^{-4} to 10^{-3}	Radio, zodiacal light, spacecraft
Meteors	0.1 to 10 cm	10^{-3} to 10	Photographic, radio, visual
Fireballs and Bolides	10 - 300 cm	–	Visual, meteorites, radio
Great Fireballs and Bolides	>300 cm	–	Meteorites, meteorite craters and geological structures, visual, radio

The terms used to describe space debris are defined in the glossary; however, for convenience the terms will be briefly described here. A meteor is an extraterrestrial particle originating in the solar system, the light of which, generated by interaction with the atmosphere, is detectable visually or by radio. A meteoroid is a particle traveling in space. A micrometeoroid is a small meteoroid, usually of mass smaller than 10^{-6} gm. A meteorite is a meteor that has survived the passage through the atmosphere and may be recovered on the earth's surface. A micrometeorite is a small meteorite, small fragment of a larger meteorite, or actual microscopic particles that have survived the passage through the atmosphere. The term dust is used to describe any extraterrestrial particles of microscopic size that originate in the solar system and may be applied to micrometeoroids or micrometeorites. The particles of debris are also termed "sporadic meteoroids," which are particles of close proximity having a similar but independent solar orbit (Ref. 2).

The space debris is believed to originate primarily in the solar system, caused by the following: cometary disintegration, which contributes more than 90% of the total; fragmentation of asteroids (solid bodies concentrated in interplanetary space between the orbits of Mars and Jupiter), which contributes between 2 and 10% of the total; material ejected from the surface of the moon by meteroid impact; interstellar capture, which contributes about 1% of the total; and condensation of interplanetary gas (Refs. 1 and 2).

6.1 METEOROID DENSITY

The density of the asteroids is about 3 to 9 gm/cm^3. They are composed of iron, iron-nickel alloys, or mixtures of these with metallic oxides (stones). Meteorite particles of this origin will be of relatively high density.

Meteorites of cometary origin are conglomerates of mineral particles and have low density, high porosity, and high frangibility. The conglomerate structure, with voids, will have an average low bulk density of about 0.4 gm/cm^3, which will increase to the density of a mixture of the heavier elements, iron and nickel and their oxides, which is about 3.5 gm/cm^3. A mass density of 0.5 gm/cm^3 for meteoroids has been tentatively agreed upon.

6.2 METEOROID VELOCITY

The minimum theoretical velocity of a meteoroid near the earth is the escape velocity of 11 km/sec. The maximum velocity of a heliocentric particle at 1 a.u. (1 a.u. = 93,000,000 sm), the distance of the earth from the sun, is about 42 km/sec. The earth has an orbital velocity of 30 km/sec, so the maximum velocity of a meteoroid in parabolic retrograde orbit in the ecliptic plane at 1 a.u. will be the summation of these velocities or 72 km/sec. Very few meteoroids have hyperbolic trajectories, so very few will have velocities greater than 72 km/sec.

The reflection of electromagnetic radiation causes a change in the momentum of a particle in solar orbit which imparts an outward force opposing the inward solar gravitational force. This effect of solar electromagnetic radiation pressure can cause a particle either to be forced out of the solar system or to spiral inward toward the sun.

The latter is the Poynting-Robertson effect. This effect tends to cause meteoroids to assume a circular orbit (gradually) rather than an eccentric orbit and thus influences the size and velocity in orbit. A particle of 1μ diameter and having the density of aluminum (2.79 gm/cm^3) in the vicinity of the earth is of the proper size to just balance the solar pressure and gravitational field. A particle 200 μ in diameter would spiral into the sun in 4000 years from the earth's orbit under the influence of the Poynting-Robertson effect. The solar wind also influences the size and velocity of particles orbiting the sun. Thus, there can be a sorting out of particles according to their size, the smaller particles being faster than the larger.

6.3 FLUX-MASS RELATIONSHIP

All of these factors have an influence on the flux-mass and size-velocity relationships of meteors observed. The velocity variation with visual magnitude assumes a velocity of 28 km/sec for magnitude 0 to 7. The increasing influence of radiation pressure with decreasing size reduces the velocity by 1 km/sec for each visual magnitude to a constant velocity of 15 km/sec at visual magnitude 20. The velocity of 15 km/sec is assumed constant for all larger visual magnitudes. A normal impact velocity for meteoroids of 25 km/sec has been tentatively agreed upon (Refs 2 and 3).

Increases in the average hourly rate of meteor influx are observed at regular intervals during the calendar years. These increases are caused by the passage of the earth in its orbit through the orbit of a stream of particles, probably of cometary origin, that are traveling in similar heliocentric orbits. The ratios of the meteoroidal stream flux to the sporadic background can increase by as much as a factor of 20 during a meteor shower. In some streams the peak flux will increase to 15% of the maximum in about 1-3/4 hr, then decrease in the next 1-1/2 hr and reduce to the sporadic background in another 1-1/4 hr for a total stream lifetime of 4-1/2 hr. Some of these streams have a period of about 1.5 years, whereas others recur in about 100 years. The flux generally decreases with increasing mass of the meteoroid in the stream fluences. The sporadic fluence also decreases in flux with increasing mass.

The tentatively established flux-mass relationship is shown in Table 6-2 (Ref. 3). These data are plotted as the log of the flux versus the log of the mass in Fig. 6-1. Meteor photographic, Explorer 16 and 23, Pegasus 1, 2, and 3 penetration, and Gemini window crater data were used to establish the curve (Refs. 3, 4, and 5). Influx rates based on radio observation or spacecraft microphone sensors were considered for the derivation of this model but were not included. A complete discussion of the meteoroid environment, with over 300 references, is given in Refs. 1 and 2.

6.4 METEOROID IMPINGEMENT

The impingement of high-velocity particles on thin-skinned pressurized structures can cause small punctures that could result in gradual loss of pressure of the space vehicle or actual rupture by explosive decompression. The kinetic energy of the impinging particle is absorbed by the particle and the skin to cause fragmentation and vaporization of both. Interaction of these fragments with the spacecraft atmosphere can result in oxidative explosions to produce high-temperature and high-pressure fluctuations. The penetration, impingement, or erosion of other spacecraft components could

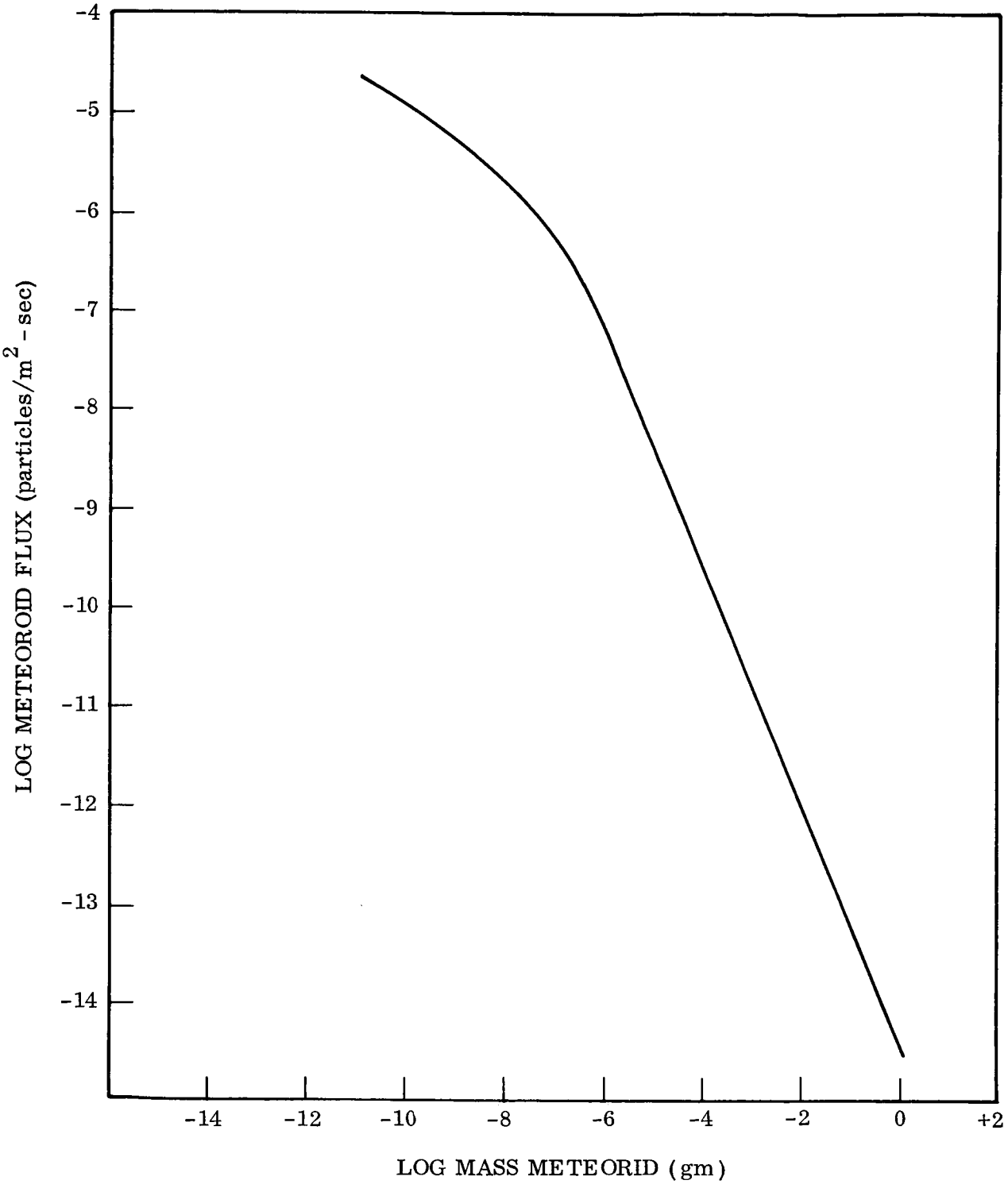

Fig. 6-1 Tentative NASA Annual Average Sporadic Meteoroid Environment Model for 1 A.U. (Refs. 3 and 4)

result in nonstandard operation, malfunction, or failure. The flux-mass relationship then should be converted to a flux-penetration relationship in some standard approved manner so that the meteoroid penetration hazard to spacecraft can be estimated.

Table 6-2

TENTATIVE ANNUAL AVERAGE SPORADIC METEOROID ENVIRONMENT MODEL (1 a.u.)

Mass Meteoroid (gm)	Flux ($particles/m^2$ sec)
1.0	3.89×10^{-15}
10^{-6}	8.17×10^{-8}
4.46×10^{-9}	2.86×10^{-6}
5.0×10^{-11}	1.52 × 15-5

6.4.1 Perforation of Materials

Terminal ballistics of the penetration of armor by projectiles has been studied for many years. The physical phenomenon of perforation, cratering, and spalling under hypervelocity impact simulated in the laboratory has yielded some empirical equations relating the velocity of the projectile and its mechanical and physical properties to the mecnanical and physical properties of the target plate (Refs. 1, and 6 to 10).

The major limitation of the ground-based simulation techniques of meteoroid impact has been the inability to achieve the high velocity (25 km/sec) estimated for meteoroids in space. Also the projectiles used have not been able to simulate the estimated density of meteoroids (0.5 gm/cm3). One of the simulation devices that has been used is a light gas gun which consists of a pump tube containing the light gas and a piston to compress the gas, which is separated from the launch tube by a diaphragm. When the diaphragm is ruptured, the pressurized gas accelerates the projectile down the launch tube to impact the target. Instrumentation to measure time and distance of flight of the projectile are provided so that the velocity at impact can be determined. The target plate is examined for cratering, perforation, and spalling. Velocities to about 10 km/sec with about a 0.1-gm projectile can be achieved using this technique; with a 3-gm projectile, velocities of about 5 km/sec are produced. These velocities are considerably lower than the estimated meteoroid velocity (Ref. 7).

Shaped explosive charges have also been used to accelerate projectiles to impact targets in the simulation of meteoroid impingement. Although velocities as high as 20 km/sec have been achieved, neither the shape nor the mass of the projectile can be determined (Ref. 7).

The exploding foil accelerator uses the explosive force generated by discharging a large quantity of electrical energy stored in capacitors through a thin metal foil. The foil is

heated to the molten state in less than a millisecond and the explosive force of the electrical energy punches a disk-shaped particle the size of the accelerator tube as the projectile. The size and material of the the projectile can be changed. Diameters of 1/8 to 1/2 in., with thicknesses of 0.002 to 0.050 in., have been used, and velocities of 10 to 18 km/sec have been achieved (Ref. 7).

The electrostatic accelerator has the highest potential for simulating the meteoroid environment. It is theoretically possible to accelerate an iron particle 1 μ in diameter to velocities of the order of 12 to 15 km/sec at about 20 to 30 million volts (Ref. 7).

By the use of several of these simulation techniques and comparison of the empirical equations developed from them, a tentative relationship between thickness of material just perforated (sometimes called the ballistic limit), its properties, the properties of the meteoroid, and its velocity have been established as shown in the following equation (Ref. 3):

$$t = 0.65\left(\frac{1}{\mathcal{E}_t}\right)^{1/8}\left(\frac{\rho_m}{\rho_t}\right)^{1/2}\left(V_m\right)^{7/8}\left(d_m\right)^{19/18} \qquad (1)$$

where

t = thickness of sheet just perforated (cm)

$\mathcal{E}_t$ = percentage elongation of sheet material (%)

ρ_t = mass density of sheet material (gm/cm^3)

ρ_m = mass density of meteoroid ($gm/cm^3 = 0.5\ gm/cm^3$)

V_m = normal impact velocity (km/sec = 25 km/sec)

d_m = meteoroid diameter (cm) assuming a spherical particle

Inserting the material constants for 2024-T3 aluminum alloy and the meteoroid constants into Eq. (1) results in

$$t = 3.30\ (d_m)^{19/18} \qquad (2)$$

A plot of the logarithm of the thickness of 2024-T3 aluminum alloy calculated from Eq. (2) as a function of the logarithm of the flux of meteoroid penetrations per square foot per day is shown in Fig. 6-2. For comparison, the data of the Gemini window crater, the Explorer 23, and the Pegasus spacecraft meteoroid penetration experiments as evaluated by Nauman (Ref. 5) are also shown in Fig. 6-2.

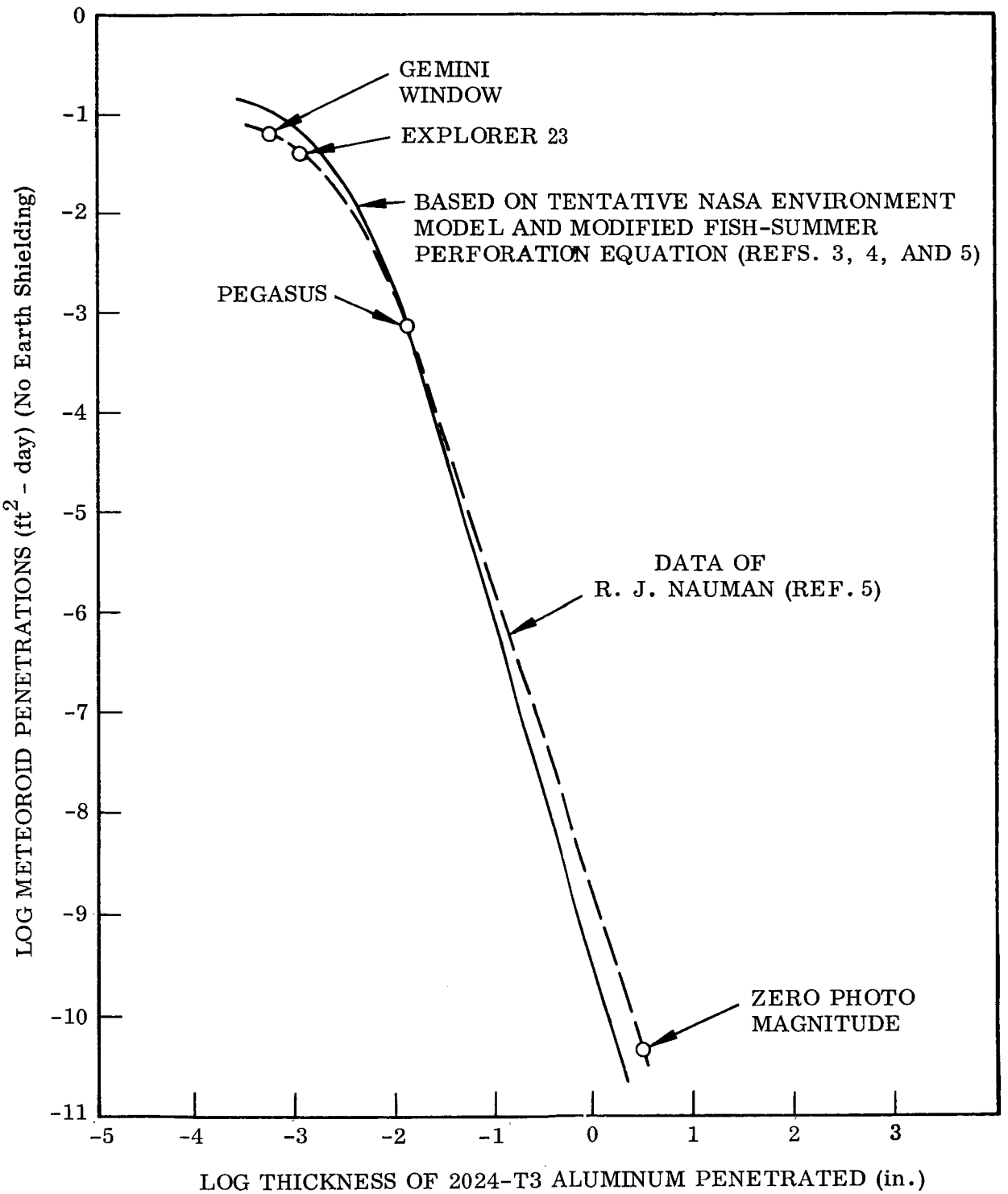

Fig. 6-2 Upper Limit of Meteroid Penetrations Through 2024-T3 Aluminum

6.4.2 Single-Wall Perforation

The meteoroid environment in terms of penetration flux and the thickness of sheet material just perforated permits the selection of the single-wall thickness of a spacecraft based upon the desired reliability for no perforations in a given area in a given time. A Poisson distribution of penetrations permits the calculation of the probability p(n) for penetration of area A in time τ by the meteoroid flux ϕ from the following equation:

$$p(n) = e^{-\phi A \tau} \sum_{n=0}^{n} \frac{(\phi A \tau)^n}{n!} \tag{3}$$

The flux corresponding to a probability p(0) of no penetrations is then

$$\phi = \frac{A\tau}{-\ln p(0)} \tag{3a}$$

The probability of 0.99, 0.95, 0.90 for no perforations by meteoroids through a given single-sheet thickness of 2024-T3 aluminum alloy for a given area-mission duration product is shown in Fig. 6-3. These data were derived from the flux-penetration curve of Fig. 6-2 and Eq. (2) and (3a).

6.4.3 Multiple-Wall Penetration

To design a single-wall spacecraft for a high probability of no perforations for a large area-duration product may impose an unacceptable weight penalty. To avoid this and achieve optimum weight, the spaced armor principle has been studied to afford protection of the main spacecraft wall by a thin sheet spaced away from it a given distance. The thicknesses of the main wall sheet, the front wall sheet (sometimes called the bumper or shield), and the spacing of the front wall from the main wall depend upon the meteoroid velocity, its mass, and the material of the spaced sheets. Structural and load consideration also enter into the configuration.

In simulation tests, it was found that more than two sheets did not provide as much protection as two properly designed spaced sheets (Ref. 11). It was also found that honeycomb or other filler material between the two walls was not as protective as two walls with proper spacing and thickness distribution between them without filler.

Three possibilities for the behavior of a particle upon impacting the front sheet are: it is stopped; it perforates without damage to the particle to travel on to impact the second sheet; or it can pass through the sheet and become fractured, molten, or vaporized. The meteoroid velocities are large enough to cause melting and vaporization.

If the meteoroid should penetrate the front sheet and impact the second sheet, a shock wave is generated within the second sheet that can cause formation of an internal fracture or spall. If the shock is intense enough, material may fracture from the inner

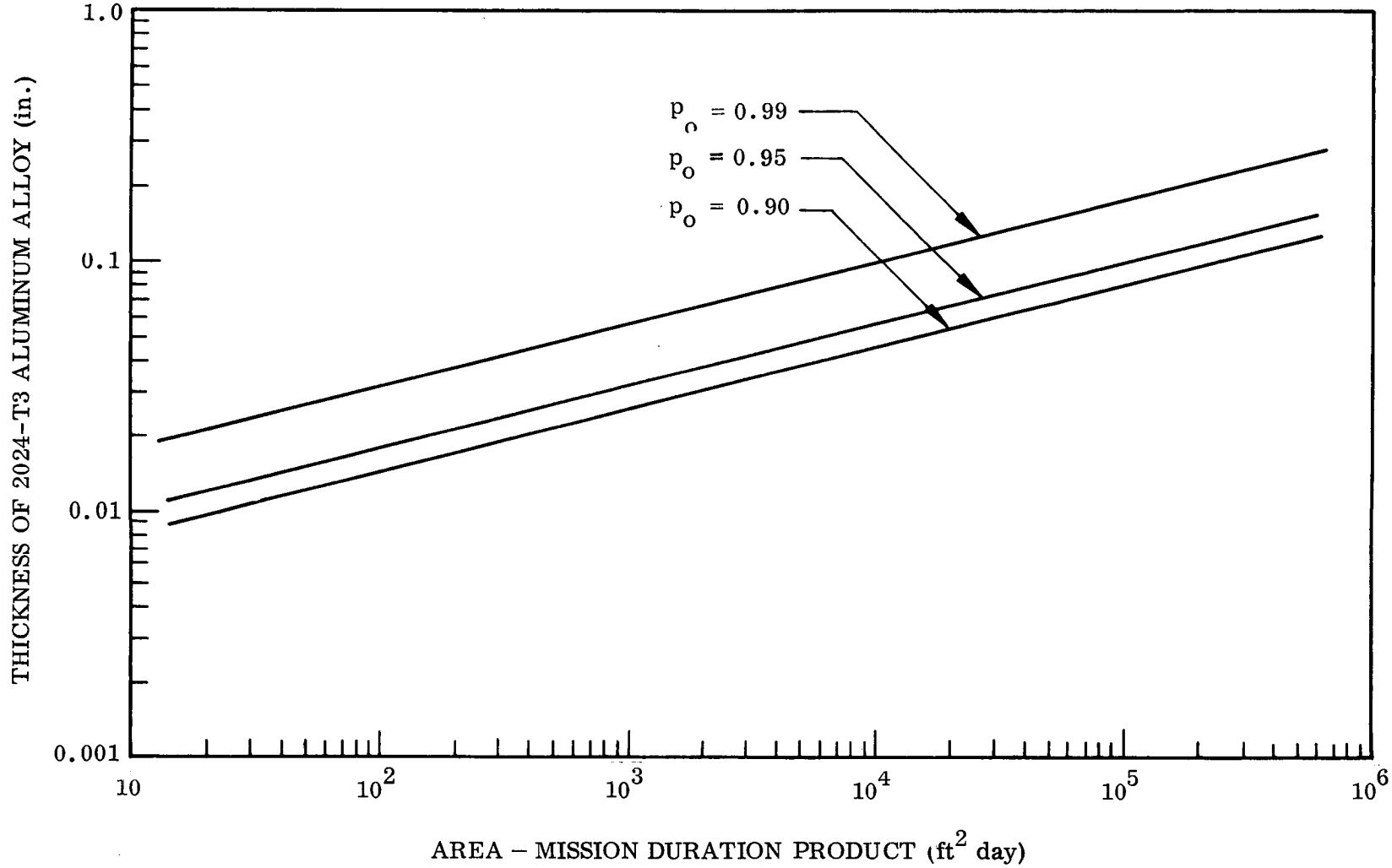

Fig. 6-3 Probability, p_o, of No Meteoroid Penetrations Through A Single Sheet of 2024-T3 Aluminum Alloy

surface of the main wall and be propelled about the inside of the spacecraft to damage components or occupants. The impact of the meteoroid debris on the second sheet can produce an impulsive load (for a few microseconds) that can cause deformation of the material and failure in tension or shear.

Theoretically, it is believed that at meteoroid velocities the material behaves hydrodynamically and the meteoroid becomes molten or vaporized as it passes through the shield. The hole in the sheet has the same diameter as the meteoroid; the shock is absorbed in the small volume about the hole; the shield debris, although traveling at slower velocities than the meteoroid fragments, can be ignored; and the meteoroid fragments are distributed in a Gaussian manner (Refs. 10 and 12).

Investigators have shown experimentally that the spacing between sheets can be from 1 to 10 in. The outer and inner sheets can be configured to give the best distribution for protection of the inner sheet. Two empirical equations have been proposed, shown below as Eq. (4) (Refs. 10 and 12) and Eq. (5) (Ref. 12).

$$V = \left[\frac{4\pi\sigma}{E} - \sqrt{\frac{1-\nu}{3(1+\nu)}}\, C\right]\left(\frac{\rho_o d}{m_p}\right)^2 S^2 t_0 t_1 \tag{4}$$

where

V = velocity of meteoroid (km/sec)

m_p = mass of meteoroid (gm)

d = diameter of meteoroid (cm)

ν = Poisson's ratio of sheet material

ρ_o = density of sheet material (gm/cm^3)

σ = critical stress in sheet

C = velocity of sound in sheet (cm/sec)

E = modulus of elasticity of sheet (dynes/cm^2)

S = sheet spacing (cm)

t_0 = thickness of shield (cm)

t_1 = thickness of spacecraft sheet (cm)

$$t_f = \frac{m_p}{0.045}\left(\frac{5.08}{S}\right)^2\left[\frac{0.0102}{(t_s/d)^2} + 0.079\right] \tag{5}$$

where

t_f = second sheet fracture thickness (cm)

s = sheet spacing (cm)

t_s = shield thickness (cm)

m_p = meteoroid mass (gm)

d = meteoroid diameter (cm)

The critical meteoroid mass for fracture of the second sheet has been calculated from Eq. (5) for the Lunar Excursion Module; it was found to be 2.6×10^{-3} gm when the spacing was 2 in., the aluminum alloy (assumed to be 7075-T6) outer sheet was 0.004 in. thick, and the inner sheet was 0.025 in. The equivalent single sheet thickness, when combined with a 0.99 probability of no penetrations and referred to the tentative NASA environment flux-mass relationship corresponds to an area time product of 66,200 ft^2-day (Ref. 12).

This treatment assumes a ratio of $t_s/d = 0.1$. Under these conditions, an efficiency factor of about 7 of the spaced double wall over the single-wall configuration is achieved. This configuration is for the case where the wall spacing is 2 in., and the thickness of the inner wall is about 5 times the thickness of the shield.

For the Apollo program, the empirical equation currently being used to estimate the double-wall configuration makes the assumption that in actual meteoroid penetration through the first sheet (the shield) the particle is not vaporized. It is assumed that since there is vacuum in the spacing between the shield and the spacecraft wall (the second sheet), some meteoroid particulate matter will strike the second sheet and some impulsive loading on it will occur.

To account for this behavior, the tentatively accepted Eq. (6) is used, where it is assumed that t_s/d is equal to 0.1 and that t_b remains constant when s/d is greater than 25.

$$t_b = \frac{K(\rho_m)^{0.15}(M_m)^{0.35} V_m}{\sqrt{S}} \qquad (6)$$

t_b = thickness of second sheet (cm)

K = constant of sheet material, for aluminum alloy $K = 0.06$

ρ_m = density of meteoroid (gm/cm^3)

M_m = mass of meteoroid (gm)

V_m = velocity of meteoroid (km/sec)

S = sheet spacing (cm)

This equation is also a specialized one and has certain limitations. Thus, as for the other equations for double-wall penetration, Eq. (6) does not completely cover all conditions. Equations (4), (5) and (6) should be used with complete awareness of their limitations.

To correct the materials parameters of Eq. (6) for other materials, Eq. (6a) is tentatively proposed.

$$t_b = \frac{K(\ell_m)^{0.15}(M_m)^{0.35} V_m}{\sqrt{S}} \sqrt{\frac{70000}{\sigma_y}} \qquad (6a)$$

Where σ_y is the 0.2% offset yield strength of the substituted material in pounds per square inch and all other parameters are as in Eq. (6) (Ref. 13).

Assume a critical meteoroid mass of 2×10^{-3} gm for a 0.99 probability of no penetrations and no back surface spalling. The meteoroid diameter d equals 0.0197 cm, since $\rho_m = 0.59$ gm/cm^3 and a spherical particle is assumed. With $t_s/d = 0.1$, the front sheet thickness t_s becomes 0.0197 cm (0.008 in.). Assuming a spacing of 5.08 cm (2 in.), then from Eq. (6) t_b equals 0.075 cm (0.03 in.). In this configuration, S/d = 25.8.

From the flux-mass relationship of Fig. 6-1, a flux of 7×10^{-12} particles/m^2-sec is determined. This is equivalent to 6.5×10^{-8} penetrations per square foot per day in Fig. 6-2, and a single-sheet aluminum alloy thickness of 0.22 in. From Fig. 6-3, this equivalent thickness gives a 0.99 probability of no penetrations for an area-duration product of 2.5×10^5 ft^2-day.

6.5 REFERENCES

1. W. A. Cosby and R. G. Lyle, The Meteoroid Environment and Its Effects on Materials and Equipment, NAS-ASP-78, Prevention of Deterioration Center, National Academy of Sciences–National Research Council, 1965

2. P. B. Burbank, B. G. Cour-Palais, and W. E. McAllum, A Meteroid Environment for Near-Earth, Cislunar and Near-Lunar Operations, NASA-TN-D-2747, Manned Spacecraft Center, Houston, Tex., April 1965

3. Mason Charak, NASA Design Criteria Branch, Office of Advanced Research Technology, Washington D. C., Personal Communication, 8 April 1968

4. M. T. Charak and S. A. Mills, "The NASA Vehicle Design Criteria Program; Engineering Models of the Environment," Third National Conference on Aerospace Meteorology, 6–9 May 1968, New Orleans, La.

5. R. J. Nauman, The Near Earth Meteoroid Environment, NASA-TN-D-3717, George C. Marshall Space Flight Center, Huntsville, Alabama, November 1966

6. J. L. Summers, Investigation of High-Speed Impact; Region of Impact and Impact at Oblique Angles, NASA-TN-D-94, Ames Research Center, Moffet Field, Calif., October 1959

7. E. T. Kruszewski, "Meteoroids; Need for Penetration Scaling Laws and The Potentials of Simulation Techniques," Conference on the Role of Simulation in Space Technology, Blacksburg, Va., 17–21, August 1964

8. R. G. Thomson and E. T. Kruszewski, "Effect of Target Material Yield Strength on Hypervelocity Perforation and Ballistic Limit," Hypervelocity Impact Symposium, Tampa, Fla., 17–19, November 1964

9. R. G. Thomson, Analysis of Hypervelocity Perforation of a Visco-Plastic Solid Including the Effects of Target-Material Yield Strength, NASA TR-R-221, Langley Research Center, Langley Station, Hampton, Va., April 1965

10. E. T. Kruszewski and R. T. Hayduk, "Implications of the Meteoroid Environment on the Design of Spacecraft," EighthAIAA/ASME Strcutures, Structural Dynamics, and Materials Conference, Palm Springs, Calif., 29–31, March 1967

11. A. R. McMillan, Experimental Investigations of Simulated Meteoroid Damage to Various Spacecraft Structures, NASA-CR-915, General Motors Corp., Santa Barbara, Calif., January 1968

12. R. Madden, Ballistic Limit of Double-Walled Meteoroid Bumper Systems, NASA-TN-D-3916, Langley Research Center, Langley Station, Hampton, Va., April 1967

13. B. G. Cour-Palais, NASA Manned Spacecraft Center, Houston, Texas, Personal Communications, 22 May 1968

PART 2

EFFECT OF SPACE ENVIRONMENT ON MATERIALS

Chapter 7

THERMAL CONTROL MATERIALS

M. E. Sibert*

Since the conception and design of the first space vehicles, it has been recognized that a prime engineering requirement is a system for temperature control that permits optimum performance of many components. Reliable long-term performance of most spacecraft components takes place at or near room temperature. Temperature extremes may also be required in the form of cryogenic fluids stored at less than -300°F (Ref. 1) or in the form of nuclear reactors operating at greater than 1000°F for future vehicles (Ref. 2). Temperature limits for typical spacecraft components are shown in Fig. 7-1.

Heat is generated both within the spacecraft and by the environment. Components producing heat include engines, electronic devices, and batteries. Heat from the environment is largely the result of solar radiation; initial ascent heating effects are largely compensated for by use of suitable shrouds. Thus, any form of spacecraft thermal control makes use of suitable materials or devices to achieve a balance between the heat absorbed and the heat emitted to result in some required temperature.

The basic thermophysical properties of materials to be considered in the design of any thermal control system are the absorptance α and emittance ϵ. Absorptance is defined as the ratio of the absorbed radiant flux to the incident flux. Emittance is the ratio of the thermal radiant excitance (radiant flux density emitted) of a radiator to that of a perfect radiator (blackbody) at the same temperature. When the sun is the primary radiation source as in the case of a spacecraft, the solar absorptance α_s is employed. This is defined as the ratio of absorbed solar irradiance to the total solar irradiance. The basic design parameter for a thermal control material is then the ratio of solar absorptance to emittance, α_s/ϵ. Both α_s and ϵ vary from 0 to 1.0. Thus, the ratio of these two properties for a given material allows estimation of vehicle temperature for given locations of a spacecraft. A low value of α_s/ϵ results in relatively low temperatures, since the material has little ability to absorb solar energy compared with its ability to radiate energy into space. Similarly, a material with a high α_s/ϵ has a high temperature, since it has a high ability for absorbing energy but little ability to release energy into the space environment.

Generally, all absorptance and emittance measurements on thermal control materials have been carried out by irradiation under simulated ultraviolet or other radiation in

---

*Other major contributors to this chapter were R. A. Breuch and S. A. Greenberg of the Aerospace Sciences Laboratory. This chapter is based on Chapter 10, by T. F. Vajta, SSD Materials Engineering, in the Second Edition of the Handbook.

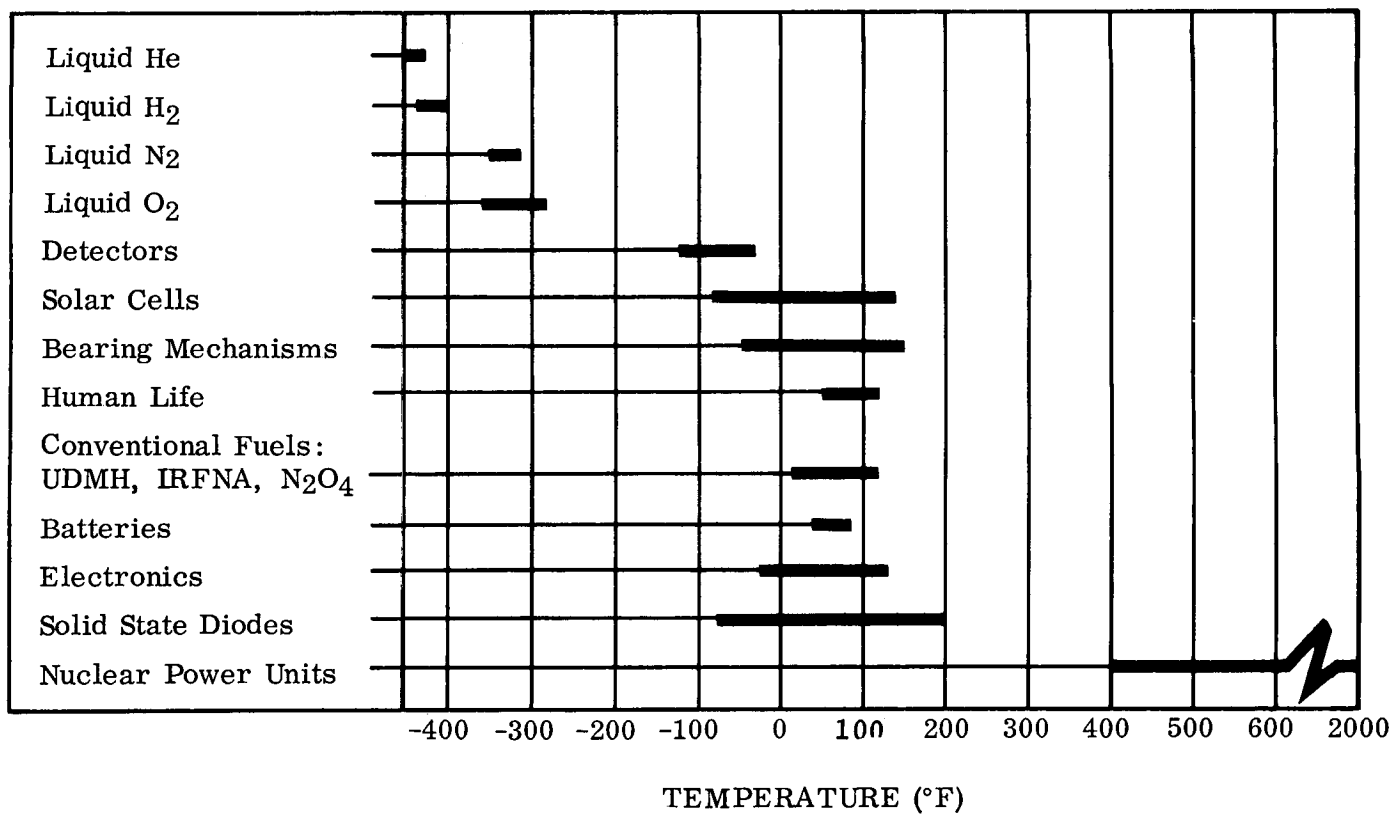

Fig. 7-1 Temperature Tolerances of Typical Spacecraft Components

vacuum under 10^{-6} to 10^{-7} Torr, followed by removal of the specimen to the normal atmosphere where it is evaluated by suitable reflectance, calorimetric, or radiometric techniques. However, during 1965, LMSC made the first measurements in situ of the absorptance change of Thermatrol (TiO_2-silicone), and S-13 materials (ZnO-silicone), wherein the change was measured with the specimen still under vacuum conditions (Ref. 3). It was found that this change was of the order of 7 to 10 times what had been observed when the measurements were not made in vacuum. Similar changes were observed for other ZnO and TiO_2 pigmented materials. These materials containing semiconductor pigments undergo darkening in the ultraviolet-vacuum environment but bleach out in seconds to minutes when reexposed to air. The most common explanation for this behavior is that loss of oxygen creates active vacancies during the ultraviolet exposure (Refs. 4 and 5). Other insulating ceramic materials such as $ZrO_2 \cdot SiO_2$ and ZnO-silicate combinations are much less subject to this bleaching effect. Even the latter class of materials may be subject to bleaching effects after exposure to proton or solar wind bombardment in vacuum and evaluation in air. Thus, in this chapter in situ measurements and flight test data are emphasized wherever available. Current thermal control material evaluation is rapidly shifting to all in situ evaluation. Observations reported by LMSC have been confirmed by others (Refs. 6 and 7). As a result of these investigations, there is at present no fully qualified white thermal control material available for other than short-term and near-earth missions.

Several current programs are concerned with preventing the significant damage to the S-13 (ZnO-silicone) and other materials revealed in laboratory in situ and flight test evaluations. The Illinois Institute of Technology Research Institute (IITRI) has a NASA-sponsored program for developing improved shelf life for the S-13 coating. An S-13G material has been developed by IITRI which employs treated zinc oxide pigments with reported improved stability. Stanford Research Institute is working toward techniques for stabilizing zinc oxide. Hughes Aircraft Company has reported a silicate-rutile material with improved performance over S-13G. LMSC is conducting an Air Force program on development and scale-up of high-stability silicate-based formulations. Essentially all the NASA research centers have active programs in the thermal control materials area. The Air Force Materials Laboratory has a long history of work in this area. Aerospace organizations known to have active programs include Boeing, McDonnell-Douglas, General Electric Space Division, North American-Rockwell, TRW Systems, Aerojet General, Minneapolis-Honeywell, and AVCO.

7.1 THE THERMAL ENVIRONMENT IN SPACE

The thermal environment in space is completely different from thermal conditions in the terrestrial environment. A spacecraft in orbit beyond the earth's atmosphere can exchange thermal energy only by thermal radiation. Atmospheric pressure and air density at even moderate altitudes are so low that aerodynamic heat transfer is essentially nonexistent.

In the case of an earth satellite, exchange of energy can take place by means of the following:

- Direct solar radiation
- Albedo radiation, solar radiation reflected from nearby planets
- Thermal energy reflected from nearby planets
- Radiation to space from the spacecraft

In the case of space probes not near planetary objects, only the direct solar radiation and spacecraft radiation to space become significant. In addition to these basic considerations, internal heat generated by the spacecraft must also be considered in the overall energy equilibrium.

Temperature dependence of a spacecraft on the basic parameters of solar absorptance and emittance can be expressed by

$$\sigma\epsilon T^4 = \alpha_s F_s S + \alpha_s F_R R + \epsilon F_E E + Q \qquad (7.1)$$

where

σ = Stefan-Boltzmann constant

ϵ = infrared emittance; the ratio of the energy emitted by the satellite outer surface to that which would be emitted by an ideal radiator (blackbody) at the same temperatures

T = absolute temperature of satellite

α_s = solar absorptance; the fraction of incident solar energy that is absorbed by a satellite surface

F_s = satellite view factor for insolation

S = local solar constant

F_R = satellite view factor for planetary albedo

R = planetary albedo

F_E = satellite view factor for planetary emission

E = magnitude of planetary emission (σT^4 planet)

Q = satellite internal energy dissipation

Dividing Eq. (7.1) by ϵ gives

$$\sigma T^4 = \alpha_s/\epsilon \left(F_s S + F_R R\right) + F_E E + Q/\epsilon \qquad (7.2)$$

When averaged over a complete orbit, the earth emission and the internal power dissipation terms are generally small compared with the insolation. The dominant terms of Eq. (7.2) dictate that the fourth power of satellite temperature be proportional to the insolation times the ratio of solar absorptance to infrared emittance. This is illustrated schematically in Fig. 7-2.

The solar radiation parameters of interest to the thermal designer are (1) spectral distribution, (2) intensity, and (3) degree of collimation. The spectral distribution may be considered constant throughout the solar system. The intensity varies as indicated in Table 7-1 (Ref. 8). The angle subtended by the sun is 0.53 deg at the

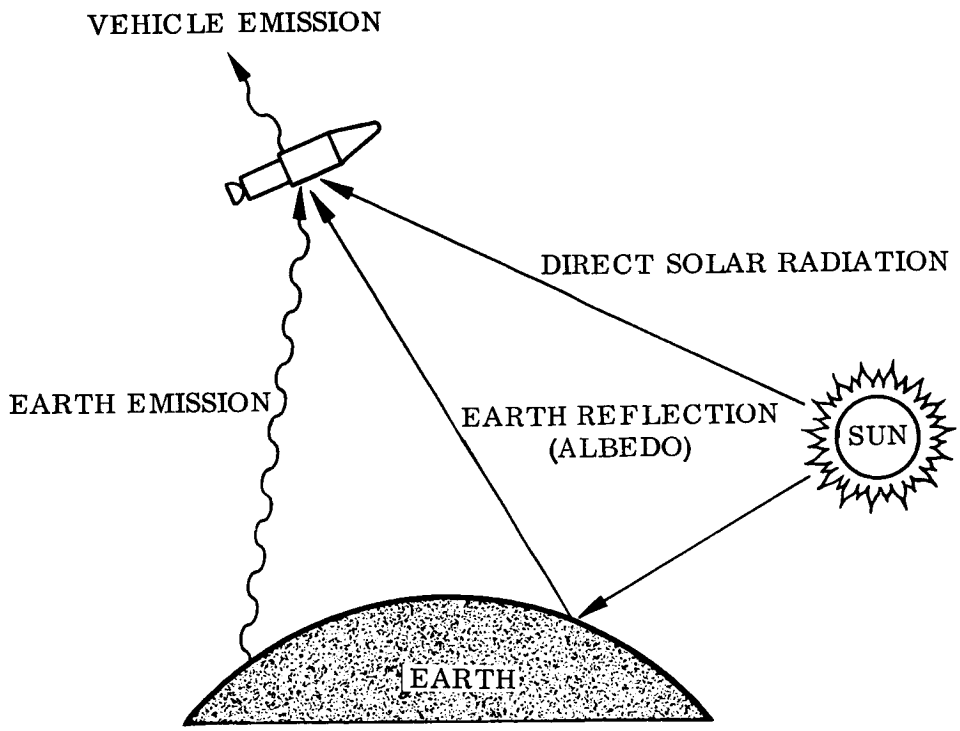

Fig. 7-2 Spacecraft Heat Balance

average earth-sun distance and varies to 1.35 deg for the average distance between the sun and its nearest planet, Mercury.

Table 7-1

INTENSITY OF SOLAR RADIATION IN THE SOLAR SYSTEM

Planet	Intensity (Percent of Solar Constant[a] at 1 A. U.)
Mercury	667
Venus	191
Earth	100
Mars	43.1
Jupiter	3.69
Saturn	1.10
Uranus	0.27
Neptune	0.11
Pluto	0.064

(a) 2.002 cal/cm^2 ± 3% with a 3.4% seasonal variation caused by the varying earth-sun distance.

Earth albedo and emission are discussed in Chapter 4. For most spacecraft heat-transfer calculations, the spectral distribution of the earth albedo may be assumed to be equivalent to that of the sun. In the absence of data on the spectral distribution of albedo of other planets, these are also assumed to be the same as the solar spectral distribution. Some albedos are estimated to be (Ref. 9):

Mercury	0.056
Venus	0.76
Mars	0.16
Earth	0.36
Moon	0.067

The emission from the planets may be assumed to be that of a blackbody at the temperature of the planet. Any significant variation in temperature over the surface of the planet must be taken into account.

7.2 THERMAL CONTROL SYSTEMS

There are two fundamental approaches to spacecraft thermal control, active and passive. In active systems, the conventional terrestrial thermal control mechanisms employ mechanical or thermoelectric devices that require a power input and generally the use of moving parts. Any such system operates with temperature as the controlled variable. A passive control system operates entirely by material and geometric considerations, resulting in thermophysical properties that satisfy the given thermal design requirements; also included is the employment of temperature- or radiation-induced changes in physical properties of materials. Passive systems require no power input or use of moving parts.

This chapter is concerned almost exclusively with passive thermal control systems for several reasons. Most active systems are made up of standard components or they are in a laboratory state of development with no immediate prospects for usage. On the other hand, passive systems have been employed on most space vehicles to date, and these are in a continuous state of development. These have been given preference over active systems largely because of greater reliability factors and overall weight considerations. The best known systems for both active and passive control are briefly described in this chapter.

7.2.1 Active Thermal Control Systems

Active thermal control systems are of various designs and are therefore not amenable to a general presentation. Various examples and methods of active control are described in the following paragraphs.

7.2.1.1 Thermostatically Controlled Heaters

Thermostatically controlled heaters constitute probably the simplest and most obvious active thermal control system. The passive thermal design of the spacecraft may be so accomplished that the lower level of temperature excursions (due to cycles and orbit variations) will lie below the permissible temperature limits but the component will remain below its upper temperature limit. The thermostatically controlled heater may then be used to keep the component temperature within tolerances. This technique, while simple for the thermal designer, may impose excessive demands on the overall system because of power limitations. However, a system of this sort was used in the Surveyor spacecraft to keep the batteries warm during the lunar night, and the Surveyors were able to resume functioning after the period of darkness because the batteries were warm enough to accept the charge when the solar panel was reilluminated.

7.2.1.2 Variable External Radiation Characteristics

The thermal control system utilized on the Able-4-Atlas lunar satellite exemplifies this type of active thermal control (Ref. 10). In brief, the system consists of a number of rotatable four-blade masks, each actuated by a spirally wound bimetallic strip; the rotation of the masks (which cover 20% of the satellite surface) exposes surface areas having differing absorbing and emitting characteristics. The system was designed to

sense internal temperatures and alter the effective radiation properties of the satellite so as to maintain the internal temperature within the specified range (45° to 70°F), even in the event of adverse effects of the space environment on the radiation properties.

Another example of this type of system has been proposed for control of the temperature of solar arrays. This system consists of a slotted shield that is moved across a pattern of alternating high and low α_s/ϵ. This sort of active thermal control system has been used by the Soviet Union (Ref. 11).

The concept of movable louvers or shutters has been reviewed in some detail (Refs. 12 and 13). This type of system was employed on the Mariner and Pioneer spacecraft (Ref. 14). In the Mariner louver thermal control system, the movable elements were polished aluminum foil panels mounted on an aluminum shaft. The shaft was supported by double sealed AISI440C ball bearings using synthane ball retainers impregnated with F50 silicone oil. A bimetallic thermal switch was used as the actuator to turn each panel in the support bearings through 90 deg. The thermal switches were attached to the instrument container in such a manner as to sense its temperature and appropriately actuate the louver. The outer surface of the instrument container, underneath the louvers, was coated with ZnO pigmented silicone white paint. With the louvers closed, a polished aluminum surface having an α/ϵ of about 4.0 controlled the temperature of the instrument container; with the louvers open, a surface having an α/ϵ of about 0.24 controlled the temperature. When the louvers were partially open, a striped pattern of intermediate α/ϵ was produced. Thus, a solar reflecting white paint or a solar absorbing polished aluminum surface or a combination of the two was the temperature control surface.

The Telstar satellites used a white coated ZK 21A magnesium alloy shutter over the top and bottom of the electronics canister as a thermal control mechanism. The dome of the electronics canister was painted with Cat-a-Lac black. A stainless steel piston in an aluminum cylinder which was sealed by a flexible brass bellows was used to open or close the shutters, depending upon the temperature of the working fluid, pentane. A 20-lb force of a steel spring against the pentane determined the opening and closing temperatures of 80°F fully open and 50°F fully closed. The stainless steel piston and aluminum cylinder were lubricated with molybdenum disulfide in an epoxy binder. The temperature of the Telstar 1 varied from 83°F before launch to 74°F after nine orbits and about 65°F after 4-1/2 months in space (Ref. 17).

7.2.1.3 Fluid Transport Refrigeration Systems

In this type of system, the cooling medium (liquid or gas) is circulated in a closed system by a pump or blower and the hot discharge fluid is cooled to the desired temperature by a radiator. A modulating bypass temperature valve controls the flow through the radiator to aid in reaching the desired intermediate temperature for the fluid. Leakage of the circulating fluid and zero-gravity pumping are problem areas in such a method (Ref. 15).

7.2.1.4 Variable Thermal Resistance Devices

Thermal resistance may be varied by altering conductivity, heat path, or radiation characteristics or a combination of these.

Variable conduction is accomplished by varying the quantity of gas in a powder or fiber insulation and thereby altering and controlling the effectiveness of the insulation (Ref. 15). An inherent weakness of this technique is the necessity of keeping the powder or fibers uniformly distributed within the insulation in order to prevent agglomeration. A variable heat path technique might consist of varying the contact area between two surfaces. In the extreme, these two surfaces could be either in full contact with one another or completely separated. However, such a system presents inherent design and reliability problems, and, in addition, accurate determination of the contact resistance under vacuum may prove difficult. A thermal switch which is activated by the movement of a temperature-sensitive fluid-filled bellows has been built at LMSC (Ref. 16). The bellows movement compresses multiple layers of reflective insulation to close the conductive thermal path.

7.2.1.5 Thermoelectric Cooling

Thermoelectric devices utilize the principle of current flowing in a circuit of two dissimilar metals; heat is evolved at one end and absorbed at the other. Practical application of these devices is limited at present because of lack of materials having a sufficiently large conversion efficiency (Ref. 18).

7.2.2 Passive Thermal Control Systems

Passive thermal control is achieved by use of one or more surfaces to provide the required energy absorption/emission in a particular environment to result in a specified temperature range. A component requiring low temperature in the solar earth environment utilizes a highly reflecting, highly emitting white surface (low α_s, high ϵ); similarly, a component operating at higher temperature might use a high absorptance α and a low-emitting metallic surface ϵ. Most space vehicles employ combinations of surfaces to produce the required temperatures for specific equipment areas. In many cases, mosaics such as checkerboard or polka dot patterns have been employed to produce an average temperature that is intermediate between the temperatures produced by the two materials alone.

Passive thermal control materials may be conveniently divided into four general categories:

- Solar Reflector – Surface which reflects the incident solar energy while emitting infrared energy, low α_s, high emittance ϵ, low α_s/ϵ
- Solar Absorber – Surface which absorbs solar energy while emitting only a small percentage of the infrared energy, high α_s, low ϵ, high $\alpha_s/\epsilon > 1$
- Flat Reflector – Surface which reflects the energy incident on it throughout the spectral range from ultraviolet to far infrared, low α_s and ϵ, $\alpha_s/\epsilon = 1$
- Flat Absorber – Surface which absorbs the energy incident on it throughout the spectral range from ultraviolet to far infrared, high α_s and ϵ, $\alpha_s/\epsilon = 1$

The curves in Fig. 7-3 represent both the idealized surface and the surfaces of the practical optimum available materials. A number of review references are available on passive thermal control materials (Refs. 19 through 23).

7.2.2.1 Solar Reflector

The solar reflectors characterized by very low α_s/ϵ ratios are generally white paints. Practical current operational ratios are in the vicinity of 0.20, but there are indications that the ratio may be reduced to less than 0.10 for a paint (Ref. 24). Values of < 0.10 are obtainable today through use of the second surface mirror concept (Refs. 25 and 26).

The Z-93 ($ZnO-K_2SiO_3$) inorganic-based materials have given excellent performance in near earth orbits (Ref. 6) but have shown serious degradation of properties in extra-terrestrial missions. Other materials exhibiting promise from this general class include the pigments $ZrO_2 \cdot SiO_2$ (Ref. 24), $LiAl \cdot SiO_4$ (Ref. 24) and Plasmo Clay (Ref. 27), all in potassium silicate binders. The SnO_2-$AlPO_4$ system (Ref. 28) also appears to be promising, particularly in nuclear radiation environments.

Of the organic-based materials silicone binders with ZnO (Ref. 6), and TiO_2 pigments (Ref. 26), are the most commonly used. These exhibit α_s/ϵ values of 0.2 to 0.3. They have both been shown to exhibit appreciable changes in properties when exposed to near-earth orbits. Recent work on the ZnO-silicone system has resulted in the S-13G coating, which is reported to possess appreciably enhanced ultraviolet stability (Ref. 29).

The third class of solar reflector coatings is the second surface mirrors. These are in the form of silver- or aluminum-coated fused quartz. The second surface reflects incident solar energy, while the front surface controls the emittance. These mirrors must be attached to a surface by suitable space-stable adhesives (discussed in Chapter 10). They possess α_s/ϵ values of 0.06 to 0.14 and exhibit essentially complete stability in all space environments (Refs. 25 and 26).

The present goal of work with solar reflector materials is development of an easily applied paint that is stable in the space environment for periods of a year or longer. Paint is the most commonly used thermal control material but is the material that has shown the most unstable properties in both simulated and actual space environments. This material is needed for maintaining spacecraft skins and adjacent internal components at very low temperatures during the mission or to reduce cryogenic refrigeration loads.

Most initial efforts to develop a suitable white solar reflector material have centered about the use of silicone, acrylic, and epoxy organic vehicles. There are strong indications that these systems will never be suitable for use on extended missions that require fairly precise temperature control. Among the coatings developed are the S-13 coating (ZnO-silicone), Thermatrol (TiO_2-silicone), Skyspar (TiO_2-epoxy), and Kemacryl (TiO_2-acrylic), several of which showed promise up to 1965. Prior to this time, specimens had been irradiated and then removed into the atmosphere for evaluation. It was found that semiconductor materials such as ZnO and TiO_2 underwent bleaching effects

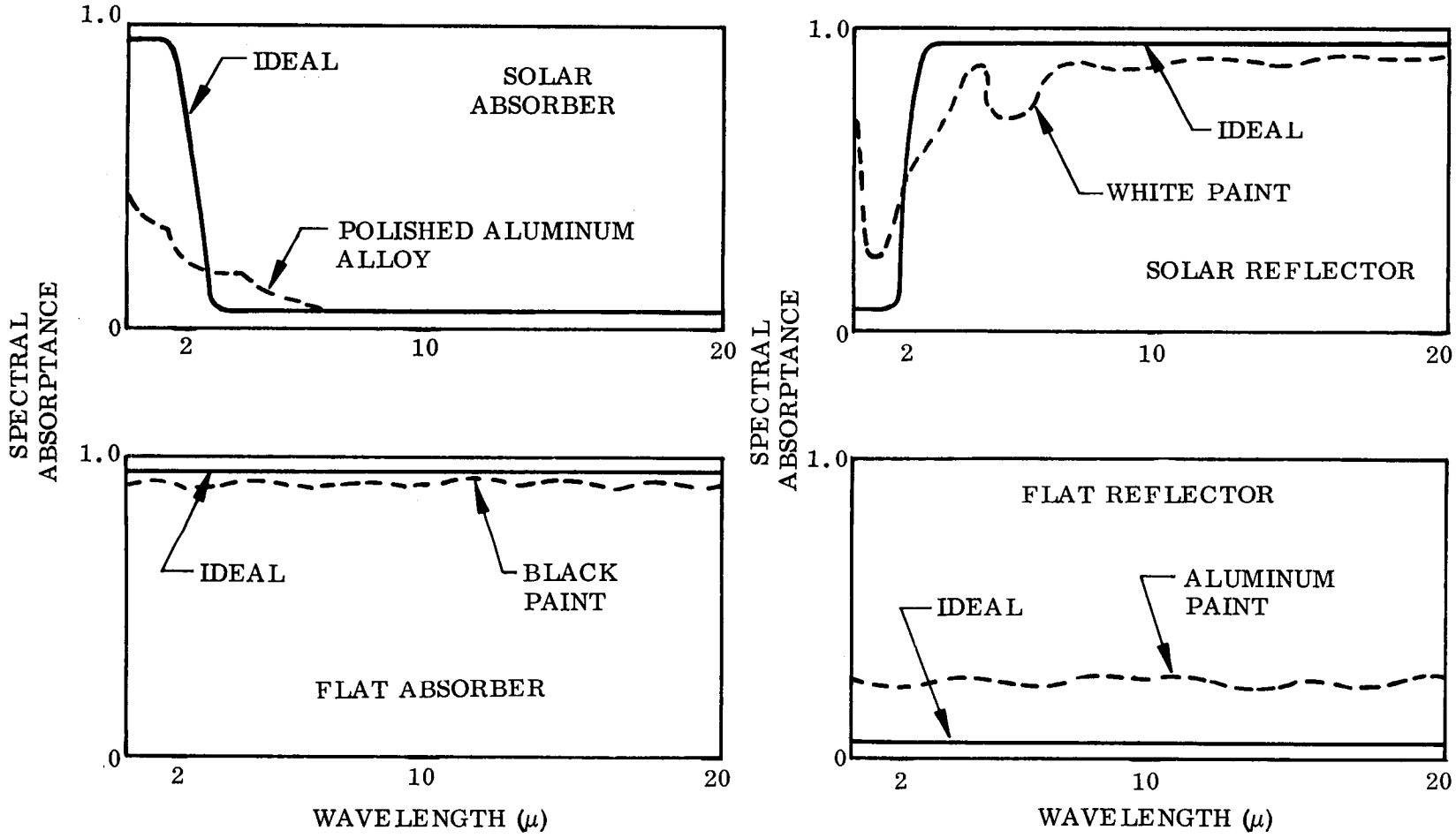

Fig. 7-3 Ideal Representation of Four Basic Surfaces and Production Materials Approximating Them

upon reexposure to air so that damage due to ultraviolet radiation was not observed. Since 1965, the properties of the materials have been measured in vacuum (in situ) after exposure to the simulated space environment, and the bleaching effects were not observed (Ref. 29).

With such a strong indication of the instability of organic-based coatings, a large amount of effort has been devoted to all-inorganic systems. This work has been concerned primarily with development of stable inorganic pigments for use in alkali silicate vehicles. This approach was initiated by LMSC (Refs. 30 and 31), and major work has since been done by IITRI, Hughes, and Goddard Space Flight Center. In the Z-93 silicate material developed by IITRI, the ZnO pigment does not undergo the same changes under ultraviolet radiation as it does in the S-13 (ZnO-silicone), probably because it reacts with the binder to produce a zinc silicate. The plasmo clay-pigmented potassium silicate developed by Hughes and used on the Surveyor has been reported to show good performance. The $LiAlSiO_4$-pigmented-K_2SiO_3 coating developed at LMSC shows stability in ultraviolet but is not too satisfactory in other radiation environments. A $ZrO_2 \cdot SiO_2$-pigmented-K_2SiO_3 system currently being developed at LMSC shows promise as a material with high stability in all environments. A good cross section of thermal control materials information is given in Refs. 19-23, 32, and 33.

Use of second surface mirrors has been developed by LMSC, as well as by the Applied Physics Laboratory and Hughes. At present, these mirrors provide the most stable solar reflecting surfaces available and are ideal for some applications; however, they do not solve the problem of applications to complex or very large surfaces because attachment is tedious.

7.2.2.2 Solar Absorbers

The solar absorbers generally used are polished or electroplated metals or specially prepared metal foils suitably attached to a surface. In a few cases, multilayers have been used, such as the Minneapolis-Honeywell Co. composite consisting of CeO_2 over Mo over MgF_2 (Ref. 34). All such materials possess high values of absorptance/emittance ratio to give α_s/ϵ values greater than 1. When silver is used as part of a mosaic containing a large percentage of white paint, the silver depresses the overall emittance, resulting in a net α_s/ϵ value of 5 to 10, depending on relative areas of silver and paint.

Solar absorptance values for solar absorbers are generally less than 0.5; emittance values are very low, from perhaps 0.3 to 0.1, resulting in high values for α_s/ϵ. This results in high surface temperatures when solar absorbers are employed. There are also potential applications for surfaces with α_s/ϵ values of the order of 0.8/0.1 in conjunction with proposed solar energy conversion devices. For such purposes, a thin coating of metal oxide is deposited on a polished metallic surface. Such a visually black coating is highly absorbent to solar energy but maintains the low emittance of the base metal (Refs. 35 – 39).

7.2.2.3 Flat Reflectors

Relatively few materials with low values of both absorptance and emittance are suitable for use as flat reflectors. Polished silver is possibly the simplest flat reflector surface

but is subject to severe atmospheric corrosion. When this type of surface is required, paints pigmented with metal flakes (aluminum) are most commonly used; very highly polished metallic surfaces can also be prepared to serve in this capacity, but they require careful handling.

7.2.2.4 Flat Absorbers

The purpose of flat absorbers is to absorb essentially all incident solar energy. Generally a black paint is used. Alternatives are anodic coatings such as Dow 17 and Alodine; some sandblasted metals; and deposited platinum or carbon blacks (which are very fragile, however). All such surfaces exhibit α_s/ϵ values of approximately 0.9/0.9 for a net value of 1. The surfaces are generally stable in the space environment, but small changes (about 3%) in the solar absorptance of the black paint have been noted in the Mariner 5 thermal control materials experiment (Ref. 40). It is expected that the largely organic-based vehicle for the carbon black pigments used to date would show some change in properties under more penetrating radiations or under severe ascent heating conditions. These materials have been selected more on the basis of thermal properties, application, and adhesion characteristics than on the basis of radiation resistance.

7.2.3 Special-Purpose Passive Thermal Control Systems

Generally, passive thermal control will be effected through proper selection of geometries and materials with fixed thermal radiation characteristics. However, other potential approaches are available, some of which are described below.

7.2.3.1 Thermal Wick

The use of a thermal wick has been proposed for cooling spacecraft components. A heat transfer fluid is contained by a housing that contains capillary channels. The fluid is evaporated at the equipment that is to be cooled and is condensed at the vehicle skin. The liquid is then returned to the hot end of the system by capillary pumping action. Typical engineering data for such a system are given in Ref. 41.

7.2.3.2 Solid Cryogenic Refrigeration

Solid cryogenic refrigeration is suited to control of components at low temperatures. The component temperature is essentially fixed by the refrigerant temperature, which in turn is determined by the ambient pressure. Since ambient pressure can readily be maintained by suitable sizing of vent lines, a simple and precise means of constant component temperature regulation is available (Refs. 1 and 42).

7.2.3.3 Interference Filters

Constructive or destructive interference can occur when electromagnetic energy is incident upon surfaces covered with films whose thickness is of the same order of magnitude as the wavelength of the incident energy. Through precise control of film thickness and proper selection of materials, one may take advantage of these effects to tailor surfaces with desired values of α_s and ϵ, and thus control temperatures to either high or low levels.

This approach to space vehicle thermal control was first employed in the Vanguard satellite program. The exterior thermal control surface of these satellites consisted of evaporated aluminum covered with a 0.65-μ-thick film of silicon monoxide (Refs. 43 and 44). The silicon monoxide film is essentially transparent to solar radiation but has a strong absorption band at about 10 μ (Ref. 45). By controlling the film thickness, infrared emittance can be controlled independently of solar absorptance. The α_s/ϵ ratio can be varied from about 4.0 to about 0.5. For the system employed in Vanguard, α_s/ϵ equals 1.3. Vanguard continued to transmit for about 6 years. The material has been used on some Explorer spacecraft and apparently was stable in the space environment.

These films are generally applied only to simple geometries. To use this method for thermal control of a large satellite with several different geometrical shapes might be costly, and such a thermal control system would be difficult to manufacture.

7.2.3.4 Surfaces for Control of Solar Cell Temperature

The silicon solar cells commonly used as satellite power sources operate most efficiently at temperatures below 0 °F. This is lower than the temperature encountered by most space vehicles. Consequently, the primary aim of thermal design is to lower the cell operating temperature.

The spectral response of solar cells is such that an appreciable amount of the incident solar radiation is not of wavelengths that are converted into electrical energy by the photovoltaic action of the cell. In a silicon cell, for example, the solar energy of wavelengths less than 0.4μ or greater than 1.1μ contributes very little to the power conversion. If a filter that will not transmit these wavelengths is used on the bare silicon, less thermal energy will be absorbed by the cell. Filters of vacuum-deposited multilayer coatings which will reduce the α_s of a given silicon solar cell from 0.82 to 0.43 while reducing the energy available for power conversion by only 10% have been reported.

If thin glass, fused silica, or sapphire covers are also used on the cells, ϵ will be on the order of 0.9 instead of 0.3 for the bare cell, thus allowing more effective reradiation of thermal energy. These thin covers are transparent to the bulk of the solar energy, reducing it by only about 5%. They also protect the solar cell from penetrating radiation. If an antireflective coating, such as magnesium fluoride film, of the proper thickness is applied to the under surface of the cover, the energy available for conversion will be reduced by only 3% instead of 5%.

For the case of an isolated solar cell facing the sun at one mean earth-sun distance, the bare cell would have an equilibrium temperature of 300 °F. With the cell cover, antireflective coating, and an ϵ of 0.9 on the back side of the cell, the temperature would be 125 °F. Addition of the filter would further reduce this temperature to 40 °F. For some silicon cells, this temperature reduction means an increase in conversion efficiency from 6% at 300 °F to 11% at 40 °F, and a consequent increase of about 60% in power per unit area.

7.2.3.5 Self-Thermostatic Materials

In many designs the thermal capacity of the satellite is such as to restrict to some tolerable value the amplitude of internal temperature fluctuations encountered in a given orbit. Commonly, this amplitude is from 5° to 20°F, a range that is satisfactory for many electronic components. However, variations in the level of internal temperatures due to precession of the satellite orbit plane from one containing the solar vector (noon orbit) to one perpendicular to the solar vector (twilight orbit) may be as great as 70°F.

A constant-temperature surface is considered to be one where the temperature is self-regulating to within 40°F, regardless of the net power supplied to the surface from inside the satellite or the amount of incident radiation of any of the three common kinds: solar, albedo, and planetary emission.

Most efforts toward development of practical materials of varying thermal control properties have attempted variation of the solar absorptance. Most commonly, dyes or other organic materials have been incorporated into standard materials (Refs. 46 and 47). General Electric has developed a practical phototropic surface reported to undergo a 2:1 α_s change over about 10°F. This material utilizes a dioctadecylphosphate pigment in polyvinylbutyral (Ref. 48).

One approach to practical variable emittance materials entails the use of semiconductors as pigments in a vehicle. Many of these materials exhibit absorption edge effects that shift as a function of temperature. These effects can potentially be translated into a variable emittance material. Semiconductors of this type have absorption peaks from 5 to 15μ in the infrared at room temperature. As temperature increases or decreases, shift of the blackbody spectral distribution can cause an increase or decrease in the total emittance. The integral of the spectral distribution curve is a measure of the total emittance of the semiconductor at that temperature (Ref. 49).

7.3 SELECTION OF SPACECRAFT THERMAL CONTROL MATERIALS

The procedure for selection of thermal control materials for a spacecraft requires consideration of many factors through a series of steps:

- A spacecraft thermal load analysis is made for the entire spacecraft.
- Detailed analyses are made for component areas where precise temperature control is required.
- Based on these analyses and the mission requirements, the thermal design is formulated in terms of materials, geometries, and devices.
- Application and development test work is performed as required.
- The complete spacecraft engineering model is subjected to development tests.
- Qualification tests are conducted for spacecraft and components.
- Acceptance tests are conducted for spacecraft and components.

Major considerations in the thermal analysis are discussed in the following paragraphs.

7.3.1 Determination of Spacecraft Thermal Load

Thermal analysis of a space vehicle is generally arrived at by use of computer techniques. Temperature requirements and thermal outputs, if any, must be accurately known for such components as electronic systems, power sources, antennas, control systems, and solar arrays. A model is then constructed consisting of all these elements connected by a thermal network specified by thermal conductivities and radiation. Heat inputs are specified for all elements that emit heat or are subject to radiative heating. Permissible temperature fluctuation of all elements is then considered.

The thermal balance for a vehicle orbiting a planet was depicted in Figs. 7-1 and 7-2. It is apparent that the only first-order adjustment of vehicle temperature possible for a given vehicle and orbit is by variation of the α_s/ϵ ratio for the surface, since the incident solar energy is fixed.

Determination of the thermal load is usually quite complex. Determination of incident irradiance is complicated by shadowing by vehicle projections. The incident albedo irradiance is still more complex because the albedo magnitude varies with vehicle orientation and position relative to the planet. Approaches to the problem have included assuming the earth to be a diffuse reflector of collimated energy, resulting in a modified double cosine intensity decay from the subsolar point (Ref. 50), and assuming the albedo view factor to be equivalent to that of a diffusively radiating sphere with a cosine intensity variation from the subsolar point (Ref. 51). No approach to albedo shadowing is completely adequate. This may or may not be the case for other planets, depending on the extent to which rotation and atmosphere affect temperature variations.

In the basic thermal analysis for the overall spacecraft, the thermal loads are determined for the hottest and coldest orbits. Using the desired temperature, Eq. (7.2) is solved to determine the required α_s/ϵ. Preliminary specifications for the vehicle surface may then be made, using the known thermal properties of materials. Many references provide further details on thermal design of spacecraft (Refs. 50 and 52).

7.3.2 Internal Component Areas

Once the overall vehicle temperature has been estimated with the preliminary α_s/ϵ materials, the temperature and the heat transferred by the internal components of the spacecraft must be determined. Separate energy balances as a function of component temperatures must be written for each component of interest. The energy balances are in the form of nonlinear partial differential equations and generally are solved simultaneously by digital or analog computer. The solution yields a temperature history for each component based upon the average thermal load and the α_s/ϵ ratio of the materials. If the resulting temperature levels are within design tolerances, further refinements of the analysis are made to determine the extent of temperature excursions caused by the actual transient thermal input. If the temperature excursions are within allowable limits, the design may be fixed.

If the temperatures thus computed are not satisfactory, it may be possible to change such factors as surface radiation characteristics (α_s, ϵ, or α_s/ϵ), internal web thickness, and equipment location in order to alter the temperature levels. If such a parameter change is not possible, some form of active thermal control must be utilized.

The accuracy of the predicted temperatures is difficult to assess owing to the complexity of the thermal analysis. Techniques for estimating errors in predicted temperatures are based on the work of Kline and McClintock (Ref. 53).

7.3.3 Example of Selection of Spacecraft Thermal Control Materials

The following example illustrates the use of the ratio of solar absorptance to infrared emittance, α_s/ϵ, in selecting thermal control materials.

Table 7-2 lists the flux incident on portions of a cylindrically shaped vehicle in a polar earth orbit with its axis coincident with the local vertical. The segments are 30-deg-wide portions of the vehicle skin. The angle between the orbit plane and the earth-sun line as viewed looking down at the earth, normal to the ecliptic plane, is denoted by β: β = 0 deg is a noon or day-night orbit; β = 90 deg is a twilight orbit.

From the ratio α_s/ϵ, combined with the incident flux from Table 7-2, vehicle equilibrium temperatures at specific points in space can be estimated. A vehicle with low α_s/ϵ external surfaces experiences relatively low temperatures, since it does not absorb solar energy very effectively (low α_s) compared with its ability to lose energy to space by thermal radiation (high ϵ). Conversely, high α_s/ϵ surfaces tend to become hot. This is illustrated in Fig. 7-4, which represents the average temperature of a cylindrical earth satellite orbiting in a stabilized nose-down position at an altitude of 300 sm. The three curves are for three different types of orbits. It is apparent that the temperature increases with increasing α_s/ϵ. Values of α_s/ϵ vary roughly as follows:

Type of Material	Approximate α_s/ϵ
White paints or ceramics	0.2
Black paints or ceramics	1.0
Metallic paints	0.8 - 1.2
Bare metals	>2

The curves in Fig. 7-4 diverge as α_s/ϵ is increased. This happens because when β becomes larger the vehicle spends more of each orbital period in the sun; consequently, it receives more insolation and α_s becomes more dominant in controlling vehicle temperature. Figure 7-5 shows, for one value of β, the effect of adding an internal power dissipation term to Eq. (7.2):

$$\sigma T^4 = \alpha_s/\epsilon (F_s S + F_R R) + F_E E + P/A\epsilon \qquad (7.3)$$

Table 7-2

SPACE-TIME AVERAGE IRRADIATION OF SEGMENT OF VERTICAL CYLINDER AT 300-sm ALTITUDE

Segment[b]	β[a] = 0 deg			β = 45 deg			β = 90 deg		
	$\overline{F_s S}$[c]	$\overline{F_e E}$[d]	$\overline{F_r R}$[e]	$\overline{F_s S}$[c]	$\overline{F_e E}$[d]	$\overline{F_r R}$[e]	$\overline{F_s S}$[c]	$\overline{F_e E}$[d]	$\overline{F_r R}$[e]
1[f]	95.4	18.8	15.7	75.5	18.8	11.2	28.8	18.8	1.36
2	82.6	18.8	15.2	125.9	18.8	12.1	219.2	18.8	2.61
3	47.7	18.8	15.0	180.4	18.8	13.2	379.1	18.8	3.76
4	12.6	18.8	14.9	208.5	18.8	13.6	438.0	18.8	4.27
5	47.7	18.8	15.0	180.4	18.8	13.2	379.1	18.8	3.76
6	82.6	18.8	15.2	125.9	18.8	12.1	219.2	18.8	2.61
7	95.4	18.8	15.7	75.5	18.8	11.2	28.8	18.8	1.36
8	82.6	18.8	15.2	22.4	18.8	10.1	0	18.8	0.466
9	47.7	18.8	15.0	0	18.8	9.2	0	18.8	0.085
10	12.6	18.8	14.9	0	18.8	8.8	0	18.8	0
11	47.7	18.8	15.0	0	18.8	9.2	0	18.8	0.085
12	82.6	18.8	15.2	22.4	18.8	10.2	0	18.8	0.466
Average	61.4	18.8	15.2	84.7	18.8	11.2	141.0	18.8	1.73

(a) β = angle between orbit plane and earth-sun line

(b) Segments are measured counterclockwise looking down

(c) Insolation

(d) Earth emission = 18.8 Btu/hr-ft^2

(e) Albedo

(f) Midpoint of segment 1 is at ψ = 0 (leading edge)

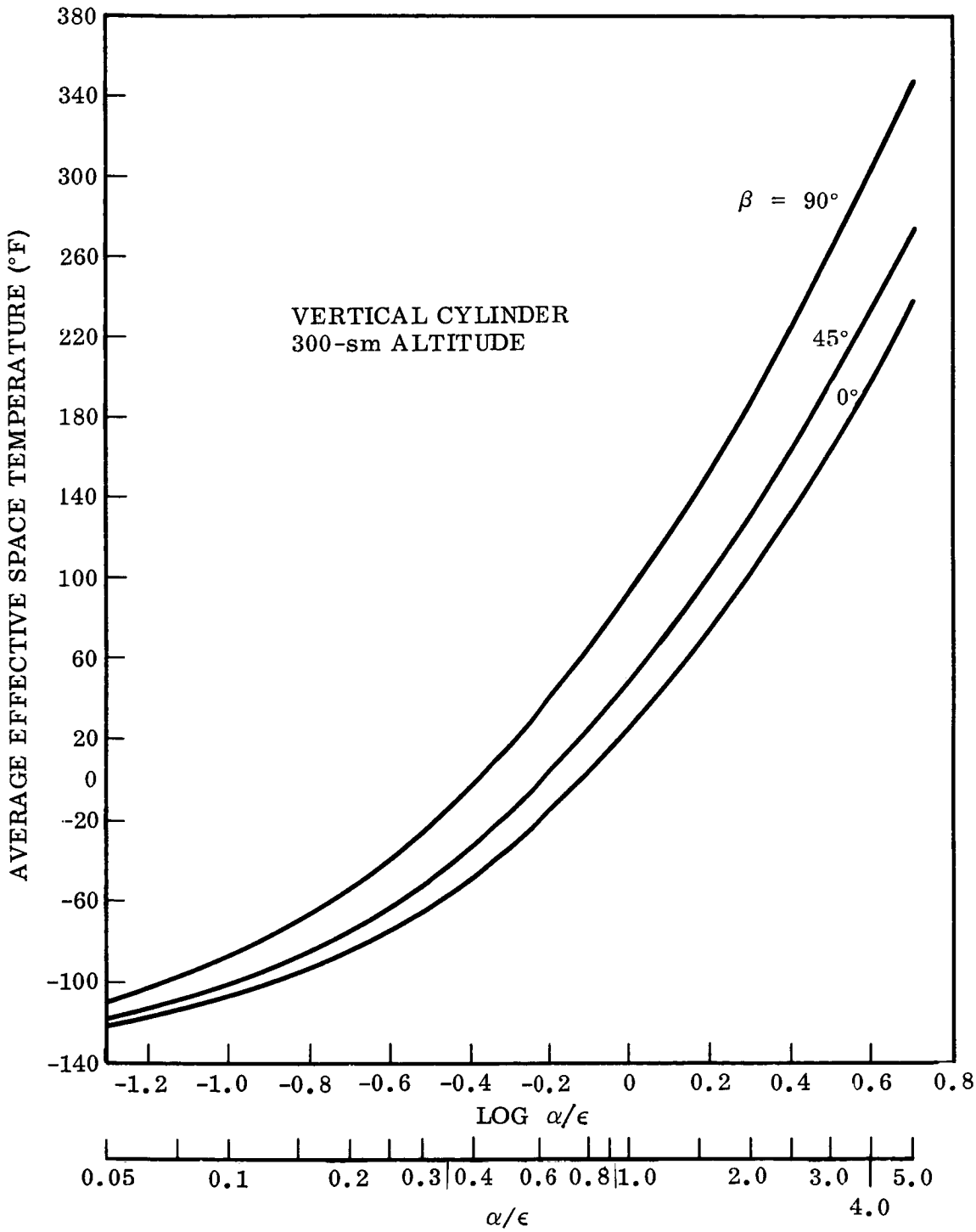

Fig. 7-4 Space-Time Average Effective Temperature as a Function of Surface Type and Orbit Inclination

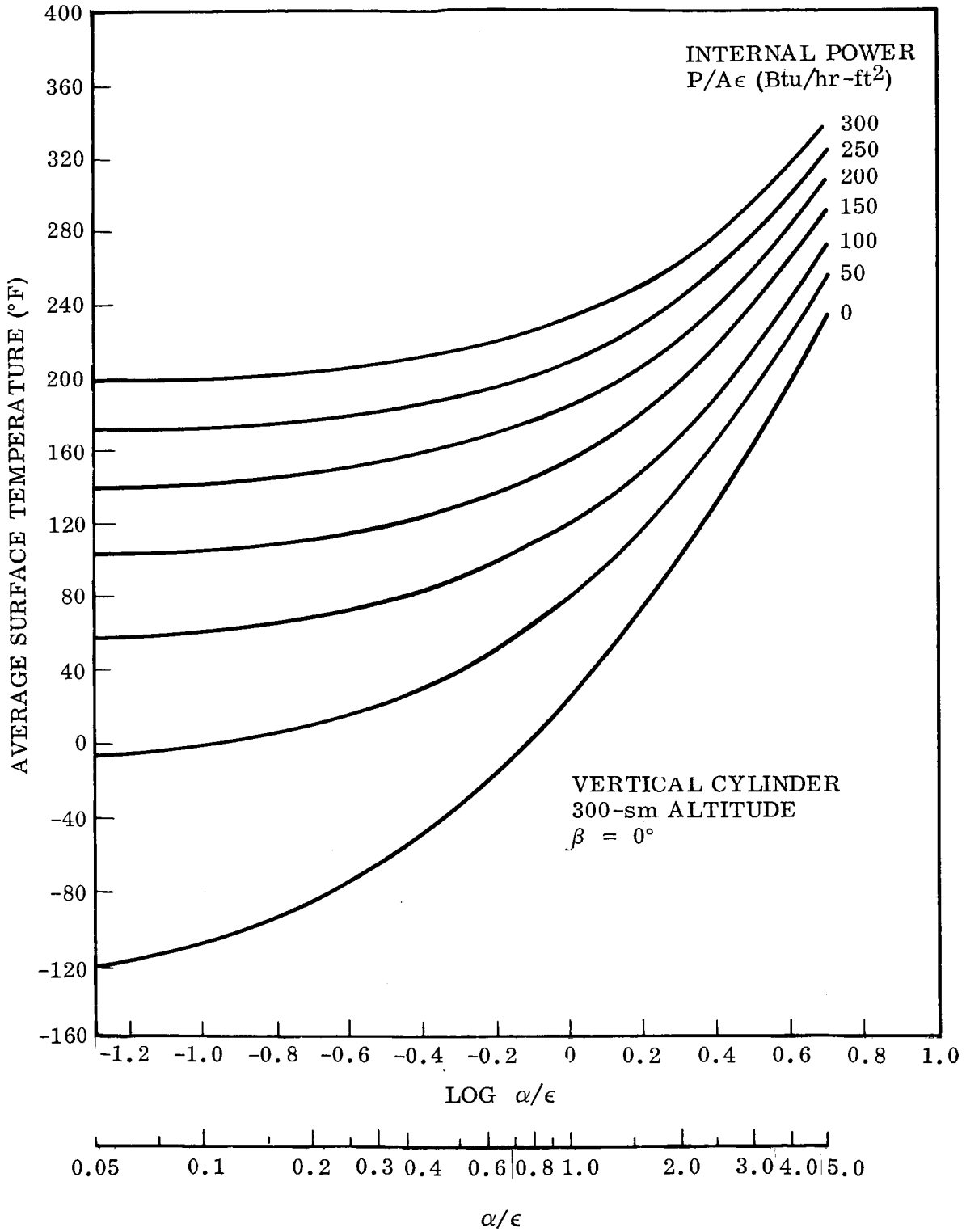

Fig. 7-5 Space-Time Average Surface Temperature as a Function of Surface Type and Internal Power Dissipation

As an example of the use of Eq. (7.3), Table 7-2, and Figs. 7-4 and 7-5 in the selection of thermal control materials, consider an earth satellite operating in a 300-sm circular polar noon orbit where the angle β between the orbit plane and the sun is zero. The satellite is a right cylinder 5 ft in diameter and 5 ft long, the skin of which is fabricated from HM21A magnesium alloy sheet. An electronic component of the satellite has an optimum operating temperature of 70°F and must be controlled for 1 month in space between 0° and 140°F. This section of the spacecraft does not view any other section and is insulated from other parts of the vehicle. During ascent the maximum peak temperature is 600°F for a duration of 1 min.

The electronic component dissipates 200 W of power continuously. The emittance for the component is assumed to be 0.85. The internal power dissipation factor $P/A\epsilon$ [Eq. (7.3)] (P = electrical power in watts, A = area of component, ϵ = infrared emittance of the component surface material) is 10 Btu/ft^2-hr. An interpolation in Fig. 7-5 results in a value of $\alpha_s/\epsilon = 0.7$ to produce a space-time average of 0°F for the external spacecraft skin. If the conductance between the electronic component and the vehicle skin is 10 Btu/°F-hr, the selected $\alpha_s/\epsilon = 0.7$ will result in an average temperature for the component of 70°F. Since Tables 7-9 through 7-14 indicate that no single material has an $\alpha_s/\epsilon = 0.7$, it is necessary to select a mosaic. Actually, this procedure results in a more flexible approach, permitting adjustment of the thermal control mosaic pattern in response to results of thermal-vacuum solar simulation tests at the subsystem level which can later be verified at the system test level. The following points are selected for the mosaic: White Thermatrol 2A-100 TiO_2 in silicone elastomer, a solar reflector with properties $\alpha_s/\epsilon = 0.24$, $\alpha_s = 0.20$, and $\epsilon = 0.85$; and Cat-a-Lac black epoxy paint, a flat absorber with properties $\alpha_s/\epsilon = 1.13$, $\alpha_s = 0.96$, and $\epsilon = 0.85$. By adjusting the respective areas in the mosaic, an approximation of the selected α_s/ϵ can be attained.

This choice of materials is preliminary; the final choice of materials and striping pattern depends upon a detailed analysis which includes the effects of circumferential variations of temperature around the cylinder and the orbital temperature fluctuations. The data on space environment resistance for the white silicone indicates that the striping pattern should allow for the increase in average α_s/ϵ resulting from exposure to the space environment. The overall change in the thermal control properties of the black paint is not as great as the change in the white. The detailed analysis would probably result in selection of the same materials, with perhaps a modification of the striping pattern.

7.3.4 Material Properties Affecting Materials Selection

Although thermal radiation properties are the most critical characteristics of the materials, other factors must also be evaluated, for example, thermal conductivity, specific heat, and thermal diffusivity.

Thermal conduction can be employed both to reduce the instantaneous temperature gradients experienced by exterior spacecraft skins and to direct the dissipation of internal power to skin areas experiencing favorable temperature ranges. In some spacecraft,

the major mode of internal heat transfer is conductive; uncertainties in values of thermal conductivity will be reflected as uncertainties in temperature prediction. The orbital temperature variations experienced by earth-satellite components are directly related to the thermal capacity of the materials used in satellite construction. Through knowledge of specific heat and proper design, thermal strains, fatigue, and other temperature-induced effects may be avoided.

Data are required on the thermodynamic and transport properties of fluids, and in some instances the absorption coefficients and index of refraction are also required. These data are employed for control of propellant temperatures, design of fluid transport heat exchangers, and design of propellant venting and dumping systems. The temperature range of interest for these properties varies from the low cryogenic levels to the elevated levels required for nuclear power systems.

7.3.5 Radiation Characteristics of Materials

Internal spacecraft temperatures are predominantly controlled by the radiation characteristics of the external satellite surfaces. In addition, heat transfer within the interior of satellite vehicles is controlled in part by the emittance of internal surfaces.

Typical depths beyond which thermal radiation is in effect totally absorbed are on the order of 0.0004 in. in metals and 0.004 in. in opaque dielectrics. The radiation characteristics exhibited by materials of interest are markedly affected by the presence of such films and by both macroscopic and microscopic surface roughness. With film-forming materials such as paints, consisting of pigment-vehicle mixtures, parameters such as pigment particle size, pigment-vehicle ratio, and the optical properties of both pigment and vehicle become important, particularly in their effect on solar absorptance.

7.3.6 Evaluation of Thermal Control Materials

Essentially all current evaluation of solar absorptance for thermal control materials is being done by sample evaluation in vacuum after irradiation. In some cases, emittance values are also obtained by this technique, but generally changes in emittance are minor.

LMSC has developed a system using a fiber optics light pipe for transmission of radiant energy to the spectrophotometer. IITRI uses an integrating sphere and a mechanical system for transfer of any of 12 samples from the radiation chamber to the integrating sphere (Refs. 6 and 54). Hughes has also employed an integrating sphere-based system with reflectance measurements made through a window in the sphere (Ref. 55). General Dynamics also uses an integrating sphere, with the sphere housed in a vacuum-irradiation measurement chamber. Samples are moved from the irradiation position to the sample aperture of the sphere by a rotating, thermostatted sample drum; a special transfer optics system delivers radiant energy to the spectrophotometer (Ref. 7). General Electric in Valley Forge, Pa., has developed a system which is equipped for proton and electron radiation as well as ultraviolet (Ref. 56). Most systems generally employ ion and titanium adsorption pumping. At this time, there is no standard established for these measurements, but in general the effects observed by various investigators for the same materials correspond quite well.

These measurement techniques are summarized in Table 7-3. Since such factors as surface roughness, surface films, paint vehicle and pigment contamination, and pigment-to-vehicle ratio affect radiation characteristics, it is necessary to describe both the physical condition of a surface and the fabrication processes used in order to specify adequately either a surface measured or one to be manufactured. For combinations of transparent and opaque materials (such as a glass and aluminum second-surface mirror), the material boundaries and interfaces must also be characterized. In the physical description of radiative surfaces, it is convenient to group materials as electrical conductors, semiconductors, or dielectrics. Specialized films or coatings on metals (e. g. , various chemical and electrochemical conversion coatings, diffusion coatings, and vacuum-deposited films) have been used as thermal control surfaces. The physical nature of such coatings and the thickness and variations must be specified. For an electrochemical coating (e. g. , anodized), the metal surface condition prior to treatment, the temperature and composition of the anodizing bath, the current-density employed, the duration of exposure, and any postanodizing treatment must be specified.

Generally, a spacecraft thermal control surface material is required to do more than just exhibit the desired thermal behavior. For example, corrosion resistance or transparency to rf electromagnetic energy is sometimes required of the coating materials. The requirement for visual tracking also affects the selection of thermal control surfaces. Range safety precautions at the launch site normally dictate the liberal use of white paint on exterior surfaces for visual tracking during ascent.

7.4 EFFECTS OF THE PRELAUNCH ENVIRONMENT

The prelaunch environment is defined as including the entire history of a vehicle prior to launch, from manufacturing to test, transportation, and launch site.

7.4.1 Material Quality Control

Quality control over the constituents of thermal control material is mandatory if consistent standards are to be maintained. There are no industry standards or specifications for paints that ensure the thermophysical properties. Properties such as viscosity or pigment/vehicle ratio may be guaranteed but seldom is extraterrestrial solar absorptance specified. It is necessary, therefore, to verify that each batch of paint displays the required thermophysical properties.

7.4.2 Manufacturing Parameters

The requirements for precise thermophysical properties of thermal control materials necessitate very refined plating, polishing, painting, and application techniques to achieve reproducible and uniform surfaces on a production scale.

Spacecraft paint thermal control coatings are obtained either as research coatings prepared by various industrial or research organizations or as commercial products obtained through industrial paint companies. Each new lot must be checked to ensure that it meets thermal control specifications. Many paints have shelf life limits. To avoid contamination, the container should not be opened prior to use; even minute amounts of

Table 7-3

MEASUREMENT TECHNIQUES FOR PROPERTIES OF THERMAL CONTROL MATERIALS

Technique And Property	Temperature (° F)	Sample Configuration	Results	Accuracy	Remarks
Calorimetric ϵ	-230 to 2000	Approx. 1-in. square hollow prism with 1/16 – 1/8-in. wall	ϵ_H, α_H at sample temperature	5% for -230° to 900° F; 10% above 900° F	Provides final design information on total hemispherical properties. Samples must be machined to close tolerances; measurement is time consuming.
Radiometric ϵ_N from 0.25 μ to 20 μ or total spectrum	1000 to melting point	Thin metal strip for resistance heating	Spectral normal emittance	5% for 1000 to 2500° F; 15% above 3000° F	Provides spectral information on material surface for design or development program. Sample preparation and measurement are time consuming.
Radiometric total normal ϵ in air	300 to 1700	Approx. 4 × 4-in. flat plate	ϵ_N, α_N	5%	To determine energy-dissipation capacity of high-temperature materials when oxidized in air. Design information. Time consuming.
Calorimetric α/ϵ device	-100 to 400	1-in. disk, both sides identical	α/ϵ and ϵ	α/ϵ 5%; ϵ 7%	Samples are easily prepared; test time not lengthy. Good solar simulation for α/ϵ or must be combined with spectral reflectance measurements.
Reflectance $\rho_{N\lambda}$; $\lambda < 2\mu$	70	1-in. disk	$\rho_{N\lambda}$ $\alpha_{N\lambda}$ α_s $.28\mu < \lambda < 1.8\mu$	$\rho_{N\lambda} = 0.8: 3\%$ $\rho_{N\lambda} = 0.1: 1\%$ accuracy of reflectance	Rapid technique to check production surfaces. Samples easily prepared. Special procedures may be used to heat or cool sample over temperature range 70° F ≤ t ≤ 400° F.
Reflectance $\rho_{N\lambda}$; $\lambda < 2\mu$	70	1-in. disk		$\rho_{N\lambda} = 0.1: 3\%$ $\rho_{N\lambda} \geq 0.9: 3\%$ accuracy of reflectance	Rapid technique for checks on production or developmental surfaces. Sample is placed in water-cooled holder and placed in 1500° F Hohlraum furnace. Sample temperature is not varied.

organic materials in a room atmosphere can be sufficient to cause change in the properties of many paints when exposed to the space environment. The thickness required for complete opacity must be known to achieve optimum properties. Generally, thin coats are opaque to infrared radiation, but thicker coats (4 to 6 mils) are required for complete opacity. Specifications will usually differentiate between the thickness for external spacecraft surfaces and that for internal surfaces which are subject to infrared radiation only.

Application of most paints of this type is done by spray processes. It is essential that spraying be done under near-clean room conditions. White inorganic surfaces which are otherwise stable may degrade under ultraviolet radiation when they are applied in an atmosphere containing volatile organic solvents or even excessive pump oil vapors from vacuum pump exhaust.

7.4.2.1 Refractory Coatings

Rokide-A (aluminum oxide) and Rokide-C (chromium oxide) were initially proposed for use as thermal control surfaces because of their high-temperature stability, which suggests stable radiation characteristics throughout an extensive temperature range. Because thin coatings have better adhesive properties under conditions of thermal shock and at the same time provide for a minimum weight thermal control surface, measurements were made to determine the minimum coating thickness required for thermal radiation opacity. As in the case of paints, once the thickness required for opacity is determined, oxide coatings with known and reproducible radiation properties can be assured by simply specifying a minimum thickness. In Ref. 48, values of solar absorptance and infrared emittance are given as a function of thickness for Rokide-A and Rokide-C. The radiation characteristics of Rokide-A were variable throughout the range of thicknesses from 0.006 to 0.015 in. Thus, a thickness greater than 0.015 in. is required to ensure opacity. On the other hand, Rokide-C appears to be opaque at a thickness of 0.005 in. or less.

Rokide requires mechanical bonding to the substrate since it is necessary to grit-blast substrates prior to application. The use of a 2-mil flame-sprayed nichrome layer between the Rokide and the metallic substrate provides a very rough surface with improved adhesion. Coating thicknesses and substrate temperatures are controlled during application by varying the rate at which the substrate passes before the flame-gun nozzle.

An aluminum oxide (Al_2O_3) coating plasma sprayed over a grit-blasted and ultrasonically cleaned 6061-T-6 aluminum alloy substrates that had been plasma sprayed with nichrome powder prior to application of the Al_2O_3 was used on Telstar 1 and 2. The α/ϵ of 0.24 changed to 0.27, an increase of 11%, after an exposure in simulated ultraviolet radiation in vacuum equivalent to 4 months in space (Ref. 17).

7.4.2.2 Polished Metals

In general, chemical and electrochemical metal polishing techniques have resulted in methods that give better optical reproducibility on a production scale. Reproducibility of properties when chemical or electrochemical techniques are used is obtained by

accurately controlling the solution concentrations, polishing times, and current densities. The success of chemical or electrochemical techniques, however, is very often dependent on the initial homogeneity of the surface to be polished. Preliminary mechanical roughening or polishing can be utilized to enhance surface homogeneity prior to chemical or electrochemical polishing operations.

7.4.2.3 Anodic Coatings

Since it is often necessary to apply anodic coatings to certain metallic components for better corrosion resistance, it would be desirable if such coatings could concurrently serve as thermal control surfaces. The radiation properties are a strong function of the anodizing solution concentration, current density, and time. Reference 48 indicates the wide spread in thermal radiation properties possible for the Dow 17 anodize on HM21A magnesium. Infrared emittance varies from 0.50 to 0.72. Efforts have been made to control this anodizing process to the extent of controlling the resulting infrared emittance. Investigations have shown that once a certain anodic coating thickness is reached, the emittance does not vary appreciably.

7.4.2.4 Metallic Films

Although plated or deposited metallic films have been used for the attainment of specific thermal radiation properties for many years, most of the early work in this area was primarily in the development of highly reflective coatings for optical systems. The use of such coatings on many satellite components is desirable for minimum-weight radiative thermal control systems.

Because of inherently high extinction coefficients, metal films only a few microinches thick are opaque to thermal radiation. Opacity has been demonstrated for a film having a thickness of 600 to 700 Å of vacuum-deposited aluminum (Ref. 58). Since the thickness of metallic films on typical satellite substrates usually exceeds that required for opacity, such films should exhibit approximately the same radiation characteristics as in their bulk form. Radiation property measurements made on several different combinations of metallic film and substrate systems (Ref. 57), however, have indicated that the resulting radiation characteristics are strongly influenced by the roughness of the substrate and by the variables of the process. For example, infrared emittance values for opaque gold films varied from 0.03 to 0.31 depending on the method of application. In one experiment (Ref. 58), the rate of application, ambient pressure, angle of vapor incidence, and substrate temperature were individually varied during the application of opaque films of evaporated aluminum (600 to 700 Å thick) on glass (Table 7-4). A change in any one of the parameters caused variations in reflectivity, especially in the shorter wavelengths, but the most marked variations resulted from the changes in ambient pressure and speed of evaporation.

7.4.3 Handling and Protection of Thermal Control Surfaces

Any change in the composition or the physical state of any deposit on thermal control surfaces can radically alter the thermal radiation characteristics. The deposition of reactive or nonreactive chemicals that can result from contact with bare hands or with

Table 7-4

EFFECT OF COATING SPEED ON REFLECTANCE OF ALUMINUM ON GLASS[a]

Pressure (Torr)	Coating Speed (sec)	Reflectance (%)
1.2×10^{-5}	7	92
1.2×10^{-5}	180	62
1×10^{-3}	4	90
1×10^{-3}	60	33
1×10^{-3}	145	12

(a) 0.22 to 0.60μ

contaminated tools and rags, or from condensation of contaminants from the ambient environment, is probably the most potentially damaging to thermal control surfaces in the prelaunch sequence. The chemical deposits left by an apparently clean hand on the surface of a metal are usually sufficient to cause localized corrosion and a change in emittance. Although a thin film of oil or grease may not react with a particular substrate, the radiation characteristics of the composite system will differ markedly from those of the pure substrate. Since such deposits are often very difficult to detect visually, it is important that their formation be totally prevented or that adequate means of inspection be used to detect their presence. A device has been developed for measuring the α_s and ϵ of thermal control materials in the field nondestructively (Ref. 59). Cleaning procedures that will not damage the substrate must then be used for removal of the deposits. Of course, deposits such as dust, or such as adhesive residue left from identification or inspection stickers, must also be prevented or removed.

Installation of components in confined spaces during satellite assembly introduces the problem of abrasive damage to thermal control surfaces. Scratches and other identations resulting from either required or accidental contact with working tools or supporting jigs and fixtures can also alter the radiation characteristics of the affected surfaces.

Probably the most important single means of eliminating degradation of thermal control surfaces in the prelaunch environment is careful indoctrination of all personnel working with these surfaces. The indoctrination should include at least the following:

- What thermal control surfaces are
- Why they are used
- How they are damaged
- The consequences of the damage
- If, when, and how thermal control surfaces can be repaired
- How damage can be avoided

7.5 EFFECTS OF THE ASCENT ENVIRONMENT

During ascent, if thermal control materials are not protected by a properly designed shroud, they can be exposed to aerodynamic heating, aerodynamic pressure and shear forces, and possibly ionized or dissociated gases. During the boost phase, the spacecraft is also subjected to vibration and shock forces, to acoustic pressure, and to stage separation shocks (Refs. 57 and 60).

7.5.1 Thermal Damage During Ascent

Aerodynamic heating during ascent can have several possible effects: discoloration, loss of adhesion, and offgassing, volatilization, or pyrolysis of materials, with possible condensation on critical vehicle components.

Discoloration of materials exposed to aerodynamic heating is most commonly found in the organic-based solar reflectors. This behavior may be due to either pigment or vehicle. Semiconductor pigments (e.g., ZnO, TiO_2) can change properties through the loss of oxygen under vacuum and heat. Organic vehicles, notably acrylics and epoxies, will degrade under like conditions. Pigment-vehicle interactions may also occur but are negligible for most inorganic systems. Discoloration is also not significant with aluminum pigmented paints (flat reflectors) or with black paints (flat absorbers).

Adhesion of materials exposed to aerodynamic heating is primarily a function of the organic or inorganic vehicle, since this is the binder holding the material to a surface. Silicate-bonded surfaces retain adhesion. Many organic-based materials such as acrylics suffer loss of adhesion due to decomposition reactions; all acrylics are subject to bubbling when heated.

The offgassing, volatilization, or pyrolysis of materials during ascent has commonly been called smoking. This behavior is often demonstrated by materials such as wire insulation, adhesives, lubricants, potting compounds, nosecone binding materials, and sealants. The possible recondensation of the gaseous products released by these materials on thermal control or optical surfaces may cause uncontrollable changes in the optical or thermal characteristics of such surfaces. The failure of the Explorer 10 payload has been traced to the recondensation of gases released by the shroud during ascent. The condensate approximately doubled the solar absorptance of the payload (Ref. 61).

The problem is compounded by the fact that smoking may not alter the desired properties of the offending material. For example, although a wire insulation may start smoking at 150°F, it may retain its insulating characteristics until 600°F. The wire would be rated stable to 600°F and would be able to meet existing industry or Federal specifications for wire insulation up to this temperature. Nevertheless, use of such wire in a space vehicle in an area heated above 150°F might result in abnormal performance of the spacecraft because of contamination of nearby thermal control surfaces.

7.5.2 Laboratory Simulation of the Ascent Condition

Because heating rates during ascent are strongly dependent upon vehicle trajectories and, to some extent, upon atmospheric conditions, representative test conditions cannot be specified completely. Thus, the data obtained in specific ascent heating tests cannot be extended beyond the experimentally obtained limits.

The test procedure requires the sequencing of local ambient pressures and test temperatures. The material to be tested is mounted on a suitable holder in a vacuum system; heat is introduced from an external source. Temperature, heat input rate, and pressure are programmed in such a way that the test system pressure is approximately that of the ambient pressure at the altitude at which the spacecraft experiences the predicted peak temperature. Simulation is based either on a predicted heat rate as a function of time or on a predicted temperature level at a particular location as a function of time. The temperature history is programmed, since temperature is much more easily measured and since the geometry need not be exactly that of the actual vehicle application. The effects of ascent heating on thermal control materials are detected as changes in solar absorptance. For materials such as sealants and wire insulations, degradation by the ascent environment is indicated by the condensation of gaseous products from the test specimen onto cooled front surface mirrors.

Test results have shown that a material that can withstand 600° F for 2 min after a 250° F/min temperature rise will not necessarily withstand a peak temperature of 550° F for 10 min with the same initial temperature pulse. Therefore, it must be emphasized that unless a proposed system of materials is tested under conditions approximating those encountered in service, considerable uncertainty in performance will result.

Typical test data for materials that have been subjected to ascent heating effects are shown in Figs. 7-6 through 7-11 and in Tables 7-5, 7-6, and 7-7 (Ref. 62). (Materials for which effects or data are not available are not listed in the tables.) Data are shown primarily for organic-based materials because they are the most subject to this type of damage. Currently used silicate or inorganic formulations are generally not subject to appreciable damage up to 800° F. Maximum specimen temperatures were held from 2 to 12 min unless otherwise specified. The data in the three tables are tabulated according to three of the four classes of thermal control surfaces. Thermal stability of solar absorbers is not listed since these materials are principally metals which are limited only by structural considerations (~1000° F). Numbers in the "Material" column refer to the complete tabulation of materials under radiation effects given in subsection 7.7.1. Some additional data on ascent heating properties for aluminum tapes are given in Table 7-8.

Thermal cycling is not actually an ascent condition, but it is a related thermal effect; therefore, thermal cycling data are included in Tables 7-5, 7-6, and 7-7. These data were obtained in an effort to simulate action on an orbiting vehicle alternately leaving and entering the earth's shadow. The consequent temperature variation results in thermal stresses which vary with time and location of the vehicle. The number of

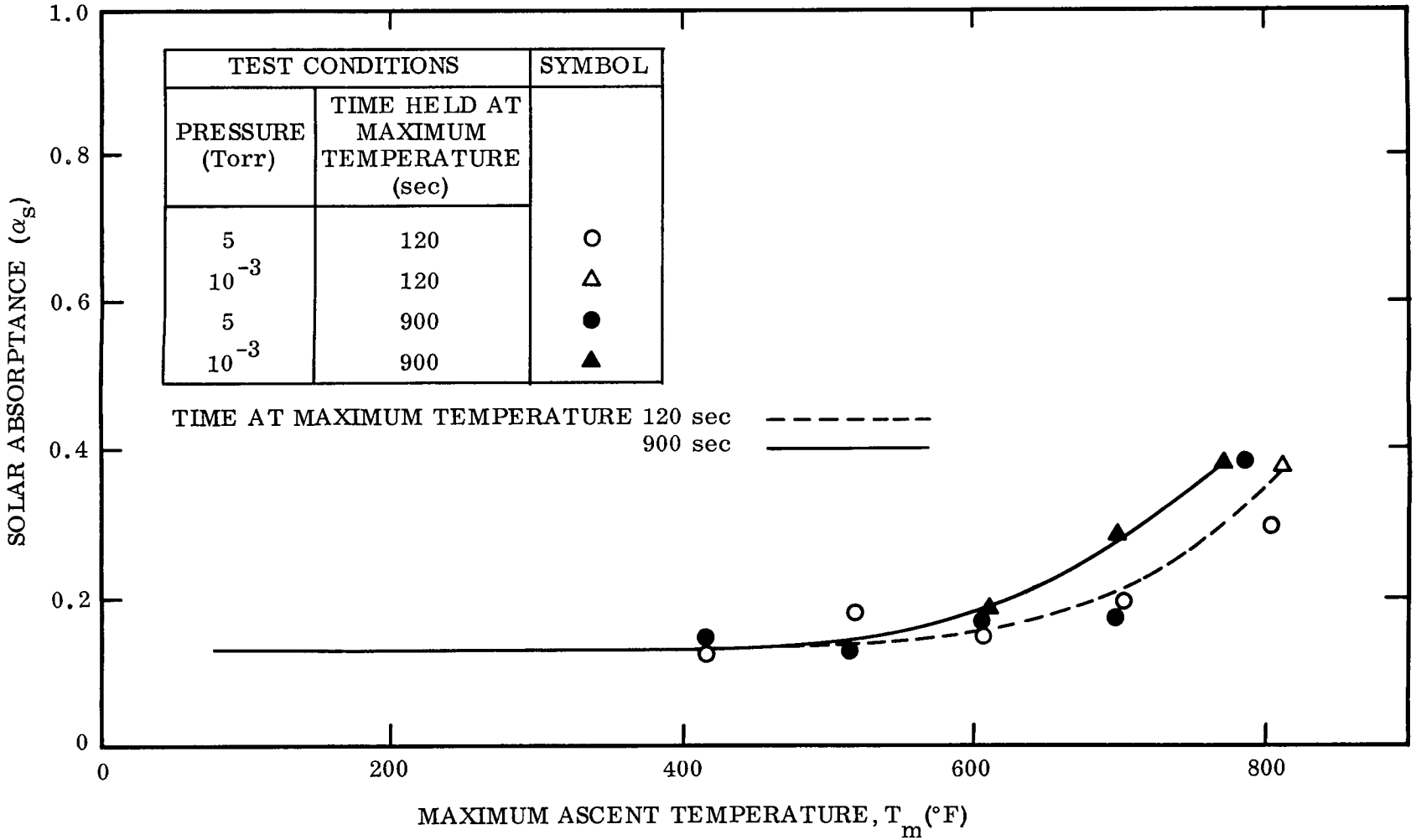

Fig. 7-6 Effect of Ascent Heating on Solar Absorptance of Lithafrax (Lithium Aluminum Silicate) in Sodium Silicate D (Baked) on 1100 Aluminum

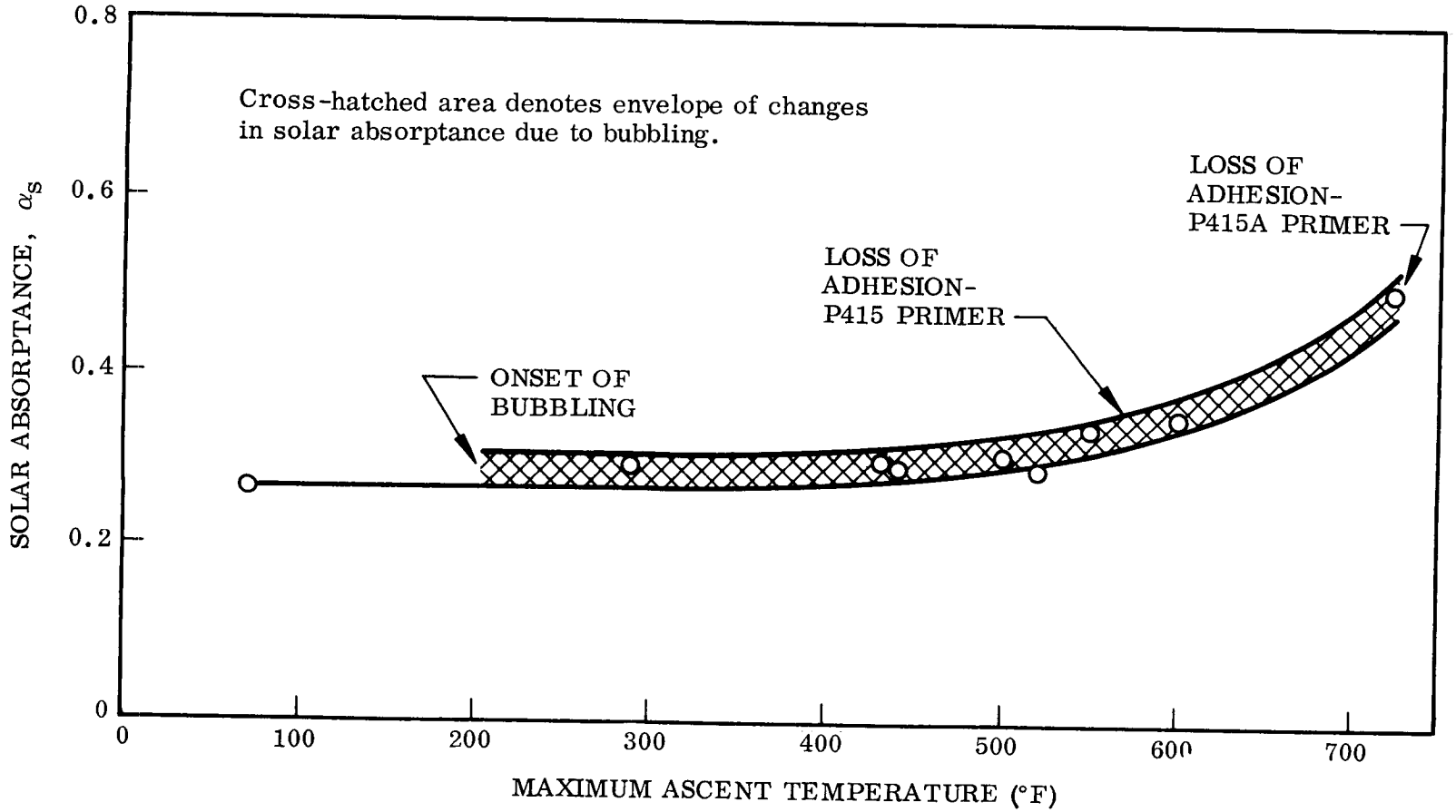

Fig. 7-7 Effect of Ascent Heating on Solar Absorptance of Sherwin-Williams White Kemacryl Lacquer

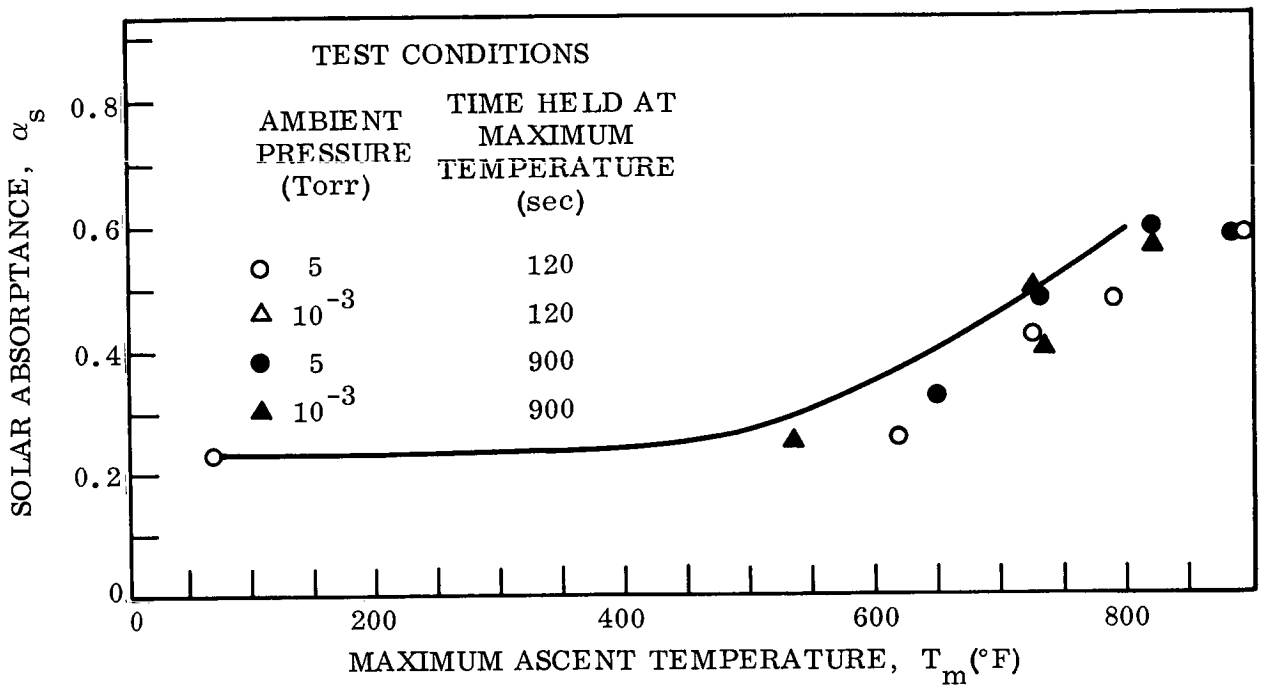

Fig. 7-8 Effect of Ascent Heating on Solar Absorptance of Fuller Gloss White Silicone Paint on 6061 Aluminum

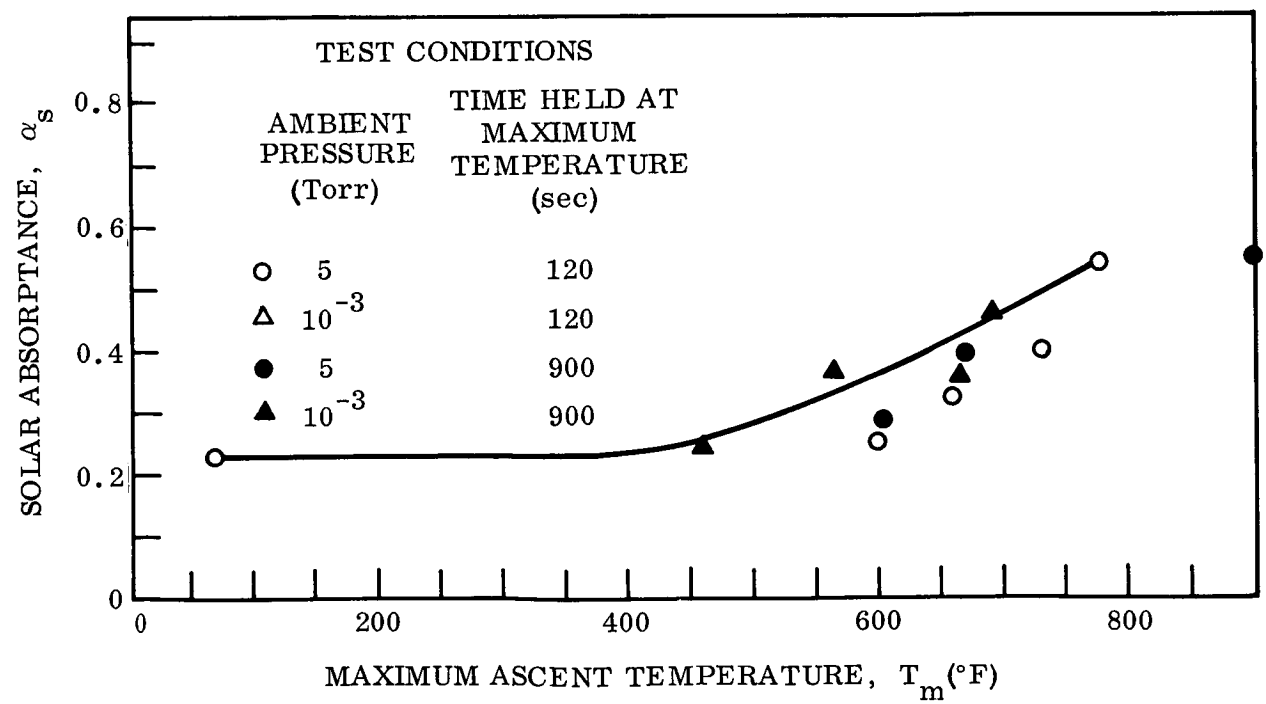

Fig. 7-9 Effect of Ascent Heating on Solar Absorptance of Fuller Gloss White Silicone Paint on Dow-17 Coated HM21A Magnesium

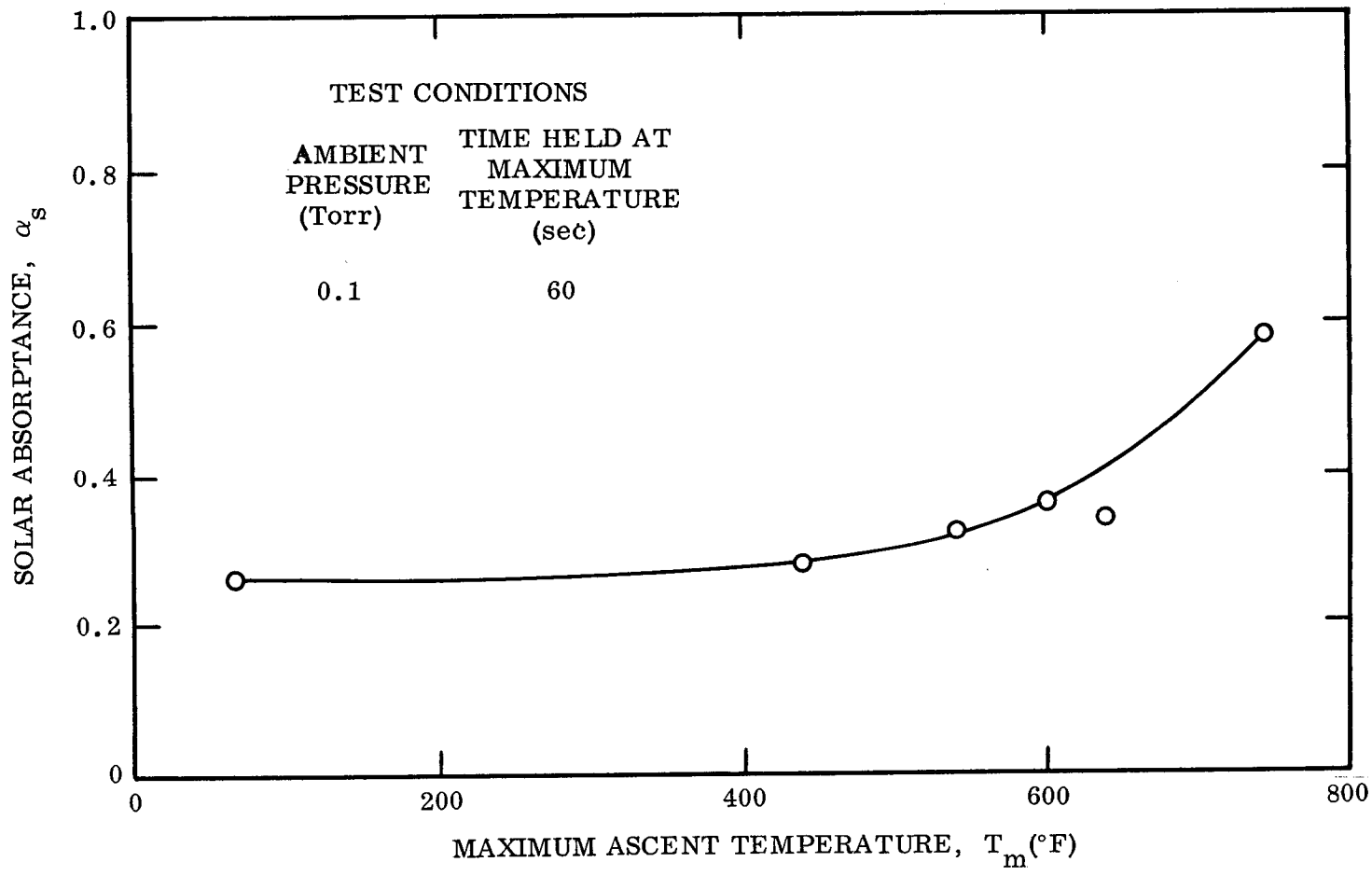

Fig. 7-10 Effect of Ascent Heating on Solar Absorptance of White Skyspar Enamel on Dow-15 Coated HM21A Magnesium

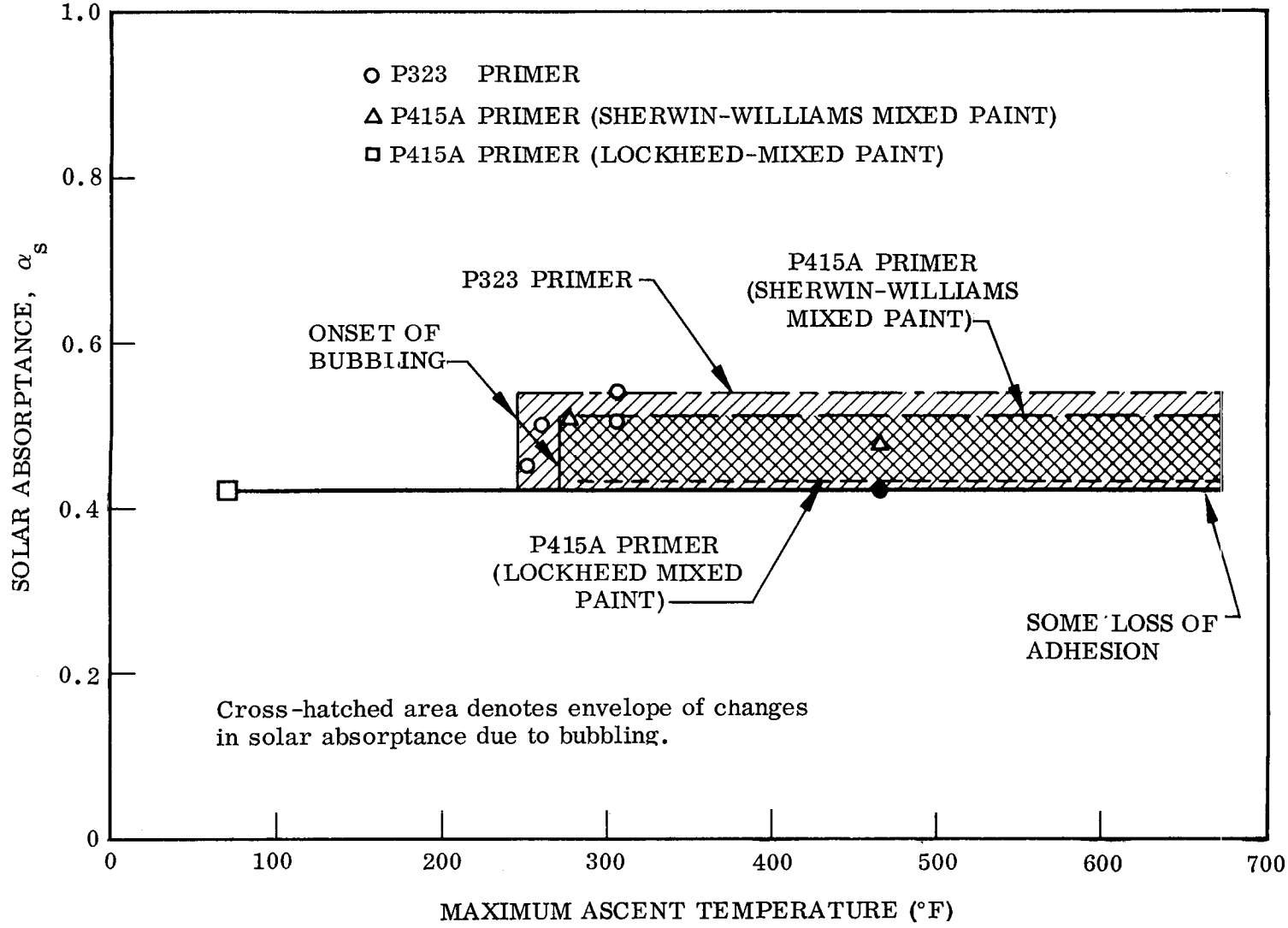

Fig. 7-11 Effect of Ascent Heating on Solar Absorptance of Sherwin-Williams Nonleafing Aluminum Acrylic Paint

Table 7-5

THERMAL STABILITY OF SOLAR REFLECTORS

No.	Material	Ascent Temp. Limits (°F)	Thermal Cycling Resistance				Remarks
			Temp. Range Limits (°F)	No. of Cycles	Length of Cycle (min)	Effect	
1A-1	Z-93	>700	-80 to 200	8	30	None	
1A-7	$ZrSiO_4$-K_2SiO_4	>700	-155 to 90	8	30	None	
1A-8	$ZrO_2 \cdot SiO_2$-K_2SiO_3	>700				None	
1A-9	$LiAlSiO_4$-K_2SiO_3	600	-240 to 70	1,040		None	Slight edge chipping on first cycle
1A-10	$LiAlSiO_4$-K_2SiO_3 (synthetic)	>700				None	
1A-12	Spodumene Na_2SiO_3	>600				None	
1A-13	Cr-Ni Spinel phosphate	700	70-770	10	2.3	None	
1A-14	SnO_2-$AlPO_4$	700	70-770	10	2.3	None	

Table 7-5 (Cont.)

No.	Material	Ascent Temp. Limits (°F)	Thermal Cycling Resistance				Remarks
			Temp. Range Limits (°F)	No. of Cycles	Length of Cycle (min)	Effect	
1A-18	H_2SO_4 Anodize-Al	Structural only				Probably none	
1A-19	Rokide A	> 1000				None	
1B-1	S-13	650	RT-LiqH_2 RT-200	10	—	None	
1B-7	Therma-trol 2A-100	650	-80 to 200	30		Minor	Simultaneous 450 ESH UV and 4×10^{14} electrons/cm^2
1B-8	Therma-trol 6A-100	700				None	
1B-12	Fuller Silicone		-240 to 70	1,210	18	Cracking increased in severity up to 330 cycles; peeling at 430 cycles	
		450	-240 to 70	170	18	Cracking, loss of adhesion	
			-80 to 200	30	18	None	Also 450 ESH UV and 4×10^{14} electrons/cm^2
1B-13	Kemacryl	450	-240 to 70	1,040	18	None	

Table 7-5 (Cont.)

No.	Material	Ascent Temp. Limits (°F)	Thermal Cycling Resistance				Remarks
			Temp. Range Limits (°F)	No. of Cycles	Length of Cycle (min)	Effect	
1B-13	Kemacryl	450	-150 to 70	385	18	None	
		Blisters at 200	-80 to 200	30	18	None	Also 450 ESH UV and 4×10^{14} electrons/cm^2
1B-16	Silicone Tape	700	RT-200	25	.04	None	
			RT to -65	15	.07	None	
1B-17	Skyspar	450	-150 to 70	385	18	None	
		200−450 $\Delta\alpha_s \sim 0.04$	-80 to 200	30	18	None	
1C-1	Optical Solar Reflector	Not qualified	-150 to 200	20		None	
			-320 to 25	20		None	

Table 7-6

THERMAL STABILITY OF FLAT REFLECTORS

Material		Ascent Temp. Limits (°F)	Thermal Cycling Resistance				Remarks
			Temp. Range (°F)	No. of Cycles	Length of Cycle (min)	Effect	
3-1	Kemacryl on Al	650	-150 to 70	385	18	None	$\Delta\alpha_s$ 0.03, 240−650°F Bubbling ~ 260°F
3-3	Fuller Leafing Al	800	-240 to 70	170	18	Cracking, loss of adhesion	
			-80 to 200	30	18	None	Also 450 ESH UV and 4×10^{14} electrons/cm^2
3-4	Fuller Leafing Al	880	-240 to 70	170	18	Cracking, loss of adhesion	
			-80 to 200	30	18	None	Also 450 ESH UV and 4×10^{14} electrons/cm^2

Table 7-7

THERMAL STABILITY OF FLAT ABSORBERS

Material	Ascent Temp. Limits (°F)	Thermal Cycling Resistance			
		Temp. Range (°F)	No. of Cycles	Length of Cycle (min)	Effect
4-4 Fuller Silicone Black	1070 or more	-240 to 70	170	18	Cracking, loss of adhesion
4-5 Micabond Black					None
4-9 Kemacryl Black	450 or more	-150 to 70	385	18	None
4-11 Dow 17	500 or more				None
4-12 Cr_2O_3-Rokide C	1660 or more	70 to 1600	1	5	None
4-13 QMV Be-Pt Black	1200 or more				Probably none
4-14 Stainless Sand-blasted	>1200				Probably none

Table 7-8

ASCENT-HEATING RESISTANCE OF SELECTED ALUMINUM TAPES

Surface	Maximum Ascent Temperature (° F)	Ambient Pressure (Torr)	Results
Permacell P-112 Aluminum Tape	409 – 590	1.1	Physical characteristics appeared to remain unchanged.
3M FP2 Aluminum Foil With Thermo-setting Pressure-Sensitive Adhesive	251 – 495	1.1	Surface properties remained unchanged; adhesion poor.
Mystik 7455 Aluminum Tape(a)	645 – 990	1×10^{-3}	Slight loss of adhesion.
Permacell EE6100 Aluminum Tape	670 – 810	0.01 – 0.8	Very slight loss of adhesion.

(a) $\alpha_s = 0.16$

cycles to failure has been found to be inversely proportional to the square of the amplitude of the stress for a given average temperature. Simulation of thermal cycling on a laboratory scale is carried out on a reduced time scale in order to shorten the test. The key principle in the simulation requires conformance only to transient portions of the curve, with some time allowance for temperature and stress equilibration between transients.

The reentry environment is similar to the ascent environment but is generally more severe (Refs. 63 and 64). To protect the vehicle from the reentry environment, the designer must often employ special devices such as ablative heat shields or sublimation cooling. Consequently, a wide range of physical and chemical properties must be known in addition to the surface radiative properties (Ref. 65). A detailed treatment of reentry effects is beyond the scope of this handbook. Such data are presented in Ref. 66.

7.6 EFFECTS OF THE SPACE ENVIRONMENT

The thermal environment of space was described in subsection 7.1. The space environment consists of both natural and artifical radiation, physical impact, and thermal effects. Natural radiation may consist of solar electromagnetic radiation, protons, electrons, or alpha particles in any combination. Artificial radiation environments may include injected electrons from high-altitude nuclear detonations or radiation resulting from nuclear reactors or isotope power supplies carried by spacecraft.

The major portions of the space environment are listed below. Those having the greatest effect on performance of thermal control materials are identified by asterisks. The space environmental factors are discussed in Chapters 4, 5, and 6.

NATURAL

Particle Radiation

• Protons	Galactic Van Allen* Solar Flare Solar Wind* Auroral
• Electrons	Van Allen* Auroral*
• Alpha Particles	Solar Wind Solar Flare
Electromagnetic	Solar Ultraviolet* Solar Infrared Solar X Rays
Physical Impact	Atmospheric Atoms or Ions Micrometeoroid Dust

ARTIFICIAL

Persistent

• Electrons	High-Altitude Nuclear Detonations*
• Neutrons/Gammas	Spacecraft-Borne Nuclear Reactors*
• Electrons/Gammas	Spacecraft-Borne Isotope Power Supplies

Transient

• Plume Contaminants	Rocket Exhaust Impingement on Surfaces

This subsection gives specific data on performance of spacecraft thermal control materials under the influence of the various environments. Available data are given for most of these materials. All data are divided into four general classes: solar reflectors, solar absorbers, flat reflectors, and flat absorbers. Solar reflectors are in turn divided into inorganic materials, organic materials, and mirror materials.

Material Type	Class	Table
Solar Reflectors		
Inorganic	1A	7-9
Organic	1B	7-10
Mirrors	1C	7-11
Solar Absorbers	2	7-12
Flat Reflectors	3	7-13
Flat Absorbers	4	7-14

Numbers assigned to the materials are used in all data presentations so that data for a given material can be readily located.

Radiation environmental effects are shown in Tables 7-9 through 7-14 for the four classes of thermal control materials. Wherever possible, test data for changes in properties measured in situ in vacuum are given, as opposed to conventional measurements made in air. Second priority is given to flight test data. For any given material the order of tabulation is ultraviolet, particulate, combined radiation, and nuclear radiation. Not all data are available for all materials, of course. Post-exposure emittance values are not shown because in most cases data are not available. The emittance is known to change very little. All emittance values (ϵ) are total hemispherical values as opposed to normal values (ϵ_N) unless otherwise stated. All radiation-induced changes are expressed as changes in solar absorptance unless otherwise noted. Accuracy of absorptance measurement is generally less than 10% for values less than 0.3 and less than 5% for values less than > 0.8. Representative curves are shown to illustrate typical changes in properties in both organic-based and inorganic-based materials and to show the significance of ultraviolet radiation damage when the changes in properties are measured in vacuum. The emittance values given are those for total hemispherical emittance ϵ_{TH}.

Table 7-9

RADIATION STABILITY OF SOLAR REFLECTORS – INORGANIC-BASED

Material	Initial Values – 70°F			Type[a]	Radiation Exposure		ESH	$\Delta\alpha_s$	Remarks	Ref.
	α_s	ϵ_{TH}	α_s/ϵ		Intensity	Integrated Flux[b]				
1A-1: SP-500 ZnO in PS-7 K_2SiO_3 (Z-93)	0.17	~0.90	~0.19	UV in situ			800	0.01	IITRI	6, 29
	0.16	0.86	0.19	Flight Mariner IV	–	–	3800	0.11		67
	0.19	0.92	0.21	Flight OSO-2	–	–	300	<0.01		68
	0.16 to 0.18	0.92 to 0.93	0.17 to 0.19	UV in situ			200	0.02	Douglas MD-22	69
	0.17			Proton	20 keV	1×10^{16}	–	0.13	Atomics Intl.	28
	0.17			Electron	2 MeV	1×10^{16}	–	0.03	Atomics Intl.	28
	0.17			Proton	150 keV	1×10^{14}		0.02		28
	0.15			SW-H_2^+	1 keV	1.6×10^{17}		0.11	MSFC-Litton	70
	0.15			SW-H_2^+	1 keV	4.25×10^{17}		0.35	MSFC-Litton	70
	0.15			SW-H_2^+	1 keV	1.9×10^{18}		0.67	MSFC-Litton	70
	0.21			Near UV Far UV Proton	10× 10× 10 keV	– – 1×10^{15}	500 500 –	0.01	Avco	71
	0.20			Near UV Far UV	10× 10×	– –	500 500	<0.01	Avco	71
				Proton in situ	2 keV	3×10^{15}	–	<0.01	LMSC	26
				Proton in situ	2 keV	5×10^{16}	–	0.26	LMSC	26
1A-2: Plasmo Clay in PS-7 K_2SiO_3 (Hughes – H-10)	0.18	0.93	0.18	UV Air			500	0.05		27
	0.17			Flight Surveyor I			600	0.06		72
1A-3: $SrMoO_4$-K_2SiO_3 in PS-7 (AFML)	0.25			Near UV Far UV			500 500	0.03	Avco	71
	0.24			Proton	10	1×10^{15}	–	<0.01	Avco	71
	0.24			Near UV Far UV Proton	10× 10× 10 keV	– – 1×10^{15}	500 500 –	<0.01		71
1A-4: TiO_2-Al_2O_3-K_2SiO_3	0.17	0.83	0.20	Flight ATS-1	–	–	1300	$\Delta\alpha_s/\epsilon$ 0.18		73

Table 7-9 (Cont.)

Material	Initial Values – 70°F			Type[a]	Radiation Exposure		ESH	$\Delta\alpha_s$	Remarks	Ref.
	α_s	ϵ_{TH}	α_s/ϵ		Intensity	Integrated Flux[b]				
1A-5: $ZnO-TiO_2-Al_2O_3-K_2SiO_3$	0.17	0.83	0.20	Flight ATS-1	–	–	1300	$\Delta\alpha_s/\epsilon$ 0.17		73
1A-6: $Al_2O_3-K_2SiO_3$	0.11	0.82	0.14	Flight ATS-1	–	–	1300	$\Delta\alpha_s/\epsilon$ 0.30		73
	0.08	0.89	0.09	UV in situ			700	0.07		24
1A-7: $ZrSiO_4-K_2SiO_3$ (Ultrox)	0.15	0.89	0.17	Flight OSO-2	–	–	300	0.04	LMSC	68
1A-8: $ZrO_2 \cdot SiO_2-K_2SiO_3$ (Synthetic)	0.07	0.85	0.08	UV Air	5.5×	–	485	0.04	LMSC	24
	0.085			UV Air	6.2×		265	0.025		24
	0.07			Proton	1 keV	5×10^{16}	–	0.02		24
	0.09			Proton	1 MeV	2×10^{15}		0.01		24
	0.10			UV in situ Proton in situ	6.5× 1 MeV	– 2×10^{15}	45 –	0.02		24
	0.09			UV Proton	6.5× 1 MeV	– 1×10^{15}	45 –	0.03		24
	0.07			Neutron γ		4×10^{14} $n_f vt$ 2×10^8 rads		0.03		74
	0.12	0.89	0.13	UV	6×	–	600	0.09		31
	0.11			Neutron, γ		1×10^8 rads		0.03		74
1A-9: $LiAlSiO_4$ (Lithafrax)-Na_2SiO_3	0.13 (0.12 to 0.14)	0.85	0.15	UV Air	6×		600	0.04	LMSC	31
	0.10			γ		1×10^8 rads		0.15		74
				Neutron		1×10^{14} $n_s vt$ 1×10^{15} $n_f vt$				74
	0.15			Electron	0.8 MeV	1×10^{15}	–	0.15		75
	0.15			Electron, UV	0.8 MeV/10×	1×10^{15}	485	0.10		75

Table 7-9 (Cont.)

Material	Initial Values – 70°F			Type[a]	Radiation Exposure		ESH	$\Delta\alpha_s$	Remarks	Ref.
	α_s	ϵ_{TH}	α_s/ϵ		Intensity	Integrated Flux[b]				
1A-10: $LiAlSiO_4$ (Synthetic)-K_2SiO_3	0.12	0.90	0.13	UV Air	6×		600	0.04	LMSC	24
	0.11			γ		3×10^8 rads		0.13		74
				Neutron		3×10^{14} $n_s$vt 1×10^{15} $n_f$vt				74
	0.16			Electron	0.8 MeV	1×10^{15}	–	0.16		75
1A-11: Evaporated SiO_x (1.5 μ) Over Evaporated Opaque Al (GSFC)	0.15	0.30	0.48	Flight ATS-1	–	–	370	$\Delta\alpha_s/\epsilon$ 0.07		73
1A-12: Spodumene-Na_2SiO_3	0.18	0.88	0.20	Flight OSO-2	–	–	300	0.045		68
1A-13: CrNi Spinel Phosphate Bonded; SnO_2 Silicate Bonded (Ames)	0.24	0.94	0.255	Flight OSO-2	–	–				68
1A-14: SbO_3-K_2SiO_3 (Ames)	0.22	0.87	0.25	Flight OSO-2	–	–	300	0.02		68
1A-15: SnO_2, $AlPO_4$ (AI93)	0.35	0.91	0.38	UV Air	10×		3000	0.10		28
	0.35			Proton	150 keV	1×10^{16}	–	0.15		28
				Proton	150 keV	1×10^{15}	–	0.07		28
1A-16: ZrO_2(TAM)CP-K_2SiO_3	0.22			UV in situ		–	800	0.08	IITRI	29
ZrO_2 (High Purity)-K_2SiO_3	0.07			UV in situ	7×	–	300	0.04	LMSC	24
	0.07			Proton in situ	1.4 keV	4.7×10^{16}	–	0.03		24
	0.07			UV Proton in situ	7× 1.4 keV	– 4.7×10^{16}	300 –	0.055		24
	0.09			Electron in situ	1 MeV	1.3×10^{15}		0.02		24
	0.09			UV Electron in situ	10× 1 MeV	– 1.4×10^{15}	135 –	0.04	2000–4000 A	24
1A-17: Barrier Anodize on Al (Boeing)	0.14						3000	0.01		76
	0.12	0.35[c]	0.34				~350	0.15		76

Table 7-9 (Cont.)

Material	Initial Values – 70°F			Type[a]	Radiation Exposure		ESH	$\Delta\alpha_s$	Remarks	Ref.
	α_s	ϵ_{TH}	α_s/E		Intensity	Integrated Flux[b]				
1A-18: H_2SO_4 Anodize on Al (AFML)	0.12						3000	0.06		
	0.15	0.90	0.17	Near UV Far UV	10×		500 500	0.03		71
	0.15			Proton	10 keV	1×10^{15}	–	< 0.01		71
	0.15			Near UV Far UV Proton	10× 10× 10 keV	– – 1×10^{9}	500 500 –	0.03		71
1A-19: Al_2O_3, Flame Sprayed (Rokide A) (Norton)	0.27	0.75	0.36						Explorers 1, 3, and 7	79
	0.23	0.75	0.31	Neutron, γ		2×10^{8} rads	–	0.04	Tiros 2	
1A-20: Evaporated Al_2O_3 (1.1 μ) on Evaporated Opaque Al (ECOM, Ft. Belvoir)	0.15	0.25	0.57	Flight ATS-1	–	–	1300	$\Delta\alpha_s/\epsilon$ 0.08		73, 77
1A-21: Aluminized FEP Teflon (2 mil)	0.16	0.66	0.24	UV Air			100	0	ATS Surveyor	27
			0.24	Flight Mariner 5			126 days	$\Delta\alpha_s/\epsilon$ 0.08		78

(a) SW = Solar wind protons.
(b) Flux is expressed in particles/cm^2 (electrons or protons) except where specific other units are given for neutron- or gamma-irradiation.
(c) Epsilon can be varied from 0.05 – 0.48.

Table 7-10

RADIATION STABILITY, SOLAR REFLECTORS – ORGANIC-BASED

Material	Initial Values – 70°F			Type[a]	Radiation Exposure		ESH	$\Delta\alpha_s$	Remarks	Ref.
	α_s	ϵ_{TH}	α_s/ϵ		Intensity	Integrated Flux[b]				
1B-1: ZnO (SP-500) in Methyl Silicone (GE RTV-602) (IITRI S-13)			0.2	Flight Mariner 5			48 days	$\Delta\alpha_s/\epsilon$ 0.21		78
	0.21			UV in situ		–	800	0.08	IITRI	6, 29
	0.18	0.87	0.21	Flight ATS-1	–	–	1300	$\Delta\alpha_s/\epsilon$ 0.29	GSFC	73
	0.18	0.82	~0.22	Flight Pegasus	–	–	1800	$\Delta\alpha_s/\epsilon_T$ ~0.18		80
	0.21			SW-H_2^+	1 KeV	2.1×10^{16}	–	0.01	MSFC-Litton	70
	0.21			SW-H_2^+	1 KeV	2.1×10^{17}		0.03	MSFC-Litton	70
	0.21			SW-H_2^+	1 KeV	1.7×10^{18}		0.07	MSFC-Litton	70
	0.21			Proton in situ	2 KeV	3×10^{15}		0.11	LMSC	26
	0.21			Proton in situ	2 KeV	5×10^{16}		0.16	LMSC	26
	0.21			UV in situ	20×	–	1330	0.10	LMSC	26
	–	–	0.22	Flight Saturn IV	–	–	<50	$\Delta\alpha_s/\epsilon$ ~0.3	Pegasus MSFC	80, 81
1B-2: ZnO (SP-500) in Toluene-Methyl Silicone (IITRI S-13G)	0.21			UV in situ			600	0.01	IITRI	6, 20
			0.2	Flight Mariner 5			39 days	$\Delta\alpha_s/\epsilon$ 0.12		78
1B-3: ZnO in Silicone (Boeing SC/5); Similar to S-13	0.18			Flight L.O. II	–	–	700 hr	0.11	Lunar Orbiter II	82
1B-4: Unspecified (Boeing SC/7)	0.21			Flight L.O. II	–	–	700 hr	0.10	Lunar Orbiter IV	82
1B-5: 80% SC/7, 20% Mirrors (Boeing)	0.18			Flight L.O. II	–	–	800 hr	0.08	Lunar Orbiter IV	82
1B-6: TiO_2 in Methyl Silicone (DC Q92-090) (GSFC)	0.19	0.86	0.22	Flight ATS-1	–	–	700	$\Delta\alpha_s/\epsilon$ 0.32		73

Table 7-10 (Cont.)

Material	Initial Values – 70°F			Type[a]	Radiation Exposure		ESH	$\Delta\alpha_s$	Remarks	Ref.
	α_s	ϵ_{TH}	α_s/ϵ		Intensity	Integrated Flux[b]				
1B-7: TiO_2 in Silicone Elastomer (LMSC/Dow Corning Thermatrol 2A-100, Also Q90-090)	0.20	0.85	0.24	UV Air	1×	–	500	0.12		24, 68
	0.20	0.85	0.24	UV Air	10×	–	1000	0.05		
1B-8: TiO_2 Titanox RANC in Polymethyl Vinyl Siloxane (Dow Corning Q92009)(LMSC 6A-100 Thermatrol)				Electron	0.8 MeV	1×10^{15}	–	0.01		75
	0.17	0.88	0.19	UV in situ	20×		1330	0.15		26
	0.17	0.86		UV Air	11×	–	2530	0.06		68
	0.165			Proton	10 KeV	1×10^{16}	–	0.13		85
	0.165			Proton	10 KeV	5×10^{16}	–	0.42		85
	0.165			Proton UV	10 KeV 10×	1×10^{16} –	– 190	0.18		85
	0.165			Proton UV	10 KeV 10×	5×10^{16} –	190	0.46		85
	0.165			UV	10×	–	190	0.02		85
	0.165			Proton in situ	2 KeV	3×10^{15}	–	0.02	LMSC	26
	0.165			Proton in situ	2 KeV	5×10^{16}	–	0.11	LMSC	26
	0.22			Proton	10 KeV	1×10^{15}	–	0.01		26
1B-9: TiO_2 in Silicone Alkyd (Vita-Var Paint Co. PV-100)	0.211	0.88	0.27						Gravity gradient test satellite (GE)	82
	0.21			Near UV Far UV Proton	10× 10× 10 KeV	– – 1×10^{15}	500 500 –	0.05	AVCO	71
1B-10: TiO_2 (Rutile) in Methyl Silicone (IITRI)	~0.23	~0.77	0.30	Flight Pegasus	–	–	1800	$\Delta\alpha_s/\epsilon_T$ ~0.27		80
1B-11: TiO_2 in Phenyl-Methyl Silicone	0.23			SW-H_2^+	1 KeV	2.1×10^{16}	–	0.15	MSFC-Litton	70
	0.23			SW-H_2^+	1 KeV	4.25×10^{17}		0.37	MSFC-Litton	70
	0.23			SW-H_2^+	1 KeV	1.9×10^{18}		0.46	MSFC-Litton	70

Table 7-10 (Cont.)

Material	Initial Values – 70°F			Type[a]	Radiation Exposure		ESH	$\Delta\alpha_s$	Remarks	Ref.
	α_s	ϵ_{TH}	α_s/ϵ		Intensity	Integrated Flux[b]				
1B-12: TiO_2 in Silicone Alkyd (W. P. Fuller 517-W-1)	0.29	0.90		Electron	0.8 MeV	1×10^{16}		<0.01		
	0.29			Electron/UV	0.8 MeV/ 10×	1×10^{16}	485	0.10		79
	0.26	0.81	0.32	UV Air	10×		1000	0.17	5 mils for solar opacity	
	0.21			Near UV Far UV			500 500	0.03	1 mil for IR opacity Peak cure temperature 465°F	79
	0.26	0.84	0.31	Neutron, γ		2×10^8 rads		0		
1B-13: TiO_2 in Acrylic (Sherwin Williams Kemacryl M49W C17)	0.27	0.86	0.31	UV Air	10×		1000	0.24	5 mils for solar opacity	
	0.21			Near UV Far UV	10× 10×		500 500	0.04	1 mil for IR opacity	
	0.24			Electron/UV	0.8 MeV/ 10×	1×10^{16}	485	0.20		
	0.21			Proton	10 KeV	1×10^{15}		<0.01		
	0.21			Near UV Far UV Proton	10× 10× 10 KeV	– – 1×10^{15}	500 500 –	0.06		71, 75
	0.24			Electron	0.8 MeV	1×10^{15}	–	0.02		
	0.27	0.89	0.30	Neutron, γ		2×10^8 rads		0.06		74
1B-14: TiO_2 in Silicone-Acrylic (GE C-2-A)	0.19	~0.85	~0.22	UV in situ			300	0.23		56
				Proton in situ		7.4×10^{14}		0.01		56
				Proton in situ		4.5×10^{14}		0.11		56
1B-15: White Velvet (3M)	0.21	0.86	0.24	UV in situ			400	0.17	Applications Technology Satellite	77
	0.21	0.86	0.24	UV Air			350	0.09	Surveyor	27
1B-16: Silicone TiO_2 Tape (LMSC 1A48)	0.16	0.86	0.18	UV Air	10×	–	500	0.03		79
	0.189	0.86	0.22	Flight OSO-2	–	–	300	0.07		66

Table 7-10 (Cont.)

Material	Initial Values – 70°F			Type[a]	Radiation Exposure		ESH	$\Delta\alpha_s$	Remarks	Ref.
	α_s	ϵ_{TH}	α_s/ϵ		Intensity	Integrated Flux[b]				
1B-17: TiO_2 in White Epoxy (A. Brown Skyspar, SA9185)	0.25	0.91		Electron	0.8 MeV	1×10^{15}	–	0.03		75
	0.25			Electron, UV	0.8 MeV/ 10×	1×10^{16}	485	0.24		75
	0.22	0.89	0.25				1000	0.25		79
	0.23			SW-H_2^+	1 KeV	6.4×10^{16}	–	0.018	MSFC-Litton	70
	0.23			SW-H_2^+	1 KeV	6.4×10^{17}		0.039	MSFC-Litton	70
	0.23			SW-H_2^+	1 KeV	2.1×10^{18}		0.119	MSFC-Litton	70
	0.23			Neutron, γ		2×10^8 rads		0.12		74
1B-18: TiO_2 in Polyvinyl Butyral and Hexamethoxy Methyl Melamine (American Cyanamid S7094-3)	0.21			UV Air	11×	–	2530	0.07	LMSC	83
1B-19: TiO_2 in Methyl Methacrylate, Ethyl Acrylate, Methacrylic Acid, and Epon 201 (American Cyanamid S7094-4)	0.20			UV Air	11×		2530	0.10	LMSC	83

(a) SW = Solar wind protons.
(b) Flux is expressed in particles/cm^2 (electrons or protons) except where specific other units are given for neutron- or gamma-irradiation.

Table 7-11

RADIATION STABILITY, SOLAR REFLECTORS – MIRRORS

Material	Initial Values – 70°F			Type	Radiation Exposure		ESH	$\Delta\alpha_s$	Remarks	Ref.
	α_s	ϵ_{TH}	α_s/ϵ		Intensity	Integrated Flux				
1C-1: Optical Solar Reflector (LMSC); Ag Coated Fused Silica-Overcoated With Vapor Deposited Inconel	0.05	0.80	0.0625	UV in situ			2000	0		26
				Electron	800 KeV	10^{16}	–	0		26
				Electron	800 KeV	3×10^{15}	–			
				UV	–	–	150	0		26
				Proton	987 KeV	5×10^{15}	–	0		84
				Proton	500 KeV	6×10^{15}	–			
				UV	–	–	150	0		84
				SW	2 KeV	8×10^{15}	–	0		84
				SW	2 KeV	8×10^{15}	–			
				UV	–	–	1100	0		84
1C-2: Optical Solar Reflector (LMSC); Al Coated Fused Silica, Overcoated With SiO	0.10	0.80	0.125	UV Air				0		26
1C-3: Al on Vycor Mirror (Hughes)	0.11	0.79	0.14	UV Air				0	Surveyor	27
1C-4: Mirror Coating (Applied Physics Labs); Ag Deposited on Glass or Fused Silica	~0.04	~0.85	~0.05	No Information						95

Table 7-12

RADIATION STABILITY, SOLAR ABSORBERS

Material	Initial Values – 70°F			Type	Radiation Exposure		ESH	$\Delta\alpha_s$	Remarks	Ref.
	α_s	ϵ_{TH}	α_s/ϵ		Intensity	Integrated Flux				
2-1: Vapor Deposited Al	0.10	0.04	2.5	UV Air				0	ATS, Surveyor Use – Hughes	27,77
2-2: Polished Al	0.21	0.04	5.25	UV Air				0	Surveyor Use – Hughes	27,67
	0.20	0.05	4.0	Flight Mariner IV	–	–	3800	0.04		27,67
2-3: Chem. Cleaned Al 6061 as Rolled	0.16	0.06	2.7	UV Air				0		79
2-4: Chem. Cleaned Al 6061 Forgings or Welds	0.29	0.09	3.2	UV Air				0		79
2-5: Chem. Cleaned Al 2024 Non-Clad, as Rolled, Hand Sanded	0.20	0.06	3.3	UV Air				0		79
2-6: Chem. Cleaned Al 2024, Clad, as Rolled	0.22	0.06	3.7	UV Air				0		79
2-7: Al Foil, Plain, Dry, Annealed	0.12	0.05	2.4	UV Air				0	MIL-A-148C	79
2-8: 2024 Al, Sandblasted	0.42	0.21	2.0							79
2-9: Alodine, 1200S-MTL-3, Am Chem Products Co. - MSFC	0.40 to 0.49	0.05 to 0.10	8.6 to 5.2	Flight Pegasus			1800	$\Delta\alpha_s/\epsilon$ ~ 0.09		80
2-10: Inconel Foil, Quilted (H. I. Thompson TPS0101B)	0.38	0.12	3.2	UV Air				0	MIL-N-6840	88
2-11: Inconel X Foil	0.66	0.10	6.6	UV Air				0	MIL-N-7786	88
2-12: Chem-Polished QMV Be	0.50	0.10	5.0	UV Air				0		79

Table 7-12 (Cont.)

Material	Initial Values – 70°F			Type	Radiation Exposure		ESH	$\Delta\alpha_s$	Remarks	Ref.
	α_s	ϵ_{TH}	α_s/ϵ		Intensity	Integrated Flux				
2-13: $CeO_{2x}/Mo_x/MgF_2$ (1000–2000A)(500–1000A)	0.85	0.11	7.7	Far UV Near UV	10× 10×		500 500	0.01		71 86
	0.87			Near UV Far UV Proton	10× 10× 10 KeV	– – 1×10^{15}	500 500 –	<0.01		71
2-14: Gold Plate (MILG-45204 Type II CL2	0.28	0.04	7.0	UV Air				0	Surveyor Use	27
2-15: Hanovia Gold 6518 on René 41	0.53	0.09	6.0	UV Air				0		79
2-16: High Purity Gold-Temperex HD on Al 6061	0.27	0.03	9.0	UV Air Electron, Proton				0 0		79
2-17: Lockspray Gold on Anodized Mg or Al Alloys Coated With Epoxy	0.22 to 0.24	0.03 to 0.05	7.3 to 4.8	UV Air	6×	–	2000	<0.01	Visor Coating Gemini missions also interior coating, adapter section	79
2-18: Electroplated Ag on Be-Cu (GE)	0.15	0.05	3.0	Flight ATS-1	–	–	1300	$\Delta\alpha_s/\epsilon$ 1.10	Gravity Gradient Exp. ATS-2	72
2-19: Al_2O_3 Overcoat (1000 Å) Over Evap. Ag on Mill Finish Al Alloy (LMSC)	0.07	0.06	1.26	UV Air	10×	–	2000	<0.01		3

Table 7-13

RADIATION STABILITY, FLAT REFLECTORS

Material	Initial Values – 70°F			Type	Radiation Exposure		ESH	$\Delta\alpha_s$	Remarks	Ref.
	α_s	ϵ_{TH}	α_s/ϵ		Intensity	Integrated Flux				
3-1: Al Acrylic Paint, Non-Leafing (Sherwin Williams)	0.44			Electron	0.8 MeV	1×10^{16}	–	0.01	Spray technique results in wide variations in α_s and ϵ; final α_s/ϵ = 1.33; material used on Surveyor.	75
	0.27	0.31	0.87	UV Air			100	0.03		27
	0.45	0.50	0.90	UV in situ	6×	–	1600	0.07		24
	0.42	0.47	0.89	Neutron, γ		5×10^7 rads		0.01		87
3-2: Leafing Al D4D	0.26	0.25	1.0						Used on Gravity Gradient Test Satellite.	86
3-3: Al-Silicone Paint, W. P. Fuller 172-A-1, Leafing Al	0.25	0.28	0.89	UV Air	6×	–	600	0.09	3 mils required for solar opacity, 1 mil for IR opacity.	79
	0.22	0.24	0.92	Neutron, γ		2×10^8 rads		0.02		74
3-4: Al-Silicone Paint, W. P. Fuller 171-A-152, Leafing Al	0.22	0.24	0.92	UV Air	6×	–	600	0.09	3 mils required for solar opacity, 1 mil for IR opacity; peak cure temp. 456°F	79
3-5: Al Silicone-JPL	0.26	0.28	0.93	Flight Mariner IV	–	–	3800	0.02		67
3-6: Cat-a-Lac Al Paint (Finch Paint and Chem.)	0.25	0.25	1.0							24
3-7: Silica Overcoat (1000 Å) Over Evap. Ag on Polished Al Alloy (LMSC)	0.06	0.085	0.74	UV Air	10×		2000	0.02		3

Table 7-14

Material	Initial Values – 70°F			Type	Radiation Exposure		ESH	$\Delta\alpha_s$	Remarks	Ref.
	α_s	ϵ_{TH}	α_s/ϵ		Intensity	Integrated Flux				
4-1: 3M Black Paint 101-C-10, Modified Alkyd	0.97	0.85	1.14	UV Air			600	0	Surveyor Use	27
4-2: Lowe Bros. Black Paint (Glyceryl-Phthalate)		>0.9							Gravity Gradient Test Satellite (GE)	86
4-3: Cat-a-Lac Black 433-1-8 Epoxy (Finch Paint and Chem.)	0.96	0.85	1.10	Flight Mariner 4	–	–	3800	<0.01		67
			1.10	Flight Mariner 5			50 days	-0.03		78
4-4: Black Silicone (W. P. Fuller 517-B-2)	0.89	0.77	1.15	UV Air	6×		600	<0.05		79
4-5: Black Micabond (L6X962)(Midland Ind. Finishes)	0.93	0.84	1.11							79
4-6: Grey Silicone Acrylic	0.74	0.86	0.86							86
4-7: Conductive Black (Epoxy Black)(Applied Physics Labs)	>0.9	>0.8	~1							87
4-8: Carbon-Dow Corning Silicone (LMSC)	0.96	~0.85	~1.1	UV Air	6×	–	420	<0.01		85
4-9: Black Acrylic (Sherwin Williams M49BC12)	0.93	0.88	1.06	UV Air	6×	–	600	<0.05		79
	0.93	0.83	1.12	Neutron, γ		5×10^7 rads 2×10^8 rads		0 –	Moderate to Severe Mech. Damage	74
4-10: Alodine 401-41 (Amchem Product Co.)	0.33 to 0.41	0.04 to 0.51	7.1 to 0.8						α_s/ϵ dependent on thickness and density	21
4-11: Dow 17 on HM21 Mg (Dow Chem. Co.)	0.78	0.70	1.11	UV Air	6×		600	0		79
4-12: Cr_2O_3 (85%) Flame-Sprayed (Norton Co. Rokide C) on 2 mil Nichrome-Coated René 41	0.90	0.85	1.06	UV Air	6×		600	0		79

Table 7-14 (Cont.)

Material	Initial Values – 70°F			Type	Radiation Exposure		ESH	$\Delta\alpha_s$	Remarks	Ref.
	α_s	ϵ_{TH}	α_s/ϵ		Intensity	Integrated Flux				
4-13: QMV Be, Pt Black-Coated	0.94	0.85	1.11	UV Air	6×		600	0	Stable High Temp ϵ; fragile	79
	0.95	0.87	1.09	Neutron, γ		5×10^7 rads 2×10^8 rads		0 0.03		
4-14: Stainless Steel, Sand-Blasted	0.75	0.85	0.88	UV Air						79
4-15: Clear Teflon (2 mil) (MIL P-22241)	0.80	0.88	0.91				100	0.04	Surveyor Use	27

7.6.1 Solar Electromagnetic Radiation

The intensity of the unfiltered solar ultraviolet radiation (extending from 100 to 3800 Å in wavelength) in space is sufficient to induce appreciable changes in the chemical and physical structure of many thermal control materials. Experiments have established that ultraviolet radiation damage is a primary consideration in the selection of thermal control materials.

Ultraviolet radiation exposure data are obtained in the laboratory by irradiating the test specimen in a vacuum system. The source and sample holder are cooled to maintain desired operating temperatures. The ultraviolet sources used vary among investigators but high-pressure mercury-argon lamps such as G.E. Type AH-6 are typical. It is essential that reflectance or absorptance measurements be made in situ, while the sample is in vacuum. The specimen is removed from the radiation area or the source is turned off during measurement. To minimize experimental time, sources are used which can impress intensities incident on the samples as high as 25 suns (one sun equals zero air-mass solar intensity at the distance of the earth from the sun, 2.0 cal/cm^2-min). Six to ten sun intensities are commonly employed.

The most important questions concern the effects of intensity, integrated dose, and spectral distribution of incident energy on the material. Schmitt and Hirt (Refs. 89 and 90) have presented data to establish the validity of the exposure time-intensity reciprocity law for a variety of organic materials (Refs. 91, 92, and 93). Other investigators, however, have found that simple reciprocity laws are inapplicable (Refs. 94 and 95). Work performed at LMSC indicates that both time of exposure and intensity increase the effects but not necessarily according to a simple reciprocity. This work seems to indicate that changes in properties may reach a saturation level with time, and the reciprocity law appears valid as a first engineering approximation.

The literature on ultraviolet radiation effects on thermal control materials is extensive. However, recent findings on the bleaching effect when changes in properties were measured in air after ultraviolet irradiation in vacuum cast considerable doubt on the reliability of the data in the literature. Results of recent test data of measurement of properties in vacuum after irradiation show that organic-based materials suffer greater ultraviolet damage than do inorganic materials because organic materials possess weaker bond strengths and less thermal stability. Among presently used organic paint vehicles, the silicones are the most stable in the ultraviolet environment (Ref. 96).

Figures 7-12 through 7-15 illustrate typical reflectance curves for four materials. In each case the measurements in vacuum are shown together with the original unirradiated measurements. Finally, a curve is shown for each sample after exposure to air, illustrating the bleaching or reoxidation and recovery of the absorptance properties. The data in Figs. 7-14 and 7-15 are plotted in terms of equal increments of the energy in the solar spectrum. In this form it may be consulted to ascertain general trends but not to read a reflectance value for a particular wavelength (except for the specific wavelength values of the abscissa).

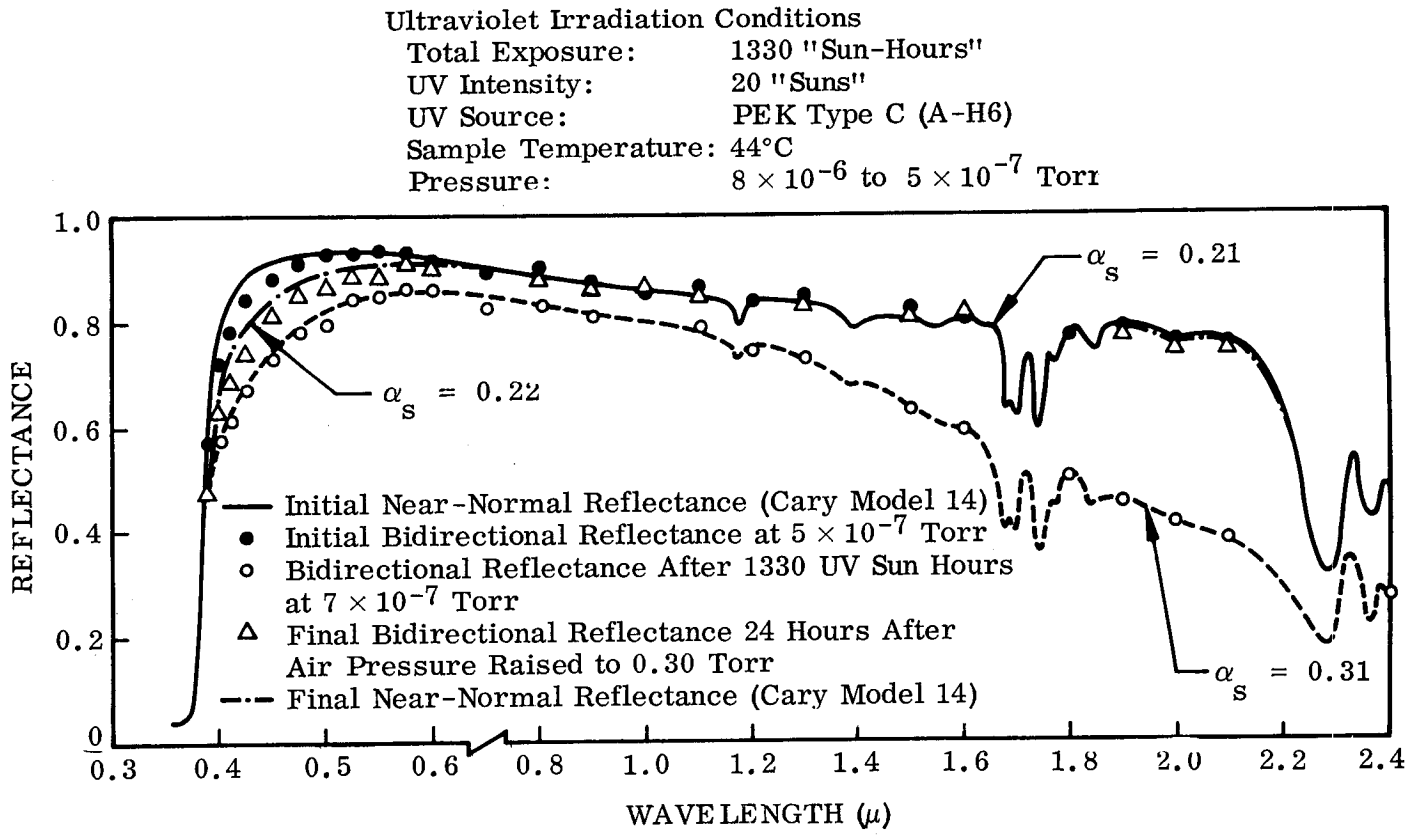

Fig. 7-12 Ultraviolet Damage and Recovery of a ZnO Pigmented Silicone Thermal Control Coating (S-13, Manufactured by IITRI)

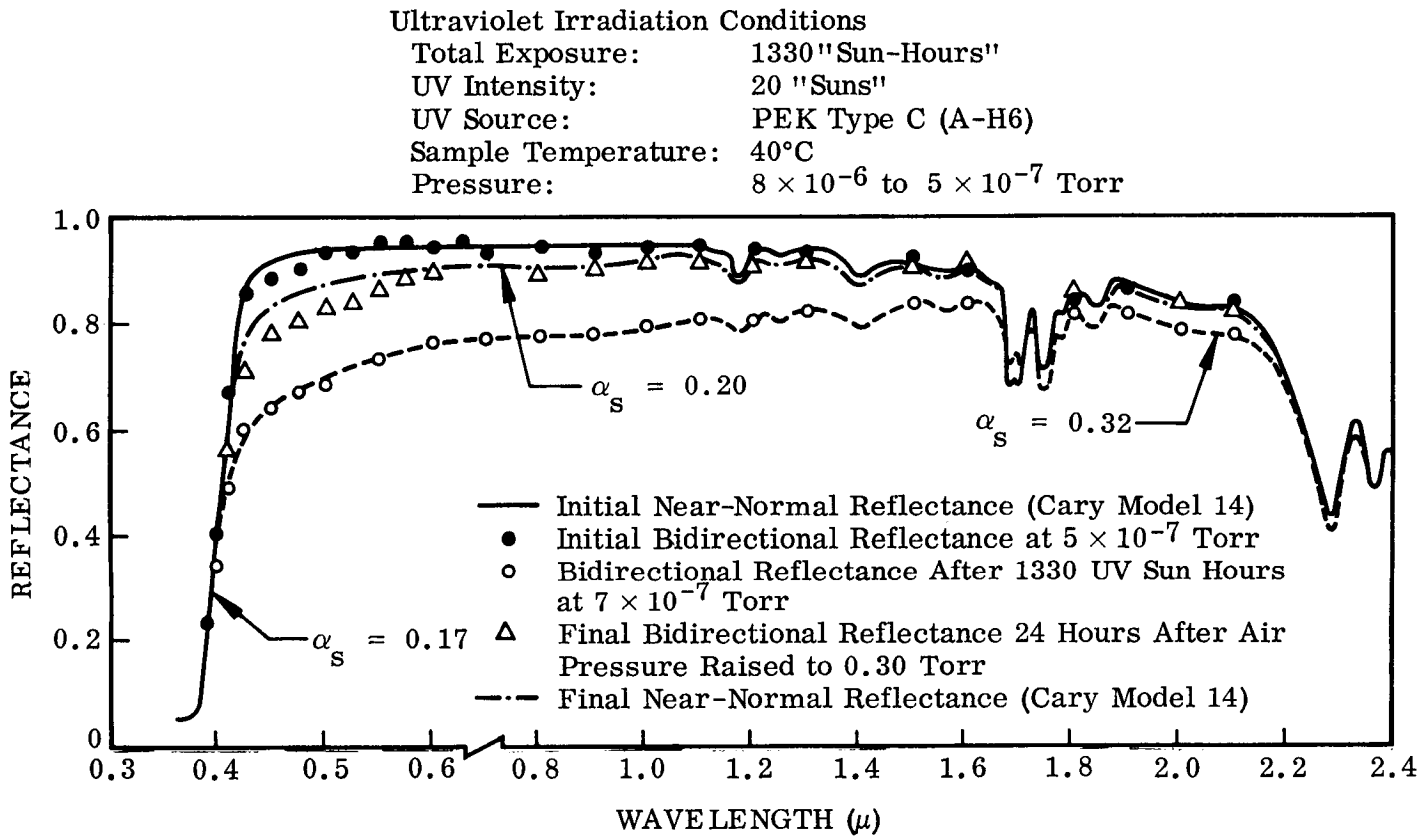

Fig. 7-13 Ultraviolet Damage and Recovery of a TiO_2 Pigmented Silicone Thermal Control Coating (Thermatrol 2A-100, Manufactured by Dow Corning Corp.)

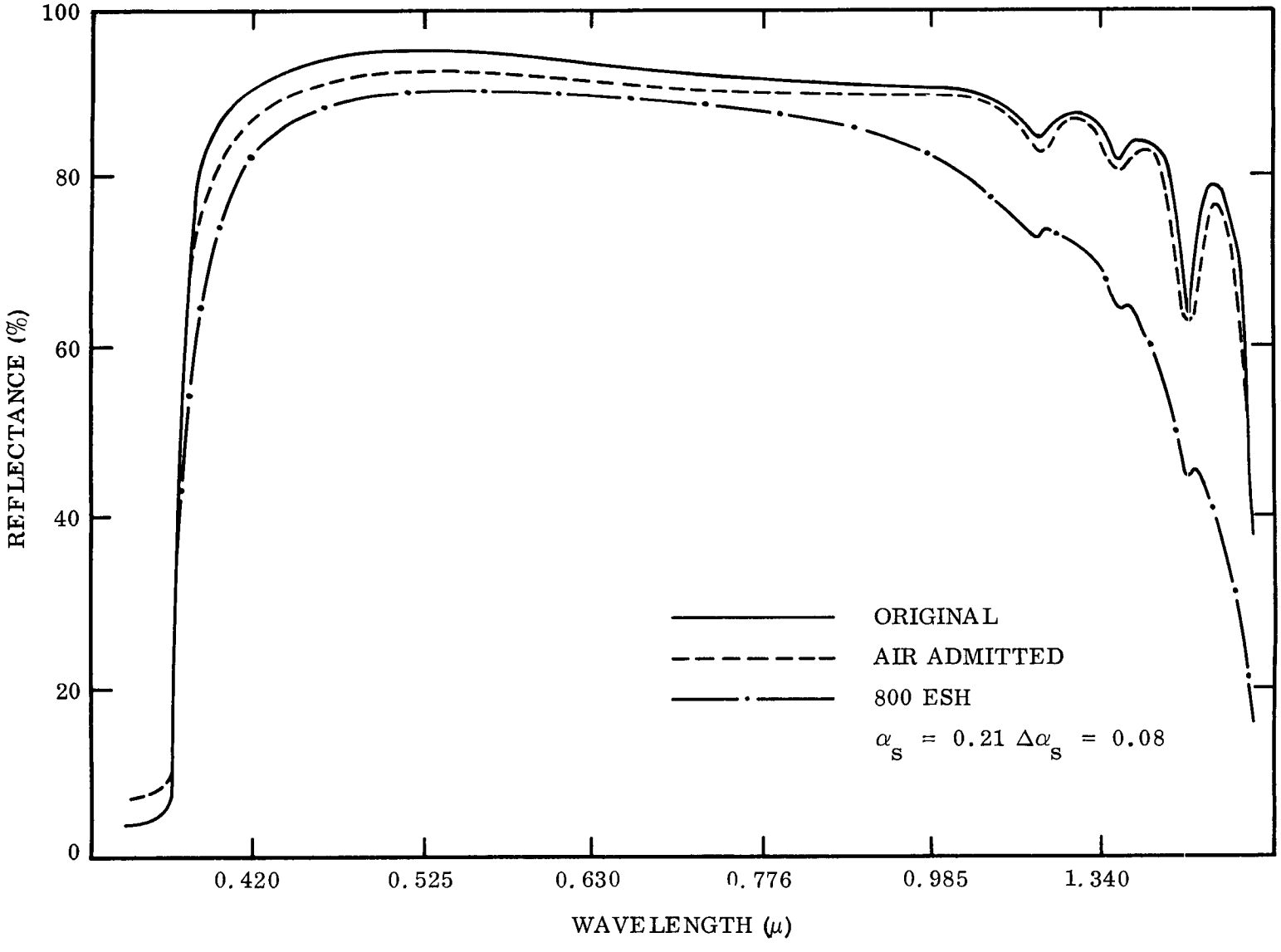

Fig. 7-14 Effect of Ultraviolet in Vacuum on S-13 Material (ZnO Silicone) (Ref. 29)

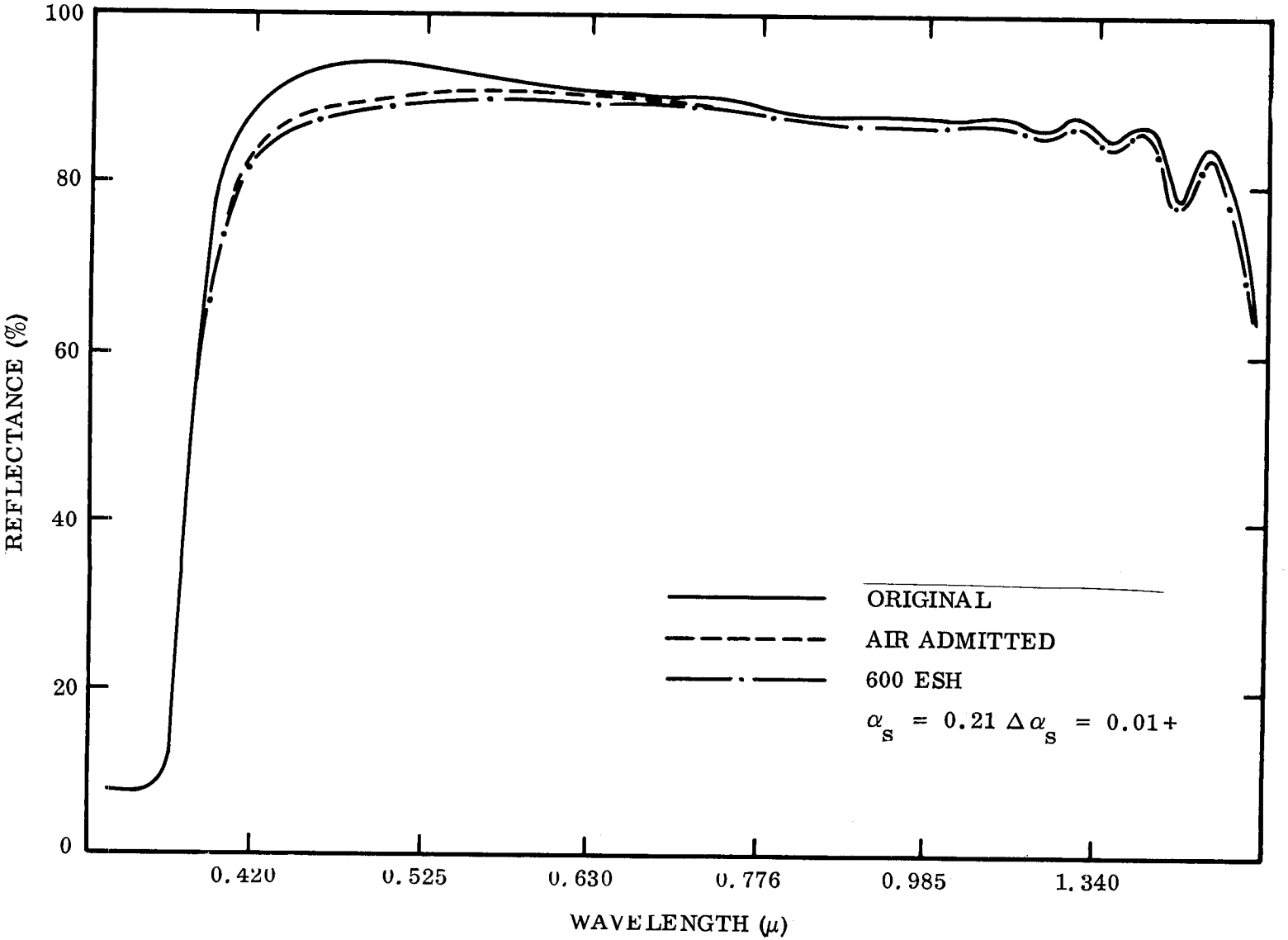

Fig. 7-15 Effect of Ultraviolet in Vacuum on S-13G Material (Sweated ZnO Pigment; Toluene Only) (Ref. 29)

The stability of various organic materials has been studied as a function of molecular structure, the number of cross-linked bonds per molecule, the identity and number of substituted side groups or chains, and the polymeric molecular weight (Refs. 97 through 100). A number of theoretically useful correlations have been achieved, but these findings cannot now be applied to untested materials because of lack of experimental verification. In general, ultraviolet should have no appreciable effect on pure metals and alloys, since the threshold energy for significant damage mechanisms is well above the predominant energy level of solar ultraviolet.

A program was carried out at LMSC to study ultraviolet-vacuum effects on solar reflector materials at cryogenic temperatures (-230° F) (Ref. 83). Solar absorptance was measured calorimetrically between cryogenic and room temperatures. The results showed that stability in the near-ultraviolet and the physical properties of the solar reflector materials were improved at cryogenic temperatures. The solar absorptance is a very weak function of the temperature of the material between cryogenic and room temperature. Some of the more significant results from this program are summarized in Tables 7-15 and 7-16. (See also Refs. 101 and 102.)

7.6.2 Particulate Radiation: Protons

The change in properties caused by high-energy protons was originally estimated by application of radiation damage models and by comparison of estimated maximum absorbed doses with published radiation effects data. The resistance of materials to space-penetrating radiation was frequently based on gamma source or nuclear reactor irradiation data. Analysis in these terms indicated that damage from the natural space radiation environment would be small except for long-term exposure to trapped radiation (Van Allen) belts. It is now apparent from both laboratory proton and solar wind proton evaluations in vacuum, together with flight data, that these assumptions and extrapolations were in error. Significant damage from high-energy protons has been observed on both organic- and inorganic-based systems.

LMSC-reported exposures of materials to simulated quiescent solar plasma, solar ultraviolet, and simultaneous solar wind-plus-ultraviolet environments indicated only minor damage to Thermatrol and Z-93 coatings (Ref. 84). These results, based on measurements of properties in air after radiation exposure in vacuum, indicated that the maximum changes expected in solar absorptance from a combined ultraviolet-proton environment would be no greater than those expected from the most damaging single environment. These results differed from the data of Gillette (Refs. 104 and 105). Gillette used 8-keV protons; LMSC used 2-keV mass 1 and 2 particles. More recent data of Jorgenson, using a plasma method for simulation of the solar wind, indicated significant changes in absorptance for several thermal control materials (Ref. 70). The Z-93 and TiO_2-phenyl methyl silicone materials were very susceptible to damage, while Skyspar enamel and S-13 were resistant to damage, as indicated by solar absorptance change.

Laboratory studies using hydrogen ion generated at a 2000-eV energy simulating the solar wind, have produced changes in the solar absorptance of the white pigmented

Table 7-15

NEAR-ULTRAVIOLET EXPOSURE AT CRYOGENIC TEMPERATURES

Material		Nominal Minimum Substrate Temperature (°F)	Nominal Maximum Substrate Temperature (°F)	Near Ultraviolet Exposure (sun-hr)(a)	Exposure (hr)	Nominal Exposure Flux Density (suns)	Number of Temperature Cycles	Initial Solar Absorptance(b)	Solar Absorptance Change(c) $\Delta\alpha_s$	$\Delta\alpha_L$ Determined During Exposure(d)
1A-1	IITRI Z-93	-215	+75	2560	211	12	275	0.18	0.01	0.09
1A-7	LMSC Ultrox Coating (Room-Temperature Cure)	-235	+75	3130	243	13	332	0.13	0.07	0.12
1A-7	LMSC Ultrox Coating (High-Temperature Cure)	-235	+80	3130	243	13	332	0.14	0.08	0.14
1A-9	LMSC Lithafrax Coating (Room-Temperature Cure)	-225	+75	3130	243	13	332	0.20	0.06	0.14
1A-9	LMSC Lithafrax Coating (High-Temperature Cure)	-230	+75	3130	243	13	332	0.19	0.05	0.14
1A-18	RTD Anodized Aluminum (1199Al Substrate)	-210	+75	2560	211	12	275	0.14	0.18	0.40
1B-1	IITRI S-13 Silicone	-220	+75	2560	211	12	275	0.20	0.03	0.08
1B-8	LMSC Thermatrol 6A-100 Silicone	-215	+75	2560	211	12	275	0.20	0.04	0.08
1B-13	TiO_2-Acrylic (Not Identical to Kemacryl)	-200	+75	2560	211	12	275	0.21	0.14	0.24
1B-18	American Cyanamid S7094-3	-215	+75	2560	211	12	275	0.19	0.08	0.11
1B-19	American Cyanamid S7094-4	-215	+75	2560	211	12	275	0.19	0.08	0.10

(a) Chamber pressure = 6×10^{-8} to 1×10^{-7} mm Hg.
(b) Determined with Cary spectrophotometer; accuracy ±0.02.
(c) Accuracy ±0.01, difference between measurements before and after exposure.
(d) Determined on thumbtack calorimeter in situ; accuracy ±0.02.

Table 7-16

NEAR-ULTRAVIOLET EXPOSURE WITH SIMULTANEOUS TEMPERATURE CYCLING BETWEEN CRYOGENIC AND ROOM TEMPERATURES

Material		Nominal Minimum Substrate Temperature (°F)	Nominal Maximum Substrate Temperature (°F)	Near Ultraviolet Exposure (sun-hr)(a)	Exposure (hr)	Nominal Exposure Flux Density (suns)	Number of Temperature Cycles	Initial Solar Absorptance(b)	Solar Absorptance Change(c) $\Delta\alpha_s$	$\Delta\alpha_L$ Determined During Exposure(d)
1A-1	IITRI Z-93	-215	+75	2560	211	12	275	0.18	0.01	0.09
1A-7	LMSC Ultrox Coating (Room-Temperature Cure)	-235	+75	3130	243	13	332	0.13	0.07	0.12
1A-7	LMSC Ultrox Coating (High-Temperature Cure)	-235	+80	3130	243	13	332	0.14	0.08	0.14
1A-9	LMSC Lithafrax Coating (Room-Temperature Cure)	-225	+75	3130	243	13	332	0.20	0.06	0.14
1A-9	LMSC Lithafrax Coating (High-Temperature Cure)	-230	+75	3130	243	13	332	0.19	0.05	0.14
1A-18	RTD Anodized Aluminum (1199Al Substrate)	-210	+75	2560	211	12	275	0.14	0.18	0.40
1B-1	IITRI S-13 Silicone	-220	+75	2560	211	12	275	0.20	0.03	0.08
1B-8	LMSC Thermatrol 6A-100 Silicone	-215	+75	2560	211	12	275	0.20	0.04	0.08
1B-13	TiO_2-Acrylic (Not Identical to Kemacryl)	-200	+75	2560	211	12	275	0.21	0.14	0.24
1B-18	American Cyanamid S7094-3	-215	+75	2560	211	12	275	0.19	0.08	0.11
1B-19	American Cyanamid S7094-4	-215	+75	2560	211	12	275	0.19	0.08	0.10

(a) Chamber pressure = 3×10^{-8} to 6×10^{-8} mm Hg.
(b) Determined with Cary spectrophotometer; accuracy ±0.02.
(c) Accuracy ±0.01, difference between measurements before and after exposure.
(d) Determined on thumbtack calorimeter in situ; accuracy ±0.02.

thermal control materials Thermatrol 6A-100 (TiO_2 pigment-silicone vehicle), S13 (ZnO pigment-silicone vehicle), and Z-93 (ZnO pigment-silicate vehicle) (Refs. 85 and 107). The changes in solar absorptance in the simulated solar wind proton, simulated solar ultraviolet radiation, and the combined environment in vacuum of 10^{-7} Torr are shown in Table 7-17. The changes in solar absorptance of these materials measured in vacuum were generally greater in simulated ultraviolet radiation than in simulated solar wind proton radiation. The one exception to this behavior was the Z-93 material at 3.0×10^{16} protons/cm^2. In the combined environment, the ZnO pigmented materials at fluxes below 3.0×10^{16} of protons and less than 1000 sun-hours showed less total change than in the ultraviolet radiation alone. One possible explanation proposed for this behavior is that the paint vehicle, darkened by ultraviolet radiation, stopped the low energy protons (Ref. 107). Also, it was postulated that the paint vehicle supplied oxygen to resupply the depleted sites generated by the proton bombardment in the ZnO pigment. This bleaching behavior was observed when measurements of absorptance were made upon introduction into the system of 50μ or atmospheric pressure oxygen after exposure of the specimens to proton and ultraviolet irradiation in vacuum.

Because of the combined darkening and bleaching effects that take place in simulated environments, it is difficult to correlate these changes with those that take place in the actual space environment. The batch-to-batch variations with the complex synergistic effects make it difficult to make predictions of absorptance changes in white paints.

Studies have also been made on proton radiation effects on stretch-formed aluminum and electroformed nickel mirrors (Ref. 108). The aluminum substrates were epoxy-coated and successive layers of SiO, Al and, in some cases, Si_2O_3 vapor deposited. The electroformed nickel substrates were successively coated with Cr, SiO, Al and in some cases, Si_2O_3. Bombardment with proton intensities of 1×10^{15} to 2×10^{17} protons/cm^2 frequently produced a temperature dependent blistering. Absorptance changes as a result of blistering was highly temperature dependent. The silicon oxide surfaces, however, were made smoother by the proton irradiation.

Metallic surfaces are probably not degraded to any extent in the proton environment. The effect of 700 Mev protons on anodized Al foil and standard Al foil was studied (Ref. 109). After a flux of 10^{13} protons/cm^2, no significant changes were observed. Low energy protons have been found to damage some metals with consequent changes in thermal properties (Refs. 111, 112).

Specific proton irradiation results and absorptance change values are shown in Tables 7-9 through 7-14. Observed changes for the ZnO-K_2SiO_3, ZnO silicone and the TiO_2-silicone materials are shown in Fig. 7-16. Values obtained by measurement in air after irradiation are also shown, indicating a bleaching effect. A less pronounced effect is shown for a synthetic lithium aluminum silicate material in Fig. 7-17. Major effects are observed for proton irradiation of the two organic materials shown in Fig. 7-18 and 7-19. The major effects observed for the Z-93 material were somewhat surprising in light of demonstrated ultraviolet stability; these probably correlate with reported degradation of this material on lunar and interplanetary vehicles.

Table 7-17

CHANGES IN SOLAR ABSORPTANCE OF WHITE THERMAL CONTROL MATERIALS IN SIMULATED SOLAR WIND PROTONS AND ULTRAVIOLET RADIATIONS(a)

Material	Pigment / Vehicle	Initial Solar Absorptance α_s	Proton Exposure		Ultraviolet Exposure		UV and Proton Exposure	
			Simulated Protons/ Cm^2 at 2000-eV Energy	Change in Solar Absorptance (%)	Ultraviolet Sun-Hours (18-Sun Intensity)(b)	Change in Solar Absorptance (%)	UV Sun-Hours and Protons/ Cm^2	Change in Solar Absorptance (%)
Thermatrol 6A-100	TiO_2 / Silicone	0.17	0.43×10^{15}	41.0	90	65.0	$90/0.28 \times 10^{16}$	124.0
			1.3×10^{15}	65.0	432	82.0	$432/1.1 \times 10^{16}$	112.0
			3.0×10^{16}	88.0	1098	88.0	$1098/2.8 \times 10^{16}$	112.0
S-13	ZnO / Silicone	0.18	0.43×10^{15}	5.6	90	44.0	$90/0.28 \times 10^{16}$	33.3
			1.3×10^{15}	11.0	432	56.0	$432/1.1 \times 10^{16}$	50.0
			3.0×10^{16}	56.0	1098	61.0	$1098/2.8 \times 10^{16}$	106.0
Z-93	ZnO / Silicate	0.14	0.43×10^{15}	-7.1	90	7.1	$90/0.28 \times 10^{16}$	0
			1.3×10^{15}	0	432	36.0	$432/1.1 \times 10^{16}$	14.3
			3.0×10^{16}	14.3	1098	36.0	$1098/2.8 \times 10^{16}$	43.0

(a) Measurements of absorptance of materials at $0.5 - 1.8\mu$ in vacuum of 10^{-7} Torr.
(b) Intensity corresponds to 18 times the solar ultraviolet (2200 – 4000 Å) intensity at distance of earth in space at zero air mass.

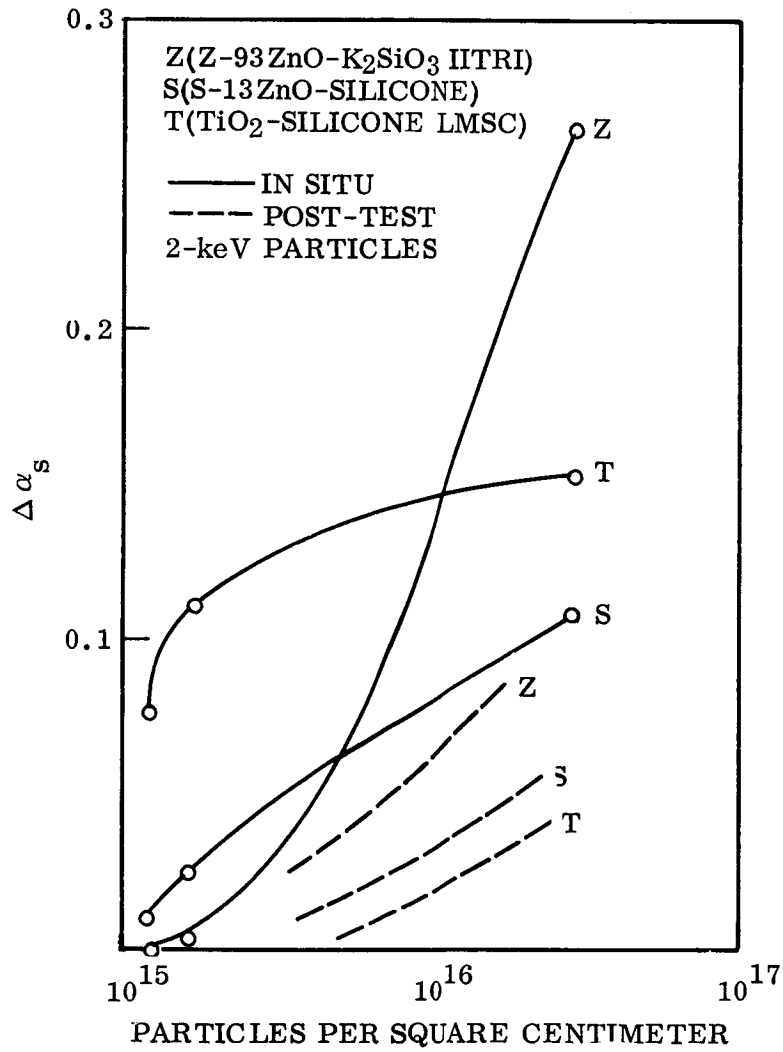

Fig. 7-16 Change in Solar Absorptance Versus Flux for Proton Only Exposure (Ref. 26)

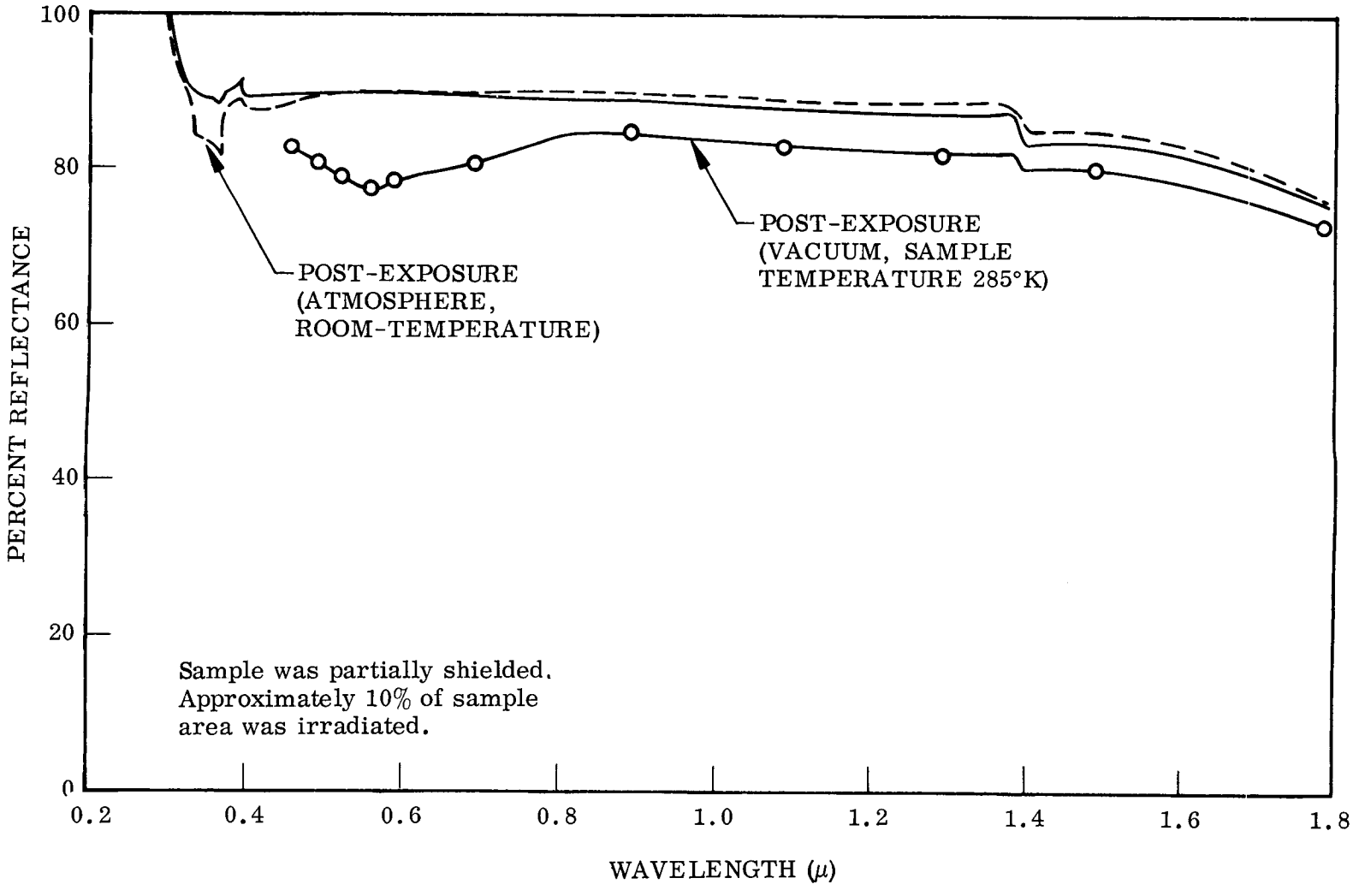

Fig. 7-17 Synthetic $LiAlSiO_4$-K_2SiO_3 Exposed to Protons Only (285°K) (Ref. 26)

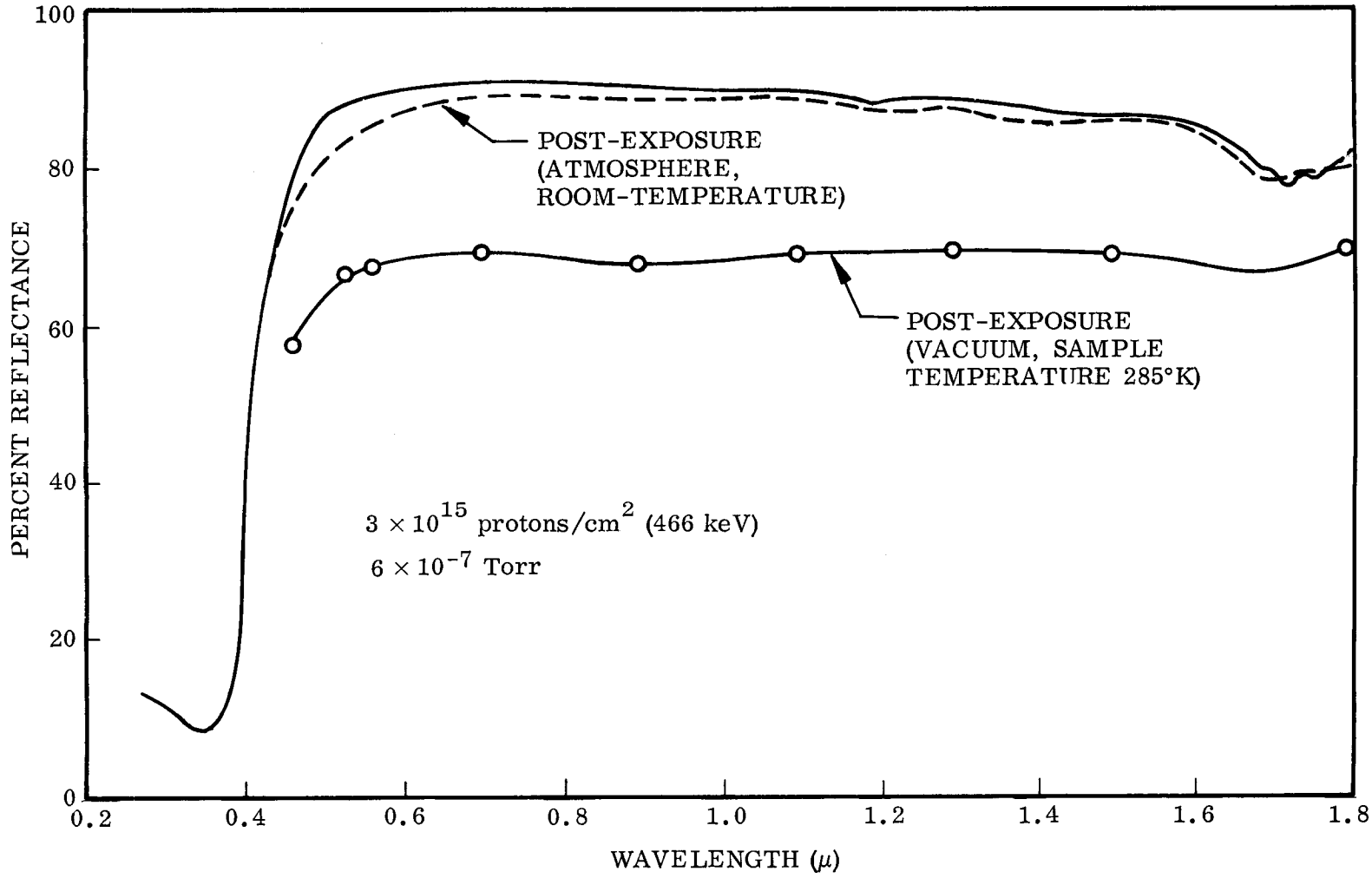

Ref. 7-18 Vita Var PV-100, Protons Only (285 °K) (Ref. 57)

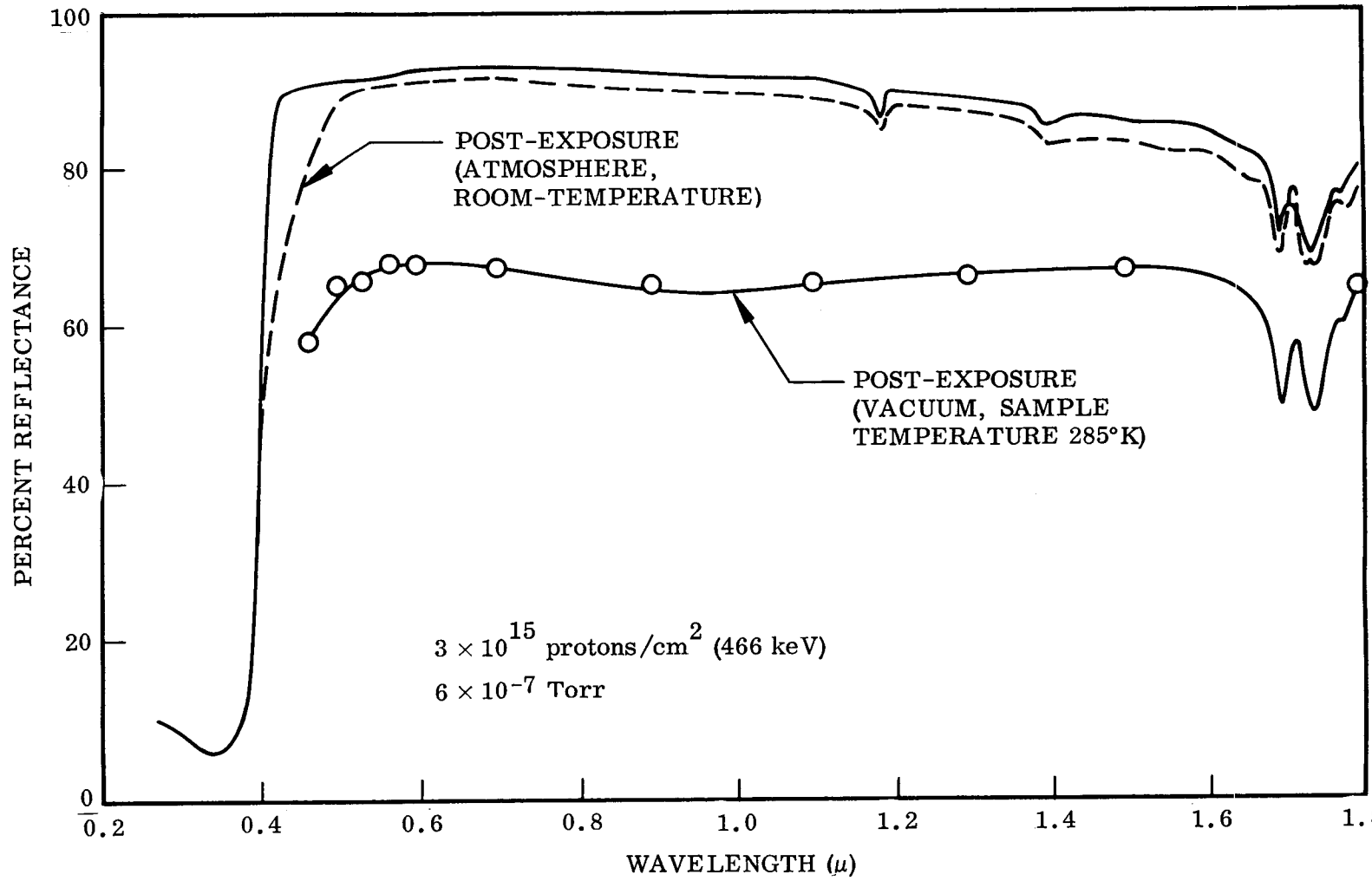

Fig. 7-19 Change in Reflectance of LMSC Thermatrol 6A-100 Exposed to Protons Only (285°K) (Ref. 26)

Only recently have there been detailed measurements of protons with energies <98 keV. Observations of low-energy protons (190 eV $\leq$ E $\leq$ 48 keV) have been reported for three outbound traversals of OGO-3 through the magnetosphere for the period 11 – 15 June 1966 (Ref. 111). The very low energy proton environment caused changes in the solar absorptance measured in laboratory simulation tests in vacuum on the order of 100% in materials exposed to 3×10^{15} protons/cm^2 at 468 keV (Ref. 83). Damage due only to particles of this energy would occur at times on the order of 1.5 years on a vehicle orbiting in the Van Allen belts at about 3.5 earth radii. When the synergistic effects of ultraviolet radiation and protons of higher energies are considered, it is possible for equivalent damage to occur in a shorter time.

7.6.3 Particulate Radiation: Electrons

Studies at LMSC have shown major changes in the solar absorptance measured in vacuum in Thermatrol (TiO_2-silicone) resulting from exposure to simulated space environment electrons. It has also been shown that the absorptance value recovers on exposure to air. The reflectance curve for Thermatrol is shown in Fig. 7-20. Work with ZrO_2-pigmented potassium silicate indicates that damage from electrons is much less severe than with the organic material.

Data on the change in solar absorptance of some organic- and inorganic-based thermal control materials, based on measurements in air after exposure to a simulated electron environment in vacuum, are shown in Fig. 7-21 (Ref. 75). Comparison of Figs. 7-20 and 7-21 shows the bleaching effect of exposure to air on the organic-based coating.

The high-altitude nuclear detonation Starfish resulted in injection of electrons trapped by the earth's magnetosphere, causing an enhancement of the existing earth's radiation belts. The integrated flux of electrons/square centimeter-day is on the order of 10^{10} to 10^{13}, dependent on altitude (Ref. 112). (Chapter 5 gives details on the electron environment in space.) Laboratory studies with simulated combined ultraviolet to 2600 sun-hr, electron radiation of 0.80 MeV, and fluxes to 3×10^{15} electrons/cm^2 have shown increases in solar absorptance of as much as 77% in white-pigmented, silicone vehicle, thermal control materials (Ref. 83). The solar absorptance change was measured with the specimen in the vacuum chamber. Measurement of the absorptance change in air after exposure to the simulated electron irradiation in vacuum has resulted in bleaching of the material and a lower estimate of the radiation damage induced by this environment.

The effect of simulated solar ultraviolet radiation and 6×10^{15} electrons/cm^2 at 0.80 MeV on two white thermal control materials is shown in Table 7-18. The changes in properties in the combined simulated environment are not additive.

7.6.4 Other Radiation Effects

The total flux of alpha particles in the natural space environment is low. For this reason, it is expected that damage to thermal control materials from this source, will not be sufficient to cause concern (Refs. 104 and 105).

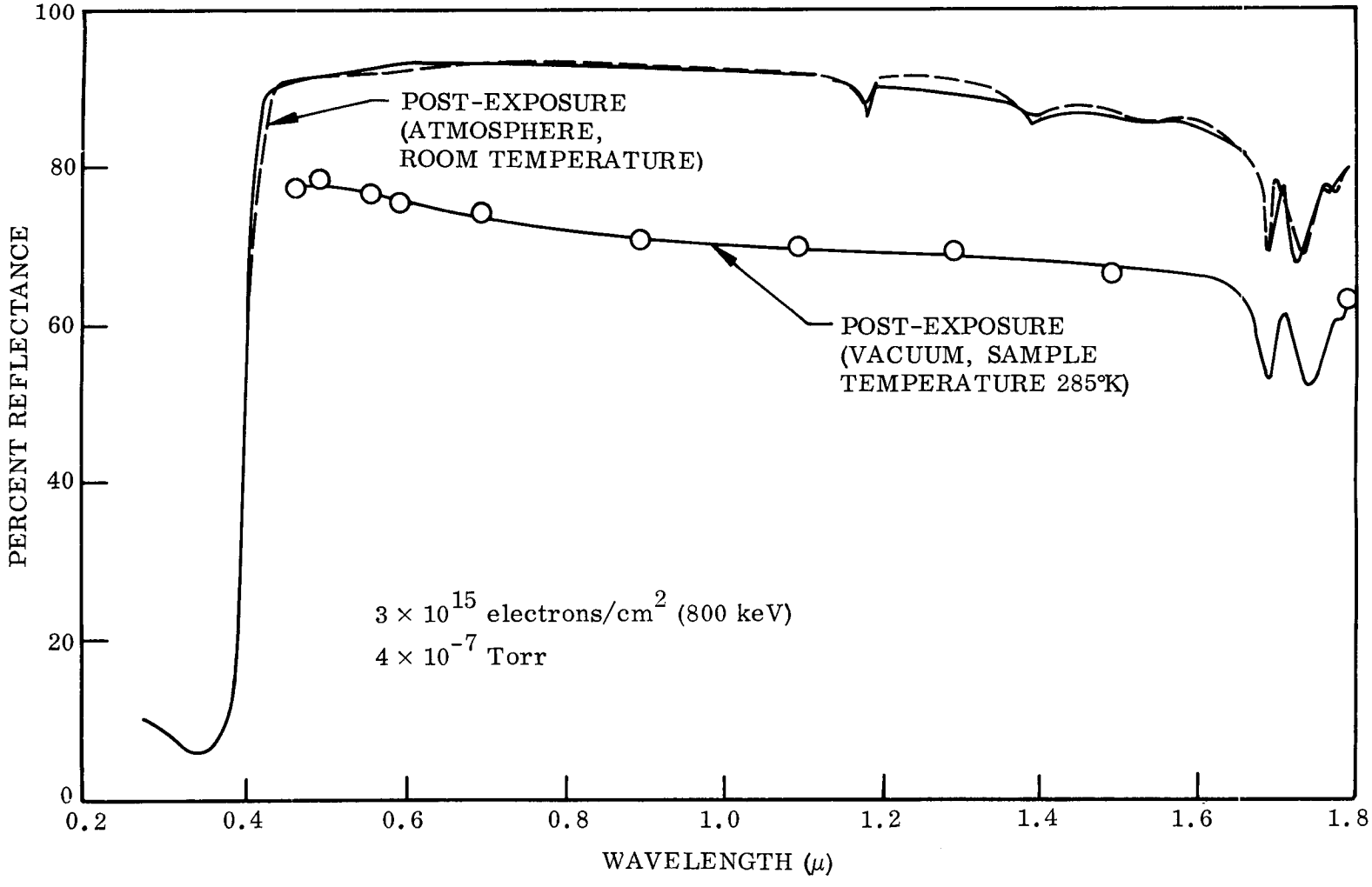

Fig. 7-20 Change in Reflectance of LMSC Thermatrol 6A-100 Exposed to Electrons Only (285°K) (Ref. 26)

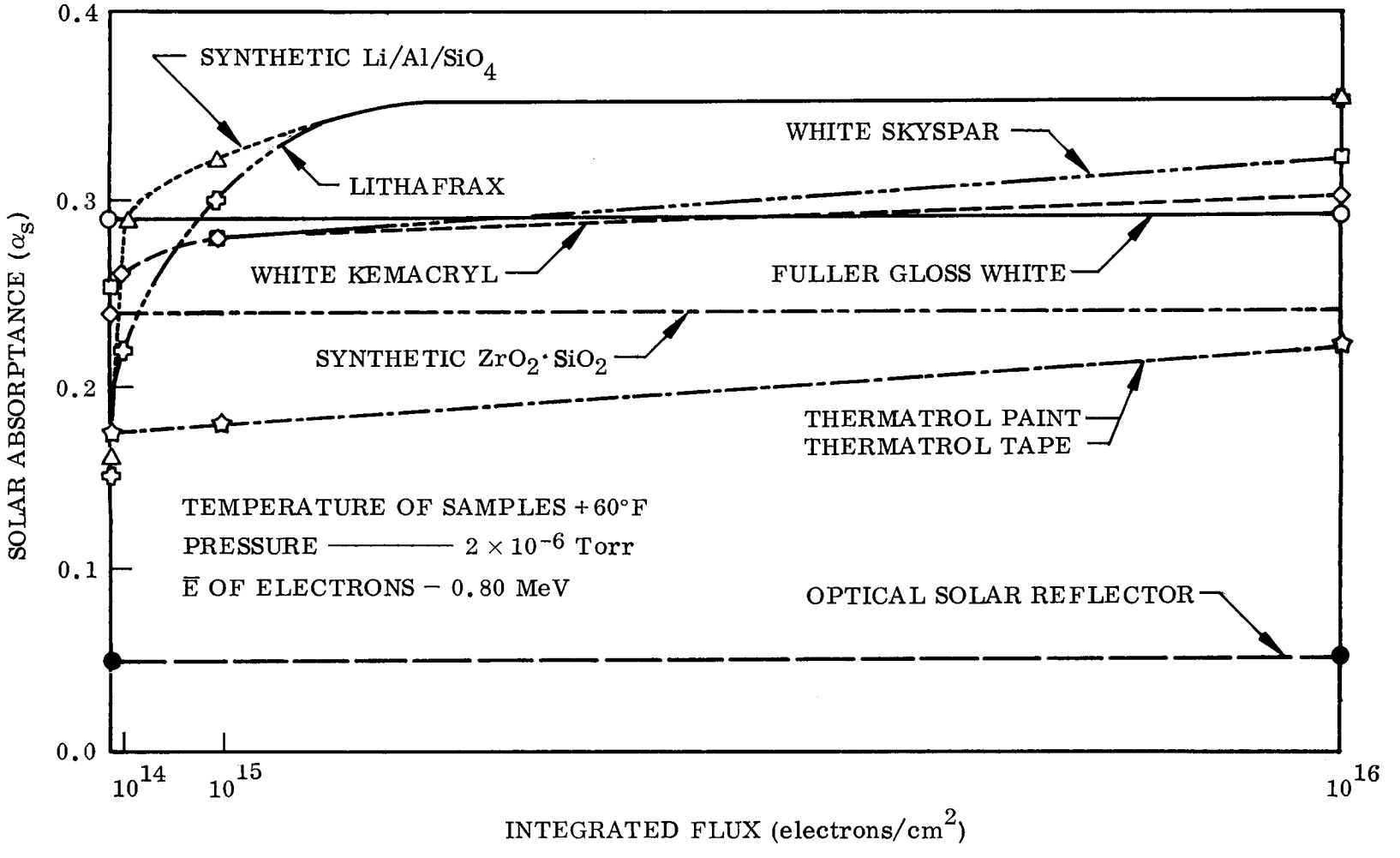

Fig. 7-21 Effect of Electron Bombardment on Solar Absorptance

A number of vehicles employing either nuclear propulsion systems or nuclear power electrical systems have been proposed. On such vehicles, leakage of nuclear radiation must be considered in terms of the effects on materials used for thermal control. Some evaluation has been done on materials under neutron and gamma radiation in conjunction with the Spacecraft Nuclear Auxiliary Nuclear Power (SNAP) programs. Some of these data are included in Tables 7-9 through 7-14. Zircon (Ultrox)-based coatings were excellent, whereas $LiAlSiO_4$ coatings were poor. Organic-based materials frequently suffered severe mechanical damage. Aluminum-pigmented materials held up well (Refs. 74 and 113). It has been found that first-order damage effects will be produced at exposures of 10^7 to 10^8 gamma radiation and 10^{14} to 10^{15} neutrons/cm^2. Damage is manifested as changes in both mechanical and absorptance properties (Refs. 101, 102, and 114). Effects in vacuum differ markedly from those in air. Absorptance properties tend to approach a saturation level which is a function of the environment.

Table 7-18

EFFECT OF SIMULATED ELECTRON[(a)] AND ULTRAVIOLET RADIATION ON TWO WHITE THERMAL CONTROL MATERIALS (REF. 14)

Pigment	Vehicle	Solar Absorptance Initial α_s	Change in Solar Absorptance After 6×10^{15} Electrons/cm^2 (%)	Change in Solar Absorptance After 436 Sun-hour UV (%)	Total Change in $\Delta\alpha_s$ UV + Electrons (%)
Thermatrol TiO_2	6A-100 Siloxane	0.19	+ 5.5	+ 15.8	+ 26.0
Fuller Gloss TiO_2	White Silicone-Alkyd	0.29	+ 3.5	+ 31.0	+ 31.0

(a) Energy of electrons = 0.80 MeV

7.6.5 Combined Radiation Effects

Ideally, any laboratory evaluation of a thermal control material should be done in vacuum using all radiation sources encountered on a mission. In the majority of laboratories, this is not feasible, but some progress is being made in evaluating materials under two radiation sources simultaneously. Work has been done at LMSC and elsewhere on combined ultraviolet-proton and ultraviolet-electron exposures. This information is included in Tables 7-9 through 7-14. Representative curves are shown in Figs. 7-22 and 7-23 for two ultraviolet-proton exposures. These measurements were

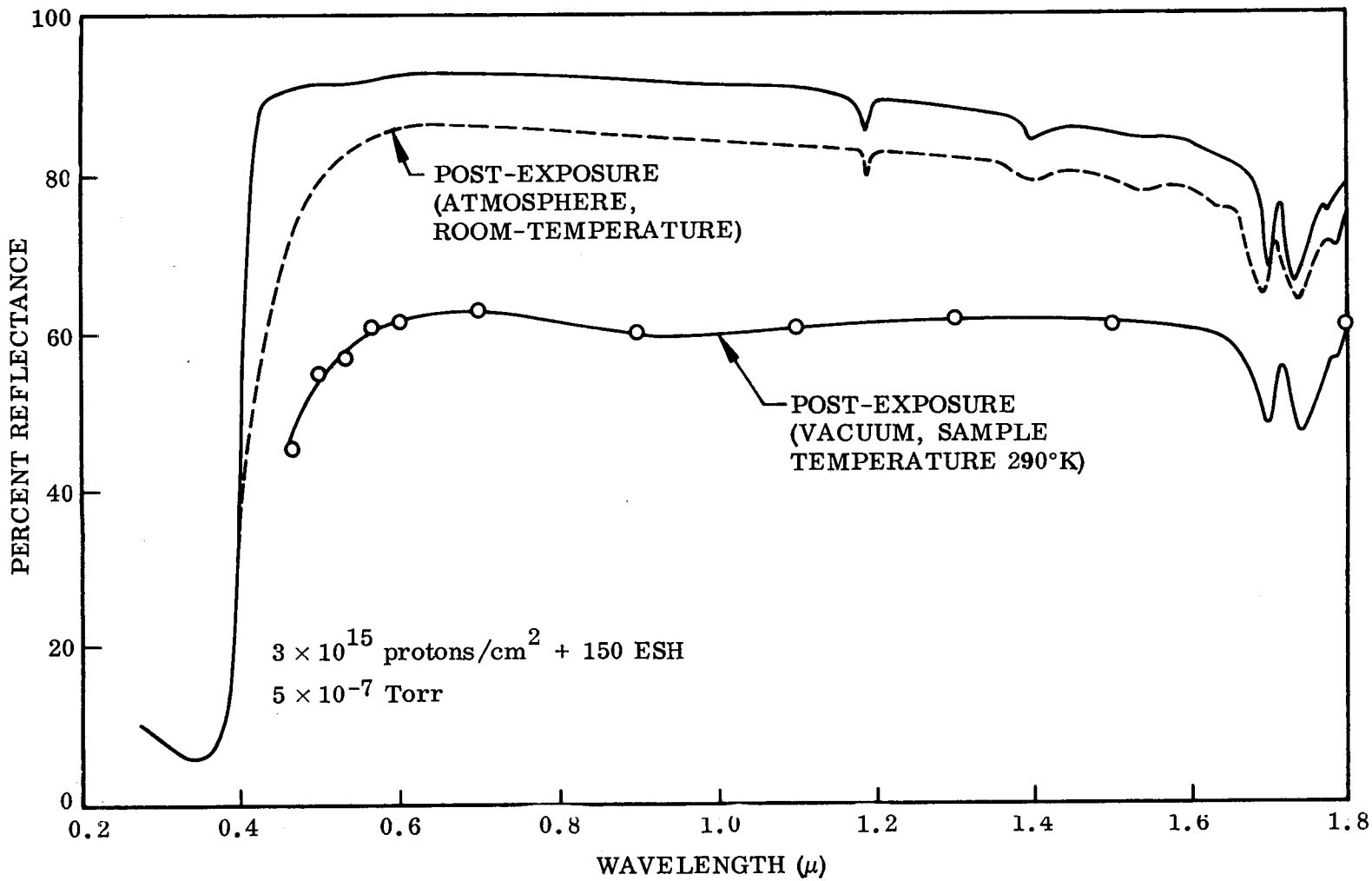

Fig. 7-22 Change in Reflectance of LMSC Thermatrol 6A-100 Exposed to Protons and Ultraviolet Radiations (320°K) (Ref. 29)

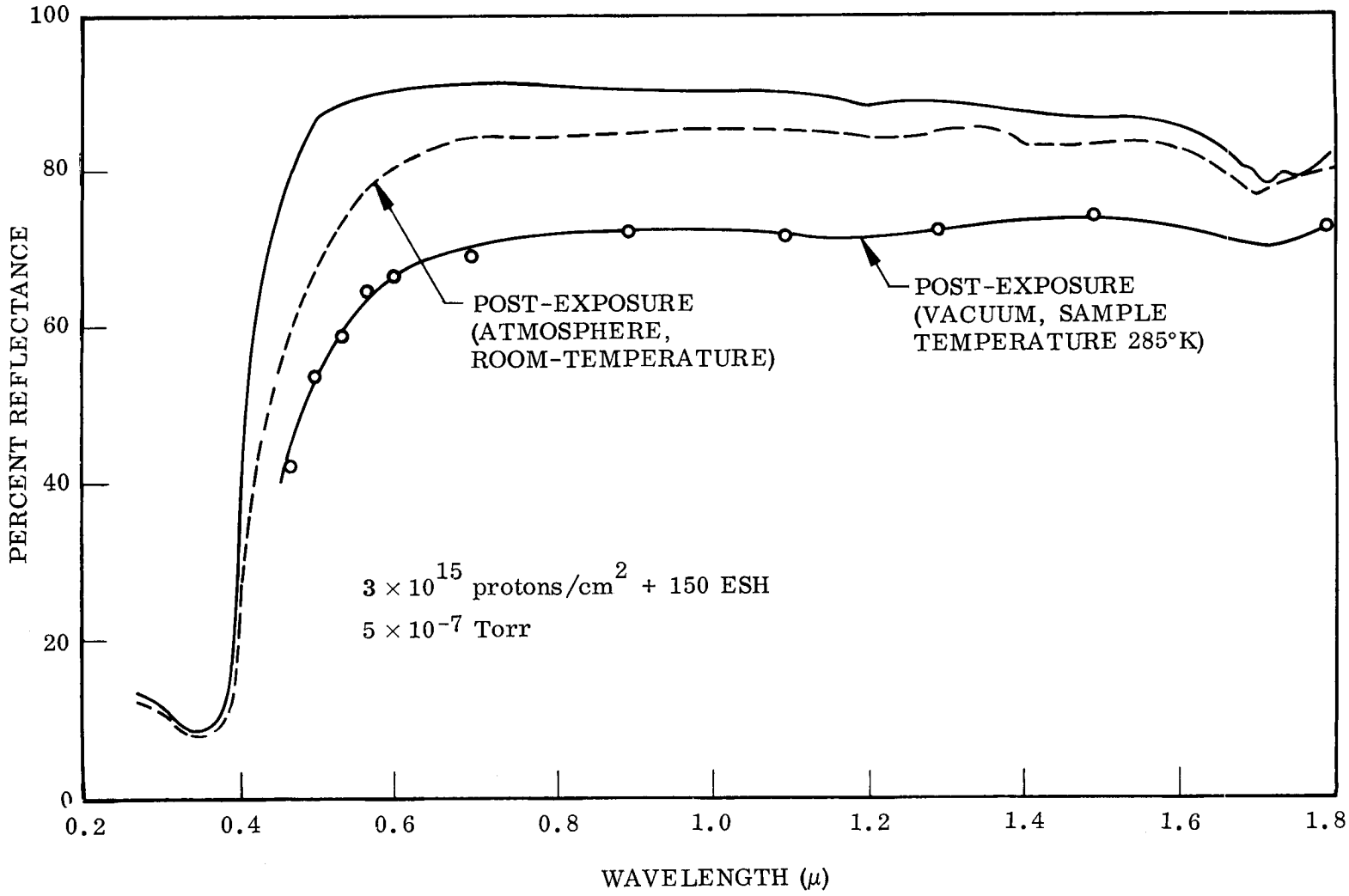

Fig. 7-23 Change in Reflectance of Vita-Var PV-100 Exposed to Proton and Ultraviolet Radiation (320°K) (Ref. 29)

made in situ for two organic-based materials, Thermatrol 6A-100 and Vita-Var PV-100. Rapid recovery of the absorptance is noted on reexposure to the atmosphere.

Flight test data and measurements in situ have been major factors in revealing previously unsuspected damage to spacecraft thermal control surfaces. The S-13 coating was employed on Pegasus, having the largest thermal control surface of any satellite to date (Refs. 81, 115, and 116). A rather sudden change in properties of the material was found during orbit. Lunar Orbiter I used S-13 material as a passive thermal control surface for all instrumentation; vehicles 2 and 3 used the same system with an S-13G overcoat. None of these performed as anticipated from laboratory evaluation (Ref. 115).

Lunar Orbiter 4 used a combination of mirrors and the S-13G material. The S-13G appeared stable for an initial period, then changed rapidly (Ref. 115). The S-13G material was also used on the Mariner (Venus) probe (Ref. 117). The change in absorptance was the same as that experienced on Lunar Orbiter. The laboratory test data for S-13G compared with the space flight data on Lunar Orbiter 4 differ by an order of magnitude, showing a 900 equivalent sun-hr change of 0.01 compared with 0.13 (Ref. 115). The most stable thermal control material used on Lunar Orbiter 4 was the Hughes silicate-rutile material. The Hughes-developed H-10 clay-based coating in a silicone binder has shown an in-flight degradation of 0.03 to 0.06 after 600 to 1000 hr (Refs. 72, 117, and 118). (See Fig. 7-24.)

Curves of the changes in solar absorptance of the flight experience from the Mariner 4 and Applications Technology Satellite are shown in Fig. 7-25 through 7-28. The Mariner 4 data in Fig. 7-25 illustrate the degradation of the Z-93 material in the interplanetary environment and a somewhat surprising absorptance change for polished aluminum. Figure 7-24 indicates that the clay-silicate material used on Surveyor behaved essentially as predicted from laboratory evaluation. Figures 7-26 through 7-28 are based on preliminary ATS-1 vehicle data. The evaporated alumina material shows essentially complete stability; the two organic materials show typical degradation in properties.

Figure 7-29 shows data from the Pegasus and Lunar Orbiter flights. The two materials are of similar composition (ZnO-silicone), but their behavior is different. It is seen that the laboratory evaluation was not adequate to predict the space environmental performance of these materials.

Data from OSO-1 and -2 flights are shown in Fig. 7-30. The curve for the change in absorptance for titanium dioxide-epoxy (Skyspar) illustrates the reproducibility of data from the two flights.

7.6.6 Effects of Physical Impact

At high altitudes (> 100 sm) the atomic species remaining of the earth's atmosphere do not greatly affect spacecraft surfaces. The kinetic energy of atomic and molecular nitrogen and of oxygen, for example, is less than the threshold energy required to initiate physical impact sputtering.

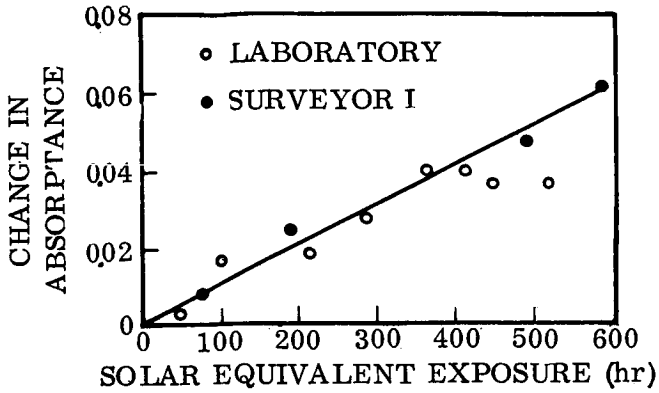

Fig. 7-24 Change in Absorptance of Inorganic White Paint (Plasmo Clay, K_2SIO_3) Used on Surveyor (Ref. 82)

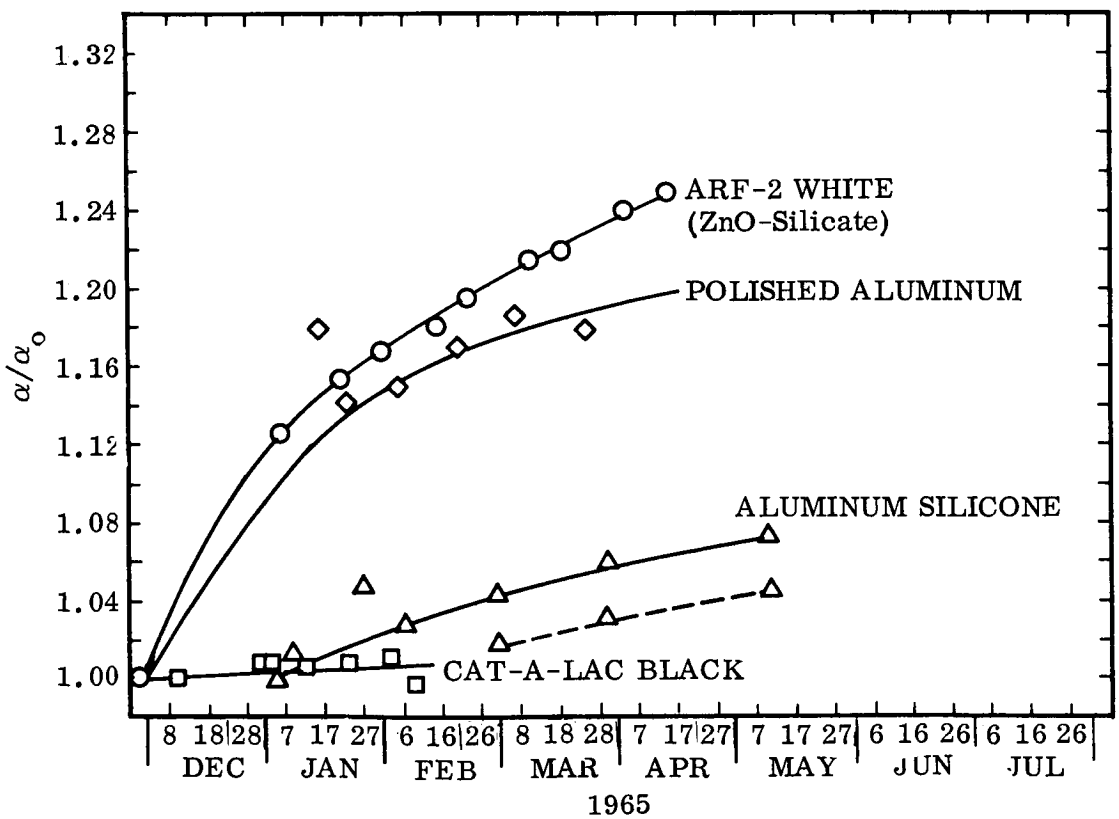

Fig. 7-25 Mariner 4 Absorptivity Standard Ratio of α to $\alpha_{initial}$ Versus Time (Ref. 82)

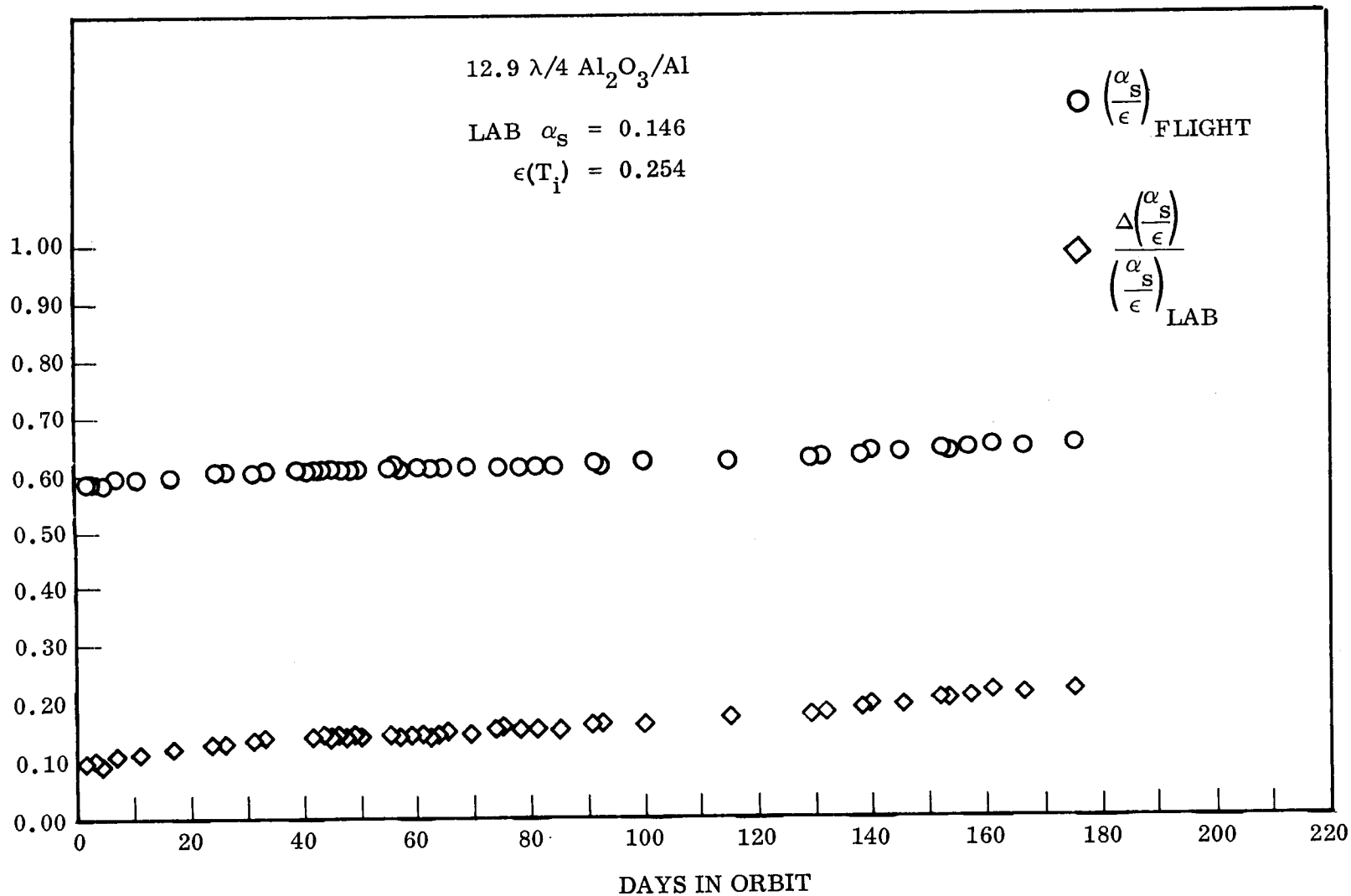

Fig. 7-26 Space Environment Behavior of 1.1 μ Al_2O_3 Evaporated Over Opaque Evaporated Aluminum (ATS-1 Data, Ref. 86)

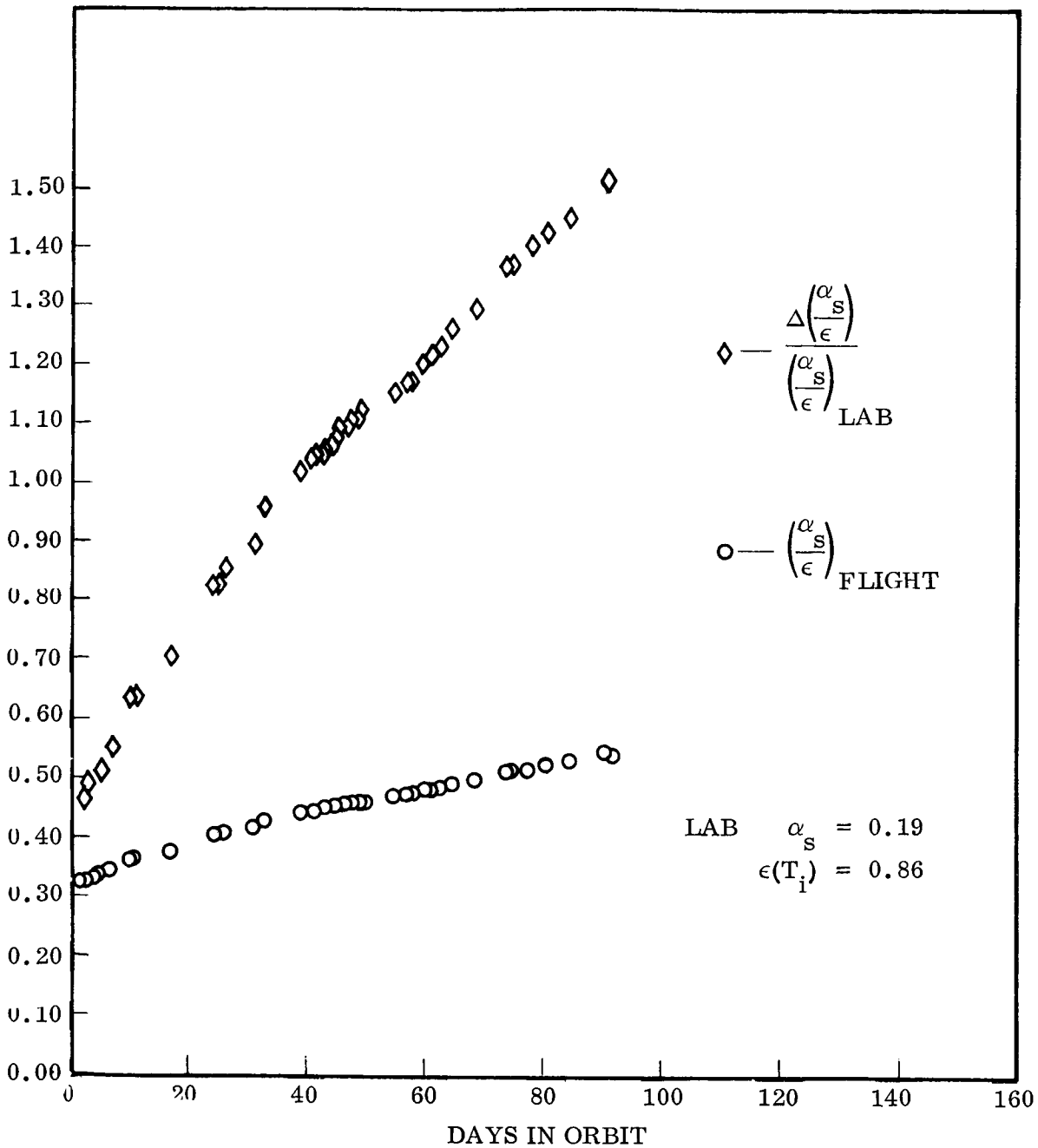

Fig. 7-27 Space Environment Behavior of TiO_2 (Anatase AMO)-Methyl Silicone (DCQ 92-090) Coating (ATS-1 Data, Ref. 14)

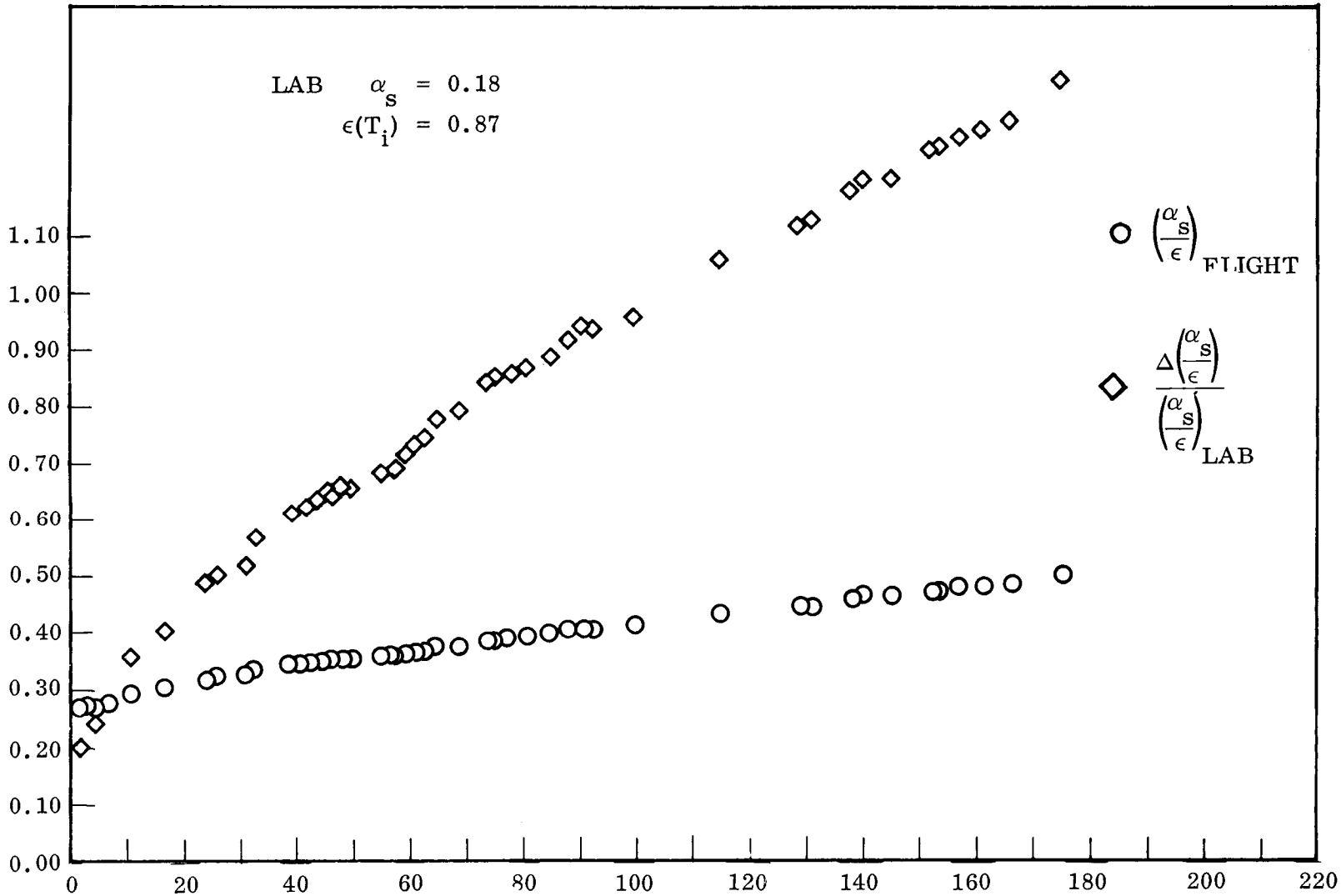

Fig. 7-28 Behavior of S-13 Coating (ZnO-Methyl Silicone) in Space Environment (ATS-1 Data, Ref. 86)

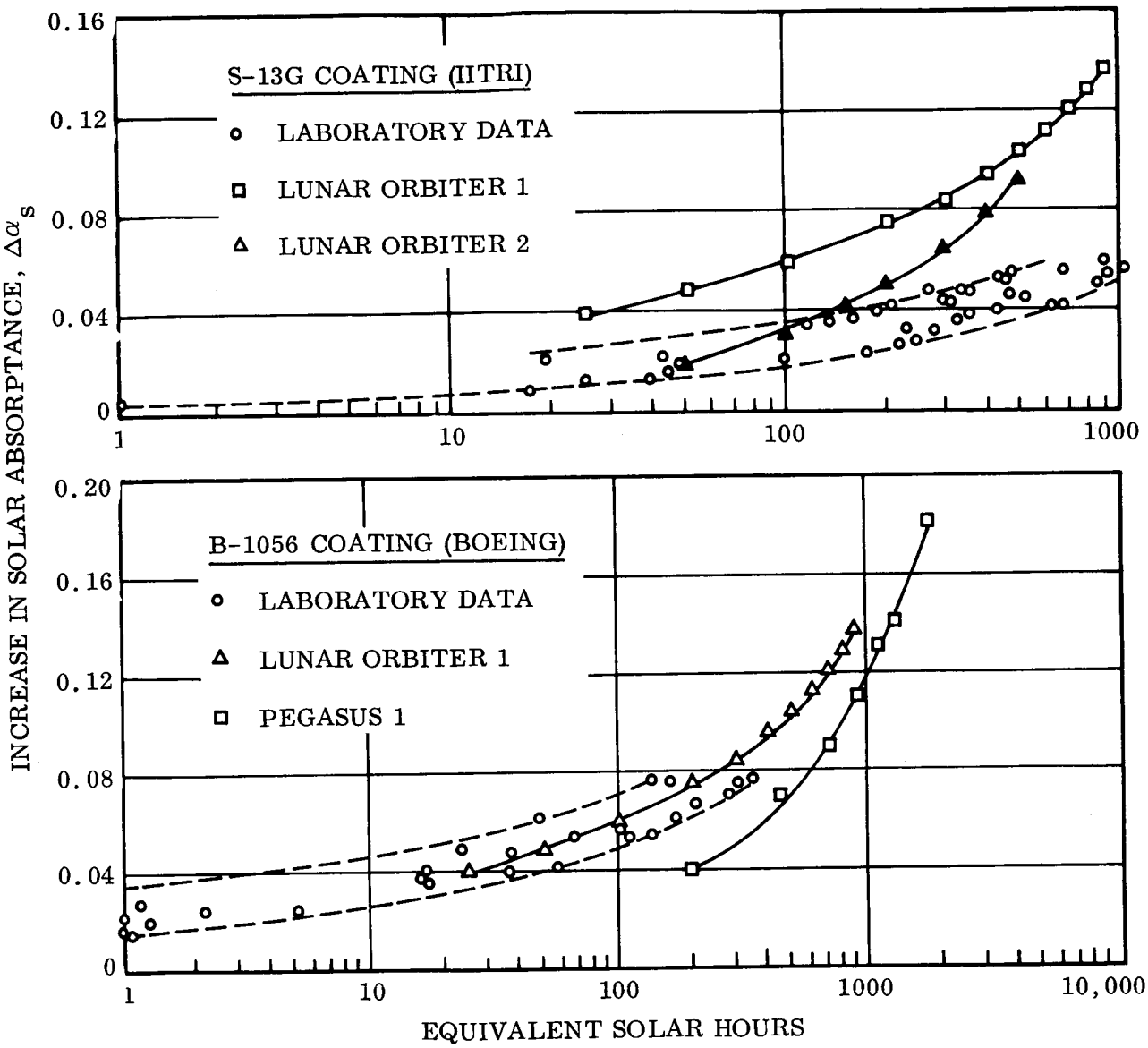

Fig. 7-29 Laboratory, Lunar Orbiter, and Pegasus Flight Data Showing Solar Absorptance Changes for S-13G and B-1056 Coatings (Ref. 55)

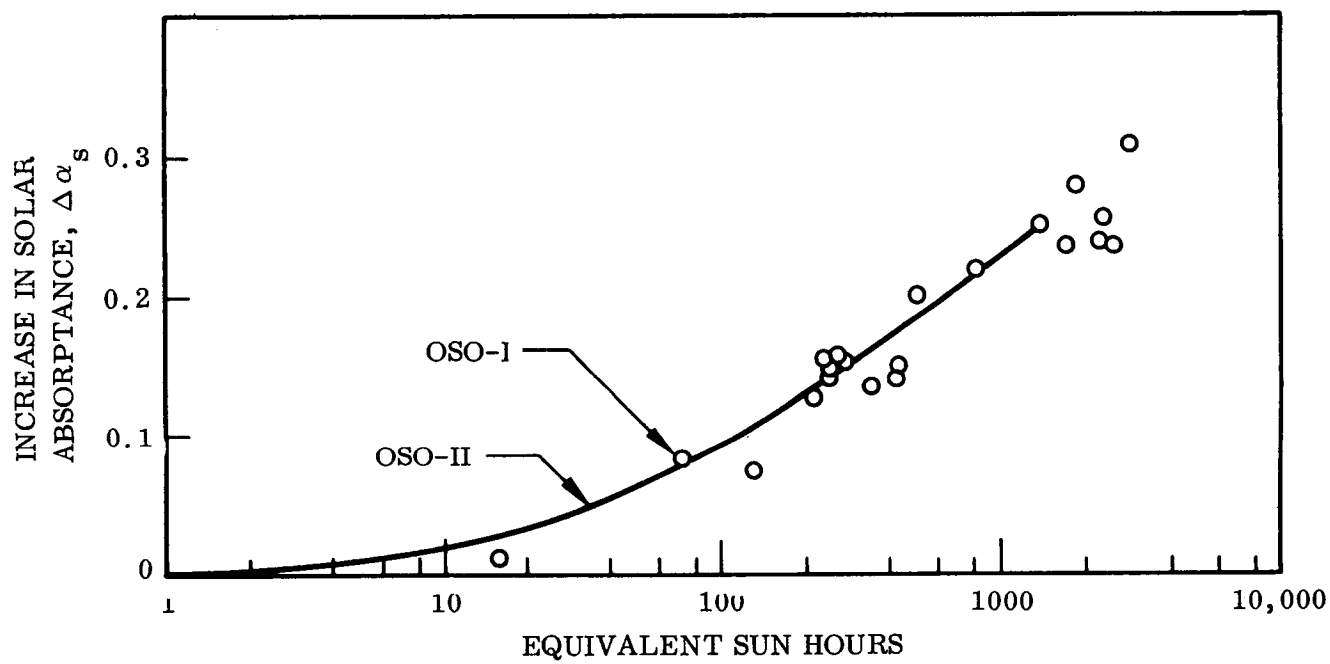

Fig. 7-30 Comparison of Changes in Solar Absorptance of Titantium Dioxide-Epoxy (Skyspar) on OSO 1 and 2 Flights (Ref. 55)

Current analysis indicates that the micrometeoroid environment does not cause changes in α_s or ϵ, or a change in the reflected angular distribution of the solar energy of thermal control surfaces, because the total flux of micrometeoroids in space is high enough to cause physical impact damage only to large areas of an exposed surface for prolonged mission times. A study of the near-earth meteoroid environment using observational data from Explorers 16 and 23, and from Pegasus 1, 2, and 3, and photographic techniques, is discussed in Chapter 6.

The effects of sputtering and erosion on the performance of a thermal control surface are considered negligible. The thermal control aspects of penetration damage are considered to be inconsequential because the fractional area affected by the meteoroid flux is found to be quite small even for long-duration missions. Theoretical and experimental penetration studies and experiments are discussed in Refs. 119 through 123.

Because of the large retro rockets used for stage separation of the Saturn propulsion system, the midcourse correction, retro, and lunar liftoff engines in the Apollo, and the attitude control rocket engines of Apollo and other systems, there has been concern recently about the effect of products of exhausts on thermal control, thermal radiators, solar cell, and optical surfaces of spacecraft. A limited number of ground-based studies have been performed, and preliminary indications are that the properties of thermal control materials may be altered. Fortunately for the spacecraft-borne optical experiments, a carefully planned sequence in which optical elements are protected during firing can reduce the contamination hazard. However, protection of thermal control and radiator surfaces and solar cells during firings is prohibitive; therefore, this aspect of the problem appears to require additional study to define in more detail the extent of damage from the contaminants, and, more important, to define the subsequent effect of the space radiation environment on these contaminant films (Ref. 124).

7.6.7 Vacuum

Metallic systems will not be affected by the vacuum environment. The vacuum stability of other inorganic materials is dependent mainly on the bond joining it to a substrate. Organic materials are unstable in a vacuum at elevated temperatures. Organic materials qualified for use as thermal control coatings in vacuum are paint formulations based on silicone, acrylic, epoxy, and phenolic. In each case, the most stable paint is a fully cured system containing essentially no plasticizers or other retained volatile components.

Significantly, in applications in which the temperatures do not greatly exceed 100°F, the organic-based thermal control materials are being used more extensively than the inorganic-based. However, there is no question that inorganic thermal control materials are basically much more stable; their chief problems are contamination and application.

7.6.8 Temperature Effects

In general, effects on thermal control materials are not significant for constant nominal temperatures, but thermal cycling between temperature extremes can result in thermal stress and contribute to changes in properties or lack of adhesion of materials to surfaces. Effects of thermal cycle testing were considered in subsection 7.6, and data are listed in Tables 7-5, 7-6, and 7-7. From these data, it is seen that nominal temperature thermal cycling generally does not affect inorganic coatings, anodic coatings, and metals. Mechanical damage is generally noted with organic-based coatings.

The effects of cryogenic temperatures and of cycling between cryogenic temperatures and room temperatures were discussed in subsection 7.6.1, and are presented in Tables 7-15 and 7-16. In this case, performance was generally improved for most materials at cryogenic temperature levels.

Investigations into the behavior of materials at high temperatures seem to indicate that actual measurements must be made and that limiting temperatures must be determined for each system of materials. Based upon experimental observations, the materials can be ranked in approximately the same order found in related areas of investigation, namely, ceramic and refractory materials, metals, nonrefractory inorganic materials, and organic materials, in order of decreasing stability. Of the organic materials tested, silicones frequently display the greatest high-temperature stability. However, recently developed polyimide, polybenzimidazole and phenyl silane resins retain good mechanical properties up to 500°F. These materials have not been used for thermal control applications. Their main application has been in adhesives and structure reinforced plastic materials. (See Chapters 10 and 12.)

7.7 SUMMARY

During the past 10 years, an immense effort has gone into research and development, simulated testing, and flight testing of spacecraft thermal control concepts and materials. A great deal of progress has been made, but much remains to be accomplished in almost every segment of this field of space technology.

Relatively little development has occurred in the area of active thermal control systems, simply because they have been used only to a limited extent on present vehicles. Some successful louver systems have been employed. With the current development of large manned vehicles, increased activity in the active thermal control systems field will be required.

In the passive thermal control area, most recent activity has been concerned with development of practical solar reflector surfaces possessing high degrees of stability in ultraviolet-vacuum environments. In general, satisfactory surfaces are available for use as solar absorbers, flat absorbers, and flat reflectors, although the choice of materials for use as flat reflectors is somewhat limited.

There is still no completely qualified material for solar reflector use. Organic-based materials which commonly have been employed on a variety of vehicles are adequate for most short-term missions. Inorganic materials have shown improved performance for some longer term missions but have also demonstrated unexpected degradation in some interplanetary and lunar missions. The recent findings of the bleaching effects when properties were measured in air after radiation exposure in vacuum and the consequent necessity of evaluating materials under vacuum conditions have resulted in a complete reevaluation of the properties of all solar reflector materials.

The foregoing comments point up the principal deficiency in the passive thermal control area: the lack of adequate, standardized testing facilities. The unexpected failure of previously qualified inorganic materials obviously resulted because the total environment had not been considered. A material for testing in situ in a vacuum-ultraviolet simulated environment cannot be considered a qualified material except for near-earth orbits. Qualification of materials must be based on simulation of the total environment for a particular mission. Researchers in this field are moving in that direction, with increasing attention not only to ultraviolet radiation evaluation but also to proton, electron, solar wind, and alpha particle evaluation. This also implies concern with solar phenomena, the micrometeoroid environment, the thermal environment, and in some cases the nuclear phenomena.

The continuing needs of spacecraft thermal control technology can be summed up as follows:

- Accurate definition of the near-earth, interplanetary, and solar space environment by astronomical, satellite, and space probe techniques
- Development of instruments and techniques for complete simulation of the particular space environment for a particular mission coupled with in situ evaluation of materials
- Continued development of new materials with long-term space environment stability and reliability, particularly solar reflectors
- Development of alternate surfaces for other classes to provide a wider choice of selections
- Development of new and more effective active thermal control systems, particularly for manned vehicles

A large amount of the information presented in this chapter will assist the designer in selecting materials for a particular spacecraft thermal design. A large amount of additional information may be obtained from the references cited. However, in all but the most straightforward cases where flight experience is available, it is still true that specification of materials for a particular vehicle for a specific mission must be done on the basis of test and evaluation under the specific conditions anticipated for that mission.

7.8 REFERENCES

1. C. H. Liebert and R. R. Hibbard, Performance of Solar Reflectors When Applied to Storage of Cryogenic Propellants in Space, NASA TN-D-2509, NASA Lewis Research Center, Cleveland, Ohio, November 1964

2. W. R. Corliss, "Survey of Space Power Requirements – 1962 to 1976," American Rocket Society Paper 2520-62, Space Power Systems Conference, Santa Monica, Calif., 25–28 September 1962

3. S. A. Greenberg, D. A. Vance, and E. R. Streed, "Low Solar Absorptance Surfaces With Controlled Emittance: A Second Generation of Thermal Control Coatings," AIAA Paper 67-343, AIAA Thermophysics Specialists Conference, New Orleans, La., April 1967

4. Solar Radiation Induced Damage to the Optical Properties of ZnO-Type Pigments, Technical Summary Report, NAS 8-18114, Lockheed Missiles & Space Company, Sunnyvale, Calif., June 1967

5. Damage Mechanisms in Thermal Control Coating Systems, Final Report, Contract AF 33(615)-5111, Lockheed Missiles & Space Company, Sunnyvale, Calif., 1968

6. G. A. Zerlaut, Development of Space-Stable Thermal Control Coatings, Triannual Reports, Contract NAS 8-5379, George C. Marshall Space Flight Center, NASA No. IITRI-U6002-36, 21 Feb 1966 (with G. A. Rubin); No. IITRI-6002-42, 11 July 1966: No. IITRI-U6002-51, 28 February 1967; No. IITRI U6002-55, 22 September, 1967, (with G. Noble and F. O. Rogers)

7. P. R. Cheever, J. K. Miles, and J. Romanko, "In Situ Measurements of Spectral Reflectance of Thermal Control Coatings Irradiated in Vacuo," AIAA Paper 67-342, Thermophysics Specialists Conference, New Orleans, La., April 1967

8. H. Strughold and O. Ritter, Solar Irradiance From Mercury to Pluto, AIRU 60-39, USAF Aerospace Medical Center, February 1960

9. K. Schocken, The Thermal Environment of the Terrestrial Planets, MTP-RP-62-7, George C. Marshall Space Flight Center, NASA, 15 September 1962

10. R. M. Acker, R. P. Lipkis, and J. E. Vehrencamp, Temperature Control System for the Atlas Able-4 Lunar Satellite, Space Technology Laboratories, Inc., 31 March 1960

11. E. Cummins, Factors Affecting the Temperature of Components Within Orbiting Space Vehicles, WADC TN-58-232, AD 155–825, Wright Air Development Center, August 1958

12. J. A. Plamondon, Analysis of Moveable Louvers for Temperature Control, NASA CR-53046, JPL-TR-32-555, January 1964; also J. Spacecraft & Rockets 1, 492497, September-October 1964

13. J. A. Wiebelt, Research on a Self-Temperature Regulating Spacecraft Skin System, NASA CR-77101, Oklahoma State University, June 1966

14. E. E. Glenn and A. Munoz-Mellowes, "Thermal Design and Testing of the Pioneer Spacecraft," Thermal Control Working Group Meeting, Dayton, Ohio, 16–17 August 1967

15. A. Gross and F. J. Sackleh, "Thermal Control of an Orbital Vehicle," pp. 235-241 in Proceedings, Annual Technical Meeting, Institute of Environmental Sciences,1961

16. T. M. Olcott and M. Ratner, Analytical and Experimental Investigation of Self Thermostatic Effects, LMSC-6-90-63-33, Lockheed Missiles & Space Company, Sunnyvale, Calif., January 1963

17. "Project Telstar," Component Reliability Symposium, Bell Telephone Laboratories, Inc., November 1962

18. E. E. Gardner and E. L. Woisard, "Thermoelectric Materials for Space Cooling," ARS Reprint 1280-60, Whirlpool Research Laboratories, St. Joseph, Mich., September 1960

19. J. D. Plunkett, NASA Contributions to the Technology of Inorganic Coatings, NASA SP-5014, National Aeronautics and Space Administration, Washington, D. C. 1964

20. E. R. Streed and J. C. Arvesen, "A Review of the Status of Spacecraft Thermal Control Materials," SAMPE J., 17-24, June-July 1967

21. Spacecraft Materials Guidebook, NASA CR-83992, JPL-TM-33-124, Jet Propulsion Laboratory, California Institute of Technology, Pasadena, Calif., December 1965

22. Search and Retrieval Guide to Thermophysical Properties Information, Thermophysical Properties Research Center, Y. S. Touloukian, Director, Lafayette, Ind.

23. LMSC Handbook of Optical Properties of Thermal Control Materials, Lockheed Missiles & Space Company, Sunnyvale, Calif., 1967

24. L. J. Bailin, Production of High Purity Thermal Control Coatings, Technical Documentary Reports IR-9-458, Contract AF 33(615)-5132, Lockheed Missiles & Space Company, Sunnyvale, Calif., I, September 19661; II, November 1966; III, and IV, February 1967; V, May 1967

25. K. N. Marshall and R. A. Breuch, "Optical Solar Reflector: A Highly Stable, Low α/ϵ Spacecraft Thermal Control Surface "(in preparation)

26. R. A. Breuch and S. A. Greenberg, "Recent Coating Developments and Exposure Parameters," Thermal Control Working Group Meeting, Dayton, Ohio, 16-17 August 1967

27. H. E. Knudson and J. S. Tuchscher, "Surveyor Spacecraft Thermal Control," Thermal Control Working Group Meeting, 16-17 August 1967, Dayton, Ohio,

28. J. R. Crosby and M. A. Perlow, "Snap 10A Thermal Control Coatings," AIAA Paper, No. 65-652, AIAA Thermophysics Specialist Conference, Monterey, Calif. 13-15 September 1965

29. G. A. Zerlaut and F. O. Rogers, "The Behavior of Several White Pigments as Determined by In Situ Reflectance Measurements of Irradiated Specimens," Thermal Control Working Group Meeting, Dayton, Ohio, 16–17 August 1967

30. L. Whitby, The Design of Paint Coatings for Spacecraft, LMSD-703026, Lockheed Missiles & Space Company, Sunnyvale, Calif., June 1960

31. M. E. Sibert, Inorganic Surface Coatings for Space Applications, LMSD 3-77-61-120, August 1961; also in Proc. Div. of Organic Coatings and Plastics Chem., American Chemical Society, Chicago, September 1961

32. G. F. Pezdirtz and R. A. Jewell, "A Study of the Photodegradation of Selected Thermal Control Surfaces," Paper No. 43, pp. 433-441, in Symposium on the Thermal Radiation of Solids, ed. S. Katzoff, NASA SP-55, National Aeronautics and Space Administration, Washington, D. C., 1965

33. R. L. Olson, L. A. McKellar, and J. V. Stewart, "The Effects of Ultraviolet Radiation on Low α_s/ϵ Surfaces," Paper No. 42, pp. 421–432, in Symposium on the Thermal Radiation of Solids, ed. S. Katzoff, NASA SP-55, National Aeronautics and Space Administration, Washington, D. C., 1965

34. R. N. Schmidt and J. E. Janssen, "Selective Coatings for Vacuum-Stable High Temperature Solar Absorbers," Paper No. 49, pp. 509–524, in Symposium on the Thermal Radiation of Solids, NASA SP-55, National Aeronautics and Space Administration, Washington, D. C., 1965

35. D. V. Edwards, et al., Basic Studies in the Use and Control of Solar Energy, UCLA Report No. 60-93, NSF G 9505 Annual Report, October 1960

36. H. Tabor, "Selective Radiation. I. Wavelength Discrimination," Trans. of Conf. on Use of Solar Energy, Vol. II, Part I, 1955

37. M. C. Mottel and T. A. Unger, "The Properties of a Copper Oxide-Aluminum Selective Black Surface Absorber of Solar Energy," Solar Energy 3, 10, 1959

38. P. Kokoropoulos, E. Salam, and F. Daniels, "Selective Radiation Coatings. Preparation and High Temperature Stability," Solar Energy 3, (4), 19, 1959

39. R. B. Gillette, "Selectively Emissive Materials for Solar Heat Absorbers, Solar Energy 4, 24, October 1960

40. W. Carroll, Jet Propulsion Laboratory, Pasadena, Calif., Personal communication, 30 October 1967

41. J. H. Laub and H. D. McGinness, Recirculation of a Two-Phase Fluid by Thermal and Capillary Pumping, JPL-TR-32-196, Jet Propulsion Laboratory, Pasadena, Calif., December 1961

42. R. E. Gaumer and A. S. Gilcrest, "Solid Cryogenic Refrigerator of Spacecraft Components," Institute of Environmental Sciences Meeting, Chicago, Ill. April 1962

43. G. Hass, L. F. Drummeter, Jr., and M. Schach, "Temperature Stabilization of Highly Reflecting Spherical Satellites," J. Opt. Soc. Am. 49, 918–924, September 1954

44. G. Hass, W. R. Hunter, and R. Tousey, J. Opt. Soc. Am. 47, 1070–1073, December 1957

45. G. Hass and C. D. Salzberg, J. Opt. Soc. Am. 44, 181, 1954

46. A. H. Sporer, "Photoionization of Triarylmethyl Leuconitriles," Trans. Far. Soc. 57, 983–991, 1961

47. E. Berman, R. E. Fox, and F. D. Thomson, "Photochromic Spiropyrans," J. Am. Chem. Soc. 81, 5605–5608, 1959

48. S. Z. Fixler, "Passive Thermal Control by Phase Change Materials," Space/Aeronautics, 45, No. 2, 104–06, February 1966

49. F. A. Grant, "Properties of Rutile (Titanium Dioxide)," Revs. Modern Phys. 31, 646–674, 1959

50. W. G. Camack and D. K. Edwards, "Effects of Surface Thermal-Radiation Characteristics on the Temperature Control Problem in Satellites," pp. 3–54 in First Symposium on Surface Effects on Spacecraft Materials, ed. F. J. Clauss, Wiley, New York, 1960

51. J. C. Grafton and J. A. Stevenson, Radiation Heat Transfer Analysis for Space Vehicles, SID 61-91, North American Aviation, Inc., December 1961

52. R. C. Gex, Temperature Control of Satellite and Space Vehicles. An Annotated Bibliography, LMSC Special Bibliography SB-61-5, Lockheed Missiles & Space Company, Sunnyvale, Calif., February 1961

53. S. J. Kline and F. A. McClintock, "Describing Uncertainties in Single-Sample Experiments," Mechanical Eng. 75, 3–8, 1963

54. G. A. Zerlaut and W. J. Courtney, "Space-Simulation Facility for In Situ Reflectance Measurements," AIAA Paper 67-312, AIAA Thermophysics Specialist Conference, New Orleans, La., 17–20 April 1967

55. P. M. Blair, Jr., G. F. Pezdirtz, and R. A. Jewell, "Ultraviolet Stability of Some White Thermal Control Coatings Characterized in Vacuum," AIAA Paper 67-345, AIAA Thermophysics Specialist Conference, New Orleans, La., 17–20 April 1967

56. J. F. Scannapieco and S. J. Babjak, "Space Environment Simulation for Thermal Control Materials," pp. 411–419 in Proc. of 13th Annual Tech. Meeting, Institute of Environmental Sciences, Vol. 2, Washington, D.C., 10–12 April 1967

57. R. E. Gaumer and L. A. McKellar, Thermal Radiative Control Surfaces for Spacecraft, LMSD-704014, Lockheed Missiles & Space Company, Sunnyvale, Calif., March 1961

58. G. Hass and J. E. Waylonis, "Optical Constants and Reflectance and Transmittance of Evaporated Aluminum in the Visible and Ultraviolet," J. Opt. Soc. Am. 51 (7), 719–722, July 1961

59. R. E. Gaumer, G. F. Hohnstreiter, and G. F. Vanderschmidt, "Inspection Tools for Measurement of the Radiation Properties of Satellite Temperature Control Surfaces," Proc. of Symposium on Measurement of Thermal Radiation Properties of Solids, Wright-Patterson Air Force Base, Ohio, 1962

60. R. E. Gaumer et al., Materials Effects in Spacecraft Thermal Control, LMSD-704019, Lockheed Missiles & Space Company, Sunnyvale, Calif., November 1960

61. "Thermodynamics of Space Flight (Heat Transfer Phenomena in Space)," X-633-63-50, Goddard Space Flight Center, NASA, Greenbelt, Md., March 1963

62. W. F. Schmidt, L. A. Haslim, and L. A. McKellar, "Effects of the Ascent Environment on Spacecraft Thermal Control Surfaces," Paper No. 57, American Society for Testing and Materials Meeting, Los Angeles, Calif., 1–5 October 1962

63. J. T. Gier, R. V. Dunkle, and J. T. Bevans, J. Opt. Soc. Am. 44, 558, 1954

64. R. V. Dunkle, "Thermal Radiation Tables and Applications," Trans. Am. Soc. Mech. Engrs. 76, 549–552, 1954

65. H. S. Schwartz et al., Properties of Thermally Degraded Ablative Materials, WADD TN-60-286, Wright Air Development Division, Wright-Patterson Air Force Base, Ohio, November 1960

66. C. J. Kateikas, G. K. Castle, and J. S. Higgins, Ablation Handbook: Entry Materials Data and Design, AFML-TR-66-262, Avco Corporation, November 1966

67. D. W. Lewis and T. O. Thostesen, "Mariner-Mars Absorptance Experiment," Paper No. 65-650, AIAA Thermophysics Specialist Conference, Monterey, Calif. 13–15 September 1965

68. B. D. Pearson, Jr., "Preliminary Results From the Ames Emissivity Experiment on OSO-2," Paper No. 65-651, AIAA Thermophysics Specialist Conference Monterey, Calif., 13–15 September 1965

69. F. D. Williamson, F. M. Smith, and V. J. Stanley, "Utilization of Inorganic Thermal Control Coating," Paper No. 4630, Thermal Control Working Group Meeting, Dayton, Ohio, 16–17 August 1967 (in press)

70. G. V. Jorgenson, "Solar Wind Damage to Spacecraft Thermal Control Coatings," AIAA J. 5 (6), 1204–05, 1967

71. J. A. Cooley, Evaluation of Thermal Control Coatings in the Space Environment, AFML-TR-67-158, AVCO Electronics Division, Tulsa, Okla., May 1967

72. W. A. Hagemeyer, Jr., "Surveyor White Paint Degradation," J. Spacecraft and Rockets 4 (6), 828–829, 1967

73. P. J. Reichard and J. J. Triolo, "Pre-Flight Testing of the ATS-1 Thermal Coatings Experiment," AIAA Paper 67-333, AIAA Thermophysics Specialist Conference, New Orleans, La., 17–20 April 1967

74. H. E. Pollard, J. E. Gilligan, and R. A. Breuch, The Development of Thermal Control Surfaces for SNAP-10A Flight Test Spacecraft, SSD-TDR-64-193, Lockheed Missiles & Space Company,, Sunnyvale, Calif., December 1964

75. R. A. Breuch, N. J. Douglas, and D. Vance, "Effects of Electron Bombardment on the Optical Properties of Spacecraft Temperature Control Coatings," AIAA J. 3 (12) 2318–2327, 1965

76. D. R. Clarke et al., Radiation Resistant Barrier-Layer Anodic Thermal Control Coatings, AFML TR-67-163, The Boeing Company, Seattle, Wash., August 1967

77. R. J. Wensley and G. A. Kane, "Applications Technology Satellite Thermal Design," Thermal Control Working Group Meeting, Dayton, Ohio, 16–17 August (in press)

78. W. Carroll, Jet Propulsion Laboratory, Private communication, October 1967

79. C. G. Goetzel, J. B. Rittenhouse and J. B. Singletary, eds., Chapter 10 and Section 21.1 in Space Materials Handbook, 2nd ed., ML-TDR-64-40 (AD 460 399), X65-14878, Lockheed Missiles & Space Company, Sunnyvale, Calif., January 1965
J. B. Rittenhouse and J. B. Singletary, eds., Section 2.2 in Supplement 1, NASA SP-3025, Lockheed Missiles & Space Company, 1966
J. Rittenhouse and J. B. Singletary, eds., Section 2.2 in AFML-TR-64-40, Supplement 2, Lockheed Missiles & Space Company, 1968

80. C. F. Schafer and T. C. Bannister, "Pegasus Thermal Control Coatings Experiment," AIAA Paper 66-419, 4th Aerospace Sciences Meeting, Los Angeles, Calif., 27–29 June 1966

81. W. C. Snoddy, "Pegasus Thermal Experimental Results," pp. 27–31 in Research Achievements Rev., Vol. II, George C. Marshall Space Flight Center, NASA, 1966

82. Boeing Airplane Co., "Lunar Orbiter," Thermal Control Working Group Meeting, Dayton, Ohio, 16–17 August 1967

83. W. F. Schmidt et al., Temperature Control Coatings for Cryogenic Temperature Substrates, AFML-TR-66-10, Lockheed Missiles & Space Company, Sunnyvale, Calif., March 1966

84. R. A. Breuch, "Studies on the Effects of the Interplanetary Space Environment on Thermal Control Coatings," pp. 104–109 in Proc. AIAA, IES, ASTM Space Simulation Conference, Houston, Tex., 7–9 September 1966; also AIAA J. 5, (9), 1650-16-54, 1967

85. J. A. Wiebelt and J. D. Pinson, Space Simulation Requirements for Proton and Ultraviolet Radiation, AEDC-TR-66-259, Oklahoma State University, Stillwater, Okla., December 1966

86. A. P. Latour, "Thermal Design of the Gravity Gradient Test Satellite," Thermal Control Working Group Meeting, Dayton, Ohio, 16–17 August 1967

87. P. R. Schrantz, Two New Coatings for Satellite Temperature Control, TG-758 (AD 630036),Applied Physics Laboratory, Johns Hopkins University, Silver Spring, Md., December 1965

88. J. Milko, NASA Lewis Research Center, Cleveland, Ohio, Personal communication, January 1968

89. R. M. Van Vliet, ed., Coatings for the Aerospace Environment, WADC TR-60-773, Wright-Patterson Air Force Base, Ohio, July, 1961

90. R. G. Schmitt and R. C. Hirt, Studies on the Protective Ultraviolet Absorbers in a High Vacuum Environment, WADC TR-59-354, January 1960

91. R. G. Schmitt and R. C. Hirt, Studies on the Protective Ultraviolet Absorbers in a High Vacuum Environment, WADC 60-704, Part II, February 1961

92. F. M. Noonan, A. L. Alexander, and J. E. Cowling, The Properties of Paint as Affected by UV Radiation in a Vacuum, NRL 5503, Part I, July 1960

93. F. M. Noonan, A. L. Alexander, and J. E. Cowling, The UV Degradation of Organic Coatings III – Effect on Physical Properties, WADD TR-60-703, Part III, December 1960

94. P. R. Cowley and E. J. Melville, "Photo-Degradation of Polymethylmethacrylate," Proc. Roy. Soc. A210, 461–481, 1952; A211, 320–334, 1952

95. L. D. Jaffe and J. B. Rittenhouse, Behavior of Materials in Space Environments, JPL TN 32-150, November 1961

96. J. E. Cowling, A. L. Alexander, and F. M. Noonan, "The Design of Organic Coatings for the Aerospace Environment," Coatings for the Aerospace Environment, WADC TR-60-773, Wright-Patterson Air Force Base, Ohio, July 1961

97. J. C. DeVos, "A New Determination of the Emissivity of Tungsten Ribbon," Physica 20, 690, 1954

98. D. K. Edwards, "Measurement of Thermal Radiation Characteristics," Proc. of 1963 Symposium of Institute of Environmental Sciences, 1963

99. J. Strong, Procedures in Experimental Physics, Prentice Hall, p. 376, 1938

100. G. E. Pride, "A Reflectance Measuring Attachment for the Beckman Spectrophotometer," J. Opt. Soc. Am. 36, 510, 1946

101. E. E. Kerlin, Investigation of Combined Effects of Radiation and Vacuum and of Radiation and Cryo-Temperatures on Engineering Materials, Vol. I, "Radiation – Vacuum Tests," FZK-161-1, 5 January 1963

102. E. T. Smith, Investigation of Combined Effects of Radiation and Vacuum and of Radiation and Cryo-Temperatures on Engineering Materials, Vol. II, "Radiation – Cryo-Temperature Tests," FZK-161-2, 5 January 1963

103. P. I. Dickson and M. C. Jones, Infrared Reflectances of Metals at Cryogenic Temperature: A Compilation From the Literature, NBS Technical Note 348, 1967

104. R. B. Gillette, et al., "Effects of Protons and Alpha Particles on Thermal Properties of Spacecraft and Solar Concentrator Coatings," p. 413 in Progress in Astronautics and Aeronautics, 18, ed. G. B. Heller 1966

105. B. Gillette and R. R. Bron, Space Radiation Tests on Reflecting Surfaces, Final Report, D2-36359-1, the Boeing Company, June 1965

106. Douglas, N. J. et al., "Solar Wind-Plus-Ultraviolet Studies on Spacecraft Thermal Control Coatings Using In Situ Optical Property Measurement Techniques," Proc. of Space Simulation Conf. Philadelphia, Pa., September 1967

107. R. B. Gillette, "Proton Radiation Effects on Solar Concentrator Reflective Surfaces," AIAA Paper 67-341, AIAA Thermophysics Specialist Conference, New Orleans, La., 17–20 April 1967

108. J. T. Bevans, A. D. LeVantine, and E. E. Luedke, Final Report on Satellite Materials and Environmental Control Systems Investigations, AFBMD-TR-61-12, December 1960

109. D. L. Anderson and G. N. Nothwang, Effects of Sputtering With Hydrogen Ions on Total Hemispherical Emittance of Several Metallic Surfaces, NASA TND-1646, January 1963

110. R. A. Miller and F. J. Campbell, Effects of Low Energy Protons on Satellite Thermal Control Coatings, Report on NRL Progress, Naval Research Laboratory, pp. 11–14, May 1966

111. L. A. Frank, "Several Observations of Low-Energy Protons and Electrons in the Earth's Magnetosphere with OGO 3, " J. Geophys. Res. 72 (7), 1 April 1967

112. J. I. Vette et al, Models of the Trapped Radiation Environment, NASA SP-3024, 1966

113. R. A. Breuch and H. E. Pollard, "Nuclear Environmental Effects on Spacecraft Thermal Control Coatings," Paper No. 39, pp. 365–379 in Symposium on Thermal Radiation of Solids, NASA SP-55, ed. S. Katzoff, 1965

114. J. Gilligan, T. Greening, and M. Sibert, "Research on Passive Thermal Control Coatings," 7th Meeting of Refractory Composites Working Group, USAF, Palo Alto, Calif., 12–14 March 1963

115. C. Mook, NASA Headquarters, Washington, D. C., Personal communication, April 1967

116. C. F. Schafer, "Thermal Control Coating Degradation Data From the Pegasus Experiment Packages," AIAA Paper 67-331, AIAA Thermophysics Specialist Conference, New Orleans, La., 17–20 April 1967

117. R. K. Refley, Temperature Control. A Case History of the Mariner Spacecraft, NASA-CR-74020, Jet Propulsion Laboratory, California Institute of Technology, Pasadena, Calif., March 1965

118. W. S. Slemp, NASA Langley Research Center, Hampton, Va., Personal communication, April 1968

119. G. V. Bull, On the Impact of Pellets With Thin Plates; Theoretical Considerations, ADL 63270-03-01 (AD 273236), Arthur D. Little, Inc., Cambridge, Mass., 1962

120. P. D. Gray et al., Rockets in Space Environment. Phase II: Individual Component Investigation, AGD Report No. 2263 (ASTIA 278055), 11 April 1962

121. R. B. Merrill, "The Effects of Micrometeoroids on the Emittance of Solids," Paper No. 45, pp. 453 – 472 in Symposium on Thermal Radiation of Solids, NASA SP-55, ed. S. Katzoff, National Aeronautics and Space Administration, Washington D. C., 1965

122. J. F. Friichtenicht, Study of Micrometeoroid Damage to Thermal Control Materials, NASA CR-62810, Space Technology Laboratories, Redondo Beach, Calif., February 1965

123. J. F. Friichtenicht et al., Study of Micrometeoroid Damage to Thermal Control Materials, NASA CR-84989, TRW Systems, Redondo Beach, Calif., October 1966

124. E. E. Luedke, Summary Report on Optical and Thermal Control Coatings Degradation of the Apollo Spacecraft, Report No. 05952-6182-R00, TRW Systems, October 1967

Chapter 8

OPTICAL MATERIALS

J. B. Singletary

Optical elements have been successfully incorporated into such spacecraft systems as communications, navigation, weather observation and astronomical observations as well as planetary and lunar probes. As is true of other types of spacecraft construction materials, careful attention is required to select optical materials that are stable in the space environment. In this chapter some of the effects of the space environment on representative optical materials will be examined.

In this chapter, the optical materials considered are those used to transmit or reflect radiation ranging from ultraviolet through the visible and infrared regions of the spectrum. Other materials whose function is the selective absorbtion and reemission of radiation to establish desired thermal balances are also termed optical materials and are frequently referred to as such in the literature. These latter materials, however, are treated separately in Chapter 7 under the heading of thermal control materials, and are not included here.

The earliest application of optical materials for space usage was probably the ultraviolet spectrographs carried aloft by captured V-2 rockets shortly after World War II. Photographic systems were later mounted on rocket probes and photographs taken of the Earth from several hundreds of kilometers altitude. Some of the more spectacular results of space photography have resulted from the various lunar programs culminating in the systematic mapping by photography of large areas of the Moon's surface from the Lunar Orbiter spacecraft. The farthest penetrations away from the Earth were the infrared radiometer carried to Venus by the Mariner 2 vehicle and the Mars photography system on Mariner 4. Many of these spaceborne optical elements have been constructed of conventional glasses and optical materials (Ref. 1); others have made use of special materials resistant to space environmental effects.

The application of optical systems may be conveniently grouped into guidance applications, in which the position of a star, planet, or other body is sensed in order to maintain vehicle attitude and position; into surveillance applications, in which a view is maintained toward space to detect and track missiles, other space vehicles, or celestial bodies.

The performance of optical materials in space is liable to degradation by much the same environmental factors that affect other spacecraft materials. These may be grouped as follows:

- Sublimation, decomposition, and offgassing of materials in vacuum and the possible deposition of products from such actions onto optical surfaces
- Cratering, spalling, and abrasion of optical surfaces by meteoroids
- Radiation- and charged particle-induced discoloration and decomposition of transmitting materials
- Changes in optical properties due to extreme temperature conditions

8.1 EFFECTS OF THE VACUUM ENVIRONMENT

The usual effects on materials associated with the vacuum environment of space are those of sublimation, and offgassing of the material or of its molecular fractions following decomposition or dissociation. A related effect is the deposition upon the material in question of offgassing products from nearby components. In the case of materials used in optical applications, the actual loss of matter as a result of vacuum exposure is likely to be of very small importance since the optical components will be constructed either of metals or of glass or ceramic materials. Both these categories of materials sublime only very slowly in space. Their rate of loss of matter has been examined and discussed in more detail in Chapter 15 of this volume in connection with their application as structural materials.

Of greater potential concern in the vacuum environment are those subsidiary materials used in connection with optical materials. For instance, a conventional material for cementing multielement lenses, Canada balsam, would likely be unsatisfactory for space usage. Such cements as the RTV silicones used for attaching solar cell covers might be indicated for this application. However, the lens designer must be concerned also with the refractive index of any cement; its selection is a more complex problem than in case of a cement for a plain transmitting element such as a solar cell cover.

The seals used for mounting optical elements such as lenses must also be carefully considered for possible contribution of offgassing contaminants. The concept of volatile condensable material (VCM) content is useful in selection of sealing materials as well as other polymeric spacecraft constituents. Tabulations of VCM content such as those of Ref. 3 and in Chapters 10 and 11 should be referred to when selecting polymeric materials which will be near optical elements. The need for such careful design was well illustrated by experience with the spacecraft windows in the Gemini vehicles. Several Gemini missions experienced an unexplained clouding of the spacecraft windows which was believed to be caused by exhaust gases from the launch vehicle engines or dirt and moisture in the air during the boost phase. However, protective covers to shield the windows through powered flight had failed to eliminate the problem. The primary reason (Ref. 4) for the problem was the offgassing of the silicone rubber used to seal the window panes in their mountings. As the silicone continued to cure under

the influence of ascent heating, gas was emitted and recondensed on the surface of the windows. Extended post curing of the silicone rubber seal at higher temperature in vacuum was successful in solving the problem in Gemini 12. A detailed analysis of sealing materials appears in Chapter 11; this problem is mentioned here only to point out the need for the optical systems engineer to be concerned, not only with the optical materials, but also with the choice of nearby materials which might possibly sublime and redeposit on optical surfaces.

8.2 SURFACE DEGRADATION IN THE SPACE ENVIRONMENT

The surface condition of optical materials is of primary importance to their function, particularly in the case of mirror elements, and must be more carefully preserved than in the case of materials whose successful functioning depends only on their bulk properties. The possibilities of erosion of optical surfaces by meteoroid bombardment and sputtering by ion bombardment have been of continuing concern to space optical designers.

At the present time, it seems that meteoroid bombardment of optical surfaces does not present a major problem to interplanetary spacecraft provided the vehicle does not encounter a meteoroid shower. The meteoroid flux in deep space appears not sufficient either to abrade the optical surfaces with small meteoroids or to crater the surface with larger particles. The cosmic dust detector on Mariner 4 registered approximately one impact per day of particles of mass greater than 10^{-13} gram on the two 22 cm $\times$ 22 cm detector plates (Ref. 5). The highest flux encountered was 3.3×10^{-4} particles/m^2-sec. Surface abrasion by meteoroids becomes more significant with deeper penetrations into regions of space containing greater particle densities such as the asteroid belts beyond Mars.

The low particle flux detected by Mariner 4 is consistent with the earlier estimates such as those of McKeown on the basis of satellite data (Ref. 6) which placed an upper limit of 100 Å/yr for erosion by dust particles. This would require about 8 yr to roughen a surface to a depth corresponding to a sufficiently large fraction of a wave length expected to cause a significant change in optical properties.

That experimental point in which the greatest reliance is being placed in the current manned spacecraft program is the experience with Gemini viewing windows. The results of one crater in all Gemini windows examined (Ref. 7) can be interpreted (Ref. 8) in terms of a much lower penetration probability for spacecraft hull materials as well as abrasion of optical surfaces than had previously been thought to be the case on the basis of microphone meteoroid detector data.

Another possible source of damage to optical surfaces is that of sputtering or erosion in which atoms or molecules are removed by impingement of high-energy particles. Redus (Ref. 9) has analyzed material removed by sputtering in the space environment. Calculations of the energies of atmospheric particles due to vehicular motion through space (the thermal energy of these particles is negligible in comparison) reveal that no sputtering will occur due to H, He, or He_2, but O_2, N_2, and N will be the prime

contributors. Tables 8-1 and 8-2 (from Ref. 9) give the estimated sputtering rates and the times required to remove 1 Å of metal from both orbital and escape vehicles at various distances from the earth.

Table 8-1

ESTIMATED RATE OF REMOVAL AND TIME TO REMOVE 1Å OF ALUMINUM BY SPUTTERING

Height (km)	Orbiting Vehicle		Escaping Vehicle	
	Rate (atom cm^{-2} sec^{-1})	Time (sec/Å)	Rate (atom cm^{-2} sec^{-1})	Time (sec/Å)
100	3.1×10^{16}	1.9×10^{-2}	3.4×10^{17}	1.8×10^{-3}
220	2.0×10^{13}	3.0×10^{1}	2.0×10^{17}	3.0×10^{-3}
700	2.2×10^{9}	2.7×10^{5}	3.4×10^{11}	1.8×10^{3}
2500	4.3×10^{5}	1.4×10^{9}	1.6×10^{8}	3.8×10^{6}

The sputtering discussed above occurs in addition to any which may be due to the solar plasma. Redus estimates that sputtering due to solar plasma from a quiet sun would remove about 30 Å/yr of silver and that a single solar flare would remove about 3 Å of silver. Though the number of solar flares per year is unpredictable, Redus estimates that the solar plasma (including solar flares) will remove 60 to 9.4×10^3 Å/yr of silver, 10^2 to 1.5×10^4 Å of copper, and 2.5×10^2 to 3.9×10^4 Å/yr of aluminum. The lower limits of these estimates imply no significant damage to reflecting surfaces in several years; the upper limits would correspond to appreciable damage in one year.

Table 8-2

ESTIMATED RATE OF REMOVAL AND TIME TO REMOVE 1Å OF SILVER BY SPUTTERING

Height (km)	Orbiting Vehicle		Escaping Vehicle	
	Rate (atom cm^{-2} sec^{-1})	Time (sec/Å)	Rate (atom cm^{-2} sec^{-1})	Time (sec/Å)
100	1.2×10^{16}	4.8×10^{-2}	2.3×10^{17}	2.5×10^{-3}
220	7.0×10^{12}	8.2×10^{1}	1.4×10^{17}	4.1×10^{-3}
700		∞	5.4×10^{9}	1.0×10^{4}
2500		∞	8.1×10^{5}	7.0×10^{8}

A space study of actual damage to surfaces which corroborates the more optimistic of the above estimates on meteoroid and sputtering erosion is that of the test coating which was installed on the OSO 1 satellite launched in March 1963. (Ref. 10) The test surface of this experiment consisted of an opaque aluminum film coated with 0.83 μ of SiO_2 and 100 Å of germanium coated over the SiO_2. Such a coating has a solar absorptance of about 0.4 and an α/ϵ ratio of about 3. If the 100 Å of germanium were removed, the solar absorptance would decrease to about 0.11 and the α/ϵ ratio would drop to about 0.8; and cause a large decrease in surface temperature. Germanium was used as the surface film because it absorbs only in the visible and not in the infrared. Therefore, the removal of such a thin germanium film changes only the solar absorptance and not the emissivity of the aluminum plus SiO_2 coating.

Over a period of 16 months following launch of the OSO 1 satellite, results of the experiment described above showed no evidence of deterioration by erosion or sputtering. Its solar absorptance was still at its initial value. Therefore, it may be concluded that for Earth satellites, erosion effects on thin films are insignificant.

8.3 RADIATION EFFECTS ON OPTICAL MATERIALS

The radiation environment of space (including the charged particle fluxes of electrons and protons) is the one of principal concern to many (but not all) spacecraft construction materials. Optical materials also may expect their greatest potential damage from this source. Although early work in this field was concentrated mostly on the damage to optical windows due to gamma rays and neutrons and much data is available on this subject (Ref. 11), more recent investigations have presented data on charged particle fluxes which more closely approximate the space environment. Some actual flight data is also beginning to become available (Ref. 12).

Those optical materials used for reflecting elements are not so likely to be damaged by space radiation; however, ionizing radiations of all types are capable of producing discoloration and loss of transparency of optical transmitting elements to a greater or lesser degree depending on the energy of the radiation, total flux, and type of material. Thus the optical reflectors or mirrors used in spacecraft may actually be less susceptible to radiation damage when designed as a front-silvered element since the metallic reflecting surface would serve to protect the glass or metallic substrate from the effects of radiation. Some glasses may begin to show coloration at doses of 600 R and nearly all glasses show a saturation of color at a level of 10^{10} R. Usually mechanical damage occurs at higher dose levels than this so that coloration is the limiting factor in design.

Coloring of glass or other transparent materials is thought to be caused when energetic bombarding particles release electrons from their equilibrium positions within the lattice, thus creating electron-hole pairs. Some of these electrons may become trapped at lattice vacancies and because they possess appropriate energy levels, create color or absorption centers which absorb electromagnetic radiation in the visible part of the spectrum. The addition of cerium to the glass may help to prevent formation of color centers, possibly through previous filling of some of the lattice vacancies. However,

irradiated cerium glasses have an absorption band in the ultraviolet region which must be taken into account. Cerium-stabilized glasses can maintain their transparency throughout the wavelength region from 0.4 to 0.7 μ under 10^6 R of cobalt-60 gamma rays and are still usable after 5×10^8 R (Ref. 13).

In some cases, other materials than glass may be preferred for such applications as viewing windows. In one study (Ref. 14) transparent materials normally employed in vehicular viewing systems were subjected to x-ray irradiation to determine how ionizing radiation affected their optical transmission. The materials tested were commercial-grade aluminate glass, polystyrene, plexiglass, allyl carbonate, and polyvinyl acetate. Figures 8-1 and 8-2 (Ref. 14) show the transmission of solar radiation at the surface of the earth as a function of dosage. Polystyrene was the least affected by radiation; the others became absorptive in the blue and ultraviolet regions. The advantages of using a plastic such as polystyrene as a window material where ionizing radiation may be encountered are obvious. However, the effects of other degrading factors may prevent such a choice.

An example of this latter situation is to be found in tests which were run on candidate materials for Apollo spacecraft windows (Ref. 15). In this case plastic materials showed a greater change in optical properties when exposed to a simulated space environment than the silica materials tested. For this study, nine samples of silica glass and transparent plastic materials were exposed to a combined environment of simulated solar radiation and charged particle flux of 50 keV protons at a rate of 1.57×10^{12} protons/cm^2-sec while being held in a vacuum of 10^{-7} to 10^{-9} Torr and cooled to maintain the specimens at room temperature. The simulated solar radiation was supplied by two sources, a xenon lamp source shaped to approximate the Johnson (Ref. 16) solar spectrum and a hydrogen discharge source simulating the extreme ultraviolet portion of the solar spectrum. Both these sources were run at a 7-1/2 sun intensity level. The protons were obtained from a Van de Graaff accelerator. Table 8-3 shows the data obtained from this study.

The silica materials performed considerably better than the plastics. Some of the plastic materials were degraded to the point of charring. It is believed that the plastics were subjected to a feedback effect in that once they had begun to darken from the radiations (probably the protons), increased absorption of the simulated solar radiation brought on their early degradation.

In another series of tests (Ref. 17) several prospective window materials were subjected to electron bombardment with generally the same favorable results for silica materials. However, although synthetic fused silica showed little sensitivity to electrons except in its ultraviolet transmission, some other silica materials varied considerably in their response. The results of this study are presented in Table 8-4 in terms of the broad band response of the materials. This is the transmission from wave lengths 0.40 μ to 1.20 μ as measured with a silicon solar cell detector and gives a good indication of the suitability of materials as solar cell covers as well as a general basis of comparison. In addition to synthetic silica, sapphire, and some radiation-shielding glasses showed

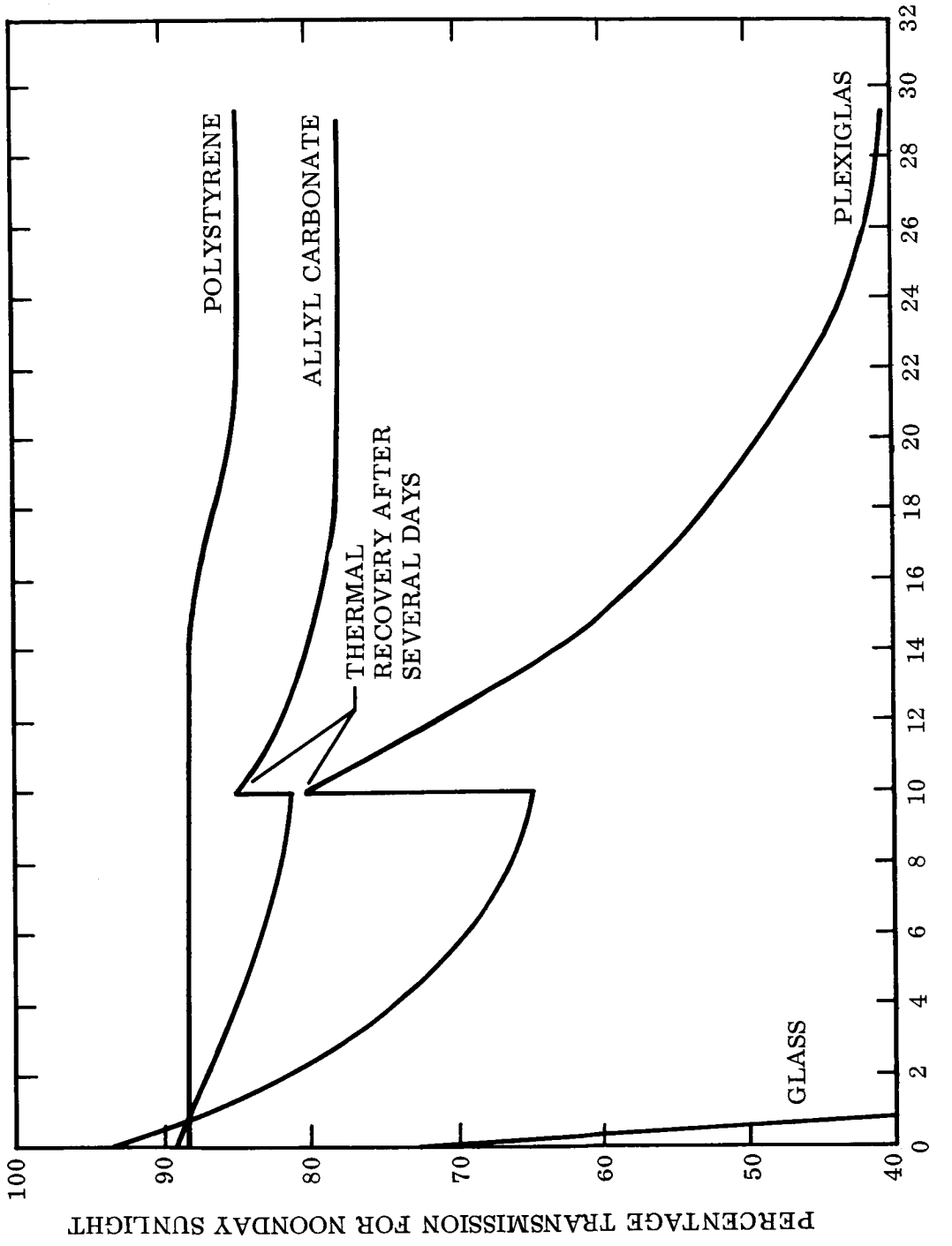

Fig. 8-1 Transmission of Various Materials After Irradiation With 150-kV X Rays for 10 hr

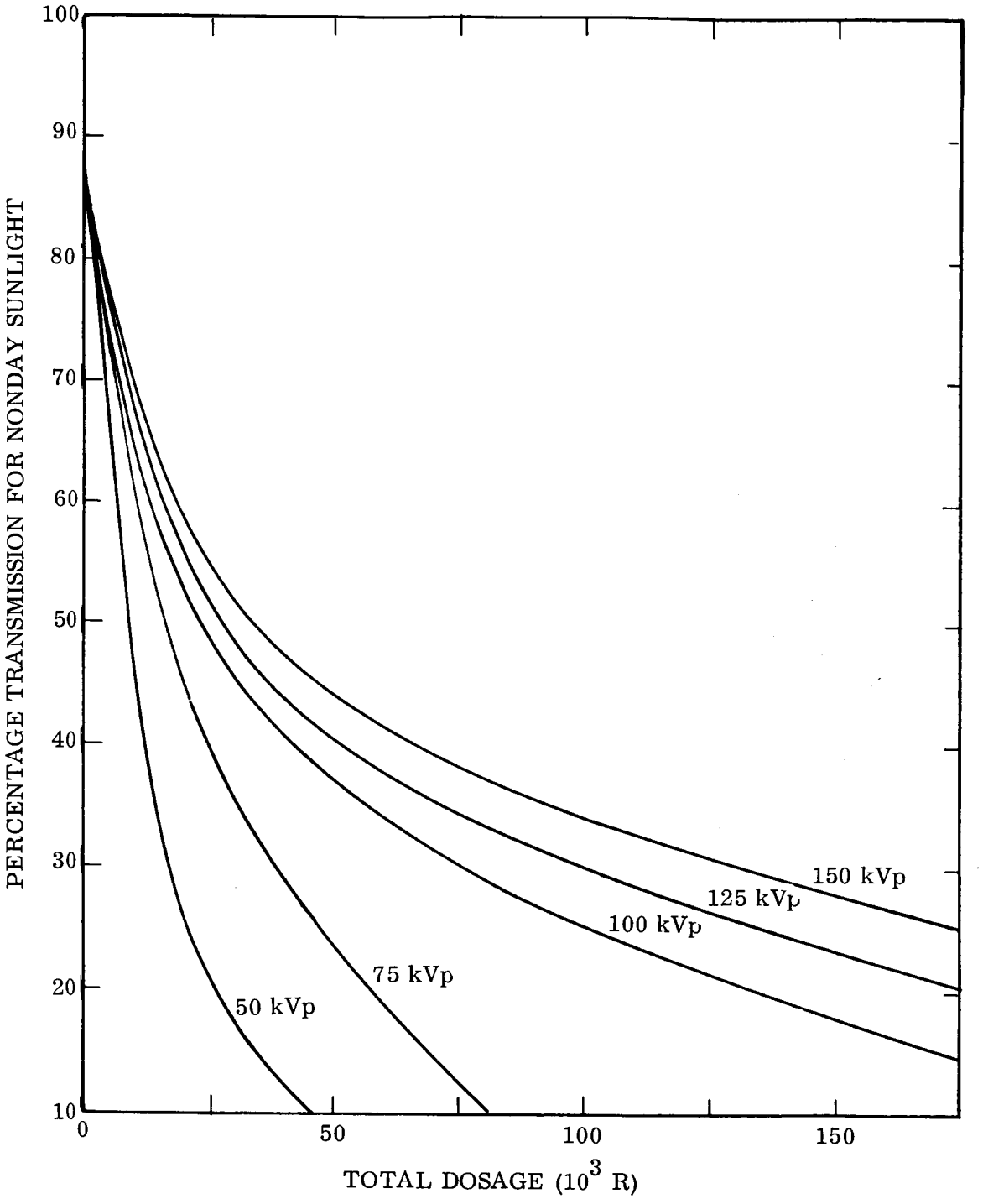

Fig. 8-2 Transmission of Commercial-Grade Alumino Silicate Glass After Irradiation by X Rays of Various Energies

Table 8-3

EFFECT OF SIMULATED SPACE RADIATION ON TRANSMITTANCE OF PROSPECTIVE APOLLO WINDOW MATERIALS

Window Material	Percent Transmission of 0.5 μ Radiation				Percent Transmission of 0.6 μ Radiation				Percent Transmission of 0.7 μ Radiation			
	Unirradiated Sample	Simulated Space Environment			Unirradiated Sample	Simulated Space Environment			Unirradiated Sample	Simulated Space Environment		
		10^{16} protons/cm^2	10^{17} protons/cm^2			10^{16} protons/cm^2	10^{17} protons/cm^2			10^{16} protons/cm^2	10^{17} protons/cm^2	
		14 sun-hr	170 sun-hr	340 sun-hr		14 sun-hr	170 sun-hr	340 sun-hr		14 sun-hr	170 sun-hr	340 sun-hr
Corning 7940, Uncoated, 1/2 in. Thick	89	86	83	82	91	87	85	85	89	87	84	86
Corning 7940 Coated, 11/16 in. Thick	91	89	81	84	95	87	81	81	93	81	69	71
Corning 1723 Coated, 1/4 in. Thick	99	93	–	77[a]	99	96	–	85[a]	92	87	–	79[a]
Owens-Illinois Inorganic Polymer 650, 3/16 in. Thick	94	59	52	48	95	74	69	64	97	82	77	71
Owens-Illinois Inorganic Polymer 100, 1/8 in. Thick	89	36	2	–	88	59	5	–	90	71	10	–
Stretched Plexiglass 1/4 in. Thick	91	22	2	–	92	40	2	–	91	47	2	–
Acrylic Sheet 1/4 in. Thick	89	34	0	–	92	67	1	–	98	87	1	–
Cross-linked Methacrylate 1/4 in. Thick	88	29	1[b]	–	91	53	1[b]	–	85	62	1[b]	–
Copolymer Styrene 5/16 in. Thick	79	15	2[c]	–	83	31	7[c]	–	78	36	12[c]	–

(a) Simulated space environment of 8×10^{16} protons/cm^2 and 340 sun-hours.
(b) Simulated space environment of 5×10^{16} protons/cm^2 and 135 sun-hours.
(c) Simulated space environment of 3×10^{16} protons/cm^2 and 39 sun-hours.

Table 8-4

RESULTS OF WIDEBAND TRANSMISSION TESTS ON SPACECRAFT WINDOW MATERIALS AFTER IRRADIATION

Manufacturer	Material	Thickness (in.)	Energy (MeV)	Dose (electrons/cm^2)	Wideband Transmission Loss (%)
Linde Co., Div. of Union Carbide Corp.	Linde sapphire	0.080	1.2	2.7×10^{15}	0
		0.120	1.2	1.0×10^{17}	0
		0.040	.30	2.7×10^{15}	0
Engelhard Ind. (Amersil Quartz Div.)	Suprasil II Synthetic fused silica	0.0625	1.2	2.7×10^{15}	0
Corning Glass Works	Corning 7940 Synthetic fused silica (uv grade)	0.125	1.2	2.7×10^{15}	0
	Corning 7940 (optical grade)	0.125	1.2	2.7×10^{15}	0
		0.250	1.2	1.0×10^{17}	2.2
	Corning 7940 (coated)	0.060	1.2	1.0×10^{16}	0
Thermal American Fused Quartz Co.	Spectrosil A	0.125/3 pcs	1.2	2.7×10^{15}	0
	Spectrosil B	0.0637	1.2	2.7×10^{15}	0
Dynasil Corp.	Optical grade Synthetic fused silica	0.125	1.2	2.7×10^{15}	0
		0.125	1.2	1.0×10^{17}	1.5
		0.125	.30	2.7×10^{15}	0
Englehard Ind. (Amersil Quartz Div.)	Optical grade fused quartz	0.0625	1.2	2.7×10^{15}	1.8
	Homosil fused quartz	0.0625	1.2	2.7×10^{15}	2.1
	Ultrasil fused quartz	0.0625	1.2	2.7×10^{15}	6.43
	Infrasil fused quartz	0.0625	1.2	2.7×10^{15}	23.4
	Unknown grade fused quartz	0.0625	1.2	2.7×10^{15}	41.6
General Electric Co.	GE 104 fused quartz	0.0935	1.2	2.7×10^{15}	0.8
		0.0935	.30	2.7×10^{15}	1.1
	GE 105 fused quartz	0.0935	1.2	2.7×10^{15}	30.0
		0.0935	.30	2.7×10^{15}	5.3
	GE 106 fused quartz	0.0935	1.2	2.7×10^{15}	28.6
		0.0935	.30	2.7×10^{15}	5.3
	Natural crystal quartz	0.292	1.2	2.7×10^{15}	26.8
Corning Glass Works	Vycor fused quartz (Corning 1913)	0.250	1.2	1.69×10^{15}	58.9
	Corning 8362 Nonbrowning lead glass	0.0625	1.2	2.7×10^{15}	2.4
	Corning 8363 High-density lead glass	0.0625	1.2	2.7×10^{15}	0
	Corning 8365 Nonbrowning lime glass	0.0625	1.2	2.7×10^{15}	0
	Corning 0211 Micro-Sheet Silica glass	0.006	1.2	2.7×10^{15}	1.8
	Corning 0211 Micro-Sheet Silica glass	0.026	1.2	2.7×10^{15}	7.6
	Corning 0211 Micro-Sheet Silica glass	0.026	1.2	1.0×10^{17}	12.2
Pittsburgh Plate Glass Co.	Solex Heat-absorbent glass	0.250	1.2	2.7×10^{15}	2.7
	Plate glass Soda lime plate glass	0.250	1.2	1.69×10^{15}	26.0
Blue Ridge Glass Corp.	Feurex Heat-resistant borosilicate glass	0.250	1.2	2.7×10^{15}	25.2

almost no damage in wide-band transmission at total doses up to 2.7×10^{15} electrons/cm^2 Examination of the complete spectral transmission curves for some of these materials, which are given in full in Ref. 18, indicates the following responses:

Sapphire showed almost no change in its transmission (at most about 1%) over the range from 0.3 to 3 μ when irradiated with 1×10^{17} electrons/cm^2. A sample of synthetic fused silica which remained unaffected throughout the infrared region, began to have its transmission reduced (up to 5%) in the visible region, and was more affected in the ultraviolet with a transmission at 0.3 μ of 92% when unirradiated, 88% when bombarded with 1×10^{15} electrons/cm^2, 80% after 1×10^{16} electrons/cm^2 and 60% after 1×10^{17} electrons/cm^2. The degree of change in transmission with irradiation was quite different in various samples of fused quartz. Vycor fused quartz was damaged so severely after 1.69×10^{15} electrons/cm^2 that it was not irradiated further. At this level, its transmission in the visible at 0.6 μ had decreased from over 90% to less than 10%.

A sample of radiation shielding glass, Corning 8365 nonbrowning lime glass, showed high resistance to irradiation with no change in transmission after 2.7×10^{15} electrons/cm^2 in the visible and infrared regions (the material does not transmit in the ultraviolet). Common glasses showed greater losses of transmission; that for a borosilicate glass is shown in Fig. 8-3 Ref. 17 and for an aluminosilicate glass in Fig. 8-4 (Ref. 18). The data of Fig. 8-4 were taken while the specimen was held at a vacuum of 10^{-6} Torr.

Measurements by Heath and Sacher (Ref. 19) corroborate the high resistance of sapphire and fused silica to electron irradiation and also present data on several crystal materials for ultraviolet transmission. These data are shown in Table 8-5. The poor resistance of lithium fluoride to electron irradiation would appear to rule it out for use in space optics while conversely barium fluoride seems to be highly suitable for this environment.

In a later experiment (Ref. 20) these ultraviolet transmitting materials were irradiated with 3 to 4.6 MeV protons to a total flux of 8.25×10^{10} protons/cm^2. The results of the proton exposure were similar to the electron experiments described above except that transmittance changes for each of the materials was somewhat less for proton irradiation than for the electron irradiation.

At the other end of the visible spectrum, data on materials transmitting in the infrared is still scarce. In an early experiment, Lusk (Ref. 21) subjected fifteen common infrared optical materials to various doses of gamma-radiation. The effects of this radiation on the infrared transmission of these materials is presented in Table 8-6 (Ref. 24). Figure 8-5 (Ref. 21) presents the changes in spectral transmission produced by gamma-irradiation of four of the materials used in space infrared optics. In a rough sense, the data for MgF_2 from Fig. 8-5 does correlate with the electron bombardment experiments shown in Table 8-5 in the spectral region in which they overlap. However, one must evaluate the effects produced by all types of radiation under varying conditions to obtain an accurate estimate of the reliability of a material in a space environment. It does appear that these materials would be stable in the space environment.

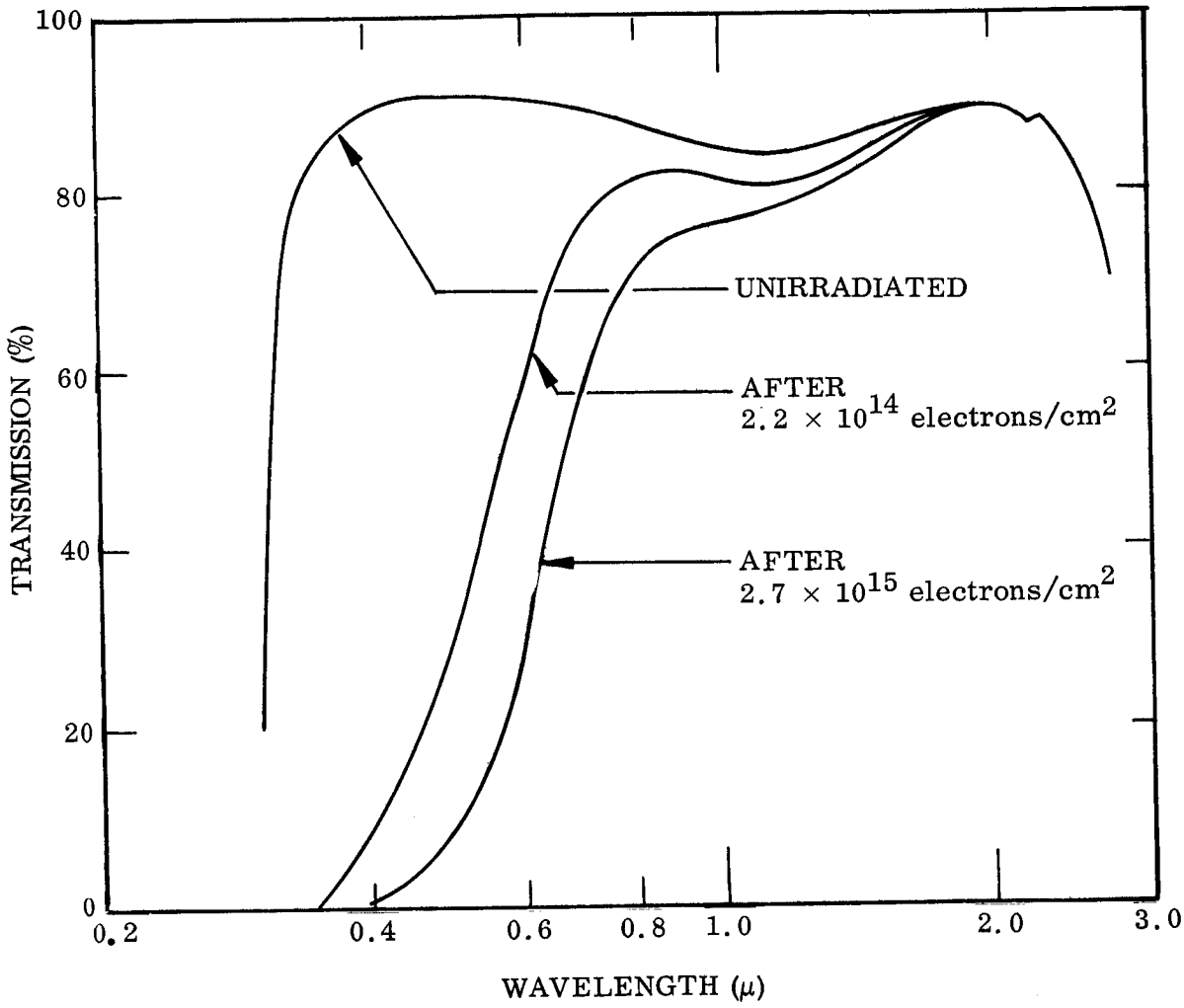

Fig. 8-3 Spectral Transmission of Feurex Before and After Irradiation With 1.2-MeV Electrons

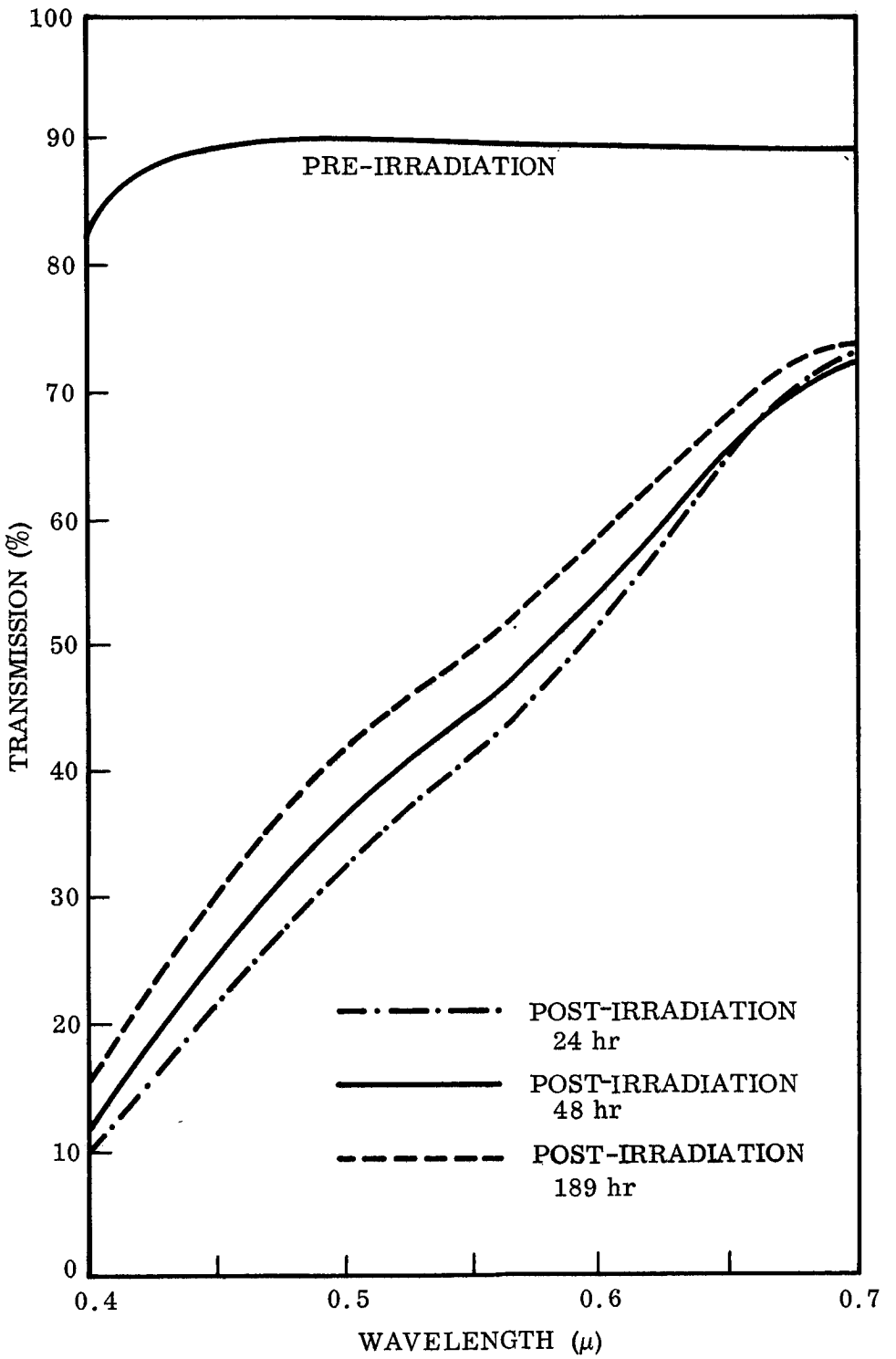

Fig. 8-4 Transmittance of Corning Type 1723 Glass After Irradiation With 1.9-MeV Electrons to an Integrated Flux of 1×10^{13} Electrons/cm^2

Table 8-5

EFFECT ON TRANSMISSION OF INFRARED RADIATION BY VARIOUS MATERIALS AFTER IRRADIATION WITH 10^{14} electrons/cm^2 AT 1.0 MeV AND 2.0 MeV

Material / Wavelength	Percent Transmission					
	1.3 μ	1.5 μ	1.75 μ	2.0 μ	2.5 μ	3.0 μ
LiF						
Unirradiated	62	77	86	87	91	92
Irradiated	6	2	0	0	0	38
MgF_2						
Unirradiated	56	70	86	91	95	95
Irradiated	55	69	82	79	41	82
CaF_2						
Unirradiated	51	63	80	85	90	92
Irradiated	45	55	53	48	64	60
BaF_2						
Unirradiated	–	58	78	82	90	90
Irradiated	–	58	78	82	87	87

Table 8-6

CHANGE IN INFRARED TRANSMISSION EFFICIENCY DUE TO RADIATION

Material	Thickness (mm)	Radiation Level (R)	Percentage Change in Transmission Efficiency (%)													
			1 (μ)	2 (μ)	3 (μ)	4 (μ)	5 (μ)	6 (μ)	7 (μ)	8 (μ)	9 (μ)	10 (μ)	11 (μ)	12 (μ)	13 (μ)	14 (μ)
Germanium Single Crystal (34.0 ohm-cm)	6.3	10^8			0	0	0	0	0	0	0	0	0	-2	-2	-2
Silicon Single Crystal	6.3	10^8		0	0	0	0	0	0	0	0	0	0	0	0	0
Silicon Boron doped	6.3	10^8	-6	-4	-4	-4	-4	-4	-6	-5	-14	-14	-8	-8		
Silicon Coated SiO for 4 μ	2.5	10^6		+14	+2	+1	-2	-5	0	0	0	0	0	0		
		10^8		+10	+1	+2	-8	-9	0	0	0	0	0	0		
Kodak 80-20 Arsenic modified Selenium	4.0	10^8	0	-2	0	-1	-2	0	-2	-2	-2	-2	-2	-4		
Kodak MgF_2	2.0	10^6	-32	-32	0	-6	-8	-4	-10	0	0					
		10^8	-32	-34	-6	-18	-14	-9	-13	-3	0					
Spinel	2.3	10^8	-5	-4	-6	-4	-2	-20								
Corning $CaAl_2O_3$ X-745 pm	2.0	10^8		-5	0	-2	0	0								
Corning 0160 Glass	2.0	10^8	-15	0	-2	+6										
Corning Pyrex 7740	2.1	10^8	-10	-6	-8	-2										
As_2S_3	3.3	10^6	-9	-10	-8	-15	-14	-12	-9	-8	-1	-14	-8	-2		
		10^8	-26	-14	-11	-16	-14	-15	-13	-11	-5	-16	-10	-4		
Mg O	5.0	10^8	-10	-8	-4	-4	-4	-6	-2	0	0					
Lox-Grade Kel-F	2.3	10^8	-6	-5	-14	0										
AgCl	6.3	10^6	0	-4	-4	-2	-6	-14	+6	+21	+10	+6				
		10^8	0	-4	-4	0	-4	-10	-6	-2	-3	-3				
Sapphire	2.0	10^8	-12	-2	0	-4	-4	-12								

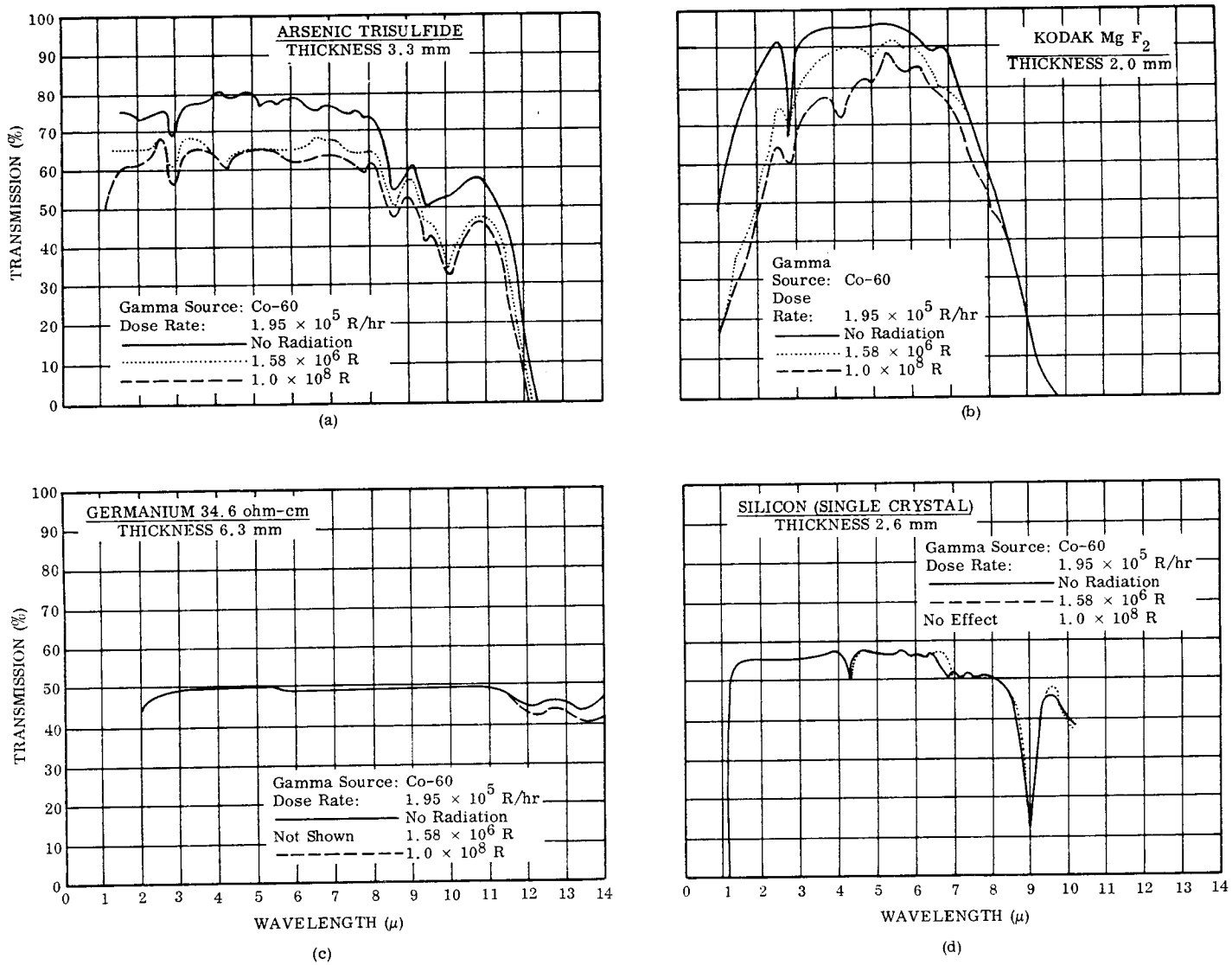

Fig. 8-5 Effects of Radiation on Transmission Efficiency of Four Materials Presently Used in Infrared Systems for Space Vehicles: (a) Arsenic Trisulfide, (b) Magnesium Fluoride (Similar to the Material Known Commercially as Intran AB-1), (c) Germanium, and (d) Single-Crystal Silicon

Both silicon and germanium are used extensively in infrared optics. An electron irradiation of 1.5 MeV induces an absorption band at 12 μ which has been associated with an oxygen impurity in silicon (Ref. 22). Vavilov (Ref. 23) found an increase in transparency in the 2.2 to 7 μ range for silicon irradiated with 1 MeV neutrons. The absorption coefficient was > 0.1 cm^{-1}. This increased transparency region is more extensive, as shown in Fig. 8-6, which is taken from Ref. 24 where it is discussed in detail.

Solar cell covers probably account for the greatest use of optical materials on spacecraft. The covers serve three major purposes. They provide protection for the sensitive silicon photovoltaic modules from damage in mishandling; although the cover material is susceptible to damage by rough usage, it is less so than the silicon semiconductor material. They also provide temperature control to the solar array because the emittance of the cover surface can be controlled by the use of antireflectance coatings. In some cases the cover sheets are attached directly to the solar cell silicon element with a compatible adhesive. This is the design most generally used. In some cases the cover sheet is held in a metal framework and is spaced away from the silicon element. In this case, the greenhouse effect has to be considered in the design and selection of materials with correct thermal radiation and conduction properties to compensate for solar heating, to ensure efficient operating temperatures for the solar array. This type of construction was used in some Vanguard, Explorer, and Telstar satellites. The third function of the cover sheet is to protect the sensitive solar cell element from cosmic dust, micrometeorite damage, and radiation damage. In the case of the cemented cover sheet, filter coatings are applied which also protect the adhesive from radiation damage, particularly UV radiation damage to the adhesive.

The lightest and most economical solar cell cover sheet material is the 6-mil thick fused silica microsheet. The material in common usage is Corning 0211 with a blue filter (OCL 207) and a magnesium fluoride antireflectance coating. This cover material is susceptible to radiation damage. Laboratory tests have shown that 500 hr in simulated sunlight (ultraviolet light from a xenon source) of five times the intensity of normal sunlight caused the glass to turn brown. A flux of 5×10^{10} electrons/cm^2 and 1 MeV energy caused a change of 4% in the solar cell output of a module covered with microsheet.

Some orbit conditions and planned mission lifetimes will permit the selection of microsheet as a solar cell cover material. The Orbiting Geophysical Observatory (OGO) and Pioneer 6 satellites designed by TRW Systems had 6-mil thick microsheet to cover solar cell modules. For OGO, the designers estimated an allowable 20 to 25% degradation of solar cell output during the mission. Microsheet was also used in Explorer 29 and Lunar Orbiter.

A fused silica (quartz) cover sheet 0.04-in. thick will shield against 400 keV electrons; 0.07 in. of quartz will shield against 800 keV electrons. Electron fluxes of 10^{14} to 10^{16} electrons/cm^2 cause slight coloration in quartz. At 22 MeV quartz cover sheet darkened with 2×10^{13} protons/cm^2. However, protons cannot be completely shielded with quartz, 0.12 in. of quartz will shield out all protons less than 20 MeV. These

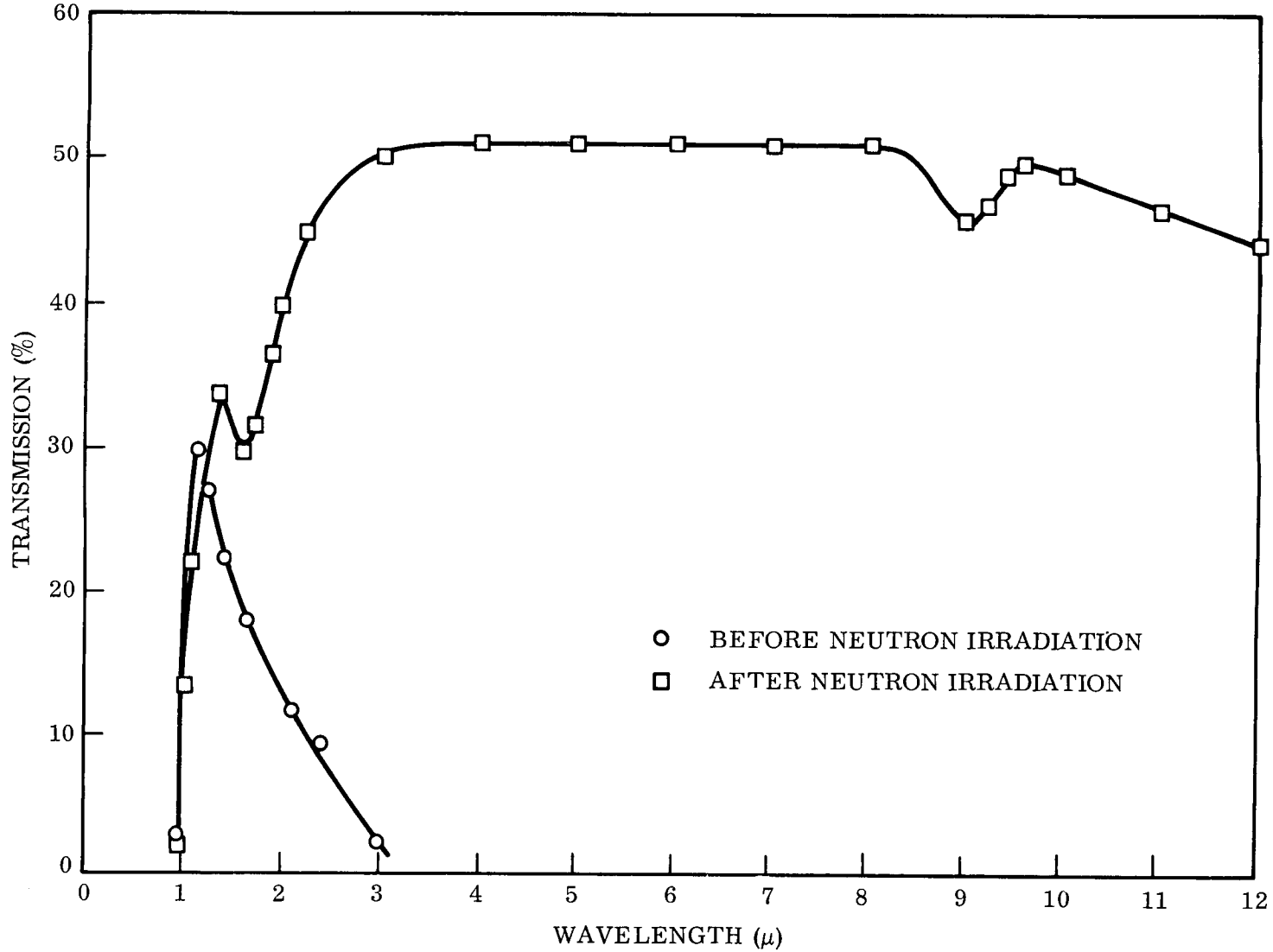

Fig. 8-6 Transmission Versus Wavelength for Irradiated and Unirradiated Silicon

results are from laboratory simulation studies (Ref. 25). Up to 500 hr and five times the sun intensity in simulated solar ultraviolet radiation caused no change in the transmittance of quartz.

Synthetic sapphire is the most radiation resistant solar cell cover sheet material. Simulation tests have shown that there was no detectable change in transmittance after 500 hr in five times the sun intensity in simulated solar ultraviolet radiation. A thickness of 0.04 in. of sapphire showed no detectable change when irradiated with 3×10^{12} protons/cm^2 at 19 MeV. A thickness of 0.030 in. of sapphire has a stopping power of 18 MeV for protons.

Results of the solar cell experiments on Explorer 15 with 10-, 30-, 50-, and 80-mil thickness of sapphire on n-on-p silicon modules gave anomalous indications of voltage loss. Such discrepancies may not have resulted from variation in the behavior of the cover or the cell module materials but might have been caused by non-uniform degradation of the adhesive. The behavior of adhesives under irradiation is discussed more fully in Chapter 10.

Fused silica, Corning 7940, has been recommended at Lockheed Missiles & Space Company for most satellite solar cell cover sheet applications. The thicknesses recommended are 0.006 in. for low orbits and 0.020 in. for higher orbits where electron and proton radiation damage are expected. The adhesive is either General Electric Silicone LTV 602 or Dow Corning Sylgard 182; the magnesium fluoride antireflectance coating and the OCL 207 (Optical Coatings Laboratory, Inc.) blue filter are also recommended (Ref. 25).

8.4 EFFECTS OF HIGH TEMPERATURES ON OPTICAL MATERIALS

The temperature which is expected to be attained by optical materials and components on spacecraft will probably be rather closely controlled by active or passive thermal control systems. However, since it may not always be possible to design the thermal control desired or since a control system may fail in usage, it is useful to examine the effects of elevated temperatures on optical materials. Spacecraft optical materials may also be exposed to high intensity thermal radiation as a consequence of nuclear device detonations (Refs. 26, 27).

A determination has been made of some physical properties of available glasses that might be used as window materials in high performance aircraft or in spacecraft (Ref. 28). The Young's modulus was measured as a function of temperature both for two chemically strengthened glasses and for two thermally tempered glasses. These data are presented in Figs. 8-7 and 8-8.

As part of its continuing research program, the U.S. Defense Atomic Support Agency is determining "degrees of degradation in functional properties of optical and infrared materials and components as a result of exposures to simulated nuclear weapon thermal pulses" (Ref. 27). The work reported in Ref. 27 consisted in exposing several specimens of optical materials to a thermal time profile corresponding to that given for a

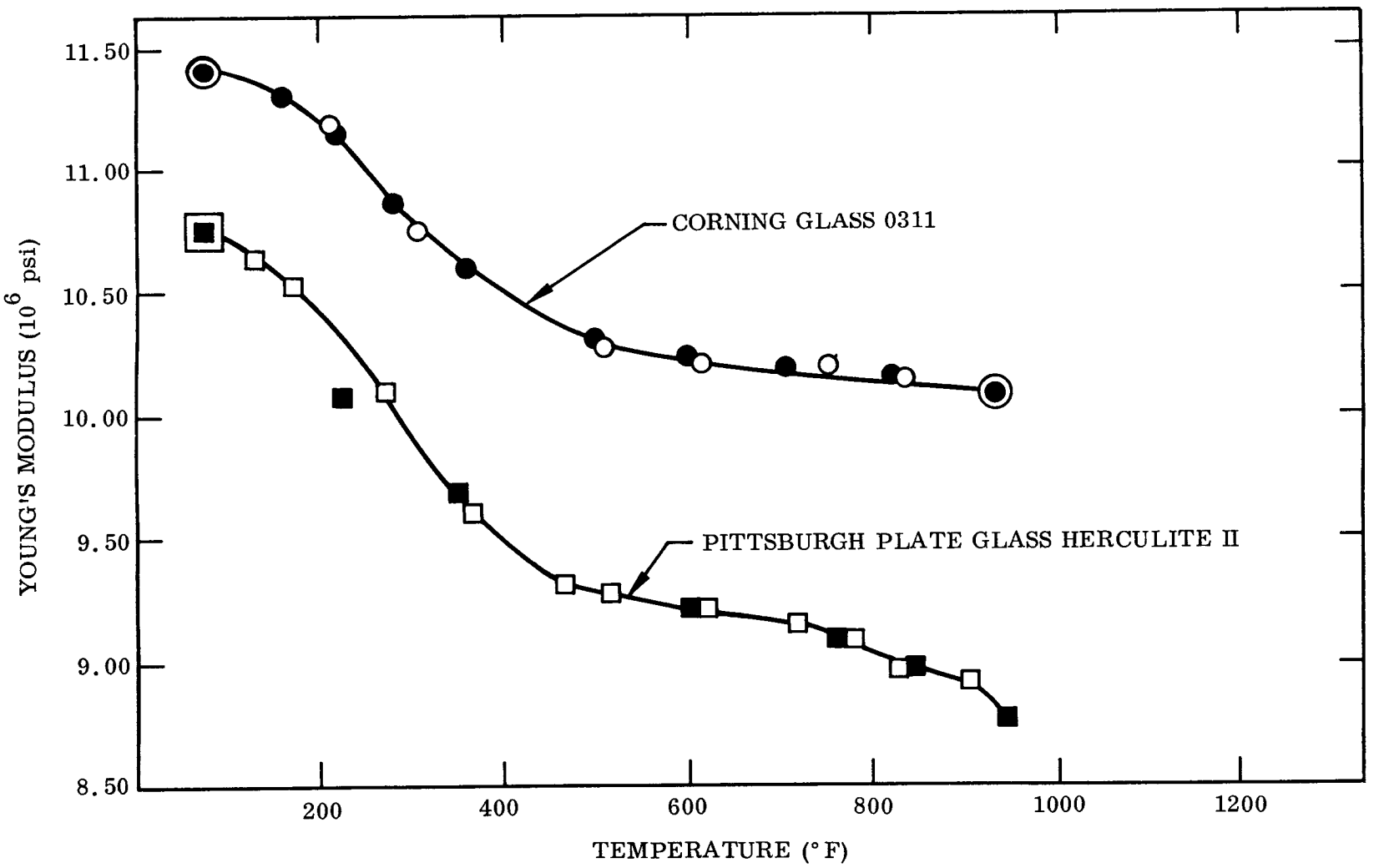

Fig. 8-7 Young's Modulus at Elevated Temperatures for Chemically Strengthened Glass

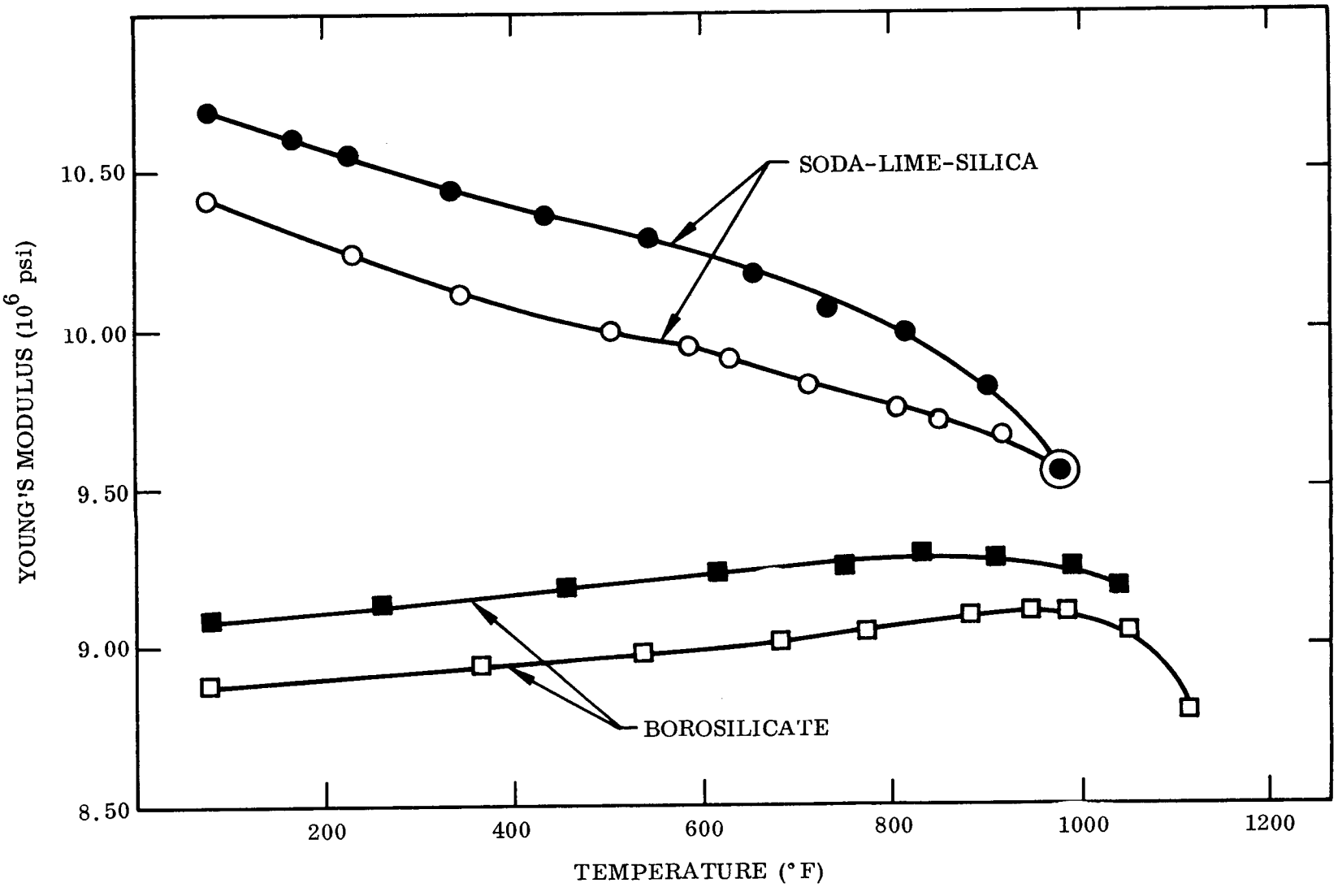

Fig. 8-8 Young's Modulus at Elevated Temperatures for Thermally Tempered Glass

nuclear device thermal pulse in Glasstone (Ref. 29). Irradiation was on one side of the material only. The results are presented in Tables 8-7 and 8-8,taken from Ref. 27. Of the materials tested in this study, it was concluded that the image converter tubes and lead sulfide detectors were most susceptible to permanent damage, while transient degradation was likely to be most noticeable in the silicon photovoltaic cells and photodiodes and in the lead sulfide detectors.

Table 8-7

DAMAGE TO OPTICAL MATERIALS EXPOSED TO HIGH-INTENSITY THERMAL RADIATION

Material	MIL-SPEC	H_{max} (cal/cm^2/sec)	Q (cal/cm^2)	t_{max} (sec)	Effect
Polaroid Filter	MIL-F-21424	22.0	13.8	0.32	No damage
		30.5	18.9	.32	Partial discoloration
		44.0	27.4	.32	Polaroid damaged – glass cracked
		10.0	19.9	1.02	No damage
		14.5	28.3	1.02	Partial discoloration
		22.0	42.9	1.02	Bubbling and scorching of material
Red Filter	MIL-F-12717	44.0	27.4	.32	No damage
		21.4	41.5	1.02	No damage
		34.1	67.1	1.02	Glass cracked
		42.3	82.5	1.02	Glass cracked
Neutral Density (0.1% transmission)	MIL-F-12717	30.8	19.6	.32	No damage
		44.0	27.4	.32	Glass cracked
		8.4	16.8	1.02	No damage
		12.8	25.4	1.02	Glass cracked
Neutral Density (10% transmission)	MIL-F-12717	44.0	27.4	.32	No damage
		21.1	41.9	1.02	No damage
		30.7	61.1	1.02	Glass cracked
		42.0	83.5	1.02	Glass cracked
Polaroid Filter	MIL-F-21424	14	33.9	1.01	Discolored
		21	50.9	1.01	Discolored
		27.6	66.9	1.01	Material burned and separated from glass

Note:
Red, Amber and Neutral Filters: No damage when exposed up to 131 cal/cm^2.
Aluminized Mirrors (Front Surface): No damage when exposed up to 218 cal/cm^2.

Dielectric Beamsplitters (ZnS and MgF_2), Cemented Doublets, and Aluminized Front Surface Mirrors: No damage when exposed up to 85 cal/cm^2.

Table 8-8

DAMAGE TO INFRARED MATERIALS EXPOSED TO HIGH-INTENSITY THERMAL RADIATION

A. Image Converter Tubes - S1 Surface

Tube No.	H (cal/cm^2-sec)	Q (cal/cm^2)	t_{max} (sec)	Ratio of Post- to Pre-exposure Conversion Index	Visual Observation
1	27.5	54.7	1.02	0	Cathode destroyed
2	14.3	28.4	1.02	.78	Central part of cathode destroyed
3	11.0	21.8	1.02	.75	No damage
3	11.0	21.8	1.02	.95	Exposed with 16 kV on tube – no damage
4	31.2	19.4	.32	.71	Central part of cathode destroyed
5	8.5	16.8	1.02	1.41	No damage
6	22.1	13.8	.32	1.00	Area near one edge of cathode destroyed
7	14.2	8.8	.32	1.21	No damage
3	4.4	8.7	1.02	1.32	No damage
8	8.5	5.4	.32	1.25	No damage
4	5.0	3.1	.32	1.00	No damage
9	0.08	.16	1.02	1.16	Exposed with 16 kV on tube – no damage

B. Lead Sulfide (PbS) Detectors

Cell No.	H (cal/cm^2-sec)	Q (cal/cm^2)	t_{max} (sec)	Ratio of Post-Exposure to Pre-exposure Response (%)
1	8.6	17.1	1.02	0
2	24.0	15.0	.32	0
3	4.6	9.1	1.02	16.7
4	12	7.5	.32	18.0
5	2.2	4.4	1.02	56.0
6	6.5	4.1	.32	58.5
7	1.0	2.0	1.02	63.5
8	2.7	1.7	.32	85.0
9	.44	0.9	1.02	75.0

C. Silicon Photovoltaic Solar Cells

Cell No.	H (cal/cm^2-sec)	Q (cal/cm^2)	t_{max} (sec)	Ratio of Post-Exposure to Pre-exposure Response (%)
1	29.6	58.9	1.02	61.0
2	14.1	28.1	1.02	95.0
3	43.8	27.3	.32	77.5
4	8.37	16.6	1.02	89.0
5	26.5	16.6	.32	100.0
6	13.8	8.5	.32	100.0
7	2.86	5.6	1.02	94.5
8	6.05	3.8	.32	100.0

D. Silicon Photodiode

Relative response remained 100% for all samples exposed to values of Q up to 51 cal/cm^2.

8.5 REFERENCES

1. C. Ellman, "The Surveyor Variable and Fixed Focal-Length Lenses, "SMPTE Preprint No. 102-34, Society of Motion Picture and Television Engineers 102nd Technical Conference, 17–22 September 1967

2. Purposely deleted.

3. R. F. Miraca and J. S. Whittick, Polymers for Spacecraft Applications, Final Report on JPL Contract 950745, Stanford Research Institute, Menlo Park, Calif., September 1967

4. "Beyond Gemini – Apollo Problems Loom," Technology Week 19, No. 21, 13–17, 21 November 1966

5. R. A. Becker, "Optical Problems of Interplanetary Space," Applied Optics 6, 955–962, May 1967

6. D. McKeown and M. G. Fox, ARS J. 32, 954–955, 1962

7. B. G. Cour-Palais, NASA Manned Spacecraft Center, Houston, Texas, personal communication, 22 April 1968

8. R. J. Naumann, The Near-Earth Meteoroid Environment, NASA TN D-3717, NASA Marshall Space Flight Center, Huntsville, Ala., November 1966

9. J. R. Redus, Sputtering of a Vehicle Suface in a Space Environment, NASA TN D-1113, Marshall Space Flight Center, Huntsville, Alabama, June 1962

10. J. T. Cox, G. Hass, and J. B. Ramsey, "Improved Dielectric Films for Optical and Space Applications," (AD 612134) pp. 193–205 in Proceedings of the 1964 Army Science Conference, (AD 611432), United States Military Academy, West Point, N. Y., June 1964

11. B. A. Gilmour and W. F. Heenan, Radiation Effects on Glass: an Annotated Bibliography, REIC Memorandum 26, Radiation Effects Information Center, Columbus, Ohio, September 1965

12. C. L. Wolff, "The Effect of the Earth's Radiation Belts on an Optical System," Paper XXXII, Conference on Optics in Space, University of Southampton, England, 27–29 September 1965

13. N. J. Kreidl and J. R. Hensler, "Gamma Radiation Insensitive Optical Glasses", J. Opt. Soc. Am. 47 No. 1, 73–75, 1957

14. G. Arutunian and F. L. Seppi, The Effects of Ionizing Radiation Upon Transparent Materials, Report No. RR-1, Ordnance Tank-Automotive Command, Detroit Arsenal, Centerline, Michigan, October 1959

15. R. H. Jones, Combined Space Environment Effects on Typical Spacecraft Window Materials, NASA-CR-65142, (N65-33370), Avco Corp., Tulsa, Okla., July 1965

16. F. S. Johnson, "Solar Radiation," Chapter 4 in Satellite Environment Handbook, 2nd Ed., ed. F. S. Johnson, Stanford University Press, Stanford, Calif., 1965

17. G. A. Haynes and W. E. Miller, Effects of 1.2 and 0.30 MeV Electrons on the Optical Transmission Properties of Several Transparent Materials, NASA-TN D-2620, National Aeronautics and Space Administration, Langley Research Center, Hampton, Va., March 1965

18. J. L. Chinn, N. M. Ewbank, Jr., and G. Gigas, "Charged Particle Radiation Effects on Selected Transparent Materials for Aerospace Enclosures," pp. 331–347 in Transparent Materials for Aerospace Enclosures, AFML TR 65-212 (AD473543L), Air Force Materials Laboratory, Wright-Patterson AFB, Ohio, September 1965

19. D. F. Heath and P. A. Sacher, Effects of a Simulated High Energy Electron Space Environment on the Ultraviolet Transmittance of Optical Materials Between 1050 and 3000 Å, NASA TM X-55337 (N66-1132), Goddard Space Flight Center, Greenbelt, Md., September 1965

20. P. A. Sacher, The Effects of a Simulated Proton Space Environment on the Ultra-Violet Transmittance of Optical Materials Between 3000 Å and 1050 Å, NASA TM X-55911 (N67-36569), Goddard Space Flight Center, Greenbelt, Md., August 1967

21. T. E. Lusk, "Infrared-Transmission Materials Would be Unaffected by Radiation in Space", Electronic Design, pp. 74–75, 26 October 1960

22. J. W. Corbett, "Defects in Irradiation Silicon: II Infrared Absorption of the Si-A Center", Phys. Rev. 121, No. 4, 1015–1022, 1961

23. U. S. Vavilov, A. F. Plotvikov, and G. V. Zakhvatin, "Infrared Absorption of High Resistivity Silicon with Radiation-Induced Defects", Soviet Physics–Solid State 1, No. 6, 894–895, 1959

24. J. Romanko, "Effects of Reactor Radiation on the Properties of Silicon and Silicon Monoxide", FZK-118, General Dynamics Corporation, Convair Div., Fort Worth, Texas, August 1959

25. Purposely deleted.

26. Purposely deleted.

27. A. J. Britten, J. R. Codispoti, and R. Wightman, Effects of High Intensity Thermal Radiation on Optical and Infrared Materials, Memorandum Report M68-1-1, United States Army Frankford Arsenal, Philadelphia, Pa., March 1967

28. M. J. Kerper, T. G. Scuderi, and E. H. Eimer, Properties of Glasses at Elevated Temperatures, WADC-TR-56-645, Part X, Air Force Materials Laboratory, Wright-Patterson AFB, Ohio, March 1965

29. S. Glasstone, The Effects of Nuclear Weapons, U. S. Atomic Energy Commission, April 1962

Chapter 9

MATERIALS FOR LUBRICATION APPLICATIONS

H. I. Silversher

The problem of selecting materials for the lubrication of advanced spacecraft systems is complicated by the unique environmental conditions surrounding the performance of a complete mission.

Three distinct sets of conditions influence the requirements for lubrication: (1) ground activities, (2) short-time operation during launch, ascent and reentry, and (3) operation in space. The optimum lubricating system should be compatible with all sets of environmental conditions. Therefore, the system should be the product of the proper selection of materials, suitable engineering design, and careful application of nondestructive test and checkout procedures.

A variety of aerospace surfaces and mechanisms require lubrication, with an attendant variance in function, speed, load, and environment. These include all contacting, rubbing, and sliding surfaces; mechanisms such as motors, gear trains, reaction wheels, gyros, and stabilizers; mechanical devices such as pin pullers, threaded fasteners, closures, and valves; equipment such as tape recorders, relays, and timing devices; electrical contact surfaces such as slip rings and brushes; and the large bearings used for positioning antennas and solar arrays or for spinning and despinning modules.

Since the most important objective of lubrication is elimination of potential failure modes induced by the wear and adhesion of adjacent cofunctional surfaces, this chapter will discuss the following:

- The mechanism of friction
- Effects of total mission environment on friction and lubrication
- Requirements for lubrication in space environment
- Materials and mechanisms for space lubrication systems
- Space simulation testing of lubricants

Materials actually used in lubrication applications in spacecraft are discussed in Chapter 17. Recommended lubricating materials are discussed in Chapter 18.

9.1 MECHANISM OF FRICTION AND ADHESION

9.1.1 The Frictional Surface

Familiar adjectives describing the physical condition of a surface, such as clean, smooth, wavy, rough, and contaminated, are meaningless under microscopic

examination where a surface with a "low" microinch finish will have its share of irregularities. Tabor (Ref. 1) states that the reason for these irregularities is the normal polycrystalline, and often polyphase, nature of real engineering surfaces, resulting in imperfections and impurities accompanied by covering films of oxides or adsorbed layers. Therefore, a seemingly smooth, clean surface is always "rough" on a microscopic scale.

Further, attempts to clean or remove a contaminating film from a surface by abrading, followed by polishing, has the effect of increasing the depth of deformation and replacing the oxide layers with an amorphous layer containing metal particles, metal oxides, polishing powders, and other foreign particles from the processing. A typical polished metal surface is never pure, smooth, or uncomplicated.

In a study of friction and wear, the irregularities of a surface are often called asperities. These are manifested in a variety of shapes such as grooves, crests, depressions, and projections roughly resembling cones and hemispheres.

9.1.2 Area of Real Contact

When two flat solid surfaces are placed in contact, the real area of contact is not the visual, superficial superimposed surfaces but rather the most prominent tips of their asperities. These discrete areas may comprise only a minute fraction of the surface Therefore, even the applied load of a few pounds is sufficient to cause a pressure of many thousands of pounds per square inch at the points of contact.

9.1.3 The Frictional Process

The welded junction theory of friction (Ref. 2) interprets frictional resistance as the net result of two concurrent conditions: the shearing of welded junctions formed between points of contact, and the ploughing out of the softer material to an appreciable depth below the surface by the harder material riding over it. For hard materials in contact with each other, analyses indicate that the influence of ploughing is relatively insignificant and friction is largely due to the shearing of welded junctions.

Three important items in the welded junction theory of friction and wear are as follows:

- The area of true contact is only a small fraction of the apparent contact area.
- High localized temperatures are generated at the points of contact by frictional heating.
- Two surfaces interact with each other to an extent that depends upon the materials themselves and the presence of surface films.

The relative values assigned to the friction of contacting surfaces are measured as a coefficient. The coefficient of friction μ can be expressed as follows:

$$\mu = \frac{F}{W} = \frac{\text{shear strength of junction}}{\text{yield strength of softer material}}$$

The purpose of lubrication, therefore, is to reduce the value of F by preventing formation of the welded junctions, by preventing the asperities from making contact, or by lowering the shear strength of welded junctions that are formed. A low coefficient of friction is desirable to prevent wear and adhesion.

9.1.3.1 Hydrodynamic Friction

Hydrodynamic friction is a viscous drag imposed by the shear within a fluid used as a hydrodynamic lubricant.

9.1.3.2 Boundary Friction

The mechanism of boundary friction is influenced by the substrate surface and the chemical nature of the lubricant material. It can be considered an extension of dry friction with the inclusion of variables through contamination. The friction and surface damage depend on chemical composition of the lubricant and the reaction products between the lubricant and the substrate. The frictional behavior may be influenced by surface roughness and contaminants.

The most prominent failure mode, common to all fluid lubricated bearing surfaces, is the existence of boundary friction conditions. The metal-to-metal contact under these conditions can result in excessive wear, severe welding, adhesion, and catastrophic seizure. In the space environment, the low ambient pressure and lack of heat conduction contribute to boundary friction by promoting evaporation of the lubricant from the bearing surface and decrease of the thickness of the lubricant film by reduction in viscosity. Therefore, comprehensive bearing design should include not only the bearing itself but also the special retainers, shields, seals, and lubricants required to assure completion of the intended mission under space conditions. Where conditions of high and low speed do not permit effective fluid lubrication, design should consider the materials specifically developed to prevent the detrimental effects of boundary friction.

9.1.3.3 Stick-Slip Friction

Stick-slip friction usually occurs at slow sliding speeds and is manifested in the discontinuity of motion. The stick phase is attributed to a higher static friction and the slip to a lower kinetic friction – each influenced by oscillations initiated by the variation of distance and speed between adjacent surfaces.

9.1.3.4 Fretting

Fretting, also known as wear oxidation and fretting corrosion, is a form of wear characterized by oscillating and reciprocating motion between adjacent surfaces. The motion is believed to break down surface films followed by formation of additional welded junctions that soon shear, resulting in abrasive particles that promote wear (Ref. 3).

9.1.3.5 Rolling Friction and Deformation Losses

Rolling friction differs from sliding friction in that it is caused by deformation of contracting surfaces during rolling with an energy loss similar to that of the ploughing term of sliding friction rather than the shearing of welded junctions. The net effect of adverse friction on a surface is the diminution or loss of function through wear. The manifestations of wear are weight loss, volume loss, chemical change, dimensional and geometric changes, and contamination.

9.1.4 Adhesion of Metals

Experiments indicate that, under the pressure acting at the surface irregularities, localized adhesion or welding and some transfer of material can take place. The metallic junctions that are formed must be sheared if the surfaces are to slide past one another, and the force required to shear the junctions and permit sliding is proportional to the product of the shear strength of the junctions and the area of real contact.

Since metals can cold weld in air when the contacting forces are sufficient to break through the surface films, as well as in vacuum, a great deal of research has been conducted to define the conditions under which cold welding is probable and to develop a satisfactory theory of the mechanism by which adhesion of metals occurs.

Research indicates that metal-metal adhesion is related to the work of adhesion of the contacting materials, expressed by the equation

$$W_{ab} = \gamma_a + \gamma_b - \gamma_{ab}$$

where

W_{ab} = work of adhesion
γ_a = surface free energy of material a
γ_b = surface free energy of material b
γ_{ab} = interface free energy

and all quantities are for a unit area.

Because the localized temperatures generated by sliding surfaces can approach the melting point of the metal, localized fusion welding might occur. A correlation between increase in adhesion and decrease of melting point has been reported.

From a metallurgical point of view, the fact that the contacting metal asperities are stressed (as a result of the load) and are probably at an elevated temperature results

in an explanation of their behavior by some considerations of high-temperature metallurgy. The relation between this behavior and cold welding is based on the reccrystallization and recovery of strain-hardened metals. Applying the reaction rate equations of Arrhenius to the process of recrystallization and recovery, the following equation for the coefficient of adhesion was derived:

$$\sigma = \sigma_o t^n e^{-Q'/RT}$$

where

σ = coefficient of adhesion
Q' = activation energy for the process
R = universal gas constant
T = absolute temperature
t = time

and σ_o and n are constants, equal to the slopes of the plots of $\ln \sigma$ versus $1/T$ and $\ln \sigma$ versus $\ln T$.

The hardness and yield strength of the metals have been considered as contributing to the metal-metal adhesion tendency because under the applied load they can govern the true area of contact and the ability of the substrate to provide a nonyielding surface on which contaminating films are supported.

Surface oxide films are normally more brittle than metals and therefore are likely to crack and expose underlying metal if it is too soft to provide a firm support under load.

In the sense that surface films reduce the possibility of metal-metal adhesion that would otherwise occur on intimate contact, these can be considered as naturally formed lubricating films. The presence and nature of these films will depend upon the reactivity of the surfaces with the surrounding atmosphere to form oxides, nitrides, or other compounds that are held by chemical bonds or to form physically absorbed gas films that are held by weaker van der Waals forces. The stability with which the films remain on the surface during sliding depends upon (1) the mechanical strength of the films and their ability to deform without cracking when the substrate below them is plastically deformed, (2) the adhesion of the film to the substrate, and (3) the thermal stability of the films (Ref. 4).

A survey of metal-to-metal adhesion by Moeller, Bossert, and Boland (Ref. 5) has been reported. Their survey was conducted in connection with experimental work on the static and dynamic coefficients of friction of candidate materials for the Apollo program which attempted to rank them according to their adhesion tendency. They indicated that

metal-metal adhesion under simulated space (high vacuum) conditions could occur only between clean, oxide-free metals. Furthermore, most metal surfaces exposed to the space environment vacuum are not likely to become clean in any reasonable time unless the rate of removal of surface films is accelerated by some electrical or mechanical means.

They concluded that there was very little correlation between the coefficients of friction, the adhesion, and the properties of the materials studies.

9.2 LUBRICATION

The purpose of lubrication is to minimize or eliminate the friction and adhesion forces that induce functional failure modes by (1) reducing wear, (2) minimizing frictional drag, (3) carrying away heat, (4) preventing corrosion, and (5) sealing against contamination.

9.2.1 Hydrodynamic Lubrication

Because hydrodynamic lubrication provides minimum friction, it has been used extensively with bearings for guidance and control systems of missiles and spacecraft.

Hydrodynamic lubrication involves a mechanical design by which the rubbing surfaces are separated by a continuous film of gas or liquid. The fluid carries the load or weight of the free member of the rubbing pair and separates it from the stationary member. It also provides a medium of very low shear strength or viscosity. The resistance to relative motion between surfaces provided with hydrodynamic lubrication is very low because of the low viscosity of the fluid.

Hydrodynamic lubrication is accomplished by either external pressurization or self-action. With external-pressurization, the fluid is supplied under pressure so that the free body can float on an externally pressurized film of oil or gas which flows within the clearance spaces of the bearing. When the clearance is adjusted to maintain the minimum safe clearance between the surfaces, only very small amounts of fluid are needed. In self-acting hydrodynamic lubrication, the bearing is its own pump maintaining the hydrodynamic film. The bearing in a leakproof container is so designed that the relative motion of the rubbing surfaces generates a film pressure within the clearance spaces and keeps the surfaces separated.

The lifting pressure increases linearly with the fluid viscosity and with the speed of relative motion between the two surfaces, and it varies inversely as the square of the film thickness. This means that the bearing requires close machining tolerances and high speeds for efficient operation. Since the viscosity of gases is low, self-acting gas bearings are limited to lighter loads than those that can be sustained by self-acting oil bearings.

9.2.2 Boundary Lubrication

The conditions for boundary lubrication exist when the contact pressure between surfaces becomes so high and the sliding speed so low that a load supporting hydrodynamic lubricant wedge is impossible to maintain. Under such conditions, films with thicknesses of molecular dimensions must serve to eliminate the welding of junctions or reduce the shear strength of welded junctions sufficiently to permit contacting asperities to slide over one another without high shearing loads with the formation of abrasive debris. Boundary lubrication is dependent on a thin film for "oiliness", and load-carrying capacity with strong film continuity adherent to the bearing surface. Boundary lubrication is provided by natural surface films such as water vapor; absorbed or chemisorbed gas films such as oxides, sulfides, and nitrides; contaminants such as dust, grease, and corrosion products or debris; low shear strength laminar solids (solid lubricants) and soft metals; and high molecular weight organic materials such as long-chain fatty acids.

Effective hydrodynamic and boundary lubrication can prevent most of the wear caused by friction.

9.3 INFLUENCE OF TOTAL MISSION ENVIRONMENT ON LUBRICATION

Primary consideration is given to the design and engineering requirements of spacecraft relevant to its intended mission and operational environment. A valid selection of structural materials, propulsion system, optical and thermal control surfaces, instruments, and appendages such as antennas, arrays, and sails establishes the baseline for lubrication. Therefore, selection of the optimum lubrication system must be correlated with both the design and the environment.

9.3.1 Ground Activities

Assembled mechanisms used in spacecraft and missiles are repeatedly tested on the ground during the checking out of various components and entire systems prior to launch. As a result, subsystems that will operate for less than a minute during the launch and ascent phases can accumulate as much as several hundred hours of test operation prior to the launching. Lubricants selected for use with these subsystems under the vacuum conditions in space will therefore have to operate for a considerable period under normal atmospheric conditions. In some instances, mechanisms that are sensitive to prolonged ground operation must be replaced by fresh units prior to launch.

Packaging and handling specifications are necessary to protect mechanisms from rough handling and harmful environments. Where such conditions are unavoidable, the qualification test specifications should require suitable testing of the mechanisms.

Materials used for gears and bearings should be made of corrosion-resistant materials or protected by suitable films of oil, grease, or other coatings. Seals should be provided around joining surfaces or couplings to exclude minute particles of dirt. These precautions are particularly important for mechanisms mounted on the exterior of a vehicle, since they are most subject to weathering.

Heavy shock and vibration loads that occur during the short-time periods of launch, ascent, and reentry can cause Brinell marks in ball and roller bearings. The rotors of most fractional horsepower motors are light enough so that Brinelling does not appear to be a real problem with such parts. However, bearings that support heavy loads and that are stationary during launch and ascent are most susceptible to this type of damage. Two methods of preventing heavy loads from causing Brinell marks are (1) rotating the shafts and bearings by having the mechanism in operation during the launch phase, and (2) blocking the load so that it is not supported on the bearings during launch and removing the blocks after the vehicle is in orbit.

Since high temperatures are generated by fuel burning and by aerodynamic heating, certain bearings (such as those used on control surfaces) and other parts must be designed to withstand high temperatures. At the other extreme, the use of cryogenic fluids for propulsion (e.g., liquid hydrogen and oxygen in propulsion and liquid helium in nuclear propulsion) means that pumps, valves, and other moving parts will require that the lubrication be kept at very low temperatures (e.g., $< -300°$ F). Since the fluids used for propulsion are very reactive and include the strongest oxidizers known, lubricants that might come into contact with such fluids must be inert.

9.3.2 Space Environment

The lubrication of spacecraft systems can be influenced by several environmental factors: weightlessness (zero gravity), penetrating radiation, temperature extremes, and ultrahigh vacuum.

9.3.2.1 Weightlessness (Zero Gravity)

Weightlessness has one beneficial effect on lubrication, but for the most part is detrimental. The beneficial effect is that once in orbit, bearings need not support a structural load. Bearing loads are reduced to levels required by initial loads associated with accelerating and decelerating mechanisms, the effects of unbalanced dynamic forces, and the centrifugal forces of balls against races in rotating ball bearings. Reduced bearing loads mean less wear. The detrimental effects are that (1) gravity-fed systems such as fluid reservoirs and hydraulic system accumulators are ineffective, and (2) in combination with ultrahigh vacuum, there is a complete absence of convection currents for cooling. The result of the latter is that frictional surfaces operate at higher temperatures than those induced by the same loading conditions in a terrestial environment.

9.3.2.2 Penetrating Radiation

Penetrating radiation from the space environment is not considered a major problem in space lubrication at this time. Not only have radiation-resistant lubricants been developed, but the concept of modern lubrication system design provides effective shielding by means of housings and retaining mechanisms. In addition, the oxygen required to accelerate radiation degradation in some lubricant materials is absent in space vacuum environments.

9.3.2.3 Temperature Extremes

The effect of temperature variations on spacecraft lubrication is more pronounced on parts that are outside the vehicle skin. The cause is direct radiation from the sun and, to a lesser extent, solar reflection from the earth. Parts such as solar array bearings, which require lubrication, can experience temperatures as low as -280° F when positioned out of the influence of solar radiation. Temperatures within the vehicle are protected from the extreme conditions by controlling the absorptivity and emissivity of the outer spacecraft skins so the only problem is the increased temperature rise on the frictional surface caused by the lack of convection heat transfer in vacuum with zero gravity.

9.3.2.4 Ultrahigh Vacuum

The factor in the space environment that most influences selection of materials for lubricated systems is ultrahigh vacuum. A complete mission may require exposure of spacecraft to pressures ranging from atmospheric to 10^{-13} Torr. (The pressures for given altitudes are given in Tables 3-2 and 3-3 of Chapter 3.) The detrimental effects on lubrication that are attributed to ultrahigh vacuum are volatilization, condensation of the volatiles, absence of reacting gases, and poor thermal conductivity.

Volatilization. The equilibrium value is a thermodynamic function of the molecular species involved and is established when the rate of molecules returning to a surface equals the rate of their leaving. In an absolute vacuum, the mean free path of molecules is large enough so that those departing can be permanently lost and equilibrium cannot be attained. Therefore, if a solid or fluid lubricant has a high vapor pressure, it may evaporate appreciably during long-time space orbits with a contingent loss of lubricative function.

Condensation of Volatiles. The detrimental effect of volatiles condensing on a cold surface is contamination, which causes changes in reflection, absorption, and emmission. Optical and thermal control surfaces are particularly vulnerable. Electrical contacts, slip-rings, and brushes are also detrimentally affected by changes in conductivity due to contaminating films.

Absence of Reactive Gases. Absorbed or chemisorbed gas films, such as oxides, are normally present on even the cleanest metal surfaces in the normal atmosphere. Such films prevent bare metal-to-metal contact and formation of strong welded junctions, thereby decreasing the coefficient of friction. However, surface films of absorbed or chemisorbed gases that are removed by wear will not reform in space, so that films present on even the cleanest surfaces in the terrestrial atmosphere will not be replenished in orbit. Under these conditions, seizure or cold-welding may occur between the surfaces. (Adhesion and cold-welding are discussed in section 9.1.4.)

Poor Thermal Conductivity. It has already been noted that the combination of vacuum and zero gravity results in absence of convection cooling. Another important effect of vacuum is poor thermal conductivity resulting from the absence of gases between

adjacent or contacting surfaces down to the asperity prominence level. In the terrestrial atmosphere, the spaces between contacting asperities are filled with air which conducts thermal energy from one substrate surface to the other, thereby producing a low gradient. In vacuum the absence of thermal conducting gas restricts the flow of heat to the real areas of contact (asperities), resulting in a high gradient. The poor conductivity coupled with the absence of convection cooling establishes higher heat resistant requirements for lubrication systems.

9.4 REQUIREMENTS OF MATERIALS AND MECHANISMS FOR SPACE LUBRICATION SYSTEMS

The requirements of materials and the design of lubrication systems for spacecraft are influenced by the total mission environment. Where the optimum material or system for one environment is not compatible with another, proper design should correlate protective devices and activity with function rather than compromise qualification.

9.4.1 Antifriction Bearings for Bearing Surfaces

In addition to bearing surfaces, the most important lubrication systems are based on antifriction bearings which serve to convert sliding friction into rolling motion.

Antifriction bearings can be divided into six generic classifications:

- Ball bearings
- Cylindrical roller bearings
- Tapered roller bearings
- Needle roller bearings
- Thrust bearings
- Self-aligning bearings (spherical raceways)

The common function of antifriction bearings is to separate a rotating shaft or wheel from the stationary parts of a mechanism by carrying the loads imposed by relative movement. These loads are either (1) radial, when the load is perpendicular to the shaft and axis of the bearing, or (2) thrust, when the axial load is parallel to the axis of the shaft and bearing. The geometry and nomenclature of each type of bearing have been standardized by the Antifriction Bearing Manufacturers Association (AFBMA).

9.4.2 Bearing Materials

The material combinations used for aerospace bearings include metals, plastics, cermets, and ceramics.

9.4.2.1 Metals

Metals used as antifriction bearings for aerospace equipment must have not only a high load capacity with high elastic limits and high fatigue strength but also good friction and wear properties in vacuum. The most commonly used metals at temperatures

below 500°F are AISI 52100 steel and 440C stainless steel that have been vacuum processed to minimize gas pockets and impurities. Other candidates include a cobalt-base alloy, a nickel-chromium alloy and nickel-bonded titanium carbide, and columbium (niobium) carbide. Antifriction properties of metals are manifested in their thermal-vacuum stability and by retaining the normal oxide film formed during processing. For continuous operation in temperatures exceeding 500°F, recommended bearing metals are 440C and 17-4 stainless steels, WD65 and WB49 alloy steels, M3 high-speed steel, M2 and M10 tool steels, Stellites 3 and 19, Haynes Alloy 25, and Hastalloys B and C, all requiring special retaining mechanisms (Ref. 6).

9.4.2.2 Plastics

Plastics have been found very useful in many applications involving friction and wear. Teflon* has been used for sleeve bearings that operate dry with little friction. Plastic bearings generally operate dry, although a few drops of oil applied initially improve their performance.

The form of plastics can be varied to meet specific needs, and many specialty grades and techniques are available that take full advantage of the special properties of plastics. In many applications, plastics can be used in pure bulk form, as in the case of cast, molded, pressed and sintered, or machined articles. In other applications, bulk plastics incorporate various fillers that improve their frictional and mechanical properties. In still other cases, plastics are used in the form of thin films or as impregnants in porous solids.

Most plastics have good friction characteristics, even when run dry. Self-lubrication can be improved by adding fillers such as MoS_2. Porous plastic bodies can be impregnated with oils to provide lubrication, as in ball-bearing retainers of Synthane (a porous paper-base phenolic composition). In other cases, a porous metal can be impregnated with a plastic such as Teflon that has outstanding antifriction properties. These characteristics of selflubrication can be used to advantage where relubrication is difficult, where operation is intermittent with long idle periods, or where temperatures are too low for oils and greases to be effective (e.g., cryogenic applications).

Some plastics have very good impact strength. They can deform elastically to absorb shock and vibration so that, during the launch phase of spacecraft, there is less danger of Brinelling with ball bearings using plastic balls than with those using steel balls.

On the other hand, plastics have some disadvantages for applications involving friction and wear. The thermal conductivity of plastics is much lower than that of metals, for example. Consequently, plastics are less able to dissipate frictional heating generated at rubbing interfaces, so that plastic parts run hotter than similar parts made of steel. For use at high speeds, it may therefore be necessary to use the plastic in the form of a thin film over a metal substrate so that the metal can conduct the frictional heat away more efficiently. Other techniques for accomplishing the same purpose include the use of metal fibers as fillers and of metal backing screens.

---

*Trade name of E. I. duPont de Nemours Co., Inc.

Bulk plastics cannot be used at temperatures as high as steels can. They soften with heat and generally should not be used above 200° to 300° F. Teflon, the most heat-resistant of the plastics, melts at 620° F and cannot be used in pure bulk form at temperatures approaching this level. Plastics have higher coefficients of thermal expansion than most metals.

Plastics are weaker than steels, so that the load-carrying capacity of plastic gears and bearings is less than for steel parts of a given size. Since plastics are strong enough for the lightly loaded applications common to spacecraft systems, however, this is not a major objection for space environment applications.

Thermoplastic materials apparently wear by softening and flow of the material at points of contact. A thermoplastic bearing surface rubbing against a metal surface will be polished and will smear material into the valleys on the metal surface. Hard particles will be embedded in the plastic and will abrade the metal; hence, cleanliness is as important as on any other bearing (Ref. 9).

Thermosetting materials apparently wear by thermal degradation at surface high spots. Rubbing against a metal surface polishes the metal. Particles embedded in a thermosetting bearing surface will cut the thermosetting material.

The plastics that show the most promise as bearing surface materials for spacecraft systems are Teflon, nylon, Delrin,* polyimides, and phenolic laminates.

9.4.2.3 Ceramics and Cermets

Ceramics and cermets are essentially hard, brittle materials, such as sapphire, glass, cemented carbides, fully dense oxides, and bonded oxides.

The advantages of some ceramics and cermets are that (1) they are hard and have generally good wear resistance; (2) they retain their hardness and strength at higher temperatures than do metal alloys; (3) they have good resistance to oxidation at elevated temperatures, good resistance to corrosion, and compatibility with liquid oxygen.

The disadvantages of ceramics and cermets are that (1) they are less ductile than most metal alloys and are more sensitive to damage by shock and vibration; and (2) the load carrying capability of some of these materials is less than that of steel, thus generally restricting their use to low speeds and light loads.

The ceramics and cermets appear to have their most promising applications as high-temperature rubbing seals and bearings, where temperatures are too high to provide an effective lubricant, although lifetimes may be limited; as parts of gas lubricated bearings, because of their ability to be precision machined to high accuracies and fine finishes and their high-temperature stability; and as jewel bearings (sapphire) in precision instruments where loads and speeds are negligible.

---

*Trade name of E. I. duPont de Nemours Co., Inc.

9.4.3 Lubricants for Spacecraft

A lubricant can be defined as a material applied to a system capable of reducing or eliminating friction-induced surface damage to rubbing solid surfaces. The lubricants used in spacecraft mechanisms can be categorized as liquids (oils and greases), solids, gases, and soft or liquid metals.

9.4.3.1 Liquid Lubricants

Liquid lubricants include (1) petroleum oils and (2) synthetics such as polyglycols, phosphate esters, dibasic acid esters, chlorofluorocarbon polymers, silicones, silicate esters, fluoroesters, neopentyl polyol esters, and polyphenyl esters.

Petroleum oils are derived from natural mineral deposits in the earth. The two most widely used types for spacecraft are the parraffinic and highly refined distillates of mineral oil. Oxidation inhibitors and load-carrying additives are usually added to petroleum oils and greases to make up natural deficiencies in properties.

Synthetic lubricants are formulated from chemicals and can have properties that are unobtainable from the petroleum oils. The synthetics can be formulated for use over an extremely wide temperature range, with high thermal and oxidative stability, and with resistance to chemicals and radiation. Properties can be improved by chemical modification and improving compatibility with additives.

Greases are classified as liquids since they are oils with an appropriate thickening agent. Greases are made from phosphate ester fluid base by using a lithium soap thickener in which the phosphate ester fluid is an additive for other base stocks such as mineral oil. Greases made from dibasic acid esters and lithium soaps exhibit good low-temperature and extreme-pressure properties. Chlorofluorocarbon greases are made using the chlorofluorocarbon oil as the base stock with an appropriate thickener, or by using other base oils with a high molecular weight chlorotrifluoroethylene polymer as a thickner. Some greases are made from silicone oils by thickening with lithium soap, carbon black, indanthrene blue, and aryl-substututed urea. Silicate ester oils and combinations of other oils are used to prepare greases by thickening with lithium soap, colloidal calcium carbonate, and phenyl alpha naphthylamine.

The most important properties of liquid lubricants to be considered for the total spacecraft mission environment include (1) volatility, (2) radiation stability, (3) thermal stability, (4) compatibility with contacting materials, (5) viscosity, (6) flammability and, especially in atmospheric environment, (7) oxidation and (8) hydrolytic stability.

Table 9-1 (Ref. 6) lists the properties of several classes of synthetic lubricants and compares them with the properties of petroleum-based materials.

Table 9-1

GENERAL PROPERTIES OF SOME CLASSES OF SYNTHETIC LUBRICANTS COMPARED WITH REFINED PETROLEUM PRODUCTS

Lubricant	Volatility	Viscosity-temperature characteristics	Oxidation resistance	Lubrication characteristics	Thermal stability	Resistance to hydrolysis (a)	Flammability characteristics (b)	Solvent effect on paints, rubber, etc.	Resistant materials available	Solubility in petroleum and other synthetics	Improvement additive compatibility	Typical Applications.
Dibasic-Acid Esters	Generally lower	Good to excellent	Fair to good	Fair to good	Fair to good	Fair to good	Poor to fair	Pronounced effect	Some	Good to excellent	Generally good	Instrument oils, low-volatility grease bases, special hydraulic fluids, jet-turbine lubricants.
Phosphate Esters	Generally lower	Fair to good	Good	Good to excellent	Poor to fair	Poor to good	Good to excellent	Pronounced effect	Yes	Good to excellent	Generally good	Fire-resistant, hydraulic fluids, low-volatility high-lubricity grease bases, lubrication additives in other synthetics, special low-temperature lubricants.
Silicones	Much lower	Excellent	Good to excellent	Poor to fair	Good to excellent	Excellent	Poor to good	Generally small effect	Yes	Poor	Poor	High-temperature bearings, condensation pump lubricant, low-volatility grease base for lightly loaded bearings, damping fluids, devices requiring minimum viscosity change with temperature.
Silicate Esters	Lower	Excellent	Poor to fair	Fair to good	Good	Poor to fair	Poor to fair	Some effect	Yes	Fair to good	Fair to good	Heat-transfer fluids, high-temperature hydraulic fluids, low-volatility, low-viscosity grease bases, components for low-viscosity hydraulic fluids.
Polyglycol Ethers	Approximately equal	Good to excellent	Poor to fair	Good	Fair to good	Fair to good	Fair to good	Pronounced effect on paint, small effect on rubber	Some	Fair to good	Generally good	Special hydraulic fluids, forming and drawing lubricants, low-temperature grease bases, vacuum-pump lubricants, component of other synthetic lubricant formulations.
Halocarbons	Some lower, some higher	Poor	Excellent	Poor to excellent	Poor to excellent	Poor to excellent	Excellent	Widely variable	–	Generally poor	Widely variable	Nonflammable, extreme oxidation-resistant lubricants for plant processes or devices handling reactive materials.
Polyphenyl Ethers	Much lower	Poor to fair, generally high pour points	Fair to good	Fair to good	Good to excellent	Fair to good	Poor to fair	Some effect	Yes	Fair	–	High-temperature fluid for reactor coolant, hydraulic applications at very high temperature. Applications not yet fully developed.
Silanes	Much lower	Fair to good	Poor to fair	Fair to good	Good to excellent	Good	Poor to fair	Generally small effect	Yes	Fair	Fair	Base stocks for high-temperature greases, hydraulic fluids and engine lubricants. Require extensive formulation.

(a) Petroleum excellent.
(b) Petroleum poor.

The film thickness in boundary lubrication is so small that there is metal-to-metal contact through asperities, and the properties of the contacting substrates are more important than those of the fluid lubricant. In hydrodynamic lubrication, there is no metal-to-metal contact and the lubricant film properties are most important.

Oils and greases are the most widely available and most commonly used. They are more easily applied than such lubricants as bonded films of laminar solids or soft metals. Not only is this true of the initial application of the lubricant, but it is especially true of replenishing the supply of lubricant as the old lubricant is exhausted. Additional oil or grease can be fed to the operating mechanisms by means of reservoirs and feed mechanisms, usually while the parts are in operation, whereas the wear-out of solid film lubricants usually requires that the mechanisms be disassembled and the parts recoated separately.

Oils are more useful in removing frictional heat than are other types of lubrication. The removal of the heat that is generated by mating parts, especially those that operate at high speeds, is an important function of lubrication, and in some cases is the primary consideration in the choice of the most suitable lubricant.

Sealing against dust, and protecting of metal parts from rusting or other forms of corrosion are functions of oils and greases during the checkout and storage periods prior to launch.

The major disadvantages of fluid lubricants in the space environment are evaporation and creepage.

Volatility. The volatility or evaporation rate is a function of the vapor pressure of the fluid lubricant at a specified temperature and is related to molecular weight. The higher the molecular weight, the lower the vapor pressure. If a fluid contains a range of molecular weights, the lower weight fractions will volatilize first.

Oils with the lowest vapor pressures and evaporation rates do not necessarily give the longest lubricating lifetimes on mechanisms operating in vacuum. An adsorption of the oil or reaction of it with the bearing surface also appears to be important (Ref. 7). The less volatile constituents that evaporate more slowly and are left behind can have different viscosity and lubricity than the original mixtures. The evaporation of lubricating oils and their possible condensation on nearby optical surfaces can obscure transmission. Films of oil that are thick enough to absorb a small fraction of the infrared radiation in the wavelength region at which horizon sensors and other equipment for stabilization and guidance operate can degrade performance.

Continued loss of oil from an oil-lubricated surface operating in vacuum means that the surface may eventually operate dry and that wear rates and the tendency for cold-welding will increase. In the case of greases, the loss of oil from the soap base or other thickener causes the greases to thicken and may eventually convert them to hard residues that do not lubricate and which can, in fact, jam ball bearings and gears.

The volatility of fluid lubricants used for space vacuum environments can be controlled by hermetrically sealing or by controlled leakage sealing.

Radiation Stability. The radiation stability of oils is lower than that of inorganic lubricants such as laminar solids and soft metals. However, based on present estimates of the amount of radiation in space and knowledge of the radiation stability of oils and greases, it does not appear that space radiation will be a limiting factor in the use of oils and greases on spacecraft with lifetimes of several years. More intense radiation from nuclear power sources can be expected to limit the usefulness of oils and greases and require alternate forms of lubrication.

When oils are exposed to penetrating radiation, the viscosity initially decreases, followed by an increase, and eventually the oil becomes a rubbery solid; the consistency of the thickener in some greases becomes thin and soupy. Eventually, polymerization of the grease-base fluid overrides the thinning effect, and the grease becomes thicker, harder, and ultimately solid. In both oils and greases, volatility generally increases; foaming tendencies increase; the flash point drops and gases are released, due to the formation of low molecular weight degradation products; and acidity and corrosiveness increase. A decrease in both oxidation stability and heat conductivity occurs in both oils and greases.

The petroleum oils, aromatic hydrocarbons, silicate esters, fluorinated compounds, and organic phosphates are stable when exposed to nuclear reactor gamma radiation to 10^8R. The polyphenyl ethers and methyl phenyl polysilaxanes (silicone oils) are stable to 10^9R.

The radiation stability of the greases depends upon the thickener as well as the fluid. Because of this effect, the greases will be a little less stable than the oil itself. For example, silicone grease thickened with copper phthalocyanine was stable to 10^9R, whereas those thickened with lithium stearate became thin at 10^8R (Ref. 8)

Thermal Stability. The thermal stability of a liquid lubricant base stock should not be confused with the physical effects of temperature extremes. At high temperatures, oils and greases have too low a viscosity to be effective lubricants: they evaporate, and in air they oxidize. At low temperatures, their viscosity becomes to high, and excessive torques result. Synthetic oils and the use of additives can extend the temperature range beyond that to which petroleum oils are limited, but the limits of temperature are still more restrictive than with some other types of lubrication. On the other hand, thermal stability relates to molecular structure of the lubricant, especially to the strength of the bond between atoms and the forces and strains imposed on the bond.

Substrate surfaces can be damaged when the fluid forms corrosive products during normal lubrication activity. The formation of acids can pit metallic surfaces.

Oils can migrate over surfaces and away from the part that they are intended to lubricate and form a contaminating film. Such creepage is more extensive under vacuum than normal atmospheric conditions.

Fluids condensing on critical surfaces can cause a malfunction. The emissivity of thermal control surfaces can be detrimentally affected, and the loss of electrical conductivity can make brushes and slip rings inoperable.

The fluid lubricant should be inert to contacting or adjacent media. Fuels and oxidizers used in propulsion systems or functional gases and chemicals should not be detrimentally affected by the presence of the fluid lubricant.

Viscosity. The viscosity of oil is a measurement of fluid friction and is the ratio of the shearing stress to the rate of shear. Molecular weight influences the viscosity of oil. The higher the weight, the higher the viscosity. Changes in temperature and pressure influence viscosity. To be effective, a lubricating oil should maintain functional viscosity for all temperatures encountered during operation. Viscosity decreases as temperature rises, and increases with decreasing temperature. Increasing pressure increases viscosity and forms the basis for hydrodynamic lubrication.

The consistency of grease (as a semisolid) is measured as a function of penetration. Penetration or penetration number is the depth, in tenths of a millimeter, that a standard cone penetrates a sample of grease under specified conditions. The higher the penetration number, the "softer" the grease. Temperature and pressure affect penetration number in a manner similar to viscosity. To be effective, a lubricating grease should maintain adequate consistency for all temperatures encountered during operation. Special additives to oils and greases provide an operable range under conditions of temperature and pressure extremes, but these should be tested for corrosiveness on a specified substrate.

Flammability. The flammability of a fluid lubricant is the chemical interaction with ambient gases, heat, and ignition sources. Typical ignitive sources are sparks, flames, and hot surfaces. Fluid lubricant additives do not influence flammability, so selection must be based on chemical composition.

Oxidation Stability. Oxidation stability is the resistance of a fluid lubricant to oxidize and become corrosive when exposed to heat and oxidizing gases in the catalytic presence of substrate metals. Additives can enhance the oxidation stability of fluid lubricants.

Hydrolytic Stability. Water can be introduced into fluid lubricants by the humidity of atmosphere and may be entrapped and present in the space/vacuum environment after launch. In terrestrial environment the water itself can corrode metallic substrates or offgas in vacuum. If the water reacts with the molecules of the lubricant (hydrolysis), it can change the properties of the lubricant and generate corrosion products. A fluid lubricant with good hydrolytic stability will not undergo detrimental changes in physical properties, generate nonfunctional masses (emulsification), react with hydrophylic additives, corrode or contaminate the metal substrate, or undergo chemical changes that cause release of volatile fractions or loss of lubricity.

9.4.3.2 Solid Lubricants.

A solid lubricant is a laminar solid capable of decreasing the amount of wear between moving surfaces by sliding under boundary conditions. The properties of a laminar solid that determine its value as a lubricant are: (1) crystal structure, (2) thermal (and oxidative) stability, (3) melting point, (4) thermal conductivity, (5) mechanical properties, (6) chemical stability, and (7) purity.

Because of the laminar crystal structure of solid lubricants, they are highly anisotropic with very pronounced isodimensional mechanical properties. These properties are usually associated with the low shear strength required for sliding and low coefficient of friction. In the laminar structure, the atoms within a plane are held together by strong chemical bonds whereas the distance between planes is relatively high and the bonding is weak. In graphite, the interatomic distance is 1.42 Å within the plane and 3.35 Å between planes. These materials lubricate due to the ease with which they can be sheared. Not all laminar solids are effective lubricants. Moreover, their lubricating effectiveness varies with such service conditions as humidity and temperature and may be contingent upon the presence of absorbed molecules on the laminar plane.

The localized frictional heat developed when one metal surface moves over another can be quite high at the real area of contact, and some of this heat is transferred to the solid lubricant. The consequent rise in temperature when in contact with gases such as O_2, CO_2, and H_2O vapor can cause decomposition of the solid lubricant and formation of corrosive or abrasive products. In the absence of atmospheric gases in the vacuum of space, the thermal stability of the solid lubricants is increased. The solid lubricant should have a high thermal conductivity because the heat generated by friction must be dissipated to prevent local welding of rubbing metal surfaces.

The melting point of solid lubricants is related to thermal stability but it is treated separately because the changes in physical properties at or near the melting point are of concern rather than the decomposition products. As the temperature is increased, the elastic vibration of the crystal lattice can become large enough to separate atoms beyond some specific critical distance, thereby opening the lattice structure and destroying the essential cohesive energy of the crystal. The result is that the lubricant can no longer give protection to the rubbing surfaces because of its deformation or its removal.

Under boundary conditions when the solid lubricant is adhering to the substrate metal, only mechanical properties of the solid lubricant that are relative to those of the metal are important. The most important properties relate to the hardness, compressibility, and tensile strength of the metal (Ref. 9).

Very often it is advantageous to prepare a metal surface so that the solid lubricant not only will adhere more effectively but also will be more compatible with the prepared substrate. Table 9-2 (Ref. 10) indicates metal treatments recommended for subsequent bonded dry solid lubricant films. These recommendations relate only to solid lubricating pigments dispersed in a resin-like binder and capable of drying (or curing)

Table 9-2

SUBSTRATE METAL AND SURFACE PREPARATION PRIOR TO APPLICATION OF SOLID FILM LUBRICANT

Material	Surface Preparation				
	Step 1	Step 2	Step 3	Step 4	Step 5
Steel, SAE 4620 Rc 58-63 Steel, SAE 4130 Rc 30 ± 3 Steel, SAE 4130 Rc 57-60	Vapor degrease	Sandblast	Vapor degrease	Acid clean; alkali clean	Manganese phosphate
Steel, CRES A-151 303 Steel, CRES 17-7 PH CRES A-286 Alloy CRES Rene 41 Alloy	Vapor degrease	Sandblast	Vapor degrease	Alkaline clean	Pickle or passivate
Aluminum, 2024-T4 Aluminum 6061-T6 Aluminum 7075-T6	Vapor degrease	Anodize (sulphuric)	Chemical conversion (allodine or iridite)		
Aluminum Bronze 1014	Vapor degrease	Vapor hone	Bright dip		
Magnesium HK 31A	Vapor degrease	Vapor hone	Anodize		

after application, to a coating not less than 0.0001 in. thick. Solid lubricant powders impinged or burnished on metallic surfaces, deposited by electrophoresis, or coated thinner than 0.0001 in. have other preparation requirements. Solid lubricant powders dispersed in fluid lubricants follow the recommendations for fluids.

The principal consideration in chemical stability is the possible formation of corrosion products as the result of interaction of a solid lubricant with the substrate, and the interaction of heat or atmosphere, resulting in decomposition products that react with the metal surface. The solid lubricant should be free from contaminants. Contaminants can be introduced by incomplete purification of natural ore, byproducts from synthesis, and products of oxidation during size reduction. Most contaminants are abrasive and counteract the low friction properties required of solid lubricants.

The advantages of solid lubricants are as follows:

- High loads – Extreme pressure causes fluid lubricants to be squeezed out from between the surfaces. With laminar solids, shearing takes place more easily when loads are high, so that laminar solids are will suited to extreme pressure lubrication.
- Low speeds – At low sliding velocities, the asperities on mating surfaces tend to penetrate the lubricating films provided by fluid lubricants, so that stick-slip action and cold-welding occur. This effect is minimized with laminar solids as long as they adhere to the surface.
- Extreme operating temperatures – Oils and greases are subject to thermal decomposition at elevated temperatures. Their viscosity varies widely with temperature, and they become viscous or solid at low temperatures. Laminar solids have better thermal stability and do not become viscous at low temperatures or "thin out" at elevated temperatures, so that they provide a wider service temperature range.
- Dirty or abrasive environments – The tacky surfaces of oils and greases tend to collect particles so that the lubricant can act as a grinding compound. Laminar solids may, therefore, be better in dusty applications where complete sealing is impractical.
- Fretting wear – Vibration in many machine joints can cause fretting wear, even though there is no apparent motion between the parts. Solid lubricants can aid in preventing this behavior in extreme pressure applications.
- Simplified design – Designs can be simplified and costs reduced by eliminating machined oil passages, oil cups and other reservoirs, filters, and recirculating pumps.
- Inadequate or unreliable maintenance – Relying on mechanisms to pump or recirculate lubricating oils may not be desirable
- Intermittent action with long periods of part disuse – Oils and greases may be inadequate where a part is subjected to intermittent action and long idle periods.

- Avoiding reaction with environment – Environments such as fuels, solvents, and liquid oxygen are reactive with some oils and greases, whereas laminar solid lubricants that are virtually nonreactive in contact with such environments can be used.
- Stability under nuclear radiation – The radiation stability of laminar solids is greater than that of oils and greases.

Lubrication by solid lubricants has the following disadvantages:

- Coefficient of friction usually higher than with oils and greases.
- Excess solid lubricant can generate debris, causing clogging or binding.
- Nonrenewable – When the lifetime of bonded film is exhausted, the coating is nonrenewable unless the mechanism is disassembled and the coated part is reprocessed. Service lifetimes should be accurately determined beforehand by simulated or actual wear tests.
- Noncooling – Unlike lubrication with oils, the solid film lubricants have low heat transfer characteristics and are inefficient in carring away heat generated during operation.
- Close control of processing variables – The precoating surface treatment needs close control if best service is to be obtained. For example, surfaces must be mechanically roughened or chemically etched to an optimum finish and must be thoroughly cleaned.
- Restrictive coating application methods – The application methods limit design; for example, holes of small inside diameter are hard to coat by spraying, tumbling, or brushing, and must be dipped; blind holes may require special injection jigs or vacuum coating.

Powdered solid film lubricants may be used as loose powders or dispersions in a volatile carrier, burnished to film form by rubbing onto the surface to be lubricated. The film is very thin and must be capable of lubricating under boundary conditions. The more common use of solid film lubricants, however, is as bonded films. The lubricant powder is attached to the bearing surface with an adhesive material that also serves as a binder for the pigment. The bonded film can be applied by spraying, dipping, or brushing onto the bearing surface or electrophoretic deposition and plasma spraying. The binder-adhesive can be an organic resin, metallic salts, or fused ceramics. The mechanical properties of a good binder are directly related to those of the film formed in combination with the lubricating solid. The binder should have high resistance to abrasion and wear, have high mechanical strength, and establish a strong adhesion bond between the film and substrate.

The organically bonded materials have a useful upper temperature limit of +450° F under atmospheric conditions. However, the development of polyimide binders can increase the temperature limit to +600° F (Ref. 11). The net effect of elevated temperature in vacuum environment is degradation of the organic binder, causing film failure and loss of adhesion to the substrate.

An investigation of inorganic binders to overcome the thermal resistance deficiency of organic resins has been conducted by several organizations. Successful solid lubricant films using a sodium silicate binder have been reported (Refs. 12 and 13). Sodium silicate formulations useful to 600° F in air can exceed 1200° F in vacuum. Another advantage of sodium silicate binders over the organics is compatibility with liquid oxygen systems.

In the absence of oxygen, the temperature resistance of solid lubricants is increased. For example, molybdenum disulphide with a useful temperature up to 650° F in atmosphere is an effective lubricant in vacuum in excess of 1800° F.

Ceramics have been used successfully for binding graphite and molybdenum disulphide solid lubricants for high-temperature use. However, the high temperatures required to fuse ceramic binders limit use to only a few substrates.

The most widely used solid lubricant pigments are graphite, molybdenum disulphide, and tungsten disulphide.

Graphite. Although fine graphite powder has been used as a lubricant for years, it is not an effective lubricant in vacuum and should not be used on spacecraft mechanisms that must operate in the hard vacuum of space. Lubricity of graphite depends upon the presence of absorbed films of condensable vapors, such as water (moisture), benzene, or ammonia. The absence of such vapors increases the lamellar shear strength of surface crystals exposed by wear, resulting in abrasive hardness with an increased friction coefficient. However, graphite has been used successfully in space vacuum as a matrix for other lubricating solids in electrical brush applications.

Several manufacturers supply silver-impregnated graphite. These materials consist of pressed graphite inwhich the pores have been impregnated with molten silver. Although silver-graphite composites have their greatest use in electrical brushes and contacts, they have also been used in self-lubricating bearings, usually in the form of bushings.

Molybdenum disulphide. The most successful of the solid film lubricants for space applications is molybdenum disulphide. This material so closely resembles graphite that the two are frequently confused. The availability of fine powders of high-purity MoS_2 has led to its widespread use as a lubricant during the past decade.

Rubbing or burnishing a film of MoS_2 onto a metal surface provides a coefficient of friction that generally is in the range 0.04 to 0.10. This range is about one-half the coefficient of friction for similar films of graphite. Although the bonded films have coefficients of friction that are at least twice the values for rubbed-in films, they have much longer wear lives. (See Table 9-3.)

Table 9-3

WEAR LIVES OBTAINED WITH VARIOUS FORMS OF MoS_2

Lubricant	Wear Life at 35,000 psi (cycles)
Resin-bonded MoS_2 film	9,860,000
Grease containing MoS_2	1,590,000
Unbonded MoS_2 powder	130,000

Bonded films of MoS_2 generally surpass bonded films of other solid lubricants at room temperature, as indicated in Table 9-4 (Ref. 14)

Table 9-4

FRICTION AND WEAR LIFE OF FILMS OF SOLID LUBRICANTS BONDED WITH A PHENOLIC RESIN

Solid Lubricant[(a)]	Kinetic Coefficient of Friction	Wear Life (cycles)
Molybdenum disulfide	0.036	103,680
Tungsten disulfide	0.034	100,460
Graphite	0.080	8,640
Cadmium iodide	0.088	4,320
Boron nitride	0.148	360

(a) Laminar solids were bonded on a manganese phosphated surface. Rotary speed was constant at 72 rpm (25.9 ft/min, surface speed). Thickness of coating varied from 0.0003 to 0.005 in. All tests were run at room temperature without atmospheric control.

Steel is the most common base material, but other metals are usually acceptable. If the film requires a high-temperature cure, the curing temperature must be below the point at which the metal or alloy softens, distorts, or becomes dimensionally unstable. Molded plastics and elastomers can also be coated, provided that the surface is properly roughened, chemically etched, or otherwise prepared and there is no adverse effect of the binder on the plastic or elastomer.

The following operating conditions affect the lives of MoS_2 bonded films: choice and size of mating parts, temperature, presence of liquid lubricants, sliding speed, norman load, and vacuum. When two wear surfaces are about the same size, it is preferable to coat both surfaces since this produces a longer life. If one surface is considerably larger than the other, however, the benefits to be obtained from coating the smaller surface are doubtful, and only the larger surface need be coated. If only one surface can be coated, the larger should be selected. When only one surface is coated, the uncoated surface should be smooth and free of burrs that might cut or abrade the coating on the mating part.

When only one of the mating surfaces is in motion, the part that is constantly presenting a fresh surface area to the point of contact should be coated, regardless of which part is in motion (e.g., coat the cam, not the follower). This minimizes contact temperatures and distributes wear of the film over the greatest area.

The harder the substrate on which the MoS_2 film is formed, the lower is its coefficient of friction and the longer it wears. When the rubbing surfaces of two parts have about equal areas and only one part is to be coated, it is usually preferable to coat the harder surface. This is because the flexing action of a soft surface disturbs the bond between the lubricant film and the substrate.

The coefficient of friction and wear life vary with the relative amounts of binder and MoS_2 in the films. Many commercially available MoS_2 films contain up to 10 or 20% of graphite mixed with MoS_2. Too low a ratio of binder to MoS_2 results in poor bonding to the substrate, and too high a ratio gives poor lubricity. For resin-bonded films, a ratio of about 1 to 1 is near optimum for normal applications in air. For sodium silicate bonded films, binder-to-MoS_2 ratios as low as 1 to 10 achieved better performance in air at elevated temperatures that the 1-to-1 ratio.

Resistance to wear is a maximum for a particular film thickness. The resistance to wear drops off rapidly at thicknesses below 1.5×10^{-4} in. (0.15 mils). The decrease in wear life at thicknesses greater than the optimum is less pronounced and is believed explainable by the fact that as the thickness increases, cohesion becomes less than adhesion of the film to the substrate, so that larger wear particles are produced. A properly applied film should be between 1.5×10^{-4} and 5×10^{-4} in. (0.15 to 0.5 mils).

Thickness can usually be controlled more satisfactorily by spraying than by dipping. By controlling the solids content and air pressure, a coating can be applied with a spray gun to within ±0.00001-in. thickness.

The thickness of the films should be taken into account in dimensioning and specifying tolerances on drawings. Allowance should be made for the thickness of the film on surfaces that show a dimension to four decimal places, which usually involve a four-decimal tolerance. If chromium or hard nickel plating is to be used, either to provide a better surface beneath the MoS_2 coating or to ensure a smooth running surface to mate with a coated part, allowance should be made for the thickness of the plate.

When used on ball bearings, only the retainers are usually coated, but both the races and retainers can be coated if care is taken to keep the thickness on the races at a minimum (e.g., 1×10^{-4} to 2×10^{-4} in.) in order to avoid jamming of the bearings. Selecting balls that are slightly undersize or on the small side of the tolerances or selecting races on the proper side of the tolerances can be helpful in providing enough clearance so that the balls are not jammed by a thick film or coating. The coating on the retainer can generally be thicker than that on the races; a thicker coat here provides a reservoir for longer life, provided that the coating is not so thick that it has poor adherence. Longer life can be achieved using a machined retainer in which there are reservoirs of the dry film lubricant. These reservoirs should be areas of maximum expected wear such as in the ball pocket.

New coatings of bonded MoS_2 films slough off slightly when first subjected to rubbing or sliding. For example, particles of the film flake off and contaminate the ball bearings so that the torque is very high. Bearings should be run-in first by slowly rotating or sliding the mating parts over each other by hand, repeating this step in the opposite direction, and then blowing off the surfaces with clean dry air or nitrogen to remove any dislodged particles. The parts should then be bench-cycled at higher speeds and cleaned by blowing. Running at gradually increasing loads is also recommended for increasing the life at the top load.

Unlike oils and greases, the viscosities of which are sensitive to temperature, the coefficient of friction for MoS_2 remains virtually constant from -100° to 650°F. This is an advantage for parts that have to operate at either high or low temperatures or over an extended temperature range. The wear life of resin-bonded films used in air is independent of temperature up to the level at which the film is cured (i.e., up to about 200° to 400°F) and then decreases as the temperature is increased further.

In many cases the use of a lubricating oil with a MoS_2 film reduces the coefficient of friction without affecting the wear life significantly. The wear life of some bonded coatings, on the other hand, can be reduced if the coating is wet with oil during operation. The coefficient of friction decreases with increasing sliding speed to about 1000 ft/min and then remains substantially constant to speeds up to 8000 ft/min. However, the wear life becomes shorter with increasing sliding speed, possibly because of the higher temperatures that are generated. Increasing the normal load lowers the coefficient of friction but shortens the wear life.

MoS_2 Composites. Many plastics and powder metallurgy compacts can be made with MoS_2 particles for gears, bearings, cams, and similar applications. With such composites, the sliding process continues to feed a thin film of MoS_2 to the surfaces so that the friction remains low even after prolonged rubbing.

The addition of MoS_2 to plastics markedly lowers the coefficient of friction (except for Teflon, which has a lower coefficient of friction than MoS_2). When MoS_2 is added to plastics, resistance to cold flow, dimensional stability, and thermal conductivity are usually improved, as well as the friction and wear characteristics.

Fine nylon powder blended with 5 to 20% MoS_2 is commercially available under the trade name Nylatron and can be cold-pressed and sintered by powder metallurgy techniques. The nylon powders are precipitated from solution and have a much higher degree of crystallinity than molded nylon, i.e., 80 to 90% crystallinity compared with 35 to 50% for injection-molded parts. The higher crystallinity reduces hygroscopic swelling and thermal expansion, increases the resistance to deformation under load, and raises the heat distortion temperature, in addition to improving the wear and abrasion resistance. Adding MoS_2 further improves the dimensional stability, reduces the friction, and increases the wear life.

Teflon that is reinforced with glass fibers and filled with MoS_2 is commercially available under the trade name Duroid or Rulon. This type of material has been used for ball bearing retainers under the trade name BarTemp. It provides its own lubrication and is intended for used with synchros, light gyros, motors, and blowers designed for high-temperature use up to 575°F.

A variety of sintered bronzes and other metals filled with MoS_2 are available commercially. Such filled metals provide lower friction and better wear than similar materials that use graphite as an impregnant rather than MoS_2, as indicated by the data in Table 9-5. The MoS_2-filled sintered bronzes have porosities on the order of 10 to 25%, which permits them to be vacuum impregnated with a lubricating oil for further reduction of the friction.

Table 9-5

FRICTION AND WEAR OF SINTERED BRONZE BEARING COMPOSITES WITH GRAPHITE AND MoS_2

Material[(a)]	Coefficient of Friction	Wear (in.)	Time (hr)
Sintered bronze	0.67	>>0.0025	70
Sintered bronze with graphite	0.47	0.002	100
Sintered bronze with MoS_2	0.34	0.001	400

(a) No oil lubrication

Sliding electrical contacts of silver-MoS_2 composites. The electrical noise of silver-MoS_2 composite slip ring brushes was compared with brushes of silver-graphite operated in air and vacuum. The two combinations that produced the least noise in vacuum were brushes of 88% silver + 12% MoS_2 on rings of fine silver and brushes of 88% silver + 12% MoS_2 on rings of rhodium-plated silver. These two combinations performed better in vacuum than they did in air. The use of brushes of 80% silver + 20% graphite on the same ring materials was better in air than in vacuum. Copper rings gave poorer performance than silver or rhodium-plated silver with both brush materials.

Soft Metals. Soft metals with low shear strength, such as silver and gold, can be vacuum deposited, plated, or burnished as thin films over hard substrates to provide lubrication. The theory behind their use is similar to that described earlier for molybdenum disulfide films; that is, the soft film reduces the amount of contact between asperities of the supporting substrate, so that the majority of welded junctions which are formed are readily sheared. The friction and wear of soft metals is greater than that with other lubricants.

Metals such as gold and silver are nonvolatile and have vapor pressures below 10^{-8} Torr up to temperatures as high at 1075° and 1420°F. Other metals that have low vapor pressures and good vacuum stability include lead and indium. The low volatility of such metals permits them to be used as lubricants in certain specialized electronic tubes, where volatilization of such lubricants as oils and greases would destroy the vacuum necessary for the operation of the tube.

Metals are more resistant to radiation damage than organic materials such as oils, greases, plastics, and the resin binders used for MoS_2 films. While the chemical stability varies with the particular metal, that of precious metals such as silver and gold is generally excellent. Gold does not oxidize in the normal atmosphere, and the oxide of silver decomposes at slightly elevated temperatures. The high-temperature stability of metals such as silver and gold makes them promising lubricants for use at elevated temperatures.

The fact that soft metals conduct an electric current can be an advantage. In one application, for example, the use of silver films to lubricate ball bearings eliminated the need for a slip ring by allowing the current to be conducted directly through the bearing elements.

The coefficient of friction is generally at a minimum at film thicknesses on the order of 10^{-5} in. Thicker films of the soft metals result in larger areas of real contact and thereby increase the coefficient of friction at a gradual rate. Thinner films cause an abrupt increase in the coefficient of friction, apparently because they do not prevent the substrate from interacting with the mating part and thus forming stronger junctions. There is also some indication that thinner films can give low coefficients of friction if the surfaces are highly polished.

The effect of temperature on the friction and wear of soft metal films appears to depend on film thickness, the relative softening of the metal film and the substrate, and the temperature level, as well as the soft metal itself. Changes may be due to a reduction in the shear strength of the metal film; the area of real contact remains constant with increasing temperature so long as the substrate remains hard and the film is not too thick. However, wear life is shortened by increasing the temperature. By holding the operating temperatures down, intermittent operation for short periods should give longer actual wear life than continuous operation. Similarly, slow speed should give longer wear than fast speeds. The coefficient of friction decreases with increasing load. The wear life, however, also decreases with increasing load.

Another composite brush material (CLB alloy) for slip-ring assemblies for conduction of high currents (75A at 430 v) has been developed. This material, nominally 82.5 – 85% Ag, 2.5% Cu, and 12.5 – 15% MoS_2, operated for 700 hr in a vacuum of 10^{-9} Torr (300 A/in.^{2} at 424 in./min) with peak electrical noise of 4 mV. There was no appreciated wear of the silver ring, and 0.015 in. total wear of the powder metallurgically produced brush material was observed (Ref. 16). The wear on the silver-graphite composite brush was 2 times greater.

Dispersions of MoS_2 in oils and greases are available commercially and are recommended for minimizing wear during the initial run-in of parts. Such dispersions must be specially prepared to prevent the coagulation of the MoS_2 powders and obtain stable colloidal dispersions.

Tungsten Disulfide. Tungsten disulfide, WS_2, has been investigated as a solid lubricant in vacuum because of its similarity in crystalline structure to molydenum disulfide. However, it has been demonstrated that the behavior of WS_2 is markedly different from that of natural MoS_2 (molybdenite) under various ambient pressure conditions. The coefficient of friction of WS_2 is not much lower in vacuum than in air and reaches a minimum value at 10^{-5} Torr. As the pressure decreases, friction increases and the shear strength curve begins to resemble that of graphite rather than MoS_2 (Ref. 17).

Plastic Thin Film Lubricants. Some solid film lubricants owe their effectiveness to sacrificial wear. Plastics such as nylon, Teflon, and Delrin are the most commonly used lubricants of this type for space applications. These materials are employed in the form of self-lubricating bearings or as retainers for ball bearings. The low compressive strength of plastics is overcome by reinforcing the polymers with glass fibers or other strengthening materials. For example, unmodified Teflon, which exhibits a very low coefficient of friction, has a very high wear rate. By adding reinforcements such as glass fibers or ceramic fibers, or fillers such as graphite, MoS_2, or ZrO_2, although the coefficient of friction is increased, the additives increase the wear life of Teflon.* However, specific applications of bulk unreinforced Teflon should be investigated because of the little understood friction transition occurring in vacuum that lends unreliability to the use of the plastics in space (Ref. 18).

Plastics are also used in sintered form (e.g., Fluorosint and Nylasint) as reservoirs for liquid lubricants, or incorporated into porous metals with other fillers. For example, Sinitex is composed of 55% sintered bronze, 27% Teflon, and 18% MoS_2. The "DU" bushing materials suitable for sleeve and thrust bearings are lead bronze-Teflon linings backed by steel.

In addition to the thermoplastics nylon, Teflon, and Delrin, thermosetting resins such as phenolic and polyimide plastics molded or laminated with fabric or paper fillers are used as bearing retainers. For example, Synthane, a porous paper-base phenolic composition, can be vacuum impregnated with an oil to provide both a retaining mecahnism and lubrication reservoir for ball bearings.

---

*Trade names of reinforced Teflon include Duroid, Fabroid, Bar Temp, and Rulon.

The use of thin films of soft metals for spacecraft applications has several disadvantages. Processing is critical. Special and careful processing is required to deposit adherent films, and the results are very sensitive to the processing treatment and quality control. Obtaining good adhesion between the metallic film lubricant and the metal substrate is the major problem in securing long wear life. Careful cleaning to remove greases, oxide films, and other contaminants prior to deposition is agreed to be an important first step. Silver and gold films adhere better to SAE 52100 steel than to 440C stainless steel. A thin film of nickel over the stainless steel can improve the adherence of vacuum-deposited silver films.

Films are sensitive to mishandling. Care must be taken to avoid disrupting the films by mishandling when the coated parts are assembled. Separable, angular contact ball bearings are used with coated balls because the balls can be easily assembled in the bearings without disturbing the films. With axial loading, this type of bearing requires careful assembly in the bearing housing or mounting. Split races have also been used to facilitate assembly.

No corrosion protection is provided to the substrate. Unlike oil and grease films, the soft metal films are in many cases too thin to protect the underlying metal substrate against corrosion. If the films are used on SAE 52100 steel, or other steels that require some protection against rusting in air, oils can be used to protect the base metal during the period that the parts are stored in a normal earth atmosphere, provided that sulfur-free oil is used in the case of silver films. Silver films can react with the sulfur in a sulfur-bearing oil to form silver sulfide, which increases the friction and wear. The subsequent evaporation of the protective oil from an exposed part in space should not present a problem, since by the time the part is spaceborne, the need for corrosion protection is past and the necessary lubrication is provided by the soft metal film.

Porous Bodies Infiltrated With Soft Metals. Another technique for forming a lubricating film of soft metal is to impregnate a hard porous substrate with the metal, and the metal is fed from the substrate to the surface. Porous bodies infiltrated with a soft metal such as silver offer the advantage of providing a reservoir from which additional soft metal can be fed to the surface to renew surface films as they are worn away. The porous body can be made of a nonmetallic material.

9.5 SPACE SIMULATION TESTING OF LUBRICANTS

The simulated space conditions most relevant to lubricant performance are the pressure and composition of the gas surrounding the bearing or mechanism tested. The effects of temperature extremes and temperature fluctuations have been tested, or determined by extrapolation, from vapor pressure and volatility data applied to standard gas flow equations. Penetrating radiation tests are important if the lubricant will not be shielded by spacecraft structure or if nuclear-powered engines are employed.

At LMSC, experiments have been conducted since 1959 to evaluate the performance of various types of lubricants on ball bearings operating in a simulated space environment (Ref 19). Lubricants evaluated have included oils, greases, bonded films of solid

lubricants such as molybdenum disulfide, and composites of self-lubricating materials such as reinforced Teflon. The lubricants have been evaluated on lightly loaded, instrument-size ball bearings operating 8000 rpm. Simulated space conditions have included vacuum down to 10^{-9} Torr, temperatures up to 300° F and radiation doses up to 5×10^7 roentgens.

9.5.1 Oils

Tests have been completed on 35 different petroleum, silicone, diester, and synthetic oils. Failures have occurred in as little as 164 hr (1 week), whereas one test was discontinued after operating satisfactorily for 48,586 hr (5.5 years). Approximately one-half of the oils failed to lubricate in vacuum in less than half a year. Sufficient tests have been conducted to demonstrate the feasibility of lubricating small ball bearings with certain oils for more than 4 years of continuous operation under light loads.

The radial loads on the bearings were those due to the weights of the rotors. The radial loading ranged from 155 gm (5.6 oz) to 275 gm (9.7 oz). These loads were divided between the two bearings and were of the same order of magnitude as the equivalent radial loads transmitted to the bearings when the torque output of the motors was transmitted through small gears, as in fine-pitch gear trains used for servomechanisms.

Most of the tests with oils were conducted in systems employing oil diffusion pumps and liquid nitrogen traps or zeolite traps, and a number of tests were conducted with ion pumps. Lubricants were evaluated in a combined environment of vacuum and radiation from a cobalt-60 radioisotrope source. The lubricants were not irradiated continuously during testing, since periodically the equipment had to be withdrawn to accommodate other tests. Therefore, the average dose rates over the total test duration may have been less than the total operating time in vacuum.

At the start of the first test under combined vacuum and radiation, the source strength was 560 curies; it decayed to a strength of approximately 400 curies. As a result, dose rates decreased from 4200 ± 10% R/hr to a rate of approximately 300 R/hr. The energy of the two gamma rays emitted from cobalt-60 source are 1.17 and 1.33 MeV, giving an average energy level of 1.25 MeV.

Organic materials such as oils and greases undergo both radiation-induced polymerization, leading to increases in viscosity, and fragmentation, frequently leading to acidic and corrosive products. These chemical changes are initiated by ionization, provided the dose rate is not so high as to cause secondary effects such as overheating.

The results of some of these tests are shown in Table 9-6. Most of the data are for bearings that operated for more than 1 year in vacuum (Ref. 10). Bearings with machined retainers of Synthane have had longer operating times than those with either steel ribbon retainers or balanced, crown-type retainers of a linen-base phenolic laminate.

Table 9-6

LONG-TERM SIMULATED SPACE ENVIRONMENT TESTS OF OIL AND GREASE LUBRICANTS

Materials		Temperature (°F)	Pressure (Torr)	Running Time[b] (hr)	Remarks[c]
Lubricant	Bearings[a]				
Versilube F50 Oil, (General Electric Co.)	1	185	9×10^{-9}	F 13,652	Wear of ball pockets.
Versilube F50 Oil	2	250 max.	4×10^{-9}	F 13,575	
Versilube F50 Oil	2	160	3×10^{-9}	F 16,085	Radiation in vacuum 5.5×10^{7} R, 16,085 hr; 8,726 hr of idle time in vacuum and radiation environment; ion pumped system.
Versilube F50 Oil,	2	250 max.	4×10^{-9}	F 23,460	Bearings heavily worn.
Apiezon J	2	320 max.	10^{-9}	D 41,165	Bearings in good condition; oil present in bearings.
Apiezon K Oil, (Associated Electronic Industries, Limited)	2	215 max.	1×10^{-8}	D 20,019	Bearings not worn; oil present in bearings; no change in torque.
USAF Oil, ML061-97 (DC7024) supplied by Aeronautical System Division, USAF	2	205 max.	4×10^{-7}	D 38,157	Bearings in good condition; oil present in bearings.
XRM 128C, Socony Mobil Oil Co., experimental paraffinic-base petroleum oil	1	170	10^{-8}	F 32,047	One bearing had wear debris; other in good condition.
XRM 141-C; same as XRM 128C but with oxidation inhibitor and lead-carrying additive	1	175	10^{-8}	D 38,254	Bearings in good condition; oil present in bearings.
FS-1265 fluoro-silicone oil (250 centistokes), (Dow Corning)	2	190 max.	1×10^{-3} to 1×10^{-8}	D 48,586	Bearings in good condition; oil present in bearings.
FS-1265 (1600 centistokes)	2	200 max.	1×10^{-3} to 1×10^{-8}	F 17,492	One bearing worn ball pockets; other in good condition, without oil present.
FPPN-10802-77 trifluoro-methylphenoxy phosphonitrile, (E. I. DuPont)	2	170	4×10^{-8}	F 9,640	Ion-pumped system; worn and broken retainer, worn balls and bearing; other bearing dry.
KG 80 paraffinic-base petroleum oil with additive, Kendall Refining Co.	2	170 max.	1×10^{-8}	D 6194	Bearings in good condition, oil still present. Tested as replacement for Terrestic V78, which is no longer available commercially.
FPPN-10802-77, trifluoromethyl-phenoxy phosphonitrile,	2		1×10^{-8}	D 30,576	In diffusion pumped system, oil present, bearings in good condition.
Versilube G-300 Grease, F50 oil in Lithium-Soap Thickener (General Electric Co.)	3	175 max.	2×10^{-7}	D 23,829	Bearings nonrotating 5,488 hr in vacuum; startup after max. 642-hr idle period; satisfactory after each idle period.
Versilube G-300 Grease	3	230 max.	1×10^{-7}	F 22,694	Including 5,488 hr nonrotating; startup after max. 648-hr idle period; satisfactory after each idle period.

Table 9-6 (Cont.)

Materials		Temperature (°F)	Pressure (Torr)	Running Time[b] (hr)	Remarks[c]
Lubricant	Bearings[a]				
Versilube G-300 Grease	3	300 max.	4×10^{-7}	F 4,354	Grease hardened.
Versilube G-300 Grease	3	165	3×10^{-9}	F 12,607	Ion-pumped system; 12,607 hr cobalt-60 radiation in vacuum, 4×10^{7}R.
Aeroshell 15,(Shell Oil Co.) (meets MIL-G-25013 and MIL-G-27343), methypenyl silicone oil with dye thickener	3	250 max.	2×10^{-7}	D 20,147	Grease in bearings not hardened; bearings in good condition.
Aeroshell 15	3	195	7×10^{-9}	F 5,518	Ion-pumped system; 4,097 hr cobalt-60 radiation 1.7×10^{7}R.
Aeroshell 15	3	12,000 hr at 250 then 160	2×10^{-7}	D 19,437	Test discontinued at 16,610 hr; exposed to air for 8 months and restarted in vacuum.
Martin-Rockwell, EG 509, silicone oil with organic thickener and solid lubricant	3	200	1×10^{-8}	F 33,744	Grease dried; bearing had wear debris.
USAF MLG-61-92, aryl urea thickened high phenyl content methylphenyl silicone, supplied by Aeronautical Systems Division, USAF	3	200	1×10^{-9}	D 38,194	Stopped at 25,319 hr, idle in vacuum 5 months, restarted; bearing in good condition; grease present.
USAF MLG-62-142, ammeline thickened inhibited, high phenyl content silicone oil, supplied by Aeronautical Systems Division, USAF	3	195	1×10^{-9}	D 38,539	Test stopped at 25,223; restarted after 5 months.
Andok C, (Humble Oil and Refining Co.)	3	150	2×10^{-8}	F 13,362	Bearings badly worn and dry.
Super-mil ASU Grease No. 31052 (American Oil Co.) (meets MIL-G-25013), silicone oil with aryl substituted urea thickener	3	175 max.	2×10^{-8}	F 28,530	Bearing jammed with dried grease and wear debris.
EG 429, Marlin-Rockwell Corp., silicone oil with organic thickener and solid lubricant	3	200 max.	1×10^{-8}	F 12,889	Grease hardened, bearing worn; one bearing satisfactory.
FS 1290, fluorosilicone oil with soap thickener, (Dow Corning)	3	195 max.	1×10^{-8}	D 13,835	Both bearings in good condition; grease turned dark color, beginning to degrade.
DC 40, silicone oil with metallic soap thickener, (Dow Corning)	3	168 max.	1×10^{-8}	D 14,601	Bearings and grease in good condition.

(a) Deep-groove, double-shielded R3-size ball bearings (3/16-in. bore, 1/2 in. o.d.), 8000 rpm. Load on bearing is weight of motor-rotor, typically 160 to 278 grm.
1: AISI 52100 synthane retainer. 2: AISI 440C synthane retainer. 3: AISI 440C ribbon retainer. 4: AISI 52100 linen-based phenolic retainer.

(b) Total running time in vacuum; tests discontinued because evaluation considered complete (1 year = 8760 hr). Data to 1 May 1968
F: failed. D: discontinued.

(c) Average energy of γ-radiation is 1.25 MeV. Diffusion-pumped vacuum systems unless otherwise noted.

The dominant mode of failure with oils has been the partial or complete loss of lubricant, with resultant wear and formation of fine wear particles, principally from the retainer. It is not clear whether the loss of lubricant is due to evaporation or creepage, although it is worth noting that no general correlation has been found between vapor pressure and lifetime and that silicone oils, which are generally regarded as being most subject to creep away from lubricated areas, have given long lifetimes. A second failure mode has been the partial loss of oil together with the decomposition of part of the remainder, leading to the formation of large oil residue particles bonded together with retainer wear debris.

A bearing test with a silicone oil, which was the same oil as used in the diffusion pumps, gave a lifetime of 2603 hr in vacuum. Thus, even under the most favorable conditions, the diffusion pump oil provides a lifetime that is an order of magnitude less that that obtained with the longest lived lubricants.

In another test to verify this conclusion, a motor with two unshielded, dry bearings with Synthane retainers was mounted in the position closest to the pump in a vacuum chamber with an oil diffusion pump. The motor was allowed to remain idle in this position for 1000 hr, which should have been sufficient to collect some migrating oil vapors from the system, and was then started and operated until failure. The bearings failed in 2400 hr, and both retainers were severely worn. A second motor was operated in a similar manner in an ion pumped system, and again the bearings suffered severe retainer wear over a period of 2400 hr.

Halogenated and high-phenyl silicone oils have given longer lifetimes in vacuum than either dimethyl or phenylmethyl silicone oils with low or medium phenyl contents, as indicated in Fig. 9-1. This observation supports the conclusion that increasing the polarity of the oils increases the tenacity with which they attach themselves to metal surfaces and provides better lubricant films. Dimethylsilicone, being a symmetrical chain molecule, has the lowest polarity of the oils indicated. Replacing some of the methyl groups with phenyl groups gives higher polarity, and partial halogenation of the phenyl group gives the highest polarity of all. The improved performance in vacuum noted with increasing polarity roughly parallels similar improvements in air.

9.5.2 Greases

Tests on bearings lubricated with 15 different greases, similar to those with oils, have been conducted to evaluate their performance in vacuum. Lifetimes have varied from 340 hr (2 weeks) to over 38,000 hr (4.75 years). Approximately one-half of the greases tested failed in less than 6 months. Greases based on halogenated silicones and phenylmethyl selicones have given the longest operating times in vacuum, including operation in vacuum at moderately elevated temperatures and exposure to gamma radiation. They have also operated with acceptably low torque levels at the test temperatures (Table 9-6).

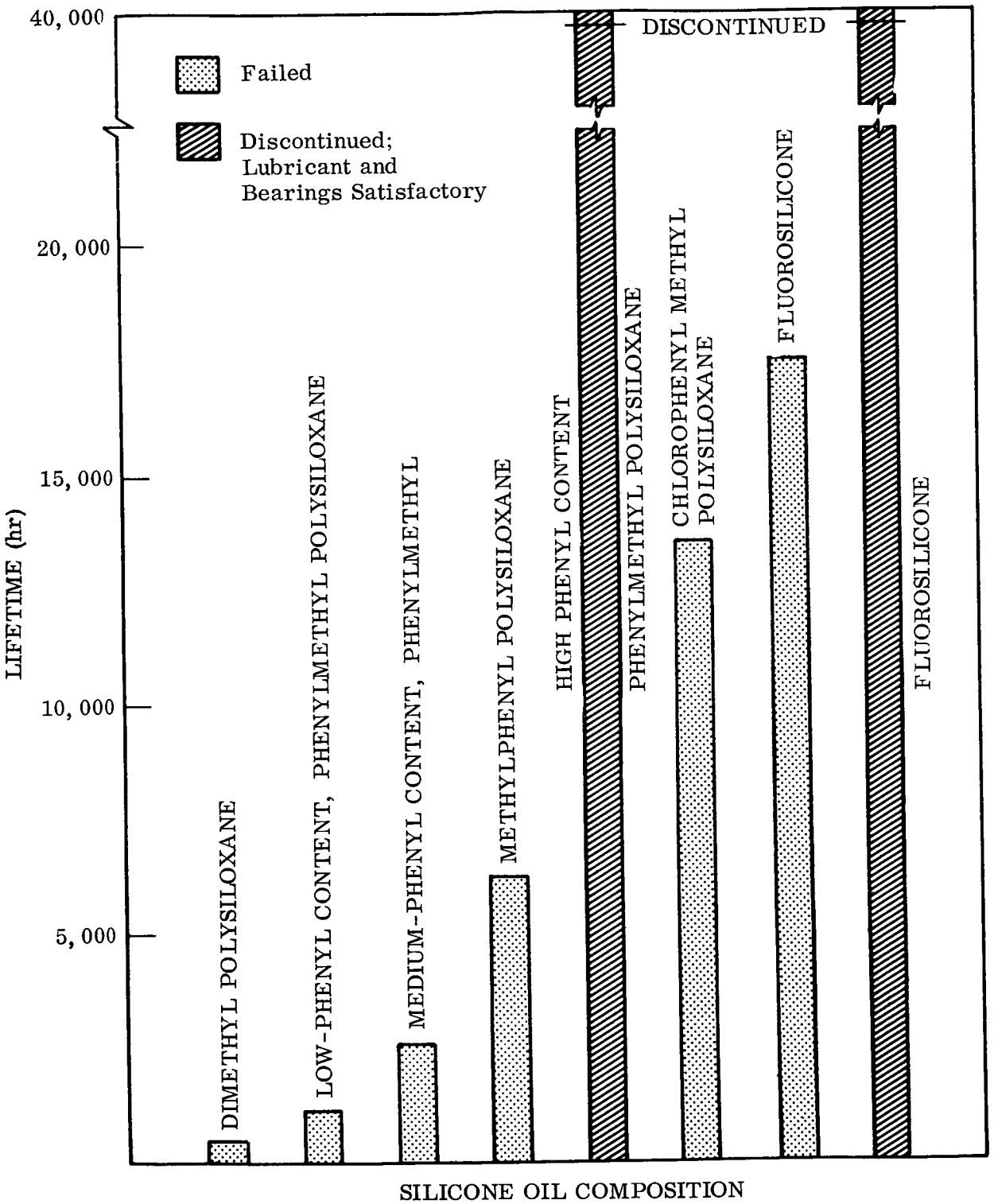

Fig. 9-1 Effect of Silicone Oil Composition on Bearing Lifetime in Vacuum

9.5.3 Bonded Films

Tests have been completed on ball bearings lubricated with 10 different bonded films of solid lubricants, most of them containing molybdenum disulfide. Lifetimes in vacuum have ranged from as short as 7.8 hr to as long as 2554 hr (less than 3.5 months), except for one test that had additional lubrication from a Teflon retainer (Table 9-7). The performances of the bonded solid films on instrument-size ball bearings have been relatively poor; these lubricants are characterized by short lifetimes and poor reproducibility (Table 9-7).

9.5.4 Special Retainer Materials

Ten different special retainer materials have been tested for use with ball bearings; these include both reinforced plastics and powder metal composites, some inherently self-lubricating and others impregnated with oil to make them self-lubricating. Reinforced Teflon composite retainers have given lifetimes in excess of 8,000 hr at axial preloads below 1 lb. Two tests with 1-lb preloads gave life times of 3,180 and 11,248 hr. Failures have been due to wear of the ball pockets, resulting in enlargement of the pockets, jamming of wear particles between bearing parts, and sometimes breaking of the retainer.

Generally, it appears that the performance of all the special retainer materials tested is limited by wear resistance and strength, even for materials that have low coefficients of friction (Table 9-7).

9.5.5 Summary of Simulation Tests of Bearings

Conclusions regarding the performance of ball bearings in vacuum and combined space environments include the following:

- Operation in vacuum can reduce lubricant lifetime to less than that obtained for operation in air. To operate equipment in space for long periods, the mechanisms must be housed in pressurized and sealed units, some means of lubricant replenishment must be provided, or the lubricants must be carefully selected from those that have demonstrated satisfactory operation in vacuum.
- Oils and greases provide the best lubrication for ball bearings exposed to vacuum. Special considerations that may favor other lubricants (e.g., molybdenum disulfide films and reinforced Teflon) include cryogenic temperatures, high temperatures, and exposure to nuclear radiation.
- Selected oils and greases have demonstrated lifetimes in vacuum of up to 5 years. They have also demonstrated lifetimes in vacuum up to 2 years when exposed simultaneously to a dose of 10^7 R of gamma radiation from a cobalt-60 source.
- Generally, ball bearing lifetime with oil lubrication increased with viscosity, and the increase was most pronounced at low viscosities. The use of oils with extremely high viscosities is limited, however, by excessive bearing torque

Table 9-7

LONG-TERM SIMULATED SPACE ENVIRONMENT TESTS ON SOLID LUBRICANTS AND SPECIAL RETAINER MATERIALS

Material	Maximum Temperature (°F)	Pressure[a] (Torr)	Running Time[b] (hr)	Remarks
Hi-T Lube, General Magnaplate, Inc., solid film, molybdenum disulfide, which was applied to bearing races and balls with modified Teflon retainers;[c] rotor weight, 275 gm.	145	2×10^{-7}	D 8,117	Ball pockets of both retainers badly worn.
	170	2×10^{-8}	F 1,198	Start-stop-reverse; broken retainers.
Applied to races and balls with paper-based phenolic retainers; rotor weight, 275 gm.	140	7×10^{-7}	F 2,554	Worn and broken retainers; ball pocket wear.
Everlube 811, Everlube Corp., sodium silicate bonded MoS_2 applied to races and retainers only, after grit blasting;[d] rotor weight, 275 gm.	180 200 at failure	1×10^{-9}	F 2,213	Bearing worn; balls were being forced from retainer pockets; high final torque.
	170	8×10^{-7}	F 1,862	Broken retainer.
	185	2×10^{-7}	F 772	Start-stop-reverse; jammed by wear debris.
Rulon C, modified Teflon, Dixon Corp.; single-piece retainer machined of material, balls and races of AISI 440C steel, double shielded; rotor weight, 275 gm.	210	2×10^{-8}	D 12,636	Ball pockets worn; wear debris buildup in pockets; 0.25 axial thrust load; start-stop-reverse; restarted in vacuum several times after stopped for 3 weeks; wear debris in worn ball pockets; 0.25-lb axial thrust load.
	180	2×10^{-8}	F 8,624	
	170	6×10^{-8}	F 3,180	No load first 518 hr; 1-lb axial thrust load; 2662 hr; ball pocket worn.

Table 9-7 (Cont.)

Material	Maximum Temperature (°F)	Pressure[a] (Torr)	Running Time[b] (hr)	Remarks
	145	3×10^{-8}	F 10,771	0.5-lb axial thrust worn ball pockets and broken retainer.
	140	3×10^{-8}	F 11,248	1-lb axial thrust load; worn ball pockets.
Duroid 5183, Rodgers Corp. 60% Teflon, 40% glass fibers with molybdenum disulfide; single-piece retainer machined of material, balls and races of AISI 440C steel, double shielded; rotor weight, 275 gm	200	10^{-8}	F 5,110	0.25-lb axial thrust load; tests at 0.5; failed at 62 hr; start-stop-reverse; failed at 90 hr, 90 reversals.

(a) Ion-pumped vacuum chambers
(b) Total running time in vacuum; tests discontinued because evaluation considered complete (1 year = 8,760 hr). Data to 1 May 1968. F: failed. D: discontinued.
(c) Deep-groove ball bearings of AISI 440C balls and races, not shielded.
(d) Deep-groove ball bearings of AISI 440C balls and races, and ribbon retainers, not shielded.

and inability to operate at low temperatures. Oils with room-temperature viscosities of 50 to 250 centistokes appear most useful for providing both long lifetimes and good torque characteristics.

- Ball bearings with retainers of reinforced Teflon, a self-lubricating material, have operated successfully in vacuum for over 10,000 hr, provided that bearing loads were light. Bonded solid film lubricants have given shorter lifetimes and generally poor reproducibility of results, although under good conditions they have given lifetimes up to 1-1/3 years.
- Bearing failures have been preceded by lubricant failures. With oils, the lubricant failure has been due to the partial or complete loss and decomposition of the lubricant followed by rapid wear; with greases, to the drying out of the greases and stoppage of the bearings by the hard, soapy residue; with bonded films of solid lubricants, to wear-through of the films followed by rapid wear and jamming; and with reinforced Teflon retainers, to excessive wear of the ball pockets.

9.6 GEAR MATERIALS AND LUBRICATION

For instrument-sized gears for scanner, actuators, and solar array drives for spacecraft subsystems, the usual metal alloys have been used. Such steel alloys as carburized and hardened AISI 1020, modified 135 Nitralloy nitrided, carburized and hardened AISI 8620 and AISI 9320 have been used in a variety of spacecraft systems in sealed gear boxes. The high-strength steel alloys such as AISI 4340 have also been used in the heat-treated condition, particularly as output gears or pinions. Dry film molybdenum disulfide lubricants burnished or in organic or silicate binders mixed with graphite have been applied to the gear teeth. Fluid lubricants such as oil and grease have also been used.

Several nonferrous gear materials have been used on spacecraft where it was necessary to keep the magnetic field of the spacecraft low. The aluminum alloys 2024-T3 and 7075-T6, the beryllium-copper alloy 25 (nominally 2.5% Be, balance Cu), and phosphorbronze-MoS_2 composites have been used. The phosphorbronze-MoS_2 composite is self-lubricating; the aluminum alloys were coated with light or hard anodize and lubricated with MoS_2 films or oil and grease. The beryllium-copper gears have been heat treated to 41-44 Rc and lubricated with oil or grease.

The corrosion-resistant stainless steels AISI 303, 415, and 440C have also been used for gear applications. The 416 and 440C are magnetic materials; the 303 is low in magnetic properties. The gears are usually lubricated with oil or grease, although some MoS_2 solid films have also been used (e.g., Lubeco 905 on the Surveyer TV camera drive mechanism.

The plastic gear materials nylon (Zytel*) and Nylasint, reinforced Teflon, and Delrin* (an acetal plastic) have been used for low-speed, lightly loaded gears. The plastic gears can be unlubricated, although it is better to apply a little oil or grease. The

---

*Trade name of E.I. duPont deNemours Co., Inc.

reinforced Teflon composite is self-lubricating; however, to improve the friction behavior and cold-flow resistance of the composite, MoS_2 is sometimes added. These plastic gears are lightweight and corrosion resistant, but for precision gearing they do not have the required dimensional stability and their wear life is short compared with that of a properly designed and lubricated metal gear.

Some recent work on the wear in vacuum of instrument-sized gears has been done (Ref. 20). In this work the wear of the gears was evaluated using four-square gear testers in a ion-pumped vacuum system. The speed was 1800 rpm with a 20 in.-oz torque load. Testing in a dust-free laboratory atmosphere was also done for comparison. Evaluation was based on 10% reduction of tooth profile – the percentage of wear on three adjacent teeth after 720 hr of continuous operation.

Materials tested were:

Carburized AISI C1020 Steel – case depth 0.002 to 0.003 in.
Nitrided Nitralloy 135 Modified Steel – case depth 0.002 to 0.003 in.
Beryllium – Copper alloy 25
7075 Al Alloy Deep Anodized (Martin Hard Coat) – case depth 0.002 to 0.003 in.
AISI 440C Stainless Steel – heat treated to R_C 55–60
Phosphor Bronze – 15% MoS_2 Composite
AISI C1085 Steel – heat treated to R_C 50, silver plated 0.0001 and 0.0001 in.
E_3C Molykote Film (MoS_2 film applied by Alpha Molykote Corp.)

In some of the early testing, it was found that the 7075 aluminum alloy gears with the Martin Hard Coat anodize treatment wore the ultimate 10% in 20 hr in the laboratory dust-free environment but showed only 2.5% wear in 720 hr in vacuum. A test was repeated where the maximum wear was 2.5% in 720 hr in vacuum, but when the same gears in the same test fixture were operated an additional 20 hr in dust-free laboratory air the maximum wear was 75%. The mating gears were nitrided Nitralloy 135 modified steel. This behavior was true to a lesser extent with the gears of AISI 440C stainless steel mating with the nitrided Nitralloy. The wear on the 440C, which was the softer material of the pair, was about 2.6% for 720 hr in vacuum and 5.2% for the same material operated in dust-free laboratory air (Table 9-8). In this case, even the wear in dust-free air was not considered excessive.

The indications are that there probably could be more wear of some unlubricated metallic gear materials during operation in dust-free laboratory air than in vacuum. Exposed gears on spacecraft mechanisms are often required to operate for long periods (> 20 to ~ 720 hr) during prelaunch subsystems and systems tests. These tests are usually in air, sometimes dust free. Apparently as much if not more wear can occur in this environment as in space. Spacecraft designers should select materials with the entire prelaunch environment and test program in mind as well as the space environment.

Table 9-8

WEAR OF INSTRUMENT-SIZED FINE-TOOTH GEARS, UNLUBRICATED, IN VACUUM AND DUST-FREE LABORATORY AIR

Material Pairs	Average Wear (%)		
	After 720 hr in vacuum	After 720 hr in air	After 720 hr in vacuum + 20 hr in air
Nitrided Nitralloy – AISI 440C			
Nitralloy	2.9	1.0	
440C	2.6	5.2	
Nitrided Nitralloy – Carb. C1020			
Nitralloy	4.5		
Carb. C1020	2.6		
Nitrided Nitralloy – 7075 Al-MHC(a)			
Nitralloy	2.0		3.1
7075 Al MHC	2.2		62.5

(a) Martin Hard Coat anodize.

9.7 REFERENCES

1. D. Tabor, "Friction and Wear," Proc. of Internat. Symposium of Lubrication and Wear, eds. D. Muster and B. Starrlicht, McCutchan Pub. Corp., Berkeley, Calif., 1965

2. F. P. Bowden and D. Tabor, The Friction and Lubrication of Solids, Oxford Univ. Press, London, 1954

3. C. Lipson and L. V. Colwell, Handbook of Mechanical Wear, Univ. of Michigan Press, 1961

4. J. B. Rittenhouse, "Space Simulation Testing of the Adhesion of Metals," pp. 88–109 in Adhesion or Cold Welding of Materials in Space Environments, STP 431, American Society for Testing and Materials, Dec 1967

5. C. E. Moeller, J. Bossert, and M. Boland, Cold Molecular Welding Study in Ultrahigh Vacuum, Final Report, Project No. 2817E, Midwest Research Institute, Kansas City, Mo., Dec 1965

6. E. E. Bisson and W. J. Anderson, Advanced Bearing Technology, NASA SP-38, 1964

7. S. Sadjian and H. Gisser, "Evaporation of Organic Compounds From Metal Surfaces at High Vacuum," Symposium on Behavior of Petroleum Products and

Derivatives in Space, sponsored by Division of Petroleum Chemistry, American Chemical Society, Los Angeles, Calif. 4–5 April 1963

8. E. E. Kerlin and E. T. Smith, Measured Effects of the Various Combinations of Nuclear Radiation, Vacuum and Cryotemperatures on Engineering Materials, Biennial Report R2K 290, General Dynamics, Fort Worth Division, 1 July 1966

9. E. R. Braithwaite, Solid Lubricants and Surfaces, the McMillan Co. New York, 1964

10. H. I. Silversher and S. P. Drake, Lubrication Evaluation, MRI 503.02, Lockheed Missiles & Space Company, Sunnyvale, Calif., April 1968

11. M. E. Campbell, "Solid Lubrication Technology: A Review," Mechanical Engineering, February 1968

12. M.J. Devine et al., "Inorganic Solid Film Lubricants," J. Chem. Eng. Data 6 (1), 79, January 1961

13. V. Hopkins et al., "MLF-5, An Inorganic Solid Lubricant Film," Proc. of USAF–SwRI Aerospace Beaming Conf., 30 September 1964

14. M. J. Devine, E. R. Lamson, and J. H. Bowen, "The Effect of the Chemical Composition of Metals in Solid Lubrication," Symposium on Behavior of Petroleum Products and Derivatives in Space, sponsored by Division of Petroleum Chemistry, American Chemical Society, Los Angeles, Calif., 4–5 April 1963

15. E. R. Lamson and M. J. Devine, "Navy Dry Film Development," pp. 17–19 in Symposium on Materials Research in the Navy, Philadelphia, Pa., March 1959

16. F. J. Clauss, Electrical Transmission Components for a Large Aerospace Environmental Chamber, AEDC TR-65-40, Arnold Engineering Development Center, Tallahoma, Tenn., February 1965

17. A. J. Haltner, Friction of Tungsten Disulfide Sliding in an Ultrahigh Vacuum System, Report R 67 SD 63, General Electric Co., Missiles and Space Division, Philadelphia, Pa., Nov 1967

18. D. G. Flom and A. J. Haltner, Lubricants for the Space Environment, Report R 68 SD 6, General Electric Co., Missiles and Space Division, Philadelphia, Pa. March 1968

19. F. J. Clauss and W. C. Young, "Materials for Lubricated Systems," Chapter 12 in Space Materials Handbook, 2nd ed., eds. C. G. Goetzel, J. B. Rittenhouse, and J. B. Singletary, ML-TDR-64-40 (AD 460-399), X65-14878, Lockheed Missiles & Space Company, Sunnyvale, Calif., January 1965

20. S. Guzder, Vacuum Test of Instrument Size Gears, Periodic Progress Report K6088, Illinois Institute of Technology Research Institute, February 1967

Chapter 10

ADHESIVES

R. E. Mauri

As spacecraft have become more sophisticated in design and construction, the requirements have steadily increased for adhesives that perform with high strength retention and reliability in the space environment. The use of structural adhesives rather than mechanical fasteners or fusion welding in spacecraft makes possible more efficient load distribution (e.g., lessened stress concentrations, which result in longer fatigue life under cyclic or static loads). Thus, thinner sections can be used, resulting in significant weight savings, which can be a critical factor in space technology.

Adhesives for bonding of structural and nonstructural spacecraft components must function predictably and reliably for durations up to 5 years under the operational and environmental conditions associated with their mission in space. High strength, strength retention, chemical inertness with materials to be bonded, low volatility or degassing, and ease of fabricability are the foremost design and manufacturing considerations in selecting the proper adhesive for a particular application. The space environmental conditions of high-energy particulate and electromagnetic radiation, vacuum, and solar ultraviolet radiation, as well as elevated and cryogenic temperature extremes, can produce profound changes in the chemical and physical properties of adhesive bonds that result in alterations of their mechanical properties. To select the proper adhesives for given applications, the spacecraft designer must, therefore, know and consider the effects of the individual and combined environments, because effects are often synergistic. Equally important considerations are the nature of the substrates or adherend surfaces, component configurations and size, and producibility of the bonded structure.

Fortunately, a large number of adhesives offering a wide range of properties and resistance to such environments are available commercially. Generally, an adhesive is formulated to give an enhanced property or processing advantage, e.g., low-temperature impact strength or ambient temperature-contact pressure cure or both. No single adhesive can be used for all spacecraft structural or nonstructural applications. It is exceptional that an adhesive having excellent properties and strength retention under one set of environmental conditions will excel under another set of conditions. Hence, the designer must have at hand sufficient information to make selection of an adhesive for a given application.

A great deal of information is available in the literature on the effects of the simulated space environment on adhesives. Most of the data is on structural adhesives, since this is the application of principal concern. This chapter summarizes the more recent data on the separate and combined effects of elevated temperatures to 500° F, cryogenic temperatures to -423° F, high-energy particulate and electromagnetic

radiation, and vacuum on the more important chemical classes of structural adhesives used in aerospace technology. No attempt has been made to cover the extremes of high temperature encountered by adhesives in such applications as supersonic and hypersonic aircraft, missile structures, and reentry bodies.

Adhesives are used in spacecraft programs in many ways. The principal uses are in metal-to-metal bonding and in bonding of plastics such as honeycomb core to metal or reinforced plastic skins. Brackets, reinforcing panels, and auxiliary equipment can be adhesive bonded to major structures with resultant weight savings and without disturbing or weakening the structure.

Emphasis on polymer and adhesives development in recent years has resulted in excellent progress in improvement of properties and resistance at temperature extremes. Many of these materials have been adapted by the adhesives industry into structural adhesive formulations offering high strength, long-term strength retention, and stability at temperatures from -423°to 500° F, and up to 1000° F for short-duration exposures. In inert gas environments or vacuum, the maximum use temperature and time at temperature can usually be extended over those in air since oxidative degradation, an important effect in organic systems above 400° to 500° F, is reduced or eliminated.

10.1 CLASSES OF ADHESIVES

Most of the structural adhesive systems used in aerospace technology are proprietary products, the compositions of which are usually defined by identification of their polymeric chemical classes. Commercial structural adhesives can be cured from ambient room temperature to elevated temperatures up to 800° F and may be in one of three forms: (1) nonsupported calendered or cast film, (2) resin-impregnated carrier cloth supported film, or (3) paste or putty. Table 10-1 (Ref. 1) lists some of the adhesives that are most commonly used in the aerospace industry today. This table defines the chemical class of each adhesive, gives its form, and includes a few special-use features for each type.

10.1.1 Unsupported Film Adhesives

10.1.1.1 Phenolic Nitrile

The phenolic nitrile adhesives are intended primarily for bonding of metal-to-metal joints or continuous faying surfaces. The system consists of two parts: an elastomeric modified phenolic in the form of an unsupported tape, and a metal primer. The material requires curing temperatures ranging from 275° to 350° F. Curing pressures ranging from 15 psi (produced by vacuum-bagging) to 100 – 200 psi are customarily used.

10.1.1.2 Nylon-Epoxy

The nylon-epoxy systems were developed as a dual-purpose metal-to-metal and sandwich construction adhesive. They provide high tensile-shear strengths of

Table 10-1

CHEMICAL CLASSES OF STRUCTURAL ADHESIVES

Class of Adhesive	Form	Short-Time Service Temperature Range (°F)	Special Features
Phenolic Nitrile	Calendered film	-67 to 260	Provides high shear properties when aged for 2-1/2 years at 250° and 350°F.
Nylon Epoxy Type I	Liquid	-423 to 180	Provides high shear properties and assembly-line fast cures.
Nylon Epoxy Type II	Cast film	-423 to 180	Combines high shear properties with good humidity resistance.
Nylon Epoxy Type III	Calendered film	-423 to 180	Provides high shear properties.
Rubber-Phenolic MIL-A-8431 Type I	Liquid	-20 to 220	For bonding vulcanized synthetic rubber to itself or metals.
Polyimide and Polybenzimidazole (Polyaromatic)	Supported film	-423 to 1000	High-temperature-resistant adhesive. Requires high curing temperature and pressure. Difficult to process.
Modified Epoxy MIL-A-5090 Type I	Supported film	-67 to 180	Provides MIL-A-5090 and MIL-A-25463 properties when cured at 200°F.
Modified Epoxy Type II	Supported film	-423 to 300	Provides structural properties up to 300°F and better peel resistance than the epoxy phenolics, with no blowing during cure.
Modified Epoxy Type III	Supported film	-423 to 400	Provides structural properties for 10 min up to 400°F and better peel resistance than the epoxy phenolics, with no blowing during cure.
Vinyl-Phenolic MIL-A-5090	Supported film	-67 to 180	General-purpose high shear strength adhesive.
Epoxy Phenolic	Supported film	-423 to 500	Provides uniform shear strength throughout its temperature range.
Phenolic Neoprene	Supported film	-300 to 180	Bonded joints resist extreme bending and shock loads.
Phenolic Butyral	Supported film	-67 to 180	Low-cost commercial sandwich adhesive.
Epoxy Polyamide	Two-part paste	-423 to 180	Room-temperature curing cryogenic adhesive.
Epoxy Nylon Polyamide	Two-part paste	-423 to 160	Good peel properties at cryogenic temperatures when cured at room temperature.
Polyurethane	Two-part paste	-423 to 140	Best peel properties and shock resistance at cryogenic temperatures when cured at room temperature.

5000 to 7000 psi and peel strengths of 22 to 40 in.-lb per 3 in. width. No release of solvents or condensation products are evolved during the cure. Thus, nonperforated sandwich core may be used without danger of rupturing the core due to the pressures generated by the evolution of excess volatiles. The nylon-epoxies also have good cryogenic temperature strengths to -423° F. They provide good sandwich core filleting and produce high strength-to-weight ratio in sandwich structures. These systems cure under contact pressure to 15 psi, and at temperatures ranging from 300° to 350° F.

10.1.1.3 Rubber Phenolic

The rubber phenolic systems can be obtained as pressure-sensitive systems and were developed as fuel cell tank and bulkhead adhesives where wide mismatches in joints were evident. These materials can be cured under contact pressure and at temperatures below 250° F.

10.1.2 Supported Film Adhesives

10.1.2.1 Polyaromatics

The polyaromatics are a class of adhesives of which the polybenzimidazoles (PBI) and polyimides (PI) are of chief commercial importance. The PBI adhesives were the first structural adhesives having the capability of withstanding short-term exposures of up to 1000° F and long-term use at 500° F. These adhesives allow effective use of such temperature-resistant metals as beryllium, stainless steel, and titanium in bonded structures.

10.1.2.2 Modified Epoxy

New developments have recently been made that permit the temperatures of modified epoxies to be extended to the range -423° to +400° F. These are 100% solids, non-volatile systems developed specifically for use with unperforated sandwich core for high-temperature use. These systems provide higher temperature properties than the former epoxy adhesives, which were limited to about 200° F, and give better tensile-shear and peel strength properties than the high-temperature-resistant adhesives for short-term exposure at temperatures up to 400° F.

10.1.2.3 Vinyl-Phenolic

The vinyl-phenolics were the first adhesives used extensively for sandwich construction. These systems are suitable for low-cost sandwich structures, and for low-density parts with large-cell-size aluminum core and honeycomb core. They are finding wide use in manufacturing of aircraft decoys, and in industrial and architectural building.

10.1.2.4 Epoxy-Phenolic

The epoxy-phenolic adhesives are used for both metal-to-metal and sandwich construction where temperatures for very short-time exposures up to 1000° F, intermediate duration exposures of 500° F, and low temperatures to -423° F are encountered. They are generally available on a glass fabric supported film. They have good bond strength with the temperature-resistant metallic alloys such as stainless steel, titanium, and beryllium but are subject to oxidative degradation when aged for long periods at temperatures in the vicinity of 500° F.

10.1.2.5 Neoprene-Phenolic and Butyral-Phenolic

The neoprene-phenolic structural adhesives were the first to be developed in the United States. They were used in the construction of the B-36 and are still in use today in modern jet aircraft. Not only did their systems succeed in transferring loads from one component to another, but they did this so efficiently that former problems associated with stress concentrations in and around rivets, resulting in fatigue cracking, were reduced. They have high resistance to vibration and fatigue loading and have been used for bonding dissimilar materials, particularly aluminum to magnesium. The butyral-phenolic adhesives have similar applications.

10.1.3 Paste or Putty Adhesives

10.1.3.1 Epoxy-Polyamide

The liquid and putty adhesives are normally desired where curing at room temperature is required, in areas with large mismatches, and where only contact pressure can be used. They are also adaptable for fairing and caulking applications. The epoxies combine the properties of good wetting action, low shrinkage, high tensile and tensile-shear strengths, toughness, and chemical inertness, providing a very versatile class of adhesives. Most of the epoxy systems, however, have comparatively low peel strengths when compared with the elevated-temperature curing systems. Joints must be designed in such a manner that they are not subject to peeling.

10.1.3.2 Polyurethanes

Polyurethane adhesives have been developed for cryogenic applications. This class of adhesives provides high tensile strength, high resilience, resistance to abrasion and oxidation, and resistance to most oils and solvents. Polyurethanes are generally two-part systems that provide higher ultimate shear and tensile strengths and also higher peel and shock properties at -423° F than at ambient room temperature, which is the inverse of most structural adhesives.

10.2 EFFECTS OF TEMPERATURE

The use of active or passive thermal control systems on spacecraft, as required for long-term reliability of sensitive electronic components, minimizes extreme temperature

variations and the maximum service temperature requirements of adhesive-bonded spacecraft components. Generally, temperature extremes for orbiting spacecraft are held to within the range -100° to +250°F, depending on operational use and location within the spacecraft. Exceptions are applications where bonded structures are used to contain or are in the proximity of cryogenic fuels and oxidizers which may be at temperatures as low as -423°F, the boiling point of liquid hydrogen. Structures such as nosecones and shrouds which experience ascent heating may reach temperatures as high as 600° to 700°F. The use of adhesives in rocket nozzle exit cones and ablative heat shields is beyond the scope of this handbook.

10.2.1 Effects of Elevated Temperature on Mechanical Properties

10.2.1.1 In Air

Generally, elevated temperatures cause one or more of the following effects on organic adhesive bonds:

- Changes in their properties, such as softening, flow, and attendant decrease in the cohesive strength of the resin in the glue line
- Porosity due to evolution of volatiles
- Chemical decomposition through pyrolytic degradation of the organic skeletal structure of the adhesive resin
- Decomposition through reaction with the adherend surfaces or with an oxidative environment

These effects are manifested by a decrease in such important mechanical property design parameters as ultimate tensile-shear and peel strengths. Some, but generally not all, the strength decrease is recovered when the temperature of the adhesive bond returns to ambient, if the maximum exposure temperature and time are such that no significant thermal decomposition has occurred. In the vacuum of space, oxidative degradation is not of primary consequence, although trapped residual air in the glue line can produce minor effects until it is exhausted in the reaction.

Polybenzimidazole Adhesives. The polybenzimidazole adhesives are based on polyaromatic compounds which are the reaction products of a tetramine and bis-phenyl ester. They provide tensile-shear strengths at very short exposures (1 to 2 min) to temperatures up to 1000°F. The PBI adhesives have better heat stability than the epoxy phenolics and provide better bond strength retention between 300° and 1000°F. Long-time aging characteristics of the bonds with stainless steel and titanium can be further improved by incorporating an inorganic arsenic compound into the adhesive (Ref. 2). Figure 10-1 (Ref. 1) shows the effect of elevated temperature on epoxy-phenolic, modified epoxy, and high-temperature-resistant polybenzimidazole (PBI) adhesives.

Figure 10-2 shows the thermal stability properties of a PBI adhesive stabilized with an inorganic arsenic compound. The material has a strength retention of about 1500 psi at 800°F. In Fig. 10-3 the tensile-shear strength degradation of material

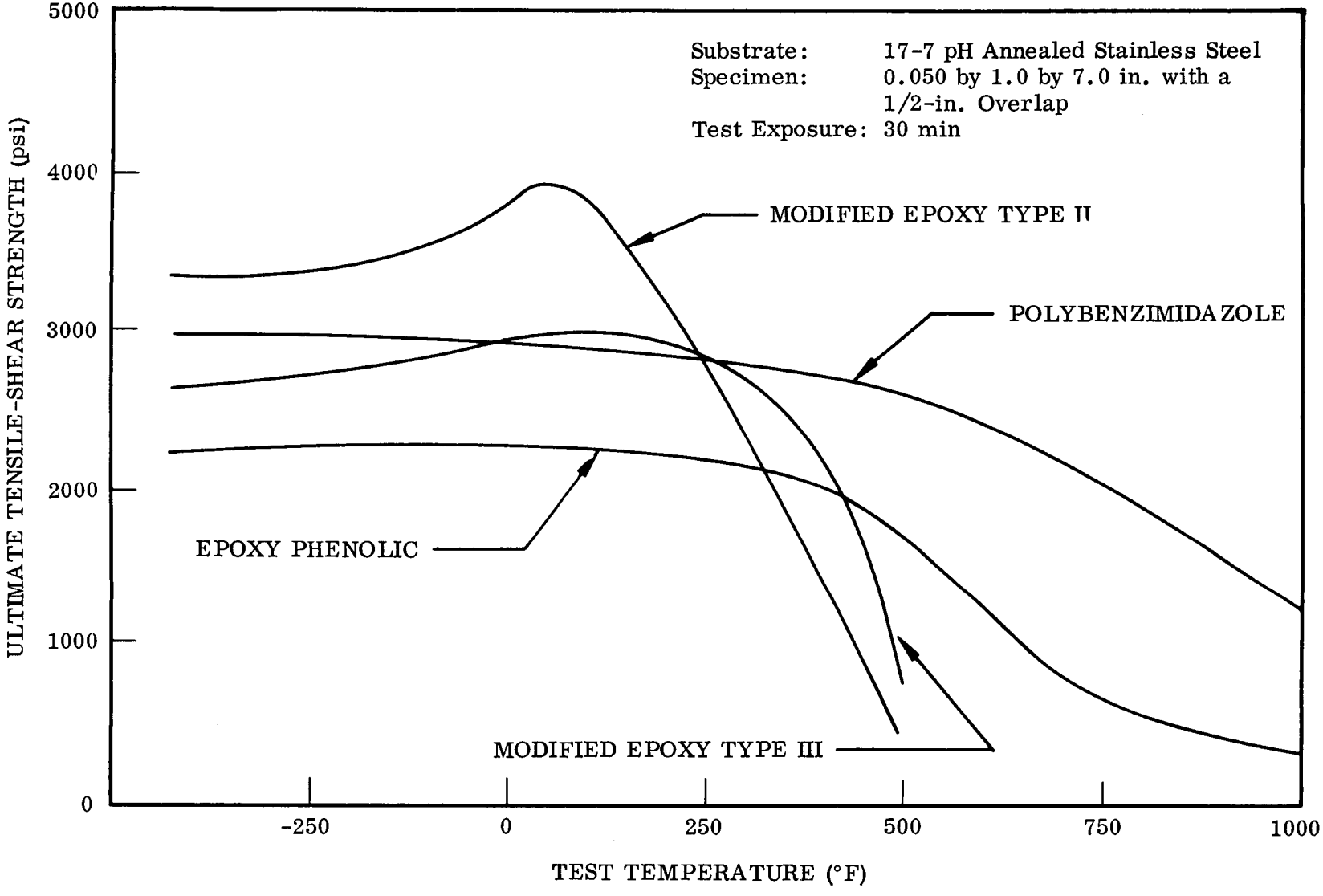

Fig. 10-1 Effect of Elevated Temperature on Various Classes of Structural Adhesive (Data of Narmco Materials Div., Whittaker Corp.)(Ref. 1)

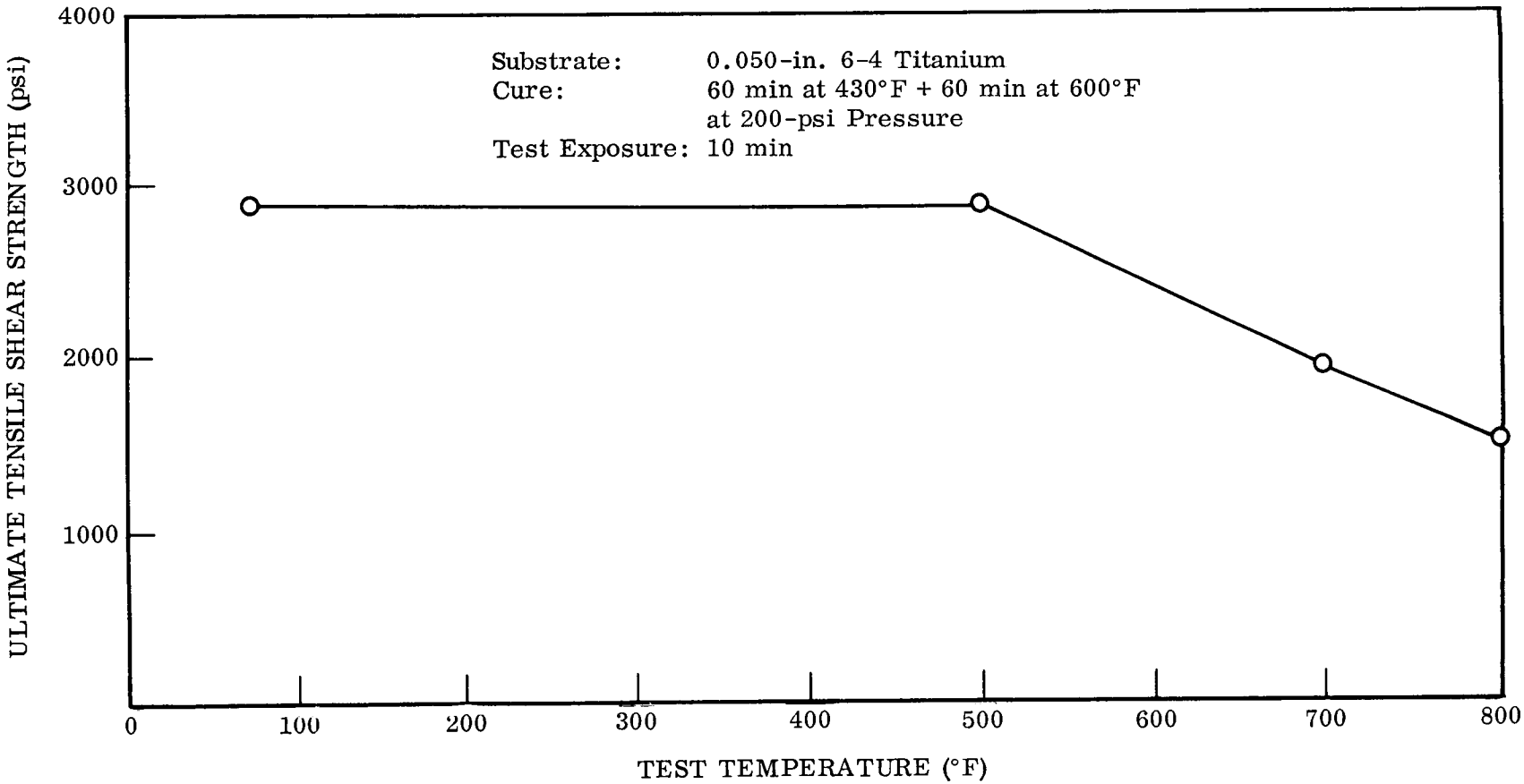

Fig. 10-2 Effect of Temperature on a Polybenzimidazole Adhesive (Ref. 2)

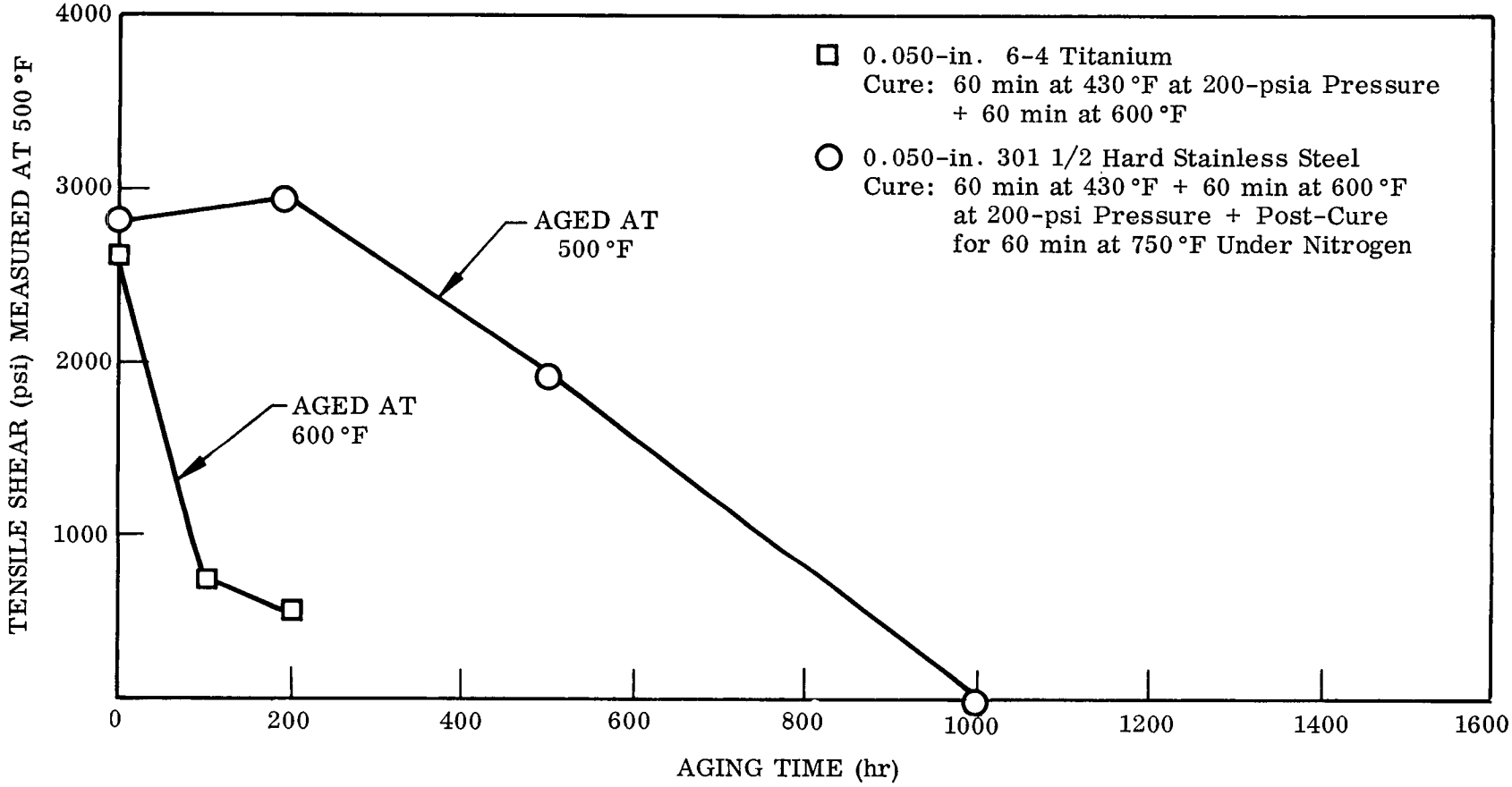

Fig. 10-3 Effect of Elevated-Temperature Aging on a Polybenzimidazole (PBI) Adhesive

aged at 600°F is shown after 100-hr exposure at 500°F. However, the strength retention is improved when the material is aged at 500°F (Ref. 2).

Polyimide Adhesives. Polyimide adhesives are based on the resinous reaction products of aromatic diamines and dianhydrides. This class of adhesives has good thermal stability and resistance to oxidation. The polyimides have good strength retention after short-time exposure up to 1000° F and after long-time exposures to temperatures above 500° F. As was found to be the case with the PBI adhesive (Ref. 2), long-time aging properties of the polyimides on stainless steel and titanium substrates are improved through the addition of an inorganic arsenic compound, which acts as a thermal stabilizer. Without the arsenic addition, the adhesive is stable at 500° F and shows good strength retention when aged 4000 hr at 500° F. Without arsenic, substantial degradation occurs within 200 hr at 600° F. With arsenic, the adhesive shows no loss of strength after 1000 hr at 600° F and shows substantial strength retention after 2000 hr at 600° F. The tensile-shear strength of an arsenic-modified polyimide adhesive (FXM34B-25A) after exposure to temperatures varying from -320° to 1000° F is illustrated in Fig. 10-4.

Modified Epoxy Adhesives. The newer, modified epoxy adhesives with latent curing agents provide the best cryogenic properties of the intermediate-high-temperature-resistant adhesive systems and also provide good long-term strength retention at temperatures up to 400° F. Figure 10-5 (Ref. 1) shows the effect of temperatures on a nylon-epoxy, the modified epoxies with latent curing agents, a nylon-phenolic, and a phenolic butyral.

Polymer modified epoxies, such as the nitrile-epoxies and nylon-epoxies, give high tensile-shear strength in metal-to-metal bonding and sandwich peel strength, but these adhesives do not have good strength retention at temperatures above the range 350° – 400° F.

Epoxy Adhesives. The high-modulus epoxies designed for use at elevated temperatures have poor peel strength compared with the polymer modified epoxies. The modified epoxies are capable of giving good sandwich properties. Sandwich peel strengths of 50 in.-lb per 3-in. width and flatwise tension values of 1000 psi at 350° F have been obtained (Ref. 2).

Figure 10-6 (Ref. 2) shows the effect of temperature on the tensile-shear strength of two high-temperature-resistant, high-modulus epoxy adhesives, a dianhydride cured paste adhesive, and a supported film adhesive. The dianhydride cured paste is a two-part system that is mixed just before use and can be cured at 125° F under contact pressure. This adhesive gives rather brittle bonds and is generally used in areas not subjected to stress, such as bonding ablative materials to metallic substrates. The supported film epoxy adhesive is cured at 350° F. When compared with epoxy-phenolics (Fig. 10-1), the epoxy adhesives have inferior tensile-shear strengths at

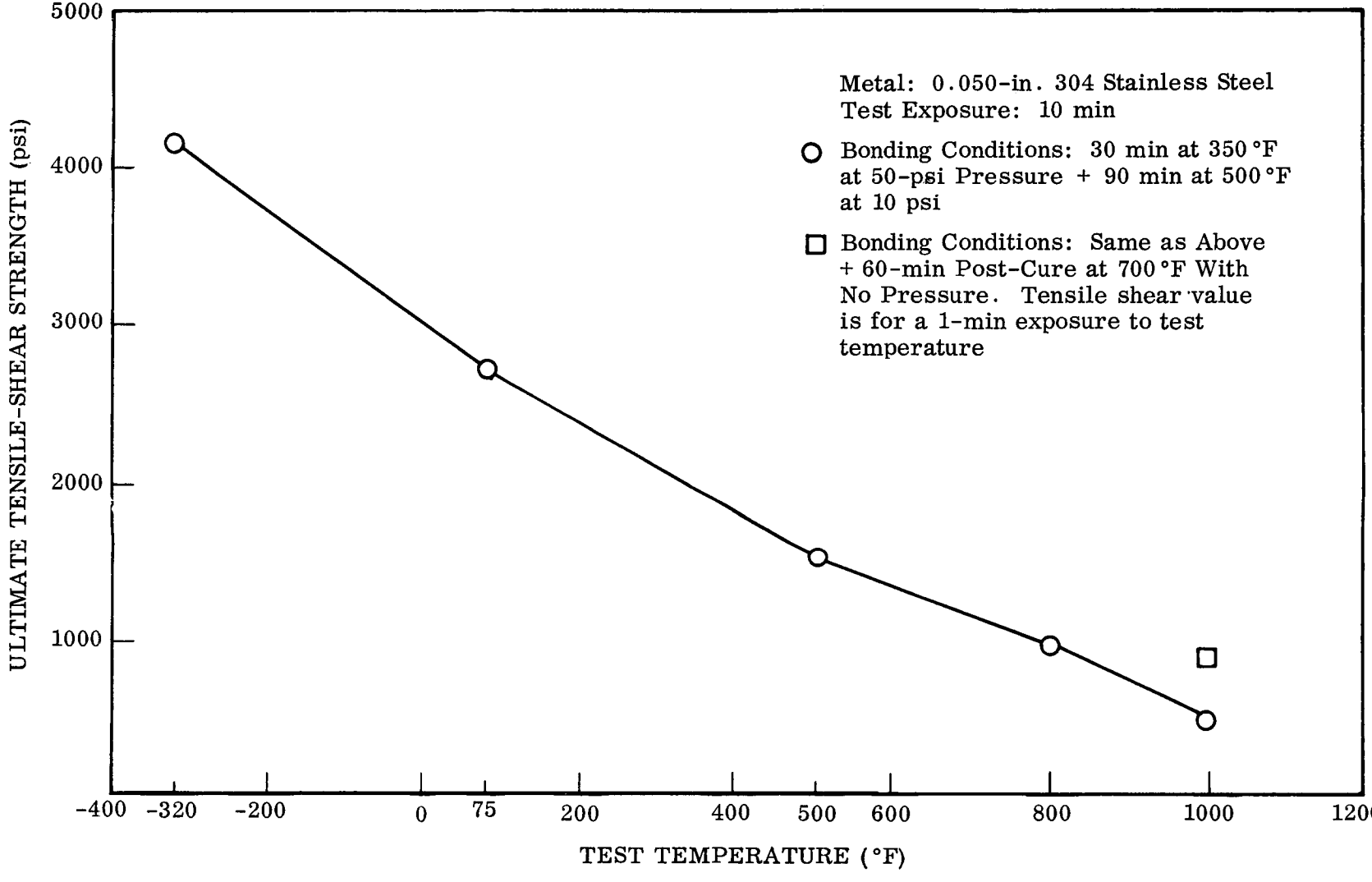

Fig. 10-4 Effect of Temperature on FXM-34B-25A Polyimide Adhesive (Manufacturer: Bloomingdale Rubber Div., American Cyanamid Co.)(Ref. 2)

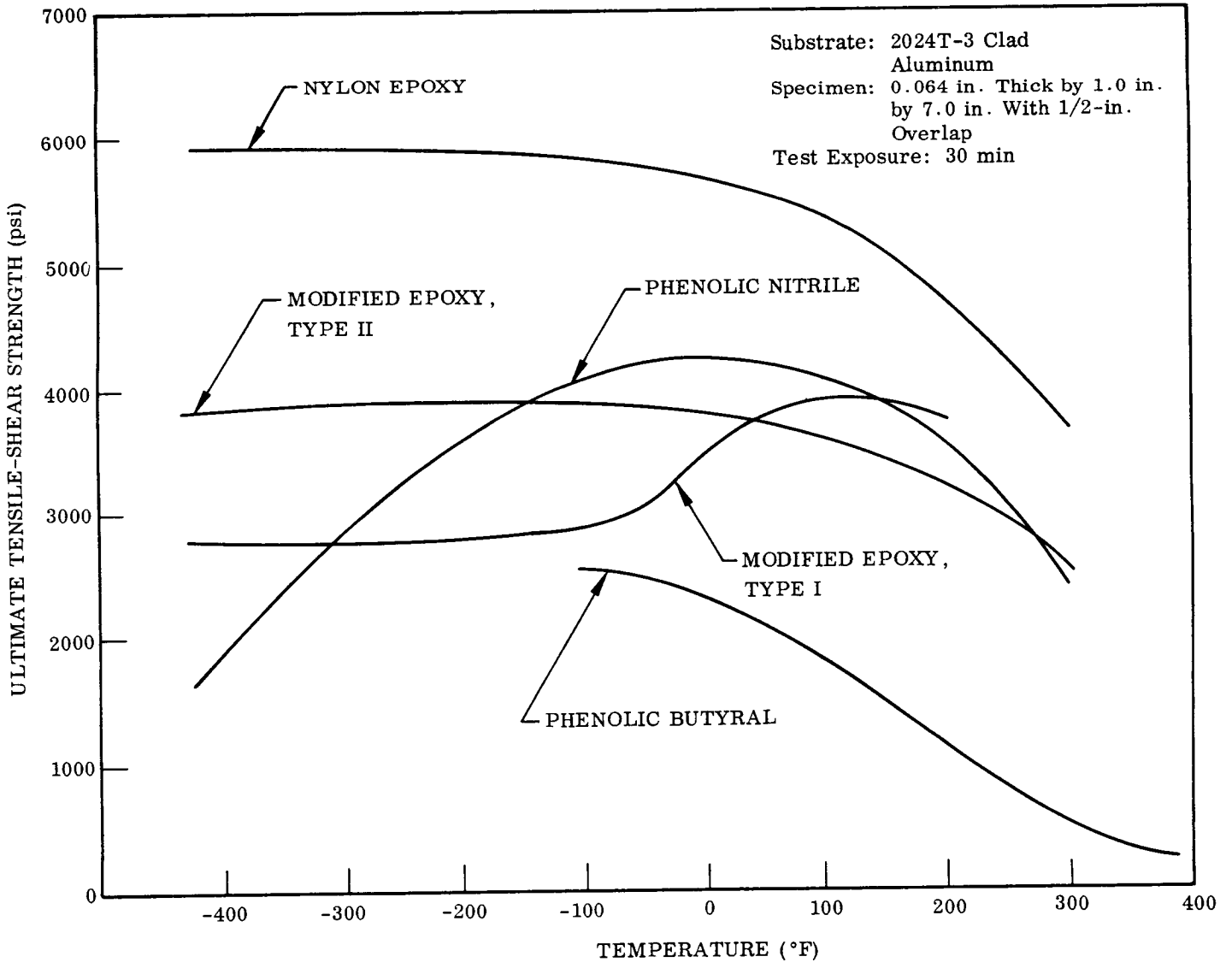

Fig. 10-5 Effect of Temperature on Various Classes of Structural Adhesives (Data of Narmco Materials Div., Whittaker Corp.)(Ref. 1)

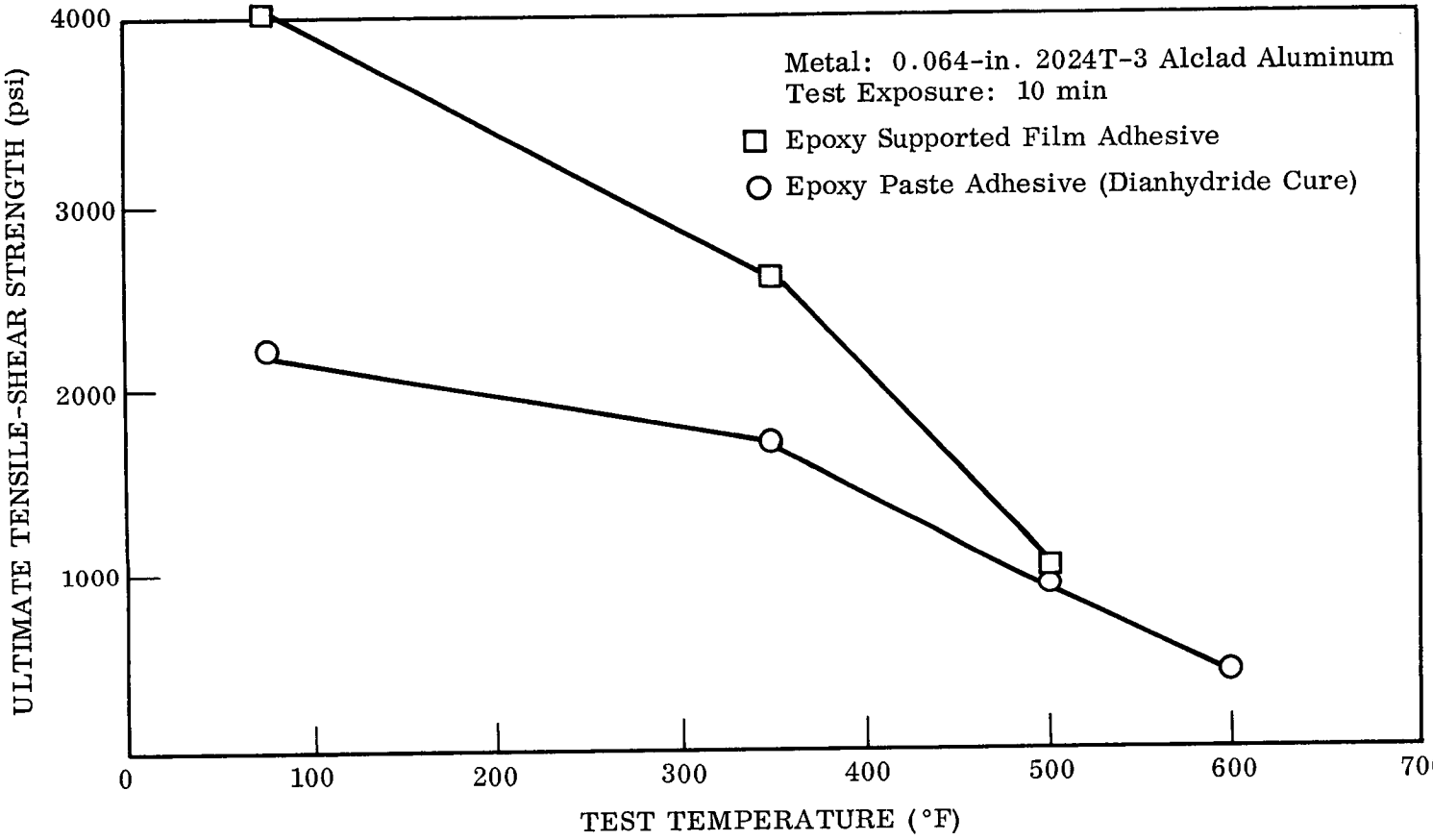

Fig. 10-6 Effect of Temperature on Epoxy Adhesives (Ref. 2)

temperatures above 500°F. However, properly formulated epoxy resins are less susceptible to oxidation degradation than the epoxy-phenolics and show better strength retention after prolonged exposure to temperatures in the 350° to 400° F region.

Epoxy-Phenolic Adhesives. The epoxy-phenolics are well suited for applications involving very short exposures (1 min) at temperatures up to 1000° F and long-term exposures at 500° F in the absence of oxygen. Figure 10-7 (Ref. 2) shows the effect of very short term (1 min) thermal exposures on the lap shear strength of a typical epoxy-phenolic (HT 424 adhesive meeting the requirements of MIL-A-8431, Type II, manufactured by Bloomingdale Rubber Div. of American Cyanimid Co.). As is the case with many highly cross-linked systems, epoxy-phenolics have good properties at cryogenic temperatures.

Epoxy-phenolics are not suitable for applications requiring prolonged exposure in air to temperatures in the vicinity of 500° F. The reason is that phenolic resins are quite susceptible to oxidative degradation at or above this temperature. The adhesive on a stainless steel substrate will have a low loss of tensile-shear strength after 500-hr exposure in nitrogen but will lose most of its strength in 100 hr in air. Some structural adhesives exhibit better thermal stability when used to bond aluminum alloys than when used with stainless steels or titanium. This is true of epoxy-phenolics.

10.2.1.2 Effect of Thermal Cycling in Air on Mechanical and Physical Properties

Thermal sterilization of organisms present in the earth's environment is often required of spacecraft before launching. Bactericidal methods used include treatment with gases such as ethylene oxide, ultraviolet and high-energy irradiation, and thermal sterilization. Such methods, while effective in varying degrees in destroying microorganisms, can affect the properties of materials and the functional reliability of components. Spacecraft and component sterilization is treated more completely in Chapter 22. For the adhesives, only thermal sterilization effects will be considered.

A summary of thermal sterilization exposure test results for adhesives is given in Table 10-2 (Ref. 3). Tensile-shear-strength retention on aluminum-to-aluminum lap bonds, and weight loss results were used to rate the compatibility of adhesives to the thermal sterilization treatment. After thermal exposure, adhesives were arbitrarily rated as follows:

1. Compatible (C) if
   a. they retained 80% or more of their original tensile-shear strength, and
   b. weight loss was less than 1%.
2. Marginal (M) if either
   a. the tensile shear-strength retention was 70 to 80%, or
   b. weight loss was 1 to 4%.
2. Not compatible (NC) if either
   a. the tensile-shear strength retention was below 70% or
   b. weight loss was more than 4%.

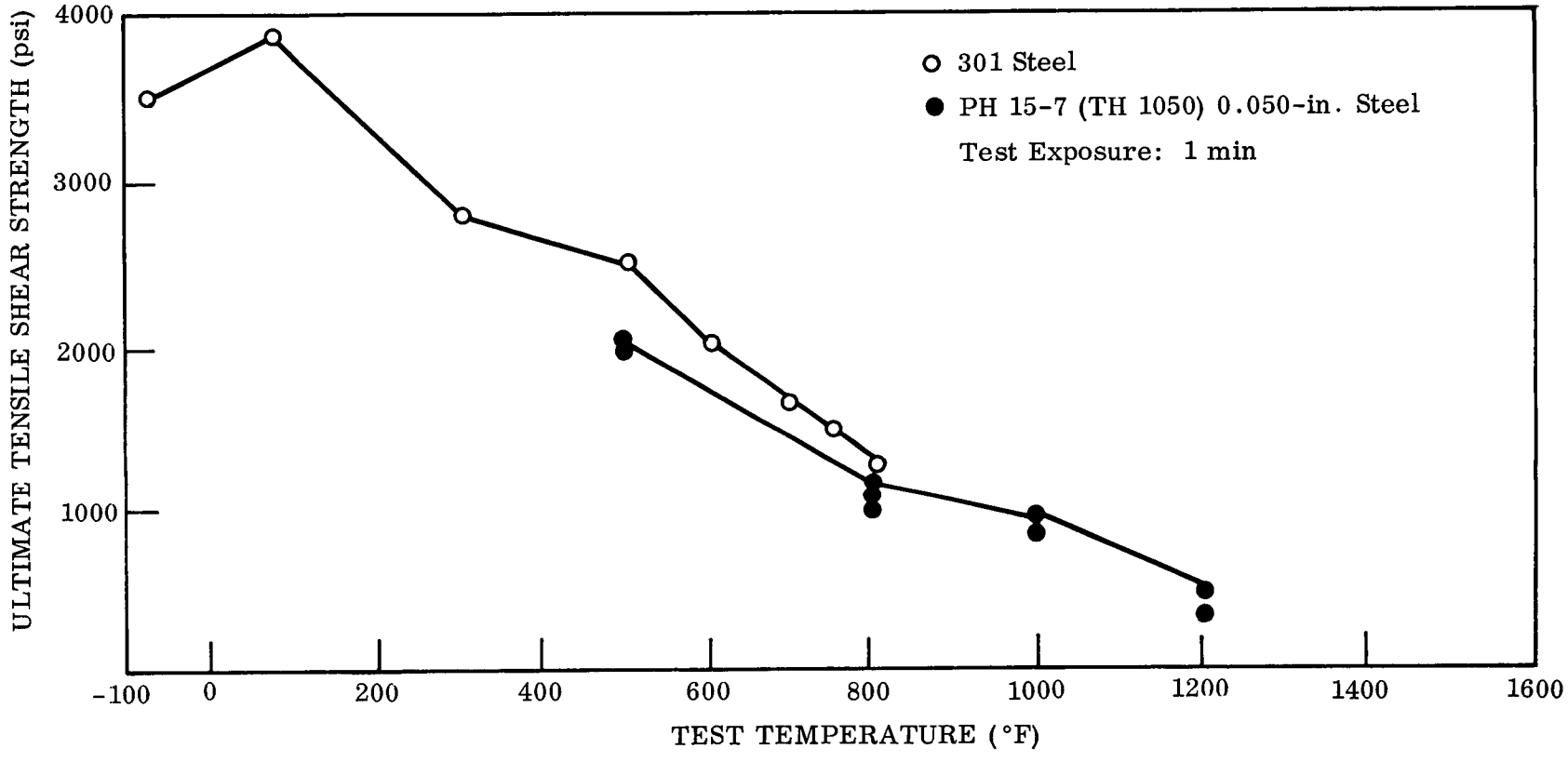

Fig. 10-7 Effect of Temperature on an Epoxy-Phenolic Adhesive, MIL-A-8431 (Ref. 2)

Table 10-2

SUMMARY OF EFFECT OF THERMAL STERILIZATION PROCEDURE ON ADHESIVES (Ref. 3)

Adhesive/Curing Agent	Chemical Class	Manufacturer[c]	Tensile-Shear Strength[a] (psi)		Comments	Compatibility Rating
			Control	After Thermal Sterilization Procedure[b]		
A-4000 Dow Corning Adhesive	Silicone	17	157	206	System evolves hydrogen.	C
Bonding Agent R-823	Epoxy/amine	16	784	1065	High weight loss (> 75%); darkens.	NC
Caram No. 206 Cement	Neoprene	18	162	176	Over 2% weight loss.	NC
EC 1103	Vinyl	4	110	820	Softens and flows; slight darkening.	NC
EC 1614 B/A	Epoxy/polyamide	4	2050	1620	Darkens.	M
EC 2216 B/A	Epoxy/modified amine	4	505	972	Darkens.	C
Eccobond 26A/B	Epoxy	12	970	741	High weight loss; darkens.	NC
Eccobond 55/9	Epoxy/amine	12	172	1003	Darkens.	C
Eccobond 55/11	Epoxy/amine	12	220	660	Weight loss over 1%.	M
Eccobond Solder 56C/9	Epoxy/amine	12	245	290	Darkens.	C
Eccobond Solder 57C A/B	Epoxy/amine	12	565	630	Darkens.	C
Epon 8/A	Epoxy/amine	1	455	1910	Thixotropic.	C
Epon 422	Epoxy/phenolic-glass fabric	1	1123	1101	Glass fabric-supported tape adhesive; weight loss > 1%.	M
Epon 828/A	Epoxy/amine	1	1174	1540	–	C
Epon 828/Z	Epoxy/amine	1	1435	1430	–	C
Epon 901/B-1	Epoxy	1	516	1220	Thixotropic.	C
Epon 901/B-3	Epoxy	1	740	1040	Thixotropic.	C
Epon Pipelok 924A/B	Epoxy	1	1849	2250	Thixotropic.	C
E-Solder 3022	Epoxy-silver/amine	15	932	1210	Weight loss > 1%; darkens.	M
FM 96	Epoxy/polyamide nylon fabric	3	945	1120	Nylon fabric-supported tape adhesive.	C
FM 1044	Epoxy/polyamide	3	2310	2625	Unsupported film adhesive.	C
GT 200	Polyester	14	157	164	Chlorinated solvent; low solid content; Mylar adhesive.	C
HT 424	Epoxy-phenolic	3	1672	1340	Nonsupported adhesive film.	M
Hysol 5150/3690	Epoxy-modified amine	13	1720	2537	Darkens.	C
Number A2/A	Epoxy-aluminum	6	804	1440	Yellows.	C
PC 12-007 A/B	Epoxy/amine	13	705	456	Used as circuit board coating; slight darkening.	NC
Proseal 501	Polysulfide	19	174	64	High weight loss (> 10%).	NC
RTV 102	Silicone	20	172	361	One part material. Thixotropic; weight loss > 2%.	M
RTV 108	Silicone	20	115	190	One part material.	C
RTV 140	Silicone	17	180	235	One part material.	C
RTV 891	Silicone	17	175	240	One part material.	C

(a) FTMS No. 175, Method 1033-1T.
(b) Three cycles of 40 hr each at 300°F in nitrogen.
(c) See Appendix at end of this chapter.

The tensile-shear strength of some of the adhesives tested increased after a heat exposure simulating a typical thermal sterilization cycle of three cycles of 40 hr each at 300° F in a nitrogen atmosphere. This behavior may have resulted because of additional curing or postcuring, volatilization of additives at the adherend-adhesive interface, or better wetting of the adherend surfaces by the adhesive at the higher temperatures.

Summary of Elevated-Temperature Effects. The high-temperature properties of several classes of structural adhesives have been given. The epoxy-phenolics, polybenzimidazole, and polyimide adhesives exhibit comparable strength retention at temperatures up to 1000° F for very short time exposures. The epoxy and modified epoxy adhesives are clearly inferior to the PBI and PI adhesives in strength retention at temperatures above 400° F.

For applications requiring intermediate and long-time aging to temperatures in the 400° to 600° F range, the polyimides are far superior to the other classes of adhesives. The polybenzimidazoles are the next most stable class of adhesives, followed by the epoxies and epoxy-phenolics. In the absence of air, the relative rankings of the epoxies and epoxy phenolics are reversed.

10.2.1.3 In Vacuum

The effects of elevated temperature in a vacuum environment are generally somewhat less severe, since no significant oxidative degradation of the adhesive can occur. Table 10-3 (Ref. 4) summarizes the effects of thermal-vacuum and thermal-air (ambient to 200° C) environmental exposures of several commonly used epoxy, epoxy-phenolic, epoxy-nylon, vinyl-phenolic, and nitrile-phenolic structural adhesive aluminum-to-aluminum bonds. Vacuum exposure at ambient temperature did not greatly affect the strength of these structural adhesive bonds. Slight decreases are shown in the tensile-shear strength after 24-hr vacuum exposure. High strength retention for all adhesives tested resulted after thermal-vacuum aging up to 200° C. This effect is due to more complete curing of the adhesive at the elevated temperature and evolution of volatile cure reaction products in vacuum.

Degassing. Adhesives are mainly organic in nature and are heterogeneously complex materials by design and formulation. This means that they generally contain additives which may not be chemically united to the polymer but which are incorporated during manufacture to impart stability, or to facilitate cure and processing during the bonding operation.

Unpolymerized fractions and residual additives that are unreacted during cure can remain in the adhesive. Generally these materials are volatile. The residual volatiles in the glue line of a bonded structure or component which may be present even after extended cure at elevated temperatures can be evolved under the vacuum conditions of

Table 10-3

EFFECT OF ELEVATED TEMPERATURES IN AIR AND IN VACUUM OF 10^{-6} TORR ON MECHANICAL PROPERTIES OF STRUCTURAL ADHESIVE BONDS (Ref. 4)

Adhesive (Commercial Designation)	Manufacturer(a)	Chemical Class	Environmental Conditioning (Aging)	Average Tensile-Shear Strength(b) (psi)
Epon 8	1	Epoxy	Control	2880
			24 hr in vacuum at RT	2690
			24 hr in vacuum at 200°C	2620
			24 hr in air at 200°C	1650
Metlbond 406-1	2	Epoxy-phenolic	Control	5650
			24 hr in vacuum at RT	5390
			24 hr in vacuum at 200°C	6020
			24 hr in air at 200°C	4590
FM-1000	3	Epoxy-nylon	Control	6690
			24 hr in vacuum at RT	7090
			24 hr in vacuum at 200°C	8020
			24 hr in air at 200°C	6980
Epon 422 J	1	Epoxy-phenolic	Control	2200
			24 hr in air at 200°C	1590
FM-47	3	Vinyl-phenolic	Control	4230
			24 hr in vacuum at RT	4220
			24 hr in vacuum at 200°C	4410
			24 hr in air at 200°C	3110
Metlbond 302A	2	Epoxy-phenolic	Control	2670
			24 hr in vacuum at RT	2680
			24 hr in vacuum at 200°C	2690
			24 hr in air at 200°C	1970
AF-6	4	Nitrile-phenolic	Control	2650
			24 hr in vacuum at RT	2490
			24 hr in vacuum at 100°C	2590
			24 hr in vacuum at 200°C	4370
Metlbond 408	2	Vinyl-epoxy-nylon	Control	5270
			24 hr in air at 200°C	5140

(a) See Appendix at end of this chapter.
(b) Tested at ambient room temperature (20°C) after environmental conditioning as indicated.

space and at elevated temperatures. Such volatiles can have much higher vapor pressures than the cured polymer and may be one or more of the following:

- Products of the condensation reaction that phenolics, polyimides, and epoxy-phenolics undergo during cure
- Processing additives
- Stabilizers
- Residual solvents
- Products of thermal decomposition
- Unreacted curing agents
- Impurities
- Low molecular weight fractions of the polymeric adhesive

These evolved volatiles can deposit on cold surfaces in the line of sight of the polymer within the spacecraft to form optically refracting and electrically insulating films or coatings that can be detrimental to the performance of sensitive optical surfaces and electrical contacts and junctions within the spacecraft. Second, critical steady-state pressures may be generated by the degassing of volatiles within an enclosed electronic container and may induce corona discharges or arcing, thus causing failure of a component subsystem. There is a possibility that evolution of volatiles from the external surfaces of the spacecraft may produce very small thrusts, with torques and moments that could affect the orientation and attitude of the vehicle in orbit.

In the case of adhesives, the potential problem of volatile evolution is considerably reduced in magnitude from that encountered with bulk plastics, films, seals, electrical insulation, and encapsulating compounds. The reason is that the path for escape of volatiles is less probable through the relatively nonporous adherend substrates and is more likely to be through the glue line edges. Since the surface area of the edges is small and the migration path is large from the interior of the glue line to the edges, degassing rates are considerably reduced by this geometry.

Laboratory studies of weight loss rates of adhesives, elastomers, and plastics in vacuum environment at ambient and elevated temperatures to 200°C, of the condensation of volatiles on various surfaces at ambient temperature, and identification of volatile species evolved for several commercial materials have been performed by the Stanford Research Institute under NASA contract from the Jet Propulsion Laboratory. These studies have led to the development of data of the minimum condensable materials evolved from adhesives and polymers. These data resulted in the writing of spacecraft materials specifications controlling the qualified materials to established chemical formulations, manufacture, and production processing of adhesives and polymers.

Results of tests (Ref. 5) indicate that the evolution of volatile condensable materials can be minimized by restricting or eliminating the use of certain additives or formulated materials, and, where feasible, controlling processing, in applications where potential contamination problems may exist. In addition, postcuring of adhesives at elevated temperatures for prolonged durations, or in vacuum, minimizes volatile evolution.

In Table 10-4 (Ref. 5) a summary of the degassing characteristics at 150°C and 200°C in vacuum of 10^{-6} Torr of one manufacturer's epoxy structural adhesives commonly used

Table 10-4

DEGASSING CHARACTERISTICS OF SOME EPOXIDE ADHESIVES AT ELEVATED TEMPERATURE IN VACUUM (10^{-6} TORR)[a]

Adhesive[b]	Description	150°C		200°C	
		Initial Weight Loss (%)	Steady-State Loss Rate (% per hr)	Initial Weight Loss (%)	Steady-State Loss Rate (% per hr)
901-B3	Two-part adhesive: (1) a gray thixotropic paste identified as Epon 828 with a metallic filler; (2) a dark-colored liquid curing agent identified as an aromatic amine or amine mixture.	–	–	0.51[c]	0.005
903	A one-part adhesive in the form of a viscous gray paste. Identified as based on Epon 828 and containing an unidentified catalyst and a mixed metallic-inorganic filler.	0.78	0.001	1.77	0.008
914	A one-part dark-gray thixotropic paste, reported stable indefinitely at room temperature. Identified as based on Epon 828 with a dicyandiamide curing agent and metallic filler.	0.49	–	1.84	0.01
917	A one-part adhesive based on an epoxy-anhydride system with a metallic filler. It is a free-flowing powder which melts at about 49°C(150°F) and does not resolidify on cooling.	1.35	0.003	2.70	0.002
924	Pipe joint sealer and adhesive compound. Composition not identified.	3.18	0.007	5.51	0.042
931	A two-part adhesive: (1) a gray-black paste based on a novel epoxy system other than the diglycidyl ether of Bisphenol; (2) a red liquid curing agent identified as an aromatic amine.	0.61	–	2.23	0.008
934	A room-temperature curing two-part adhesive that meets the MIL-A-5090D, Type I, requirements. Consists of a gray epoxy paste similar to that used in Epon 931 and an amber amine curing agent identified as a polyamide. The filler is metallic.	1.18	0.002	2.22	0.014
941	Similar to 934 but has poorer quality control.	1.10	0.002	2.29	0.009
422J	A gray tape adhesive meeting the MIL-A-5090D, Type III, Class F, requirements. A blend of epoxy and phenolic resins containing a metallic filler and dicyandiamide as curing agent. This blend is applied to 112-Volan A glass fabric support. The adhesive cures with evolution of volatiles to form a porous bond.	3.97	0.003	4.40	0.002

(a) Data extracted from Ref. 5.
(b) Shell Chemical Company.
(c) Pretreated at ambient temperature for 55 hr in vacuum (10^{-6} Torr).

in aerospace construction are given. The nine adhesives are identified by usage, chemical class, and form.

The data of percent weight loss are presented in graphic form in Figs. 10-8 and 10-9. These curves show an initial rapid evolution of volatile material in a relatively short time, of the order of 10 to 20 hr. Following the rapid evolution, a gradual transition to a steady-state rate of nearly constant degassing for some materials is shown. The range of error of the weight loss determination has been estimated to be about 1% (Ref. 5). The error of the initial weight loss measurement was about 5%, while the error in the measurement of the steady-state loss rate was somewhat higher since the steady-state loss rate was about two orders of magnitude lower than the initial weight loss.

The initial weight loss appears to be diffusion controlled, since it increases with decreasing thickness of the Epon 914 adhesive, as shown in Fig. 10-10, which was developed from the data of Ref. 5. The steady-state rate did not appear to be affected by the specimen thickness, since this rate was constant for the range of thicknesses from 0.00034 in. to 0.00383 in. of the Epon 914 material.

The postcuring conditions of the adhesive prior to thermal-vacuum exposure affect the amount of initial degassing of the epoxy adhesives. The Epon 901 had 55-hr pretreatment in vacuum (room temperature – 10^{-6} Torr) prior to thermal-vacuum exposure at 200°C and 10^{-6} Torr. The initial weight loss percent for this material was 0.5; the lowest value of materials that had no prior vacuum treatment was about 1.8 (Table 10-4).

The duration of the postcuring cycles also influences the thermal-vacuum weight loss. As shown in Figs. 10-11 and 10-12, the percent weight loss of the Epon 422J adhesive in 10^{-6} Torr vacuum at 200° C was reduced by about a factor of 3 after a 48-hr postcure in air or nitrogen.

In addition to the weight loss and rate measurements, the amount of vacuum-condensable materials (VCM) was also determined in the Stanford Research Institute work for the Jet Propulsion Laboratory (Ref. 6). In Table 10-5 the VCM evolved from several adhesives and deposited on mirror surface collector plates at 25° C are listed. The adhesives were held 24 hr at 125° C in 10^{-6} Torr vacuum for these determinations. Although in the actual application the adhesive is exposed to vacuum only at the glue line, thus minimizing the total surface area exposed, it is advisable to use only materials that have the lowest total weight loss and vacuum-condensable materials evolved for most spacecraft adhesive applications.

The epoxy-nylon (polyamide) adhesive films have been shown to release low-molecular-weight resin fractions under thermal-vacuum conditions. Better performance of most adhesives is achieved by extending the curing time at the maximum recommended temperature. It was found that curing at temperature in vacuum, particularly for silicone polymers, was effective in minimizing the amounts of vacuum-condensable materials evolved in service. The time devoted to curing prior to a space mission is well spent if ultimate low-degassing performance can be assured to maintain critical surfaces clean and free from contamination by evolved condensable volatiles (Ref. 6).

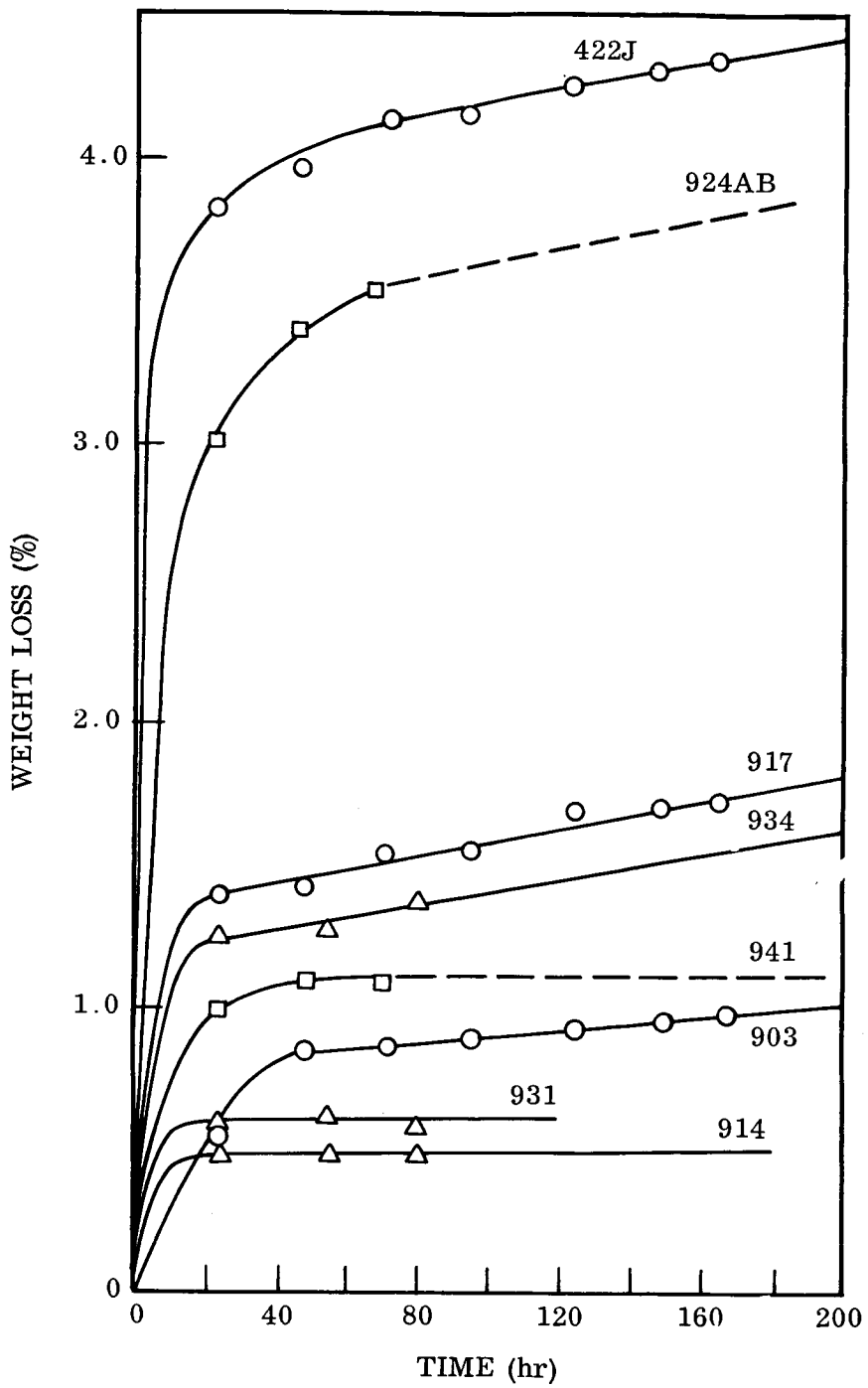

Fig. 10-8 Percent Weight Loss of Epon (Shell Chemical Co.) Adhesives at 150 °C and 10^{-6} Torr (Ref. 5)

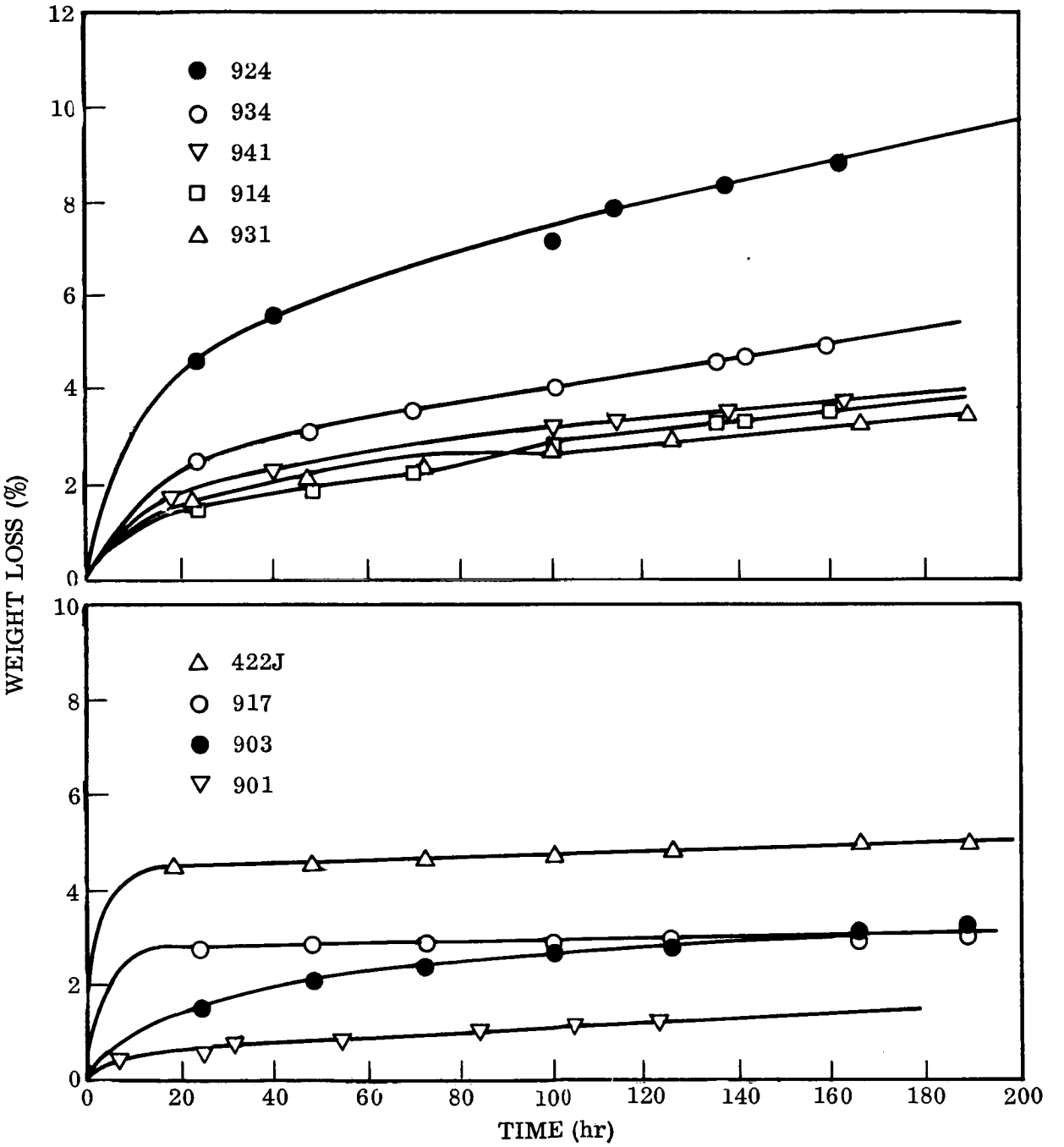

Fig. 10-9 Percent Weight Loss of Epon (Shell Chemical Co.) Adhesives at 200 °C and 10^{-6} Torr (Ref. 5)

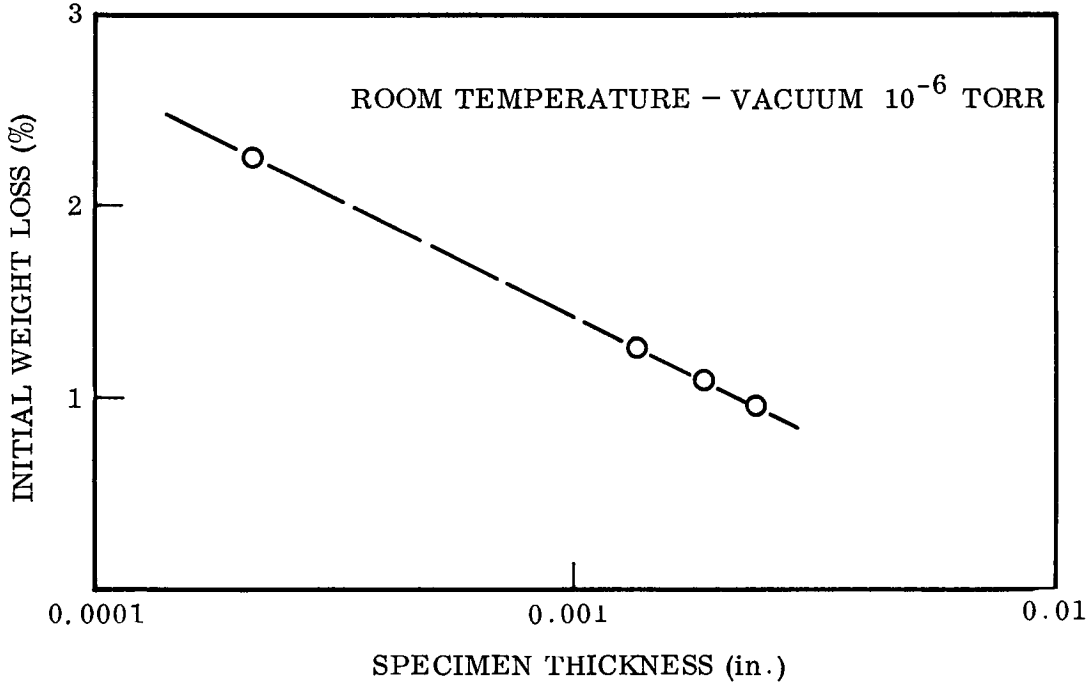

Fig. 10-10 Effect of Specimen Thickness on Initial Weight Loss of Adhesive Epon 914 (Ref. 5)

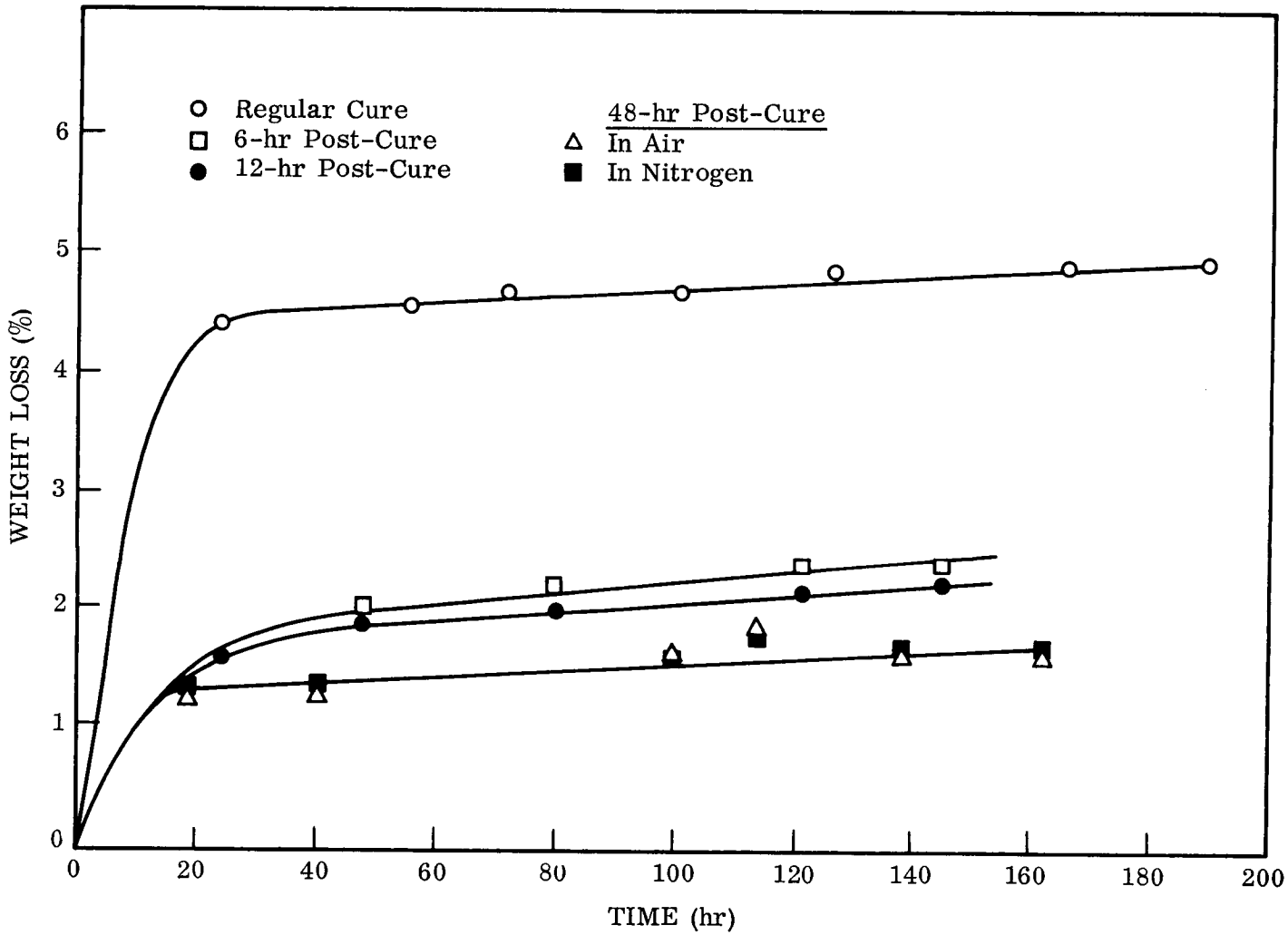

Fig. 10-11 Percent Weight Loss of Epon 422 (Shell Chemical Co.) After Various Post-Curing Conditions (Ref. 5)

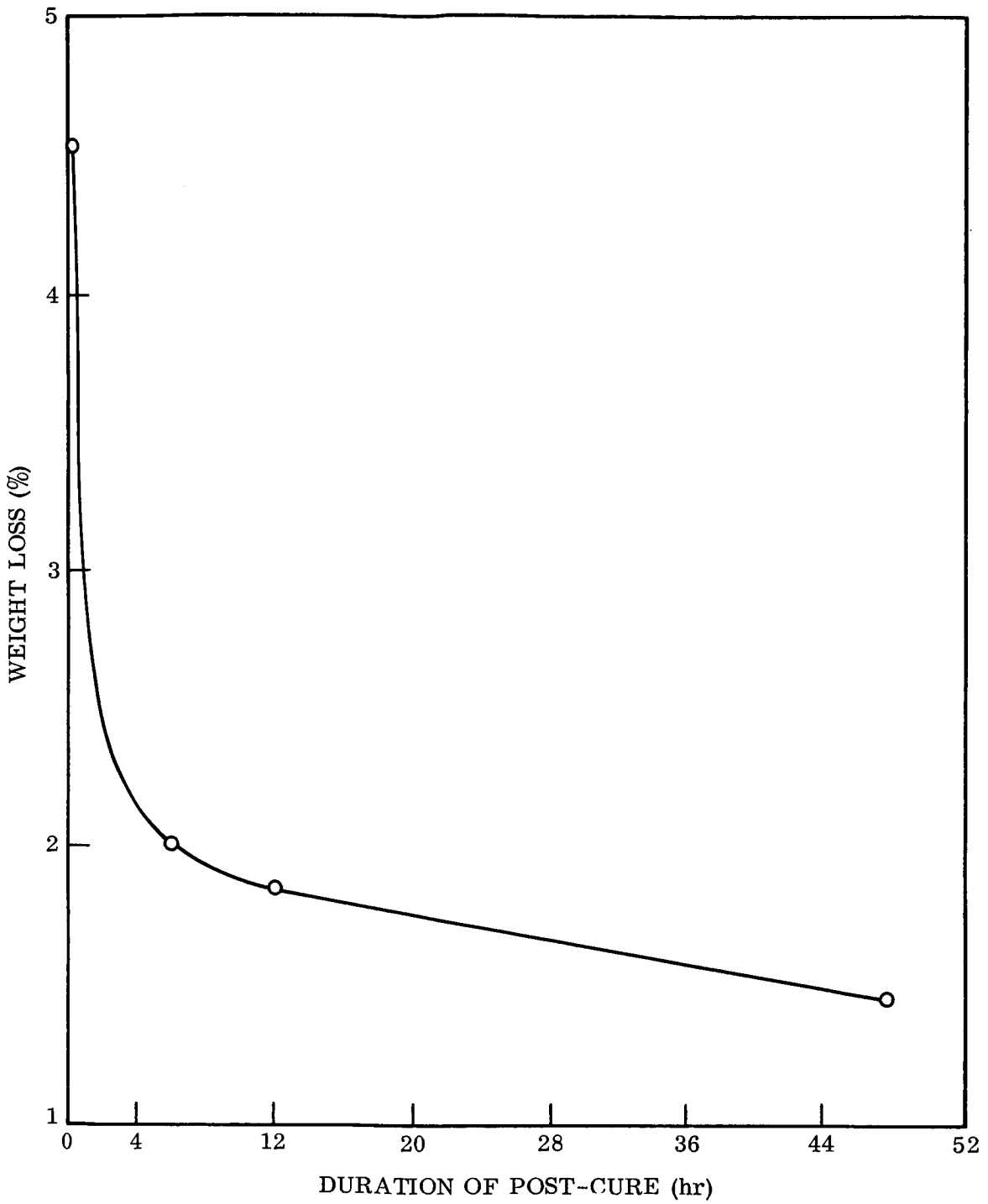

Fig. 10-12 Effect of Duration of Post-Cure on Cumulative Percent Weight Loss of Epon 422 (Shell Chemical Co.) After 48 hr at 200 °C and 10^{-6} Torr (Ref. 5)

Table 10-5

WEIGHT LOSS AND VACUUM CONDENSABLE MATERIAL (VCM) EVOLVED FROM SEVERAL ADHESIVES[a] (Ref. 6)

Adhesive/Curing Agent	Manufacturer[b]	Cure	Total Weight Loss (%)	VCM[c] (wt. %)
Armstrong A-2/A	6	45 min at 74°C + 45 min at 93°C	0.17	0.03
Armstrong A-2/E		45 min at 93°C	0.26	0.03
Eccobond 45/15		16 hr at 52° C	6.06	0.63
Eccobond 55/9		24 hr at 25°C	0.40	0.06
Eccobond 55/9		16 hr at 65°C	0.17	0.07
Eccobond 55/9		24 hr at 150°C	0.15	0.10
Eccobond 55/11		1/2 hr at 150°C	3.76	3.40
Eccobond 55/11		24 hr at 150°C	0.43	0.43
Eccobond 56C/9		16 hr at 50°C	0.30	0.03
Eccobond 56C/9		16 hr at 65°C	0.42	0.03
Eccobond 104 A/B		3 hr at 150°C	0.30	0.24
Epon 828/Versamid-125	1	1 hr at 65°C + 1 hr at 95°C + 24 hr at 150°C	0.51	0.12
Epon 828/Versamid-125		1 hr at 65°C + 1 hr at 95°C + 1 hr at 150°C	1.65	0.77
Epon 901/B-1		1 hr at 93°C	0.34	0.14
Epon 901/B-3		1/2 hr at 115°C + 1-1/2 hr at 175°C	0.19	0.01
Epon 903		1 hr at 175°C	0.36	0.21
Epon 914		1 hr at 175°C	0.24	0.15
Epon 917		15 min at 175°C	0.17	0.03
Epon 919 A/B		3 hr at 82°C	1.45	0.23
Epon 931 A/B		1 hr at 125°C	0.13	0.01
Epon 934 A/B		1 hr at 82°C	0.10	0.08
FM-1000	3	1 hr at 150°C	8.31	4.64
FM-1000		2 hr at 150°C	6.22	5.08
FM-1000		2 hr at 170°C	5.39	4.35
FM-1000		2 hr at 200°C	5.55	4.71
FM-1044		1 hr at 150°C	7.95	3.76
FM-1044		24 hr at 150°C	5.84	2.99
EC-2216 A/B	4	8 hr at 25°C + 1/2 hr at 125°C	0.60	0.24

(a) 24 hr at 125°C and 10^{-6} Torr.
(b) See Appendix at end of this chapter.
(c) VCM collector plates at 25°C.

10.2.2 Reduced/Cryogenic Temperature Effects

At temperatures below ambient room temperature, the tensile-shear strength of organic structural adhesives gradually increases and may reach a maximum at about -100° F. At cryogenic temperatures – in the vicinity of the boiling points of nitrogen (-320° F) and hydrogen (-423° F) – the bond strength gradually decreases from the maximum but may still be above the room-temperature values. This increase in the strength of bonds at reduced temperatures is partially attributed to the degree of crystallinity of the polymer and transitions from the plastic to the glassy state. Bonds at these temperatures are generally quite brittle and have reduced impact strength, resistance to vibration, and cyclic tensile-compressive fatigue life.

Today adhesives are used for many cryogenic applications as well as for elevated-temperature use. The major use of adhesives at cryogenic temperatures has been in the bonding of external thermal insulation for both metallic and nonmetallic substrates. Several classes of structural adhesives are used in cryogenic applications. These include the epoxy-phenolics, which have a useful temperature range of -423 to +500° F, and the polyurethane adhesives, which steadily increase in strength at reduced temperatures until their highest strength at any temperature is achieved at -423° F. This behavior is contrary to that found among the other common types of structural adhesives. Figure 10-13 (Ref. 1) shows the effect of cryogenic temperatures on a nylon-epoxy, modified epoxy, phenolic-nitrile, epoxy-phenolic, and polyurethane adhesive.

The tensile-shear strengths of several structural adhesives in the temperature range 180° to -423° F with some typical metal adherends are shown in Table 10-6 (Ref. 7). Although there are some gaps in the data, quite a few adhesives have favorable properties through the temperature range. Another parameter of interest in structural adhesive bonding is the peel strength for a given width of bond. Some limited data (Ref. 7) on the peel strength of some of the adhesives of Table 10-6 are shown in Table 10-7 for the temperature range 180° to -423° F. Since the data are rather sparse, it is difficult to draw conclusions or make comparisons.

Table 10-8 (Ref. 7) presents a summary of the coefficients of linear thermal expansion of some common structural adhesives at cryogenic temperatures (-320 to +32° F).

Room-temperature tensile-shear tests of most structural adhesives with proper adherend cleaning and preparation show cohesive failure at the glue line. Such failures indicate that the resin shear strength, rather than the resin-substrate bond, is the limiting factor. Below room temperature, all polyurethane bond failures were cohesive in nature, whereas the epoxy bond failures were of the adhesive-to-adherend mode. At elevated temperatures the reverse has been found to be true. These failure modes indicate that polyurethane adhesives have their greatest bonding efficiency at cryogenic temperatures, whereas most epoxy adhesives perform best at slightly below or above room temperature.

Tension-compression cyclic fatigue tests, with an 1800-psi applied load, of a polyamide epoxy, a flexibilized epoxy, and a polyurethane are presented in Table 10-9 (Ref. 8). The epoxy-polyamide adhesive withstood more tension-compression cycles

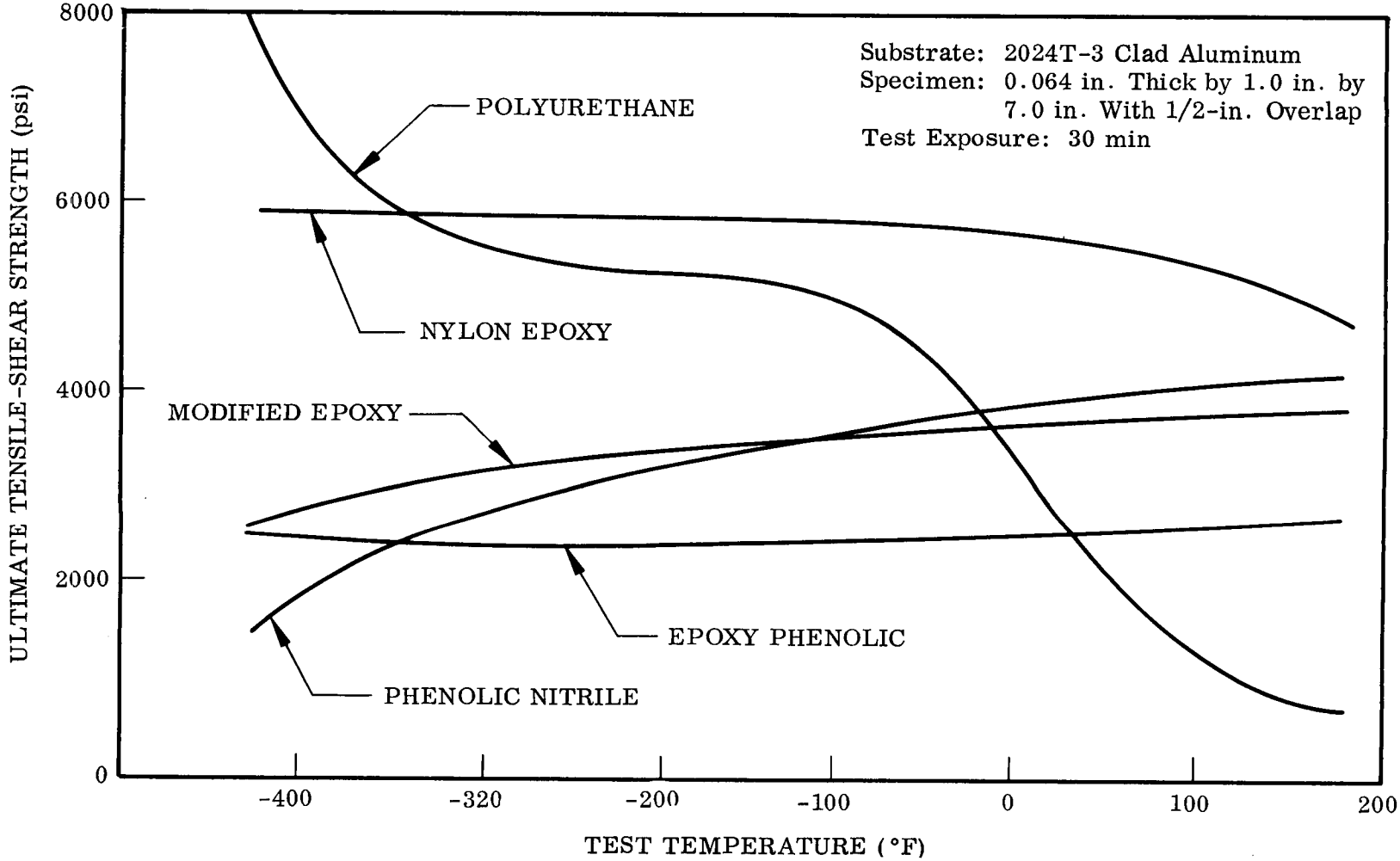

Fig. 10-13 Effect of Cryogenic Temperatures on Various Classes of Structural Adhesives (Ref. 1)

Table 10-6

TENSILE SHEAR STRENGTH OF SOME STRUCTURAL ADHESIVE BONDS TO SEVERAL ADHEREND AT TEMPERATURES FROM 180° TO -423° F (Ref. 7)

Adhesive and Manufacturer[a]	Class	Cure	Adherend	Tensile Shear Strength (psi)					
				+180	RT	-67	-100	-320	-423
Metlbond 406 (2)	Nylon-Epoxy	Room temperature to 350°F in 20 min; 1/4 hr, 350°F, 25 psi	0.064 in. 2024T3 Clad	3860	5980	5620	–	4360	–
			0.064 in. 2024T3 Bare	–	5790	–	5470	5050	4580
			0.064 in. 7075T6 Bare	–	–	–	–	4840	3813
			0.100 in. 5456 Bare	–	4110	–	–	–	–
			0.020 in. EFH 301 S/S	–	5810	–	7790	6020	6730
			0.020 in. A-110-AT Ti	–	4160	–	6110	5230	3440
Metlbond 408 (2)	Nylon-Epoxy	Room temperature to 350°F in 20 min; 1 hr, 350°F, 25 psi	0.064 in. 2024T3 Clad	3110	6490	6480	–	2800	–
			0.064 in. 7075T6 Bare	–	–	–	–	4090	2004
AF-40 (4)	Nylon-Epoxy	Room temperature to 350°F, 10°F/min; 1 hr, 350°F, 50 psi	0.064 in. 2024T3 Clad	4080	5000	5800	–	–	–
			0.064 in. 7075T6 Bare	–	–	–	–	5990	5743
			0.020 in. EFH 301 S/S	–	3050	–	8550	5480	5200
AF-41 (4)	Nylon-Epoxy	Room temperature to 350°F, 10°F/min; 1 hr, 350°F, 50 psi	0.064 in. 2024T3 Clad	3135	5700	6600	–	–	–
			0.064 in. 7075T6 Bare	–	–	–	–	5010	3402
FM-1000 (3)	Nylon-Epoxy	Room temperature to 350°F, 10°F/min; 1 hr, 350°F, 25 psi	0.064 in. 2024T3 Clad	4320	7090	7400	–	–	–
			0.064 in. 2024T3 Bare	–	6110	–	5210	3790	3370
			0.064 in. 7075T6 Bare	–	–	–	–	4310	2347
			0.020 in. EFH 301 S/S	–	3730	–	7450	4310	3750
Resin 3135 (2)	Epoxy-Polyamide	1/2 hr, 200°F, contact; 24 hr contact	0.064 in. 2024T3 Clad	(200°F) 3000	4500	–	–	–	–
			0.064 in. 2024T3 Bare	–	2180	–	1850	1760	1640
			0.064 in. 7075T6 Bare	–	–	–	–	1514	1552
			0.020 in. EFH 301 S/S	–	1310	–	1830	1350	940
			0.020 in. A-110-AT Ti	–	1040	–	1790	1020	1020
EC-1933B/A (4)	Epoxy-Polyamine	2 hr, 150°F, contact	0.064 in. 2024T3 Clad Prime	3500	4000	3100	–	–	–
			0.064 in. 7075T6 Bare	–	–	–	–	1775	1649
Resiweld No. 4 (5)	Epoxy-Polyamide	24 hr, room temperature, contact	0.064 in. 2024T3 Bare	–	2460	–	2380	1900	2010
EC-1469 (4)	Epoxy	1 hr, 350°F, 25 psi	0.064 in. 2024T3 Clad	–	2715	–	2715	2535	2345
Alumina Filled Epoxy	Epoxy	None	Copper	–	3500	–	–	1000	1000
XL967045-B/A (4)	Epoxy	48 hr, room temperature, contact	0.064 in. 2024T3 Clad	–	2390	–	2200	–	–
Metlbond 302 (2)	Epoxy-Phenolic	1 hr, 350°F, 25 psi	0.064 in. 301-1/2H-2B S/S	–	2595	–	2585	3135	3000
			0.020 in. EFH 301 S/S	–	2490	–	2780	2800	2690
			0.020 in. A-110-AT Ti	–	800	–	1440	1920	1560
Epon 622J (1)	Epoxy-Phenolic	1 hr, 350°F, 25 psi	0.064 in. 301-1/2H-2B S/S	–	3315	–	3650	3145	3240
Metlbond 4021 (2)	Nitrile Phenolic	1 hr, 350°F, 100 to 200 psi	0.064 in. 2024T3 Bare	2900	3750	3400	–	–	–
			0.020 in. 2024T3 Bare	–	–	–	–	–	–
			0.064 in. 2024T3 Clad		4295	–	4125	1620	1085
Metlbond 4041 (2)	Nitrile Phenolic	1 hr, 350°F, 100 to 200 psi	0.064 in. 2024T3 Bare	2500	3750	6200	5020	4400	1710
			0.020 in. EFH 301 S/S	–	2580	–	8700	5810	2070
			0.020 in. A-110-AT Ti	–	1590	–	6220	3690	1420
AF-32 (4)	Nitrile Phenolic	1 hr, 350°F, 100 psi	0.020 in. EFH 301 S/S	–	3650	–	8490	3600	2750
AF-5930 (4)	Nitrile Phenolic	1 hr, 350°F, 150 psi	0.064 in. 2024T3 Clad	–	3920	–	3795	1225	–
Bondmaster M24B (7)	Rubber-Epoxy-Phenolic	2 hr, 350°F, 50 psi	0.064 in. 2024T3 Clad	–	3625	–	1635	1230	1045
Plastilock 601 (8)	Rubber Resin	Manufacturer recommended	0.064 in. 2024T3 Bare	2000	3750	1250	–	–	–
Metlbond 303(MN3C (2)	Neoprene Nylon Phenolic	3/4 hr, 330°F, 40 psi; 3/4 hr, 330°F, 150 psi	0.064 in. 2024T3 Clad Na-amide-treated Teflon to SAE 52100 steel	1620	2930	5430	–	3750	–
Narmtape 111 (2)	Nylon Phenolic Epoxy	1 hr, 350°F, 25 psi	0.064 in. 2024T3 Bare	2750	3500	1500	–	–	–
APCO-1261 (9)	Polyurethane	1/2 hr, 300°F, contact under 100 psi nitrogen	0.064 in. 7075T6 Bare	–	1332	–	–	1940	–
APCO-1219 (9)	Polyurethane	24 hr, room temperature contact	0.064 in. 2024T3 Bare	–	1310	–	3100	2980	2710
			0.020 in. EFH 301 S/S	–	840	–	2210	1640	1020
Swedlow 371W (10)	Vinyl Phenolic	1/2 hr, 340°F, 5 psi	0.064 in. 2024T3 Clad	–	4855	–	2450	1795	1395
FM-47 (3)	Vinyl Phenolic	1 hr, 350°F, 200 psi	0.064 in. 2024T3 Clad	–	4600	–	3040	2325	1915
Redux 775 (11)	Vinyl Phenolic	1/2 hr, 340°F, 100 psi	0.064 in. 2024T3 Clad	–	3995	–	3200	2035	–
EC-1471 (4)	Vinyl Phenolic	1 hr, 350°F, 150 psi	0.064 in. 2024T3 Clad	–	5725	–	3455	2070	–

(a) See Appendix at end of this chapter.

Table 10-7

TEE PEEL STRENGTH OF SOME STRUCTURAL ADHESIVE BONDS TO ALUMINUM ALLOY ADHERENDS AT TEMPERATURES FROM 180° TO -423° F (Ref. 7)

Adhesive and Manufacturer(a)	Class	Cure	Adherend	Tee Peel Strength/lb-in. Width						Peel Rate in./min
				+180	RT	-40	-67	-320	-423	
Metlbond 406 (2)	Nylon-Epoxy	Room temperature to 350°F in 20 min; 1/4 hr, 350°F, 25 psi	0.020 in. 2024 T3 Clad	49.6	60 – 70	–	26.6	–	–	2
			0.020 in. 7075T6 Bare	–	–	–	–	8.33	8.2	2
Metlbond 408 (2)	Nylon-Epoxy	Room temperature to 350°F in 20 min; 1 hr, 350°F, 25 psi	0.020 in. 2024 T3 Clad	–	50 – 60	–	15	–	–	2
			0.020 in. 7075T6 Bare	–	–	–	–	4.33	5.3	2
AF-40 (4)	Nylon-Epoxy	Room temperature to 350°F, 10°F/min; 1 hr, 350°F, 50 psi	0.032 in. 2024 T3 Clad	90	118	54	38	–	–	20
			0.020 in. 7075T6 Bare	–	–	–	–	11.7	13.0	2
AF-41 (4)	Nylon-Epoxy	Room temperature to 350°F, 10°F/min; 1 hr, 350°F, 50 psi	0.032 in. 2024T3 Clad	71	111	–	11	–	–	20
			0.020 in. 7075T6 Bare	–	–	–	–	5.25	4.2	2
FM-1000 (3)	Nylon-Epoxy	Room temperature to 350°F, 10°F/min; 1 hr, 350°F, 25 psi	0.020 in. 2024T3 Clad	–	60	–	–	–	–	3
			0.020 in. 7075T6 Bare	–	–	–	–	3.1	5.5	2
Resin 3135 (2)	Epoxy-Polyamide	1/2 hr, 200°F, contact; 24 hr contact	0.020 in. 7075T6 Bare	–	–	–	–	0	0	2
EC-1933B/A (4)	Epoxy-Polyamine	2 hr, 150°F, contact	0.020 in. 7075T6 Bare	–	–	–	–	1.7	2.25	2
Metlbond 302 (2)	Epoxy-Phenolic	1 hr, 350°F, 25 psi	0.020 in. 7075T6 Bare	–	3.33	–	–	3. 66	–	2
Metlbond 4021 (2)	Nitrile Phenolic	1 hr, 350°F, 100 – 200 psi	0.064 in. 2024T3 Bare	–	–	–	–	–	–	
			0.020 in. 2024T3 Bare	–	45	5.0	5.0	–	–	2
			0.064 in. 2024T3 Clad	–	–	–	–	–	–	
Metlbond 4041 (2)	Nitrile Phenolic	1 hr, 350°F, 100 – 200 psi	0.020 in. 2024 T3 Bare	12	22	32	14	–	–	2
Plastilock 601 (8)	Rubber Resin	Manufacturer recommended	0.020 in. 2024T3 Bare	17	18	1.0	1.0	–	–	2
Narmtape 111 (2)	Nylon Phenolic Epoxy	1 hr, 350°F, 25 psi	0.020 in. 2024T3 Bare	45	22	3	3	–	–	2
APCO-1261 (9)	Polyurethane	1/2 hr, 300°F, contact under 100 psi nitrogen	0.020 in. 7075T6 Bare	–	1.92	–	–	3.33	–	2

(a) Numbers in parentheses are coded to the list of manufacturers given in the Appendix at the end of this chapter.

Table 10-8

COEFFICIENT OF LINEAR THERMAL EXPANSION OF SOME STRUCTURAL ADHESIVES AT CRYOGENIC TEMPERATURES (Ref. 7)

Adhesive	Manufacturer	Class	Coefficient of Linear Expansion From -320° to 32° F (in./in. $-^{\circ}F \times 10^{5}$)
APCO 1261	Applied Products Div., Hexcel Products Co.	Polyurethane	4.10
Metlbond 408	Narmco Materials Div., Whittaker Corp.	Epoxy-Nylon	3.24
AF-40	Minnesota Mining and Manufacturing Co.	Epoxy-Nylon	3.08
Metlbond 406	Narmco Materials Div., Whittaker Corp.	Epoxy-Nylon	3.06
Resin 3135	Narmco Materials Div., Whittaker Corp.	Epoxy-Polyamide	3.21
FM-1000	Bloomingdale Rubber Div., American Cyanimid Co.	Epoxy-Nylon	2.88
AF 41	Minnesota Mining and Manufacturing Co.	Epoxy-Nylon	2.79
EC 1933B/A	Minnesota Mining and Manufacturing Co.	Epoxy-Polyamide	2.28

Table 10-9

FATIGUE BEHAVIOR OF ADHESIVES

Adhesive	Room Temperature		-320° F	
	Cycles to Failure	Remarks	Cycles to Failure	Remarks
Epoxy-Polyamide	3,600	All bond failures	600,000	Metal failures
Flexibilized Epoxy	280	All bond failures	130	All bond failures
Polyurethane	–	Will not support 1800 psi	1,000,000	No failures
Modified Epoxy-Phenolic Glass Cloth Supported; Primed	4,075	All bond failures	470,000	All bond failures
Nylon-Epoxy, Unsupported Film, No. 3, Primed	221,000	All bond failures	244,000	All metal failures
Modified Epoxy, Fabric Supported, Primed	253,000	All bond failures	1,000,000	No failures

at room temperature than either the flexibilized epoxy or the polyurethane adhesive. The polyurethane adhesive was not able to withstand the applied 1800-psi pre-load at room temperature. At the temperature of liquid nitrogen (-320° F), however, the polyurethane system withstood 1,000,000 cycles without failure but the epoxy-polyamide sustained a metal failure at 600,000 cycles.

The polyurethane adhesive also proved to be quite compatible with cryogenic liquids used as space vehicle fuels and oxidizers. In one investigation (Ref. 8), a polyurethane adhesive was used to fasten a 3-in.-diameter aluminum disc over a hole separating a vacuum chamber and a liquid hydrogen (-423° F) reservoir. The area of the adhesive bond was 3.9 $in.^2$. After 6 hr of continuous monitoring, no change in vacuum pressure was observed. When hydrogen permeability was measured by a gas chromatograph, an 11-mil-thick film of polyurethane adhesive showed a permeation rate of 7.6×10^{-8} gm/cm^2-min.

The effect of liquid oxygen on the polyurethane adhesive was determined by immersing lap-shear test specimens of the adhesive for 72 hr (Ref. 8). After this soak period, there was no decrease in the tensile-shear strength of the bond when removed from the liquid oxygen (-300° F) and tested in liquid nitrogen (-320° F).

The heat-cured adhesive films, as a class, show tensile-shear strengths and "T" peel strengths at slightly elevated and cryogenic temperatures somewhat better than the room-temperature-curing systems. The room-temperature-cured polyurethane adhesive does exhibit favorable properties at cryogenic temperatures.

In comparing the structural film adhesives, it should be recognized that the difference between their film weight-per-unit area can influence the results. This variable influences the properties of honeycomb-core-to-facing sheet bonding in sandwich construction because of the increased thickness of the glue line and contact area (fillet depth) of the adhesive on the honeycomb core. Thus, higher strengths are obtained for honeycomb sandwiches made from the 3 to 4 times heavier epoxy-phenolic film adhesive than with specimens made with nylon-epoxy film. In another instance cited, three layers of an unsupported nylon-epoxy adhesive film were found to increase the climbing-drum peel strengths over the one-layer values (Ref. 8).

The epoxy-nylon adhesives show the highest lap-shear strengths with all adherends over the entire temperature range -423° to 78° F. The nitrile-phenolic adhesives show good properties over the temperature range -320° to +78° F, but strength values drop off sharply at -423° F. The epoxy phenolic adhesives have lower properties than those obtained with the epoxy-nylon and nitrile-phenolic adhesives at -320°, -100°, and +78° F. At -423° F the epoxy-phenolic is superior to the nitrile-phenolics. Room-temperature-cured adhesives are generally inferior to those that are heat cured. Of the three room-temperature-cured adhesives tested, the polyurethane gave higher lap-shear strengths than the epoxy-polyamides with an aluminum adherend, and approximately the same strengths with stainless steel adherends. For all the adhesives tested, the highest lap-shear strength was at -100° F (Ref. 9).

10.3 EFFECTS OF HIGH-ENERGY RADIATION ON ADHESIVES

The effects of high-energy particulate (neutrons, electrons, and protons) and electromagnetic (x-ray and gamma-ray) radiation on adhesives have been studied since about 1955. Exposure to charged particles, electrons, and protons is the principal concern in the natural space environment. The short-wavelength electromagnetic radiation (x rays), although more penetrating than particulate radiation, is generally of much lower intensity in space orbits and trajectories of current importance. However, some simulated radiation-effects tests utilize low-wavelength electromagnetic radiation and neutron radiation from nuclear reactors to ascertain the effects of radiation on adhesives and other nonmetallic materials.

The effects of high-energy electromagnetic, neutron, and charged-particle radiation on structural adhesive bonds are similar. There can be an increase in the temperature of the adhesive glue line because of the absorption of the incident energy by the adherends, the surrounding structure, or the adhesive itself. This increase in temperature can be predicted or determined if the incident flux intensity, the type of particle, the absorption coefficients, and the thermal properties of the various materials being irradiated are known.

Another effect of radiation on polymeric materials is cross-linking, or chain scission, of the adhesive. The occurrence of chemical intermolecular, free radical, or atomic processes is dependent on the chemical nature of the polymer and on the radiation dose absorbed.

Cross-linking involves the formation of bridges or chemical bonds between adjacent chains in the polymer to form a more complete three-dimensional network. It is associated with an increase in molecular weight. Cross-linking in polymers causes an increase in hardness, rigidity, tensile modulus of elasticity, ultimate tensile strength, density, and brittleness of the material. These changes in properties are detrimental because they increase the tendency to fracture under structural load, particularly with shock or vibration. Polymers used in structural adhesive formulations of the thermosetting type usually undergo a cross-linking intermolecular reaction during cure and are further cross-linked by incident high-energy radiation.

Chain scission of polymers is the radiation damage mechanism in thermoplastics and some elastomers, including ethylenic or vinylic types, particularly those containing halogen atoms. Such polymers are sometimes used as resins in nonstructural adhesives or solvent-based rubber cements. They generally do not possess sufficient adhesive or cohesive strength and are not sufficiently temperature resistant themselves to be used for structural applications. They are used as additives or coreactants with thermosetting resins for structural adhesive formulations to modify a processing characteristic or mechanical-thermal-physical property of the uncured or cured adhesive. Examples of such formulations are vinyl-phenolics and epoxy-nylons (polyamides).

Chain scission involves depolymerization or "unzipping" of the main skeletal polymer chains into low molecular weight fractions. Such polymers can degas, undergo weight

losses, and become porous, particularly in a vacuum-radiation environment. Chain scission in a polymer can cause softening (e.g., butyl rubber becomes a tarry liquid at 10^5 rad), reduced tensile strength and tensile modulus of elasticity, large volatile inclusions (even foaming in the case of Teflon TFE at high irradiation doses), decrease in density, depression of molecular weight and the glass-transition temperature, and sometimes color changes. Polyvinyl chloride (PVC) is used as a dosimeter for accurate measurement of gamma radiation dose; its darkening is a function of the absorbed dose.

The effects of radiation on a polymeric material are to a very large extent dependent on the temperature and surrounding atmosphere. Since changes occurring in a polymer are chemical, the presence or absence of air (or other reactive gases) has a bearing on the type of reaction and the reaction rate induced by the absorbed radiation. As an example of this effect on Teflon (TFE) in vacuum or in an inert atmosphere, the damage threshold is about 10^7 rad, whereas, when irradiated in air, it is about 10^5 rad. The reason for the two orders of magnitude difference in radiation damage threshold is that oxygen in the air can enter into the depolymerization reaction and catalyze the decomposition.

In the case of thermosetting materials such as those used in structural adhesive formulations, the effects are not as pronounced between irradiation in vacuum (or in an inert atmosphere) and irradiation in air, but difference effects have been shown; they are important and should be considered by the designer. The effect in vacuum is generally less than in air.

The effects of temperature extremes, the presence of air, inert or reactive atmospheres, or vacuum, and high-energy radiation on polymers are extremely complex and synergistic. These effects should not generally be considered individually by the designer. However, because combined-effects data often are not available, it sometimes becomes necessary to estimate from the individual effects.

Table 10-10 (Refs. 9 and 10) summarizes the effects of mixed gamma-neutron radiation from a reactor in air and in vacuum on various classes of structural adhesives. The adhesives were irradiated in vacuum at various exposure doses and tested in air after irradiation in vacuum.

The effect of increasing temperature on a typical epoxy-phenolic adhesive is shown in Table 10-11 (Ref. 10). The percent change in tensile-shear strength is greater by nearly a factor of 3 at double the temperature for almost the same radiation dose. At increased temperature, but at a factor of 2 decreased radiation dose, the percent change in strength decreases by about a factor of 8.

Data on the effect of mixed neutron-gamma reactor radiation on another typical epoxy-phenolic adhesive at temperatures from 75° to 450° F in air are presented in Table 10-12 (Ref. 11).

Table 10-10

EFFECT OF NUCLEAR REACTOR IRRADIATION IN AIR AND VACUUM ON ULTIMATE TENSILE SHEAR STRENGTH OF SOME ADHESIVES AT ROOM TEMPERATURE (Refs. 4, 9, 10)

Adhesive Type	Manufacturer(a)	Class	Tensile Shear Strength Before Irradiation (psi)	Irradiation in Air (rads)	Tensile Shear Strength After Irradiation in Air (psi)	Irradiation in Vacuum (rads)	Tensile Shear Strength After Irradiation in Vacuum (psi)	Percent Change in Tensile Strength
Epon 929	1	Epoxy	2264	3.9×10^8	2510	2.9×10^8	1973	-12
Epon 934	1	Epoxy	2562	3.9×10^8	2840	2.9×10^8	2320	-9
Epon 8	1	Epoxy	2361	–	–	1.7×10^8	2072	-12
FM-1000	3	Epoxy-polyamide (nylon)	6065	–	–	1.7×10^8	6121	Negligible
			6283	3.9×10^8	6086	2.9×10^8	6117	Negligible
Metlbond 406	2	Epoxy-polyamide (nylon)	4823	1.1×10^8	5940	–	–	–
				4.9×10^8	752	–	–	–
HT-424	3	Epoxy-phenolic	3605	3.9×10^8	2599	2.9×10^8	3303	-8
Epon 422 J	1	Epoxy-phenolic	2362	–	–	3.9×10^8	2452	Negligible
Narmco A	2	Modified epoxy	4157	3.9×10^8	3634	2.9×10^8	4959	+16
Metlbond 408	2	Vinyl epoxy-nylon	4083	–	–	3.9×10^8	896	-78
FM-47	3	Vinyl-phenolic	4315	3.9×10^8	3716	2.9×10^8	2561	-42
			4180	–	–	3.9×10^8	2415	-40
Metlbond 4021	2	Nitrile-phenolic	4370	3.9×10^8	3234	2.9×10^8	3250	-25
AF-6	4	Nitrile-phenolic	2578	–	–	3.9×10^8	2410	-6
				11×10^8	3814	–	–	–
APCO 1252	9	Polyurethane	2743	3.9×10^8	3262	2.9×10^8	3181	+12
				6×10^8	5028	–	–	–
Narmco C	2	Polyurethane	883	3.9×10^8	20.8	2.9×10^8	454	-48

(a) See Appendix at end of this chapter.

Table 10-11

EFFECT OF NUCLEAR REACTOR RADIATION IN VACUUM AT ELEVATED TEMPERATURE ON THE ULTIMATE TENSILE SHEAR STRENGTH OF AN EPOXY-PHENOLIC ADHESIVE (Ref. 10)

Adhesive	Manufacturer	Class	Temp. (°F)	Vacuum (Torr)	Tensile Shear Strength Before Irradiation (psi)	Irradiation in Vacuum (rads)	Tensile Shear Strength After Irradiation (psi)	Percent Change
Metlbond 302	Narmco Materials Div., Whittaker Corp.	Epoxy-Phenolic	77	3×10^{-1}	2482	1.6×10^{8}	2856	15
			157	5×10^{-6}		2.1×10^{8}	3511	41
			207	3×10^{-1}		9.2×10^{7}	2507	5

Table 10-12

EFFECT OF NUCLEAR REACTOR RADIATION AT ELEVATED TEMPERATURES IN AIR ON AN EPOXY-PHENOLIC ADHESIVE (AEROBOND 422J)[a] (Ref. 11)

Radiation Exposure Dose		Irradiation Conditions		Storage Conditions After Irradiation		Test Temperature (°F)	Average Tensile – Shear Strength (psi)	Standard Deviation	No. of Specimens
Gamma (rads)	Neutrons (per cm^2) (E>2.9 MeV)	Temperature (°F)	Time (hr)	Temperature (°F)	Time (days)				
Control	–	–	–	75	–	75	2,490	51	16
Control	–	–	–	75	–	350	2,690	102	8
Control	–	110	33	–	–	75	2,666	160	20
2.5×10^8	2.2×10^{15}	110	33	–	–	75	2,782	123	20
Control	–	140	33	–	–	75	2,742	171	20
9.1×10^8	1.0×10^{16}	140	33	–	–	75	2,606	137	20
Control	–	250	33	350	7	350	734	88	20
6.8×10^8	5.9×10^{15}	250	31	350	7	350	2,240	156	16
6.8×10^8	5.9×10^{15}	250	31	350	8	350	1,937	131	4
Control	–	310	31	350	7	350	816	80	20
2.2×10^9	2.4×10^{16}	310	31	350	7	350	2,400	189	3
2.2×10^9	2.4×10^{16}	310	31	350	8	350	1,853	62	17
Control	–	–	–	–	–	75	2,542	195	10
5.6×10^8	5.2×10^{15}	120	55	–	–	75	2,661	199	20
1.7×10^9	1.7×10^{16}	130	55	–	–	75	2,590	180	20
Control	–	450	55	–	–	450	1,430	136	9
6.0×10^8	7.2×10^{15}	445	55	–	–	450	1,280	74	9
Control	–	445	55	450	7	450	920	83	10
6.0×10^8	7.2×10^{15}	445	55	450	7	450	809	78	10

(a) Manufactured by Applied Products Div., Hexcel Products Co.

Lap-shear specimens were prepared with epoxy, epoxy-phenolic, vinyl-phenolic, and nitrile-phenolic adhesives (Ref. 12). These were irradiated in air and in vacuum (10^{-6} Torr) to a gamma exposure dose of 10^7 rads at a temperature of 100° F maximum. The specimens were than tested for tensile-shear strength at a temperature of -320° F. In all cases, the change in strength was small (Fig. 10-14).

In Table 10-13 (Ref. 13), data on the effects of gamma radiation (nuclear reactor) on representative structural adhesives are given. The specimens were irradiated and tested in tensile-shear in air and immersed in cryogenic fluid. The cryogenic fluids were liquid nitrogen (-320° F) and liquid hydrogen (-423° F). A summary of the results for each adhesive class is given in the following paragraphs.

10.3.1 Epoxy-Nylon

Gamma irradiation up to 1.0×10^8 rads, in air at 75° F, did not affect the ultimate tensile-shear strength of these adhesives. At a gamma dose of 1.7×10^9 rads, there was a loss of about two-thirds of this strength.

Specimens irradiated and tested in the cryogenic liquid nitrogen (LN_2) fluid were about two-thirds as strong as were those in air at ambient temperature. In liquid hydrogen the specimens were about one-half as strong as in air.

10.3.2 Epoxy-Phenolic

Radiation levels up to 1.7×10^9 rads in air, and $2.5 + 10^8$ rads in cryogenic fluids caused less than a 20% decrease in the strength of the epoxy-phenolic adhesive. The epoxy-phenolic materials are good radiation-resistant structural adhesives for cryogenic applications.

10.3.3 Epoxy

The epoxy adhesive was stable when irradiated in air and in cryogenic fluids. Up to the maximum gamma dose exposures, there was very little change in the tensile-shear strength adhesive in any of these environments.

10.3.4 Modified Epoxy

The modified epoxy adhesive did show significant change in tensile strength under radiation in air up to a gamma dose of 1.7×10^9 rads. There was little radiation effect on the strength in air at 3.3×10^8 rads. This adhesive lost 50% of its strength when exposed to radiation and the LH_2 environment.

10.3.5 Polyurethane

The polyurethane adhesive increased in strength under irradiation in air but decreased in strength when irradiated in the cryogenic fluids LN_2 and LH_2.

Notes:

1. Data are for lap-shear specimens of the materials listed.
2. Each point is the actual ultimate tensile-shear strength of the test specimen.
3. Temperature of specimens during test was -320 °F.

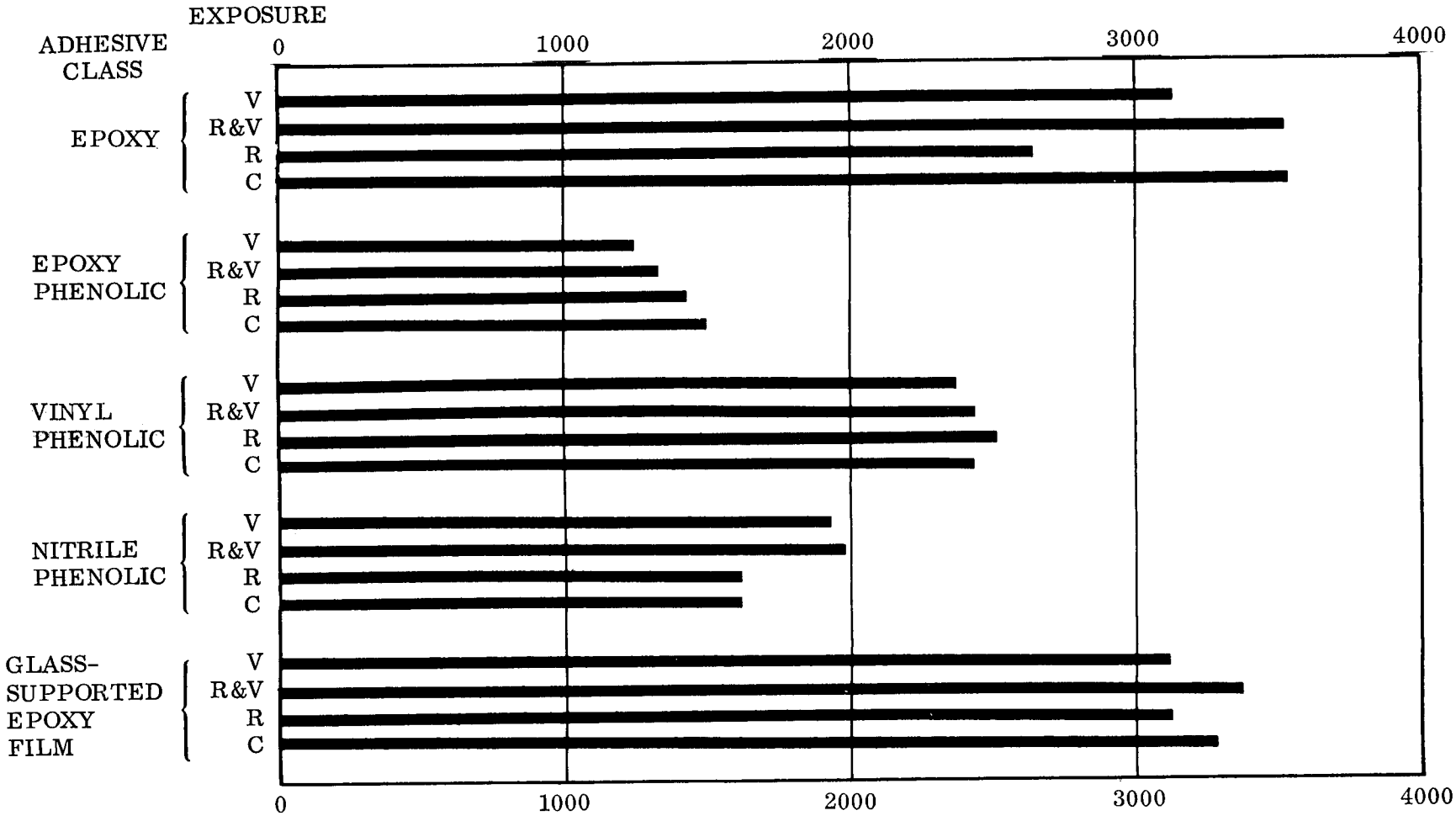

V = Vacuum (10^{-6} Torr)
R = Radiation (10^{7} rads)
C = Controls

Fig. 10-14 Effect of Radiation and Vacuum on Tensile-Shear Strengths of Structural Adhesives Tested at Cryogenic Temperatures (Ref. 12)

Table 10-13

EFFECT OF GAMMA (NUCLEAR REACTOR) RADIATION IN AIR AND IN CRYOGENIC FLUIDS ON TENSILE SHEAR STRENGTH OF SOME STRUCTURAL ADHESIVES (Ref. 13)

Adhesive	Manufacturer(a)	Class	Ultimate Tensile Strength (psi) Measured at Indicated Temperature After Gamma-Irradiation in Rads Shown in Column Headings									
			Ambient Air (75° F)					Liquid Nitrogen (-320° F)		Liquid Hydrogen (-423° F)		
			0	6.0×10^{7}	1.1×10^{8}	3.3×10^{8}	1.7×10^{9}	0	1.5×10^{8}	0	7.5×10^{7}	2.4×10^{8}
AF-40	4	Epoxy Nylon	5606	–	6170	–	–	4110	2720	–	–	–
FM 1000	3	Epoxy-Nylon	6265	6165	6351	5991	2201	4669	2096	2991	2137	1726
Metlbond 406	2	Epoxy-Nylon	4823	–	5940	–	–	2990	2292	3250	–	1978
Epon 934	1	Epoxy Nylon	2756	2873	2246	2934	2766	1983	1908	1899	1831	1684
Narmco A	2	Modified Epoxy	4157	4311	4324	4140	1313	–	–	2048	1605	1676
HT-424	3	Epoxy Phenolic	3500	3529	3363	2639	2193	4471	3339	3593	3125	2893
Aerobond 422J	9	Epoxy Phenolic	2520	–	2520	–	2361	3030	2910	2436	2244	2209
Aerobond 430	9	Epoxy Phenolic	2627	2541	2404	2685	2213	–	–	–	–	–
APCO 1252	9	Poly-Urethane	3228	–	3416	3409	2750	5040	4592	5928	–	4536

(a) See Appendix at end of this chapter.

Some of these adhesives were also irradiated and tested in vacuum (Ref. 14); this combined environment had little effect on the tensile-shear strengths of these materials. The polyurethanes, epoxies, and phenolics have relatively high radiation resistance compared with the other classes of polymers. Polyurethanes have good resistance to the effects of nuclear radiation and cryotemperatures. Furthermore, some polyurethanes can be cured at room temperature for the adherence of cryogenic insulations to the liquid containers. All of these adhesives should be considered for service in radiation and cryogenic environments for structural components of a spacecraft.

The typical specifications applicable to the structural adhesives are shown in Table 10-14.

10.3.6 Nonstructural Adhesives

Adhesives for bonding transparent cover materials to silicon solar cell elements are considered as nonstructural adhesives. Those for bonding of the solar array subpanels to the honeycomb panel structural substrate are also in this category.

For the bonding of the transparent covers to the solar cell, a transparent adhesive is required. The spectral transmittance is usually specified to be a minimum of 90% in the spectral wavelengths of 0.5, 0.7, 0.9, and 1.1 μ. The cured material must meet the spectral transmittance characteristics after a thermal soaking at 200° F for 24 hr followed by 24 hr at -100° F. The cured adhesive should not exhibit cracking, blistering, or peeling when undergoing 30 cycles of temperature, with a 15-min dwell, at -70° and +175°F. It should also withstand exposure to saturated humidity at 140° F for 6 hr.

Although penetrating particle radiation, electrons and protons, can cause a loss in transmission of the solar cell cover, laminate tests indicate that the quartz cover material may absorb most of the energy of this radiation. Thus, the factor of the solar radiation that can cause darkening (loss of transmission) in the transparent adhesives is the ultraviolet radiation component. Minimum spectral transmittance stability under ultraviolet radiation of a high-intensity (1 kW), high-pressure mercury-arc-light source provided by a General Electric AH-6 lamp or the equivalent is shown in Table 10-15.

For these measurements, specimens are made of two 0.02- or 0.005-in.-thick quartz slides about 3/4 in. long and 3/8 in. wide, cemented together with the adhesive (Ref. 14). Generally, the cover slides are coated with an antireflectance layer, which enhances the transmission characteristics in the 0.6 to 0.8 μ wavelength region. A blue-red filter coating is also applied which is designed to provide protection against damage to the adhesive by ultraviolet radiation and to reduce the operating temperature of the solar cell (Ref. 15). The adhesives in general use are either clear silicone rubbers or clear epoxy materials. Some clear polyurethane adhesives were used formerly, but the silicone and epoxy adhesives have proved to have more reproducible batch-to-batch properties.

Table 10-14

STRUCTURAL ADHESIVE SPECIFICATIONS

Material	Specification	Tensile Shear Strength (psi)	Temperature (°F)	Duration (min)	Useful Temperature Range (°F)	Remarks
Adhesive, Epoxy, Heat-Resistant Air Frame Structure	MIL-A-5090, Type I	2500 2500 1250	-67 75 180	10 — 10	-67 to 180	General-purpose structural bonding.
	MIL-A-5090, Type II	2250 2250 2000	-67 75 300	10 — 10	-67 to 300	General-purpose structural bonding at 300°F.
	MIL-A-5090, Type III	2250 2250 1850	-67 75 500	10 — 10	-67 to 300 and 10 min at 500	General-purpose structural bonding to 300°F, with capability to 500°F for 10 min.
Adhesive Structural Metal-to-Metal	MIL-A-8623, Type I	1300 2500 1250	-67 75 180	— —	-67 to 180	General-purpose epoxy or silicone adhesives, room-temperature cure, Type I.
	MIL-A-8623, Type II	2500 2500 1250	-67 75 180			Type II cures between 87° and 210°F epoxy.
	MIL-A-8623, Type III	2500 2500 1500	-67 75 180			Type III cures at > 210°F.

Table 10-15

MINIMUM SPECTRAL TRANSMITTANCE OF SOLAR CELL COVER ADHESIVES

Wavelength (μ)	Transmittance After Ultraviolet Exposure (%)	
	300 Sun Hours	600 Sun Hours[a]
0.5	80	72
0.7	90	88
0.9	90	90
1.1	90	90

(a) 6 times simulated solar ultraviolet intensity for 100 hr.

The effect of simulated solar ultraviolet radiation and environmental testing (thermal soak, cycling, and humidity) on three typical solar cell adhesives is shown in Table 10-16.

Table 10-16

EFFECT OF SIMULATED SOLAR ULTRAVIOLET RADIATION ON SPECTRAL TRANSMITTANCE OF ADHESIVE QUARTZ LAMINATE

Material[a]	Transmittance (%)									
	Before			After[b]			Change			
	0.5μ	0.7μ	0.9μ	0.5μ	0.7μ	0.9μ	0.5μ	0.7μ	0.9μ	Ave.
Epocast H-1377/C	91.9	92.3	92.8	64.1	91.7	92.3	27.8	0.6	0.5	9.6[c]
LTV602/SRC 05	92.1	93.5	94.6	73.6	89.6	91.3	18.5	3.9	3.3	8.6[c]
XR63488 (Sylgard 182)	93.2	94.0	95.3	84.3	94.1	95.0	8.9	0	0.3	3.1[d]

(a) Adhesive cemented two uncoated 0.04-in.-thick, 0.4-in.-wide, 0.8-in.-long Corning No. 7940 fused silica cover slides, adhesive about 1 mil (0.001 in.) thick.
(b) After thermal soak (200° and -100° F, 24 hr each), humidity (140° F, 95% RH, 48 hr), thermal cycling (30 cycles, 15-min dwell at 170° and -70° F), and ultraviolet irradiation in vacuum.
(c) Simulated solar ultraviolet radiation for 100 hr in vacuum (10^{-6} Torr) of 6 times sun intensity. Solar intensity 0.0126 W/cm^2 normal incident ultraviolet flux from 2000 to 4000 Å (0.2 to 0.4 μ) at zero air mass (AMZ) at the earth's mean distance from the sun = 600 sun-hr.
(d) 100 hr at 5 times solar intensity = 500 sun-hr.

The antireflectance and blue filter coatings do reduce the change in transmittance of the silicone adhesive laminates. The change in transmittance of the coated No. 7940 laminates bonded with LTV 602 and Sylgard 182 is shown in Table 10-17 (Ref. 14). In these tests, the specimens did not have the thermal soak, cycling, and humidity exposures prior to ultraviolet irradiation.

Table 10-17

EFFECT OF SIMULATED SOLAR ULTRAVIOLET[a] ON SPECTRAL TRANSMITTANCE OF SILICONE ADHESIVE BONDED NO. 7940 QUARTZ[a] LAMINATES

Material	Transmittance (%)									
	Before			After			Change			
	0.5μ	0.7μ	0.9μ	0.5μ	0.7μ	0.9μ	0.5μ	0.7μ	0.9μ	Ave.
LTV 602	89.0	92.0	93.6	85.2	91.2	92.4	-3.8	-0.8	-1.2	-1.9
XR63488 (Sylgard 182)	89.0	93.5	95	89.6	92.6	91.5	+0.6	-0.4	-3.5	-1.1

(a) 5 times solar intensity for 100 hr in vacuum 10^{-6} Torr.

A study was undertaken of radiation effects on various adhesives used for bonding the cover to the solar cells of the Explorer 26 (EPE-D). The four adhesives used to laminate solar cell cover materials for the tests follow.

Resin Trade Name	Class	Manufacturer
LTV 602	Clear silicone rubber	General Electric
Sylgard 182	Clear silicone rubber	Dow Corning
Ciba 502	Clear epoxy	Ciba Plastics
Maraglas 656	Clear epoxy	Marblette Corp.

The adhesives were used to bond 60-mil covers to a 60-mil base of No. 7940 fused silica. In this study, a 500-W Hanovia mercury vapor lamp was used as an ultraviolet radiation source in a vacuum of 10^{-7} Torr. The results of the change in transmission for the 300-hr exposure of the four adhesives is shown for the spectral range of 0.35 to 0.8 μ in Fig. 10-15. If one assumes that the transmission before exposure for the Sylgard 182 laminate (XR63488) was about 95%, as was the case in Table 10-14 (Ref. 14), then the change at 0.5 μ was 11%; at 0.7 μ, 1%; and at 0.8 μ, 0% – for an average of about 4%, which is not too different from that reported in Ref. 14. This behavior has resulted in the choice of this material for a number of solar cell cover bonding applications. However, in the 0.35 μ to 0.5 μ range, all the adhesives had as much as 80% to 20% transmission loss, resulting from ultraviolet radiation exposure. A more ultraviolet radiation resistant adhesive is needed for this application.

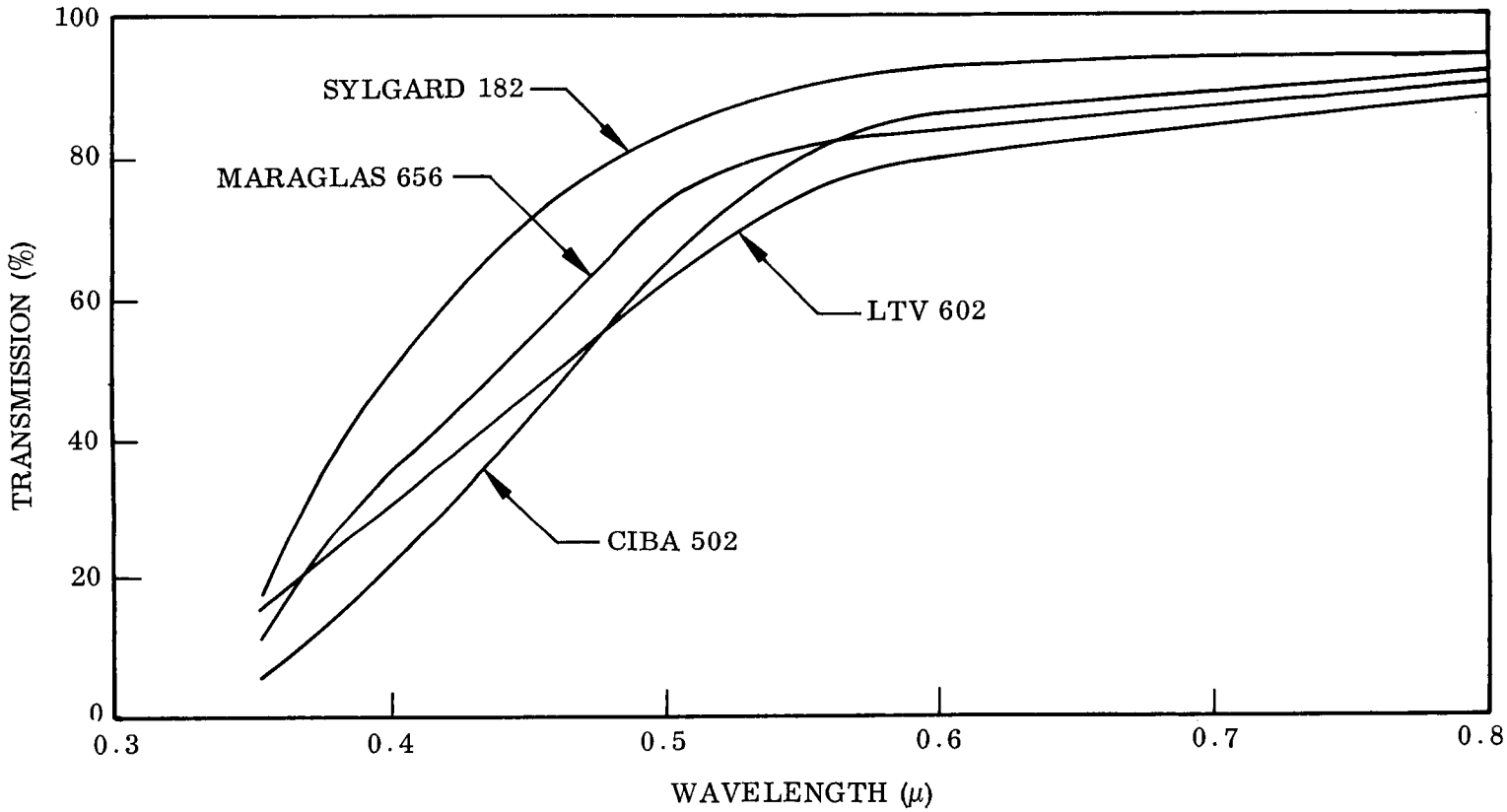

Fig. 10-15 Transmission of Adhesives After 300 hr at Exposure to Ultraviolet Radiation (500-W Hanovia Lamp, Vacuum 10^{-7} Torr)(Ref. 16)

The effect of the thermal soak, cycling, and humidity, as well as vibration environments, was also investigated in the work of Ref. 16. It was found that the epoxy-based, adhesive-bonded laminates had cracked covers or had bubbles in the adhesive. The silicone-based laminates had delaminations. In these tests the Sylgard 182 silicone material had the fewest defective laminates.

Charged-particle radiation exposure of the adhesive-bonded fused silica laminates was also conducted (Ref. 16). In these tests the specimens were OCLI (Optical Coatings Laboratory) 6-mil microsheet (Corning 0211) with antireflectance and blue filter coatings bonded to a 60-mil No. 7940 fused silica base with 1- to 2-mil-thick adhesive. These specimens were irradiated with 4×10^{11} protons/cm^2 of 4.6 MeV energy or 10^{15} electrons/cm^2 of 1-MeV energy in a 10^{-4} Torr vacuum. The spectral transmittance measurements of the silicone adhesive-bonded specimens before and after exposure showed that the change in the laminates was nearly the same as that in the 6-mil microsheet alone. This behavior resulted in experiments with the adhesive alone, the 6-mil cover ("filter glass"), and the laminates which are shown in Fig. 10-16. As can be seen in the figures, the electron and proton irradiation does not affect the transmission of the silicone adhesives (LTV 602 and Sylgard 182) but does affect the transmission of the 6-mil microsheet. The 0211 is Vycor fused silica.

From the results of these simulated space environment exposures, it would appear that the short-wavelength electromagnetic radiation caused a decrease in the transmittance of the transparent epoxy and silicone solar cell cover adhesives. The charged-particle radiation consisting of 4-MeV protons and 1-MeV electrons caused a decrease in the transmittance of the fused silica cover material but not in the adhesive.

The other element in the adhesive bonding of solar cell covers is the active silicon solar cell itself. The contribution of the total solar power degradation in space, measured by spacecraft solar panels, by the radiation damage to the silicon is difficult to determine. From the experiments discussed, it would appear that the total solar panel power loss is contributed to by all of the following: each element of the adhesive, darkened by solar ultraviolet; the cover sheet, darkened by the charged particles, electrons, and protons; and the silicon itself, damaged by charged-particle or high-energy, short-wavelength electromagnetic radiation not absorbed by the cover or the adhesive.

For the bonding of the solar cell insulating substrate to the solar panel, a number of adhesives have been used. These fall into the classes of room-temperature curing epoxy or silicone materials. Some epoxy-nylon and phenolic-nitrile adhesives have been used for this application.

It has been found that the silicone adhesives have somewhat better peel strength properties and resist vibration better than the others. Those that have been used are the room-temperature curing silicone elastomers and resins that conform to Specifications MIL-A-25457 and MIL-A-8623, Type I.

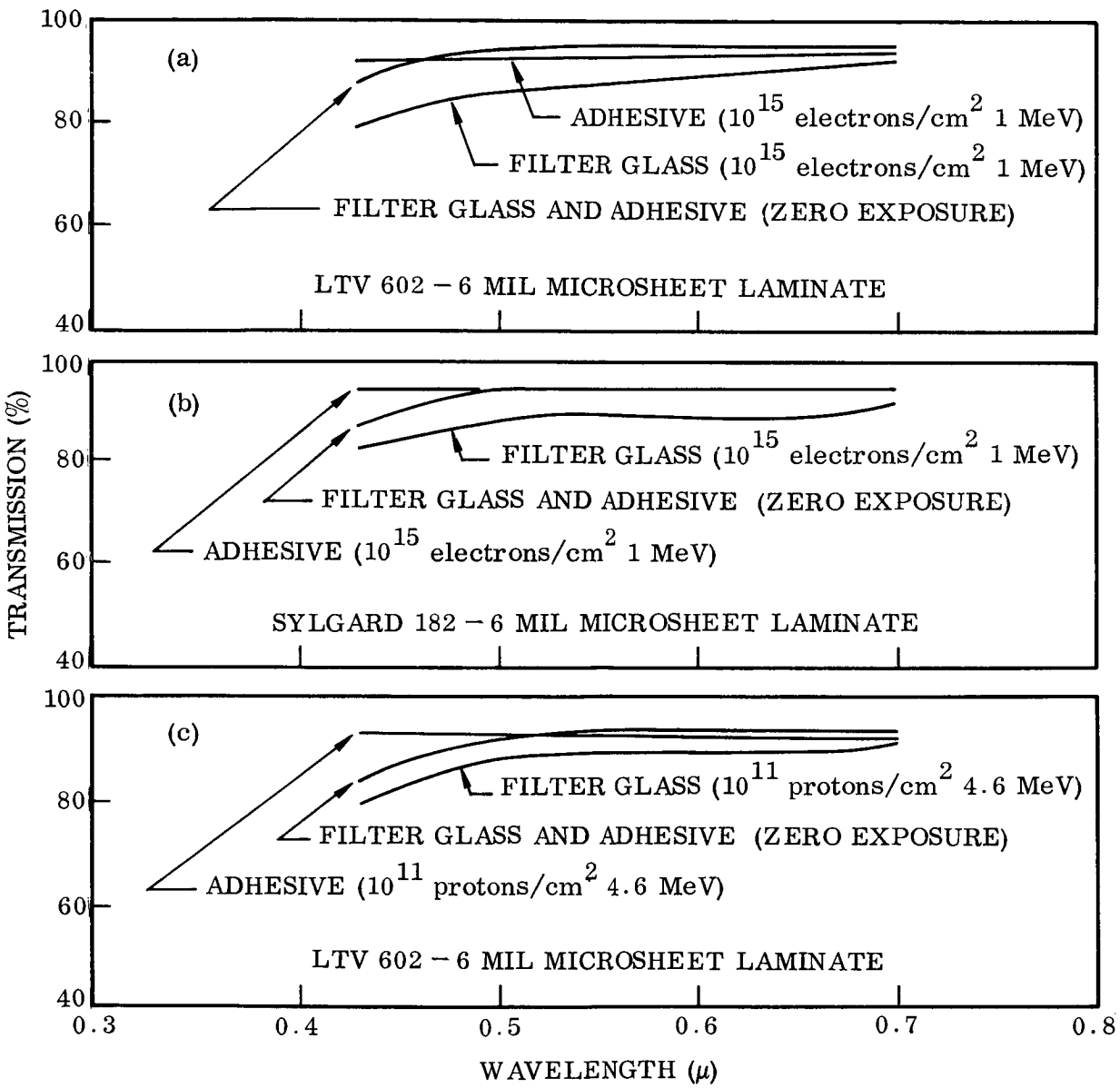

Fig. 10-16 Electron (a and b) and Proton (c) Irradiation Effects on Laminate Components (Vacuum 10^{-4} Torr)(Ref. 16)

The commercial designations used in recent spacecraft were the GE RTV40 and RTV60, Dow Corning 92024, Minnesota Mining and Manufacturing Company adhesive AF30, and Bloomingdale Rubber Company (a Division of American Cyanimid Co.) FM1000.

Another method that was found to be effective for bonding the insulating substrate to the solar panel structure was to keep the modified epoxy resin of the glass cloth reinforced substrate in a slightly tacky state ("B" stage). When the glass reinforced resin in this "B" state was applied to the solar panel structure, it acted, when cured, as its own adhesive for attachment of the insulation substrate to the panel (Ref. 17).

These adhesives are intended for use in the temperature range -67° to 300°F. The tensile-shear properties are a minimum of 1050 psi at 75°F and a peel strength of 3.2 lb/in. width.

10.4 REFERENCES

1. J. K. Kuno, "Comparison of Adhesive Classes for Structural Bonding at Ultra-High and Cryogenic Temperature Extremes," Seventh Annual SAMPE (Society of Aerospace Materials and Process Engineers) National Symposium Transactions, pp. 11-1 to 11-36, Los Angeles, Calif., 20-22 May 1964

2. R. B. Krieger and R. E. Politi, "High Temperature Structural Adhesives," Ninth Annual SAMPE National Symposium Transactions, Dayton, Ohio, 15-17 November 1965

3. S. H. Kalayan and B. A. Campbell, Effects of Thermal Sterilization Procedure on Polymeric Products, NASA Jet Propulsion Laboratory Technical Report No. 32-973, 15 November 1966

4. E. E. Kerlin, Investigation of Combined Effects of Radiation and Vacuum and of Vacuum and Cryotemperatures on Engineering Materials, Vol I, "Radiation-Vacuum Tests," Report No. FZK-161-1, General Dynamics, Fort Worth, Tex., 5 January 1963

5. J. A. Black, D. J. Lyman, and D. B. Parkinson, Development of Material Specifications and Qualification of Polymeric Materials for the J. P. L. Spacecraft Materials Guidebook: Epoxide Adhesives, Special Report No. 1 (PRD-5046), Stanford Research Institute, Menlo Park, Calif., 15 June 1965

6. R. F. Muraca et al., Polymers for Spacecraft Hardware: Materials Characterization, Interim Report No. 3 – Part I (A5D-5046), Stanford Research Institute, Menlo Park, Calif., 9 December 1966

7. M. B. Smith and S. E. Susman, Development of Adhesives for Very Low Temperature Applications, NASA Final Summary Report No. CR 52879, May 1963

8. L. M. Roseland, "Evaluation of Structural Adhesives for Potential Cryogenic Usage," Seventh Annual SAMPE National Symposium Transactions, pp. 7-1 to 7-17, Los Angeles, Calif., 20-22 May 1964

9. N. J. Broadway and S. Palinchak, The Effect of Nuclear Radiation on Elastomeric and Plastic Components and Materials, REIC Report No. 21 (Addendum), pp. 11–22, Radiation Effects Information Center, Battelle Memorial Institute, 31 August 1964

10. E. E. Kerlin and E. T. Smith, Measured Effects of the Various Combinations of Nuclear Radiation, Vacuum and Cryotemperatures on Engineering Materials, Report No. FZK-172, General Dynamics, Fort Worth, Tex., 30 September 1963; and Report No. FZK-290, 1 July 1966

11. NARF Final Progress Report, Report No. NARF 62-18P-FZK-9-184, Final Progress Report, General Dynamics, Fort Worth, Tex., 1 October 1961, 30 September 1962

12. P. D. Gray et al., Rockets in Space Environment, Vol. I, "The Experimental Program," Report No. RTD-TDR-63-1050, Aerojet General Corporation, February 1963

13. R. P. Lightfoot and E. E. Kerlin, "Measured Effects of Various Combinations of Nuclear Radiation, Vacuum and Cryotemperatures on Aerospace Adhesives," Eleventh Annual SAMPE National Symposium Transactions, pp. 279-290, St. Louis, Missouri, 10-21 April 1967

14. R. E. Mauri, Evaluation of Optical Properties and Environmental Stability of Solar Cell Adhesives, LMSC-A-034229, April 1964

15. D. C. Briggs, "Experimental Study of Coatings for Temperature Control of Solar Cells," NASA CR73030, Philco Corporation, WDL Division, June 1966

16. J. C. Haynos, "Investigation of Resinous Materials for Use as Solar Cell Glass Adhesive," NASA TMX55333, N66-11228, Goddard Space Flight Center, September 1955

17. J. B. Rittenhouse and J. B. Singletary, Space Materials Handbook, Suppl. 2, Table 1-10, AFML-TR-64-40, Supp. 2, 1968

Appendix A

CODE NUMBER OF ADHESIVE MANUFACTURERS REFERRED TO IN THIS CHAPTER

Code Number	
1	Shell Chemical Co.
2	Narmco Materials Div., Whittaker Corp.
3	Bloomingdale Rubber Div., American Cyanimid Co.
4	Minnesota Mining and Manufacturing Co. (3M Co.)
5	H. B. Fuller, Co.
6	Armstrong Products Co.
7	Rubber and Asbestos Corp.
8	B. F. Goodrich Co.
9	Applied Products Div., Hexcel Products Co.
10	Swedlow Plastics Co.
11	Ciba Co., Inc.
12	Emerson and Cuming Co.
13	Hysol Co.
14	G. T. Schjedahl Co.
15	Epoxy Prod. Co.
16	C. H. Biggs Co.
17	Dow Corning
18	Caram
19	Coast Pro Seal
20	General Electric

Chapter 11

MATERIALS FOR SEALING APPLICATIONS

R. F. Betts

Seals for aerospace applications consist of plastic and elastomeric formulations, metallics, and composites of metals and nonmetals. Of these, elastomers have the most applications because of their high degree of resilience and conformability, their relatively low cost, and the simplicity of the integrated seal configurations. The discussion in this chapter emphasizes the general material properties of elastomers and plastics currently used for seal applications and the effects of the space environment on such properties.

Although this information will assist the designer in selecting the best materials for a particular application, the final choice to ensure optimum performance and reliability should, whenever possible, be based on experimental evaluation of the seal unit under the actual or simulated service and environmental operating conditions. Seals considered in this chapter include preformed types such as flat gaskets and O-rings and, to a lesser extent, elastomeric sealants or calking compounds which are applied in a resinous uncured form to the mating surfaces.

The properties of elastomers are greatly influenced by the additives (e.g., fillers, curing agents, accelerators, and blending agents), processing techniques, and cure used in their manufacture. Many elastomer formulations are commercially available for common and specialized applications, many of which are proprietary. These are derived from relatively few chemical classes comprising the base resins. In the case of plastics, the variations in properties arising from processing and cure are less than in the case of elastomers. The properties of a plastic are generally defined by its chemical type, molecular weight, and degree of crystallinity.

Material data are reported for representative chemical classes of elastomers and plastics used in seal applications. These are identified in the text by the generic, trade, or chemical name associated with their principal or base resin (polymer). In many cases, the mechanical property values and the effects of the environments given are typical for a particular material tested and may differ widely for different formulations based on other resins of the same chemical class. Hence, the designer must exercise care in the selection of elastomers for sealing applications. Behavior trends and relative effects are, therefore, the main considerations to be evaluated.

Since references in the literature do not, in all cases, accurately define the test material or specify the exact conditioning and variables to which that material has been subjected, direct comparison is difficult between two or more sources of information on elastomers and plastics.

11.1 SEALING APPLICATIONS IN AEROSPACE VEHICLES

Seals may be considered as either dynamic or static depending on whether there is relative motion between the contacting surface of the sealing element and the component it is sealing. The sealing function in an aerospace vehicle may be accomplished by one or a combination of the conventional methods of sealing-in-place, the use of pre-molded seals, or bonding.

In this section, the first two methods will be considered as applicable to sealants and elastomers. Seal design details will not be discussed. Examination of present design concepts indicates that areas in which there are seal and sealant requirements may be broadly classified as follows:

- Cabin areas including crews' quarters
- Fluid storage and distribution systems
- Electronic components housing

11.1.1 Cabin Sealing

The structural components of a space vehicle will have to be sealed primarily to maintain the integrity of the pressurized cabin areas. The sealant will be applied along structural seams, joints, and other areas where loss of cabin atmosphere may occur. Other areas are cutouts or openings in the shell and the seals used around them are usually exposed to the pressure differential of 1 atm maximum between the interior of the cabin and the exterior. The seals will be subjected to both thermal and radiation levels which will depend on the shielding characteristics of the outer shell and the insulation between the shells. The principal cabin sealing applications are pressure bulkheads, firewalls, access doors and hatches, observation windows, airlocks, and feed-throughs for ducts, plumbing, or wiring.

In application where the seal is against the escape of cabin atmosphere into outer space or an unpressurized area of the vehicle, the inside surface of the sealant will be exposed to the cabin pressure while the outside surface is exposed to a vacuum. Over a period of time the volatile constituents of the sealant may evaporate from the exposed surface. However, in most cases the exposed area is quite small, therefore the probable evaporation losses are minimized. In applications that involve opening doors and hatches to outer space for extravehicular operations, the seal may be exposed to the total space environment for periods of 10 to 30 min.

Aerodynamic heating during reentry will generate skin temperatures that may range from 900° to 3000°F. Because these temperatures are beyond the capabilities of current elastomeric sealants, adequate thermal protection will be needed for any sealants applied in the "hot" areas of a reentry vehicle.

11.1.2 Fluid Storage and Distribution System Sealing

The storage and distribution of fluids for the operation and maintenance of a space vehicle depends primarily on the reliability of the seal and sealants used in the system

components. In a space vehicle, these include the following: propulsion systems, hydraulic systems, and pneumatic systems.

Propulsion Systems. This category, including thrust devices required for orbital corrections or deceleration for landing on celestial bodies, has, by far, the largest tankage requirements. The chemical and other induced environments to which these tanks, plumbing, pumping components, and sealing materials will be exposed depend on the propellants and specific propulsion system. Seals or sealants used in these applications must be capable of withstanding the environment of the contained fluid, and the pressure differential between the internal container and the external compartment in which the component is located.

Hydraulic Systems. Component limitations presently restrict hydraulic systems to a maximum operating temperature of ~ 400°F. The hydraulic system for the B-70 and supersonic transport will vary between 400° and 700°F. Reentry vehicles will have requirements that range from 700° to 1200°F with short time exposures up to 1500°F for actuating equipment in the nozzle area of the rocket engines.

Pneumatic Systems. Such systems have been proposed for performing some of the functions currently allocated to the hydraulic system. The high-temperature problems that exist with hydraulic fluids are minimized in pneumatic systems, and no deterioration of the working fluid is encountered at the anticipated operating temperatures.

11.1.3 Electronic Components Housing

In those components operating under high voltages in systems such as radio, radar, and guidance, it is common practice to enclose the assemblies in pressurized containers charged with an inert gas. Besides protecting the component from a contaminating or corrosive atmosphere the tendency for the high voltage elements to arc is greatly reduced. These equipment containers usually have domed ends or covers which are sealed with O-rings or gaskets, against gas pressure of ~ 40 to 50 psi. The gas normally used is nitrogen. Although these units are normally mounted on shock absorbing mounts and are usually inside the spacecraft skin, they may be exposed to both natural and induced radiation in addition to the thermal environment created by the electric and electronic components.

Potting sealants are used around current conducting wire junctions, splices, connectors, terminals, or other places where normally exposed electric wires must be protected against contamination and power drain resulting from shorting by metallic objects or arcing under reduced pressure. Environmental exposure for potting compounds will be equivalent to that found in the compartment or console in which they may be enclosed and the thermal effects induced by the electric or electronic components.

11.2 SEALING MATERIALS

11.2.1 Elastomers

The American Society for Testing and Materials defines an elastomer as: A) capable of being stretched 100%; B) after being stretched 100%, held for five (5) minutes and then released, it is capable of retracting to within 10% of its original length within 5 minutes after release.

Table 11-1 presents the generic name, chemistry, and typical properties of the principal elastomeric seal materials employed in spacecraft engineering systems.

The choice of a seal material depends upon the basic engineering properties which can reasonably be predicted from each class of elastomers and in many cases would involve service testing of a particular seal if its intended use involves a critical engineering application.

11.2.1.1 Buna-N Elastomers

The Buna-N or Nitrile elastomer is formed by co-polymerizing butadiene and acrylonitrile. The acrylonitrile content of Buna-N is varied in commercial products from 18% to 48%. As the nitrile content increases, resistance to petroleum base oils and hydrocarbon fuels increases, but low temperature flexibility decreases (Ref. 1).

It can be compounded for service over a temperature range of -65°F to +275°F, and is a widely used elastomer in the aerospace industry. Most military rubber specifications requiring fuel and oil resistant O-rings can be met with nitrile base compounds. In order to obtain good resistance to low temperature with nitrile compounding, it is necessary to sacrifice some high temperature fuel and oil resistance.

Nitrile compounds have better compression set or cold flow, tear and abrasion resistance than other elastomers. Buna-N is the preferred elastomeric sealing material in pneumatic systems using either nitrogen or helium gases.

Nitrile compounds are not resistant to the swelling action of oxygenated solvents (e.g., acetone or methyl ethyl ketone) and phosphate ester hydraulic oils such as Skydrol, Cellulube, or Pydraul. It is also not resistant to ozone, strong oxidizing acids or the halogenated solvents such as carbon tetrachloride or trichloroethylene (Refs. 2, 3).

11.2.1.2 Polychloroprene Elastomers

Polychloroprene (Neoprene) is one of the first synthetic rubbers used commercially in the rubber industry. It is formed by the polymerization of 2-chlorobutadiene 1,3. Neoprene products have good resistance to weather, ozone and natural aging (Ref. 1).

This elastomer has good mechanical properties and resistance to non-aromatic petroleum products. It is flame resistant, and will not support combustion. It has good resistance to the corrosive action of chemicals such as organic acids, Freon, alcohols,

Table 11-1

ELASTOMERIC SEAL MATERIALS FOR AEROSPACE ENGINEERING APPLICATIONS

Generic Name	Chemical Nomenclature	Typical Properties
Buna-N (Nitrile)(NBR)	Butadiene acrylonitrile copolymer	Very good resistance to petroleum products. Fair resistance to acids and alkalis. Fair radiation stability.
Neoprene	Chloroprene polymer	Resistant to nonaromatic petroleum products, ozone sunlight and oxidation. Excellent mechanical properties but poor resistance to aromatic, ketone or chlorinated solvents.
Butyl	Isobutylene isoprene copolymer	High impermeability to gases. High resistance to organic and mineral acids and alkalis.
Silicone	Dimethyl polysiloxane polymer	Resistant to high and low temperature. Poor resistance to oils or solvents; high permeability to gases. Good resistance to vacuum degassing fair radiation stability.
Fluorosilicone	Trifluoropropyl-dimethyl polysiloxane polymer	Good mechanical properties when exposed to petroleum fuels at both high and low temperatures.
EPR	Ethylene-propylene copolymer	Resistant to heat degradation, ozone, abrasion, compression set, water-phosphate esters, glycols and ketones. Poor petroleum resistance.
Fluorocarbon	Vinylidene fluoride hexafluoropropylene copolymer	Resistant to ozone, oxygen, weather, high temperature petroleum, synthetic lubricants, solvents, fuels and chemicals. Used for vacuum seals. Fair radiation stability.
Polysulfide (Thiokol)	Ethylene dichloride sodium tetrasulfide copolymer	Resistant to highly aromatic oils, greases, and solvents. Low mechanical properties with poor abrasion and temperature resistance.
Polyurethane	Organic polyester or polyether tolylene 2, 4-di-isocyanate cop-copolymer	High mechanical properties and abrasion resistance. Poor resistance to water, acids, ketones, and chlorinated solvents. Temperature service limit is 200° to 250°F.
Nitroso	Nitroso perfluorobutyric acid trifluoronitrosomethane tetrafluoroethylene terpolymer	Resistant to nitrogen tetroxide rocket oxidizer. Good mechanical properties over wide temperature range. Material is nonflammable.
KEL-F (elastomer)	Chlorotrifluoroethylene vinylidene fluoride copolymer	Resistant to high temperature strong oxidizing agents and solvents. Material is useful for service in red fuming nitric acid.

glycerine, and glycols. It has service temperature between -30°F and +200°F. Neoprene does not soften as does natural rubber when exposed to heat, but instead it will harden slowly.

Neoprene is not recommended for engineering applications involving contact with such strong oxidizing agents as concentrated chromic, nitric, or sulfuric acids, hydrogen peroxides, and hypochlorites. Neoprene should not be allowed to come in contact with aromatic organic hydrocarbons, ketones, or phosphate ester hydraulic fluids because of softening and swelling accompanied by degradation of mechanical properties (Refs. 2, 4).

11.2.1.3 Butyl Elastomer

Butyl rubber is prepared from 97 parts of isobutylene and approximately 3 parts of isoprene. Both of these polymers are obtained from cracked refinery gases and the small ratio of isoprene (diolefin), varying from 0.5% to 4.5%, provides enough unsaturation in the final copolymer to allow vulcanization with sulfur. The copolymerization is carried out at approximately -140°F in the presence of aluminum chloride and a trace (0.002%) of water (Ref. 1).

Butyl rubber has high impermeability to gases. For this reason it has been used in the aerospace industry for vacuum sealing applications down to 1×10^{-7} Torr. Preformed packings (O-rings) fabricated from a butyl compound have been successfully used in propellant systems using UDMH and Aerozine 50 (50% UDMH - 50% Hydrazine) because the material possesses resistance to both organic and inorganic acids and alkalies. Recently various butyl compounds have been chosen for expulsion bladders or diaphragms in aerospace vehicles because the material had to be resistant to hydrazine fuels on one side and impermeable to pressurized nitrogen gas on the opposite side.

Butyl has also been used in successfully sealing hydraulic systems that use phosphate ester fluids such as Skydrol 500.

Because of the very small amount of unsaturation present in the butyl polymer, the material possesses high ozone and weather resistance. These properties in addition to the low water absorption characteristics have increased its use for sealing materials in electrical applications. Mechanically, butyl rubber is resistant to flexing, abrasion, and tearing. Chemically, certain formulations will withstand contact with concentrated hydrochloric, 50% sulfuric, 50% phosphoric, and 70% nitric acids.

Butyl rubber should never be used in applications that require resistance to either aliphatic or aromatic hydrocarbons. It swells in hydrocarbon solvents and paraffin oils. Polar solvents, such as esters and ketones also swell and degrade the material. Butyl will not perform satisfactorily in any engineering applications that require contact with petroleum products, diester base synthetic lubricants, ketones such as acetone or methyl ethyl ketone (MEK), or silicone fluids and greases. When choosing butyl as a sealing material designers should also keep in mind that it is subject to cold flow

(compression set). This poor rebound characteristic limits the choice of butyl sealing materials to applications where specific fluid resistance is of prime importance (Ref. 2).

11.2.1.4 Silicone Elastomer

Silicone rubber is one of a family of semi-organic materials that look and feel like organic rubber, yet have a completely different type of structure from other elastomers. In the preparation, dimethyl dichlorosilane is hydrolyzed to form dimethyl silanol which is then condensed to dimethyl siloxane, and this, upon further condensation yields dimethyl polysiloxane.

Various silicone rubbers are produced by substituting some of the methyl groups in the polymer with other groups such as phenyl or vinyl groups. The presence of phenyl groups in the polymer chain gives improvement in low temperature properties (Ref. 5).

Silicone rubber is flexible below - 135°F and it can be compounded to resist a temperature of 700°F for short periods. The maximum temperature at which silicones retain optimum mechanical properties for continuous service in dry air is 450°F.

Silicone rubbers have a moderate resistance to most chemical reagents. They are relatively unaffected by cold dilute solutions of acids and alkalis, but disintegrate in contact with these reagents in concentrated form.

Silicone rubber is suited for use as a sealing and gasketing material in electrical applications. It has good resistance to ozone, corona discharge, and weather.

Silicone rubber also has an unlimited shelf life and is of special importance in military applications due to its resistance to fire. Although it will burn as long as flame is applied, its combustion is not self-propagating.

Silicone rubber swells appreciably in certain oils, silicone fluids, and in aromatic and chlorinated aliphatic solvents. The mechanical properties of silicone rubber at room temperature are relatively poor when compared with the other synthetic elastomers. Manufacturers do not recommend the use of O-ring dynamic silicone seals because of the inherently weak tear and abrasion resistance of the material (Ref. 6).

11.2.1.5 Fluorosilicone Elastomers

Fluorosilicone rubber is a silicone elastomeric material with the high and low temperature resistance of the polymethylsiloxanes, but has much higher resistance to nonpolar materials such as petroleum oils or fuels. By substituting a trifluoropropyl group in place of one of the methyl groups in the normal polysiloxane monomer enough polarity is introduced into the polymer to create inherent resistance to nonpolar fluids (Ref. 5).

Fluorosilicone rubber has a wide operating temperature range (-100°F to +350°F) and good chemical resistance to nonpolar fluids. It will resist petroleum fuels, gasoline, chlorinated solvents, jet fuel (such as JP-4), diester oils (such as MIL-L-7808), and

ozone. In aerospace applications where seals are required to operate in contact with petroleum fluids at very low temperatures, and still maintain resistance to vacuum and radiation environments, fluorosilicone materials offer the best choice.

Fluorosilicones should never be used in contact with strong oxidizing acids or alkalies, such as hydrazine-based fuel. Concentrated sulfuric acid will dissolve both silicone and fluorosilicone materials while concentrated solutions of strong bases will cause softening and subsequent loss of mechanical strength.

Fluorosilicones are also not resistant to solvents such as acetone and other lower molecular weight ketones or esters.

Preformed packings (O-rings) fabricated from either silicone or fluorosilicone materials should not be used for dynamic sealing applications because both materials possess inherently low tear and tensile strength (Ref. 2).

11.2.1.6 Ethylene Propylene Rubber

Chemically, two different types of ethylene propylene are being produced, ethylene-propylene-diene terpolymer and ethylene-propylene copolymer. The terpolymer is being developed as a sulfur vulcanizable elastomer having a basic monomeric structure.

The main polymer chain is saturated and consists of randomly arranged ethylene and propylene units, with diene units spaced at less frequent intervals. The diene adds to the chain through one of its double bonds, leaving a second double bond in the side chain. The pendant double bond is of sufficient reactivity to permit crosslinking with sulfur-based curing systems (Ref. 7).

The ethylene propylene elastomer most commonly used in the aerospace industry is vulcanized with an organic peroxide such as benzoyl peroxide and chemically is the copolymer of ethylene-propylene.

This copolymer, because of its saturated chain possesses resistance to the effects of ozone, oxygen, weather, heat, and chemicals. In ozone tests ethylene propylene has resisted attack, both at the normal test concentration (50 ppm) and at a concentration 200 times the normal test exposure. Outdoor weathering specimens showed no crazing or discoloration after two (2) years exposure in Florida sunlight. Ethylene propylene seals have operated successfully in phosphate ester fluids such as Skydrol at 350°F for extended time periods and have also withstood a steam/air/water environment at 380°F.

Tests in the hydrazine fuels have shown that peroxide cured ethylene-propylene O-rings have a minimum amount of volume swell and loss of original mechanical properties after immersion periods of 120 days at a propellant temperature of 70°F. The EPR seals are used instead of butyl rubber seals in propulsion systems (Ref. 8).

Ethylene propylene is unsuitable for exposure to petroleum products or nonpolar solvents. The flame resistance and permeability to gases of ethylene propylene are relatively poor when compared with other elastomers.

11.1.1.7 Fluorocarbon Rubber

Technically there are two types of fluorocarbon rubber. Both have high percentages of fluorine in their structure. Chemically, they may be classified as a copolymer of hexafluoropropylene and vinylidene fluoride and a copolymer of chlorotrifluoroethylene and vinylidene fluoride.

The first elastomer is commercially available from either DuPont as Viton rubber or Minnesota Mining and Manufacturing Company as Fluorel rubber. The second copolymer is commercially available under the trade name Kel-F Elastomer and is available from 3M.

The highly fluorinated structure of the fluoroelastomers accounts for their resistance to high temperature and corrosive media. The working temperature range of these materials is from -20°F to +400°F with temperatures up to +500°F for very short periods of time. Both copolymers are resistant to atmospheric oxidation, sun and all kinds of weather in a wide range of climates. When tested under concentrations of 150 ppm of ozone no cracking was observed after 200 hours.

Viton, Fluorel and KEL-F also have high resistance to petroleum fluids as well as strong acids and rocket propellants. They are recommended for service with air, exhaust gases, silicone greases and oils (such as Versilube or DC 200), silicate-ester base hydraulic fluids (such as MLO-8200 or MIL-H-8446), and all diester synthetic fluids such as MIL-L-7808, MIL-L-6085 and MIL-L-6387.

The KEL-F elastomer has high resistance to acids and water. For example, this polymer had good retention of physical properties after immersion in red fuming acid for 27 days at 77°F with volume swell of 24%.

Viton and Fluorel have high resistance to the effects of either hydrochloric, hydrofluoric, or sulfuric acids. Fluorel elastomers in a 7 day immersion in fuming sulfuric acid at 77°F had a volume swell of 12% and a tensile strength of 1780 psi.

For any elastomer to provide an efficient seal under vacuum conditions it must have low permeability to gases. The helium permeability of the Viton material at 75°F is 0.77×10^{-8} $cm^3/sec\text{-}cm\text{-}cm^2\text{-}atm$. This allows the material to seal down to a vacuum of 10^{-9} Torr. The weight loss of Viton at 1.8×10^{-9} Torr is 2.1% (Ref. 8).

11.2.1.8 Polysulfide (Thiokol) Rubber

The polysulfide elastomeric materials are produced by reacting an organic dihalide, ethylene dichloride, with an inorganic polysulfide.

The use of different dihalides and different sulfur concentrations alters the physical properties of the resulting polymers by altering the length of the aliphatic group and the number of sulfur atoms in the polymer chain. Increased sulfur concentration improves solvent and oil resistance, and also reduces the permeability to gases. Low-temperature flexibility is tied to the structure of the hydrocarbon chain.

These rubbers have high resistance to solvents and oils, and to aging, ozone, and sunlight, along with low permeability to gases and vapors (Ref. 9).

Thiokol ST rubber is a branched-chain aliphatic high molecular weight polysulfide polymer that is vulcanized by oxidizing the mercaptan terminals. This material has good flex-crack resistance and flexibility down to -65°F. It is used in making molded O-rings and gaskets.

The heat resistance, mechanical strength, compression set, and abrasion resistance of the polysulfide elastomers are lower than many of the other synthetic elastomers. Service temperature range is -65°F to +225°F. Typical compression set after loading for 22 hours at 158°F is approximately 40% to 45% of original thickness. Abrasion resistance is about half that of natural rubber or SBR (sytrene-butadiene rubber). The typical strength of the Thiokol elastomers is 1200 to 1400 psi maximum. Because of their unpleasant odor, particularly during processing, the Thiokol polymers are not used as much as the two major oil resistant synthetic rubbers – the nitriles and neoprenes (Ref. 4).

11.2.1.9 Polyurethane Elastomers

The polyurethane elastomers are formed in three separate polymerization steps: (1) preparation of a polyester or polyether, (2) chain lengthening by reacting the above products with a di-isocyanate, (3) chain extension and cross-linking to effect the final vulcanized material. The first step involves the preparation of a polyester by reacting ethylene glycol with adipic acid. The polyester is then reacted with a di-isocyanate to lengthen the chain.

The third step in the formation of a vulcanized polyurethane elastomer involves the addition of more di-isocyanate groups which may react either with the terminal hydroxyl (OH) groups to extend further the length of the polymer chain or more importantly the excess di-isocyanate reacts with hydrogen atoms that are attached to the nitrogen atoms in the linear chain to form cross links at periodic intervals.

Polymer chemists attribute the high mechanical properties, particularly the tear resistance, of polyurethane rubber to the fact that cross links are regularly spaced and separated by linear chain sections of considerable length (Ref. 6).

Vulcanized polyurethane elastomers have good resilience, resistance to abrasion, ultraviolet light, oxygen, ozone, petroleum products, and flex cracking.

Polyurethane rubber should not be used in contact with water, acids, ketones and chlorinated or nitro - hydrocarbons. In addition they have poor compression and permanent set properties. The vulcanized polyurethane materials undergo a decrease of mechanical properties at temperatures above 225°F; consequently they must be used in engineering applications that do not require high temperature resistance.

Table 11-2 provides the trade name, chemistry, and manufacturer of polyurethane elastomer materials which are readily available and most commonly used.

Table 11-2

COMMERCIAL POLYURETHANE ELASTOMERS

Manufacturer	Trade Name	Chemical Type	Cure Agent
DuPont	Adiprene C	Polyether	Sulfur or Peroxide
General Tire & Rubber	Genthane	Polyester	Peroxide
B.F. Goodrich Co.	Estane	Polyester	Thermoplastic
Mobay Chemical Co.	Texin	Polyester	Thermoplastic
United States Rubber	Vibrathane	Polyester	Peroxide
Thiokol Chemical Co.	Elastothane	Polyester	Sulfur or Peroxide
Isocyanate Products Co.	Castomer	Polyester	Amine
American Cyanamid	Cyanaprene	Polyester	Sulfur or Peroxide

11.2.1.10 Carboxy Nitroso Elastomer

Nitroso rubber sealing material was developed under contract to the Air Force Materials Laboratory at Wright-Patterson Air Force Base. It is formed by the terpolymerization of tetrafluoroethylene (49%), trifluoronitrosomethane (49%), and perfluoronitrosobutyric acid (2% by weight).

This terpolymer (commonly referred to as nitroso gum) is then cross-linked with chromium trifluoroacetate using a silica material as the reinforcing filler. This finalized crosslinked and vulcanized material is the only elastomer presently available which can be successfully used in engineering applications requiring long term resistance to the solvent effects of nitrogen tetroxide (N_2O_4) or inhibited red fuming nitric acid (IRFNA) (Refs. 10, 11).

Nitroso rubber has a low temperature serviceability of -40°F while the high temperature limit for continuous service is 375°F. Thermogravimetric analysis shows no weight loss up to 480°F. Decomposition of the material occurs at approximately 520°F.

When subjected to a direct flame, carboxy-nitroso rubber will not ignite or char, but does evolve heavier-than-air gases which tend to extinguish the flame. Nitroso rubber has good resistance to ozone and sunlight. No cracking was observed after exposure to 175 ppm ozone concentration for 24 hours at 150°F, and no visible cracks appeared in the material after a sunlight exposure period of 60 days at 20% elongation. The material has also been shelf aged in a warehouse for a period of 18 months with no appreciable change in mechanical properties.

Nitroso rubber should never be used where it will come in contact with amines such as hydrazine, unsymmetrical dimethyl hydrazine or monomethyl hydrazine. Some highly

fluorinated solvents such as Freon 113 will dissolve the nitroso gum; therefore the use of nitroso rubber in contact with Freon materials should be thoroughly investigated for compatibility prior to usage.

The nitroso material has been completely developed since 1964 and the capacity to produce quantities of the gum material is still very limited; however, enough material will be available in 1968 to produce the vulcanized rubber in production quantities (Ref. 12).

11.2.2 Plastics

Many of the thermoplastic materials have been successfully used as sealing materials in the aerospace industry. In general, they are chosen for particular engineering applications because none of the organic elastomeric materials will perform satisfactorily. The thermoplastics, as a class of materials, have good mechanical properties and strength retention at low temperatures; however, they lack the resilience, conformability, and memory of the elastomeric materials.

The almost complete chemical inertness of the highly fluorinated plastic materials, such as polytetrafluoroethylene (TFE), fluorinated ethylene propylene (FEP), polychlorotrifluoroethylene (KEL-F), and polyvinylidene fluoride (Kynar) led to their use in seals of all types and configurations.

Both TFE and FEP are chemically inert to essentially all industrial chemicals and solvents, even at elevated temperatures and pressures. This chemical compatibility stems from three causes:

- Strong interatomic bonds between carbon-carbon and carbon-fluorine atoms.
- Almost perfect shielding of the polymer carbon backbone by fluorine atoms.
- High molecular weight (or long polymer chain length) compared with many other polymers.

Table 11-3 lists the chemistry, generic name, and typical properties of plastic seal materials employed in spacecraft engineering systems.

11.2.2.1 Polytetrafluoroethylene Plastic (PTFE)

PTFE is formed by the addition polymerization of tetrafluoroethylene. It is a linear polymer free from any significant amount of branching. Because the carbon atoms of the polymer are completely sheathed by fluorine it is inert to chemical attack. The only chemicals which attack Teflon (TFE) are chlorine trifluoride and fluorine at high temperatures and molten alkali metals such as molten sodium.

Because of its wide operating temperature range (-423°F to +500°F), chemical inertness, and low coefficient of friction, TFE Teflon has been extensively used as a sealing material. Teflon (TFE) static seals are used in missile systems with liquid

Table 11-3

PLASTIC SEAL MATERIALS USED IN AEROSPACE ENGINEERING APPLICATIONS

Generic Name	Chemical Nomenclature	Typical Properties
Teflon[a] (TFE)	Polytetrafluoroethylene	Good chemical resistance, low coefficient of friction. Cold flow, compression set, and radiation stability are poor.
Teflon[a] (FEP)	Copolymer of Tetrafluoroethylene and Hexafluoropropylene	Good chemical resistance and low coefficient of friction; however, compression set and cold flow are poor.
KEL-F[b] (plastic)	Polychlorotrifluoro-ethylene	Chemical resistance not as good as FEP or TFE Teflon. Cold flow is much less than FEP or TFE Teflon; however, compression set and radiation resistance are poor.
Kynar[c]	Polyvinylidenefluoride	Higher tensile strength abrasion resistance and resistance to cold flow than TFE Teflon. Chemical resistance and coefficient of friction are not as good as TFE.
Poly-ethylene	Ethylene Homopolymer	Resists most solvents. Poor heat resistance. Good radiation stability.
Vinyl	Polyvinyl chloride	Good compressibility, resiliency; resistant to water, oils, gasoline, and many acids and alkalis. Mechanical properties depend on type used and plasticizer. Fair radiation stability.

(a) Trade name of E. I. DuPont de Nemours Co., Inc.
(b) Trade name of Minnesota Mining and Manufacturing Co.
(c) Trade name of Pennsalt Chemical Co.

cryogenic propellants, liquid oxygen, liquid nitrogen, or liquid hydrogen. Liquid oxygen impact sensitivity tests have shown that Teflon (TFE) was one of the few organic materials which would withstand a 70 foot-pound impact without exploding when it is immersed in liquid oxygen. Liquid oxygen forms explosive mixtures with almost all other organic materials.

11.2.2.2. Fluorinated Ethylene-Propylene Plastic

This completely fluorinated thermoplastic, fluorinated ethylene propylene (FEP), is formed by copolymerizing hexafluoropropylene with tetrafluoroethylene. Teflon (FEP) is very highly fluorinated and closely resembles Teflon (TFE) with the exception of some branching at periodic intervals. This material has properties similar to TFE; however, its upper temperature service limit is 400°F while TFE has a 500°F continuous thermal rating. One of the major advantages associated with the use of FEP Teflon is that the material is melt processable and as such can be injection molded whereas TFE is fabricated by processes similar to powder metallurgy where compression molding and sintering must be used.

Teflon FEP is used where performance conditions require high chemical resistance, or retention of properties at both low and high temperatures. It is unaffected by rocket fuels and oxidizers, liquid oxygen and liquid hydrogen, and most chemical reagents except molten alkali metals, fluorine at high temperatures, and several halogenated compounds.

11.2.2.3 Polychlorotrifluoroethylene (PCTFE) Plastic

Polychlorotrifluoroethylene (PCTFE) resins are fluorocarbons in which a chlorine atom is substituted for a fluorine atom to produce a melt-processable thermoplastic linear polymer.

The PCTFE differs from TFE in that every fourth fluorine atom on the backbone chain of carbon atoms is replaced with a chlorine atom. This inclusion of the chlorine atom is beneficial in its effects on the mechanical, rheological and optical properties. However, it is somewhat detrimental in its effects on chemical, electrical and frictional properties and thermal stability.

In common with all fluorocarbons, the PCTFE resins retain their mechanical properties over a wide range of temperatures (-423°F to +390°F).

The chemical resistance of PCTFE is good but not as good as TFE Teflon. Substances such as chlorosulfonic acid, molten caustic alkalis and molten alkali metal will adversely affect the material. Alcohols, acids, phenols, and aliphatic hydrocarbons have little effect but certain aromatic hydrocarbons, esters, halogenated hydrocarbons, and ethers may cause swelling at elevated temperatures.

For sealing applications PCTFE has been used specifically because it has better strength than TFE Teflon below 210°F, much greater resistance to cold flow than TFE, and better radiation resistance than either FEP or TFE Teflon under atmospheric conditions.

The polychlorotrifluoroethylene plastic (PCTFE is marketed under the trade names of KEL-F (Minnesota Mining and Manufacturing Co.), and Halon (Allied Chemical Corp.).

11.2.2.4 Polyvinylidene Fluoride

Polyvinylidene fluoride, under the trade name Kynar, is presently marketed by the Pennsalt Chemicals Corportation and is formed by the polymerization of vinylidene fluoride.

Polyvinylidene fluoride has two fluorine atoms in the monomeric unit; both being attached to the same carbon atom. It contains about 59% fluorine by weight as compared with 75% for TFE and FEP Teflon.

When compared with TFE Teflon, polyvinylidene fluoride has several advantages; higher tensile strength, resistance to abrasion, and higher resistance to cold flow under load up to about 200°F. Also, it has a 20% lower specific gravity, hence greater production per pound. Its disadvantages include: a lower service temperature (-80°F to +300°F) than PTFE or PCTFE, and a higher dielectric constant and dissipation factor that reduces its application as insulation, especially at high frequencies. Likewise, its coefficient of friction is slightly higher, hence its antistick properties are not as good as those of TFE. Although it has generally good chemical resistance, strongly polar solvents such as dimethyl acetamide tends to dissolve the polymer, while some strongly basic primary amines such as n-butylamine cause discoloration and embrittlement.

11.2.2.5 Polyethylene Plastic

Polyethylene is a wax-like thermoplastic softening at about 180° to 270° F with a density less than that of water. It is formed by either high pressure or low pressure polymerization techniques from ethylene gas.

In commercial practice, three types of this thermoplastic material are available. These resins are known as either low (0.910 to 0.925 g/cm^3), medium (0.926 to0.940 g/cm^3) or high density (0.941 to 0.965 g/cm^3) polyethylenes. In general, as the density increases, the stiffness, ultimate strength, softening temperature, degree of crystallinity, and impermeability to liquids and gases increases.

The chemical resistance of the various density grades of polyethylene is good. Most acids, bases, and salts that attack metals such as hydrochloric, hydrofluoric, chromic, and sulfuric acids; ammonia; sodium hydroxide (10%); hydrogen peroxide, and salt water will have little or no effect on the various polyethylenes at normal temperatures.

Polyethylene is, however, affected by nitric acid and similar strong oxidizing agents. In addition, it is affected by many hydrocarbons and solvents, such as benzene, and xylene. Chlorine and some chlorinated compounds affect polyethylene, yet the degree of attack is relatively slight.

The disadvantages of the polyethylenes include a tendency to fail under a combination of mechanical and electrical stress, plus a high thermal coefficient of expansion.

11.2.2.6 Vinyl Polymers

The largest group of plastics produced are those which depend for polymerization on the presence of a double bond. This leads to a carbon chain similar to that found in natural rubber. These are the vinyl resins.

Polyvinyl chloride results from the polymerization of vinyl chloride. The vinyl chloride polymer is linear and therefore substantially thermoplastic. The presence of the chlorine atom causes an increase in the hardness and stiffness of the polymer.

The polyvinyl chloride thermoplastic materials have good physical properties, ability to be compounded for a wide range of applications, ease of processing, and relatively low cost.

Properties of PVC include good water and chemical resistance, strength, and abrasion resistance. Polyvinylchloride is also one of the few thermoplastic materials which is self-extinguishing.

Polyvinylchloride is resistant to most acids, salt solutions, petroleum products, fats, and fungus-producing atmospheres. Products taking advantage of this chemical resistance include acid-in-salt-solution tubing and tubing and gaskets used in chemical processing equipment.

One of the poor properties of the vinyl polymers is a rather limited thermal stability. Heating polyvinylchloride at temperatures above 170°F has adverse effects on the properties of the polymer. There is some uncertainty as to the mechanism of degradation of the polyvinylchloride materials. There is some infrared evidence that as hydrogen chloride is removed a long chain diene structure is formed. The first physical manifestation of thermal degradation is a change in the color of the material. Initially water-white, on heating it will turn, in sequence, pale yellow, orange, brown, and black. Further degradation causes adverse changes in mechanical and electrical properties. For most commercial purposes, however, the end point is the change in color (Refs. 13, 14).

11.2.3 Metals and Composites

Metallic and composite seals have been developed in an attempt to bypass the inherent limitations of organic polymers for withstanding some environmental conditions encountered in spacecraft seal applications. The advantages of such seals over elastomeric seals are (1) their wide temperature range (-423°F to 1800°F), (2) they are not affected by electromagnetic or particulate radiation, and (3) their chemical resistance to propellants, synthetic lubricants, and hydraulic fluids.

11.2.3.1 Metallics

The leakage rates of metallic seals are low, comparable to those of the better elastomeric seals. Some designs are available in which no appreciable weight penalty is incurred. A wide range of gasket materials and configurations are available to the designer; gaskets may be obtained in such shapes as: plain solid, deeply corrugated, corrugated core with metal shell, solid metal with V-shaped grooves, grooved metal core with metal jacket, serrated, cross-ribbed, oval, and many others. The extent of chemical and heat resistance obtainable with metal gaskets depends on the metal. Available gasket metals and their properties are given in Table 11-4 (Ref. 15).

Table 11-4

PROPERTIES OF METALLIC SEAL MATERIALS

Material	Operating Temperature (°F)	Properties
Lead	-300 to 200	Good chemical resistance; best conformability of metal seals; not for vacuum use due to high vapor pressure at moderate temperatures
Indium	-300 to 250	Low vapor pressure at temperatures up to 125°C but low melting; very useful for high vacuum systems not requiring bake-out; used as wire; does not require fusion joint to form gasket; loose ends will flow together under pressure.
Tin	-300 to 250	Good resistance to neutral solutions; attacked by acids, alkalis; not for vacuum use due to relatively high vapor pressure at moderate temperatures.
Aluminum	-423 to 800	High corrosion resistance; slightly attacked by strong acids, alkalis
Copper, Brass	-300 to 600	Good corrosion resistance at moderate temperatures (except to strong oxidizing agents, acids)
Nickel	-300 to 1400	High corrosion resistance
Monel	-300 to 1500	High corrosion resistance; good against most acids and alkalis, but attacked by strong hydrochloric and strong oxidizing acids
Inconel	-300 to 2000	Excellent heat, oxidation resistance
Stainless Steel	-423 to 1200	High corrosion resistance; properties depend on type used

11.2.3.2 Metal Composites

The chief limitations of the harder metals as gasket materials are their relatively poor compressibility and sealing properties. These limitations can be overcome by combining the metal with softer materials such as asbestos, Teflon,or rubber, to produce a composite material which, with little sacrifice in chemical and heat resistance, has good compressibility and sealing properties. Gasket manufacturers have designed a great many composite gaskets. The most commonly used is the spiral-wound metal gasket. Many other designs are available which should be investigated if the spiral-wound type does not appear suitable.

11.3 SEAL LEAKAGE

A seal confinging a fluid at a given temperature and pressure differential can leak under normal service because of (1) limitations in seal design and mechanical imperfections in seal construction and assembly and (2) permeation of the gas or liquid through the seal material in contact with it. Of these, the former is by far the most important from the standpoint of the magnitude of leak rates. Although seal leakage rates can be made small by proper selection of materials and design configuration for a particular application, they cannot be completely eliminated. For many space applications requiring long-term seal service, leakage rates must be determined in order to estimate container volume for enough fluid to last out the mission lifetime and assure reliability.

Leakage rates resulting from mechanical defects are nonpredictable and vary widely from one seal design to another depending upon configuration and materials of construction under fixed operating conditions. The degree of such leakage, the suitability of a particular design and materials, and the seal system reliability must be experimentally determined under actual or simulated environmental and operating conditions encountered in service. Generally, the leak rate is increased at elevated temperatures and greater pressure differentials. Dynamic seals such as those used for reciprocating and rotating shafts show somewhat greater leakage rates than static seals at similar temperatures and pressure differentials. Under continuous operations, the leak rates of dynamic seals generally increase with time because of wear of sliding and rotating surfaces in the seal assembly (Ref. 16).

Elastomers examined for use as seals in reciprocating motion included neoprene, silicone, Viton-A, nitrile (Buna-N), and Butyl rubbers. Also tested were KEL-F, polyethylene, and polyvinyl chloride. Materials tested for rotating seals were silicone rubber, Viton-A, KEL-F elastomer, Teflon, and KEL-F (Ref. 17).

Polyethylene and silicone rubber were the most effective seals for reciprocating service. Leak rates were very low, 5×10^{-5} standard cubic centimeters of helium gas, after test durations of 30 minutes. It was found that a dry lubricant such as molybdenum disulfide improved performance. Silicone rubber and Viton-A proved to be good materials for rotational motion. Again, small amounts of dry lubricants were beneficial. Seal positioning and loading were found to be critical, and have to be carefully designed.

Teflon, because of its relatively rigid, inflexible properties wore rapidly since it was not as porous as the elastomers and would not accept a surface coating of lubricant such as molybdenum disulfide to reduce friction and wear. The self-lubricating properties of a material apparently do not increase its life when operated as a dynamic vacuum seal.

Static seal tests were conducted on the same elastomers used for the dynamic tests. Seals were loaded to obtain the deflections and contact pressures recommended by the manufacturers. Leak rates were measured before and after operation. Some seals such as silicone rubber exhibited a reduced leak rate for static sealing after being subjected to dynamic operation.

Polyethylene and polyvinyl chloride (Vinylite) in an O-ring configuration were very effective in static applications. These materials as well as the remainder of the elastomers tested were not appreciably affected by a 2-week vacuum exposure at 1×10^{-7} Torr.

In a study of seven elastomer materials for use as O-ring-type door seals the offgassing and leakage rates in a high vacuum were compared. Butyl rubber, Viton-A, neoprene, and Buna-N were roughly comparable in combined gas load leakage plus offgassing with preference in the order named. Natural rubber was eliminated in the tests because of excessive physical damage, and Teflon was rejected because of permanent deformation. The outgassing studies rated the silicones as lowest in offgassing with Butyl, Viton-A, and Neoprene in descending order of merit. However, the silicone O-rings were poorest in offgassing and leakage. The degree of compression of the O-rings was found to be an important factor and the effect of compression was approximately the same for all the materials used.

The effect of temperature was explored in the range from 25° to 100°C. Helium leak rate increased, at first, with increase in temperature for all the elastomers studied. However, different elastomers reacted differently to long exposure at 100°C. The leak rate of the silicones ultimately decreased by a hundredfold, but the deformation made it impossible to re-use the O-ring. Butyl rubber is not deformed by prolonged heating and the leak rate remains at the level initially reached. Neoprene and Viton-A performed in a manner intermediate to these two extremes.

Table 11-5 shows the air leak rates of some elastomers at 20°C and at 100°C. The effect of temperatures to 400°F on air permeability of some sealing materials is shown in Table 11-6. The effect of permeability and of loading on leakage rates are shown in Tables 11-6 through 11-8 (Ref. 17).

11.4 ENVIRONMENTAL EFFECTS ON SEALING MATERIALS

11.4.1 Compatibility With Reactive Fluids

Solution and reaction are of importance in the interaction of chemical fluids with elastomeric sealing materials. Some liquids may be solvents for particular elastomers, but do not react; these liquids when in contact with the material cause reversible swelling and property changes. Other liquids may not be solvents but may be reactive;

Table 11-5

AIR LEAK RATE OF ELASTOMER COMPOUNDS (Ref. 17)[a]

Compound	Leak Rate, std cc air/inch-year	
	20°C	100°C
Silicone (Compound 76-128)	2.2	3.6
Neoprene	0.03	0.29
Viton-A	0.022	0.44
Butyl	<0.001	0.37

(a) Elastomer was loaded by four clamps with 40 ft-lb torque on each clamp in addition to atmospheric pressure.

these liquids cause both swelling and irreversible changes in the properties of elastomers at rates dependent on both solubility and reactivity with the material. The compatibility of a specific elastomer in a particular fluid may be determined by standard immersion tests.

The fluid resistance of elastomers is characterized by the degree of swelling which occurs in the presence of the fluid. The smaller the swelling or volume growth, the greater the resistance to the particular fluid. A volume change less than 16%, indicates elastomer-liquid compatibility; changes greater than 40% indicate elastomer-liquid incompatibility.

Swelling is an important consideration from two standpoints. First, the ensuing volume increase must be accommodated, and second, the effects of deterioration of properties must be considered. Swelling is not necessarily associated with destructive effects.

Although some fluids cause swelling of an elastomer by as much as 200%, the properties may remain essentially unchanged upon evaporation of the liquid. Some fluids have a slow deteriorating influence, causing irreversible and permanent damage. Typical curves for loss in tensile strength, elongation, and hardness for a nitrile elastomer as a function of percent volume swell are shown in Fig. 11-1 (Ref. 18).

11.4.1.1 Hydrocarbon Fluids

Aromatic hydrocarbons cause greater swelling in elastomers than the straight chain hydrocarbons; consequently, a petroleum product having a high aromatic content (aromaticity), will cause greater swelling. The aromatic content of a petroleum hydrocarbon may be accurately measured by determining the aniline point or mixed aniline point of a specific petroleum fluid. Since a decrease in aniline point of any hydrocarbon fluid corresponds to an increase in aromatic content; this method can be used to

Table 11-6

AIR PERMEABILITIES OF ELASTOMERS AT VARIOUS TEMPERATURES

Elastomer	Permeability (STP) $cm^3/sec\text{-}cm^2\text{-}cm\text{-}atm$				
	75°F	176°F	250°F	350°F	400°F
Natural Rubber	0.49	4.4	7.1	20.7	26.2
Buna-S (SBR)	0.25	2.9	4.7	15.4	
Neoprene	0.09−0.10	0.98−1.7	2.6−3.0	7.3	
Butyl	0.02	0.32−0.46	1.3−1.8	5.6−6.1	
Nitrile	0.13	0.8	2.2	6.6	
Polysulfide	0.02	0.37	1.6	melted	
Hypalon	0.72	0.73	2.3	6.2	
Polyurethane (polyester type)	0.05	0.97	3.1	7.1	Melted
Silicone	11−33	35−47		69−113	74
Vyram	0.007	0.24	0.56	5.1	
Kel-F 3700		0.8	3.4	15.6	
Viton A		0.88	3.6	14.6	
Acrylic (Acrylon EA-5)	0.16	1.5	3.7	10.2	
Polyester (Hycar 4021)	0.19	1.8	4.8	9.4	
Methacrylate					16.3
Polyurethane (Adiprene C)		2.3	3.8	16.6	
Carboxy		2.4−2.6	2.3−6.2	7.1−14	

Table 11-7

COMPARISON OF AIR LEAK RATES OF ELASTOMERS
EXPERIMENTAL AND CALCULATED

Material	Permeability[a]	Leak Rate at 100 C, std cc air/in.-yr	
	std cc/cm^2-cm-atm-sec	Calculated	Experimental[b]
Viton-A	8.8×10^{-8}	0.36	0.44
Neoprene	7.0×10^{-8}	0.29	0.29
Silicone	450×10^{-8}	18.40	3.60
Butyl	3.2×10^{-8}	0.13	0.37

(a) Obtained from WADC Technical Report 56-331 cm refers to thickness of material.

(b) The clamp torque was approximately 40 foot-pounds during these measurements.

Table 11-8

RELATION OF AIR LEAK RATE OF GASKET
MATERIAL TO LOADING (Ref 17)

Torque on Clamps (ft-lb)	Air Leak Rate, std cc air/in.-yr			
	Neoprene	Silicone	Butyl	Viton-A
0 (atmospheric pressure)	1.28	10.0	<0.001	1.1
10	0.22	4.0	<0.001	0.2
20	0.09	2.8	<0.001	0.08
30	0.03	2.4	<0.001	0.04
40 (normal operating torque)	0.03	2.2	<0.001	0.022
60	0.03	2.2	<0.001	0.02
80	0.03	2.0	<0.001	0.02
100	0.018	1.6	<0.001	0.01
150	0.002	1.4	<0.001	0.01

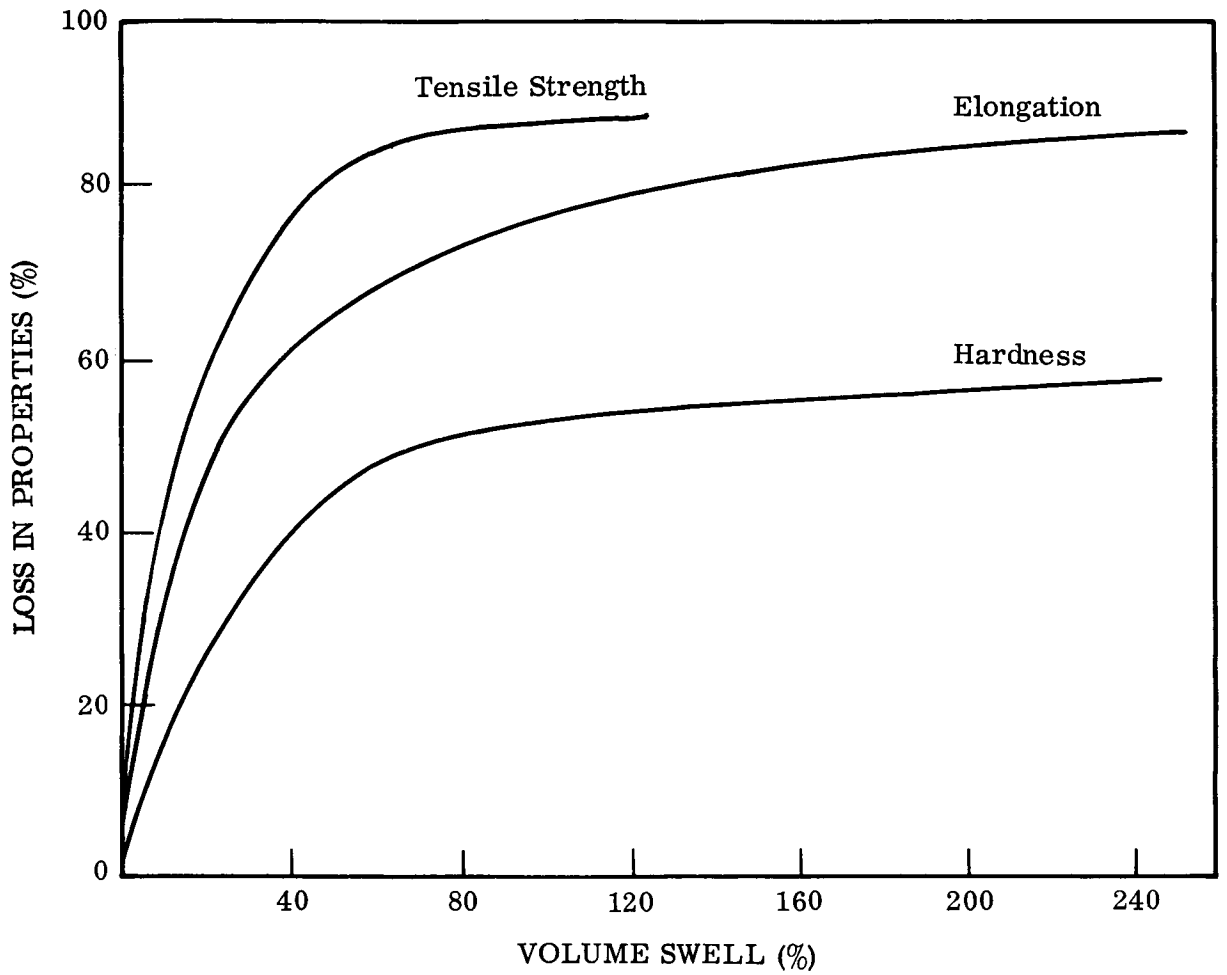

Fig. 11-1 Loss of Properties of Buna-N Elastomer Due to Volume Swell (Ref. 18)

predict accurately if a fluid is a high, medium, or low swelling material when it is exposed to rubber products. The procedure used to determine aniline point of a hydrocarbon fluid is ASTM-D-611.

Test method ASTM-D-471 is used in exposing elastomers to the influence of liquids under definite conditions of temperature and time for the purpose of measuring the resulting deterioration in the mechanical properties. The deterioration is measured by the changes in mechanical and physical properties before and after immersion in the test liquid. Weight, volume, tensile strength, ultimate elongation, and durometer hardness are the properties measured.

There are many aerospace engineering systems which require the use and transfer of all types of hydrocarbon fluids including petroleum products as well as the large variety of synthetic fluids which have been developed for specific applications. Accordingly, it is important that design engineers take into consideration the type of fluid that is going to be used in a particular service application and specify the material which is the least affected by that fluid. Fortunately, work has been done on the compatibility of elastomers with hydrocarbon fluids. Table 11-9 lists some of the fluids and elastomers which are compatible.

11.4.1.2 Liquid Propellants – High Energy Fuels and Oxidizers

The high specific impulses required of propulsion systems of spacecraft and missiles has led to the development of fuels and oxidizers of inherently high reactivity toward materials of construction. Particularly susceptible to attack and subsequent degradation are organic elastomeric materials, such as seals and hoses. Degradation of an elastomeric seal leads quickly to failure of the seal system and thus to leakage and loss of fuel or oxidizer.

Propellants of current interest include hydrazine fuels, nitrogen tetroxide, and fluorine-containing oxidizers.

For hydrazine fuels, the only commercial elastomers found useful, Table 11-10, are peroxide cured ethylene propylene, butyl rubber, and cis-1, 4 polybutadiene. Table 11-11 shows the changes in properties of three elastomers immersed in hydrazine-unsymetrical dimethyl hydrazine mixture (Ref. 19).

Nitrogen tetroxide, N_2O_4, is a strong oxidizer which affects most organic polymers. Table 11-12 shows the resistance of elastomers, to nitrogen tetroxide. Table 11-13 gives the results of immersion testing with Viton, butyl, and nitroso elastomers in N_2O_4 (Ref. 19). Tests conducted at 165°F with nitroso elastomer show that it will effectively withstand long term constant contact with N_2O_4 without serious loss of mechanical properties.

Many immersion tests have been conducted in order to ascertain the compatibility of the fluorine containing oxidizers with various elastomeric and plastic sealing materials.

Table 11-9

COMPATIBILITY OF ELASTOMERS WITH FLUIDS BASED ON PERCENTAGE SWELL

FLUIDS	Silicone	Butyl	Natural Rubber	Buna-S (GR-S)	Neoprene	Hypalon	Kel-F-Elastomer	Thiokol (polysulfide)	Philprene VP (polyisoprene)	Buna-N (Low nitrile) (acrylonitrile)	Buna-N (High nitrile) (acrylonitrile)	Acrylates (Hycar 4021)	Viton A	LS-53 (fluorosilicone)	IF 4-(FBA) (perfluorobutyl acrylate)	Vyram
MIL-H-5606 (Hydrocarbon)	U[(a)]	U	U	U	D	D	S	S	S	S	S	S	S	S	S	S
Engine Oil (Hydrocarbon)	U	U	U	U	D	D	S	S	S	S	S	S	S	S	S	S
OS-45 (Silicate)	U	U	U	D	S	s	S	D	d	D	D	D	S	U	S	D
MLO-8200 (Silicate)	U	u	u	d	s	s	S	d	d	d	d	d	S	u	s	d
Fuel, Gasoline, JP-4 (Hydrocarbon, Napthenics, and Aromatic)	U	U	U	U	U	U	S	S	D	D	S	S	S	S	S	S
MIL-L-7808 (Diester, Organic)	D	U	U	U	U	U	U	S	D	D	S	S	D	U	S	S
Skydrol-7000 (Phosphate)	S	S	D	U	U	U	U	U	U	U	U	U	u	S	S	S
Skydrol-500 (Phosphate)	S	S	D	U	U	U	U	U	U	U	U	U	U	S	D	S

(a) Key:

Evaluation	Symbol Observed	Symbol Estimated
Satisfactory, 0–15% Swell	S	s
Doubtful, 16–40% Swell	D	d
Unsatisfactory 40% Swell	U	u

Many factors affect percentage swell which are not reflected in this tabulation. The manufacturer should be consulted for accurate information on specific compounds.

Table 11-10

RESISTANCE OF ELASTOMERS TO HYDRAZINE FUELS (Ref. 19)

Material	Resistance
Styrene-butadiene copolymer	Disintegrates
Acrylonitrile-butadiene copolymers	Softens, swells, gummy
Polychloroprene	Blisters, swells
Silicone elastomers	Softens, loses properties
Fluorosilicone elastomers	Dissolves
Viton-A	Embrittles, flakes
Kel-F elastomer	Blisters, becomes tacky
Ethylene propylene copolymer	Recommended
Butyl rubber	Recommended
cis-1, 4-Polybutadiene	Recommended

Table 11-11

PROPERTIES OF ELASTOMERS AFTER 38-WEEK IMMERSION IN HYDRAZINE/UDMH (Ref. 19)

Material	Condition	Tensile Strength (psi)	Elongation (%)	200% Modulus (psi)	Shore A Hardness	Volume Swell (%)
cis-1, 4-Polybutadiene 35	Original	1650	200	1650	75	–
	Exposed	1140	160	–	75	–
	Percent change	-31	-20	–	0	25
Butyl 112	Original	1670	230	1000	80	–
	Exposed	1340	160	–	70	–
	Percent change	-20	-31	–	-13	25
EPR 132	Original	1910	420	540	50	–
	Exposed	1600	370	495	50	–
	Percent change	-16	-12	-8	0	20

Table 11-12

RESISTANCE OF CURED ELASTOMERS TO NITROGEN TETROXIDE
(Ref. 19)

Material	Resistance
Acrylonitrile butadiene copolymers	Dissolves
Polychloroprene	Blisters, dissolves
Hypalon (chlorosulfonated polyethylene)	Swells excessively
Silicone elastomers	Hardens, disintegrates
Viton-A	Swells excessively
Kel-F	Swells, becomes tacky
Unsaturated hydrocarbon elastomers	Degrades
Saturated hydrocarbon elastomers	Variable, some suitable for short exposure
Nitroso rubber	Poor to excellent

Table 11-13

RESISTANCE OF ELASTOMERS TO LIQUID N_2O_4 FOR 14 DAYS AT 120°F (Ref. 19)

Elastomer	Immersion Period (days)	Tensile Strength (psi)	Elongation (%)	200% Modulus (psi)	Hardness Shore A	Volume Swell (%)	Remarks
Nitroso compound	0	1050	250	960	70	–	–
	14	1040	250	860	65	30	–
Viton compound	0	2450	150	–	80	–	–
	14	1120	300	880	70	265	–
Butyl compound	0	2100	250	1800	90	–	–
	14	–	–	–	–	–	Degraded

These studies determined that fluorocarbon plastics such as TFE, FEP, and KEL-F 81 and silicone elastomers retained adequate sealing properties after being immersed in oxygen difluoride for a period of 30 days at a propellant temperature of - 100° F.

In similar tests TFE, polyethylene, and ethylene propylene rubber were found to be compatible with a perchloryl fluoride-tetrafluorohydrazine mixture and TFE, KEL-F 81 and uncured nitroso rubber gum were found to be suitable sealing materials in chlorine trifluoride only for a limited time (Ref. 19). The compatability of plastics with some reactive fuels and oxidizers is shown in Table 11-14. These materials have been used in aerospace scaling applications.

11.4.2 Effects of Elevated Temperatures

Until recently, the only effects commonly measured on elastomeric materials were changes in room temperature properties. The high operating temperatures of many aircraft and missile parts require the designer to consider response of elastomers at elevated temperatures.

Elastomers exposed to elevated temperatures exhibit two types of response: reversible and irreversible, caused by changes in the material. It is difficult to separate the two types of response. The low thermal conductivity of most elastomers, the high rate of the irreversible changes, and the similarity of the rate equations of the two types of response make separation impractical. Reversible response is time and temperature dependent, and irreversible response has been termed aging.

Mechanical and physical properties of elastomers depend on (a) the strength of the bonds linking the polymer chains, (b) the tendency of the polymer chains to form crystallites on stretching, and (c) the strength of the filler-polymer linkages.

Increasing the temperature of a crystallizing elastomer causes it to become amorphous which causes a loss of the portion of strength derived from the formation of crystallites. The interchain bonds and the bond between the polymer chains and the fillers are decreased in strength by the increase in temperature. Consequently, any improvement in the elevated temperature properties of an elastomer would involve the creation of new connective forces or the protection of existing ones.

As an elastomer is held at temperature, the polymer chain may break or a portion may cleave off the side chains to create free radicals. If free radicals on alternate chains react, additional cross links are created and the elastomer increases in modulus and hardness, but usually decreases in elongation and tear strength. If the cleavage occurs in the polymer chain and reactions occur to prevent the relinking of the ends of the chain, scission occurs and the product decreases in modulus and hardness. Heating in the presence of oxygen usually increases the rate of chemical reaction between oxygen and the polymer chains.

The deterioration of polymers at elevated temperatures is determined by tensile tests, compression-set characteristics, and the behavior of the material in contact with fluid.

Table 11-14

COMPATIBILITY OF PLASTICS WITH LIQUID PROPELLANT FUELS AND OXIDIZERS

Material	Commercial Designation	Fuel[a]						Oxidizer[a]									Recommended Application
		Unsymmetrical Demethylhydrazine			Hydrazine			Nitrogen Tetroxide			Inhibited Red Fuming Nitric Acid			Propyl Nitrate			
		Splash[b]	Short Term[c]	Long Term[d]	Splash	Short Term	Long Term	Splash	Short Term	Long Term	Splash	Short Term	Long Term	Splash	Short Term	Long Term	
Polyvinyl Fluoride	Tedlar[e]	S	S	U	S	S	U	S	U	U	U	U	U				Not for seal service (film)
Polycarbonate	Lexan[f]	S	U	U	U	U	U	U	U	U	U	U	U	S	U	U	Not for seal service (sheet or molding, rigid)
Polytetrafluoroethylene	Teflon, FEP[e]	S	S	S	S	S	S	S	S	S	S	S	S	S	S	S	Dynamic or static seals. Long-term service with fuel and oxidizer
Polytetrafluoroethylene	Teflon, TFE (Filled and Unfilled)[e]	S	S	S	S	S	S	S	S	S	S	S	S	S	S	S	Dynamic or static seals. Long-term service with fuel and oxidizer
Polyethylene (Branched)	Alathon (Low Density[e]	S	S	U	S	S	U	S	U	U	S	S	U	S	S		Dynamic or static seals, retainers Short-term fuel service only
Polyethylene (Linear)	Marlex or Hi-Fax (High Density)[g]	S	S	U	S	S		S	M	U				S	S		Dynamic or static seals, retainers. Short-term fuel service only
Polyethylene (Irradiated)	Irrathene[f]	S	S	U	S	S	U	S	U	U	S	U	U	S	S		Dynamic or static seals, retainers. Short-term fuel service only
Polytrifluorochloroethylene (Modified)	Genetron, Modified (Kel-F)[h]	S	U	U	S	U	U	S	M	U	S	S		S	S		Dynamic or static seals. Short-term oxidizer service only
Polytrifluorochloroethylene	Trithene (Kel-F)[i]	S	S	U	S	U	U	S	M	U	S	S		S	S		Dynamic or static seals. Short-term oxidizer service only
Polyvinylchloride (Plasticized)	Tygon[j]	S	M	U	S	M	U	S	U	U	S	U	U	U	U	U	Static seals. Short-term service with fuels only
Hexamethylenediamine adipimide	Nylon (Zytel)[e]	S	S	S	S	U	U	U	U	U	U	U	U	S	U	U	Dynamic or static seals. Long-term with UDMH fuel only

(a) S – Satisfactory
M – Marginal
U – Unsatisfactory

(b) 1 min at 77°F

(c) 1–60 days at 77°F–160°F

(d) <1 year

(e) E. I. du Pont Co.

(f) General Electric Co.

(g) Hercules Powder Co., Inc.
Phillips Petroleum Co.

(h) Allied Chemical & Dye Corp.

(i) Visking Corp.

(j) U.S. Stoneware Co.

In actual service, such properties as hardness, resilience, modulus, and permeability to gases and liquids may be factors determining the usefulness of the material at elevated temperatures.

At elevated temperatures, the tensile strength of all vulcanized elastomers decreases. After aging at elevated temperatures, most compounds show an increase in Shore A hardness and a decrease in flexibility or elongation. Figure 11-2 shows the effect of temperature on the tensile strength, modulus, and breaking elongation of a vulcanized natural rubber stock (Ref. 19).

Figure 11-3 shows the effect of elevated temperature on the tensile strength, modulus and breaking elongation of a vulcanized butyl rubber. The breaking elongation curve shows a very high maximum at about 130°F.

Table 11-15 shows the tensile and elongation properties of 21 rubber compounds before and after heat aging at temperatures ranging from 73°F to 550°F.

Table 11-16 shows elastomers arranged in order of decreasing temperatures at which 25% loss of room-temperature tensile strength results from heat aging for eight hours. A typical natural rubber loses 25% of its strength after eight hours of exposure at 215°F.

Table 11-17 lists some elastomers and the temperature at which they lose 50% of original tensile values.

In Table 11-18, the changes in tear resistance at elevated temperatures are noted for various elastomeric materials. Neoprene and natural rubber retain the highest tear resistance at elevated temperature.

Elastomers may be grouped by characteristic behavior at elevated temperatures in three categories:

1. Rapid loss of strength with temperature increase is exhibited by natural, polyurethane, Neoprene, and butadiene-acrylonitrile (NBR) rubbers.
2. Lower percent loss of strength with increasing temperatures is exhibited by silicone, polysulfide, and fluorocarbons.
3. Sharp drop in tensile properties is exhibited by KEL-F and VITON elastomers in the temperature range from 200 to 250°F, with a much smaller loss with further temperature rise.

Silicones or fluorocarbons are the best choice as flexible materials where prolonged exposure to oxidation, ozone, sunlight, and other environmental conditions occur at high temperature. At very high temperatures some silicone compounds offer serviceability for very brief periods. For comparison: at 500°F vinylidene fluoride-hexafluoropropylene (Viton rubber), methyl vinyl silicone, and methyl phenyl silicone are serviceable for 28 days. At 600°F they are serviceable for 72 hours. At 700°F only vinylidene fluoride/hexafluoropropylene remains usable for several hours, and at 800°F for only 10 minutes (Ref. 20).

Effects of elevated temperatures on plastics are covered in Chapter 12 and in Ref. 20.

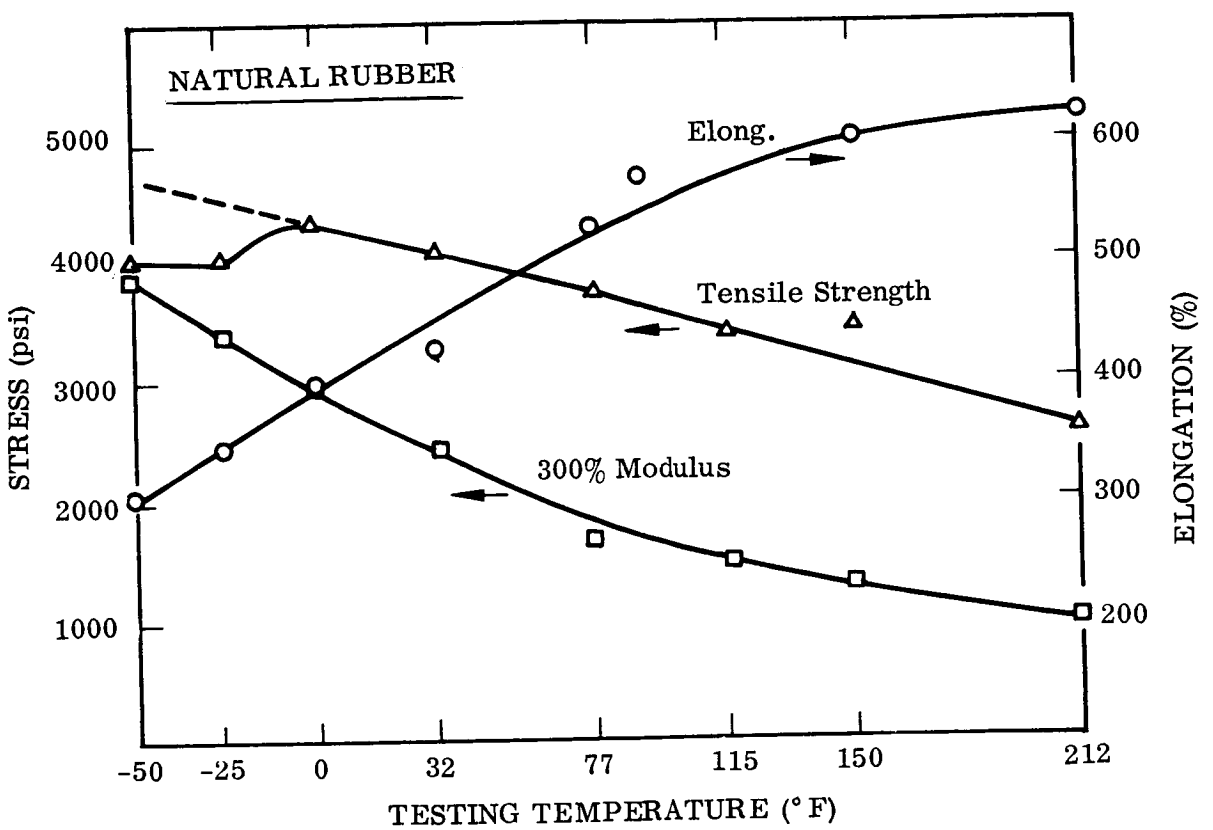

Fig. 11-2 Effect of Testing Temperature on Stress-Strain Properties (Ref. 18)

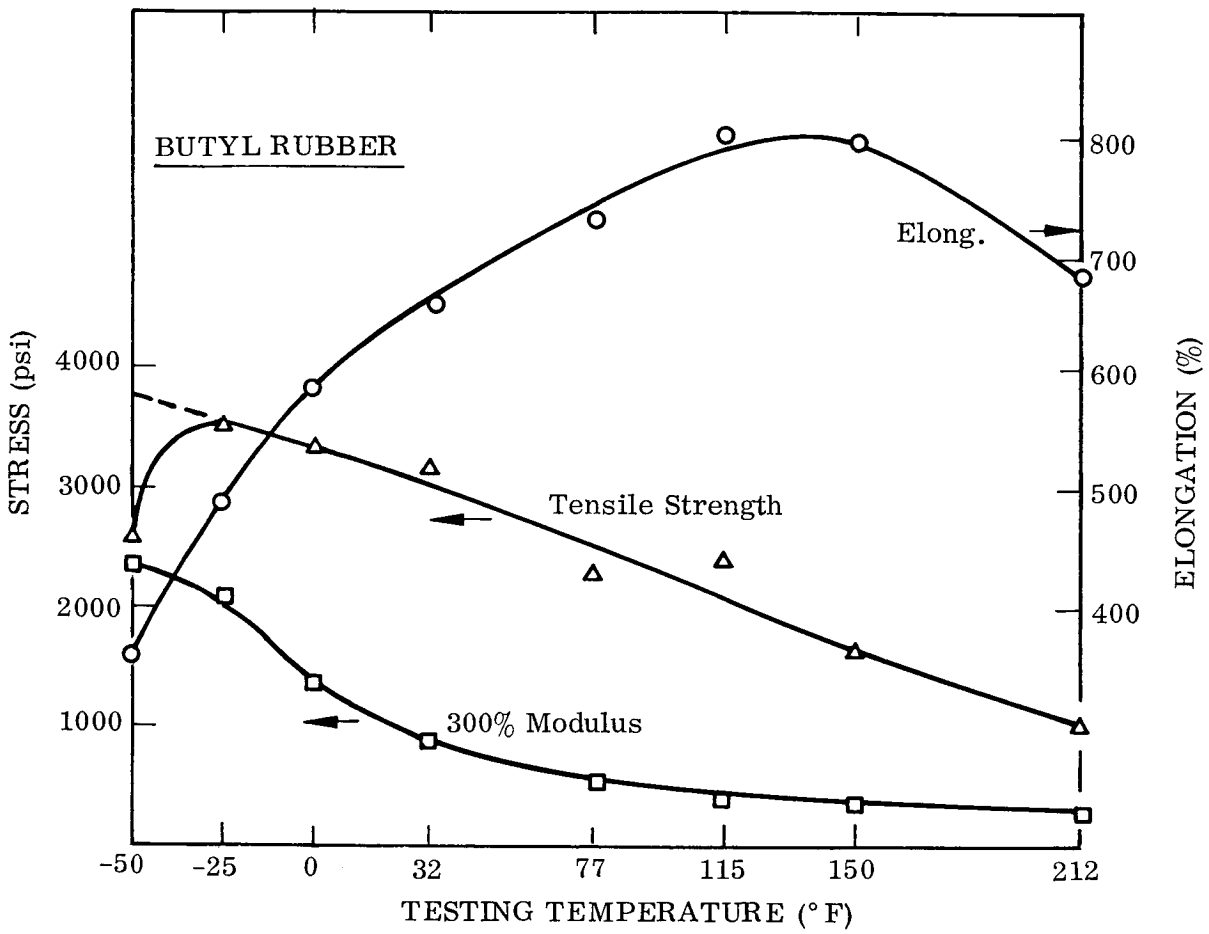

Fig. 11-3 Effect of Testing Temperature on Stress-Strain Properties (Ref. 18)

Table 11-15

SUMMARY OF TENSILE PROPERTIES OF ELASTOMER COMPOUNDS AT ELEVATED TEMPERATURES BEFORE AND AFTER HEAT AGING (Ref. 20)

Tests: Tensile strength (T) in psi, and % elongation at break (E), measured at temperatures shown. All samples, both aged and unaged, were allowed to come to equilibrium temperature prior to actual test.

Heat-aging period: 8 hr at temperatures shown (°F)

Aging temp. (°F) / Test temp. (°F)		– 73	– 200	200 200	– 250	250 250	– 300	300 300	– 350	350 350	– 400	400 400	– 450	450 450	– 500	500 500	– 550
Rubber	Test																
Natural[a]	T	3850	2980	2730	2460	800	1530	690	770	400	500	125	270	–	20	–	–
	E	480	500	480	480	180	400	440	520	260	500	80	300	–	10	–	–
Neoprene[a]	T	3550	1920	1980	1570	1680	1410	1020	1320	330	770	180	360	–	215	–	–
	E	480	360	320	320	240	320	100	350	20	100	10	30	–	10	–	–
Butyl (Phenol Dialcohol cure)[b]	T	2050	1550	1470	1320	1270	1140	850	940	500	790	360	600	–	440	–	–
	E	440	330	330	340	300	260	180	200	120	150	90	120	–	100	–	–
Butyl (Sulfur cure)[b]	T	2325	1170	1240	930	730	750	600	710	410	640	–	440	–	–	–	–
	E	400	270	200	210	140	190	160	210	230	260	–	330	–	–	–	–
Butyl (Sulfur plus quinone cure)[b]	T	1925	860	870	690	520	500	400	380	260	290	–	170	–	–	–	–
	E	360	210	200	190	130	170	100	130	110	100	–	120	–	–	–	–
Nitrile[a]	T	2500	860	925	700	630	640	410	440	300	230	130	160	160	100	–	–
	E	300	140	170	120	80	100	80	70	20	40	20	20	10	10	–	–
Hypalon[a]	T	2175	660	740	470	720	460	670	470	400	440	200	380	270	170	400	–
	E	260	160	100	60	60	50	40	50	20	100	20	80	10	10	20	–
Polysulfide[a]	T	1350	800	740	690	580	550	200	210	–	30	–	–	–	–	–	–
	E	240	180	140	140	120	120	60	110	–	50	–	–	–	–	–	–
Polyurethane[a]	T	5775	3220	3450	2320	2110	1260	1340	1090	580	750	100	–	–	–	–	–
	E	420	310	310	300	280	190	250	180	300	160	160	–	–	–	–	–
Polyurethane[b]	T	4240	1570	1550	1320	1180	810	800	690	530	515	240	380	65	–	–	–
	E	360	240	210	210	200	140	140	110	140	110	130	200	110	–	–	–
Polyurethane[b] (Adiprene C)	T	4650	1130	770	580	470	260	290	270	30	60	–	–	–	–	–	–
	E	480	220	120	140	70	60	80	80	70	160	–	–	–	–	–	–
Silicone[b,d] (Silastic 916U)	T	1650	960	870	–	–	720	660	–	–	430	410	390	390	350	290	310
	E	580	390	390	–	–	330	340	–	–	240	220	200	180	190	160	180
Silicone[b,d] (Silastic 50)	T	1000	830	760	–	–	500	560	–	–	480	420	280	340	330	270	270
	E	300	190	200	–	–	130	130	–	–	110	110	70	80	80	60	70
Fluorocarbon (Viton A)[c]	T	1625	440	420	–	–	260	–	–	–	180	200	180	200	150	110	90
	E	230	150	140	–	–	100	–	–	–	70	80	80	70	70	50	60
Fluorocarbon (Kel-F 3700)[b]	T	2650	710	900	–	–	500	–	–	–	420	280	250	500	410	300	440
	E	300	130	120	–	–	100	–	–	–	90	70	50	110	80	90	90
Fluorocarbon (Kel-F 5500)[b]	T	1775	340	370	300	190	230	220	–	–	165	160	–	–	150	155	–
	E	390	400	380	320	310	230	220	–	–	190	160	–	–	160	190	–
Fluorocarbon[b,e]	T	1200	450	475	345	360	225	265	210	215	225	140	165	135	–	–	–
	E	160	90	90	60	70	60	60	50	10	50	40	50	50	–	–	–
Polyacrylic[a]	T	1825	1330	1090	940	840	630	610	610	580	495	330	460	370	370	50	290
	E	370	240	180	200	120	160	100	150	80	100	20	100	20	60	20	20

(a) Preheat period of 30 minutes used for bringing test strips to test temperature.
(b) Preheat period of 6 minutes used for bringing test strips to test temperature.
(c) Post-cure: 1 hr at 300°F; 8 hr at 480°F
(d) Post-cure: 1 hr at 300°F; 1 hr at 350°F; 8 hr at 400°F
(e) Post-cure: 24 hr at 300°F

Table 11-16

SHORT TERM AGING RESISTANCE OF ELASTOMER COMPOUNDS (Ref. 20)

Aging period: 8 hr.
Temperature: room temperature.
Basis for comparison: Aging temperature which causes 25% loss in tensile strength.

Elastomer	Temperature (°F)
Vinylidene fluoride/ hexafluoropropylene	530
Methyl silicone	450
High strength silicone	450
Monochlorotrifluoroethylene/ vinylidene fluoride	450
Vinyl silicone	430
Fluorinated silicone	430
Nitrile silicone	430
Isobutylene/ isoprene (IIR)	410
Ethyl acrylate/ chloroethyl vinyl ether	390
Chlorosulfonated polyethylene	370
Poly 1, 1 dihydroperfluoro butyl acrylate	370
Chlorinated isobutylene/ isoprene	350
Brominated isobutylene/ isoprene	340
Polychloroprene (CR)	330
Butadiene/acrylonitrile (NBR)	310
Butadiene/acrylonitrile/ acrylic acid	310
Polyurethane	310
Pale crepe (NR)	300

Table 11-17

TEMPERATURES AT WHICH ELASTOMERS RETAINED 50% OF ORIGINAL TENSILE STRENGTH AT TEST TEMPERATURE (Ref. 20)

Elastomer	Temperature (°F)
Methyl silicone	+450
Vinyl silicone	+450
High strength silicone	350
Brominated isobutylene/ isoprene	300
Nitrile silicone	290
Chlorinated isobutylene/ isoprene	270
Isobutylene/ isoprene	270
Pale crepe	230
Polychloroprene	210
Polyurethane	200
Butadiene/ acrylonitrile/ acrylic acid	200
Butadiene/ acrylonitrile	200
Chlorosulfonated polyethylene	200
Fluorinated silicone	190
Poly1, 1 dihydroperfluoro butyl acrylate	180
Ethyl acrylate/ chloroethyl vinyl ether	180
Vinylidene fluoride/ hexafluoropropylene	180
Monochlorotrifluoroethylene/ vinylidene fluoride	170

Table 11-18

CRESCENT TEAR STRENGTH OF ELASTOMER COMPOUNDS AT ELEVATED TEMPERATURES (Ref. 20)

	Crescent Tear (lb/in.)				
Test Temperature (°F)	73	200	300	400	500
Natural	864	362	311	204	(a)
Butyl	332	195	165	72	35
Butyl	234	163	137	91	–
Butyl	166	100	70	25	–
Neoprene	696	323	218	101	13
Hypalon	256	56	36	19	16
Nitrile	228	98	63	49	18
Acrylon EA-5	216	109	58	60	26
Hycar 4021	226	117	65	37	18
Fluorocarbon	118	34	16	11	6
Vyram N-5400	194	70	40	14	–
Polysulfide	218	182	148	12	–
Polyurethane	308	155	101	92	(a)
Polyurethane	214	79	45	32	–
Adiprene C	211	68	33	20	–
Silastic 916 U[(b)]	187	83	54	42	–
Silastic 50[(b)]	68	39	32	18	–
Viton A[(c)]	179	62	23	4	–
Kel-F 3700[(d)]	134	69	38	24	–

(a) Melted.
(b) Post-cure: 1 hr at 300°F; 8 hr at 480°F.
(c) Post-cure: 1 hr at 300°F; 1 hr at 350°F; 8 hr at 400°F.
(d) Post-cure: 16 hr at 300°F.

11.4.3 Effects of Very Low Temperatures

A number of changes can take place in elastomeric materials as a result of exposure to low temperature. Low temperatures cause loss of resilience and hardness; these changes are reversible. Returning the elastomers to room temperature, or slightly elevated temperatures, results in a restoration of its original properties. This is in contrast to the effects of high temperature exposure which permanently changes the composition of the material.

If the modulus of an elastomeric specimen is measured at successively lower temperatures, being held at each temperature only long enough for thermal equilibrium to be established, its stiffness will increase as a function of temperature. As the temperature is decreased, the specimen becomes progressively stiffer at a gradual rate until a particular temperature is reached. At this point, stiffness increases sharply with a decrease in temperature, so that within a range of about 20°F stiffness may increase a hundredfold or more. Further cooling produces little additional increase in stiffness.

At some temperatures, under impact, the elastomeric specimen becomes brittle or will shatter. The temperature at which this occurs depends on the rate of application of load. It is known as the brittle temperature or the brittle point. The brittle point determination bears no definite relationship to the stiffness test, because of the difference in time scale between the stiffness and impact tests.

Long-time exposure of an elastomer to low temperatures produces crystallization. Crystallization results in stiffening that is only evident after prolonged exposure. It may require hours, days, or even weeks, depending upon the exposure temperature and on the particular composition involved. While crystallization results in an increase in stiffness, it does not necessarily result in brittleness. Nor does the fact that crystallization has taken place appear to affect the brittle point of the material.

Among the common elastomers, natural rubber, butyl rubber, and Neoprene are crystallizable. Among all of these the rate of crystallization is increased by placing the vulcanizate under strain. For each elastomer there is a temperature at which crystallization takes place most readily. Since crystallization is time dependent rather than temperature dependent, it does not occur if the elastomers are cooled more or less rapidly through the range in which crystallization ordinarily can occur.

The second effect is known as the plasticizer-time effect. Many compounds designed for low temperature service contain substantial quantities of special plasticizers which are used to improve low temperature flexibility and to depress the brittle point of the material. Under ordinary temperature conditions such plasticizers are soluble in the elastomers. Upon prolonged exposure to low temperatures in the range of -40°F, however, the solubility of the plasticizer is reduced and a portion of it is thrown out of solution. This portion, of course, is of no value in reducing the brittle point or in promoting flexibility; consequently, plasticizer-time effects may result in two changes in the material. First, its flexibility at temperatures above the brittle point may be reduced; second, its brittle point may be raised several degrees.

Figure 11-4 illustrates the low temperature stiffening of several elastomeric materials as measured by the Gehman test. The graphs of the degrees twist versus temperature of most of the organic elastomer compounds in common use fall in the narrow range between natural rubber and fluorocarbon elastomers.

Figure 11-5 depicts low temperature retraction characteristics of several elastomers. Not only are the temperatures at which significant change in retraction behavior occurs considerably different from stiffening temperature, but the order of merit is different. Results of these tests are highly dependent on differences in both elastomer processing and test technique.

Figure 11-6 depicts low temperature resilience characteristics of several elastomers. It further demonstrates that minimum service temperature is a function of both the elastomer and the type of response required of the elastomer in service. The change in behavior at low temperatures, measured by the various tests, marks the change in response of the material from that of an elastomer to that of a plastic material and, in this transition region, responses are especially strain rate sensitive. This is the reason, not only for the differences in temperature of marked change in response as measured by the various tests, but also for the variations in recommended minimum service temperatures for different service applications (Ref. 18).

11.4.4 Effects of High Vacuum

Polymeric plastic or elastomeric sealing materials, can offgass and suffer weight loss in the high vacuum of space. This loss can result in changes in the mechanical or electrical properties of the material. This behavior is true when the material contains volatile additives or plasticizers. One consideration of this effect is the possible condensation of volatile offgassing constituents on an optical surface which may cause loss of resolution or control. The offgassing products may also limit the effectiveness of passive thermal control coatings, contaminate electrical contacts; and, if the volatile by-products enter the manned spacecraft, they can often be noxious or even toxic to the occupants.

Exposure of elastomer or plastic materials to vacuum causes changes in mechanical properties, such as elongation, tensile strength, hardness and elasticity as a function of the relative rates of cross linking (or chain lengthening) and cleavage (chain scission).

Offgassing of most materials increases considerably at elevated temperatures. The greater weight loss is probably due to the offgassing of larger molecules which do not escape or which are removed very slowly at lower temperatures. Weight losses of materials under vacuum at temperatures above ambient may be more than or less than weight losses experienced at similar temperatures in air. The result depends upon the temperature at which the specific polymer being examined starts to oxidize. At sufficiently elevated temperatures some plastic and elastomeric materials will tend to oxidize in air, showing a net weight loss greater than that experienced at the same temperature under vacuum. Other organic sealing materials, more resistant to oxidation, may lose plasticizer or other constituents under vacuum and exhibit a net loss greater than that in air.

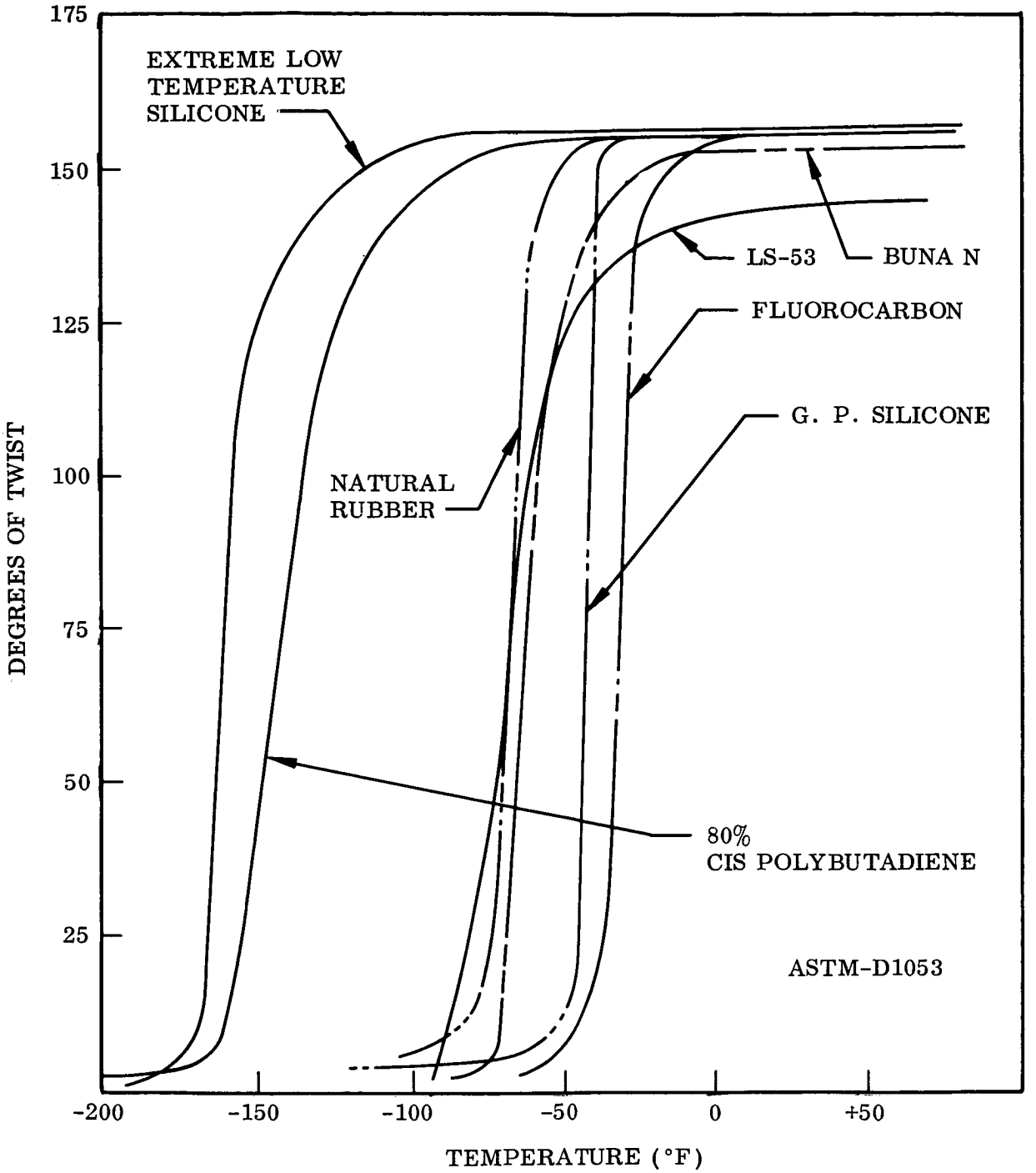

Fig. 11-4 Stiffening of Elastomers at Low Temperatures (Ref. 18)

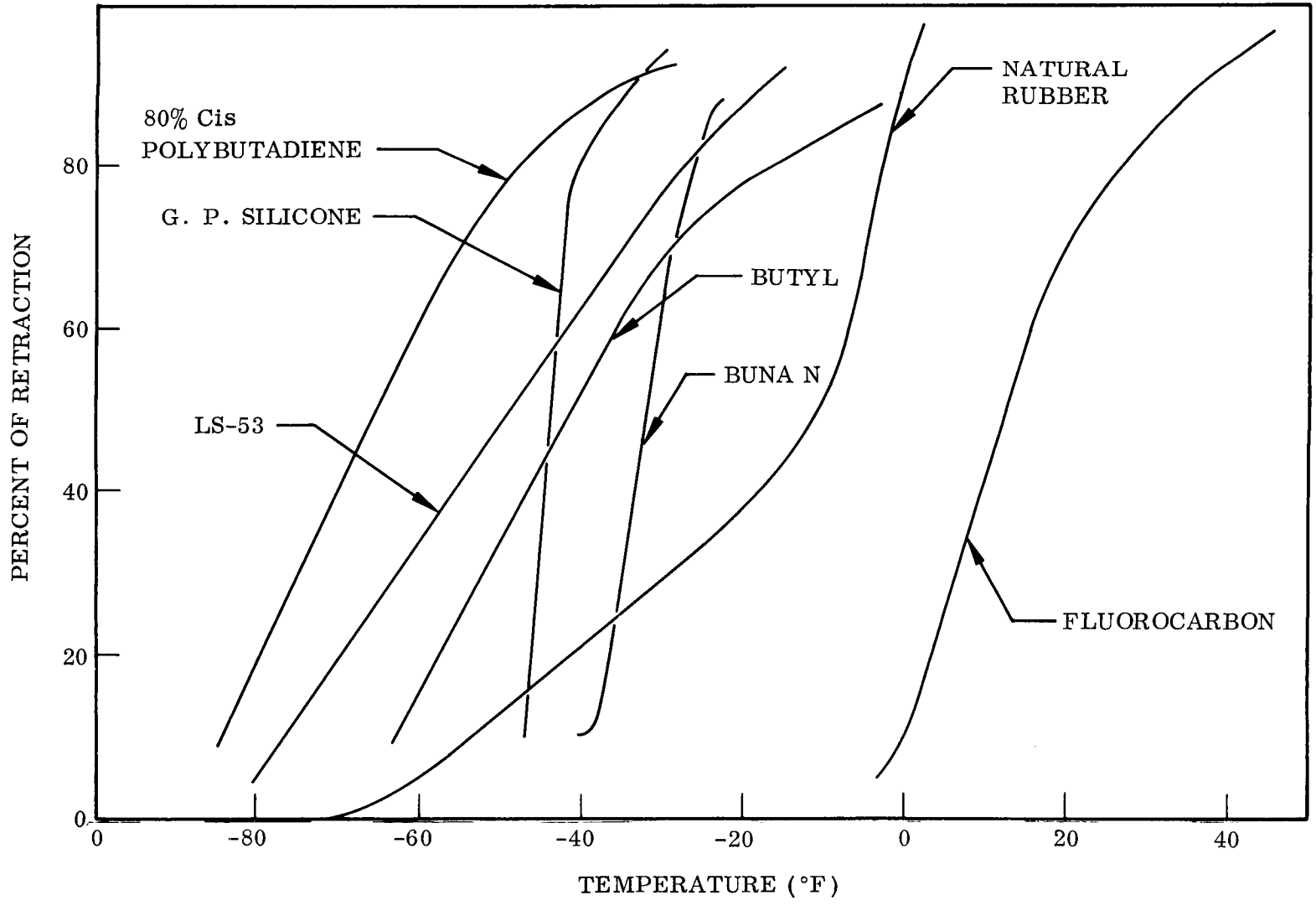

Fig. 11-5 Stiffening of Elastomers at Low Temperatures (Ref. 18)

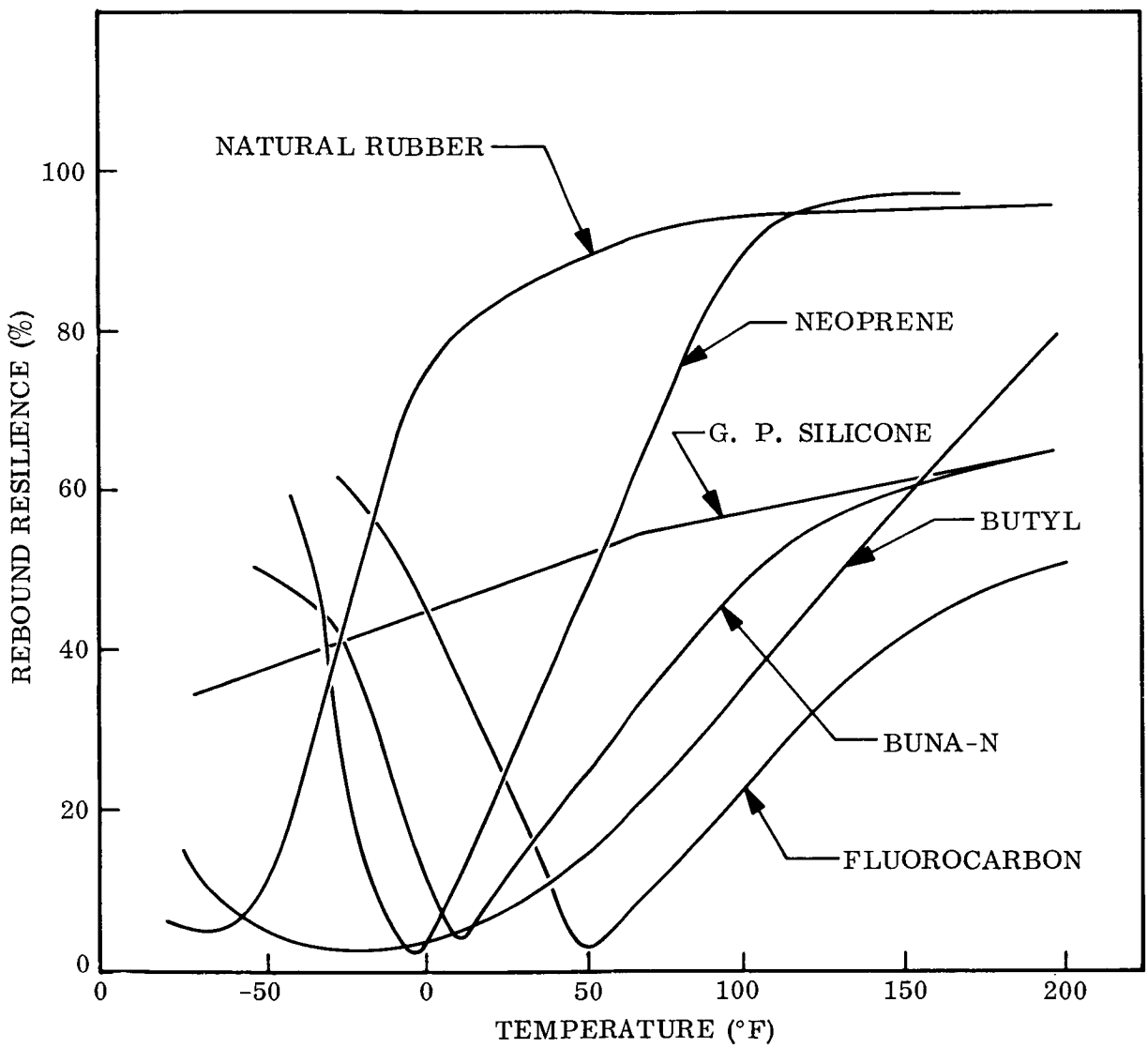

Fig. 11-6 Stiffening of Elastomers at Low Temperatures (Resilience)(Ref. 18)

Seventeen elastomeric sealing materials were tested at Marshall Space Flight Center at less than 10^{-5} Torr at various temperatures. The results of these tests are shown in Table 11-19.

Six plastic sealing materials were also tested at Marshall Space Flight Center. The results of these tests are shown in Table 11-20 (Ref. 21).

About 350 commercial polymeric products were screened for offgassing characteristics at Stanford Research Institute under contract to Jet Propulsion Laboratory. About 100 materials qualified within the limits of < 0.1% weight loss and < 0.1% volatile condensable material (VCM), when exposed in a vacuum of 10^{-6} Torr at 125°C (255°F). Table 11-21 lists some of the commercial seal and gasket materials that were exposed for 24 hours.

Table 11-22 shows the degradation in some of the mechanical properties that resulted after exposure to a temperature of 125°C (275°F) at 10^{-6} Torr for a period of 500 hours.

Table 11-23 gives total percentage weight losses and percentage of volatile condensable material (VCM) measured on some of the commercial sealants which are used for encapsulant or trowelling applications in spacecraft (Ref. 22).

Generally, the room temperature vulcanizing (RTV) silicone sealants and encapsulants shown higher weight losses and VCM than most of the polyurethane materials.

11.4.5 Effects of Penetrating Radiation

In most seal applications the material will be shielded by metallic structural elements of sufficient mass to prevent exposure to all but the most penetrating radiation in space. Nuclear reactors on board, nuclear detonations, or a solar flare may have particles with enough energy to penetrate the spacecraft structure and seal housing elements. In the case of solar flare, the duration of peak flux intensity may not be long enough to cause damage by the energetic protons accompanying it so little damage to polymeric sealing materials should be expected from this source.

The external window seals of manned spacecraft will be partially exposed to the unfiltered space radiations. During the extravehicular activities of manned spacecraft missions portions of the hatch seals may also be exposed to the space environment. This latter exposure is of comparatively short duration. For Apollo missions, the exposure of the window seals externally will be of the order of 500 hours. Such sealing materials as the silicone elastomers may be selected for this application.

Most of the testing of seal materials has been done by exposure to nuclear reactor gamma and neutron radiation. The effect of reactor gamma radiation was to decrease elongation; tensile strength may increase or decrease to the threshold dose and then decrease to unusable levels, the compression set tended to increase from 50 to 100% for most elastomers. The changes in most materials were generally the same in air as in vacuum. The doses to affect the threshold change in elongation in four elastomers

Table 11-19

EFFECTS OF THERMAL VACUUM ON VARIOUS ELASTOMERIC MATERIALS (Ref. 21)
(10^{-5} Torr at Temperature Shown)

Material	Sample Thickness (cm)	Surface Area (cm^2)	Time at Temp. (hr)	Temp. (°C)	Initial Weight (gm)	Total Weight Loss (%)	Change in Physical Appearance
Kel-F	0.178	4.85	15	R.T.	–	0.0	None
			15	100	–	0.0	None
			25	199	0.9063	1.1	Turned black
Viton-B	0.254	5.17	20	100	1.1162	0.1	None
			20	149	–	0.2	None
			52	198	–	1.2	None
Viton-A	0.178	4.85	15	R.T.	0.7644	0.0	None
			15	100	–	0.1	None
			136	199	–	4.9	Turned black
Polyacrylic	0.178	4.85	12	R.T.	0.4849	0.0	None
			15	101	–	0.3	None
			16	152	–	0.8	None
Fluorinated Silicone	0.229	5.05	15	R.T.	0.5469	0.0	None
			20	100	–	0.3	None
			138	200	–	2.3	None
Silicone	0.178	4.85	12	R.T.	–	0.0	None
			15	102	–	0.4	None
			138	201	0.4575	3.3	None
Hypalon	0.178	4.85	12	R.T.	–	0.0	None
			117	102	0.5393	0.5	None
			235	150	–	8.5	Cracked at surface
Neoprene	0.178	4.85	150	R.T.	0.5634	0.1	None
			17	102	–	1.6	None
			17	150	–	1.8	None
Polyurethane	0.178	4.85	12	R.T.	–	0.8	None
			46	100	–	2.2	None
			216	152	0.5156	6.0	None
Butyl	0.178	4.85	16	R.T.	–	0.0	None
			130	99	–	3.0	None
			140	150	0.4506	3.6	None
Styrene-Butadiene	0.178	4.85	75	R.T.	–	0.3	None
			75	100	0.4774	4.6	None
			115	149	–	6.2	None
Natural Rubber	0.178	4.85	226	R.T.	–	1.3	None
			96	100	–	4.8	None
			96	149	0.4880	6.6	None
Buna-N	0.178	4.85	16	R.T.	–	0.0	None
			60	101	0.4219	5.7	None
			60	150	–	7.1	None
Neoprene, 5PPH Antiox 4010 Compound 2277 Precision Rubber Products	0.178	4.85	–	100	–	7.3	None
			–	152	0.5621	8.3	None
Neoprene WRT Compound 3046-70 Plastics & Rubber Products	0.178	4.85	–	R.T.	0.6520	0.2	None
			–	100	–	7.5	None
			–	152	–	8.5	None
Buna-N Compound 66-581 Parker-Hannifin	0.178	4.85	–	R.T.	0.5353	0.0	None
			–	96	–	7.4	None
			–	154	–	11.7	None
Polysulfide	0.178	4.85	12	R.T.	–	0.0	None
			20	100	–	15.3	None
			20	125	–	27.3	Cracked at surface
			6	150	0.55445	39.0	Cracked at surface

Table 11-20

EFFECTS OF THERMAL VACUUM ON VARIOUS PLASTIC MATERIALS (Ref. 21)
(10^{-5} TORR AT TEMPERATURE SHOWN)

Material	Thickness Sample (cm)	Surface Area (cm^2)	Time at Temp. (hr)	Temp. (°C)	Initial Weight (g)	Weight Loss		Change in Physical Appearance
						Total (g)	Total (%)	
Teflon-TFE DuPont	0.076	12.2	200	R.T.	0.9887	0.0000	0.0	None
			200	100	0.9865	0.0000	0.0	None
			200	200	0.9500	0.0000	0.0	None
Mylar DuPont	0.0025	25.0	16	R.T.	0.0397	0.0000	0.0	None
			16	100	0.0397	0.0000	0.0	None
			—	—	—	—	—	(a)
Polyethylene Source Unknown	0.409	5.87	72	R.T.	0.6700	0.0000	0.0	None
			72	50	0.6750	0.0013	0.2	None
			18	100	0.6705	0.0005	0.1	Sample melted
Polyimide Tape M DuPont	0.0051	116.	12	R.T.	0.4135	0.0000	0.0	None
			20	103	0.4135	0.0005	0.1	None
			20	201	0.4125	0.0015	0.4	None
Polyamide Film HT-1 DuPont	0.0087	20.6	15	R.T.	0.0595	0.0018	3.0	None
			20	201	0.0599	0.0022	3.7	None
Polyvinyl Chloride (PVC) Film Marshall Space Flight Center	0.023	6.45	44	R.T.	0.0880	0.0030	3.4	None
			—	100	0.0870	0.0262	30.1	Became hard and began to decompose

(a) Test was started at 200° C but sample melted with no apparent decomposition.

Table 11-21

EFFECT OF THERMAL-VACUUM EXPOSURE AND POSTCURE ON VARIOUS SEAL AND GASKET MATERIALS (Ref. 23)
(24 hr at 125° C and 10^{-6} Torr)
(VCM collectors at 25° C)

Material	Mfr. (a)	Cure	Total Wt. Loss (%)	VCM, (b) Wt. (%)
Acrylic				
Hycar 520-67-108-1	BFG	As received	1.90	0.17
Butyl				
EX-1090	ENJ	Postcured 4 hr/150° C	0.80	0.24
EX-1091	ENJ	Postcured 4 hr/150° C	0.70	0.20
EX-1092	ENJ	Postcured 4 hr/150° C	0.86	0.10
FR-60-26	FRC	As received	4.06	0.10
SR-613-75	SIS	As received	2.39	0.39
SR-634-70	SIS	As received	1.40	0.18
805-70	PRP	As received	1.30	0.48
Ethylene-Propylene				
SR-722-70 A	SIS	As received	2.00	0.85
SR-722-70 B	SIS	Postcured 24 h4/150° C	0.98	0.60
Fluorosilicone				
1050-70	PRP	As received	0.50	0.03
L-449-6	PSC	As received	0.53	0.07
Neoprene				
C526-7	PSC	As received	3.01	1.72
Silicone				
Hadbar 28-80	PPH	As received	0.86	0.21
Hadbar 4000-80	PPH	As received	0.54	0.14
SE-555 (white)	GES	As received	0.55	0.33
SE-555 (gray)	GES	As received	0.53	0.30
SE-555 (red)	GES	As received	0.76	0.53
SE-556	GES	Postcured 24 hr/250° C	0.10	0.01
SE-3604 (24/480)	GES	As received	0.51	0.12
SE-3613 (24/480)	GES	As received	0.09	0.06
SE-3713 (24/480)	GES	As recieved	0.20	0.09
SE-3813 (24/480)	GES	As received	0.27	0.04
SE-4511 (24/480)	GES	As received	0.19	0.10
Vinylidene fluoride-hexafluoropropylene				
Viton A4411A-990	DUE	As received	0.54	0.03

(a) Manufacturer Code:
BFG – B. F. Goodrich
ENJ – Enjay
FRC – Fargo Rubber
SIS – Stillman Rubber
PRP – Plastics & Rubber
PSC – Parker Seal
PPH – Hadbar Rubber
GES – General Electric
DUE – Dupont

(b) Volatile Condensable Material = VCM

Table 11-22

EFFECTS OF THERMAL-VACUUM EXPOSURE ON THE MECHANICAL AND PHYSICAL PROPERTIES ON SEAL AND GASKET MATERIALS (Ref. 23)
(500 hr at 135°C and 10^{-6} Torr)

Material	Dimensional Change (%)	Weight Change (%)	Shore Hardness		Tensile (psi)		Elongation at Break (%)	
			Control	Test	Control	Test	Control	Test
Acrylic								
Hycar 520-67-108-1	L, n.c.	-1.06	86.3	89.1	1860	2140	128	88
Butyl								
805-70	L, -1.00	-2.42	77.2	79.9	1120	1100	295	208
EX-1090	L, -0.39	-1.57	70.7	86.6	2240	1710	550	129
EX-1091	L, -0.50	-1.49	71.0	79.8	1800	1840	380	200
EX-1092	L, -0.96	-2.11	76.2	85.7	1880	1380	210	78
FR 60-26	L, -1.60	-4.30	62.5	78.8	2292	1520	554	228
SR 613-75	L, -0.81	-2.15	82.1	81.6	1108	1011	150	216
SR 634-70	L, n.c.	-1.78	71.1	93.1	2058	996	400	97
Ethylene-Propylene								
SR 722-70 (A)	L, -0.95	-1.68	77.0	80.5	2488	2294	269	245
SR 722-70 (B)	L, -0.76	-1.44	77.5	82.5	1571	1990	195	182
Fluorocarbon								
Viton A4411A-990	L, n.c.	-0.54	85.4	86.7	2030	2220	358	273
Silicone								
Hadbar 28-80	L, -0.43	-0.67	85.6	88.6	971	866	116	100
Hadbar 4000-80	L, -0.26	-0.56	77.0	80.8	1108	910	331	282
SE-555 (red)	L, -0.08	-0.76	70.6	69.6	1080	1440	500	512
SE-555 (gray)	L, -0.26	-0.95	60.1	66.8	1115	1380	442	347
SE-555 (white)	L, +0.21	-0.85	60.8	69.0	1640	1461	480	425
SE-556	L, -0.31	-1.04	54.6	65.3	1390	1390	515	458
SE-3604 (24/480)	L, n.c.	-0.18	77.4	78.4	849	917	142	105
SE-3613 (24/480)	L, n.c.	-0.13	70.6	70.7	1020	977	212	122
SE-3713 (24/480)	L, n.c.	-0.25	77.9	77.9	1090	1176	126	117
SE-3813 (24/480)	L, n.c.	-0.33	87.4	88.2	1074	1230	79	80
SE-4511 (24/480)	L, -0.03	-0.21	52.1	57.4	733	753	312	253

Table 11-23

EFFECT OF THERMAL VACUUM EXPOSURE AND POSTCURE ON ENCAPSULATING MATERIALS (Ref. 73)
(24 hr at 125°C and 10^{-6} Torr)
(VCM Collectors at 25°C)

Material[a]	Mfr.[b]	Mixture	Cure	Total Wt. Loss (%)	VCM,[c] Wt. (%)
Epoxy					
BR-617 A/B	ACB	100pA/25pB	48 hr/25°C	31.02	0.91
BR-617 A/B	ACB	1001A/25pB	48 hr/25°C + 16 hr/52°C	30.82	0.89
Corfil 615/Z	ACB	100p615/14.5pZ	16 hr/50°C + 1 hr/150°C	2.00	0.07
Epocast 168/995	FPI	90p168/10p995	16 hr/50°C + 1 hr/150°C	1.53	0.06
Hysol 5150/3690	HYS	100p5150/100p3690	24 hr/25°C	1.82	0.17
Hysol C7/4248	HYS	100pC7/100p4248	2 hr/25°C + 16 hr/175°C	0.66	0.23
Maraset 655/553	MRC	100p655/20p553	16 hr/82°C	0.59	0.00
Maraset 655/533	MRC	100p655/20p553	16 hr/82°C + 24 hr/150°C	0.32	0.00
Maraset 655/555	MRC	100p655/7p555	16 hr/82°C	0.41	0.00
Maraset 655/555	MRC	100p655/7p555	16 hr/82°C + 24 hr/150°C	0.25	0.00
Scotchcast 235 A/B (brown)	MME	50pA/100pB	6 hr/93°C	6.20	0.31
Scotchcast 241 A/B (brown)	MME	50pA/100pB	16 hr/93°C	2.78	0.02
Scotchcast 241 A/B	MME	50pA/100pB	6 hr/95°C	2.97	0.04
Scotchcast 241 A/B	MME	50pA/100pB	3 hr/121°C	1.93	0.05
Scotchcast 260	MME	As received	30 min/150°	0.52	0.03
Scotchcast 281 A/B	MME	100pA/150pB	20 hr/75°C	0.36	0.05
Stycast 1210 A/B	EMC	100pA/50pB	24 h4/150°C	1.67	0.05
Stycast 1263/31	EMC	100p1263/3p31	16 hr/107°C + 24 hr/150°C	0.12	0.01
Stycast 1264 A/B	EMC	100pA/45pB	48 hr/25°C	2.80	0.14
Stycast 1269 A/B	EMC	100pA/55pB	16 hr/75°C + 4 hr/100°C + 4 hr/120°C	2.02	1.10
Stycast 1269 A/B	EMC	100pA/100pB	16 hr/100°C + 24 hr/150°C	0.18	0.05
Stycast 2741/15	EMC	100p2741/150p15	8 hr/25°C	10.63	2.00
Stycast 2741/15	EMC	100p2741/150p15	8 hr/25°C + 24 hr/150°C	1.65	0.10
Stycast 2850 FT/9	EMC	100p2850/3.5p9	16 hr/25°C	0.34	0.04
Stycast 2862 A/B	EMC	100pA/100pB	16 hr/120°C	0.32	0.04
Stycast 2862 A/B	EMC	100pA/100pB	16 hr/120°C + 24 hr/150°C	0.00	0.00
Stycast 3050/11	EMC	100p3050/9.5p11	16 hr/77°C	0.68	0.06
Polyester					
Stycast 40/7	EMC	100p40/2p7	16 hr/25°C + 2 hr/85°C + 24 hr/150°C	2.26	0.35
Polyethylene					
TPM-2/10	EMC	100pTPM-2/1p10	12 hr/50°C + 4 hr/80°C	6.41	0.42
TPM-3/10	EMC	100pTPM-3/1p10	12 hr/50°C + 4 hr/80°C	3.33	0.90
TPM-6 A/B	EMC	100pA/4pB	16 hr/105°C + 4 hr/145°C + 4 hr/175°C	2.29	0.47

Table 11-23 (Cont.)

Material[a]	Mfr.[b]	Mixture	Cure	Total Wt. Loss (%)	VCM,[c] Wt. (%)
Polyurethane					
Ecco CP6/R6	EMC	100pCP6/17pR6	3 hr/105°C	5.78	2.01
PR-1527 A/B	PRC	26pA/100pB	6 hr/82°C	1.65	0.44
PR-1527 A/B	PRC	33pA/100pB	7 days/25°C	1.14	0.23
PR-1538 A/B	PRC	32pA/100pB	6 hr/82°C	2.07	0.56
PR 1538 A/B	PRC	33pA/100pB	3 hr/25°C + 3 hr/82°C	1.15	0.16
Stycast CPC-21 A/B	EMC	100pA/60pB	6 hr/95°C	17.33	4.18
Stycast CPC-21 A/B	EMC	100pA/60pB	6 hr/95°C + 24 hr/150°C	15.32	4.03
Stycast CPC-22 A/B	EMC	100pA/60pB	40 hr/65°C	29.86	5.48
Stycast CPC-22 A/B	EMC	100pA/60pB	40 hr/65°C + 24 hr/150°C	28.25	5.12
Stycast CPC-41 A/B	EMC	100pA/120pB	48 hr/65°C	0.66	0.14
Stycast CPC-41 A/B	EMC	100pA/120pB	48 hr/65°C + 24 hr/150°C	0.58	0.10
Silicone					
RTV-30/T-12	GES	100p30/0.1pT-12	24 hr/25°C + 24 hr/135°C	0.74	0.34
RTV-40/T-12	GES	100p40/0.1pT-12	24 hr/25°C	1.49	0.43
RTV-40/T-12	GES	100p40/0.1pT-12	24 hr/25°C + 24 hr/150°C	1.07	0.56
RTV-40/T-12	GES	100p40/0.1pT-12	7 days/25°C	1.07	0.33
RTV-41/T-12	GES	100p41/0.1pT-12	8 hr/25°C + 4 hr/50°C	2.06	0.45
RTV-41/T-12	GES	100p41/0.1pT-12	8 hr/25°C + 24 hr/150°C	1.09	0.60
RTV-41/T-12	GES	100p41/0.1pT-12	8 hr/25°C + 24 hr/250°C	0.17	0.12
RTV-77/T-12	GES	100p77/0.1pT-12	8 hr/25°C + 24 hr/150°C	1.69	1.02
RTV-88/T-12	GES	100p88/0.1pT-12	24 hr/25°C + 24 hr/135°C	0.66	0.36
RTV-102 (white)	GES	As received	24 hr/25°C	5.45	1.63
RTV-102 (white)	GES	As received	24 hr/25°C + 24 hr/125°C	2.97	1.55
RTV-103 (black)	GES	As received	24 hr/25°C	5.35	1.72
RTV-103 (black)	GES	As received	24 hr/25°C + 24 hr/150°C	2.92	1.65
RTV-108 (clear)	GES	As received	24 hr/25°C	5.52	1.60
RTV-108 (clear)	GES	As received	24 hr/25°C + 24 hr/150°C	3.11	1.60
RTV 580/T-12	GES	100p580/0.1pT-12	24 hr/25°C + 24 hr/150°C	1.81	0.81
RTV-602/SRV-05	GES	100p602/0.25pSRC-05	24 hr/25°C	3.10	0.96
RTV-602/SRC-05	GES	100p602/0.25pSRC-05	24 hr/25°C + 24 hr/150°C	2.07	1.04
RTV-630 A/B	GES	100pA/10pB	48 hr/25°C + 24 hr/150°C	1.30	0.81
RTV-632 A/B	GES	100pA/10pB	48 hr/25°C + 24 hr/150°C	1.25	0.74
Silastic-501/T-12	DCC	100p501/4pT-12	7 days/25°C	5.32	3.62
Silastic-501/T-12	DCC	100p501/4pT-12	7 days/25°C + 24 hr/125°C	4.12	3.01
Silastic-732 (clear)	DCC	As received	24 hr/25°C	2.39	0.75
Silastic-732 (clear)	DCC	As received	24 hr/25°C + 24 hr/150°C	1.59	0.80
Silastic-732 (black)	DCC	As received	24 hr/25°C	2.50	0.84

Table 11-23 (Cont.)

Material[a]	Mfr. [b]	Mixture	Cure	Total Wt. Loss (%)	VCM, [c] Wt. (%)
Silastic-732 (black)	DCC	As received	24 hr/25°C + 24 hr/150°C	1.76	0.85
Silastic-732 (white)	DCC	As received	24 hr/25°C	2.96	0.96
Silastic-732 (white)	DCC	As received	24 hr/25°C + 24 hr/150°C	1.73	0.93
Silastic-881/Cat	DCC	100p881/4.6pCat	24 hr/25°C	2.95	0.78
Silastic-881/Cat	DCC	100p881/4.6pCat	24 hr/25°C + 24 hr/125°C	1.43	0.80
Silastic-881/Cat	DCC	100p881/4.6pCat/0.32pT-12	24 hr/25°C	3.15	1.07
Silastic-881/cat	DCC	100p881/4.6pCat/0.32pT-12	24 hr/25°C + 24 hr/125°C	1.66	0.88
Silastic-3116/T-12	DCC	100p3116/4.0pT-12	7 days/25°C	1.84	0.61
Silastic-3116/T-12	DCC	100p3116/4.0pT-12	7 days/25°C + 24 hr/125°C	1.05	0.63
Silastic-3116/T-12	DCC	100p3116/4.24pT-12	7 days/25°C	1.77	0.51
Sylgard-184/Cat	DCC	90p184/10pCat	4 hr/65°C	1.77	0.89
Sylgard-184/Cat	DCC	90p184/10pCat	4 hr/65°C + 24 hr/150°C	0.94	0.62

(a) Resin/curing agent
(b) Manufacturer's Code:
ACB – American Cyanamid
FPI – Furane Plastice
HYS – Hysol Corp.
MRC – Marblett Corp.
MME – Minnesota Mining Mfg.
EMC – Emerson & Cuming, Inc.
PRC – Products Research
DCC – Dow Corning
GES – General Electric
(c) Volatile Condensable Materials = VCM

in air and vacuum are shown in Table 11-24 (Ref. 17). There is little difference, for those materials, between the effect of radiation in air or vacuum.

Table 11-24

EFFECT OF REACTOR GAMMA RADIATION ON SOME ELASTOMERS EXPOSED AND TESTED IN AIR OR VACUUM (Ref. 17)

Elastomer	Gamma Radiation Dose (Rads)	% Change in Elongation Exposed in	
		Air	Vacuum to 10^{-7} Torr
Natural Rubber	7×10^6	- 7	-10
	6×10^7	-37	-37
Buna-N	1.5×10^6	- 6	- 8
	1.3×10^7	-18	-10
Neoprene	1.5×10^6	+ 3	+ 7
	1.3×10^7	-15	- 6
Viton B	1×10^7	-50	—
	5×10^7	-82	-88
	5×10^6	—	-27

The temperature and radiation resistance of several elastomeric sealing materials is summarized in Table 11-25 (Ref. 17).

Antirad materials have been used to increase the radiation stability of polymers. They function by preferentially absorbing the energy induced in the polymer by the radiation and releasing it in less damaging form as heat. Phenyl compounds, because of their ring structure, can absorb more energy than the straight chain compounds and thus are used as antirad additives to elastomers.

The radiation resistance of most of the plastics used in sealing applications is about the same as that of the elastomers. The effect of reactor gamma radiation on several plastic materials is shown in Table 11-26 (Ref. 17). The changes in mechanical properties are usually a decrease in both tensile strength and elongation above the radiation damage threshold. With the exception of the fluorocarbon plastics, Teflon TFE, FEP, the radiation resistance is about the same in air as in vacuum. In the case of the Teflon TFE and FEP the radiation resistance, as indicated by changes in mechanical properties, is increased about one to two orders of magnitude in vacuum over that in air. The KEL-F material is slightly stronger than the Teflon materials and is not as greatly affected by gamma radiation. There is little improvement in vacuum.

Table 11-25

TEMPERATURE AND RADIATION RESISTANCE OF TYPICAL ELASTOMERS FOR SEAL SERVICE (Ref. 17)

Material	Temperature (° F)		Reactor Gamma Radiation Dose (rad) in Air		Remarks
	Continuous Operation	Maximum Tolerable (Short Time)	Continuous Operation, Maximum	Maximum Tolerable[a]	
Neoprene MIL-S-6855 Type II MIL-R-15624 Type I	-40 to 200	300	5×10^7	5×10^8	Good radiation stability for most formulations, retains hardness better than most elastomers; overall damage threshold for change in mechanical properties is 5×10^7R; tensile strength is reduced at dose up to 10^8R and then increases at higher doses; elongation gradually decreases to 5×10^7 and then rapidly decreases; stability of neoprenes is very dependent on formulation (e.g., fillers, plasticizers, additives); little difference between effects of radiation in air or vacuum above 10^7R undergoes a considerable compression set; above average temperature stability is characteristic of neoprenes
Fluorocarbon Viton-A	-20 to 400	600	5×10^6	5×10^7	Poor radiation stability; overall damage threshold for change in mechanical properties affecting use as seal is 5×10^6R; 25% change occurs at 6×10^7R; possesses poor stability when irradiated in air at temperatures above 250° F; does not degrade as rapidly when irradiated in inert atmosphere environment or in contact with diester oils; Viton gradually hardens, undergoes considerable compression set and becomes brittle at higher doses, but at 5×10^7R (in oil) it reportedly retains its sealing ability; has very good temperature resistance and low permeability to gases. Damage threshold 10^8 rad in vacuum.
Viton-B MIL-R-25897 Types I & II	-20 to 400	600	5×10^6	10^7	
Silicone ZZ-R-765 Class III	-100 to 400	600	5×10^7	10^8	Good radiation stability; undergoes rapid degradation in elongation, tensile strength, compression set, and hardness at doses higher than 10^7R (25% damage level); useful immersed in most fluids except MIL-7808 to 5×10^8R; little difference between effects in air and vacuum; 50% loss in mechanical properties at 5×10^6 rad at 400° F.
Butyl MIL-G-1149 Type I Class 3 MIL-R-43109	210	300	10^6	10^7	Least radiation resistant elastomer; softens and undergoes considerable set until, at 6×10^7R, becomes a tarry fluid; 25% change in mechanical properties at 4×10^6R; poor elevated temperature resistance (except special formulations which can operate up to 350° F); have low permeability to gases.
Buna-N Butadiene-Acrylonitrile Rubber, Mil-P-5315, or MIL-P-5516, 60 Durometer)	-65 to 160	300	10^7	10^8	Comparable to neoprene in radiation stability (average for elastomers); 25% change in useful seal mechanical properties at 7×10^6R; has higher radiation stability when irradiated in inert atmosphere vacuum, or in contact with diester oils; fair heat resistance with low permeability to gases. Becomes brittle at higher radiation doses
Polyurethane	-423 to 240	350	10×10^7	10^9	No changes in hardness at 10^9; 25% change in tensile strength and elongation with irradiation at 5×10^9R; little difference between effects in air or vacuum; stable in radiation to 260° F. Electron irradiation equivalent to 10^8R causes complete loss in strength.

Table 11-25 (Cont.)

Material	Temperature (°F)		Reactor Gamma Radiation Dose (rad) in Air		Remarks
	Continuous Operation	Maximum Tolerable (Short Time)	Continuous Operation, Maximum	Maximum Tolerable[a]	
Polysulfide MIL-S-8802 Fuel Tanks	-65 to 250	–	10^6	10^8	Loses tensile strength at 10^6R, but retains elongation; loss in elongation at 10^8R; changes in air or vacuum similar. Ultraviolet radiation increased temperature so heat effect masked UV radiation effect.
Mil-S-7124 Structural Seal	-65 to 180	–			
Mil-S-7126 Glass and Plastic Seal	-40 to 225	–			
Natural Rubber	–	–	10^7	10^8	Loss in tensile strength and elongation at 10^7R; damage threshold for loss in greater than 25% of mechanical properties about 10^8R; little difference between irradiation in air or vacuum.

(a) More than 25% change in most sensitive property.

Table 11-26

TEMPERATURE AND RADIATION RESISTANCE OF PLASTIC MATERIALS FOR SEALING APPLICATIONS
(Ref. 17)

Material	Service Temperature Range (°F)	Reactor Gamma Dose (Rad) in Air		Remarks
		Continuous Operation Maximum	Maximum Tolerable[a]	
Polytetrafluoro-ethylene Teflon (TFE) MIL-P-22242 AMS 3651	-423 to +500	1×10^5	1×10^6	Resistance to radiation better in air than in vacuum; 8×10^7 rad causes 25% loss in tensile strength in vacuum. Fiberglass reinforced showed loss of 40% in strength in air at 10^8 rad.
Fluorinated ethylene propylene Teflon (FEP) AMS 3647	-423 to +400	1×10^6	1×10^7	Radiation resistance somewhat better than Teflon TFE. About the same in vacuum as TFE. Both TFE and FEP are about one to two orders of magnitude more radiation resistant in vacuum than in air.
Polychlorotrifluoro-ethylene KeLF MIL-P-46036 AMS 3646	-423 to 350	5×10^6	5×10^7	Slightly more radiation resistant in air and vacuum than TFE and FEP Teflon. Little improvement in properties in vacuum. Showed no change in properties in liquid N_2 at -320°F and 5×10^6 rad.
Polyvinylidene fluoride Kynar MIL-P-46122	-80 to +300	1×10^7	5×10^7	Radiation resistance about the same in air as in vacuum. Resistant to ultra-violet radiation damage.
Polyethylene MIL-P-23536 MIL-P-43081 MIL-P-22748 (High Density)	-100 to +180	2×10^7	9×10^7	Resistance to radiation is better in vacuum than in air. Threshold for damage in vacuum is about 5×10^8 rad.
Polyamide Nylon	-320 to +300	9×10^5	5×10^6	Radiation resistance a little better than the fluorocarbon Teflon TFE and FPE. Threshold in vacuum about 5×10^8 rads tensile strength increases at 10^9 rads then increases substantially at higher doses.
Polyimide Nomex HT-1	-423 to +500	3×10^8	2×10^9	Has good strength retention to 10^7 rads at 500°F
Polyvinyl Chloride PVC L-P-535 L-P-510 MIL-P-6264	-100 to +200	2×10^7	1×10^8	Releases HCL when irradiated at 10^8 rads. Corrosive gas could be detrimental to mating parts and dangerous in cabin atmosphere.

(a) More than 25% change in most sensitive property.

The important changes in properties of the plastic sealing materials are the drastic decrease in tensile strength and elongation. Generally the change in elongation is the most sensitive property. It will begin to decrease slightly at the minimum dose shown in Table 11-26. The conservative selection condition would be to ensure that the radiation exposure stays perhaps a factor of 2 to 5 below the minimum level to assure no change in the most significant property.

The effect of reactor gamma radiation on materials for sealing applications is summarized in Figs. 11-7, 11-8, and Table 11-27.

11.4.5 Effect of Solar Radiation

Because seals are generally confined within a component inside the spacecraft structure, they are not directly exposed to solar infrared or ultraviolet radiation. For seals that may be used externally on the spacecraft and that may be directly exposed, surface degradation, cracking and discoloration can occur. Such degradation does not affect the bulk mechanical properties of a plastic and elastomer when used in thick sections (e.g., > 0.060 in.) because of the short penetration range of ultraviolet radiation in the materials. However, cracking can result in increased permeability to gases. Discoloration may lead to higher equilibrium temperatures in space because of an increase in solar absorptivity of the surface.

The ultraviolet stability of some common elastomers is listed in the order of decreasing stability: (1) silicone, (2) butyl, (3) Neoprene, (4) polysulfide, (5) natural rubber. Cross linking is the predominant mechanicsm causing changes in the properties of natural rubber, Neoprene and silicone elastomers. These polymers become harder and progressively more brittle, and are susceptible to cracking and decreased elongation. Butyl, polysulfide and fluoro-rubbers undergo a chain scission process wherein depolymerization and softening are characteristic. Polymer stability is maximized by incorporation of small fractions of ultraviolet absorbers into the formulation which preferentially or selectively absorb the incident radiation and convert and emit it as thermal energy. A second approach is based on the high reflectivity and inertness of metallic coatings to ultraviolet. It embodies the plating or vacuum deposition of materials such as aluminum and metallic oxides on the surface of the elastomer or plastic to be exposed to sunlight. Generally the heat effects of heat-sensitive elastomers exposed to ultraviolet radiation masks the effect of the UV radiation (Ref. 17).

A summary of the effects of ultraviolet radiation on some polymeric materials used in sealing applications is shown in Table 11-28.

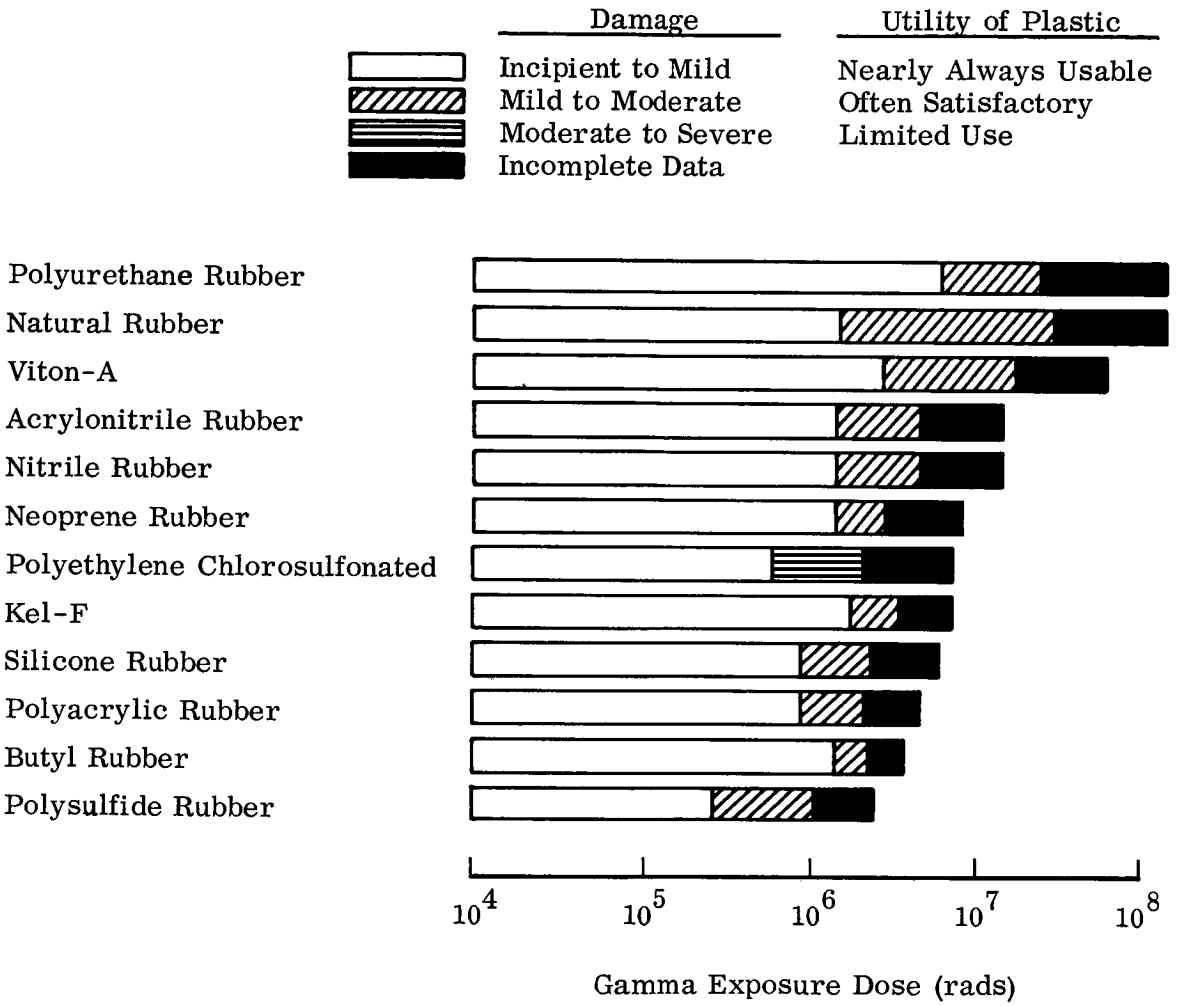

Fig. 11-7 Relative Reactor Gamma Radiation Stability of Elastomers for Seals (Ref. 17)

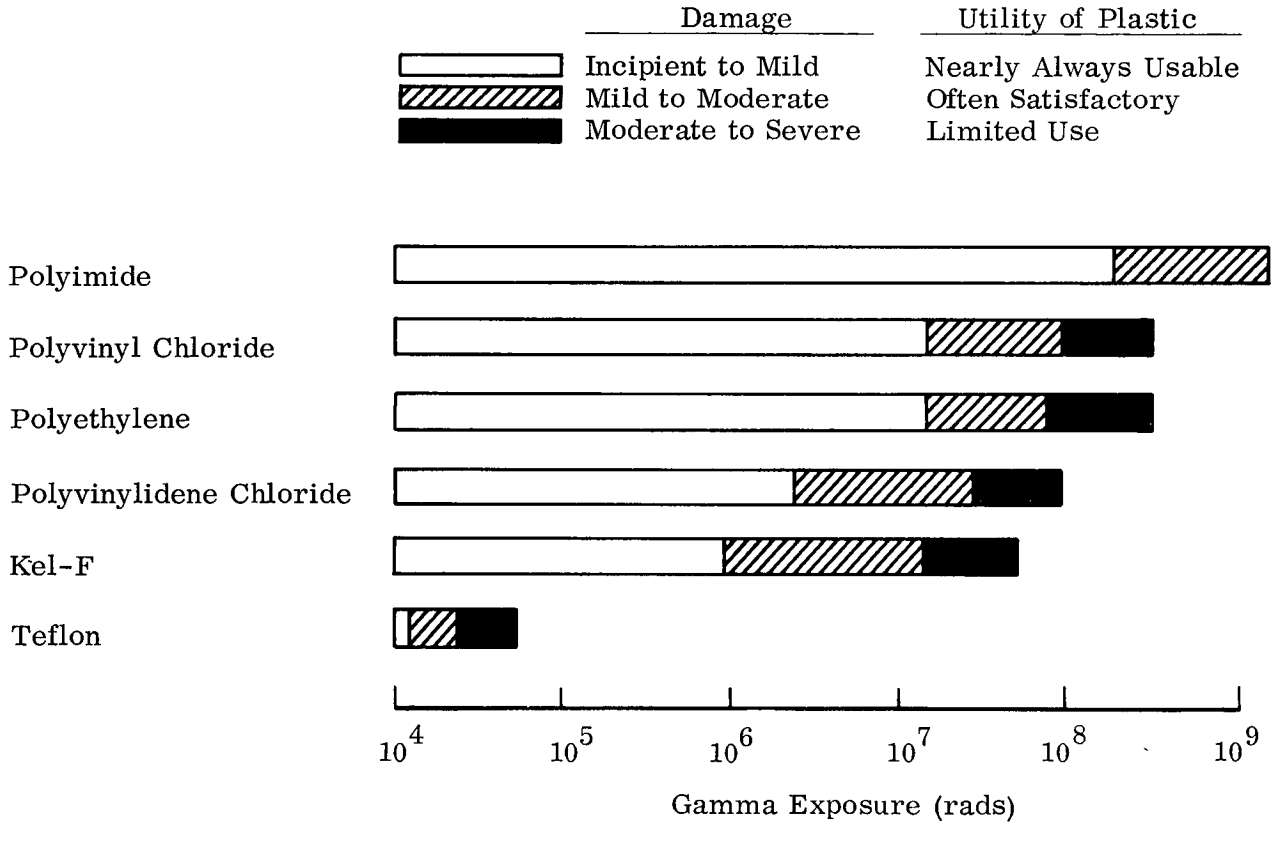

Fig. 11-8 Relative Reactor Gamma Radiation Resistance of Thermoplastic Materials for Seals

Table 11-27

EFFECT OF VACUUM ON REACTOR GAMMA RADIATION STABILITY OF SEVERAL POLYMERS (Ref. 17)

Polymer	Effect of Vacuum[a]
Plastics	
Diallylphthalate	No significant effect
Epoxy	No significant effect
Mylar	Improves stability
Polyamide (nylon)	No significant effect
Polycarbonate	Slight improvement
Polyethylene	Improves stability
Polyvinyl chloride	Decreases stability
Silicone	Improves stability
Teflon	Improves stability substantially
Kynar (polyvinylidene fluoride)	No significant effect
Tedlar (polyvinyl fluoride)	No significant effect
Kel-F (trifluoromonochloroethylene)	Improves stability
Elastomers	
Polyacrylic	No significant effect
Butyl	No significant effect
Hypalon (chlorosulfonated polyethylene)	Decreases stability
Neoprene	No significant effect (conflicting data)
Nitrile	Decreases stability
Polysulfide	No significant effect
Polyurethane	No significant effect
Silicone	No significant effect
Viton-A	Improves stability

(a) These effects are only general; individual compositions may behave differently at different energy levels. Particulate radiation (protons, electrons) can have different effects.

Table 11-28

EFFECT OF ULTRAVIOLET RADIATION ON POLYMER STABILITY (Ref. 17)

Polymer	Effect of Ultraviolet Energy[a]
Plastics	
Mylar	Decreases tensile strength and elongation
Polyamide (nylon)	No significant effect
Polymethyl methacrylate	Surface discoloration and crazing
Polyethylene	Embrittlement
Polypropylene	Embrittlement
Polyimide	No significant effect
Polystyrene	Yellows
Plasticized polyvinyl chloride	Develops tacky and discolored surface
Teflon	No significant effect
Elastomers	
Butyl	Increases tensile strength and elongation
Hypalon (chlorosulfonated polyethylene)	No significant effect
Neoprene	Increases tensile strength, decreases elongation
Nitrile	Decreases tensile strength and elongation
Styrene-butadiene (SBR)	Decreases tensile strength and elongation
Silicone	Surface crazing
Viton A	No significant effect

(a) Relative only, since spectral distribution and total exposure in equivalent sun hours not specified.

11.5 REFERENCES

11.5.1 Cited References

1. H. L. Fisher, Chemistry of Natural and Synthetic Rubber, Reinhold Publishing Corp., New York, 1957

2. W. E. Burton, Engineering with Rubber, McGraw-Hill Book Company, Inc., New York, N.Y., 1949

3. G. G. Winspear, Rubber Handbook, R. T. Vanderbilt Company Inc., 230 Park Ave., New York, N. Y., 1958

4. M. Morton, Introduction to Rubber Technology, Reinhold Publishing Corp., New York, N.Y., 1963

5. E. G. Rochow, Chemistry of the Silicones, John Wiley and Sons, New York, N.Y., 1951

6. P. J. Larsen, "Engineering Elastomers," Product Engineering, 8 January 1962

7. L. A. Wood, Ethylene-Propylene Co-Polymers, National Bureau of Standards Report 7562, 20 July 1962

8. W. R. Sheehan, N. B. Levine, and J. Green, Elastomeric and Compliant Materials for Liquid Rocket Fuel and Oxidizer Application, ML-TDR-64-107, Part IV, April 1967

9. G. S. Whitby, C. C. Davis, and R. F. Dunbrook, Synthetic Rubber, John Wiley & Sons Inc., New York, N.Y., 1954

10. "Process Development Program Nitroso Rubber Terpolymer," Parts I through III, Air Force Materials Laboratory Wright-Patterson AFB, Ohio (IR-9-363 I through III), July 1966, Oct 1966, Jan 1966

11. E. C. Stump, W. H. Oliver, and C. D. Padgett, "Synthesis and Polymerization of Fluorinated Sulfur Modified Nitroso Rubber," U.S. Army Natick Laboratories, 23 April 1964

12. "Carboxy Nitroso Rubber Data Brochure," PD 10-2, PD-10-3, Thiokol Chemical Corp., Reaction Motors Division, Denville, New Jersey

13. A. G. Pickett and M. N. Lemmcoe, "Handbook of Design Data on Elastomeric Materials," Southwest Research Institute, ASD-TR-61-234, June 1961

14. J. A. Brydson, Plastics Materials, D. Van Nostrand Company Inc., Princeton, New Jersey, 1966

15. R. Fabian, "Materials for Gaskets, Packings and Seals," Materials in Design Engineering, December 1959

16. J. S. Islinger, "Sealing Against Vacuum," Institute of Environmental Sciences, 1963 Proceedings, Los Angeles, California, April 1963

17. N. J. Broadway and S. Polinchak, "The Effect of Nuclear Radiation on Elastomeric and Plastic Components and Materials," Radiation Effects Information Center, Battelle Memorial Institute, REIC Rept. No. 21 Addendum, 31 August 1964

18. A. G. Pickett and M. M. Lemmcoe, "Handbook of Design Data on Elastomeric Materials Used in Aerospace Systems," ASD TR-61-234, June 1961

19. C. L. Ballanca and I. O. Salyer, "Effect of Liquid Rocket Fuels and Oxidizers on Elastomeric O-ring Seals," Rubber Chemistry and Technology, Vol. 39, 4, Part 2, September 1966

20. Military Standardization Handbook – Rubber and Rubber-Like Materials, MIL-HDBK-149 (MR), U.S. Army Materials Research Agency, Watertown, Mass., 21 August 1962

21. W. G. Jurevic and J. B. Rittenhouse, "Structural Plastics Handbook," Lockheed Palo Alto Research Laboratory, AFML-TR-67-332, Lockheed Missiles & Space Co., Palo Alto, California, October 1967

22. J. B. Gayle, S. V. Caruso and C. T. Egger, "Vacuum Compatibility of Engineering Materials (Solids)," MTP-P & VE-M-63-11, George C. Marshall Space Flight Center, Huntsville, Ala. 16 September 1963

23. R. F. Muraca and J. S. Whittick, "Polymers for Spacecraft Applications," Final Report, Stanford Research Institute, SRI Project No. ASD-5046, 15 September 1967

11.5.2 Uncited References

J. G. Austin and J. B. Gayle, Vacuum Compatibility of Engineering Materials (Liquids and Semi-Solids), NASA-TM-X-53207, 5 February 1965

J. H. Baldridge and M. R. Inskeep, "Research on Rubberlike Materials for Applications Involving Contact with Liquid Rocket Propellants," WADC-57-651 May 1960

J. R. Bos and E. B. Weber, "Composite Elastomer-Metal O-Ring Seals," Chance Vaught Aircraft, Inc., WADC-TR-59-749, April 1960

C. S. Marvel, "Synthesis of Thermally-Stable Polymers," Air Force Materials Laboratory, Wright-Patterson AFB, Ohio (ML-TDR-64-39), January 1967

"Evaluation of Elastomers as O-Ring Seals for Liquid Rocket Fuel and Oxidizer Systems," ASD-TDR-63-496, September 1963

"The Language of Rubber," Elastomer Chemicals Department, E. I. DuPont de Nemours and Co., Inc., Wilmington, Delaware, January 1963

Chapter 12

ORGANIC MATERIALS FOR STRUCTURAL APPLICATIONS

R. E. Mauri

In this chapter, data on the effects of space environment on reinforced plastics are presented and discussed. For spacecraft structural applications, the changes in mechanical properties occurring in these composite materials from exposure to the individual and combined environments of penetrating radiation, temperature, vacuum, and solar ultraviolet radiation are some of the design considerations. Space environmental effects on polymeric materials for other functions such as adhesives, seals and sealants, and dielectrics and on spacecraft applications where optical, thermal and electrical properties are of principal concern are discussed in Chapters 7, 10, and 13.

Structural reinforced plastics are composite materials that consist of a binder, usually an organic resin, and the reinforcement material which can be a continuous or a discontinuous fiber. For most structural applications, continuous fiber reinforcements are used. The most common reinforcement used is glass fiber. There are several grades and configurations of fiberglass in use. Other fiber reinforcements that have been developed for use in aerospace structural applications are boron, carbon, graphite, and silica. The resin binders used are epoxy, epoxy-phenolic, phenolic, silicone, polyester, polyimide, and polybenzimidazole. A more complete treatment of the properties of reinforced plastics is given in Ref. 1.

12.1 PENETRATING RADIATION EFFECTS

The general effect of penetrating radiation on reinforced plastic composites consists of additional cross-linking in the thermosetting resin binder. This is manifested by increasing tensile strength, density, modulus of elasticity, and decreasing impact strength and ultimate elongation. The fibrous reinforcement is generally inorganic such as glass, asbestos, or silica and is not affected by radiation doses up to 10^{12} rads. Reinforced plastics are more radiation resistant than nonreinforced or unfilled plastics of the same chemical class. In general, the mechanical properties of reinforced plastics such as epoxy, phenolic, silicone, and polyester-glass fabric laminates are not significantly changed at doses up to 10^8 rads, and some retain useful properties up to 10^{10} rads. The general ranking in decreasing order of radiation resistance (damage threshold) is: phenolics, epoxies, polyesters, and silicones.

The effects of radiation on reinforced plastics as well as other polymeric materials is dependent on the other ambient environments to which the material is exposed, such as elevated or reduced temperatures and vacuum or air atmospheres. Generally, the effects are not additive and must be determined by experiment for a given material. As a rule, the effects of penetrating radiation and elevated temperature on a polymer in air are more severe than the effects of the same dose of radiation and elevated temperature in vacuum or inert atmosphere.

Table 12-1 (Refs. 2, 3, and 4) summarizes the effects of reactor (gamma) radiation on typical phenolic, epoxy, silicone, and polyester glass fabric reinforced plastic laminates. Ultimate tensile strength and elongation are reported before and after irradiation in vacuum and air. Radiation doses were of the order of 10^7 to 10^8 rads (10^9 to 10^{10} ergs g^{-1}(C)); measured temperatures during irradiation ranged from ambient to 200 °F; and pressures during irradiation were from atmospheric to 5×10^{-7} Torr. The data indicate that the tensile strengths of epoxy, phenolic, polyester, and silicone laminates generally increased at radiation doses up to 10^8 rads (1×10^{10} ergs g^{-1} (C)) in vacuum; epoxy had the greatest increase, followed by Mobiloy 81-AH7 phenolic. At 3×10^8 to 6×10^8 rads (3×10^{10} to 6×10^{10} ergs g^{-1} (C)), decreasing tensile strengths were evident for all laminates except the CTL-91LD phenolic. The silicone and polyester laminates showed the greatest change. Laminates irradiated in air at doses up to 4×10^8 rads (4×10^{10} ergs g^{-1} (C)) generally showed decreasing tensile strengths (with the exception of the epoxy laminate) compared with the unirradiated controls. The best strength retention in air at such doses was exhibited by the epoxy and phenolic laminates. Silicones and polyesters show the least strength retention after irradiation in air. Ultimate elongations were not significantly changed for any of the laminates irradiated in air or in vacuum at doses up to 6×10^8 rads.

Effects of radiation on phenolic, epoxy, polyester, and silicone-glass fabric laminates at ambient and cryogenic temperatures (liquid hydrogen immersion at -423 °F) are given in Table 12-2 (Ref. 4). These data indicate that the tensile strengths of all the laminates except the epoxy increased when irradiated in air at the dosage indicated. The 1.5×10^8 rad dose on the laminates immersed in liquid hydrogen produced an increase in the tensile strengths of the phenolic and silicone laminates. The polyester and epoxy laminates decreased about 25% and 3.0%, respectively. At this temperature and dose, however, the tensile strengths were from 40 to 110% greater than those of the laminates tested in air at 77 °F.

Additional data on the effects of radiation at cryogenic temperatures on a phenolic glass fabric laminate (Conolon 506) and a polyester glass fabric laminate (Paraplex P-43) are given in Figs. 12-1, 12-2, and 12-3 (Ref. 5). At exposure doses of 6×10^8 rads, no change in the ultimate tensile strength occurred at liquid nitrogen temperature (-320 °F). Although tensile strength increased at -423 °F, this was believed to be caused by chemical reactions between the ionized or dissociated hydrogen atoms and the resin rather than the lower temperature.

The phenolic glass laminate and polyester glass laminate changed little in strength and modulus of elasticity at cryogenic temperatures, but the ultimate elongation increased. This effect may be due to the breaking of resin-to-glass adhesion because of differential thermal contraction.

Figures 12-4 through 12-7 (Ref. 6) compare the tensile and flexural strength retention of epoxy and phenolic laminates and moldings reinforced with woven and unwoven fibers of glass, silica, asbestos, and graphite under individual and combined environments of radiation and vacuum when tested at 78 ° and -300 °F.

Table 12-1

EFFECTS OF REACTOR RADIATION ON TENSILE PROPERTIES OF GLASS FABRIC LAMINATES IN AIR AND VACUUM

Loading Rate	Material and Trade Name	Gamma Dose (rads)	Ultimate Tensile Strength (psi)	Ultimate Elongation (percent)	Temperature (°F)	Pressure (Torr)
Low	Epoxy Epon 828 (Shell Chemical Co.)	0	37,452	1.40	77	760
High		1.38×10^{8} (a)	47,715	2.0	153	0.3
High		1.97×10^{8} (a)	55,489	–	205	5×10^{-6}
Low		8.6×10^{7} (a)	42,141	1.5	158	0.3
Low	Phenolic Conolon 506 (Narmco Div., Whittaker Corp.)	0	41,333	1.5	77	760
High		1.25×10^{8} (a)	53,568	2.25	153	0.3
High		1.97×10^{8} (a)	64,250		77	5×10^{-6}
Low		9.7×10^{7} (a)	41,765	1.45	158	0.3
Low		10^{8}	41,850	1.91	77	760
Low	Silicone DC-2106 (Dow Corning Corp.)	0	23,914	1.42	77	760
Low		4.48×10^{8} (a)	21,276	1.32	104	5×10^{-7}
Low	Phenolic CTL-91-LD (U.S. Polymeric Co.)	0	26,170	1.11	77	760
Low		4.48×10^{8} (a)	29,815	1.23	110	5×10^{-7}
Low	Phenolic Mobiloy 81-AH7 (Cordo Molding Products, Inc.)	0	49,238	1.60	77	760
Low		6.0×10^{7}	46,381	1.52	100	760
Low		1.07×10^{8}	49,380	1.54	100	760
Low		3.9×10^{8}	47,368	1.51	100	760
Low		4.1×10^{7} (a)	55,838	1.63	160	8×10^{-7}
		1.4×10^{8} (a)	58,741	1.51	160	8×10^{-7}
		3.1×10^{8} (a)	42,317	1.25	200	6×10^{-7}
	Polyester Paraplex P-43 (Rohm & Haas Co.)	0	39,173	1.88	77	760
		6.0×10^{7}	32,941	1.66	100	760
		1.07×10^{8}	35,445	1.63	100	760
		3.9×10^{8}	36,773	1.80	100	760
		4.1×10^{7} (a)	42,768	1.94	160	8×10^{-7}
		1.4×10^{8} (a)	40,356	1.88	200	6×10^{-7}
		3.1×10^{8} (a)	31,908	1.53	–	–
	Silicone DC-2104 (Dow Corning Corp.)	0	19,406	1.05	77	760
		6.0×10^{7}	20,515	1.05	100	760
		1.07×10^{8}	19,423	1.02	100	760
		3.9×10^{8}	20,734	1.17	100	760
		3.8×10^{7} (a)	21,099	1.28	160	8×10^{-7}
		1.4×10^{8} (a)	21,820	1.20	160	8×10^{-7}
		2.85×10^{8} (a)	16,400	1.06	200	6×10^{-7}
	Polyester Selectron 5003 (Pittsburgh Plate Glass Co.)	0	45,429	1.99	77	760
		6.0×10^{7}	47,805	1.86	100	760
		1.07×10^{8}	41,879	1.69	100	760
		3.9×10^{8}	45,815	1.79	100	760
		7.2×10^{7} (a)	52,657	2.05	130	10^{-3}
		1.05×10^{8}	46,080	1.97	150	10^{-3}
		2.85×10^{8} (a)	44,786	1.92	200	6×10^{-7}

(a)Irradiated in vacuum; others irradiated in air.

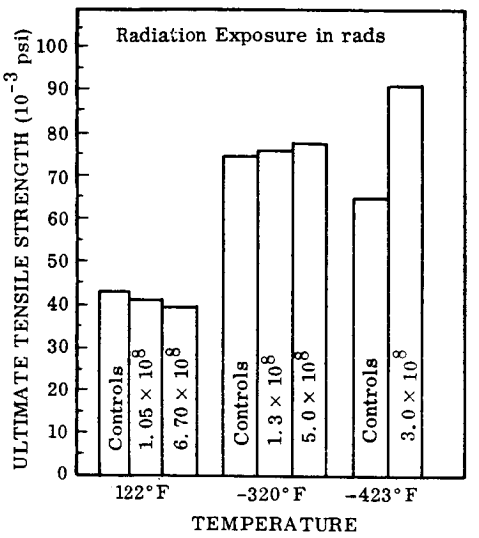

Fig. 12-1 Radiation-Cryogenic Temperature Data for a Glass-Fabric Phenolic Laminate (Conolon 506)

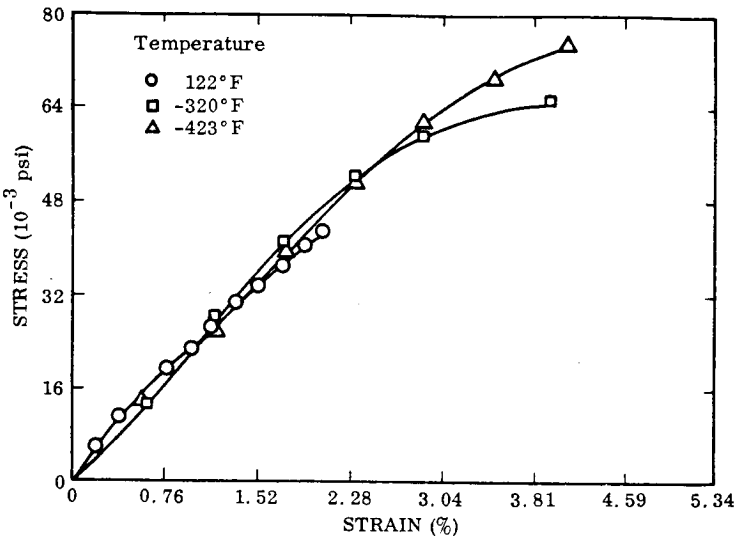

Fig. 12-2 Typical Stress-Strain Temperature Response Curve for a Structural Laminate (Conolon 506)

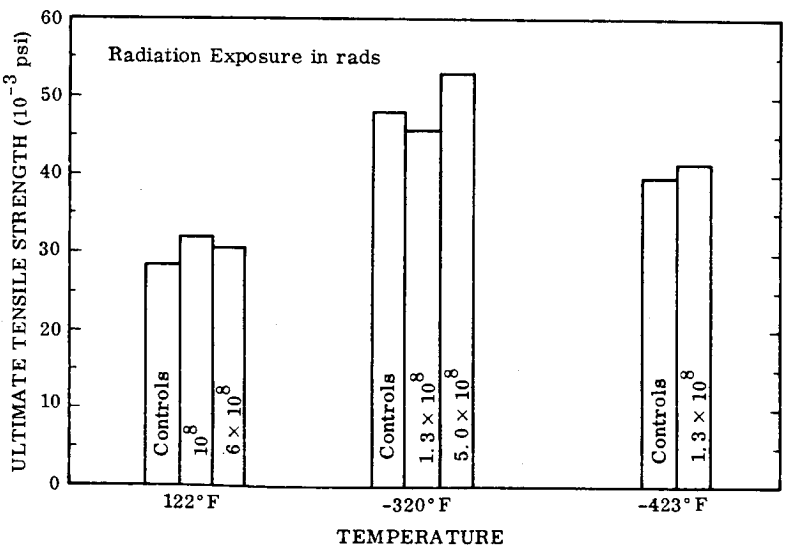

Fig. 12-3 Radiation-Cryogenic Temperature Data for a Glass-Polyester Laminate (Paraplex P-43)

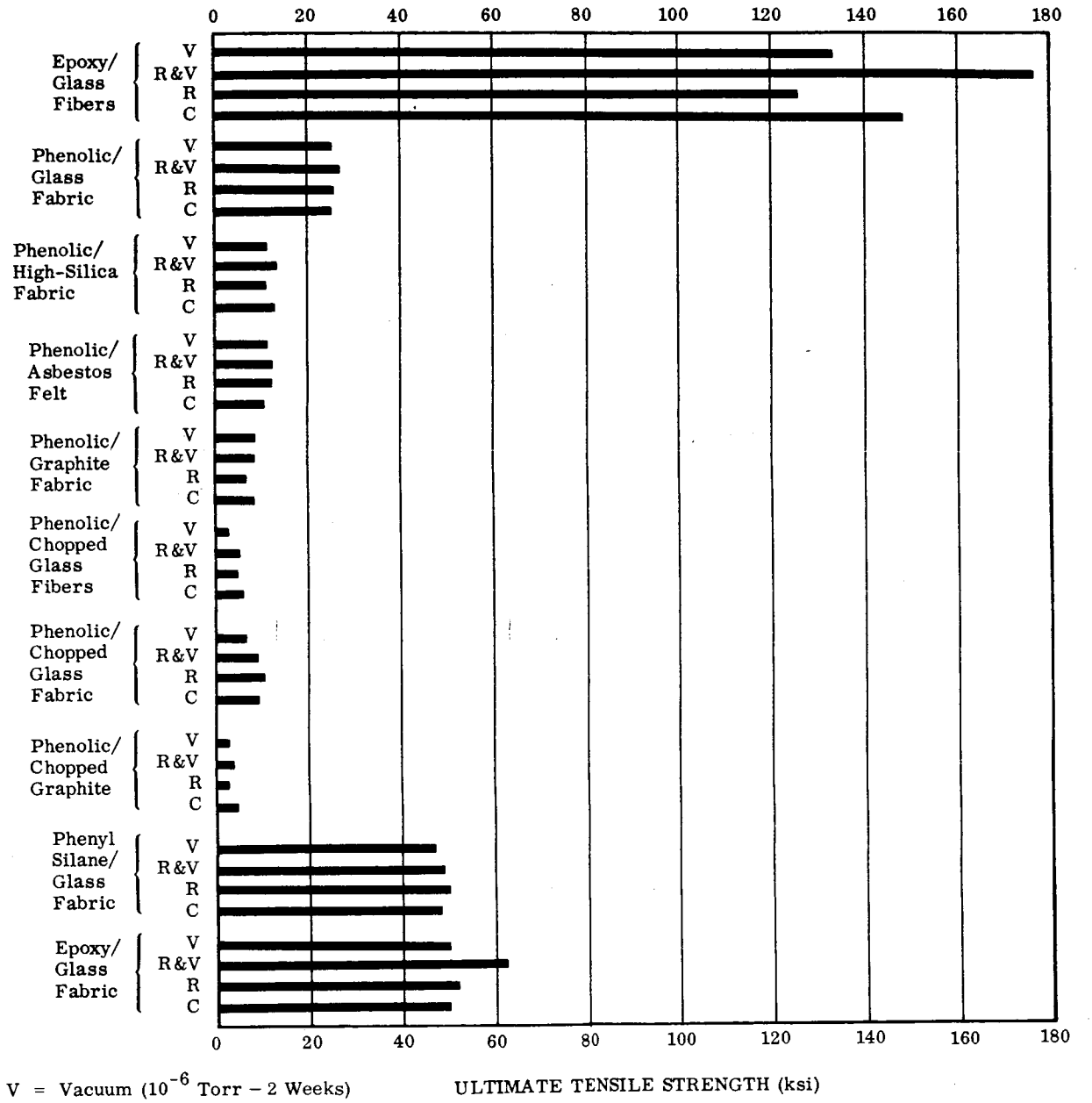

Fig. 12-4 Comparison of Ultimate Flexure Strength Retention of Reinforced Plastics

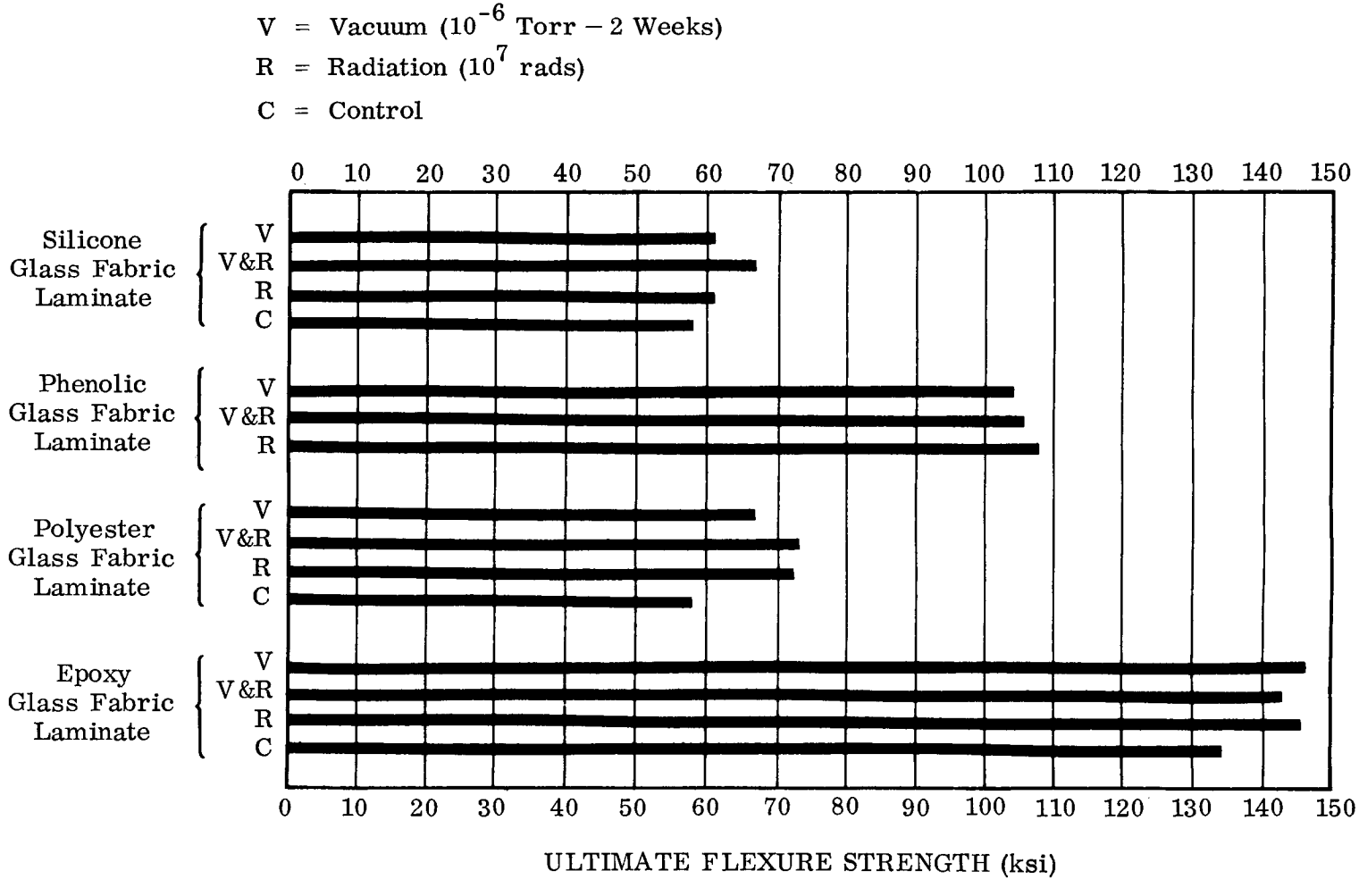

Fig. 12-5 Comparison of Ultimate Flexure Strength Retention of Reinforced Plastics at -300°F

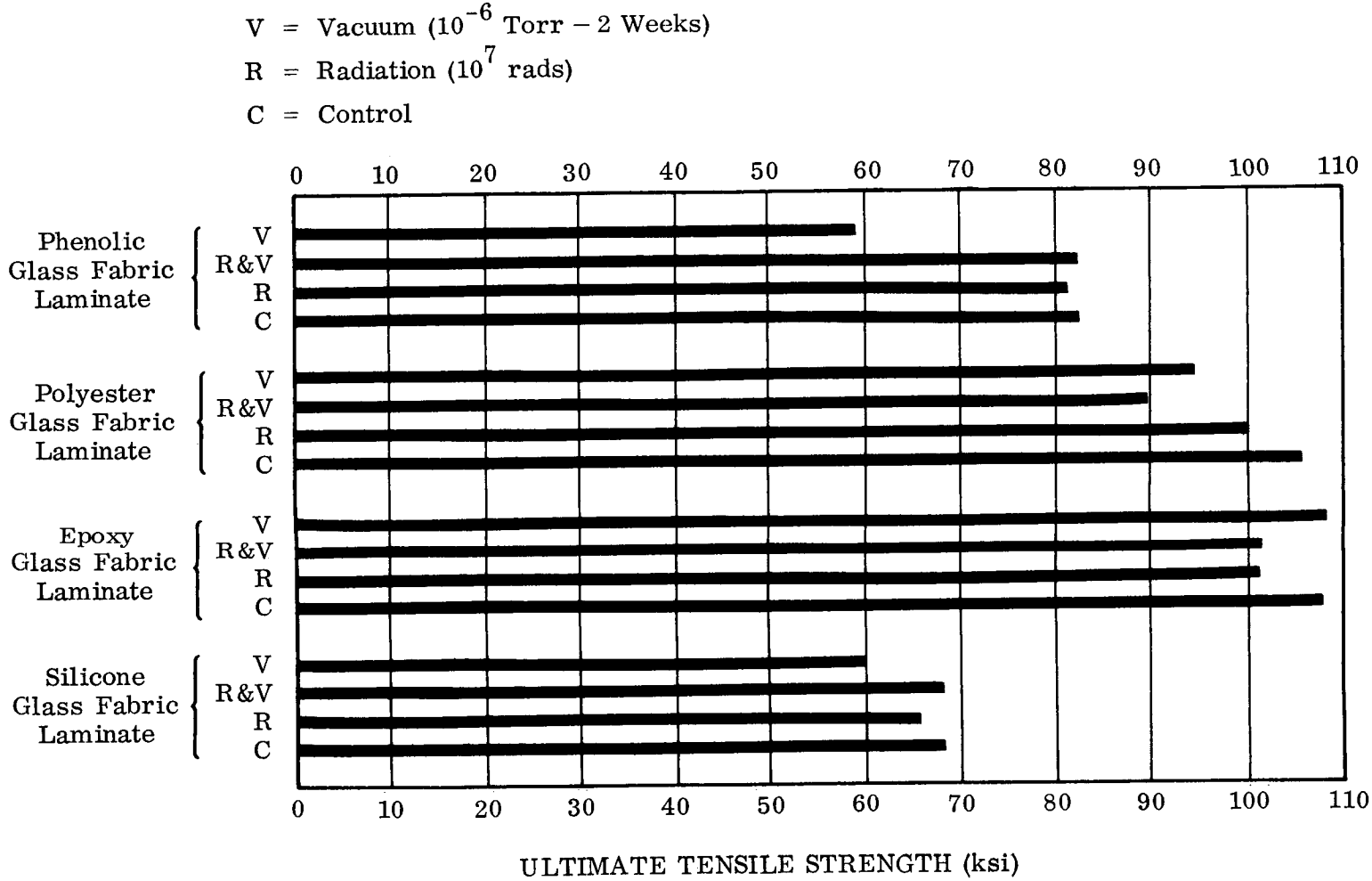

Fig. 12-6 Tensile Strength Retention of Laminates at -300°F

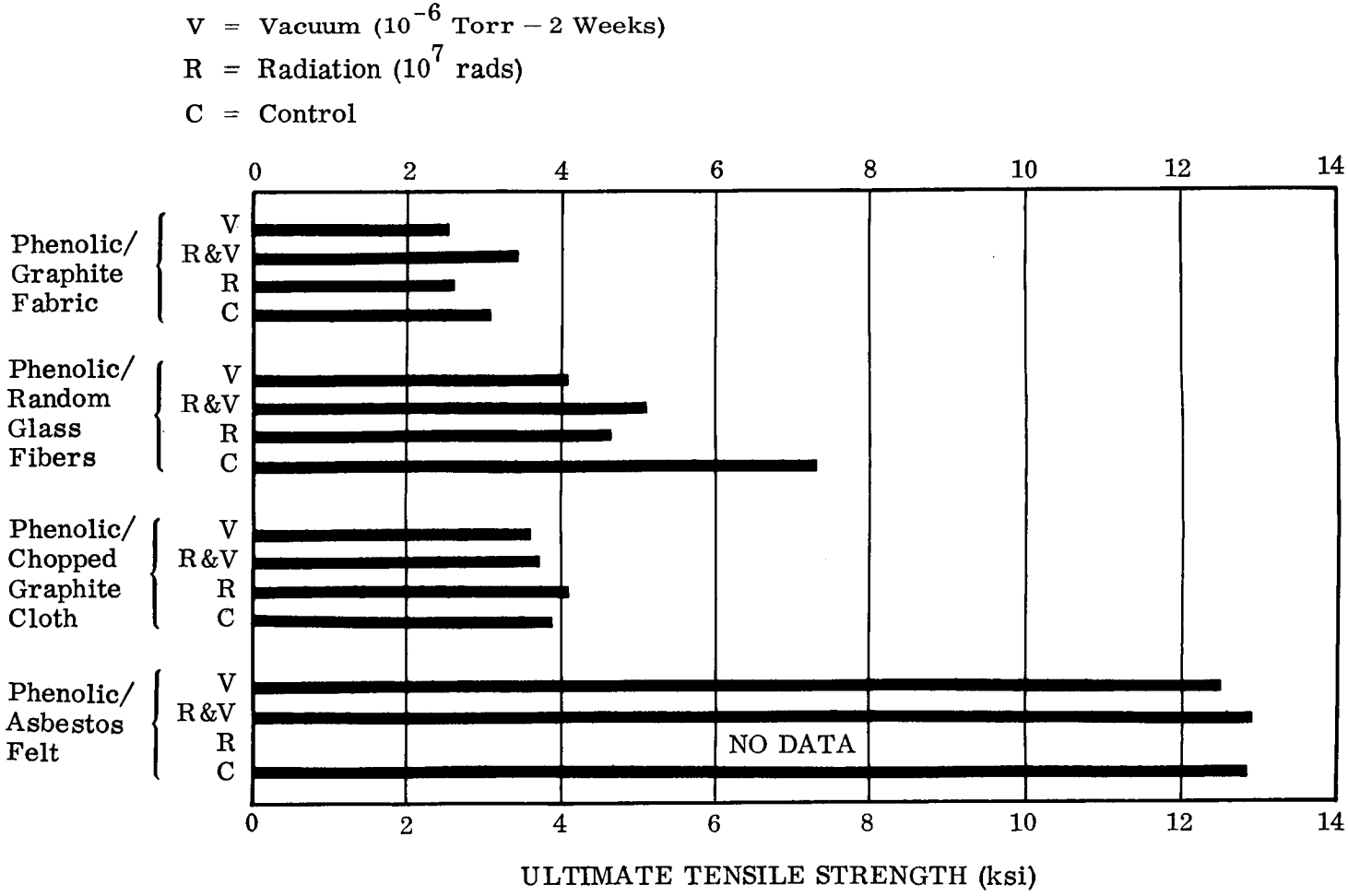

Fig. 12-7 Ultimate Tensile Strength Retention of Reinforced Plastics at -300°F

Table 12-2

EFFECT OF REACTOR RADIATION ON ULTIMATE TENSILE STRENGTH OF GLASS FABRIC LAMINATES

Material	Ultimate Tensile Strength (psi)			
	Ambient Air (77 °F)		Liquid Hydrogen (-423 °F)	
	Control	Gamma Dose 1.7×10^9 rads	Control	Gamma Dose 1.5×10^8 rads
Phenolic Mobaloy 81-AH7 (Cordo Molding Products, Inc.)	36,100	36,800	50,700	57,150
Silicone DC 2104 (Dow Corning Corp.)	24,200	32,000	55,000	56,300
Epoxy Epon 828/A (Shell Chemical Co.)	39,800	37,700	87,350	84,700
Polyester Selectron 5003 (Pittsburgh Plate Glass Co.)	39,000	43,900	70,800	53,200

12.2 SOLAR ULTRAVIOLET RADIATION EFFECTS

Ultraviolet radiation can produce photochemical reactions in the polymeric resin binder of reinforced plastics which are similar to the reactions taking place during exposure to penetrating radiation (i.e., cross-linking and chain scission). Because of the high absorptivity of the resins in the ultraviolet region of the spectrum, however, most of the energy is deposited near the exposed surfaces and damage effects are limited to changes in spectral properties such as darkening or an increase in solar absorptivity. The bulk of the material is not affected and mechanical properties of typical cross-sectional thicknesses used for structural applications on the external surfaces of a spacecraft are not significantly changed. Data on ultraviolet effects on reinforced plastics have been presented in Chapter 15 of the previous edition of this book (Ref. 7). The damage effects noted appear to have been due principally to the elevated temperatures produced by energy absorption during the accelerated ultraviolet irradiation rather than to the ultraviolet photolysis itself.

Solar ultraviolet radiation is judged to be an environment of minor importance insofar as its effects on the mechanical properties of reinforced plastics are concerned. Complete protection to external exposed spacecraft surfaces can be achieved by means of applying properly selected passive thermal control coatings such as are described in Chapter 7.

12.3 EFFECTS OF TEMPERATURE EXTREMES

The use of active and passive thermal control systems on spacecraft to balance the rates of solar energy absorption and the emission of internal heat to space narrows the range of maximum to minimum temperatures which spacecraft materials and components must encounter in service. Such temperature ranges are about -100° to 250°F. At these temperatures, strength properties are changed reversibly, and more drastic effects such as chemical degradation do not occur. Higher temperatures result from aerodynamic heating in reentry, but a discussion of the effects is beyond the scope of this book. A treatment of the data for heat shield (reentry) materials is given in Ref. 8. Temperatures as low as -423°F, the boiling point of liquid hydrogen, are attained by reinforced plastics in contact with cryogenic fluids (e.g., propellant storage).

12.3.1 Elevated Temperature Effects

Moderately elevated temperatures up to 250°F reduce the mechanical strength properties of reinforced plastics and accelerate the rate of outgassing of entrapped gases and volatiles with accompanying weight loss by the material. Synergistic effects are generally produced with combined environments such as penetrating radiation which cannot be predicted from the effects produced by each environment acting alone. The effects of combined environments are greatly dependent on the exposure conditions and type of material and must be determined experimentally. At temperatures above 400° to 500°F, depending on the chemical structure of a polymer, the ambient atmosphere, and the exposure time, chemical decomposition or pyrolysis can occur which drastically and irreversibly causes a reduction in its useful mechanical properties. In a vacuum or inert atmosphere, the effects of elevated temperature on a polymer are generally less than at the same temperature-time conditions in air because only purely thermally induced decomposition or unzipping of molecular chains can occur in the absence of air, whereas in air the polymer can undergo both oxidation and pyrolysis degradation. (See Refs. 9 and 10.) Because the rate of degradation of polymers at elevated temperatures is less in vacuum than in air, their upper temperature service limit is increased for extended missions.

The effects of elevated temperature on reinforced plastics have been reviewed and summarized in Ref. 1. Mechanical and physical property data on commercially available phenolic, epoxy, and silicone resin composites with various combinations of glass, silica, carbonaceous, and asbestos fibrous reinforcements in woven and unwoven form are presented. These resin-reinforcement systems find widespread aerospace applications in which long-term thermal resistance, exhibited by high strength retention to temperatures as high as 500°F, is required. The more recently developed high-temperature-resistant resin-reinforcement systems, capable of withstanding 1000°F for short exposures, such as the polymides, diphenyl oxides, and polybenzimidazoles, are discussed in Ref. 1. Some discussion of the properties of reinforced plastics using these new resins will be presented here. A representative presentation in Fig. 12-8 compares the flexural strength at elevated temperature of the new heat-stable resins.

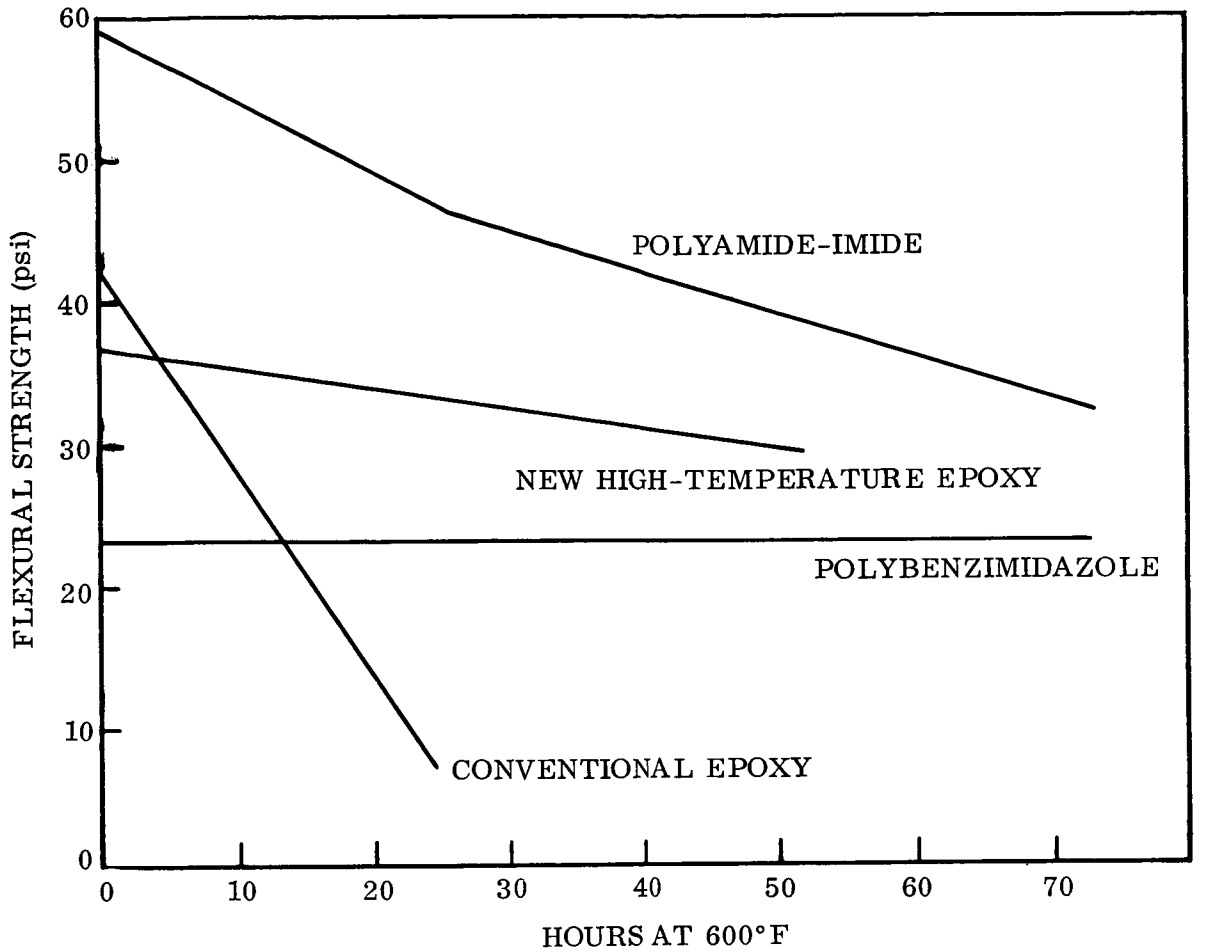

Fig. 12-8 Flexure Strength Versus Time of Glass-Reinforced Laminates at 600°F

12.3.1.1 Polybenzimidazoles (PBI)

These resins consist of a totally aromatic chemical structure with improved thermal and oxidation stability. They are produced by the condensation reaction of aromatic dicarboxylic compounds of diphenyl esters and aromatic tetramines such as diaminobenzidine. As a result of their complete aromaticity, the polymers have high glass transition temperature (T_G), are infusible below 750°F, and are soluble only in high boiling, highly polar solvents. Because of their infusibility and intractability, use of these polymers as laminating resins for the preparation of reinforced plastics requires the synthesis of a pre-polymer stage which can be melted or dissolved into a lacquer in order to wet and impregnate the fibrous reinforcement. During the subsequent cure, the polymer becomes infusible and achieves its ultimate high-temperature-resistant properties.

In Table 12-3 (Ref. 11), the typical mechanical properties at ambient and elevated temperatures of PBI structural reinforced laminates made with 181 – AF-994-HTS glass fabric reinforcement are presented.

Table 12-3

TYPICAL ELEVATED-TEMPERATURE MECHANICAL PROPERTIES OF POLYBENZIMIDAZOLE RESIN – GLASS FABRIC REINFORCED LAMINATES (Ref. 11)

Temperature (°F)	Flexural Strength (psi)	Compressive Strength (psi)
77	130,000	68,000
2 hr water boil	94,000	42,000
600 for 200 hr	37,000	10,000
700 for 1 hr	83,000	48,000
700 for 24 hr	53,000	–
800 for 1 hr	47,000	21,000

12.3.1.2 Polyimides and Diphenyl Oxides

Two other recently developed heat-resistant resins, the polyimides and the diphenyl oxides, are finding increasing usefulness for long-term high-temperature applications (up to 600°F). The polyimides are the reaction product of aromatic dianhydrides and aromatic diamines, with small quantities of trifunctional reactants included to promote cross-linking. The diphenyl oxide resins are reaction products of diphenyl oxide derivatives and formaldehyde. Recommended glass fiber coating or coupling agents for glass fabric reinforcements to obtain the best mechanical properties and high-temperature strength retention in structural reinforced plastic laminates are: A-1100 (Union Carbide Co.) and F-1A (Ferro Corp.) for the polyimides, and Y-2967 for the diphenyl oxide resins. Polyimide laminates can be fabricated using either vacuum bag or press molding techniques. The vacuum bag technique has the advantages of ease of fabrication and greater reproducibility in properties. The strength properties of polyimide (PI) laminates are unaffected by prolonged heating at 500°F in air as shown from the data in

Table 12-4 (Ref. 11) but lose considerable strength in air at service temperatures above 600°F. The strength properties of diphenyl oxide (DPO) laminates are little affected by heat aging in air at 400°F for long times as shown by the data in Table 12-5 (Ref. 11). At temperatures above 500°F in air, the strength properties of DPO resin laminates decrease at a fairly rapid rate.

When making a choice between the PI and DPO resins, the operating temperature and strength requirements must be taken into consideration to select optimum properties. The DPO resin laminates are stronger at room temperature but decrease in strength at a more rapid rate than PI resin laminates.

Reinforced plastics made from PBI, PI, and DPO resins are finding increased usage in structural aerospace applications where high strength-to-weight ratio and strength retention at elevated temperatures to 700°F for long durations, and low thermal conductivity are required. Current applications are mainly for supersonic aircraft and rockets which include: (1) structural dielectric materials for radomes and radio antenna housings, (2) motor cases and nozzles for solid propellant rockets, (3) structural parts such as leading edges, (4) turbine compressor blades in jet engines, and (5) adhesives in the case of PI and PBI resins. (See Chapter 10.) In general, they are relatively expensive and more difficult to process, since cure and post-cure times and temperatures are longer and higher than the conventional resin-reinforced plastics such as epoxies and phenolics but are finding new applications where their high strength and strength retention properties at high temperatures will give significant advantages over more conventional metallic and nonmetallic materials.

Another effect of elevated temperature on structural plastic materials is the offgassing of volatile constituents which results in a loss in weight of the composite.

Table 12-6 (Ref. 12) presents data on the weight loss of two types of phenolic laminates and an epoxy-glass fiber laminate at temperatures from 75° to 300°F in vacuum for periods up to 8 days. Results indicate that the epoxy laminate had 25 to 50% of the weight loss of the phenolic glass laminate at each test temperature, and up to 50% of the weight loss of the phenolic-cotton laminate. This behavior is to be expected since phenolics produce water of condensation during the curing reaction and have high initial volatile content, whereas epoxies do no cure by this mechanism.

Table 12-7 (Ref. 13) presents data on the weight loss of polyester, phenolic, epoxy, and silicone glass fabric laminates at elevated temperatures to 150°C (300°F) in vacuum. These data indicate that phenolics have among the highest weight losses (or volatile evolution) at elevated temperatures. The two types of polyester laminates gave mixed results, and the silicone and epoxy laminates had the least weight loss. The effect of specimen surface area on weight loss showed no definite trends. Usually the evolution of volatile constituents from polymers is diffusion controlled, and thus the initial weight loss is a function of the material thickness. (See Chapter 10.)

12.3.2 Reduced Temperature Effects

Some important effects of reduced temperatures on plastic materials are the increase in mechanical strength properties and the decrease in impact strength and fatigue life

Table 12-4

STRENGTH PROPERTIES OF POLYIMIDE-E GLASS (A-1100) FABRIC LAMINATES AT 500°F (Ref. 11)

Property	Control RT	Aging Time (hr) (500°F)			
		250	500	750	1000
Tensile Strength (psi × 10^3)	58.9	53	50.9	47.4	39
Tensile Modulus (psi × 10^6)	3.2	3.2	3.1	3.1	3.2
Compressive Strength (psi × 10^3)	51.9	45.8	54.4	50.0	46.2
Compressive Modulus (psi × 10^6)	3.4	3.7	–	3.8	3.7
Flexural Strength (psi × 10^3)	74.7	55.9	54.6	56.3	54.5
Flexural Modulus (psi × 10^6)	2.9	2.2	2.5	2.4	2.7
Interlaminar Shear Strength (psi)	1816	1888	1528	1356	1196
Bearing Strength Ultimate (psi)	60.4	54.1	40.6	39.2	33.6

Notes:

Resin – PI 2501 E. I. du Pont de Nemours Co., Inc.

Resin Content, 23.2%; specific gravity, 1.76; void content, 16.2%

Cure – Vacuum bag, 10 to 14 psia; room temperature to 350°F in 1/2 hr, hold at 350°F for 2 hr.

Post-Cure – 2 hr each at 400°, 450°, 500°, 550°F; and 8 hr at 600°F.

Table 12-5

STRENGTH PROPERTIES OF DIPHENYL-OXIDE-E GLASS (A1100) FABRIC LAMINATES AT 400°F (Ref. 11)

Property	Control RT	Aging Time (hr) (400°F)			
		250	500	750	1000
Tensile Strength (psi $\times 10^3$)	51.6	44.6	44.7	42.8	43.5
Tensile Modulus (psi $\times 10^6$)	3.3	3.2	2.8	3.2	2.8
Compressive Strength (psi $\times 10^3$)	70.9	63.2	60.5	59.4	57.3
Compressive Modulus (psi $\times 10^6$)	4.3	3.5	5.4	3.7	3.9
Flexural Strength (psi $\times 10^3$)	76.7	58.8	59.8	61.7	54.9
Flexural Modulus (psi $\times 10^6$)	3.9	2.6	2.6	1.3	2.2
Interlaminar Shear Strength (psi)	1190	1316	1354	1364	1880
Bearing Strength (psi)	94.7	59.9	71.2	68.6	52.8

Notes:

Resin – DP-94, Ironsides Co., Columbus, Ohio.

Resin content, 32.2%; specific gravity, 1.84; void content, 5.3%

Cure – Press at 310 psig at 320°F for 1 hr.

Post-Cure – 24 hr at each 50°F increment from 250° to 450°F in air.

under cyclic loads. These effects are manifestations of the tendency of these materials to undergo brittle fracture at decreasing temperatures in contrast to ductile behavior which they exhibit at ambient and elevated temperatures. The temperature at which sharp transitions occur in the mechanical, physical, and electrical properties of a material such as the change between ductile behavior and brittle-fracture vehavior in a plastic is known as the second-order transition temperature or the glass transition temperature (T_G). Polymers are glassy, brittle, and hard materials below their second-order transition temperature. As temperature is increased above T_G, the polymers become less rigid and have greater plasticity and elasticity. These physical changes are reversible with temperature and are attributed to the degree of atomic and molecular motion in the material (such as atomic rotation about a chemical bond) which is a function of the thermal energy available. Figure 12-9 shows schematically how the stress-strain properties of a polymer change as temperatures are increased from the glass transition temperature.

Table 12-6

WEIGHT LOSS FOR LAMINATES UNDER VACUUM-THERMAL CONDITIONS

Laminate	Weight Loss (%)								
	Temperature, 75 °F			Temperature, 150 °F			Temperature, 300 °F		
	Time (days)			Time (days)			Time (days)		
	1	5	8	1	4	7	1	4	7
Epoxy glass fiber	0.03	0.06	0.06	0.09	0.30	0.33	0.31	0.56	0.62
Phenolic glass fiber	0.11	0.24	0.29	0.24	0.48	0.55	0.97	1.25	1.32
Phenolic cotton	0.41	0.95	1.14	0.93	1.32	1.36	1.64	1.83	1.89

12.4 VACUUM EFFECTS

Polymers exposed to the high vacuum of space lose weight by two possible mechanisms. The first of these is evaporation or offgassing of volatile materials and entrapped gases. Volatiles can consist of low molecular weight polymer fractions or monomers, impurities, and additives. The latter are frequently incorporated to modify handling and cure properties and to obtain certain desirable properties in the finished product. This mechanism is relatively unimportant for long-chain, high-molecular-weight polymers of a high degree of purity. The second mode of weight loss consists of thermal or radiation induced decomposition of the polymeric structure into much lower molecular weight fragments. These fragments diffuse to the surface of the material and escape through evaporation. The evaporation rate is dependent upon the mean free path of the molecules. If this is large, none of the molecules leaving the surface encounter collisions and return to the surface. At high vacuums, such behavior is approached. Estimated rates of offgassing and weight loss of simple pure materials can be predicated by the Langmuir equation from a knowledge of the vapor pressure and the molecular weight of the gas species evolved. For most polymeric compositions, these paramaters are not defined

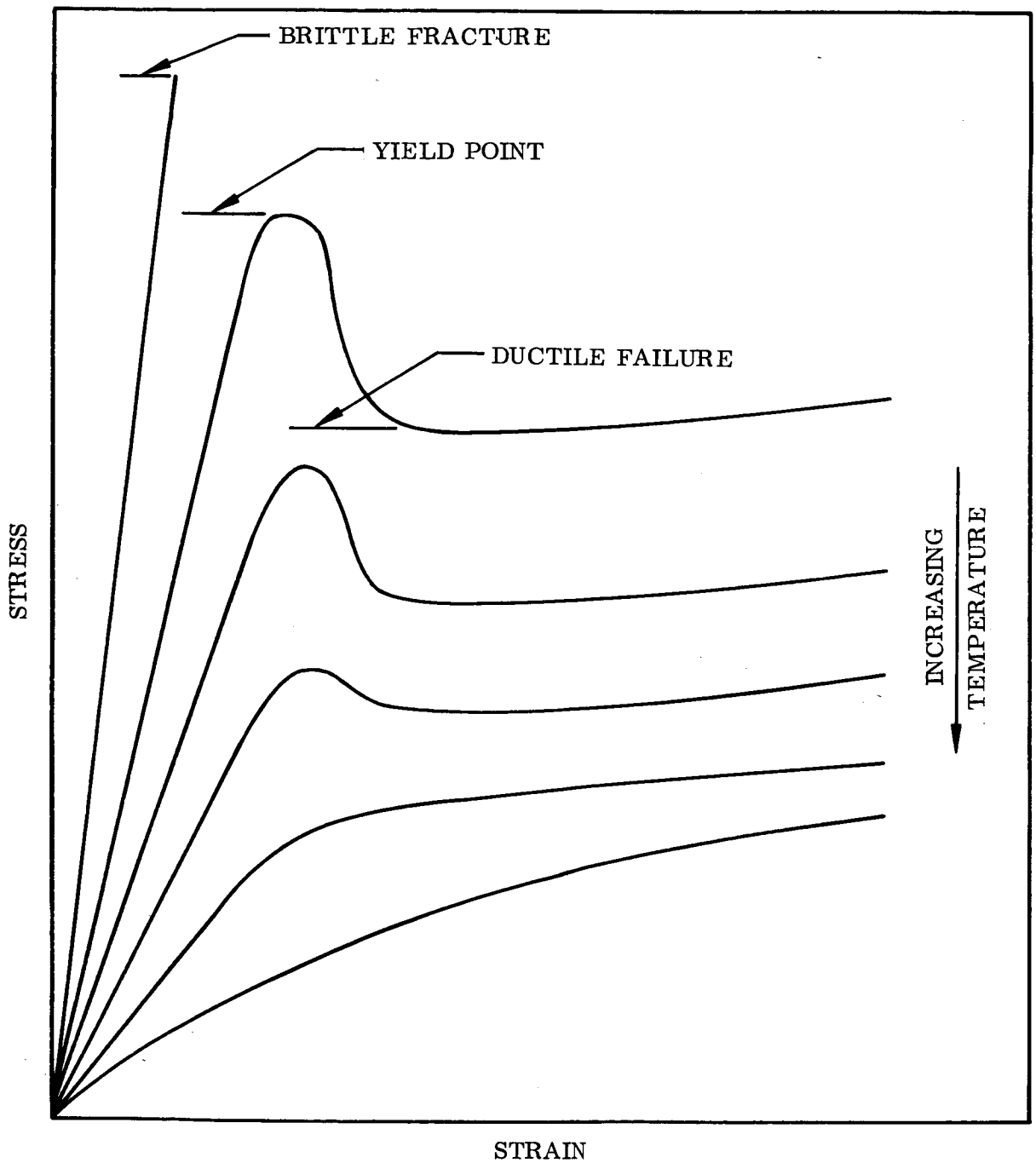

Fig. 12-9 General Stress-Strain Behavior of Polymers

and must be determined experimentally. For this reason, the Langmuir equation finds very limited application in predicting rates of polymer offgassing, and weight losses are usually determined directly by experiment.

Table 12-7

WEIGHT LOSS OF REINFORCED PLASTICS AT ELEVATED TEMPERATURES IN VACUUM

Material	Surface Area (cm^2)	Temperature (°C)	Weight Loss (%)	Pressure (Torr)
Paraplex P-43, polyester-glass fabric laminate	1.500	58	0.37	10^{-4}
	2.759	50	0.13	10^{-6}
	1.010	105	2.03	
	3.264	99	2.60	10^{-6}
CTL-91-LD, phenolic glass fabric laminate	3.207	54	0.90	10^{-5}
	2.027	105	1.78	10^{-5}
	2.061	104	1.55	10^{-6}
Epon 828, epoxy glass fabric laminate	2.979	55	0.16	10^{-5}
	3.210	48	0.08	10^{-6}
	2.121	101	0.27	10^{-6}
DC-2104, silicone glass fabric laminate	1.141	50	0.00	10^{-6}
	1.742	100	0.15	10^{-6}
DC-2106, silicone glass fabric laminate	2.285	41	0.13	10^{-5}
	2.382	47	0.12	10^{-6}
	2.087	103	0.32	10^{-6}
	1.434	105	0.21	10^{-6}
	8.410	150	0.08	
Selectron 5003 polyester glass fabric laminate	3.851	50	0.05	10^{-6}
	2.732	95	0.41	10^{-6}

In the case of weight loss which occurs through thermal or radiation-induced decomposition or depolymerization, there are no simple mathematical models or relationships which can be used to predict weight loss. Materials decompose by many different mechanisms; the products of degradation are often complex and depend on the temperature, radiation species, and the dose rate. Such cases must be studied experimentally. In most studies reported in the literature involving the thermal degradation of polymers

in vacuum, the temperatures at which the materials were studied have been much higher than those at which the materials are used in spacecraft service. These higher temperatures have been used to accelerate the degradation process so that experiments can be carried out in relatively short times. There have been few reports on the weight loss of polymers at relatively low temperatures and for periods of time which simulate or approach those expected in space vehicle applications. In most of the studies conducted, there has been little attention given to the dependence of the polymer degradation rate as a function of pressure; it has been assumed that the vacuum was sufficiently low to eliminate or minimize the reactions between the residual gas species and the polymer.

Studies of weight loss of polymers in vacuum have varied considerably in experimental technique. In many of the studies, weight loss has been measured after a given vacuum exposure for a fixed time. The data have often been extrapolated to much longer times. This has resulted in weight losses which are erroneously high.

A plot of weight loss versus time for polymers exposed to vacuum at ambient and elevated temperatures shows that the resulting curve has two characteristic parts. In the initial part of the curve, there is a high offgassing rate which is due to the loss of adsorbed and absorbed water and other atmospheric species as well as the evolution of polymeric fragments. Once these constituents have been released, the offgassing rate decreases to an equilibrium value. In this part of the curve, the loss of weight is due principally to volatiles released through degradation of the polymeric structure. Generally, this weight loss rate will remain invariant with time. If extrapolation of data obtained over relatively short times is made, care must be taken to assure that only the equilibrium weight loss rate is used.

The use of plastics in space vehicles introduces the possibility of another design consideration: condensation of offgassed products on critical optical and electrical components. Such condensation could impair their function during a space mission. Information on the volatile condensable material (VCM) offgassed from several polymeric materials is given in Chapters 10 and 11 and Ref. 14. When the products are noncondensable on a "cold"surface, they are unimportant in this respect.

The steady-state weight loss rate values at 350 °F as a function of pressure for cured phenolic, epoxy, and silicone resins are given in Fig. 12-10 (Ref. 15). In the case of the phenolic, weight loss data obtained for a single specimen are shown for both decreasing and increasing pressures. The data show the reversible nature of weight loss. Figure 12-11 (Ref. 15) illustrates the effect of temperature on the weight loss rate of a cast epoxy resin at atmospheric and reduced pressures.

A summary of steady-state weight loss rates for various plastic materials is presented in Table 12-8 (Ref. 15). The steady-state weight loss rates for the phenolic exposed at 350 °F were higher than the rates observed at 400 °F. To determine if the comparatively large weight loss rates observed at atmospheric pressure were due to the oxygen or water vapor present in the system, the weight loss rates were measured in helium and nitrogen at 760 Torr. It is seen from the data presented in Table 12-9 (Ref. 15) that the weight loss rates of the specimens exposed to helium and nitrogen at atmospheric pressure were identical to those obtained in vacuum at 0.046 and 1.2×10^{-5} Torr. The

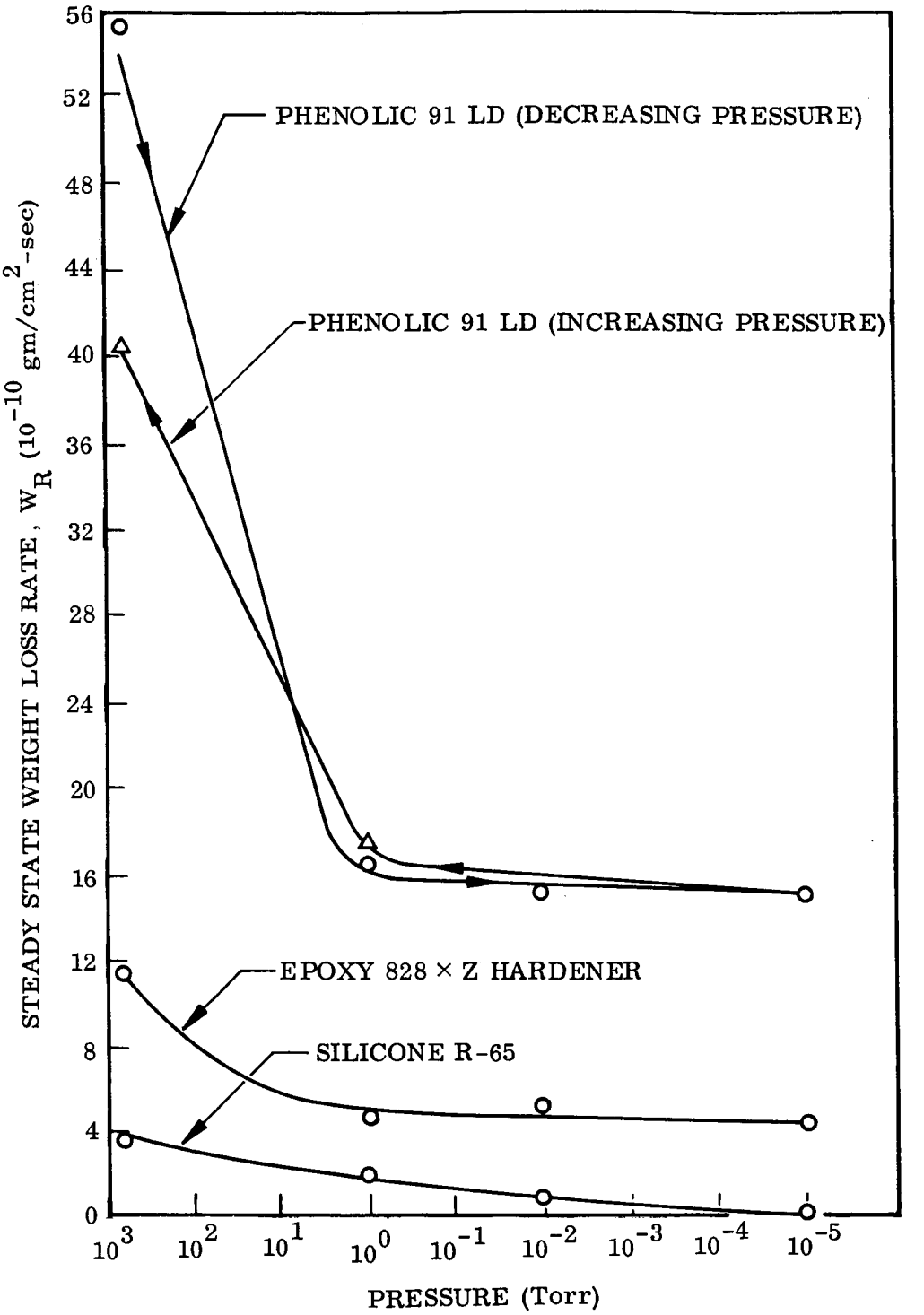

Fig. 12-10 Effect of Residual Pressure on Weight Loss Rates at 350° F

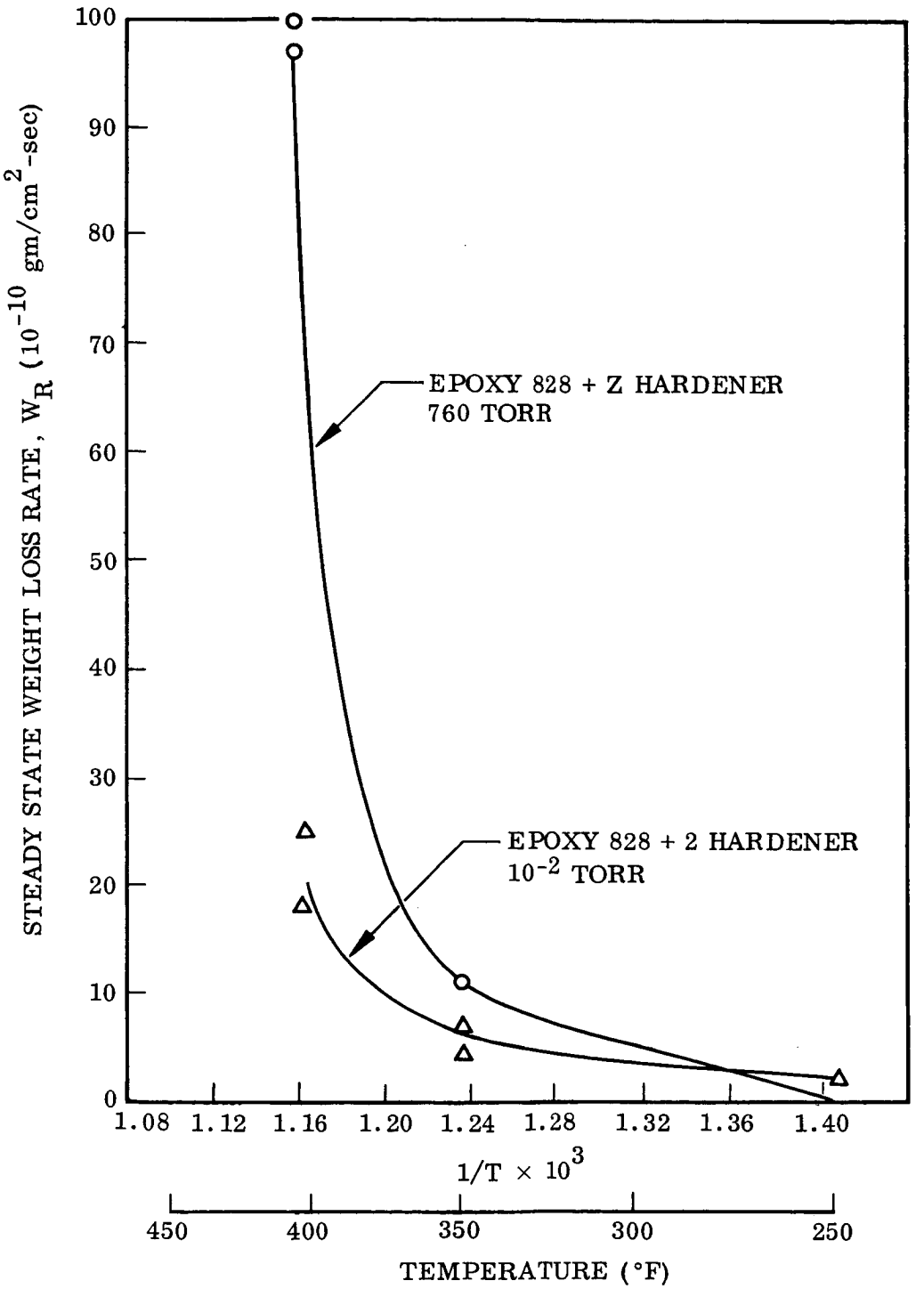

Fig. 12-11 Effect of Temperature on Weight Loss in Air and in Vacuum

Table 12-8

SUMMARY OF STEADY STATE WEIGHT LOSS DATA

Specimen	Temperature (°F)	Pressure (Torr)	Decreasing Pressure Weight Loss Rate (10^{10}g/cm^2-sec)	Increasing Pressure Weight Loss Rate (10^{10}g/cm^2-sec)
Phenolic CTL-91 LD	250	760		
	250	9.5×10^{-1}	0.4	
	250	2.2×10^{-2}	0.9	
	350	760	56.1	
	350	760		40.2
	350	9.5×10^{-1}	16.0	
	350	9.5×10^{-1}		17.3
	350	4×10^{-2}	15.3	
	350	5×10^{-2}		13.8
	350	10^{-5}	15.0	
	400	760	30.1	
	400	9.5×10^{-1}	8.6	
	400	4.6×10^{-2}	6.5	
	400	1.2×10^{-5}	6.5	
Epoxy Shell 828-hardener Z	250	760		
	250	9.5×10^{-1}	1.1	
	250	7×10^{-2}	1.0	
	350	760	11.4	
	350	760		
	350	9.5×10^{-1}	4.7	
	350	9.5×10^{-1}		6.9
	350	4×10^{-2}	5.0	
	350	2×10^{-2}		6.0
	350	10^{-5}	4.3	
	400	760	97	
	400	760		100
	400	9.5×10^{-1}	25	
	400	9.5×10^{-1}		18
	400	3.6×10^{-2}	20	
	400	5.2×10^{-2}		24
	400	10^{-5}	19	
Teflon R/M-820	300	760		
	400	760		
		9.5×10^{-1}	0.2	
Diallyl-phthalate Acme 1-520	300	760	12.1	
	300	9.5×10^{-1}	3.5	
	300	2.3×10^{-2}	3.0	
	300	10^{-5}	1.1	
	350	760		20.9
	350	9.5×10^{-1}	8.6	
	350	9.5×10^{-1}		5.9
	350	1.6×10^{-2}		12.1
	350	10^{-5}		7.7

Table 12-9

EFFECT OF GAS COMPOSITION ON STEADY STATE WEIGHT LOSS RATES OF PHENOLIC 91 LD (400 °F)

Exposure Condition	Weight Loss Rate (10^{-10} g/cm^2-sec)
1.2×10^{-5} Torr	6.5
0.046 Torr	6.5
0.95 Torr	8.6
760 Torr helium	6.5
760 Torr dry nitrogen	6.5
760 Torr air	30.1

Table 12-10

EFFECT OF INERT GLASS FIBER FILLER ON STEADY STATE WEIGHT LOSS RATE OF SILICONE R-65 (450 °F)

Percent Filler	Weight Loss Rate (10^{-10} g/cm^2-sec)	Weight Loss Rate per Unit Mass of Silicone R-65 (10^{-10} g/cm^2-sec)
0	5.7	5.7
48	9.7	18.7
73	6.6	24.8

weight loss tests of Tables 12-8 and 12-9 were conducted on resins containing no fillers; a series of tests was also performed to determine the effect of filler content at 450° F. The data of Table 12-10 (Ref. 15) indicate that the weight loss rate per unit mass of resin increases with filler content. The filler is believed to promote leak paths for outgassing of volatiles in the resin matrix.

The effect of thermal-vacuum exposure and reexposure to air at atmospheric pressure on the flexural strengths of polyester, phenolic, phenyl-silane, and epoxy laminates are shown in Table 12-11 (Ref. 15). The strength of the polyester laminate decreased in thermal-vacuum exposure. The strengths of the phenolic, phenyl-silane, and epoxy laminates increased in thermal vacuum exposure. After exposure to air following the thermal-vacuum exposure, there was a decrease in strength of the phenolic, phenyl-silane, and epoxy laminates that appeared to be time dependent. As shown in Fig. 12-12 (Ref. 15), most of the strength loss for the phenolic and phenyl-silane laminates seemed to occur in the first 10 hours of exposure to air after the thermal-vacuum exposure. The strength of the polyester laminate was not affected by the exposure to air after the thermal-vacuum exposure.

Mechanical properties of glass-fiber reinforced plastics are known to be altered by varying the moisture content of the composite. It is believed that a slight increase in moisture content can cause an appreciable decrease in the strength of the resin-to-glass bond in many laminates. Thus, vacuum exposure can, by eliminating the moisture, increase the strength of reinforced plastics.

Table 12-11

AVERAGE MAXIMUM FIBER STRENGTH OF LAMINATES IN VACUUM AND AIR AFTER VACUUM-THERMAL EXPOSURE

Material	Exposure	Control Specimens[a]	Exposed Specimens[b]	Change (%)	After 4 hr Atmospheric Pressure[a]	Change (%)	After ≥ 100 hr Atmospheric Pressure[a]	Change (%)
		Stress (psi)	Stress (psi)		Stress (psi)		Stress (psi)	
Polyester MIL-P-3013A	300°F 2×10^{-6} Torr	72,000	5,674	-92.1	5,933	-91.8	5,576	-92.3
Phenolic CTL-91LD	470°F 1×10^{-6} Torr	59,300	118,200	+99.3	104,800	+76.7	91,900	+55.0
Phenyl-Silane CTL-37-9X	450°F 1×10^{-6} Torr	51,400	94,700	+84.2	66,700	+29.8	53,400	+3.9
Epoxy 828 With CL hardener	400°F 1×10^{-6} Torr	69,500	81,840	+17.7	85,600	+23.2	63,200[c]	-9.1
No. of Specimens Tested		6	6		3		3	

(a) Measured in air.
(b) Measured in vacuum.
(c) 600 hr.

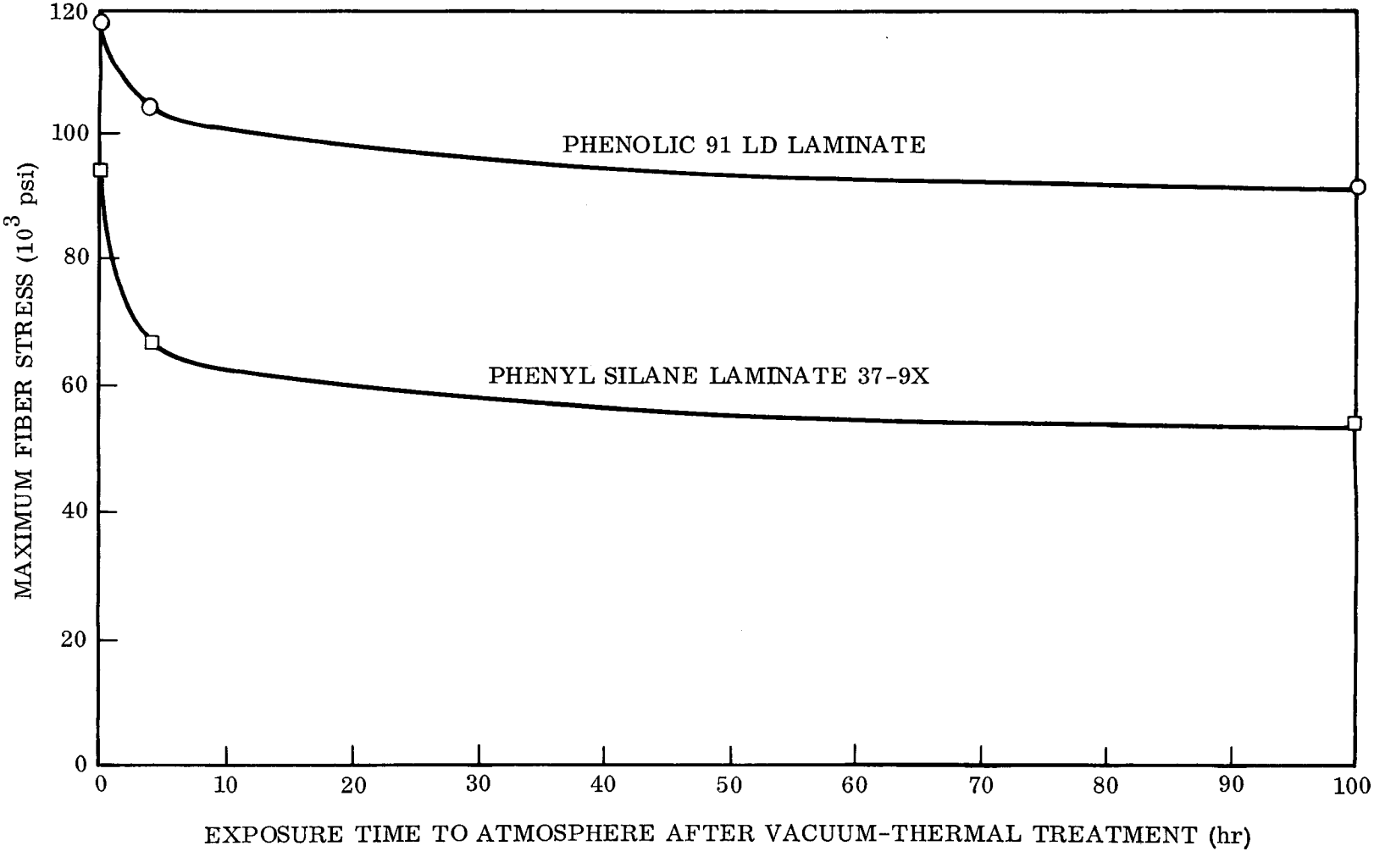

Fig. 12-12 Effect of Atmospheric Exposure on Flexure Strength After Vacuum-Thermal Treatment

12.5 REFERENCES

1. W. G. Jurevie and J. B. Rittenhouse, Structural Plastics Applications Handbook, AFML TR 67-332, Lockheed Palo Alto Research Laboratory, Palo Alto, Calif., September 1967

2. E. E. Verlin, Investigation of Combined Effects of Radiation and Vacuum and of Radiation and Cryotemperatures on Engineering Materials, FZK-161-1, General Dynamics Corp., Fort Worth, Tex., 5 January 1963

3. E. E. Kerlin and E. T. Smith, Measured Effects of the Various Combinations of Nuclear Radiation, Vacuum and Cryotemperatures on Engineering Materials, FZK-172, General Dynamics Corp., Fort Worth, Tex., 30 September 1963

4. E. E. Kerlin and E. T. Smith, Measured Effects of the Various Combinations of Nuclear Radiation, Vacuum and Cryotemperatures on Engineering Materials, FZK-290, General Dynamics Corp., Fort Worth, Tex., 1 July 1966

5. E. C. McKannon and R. L. Gause, "Effects of Nuclear Radiation and Cryogenic Temperatures on Non-Metallic Engineering Materials," J. Spacecraft 2, No. 4, 558 – 564, July – August 1965

6. P. D. Gray, G. K. Corneluis, J. D. O'Donnell, and W. W. Howard, Rockets in Space Environment, Vol. 1, "The Experimental Program," RTD-TDR-63-1050, Aerojet General Corp., Azusa, Calif., February 1963

7. C. G. Goetzel, J. B. Rittenhouse, and J. B. Singletary, Space Materials Handbook, 2nd Ed., ML-TDR-64-40 (AD 460399) (X65-14878), Lockheed Missiles & Space Co., Sunnyvale, Calif., January 1965

8. C. J. Catsikas, G. K. Castle, and J. S. Higgins, Ablation Handbook, Entry Materials Data and Design, AFML-TR-66-262, Avco Corp., November 1966

9. S. Podlaseck and J. Suhorsky, "The Stability of Organic Materials in Vacuum," pp. 593 – 603 in 1963 Proceedings of the Institute of Environmental Sciences Annual Technical Meeting, 17 – 19 April 1963

10. S. Podlaseck, J. Suhorsky, and A. Fisher, "The Behavior of Organic Materials at Elevated Temperatures in a Vacuum," 9th National Symposium of the American Vacuum Society, Los Angeles, Calif., 31 October – 2 November 1963

11. A. Olevitch, Emerging Aerospace Materials and Fabrication Techniques, WADC Technical Report No. AFML-TR-67-1, January 1967

12. R. A. Boundy, "Spacecraft Applications of Polymeric Materials," 18th Annual Meeting of the Reinforced Plastics Division, Society of the Plastics Industry, Chicago, Ill., 1963

13. Vacuum Compatibility of Engineering Materials, NASA Technical Report TMX 53286, 24 June 1965

14. R. F. Muraca and J. S. Whittick, Polymers for Spacecraft Application, Final Report, SRI Project ASD-5046, JPL Contract No. 950745, Menlo Park, Calif., 15 September 1967

15. C. C. Bailey, The Behavior of Organic Materials Under Simulated Space Environmental Conditions, RM-130, Martin-Marietta Corp., Baltimore, Md. 30 August 1964

Chapter 13

MATERIALS FOR ANTENNA SYSTEMS

A. S. Dunbar

Among the many applications of spacecraft antennas are: communication, telemetry, command and control, beacon, navigation, observation, rendezvous, radar, and radio astronomy. These applications encompass the radio spectrum from about 100 kHz to frequencies greater than 100 GHz. The designs of the antennas used are as greatly varied as the sizes and shapes of the spacecraft for which they are made.

The two major challenges in the design of spacecraft antennas are the interrelated problems of mechanical and electrical feasibility together with their compatibility with the space vehicle and with the environment. The basic problem is to devise a mechanical and electrical structure that is at once small enough and light enough for utilization on the space vehicle and which, when deployed in space, will have enough structural integrity and accuracy to withstand the space environment and perform its intended function (Refs. 1 and 2). Thus, the design of reliable antennas for use on spacecraft requires an appreciation of materials properties, the evaluation of fabrication methods and mechanical devices, as well as familiarity with electromagnetic principles and techniques. The materials selected for spacecraft antenna fabrication and assembly must be dimensionally stable in the space environment, must be readily formed, machined and joined, and must have good electrical properties – the metals must be good conductors and the dielectrics must be good insulators with low rf dissipation factors. Selection and utilization of the proper materials is essential to an electrical and mechanical design that will achieve the mission objectives and orbital lifetime requirements. Recommended materials for spacecraft antenna applications are reviewed in Chapter 18.

13.1 ANTENNA TYPES AND APPLICATIONS

A catalog of spacecraft antennas will include simple dipoles, slots, spirals, helixes, log-periodic structures, arrays, and reflector antennas. Antennas used for telemetry on the first satellites, such as Vanguard and the early Pioneer series, were simply dipoles made from flexible wire which deployed into position upon release from a protecting cover. Telescoping dipoles actuated by an explosive device have been used. Spring-loaded dipoles of several forms are also used on many spacecraft of current design.

Slot antennas have also been used extensively. These antennas consist of three major parts: the input section, a cavity, and a window in the half-wave slot. The window performs three functions: its size and shape aid in matching the antenna; its dielectric forms a bridge in the vehicle skin for structural integrity; and maintains the vehicle aerodynamic contour required during ascent.

Booms must be used on satellites to erect ground-plane antennas at a reasonable distance from the vehicle to minimize the pattern distortion caused by its body. Such booms may be erected by springs placed under compression for the exit phase and released when the vehicle is in orbit. By the use of an erected boom, many antennas that would not operate flush-mounted in the vehicle skin become feasible. Some examples are multipurpose monopoles, whip antennas, biconicals, discones, and crossed dipoles. Where ground planes are required, radials unfurled from spring steel tape are used.

Helix, spiral, Yagi, and many similar familiar antenna forms have been employed for various space vehicle communication, command, and data system functions. For high-gain data transmission, such as from the Venus probe (Mariner 2), steerable paraboloidal reflector antennas were used, as illustrated in Fig. 13-1, which also shows the omnidirectional antenna at the top of the spacecraft and the two command antennas, one on either side of the solar panels (Refs. 3 and 4). These paraboloid reflector antennas were made of an aluminum alloy framework (structural shapes of 2024-T4) with aluminum alloy screening for the reflective surface (1/4-in. mesh ECH 19).

Other examples of antenna uses include the Lunar Orbiter, which employed a biconical discone low-gain antenna mounted at the end of a 82-in. boom. For high-gain transmission, a 36-in. parabolic dish of a lightweight honeycomb structure was extended on a 52-in. boom that acted as a coaxial transmission line (Ref. 5). The Apollo program required antennas of great flexibility – the ability to transmit at high and low altitudes. In addition, rocket engines imposed mechanical and thermal loads on the antennas. An open-cell surface construction of welded and brazed René-41 metal (a nickel alloy capable of withstanding high temperatures) was selected to minimize torques produced by impinging gases and to reduce stresses due to thermal gradients. This construction afforded high mechanical stiffness with reduced weight (Ref. 6). The British Ariel 3 satellite utilized a four-rod circularly polarized turnstile antenna system to simultaneously transmit and receive data (Ref. 7). Surveyor 4 used a communications system of three antennas: a single planar-array, high-gain directional; and two omnidirectional, conical antennas. A surface coating is used for passive thermal control of this system (Ref. 8). The ATS-4 program employed an aluminum petal honeycomb core with titanium face sheets and reflective screens. The bonding in this structure was performed with FM-1000 adhesive (Ref. 9).

The antenna of Explorer 29 was a fiberglass-reinforced resin hemisphere containing on its surface a spiral of silver-loaded epoxy C-93 paint applied over the Vita Var PV100 white thermal control surface.

In the Tetrahedral Research Satellites, now called Environmental Research Satellites, steel measuring tapes were used as antennas. A coiled tape was enclosed in small housings at two corners of the satellite. The cover of the housing was removed by command after the satellite was injected into orbit, thereby permitting the tape coil to deploy. These antennas performed satisfactorily in some instances (one was reported to be slow in deployment) and permitted the satellites to transmit data about the space radiation environment and its effects on solar cell and propulsion valve materials.

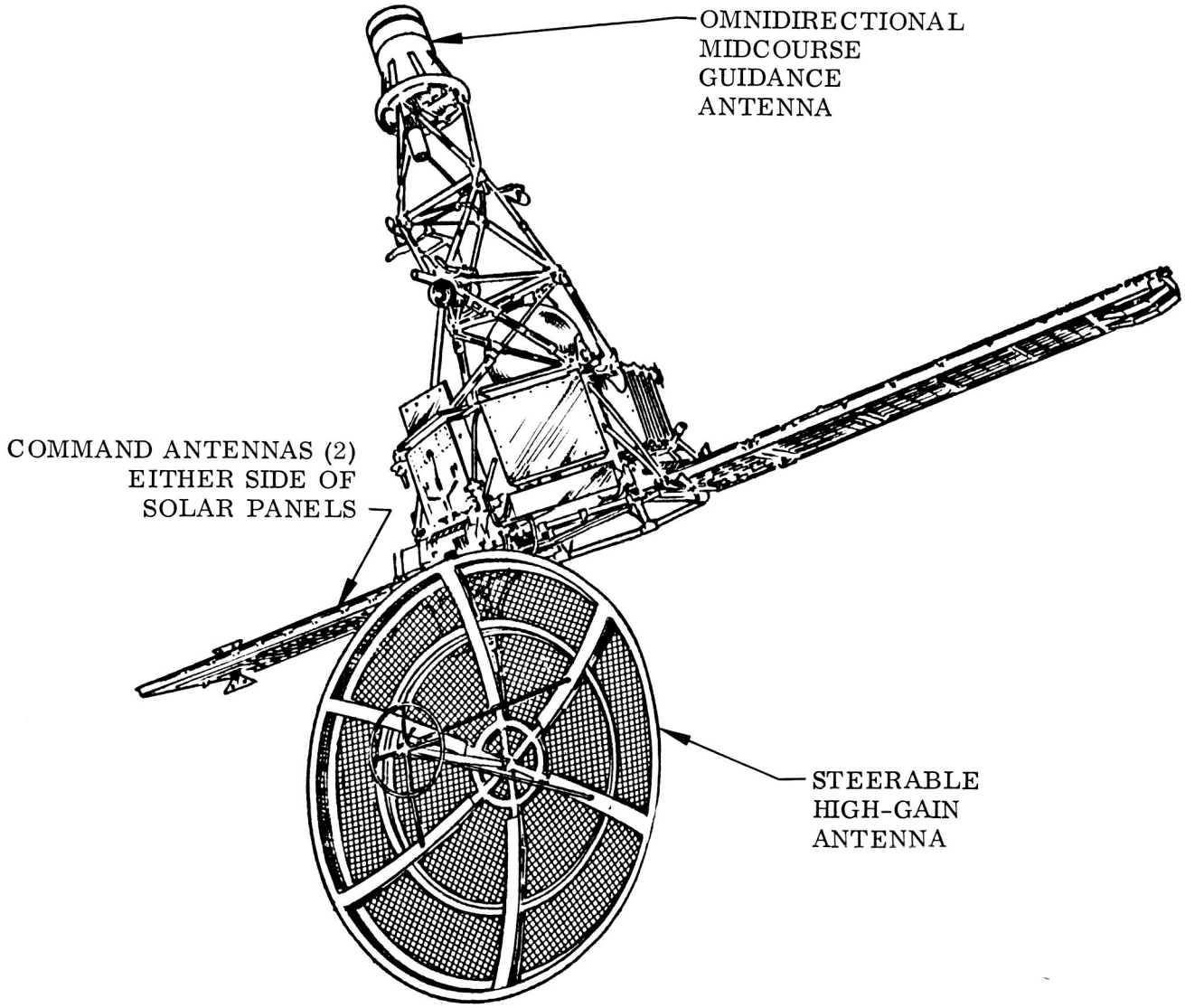

Fig. 13-1 Mariner 2 Steerable Paraboloidal Reflector Antenna

Actually, the material is the replacement steel tape for the Stanley retractable pocket rule, commonly called a "yo-yo." It is purchased in a sealed plastic bag, is painted white with black ruling and numerals, and has a coating of 0.5-mil Mylar to protect it in service. It is taken out of the sealed bag and installed in the spacecraft. Thermal-vacuum tests have shown that the tape coated with Mylar performs better than tapes that are gold-plated.

The 46 × 21 in. Mariner Mars high-gain antenna was made of aluminum honeycomb. The reflector skins were 0.004 in. thick and the honeycomb core was of 0.0007 in. aluminum. The total weight of the reflector and backing structure was 2.1 lb.

Extensive use has been made of automatically erected reflector antennas in which the parabolic surface consists of nylon or Dacron fabric coated with gold or copper. The fabric is stretched into the proper shape by thin metallic ribs (Ref. 10).

Use has been made of an electrically steerable high-gain array antenna consisting of a cylindrical array and a rotary rf switch. Electronically steerable arrays have been designed for satellite applications that make use of transmission line networks and diode switches. Many more applications of phased array antennas can be confidently expected (Ref. 11).

Antennas for radio astronomy from space platforms are required in two broad-frequency bands for which earth-based observations prove difficult. One of these is the region of the radio-frequency spectrum where the ionosphere acts as a shield to prevent observation of radio waves that reach the vicinity of the earth, roughly from a few megahertz down to a few hundred kilohertz. The other is the wavelength range from about 1 cm to the far infrared, corresponding to the frequency range from 30 GHz to a few hundred GHz. Lying between these two bands is the radio window extending from the frequency at which the ionosphere becomes transparent to the frequency at which the atmosphere becomes highly absorbing.

To achieve the directivity necessary for observing discrete radio sources in the long-wave part of the spectrum, very large antennas will be required. For example, at a frequency of 1 MHz (300-m wavelength) the effective aperture of an antenna must be 2 km to give a beamwidth of 10 deg. Correspondingly larger apertures will be required for longer wavelengths to give the same beamwidth.

At the other end of the spectrum, in the millimeter wavelength and long infrared region, size is not the problem. However, precision in antenna structure, surface finish, and pointing will be needed. Thermal deflections are a serious problem and require sophisticated solutions (Ref. 12).

Deep space missions, manned space stations, space observatories, lunar and planetary explorations, and other future space operations require antenna systems of large size, high gain, and construction suitable for assembly in space. For efficient and reliable operation, the antenna designs for each mission must be selected in terms of the application, the environment, the available materials for construction, and the operational conditions.

Increasing the gain of a spacecraft antenna can necessitate one of two things: increasing the size of the radiating aperture or increasing the frequency. Large radiating apertures for spacecraft applications require that the antenna be folded or otherwise packaged during launch and ascent and unfolded or automatically erected when the vehicle is in orbit.

The use of a directional antenna usually complicates the design of the satellite, since provision must be made for aiming its beam. Steering requirements for aiming vary greatly, according to the orbital altitude, method of stabilization, and antenna size or gain. Satellite altitude determines to a great extent the steering requirements. As the altitude increases, both the required angular ranges and rates decrease until, in the stationary orbit, fixed narrow-beam antennas can be used. Space probes require moderate steering angles and low angular rates.

The mode of stabilization of the satellite also has a strong influence on the steering requirements of directional antennas. The attitude-stabilized vehicle provides a platform for the antenna. Maximum steering angles and rates are determined by the orbital parameters. An unstabilized vehicle, on the other hand, may present any aspect to an earth observer, with no control of the vehicle orientation. Steering required to maintain communication with an earth station in this case covers the entire sphere. Spin-stabilized vehicles require steering about the spin axis as well as yaw and pitch to keep the antenna pointed toward the earth.

There are three techniques for designing automatically erectable antennas: mechanical folding, inflating, and pressure erecting. Mechanically folding an antenna generally results in a bulky package, but high precision can be maintained in the erected structure. Inflated antenna structures result in good stowed-to-erected size ratio, but they are subject to leaks and the constant threat of puncture by meteoroids. Pressure-erected devices, which do not depend upon retaining internal pressure after erection for maintaining the structural shape, provide good packaging, small stowed volume, and reliable performance. The method selected for antenna erection will depend upon the complete system requirements – antenna frequency and size, structural precision, vehicle stabilization, and weight limitations.

13.2 SPACE ENVIRONMENT FACTORS IMPORTANT TO ANTENNA DESIGN

The space environment factors that are of primary importance in antenna design are generally the same as those encountered in the design of other spacecraft, i.e., evaporation and sublimation due to high-vacuum exposure, erosion and puncture by meteoroids, and heating and materials property degradation resulting from ultraviolet and penetrating radiation. The most important aspects of the environments and their influence on antenna design considerations and the choice of materials for fabricating antennas are reviewed here.

13.2.1 Vacuum Effects

The significant aspects of the extremely low pressure in space are the possibility of material loss through evaporation or sublimation, change in dielectric properties, and problems of lubrication. The rate of mass loss of materials at low pressure is

governed by the molecular weight of the material, its absolute temperature, and its vapor pressure. It has been found that an appreciable loss of cadmium and zinc will occur at temperatures likely to be encountered in spacecraft applications. Consequently, they should not be used in any antenna where they may be exposed to high vacuum. Magnesium may experience some sublimation, but only at high temperatures. Most other metals, such as aluminum, copper, or silver, will not lose significant thickness except at very high temperatures. For example, copper and silver would have to remain at a temperature over 1400° F to lose 10^{-3} cm/yr (4×10^{-4} in./yr).

Although any structural metals may be used for spacecraft antenna design and fabrication, aluminum and magnesium are the most common. The selection of metals for antenna construction is governed primarily by good engineering practice.

Most of the organic materials used for dielectrics are long-chain polymeric compounds which degrade in a vacuum by chemical breakdown into more volatile fragments rather than by evaporation or sublimation. Such polymers as nylon, acrylics, polysulfides, and neoprene show high decomposition rates in vacuum. On the other hand, such plastics as tetrafluroethylene and polyethylene are quite stable in high vacuum. Epoxy-glass laminates and polyester-glass laminates have been used successfully for long periods. This is discussed more fully in Chapters 11 and 12 and in Ref. 13.

There seems to be no good evidence of any important change in the properties of inorganic dielectrics, such as glass and ceramics, in vacuum. Some glasses turn brown under intense radiation, but this apparently has little effect on the dielectric properties. Chapter 8 presents more complete data on these materials.

For lubrication in space of antenna mechanisms, low-vapor pressure greases or oils in enclosed containers may be the best solution. Evaporation of the lubricant is inevitable, of course, but effective sealing will minimize the escape of the lubricant vapor. Solid lubricants, such as molybdenum disulfide and silver or gold plate, have been used successfully at low speeds. Molybdenum disulfide, however, tends to flake off small bearings. Graphite is of no value for lubrication in a vacuum because it depends upon the presence of water vapor for its lubricating properties. A complete discussion of lubricants and space environmental effects on them is given in Chapter 9.

At low pressure, antennas are susceptable to voltage breakdown. When such breakdown occurs, the observed effect is fourfold: the radiated power decreases, the radiation pattern changes, the input impedance changes, and, in the case of pulse modulation, the pulse shape changes (Refs. 14 and 15). Studies of rf breakdown show that a minimum breakdown voltage exists where the electron collision frequency in the air is approximately equal to the radio frequency. This may be expressed by

$$P_{Torr} = f_{GHz}$$

That is, the minimum breakdown condition corresponds to the pressure measured in Torr being equal to the radio frequency measured in gigahertz. The power at which breakdown occurs is a function of both the radio frequency and the antenna geometry. The theoretical minimum electric field strength at which breakdown will occur is given by

$$E/p = 165 \text{ V/cm-Torr}$$

Experimental results obtained by measurements on a wide variety of antennas have verified this formula. Generally, antenna breakdown will not be a problem on satellites and space vehicles. The minimum breakdown condition occurs in the atmosphere during ascent and must be considered in the design of telemetry and beacon antennas for the ascent. However, the problem of voltage breakdown in transmission lines and connectors cannot be dismissed so easily.

Dielectric-core flexible cables are not subject to ordinary gaseous discharge breakdown, since the solid dielectric core will break down only when the power is so high that the voltage exceeds the dielectric strength. Cable connectors, however, suffer breakdown in the air gap between the dielectric interface of the connector parts. This discharge is caused by the high electric field tangential to the dielectric faces of the connector, and a minimum breakdown condition occurs, similar to that previously discussed. Unfortunately, since the connectors are not usually vented, the leakage of air may occur at a slow rate, with the result that the minimum condition occurs, without regard to the external pressure, when the internal pressure falls to the critical level. The practical solution to this problem is to fill the connector air space with a suitable dielectric grease, such as Dow-Corning DC-4.

Gas discharge at microwave frequencies in waveguides has been extensively investigated. Theoretical and experimental data of the breakdown field in waveguides have been published by Brown (Ref. 16) and Gould and Roberts (Ref. 17). These data provide accurate predictions of breakdown fields in the pressure range from atmospheric to about 1 Torr. The waveguide breakdown exhibits a minimum condition similar to that for antennas. Recent calculations and experiments have extended the data on waveguide breakdown to a pressure less than 10^{-2} Torr (Ref. 18). These results show that at very low pressure the waveguide will support large peak power without breakdown, so long as the electric field strength remains less than a critical magnitude that will cause secondary emission from the waveguide walls.

13.2.2 Micrometeoroids

The presence of meteoroidal particles and dust in space is a unique environmental factor in design for space applications. Although the data giving the number of particle impacts per unit area show considerable variation, the general mass distribution curves confirm theoretical predictions. This is discussed more fully in Chapter 6. There is an increase in flux with decrease in particle size, and one must expect an exposed

surface to be struck many times a day by particles of 100 μ and smaller diameter. Damage to vehicle or antenna structure, such as extendable booms, reflectors, and the like, does not appear to be a serious problem. This is most readily confirmed by the fact that no large particles seem to have damaged any orbiting vehicle, with the possible exception of 1958 Gamma (Explorer III). Failure of both transmitters coincided with a high measured rate of meteoroid hits during a shower, and it has been suggested that the failure may have been caused by meteoroid damage. Mariner 4 (Mars) telemetered 16 indications on the microphone meteoroid detectors in August 1967. However, communication continued with the spacecraft from January 1967 through November 1967 after the spacecraft had been in solar orbit for about 3 years.

Surface erosion by micrometeoroidal particles and dust will most certainly occur. However, the erosion rate will be, on the average, less than a few microinches per year. Impact and puncture of thin wall structures can be predicted. Consequently, a thin wall structure will necessarily depend upon its own structural rigidity to maintain its shape; that is, because of micrometeoroid puncture, a pressure-erected device cannot be depended upon to maintain structural shape unless it is sufficiently self-rigid under space environmental forces.

For example, Echo I has suffered sufficient puncture and erosion to cause some surface contour distortion. By mid-1963, after 3 years in orbit, Echo was still useful for limited bandwidth communications. The optical brilliance had not been destroyed, although some scintillations occur which show that the surface is somewhat wrinkled. The combined effects of micrometeoroidal erosion and puncture and the material stresses in the Mylar spherical balloon have caused surface distortions upon loss of internal pressure.

13.2.3 Radiation Effects

Any space structure may be subjected to radiation of several kinds: electromagnetic, which is chiefly of solar origin, including infrared and ultraviolet; penetrating radiation such as protons, electrons, and cosmic rays, all of natural origin; and nuclear radiation generated by a nuclear power source aboard the vehicle or by a high-altitude nuclear explosion. The solar radiation is the major heat input to the space vehicle, and its control depends almost entirely upon radiative heat transfer on the vehicle and antenna surfaces. Temperature-control problems are discussed more fully in Chapter 7. Experience has shown that it is possible to design for any reasonable steady temperature desired, since existing materials applied in proper thickness and positions will provide the necessary radiation control. For instance, although polished aluminum has a high reflectivity constant of 0.95, its equilibrium temperature under solar radiation is 400° F because its emissivity in the infrared is low. Special paints and coatings can be used to reduce the temperature to approximately 44° F. On close-to-earth orbits, during the dark portion of the orbit where earth radiation is predominant, the low-temperature extreme can reach - 86° F. A more serious problem is the temperature variations that may occur as the space vehicle passes into the earth's shadow or the antenna becomes partially shadowed by the vehicle itself. Temperature changes may also occur in a mechanically steered antenna whose aspect angle to the sun changes with time.

Consequently, although the surface may be treated for temperature control under any assumed steady-state condition, variations in the solar energy falling on the antenna surface may produce temperature gradients. Accordingly, careful attention must be given in the design to the effect and techniques for minimizing the influence of temperature variations and gradients in the antenna structure. Design procedures have been developed and applied to meet the exacting requirements of high-gain space-vehicle antennas.

Damaging ultraviolet radiation in the region of 2200 to 3100 Å is ordinarily completely absorbed by the atmosphere. Consequently, for spacecraft applications above the atmosphere, plastics, which in general are sensitive to ultraviolet, must be chosen with care. Mylar (polyethylene terephthalate), will show a slight loss in plasticity after exposure time of 1 year. H film and FEP Teflon are preferred because of Mylar's low resistance to ultraviolet. Polystyrene, on the other hand, may become severely striated.

Exposure to penetrating radiation, whether occurring naturally in space or produced artificially, must be taken into account, because of the effect of this radiation upon the physical, chemical, and dielectric properties of materials. Among the materials most sensitive to damage by particle radiation are semiconductors. Metals and alloys are not affected except in a shallow surface layer in which there may be a change in ferromagnetic properties. Oils and greases are little affected by space radiation. The flexibility, strength, and dielectric properties of most plastic materials will be detrimentally affected by radiation in varying degrees. (See Chapter 12.) Discussions and data relative to materials for antennas are given in other chapters of this handbook. This information may be used to determine the sensitivity of materials to radiation damage and to aid in the selection of materials most suitable to the application and the expected environment.

Several types of rf cables and components are suited to spacecraft applications, but certain environmental factors in addition to the external space environment must be considered in the selection of cables. The vehicle environment will differ from the external environment, due to the temperature of the skin, the temperature gradients, and the internal electronic package environment. Attention must be given to the electromagnetic compatibility environment also.

The characteristics of various cable core materials have been extensively studied. These materials are Teflon, polyethylene, and other polyolefins. Polyethylene has the greatest resistance to penetrating radiation but the lowest softening temperature. Polyolefins in general show a strong tendency to degas at high vacuum and have to be used with caution. Teflon in the bulk form has good radiation resistance but suffers severe radiation damage at high radiation dose rates ($> 5 \times 10^8$ R) when in thin film or tape form. Teflon also has the highest softening point of the three materials.

13.3 GENERAL SYSTEMS CONSIDERATIONS

An important part of the overall environment affecting spacecraft telecommunication system design is determined by the technical characteristics of the earth-space radio propagation link. The basic physical laws that govern the transmission of all types of information by rf electromagnetic wave propagation are well known and have been discussed in detail in the technical literature (Refs. 19 and 20). Of primary interest here are the factors affecting antenna design which result directly from technical characteristics of the earth-space or space-space links. Thus, it is evident that the signal-to-noise power ratio of the one-way link is directly proportional to the gain and effective area of the transmitting and receiving antennas, which depend upon size, dimensional tolerances, and operating frequency; and inversely proportional to the effective noise temperature of the receiving system, which depends upon the receiver antenna noise temperature and the operating frequency.

The subject of suitable frequencies for the earth-space communication links has been covered in detail in the literature. Several technical factors influence the choice of operating frequencies. The result of analyses shows that the range of suitable frequencies from the noise and attenuation standpoint is wider for the earth-space direction than for the space-earth direction. For the former, most of the frequency spectrum from below 100 MHz to 50 GHz appears suitable. For the latter, however, frequencies in the range of 0.5 to 15 GHz appear best. Therefore, the range of primary interest is 0.5 to 15 GHz. In the future, some higher frequencies (perhaps in the millimeter-wave region) will be used, but the choice of such frequencies will have to be based on demonstrable improvement in system performance. The advantage of such higher frequencies, say in the 100 GHz region or higher, would include broader usable bandwidth to permit carrying more information per unit time, and narrower beamwidths (higher gain). However, further research is needed on atmospheric attenuation and scattering above 30 GHz. The use of millimeter-wave telecommunications will also cause the antenna engineer to face a broad range of problems that include new materials and structural and environmental constraints.

Stability equations indicate that antenna locations are important to vehicle stability. Although large satellites may have an active system for maintaining a specified orientation relative to earth, it is desirable to minimize the energy used by such a system. Stability equations suggest antenna locations having the least effect on satellite stability, based on an optimum relation among the three moments of inertia. The solution to these equations shows that $I_y > I_x > I_z$, where I_y is the moment of inertia about the pitch axis, I_x is the moment of inertia about the yaw axis, and I_z is the moment of inertia about the roll axis.

This condition may not always be possible for the satellite alone, but when it exists it should not be disrupted by erection of an antenna. In some instances, the addition of antennas may help create this condition of stability. As illustrated in Fig. 13-2, I_y is maximized by placing the antennas in the orbital plane (Ref. 21).

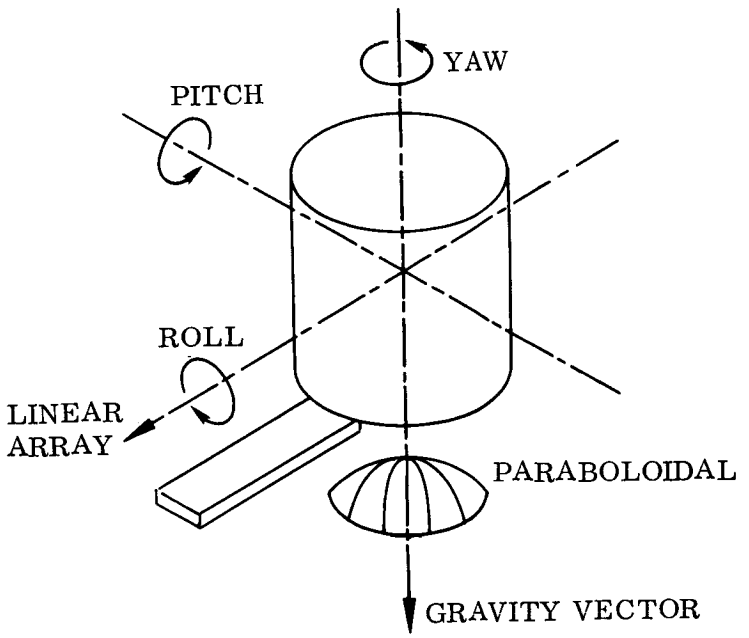

I_x = moment of inertia about yaw axis
I_y = moment of inertia about pitch axis
I_z = moment of inertia about roll axis

Fig. 13-2 Satellite Orientation for Maximum Stability

Another effect of the antenna on stabilization is the reactive torque imparted by antenna rotation, which in turn will rotate the vehicle. One obvious compensation is to have the vehicle inertia much larger than that of the antenna, but this is not the only recourse. Reactionless gear drives can be constructed, i.e., gear trains in which the inertia of one of the members counteracts the torque rotating the antenna. The equilibrium of all inertial forces with no net torque on the vehicle frame occurs when the load inertia is equal to the product of motor inertia and the gear ratio.

13.4 MECHANICAL REQUIREMENTS AND MECHANISMS

Omnidirectional spacecraft antennas are required for many applications. The design of such antennas depends upon the size and shape of the vehicle in terms of the operating wavelength. Where such coverage is required for systems on large space vehicles, it may be necessary to place the antenna on a boom extended from the vehicle.

The considerations involved in the design of directive antennas are essentially the same as those for similar ground-based applications. However, some of the problems encountered with high-gain antennas are unique to the space environment. Furthermore, the mechanical design may be simpler because gravitational, wind, and ice loading forces will be absent. On the other hand, considerations of dimensional accuracy may be more important and protection against micrometeoroidal damage must be considered.

13.4.1 Basic Structural Requirements

At least until antennas can be designed and fabricated in orbiting space stations, one must approach the design of spacecraft antennas with two sets of structural requirements in mind. First, the antenna must survive the shock, acceleration, and vibration of the launch, exit, and orbit-injection phases of flight, and it must also permit testing in the laboratory and the simulated space environment. Second, the antenna must perform the required functions when it is placed in operation on the orbiting spacecraft. These two sets of conditions are, in certain respects, quite different. The laboratory and simulated space environment impose the condition that the antenna operate under the forces of gravity during test. When the environment is in orbit, this force is virtually absent. The shock and vibration at launch far exceed any forces that the antenna will experience under operational conditions in orbit. Force on the antenna above an altitude of 300 nm (346 sm) are negligible compared with the steering torques of the satellite itself, but these are small compared with the forces of gravity encountered in the laboratory.

Antennas of a wide variety of sizes and shapes will be required for various applications. The mechanical requirements for omnidirectional antennas are simple. In some cases, the design is complicated by the need for an extensible boom, which may be extended mechanically or by pressure-erection. High-gain steerable antennas may require the application of automatic erection or unfurling techniques.

13.4.2 Antenna Unfurling

By definition, an unfurlable antenna must be capable of being unfolded from a small package into a structure of significant size. Either mechanical or pressure-erection techniques may be used. In mechanical erection, an assembly of essentially rigid parts whose shape is not changed during erection is placed in position and locked. In pressure erection, a relatively thin-skinned container is inflated. Its shape, size, and condition may be changed in the process, and it supports itself after the inflation, remaining stable after the inevitable loss of internal pressure. Each technique results in problems of antenna performance not present in completely rigid antennas (not unfurlable).

Pressure-erected reflectors and space structures may be rigidized by means of foam-in-place techniques. The reflector or space structure is made from flexible material, such as Mylar film, rubberized fabric, or aluminum foil. In the case of a parabolic reflector, two skins are made and joined together, one for the reflector surface and one for the back reinforcement. Upon inflation, the hollow space is filled by a foam-in-place plastic (Ref. 22).

13.4.3 Reflector Tolerances

The mechanical requirements of unfurling, particularly of cutting the antenna into sections, may cause some form of systematic deformation of the antenna surface. Certain types of irregular deformations, however, may occur on any structure. These irregularities are contour accuracy of the reflector; local depressions or bumps; isolated screwheads, rivets, or holds; and perforations.

Because the minor lobes of the antenna radiation pattern are extremely sensitive to antenna phase errors, the magnitude of the minor lobes is a key to antenna performance. Analyses of the effect of aperture phase errors on antenna gain and minor lobe level have shown that very close tolerances must be maintained if low minor lobes are required. Figure 13-3 shows the reduction in relative gain G/G_o versus root mean square phase error and the minor lobe level for the case of an antenna designed to yield minor lobes 29 dB down from the peak of the antenna beam. The curves show that some of the minor lobes will be above - 20 dB if the root mean square phase error is 0.25 rads (Ref.23).

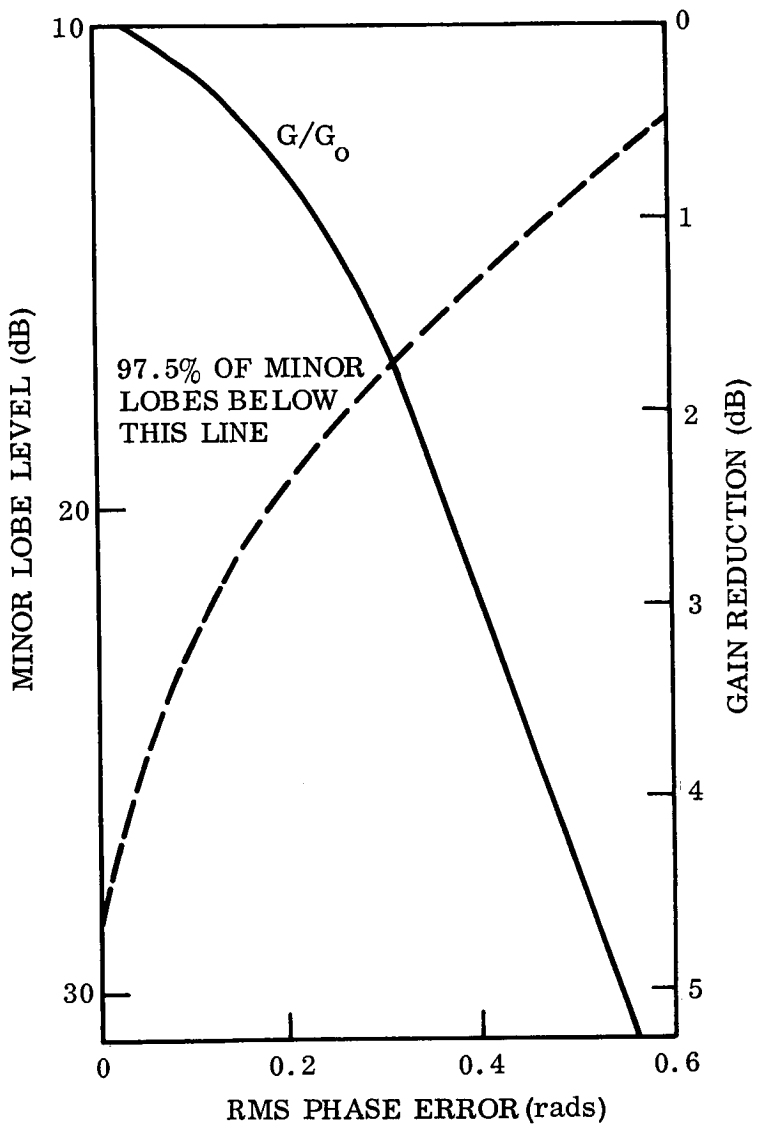

Fig. 13-3 Antenna Gain and Minor Lobes Versus Root Mean Square Phase Error

Local deformations, either projections or indentations that extend a distance no more than $\lambda/4$ from the average surface, can be allowed if they are small compared with the total antenna area. Small screwheads or rivets have negligible affect unless there are a great many forming a regular array. Perforations have no appreciable effect if the holes are less than about $\lambda/2$ in circumference, in which case the loss caused by transmission through them will be less than 1%.

A theoretical study was made of the degradation of antenna characteristics resulting from the use of a sectioned reflector, not perfectly parabolic, which was formed of flat or singly curved sheets (Ref. 20). For mechanical reasons, it may be desirable to reduce the number of sections; however, the larger areas of deviation from the ideal contour might cause excessive radiation pattern distortion if there were too few sections. This problem can be studied by the well-known methods of calculating a radiation pattern from the aperture excitation.

Computations have been made for a number of types of sectioned antenna reflectors: segmented cylindrical reflectors, and conically segmented and radially segmented paraboloidal reflectors. The number and type of segments influence the gain of the antenna and the magnitude of the minor lobes. Detailed studies by computer have been made for reflector sizes up to 50-ft-diameter paraboloids.

13.4.4 Booms and Erection Mechanisms

For support of small omnidirectional antennas or scientific experiment packages at a distance from the space vehicle to avoid interference with or shadowing by the vehicle, extensible booms are required. In addition, low-frequency (300 kHz to 30 MHz) dipole antennas require a means of extending the dipole elements from the vehicle. While a long-wire antenna has been shown to be suitable under certain controlled conditions on a spinning satellite, boom mechanisms have more general application for low-frequency antennas as well as for other antennas and devices.

Folded, self-latching, hinged, spring-actuated mechanisms have been used on a number of satellites, for both antennas and instrument booms. An interesting and useful method for obtaining long booms or antennas is the system shown in Fig. 13-4. This device consists of wide beryllium-copper tapes that have been preformed into tubes. In the packaged condition, the tapes are rolled on spools, and when extended they form a cylinder. With this method, low-frequency antennas 150 ft long have been constructed for the S-27 satellite (Topside Sounder). V-antennas 750 ft long were constructed by this method for use on the Radio Astronomy Explorer Satellite in 1967 (Ref. 11).

The major problem in the use of this antenna is bending of the extended cylinder, caused by solar heating. This problem is caused by the temperature difference across the cylinder when one side is receiving direct solar radiation and all sides are radiating heat to outer space.

The amount of bending varies directly with the temperature difference across the cylinder and with the square of the length of the cylinder. If long cylinders are to be used, then the temperature difference must be controlled to very narrow limits. For example, a 1,000-ft aluminum boom of 1-in. cross-sectional diameter would have a 74-ft deflection at the tip or an angular deviation of over 4° for a 1° F temperature gradient. Methods of minimizing this bending have been devised. One method is to perforate the tape, painting the inside black and the outside white. This approach can be very effective, provided the concentricity of perforations can be maintained. The major design problem is to provide equal temperatures to each side of the cylinder under various angles of solar incidence.

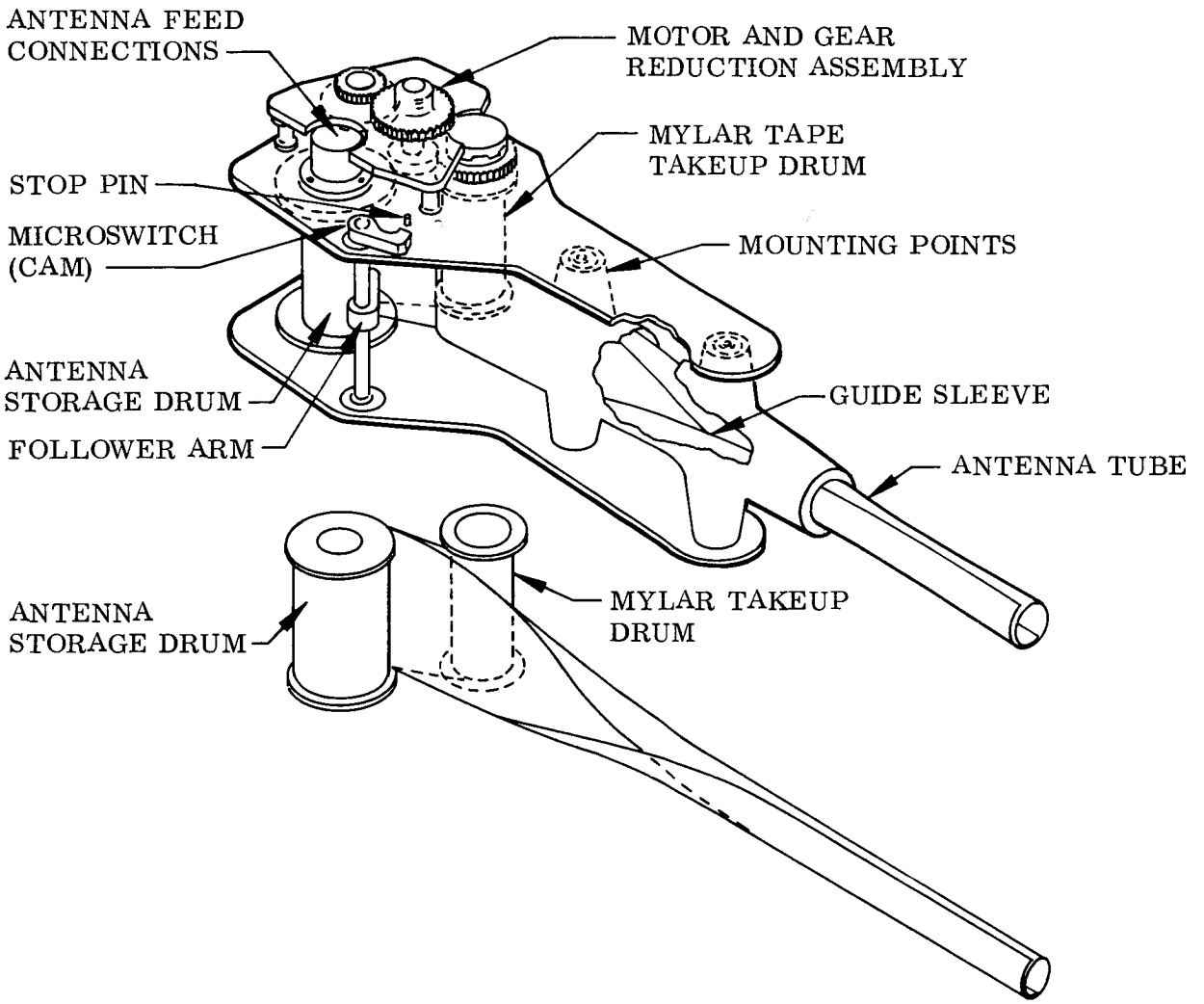

Fig. 13-4 Extensible Tube Antenna

Pressure-erected foil tubing booms have been designed and used on satellites also. The tubes were formed on mandrels from Mylar – aluminum foil – Mylar laminate and joints were sealed with thermally cured plastic adhesive tape. When inflated by gas pressure, the boom or antenna structure is erected. After erection, the gas may be released by means of a relief valve. Because there are only minor forces tending to deform the tubular structure, it will retain its shape and will not be affected by meteoroid punctures.

A variety of structures, ranging from complicated tubular frames to large curved surfaces, reinforced by tubular members, can be constructed with pressure erection techniques. As one example, an aluminum foil tube log-periodic antenna was designed to operate over the frequency range 70 to 700 MHz. Its total weight including the gas bottle and valve mechanism is 4 lb.

Methods for constructing foil tube structures have been investigated and tested (Ref. 10). Tubes of various laminations were constructed and beam-strength tests performed in tubes stretched with various hoop stresses.

Self-erection techniques that use the material in the structure as the erecting mechanism have been developed. For example, this technique has been demonstrated with erectable Yagi disc antennas (Ref. 24). The antenna consists of dipole ground-plane units for the feed, made of formica printed-circuit board, and director assemblies of aluminum foil discs. The discs were separated by polyether flexible urethane foam spacers. The precut and shaped foam acted as the supporting structure for the discs and as the erecting mechanism. The antenna is packaged with the foam compressed, and upon release, the foam returns to its original shape. Packaging ratios of 10 or 15 to 1 can be achieved.

13.4.5 Millimeter-Wave Antennas

The problem of designing a very accurate reflector for operation at millimeter wavelengths in space appears to be twofold. The first requirement of the design is that it lend itself to fabrication techniques that will initially produce the required accuracy. Once the reflector has been manufactured to the required accuracy, the second requirement is to maintain this accuracy in the operating environment.

To achieve high initial accuracy, several techniques are available. Computerized milling, precision stretch forming, and molding are manufacturing methods that can be used to form accurate paraboloidal segments. For positioning and alignment of the segments, optical techniques are available.

The question of available space for stowage of the reflector aboard the vehicle during launch greatly influences and frequently dictates the design approach. It is evident that the required apertures are not too different from the diameters of coming generations of spacecraft, say 10 to 30 ft. It appears possible and certainly advisable, then, to use a solid, nonfolding design, thus avoiding complication and improving the accuracy potential. Should an aperture greater than the vehicle diameter be required, then a folding design is needed. In one design, a solid-center section of a maximum diameter as allowed by the spacecraft booster envelope is surrounded by folding petal-type sections that can be deployed in space to form a paraboloid.

The problem of maintaining the surface accuracy of parabolic reflectors in the space environment has been studied extensively (Ref. 21). Solar heating and shadowing causing thermal gradients throughout the structure is the primary problem. If the structure were to be uniformly heated and cooled, the surface accuracy would not be

greatly altered. This is not the case, however, and severe gradients can occur as the solar illumination varies throughout the orbit. These gradients, of course, cause deflection and distortions of the reflector surface. The following solutions are available, the choice of which would be determined by the particular mission:

- Using a design as "open" as possible to reduce mutual shadowing (applies to the primary rib structure as well as the reflector surface)
- Using materials with low thermal coefficient of expansion such as Invar
- Rotating the structure to ensure uniform temperature
- Using surface finishes and perforating techniques to reduce thermal gradients

13.4.6 Steering High-Gain Antennas

The steering requirements of a high-gain antenna, a function of the satellite altitude, will be an important factor in the overall antenna design. Whether the pointing of a particular antenna is feasible will be determined by the angular rates, angular accelerations, and drive-power limitations.

Low-altitude orbits involve a range of steering angles of about 140° and angular rates approaching 1° per second to maintain contact with a station on earth. As the altitude increases, both the required angular range and the angle rate decrease until at an altitude of 22, 000 nm, where a satellite in an equatorial orbit appears to stand still, the included earth angle is only 18°. A fixed narrow-beam antenna can then be used.

Two of the possible methods for steering are the azimuth-elevation system and the roll-pitch system. Because of the lower angular accelerations involved, the roll-pitch system of beam steering is more desirable.

Even for very-low-altitude satellites, the rate and acceleration are quite small; in fact, the theoretical maximum drive power for the antennas studied is less than 1 W. This comment applies to continuous tracking of a single ground station but would probably not be true if rapid steering between several stations were required.

13.5 REFERENCES

13.5.1 Cited

1. A. S. Dunbar, "Spacecraft Antennas," Chapter 4 in Electromagnetics in Space, ed. K. R. Spangenberg, McGraw-Hill Book Company, Inc., New York, 1965

2. A. M. Berkman and W. M. Young, "Advanced Antennas for Space Application," Paper 14.1, Wescon Technical Papers, 1965

3. Mariner, Mission to Venus, Jet Propulsion Laboratory, California Institute of Technology, McGraw-Hill Book Company, Inc., New York, 1963

4. R. V. Meghreblian, F. L. Schutz, and W. G. Fawcett, "Science Payloads From Mariner II to Mariner IV," Conference on the Exploration of Mars and Venus, XIII-8 to XIII-10, Virginia Polytechnic Institute, August 1965

5. W. T. Bundick, C. H. Green, and E. A. Brummer, "The Lunar Orbiter Telecommunications Systems," IEEE Transactions on Communication Technology, Vol. COM-15, June 1967, pp. 433–443

6. A. P. Notthoff, "Apollo Antenna Fastens on the Beam to the Moon," Electronics 40, 80–86, 1 May 1967

7. "Ariel 3, the First All-British Satellite," Industrial Electronics 5, No. 7, 297–300, July 1967

8. "Surveyor IV Goes Dead," Space World, D11-47, 5–13, November 1967

9. An Advanced Study of an Application Technology Satellite (ATS-4) Mission, Final Study Report, 1, Book 1, Contract NASw-1410, General Electric Company, Philadelph Pa., November 1966

10. E. A. Blasi, "Antennas for Space Application," 12th Symposium of AGARD, Avionics Panel, Düsseldorf, W. Germany, July 1966

11. W. Korvin and R. B. Jackson, "Antennas for Space Vehicles," Space/Aeronautics 42, 60–67, November 1964

12. G. E. Fisher et al., "Design Features of Large Antennas in Space," AIAA Paper No. 66-848, AIAA Third Annual Meeting, 29 November–2 December 1966

13. "The Nature of Materials Failure Under Sapce Conditions," Electro-Technology 72, 128–132, September 1963

14. W. E. Scharfman and T. Morita, "Power-Handling Capability of Antennas at High Altitudes," IRE International Convention Record, Part I, 103–114, 1960

15. A. D. MacDonald, Microwave Breakdown in Gases, Chapter 8, John Wiley and Sons, Inc., New York, 1966

16. S. C. Brown, Basic Data of Plasma Physics, John Wiley and Sons, Inc., New York, 1959, pp. 142–187

17. L. Gould and L. W. Roberts, "Breakdown in Air at Microwave Frequencies," J. Appl. Phys. 27, 1162–1170, October 1956

18. A. S. Dunbar, "Breakdown in Air at Very Low Pressure in a Waveguide," J. Appl. Phys. 35, 3047–3047, October 1964

19. R. C. Hansen and R. G. Stephenson, "Communication at Megamile Ranges," Microwave J., Part 1, p. 79, December 1961; Part 2, p. 79, January 1962

20. L. C. VanAtta, "Interplanetary Communication," Sci. and Technol., No. 59, pp. 50-61, November 1966

21. Study and Design of Unfurlable Antennas, Final Report, Contract AF 33(616)-6022, WADD Technical Report 6-62, Vol. II, 1960

22. Solar Concentrator Development and Evaluation Program, Report GER-10084, Goodyear Aircraft Corporation, Akron, O., Vol. I, 1961

23. J. Ruze, "Effect of Aperture Errors on Antenna Radiation Pattern," Nuovo Cimento, Suppl. 9, 364 – 380, 1952

24. W. F. Croswell, M.C. Gilbreath, and V. L. Vaughn, Jr., "Self-Erecting Space Antennas," IRE Trans. Space Elect. Telemetry 8, 139, 1962

13.5.2 Uncited

M. E. Devane and M. L. Rosenthal, Telemetry Antenna for Lincoln Experimental Satellites LES-1 and LES-2, TR-394, June 1965

P. L. Uslenghi, Studies of Antennas for Space Vehicles, NASA-CR-159, National Aeronautics and Space Administration, Washington, D.C., March 1965

K. Woo, "High Impact Antenna Study: Coaxial Cavity Radiator," Space Programs Summary, Paper 37-40, Vol. 4, 201-206, Jet Propulsion Laboratory, California Institute of Technology, Pasadena, Calif., 31 August 1966

G. E. Fleischer, "Spacecraft Antenna Pointing," Space Programs Summary, Vol. 4, Paper 37-40, pp. 16 – 19, Jet Propulsion Laboratory, California Institute of Technology, Pasadena, Calif., 31 August 1966

A. T. Villeneuve, Study of Advanced Antenna Systems Problems for Space Vehicles – Final Report, Hughes Aircraft Company, Culver City, Calif., 31 December 1964

H. S. Jones, Jr., A Flush-Mounted Composite Radome Antenna System, Harry Diamond Labs., Washington, D.C., August 1966

Symposium on Passive Gravity-Gradient Stabilization, Ames Research Center, Moffett Field, Calif., pp. 179 – 183, 10 – 11 May 1965

Chapter 14

ELECTRONIC MATERIALS AND COMPONENTS

P. S. Castro
R. A. Glass
J. C. Lee
P. V. Phung
F. F. Stucki

Penetrating radiation constitutes the most important direct space environmental parameter affecting the operation of electronic components in space. The nature of applications of electronic components generally results in their being protected from other aspects of the space environment.

14.1 RADIATION EFFECTS

The designer of electronic components and devices for space applications is interested in how the radiation environment will change the properties of these components and devices and at what level of radiation dose and under what environmental conditions the components and devices will cease to operate satisfactorily. Data needed to answer these questions fall into two general categories: those concerning the materials of which a component or device is built and those concerning the entire component or device. Data on radiation effects on components and devices are of greater usefulness to the aerospace designer, but unfortunately, these data are still incomplete, partially because the many types and varieties of electronic components and devices would require a much greater investment of time and equipment for testing than has heretofore been expended. Furthermore, advances in electronic technology are introducing novel and modified varieties of components at a fast rate, and test data for these new items are necessarily scarce at best.

14.1.1 Radiation Response of Electronic Materials

Since direct data on radiation effects on components and devices will frequently be unavailable to the designer of aerospace equipment, he must then resort to the other category of data mentioned – the individual materials of which the component is made. On the basis of radiation effects on materials, some extrapolation can be made as to the behavior of components and the limiting conditions that a component can withstand.

This section presents a discussion of the general effects of space radiation on materials used in the manufacture of electronic components (Refs. 1 to 8). Available information on the components and devices themselves will be presented in subsequent sections, and finally the effects of other environmental factors will be summarized.

14.1.1.1 Metals and Alloys

Of all the materials used in electronics, metals and their alloys are probably the most resistant to the effects of radiation. Changes in their mechanical properties are of little concern in electronics because they are comparatively small and a large percentage of these changes anneal out at rather low temperature.

Effects of radiation on electrical resistivity have been studied extensively. Changes in this property are essentially due to lattice imperfections, which are more efficiently produced by heavy particles than by electrons or gamma radiation. Neutron irradiation at temperatures between 30° and 300°C causes small permanent changes in most metals. At room temperature, increases in resistivity range from 0 to a few percent for an integrated slow neutron flux of 10^{19} neutrons/cm^2 for metals commonly used in electronics such as copper, silver, nickel, platinum, and their alloys. Substantial effects are observed, however, in metals having a high melting point: about 10% for the same neutron dose in tungsten and molybdenum at room temperature.

During exposure to an integrated fast neutron flux of 2×10^{18} neutrons/cm^2, copper-nickel and nickel-chrome, commonly used in wire-wound resistors, showed a maximum increase in resistance of 0.8%. However, no permanent effect was observed. The effects of radiation on the work function and emitting property of metals and alloys used for thermionic and photo cathodes have not been studied.

A more detailed treatment of the effects of the space environment on metallic materials for all applications is given in Chapter 15.

14.1.1.2 Ceramic Materials

In general, ceramic materials used in capacitors, including those containing some organic binder, can withstand appreciable doses of radiation. Only negligible degradation of electrical and physical characteristics occurs up to 10^{15} to 10^{18} neutrons/cm^2.

In thermistors made of metal oxides, the most susceptible constituent is the organic binder. Gas evolution may cause some decay of mechanical characteristics. However, exposure to fast neutrons up to 5.5×10^{10} rads produces no change in the negative temperature coefficient. In one test with slow neutrons, a dose of 2×10^{15} neutrons/cm^2 did not produce any significant effect.

Silicon thermistors are preferred in some applications because of their positive temperature coefficient. Their resistance, however, is very sensitive to radiation. At a dose of 10^{17} neutrons/cm^2, the resistance increases by a factor 10^6, of which only a negligible fraction can be attributed to irradiation temperature.

Prolonged irradiation in all oxides leads to permanent displacement effect and loss of oxygen, especially near the surface.

In glasses, radiation-induced changes of concern in electronics are electrical conductivity, mechanical degradation, and absorption of visible light. No quantitative information is available on increased conductivity, although some test data seems to indicate that this effect is unimportant in lead glass irradiated with 1-Mev electrons.

Coloration in most glasses saturates at 1×10^{10} rads or less. High-purity vitreous silica remains transparent at 1×10^{8} rads. Addition of 1 or 2 percent CeO_2 increases resistance to coloration. The cerium ion is efficient in removing radiation-produced free electrons which would otherwise form color centers.

Electrons or gammas are more efficient in creating color centers than in displacing atoms. Consequently, degradation in mechanical properties occurs at higher doses than does coloration. Bombardment with neutrons and heavy particles leads to mechanical failure at rather low doses. The presence of boron in borosilicate glasses makes them particularly susceptible to neutrons because of the transmutation reaction in boron during which its nucleus absorbs a neutron, then breaks up into an alpha particle and a lithium atom. Cracking and chipping are observed in these glasses at doses ranging from 10^{15} to 10^{20} neutrons/cm^2 depending on the boron content, the initial annealing, and the particular device.

The effects of space radiation on glasses for optical applications in spacecraft are considered in more detail in Chapter 8.

14.1.1.3 Semiconductor Materials

Nuclear radiations produce permanent effects on semiconductors, mainly through displacement of individual atoms of the bombarded material. The minimum energy which a bombarding particle would require to displace one atom is usually estimated at 30 eV for germanium and 25 eV for silicon. Most displaced-atoms defects anneal out at room temperature or form secondary associations with each other and with impurities initially present in the lattice. Those that are thermally stable, however, can affect electronic properties of semiconductors by increasing the concentration of trapping, scattering, and recombination centers. Trapping centers remove carriers that would otherwise be available for conduction. Silicons of n- and p-type gradually change to the intrinsic materials; n-type germanium may convert to p-type. Creation of scattering centers shortens the mean free path of free carriers, whereas additional recombination centers reduce the minority carrier lifetime.

Solar cells suffer two main types of damage: decrease in minority carrier lifetime and interaction of vacancies with impurities such as oxygen and phosphorus. Altering the concentration and nature of impurities can reduce the extent of damage appreciably.

Silicon n-p cells are more radiation resistant than silicon p-n cells. The reason is probably that the recombination length in the p region of the first category is larger than the recombination length in the n region of the second category after prolonged bombardment. For proton irradiation the threshold for 25% degradation is about 10^{11} protons/cm^2 at a primary energy of 240 MeV.

Silicon lithium-drift p-i-n diodes suffer the usual degradation in minority carrier lifetime. In addition, however, a redistribution of lithium ions occur in the drifted region. The increased lithium gradient at the junction leads to a narrower depletion width, causing the lithium drift p-i-n diodes to be more vulnerable to radiation than the p-n type.

14.1.1.4 Dielectric Materials

At a total gamma dose of 1×10^8 rads, polytetrafluoroethylene, polytrifluorochloroethylene, polystyrene, and polyethylene decrease in volume resistivity by a factor of about 10, and polyethylene terephthalate (Mylar) by a factor of about 6.

Changes in mechanical properties are generally more serious. At gamma doses as low as 8.7×10^3 rads the melt viscosity of Teflon decreases by several orders of magnitude (due to predominant scission). Approximately 3.6 μgm of corrosive fluorine gas per gram of Teflon is evolved at a dose of 4.35×10^6 rads. The influence of the space environment on mechanical properties of plastics for structural applications is described more fully in Chapter 12.

Teflon capacitors exposed to 10^{14} neutrons/cm^2 increase in capacitance by about 10% and the leakage resistance drops from 6×10^{11} to 6×10^8 ohms. In capacitors, the oriented film Mylar shows no objectionable degradation in electrical properties up to 10^8 rads and in mechanical properties up to 10^9 rads of gamma radiation. During irradiation, the dielectric constant undergoes some changes but recovers after irradiation.

Mica used in capacitors behaves satisfactorily up to a neutron dose of 5×10^{18} neutrons/cm^2. Epoxy binders used in carbon composition resistors become increasingly conductive under irradiation, with no recovery. A fast neutron dose of 2.4×10^{17} neutrons/cm^2 decreases the resistance of a 100-ohm resistor by 4%.

Damage in metallized paper capacitors is primarily due to gas evolution from the impregnants (mineral oil, wax, castor oil, petroleum jelly, chlorinated compounds), causing pressure buildup, bursting, and short circuit. For fast neutrons, the threshold of damage is around 10^{13} neutrons/cm^2.

The main radiation effects on circuit boards are increased leakage current and mechanical damage in the form of blistering and warping. The extent of damage depends critically on the manufacturing process, but test data seem to indicate that the glass-melamine type is more susceptible to blistering and warping than the glass-epoxy, paper-phenolic, steatite, and nylon-phenolic types.

Increase in leakage current is believed to be due to radiation-induced ionization in air, establishing conductive paths between exposed copper conductors. Coatings reduce this leakage, and the most efficient one seems to be silicone varnish. The leakage current in an uncoated board was less than 10^{-12} amp before exposure and 1.09×10^{-7} amp during exposure to gamma radiation at a rate of 70 rads/sec. Under the same irradiation condition, a board coated with silicone varnish showed a leakage current of less than 10^{-12} amp before exposure and 5.6×10^{-10} amp during exposure.

14.1.1.5 Insulating Materials

Organic dielectrics, encapsulants, and other types of insulating materials are relatively sensitive to radiation damage with respect to their physical strength and dimensional stability as well as their electrical properties. The most sensitive organic insulation possesses a radiation tolerance of up to 1×10^7 rads (Ref. 9). Radiation-resistant organic materials of certain types have been known to perform satisfactorily in an environment up to 10^{10} rads, whereas inorganic insulation and dielectrics may be usable to radiation levels up to 5×10^{12} rads. Table 14-1 (Refs. 9 and 10) presents some of the changes in electrical properties of fluorocarbon materials on irradiation. Silicone dielectrics are generally resistant to particle radiation (Ref. 11). In one study, it was found that although crosslinking occurred at 10^6 rads in dimethyl-based silicones and at 10^8 rads in methyl phenyl-base silicones, with accompanying brittleness, no significant changes were observed in the electrical properties.

Wire insulations of alternate laps of polyimide, H-film, and Teflon FEP of 3, 4, and 6 mil (0.006 in.) total thickness, and polyolefin with a polyvinylidene fluoride jacket of about 9-mil total thickness were irradiated for 10 hr at 6000 rads/hr of x rays in vacuum at 150° C (300° F). The voltage breakdown and insulation resistance of twisted pairs of the wires were measured before and after exposure. No significant changes in these properties occurred as a result of the x-ray radiation. The insulation resistance of some combinations increased about one order of magnitude after irradiation. For example, the resistance of the polyolefin-polyvinylidene fluoride combination increased from 6.3×10^{13} ohms before to 3.1×10^{14} ohms after irradiation (Ref. 12).

Several encapsulating compounds have been found serviceable for space applications. The cure is an important factor in space stability, a higher temperature cure being preferred to room-temperature cure. Solvent systems are generally not satisfactory as they tend to dissolve the insulation of imbedded wires. Some of the classes of encapsulating materials and the temperature and radiation environments in which they can be used are shown in Table 14-2 (Ref. 13).

14.1.2 Semiconductor Devices

Over the past decade, the amount of radiation effects data on semiconductor devices has increased by about three orders of magnitude and the degree of sophistication in radiation effects information has also increased to a large extent. Yet the designer is still not able to achieve reliably hardened designs by selecting components and materials from various compendia of radiation effects information. The reason for this apparent paradox lies in the basic limitation in the component selection approach to hardening, an approach which is only one of the major factors in evaluation and circumvention of system and subsystem vulnerability. The complexities which broaden the scope of the problem of radiation vulnerability and circumvention results from (1) multiplicity in degradation modes, and corresponding multiplicity in tolerance levels, (2) possible interaction between modes, (3) dependence on secondary environments, (4) damage to circuits or degradation of system performance by transient effects, (5) dependence on nonradiation ambients such as temperature, pressure, mechanical stress, and electrical stress, (6) wide variations in radiation tolerance

Table 14-1

CHANGES IN ELECTRICAL PROPERTIES OF ELECTRICAL INSULATORS DUE TO RADIATION AND VACUUM EXPOSURE

Material	Radiation Exposure (rads)	Dissipation Factor[a]		Dielectric Constant[a]		Volume Resistivity (10^{17} ohm cm)	
		Before	After	Before	After	Before	After
Polytetrafluoroethylene, TFE-6	4×10^7	<0.001	0.081	2.08	2.12	>10.0	0.31
Polytetrafluoroethylene, TFE-7	4×10^6	<0.001	0.019	2.09	2.13	>10.0	0.28
Fluorinated Propylene, FEP-100	1.6×10^6	–	–	–	–	>10.0	0.048
Monochlorotrifluoro-ethylene, K-4	2.5×10^6	0.008	0.005	–	–	>10.0	0.38
Monochlorotrifluoro-ethylene, K-5	2.5×10^6	0.011	0.004	–	–	>10.0	2.30
Kynar 400	$6.6 > 10^7$	0.0042	0.0100	1.00	0.988	0.04	0.0005

(a) Measurements taken at 60 Hz.

Table 14-2

ELECTRICAL ENCAPSULANT MATERIALS

Material	Continuous Temperature Range for Successful Use (°F)	Radiation Level at Which Electrical Properties May Begin to Change (rad)
Polyurethanes	-65 to 165	$10^8 - 10^9$
Silicone Rubbers	-85 to 500	5×10^6
Polysulfide	-70 to 300	10^6
Epoxies	-65 to 200	$10^7 - 5 \times 10^8$

of devices of similar electrical characteristics fabricated by different manufacturers or even by the same manufacturer, (7) very rapid developments and changes in electronic device technology and application, and (8) proximal or interface effects related to configuration rather than basic transducer properties.

To cope with this broad scope of problems, it is necessary to adopt a broad approach which seeks to utilize indirect as well as direct methods of hardening and circumvention. The designer must incorporate radiation vulnerability – its assessment and circumvention – into his planning and design at very early stages in order to maximize his flexibility in circumvention through circuit design, programming, device selection, packaging, and location. He must understand the manner in which radiation affects the functional parameters of interest; he must know how these changes will affect his subsystem and the overall system; he must think of alternatives, tradeoffs, possible relocations, and, finally, possible device selection or hardening. In short, the designer must consider radiation as an added ambient environment along with and in context with temperature, pressure, etc. Hardening by comparing environmental specifications with previously reported data on specific components is very risky unless such information is taken only as a guideline and in specific context with application and service conditions.

14.1.2.1 Diodes, Transistors, and Solar Cells

In context with the above discussion of the nature of radiation vulnerability and the approach to circumvention and hardening, the radiation tolerance information in this section is presented in terms of "useful range" in Figs. 14-1 and 14-2 and by specification of dominant modes of degradation in Table 14-3. The generic categories have been selected on the basis of conventional usage and transducer configuration. The dominant failure modes are based on radiation response and parameters of importance in common applications. It is intended that the designer use Table 14-3 as a guide to the useful range or the range of radiation in which a particular generic class of devices is expected to suffer significant changes in one or more of the commonly used characteristics but not to the extent of degradation beyond usefulness in conventional application. If it can be ascertained from Fig. 14-1 that a particular device under consideration belongs to a class well below the useful range (significant change, but still useful), perhaps the vulnerability problem can be regarded as minor or nil unless an unusually tight requirement is imposed. If the application is a critical one or if the radiation level is expected to fall into or close to the range of significant damage, Table 14-3 should be consulted to find the dominant mode of degradation and to help assess the systems implications of these anticipated effects. Although the format chosen gives only approximate information and some devices in a given category may fall well outside the average envelope indicated for the group, it is clear that the measured radiation tolerance of a specific device in a particular test is subject to wide variation in other applications and under different conditions of use. Furthermore, specifying the measured radiation tolerance or performance in a test to the observed degree of precision often tends to mislead because there is a natural tendency to infer the spread of the tolerance range from the precision of a set of measurements.

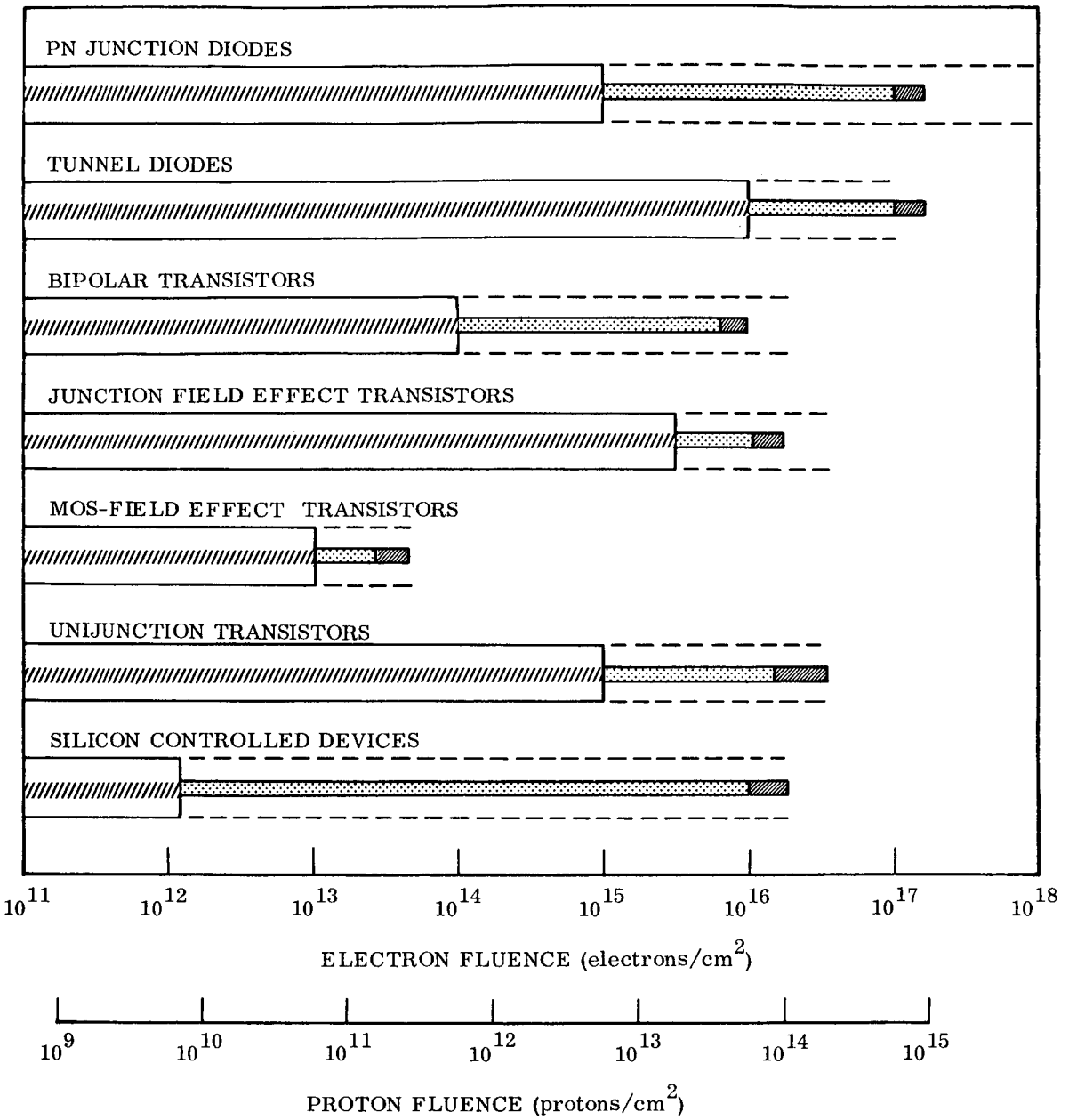

Fig. 14-1 Useful Ranges for Semiconductor Devices Exposed to Space Radiation (Correlated With Table 14-3)

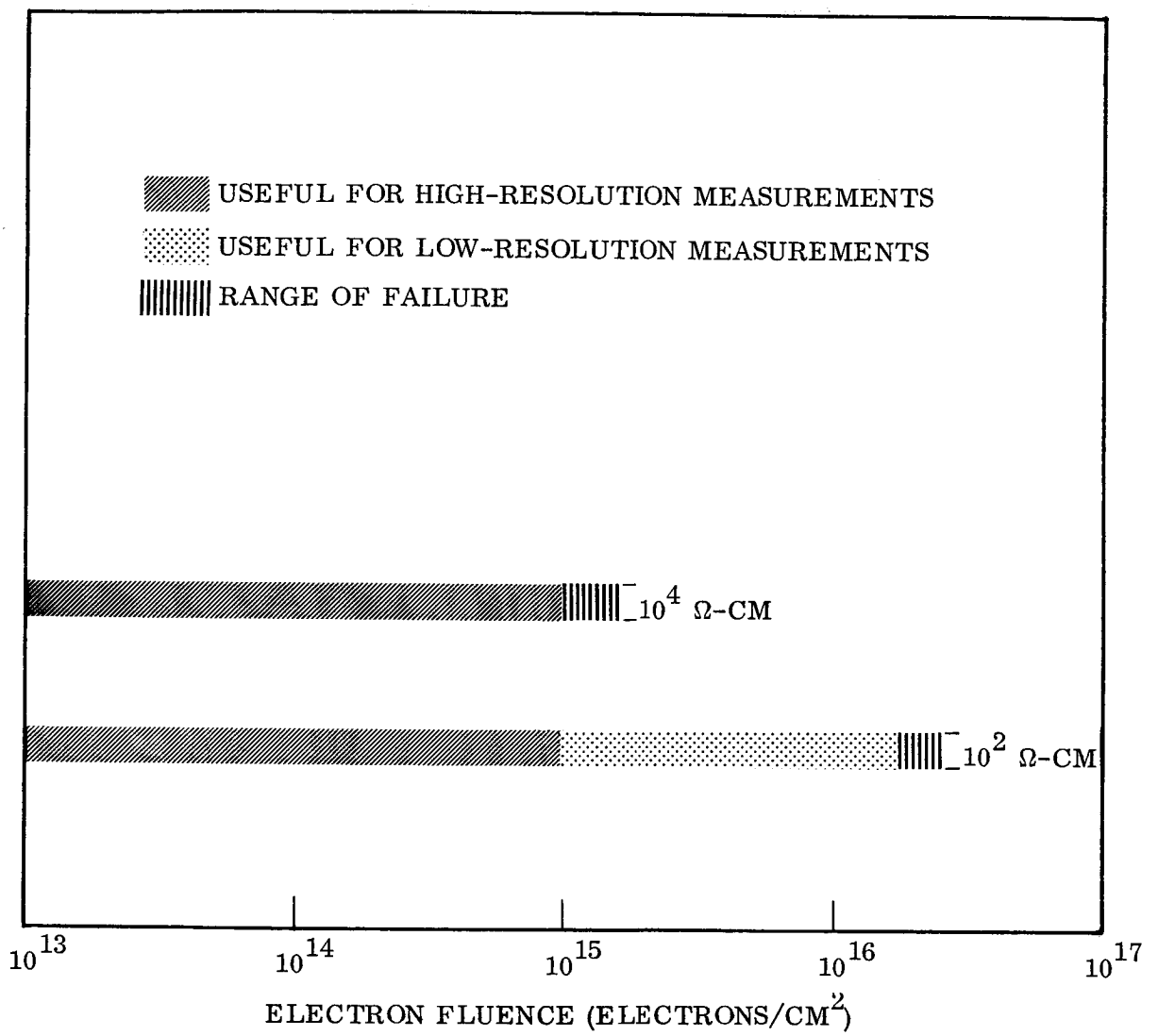

Fig. 14-2 Useful Ranges for Silicon Charged Particle Detectors Exposed to Space Radiation (Phosphorous-Diffused Devices)

Table 14-3

TRENDS OF RADIATION DAMAGE IN SEMICONDUCTOR DEVICES

Device Type	Operating Parameter	Parameter Change With Increasing Fluence	Comments
Diodes, PN Junction	Forward voltage (V_F) Reverse breakdown voltage (V_R) Reverse leakage current (I_R) Rise time (T_R) Storage time (T_S)	Increase Slight increase Increase Increase Decrease	Fast diodes with low breakdown voltages are less sensitive to permanent effects because of doping profiles.
Diodes, Tunnel	Peak current (I_P) Valley current (I_v)	Slight decrease Increase	Because of high doping, this device is not affected until relatively high dose levels.
Transistors, Bipolar	Current gain (h_{FE}) Reverse leakage current (I_{co}) Saturation voltage $(V_{CE})_{(sat)}$	Decrease Increase Increase	High-frequency, low-breakdown voltages, characteristic of epitaxial devices, provide better radiation resistance. Some manufacturers advertise radiation-resistant devices incorporating these features.
Transistors, Junction Field Effect	Transconductance, in grams Drain current with $V_{gs} = 0$ (I_{DSS}) Pinch-off voltage (V_p)	Decrease Decrease Decrease	Gain parameter (transconductance) is not appreciably degraded until relatively high radiation dose levels, making the device less sensitive than comparable bipolar devices.
Transistors, MOS Field Effect	Transconductance, in grams Threshold voltage (V_r) Channel resistance (r_{DS})	Decrease Increase Increase	Very easily degraded in an ionizing radiation environment via charge storage in the oxide layer.
Transistors, Unijunction	Interbase resistance (R_{BB}) Valley current (I_v) Valley voltage (V_v) Intrinsic standoff ratio	Increase Decrease Increase Remains same	Interbase resistance very sensitive to neutron-induced permanent radiation damage due to doping concentrations.
Silicon – Controlled Devices	Gate current for triggering (I_{GF}) Gate voltage required for I_{GF} (V_{GF})	Increase Increase	New device designs, employing selective current gains in the analog of the device, claim greatly increased radiation tolerance.
Solar cells	Short-circuit current (I_{SC}) Open-circuit voltage (V_{oc}) Maximum available power ratio $\left[P_{max}/\left(P_{max}\right)_o\right]$	Decrease Decrease Decrease	n-on-p are approximately one order of magnitude more resistant than the p-on-n devices. Cadmium sulfide thin-film cells look promising, but extensive degradation data are not available at this time.

The specific intent of the tabular information presented is only to provide the designer with a warning signal of situations of potentially marginal performance and reliability and to give indications of the nature of the malfunction. When a potentially marginal situation arises, the designer may choose to circumvent by alternate design or functional requirement, to circumvent by temporary overrides or disconnects, to modify the design to allow substantial degradation in pertinent parameters without major system compromise, to relocate or repackage or provide additional shielding if reasonable, or to undertake a systematic test program to establish and proof-test a given level of system performance under appropriate test conditions.

The best conditions for such testing, would, of course, be those of actual usage – the space environment. One example of such tests carried out in space is the extensive study of radiation damage to solar cells and transistors performed by the Applied Physics Laboratory beginning in 1961 (Ref. 14). In particular, the influence of shielding of various types of thicknesses was studied in detail. Shielding used on the solar cells studied ranged from none up to 0.125-in. quartz (0.700 gm/cm^2) and up to 0.3-in. aluminum (2.057 gm/cm^2) for the transistors. The results of these flight experiments indicate that optimum power-to-weight ratio solar arrays will be obtained by use of n-on-p solar cells with 6-mil quartz covers. In one experiment, for example, n-on-p solar cells with 0.125-in. quartz covers decreased in current output by 10.5% in 500 days whereas the same type cells decreased by only 8% in the same time under 0.006-in. covers. This difference is attributed to discoloration of the thick cover slide.

The transistor reliability studies, performed on satellite 1964-83C, are summarized in Table 14-4.

The lower damage shown by the 2N1711 transistor with punctured case as compared with transitors with unpunctured cases is ascribed to ionization of gases with consequent surface damage in the unventilated transistors.

Solar cells have been considered separately in Fig. 14-3 and Table 14-3 because of their importance in space vehicle applications in the foreseeable future and because they are by function and by mechanism substantially different from the circuit component devices. Experimental data on actual exposure to the space environment have been obtained for solar cells on a number of spacecraft flights. The early data from ATS-1 given in Table 14-5 show response of a variety of cell types and shielding combinations (Ref. 15).

Some serious thought is now being given to pre-irradiation of solar cells before flight. Since the most serious loss of solar cell output occurs in the first few days or weeks in orbit, pre-irradiation would result in cell outputs more constant with time (although lower). Since solar cell arrays must now be designed to give sufficient power after radiation degradation, their excess power during the early times in orbit must be dissipated; pre-irradiation would reduce this requirement.

Table 14-4

EFFECT OF SPACE RADIATION IN ORBIT ON TRANSISTORS

Transistor Type	Shielding	Percent of Original Value of Transistor β Retained After Indicated Days in Orbit			
		10 Days	50 Days	100 Days	200 Days
2N2222[a]	None	93	85	80	74
	0.1 in Al (0.685 gm/cm^2)	99	98	97.5	97
2N2586[a]	None	100	98	97.5	97
	0.1 in Al (0.685 gm/cm^2)	98	96	94	93
2N2907-A[a]	0.1 in Al (0.685 gm/cm^2)	100	100	99	98
2N1711[b] (Unaltered)	Epoxy glass honeycomb (0.28 gm/cm^2)	92	72	68	66
2N1711[b] (Punctured Case)	Epoxy glass honeycomb (0.28 gm/cm^2)	98	91	87	83

(a) Exposed to environment of satellite 1964-83-C, apogee 1070 km, perigee 1027 km, inclination 89.99 deg, launch date 12 December 1964.

(b) Exposed to environment of satellite 1963-38C, apogee 1120 km, perigee 1070 km, inclination 89.9 deg, launch date 28 September 1963.

(A) Electron Irradiation

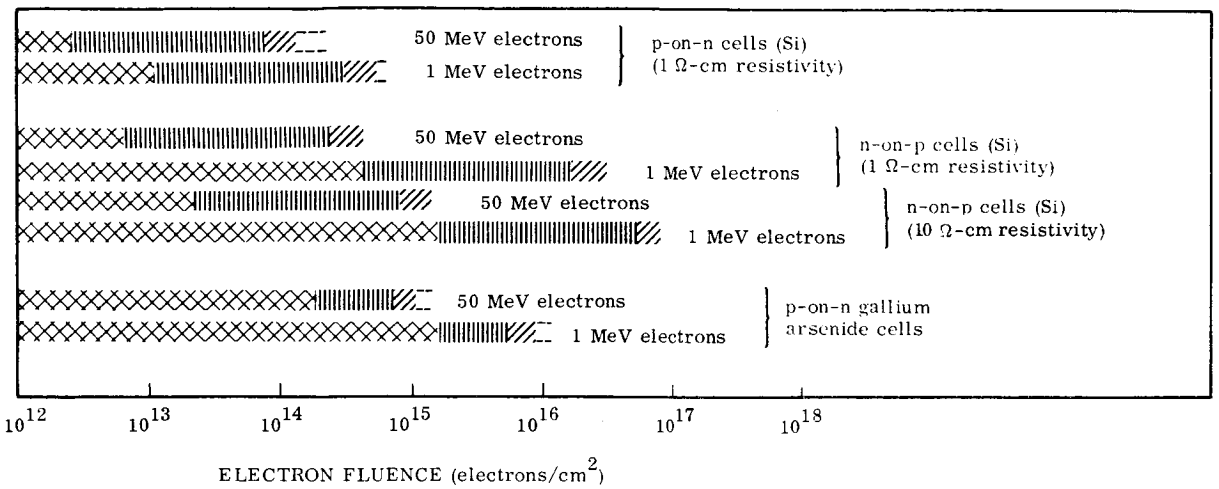

(B) Proton Irradiation

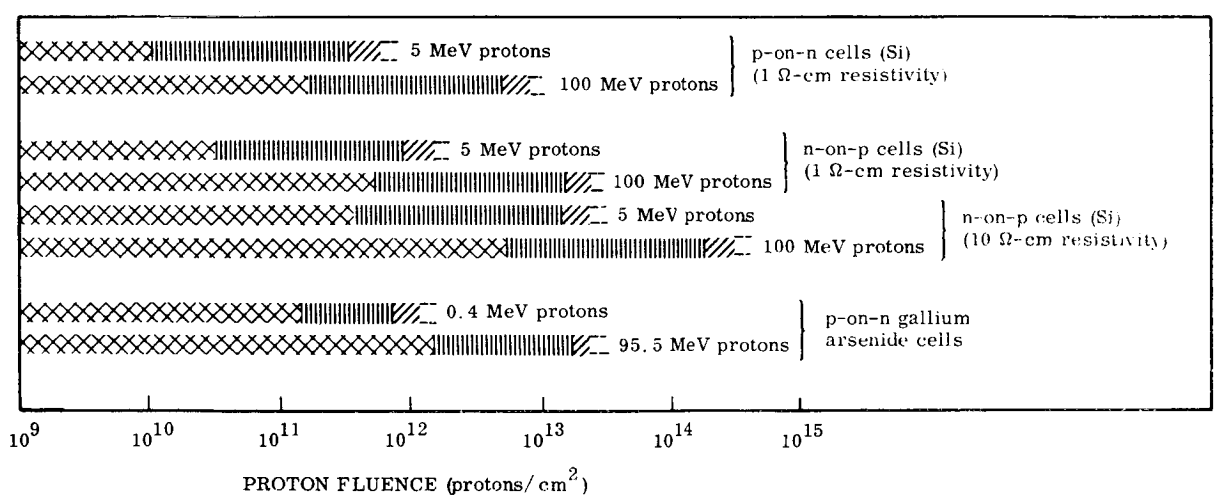

DEGRADATION IN MAXIMUM AVAILABLE POWER RATIO

≤ 20%

≤ 50%

> 50%

Fig. 14-3 Useful Ranges for Solar Cells Exposed to Space Radiation

Table 14-5

CHANGES IN CHARACTERISTICS OF EXPERIMENTAL SOLAR CELLS ABOARD ATS-1 SPACECRAFT

Solar Cell Type	Base Resistivity (ohm-cm)	Dopant	Shield Material	Shield Thickness (mils)	Cell Short Circuit Current (mA)		Percent Change	Cell Voltage (mV)		Percent Change
					At Liftoff	After 3.3 Days in Orbit		At Liftoff	After 3.3 Days in Orbit	
n/p	10	Al	Sapphire	30	46.4	46.8	+ 0.9	531	522	- 1.7
n/p	13	B	7940 Silica	6	63.4	63.8	+ 0.6	554	547	- 1.3
n/p	10	B	7940 Silica	6	67.5	67.0	- 0.7	567	565	- 0.4
n/p	7	B	7940 Silica	6	62.7	62.4	- 0.5	573	566	- 1.2
n/p	3	B	7940 Silica	6	62.4	62.4	0	586	580	- 1.0
n/p	Graded	B	7940 Silica	6	55.5	55.9	+ 0.7	600	597	- 0.5
p/n	1	P	None	0	58.7	21.9	-62.7	563	435	-22.7
n/p	1	B	None	0	53.7	40.0	-25.5	569	474	-16.7
n/p	10	B	7740 Glass	1	62.0	60.9	- 1.8	554	545	- 1.6
n/p	10	B	0211 Glass	6	66.4	67.2	+ 1.2	575	567	- 1.4
n/p	10	B	7940 Silica	60	68.0	68.5	+ 0.7	576	570	- 1.0
n/p	10	B	7940 Silica	30	68.4	68.9	+ 0.7	570	565	- 0.9
n/p	10	B	7940 Silica	15	67.0	67.6	+ 0.9	572	575	+ 0.5
n/p	10	B	None	0	69.5	60.2	-13.4	559	431	-22.9
n/p	10	Al	7940 Silica	30	66.9	67.5	+ 0.9	570	561	- 1.6
n/p	10	Al	7940 Silica	6	64.0	63.0	- 1.4	568	557	- 1.9

The term "threshold of failure" or "degradation" was avoided in the previous discussion and is avoided in the illustrations because these terms and their variations have been used in a variety of different ways in the radiation effects literature and because the concept of the word "threshold" implies a sharp boundary which is inappropriate in most applications of radiation damage data. However, the commonly used meanings of "threshold" are described and compared in the following paragraphs for purposes of clarification and to indicate the context in which the tabular information is presented.

In the simplest case, failure behavior can be described in terms of a step function; i.e., zero failures occur up to a certain critical level of radiation and 100% failure is encountered beyond this level. This behavior can thus be characterized by a discrete threshold. However, failure data conforming to such go or no-go response are rather rarely encountered in radiation-induced failure processes. More often, the failure behavior is characterized by a frequency distribution in the failure probability versus dose. Accordingly, the failure threshold can be defined in various arbitrary ways:

- The maximum permissible radiation constraint which, within a set of nominally identical specimens, produces an average absolute or percent change in an operating characteristic such that the latter is still within prescribed limits of tolerance. (This definition neglects to consider the statistical spread in degradation behavior. As a consequence, some outlying members of the set may actually exceed the design specifications.)
- A definition similar to the above but superior in its usefulness assumes the thresholds to be given by the maximum permissible radiation constraint which, among a set of nominally identical specimens, produces a given maximum but still acceptable change in an operating characteristic such that this maximum change is not exceeded by more than some specified small proportion of nominally identical specimens. This is the concept used in establishing the approximate endpoints of the useful ranges in Fig. 14-1.
- The maximum permissible radiation producing a still acceptable proportion of defective specimens in a given set of nominally identical specimens.
- The radiation level at which a given radiation-induced effect becomes barely detectable by means of a specified technique of measurement.

14.1.2.2 Integrated Circuits

Owing to the wide variability in the structural and functional design of integrated circuits or microcircuits, their response to radiation is discussed here only in general terms. Moreover, there is, to date, a paucity of experimental data on specific integrated circuits to permit a comprehensive evaluation of the behavior of generically related systems. However, one study of commercially available circuits reveals that the better constructed circuits are immune to transient radiation disturbances to over 10^9 rad and to permanent damage up to at least 10^{13} neutrons/cm^2 (Ref. 16).

In a space radiation environment, the principal modes of degradation expected will arise from (1) cumulative displacement damage, (2) leakage currents, (3) surface and interface effects, and (4) effects of charge storage in the oxide layer of metal-oxide-silicone-type structures. These modes of damage are, to a greater or lesser degree, also in evidence upon irradiation of discrete components, but they are less accessible to study at the locus of their occurrence in microcircuits because of their small scale and peculiar geometries.

The high surface-to-volume ratio of the constituent circuit elements generally contributes a predominance of the role of surface and interfacial phenomena. As a consequence, the radiation response of these structures is very sensitive to subtle configurational, topological, and compositional variations – factors currently not adequately understood or adequately controlled during the fabrication process. These difficulties are compounded by the fact that the performance of microcircuits and hence their response to radiations are of necessity a function of the circuit parameters.

One approach to predicting microcircuit performance upon irradiation has been to treat the constituent circuit elements as if they were discrete devices. This practice yields, at best, crude estimates of performance for preliminary design purposes and definitely does not eliminate the need for testing. Two general rules for maximizing radiation stability of microcircuits can be given:

- The circuit selected should be relatively insensitive to transistor gain degradation
- The transistor elements should have the highest circuit-compatible gain-bandwidth product.

However, the trend toward development of large-scale monolithic arrays will progressively preclude the application of this approach and will pose new problems in the formulation of effective and economical techniques of predicting and testing circuit response.

14.1.3 Electron Tubes

Until about a decade ago the electron tube was the "work horse" in active electronic circuitry while the proportionate use of transistors was increasing but remained relatively low. In the past 4 years, the solid state electronic device for general circuit application has virtually replaced electron tube devices in ground-based equipment and in space vehicle instrumentation except for special-purpose applications. This trend has had a strong effect on the manufacturing and development of electron tubes and on the radiation testing programs. The radiation damage data on electron tubes remain fragmentary and in a sense have been abandoned as a result of the rapid increase in the use of semiconductor devices. Moreover, most of the tests on electron tubes were performed during a period when the use of nuclear reactor facilities was prevalent and many experimenters reported results in total dose of neutrons integrated over time and large portions of the energy spectrum plus the associated reactor gamma environment. Because of their greater physical dimensions, very few data are available on the response of electron tubes in electron and proton accelerator beams. The combination of these factors makes it difficult to correlate precisely to obtain highly reliable information on the tolerance of electron tubes to natural space radiation.

As a rule of thumb, it is probably safe and conservative to assume that electron tube devices as a class are at least two orders of magnitude higher in tolerance to permanent effects of penetrating radiation than the semiconductor component group. It is recognized that there is wide variation in both categories, and this comment is made

only to indicate a general trend. Reactor experiments indicate usable ranges of 10^{15} to 10^{17} neutrons/cm^2 (plus associated gamma doses of 10^5 to 10^7 rad) for general-purpose tubes of conventional construction. The General Electric TIMMS (thermionic integrated micro modules) units, developed for high-temperature application, were found to be about two orders of magnitude more resistant than those of conventional construction.

The permanent failure of hard vacuum tubes is generally due to cracking of the glass envelope or separation at the Kovar-to-glass seals. The optical darkening of the glass in the ultraviolet and visible range after relatively low exposures is of little consequence except for tubes with optical applications. Cracking in the envelope and breaks in the seal occur in fairly wide statistical distributions and at levels well below the range of serious catastrophic damage to the individual materials, glass and Kovar. This leads to the conclusion that these failures are due in part to mechanical stresses, and to interface stresses which are probably aggravated by variations in fabrication control. There are indications that tube life (active) is diminished after irradiations in the range of 10^{15} to 10^{17} neutrons/cm^2 plus associated gammas but the statistics are poor. Transient effects on the operating characteristics are not serious at 10^6 rad/hr and 10^{11} neutrons/cm^2.

Gas tubes are similar to vacuum tubes in most respects and can be expected to suffer permanent damage due to glass envelope failure and seal failure in about the same range. The characteristic differences in gas tubes are the partial pressure of filling gas and the somewhat different electrode configurations. The presence of the filling gas and its function give rise to two additional failure modes. At high ionization dose rates, transient currents are produced but no permanent damage is expected. Neutron-induced transmutations in the gas are possible and would tend to produce a change in gas pressure at a rate dependent on the half-life of the unstable isotope produced. However, this mode is relatively unimportant in space application unless reactor power units are used in the immediate vicinity.

Light-sensitive tubes are probably the most important class of vacuum tubes remaining in extensive use in space vehicles, although the solid state electro-optical devices are also gaining rapidly in use and performance. The basic construction is closely related to the hard vacuum tube, and the mechanical failure problems are expected to be similar in kind and in exposure range. Glass darkening occurs in the range of 10^3 to 10^8 rad and tends to saturate at about 10^{10} to 10^{11} protons/cm^2. Quartz and fused silica are about two decades more resistant. Most of the coloration induced by radiation can be annealed by moderate-temperature immersions but might prove to be inconvenient in operational equipment. Another problem encountered in photosensitive tubes is the radiation-induced transient response because many applications involve low signal-to-noise ratios which are close to the capability of the device and its ancillary equipment. Among the suspect modes are luminescence of the glass envelope, secondary electrons produced in the photocathode region, recoil electrons produced in the dynode region, and leakage across insulators. A recent report (Ref. 7) indicates that glass luminescence appears to dominate under exposure to 2.6-MeV electrons (or bremsstrahlung formed in aluminum by 2.6-MeV electrons). The dark current attributable to luminescence was about four times that due to photocathode recoil electrons; and the effects

due to recoil electrons produced in the dynode section were another half decade below the photocathode effects. No leakage across insulators was indicated, presumably because of the geometric configuration of the electron beam.

Except for the filament-less TIMMS construction, which is probably practical for applications on reactor-powered vehicles, the radiation response of electron tubes is characterized by their general construction, which involves a glass envelope and vacuum seals, insulation, filling gas in the case of gas tubes, photosensitive surfaces, and dynode structures in the case of light-sensitive tubes. This range of general characteristics covers most conventional and special-purpose tubes, including microwave power tubes which may have specialized applications in space. Therefore, the behavior of tube types not specifically discussed can probably be inferred from their general construction and functions.

In summation, it appears that electron tubes in space applications will be relegated to highly specialized functions only and that solid state devices will continue to dominate until important breakthroughs are achieved in other approaches such as fluidics. The continued domination by solid state systems is guaranteed by the low power requirements and the rapid trend toward LSI (large-scale integration) and other forms approaching the ultimate limits in semiconductor device compactness.

14.1.4 Resistive Components

Comparatively little work has been done recently concerning radiation effects on resistors and capacitors, probably because of the greater radiation resistance of these elements compared with that of the semiconductor devices with which they are used. The resistive components examined fall into three general categories: carbon composition, film, and wirewound. The resistors in each category may be either fixed or variable.

Of the fixed resistors, the wirewound resistors are the least radiation sensitive, requiring fluences of 10^{15} to 10^{16} neutrons/cm^2 for significant changes. Oxide film resistors are the most sensitive, showing degradation at fluences of 10^{12} neutrons/cm^2. Resistances of carbon composition begin to show damage at fluences of about 10^{13} neutrons/cm^2. In general, the larger the value of resistance, the greater the percentage of change in resistance under radiation, with 1-megohm resistors changing by a factor of 3 to 4 over 100-ohm resistors.

The variable resistors are the potentiometer and trimmer resistance type and are either wirewound or composition-film. In general, these resistive elements show performance similar to that of their fixed resistor counterparts.

The effects of gamma radiation on resistive components is generally insignificant compared with the effects on semiconductors and capacitors. Gamma-rate effects are momentary, lasting only a few microseconds, and are usually due to ionization causing a shunt leakage path. Therefore, these effects will be more significant for high-value rather than low-value resistors. Although gamma-rate effects are small in resistors, these effects may become significant for rates as low as 10^7 R/sec.

A summary of radiation effects on resistive components is shown in Fig. 14-4 (Ref. 4). These data are of a general nature, of course, so that if information is desired on a particular resistive component, it is advisable to run laboratory tests on that component.

Because of the radiation insensitivity of resistors, all wirewound, carbon, and composition resistors and potentiometers tested are suitable for all 1-year circular-orbit space missions.

The trends of radiation influence on resistors are summarized in Table 14-6 (Ref. 21).

Table 14-6

TRENDS OF RADIATION DAMAGE IN RESISTIVE ELEMENTS

Resistor Parameter	Dependence on Radiation	Specific Examples
Transient leakage resistance (R_s)	Inversely as gamma dose rate	2×10^3 kilohms at 10^{10} rads/sec for carbon composition
Compton replacement current (I_R)	Directly as gamma dose rate	5 ma at 10^{10} rads/sec for carbon composition
Permanent resistance changes (ΔR)	Directly as neutron fluence	2% reduction at 10^{14} neutrons/cm^2 (fast) for carbon composition

14.1.5 Capacitive Elements

Comparatively little recent work has been reported on capacitors, again probably because of their relative insensitivity compared with semiconductors. Capacitors are divided into six categories, according to the type of dielectric used: ceramic, glass/porcelain, mica, paper, plastic, and electrolytic. The parameters affected by radiation are capacitance, dissipation factor, and leakage resistance. Although changes in capacitance may be either positive or negative, the dissipation factor invariably increases and the leakage resistance invariably decreases. In addition, oil-impregnated paper capacitors are subject to failure by case rupture due to evolved gas from the oil during radiation.

Paper and paper/plastic capacitors appear to be the most sensitive to radiation of the types tested, being worse than the inorganic dielectric types by a factor of about 1000. Of all capacitors, it appears that glass capacitors have the greatest radiation resistance, followed by mica and ceramic. Both tantalum and aluminum electrolytic capacitors have relatively low radiation thresholds; however, they appear capable of withstanding extended exposure to radiation before suffering severe damage.

Transient radiation is principally manifested as a transient drop in the dielectric resistance of the capacitors. The capacitors invariably recover to their initial state.

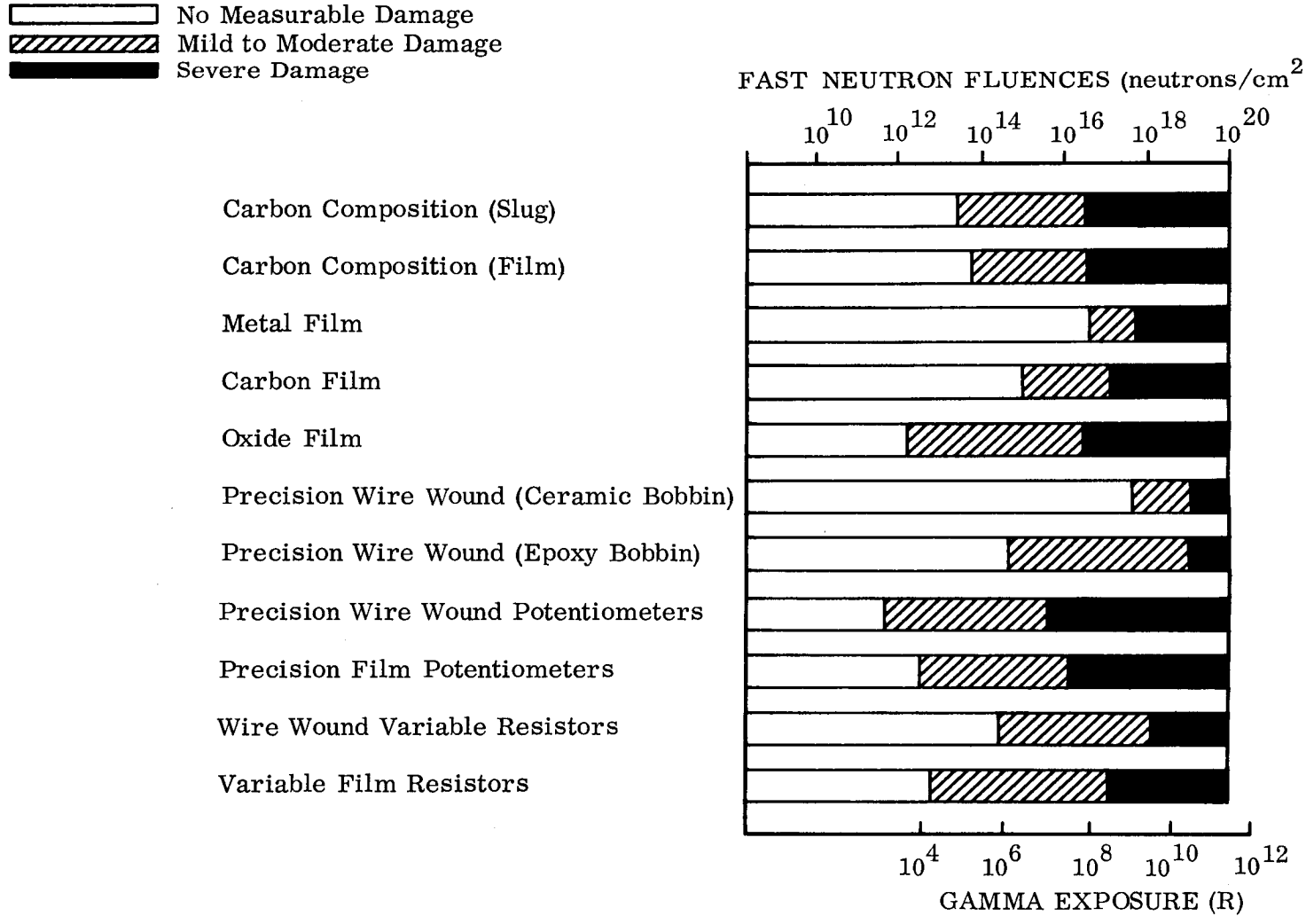

Fig. 14-4 Estimated Effects of a Radiation Environment on Commonly Used Resistance Devices

The relative radiation sensitivity of the six basic categories of capacitors is shown in Fig. 14-5 (Ref. 22). The data given are approximate only. If detailed information concerning radiation effects on a particular capacitor is desired, it is advisable to make radiation tests on that particular type.

Because of the relative insensitivity of capacitances, all capacitors of the types discussed are suitable for all 1-year circular-orbit space missions.

14.1.6 Inductive Components and Electromechanical Devices

14.1.6.1 Inductors

Very few data are available concerning radiation effects on inductors, and these data appear to be confined to high-frequency chokes, with an inductance range of 0.1 to 10,000 microhenries (Refs. 1 and 20). The chokes are of the molded type, having phenolic cores for low inductances, powdered iron cores for medium inductances, and ferrite cores for the higher inductances.

The extent of radiation damage to these components depends upon the type of resin used for coil encapsulation. For an integrated fast neutron exposure of up to 4×10^{16} neutrons/cm^2, radio-frequency chokes encapsulated in either diallylphalate or epoxy have inductance changes of about 5% and resistance changes of about 10%. For an integrated fast flux of 10^{14} neutrons/cm^2 and a gamma exposure of 5×10^6 rads, the changes reported are insignificant.

No data appear to be available for air coils or for low-frequency inductors. However, it is anticipated that, at least for air coils, very little sensitivity would be noticed except for perhaps inductance variations due to dimensional changes and for transient effects due to ionization of the air surrounding the coil. Low-frequency inductors in the range of 0.001 to 200 H are generally constructed similar to transformers, and it is expected that their radiation characteristics would be similar.

14.1.6.1 Transformers

The principal effect of radiation on transformers appears to be physical damage rather than a direct effect on their electrical operation. The usual physical damage is case rupture of hermetically sealed units caused by gas evolved from the potting compound. In some instances, the case rupture caused shorting of the terminals of the transformers. The experimental data, however, show that no significant degradation of the electrical characteristics of transformers occurs as a result of irradiation, at least up to 5×10^{17} neutrons/cm^2 and 2×10^9 rads.

14.1.6.3 Relays and Switches

The primary damage occurring in relays and switches due to nuclear radiation is damage to the insulating and construction materials used in these devices. Their radiation resistance is considerably enhanced by the use of such materials as Mycalex and

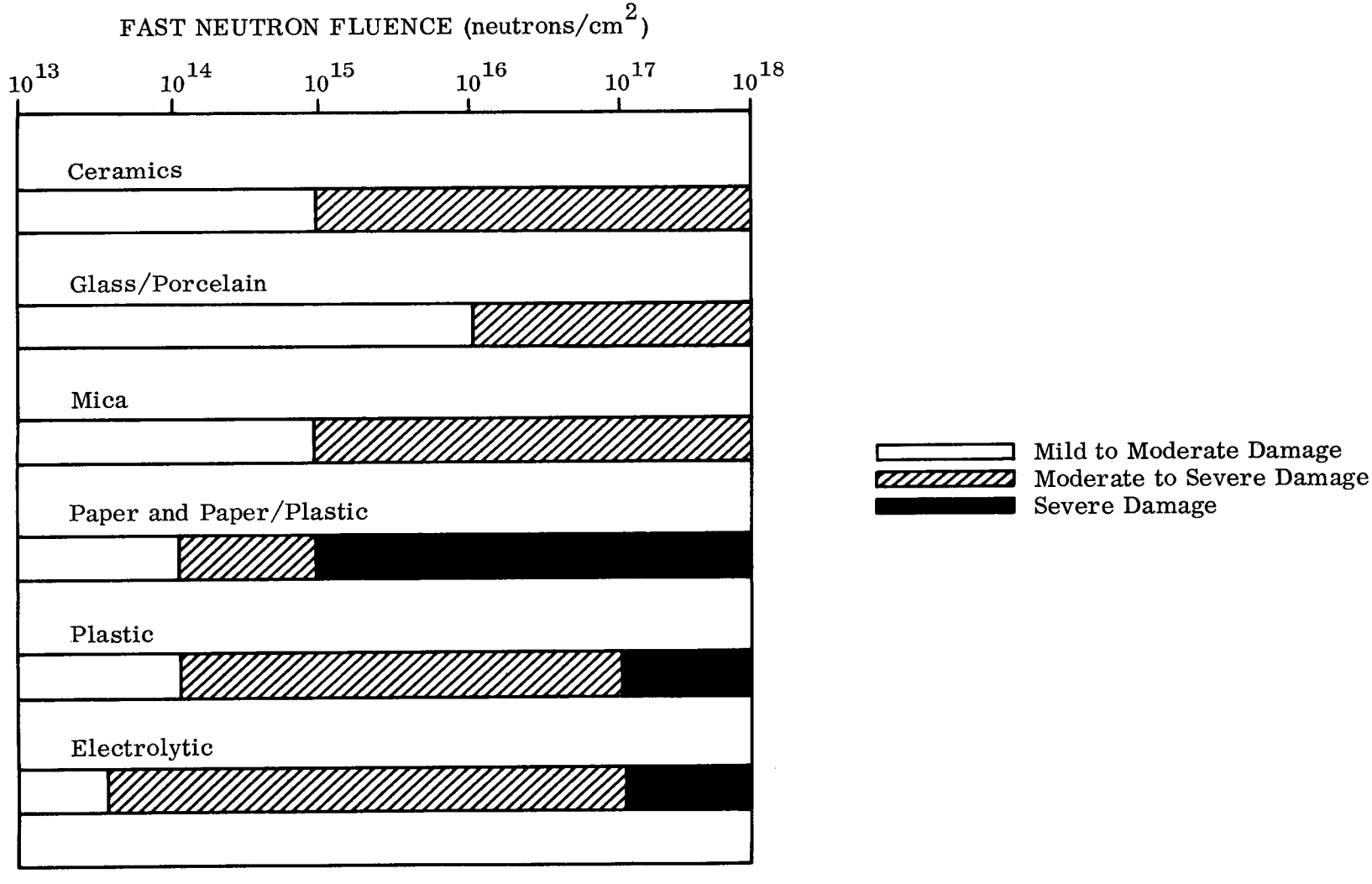

Fig. 14-5 Relative Radiation Sensitivity of Capacitors

fiberglass. With proper materials, relays have operated satisfactorily at fast neutron fluxes of us to 6.5×10^{14} neutrons/cm^2. Some microswitches have shown case damage at gamma-ray exposures as low as 4 to 6×10^6 rads or neutron fluxes of 10^{15} neutrons/cm^2. However, in general, these switches can withstand gamma radiation exposures of 10^7 rads with only minor deterioration but major case embrittlement occurs at gamma radiation exposures of 1.2×10^8 rads.

Since a major factor in the radiation resistance of relays and switches is insulation and construction materials, additional information concerning the effects of radiation on these devices can be determined by obtaining information on these materials.

14.1.7 Magnetic Materials

The two main classes of magnetic materials used in the construction of magnetic devices and circuits are metallic and nonmetallic. Metallic magnetic materials are specialized conductors which at higher operating frequencies show eddy current effects. This then leads to the lamination of metallic sheets to form useful magnetic devices. To prevent magnetic short circuits, the thin metallic sheets are separated by an insulator such as paper, mica, lacquer or metallic oxides.

Metallic conductors are little affected by radiation effects. The insulation may be affected if exposed to high enough fluences of energetic penetrating radiation. Above the Curie temperature, metallic magnetic materials lose their intrinsic magnetic capabilities, and the ordered domain structure of the material is changed to an unordered or random arrangement of the magnetic domains.

For many ferromagnetic materials, the Curie temperature is above 500°C (932°F). The specialized magnetic materials such as permanent magnets and magnetic materials used to store information operate only in the small temperature range -10°C to 100°C and may lose their magnetic capability well below their intrinsic Curie temperature.

Local magnetic heating which develops hotspots can produce localized demagnetization. Such a change in the local order of the domains results in a pronounced change of the electromagnetic behavior of the magnetic material.

Nonmetallic magnetic materials are separated into two classes: powder cores and solid state ferric-oxide cores. Powdered cores overcome the frequency limitations of metallic magnetic materials. Fine magnetic metallic or magnetic ferric oxide powders are pressed with a binder into a suitable shape, and fired to form a hard compact. This powder core is mounted into a nonconducting container and wound with the required windings. Changes in the properties of these powdered cores are mainly due to changes in the binder.

Solid state ferric oxides or ferrites are widely used for high-frequency inductors and with a specialized magnetic nonlinear characteristic as information storage elements. Ferrite materials are not affected by penetrating radiation. The square loop ferrite

cores used to store information are temperature sensitive. This is a secondary temperature effect, which can be induced by the penetrating radiation.

The effects of reactor neutron and gamma radiation on some components containing magnetic materials are shown in Table 14-7 (Ref. 23). The majority of the failures occurred at high neutron fluences and were attributed to short circuits caused by insulation embrittlement or loss in integrity of a powder metallurgically produced compact. Only transient changes in magnetic properties of the material occurred.

Threshold damage to iron and 5-molybdenum Permalloy magnetic components occurs at about 10^{16} protons/cm^2 of 1.5 MeV. At 10^{17} protons/cm^2, the maximum permeability was decreased 22 and 36%, respectively. At 10^{17} protons/cm^2 and 4 MeV, the maximum permeability of the 5 Mo-Permalloy was reduced 49%.

An optically polished yttrium-iron garnet single crystal for a ferromagnetic power limiter was irradiated with 10-MeV protons, -1MeV electrons, and low-intensity cobalt-60 gamma radiation. The changes in electrical and magnetic properties detected were attributed to the electron- and proton-induced radiation damage of the Teflon holder which supported the magnetic device in the resonant transmission cavity (Ref. 9).

14.1.8 Batteries

One aspect of electrical equipment that has been of considerable interest recently is the operating temperature of spacecraft batteries. Generally, these batteries are made up of several cells of 1.2 V (20−30 A) each. The active elements of the cells are enclosed in a case of acrylonitrile-butadiene-styrene for silver-zinc or nylon or nickel for nickel-cadmium. For primary cells, the active elements are silver, silver oxide, and zinc electrodes with cellophane spacers and insulators; the electrolyte is potassium hydroxide. For rechargeable cells, the active elements are nickel, nickel oxide, and cadmium; the other elements are similar to those in the primary silver-zinc cell. Cells generate gas during their operation (hydrogen when in use, and oxygen when completely discharged), so they are vented to prevent excess internal pressure. The charge and discharge rates of the cells, and consequently of the battery, are sensitive to the operating temperature. To maintain proper operating temperatures in the range of 30° to 100°F, batteries require thermal control in the form of insulation or heaters to keep them warm or radiating elements or surfaces to reduce the operating temperature. If the battery runs too cold (below 20°F), insufficient power will be developed. If the battery gets too hot (above 120° to 130°F), irregular charge-discharge characteristics are developed which, if not corrected, can force the battery into irregular cycles that can become cumulative in their effect and ultimately destroy the battery. One reason for this behavior is that at higher temperature the internal resistance decreases and the electrical heating of the cell increases, which causes a runaway increase in the battery temperature.

14.2 OTHER ENVIRONMENTAL EFFECTS

Penetrating radiation constitutes the most important direct space environmental parameter of significance to the operation of electronic components and materials in

Table 14-7

EFFECT OF REACTOR RADIATION ON ELECTRONIC COMPONENTS CONTAINING MAGNETIC MATERIALS

Component	Neutrons/cm^2	Gamma Radiation	Remarks
Plate Transformer	4×10^{17}	2×10^9	Windings failed at 4×10^{17} neutrons/cm^2. Irradiated at 932°F (500°C). Failure attributed to effect of elevated temperature.
Filament Transformer	4×10^{17}	2×10^9 2×10^6/hr	Of two units irradiated, one did not fail and one developed an open circuit in primary winding at 1×10^{17} neutrons/cm^2. Irradiated at 932°F (500°C).
Inductor (Reactor)	4×10^{17}	2×10^9	Of two units irradiated, one did not fail, and one developed an open circuit at about 5×10^{16} neutrons/cm^2. Irradiated at 932°F (500°C).
Magnetic Coils	2.5×10^{18}	–	Polymeric insulation materials, Bakelite varnish, polystyrene, rubber and friction tape, embrittled.
Magnetic Core Materials 2V Permendur Laminated	2.5×10^{18}	3×10^8	Little change in magnetic properties at direct current, 60 and 400 cycles/sec alternating-current frequencies. Cobalt-containing alloy, Permendur, had induced radioactivity.
2-81 Mo Permalloy (Powder Metallurgy Process);50-50 Ni-Ferrite Ceramic, Linear	2.5×10^{18}	3×10^8	Changes in magnetic properties of 2-81 Mo Permalloy because of radiation effects on binder increased air gaps with loss of magnetic flux density. No change in ceramic material.
Nickel Ferrite, Yttrium-Iron Garnet	1×10^{17}	5×10^9	No change in magnetic properties of square hysteresis loop materials.
Ferrite Core	4×10^{17}	2×10^{19}	No change in magnetic properties.

space. Some other environmental factors of less direct consequence are enumerated and discussed briefly below.

14.2.1 Vacuum

Exposed insulators, such as wire insulation, connector insulation, and encapsulating materials may be subject to outgassing, sublimation, and perhaps vacuum decomposition in some cases. Very few cases would have serious consequences because low vapor pressure and vacuum stable materials for electrical functions are readily available.

High voltage breakdown problems were reported during the thermal-vacuum testing of satellites Ariel 1 and 2, Explorer 17, Nimbus, OAO, and OGO. In the OSO 1 and 2, there was no evidence of this problem in thermal-vacuum test but it did occur in orbit. This behavior indicates inability to completely simulate the space environment. The major difference is the ionized elements, energetic particles, and ultraviolet and gamma radiation that are not normally present in thermal-vacuum acceptance testing of spacecraft subystems or systems. It is probable that adequate space simulation could be provided at the subsystem level to detect the potential problem area before flight.

14.2.2 Humidity and Other Contaminants

In most cases, the operation of electrical equipment is unimpaired or even improved by lowering the water content and other contaminants of the atmospheres. In exceptional cases, such as carbon brush contacts, the component can be sealed with an optimized atmosphere, or another brush material can be substituted.

14.2.3 Zero Gravity

The number of electronic devices depending on a gravitational field is very small. Such devices are usually specialized equipment for experimental purposes and are not generally included among the electronic components of missiles.

14.2.4 Micrometeoroids

Most electronic components are protected mechanically from physical impact with micrometeoroids, but exposed insulators and optical surfaces may sustain damage. Solar cell cover plates may be damaged optically in time, but sandblasted plates do not seem to reduce the cell output seriously. Light shields on phototubes and other light-sensitive devices may be subject to puncture, but such applications are usually of a special nature and the problem is treated as a prime one.

The effect of simulated exposure to micrometeoroids has been studied in connection with specific space programs. In one such study (Ref. 24), it was concluded that the damage to protected solar cells would be very low after 55 days in space, with the extent of damage strongly dependent upon the meteoroid model chosen.

14.2.5 Magnetic Fields

The magnitude of the magnetic intensity and the variations anticipated are not expected to have serious effects on electronic components. Although some electrical equipment does depend upon magnetic fields, the magnitude of these fields is very high compared with those in space. Possibly the magnetic field changes in the vicinity of a nuclear detonation would be sizable, but it appears that other catastrophic effects would be present and possibly overwhelming. Sensitive scientific instruments such as magnetometers are exceptions to this discussion, but these are used for special purposes and should not be classified with normal engineering components.

14.2.6 Visible Light

Except for special devices such as phototubes, fluorescent devices, and photovoltaic systems, light in the visible region is not of serious consequence. Light shields and baffles for these types are generally considered as primary design parameters.

14.2.7 Ultraviolet Radiation

Ultraviolet radiation can affect electrical components by inducing a spurious photo response or by degrading such surface materials as organic dielectrics and optical filters. Data on the combined effects of ultraviolet, vacuum, and penetrating radiation are still very scarce, but it should be emphasized that ultraviolet radiation must be considered carefully in the selection of surface insulators and dielectrics for long-term operation. The production of spurious responses by direct interaction or through intermediate mechanisms such as fluorescence is subject to considerations similar to those for visible light.

14.2.8 Temperature

Not rightfully a primary parameter of space, temperature is a phenomenon in a spacecraft that results from a number of other factors. Electrical components are sensitive to temperature, and many components such as transistors and resistors have temperature-dependent parameters. These effects are well known and are generally compensated in circuit design and by means of spacecraft thermal control, as described in Chapter 7. That this has not always been completely achieved in the past, however, is indicated by the experience with transistors on the Relay 1 Satellite which were mounted so that they received no transferred heat from the rest of the power supply and thus were at about -20°C. Since this was a critical temperature for the material, a power drain resulted because of a change in transistor parameters. After several days in space, these transistors cooled further, to -30°C, and at this less critical temperature their characteristics became favorable and offset the power drain. At warmer temperatures, this power drain would not occur. The solution to the problem was to provide a heat conduction path from the power supply to the transistor mounting to keep the transistors at a temperature above the critical temperature.

14.3 REFERENCES

1. D. J. Hamman et al., Space Environment Effects on Materials and Components, (AD 601 876), Vol. II, "Electronic and Mechanical Components," Redstone Arsenal, Ala. 1 April 1964

2. W. C. Hulten et al., Irradiation Effects of 22 and 240 MeV Protons on Several Transistors and Solar Cells, NASA-TN-D-718, NASA-Langley Research Center, Langley Field, Va., April 1961

3. P. Lamond and P. Berman, High Efficiency Silicon Solar Cells, ARDA-80-59, Report No. 3, Transition Electronic Corp., Wakefield, Mass., 1 July and 31 December 1960

4. B. C. Spradin, Nuclear Radiation Effects on Resistive Elements, Radiation Effects Information Center, Battelle Memorial Institute, July 1966

5. B. W. Kennedy, Effects of Gamma on Selected Potting Compounds and Insulating Materials, NASA-Marshall Space Flight Center, Huntsville, Ala., November 1963

6. N. J. Gri, "Radiation Damage in Silicon p-i-n Lithium-drift Solar Cells," pp. 464 – 471 in IEEE Trans. on Nuclear Science, NS-12, February 1965

7. TREE Handbook (Transient-Radiation Effects on Electronics), DASA 1420, Battelle Memorial Institute, August 1967

8. J. F. Kircher and R. E. Bowman, Effects of Radiation on Materials and Components, Reinhold Publication Corp., 1964

9. J. E. Drennan and D. J. Hamman, Space Radiation Damage to Electronic Components and Materials, REIC Report No. 39, Battelle Memorial Institute, Columbus, Ohio, January 1966

10. E. E. Kerlin and E. T. Smith, Measured Effects of the Various Combinations of Nuclear Radiation, Vacuum, and Cryotemperatures on Engineering Materials, FZK-290, General Dynamics Corp., Fort Worth, Tex., July 1966

11. A. F. Ringwood, "Behavior of Plastics in Space Environment," Modern Plastics, 41, 173, January 1964

12. L. J. Frisco and K. N. Mathes, Evaluation of Thin-Wall Spacecraft Electrical Wiring, Final Report on Contract NAS 9-4549, Vol. I, General Electric Co., Schenectady, N.Y., September 1965

13. Program 461 Spacecraft Materials Handbook, LMSC-A327227, Lockheed Missiles & Space Company, Sunnyvale, Calif., May 1964

14. R. E. Fischell et al., Radiation Damage to Orbiting Solar Cells and Transistors, TG-886 (AD 657 155) (N67-38181), Applied Physics Laboratory, Johns Hopkins University, Silver Spring, Md., March 1967

15. R. C. Waddel, Early Results From the Solar Cell Radiation Damage Experiment on ATS-1, NASA-TM-X-55772 (N67-26568), NASA Goddard Space Flight Center, Greenbelt, Md., April 1967

16. C. W. Perkins, R. W. Marshall, and A. M. Liebschultz, Radiation Effects on (Monolithic) Microelectronic Circuits, Report No. 5 (AD 642 301) (N67-15500), Hughes Aircraft Co., Fullerton, Calif., November 1966

17. A. J. Favale, F. J. Kuehne, and M. D. D'Agostino, "Electron Induced Noise in Star Tracker Photomultiplier Tubes," IEEE Trans. on Nuclear Science NS-14, 190, December 1967

18. Radiation Effects, Survey of Soviet-Bloc Scientific and Technical Literature, 1960-1963, Aerospace Technological Division, Library of Congress, Washington D.C., 24 March 1965

19. D. J. Hamman et al., Radiation Effects, State of the Art, 1961-1965, REIC Report No. 38, Battelle Memorial Institute, Columbus, Ohio, 30 June 1965

20. J. F. Kircher and R. E. Bowman, eds., Effects of Radiation on Materials and Components, Reinhold Publishing Corp., New York, N.Y., 1964

21. J. T. Finnell and F. W. Karpowich, "Skipping the Hard Part of Radiation Hardening," Electronics, 122–127, 4 March 1968

22. C. L. Hanks and D. J. Hamman, The Effect of Nuclear Radiation on Capacitors, REIC Report no. 44, Battelle Memorial Institute, Columbus, Ohio, 30 December 1966

23. C. G. Goetzel, J. B. Rittenhouse, and J. B. Singletary, eds., Space Materials Handbook, 2nd ed., ML-TDR-64-40 (AD 460 399), X65-14878, Lockheed Missiles & Space Company, Sunnyvale, Calif., January 1965

24. M. J. Mirtich and R. L. Bowman, "Effect of Simulated Micrometeoroid Exposure on Performance of n/p Silicon Solar Cells," AIAA J. 5, 1364-1466, July 1967

Chapter 15

METALLIC AND CERAMIC MATERIALS FOR STRUCTURAL APPLICATIONS

R. W. Parcel

Metallic structural materials are used in spacecraft applications for load-carrying components such as structural shells, membranes, and fuel tanks. In this usage, maximum strength at minimum weight compatible with acceptable manufacturing technique is desired, as with other airborne structures. Those high-strength alloys which are based on magnesium, aluminum, titanium, beryllium, and steel (principally stainless) are candidate structural materials. The effect of the space environment on the load-carrying capabilities of these materials and thus their suitability for spacecraft usage is discussed in this chapter. The discussion is presented separately for the environmental factors of temperature, vacuum, meteoroid bombardment, radiation, and compatibility with liquids. Data are presented on other potential structural materials, such as the refractory metals and ceramics, which may be used presently for specialized items, or have future applications.

The refractory metals, columbium, molybdenum, tantalum, and tungsten suffer severe disadvantages in cost and weight when considered for structural purposes; Mo and W also exhibit very low ductility and pose serious fabrication problems. At service temperatures above 2200° F, however, no other metals will serve, therefore these disadvantages must be tolerated.

Spacecraft have no structural need for the refractory metals except in propulsion systems or during reentry. Under these categories, there are three common applications of refractory metals where the influence of space environment must be known:

- Rocket engines with restart capability will be subject to the space environment between firings, for very short intervals at high temperature after a firing, and for long periods before another operation.

- Retrorockets used to brake for reentry or for landing on another planetary body will spend periods in space before use.

- Reentry structures (e.g., heat shields) may spend long periods in space, and may or may not have been subjected to thermodynamic heating during ascent.

It is essential that materials in such applications withstand the space environment sufficiently well to function at the designated time.

Ceramic materials, because of their brittleness at ordinary temperatures, are limited by present design technology (Ref. 1) to special circumstances, such as:

- Structures in which the material is stressed in compression only
- In a composite arrangement which distributes tensile loads and precludes high stress concentration
- For very high-temperature service, such as reentry leading edges or surfaces and nuclear reactors
- In electronic applications, where electrical or thermal properties are paramount but structural integrity is nevertheless necessary

Of particular interest to space technology are graphites, carbides, oxides, nitrides, borides, beryllides, and silicides. Most of the physical and thermal properties presently known about these and other ceramics have been collected in Ref. 2.

Various forms of graphite are showing great promise for very high temperature applications (Ref. 3). These are mostly carbon-carbon composites, which are not within the scope of this chapter.

Although these materials are generally unaffected structurally by the space environment, it is necessary to study each material for possible adverse effects before deciding on an application.

15.1 TEMPERATURE EFFECTS

The temperature at any level in the atmosphere is affected by the altitude, time of day, season, and latitude. The general variation of temperature with altitude is shown in Tables 3-2 and 3-3 in Chapter 3. The temperature scale is the kinetic temperature, which is a measure of the kinetic energy of the molecules and atoms in the atmosphere at the indicated altitude. The actual temperature of a body at the location would depend on solar and aerodynamic heating, and on the radiative characteristics of the surface of the body as discussed in Chapter 7. For example, the temperatures expected for Agena satellite programs are -100° to 200° F. It is considered here that actual satellite body temperatures will be controlled with the range of -150° to 300° F. Ascent heating can produce 700° to 800° F in certain areas. The high temperatures attained in propulsion systems will not be discussed except as space environment alters their influence.

Temperature can have important effects when metals of widely different coefficients of expansion are joined. The low coefficient of thermal expansion of beryllium compared to aluminum or magnesium is a potential source of high thermal stresses when these metals are joined. Uncontrolled solar heating can cause excessive differential expansion. To control this effect, the basic design must allow for such expansion, or thermal control techniques must be carefully applied, or both measures may be taken. Similarly, the low expansion coefficients of ceramics as shown in Table 15-1 (Ref. 3) will require careful design allowance when they are joined to metals.

Table 15-1

PROPERTIES OF SOME CERAMIC MATERIALS

Material	Theoretical Density (gm/cm^3)	Bulk Density (gm/cm^3)	Melting Point (°F)	Coefficient of Thermal Expansion ($°F^{-1}$)	Thermal Conductivity at Room Temp. [Btu/(hr)(ft)(°F)]	Specific Heat at Room Temperature
Al_2O_3 – Single Crystal	3.9		3720	4.4 70 – 1000°F	26	0.18
Al_2O_3 – Polycrystalline		3.7 – 3.9		4.4 70 – 1000°F 5.0 1000 – 1800°F	19.8	
BeO	3.00	2.7 – 2.9	4658	4.1 70 – 800°F 5.7 800 – 2200°F	130	0.238
SiC (Self-Bonded)	3.217	< 3.2	Sublimes	2.4 70 – 1600°F	100	
SiO_2 – Fused (Vitreous)	2.21		3140	0.3 70 – 1800°F	0.7	0.18
MgO	3.58	3.3 – 3.5	5166	6.45 70 – 1000°F 8.75 1000 – 1800°F	25 – 35	0.20
ThO_2	10.00 ± .01	< 10	5830 ± 130	5.3 80 – 1400°F	6	0.055
ZrO_2 (a)	5.6		5010 ± 150	4.16 80 – 800°F 6.67 800 – 1400°F	0.9	0.11

(a) ZrO_2 stabilized in the cubic phase with additions of up to 15 wt% CaO or MgO. Stabilized ZrO_2 has a smooth thermal expansion and good thermal shock resistance. Unstabilized ZrO_2 undergoes a transformation, on heating, from the monoclinic to a tetragonal phase at about 1000°C. The reverse transformation occurs on cooling. These transformations are accompanied by large volume changes which result in poor thermal shock resistance.

15.2 VACUUM EFFECTS

Expected pressures will range from about 10^{-6} Torr at 100 miles elevation to about 10^{-10} Torr at an altitude of 500 miles, and will be progressively lower with increasing altitudes, as shown in Tables 3-2 and 3-3 of Chapter 3.

There are, potentially, three major effects on materials associated with very low-pressure environment:

1. Reaction of the surface with high-energy atomic and molecular particles causes localized loss of material through sputtering.

2. Material is lost by evaporation when the atmospheric density is sufficiently low.

3. Mechanical properties of the structural material are affected by the partial loss of the surface film of gas which covers all material at normal atmospheric pressures.

15.2.1 Sputtering

The sputtering process is associated with a minimum threshold energy value for atomic or molecular particles striking the vehicle surface. Typical values that have been obtained for this threshold energy are 6, 11, and 12 eV for atomic oxygen, a nitrogen molecule, and an oxygen molecule respectively to remove one or more atoms of the surface materials upon which they impinge (Ref. 4.). Loss of metal by this mechanism can vary over a wide range; e.g., a 300 Å coating of aluminum (10^{-5} gm/cm^2) can be removed in one month during a period of low-intensity solar wind or in several hours during a solar storm (Ref. 5). Other estimates increase these time spans by a factor of ten (Ref. 6.). Although loss of metal by sputtering may seriously affect optical and emissive properties of surfaces, it has little structural significance.

Surface blistering of plated metals is another effect associated with the impingement of particles from the space environment. Hydrogen ions at 1/2 to 2 keV have been shown to penetrate gold plating with resulting nucleation of molecular hydrogen at the gold-substrate interface. After the equivalent of one year in space, gold-coated aluminum increased its solar absorption by 17% from this effect (Ref. 7). Microcircuits formed by evaporation of metallic traces might suffer from this effect, except that all known applications are protected for other reasons. Other work (Ref. 8) shows that protons can cause blisters in pure, annealed aluminum, at energies below 100 keV. Even small blisters would seriously impair the optical figure of an aluminized mirror, causing far greater effect than mere pitting.

15.2.2 Evaporation

Loss of material by direct evaporation can occur only after loss of a surface film, or penetration of the film by the evaporating metal atoms or molecules. All metals

will necessarily be covered by a surface film prior to being placed in orbit as part of a space vehicle. The time for loss of any specific amount of material from the surface of an initially film-covered metal must therefore be equal to or greater than the time for evaporative loss of the film-free metal. Such loss will be in accordance with kinetic theory and a maximum value for this loss can be determined by applying the Langmuir equation under conditions of a negligible number of escaping atoms returning to the material surface. The sublimation or evaporation rates of some metals are shown in Fig. 15-1 (Refs. 9 and 10).

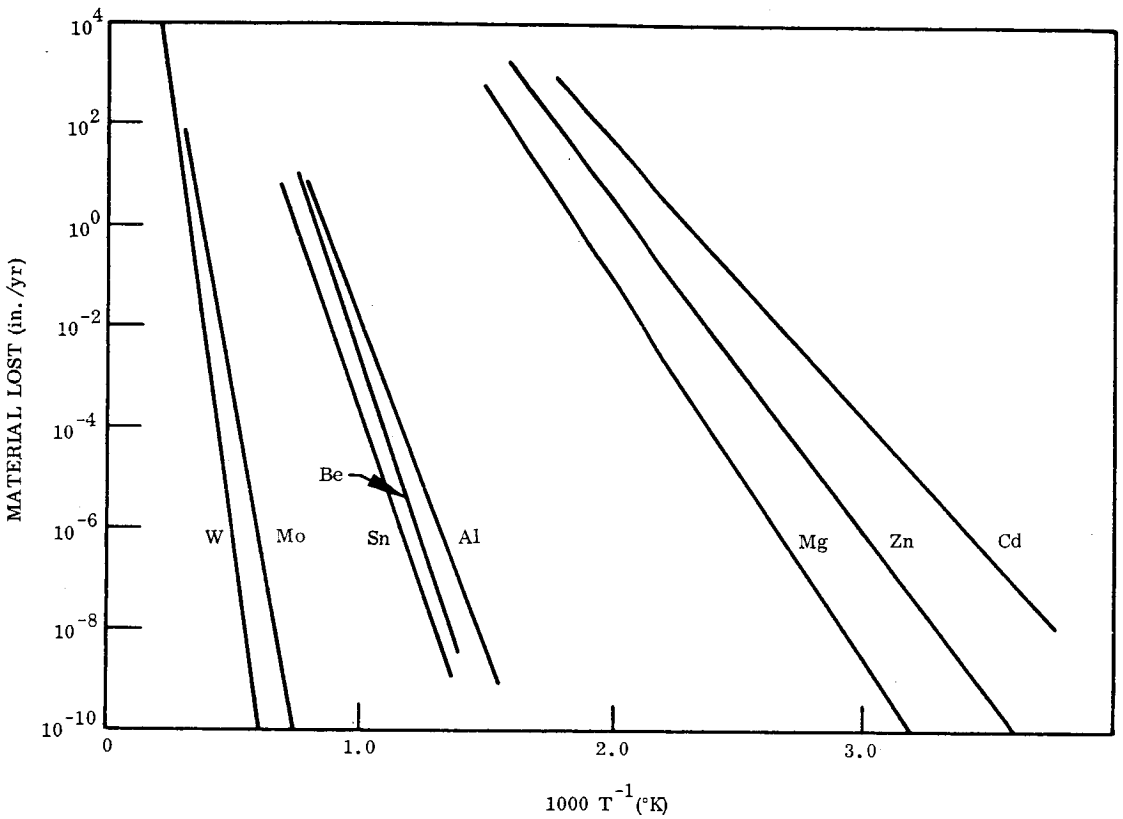

Fig. 15-1 Evaporation Rates for Some Metals

Loss of one component from an alloy is more difficult to predict. For solid solutions, Raoult's law gives a close approximation. For other systems, especially eutectics, the vapor pressure of the alloy can be higher than that of its component elements. This is of little concern in most alloy systems except some of the castings used for instruments and their housings. When the low vapor pressure element is in a much higher concentration, sublimation will proceed from grain boundaries and surfaces until the volatile element is depleted; henceforth the process will be diffusion controlled. Appreciable diffusion will not take place below creep temperatures. Thus, the net effect will be a surface roughening, from grain orientation effects, which will not have structural significance, but can eventually affect the reflectivity.

Loss of material by direct evaporation in the low-pressure environment of space is insignificant for aluminum, beryllium, titanium, steel, or the refractory metals and their alloys. In the case of magnesium, evaporative losses computed from the Langmuir equation would be appreciable (0.004 in.) in the course of a year for a structure above 400° F. However, many factors enter to reduce the probability of such losses. Mean temperatures are usually much less than 400°; protective coatings or oxides also tend to reduce evaporation. The Langmuir equation predicts the maximum rate, but the actual rate observed is always lower; very careful experimental techniques are needed to achieve the theoretical maximum. References 11 and 12 confirm the equation for liquid magnesium and for solid magnesium at 470° F; Ref. 13 notes that magnesium sublimation fell far short of the theoretical prediction at 275° F. There is evidence (Ref. 14) that under certain conditions sublimation increased drastically at about 400° F. These divergent results are not necessarily contradictory. Evaporation losses of magnesium can be substantially reduced and the useful time and temperature limits greatly prolonged with little weight penalty by applying a barrier coating only a few molecules thick of some metal of much lower evaporation rate.

Similarly, recent work has shown that cadmium sometimes evaporated at a rate much lower than predicted from the Langmuir equation. This report indicated (Ref. 15) that both bulk cadmium and electroplated cadmium sublimed at about one-fiftieth the predicted rate, over the range from 200 to 400° F. The bulk material could be brought up to the theoretical rate by flashing the surface at 500° F. It is believed (Ref. 16) that cadmium oxide is responsible for the low rate, and that this oxide exists throughout an electroplated layer. Vapor deposited cadmium might not enjoy this advantage.

The temperature calculated from the Langmuir equation at which some of the most common structural materials will lose 0.040 in./yr in vacuum is shown below:

Material	Temperature (C°)
Cd	120
Mg	240
Sn	800
Al	810
Be	840
Fe	1050
Ti	1250
Mo	1900
Ta	2300
W	2500
MgO	1090
BeO	1700
ZrO_2	1480

In the case of tungsten, a nozzle which is at 5000° F (2760° C) at the end of a firing cycle in space will cool long before it loses significant metal by sublimation.

15.2.3 Protective Coatings

Some protective coatings, such as certain oxides used on structural metals, may be appreciably degraded in vacuum. The hydrated oxides used to coat light metals (anodizing) may be changed after long exposure at very low pressure. Where the coating serves no purpose except corrosion protection, the loss is inconsequential since the purpose was served before flight. Where the thermal or electrical properties of the surface are important the situation may require more study. In a space radiator such surface change could be critical. Very little work has been reported in the area of hydrated oxides. Protective coatings on refractory metals are intended to reduce oxidation at elevated temperatures. They serve no function in space, hence their integrity is no longer important after ascent.

Metallic coatings of cadmium and zinc, used to protect structural units such as fasteners and frames have appreciable sublimation rates at temperatures of interest. The evaporated metal can, in some instances, redeposit on optical surfaces or electronic components. There is increasing evidence, as mentioned in the previous section, that this possibility has been overemphasized although it remains a genuine concern. The evaporating atoms will travel in straight lines at the partial pressures encountered in space. They can therefore accumulate only on surfaces in an optical line of sight. If the surroundings of an enclosure are at a uniform temperature, the volume quickly reaches equilibrium vapor pressure, and sublimation ceases. Furthermore, deposition on an optical surface is probably controlled by nucleation rates for the deposited film. Film formation seems to require an overpressure analogous to overvoltage in an electrolytic deposition process. At any rate, rough surfaces can acquire a deposit more quickly than an optical surface at the same temperature. It is possible to coat such surfaces (e.g., anodized aluminum) at temperatures where optical surfaces are unaffected. It is probable that the extreme measures for cleanliness needed to ensure an adherent coating on telescope mirrors also influence the deposition rate. The rate of evaporation also influences the nature and extent of deposited coatings (Ref. 17). Metal films several atoms thick can be virtually transparent and nonconductive (Ref. 10).

In spite of the evidence that sublimation of cadmium and zinc may not be as deleterious as theory predicts, use of these materials in the interior of long-lived vehicles should be restricted. Protective coating of low vapor pressure metals, or conversion coatings such as phosphate should be substituted. The economics of plating even the expensive metals are entirely reasonable for the degree of temporary protection needed.

Sublimation of the refractory metals is essentially zero at their temperature in space. Most ceramics and refractory compounds have very low vapor pressures at ordinary temperatures. As temperatures are raised, most decompose rather than vaporize. Table 15-2 gives the vacuum stability of some of these materials (Ref. 18). The very low oxygen pressures found in space may influence creep strength of oxide ceramics by creating vacancies in the lattice, hence influencing movement of dislocations. Any bulk effect would be diffusion controlled, however, and therefore inoperable below about 600°C (Ref. 19).

Table 15-2

VACUUM STABILITY OF SOME CERAMIC MATERIALS

Material	Temperature at Which Appreciable Vaporization Occurs	
	°C	°F
Al_2O_3	(a)	
BeO	2100	3800
SiO	2000	3600
SiO_2	(a)	
MgO	1600	2900
ThO_2	2300	4200
ZrO_2	2300	4200

(a) Stable to its melting point.

15.2.4 Influence of Vacuum on Mechanical Properties

In some cases, removal of the adsorbed gas layer from a metal surface affects the strength of the metal. Under one set of conditions, a metal may be stronger in an oxidizing environment; with a change of stress or temperature, it may become stronger in a neutral or vacuum environment. Reduction of strength from that found in a neutral atmosphere has been attributed to the decrease of surface energy accompanying gas adsorption, which lowers the work required for crack propagation. On the other hand, diffusion of oxygen and other gases into a metal hardens and strengthens it (Ref. 20). Data of Forestier and Clauss (Ref. 21) indicate that environmental effects on tensile strength are insignificant except perhaps for very thin sections of 100 μ or less. Unless the test specimen is altered in composition or structure by diffusion inward of the gaseous environment, or by diffusion outward of hydrogen or other volatile constitutents, it will be stronger in vacuum than in a gas (Ref. 22). However, except for fatigue life, no large strengthening effect of vacuum on mechanical properties of metals has been reported.

Fatigue life is variously reported as changed or as unchanged by vacuum, depending on the conditions of test (Ref. 23). In no case, however, has a loss in fatigue strength been sufficiently demonstrated. The influence of vacuum on fatigue life must be judged from tests tailored to the intended application at the present state of knowledge. On aluminum, for example, whether in atmospheric or low pressure, water vapor has a significant effect on fatigue life (Ref. 24).

It is well established that vacuum can increase fatigue life; there is also evidence that it can decrease it, at least slightly (Ref. 25). Mechanisms have been proposed, but not substantiated for each effect. The benefits of vacuum may not persist upon long exposure (Ref. 26).

Most of the data collected were for smooth, unnotched specimens, and low strength metals; hence they may not apply to a real structure.

Alloys such as brass which have a volatile component might lose surface strength by evaporation of some alloy component and hence lose fatigue strength. At temperatures characteristic of satellite interiors, this effect would be confined to a very thin surface layer.

15.2.5 Cold Welding

Laboratory experiments (Refs. 27 and 28) have shown that metals may join by solid state welding under simulated space environments (vacuum). Most metals would be expected to weld under suitable conditions, such as high pressure between contacting surfaces, extreme cleanliness, and long time. Nevertheless, no instances have been reported where unintended cold welding has occurred in an actual space flight.

It is demonstrated (Ref. 27) that common heat-and-corrosion resisting steels and Ti-6Al-4V alloy did not adhere under static load at temperatures below 500° C under high vacuum. Copper and 2014 aluminum alloy bonded to like and unlike metals at 300° C but not at 150° C. Under dynamic loading, which promotes cleaner surfaces and better contact, these minimum bonding temperatures are lowered. Tenacity and abrasion resistance of natural oxide films would be expected to play a decisive role. The 2014 aluminum alloy and Ti-6Al-4V alloy did not bond until 150° C, whereas A286, René 41, and 304 stainless steel could be made to bond at room temperature under dynamic conditions where the abrading of contacting surfaces removed the barrier film.

In summary, static bonding requires that one of the metals in contact be loaded above its yield point, so that surfaces can mate intimately, that the surfaces be atomically clean, and that temperature be high enough to permit some diffusion. If metals of ordinary cleanliness are in contact under high pressure, degassing cannot occur at the interface, hence the temperature must be high enough to diffuse away the contaminated layer. Under dynamic conditions, it must be possible to remove the oxide layer under the conditions of loading which exist, and the load must cause enough yielding to allow intimate contact. Dissimilar metals may be more resitant to bonding than like metal couples, probably because of lattice mismatch. Metals pairs that are mutually soluble in the solid state may bond as readily as those pairs that are mutually insoluble in the solid state. The subject of metal-metal adhesion (cold welding) was also discussed in connection with materials for lubrication applications in Chapter 9.

15.3 RADIATION EFFECTS

Metals present no radiation damage problems except at extremely high doses (of the order of 1×10^{19} neutrons/cm^2 or greater) such as those that might be obtained from reactor fluxes (Refs. 29 through 32). At the high doses, slight embrittlement takes place, resulting in increases in hardness and some physical properties and a decrease in creep rate. These changes are caused by displacement reactions with the neutrons, and while no data are available on proton damage, it is believed that comparable doses are required to produce the same effects. Fatigue properties are among the least affected (Ref. 33). Metals are essentially undamaged by the gamma irradiation encountered from natural space sources. Effects of space radiation on metals have also been considered by Hoffman (Ref. 34) and by Hess and Badertscher (Ref. 35).

All metals might be expected to suffer damage to surface properties from solar flares and the radiation belts, but none should show damage through 1 mg/cm^2 (Ref. 36). This corresponds, for example, to about 6 μ of Mg.

A 15% decrease in hardness has been noted in beryllium, from slow neutron dosage of 4×10^{20} neutrons/cm^2 (Ref. 36). This dosage will not be encountered in space except from reactors. Corpuscular radiation will affect only the surface, to a maximum depth of about 2×10^{-4} in.

Rays of wavelength capable of appreciable penetration into ceramics constitute a very small portion of the sun's psectrum. Only one part in 10^{11} is shorter than 1 Å, and one part in 10^5 shorter than 1000 Å. The latter rays can penetrate only fractions of a micron, and the former are not present in significant amounts, hence mechanical damage is limited to surface effects.

Exposures in vacuum to x-rays of about 0.38 Å, carried out on forsterite (Alsimag-243), alumina, and steatite showed little change, even in surface electrical properties. BeO also showed little change electrically, but changed color from white to dark gray (Ref. 37). Such a change could be of importance where emissivity is concerned.

15.3.1 Whiskers

Certain metals and alloys tend to form filamentary growths (whiskers) which can cause shorts in high impedance electrical circuits. These growths, of about one micron in diameter and up to one-half inch long, are single crystals of such perfection that their strengths are about 100 times greater than macroscopic specimens (Ref. 38). A new technology for growing perfect whiskers and employing them in composites is receiving much attention but is beyond the scope of this chapter. This same perfection enables them to carry currents up to 1 million A/in.^{2} (Ref. 39), so that even their minute cross sections can pass a few milliamperes and may be capable of disabling a high-impedance circuit.

Metallic whiskers form by two distinct mechanisms: vapor deposition, which requires vacuum and metals of high vapor pressure; and microextrusion, which requires stress. Given sufficient time, very small localized stresses of magnitudes normally

ignored furnish adequate energy for whisker formation. Nucleation of whiskers by irradiation or neutron bombardment probably falls in this category.

Non-metallic filaments, such as oxides or sulfides, require an appropriate atmosphere such as humidity or sulfide gases. They are of little interest or concern. Tin, cadmium, and zinc, in that order, have the greatest inclination to form metallic whiskers. For aerospace applications, no other metals need cause concern in this respect. Thin electroplates are the worst offenders, probably because of coherency strains, but thick plates and solid metal can also produce growths, in decreasing order. Electrically isolated, high impedance circuits in close proximity (up to 1/2 in.) to these metals can be disabled by electrical shorts due to whisker growth. Eutectic alloys, where the whisker-forming metals exist as almost pure phases on a micro scale, are almost equally likely to cause trouble. Ordinary solder, fortunately, is a rare offender.

The long, unattended service required of some satellite circuits, together with microminiaturization, requires that proper precautions be taken to suppress whisker growth. The following steps are simple and effective:

- Cadmium and zinc should be eliminated from sensitive circuits and from their supports and enclosures, unless spacings are at least 1/2 in.
- All tin plate should be fused.
- Solder joints closer than 1/2 in. to bare electrical components should be coated with a conformal coating of epoxy or polyurethane plastic.
- Pure tin should be eliminated from relays, capacitors, and microcircuits, or given a plate of nonsensitive metal such as gold.

Circuits which can tolerate momentary shorts of more than 1/2 amp can be exempted from these precautions. Currents of this magnitude will vaporize the whiskers, and the resultant volume of vapor can be ignored.

A precautionary note regarding silver is in order. This metal sprouts silver sulfide whiskers with ease in the presence of sulfur compounds, and can do so when in contact with some grades of rubber. No electrical problems from this source have been reported.

15.3.2 Compatibility With Liquids

Although liquid propellants are obviously not a space environment, nevertheless a knowledge of their effects is essential to spacecraft design. Such knowledge is applicable not only to propellant tanks and fittings, but also to materials in critical applications which might be subject to vapors or spillage from such liquids.

References 40 and 41 are the most extensive references to date, providing a good survey of the compatibility problem. General rules (Ref. 42) are of value however. The following metals and alloys should not be brought into contact with hydrazine: carbon and low alloy steels, copper and its alloys, molybdenum and stainless steels containing greater than 0.5% molbdenum, 40E aluminum (a 5.5% Zn casting alloy), magnesium, zinc, and lead. Any of these materials may cause the decomposition of the hydrazine.

Most common metals can be used with chlorine trifluoride because of the formation of a passivating fluoride coating. Normally nickel, Monel,and 18-8 stainless steel are preferred. Metals must be passivated before use with hydrogen peroxide. The 300 series of stainless steels are recommended for limited use with hydrogen peroxide and also with nitrogen tetroxide containing over 0.1% water. Recent tests indicate that titanium alloys are satisfactory for use with nitrogen tetroxide provided NO (nitric oxide) content is at least 0.3%. However, it is recommended that tests be made of any proposed application of titanium alloys in the configuration where they will be used and under conditions to which they will be subjected during the life cycle of the application. At ordinary temperatures, perchloryl fluoride is not corrosive to most metals. The following metals are recommened for use with moist perchloryl fluoride: AISI 304, 310, 314, and 316 stainless steels; Hastelloy; titanium, tantalum, Durimet "T" and Durimet 20.

In general, compatibility in Refs. 40 through 42 refers to chemical effects of the combination on either the metal (corrosion) or the liquid (e.g., decomposition, contamination, or detonation). Stress corrosion is more insidious, less understood, and also less well documented. Stress corrosion depends first of all on the alloy and its mechanical or thermal treatment, the chemical environment, and the stress level. Conditions which will cause stress corrosion cracking in any metal are specific for that alloy. It is established that the stress must be tensile, so that shot peening can often be used, to put the surface in compression and thus minimize residual surface tensile stresses that may result from fabrication. Mild steels can crack in nitrates and alkalies, stainless steels in halides and caustic alkalies, etc. (Ref. 43).

Titanium is remarkably inert in a chemical sense to most chlorides at ordinary temperatures but most of its alloys can be significantly affected by stress corrosion in the same solutions (Ref. 44) at elevated temperatures (>500° F).

In this instance, the effect is equivalent to a lowering of toughness and can be treated exactly that way from the designer's standpoint. Methanol can also cause premature failure of titanium alloys (Ref. 45).

Liquid and gaseous oxygen can react violently with titanium upon impact by bullet puncture or explosive shock. Tensile rupture under gaseous oxygen at 50 to 100 psi will cause ignition. More severe conditions can cause similar phenomena in other metals, but only titanium and zirconium have exhibited catastrophic reactions (Ref. 46).

Stress corrosion is sensitive to the presence or absence of small amounts of impurity in the liquid, such as water, chloride ions, various oxides of nitrogen, etc. Extensive tests may not reveal any sensitivity if conditions are slightly different. The theory is not well developed. Therefore, for the present, when either alloy or propellant is changed, the user must review the literature extensively, and will probably need to develop specific experimental data.

15.4 METEOROID PENETRATION

Meteoroid penetration can be a problem with spacecraft structural materials. Such items as the spacecraft skin or pressurized containers for propulsion or guidance are vulnerable. The meteoroid environment and the single wall penetration parameters have been tentatively established and are discussed in Chapter 6. There still remains considerable work to be done on the double wall penetration parameters. A preliminary discussion of the double wall penetration is also presented in Chapter 6.

Much work still remains on the correlation of the penetration results from Explorers 16 and 23 and Pegasus 1, 2, and 3 spacecraft with the results from ground-based simulation experiments. Impact results from acoustical and wire grid sensors on spacecraft have been judged to be ambiguous. The main problem is the inability in ground-based tests to adequately simulate the meteoroid velocity and mass.

15.5 REFERENCES

1. P. Boland and J. D. Walton, Jr., Aerospace Ceramics – Characteristics and Design Principles, AFML-TR-171, Georgia Institute of Technology, Engineering Experiment Station, June 1965

2. J. F. Lynch et al., Engineering Properties of Ceramics – Databook To Guide Materials Selection for Structural Applications, AFML-TR-66-52, June 1966 (continuously updated)

3. W. G. Jurevic and W. G. Bradshaw, Consideration of the Characteristics of Graphites and Carbons, B-70-66-1, LMSC, 25 March 1966

4. R. P. Stein, "Atomic and Molecular Sputtering," pp. 391 – 401 in Surface Effects on Spacecraft Materials, ed. Francis J. Clauss, John Wiley & Sons, New York, 1960

5. L. Reiffel, "Structural Damage and Other Effects of Solar Plasmas," American Rocket Society J. 30, No. 3, 258, March 1960

6. F. Gronlund and W. J. Moore, "Sputtering of Silver by Light Ions With Energies From 2 to 12 KeV," J. Chem. Phys. 32, 1540, 1960

7. D. L. Anderson and R. G. Dahms, "Surface Blistering of Metals Due to Low Energy Hydrogen Ion Bombardment," 7th AIAA Structures and Materials Conference, 1966

8. L. H. Milacek and J. A. Cooley, A Study of the Blistering of Metal Surfaces by Solar System Ions, NASA-CR-78313; TR-66-G-106-F, August 1966

9. E. A. Gulbransen and K. F. Andrew, "Reactions of Metals in High Vacua," J. Phys. and Colloid. Chem. 53, 690–711, 1949

10. V. Pacalka, "The Measurement of Critical Thickness of Aluminum Films," Czeck. J. Phys. 9, No. 5, 668–669, 1959

11. "Physical Chemistry of Metallic Solid Solutions and Intermetallic Compounds," National Physical Laboratory Symposium, Teddington, England, 4–6 June 1958

12. R. A. Lad, "Survey of Materials Problems Resulting From Low Pressure and Radiation Environment in Space," Tech. Note D-477, U. S. National Aeronautics and Space Administration, Washington, D. C., 1960

13. Mariner Spacecraft, JPL Report to NASA Research, Communication on Materials, 10 September 1962

14. W. P. Gilbreath, Vapor Pressure of Mg Between 223 and 385°C, NASA TN-D-2723, March 1965

15. R. D. Wales and M. G. Lueblen, "Evaporation of Electroplated Cadmium in High Vacuum," J. Spacecraft & Rockets 2, No. 3, 467, May – June 1965

16. A. N. Nesmeyanov et al., "Effects of Oxide Films on the Plate of Evaporation," Russian J. Phys. Chem. 34, No. 7, 681, July 1960

17. Dinh-Vuong, "Influence of Evaporation Speed on the Electrical Conductivity of Thin Metallic Plates," J. de Phys. et la Radium 23, No. 2, 1962

18. W. H. Kohl, Materials and Techniques for Electron Tubes, Reinhold Publishing Corporation, New York, 1960

19. J. M. Leitnaker, M. G. Bowman, and P. W. Gilles, "Thermodynamic Properties of the Tantalum and Tungsten Borides," J. Electro-Chem. Soc. 109, 441, May 1962

20. R. L. Bjork and C. Gazley, Estimated Damage to Space Vehicles by Meteroids, RM 2332, RAND Corp., February 1959

21. H. Forestier and A. Clauss, "Influence des gas adsorbes sur la résistance mécanique d'un fil métallique," Rev. Met. 52, 961, 1955

22. J. H. Atkins et al., Effects of Space Environment on Materials, NRC Research Project 40-1-041, August 1960

23. R. H. Christensen, "Fatigue of Metals Accelerated by Prolonged Exposure to High Vacuum," Douglas Missile & Space Systems Division Engineering Paper No. 1636, ASTM Committee on Fracture Testing of High Strength Metallic Materials, Boston, Mass., May 1963

24. J. L. Nam, The Influence of Surface Phenomena on the Mechanical Properties of Structural Materials, NRC Project No. 42-1-0105, Contract No. AF 49(638)-1005, National Research Corp., 1963

25. C. M. Hudson, Problems of Fatigue of Metals in a Vacuum Environment, NASA-TN-D-2563, January 1965

26. A. J. Nachtigall et al., The Effect of Vacuum on the Fatigue and Stress-Rupture Properties of S-816 and Inconel 550 at 1500°F, NASA TN-D-2898, Washington, D.C., June 1965

27. P. M. Winslow, D. V. McIntyre, and K. E. Demorest, Adhesion of Metals in the Space Environment, 7th AIAA Structures and Materials Conference, 1966

28. J. P. Mugler and J. N. Bradford, Adhesion of Metals in Ultrahigh Vacuum, NASA Lewis Res. Center, High Vacuum Technology Testing and Measurements Meeting, August 1966

29. O. Sisman, C. D. Bopp, and R. L. Towns, Solid State Semi-Annual Progress Report ORNL-1606, December 1953

30. R. V. Steele and W. P. Wallace, The Effect of Neutron Fluxes on the Mechanical Properties of Aluminum Alloys, LRL-145, California Research and Development Company, May 1954

31. Reactor Engineering Division Quarterly Report, ANL-5208, Argonne National Laboratory, December 1953

32. The Reactor Handbook, Vol. III, USAEC, Materials Technical Information Services, April 1952

33. The Effect of Nuclear Radiation on Structural Metals, REIC Report No. 20, Battelle Memorial Institute, Columbus, Ohio, September 1961

34. R. A. Hoffman, Radiation Hazards of Primary Cosmic Particles, AFMDC-TR-59-32, Holloman Air Force Base, July 1965

35. R. E. Hess and R. F. Badertscher, Space Radiation as an Environmental Constituent, REIC Memorandum 19, Radiation Effects Information Center, 1960

36. The Reactor Handbook, Vol. 31, USAEC, Materials Technical Information Services, 3 April 1962

37. Dielectrics for Satellites and Space Vehicles, Contract DA 36039 SC 78321, Johns Hopkins University, February 1962

38. J. E. Emrick, "Studies of Iron Whiskers of High Average Strength Grown in a Hydrogen Contaminated Hydrogen Atmosphere," WADD Tech. Note 61-54, June 1961

39. S. M. Arnold, "The Growth and Properties of Metal Whiskers," 32rd Annual Convention of the American Electroplaters Society, 1956

40. DMIC Memo 201, Defense Metals Information Center, Battelle Memorial Institute, January 1965

41. Titan II Storable Propellant Handbook, Final Handbook, Rev. B., Contract No. AF 04(694)-72, Bell Aerosystems Company, March 1963

42. C. J. Thelan, "Materials Requirements for Storable Liquid Propellant Rocket Motors," ASM 1962 Golden Gate Metals Conference, February 1962

43. E. N. Pugh, On the Mechanism(s) of Stress Corrosion Cracking, AROD 50231, The Martin Company, August 1965

44. R. W. Rudy, Jr. and R. J. Good, Stress Corrosion Characteristics of Alloys of Titanium in Sea and Salt Water, NRL-6564, July 1967

45. R. L. Johnson et al., Stress Corrosion of Ti-6Al-4V Alloy in Methanol, NASA-TN-D-3868, February 1967

46. Reactivity of Metals With Liquid and Gaseous Oxygen, DMIC Memo 163, January 1963

Chapter 16

MISCELLANEOUS MATERIALS

John B. Singletary

The previous chapters have described most of the important space materials, together with their performance in the space environment, and classified them according to application. This chapter discusses some of the remaining commonly used materials, the principal classes being organic fluids, photographic emulsion, propellants, and explosives. Since most of these materials are organic, they are chiefly damaged by primary or secondary ionizing radiation particles. In general, the predominant radiations causing damage will be gamma rays, electrons of the artificial radiation belt, or high-energy Van Allen protons. Some damaging neutrons may arise from secondary emission from proton bombardment.

16.1 ORGANIC FLUIDS

Organic fluids undergo a variety of reactions when exposed to a radiation field because of the many different ions and free radicals that are formed. (See Chapter 5 for a more detailed discussion.) The principal reactions are polymerization, cross-linking, and splitting-off of small molecules. The polymerization and cross-linking cause an increase in viscosity up to a gelation point and the formation of sludge. Splitting-off of small molecules results in gas evolution, decrease in flash point, and sometimes increase in acidity (resulting in corrosion).

As is the case with all organic materials, the presence of the benzene ring in the structure of the molecules results in much improved radiation tolerance. Thus, the polyphenyls have been used successfully as reactor coolants, and polyphenyl ethers have been developed for use as hydraulic fluids, lubricants, and the base stock for radiation-resistant greases. Lubricants are treated in detail in Chapter 9.

Hydraulic fluids, like lubricants, are damaged more in a dynamic irradiation than in a static irradiation. Of the common fluids, the petroleum-based MIL-O-5606 is not as resistant as the MIL-O-8515 specification. Viscosity and acidity increases are the biggest problems with these fluids, along with a potential hazard from a lowered flash point.

Gyro fluids are generally divided, according to use, into the following categories:

- Damping fluids, in which the slope of the viscosity versus temperature curve should be as flat as possible
- Flotation fluids, which require a high density

The most common damping fluids are siloxanes; fluorinated hydrocarbons are usually used for flotation. Since siloxanes have a variety of structures, one should choose a

high-phenyl fluid, such as DC703 or DC710, in preference to a fluid, such as DC200, which contains no phenyl groups. The high-phenyl fluids have much better radiation resistance than the pure methyl siloxanes, particularly in gelation point. The silicone fluids evolve less gas than most fluids.

At present, there are no completely satisfactory flotation fluids for use in a high radiation field because all are fluorinated hydrocarbons, which have poor radiation resistance. Halocarbon 4-1 is satisfactory to a dose of 1.2×10^8 R from the standpoint of viscosity. However, any metal parts in contact with these fluids should be made of materials resistant to HCl and HF, both of which would be formed under irradiation. The design must also incorporate a solution to formation of gas during irradiation.

Research efforts on radiation effects on these materials have been at a very low level for the last few years (Ref. 1). Consequently, most of the data given in Table 16-1 on radiation damage to hydraulic fluids and gyro fluids is fairly old.

16.2 PHOTOGRAPHIC EMULSIONS

Photographic emulsions are very sensitive to space radiations and quite difficult to protect since the qualities that enable the emulsions to do their primary job of detecting visible or near-visible radiations also make them liable to blackening damage by the "detection" of gamma rays as well as ionizing particles. There is a wide variation in film speeds which, it appears, is closely related to the radiation sensitivity of the film. The films most sensitive to visible light are also most sensitive to radiation.

A recent survey of several films and their sensitivity to space radiation confirms this relative ranking of emulsions (Ref. 7). In this study, radiation damage to films is measured in terms of the equivalent gamma-ray exposure in rads required to bring each film to a state of photographic density equal to 0.3 above the background density that is inherent in any photographic emulsion. This equivalent exposure is taken as the maximum acceptable level for ordinary usage and is listed for a number of films and exposures in Table 16-2, which is adapted from Ref. 7.

16.3 EXPLOSIVES AND PROPELLANTS

High-energy nuclear radiation can produce macro- and micro-chemical and physical changes in explosives resulting in impairment of the performance and reliability of spacecraft ordnance devices. As a result, an explosive can experience changes in sensitivity to initiation through impact, temperature, vibration, and other forms of imparted energy. Ultimately, detonation can occur through the absorption of large radiation doses in very short times.

A very large part of the detailed experimental data that have been gathered on the radiation response of explosives has been in support of military projects, and either the devices tested or the radiation effects data or both have been classified. The remarks presented here are intended to give only the most general indication of radiation effects on explosive materials described in the unclassified literature.

Table 16-1

HYDRAULIC AND GYRO FLUIDS

Material	Particle Bombardment ($n_f vt$)	Gamma Irradiation (R)	Remarks	Ref.
Mil-O-5606 (Petroleum-based hydraulic fluid)	None	1.2×10^8	Viscosity (130°F) reduced from 10.2 to 4.3 Cs.	2
Mil-O-8515 (Disiloxane-diester based hydraulic fluid)	4.5×10^{13} 2.9×10^{14}	1.0×10^7 6.4×10^7	Essentially unchanged. Neutralization number[a] up from 0.2 to 1.4 (statically irradiated samples).	3
Halocarbon 4 – 11 (Polychlorotri-fluoroethylene)	None	1.2×10^8	Viscosity change slight; neutralization number changed from 0.3 to 1.9. G value[b] for gas = 2.01.	2
Dow Corning 200 (Dimethyl-siloxane)			G value for gas = 2.01.	4
Dow Corning 710 (Methyl-phenyl siloxane)	None	5×10^8 1×10^9	Viscosity very high. G value for gas = 0.07. Gelation point.	5
Dow Corning 703 (Methyl-phenyl siloxane)	None	7×10^8	Solid.	5
Halocarbon 208 (perchlorofluorobutane)	None	3×10^7	G value = 10; viscosity essentially unchanged.	6
Fluorochemical FC-43	None	1×10^7	G value = 10; viscosity increased ~ 2%.	6

(a) Neutralization number: milligrams of KOH to neutralize 1-gm sample.
(b) G value = number of molecules changed per 100-eV energy input.

Table 16-2

SENSITIVITY OF PHOTOGRAPHIC FILMS TO SPACE RADIATION

Film Type	Incident Radiation	Incident Geometry	Equivalent Exposure for Maximum Allowable Fogging (rads)
Single Emulsion, Eastman No Screen (no longer made to same specifications)	0.1 MeV Electrons	Diffuse Normal	0.50 0.25
Single Emulsion, Eastman Type A (no longer made)	0.1 MeV Electrons	Diffuse Normal	2.5 1.5
Cine Positive 5302	0.07 MeV Electrons	Diffuse	21
NTB	0.8 MeV Electrons	Normal	4.0
SWR	0.8 MeV Electrons	Normal	14
Kodak Plus X Aerial Film, Type 4401	Cobalt-60 Gamma Rays (1.25 MeV, av. energy)	Isotropic	1.7
Kodak Pantomic X Aerial Film, Type 4400			1.7
Kodak High-Definition Aerial Film, Type 4404			92
Kodak Special Fine-Grain Aerial Film, Type SO-190			34
Kodacolor Film			7
Kodak Ektachrome Aero Film, Type 8842			1
Kodak Ektachrome ER, Daylight Type			1
Kodachrome II Daylight Type (ASA 25)	Cobalt-60 Gamma Rays (1.25 MeV, av. energy)		3
Polaroid	Protons (E > 30 MeV)		0.08
Tri-X	Protons (E > 30 MeV)		0.8
Plus-X	Protons (E > 30 MeV)		2.5
Microfile	Protons (E > 30 MeV)	Isotropic	84

Explosives are nearly all complex nitrogen-containing organic compounds with a high degree of chemical instability. As is the case in nearly all organic compounds, the radiation resistance increases with the aromatic content of the compound (Ref. 8). Most explosives evolve gas during irradiation and some continue to evolve gases for a long time after being removed from the radiation field.

Considerable decomposition can occur in most explosives without seriously affecting the peak pressure, delay time, or impact test results. The decomposition has been determined by density and mass changes and by analysis of the gases evolved. Nitrogen along with some oxides of nitrogen and the oxides of carbon are the major decomposition products.

Lead styphnate and TNT have shown good properties after a gamma ray dose of 2.2×10^8 R. Others such as diazodinitrophenol at a dose of 1.1×10^8 R and nitroglycerin at a dose of 1.2×10^9 R are degraded too much to be reliable. No dose rate effect has been observed. These materials could create some concern in applications such as explosive charges employed for a separation or other critical function late in an orbital operation. Such devices, depending on the location, function, and time of use, may require some protection to prevent a change in firing characteristics or to reduce radiation-induced deterioration.

The principal micro- and macroscopic effects of radiation on explosives along with the test methods commonly used for investigating damage mechanisms and effects are summarized in Table 16-3 (Ref. 9).

Most liquid rocket propellants have shown little damage to the operating characteristics of the fluids at doses of less than 10^8 R. In one study (Ref. 10), nitrous oxide oxidant (N_2O) was irradiated to a dose of 1.4×10^7 R and a 50-50 mixture of hydrazine and UDMH (unsymmetrical dimethyl hydrazine) was irradiated to a dose of 1.4×10^7 R in the Lockheed Radiation Effects Reactor. The N_2O was not damaged by the radiation. There was some slight decomposition of the hydrazine mixture, observable as a rise in the ullage pressure. No effect was observed in the ignition properties of the mixture.

In another study, both a hydrazine and UDMH were irradiated with x rays of 0.1 to 1.0 Å wavelength with total absorbed doses ranging from 4 rads to 2.3×10^6 rads (Ref. 11). The results showed decompositions ranging from 0.3 to 31%. The order of decreasing sensitivity to x-rays was as follows: hydrazine vapor, UDMH vapor, UDMH liquid, and hydrazine liquid. In this case, as was also found for explosives, the damaging effects were related to total dose absorbed and were independent of the dose rate. The primary products evolved from hydrazine under irradiation were nitrogen, hydrogen, and ammonia. The products from UDMH included nitrogen, hydrogen, ammonia, hydrazine, methylamine, and dimethylamine.

Solid propellants may sustain large changes in physical properties under irradiation but little change in such properties as burning rate, as indicated by the data of Table 16-4 (Ref. 12). Long-term storage of solid propellants and of liquid propellants in solid form in an orbital environment has been extensively studied (Refs. 13 and 14).

Table 16-3

SUMMARY OF EFFECTS OF RADIATION INTERACTION WITH PRIMARY AND SECONDARY HIGH EXPLOSIVES

Principal Radiation Effects	Manifestations Noted (Gross Effects on Physical, Chemical and Performance Properties)	Usual Test Methods for Detecting Effects and Mechanisms Responsible	Examples of Explosives Studied Undergoing Listed Effects
Chemical			
Chemical decomposition through free radicals, ionization, and atomic and molecular excitation process	Gas evolution and postirradiation gas evolution, secondary product formation, change in detonating power, weight loss	Pressure rise (e.g., Taliani test) electron spin resonance (ESR), gas chromatography and mass spectrometry, infrared spectrophotometry, Brisance squib detonation test, thermogravimetry	Picric acid, TNT, PETN, DATB, Tetryl, $Hg(CNO)_2$, Pb Styphnate, Pb $(N_3)_2$, RDX, HMX, NG, NC, DDNP
Molecular rearrangements	Change in melting point and other phase transition and deflagration temperatures, change in thermophysical properties (e.g., specific heat, thermal conductivity)	Differential thermal-analysis (DTA)	Same as above
Physical (Solid State)			
Crystalline faults, atomic dislocations, and other solid state imperfections	Change in: brittleness, impact sensitivity, crystal size, and internal stresses	Mechanical tests, optical and electron microscopy, polarography, drop-weight test	Pb and Alkali azides
Electron-hole pair production (F-center formation)	Change in color and electrical properties	Dielectric tests, optical absorptance and reflectance	Pb and alkali azides
Thermal			
Macro- and microscopic heating	Initiation and detonation (high dose rates)	Calorimetry, optical microscopy, visual detonation	NH_3NI_3, Pb $(N_3)_2$, and other azides

Table 16-4

EFFECT OF RADIATION ON AMMONIUM PERCHLORATE PROPELLANTS

Propellant	Radiation Dose (mrad)	Burning Rate[a] (in./sec)	Tensile Strength[b] (psi)
Polysulfide, Thiokol TP-L-3014	0	0.0593	249
	10	0.0593	156
	50	0.0549	51
Polysulfide, Thiokol TP-L-3014a	0	0.0582	136
	20	0.0548	138
	50	0.0568	62
Hydrocarbon, Thiokol TP-H-3062	0	0.0422	91
	20	0.0428	168
	50	0.0425	145
Polyurethane, Thiokol TP-6-3129	0	0.0347	54
	20	0.0355	56
	50	0.0371	40
Polyacrylonitrile, Hercules HES 6648	0	0.0660	190
	10	0.0700	72
	50	0.0860	56
Polyethylacrylate, Hercules HES 6420	0	0.0412	111
	10	0.0447	67
	50	0.0486	30
Cellulose acetate, Hercules HES 5808	0	0.0325	541
	10	0.0323	341

(a)Number of determinations = 10 – 20.
(b)Number of determinations = 5.

16.4 REFERENCES

1. Radiation-Effects State of the Art, 1965 – 1966, REIC Report No. 42, Battelle Memorial Institute, Columbus, Ohio, June 1966

2. S. L. Cosgrove and R. L. Dueltgen, The Effect of Nuclear Radiation on Lubricants and Hydraulic Fluids, REIC Report 19, Battelle Memorial Institute, Columbus, Ohio, May 1961

3. H. B. Brooks et al., Effects of Radiation on Selected Materials, MR-N-239, Convair, Fort Worth, Tex., June 1959

4. E. L. Warrick, D. J. Fischer, and J. F. Zack; Radiation Resistant Silicones, Third Semiannual Radiation Effects Symposium, Marietta, Georgia, Vol. 5, Oct 1958

5. L. J. Hillenbrand, The Effect of Nuclear Radiation on Hydrocarbon Fuels, REIC TM-11, Battelle Memorial Institute, Columbus, Ohio, Nov 1958

6. R. A. Glass et al., Radiation Testing of Program-461 Gyro Fluids, LMSC 3-56-65-7, Lockheed Missiles & Space Co., Sunnyvale, Calif., March 1965

7. E. L. Noon and R. R. Brown, "Sensitivity of Photographic Film to Nuclear Radiation in Near-Earth Missions", IEEE Trans. On Nuclear Science NS-14, 200, December 1967

8. M. J. Urizar, E. D. Loughran, and L. C. Smith, "The Effects of Nuclear Radiation on Organic Explosives," Explosivstoffe, Nr. 3, 55, 1962

9. R. E. Mauri, Literature Survey on Effects of Radiation on Explosives, LMSC-A-30-65-2, Lockheed Missiles & Space Co., Sunnyvale, Calif., December 1965

10. G. Yasui, RIFT Radiation Effects Program Irradiation No. 2; Liquid Propellants, NSP-63-80, July 1963

11. H. Lucien and M. L. Pinns, The X-Irradiation of Hydrazine and 1, 1-Dimethylhydrazine, NASA TN-D-2452, Lewis Research Center, Cleveland, Ohio, August 1964

12. T. Acker et al., "Effect of Radiation on Ammonium Perchlorate Propellants," AIAA J. 2, 1165, June 1964

13. J. M. Allen, A. Levy, and J. F. Kircher, Evaluation of Solid Propellants and Solid-Propellant Systems for Space Application, BMI 1683-SR (1), Battelle Memorial Institute, Columbus, Ohio, August 1963

14. J. A. McMillan, "Possible Implications of the Damage by Radiation in the Storage of Propellants in Outer Space and Tentative Methods for Its Measurements", IEEE Trans. on Nuclear Science NS-10, 24 January 1963

PART 3

MATERIALS IN SPACE

Chapter 17

SPACECRAFT MATERIALS EXPERIENCE

J. B. Singletary

J. B. Rittenhouse

This chapter surveys the available information on materials used in the construction of successfully orbited spacecraft from the first launches up to about June 1968. This same type of materials information has been presented in the 2nd Edition of the Space Materials Handbook (Ref. 1) and in Supplements 1 and 2 to that book (Refs. 2 and 3). The present compilation summarizes, revises, and updates the information found in these earlier versions. Since the intent of this chapter is to facilitate ready access to data on materials actually used in orbit, those spacecraft that failed in launch attempts or those that have been developed but not yet launched along with classified or U.S.S.R. spacecraft where complete information is not available have been excluded from these listings.

The numbers of spacecraft successfully launched worldwide continued to increase each year through 1966 although 1967 saw a small decrease over the three preceding years. The grand total launched through 31 December 1967 stands at 780, and the number remaining in orbit at 343 (Ref. 4). The international nature of the space effort continues to expand with another nation, Australia, joining the club of spacecraft researchers with their launch on 29 November 1967 of the WRESAT vehicle. Seven nations are now represented by Earth-orbiting satellites: U.S., U.S.S.R., Canada, France, Italy, United Kingdom, and Australia.

One might expect to find that the steady increase of world experience in spacecraft development and construction would result in greater reliability and thus longer lifetimes as the space age progresses. That this is indeed the situation is indicated by the results of an analysis of spacecraft lifetimes. This analysis was performed on a sample of 103 unmanned scientific spacecraft chosen to meet the following requirements: (a) Earth-orbiting, (b) successfully transmitted information, and (c) information on their behavior available in Refs. 4 and 5.

Of the 103 spacecraft selected, 62 had ceased transmission and 41 were still transmitting up to 30 April 1968. The spacecraft that had ceased transmission could have done so for a number of reasons; some malfunction or failure in a vital component, the spacecraft was silenced by ground command, or the spacecraft was silenced by an on-board timing mechanism. Thus, the lifetimes estimated will give only an approximate indication of spacecraft reliability. These lifetimes in years from the date of launch of the 103 selected spacecraft are plotted in Fig. 17-1 against the year of the space age in which each was launched. Year one of the space age was arbitrarily chosen as 1958.

A least squares estimate of the lifetimes of the spacecraft that have ceased transmitting was determined and is also shown in Fig. 17-1. The 90% confidence of the lifetimes at the beginning of 1968 (year 11 of the space age) was also approximated

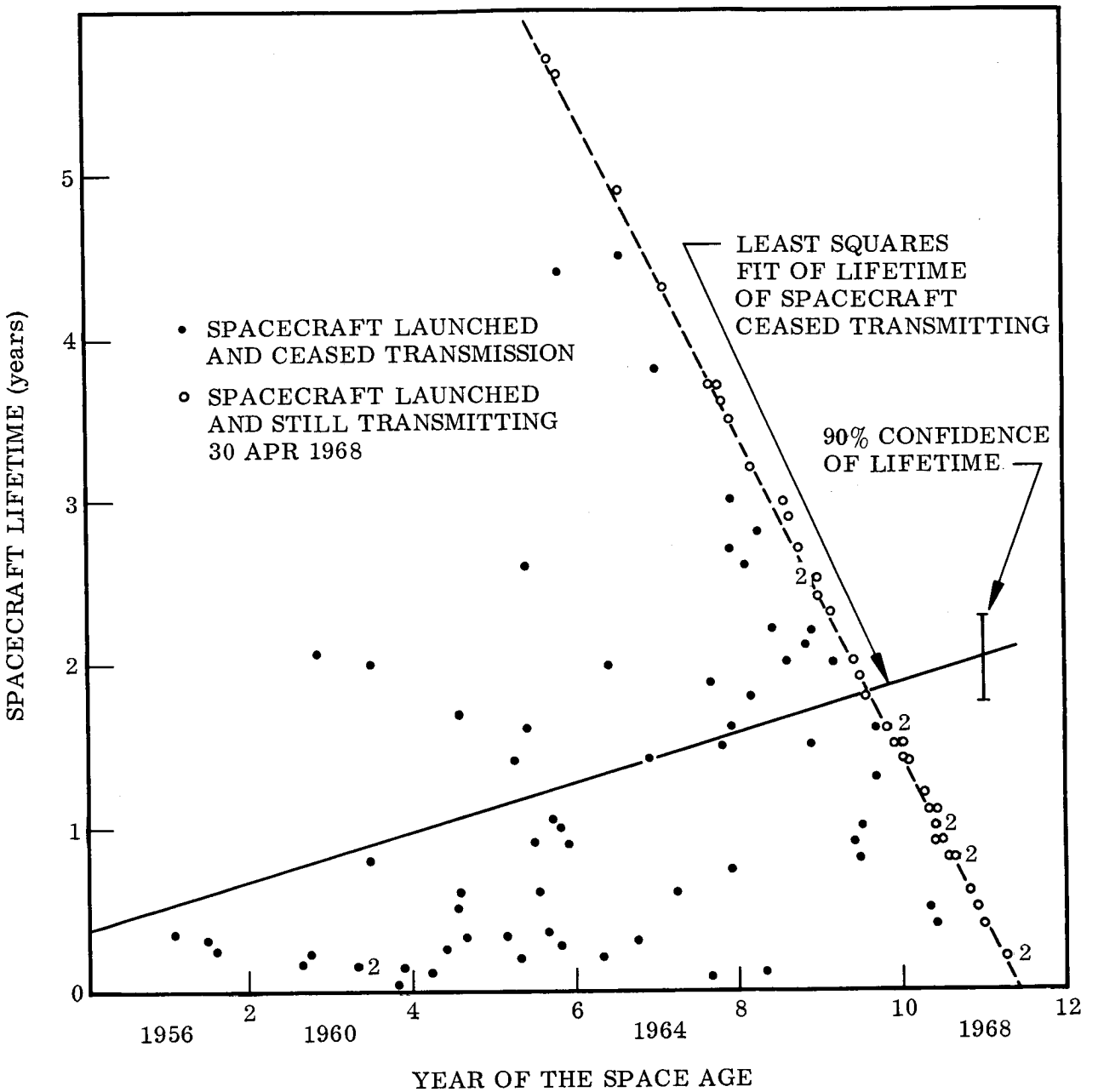

Fig. 17-1 Estimated Lifetime of Some Unmanned Scientific Spacecraft

from the least squares estimate. This treatment indicates a probable average lifetime at the beginning of 1968 of about 2.0 ± 0.25 years.

At the present time (30 April 1968) two spacecraft that were launched in 1962 are still transmitting, for an estimated lifetime of over 5.5 years.

The distributions by year launched are shown in Table 17-1 below for total spacecraft in the sample selected, for spacecraft still transmitting, and for the percentage of those selected that are still transmitting. The majority of those still transmitting have been in orbit more than two years.

Table 17-1

DISTRIBUTIONS OF SPACECRAFT BY YEAR

Year of Launch	Year of Space Age	No. Selected	No. Transmitting 30 Apr 1968	Transmitting (%)
1958	1	3	–	–
1959	2	3	–	–
1960	3	6	–	–
1961	4	8	1	12
1962	5	14	2	14
1963	6	7	1	14
1964	7	13	5	38
1965	8	16	7	44
1966	9	14	8	57
1967	10	16	14	88
1968	11	3	3	100

Information on the effects of the space environment on materials used in spacecraft must still be obtained mostly by inferences gleaned from the overall systems performance of the space vehicle since the recovery of materials from space is not a very common occurrence. A meteoroid experiment was picked up from the exterior surface of an Agena target during Gemini 10 extravehicular maneuvers; this, however, represents relatively short time space exposure. Studies which have been proposed to recover entire spacecraft or parts therefrom promise a wealth of new data on environmental effects on materials in the near future. For the present, the reported performance of a given spacecraft can only be related to the materials known to have

been used in its construction so as to give the spacecraft designer some assurance that the materials will successfully resist similar environments in the future. Some space-borne experiments with materials have been performed and are of special interest to the spacecraft designer. Particular attention is given in this chapter to relating the results of such space experience to comparable experience in space-simulation testing of materials.

The information presented in this chapter has been obtained from published technical literature, from government-sponsored reports, and from direct interviews with responsible scientists and engineers connected with the various spacecraft projects at government agencies, laboratories, and industrial organizations. This has made necessary the use of personal communication references. It is felt that the timeliness of including such late information through this device outweighs the disadvantage of these references not being immediately available to the reader.

17.1 RÉSUMÉ OF SUCCESSFULLY LAUNCHED SPACECRAFT

Spacecraft launched since 1957 are summarized in the first four tables and include their orbital parameters and some launch data (Refs. 4 and 5). Table 17-2 lists those spacecraft which were launched primarily to gather scientific data, to report on the Earth's weather conditions or to serve as a link in long-range communications systems and for which a fair amount of data have been released. These spacecraft include those in the above categories sponsored by the National Aeronautics and Space Administration, by foreign nations except the U.S.S.R., and by the U.S. Department of Defense for some unclassified projects. The U.S. manned spacecraft and closely related vehicles, such as the Agena vehicles used as targets in the Gemini program, are listed in Table 17-3. In Table 17-4 are presented the scientific satellites of the U.S.S.R. including all spacecraft launched by them except manned satellites and the Cosmos series. The manned spacecraft of the U.S.S.R. are shown in Table 17-5. Those spacecraft launched by one or another of the branches of the U.S. Department of Defense and for which no spacecraft project names have been assigned are omitted from the tables since very little information is available about them. The U.S.S.R. Cosmos spacecraft, of which 210 have been launched to date, are omitted for the same reasons.

The environmental factors affecting a spacecraft designed to operate at a given orbital altitude and inclination are necessarily complex, but, in a general manner, can be correlated with these orbital parameters. As an aid in this correlation, Table 17-6 presents spacecraft arranged according to altitude at apogee and inclination of their orbits from the equator. Not all the spacecraft launched and listed in Table 17-2 have been included in Table 17-6. Instead only a representative selection has been included based on availability of materials data for those spacecraft included, as well as including a fair representation of various programs.

By use of this table, the attention of the spacecraft designer can thus be focused readily on those satellites that have encountered the same space environment as that for which

Table 17–2

APPLIED AND SCIENTIFIC SPACECRAFT

Name	Project Direction	Launch Date	Launch Vehicle	Weight (lb)	Period (min)	Perigee (sm)	Apogee (sm)	Inclination From Equator (deg)	Status
Explorer 1	USA	1/13/58	Jupiter C	31	114.7	224	1,584	33.3	In orbit; transmitted to 5/23/58; discovered radiation belt
Vanguard 1	USN	3/17/58	Vanguard	3	134.3	405	2,462	34.5	In orbit; transmitted to 5-64; proved earth pear-shaped
Explorer 3	USA	3/26/58	Jupiter C	31	114.7	117	1,739	33.5	Decayed 6/28/58; transmitted radiation and micrometeoroid data until 6/16/58
Explorer 4	ARPA	7/26/58	Jupiter C	38	110	163	1,372	50.1	Decayed 10/23/59; mapped project Argus radiation belts until 10/6/58
Pioneer 1	NASA	10/11/58	Thor-Able	84					Lunar probe failed; reached 70, 717-sm altitude; returned radiation, magnetic field, micrometeoroid data
Pioneer 3	NASA	12/6/58	Juno II	13					Lunar probe failed; reached 63,580 sm altitude, discovered Van Allen outer belt
Score	ARPA	12/18/58	Atlas B	8,750	101.5	115	914	32.3	Entire Atlas injected into orbit; first communications satellite; relayed messages for 13 days; decayed 1/21/59
Vanguard 2	NASA	2/17/59	Vanguard	22	126 days	347	2,064	32.9	In orbit; silent
Pioneer 4	NASA	3/3/59	Juno II	13	398 days	0.9871 AU	1.142 AU	0.127	Lunar probe in solar orbit; silent
Explorer 6	NASA	8/7/59	Thor-Able	143	768	157	26,366	47	Decayed 7/61; first use of solar paddles; transmitted until 10/6/59; returned first TV photo of earth
Vanguard 3	NASA	9/18/59	Vanguard	100	130	317	2,329	33.3	In orbit: mapped earth's magnetic field; returned radiation and meteoroid until 12/11/59
Explorer 7	NASA	10/13/59	Juno II	92	101	346	676	50.3	In orbit; transmitted data until late 1961
Pioneer 5	NASA	3/11/60	Thor-Able	95	311.6	0.8061 AU	0.9731 AU	3.35	Interplanetary probe in solar orbit; silent
Tiros 1	NASA	4/1/60	Thor-Able	270	99	430	468	48.3	In orbit; silent; transmitted until 6/1/60
Transit 1B	ARPA	4/13/60	Thor-Able-Star	265	96	232	463	51.3	Decayed 10/5/67; transmitted until 7/12/60
Transit 2A/ Greb 1	USN	6/22/60	Thor-Able-Star	223 42	101.7 101.6	389 382	665 657	66.7 66.8	In orbit; transmitted until 8/62 In orbit; transmitted solar data until 4/61

Name	Project Direction	Launch Date	Launch Vehicle	Weight (lb)	Period (min)	Perigee (sm)	Apogee (sm)	Inclination From Equator (deg)	Status
Echo 1	NASA	8/12/60	Delta	166	118	941	1,052	47	In orbit; relayed voice and TV signals
Courier 1B	USA	10/4/60	Thor-Able-Star	500	107	586	767	28.3	In orbit; transmitted for 17 days
Explorer 8	NASA	11/3/60	Juno II	90	112	285	1,422	50	In orbit; transmitted until 12/27/60
Tiros 2	NASA	11/23/60	Delta	280	98.3	387	452	48.5	In orbit
Explorer 9	NASA	2/16/61	Scout	15	118	395	1,605	38.6	In orbit; silent
Transit 3B/ Lofti	USN	2/21/61	Thor-Able-Star	250 57	94.5	117	511	28.4	Decayed 3/30/61; second stage satellites failed to separate
Explorer 10	NASA	3/25/61	Delta	79	112 hr	100	145,000	33	Present position uncertain
Explorer 11	NASA	4/25/61	Juno II	82	108	304	1,113	28.8	In orbit; gamma ray counter returned data for 4 months
Transit 4A Injun/Greb 3	USN	6/29/61	Thor-Able-Star	270 (total)	103	534	623	67	In orbit; first nuclear power supply. Injun and Greb failed to separate from each other. Injun provided radiation data until 4/63; Greb x-ray data until late 1961
Tiros 3	NASA	7/12/61	Delta	285	100	461	506	47.8	Returned 35,053 photos until 2/27/62
Explorer 12	NASA	8/15/61	Delta	82	1585	180	47,800	33.3	Radiation and solar wind data until 12/6/61
Ranger 1	NASA	8/23/61	Atlas-Agena B	675	91.1	105	313	32.9	Decayed 8/30/61; attempt to reach deep space orbit failed
Explorer 13	NASA	8/25/61	Scout	187	97.3	175	606	36.4	Decayed 8/28/61; lower orbit than planned resulted in little useful data
Transit 4B/ TRAAC	USN	11/15/61	Thor-Able-Star	190 240	105	582	700	33.4	In orbit; returned geodetic data until 8/62; orientation experiment partly successful
Ranger 2	NASA	11/18/61	Atlas-Agena B	675	88.3	98	147	33.3	Decayed 11/18/61; attempt to reach deep space orbit failed
Oscar 1	USAF	12/12/61	Thor-Agena B	10	91.1	146	258	81.2	Delayed 1/1/61; first ham satellite
Ranger 3	NASA	1/26/62	Atlas-Agena B	727	406.4 days	0.9839 AU	1.163 AU	0.3988	Lunar probe in solar orbit; silent
Tiros 4	NASA	2/8/62	Delta	285	100.4	441	525	48.3	In orbit; returned 31,593 cloud cover pictures until 6/10/62
OSO 1	NASA	3/7/62	Delta	458	96.2	344	370	32.8	In orbit; transmitting solar flare and radiation data
Ranger 4	NASA	4/23/62	Atlas-Agena B	730	64 hr to moon				Impacted moon; timer failure caused malfunction of solar panels; batteries drained in 8 hr
Ariel	NASA/UK	4/26/62	Delta	132	100.9	242	754	53.9	In orbit; first NASA international satellite
Oscar 2	USAF	6/1/62	Thor-Agena B	10	90.5	129	240	74.3	Decayed 6/21/62; amateur radio satellite
Tiros 5	NASA	6/19/62	Delta	286	100.5	367	604	58.1	In orbit; returned 57,857 cloud cover photos until 5/4/63
Telstar 1	AT&T	7/10/62	Delta	170	157.8	593	3,503	44.8	First active repeater communication satellite; transmitted until 2/21/63

Mariner 2	NASA	8/26/62	Atlas-Agena B	447		in heliocentric orbit			Venus probe passed within 21,594 sm of planet, reported surface temperature of 800°F, returned data to 54.3×10^3 sm
Tiros 6	NASA	9/18/62	Delta	281	98.7	423	444	58.2	In orbit; wide angle camera operating
Alouette 1	Canada	9/28/62	Thor-Agena B	320	105.4	620	638	80.5	In orbit; active
Explorer 14	NASA	10/2/62	Delta	89	2184	174/280	61190/61106	32.9/ 33.6	In orbit; active
Ranger 5	NASA	10/19/62	Atlas-Agena B	755		in heliocentric orbit			Lunar probe missed moon by 450 sm
Explorer 15	NASA	10/27/62	Delta	98	312	194	10,760	18	In orbit; active
Anna 1B	USN	10/31/62	Thor-Able-Star	350	107.7	671	728	50.5	In orbit; active
Injun 3	USAF	12/12/62	Thor-Agena D	114	116.3	153	1,729	70.3	Pickaback on classified Air Force satellite transmitting radiation data
Relay 1	NASA	12/12/62	Delta	172	185	820	4,612	47.5	In orbit; active repeater communication satellite
Explorer 16	NASA	12/16/62	Scout	222	104	466	733	52	In orbit; micrometeorite satellite: transmitting
Transit 5A	USN	12/18/62	Blue Scout	135	99	432	455	90.6	In orbit: power supply malfunction after 1 day
Syncom 1	NASA	2/13/63	Delta	86	14265	21,268	22,974	33.5	In orbit; communication lost at injection into synchronous orbit
Explorer 17	NASA	4/2/63	Delta	405	96.4	158	570	57.6	Decayed 11/24/66; atmospheric structure satellite
Telstar 2	AT&T	5/7/63	Delta	175	225	604	6,713	42.7	In orbit; active repeater communications satellite
ERS 5	USAF	5/9/63	Atlas-Agena B	1.5	166.5	2,241	2,297	87.4	In orbit; returned solar cell damage data for 92 days
ERS 6	USAF	5/9/63	Atlas-Agena B	1.5	166.5	2,238	2,282	87.3	In orbit; duplicate of ERS 5, returned data for 89 days
Lofti 2A	USAF/USN	6/15/63	Thor-Agena D		93.7	114	449	69.9	Decayed 7/18/63; VLF experiment payload
Greb 4	USAF/USN	6/15/63	Thor-Agena D		94.1	110	480	69.8	Decayed 8/1/63; solar radiation payload
Tiros 7	NASA	6/19/63	Delta	297	97.4 97.4	385 382	401 409	58.2 58.2	In orbit; wide angle cameras, IR experiments operating; transmissions on 136.232 and 136.922 mc
Hitchhiker 1	USAF	6/26/63	Thor-Agena D	176	132.6 132.5	201 214	2,571 2,558	82.1 82.1	In orbit; pickaback to measure artificial radiation decay
Geophysical Research Satellite	USAF	6/28/63	Scout		102.1 102.1	255 262	815 807	49.7 49.7	In orbit; no details released; initial orbital data as of 6/30/63
ERS 9	USAF	7/18/63	Atlas-Agena B	1.5	167.9	2,276	2,319	88.4	In orbit; returned radiation damage data for 111 days
Syncom 2	NASA	7/26/63	Delta	86	1408	22,132	22,823	30	In orbit; active-repeater communications satellite, moved to position over Brazil; early communication tests successful

Name	Project Direction	Launch Date	Launch Vehicle	Weight (lb)	Period (min)	Perigee (sm)	Apogee (sm)	Inclination From Equator (deg)	Status
Vela 1	USAF	10/16/63	Atlas-Agena D	297	105 hr 108 hr	63,441 62,906	70,631 72,279	38.3 38.1	In orbit: nuclear detection satellite, to provide radiation background data
TRS 5	USAF	10/16/63	Atlas-Agena D	4.5	39 hr 38.7 hr	129 592	64,531 63,610	36.7 35.9	In orbit: pickaback returned radiation data for two weeks
Vela 2	USAF	10/16/63	Atlas-Agena D	297	108.7 hr 109.9 hr	62,806 64,474	72,974 72,379	38.0 37.0	In orbit: second nuclear detection satellite, initially lagged 140 deg behind Vela 1, continues to transmit
Explorer 18	NASA	11/26/63	Delta	138	96.3 hr 93.4 hr	119 2,402	122,522 119,523	33.3 36.4	In orbit: IMP-1, discovered high-energy radiation region beyond Van Allen belt, transmitting on 136.111 Mc
Explorer 19	NASA	12/19/63	Scout	18	115.9 115.4	366 382	1,487 1,454	78.6 78.6	In orbit: 12-ft balloon identical to Explorer 9, for atmospheric density studies in near-polar orbit
Tiros 8	NASA	12/21/63	Delta	265	99.3 99.4	430 437	473 467	58.5 58.5	In orbit: first Tiros to carry APT system transmitting on 136.233 and 136.924 Mc
GGSE	USAF/USN	1/11/64	TAT-Agena D		103.5 103.4	560 567	585 579	70.0 69.9	In orbit: gravity gradient stabilization experiment
EGRS	USAF/USN	1/11/64	TAT-Agena D		103.5 103.4	563 567	578 579	69.9 69.9	In orbit: payload designed to precisely locate other satellites, transmitting on 136.804 Mc
Greb 5	USAF/USN	1/11/64	TAT-Agena D	100	103.5 103.5	563 567	578 579	69.9 69.9	In orbit: solar radiation satellite monitoring x-ray and UV emissions, transmitting on 136.887 Mc
Relay 2	NASA	1/21/64	Delta	172	194.7 194.7	1,298 1,296	4,606 4,607	46.0 46.3	In orbit: active-repeater comsat, provided first Japan-France comsat link transmitting on 136.142 and 136.621 Mc
Echo 2	NASA	1/25/64	Thor-Agena B	547	108.8 108.5	642 676	816 766	81.5 81.5	In orbit: passive reflector comsat, first cooperative program with USSR, beacon transmitting on 136.021 and 136.170 Mc
Ranger 6	NASA	1/30/64	Atlas-Agena B	804	Flight time: 65.6 hr				Impacted on moon: closeup photographic experiment failed to provide data
Ariel 2	NASA/UK	3/27/64	Scout	150	101.3 100.6	180 180	843 800	51.6 51.7	In orbit: returning data from British galactic noise, ozone and micrometeoroid experiments, transmitting on 136.577 Mc
Vela 3	USAF	7/17/64	Atlas-Agena D	319	100.3 hr 101.5 hr	63,369 65,061	62,024 65,349	39.5 39.1	In orbit: experimental nuclear detection satellite to test satellite-borne sensor system, continues to transmit
Vela 4	USAF	7/17/64	Atlas-Agena D	319	100.1 hr 101.2 hr	58,766 58,772	69,482 70,292	40.9 40.9	In orbit: icosahedron identical to Vela 3, lags Vela 3 by 140 deg, continues to transmit
ERS 13	USAF	7/17/64	Atlas-Agena D	4.5	39.2 hr 39.2 hr	120 198	64,886 64,637	36.7 38.3	In orbit: tetrahedral research satellite intended to return radiation data, transmitting on 136.771 Mc
Ranger 7	NASA	7/28/64	Atlas-Agena D	806	Flight time: 68.6 hr				Impacted on moon: closeup photographic experiment returned 4316 high-quality photographs in last 13 min
Syncom 3	NASA	8/19/64	TAD	86	1436.2 1436.5	22,164 22,239	22,312 22,244	0.1 0.1	In orbit: first truly synchronous comsat, now stationed at 180°W; communication tests successful

Explorer 20	NASA	8/25/64	Scout	97	103.9 103.9	540 540	634 634	79.9 79.9	In orbit: ionosphere research satellite part of Topside Sounder Program, transmitting on 136.680 and 136.350 Mc
Nimbus 1	NASA	8/28/64	Thor-Agena B	830	98.3 98.4	263 267	579 580	98.6 98.7	In orbit: second-generation weather satellite, 27,000 photos returned until 8/28/64 when solar paddles locked
OGO 1	NASA	9/4/64	Atlas-Agena B	1073	64.0 hr 64.0 hr	175 801	92,827 92,216	31.1 32.3	In orbit: spin-stabilized rather than earth-oriented, returning data from 20 geophysical experiments on 400 Mc
Explorer 21	NASA	10/3/64	Delta	136	35 hr 34.7 hr	122 414	59,253 58,734	33.5 33.8	In orbit: IMP-2, apogee much lower than planned 126,500 sm, transmitting solar wind data on 136.145 Mc
Explorer 22	NASA	10/9/64	Scout	116	104.7 104.8	549 552	669 671	79.7 79.7	In orbit: ionosphere and geodetic research satellite, being tracked by laser at Wallops, transmitting on 136.171 Mc
Mariner 3	NASA	11/5/64	Atlas-Agena D	575					In solar orbit: shroud failure prevented planned Mars flyby
Explorer 23	NASA	11/6/64	Scout	295	99.2 99.2	288 289	610 606	51.9 52.0	In orbit: four micrometeoroid experiments wrapped around Scout fourth stage, transmitting on 136.080 and 136.857 Mc
Explorer 24	NASA	11/21/64	Scout	19	116.3 116.3	344 336	1,551 1,544	81.4 81.4	In orbit: 12-ft balloon, to continue Explorer 9 and 19 studies, first NASA dual payload launch, beacon on 136.710 Mc
Explorer 25	NASA	11/21/64	Scout	90	116.3 116.2	345 329	1,547 1,550	81.4 81.4	In orbit: radiation satellite, results integrated with Explorer 24 air density data, transmitting on 136.292 and 136.860 Mc
Mariner 4	NASA	11/28/64	Atlas-Agena D	575					In solar orbit: five interplanetary experiments operational; took first close-up pictures of Mars on July 14, 1965, passing within 5600 sm of the planet.
San Marco 1	Italy	12/15/64	Scout	254	94.9 94.8	128 126	510 499	37.8 37.8	Decayed 9/13/65: flight test of Italian ionosphere-air density satellite
Explorer 26	NASA	12/21/64	Scout	101	456 458	190 193	16,280 16,326	20.2 20.2	In orbit: repeat of Explorer 15, intended to study natural and artificial radiation, transmitting on 136.275 Mc
Tiros 9	NASA	1/22/65	Delta	305	119.2 119.2	435 437	1,602 1,606	96.4 96.4	In orbit: first "cartwheel" Tiros, elliptical rather than planned circular orbit
OSO 2	NASA	2/3/65	Delta	545	96.5 96.5	343 341	393 388	32.9 32.9	In orbit: six of eight experiments returning good solar x-ray, γ-ray, and UV data, transmitting on 136.712 Mc
LES 1	USAF	2/11/65	Titan 3A	69	145.7 145.7	1,726 1,727	1,744 1,744	32.2 32.1	In orbit: Transtage ejected experimental communications satellite after two restarts (Initial orbital data as of 2/15/65)
Pegasus 1	NASA	2/16/65	Saturn I	23,000	97.0 97.0	308 310	462 453	31.7 31.8	In orbit: meteoroid detection satellite with 2300 ft^2 of sensors, attached to S-IV second stage, transmitting on 136.41 and 136.89 Mc
Ranger 8	NASA	2/16/65	Atlas-Agena B	809		Flight time: 64.9 hr			Impacted on moon: returned 7137 photos, landed in Sea of Tranquility at 2.59°N, 24.77°E

Name	Project Direction	Launch Date	Launch Vehicle	Weight (lb)	Period (min)	Perigee (sm)	Apogee (sm)	Inclination From Equator (deg)	Status
Surcal	USN/USA	3/9/65	Thor-Agena D		103.5	564	584	70.1	In orbit: surveillance calibration satellite first 8-payload launch
GGSE 2	USN/USA	3/9/65	Thor-Agena D		103.5 103.5	562 566	583 583	70.1 70.1	In orbit: gravity gradient stabilization experiment, transmitting on 136.739 Mc (orbital data as of 3/15/65)
GGSE 3	USN/USA	3/9/65	Thor-Agena D		103.5 103.5	562 563	583 585	70.1 70.1	In orbit: gravity gradient stabilization experiment, transmitting on 136.776 Mc
Greb 6	USN/USA	3/9/65	Thor-Agena D		103.4 103.5	562 564	583 585	70.1 70.1	In orbit: solar radiation satellite, transmitting on 136.801 Mc
Secor 3	USN/USA	3/9/65	Thor-Agena D	40	103.4 103.5	562 564	583 585	70.1 70.1	In orbit: geodetic satellite, transmitting on 136.84 Mc
Surcal	USN/USA	3/9/65	Thor-Agena D						In orbit: surveillance calibration satellite
Oscar 3	USN/USA	3/9/65	Thor-Agena D	33					In orbit: amateur radio satellite, transmitted for 16 days
Secor 2	USAF/USA	3/11/65	Thor-Able Star	40	97.9	178	642	90	Decayed 2/26/68: geodetic satellite
Ranger 9	NASA	3/21/65	Atlas-Agena B	809		Flight time: 64.5 hr			Impacted on moon: returned 5814 photos, landed in crater Alphonsus
Snapshot	USAF	4/3/65	Atlas-Agena D		111.5	805	826	90.2	In orbit; SNAP-10A operated at more than 500 W for 43 days
Secor 4	USA	4/3/65	Atlas-Agena D	40	111.6	797	816	90.2	In orbit; geodetic satellite failed to operate
Early Bird 1	COMSAT Corp.	4/6/65	TAD	88	1437	21,748	22,732	359.86	In orbit: transmitting on 136.440 and 136.980 Mc
Explorer 27	NASA	4/27/65	Scout	132	107.8	595	818	41.16	In orbit: transmitting on 136.739 Mc
LES 2	USAF	5/6/65	Titan IIIA	82	315.2	1,757	9,384	31.4	In orbit: experimental comsat launched by last Titan IIIA
LCS 1	USAF	5/6/65	Titan IIIA	75	145.6	1,727	1,737	32.1	In orbit: passive aluminum sphere for radar calibration studies
Pegasus 2	NASA	5/25/65	Saturn I	23,100	97.3	314	466	31.7	In orbit: meteoroid detection satellite, provided good data
Explorer 28	NASA	5/29/65	Delta	130	8558	121	163,831	33.9	In orbit: IMP C, returning data on magnetic fields, radiation
Tiros 10	NASA	7/2/65	Delta	280	100.6	458	517	98.6	In orbit: sun-synchronous orbit, returning 400 photos daily
Vela 5	USAF	7/20/65	Atlas-Agena D	334	6713	66,476	72,234	35.2	In orbit: experimental nuclear detection satellite
Vela 6	USAF	7/20/65	Atlas-Agena D	334	6716	63,217	75,561	35.0	In orbit: lags Vela 5 by 180 deg, both continue to transmit
ERS 17	USAF	7/20/65	Atlas-Agena D	12	2595	129	69,723	35	In orbit: environmental research satellite monitoring radiation
Pegasus 3	NASA	7/30/65	Saturn I	23,100	95.3	323	336	28.9	In orbit: final Saturn I launched meteoroid detection satellite

Secor 5	USA	8/10/65	Scout	45	122.1	702	1,503	69.2	In orbit: Scout flight test carried geodetic satellite
Atlas-Centaur 6	NASA	8/11/65	Atlas-Centaur	2100	31 days	105	509,829	28.6	In orbit: Surveyor model launched on a simulated Moon trajectory
Surcal	USN	8/13/65	Thor-Able Star		108.1	680	738	90.0	In orbit: surveillance calibration satellite, failed to separate from second stage, failed to deploy 200-ft antenna
Surcal	USN	8/13/65	Thor-Able Star		108.1	680	738	90.0	In orbit: "Dodecahedron," extended twelve 25-ft antennas
Surcal	USN	8/13/65	Thor-Able Star		108.1	680	738	90.0	In orbit: "Tempsat," 14-in. sphere painted dull black
Surcal	USN	8/13/65	Thor-Able Star		108.1	680	738	90.0	In orbit: 14-in. white sphere to check Spasur system
Surcal	USN	8/13/65	Thor-Able Star		108.1	680	738	90.0	In orbit: rectangular package with beacon transmitter
OV1-2	USAF	10/5/65	Atlas D	190	125.7	256	2,146	144.3	In orbit: first successful OV1, returning radiation data
OGO 2	NASA	10/14/65	TAT-Agena D	1118	104.3	260	941	87.4	In orbit: geophysical satellite, 19 experiments returning data
OV2-1/LCS 2	USAF	10/15/65	Titan IIIC	375/75	99.7	439	492	32.6	In orbit: transtage broke up, failed to release payloads
Explorer 29	NASA	11/6/65	TAID	385	120.3	692	1,414	59.4	In orbit: GEOS geodetic satellite, all systems operational
Explorer 30	NASA	11/18/65	Scout	125	102.8	440	548	59.7	In orbit: solar radiation satellite, final IQSY monitor
A 1	France	11/26/65	Diamant	92	108.7	328	1,099	34.2	In orbit: first French satellite, transmitted for 2 days
Alouette 2	Canada	11/28/65	Thor-Agena B	320	121.4	314	1,856	79.8	In orbit: "topside sounder" ionospheric research satellite
Explorer 31	NASA	11/28/65	Thor-Agena B	218	121.3	314	1,851	79.8	In orbit: direct measurements satellite, complements Alouette
FR 1	France	12/6/65	Scout	132	99.9	458	484	75.9	In orbit: French VLF wave propagation research satellite
Pioneer 6	NASA	12/16/65	TAID	140		Heliocentric Orbit			In solar orbit: returning good solar and interplanetary data
OV2-3	USAF	12/21/65	Titan IIIC	427	589.7	110	20,903	26.4	In orbit: radiation satellite, transtage separation failed
LES 4	USAF	12/21/65	Titan IIIC	115	589.6	124	20,890	26.6	In orbit: experimental all-solid-state comsat, transmitting on X-band
Oscar 4	USAF	12/21/65	Titan IIIC	29					In orbit: amateur radio comsat, transmitting on 431.962 and 431.972 Mc
LES 3	USAF	12/21/65	Titan IIIC	35					Decayed 4/6/68: radio signal generator for comsat system tests
ESSA 1	NASA	2/3/66	Delta	305	100.2	432	521	97.9	In orbit: first ESSA operational meteorological satellite

Name	Project Direction	Launch Date	Launch Vehicle	Weight (lb)	Period (min)	Perigee (sm)	Apogee (sm)	Inclination From Equator (deg)	Status
D 1A	France	2/17/66	Diamant	44	118.6	313	1,711	34.0	In orbit: returning geodetic data
ESSA 2	NASA	2/28/66	TAID	290	113.6	843	885	101.0	In orbit: completed initial ESSA global system, APT cameras
OV1-4	USAF	3/30/66	Atlas D	193	103.9	550	630	144.5	In orbit: returned zero-g, thermal control experiment data
OV1-5	USAF	3/30/66	Atlas D	252	104.4	613	659	144.7	In orbit: optical radiation test, gravity gradient-stabilized
OAO 1	NASA	4/8/66	Atlas-Agena D	3900	100.8	492	505	35.0	In orbit: battery failed second day in orbit
OV3-1	USAF	4/8/66	Scout	152	151.7	220	3,568	82.5	In orbit: radiation research satellite
Nimbus 2	NASA	5/15/66	TAT-Agena B	912	108.1	684	734	100.3	In orbit: returning TV and infrared cloud cover photos
Explorer 32	NASA	5/25/66	Delta	495	116.0	173	1,629	64.7	In orbit: 3 aeronomy experiments returning data
Surveyor 1	NASA	5/30/66	Atlas-Centaur	596		Flight time: 63.6 hr			Landed on Moon: transmitted 11,150 photos up to 7/13/66, some data 11/8/66 after lunar night
OGO 3	NASA	6/7/66	Atlas-Agena B	1135	2907.9	170	75,768	30.9	In orbit: 21 experiments returning geophysical data
Secor 6	USAF/USA	6/9/66	Atlas-Agena D	38	125.1	104	2,266	90.1	Decayed 7/6/67: geodetic tests
ERS 16	USAF/USA	6/9/66	Atlas-Agena D	11	125.0	112	2,251	90.0	Decayed 3/12/67: carried 5 metal-to-metal bonding experiments
OV3-4	USAF	6/10/66	Scout	173	143.2	399	2,939	40.8	In orbit: radiation research satellite
GGTS 1	USAF	6/16/66	Titan IIIC	104	1334.2	20,913	21,051	0.1	In orbit: gravity gradient test satellite, 2 booms deployed
IDCSP 1	USAF	6/16/66	Titan IIIC	100	1334.7	20,923	21,053	0.1	In orbit: one of 7 initial defense communication satellites
IDCSP 2	USAF	6/16/66	Titan IIIC	100	1335.3	20,927	21,066	0.1	In orbit: initial defense comsat, all successfully separated
IDCSP 3	USAF	6/16/66	Titan IIIC	100	1336.6	20,936	21,088	0.1	In orbit: initial defense communication satellite
IDCSP 4	USAF	6/16/66	Titan IIIC	100	1338.6	20,936	21,139	0.2	In orbit: initial defense communication satellite
IDCSP 5	USAF	6/16/66	Titan IIIC	100	1340.8	20,935	21,194	0.0	In orbit: initial defense communication satellite
IDCSP 6	USAF	6/16/66	Titan IIIC	100	1344.0	20,949	21,258	0.1	In orbit: initial defense communication satellite
IDCSP 7	USAF	6/16/66	Titan IIIC	100	1347.6	20,948	21,350	0.0	In orbit: initial defense communication satellite
PAGEOS	NASA	6/24/66	TAT-Agena D	125	181.4	2,607	2,662	87.1	In orbit: 100-ft ballon, photographed in geodetic study

Explorer 33	NASA	7/1/66	TAID	206	8540	9,880	270,564	28.7	IMP satellite; injection into lunar orbit failed; transmitting on 136.02 Mc
OV1-8	USAF	7/14/66	Atlas D	74	105.2	612	635	144.2	In orbit: 30-ft wire mesh sphere for passive comsat tests
OV3-3	USAF	8/4/66	Scout	165	136.9	224	2,787	81.5	In orbit: instrumented to study Earth's radiation belts
Lunar Orbiter 1	NASA	8/10/66	Atlas-Agena D	853		Selenocentric Orbit			Took pictures of potential Apollo landing sites; intentionally crashed on Moon 10/29/66
Pioneer 7	NASA	8/17/66	TAID			Heliocentric Orbit			In solar orbit: six solar and interplanetary experiments active
Secor 7	USA	8/19/66	Atlas-Agena D	38	167.6	2,287	2,299	90.1	Transmitting on 136.8 Mc
ERS-15	USAF	8/19/66	Atlas-Agena D	11	167.5	2,280	2,300	90.1	In orbit: conducting five coldwelding experiments
Surveyor 2	NASA	9/20/66	Atlas-Centaur	644		Flight Time 62.8 hr			Crashed on Moon 9/23/66
ESSA 3	NASA	10/2/66	TAD	320	114.6	862	925	101.0	Transmitting on command on 136.77 Mc; replaced ESSA 1
Secor 8	USAF	10/5/66	Atlas-Agena D	38	167.6	2,287	2,304	90.2	In orbit: active geodetic satellite
Intelsat 2A	CSC	10/26/66	TAD	192	730.1	2,088	23,014	17.2	In orbit: active comsat, 12-hr rather than planned 24-hr orbit
OV3 2	USAF	10/28/66	Scout	177	104.2	198	993	82.0	In orbit: active radiation satellite
OV4 3	USAF	11/31/66	Titan IIIC	21300	90.6	187	188	32.8	Decayed 1/9/67: modified Titan II tank carrying 9 experiments
OV4 1R	USAF	11/3/66	Titan IIIC	300	90.4	181	181	32.8	Decayed 1/11/67: receiver in "whispering gallery" test with OV4 1T
OV1 6	USAF	11/3/66	Titan IIIC	445	90.4	180	180	32.8	Decayed 12/31/66: classified payload
OV4 1T	USAF	11/3/66	Titan IIIC	240	90.7	181	198	32.8	Decayed 1/11/67: transmitter for "whispering gallery" experiment
Lunar Orbiter 2	NASA	11/16/66	Atlas-Agena D	861	216.8	129	1,147	11.8	Decayed 10/11/67; returned 205 frames of lunar photography
ATS 1	NASA	12/6/66	Atlas-Agena D	775	660	22,277	22,920	0.2	In orbit: carrying out communication and meteorological tests
OV1 9	USAF	12/11/66	Atlas D	230	142.3	297	3,004	99.4	In orbit: radiation satellite to study biohazards, active
OV1 10	USAF	12/11/66	Atlas D	287	98.9	403	479	93.5	In orbit: gravity-stabilized radiation satellite, active
Biosatellite 1	NASA	12/14/66	TAD	940	90.7	191	197	33.5	Decayed 2/15/67: failed to return biological capsule after 3 days
Pacific 1	CSC	1/11/67	TAD	192	1436.1	22,244	22,257	1.3	In orbit: transpacific communication service initiated 1/11/67
IDCSP 8	USAF	1/18/67	Titan IIIC	100	1300	20,835	21,038	0.1	In orbit: initial defense communication satellite
IDCSP 9	USAF	1/18/67	Titan IIIC	100	1331	20,854	21,031	0.0	In orbit: initial defense communication satellite

Name	Project Direction	Launch Date	Launch Vehicle	Weight (lb)	Period (min)	Perigee (sm)	Apogee (sm)	Inclination From Equator (deg)	Status
IDCSP 10	USAF	1/18/67	Titan IIIC	100	1332	20,867	21,036	0.0	In orbit: initial defense communication satellite
IDCSP 11	USAF	1/18/67	Titan IIIC	100	1333	20,875	21,063	0.0	In orbit: initial defense communication satellite
IDCSP 12	USAF	1/18/67	Titan IIIC	100	1335	20,901	21,089	0.0	In orbit: initial defense communication satellite
IDCSP 13	USAF	1/18/67	Titan IIIC	100	1337	20,923	21,128	0.1	In orbit: initial defense communication satellite
IDCSP 14	USAF	1/18/67	Titan IIIC	100	1340	20,932	21,192	0.1	In orbit: initial defense communication satellite
IDCSP 15	USAF	1/18/67	Titan IIIC	100	1343	20,935	21,275	0.0	In orbit: initial defense communication satellite
ESSA 4	ESSA	1/26/67	TAD	290	113.4	822	894	102.0	In orbit: replaced ESSA 2, one of two APT cameras operational
Lunar Orbiter 3	NASA	2/4/67	Atlas-Agena D	850	218.6	124	1,150	21	Impacted on Moon 10/9/67: returned 182 frames of lunar photography
D 1C	France	2/8/67	Diamant	50	104.3	360	833	40.0	In orbit: geodetic satellite, operational in spite of low apogee
D 1D	France	2/15/67	Diamant	50	110.2	368	1,172	39.4	In orbit: provided good laser, doppler data until 4/5/67
OSO 3	NASA	3/8/67	Delta	627	95.9	336	354	32.9	In orbit: solar observatory, nine experiments returning data
Atlantic 2	CSC	3/22/67	TAD	192	1436.1	22,246	22,254	2.0	In orbit: third Intelsat II, stationed above Atlantic
ATS 2	NASA	4/5/67	Atlas-Agena D	815	218.9	115	6,947	28.4	In orbit: elliptical orbit prevented gravity test
Surveyor 3	NASA	4/17/67	Atlas-Centaur	625		Flight time: 65.0 hr			Landed on moon: soil sampler, photo experiments until 5/3/67
ESSA 5	ESSA	4/20/67	TAD	320	113.5	840	883	101.9	In orbit: replaced ESSA 3, two AVCS cameras operational
San Marco 2	Italy	4/26/67	Scout	285	94.9	135	498	2.9	Decayed 10/14/67: first equatorial launch, returning air density data
Vela 7	USAF	4/28/67	Titan IIIC	509	6658	67,804	69,991	32.2	In orbit: earth-oriented advanced nuclear detection satellite
Vela 8	USAF	4/28/67	Titan IIIC	509	6734	67,238	71,674	32.1	In orbit: lags Vela 7 by 180°, both continue to transmit
ERS 18	USAF	4/28/67	Titan IIIC	20	2840	5,357	69,316	32.9	In orbit: radiation research sub-satellite, active
OV5 3	USAF	4/28/67	Titan IIIC	19	2840	5,357	69,316	32.9	In orbit: radiation research sub-satellite, active
OV5 1	USAF	4/28/67	Titan IIIC	14	2840	5,357	69,316	32.9	In orbit: materials research sub-satellite, active

Lunar Orbiter 4	NASA	5/4/67	Atlas-Agena D	860	721	1,681	3,750	85.5	Decayed to Moon 10/6/67: returned 163 photos in lunar scientific survey
Ariel 3	UK	5/5/67	Scout	198	95.6	306	373	80.2	In orbit: first all-British research satellite, active
Explorer 34	NASA	5/24/67	TAD	163	6231	154	131,187	67.1	In orbit: IMP F, returning radiation, magnetic fields data
Surcal	USAF/USN	5/31/67	Thor-Agena D		103.5	570	582	70.0	In orbit: 20-in surveillance calibration sphere
GGSE 4	USAF/USN	5/31/67	Thor-Agena D		103.4	569	577	70.0	In orbit: gravity gradient stabilization experiment satellite
GGSE 5	USAF/USN	5/31/67	Thor-Agena D		103.4	570	575	70.0	In orbit: gravity gradient stabilization experiment satellite
Surcal	USAF/USN	5/31/67	Thor-Agena D		103.4	569	575	69.9	In orbit: navigation experiment satellite
Surcal	USAF/USN	5/31/67	Thor-Agena D		153.4	569	577	70.0	In orbit: 16-in surveillance calibration sphere
Mariner 5	NASA	6/14/67	Atlas-Agena D	540		Heliocentric Orbit			In solar orbit: 2480-mi Venus flyby, continues to transmit
Secor 9	USA/USN	6/29/67	Thor-Burner II	45	172.1	2,362	2,451	89.8	In orbit: geodetic satellite, continues location survey
Aurora 1	USA/USN	6/29/67	Thor-Burner II	47	172.1	2,370	2,458	89.8	In orbit: investigating formation of Aurora Borealis
IDCSP 16	USAF	7/1/67	Titan IIIC	100	1309.8	20,509	20,846	7.2	In orbit: initial defense communication satellite
IDCSP 17	USAF	7/1/67	Titan IIIC	100	1311.6	20,542	20,857	7.2	In orbit: initial defense communication satellite
IDCSP 18	USAF	7/1/67	Titan IIIC	100	1313.5	20,582	20,866	7.2	In orbit: completes global IDCSP system
DATS 1	USAF	7/1/67	Titan IIIC	100	1315	20,620	20,875	7.2	In orbit: mechanically despun antenna test satellite
DODGE	USAF	7/1/67	Titan IIIC	430	1317	20,661	20,884	7.2	In orbit: DOD gravity-gradient experiment satellite
LES 5	USAF	7/1/67	Titan IIIC	225	1319	20,692	20,894	7.2	In orbit: conducting tactical military communication tests
Surveyor 4	NASA	7/14/67	Atlas-Centaur	625		Flight time: 63.0 hr			Impacted on moon: communication lost 2.5 min before landing
Explorer 35	NASA	7/19/67	TAD	230	684	500	4,600		In lunar orbit: measures earth's magnetic tail every 29.5 days
OV1 86	USAF	7/27/67	Atlas D	260	95.5	303	390	101.7	In orbit: four experiments including cosmic ray telescope
OV1 12	USAF	7/27/67	Atlas D	311	95.6	342	344	101.6	In orbit: flare activated radiological observatory
OGO 4	NASA	7/28/67	TAT-Agena D	1240	98.1	256	564	86.0	In orbit: 18 experiments returning geophysical data
Lunar Orbiter 5	NASA	8/1/67	Atlas-Agena D	860	495	122	3,738	85	In lunar orbit: completed Lunar Orbiter photographic mapping

Name	Project Direction	Launch Date	Launch Vehicle	Weight (lb)	Period (min)	Perigee (sm)	Apogee (sm)	Inclination From Equator (deg)	Status
Biosatellite 2	NASA	9/7/67	TAD	1120	90.8	188	203	33.5	Re-entered 9/9/67: biological capsule recovered after 44.9 hr
Surveyor 5	NASA	9/8/67	Atlas-Centaur	616		Flight time: 64.8 hr			Landed on moon: returned 19,000 photos, soil analysis data
Pacific 2	CSC	9/27/67	TAD	192	1439.5	22,220	22,245	0.9	In orbit: transpacific communication service initiated 11/4/67
OSO 4	NASA	10/18/67	Delta	597	95.7	332	352	32.9	In orbit: returned first pictures of sun in extreme ultraviolet
ATS 3	NASA	11/5/67	Atlas-Agena D	805	1436.0	22,228	22,239	0.1	In orbit: returned color photos of entire earth
ESSA 6	NASA	11/10/67	TAD	290	114.8	877	923	102.1	In orbit: returning photos of cloud cover every 6 min.
Surveyor 6	NASA	11/7/67	Atlas-Centaur	617		Flight time: 65.4 hr			Landed in Moon 11/10/67
WRESAT	Australia	11/29/67	Sparta	100	98.9	106	78	83.3	Decayed 1/10/68
OV3-6	USAF	12/5/67	Scout	222	92.5	239	259	90.6	In orbit: conducted ionospheric studies
Pioneer 8	NASA	12/3/67	TAD	145		Heliocentric Orbit			In solar orbit: studying solar radiation
Explorer 36	NASA	1/11/68			112.2	673	979	105.7	GEOS-2
Surveyor 7	NASA	1/7/68							Landed on Moon 1/10/68
OGO 5	NASA	3/4/68			3795.9	168	92,079	31.1	
Explorer 37	NASA	3/5/68			98.7	318	548	59.4	
OV1-13	USAF	4/6/68			199.5	345	5,790	100.0	
OV1-14	USAF	4/6/68			207.8	348	6,173	100.0	

Table 17-3

U.S. MANNED ORBITAL SPACECRAFT

Name	Project Direction	Launch Date	Launch Vehicle	Weight (lb)	Period (min)	Perigee (sm)	Apogee (sm)	Inclination From Equator (deg)	Status
Mercury – Atlas 4	NASA	9/13/61	Atlas D	2700	88.6	100	159	32.6	Re-entered 9/13/61; recovered from ocean after 1 orbit
Mercury – Atlas 5	NASA	9/29/61	Atlas D	2900	88.5	100	148	32.5	Re-entered 11/29/61; chimpanzee Enos recovered after 3 orbits
Mercury – Atlas 6	NASA	2/20/62	Atlas D	2987	88.5	100	163	32.5	Re-entered 2/20/62; Friendship 7 with J. Glenn recovered after 3 orbits
Mercury – Atlas 7	NASA	5/24/62	Atlas D	2975	88.3	100	167	32.5	Re-entered 5/24/62; Aurora 7 with S. Carpenter recovered after 3 orbits
Mercury – Atlas 8	NASA	10/3/62	Atlas D	3030	89.0	100	176	32.5	Re-entered 10/3/62; Sigma 7 with W. Schirra recovered after 6 orbits
Mercury – Atlas 9	NASA	5/15/63	Atlas D	3000	88.5	100	166	32.5	Re-entered 5/16/63; Faith 7 with G. Cooper recovered after 22 orbits
Gemini-Titan 1	NASA	4/8/64	Titan 2	11,400	89.2	100	204	32.6	Decayed 4/12/64: unmanned boilerplate Gemini, plus second stage
Gemini-Titan 3	NASA	3/8/65	Titan 2	7,000	88.2	100	140	32.5	Re-entered 3/12/65: first manned orbital maneuvers, V. Grissom and J. Young landed after 3 orbits
Gemini-Titan 4	NASA	6/3/65	Titan 2	7,000	89.0	87	158	32.0	Re-entered 6/7/65; first US extra-vehicular activity by astronaut in orbit
Gemini 5	NASA	8/21/65	Titan 2	7,000	89.5	100	215	32.6	Re-entered 8/29/65: first extended U. S. manned flight; L. G. Cooper and C. Conrad landed after 128 orbits, 190.9 hr
REP	NASA	8/21/65	Titan 2	76	89.2	104	195	32.6	Decayed 8/27/65: radar evaluation pod ejected from Gemini 5
Gemini 7	NASA	12/4/65	Titan 2	8,000	89.2	100	204	28.9	Re-entered 12/18/65: F. Borman and J. Lovell went record 220 orbits, 330.6 hr served as Gemini 6 rendezvous target
Gemini 6	NASA	12/15/65	Titan 2	7,000	88.5	100	162	28.9	Re-entered 12/16/65: W. Schirra and T. Stafford rendezvoused within 1 ft of Gemini 7, landed after 17 orbits, 25.9 hr
Agena Target	NASA	3/16/66	Atlas-Agena D	7,000	90.4	185	186	28.9	Re-entered 9/20/67: first docking in space accomplished on fifth Gemini orbit. During powered maneuvers, short circuit in Gemini orbit and maneuvering system caused docked spacecraft to yaw and roll, forcing separation of docking

Table 17-3 (Cont'd)

Name	Project Direction	Launch Date	Launch Vehicle	Weight (lb)	Period (min)	Perigee (sm)	Apogee (sm)	Inclination From Equator (deg)	Status
Gemini 8	NASA	3/16/66	Titan 2	8,351	88.8	99	168	28.9	Re-entered 3/16/66: initial docking test; N. Armstrong and D. Scott landed after 6.5 orbits, 10.7 hr, due to short circuit
ATDA Target	NASA	6/1/66	Atlas-Agena D	1,700	90.4	185	185	28.9	Decayed 6/11/66: Augmented Target Docking Adapter Fairing separation failed, preventing docking
Gemini 9	NASA	6/3/66	Titan 2	8,268	88.8	100	169	28.9	Re-entered 6/6/66: rendezvous tests carried out by crew, T. Stafford and E. Cernan. EVA by Cernan terminated early because of helmet fogging. Landed after 47 orbits, 72.3 hr
Agena Target	NASA	7/18/66	Atlas-Agena D	7,184	91.5	214	217	28.9	Re-entered 12/29/66: first firing of Agena primary propulsion system while docked with Gemini. Docked spacecraft later approached within 50 ft of Gemini 8 Agena target vehicle
Gemini 10	NASA	7/18/66	Titan 2	8,248	95.2	185	469	28.8	Pilots J. Young and M. Collins returned to Earth 7/21/66; docked with Agena target, flew together for over 38 hr
Agena Target	NASA	9/12/66	Atlas-Agena D	7,199	90.4	180	191	28.8	In orbit; on docking with Gemini 11 was used to boost combination to 739.4 nm for two orbits, then another burn return to lower altitude. Rendezvous was first one accomplished on first Gemini orbit
Gemini 11	NASA	9/12/66	Titan 2	8,374	89.0	100	174	28.8	Returned to Earth 9/15/66 with crew C. Conrad, Jr., and R. Gordon, Jr.: Richard Gordon cut short EVA operations because of fatigue and excessive perspiration
Agena Target	NASA	11/11/66	Atlas-Agena D	7,090	90.4	182	188	28.9	Re-entered 12/23/66; three-orbit rendezvous accomplished to simulate lunar program rendezvous. Three dockings and undockings performed
Gemini 12	NASA	11/11/66	Titan 2	8,294	89.0	100	175	28.9	Returned to Earth 11/15/66 with crew J. Lovell and E. Aldrin, Jr.: set new EVA record with total of 5 hr, 37 min

Table 17-4

USSR APPLIED AND SCIENTIFIC SPACECRAFT

Name	Project Direction	Launch Date	Weight (lb)	Period (min)	Perigee (sm)	Apogee (sm)	Inclination From Equator (deg)	Status
Sputnik 1	USSR	10/4/57	184	96.2	141	588	65.1	Decayed 1/4/58; first artificial satellite; transmitted 21 days
Sputnik 2	USSR	11/3/57	1,120	103.7	140	1,038	65.3	Decayed 4/14/58; carried dog Laika; transmitted 7 days
Sputnik 3	USSR	5/15/58	2,925	105.8	140	1,168	65.2	Decayed 4/6/60; variety of data returned up to reentry
Lunik 1	USSR	1/2/59	3,245	450 days	0.9766 AU	1.315 AU	0.01	In solar orbit; lunar probe passed within 4660 sm of moon
Lunik 2	USSR	9/12/59	858		Flight time: 33.5 hr			Impacted on moon; detected lunar ionosphere, no magnetic field or radiation
Lunik 3	USSR	10/4/59	614	16.2 days	25,257	291,439	76.8	Decayed 4/20/63; lunar probe passed within 4373 sm of moon, photographed far side for 40 min from distance of 37,000 to 43,000 sm
Sputnik 4	USSR	5/15/60	10,008	91.3	194	229	65.0	Decayed 9/5/62; fragment recovered in Wisconsin; Vostok prototype cabin ejection attempted 5/19/60; separated into 8 pieces
Sputnik 5	USSR	8/19/60	10,120	90.7	190	211	64.9	Reentered 8/20/60; cabin and capsule with dogs Belka and Strelka recovered on 18th orbit
Sputnik 6	USSR	12/1/60	10,060	88.6	116	165	65.0	Decayed 12/2/60; reentry cabin with dogs Pchelka and Mushka burned up
Sputnik 7	USSR	2/4/61	14,292	89.8	139	204	65.0	Decayed 2/26/61; believed to be Venus probe abort
Venus Probe	USSR	2/12/61	1,419	300 days	0.7183 AU	1.0190 AU	0.58	In solar orbit; Venus probe; radio contact lost at 4.7×10^3 sm
Sputnik 8	USSR		14,292	89.7	123	198	65.0	Decayed 2/25/61; launched Venus probe from parking orbit
Sputnik 9	USSR	3/9/61	10,340	88.5	114	155	64.9	Reentered 3/9/61; cabin with dog Chernushka recovered
Sputnik 10	USSR	3/25/61	10,330	88.4	111	153	64.9	Reentered 3/26/61; cabin with dog Zvezdochka recovered after 17 orbits
Mars 1	USSR	11/1/62	1,965		Heliocentric Orbit			In solar orbit; Mars probe; transmissions ceased after 66×10^3 sm
Lunik 4	USSR	4/2/63	3,135		55,800	434,000		In orbit; lunar probe; missed moon by 5,281 sm; entered solar orbit
Polyot 1	USSR	11/1/63		102.3	211 212	329 863	59.0	In orbit: first Soviet spacecraft reported to have extensive maneuver capability
Elektron 1	USSR	1/30/64		169 169.3	252 251	4,412 4,421	61 60.9	In orbit: scientific satellite to study inner Van Allen radiation belt, first dual Soviet launch
Elektron 2	USSR	1/30/64		1,360 1,356.3	286 557	42,377 41,958	61 59.2	In orbit: intended to provide data on outer radiation belt, configuration differed from Elektron 1
Zond 1	USSR	4/2/64			Heliocentric Orbit			In solar orbit: only the third announced Soviet probe in long, unsuccessful interplanetary program
Polyot 2	USSR	4/12/64		92.5 92.0	193 185	311 278	58.1 58.1	In orbit: reported to have completed series of maneuver tests during first day of orbit
Elektron 3	USSR	7/11/64		168.1 168.1	251 247	4,365 4,368	61 60.8	In orbit: second Elektron dual launch, research satellite to monitor radiation in inner Van Allen belt
Elektron 4	USSR	7/11/64		1,313.8	285 379	41,076 41,078	61 60.1	In orbit: intended to make simultaneous radiation measurements in outer belt and magnetosphere

Table 17-4 (cont.)

Name	Project Direction	Launch Date	Weight (lb)	Period (min)	Perigee (sm)	Apogee (sm)	Inclination From Equator (deg)	Status
Zond 2	USSR	11/30/64						In solar orbit: Mars probe, tested plasma engine in flight
Molniya 1	USSR	4/23/65		720.5	308	23,800	65.19	
Lunik 5	USSR	5/9/65	3,500					Moon probe, failed to carry out soft landing, crashed on moon 6/12/65
Luna 6	USSR	6/8/65						Moon probe, missed moon
Proton 1	USSR	7/16/65	26,896	92.5	118	390	63.5	Decayed 10/11/65: physics laboratory, heaviest Soviet payload yet
Zond 3	USSR	7/18/65			Heliocentric Orbit			In solar orbit: retransmitting photos taken during lunar flyby
Luna 7	USSR	10/4/65	3,318		Flight time: 86.1 hr			Impacted on Moon: retros fired early, soft landing failed
Molniya 1B	USSR	10/14/65		719	311	24,855	65	Decayed 3/17/67 second Soviet comsat, USSR-France communications link
Proton 2	USSR	11/2/65	26,896	92.6	119	396	63.5	Decayed 2/6/66 heavyweight complex high-energy physics laboratory
Venus 2	USSR	11/12/65	2,123		Heliocentric Orbit			In solar orbit: planetary probe, on 3.5-month flight to Venus
Venus 3	USSR	11/16/65	2,116		Heliocentric Orbit			In solar orbit: planetary probe, backup to Venus 2
Luna 8	USSR	12/3/65	4,422					Impacted on Moon, retros fired late, soft landing failed
Luna 9	USSR	1/31/66	220		Flight time: 79.0 hr			Landed on Moon: returned photos of lunar surface for 3 days
Luna 10	USSR	3/31/66	540	178	217	621	72	In lunar orbit: lunar and circumlunar data until 5/30/66
Molniya 1C	USSR	4/25/66		710	310	24,544	64.5	In orbit: comsat, also transmitting cloud cover photos
Proton 3	USSR	6/6/66		92.3	114	361	63.5	Decayed 9/16/66
Luna 11	USSR	8/24/66	3,616	178	99	746	27	In lunar orbit: returned data until 10/1/66
Molniya 1D	USSR	10/20/66		713	301	24,668	64.9	In orbit: fourth Russian comsat, in 12-hour orbit
Luna 12	USSR	10/22/66		205	62	1,081		In lunar orbit: photographed moon, returned scientific data
Luna 13	USSR	12/21/66			Flight time: 79.7 hr			Landed on moon: returned photos, soil density data
Molniya 1E	USSR	5/25/67		319	286	24,737	64.8	In orbit: fifth Soviet comsat, in 12-hour orbit
Venus 4	USSR	6/12/67	2,438		Heliocentric Orbit			In solar orbit: ejected capsule for 10/18/67 Venus soft landing
Molniya 1F	USSR	10/23/66		712	289	24,606	65	In orbit: sixth Soviet comsat, in 12-hour orbit
Molniya 1G	USSR	10/22/67		716.2	327	24,700	64.8	
Zond 4	USSR	3/2/68			Heliocentric Orbit			
Luna 14	USSR	4/7/68			Selenocentric Orbit			

Table 17-5

U.S.S.R. MANNED ORBITAL SPACECRAFT

Name	Project Direction	Launch Date	Weight (lb)	Period (min)	Perigee (sm)	Apogee (sm)	Inclination From Equator (deg)	Status
Vostok 1	USSR	4/12/61	10,418	89.1	112	203	65.0	Reentered 4/12/61; cabin and Y. Gargarin recovered after 1 orbit.
Vostok 2	USSR	8/6/61	10,430	88.6	111	160	64.9	Reentered 8/7/61; cabin and G. Titov landed separately after 17 orbits.
Vostok 3	USSR	8/11/62	About 10,160	88.3	112	146	65.0	Reentered 8/15/62; cabin and A. Nikoloyev landed separately after 64 orbits.
Vostok 4	USSR	8/12/62	About 10,160	88.4	112	147	65.0	Reentered 8/15/62; cabin and P. Popovich landed separately after 48 orbits, 6 min after Vostok 3 reentry: initial orbit placed Vostok 4 within 3.1 sm of Vostok 3.
Vostok 5	USSR	6/14/63	About 10,160	88.3	109	138	65.0	Reentered 6/19/63; cabin and V. Bykovsky landed after 82 orbits.
Vostok 6	USSR	6/16/63	About 10, 160	88.4	114	145	65.0	Reentered 6/19/63; cabin and V. Tereshkova landed separately after 49 orbits, 3 hr before Vostok 5 landing.
Voskhod 1	USSR	10/12/64	11,070	90.1	100	255	65.0	Reentered 10/12/64; first three-man crew – V. Komarov, K. Feoktistov, and B. Yegorov – landed after 16 orbits.
Voskhod 2	USSR	3/18/65		90.9	107	308	65.0	Reentered 3/19/65; A. Leonov spent 10 min outside spacecraft, landed with B. Belyayev after 17 orbits.
Soyuz	USSR	4/23/67		88.6	125	139	51.7	Reentered 4/24/67; recovery attempt after 17 orbits, 25.2 hr, failed due to fouled parachutes; V. Komarov killed.

Table 17-6

APOGEE AND INCLINATION OF VARIOUS SPACECRAFT

Spacecraft	Launch Date	Apogee (sm)
Earth-Orbiting Vehicles With Apogees < 600 sm and Inclinations < 70 deg		
Gemini 3	3/23/65	140
BIOS 2	9/7/67	203
OSO 4	10/18/67	354
OSO 1	3/7/62	370
PEGASUS 1	2/16/65	462
TIROS 1	4/1/60	468
Gemini 10	7/18/66	469
OV2-1	8/15/65	492
San Marco 1	12/15/64	510
Explorer 30	11/18/65	548
Explorer 17	4/2/63	570
GREB 5	1/11/64	578
Earth-Orbiting Vehicles With Apogees < 600 sm and Inclinations > 70 deg		
ARIEL 3	5/5/67	373
Transit 5A	12/18/62	455
TIROS 10	7/2/65	517
ESSA 1	2/3/66	521
OGO 4	7/28/67	564
Nimbus 1	8/28/64	579
Earth-Orbiting Vehicles With Apogees Between 600 and 10,000 sm and Inclinations < 70 deg		
Explorer 23	11/6/64	610
ANNA 1B	10/31/62	728
Courier 1B	10/4/60	767

Table 17-6 (Cont'd)

Spacecraft	Launch Date	Apogee (sm)
Earth-Orbiting Vehicles With Apogees Between 600 and 10,000 sm and Inclinations < 70 deg		
D1-C	2/8/67	833
ARIEL 2	3/27/64	843
Echo 1	8/12/60	1052
SECOR 5	8/10/65	1503
Explorer 1	1/13/58	1584
LES 1	2/11/65	1744
Vanguard 1	3/17/58	2462
OV3-4	6/10/66	2939
Telstar 1	7/10/62	3503
RELAY 2	1/21/64	4606
Telstar 2	5/7/63	6713
ATS 2	4/5/67	6947
LES 2	5/6/65	9384
Earth-Orbiting Vehicles With Apogees Between 600 and and 10,000 sm and Inclinations > 70 deg		
Explorer 20	8/25/64	634
Alouette 1	9/28/62	638
Nimbus 2	5/15/66	734
Echo 2	1/25/64	816
ESSA 5	4/20/67	883
OGO 2	10/14/65	941
Explorer 24	11/21/64	1551
Alouette 2	11/28/65	1856
ERS 16	6/9/66	2251
SECOR 8	10/5/66	2304
OV3-1	4/22/66	3568

Table 17-6 (Cont'd)

Spacecraft	Launch Date	Apogee (sm)
Earth-Orbiting Vehicles With Apogees Between 10,000 and 45,000 sm		
Explorer 15	10/27/62	10,760
Explorer 26	12/21/64	16,280
LES 4	12/21/65	20,890
OV2-3	12/21/65	20,903
IDCSP 1-7	6/16/66	21,053–21,350
ATS 3	11/5/67	22,254
SYNCOM 3	8/19/64	22,312
Pacific 1	1/11/67	22,527
ATS 1	12/6/66	22,920
Explorer 6	8/7/59	26,366
Earth-Orbiting Vehicles With Apogees > 45,000 sm		
Explorer 12	8/15/61	47,800
ERS 17	7/20/65	69,723
VELA 7, 8	4/28/67	69,991
Explorer 18	11/26/63	122,522
Explorer 28	5/29/65	163,831
Explorer 33	7/1/66	270,564
Lunar and Interplanetary Probe Vehicles		
Ranger 4 – 9	Various	Lunar Impact
Pioneer 4 – 7	Various	Solar Orbit
Mariner 2	8/26/62	Venus Probe
Mariner 4	11/28/64	Mars Probe
Surveyor 1	6/30/66	Landed on Moon
Lunar Orbiter	Various	Lunar Orbit

he is designing a new satellite. Following the practice established in Refs. 1, 2, and 3, we have divided the spacecraft into the following categories:

- Earth orbiting vehicles having apogees <600 sm
- Earth orbiting vehicles having apogees <600 sm and inclinations >70 deg
- Earth orbiting vehicles having apogees between 600 and 10,000 sm
- Earth orbiting vehicles having apogees between 600 and 10,000 sm and inclinations >70 deg
- Earth orbiting vehicles having apogees between 10,000 and 45,000 sm
- Earth orbiting vehicles having apogees >45,000 sm
- Lunar probes and interplanetary vehicles

The space environments to be encountered by spacecraft in these orbits are discussed in Chapters 2 through 6.

17.2 MATERIALS USED IN SUCCESSFULLY ORBITED SPACECRAFT

Materials used in the construction of successfully launched satellites and spacecraft are tabulated in Tables 17-7 through 17-15 on pp. 485 through 528. These tables include the pertinent information from similar tables found in Refs. 1, 2, and 3. Following the procedure used in those documents, references to the literature for the materials tables are listed together in Section 17.3.2. This list will include, however, only references for the additional materials information added in this edition; references for the materials information brought forward from Refs. 1, 2, and 3 will not be repeated here.

The materials are arranged according to their class of functional application with separate tables covering thermal control materials, optical materials, materials for lubricated systems, adhesives, sealing materials, organic structural materials, materials for antennas, electronic materials, and inorganic structural materials. Within the tables, a further breakdown is made to show materials used in particular satellite and spacecraft vehicles.

The accompanying paragraphs are grouped according to spacecraft project name and are intended to form, in effect, a discussion of Tables 17-7 through 17-15 giving the results obtained from the spacecraft and correlating its performance insofar as possible with the choice of materials made during its design and the behavior of these materials under simulated and actual space environment.

17.2.1 Alouette

This satellite, the first to be built in Canada, was designed to measure electron densities and their temporal and spatial variations in the Earth's ionosphere by means of a variable frequency radio probe which was periodically swept from 1.6 to 11.5 MHz. In terms of lifetime and reliability of performance, it must be counted as a remarkably successful effort. Although the first Alouette satellite was launched in September 1962 and thus may have been affected by the artificial electron belt set up by the Starfish

high-altitude nuclear experiment of July 1962 and the subsequent high-altitude nuclear experiments of the U. S. S. R., the spacecraft performed thousands of measurements of the ionosphere and 2-1/4 yr after launching was reported to have suffered not a single failure in any of its 7000 parts (Ref. 6). As of this writing, almost 6 years after launch, it is still in orbit and transmitting ionospheric data during about 2-1/2 hours per day.

Perhaps the most interesting materials application aboard Alouette was that for the antennas used to receive reflected radio signals from the ionospheric layers. After injection into orbit, the antennas were deployed from a tape of spring steel which had been previously heat-treated, opened flat, and wound on a drum for storage. When this material was pulled off its drum and deployed into space, it formed into a tube with about 180 deg of overlap, forming a structure with considerable bending strength. On Alouette 1, four of these antennas were extended from the equator of the satellite to form a crossed dipole; the maximum extension was 75 ft. Much longer extensions than this are apparently possible and DeHaviland Aircraft of Canada, patent holder on this device, has designed antennas up to 1000 ft in length (Ref. 7). However, with a tube of even 75 ft in length and 0.85 in. in diameter, as in Alouette, the effect of solar heating of one side of the tube with consequent differential expansion and distortion of antenna alignment may become serious. On the Alouette, the antenna material selected was spring steel, but the current state-of-the-art choice would be beryllium copper alloy with a highly reflective silver plate coating (Ref. 7). Basically for high strength and good repeatability (of deployment), a material of low Young's modulus and highest possible yield strength is required; high conductivity is also required to minimize thermal distortion. The beryllium copper alloys seem to represent a reasonable compromise among these demands.

The power supply of Alouette utilized 6,480 p-on-n type silicon solar cells coupled with sealed nickel-cadmium batteries. Covers of 12-mil thick glass protected the solar cells. Power output from the solar cell array had been degraded by 20% in the first 11 days, by 33% within 3 months, by 37% by the end of 10 months in orbit, and by 43% after 3 years in orbit (Ref. 8). Part of this degradation could result from darkening of glass or adhesive cementing the glass to the silicon module. In the follow-on vehicles to Alouette, power will be obtained from the more radiation-resistant n-on-p type solar cells.

Several items may be mentioned in regard to correlation between simulation testing and performance in orbit. The solar cell degradation rate detailed above followed predictions made by NASA-Goddard scientists on the basis of previous testing and experience with p-on-n cell assemblies. Temperatures as measured on the instrumentation decks of the spacecraft followed closely the predicted values. In a 66% sun orbit the mean temperature was measured as 56°F as opposed to a prediction of 45°F; for the 100% sun orbit the spacecraft ran at 86°F as compared with a prediction of 84°F (Ref. 9).

Initial testing of a structural model of Alouette revealed a severe resonant response to vibration but the installation of eight struts between the equipment shelf and the thrust tube eliminated this problem. In a test of the antenna extension made after

thermal-vacuum testing, it was found that prolonged exposure to vacuum had caused a nylon sleeve in the deployment mechanism to shrink. This shrinking combined with possible small clearances had resulted in the binding of the mechanism. The parts were modified to provide greater clearance; thus, in this case the application of knowledge regarding space environmental effects on materials to the simulation situation resulted in a design change critical to the ultimate spacecraft mission. Another change made during the environmental testing program was to replace aluminum bushings with stainless steel bushings on certain aluminum shafts in the antenna drive train idler mechanism to prevent binding due to nylon gears running on aluminum shafts.

The second spacecraft of this series, Alouette 2, was launched on 28 November 1965 with much the same but slightly more sophisticated mission objectives as Alouette 1. It is instrumented with five experiments as follows: (a) a topside sounder which measures the distribution of electrons in the ionosphere as a function of distance from the satellite (similar to instrument on Alouette 1 but had wider frequency sweep and greater transmitter power by a factor of 3 to allow use at higher orbit), (b) a background radio noise experiment operating from 0.2 Hz to 14 MHz, (c) a VLF experiment operating from 50 Hz to 30 kHz, (d) an energetic particle experiment measuring electron and proton fluxes in several ranges, and (e) an electrostatic probe which measures electron number density and temperature near the spacecraft (Ref. 10).

After 16 months in orbit Alouette was reported (Ref. 11) to be completely free of any failures. As of this writing it is also still orbiting and transmitting data. The high reliability of this spacecraft is attributed by its designers (Ref. 11) to the use of very large operating margins in design, an extensive testing program, and care in assembly and inspection.

17.2.2 ANNA

The ANNA 1B satellite, launched 31 October 1962, is another long-lived spacecraft. Although the power available from its solar cells has been reduced over the years due to radiation damage, it is still capable of radio transmission and of flashing its xenon tube optical beacon lights on command (Ref. 12). In addition to its working complement of solar cells, ANNA 1B was one of the first spacecraft to carry a solar cell damage experiment and it was discovered, during its first 40 days in orbit that p-on-n cells had degraded 7% while n-on-p cells had degraded only 2.3% when both types of cells were protected by 30-mil sapphire covers (Ref. 13).

Signals of three types, optical, radio ranging, and radio doppler, from the ANNA 1B, as well as a number of other satellites designed by the Applied Physics Laboratory, have been used in a high-precision geodetic survey system. The NASA Explorers 22, 27, and 29 as well as the Navy navigation satellites and three French satellites have contributed to this program.

17.2.3 Apollo

The Apollo program with its goal of landing two U.S. astronauts on the Moon, has been significantly delayed by the spacecraft fire of 27 January 1967. This tragic

accident, occurring during ground testing of the Apollo-Saturn at Cape Kennedy, resulted in the death of three astronauts. In the intensive study following this event, nearly all combustible material has been removed from the spacecraft and the hatch has been redesigned for fast escape. A number of new and interesting materials developments have resulted from this reexamination of Apollo materials as well as from the program as originally planned. Although a manned Apollo spacecraft has not as yet been orbited, a preliminary listing of materials for the full Apollo payload is included in Tables 17-7 through 17-15.

Pre-Apollo flights orbiting the Saturn IV-B stage along with boilerplate payloads were carried out in 1964 with a series of three launches. After a lapse during 1965, three further missions were performed in 1966. The first, launched 26 February 1966, was designated as Apollo/Saturn IB-201 or AS-201 and carried a full Apollo Command Module 4630 sm in a suborbital maneuver. The second, AS-203, performed with the Saturn IB booster, carried the Saturn IVB stage and an Apollo boilerplate vehicle into orbit for four orbits before it was destroyed in a pressure test of the S-IVB. The third launch, AS-202, was a three-fourths orbit down-range flight carrying a full Apollo module to a 19,000 mph reentry for a test of the Command Module heat shield.

Following a long delay in launchings as a result of the Apollo 204 fire, a successful flight was made on 9 November 1967 of the first Saturn V launch vehicle which carried the Apollo 4 spacecraft to an orbital height of 11,234 miles. The next flight of Apollo 5 saw the first test of the Lunar Module vehicle on 22 January. Boost was accomplished by an uprated Saturn I rocket with no recovery of the LM vehicle. First indications were that the performance of the Apollo 5 spacecraft was sufficiently good to make unnecessary another unmanned flight before the first manned Apollo flight. An Apollo 6-Saturn V flight originally scheduled for 21 March 1968 was cancelled on the basis of this evaluation; however, Apollo 6 was rescheduled and successfully flown 4 April 1968.

The presence of man strongly influences the design and choice of materials of construction of manned spacecraft such as Apollo as compared with unmanned spacecraft (Ref. 14). Man, as a unique payload for a space vehicle, introduces requirements for a large pressurized volume and for special features such as windows and hatches needed to permit him to function. The problem of compatibility of materials with man's presence forms the subject matter for Chapters 19, 20, and 21 of this handbook.

An interesting materials problem which developed during preflight testing of the Service Module involved the rupture of propulsion tanks evidently due to interaction between methyl alcohol, used in the tank to simulate fuel, and the stressed titanium alloy tank. This phenomenon has been reported previously in the literature with HCl-methanol solutions in connection with research on the chloride stress corrosion cracking of titanium alloys (Ref. 15). Because the fuel tanks in the AS-204 vehicle had also been exposed to methanol, they were replaced. A more compatible fluid will be used for future pressure tests. More complete tests of specimens from actual Apollo hardware as well as Ti-6Al-4V forgings (Refs. 16 and 17) have confirmed the earlier findings and definitely indicate that at the operating stress levels in the Apollo fuel tanks, initial flaws or defects of undetectable size can grow to critical size and cause failure when exposed to methanol.

Table 17-7

THERMAL CONTROL MATERIALS

Alouette. Several surfaces were used to achieve the desired passive thermal control including optically coated glass-covered solar cells, anodized aluminum (α/ϵ = 0.95), black epoxy-based FeO enamel (α/ϵ = 1.0), white ultraviolet resistant polyurethane-based TiO_2 enamel (α/ϵ = 0.2), and polished aluminum (α/ϵ = 2.5).

Anna 1B. Flat black epoxy paint with FeO pigment – Mono Seal Products Co.

Apollo. Insulation: (a) Launch escape tower – titanium tubing covered with layer of Buna-N elastomer to protect from rocket exhaust heating; (b) Command Module, between inner structure and heat shield – aluminum faced nylon enclosed TG 15000 silicone impregnated glass fiber); (c) Command Module, ablative heat shield – AvCoat 5026-39 HC/G (AVCO Corp.) consisting of a phenolic honeycomb having its cells filled with an epoxy-phenolic containing phenolic microballoons and quartz fibers; (d) Service Module – cork sheet to protect against launch heating; (e) boost protective cover over Command Module – covered with 0.3-in. cork layer; (f) Lunar Excursion Module – underside of crew compartment was covered with a heat shield of about 20 alternate layers of nickel foil and Fibrafrax paper (50:50 mixture of aluminum oxide and silica) to protect it from blow-back of ascent engine during lunar lift-off.

Active Thermal Control: Command and Service Module – circulating water-ethylene glycol system carries heat to external cold plates for radiative dumping.

Passive Thermal Control: (a) Service Module skin panels – aluminum pigmented polyester except for radiating sections which are ZnO-K_2SiO_3 paint; (b) Command Module – aluminized Mylar coated with thin layer of SiO_x was bonded to exterior surface, and textured aluminum foil covered with a noncontinuous layer of K_2SiO_3 and textured aluminum foil covered with an openweave fiberglass cloth were used on the heat shield. Gold tapes, aluminum tapes, and epoxy paints were used for internal coating. (c) Lunar Excursion Module – several coatings were used for exterior: Alzak-coated 2024 aluminum alloy, H-film with vacuum deposited SiO_x, and aluminum pigmented black (Finch Paint Co.); also white paints either Z93, ZnO, or the LP 40 silicate paints. In the interior of the crew compartment the aluminum alloy surface is first deoxidized then given the Alodine coating treatment followed by the 3M velvet gray coating.

Ariel 1. Evaporated-gold coating over varnish, lacquer, conducting silver paint, electroplated copper, and lacquer substrates applied in that order. About 25% of the surface area was covered with a combination of silicone paints pigmented with either carbon black or zinc sulfide (white).

Ariel 3. The aluminum surface was nickel plated, buffed, then gold (99% Au, 1% Ag) plated over approximately 60% of the total surface area of the spacecraft. Remainder of area was covered with either black acrylic paint or a white acrylic paint covered with a white silicate.

ATS. Active thermal control – system of fixed and movable vanes which expose or cover alternate coatings of vapor-deposited aluminum (ϵ = 0.04) and acrylic base white paint (ϵ = 0.85) to control the spacecraft temperature to 70° ± 30°F.
Internal surfaces – painted black to facilitate radiation interchange.
Electronics and payload module is insulated with aluminized Mylar superinsulation.
Passive thermal control coatings – polished aluminum and black alicyclic-diamine high-temperature epoxy paint.

Bios. Adaptor section – 28-layer aluminized Mylar insulation blanket; electric heaters to hold temperature between 0° and 100°F.
Life capsule – active thermal control system with water boiler system and coolant loop used to hold temperature to ~ 70–75°F. Coolant fluid – Coolanol 25 silicate ester (Monsanto Chem. Co.).

Courier 1B. TiO_2-pigmented paint.

Echo 1. Outer surface of balloon – 2200 Å layer of vapor deposited aluminum.

Echo 2. Outer layer of balloon – Alodine 401-45, an amorphous compound consisting mainly of chromium and aluminum phosphates, of thickness 0.02 mil. Inner layer of balloon – carbon black of thickness 0.02 mil.

ERS. (Environmental Research Satellite). External – Cat-a-lac flat black epoxy paint for high-altitude polar orbits. Silver Chromatone paint for low-altitude polar orbits. Gold vacuum deposited on polymer tape 3M type Y9181. Aluminized foil tape 3M type 425. Internal – solid state commutator mounted on a boron nitride block to maintain thermal stability of commutator.

ERS 15 and 16. External surface – (mostly solar cells), gold plating, and titanium tape; coldwelding experimental valves – plastic support brackets, aluminized Mylar wrap, 3M type 850, applied over the valve bodies; contaminant gas reservoir tank – bare aluminum.

Explorer. The first Explorer made use of stripes of aluminum oxide (Rokide A) and the slightly oxidized stainless steel surface of the spacecraft. The remainder of the earlier Explorers had coatings of varying combinations of the following materials (not all on the same spacecraft): Rokide A, ZrO_2 pigmented paint, TiO_2 pigmented paint, aluminum powder pigmented paint, black anodized aluminum, evaporated aluminum, evaporated gold, and black and white epoxy paints (Cat-a-lac).

Explorers 9, 19, 24. (Atmospheric Density Explorers). White dots spotted on the aluminum outer surface of the balloon, dots made up about 17% of the surface and consisted of an epoxy (epichlorohydrin bisphenol-4) paint pigmented with titanium dioxide for Explorer 9 and a methyl silicone elastomer pigmented with zinc oxide for the Explorers 19 and 24.

Explorer 17 (Atmospheric Structure Explorer). Vapor-deposited aluminum covered with silicon oxide coating.

Explorers 12, 14, 15, and 26 – Energetic Particles Explorers (EPE). Coated first with lacquer to get a mirror finish, then finished with vapor-deposited aluminum and silicon oxide coating. Other surfaces – silicone paints (black, white, and leafing aluminum pigmented) and aluminized tape or foil tape.

Explorers 18, 21, and 28 – Interplanetary Monitoring Platform (IMP). Some parts of Explorers 18 and 21 used the lacquer, deposited aluminum, and silicone oxide finish as described for the EPE vehicles. Because of problems with paint adhesion on Explorer 15, painted surfaces on Explorer 18 onward were changed to Cat-a-lac black and a white epoxy undercoat with Naval Research Laboratory (NRL) silicone white. Due to the indicated high degradation rate of the NRL white paint, a methyl silicone paint with titanium dioxide pigment was used on Explorers 21 and 28 as well as on Explorer 26 of the EPE series. The Cat-a-lac black epoxy and the NRL leafing aluminum paint were also used on Explorers 21 and 28. Small areas were covered with aluminized or foil tape. Active thermal controls, heaters in the magnetometer package, were also used.

Explorer 29. Most of surface was painted with Vita Var PV100 White with conductive spiral for the antenna painted on the surface with silver loaded epoxy C-93 (J. F. Motson Co.). The 60-ft deployable antennas were silver plated.

Explorer 33. Insulation: aluminized H-film has replaced aluminized Mylar in places where higher temperatures are expected. Rocket engine was insulated with multilayer blanket of 10 layers of aluminized H-film interspersed with alternate layers of glass fiber Dexter paper.

Passive Thermal Control: (a) Bottom surface – 55% buffed aluminum surface and 45% Q92-090 paint, a TiO_2 elastomeric silicone also known as Dow-Corning 2A-100; (b) Lateral surface – Cat-a-lac black paint; (c) Top surface 85% buffed aluminum and 15% Q92-090; (d) Goddard magnetometer – 90% evaporated aluminum and 10% white paint; (e) Ames magnetometer – Thermatrol paint, the Dow-Corning 2A-100 (Q92-090).

Gemini. Adapter section – silicate paint pigmented with zirconium dioxide on outside, Lockspray gold over epoxy paint on the inside.
Other interior paints – Andrew Brown Co. XA silicone paints.
Instrument coolant – Monsanto silicate ester MCS-198.

Spacecraft walls were insulated with Min-K, asbestos fiber reinforced metallic oxides with opacifiers to block radiation. Reentry heat shield – a glass fiber reinforced phenolic honeycomb sandwich served as structure and another layer of the same honeycomb filled with DC-325 ablative material provided heat protection. The honeycomb and face sheets were bonded together with HT-424 and bonded to a titanium alloy structural ring with the same adhesive.

LES (Lincoln Experimental Satellite). Outer panels, where not supporting solar cells, were covered with glass microsheet backed with aluminum. Interior surfaces were painted black.

Lunar Orbiter. Passive Thermal Control – surface coating on insulation blanket was SiO_x which was in turn coated with clear RTV-602; this surface had α/ϵ of about 0.3 to meet design criteria of "less than 1.0." Surface of the upper heat shield near the rocket engine nozzle was bare 321 stainless steel. The bottom of the equipment deck, which is the sun-facing side, was painted with a white methyl silicone paint pigmented with zinc oxide (Boeing Co. B1056). Back side of the solar panels was coated with Cat-a-lac black epoxy and the same coating was used for most interior surfaces with the exception of the camera housing which was buffed 6061 aluminum. The low-gain antenna boom was painted with Laminar X500 specular black (Magna Paint and Chem. Corp.) to cut down possible reflections to the Canopus sensor.

Insulation – a blanket of multilayer aluminized Mylar and Dacron (4 to 6 layers) covered the main central section of the spacecraft.

Miscellaneous – Indium foil was used to form a good heat conducting path between Inertial Reference Unit assembly and the spacecraft mounting deck.

Mariner 2. Exposed wiring wrapped with Teflon-coated aluminum foil. Venus radiometer surface contoured to minimize heat concentration; Lexan polycarbonate insulation prevents thermal conduction; aluminized Mylar sheet and tube reinforced with Teflon (top and bottom of base); gold plate on instruments; Cat-a-lac flat black paint, carbon filled epoxy (inside electronic compartments); polished aluminum louvres (active thermal control); TiO_2-silicone base white paint on electronic compartment: Al-silicone base paint on electronic containers; Dow 7 treatment of AZ-31 Mg alloy for electronic containers.

Mariner 3 and 4. Surfaces of some electronic boxes in main bus were covered with 12-mil polished aluminum shielding. Five of the eight boxes had aluminum foil louvers over a surface of TiO_2 white paint for active thermal control. Some of the shields contain cutouts which allow heat to be radiated from local "hot spots." Upper and lower surfaces of bus were shielded with 30 layers of crinkled aluminized Mylar. The outer and inner layers of each multilayer were covered with either black Dacron, if the shield is in the sunlight, or aluminized Teflon. Cable harnesses were wrapped with aluminized polyvinylfluoride. Some exposed wiring was wrapped with aluminized Teflon. The high-gain antenna coating was a polyurethane pigmented with Cr_2O_3. Antenna feed coated with PV-100 organic base white paint. Both Dow 7 and Dow 17 conversion coatings used on various magnesium parts.

Mercury-Atlas. Rene 41 shingles, heat oxidized to a black color (conical side of spacecraft); beryllium shingles, chemically oxidized (cylindrical side); black ceramic paint (washers, bolts, etc.); gold coating on inside of beryllium shingles.
Thermal insulation: Thermoflex – Johns-Manville; Fiberfrax (carborundum), with foils of Inconel and aluminum.
Modified silicone base paint for internal use.

Nimbus 1. Two multilayer assemblies insulate the spacecraft control subsystem. One consists of 11 layers of 1/4-mil thick crinkled aluminum foil separated by 10 layers of 4-mil thick matted glass fiber paper. The assembled stack is covered on both sides by an additional layer of glass fiber paper and is enclosed with a 2-mil thick woven glass fiber fabric which is impregnated with Teflon. The second assembly consists of 34 layers of 1/4-mil aluminized Mylar. Teflon-impregnated glass fiber fabric is also used as an external cover for this assembly.

Solar power paddles – front side, solar cells, $\alpha = 0.773$, $\epsilon = 0.942$; back side PV 100 or white epoxy, $\alpha = 0.2$ and $\epsilon = 0.88$.

Faying surfaces of components and panels were coated with Eccobond 56C for more efficient conductive heat transfer.

Sensory assembly crossbeam structure on which the camera system components are mounted was painted with absorptive flat black paint to achieve an adiabatic structure.

Vita Var PV 100 was used on the outboard faces of compartments and on the bottom surfaces of batteries.

Aluminum-pigmented silicone alkyd paint (D4D) was used on the quadraloop antenna, separation ring, struts, lower section of command antenna, outer surface of insulation on three compartments and on the insulation blanket sheet.

Amfab (TV 20-60, a Teflon-impregnated glass fabric manufactured by AM&F) was used as the outer coating of the top insulation and on the control system surfaces.

In addition to passive control, Nimbus also incorporated active control in the form of louvers constructed of multilayer aluminized Mylar. They are actuated by a stainless steel AISI 302 bellows and provide control for the vidicon electronics and the attitude control servomechamisms. When open, the louvers uncovered the magnesium alloy container cover which was painted white. The expansion of Freon 114 in the vidicon thermal control mechanism and Freon 11 in the attitude control instrument system thermally actuated the louver mechanisms.

The interior of the structure was black anodized over aluminum, or black painted over magnesium with a GE proprietary carbon black pigmented formulation ($\alpha/\epsilon = 0.94$) where high temperature stability was required, or with a Lowe Bros. glycerol phthalate black in other less sensitive locations.

The truss structure was wrapped with aluminized Mylar and aluminized Teflon tape, as were the electrical cable harnesses.

OAO 1. Surface panels – Alzak Lighting sheet (3003 aluminum alloy with 99.9% aluminum cladding which is electrolytically brightened and coated with a light clear anodize); instrument bay insulation – either 10 or 25 layers of 1/4-mil thick Mylar coated with 25×10^{-6} in. of aluminum.

OGO. Back surfaces of solar panels – ZrO_2 pigmented potassium silicate inorganic paint. Other coatings used included Dow Corning DC 92-007 white paint, black Finch Cat-a-lac paint, vacuum deposited aluminum, and a chemical conversion coating per MIL-C-5541.

Except for the 2 surfaces covered with louvers and the solar panels, multiple layer aluminized Mylar is used. Five to ten layers of 1/2 mil material is used plus an inner and outer layer of 3 mils each. Most of the insulation is applied by ultrasonic welding.

Experimental package coatings – evaporated SiO_x, Mylar and Kapton blankets (aluminized), and Cat-a-lac black paint; booms – blanketed with aluminized Mylar.

Oscar 3. External surface – nonleafing aluminum paint on Mystic tape.

OSO 1. Gold plate on spectrometers on sail; aluminum paint/silicone resin (on wheel); white TiO_2 nontinted paint/silicone resin (on sail); polished aluminum solar panels; aluminum paint/silicone resin on arms and epoxy fiberglass gas containers; anti-reflectance coating on solar cells.

Coating experiment – TiO_2 in epoxy, TiO_2 in silicone, white fused porcelain enamel, aluminum powder in silicone, Al-SiO-Ge films, and Al-SiO-Ge – SiO films were tested.

OSO-2. Paints – a base of phenylmethyl silicone resin with the white version pigmented with TiO_2.
Outer rim of wheel – leafing aluminum.
Top and bottom of wheel – polished aluminum.
Internal parts – black anodized.
Heat sink – Coors BeO for power transistors.

OV3. Outer surface – buffed aluminum; internal surfaces – polished aluminum, 3M black velvet paint, and 3M white paint; insulation around spectrometer – 20 layers of a alternating aluminized Mylar and raw silk.

Pegasus 1 and 2. Back of solar panels – PV-100 white paint.
Saturn S-IV stage – S-13 paint.
Electronics boxes – PV-100, S-13, and aluminum pigmented silicone (Fuller 172-A 172-A-1) paints.
Tubing near electronics boxes – wrapped with aluminized Mylar tape.
Louvers on bottom of electron cannister – polished aluminum.
Other miscellaneous surfaces – Lowe Bros. black paint.
Aluminum surfaces of meteoroid detectors – adaptation of chromium aluminum phosphate coating used on the Echo. The change involved addition of phosphoric acid in processing. Fairchild-Hiller designation is MTL-3.
Canister area – superinsulation (aluminized Mylar) except for the bottom which is louvered.

Pioneer 5. Active temperature control: aluminum foil coated with high α/ϵ TiO_2; thin polished aluminum discs were covered with pivoted thin aluminum segments painted alternately black and white on four segments with four open segments; discs rotated by expansion of bi-metallic spring to control temperature.

Passive temperature control; lithium heat sinks; TiO_2 coating, range of temperature 35° to 85°F; infrared emissive material on transmitter; vacuum deposited interference filter on solar cells.

Pioneer 6 and 7. Passive thermal control – the end of the spacecraft opposite the antenna was painted with Lockheed LP-10A zirconium oxide-potassium silicate white paint (thermal cure). Internal surfaces of the spacecraft were coated with Cat-a-lac black paint, epoxy vehicle, carbon black pigment (Finch Paint and Chemical Co.). The booms and antennas were coated with one or the other of the two paints mentioned above. Active thermal control – spacecraft end opposite the antenna had a set of louvers actuated by a bimetallic spiral spring which alternately covered or exposed the white paint mentioned above. The louvers were A1100 aluminum foil. Insulation – antenna end of the spacecraft was covered with a blanket of multilayer aluminized Mylar superinsulation.

Ranger 1. Lexan polycarbonate insulation prevents thermal conduction between metal parts of structure, aluminized Mylar sheet and tube reinforced with Teflon (top and bottom of base); gold plate on instruments; Cat-a-lac flat black paint, carbon filled epoxy (inside electronic compartments); TiO_2-silicone base white paint on electronic compartments; Al-silicone base paint on electronic containers; Dow 7 treatment of AZ-31 Mg alloy for electronic containers.

Ranger 6 through 9. External – completely passive thermal control system used; black Cat-a-lac paint used in all surfaces where sunlight might be reflected to other parts of the spacecraft; polished surfaces used for other surfaces to reflect sunlight away from the spacecraft.
External – aluminized Mylar used for wrapping cable harnesses.
Electronic boxes – white TiO_2-pigmented silicone paints used on exteriors of some boxes; also gold plating used on exteriors and interiors of some boxes.

Relay. Coated Mylar covering ends of solar cells; anti-reflective coatings on solar cell covers maintain satellite temperature; aluminized Mylar films closing ends of assembly.

Active thermal control: Alternate sections covered with aluminized Mylar.

Surveyor. Passive thermal control surfaces – polished aluminum structure on parts facing the Moon, Hughes Aircraft Co. proprietary inorganic white paint on surfaces facing the Sun. These two coatings cover about 90% of the exterior surface of the spacecraft. Smaller areas include the back of the solar panel, which was covered with an organic white paint; the landing legs, which were coated with Minnesota Mining and Manufacturing Co. White Velvet paint; and the exterior surfaces of the vernier engines, which were gold plated to Specification MIL-G 45204.

A calibration screen for the television cameras was coated with small areas of red, green, blue, and various gray paints, all of which were specially developed inorganic coatings. The vernier engine nozzle exterior was coated with pyrochrome green paint to give high emittance at 2000°F. Active thermal control – the electronic boxes were regulated in temperature by use of a thermal switch of silver-coated Vycor which provided a conductive path to the radiating surfaces. Heating elements were also provided in the boxes to keep them above their allowable minimum temperature. Insulation – electronic compartments were insulated with 75 sheets of aluminized Mylar. The objective was to maintain one compartment between 40 and 125°F and the other between 0 and 125°F.

Syncom 1, 2, and 3. Internal surfaces – black epoxy paint or vapor deposited aluminum.
Electronics packages – silver plated.
Traveling wave tube – finished white, then encapsulted in polyurethane for heat dissipation; silver filled epoxy between electronics packages and bulkheads for better heat conduction.

Telstar 1 and 2. Outer skin – about 60% total area covered with a plasma sprayed aluminum oxide coating. Dow-17 electrodeposited chromium oxide coating on Mg antenna; Parson's black coating on electronic chassis; 750Å silicon monoxide anti-reflection solar cell coating; 1000 Å film of magnesium fluoride on sapphire solar cell covers; aluminized Mylar as insulation separated by fiberglass spacers; plasma jet deposited Al_2O_3 external coating of antenna; Vitavar (polyurethane paint with TiO_2 pigment) internal part of shell and frame; polished electroplated gold film.

Active thermal control device: Aluminum, steel spring, brass bellows, stainless steel piston, copper ring, Mg shutter activated by expansion of pentane; aluminum oxide coating on parts not covered by solar cells.

Telstar. Drifilm 88 – General Electric Co.; Martin hard coat process used on aluminum plates and rods; Iridite used on aluminum parts for corrosion resistance; black epoxy paint (RCA 1985090) – Egyptian Mfg. Co.; black epoxy paint (RCA 201600-1); anodized aluminum, black (RCA 1980039), corrosion resistant finish; antireflective coating on solar cells.

Transit. Equipment section insulation – alternate layers of aluminum foil and fiberglass filter paper. Gold film on inside surface of spherical satellite.

Vanguard. Kel-F instrument support pieces vacuum-plated with gold; silicon monoxide on 5052 aluminum surface, exterior of sphere; inner 5052S aluminum electronics package plated with zinc, copper, cadmium, and silver.

Vela. Insulation for apogee motor – honeycomb core paper phenolic with aluminum foil face sheets.

Thermal control coatings included S13-G white paint, vacuum deposited aluminum, black Cat-a-lac paint, aluminum foil tape (3M type 425), aluminized Mylar tape (3M type 850), gold anodized and gold plated aluminum, and a chemical conversion coating per MIL-C-5541.

Table 17-8

OPTICAL MATERIALS

Alouette. Solar cell covers – 12-mil thick glass.

Anna 1B. Solar cell covers on test panel – 6-mil glass, 20-mil quartz, 30-mil sapphire.

Ariel 2. Solar cell covers – 12-mil optical microslides with UV filter on one surface and antireflecting coating peaked at 0.7 μ on the other surface.

Ariel 3. Solar cell covers – 6-mil microsheet with OCLI interference filter.

ATS. Solar cell covers – 30-mil fused silica with blue filter and antireflective coatings.

Courier 1B. Solar cell covers – 6-mil Corning microsheet.

ERS (Environmental Research Satellite). Solar cell covers – 0.020-in. Corning 7940 quartz with blue filter for satellite power; test solar cells bare and having 20- and 40-mil Corning 7940 covers.

Explorer. Solar cell covers – varied from 0.003-in. glass on Explorer 6 to 0.060-in. Corning 7940 on Explorer 26, and 0.125-in. quartz on Explorer 19.

Explorer 22. Laser reflectors – 360 1-in. corner cube prisms of fused silica.

Explorer 33. Solar cell covers – 0.006-in. Corning 7940 fused silica.

French D1-A. Laser reflectors – fused silica corner cube reflectors.

Gemini. Viewing windows – Vycor panes, unsealed; aluminum silicate glass, sealed; MgF_2 coating on window surfaces.
Antenna windows – Vycor, fused silica.

Lunar Orbiter. Solar cell covers were 6-mil thick Corning 0211 microsheet. The sun sensors were made by Ball Bros. and were similar to those used on OSO. Canopus sensor was by ITT Federal Laboratories. Camera lenses were made of conventional optical glass, but were protected by a quartz window.

Mariner 3 and 4. TV camera telescope – an f/8 Cassegrainian system with beryllium primary and secondary mirrors; primary mirror is 1.62 in. in diameter. Canopus tracker assembly – lenses made of highest grades of synthetic quartz and light flint glass. Edges of lenses were polished and painted with Cat-a-lac black paint to cut down stray light. Assembly incorporates a baffle made of black-anodized aluminum coated with 3M Black Velvet paint and fabricated with sharp knife edges (1-mil radii).

Mariner 4. Magnetometer sensor lenses – crown glass; magnetometer sensor polarizer – polyvinyl alcohol sheet bonded between glass plates; magnetometer sensor 1/4-wave plate – mica sheets between glass.

Table 17-8 (Cont.)

Mercury-Atlas. Viewing windows: Vycor panes, unsealed; aluminum silicate glass, sealed; MgF_2 coating on window surfaces.
Antenna windows – Vycor, fused silica.

Nimbus 1. The horizon scanner of the Nimbus control subsystem contains a filter window design to limit energy transmission to the wavelength band of 13 to 18 μ. The window consists of a plate of germanium coated on both sides with 45 to 50 alternating layers of vapor-deposited zinc sulfide and germanium. Individual filter coating layer thicknesses range between 50 and 1000 Å. The windows are manufactured by the Optical Coatings Laboratory, Inc.
IR sensor housing window – single germanium crystal.
Prism wedge – single crystal germanium, 300 HM-CM.
Sun sensor window – Corning fused silica No. 7940.
Solar cell covers – 6-mil Corning type 7940 silica with UV filter.
Camera lenses – conventional optical glass; protected by cover plates of fused silica.

OGO. Horizon scanners windows – IRTRAN 4 zinc-selenide.
Solar cell covers – coated 6-mil-thick Corning 0211 glass.

Oscar 3. Solar cell covers – 0.020-in. fused silica glass with blue coating.

OSO-1. Solar sensor lenses – made from borosilicate crown glass.
Solar cell covers – 6-mil glass 0211 microsheet.

OSO-2. Solar sensor lenses – cerium glass with coarse sensors further protected by a cerium glass filter.
Solar cell covers – 20-mil Spectrolab quartz cover.

Pegasus 1 and 2. Solar cell covers – 60-mil-thick fused silica with polished edges and antireflection and UV blocking coatings.
Solar sensor – fused quartz block backed by a special pattern of solar cells (manufactured by Adcole Corp.).
Earth sensor – bismuth-antimony thermopile in nitrogen atmosphere behind germanium lens coated with proprietary interference filter.

Pioneer 5. 0.003-in. glass solar covers; 0.49-μ interference filter on solar cell covers to protect cement from UV.

Pioneer 6 and 7. Solar cell covers – 6-mil thick microsheet glass.

Ranger 6 through 9. Sun sensors – cadmium sulfide.
Earth sensors – three end-on photomultiplier tubes.

Relay. Solar cell covers – 0.060-in. thick Corning 7940 fused silica.

Secor. Solar cell covers – 0.060-in. thick Corning 7940 fused silica.

Soviet Spacecraft (Vostok 3 and 4). Windows – heat-resistant glass with protective blinds which are activated mechanically or electrically.

Surveyor. TV cameras incorporated a plane beryllium mirror approximately 4 in. by 6 in. The lenses of the TV camera were ordinary crown glass; however, because of the beryllium mirror, the lenses did not face directly to outer space. Solar cell covers were Optical Coatings Laboratory microsheet in 6-mil thickness.

Syncom 2. Solar cell covers – 6-mil Corning 0211 microsheet.

Syncom 3. Solar cell covers – 12-mil Corning 7940 fused silica quartz.

Telstar. 0.3 gm/cm^2 sapphire solar cell covers.

Tiros. Microsheet glass 0.006-in. on solar cells; 0.800-μ short wavelength cutoff coating on solar cell covers.

Medium resolution scanning radiometer: thermistor bolometer detectors. Various combinations of lenses and filters were used to define the wavelength regions to be observed in each of the five channels. They are as follows:
Channel 1 – germanium lenses coated with ZnS and a multilayer filter incorporating Al_2O_3, germanium, and SiO.
Channel 2 – ZnS-coated germanium lenses, filters of InSb and As_2S_3 glass.
Channel 3 – a barium fluoride lens and sapphire lens, no filters.
Channel 4 – not used.
Channel 5 – one quartz lens and a sapphire lens; filters made by Infra-Red Industries of three types: Type 259, 011, 513; Type 259, 001, 608; and Type ON-20.

Transit. 0.420-μ red-blue filter on p-n silicon solar cells; 0.006-in. microsheet glass solar cell covers.

Vanguard. 1/16-in. thick quartz solar cell covers.

Table 17-9

MATERIALS FOR LUBRICATED SYSTEMS

Alouette. Stainless steel bushings replaced aluminum bushings on certain aluminum shafts in the antenna drive train idler mechanism to prevent binding due to nylon gears running on aluminum shafts.

Apollo. Star-tracker assembly – G-300 grease and F-50 oil; Service Module main engine gimbal actuator – FS 1290, a fluorosilicone fluid FS 1265 with a lithium soap thickener.

Ariel. Escapement mechanism, gear train materials, and lubricants used for gears and bearings not disclosed.

Courier 1B. Five tape recorders – lubricated with diester oils.

Explorer 3. Cosmic ray tape recorder: diester oil – MIL-L-6085A; Winsor Lube – L-245X (a diester oil conforming to MIL-L-6085A); gears operated dry.

Explorers 7 through 26. (not all items on same spacecraft) Aluminum and stainless steel gears, teflon coated; stainless steel ball bearings, unplated or gold-plated; Teflon and brass bushings.

Gemini. Cabin area – silicones, fluorocarbons, and baked dry film lubricants.
Valves and fittings in propulsion system – fluorocarbons and heat-cured dry film lubricants.
Mechanical systems operated in the orbital environment – sodium silicate bonded dry-film lubricant.
Antifriction bearings – G-300 silicone grease or CLD 5940 dry-film lubricant.

Mariner 2. GE-F50 lubrication of ball bearings; Electro film 4396 (phenolic bonded MoS_2 with graphite) as gear lubricant; double shield-440C bearings in sealed container (antenna) drive and Lyman-α telescope mechanism).
Gear materials in antenna drive: Al 2024-T4, 303 stainless steel; beryllium-copper alloy 25; AISI-4340 steel.

Mariner 3 and 4. Solar panel actuator – silicone oil sealed internally; MoS_2 coating externally.
Solar panel hinges – single ball bearing Teflon coated.
Latch mechanisms – MoS_2 coatings.
Temperature control louvers – Teflon coated bushings.
Solar sail deployment pivots – Nylotron bushing.
IR, UV, and TV scanner mechanisms – GE-300 grease and F-50 oil lubricants.

Mariner 4. Planetary scan system bearings – asbestos-filled Teflon; louver seal bearings – glass-filled Teflon; TV camera shutter – Teflon and Nylotron (MoS_2-filled Nylon); scan mechanism gears – aluminum 2024 lubricated with Electrofilm 4396 and mated to stainless steel 303 pinions.

Mercury-Atlas. Environmental control system: greases – low odor silicones; dry film lubricants; fluorinated hydrocarbon lubricants; Kel-F lubricants; MoS_2-bonded coating on heat shield release mechanism.

Gyro Bearings, sliders, and other mechanisms – F-50 oil and G-300 grease.

Nimbus 1. Solar cell paddle bearings – large ball bearings lubricated with G-300 grease.
Slip ring assembly – brushes, 88% silver and 12% MoS_2; slip ring, rhenium plated silver.
Thermal shutters – sintered bronze bushing impregnated with F-50 oil (shaft material is aluminum).
Iris drive motor brushes – Stackpole carbon brush 566 (lithium carbonate).
Radiometer – Windsor Lube L245X (diester base oil, MIL-L-6085A) dispensed from sintered nylon reservoirs surrounding rotating shaft.
Gear motor used to drive solar panel mechanism – lubricated with G-300 grease (F-50 silicone oil in lithium soap base).
Separation ring lubricant – DC-55 silicone grease.
Other applications – DC-4 silicone grease.
Paddle deployment hinge pins – MoS_2.
Tape recorder – BarTemp bearings, gold-plated slip rings.
Solar panel drive mechanism – beryllium-copper alloy output shaft pinion mating with a Micro Mach 416 nitrided gear lubricated with G-300 grease mounted on an aluminum alloy 2014-T4 tubular shaft which was connected to a backlash clutch mechanism and to the solar panels; bearings were 440C stainless steel balls and races with crown retainers with a 25% pack of G-300 grease.

Nimbus 2. AISI 4340 alloy steel hardened to 46 to 50 Rockwell for the output shaft pinion. The pinion mates with a hard anodized 2014-T4 aluminum alloy gear on the tubular aluminum shaft. The external ring gears are now nitrided 135 M nitralloy instead of the Micro Mach 416 previously used. The R4 shaft bearings and the R2 motor bearings are 440 C stainless steel races and balls with paper base phenolic retainers. A 25% pack of G-300 grease is in the bearings and the same lubricant is used for the gears.

OAO. Sun shutter bearings – CBS Laboratories CLD 5940 lubricant (MoS_2-Ag); movable entrance slit – Teflon sheet material used and also some surfaces were gold plated; diffraction grating – Rulon sleeve bearing; stepping motor – BarTemp bearings, one type motor used synthetic sapphire pivot bearing; star tracker – Vac-Kote (Ball Bros. Research Corp.).

OGO. Thermal louvers – sleeve bearings made of 80% Ag and 20% MoS_2 with a shaft made of aluminum coated with Everlube 811 B (sodium silicate bonded MoS_2).
Solar panel orientation devices – gold-plated balls and races burnished with MoS_2.
Wabble drive – MoS_2 impregnated sintered bronze driver gear and gold-plated stainless steel output gear.
Orbital plane experimental package – gold-plated balls and races, MoS_2 plating, and G-300 grease in various applications.
Shaft assembly bearing – Synthane L retainer impregnated with 5% by volume Apiezon K.
Elgiloy springs in boom deployment mechanism – Everlube 811 B.

Table 17-9 (Cont.)

Solar array drive and shaft support bearings:
Balls and races – 440 C CRES, conforming to QQ-S-763, gold plated.
Retainer – 416 CRES, conforming to QQ-S-763, gold plated.
Gold plate – 24-carat gold plating preceded by nickel strike 0.00004-in. thick maximum in conformance with MIL-G-45204, Type 1, Class 1, 0.00008 to 0.00010-in. thick including nickel strike.
MoS_2 burnishing – application of dry, unbonded MoS_2 films.

OSO 1 and 2. Coin silver 90 Ag/10 Cu slip rings, lubricated with Apiezon-C oil vacuum impregnated; stainless steel chain and sprocket drive for spectrometer; MoS_2 lubricant; Teflon idler wheel in contact with chain; sintered bronze bushings on shafts of extended arms; MoS_2 lubricant for bushings.
Main bearing – 440 electric vacuum melted martensitic stainless steel bearing with retainers of linen and cotton reinforced phenolic impregnated with Ball Bros. proprietary lubricant.
Hinge pins – mixture of Apiezon L, SiO_2, and MoS_2.
Slip rings – 90% Ag-10% Cu impregnated with proprietary lubricant.
Brushes – 75% Ag-20% graphite-5% MoS_2 impregnated with proprietary lubricant.

Pegasus 1 and 2. Deployment mechanism – Everlube 811 and Molycote X-15.
Thermal control louvers – Fluorosint bearings.
Hinge pins on wings – not lubricated but contain Teflon bushings.
Deployment mechanism bearings – 52100 and 440C.
Output shaft bearings – Gold-plated 52100 steel races with Rulon C ball retainers and 440 stainless steel.
Gear and pinion shaft radial and thrust bearings – Torrington needle bearing with 440C needles in 1012 steel cups (electroless nickel plated) and lubricated with burnished MoS_2.

Pioneer 5. Octoil S (low vapor pressure oil) for active thermal control blades.

Ranger 1 through 5. GE-F50 lubrication of ball bearings; double shielded 440C bearings in sealed container (antenna drive and Lyman-α telescope mechanism); Electro film 4396 (phenolic bonded MoS_2 with graphite as gear lubricant.
Gear materials in antenna drive: 2024-T4; 303 stainless steel; beryllium-copper alloy 25; AISI-4340 steel; AISI-4130 steel for spur, mitre, worm gears, and pinions; 440C bearings, double shielded with fiberglass reinforced Teflon retainer impregnated with MoS_2 (friction experiment) (Ranger 1 and 2); races in friction experiment were coated with epoxy bonded MoS_2. Inboard motor bearing enclosed in motor housing, output shaft brought through double Teflon O-ring seal (Ranger 1 and 2).

Ranger 6 through 9. (Same as Ranger 1 through 5).
Solar panel actuator – silicone oil, sealed internally; MoS_2 coating externally.
Solar-panel hinges – single ball bearing, silicone grease.
Gamma-ray extension boom – silicone oil, sealed internally.
Lyman-alpha telescope scanner – low-speed stepping motor, MoS_2; high-speed actuator, F-50 silicone oil, sealed.

Latch mechanisms – MoS_2.
Omni-antenna hinge – MoS_2; actuator dash pot used silicone oil, sealed.
High-gain antenna drive – sealed actuator gears, MoS_2; shaft bearing, silicone oil; worm gears, Aero-Shell 7 grease.

Surveyor. All lubricants used on this spacecraft were the dry film type with Microseal, a proprietary material, and LubCo 905, a proprietary inorganic-resin bonded pigmented MoS_2 material.
Bushings and Bearings – Teflon coated.
Engine shutoff assembly – Kel-F 90 (later changed to DuPont PR 240AC).

Telstar 1 and 2. MoS_2 bonded with epoxy (in active thermal control device) to aluminum cylinder and steel piston.

Tiros. Camera shutter – aluminum shutter sliding in channel of graphite-impregnated nylon.
Radiometer – Windsor Lube L245X (diester base oil, MIL-L-6085A) dispensed from sintered nylon reservoirs surrounding rotating shaft.
Chromium-plated aluminum gears and R-2 size ball bearings (on infrared radiometer); anodized aluminum shutter sliding on nylon impregnated with graphite (camera shutter mechanism); Miniature bearing No. S3FCHHP25 (radiometer spindle); hardened stainless steel on 52100 steel (monorail rider on precession dampers); oil-sealed bearings; Barden races – MoS_2 impregnated (constant relay switch); tape recorder gears and motor sealed and oiled.

Transit 4A and 4B. Sleeve bearing of fiberglass reinforced Teflon in phenolic retainer (solar cell hinges); stainless steel journal SAE 302 active thermal control mechanism.

Table 17-10

ADHESIVES

Anna 1B. Epoxy resin for impregnation of glass reinforced honeycomb material for shell.

Apollo. Service Module – Type III HT-424 was used for bonding face sheets to core in outside panels. Other adhesives in Service Module and Command Module were Type I HT-424, FM123-2, and Epon 934. HT-424 tape was used for bonding the ablative heat shield to the substructure on the Command Module.

Ariel. Shell Epon 901 with B-1 hardener to bond aluminum parts to fiberglass.

Ariel 3. Solar cell bonding – I.C.I. Silcoloid 201.
Bond conical top to cylindrical body of spacecraft – Shell Versamid and Araldite 951.

ATS. Attachment of ceramic sleeves to antennas – Saureisen No. 31 ceramic adhesive.
Solar cell covers to cells – Sylgard 182 and 184 (Dow-Corning).

Courier 1B. Bonding solar cells to module skin – Dow-Corning Q-3-0120.
Bonding modules to satellite – Dow-Corning Q-3-0120.
Bonding solar cells covers – Dow-Corning Q-3-0040.

Echo 1 and 2. Bonding Mylar to aluminum in skin laminations – GT-301 adhesive (a modified polyester cement) of thickness 0.3 mil.

Explorer. Bonding of solar cells to substrate – earlier spacecraft used epoxy cements and Sauereisen cement, later ones used RTV 40 (General Electric) or RTV-602. Also, RTV-60 used to bond cell modules to skin on Explorer 29.
Bonding cover glass to solar cells – Sylgard 182.

Explorers 9, 19, 24 (Atmospheric Density Explorers). Bonding gores in construction of balloon – Goodyear Pliobond and GT-301 (made by G. T. Schjeldahl Co.).
Bonding aluminum to Mylar for skin lamination – GT-301.

Explorer 22. Bonding corner cube silica prisms to aluminum mounting bracket – epoxy cement.

Explorer 29. Honeycomb shell structural bonding was done with Epon 828. Solar cell covers bonded to cells with RTV-602. Solar cell modules were bonded to spacecraft skin with RTV-60.

Explorer 33. Bonding battery case to supporting structure – Bisphenol A epoxy;
Laminated solar paddle substrate – FM 1000;
Solar cells to substrate – RTV-40; covers to solar cells – RTV-602.

Gemini. Bonding layers of reentry heat shield and bonding heat shield to titanium substrate – HT-424.

Lunar Orbiter. The solar panel aluminum honeycomb structure was bonded with FM 1000. On the surface of the panel was a dielectric layer of fiberglass reinforced SMP 62-63. A mixture of RTV-580 and RTV-560 was used to fasten the solar cells to the dielectric layer and the solar cell covers were affixed with Sylgard 182.

Mariner 2. RTV-40 for bonding solar cells to fiberglass sheet; Versimid 125 and Epon 828 for bonding electronic components; Solithane 113 with curing agent 300 (conformal coating).

Mariner 3 and 4. 913 Epon used for bonding face sheets to core of solar panels. RTV-60 used to bond dielectric face plate for solar cell insulation. RTV-612 used to bond solar cell covers to cells.

Mariner 4. Cover plate for gimballed "Science" platform – aluminum honeycomb bonded with Metlbond 406 adhesive.

Nimbus 1. Bonding solar cell covers to cells – PD-454.
Camera lens cover glass adhesive – RTV-60 silicone with SS 4004 primer.
Other adhesives – FM-1000; Epon 815, 828; Epibond 123; Eccobond 57C, (Emerson and Cumings); Eastman 910; Dow-Corning A 4000.
Video target mount – RTV-731.
Leadwire tack bonding – RTV-102.
Solar panel honeycomb construction – F 100.

OAO. Electronics mounting honeycomb panels were bonded with epoxy-phenolic. The instrumentation was bonded to the honeycomb panels with silicone rubber RTV-40 with 25% alumina to ensure good thermal contact between the electronic package and the mounting panel.

OGO. FM 100 for bonding phenolic fiberglass face sheet to phenolic fiberglass honeycomb. EC 1469 for bonding 2024 Al alloy face sheets to 3003 Al alloy honeycomb. These laminates used for instrument and electronic module containers. EPDX 74 used to bond solar cell covers to cells. Versimid 140, Epon 6, and Epon 8 used for miscellaneous bonding.

OSO 1. Furane 15E to attach glass covers on solar cells; epoxy cement GE RTV-40 bonding of solar cells to aluminum Bondolite substrate.

OSO 2. Bonding solar cells to substrate – RTV-40; bonding solar cell covers to cells – Spectrolab ES-10; other applications – Silastic 140.

OV 3. Structural bonding – FM 1000; wiring tie-downs – RTV-732.

Pegasus 1 and 2. Laminating Mylar dielectric on capacitive detectors – GTS A-29.
Cementing detector assembly to foam substrate – GTS A-49.
Electrical connectors on detector panels – Pittsburgh Plate Glass Co. M-690.
Diode boards to detector panels – RTV-577.
Foam end plugs in structural tubing – RTV-102.

Table 17-10 (Cont.)

Solar cell cover plates – RTV-602.
Solar cells to substrate – RTV-40.

Pioneer 6 and 7. Solar cells were cemented to their substrate with RTV 602 adhesive and the solar cell covers were cemented to the cells with the same adhesive. The electronic equipment platform was aluminum honeycomb structure bonded with FM 1000 adhesive (Bloomingdale Rubber Co.). The thermal control louvers were assembled and bonded to their actuating pin with Epon 901-B3 (Shell Chemical Co.).

Ranger 1-5. RTV-60 for bonding solar cell elements to Mylar; RTV-60 (cover glass to solar cells); Versimid 125 and Epon 828 (bonding electronic components); Solithane 113 with curing agent 300 (conformal coating).

Ranger 6 through 9. RTV-602 for bonding cover glass to solar cells and RTV-60 for bonding solar cells to substrate; Versimid 125 and Epon 828 for bonding electronic components; also used Armstrong A-2/A epoxy adhesive.

Secor. Solar cell cover bonding – XR 63-489 and XR 63-466 primer
Magnetic despin rods attachment – Scotchweld EC 2216A/B epoxy.

Surveyor. Solar cells were bonded to the solar panel with Minnesota Mining and Manufacturing Co. AF 300, while the solar cell covers were bonded to the cells with Spectrolab ES 10 silicone adhesive. Most structural bonding throughout the spacecraft was done with epoxies, particularly Epiphen 825A; some use was made of Bloomingdale FM 1000. Bonding of the solar panel honeycomb structure was accomplished with Minnesota Mining and Manufacturing Co. AF 300. The thermal switch on the active thermal control system was bonded with GE RTV 11. Bonding of the battery case was done with Epon 815 cured with triethylene tetramine.

Syncom 1 and 2. Solar cells to satellite skin – RTV-731.

Syncom 3. Solar cell covers – LTV 602.
Solar cells to satellite skin – proprietary Hughes adhesive.
Other uses – Bordon Epiphen 825A and a versimide-cyclamen epoxy.

Tiros. Hysol PC 12-006 (modified) epoxy resin; Hysol 1-C-epoxy resin (bonding components to fiberglass boards); FM-97-epoxy – Bloomingdale Rubber Co., bonding of solar cells; Stycast 1095 – Emerson and Cumming, Inc., bonding of electronics; Solithane 113 with CAB-O-SIL bonding of electronics – Thiokol Chemical Corp.; Solithane 113 – Thiokol Chemical Corp.; Hysol 42-38 (conductive cement); Epon 828 Bonding epoxy fiberglass boards to camera assembly – Shell Chemical Corp.; Eccobond 55 bonding epoxy fiberglass boards to camera assembly – Emerson and Cumming, Inc.; Ciba 502 bonding resin; Stycast 2651, securing temperature sensing elements – Emerson and Cuming.

Vela. Side Panels, face sheet to cover bonding – FM 86; solar cell modules to substrate – RTV-571.

Table 17-11

SEALING MATERIALS

Apollo. Penetrations in heat shield of Command Module – gaskets of RTV-560.

Explorer 7. Sonotone glass-to-metal battery seals; silicone rubber gaskets and sides of solar cell covers.

Explorer 12. Epoxy battery seal.

Explorer 17. OFHC copper gaskets are used in the twenty-two instrument ports, and the main shell seal is formed by a 0.05-in. copper gasket.
Mass spectrometer – gold O-rings.
Other seals – glass-to-metal with rubber O-rings as backups.

Gemini. Hatch seals and window seals – silicone rubber.

Mariner 2. Viton A O-rings to seal antenna damper shaft and drive housing cover; butyl rubber O-rings on antenna drive shaft.

Mariner 4. Solar panel damper assembly seals – Teflon. Antenna damper seals – Viton O-rings and Teflon slipper seals.

Mercury. RTV-90 silicone – General Electric Co. (capsule, hatch, and window seals); silicone O-rings.

Nimbus 1. Control penumatic subsystem – Epon 8 filled epoxy, polyester base Loctite; O-rings – butyl rubber.
Cross beam edge member sealant – Stafoam 110.
Other locations in spacecraft – Loctite Sealant Grades A and C, buna-N elastomer, glyptol, RTV silicone rubber, Type IV, mica filled epoxy PRH-103.

OSO 1. Viton A O-rings for sail shaft seal in gas container.

OV3. Window seals – butyl rubber.

Ranger 1–5. Viton A O-rings to seal antenna drive shaft and housing cover; Butyl rubber O-rings on antenna drive shaft.

Surveyor. Viton A was used for O-rings in the programming valve of the gas chromatograph (to be used in future launches). Its oven made use of an all metal K-ring seal which was heavily gold-plated. Most of the other seals used on the spacecraft were also Viton A.

Telstar I and 2. Ceramic seals on battery cells; high alumina ceramic insulator-bonded to a Kovar pin provides hermetic ceramic-to-metal seal on battery cans; Kovar (Fe-Ni-Co alloy); zirconium-silver metal seal for joint between sapphire covers and platinum frame of solar cell covers; Viton O-ring, to seal canister which contained all electronics, was evacuated and back-filled with argon.

Tiros. Bondmaster M648 as a fillet and sealant around solar cells and module boards to stop vibration and fill voids.

Table 17-12

STRUCTURAL MATERIALS – ORGANIC

Alouette. Component mounting platform in electronic packages – glass base epoxy laminate, 1/16-in. thick.
Encapsulant for electronic units – polyurethane foam of density 10 lb/ft^3.
Unspecified uses – Aluminized Mylar, glass fiber paper, commercial brown wrapping paper, Micarta.

Anna 1B. Nylon lacing for supports; fiberglass epoxy honeycomb material for external shells and central support tube, 36-in. diameter sphere.

Apollo. Boost protective cover – upper section of 91LD glass reinforced phenolic HRP honeycomb 0.5-in. thick was bonded to a stainless steel honeycomb substructure with HT-424 adhesive. Lower part of the cover was a flexible layer of Teflon-impregnated glass cloth with a glass-phenolic reinforcing ring at the bottom. A separate hatch cover was also glass-phenolic and a transition ring between the upper and lower parts of the cover was HT-1 (Nomex) cloth. The entire cover was covered with 0.3 in. of cork insulation.
Cabin interior – Teflon and polyvinylidene fluoride have been substituted for nylon wherever possible to cut down fire hazard.
Attachment pads – Beta cloth (glass fiber) tape and polybenzimidazole hooks.
Astronaut couches – Teflon-coated Beta material.

Ariel 1. External skin of the spacecraft – epoxy fiberglass bonded with Epon 828; top dome is 1/16-in. thick, bottom is 1/32-in. thick, and center cylinder is 1/16-in. thick by 23 in. in diameter.
Inertia booms – epoxy bonded fiberglass tubing 30-in. long.
Encapsulants for electronic subsystems – Eccofoam FP.
Harness wire insulation – Teflon.
Nylon cord connecting experiment booms.

Ariel 2. Outer structural shell – filament wound fiberglass.

BIOS. Reentry shield – nylon phenolic with fiberglass liner.

Courier 1B. Equipment shelves – fiberglass reinforced plastic honeycomb, the reinforcement consisting of a continuing length of tubing molded into the shelf.
Outer shell – two hemispheres fabricated of fiberglass plastic honeycomb between two skins of epoxy-impregnated fiberglass. Outer skin is coated with aluminum to function as a ground plane for the antennas.
Encapsulating compounds – RTV-60 silicone rubber, Eccofoam FP of density 2 lb/ft^3.
Wire insulation – Teflon.

Echo 1. 0.0005 aluminized Mylar balloon, 100-ft diameter – G. T. Schjedahl Co.

Echo 2. Main skin of balloon consists of a laminated sandwich construction with 0.35-mil thick Mylar (polyethylene terephthalate) film between two layers of 0.18-mil thick 1080 aluminum.

Inflation was achieved by means of sublimation of 38 lb of pyrazole crystals packed in wax-sealed plastic bags inside the balloon and arranged to be unsealed by heating and inflating the balloon at a slow uniform rate.

ERS (Environmental Research Satellite). Solar cell substrate – 0.007-in. copper-clad fiberglass reinforced epoxy.

Explorer. Electronic boxes and circuit boards have made use of epoxy and nylon combined with fiberglass. Electronic encapsulating materials used have included Eccofoam FP (Emerson and Cuming), Epon 834, and silicone rubber.

Explorer 6. Dacron cord, restraining solar paddles; fiberglass laminate shrouds around explosive bolts.

Explorer 7. Laminated polyester-fiber glass for shell structure of two truncated cones 30-in. in diameter and 30-in. high.

Explorers 9, 19, 24 (Atmospheric Density Explorers). This series of spacecraft were spheres 12 ft in diameter and constructed of a four-layer laminate of two 1/2-mil layers of aluminum and two 1/2-mil layers of Mylar cemented together with GT-301 adhesive. The outside surface was aluminum and the inner Mylar. The balloons were constructed as two hemispheres with a dielectric gap between the halves. On Explorer 9 this gap (~ 1 in.) was of Mylar but on Explorers 19 and 24 it was changed to H-film.

Ten fiberglass stiffeners were equally spaced around the balloon equator and bridging the antenna gap to compensate for the weakness of the dielectric material in buckling.
Ejection bellows – flexible body, Fairprene elastomer; fixed bulkhead, fiberglass; sliding piston, aluminum.

Explorers 12, 14, 15, 26 (Energetic Particles Explorers). Equipment shelf – octagon shaped platform made from nylon honeycomb with facings of 181 glass cloth bonded with Epon 828.

Explorers 18, 21, 28 (IMP). Equipment shelf – platform of nylon honeycomb and fiberglass similar to the EPE satellites.

Explorer 22. Outer shell – nylon honeycomb and fiberglass.

Explorers 13, 16, 23 (Meteoroid Detection Explorers). Mylar strips 5-mil thick were used to insulate the heat-transfer band from the forward shell.

On Explorer 13, the stainless-steel meteoroid sensor assemblies were mounted on silicone rubber. For Explorer 16, the mounting was changed to 1/8-in. thick urethane foam.

Explorer 29. The central backbone of the spacecraft was an 8-in. diameter tube of 181 glass fiber cloth face sheets bonded to nylon phenolic honeycomb core with Epon 828 adhesive. The 24-in. diameter hemisphere was constructed of the same materials.

Explorer 33. Battery case – Bakelite C-11.
Retromotor adapter bracket – Epon 828 – 181 glass cloth composite.

French A-1. Outer shell – glass fiber-reinforced plastic.

Gemini. Reentry heat shield – one layer of Refrasil phenolic honeycomb plus another layer of the same honeycomb filled with DC-325 ablative material. The two layers are bonded together with HT-424 and to a titanium back-up plate with the same adhesive.
Heat shield edge ring – silica-cloth phenolic resin composite.
Circuit boards – epoxy glass laminate coated with epoxy.
Astronaut couches – nylon netting.
Wiring insulation inside crew cabin – Teflon.
Wiring insulation outside crew cabin – irradiated polyolefin.
Encapsulating compound – RTV silicone.

Lunar Orbiter. High-gain antenna was a 36-in. parabolic dish of lightweight plastic honeycomb construction. Bladders used to empty the fuel and oxidizer tanks through pressurization with nitrogen gas were constructed of a composite of aluminum foil and Teflon. The foil was used to cut down gas permeability of the membrane and possible dilution of the fuel or oxidizer. Fastener for the camera lens door was Velcro tape.

Mariner 2. Dacron cloth impregnated carbon filled silicone rubber, reinforced and supported with epoxy fiberglass tubular structure (end of solar panel); 828 epoxy – 181 fiberglass for omni-antenna support structure and high-gain antenna feed support tubes; 828 epoxy – 181 fiberglass cloth for structural support of radiometer reference horns; fiberglass reinforced epoxy honeycomb to support aluminized Mylar thermal control surface; epoxy fiberglass sheet bonded to aluminum Truscor for solar cell mounting.

Potting compounds: Stycast 1090 (modified epoxy); Eccofoam FP; FPH polyurethane foam; PR-1927 (elastomeric); polyurethane and silicone rubber modified RTV60-PR-1930; diallylphthalate molding compound around potted cannon type connection; MIL-P-18177 – Type CEE circuit boards; Teflon insulation on internal wiring; irradiated polyolefin on external wiring.

Mariner 3 and 4. Antenna feed – epoxy fiberglass tubing.
Solar sails – Mylar, aluminized on one side, coated with black dye on the other
Ascent fairing shroud – fiberglass honeycomb construction on Mariner 3 (changed to magnesium on Mariner 4).

Mercury. RTV silicone potting compound.

Nimbus 1. Control box top cover – fiberglass laminate.
Thermal control shutters – 30 layers of 1/4-mil aluminized Mylar.
Wiring insulation – silicone rubber-impregnated braided fiberglass (Mil-I-1805A). Some polyvinyl insulation sleeving was used but in more lately constructed equipment, change has been made to fiberglass. Other low-voltage wiring insulation was irradiated polyethylene.
Target lamp encapsulant – PD-454 (Code L), a transparent epoxy.
High-voltage wiring – silicone rubber insulated (Mil-W-16878, Type FF).
Electronic modules encapsulants – GE formulations MP 49 and MP 50 low-density filled epoxy resins (filler was silica micro-balloons). Also used for circuits carrying less than 200 V was the transparent polyurethane PR-1530 or the non-transparent silicone resin RTV-60.
Insulation of solar cells from structure – epoxy fiberglass cloth.

OAO. The electronic instrumentation was bolted to adhesive bonded aluminum alloy honeycomb panels constructed of 3003 aluminum alloy facing sheets and core.

OGO. Outboard end of short booms – fiberglass reinforced epoxy laminate torque box, rigid support for experiment assembly.
Self-locking nuts – pure nylon or nylon with non-outgassing dye.
Instrument boom insulation – 181 glass cloth reinforced Epon 828 brackets.
Electronic modules; instrument boxes – fiberglass reinforced phenolic honeycomb construction.
Thermal insulation blanket – aluminized Mylar Type W; 10 to 12 layers, ultrasonically bonded.
Electronic cable lacing – Dacron.
Wire insulation – irradiated polyolefin, also some TFE Teflon.
Encapsulants – Solithane 113 polyurethane for conformal coating, silicone RTV-11 and RTV-60 on cable clamps, relays, and switches; Scotchcast epoxy and Stycast 1090 on connectors; Epon 826, TETA cure impregnated with Al for thermal conducting applications.

Oscar 3. Encapsulation material – polyurethane foam.

OSO 1. Silicone rubber potting compounds (encapsulating electronic components; fiberglass reinforced epoxy circuit boards; epoxy fiberglass pressure bottles; epoxy coatings on battery containers.

OSO-1. Circuit board – epoxy glass laminate materials (Mil-P-18177 and Mil-P-13949B).
Wire insulation – Teflon.
Shrinkable tubing – Polyolefin.
Circuit board damper – silicone foam.
Encapsulants – Rigidlock foam to hold tuned coils of diplexer, Epon 828, Armstrong C-7, GERTV-11, GE LTV-502.
Gas bottle (attitude control system) – glass reinforced epoxy.
Lubricant reservoirs – Nylasint.

PAGEOS. Balloon satellite 100 ft in diameter with skin of aluminized Mylar 0.5 mil in thickness covered by 2200 Å of evaporated aluminum; inflated with 10 lb of benzoic acid and 20 lb of anthraquinone.

Pegasus 1. Meteoroid detecting surfaces – the capacitor sandwich has a center insulator of Mylar, laminated from 3 layers of 0 15-mil-thick Mylar. For the 1.5-mil-thick aluminum detector panels, the sandwich is attached to a 1-in.-thick core of Delta-T rigid polyurethane foam. For the 8- and 16-mil panels, the sandwich is cemented to a 0.25-in.-thick layer of soft Scott foam which in turn is cemented to a core of 0.5-in.-thick rigid NOPCO G-304 polyurethane foam. On the other side of the rigid foam an identical arrangement completes the double-sided detector.

Pegasus 1 and 2. Potting compound – PR-1538 urethane.
Isolation mounts – silicone rubber.
Wiring harness insulation – Raychem Corp. Novathene on Pegasus 1 and Raychem Corp. Spec 44 wire insulated with irradiated polyolefin and polyvinylidene fluoride on Pegasus 2.
Wire and cable ties – silicone rubber tape and nylon sta-straps.
Conformal coatings – X-81 epoxy and PR-1538 urethane.
Center section supporting angles – fiberglass.

Pioneer 4. 0.016-in. laminated epoxy-glass cloth formed into a conical section 20-in. high, 9-in. diameter at the base mounted on forward end of titanium alloy fourth-stage motor case.

Pioneer 5. Fiberglass shaft and body of epoxy with filler of Bakelite microballoons on active thermal control unit; tips of solar paddles in rubber sponge, held by prestretched Dacron cord.

Pioneer 6 and 7. Main shell solar panel substrate – face sheets of 143 glass cloth impregnated with epoxy-phenolic, 10-mil thick. Mounting inserts for attaching electronic equipment to support shelf – Epon 6 or Epon 8 filled with quartz microballoons. High-gain antenna boom and experimental and control booms – epoxy-phenolic reinforced with 143 glass cloth. Guys for high-gain antenna – glass fiber cables. Antenna elements – low-density foam dielectric coated with a conductive layer. Insulation between antenna elements – Rexolite; attitude control nozzles – Lexan.

Rangers 1 and 2. 828 epoxy – 181 fiberglass for omni-antenna support structure; high-gain antenna feed support tubes of 828 epoxy – 181 fiberglass; Mylar bonded to Al Truscor with RTV-60 (solar panels).

Rangers 3, 4, and 5. Balsa wood sphere 25-in. in diameter as impact limiter for lunar seismometer; epoxy fiberglass shell 12-in. in diameter with rubber liner inside balsa wood sphere.

Rangers 6 through 9. Supports for high gain antenna feed are four fiberglass tubular struts. Container for hydrazine fuel in the midcourse rocket motor is a rubber bladder. (Fargo Rubber compound FR-6-60-26).
Attitude control system valve seat – Teflon.
Junction connectors – silicone rubber filled in Ranger 7 and above instead of polyurethane.
Circuit boards – G11-FR4 epoxy-fiberglass.
Potting materials – Stycast 1090/11 epoxy, RCA 688 epoxy, and PR-1527 polyurethane.
Lacing cords – nylon for Ranger 6, changed to Dacron for Rangers 7, 8, and 9.
Connector conformal coatings – Solitane 113.
Shrink fit tubing for cables – Thermofil type CRN.
Wire insulation – Rayolin-N and some Teflon.
Cable clamp cushion – silicone rubber.
Electrical insulation between structure and cells in solar panel – laminar sheet of 4-mil-thick epoxy fiberglass.
Fasteners – KEL-F was used to minimize galling and nylon caps were bonded to the back of nuts as a dust cover.
Linings for wire cable clamps – silicone rubber.
Encapsulant – for connector pins, Silastic 881; flexible, epoxy compound Bondmaster 688; rigid, Stycast 1095, an epoxy compound filled with glass microspheres. Rangers 7 through 9 and Mariners 2 and 4 organic structural materials were given a vacuum outgassing treatment prior to application in spacecraft.

Relay 1. Dry-friction damper – polished, phenolic fiberglass rod sliding in a stainless steel tube.

Surveyor. Vernier propulsion system thrust chamber liner – mostly glass-phenolic composite with JTA graphite used for the nozzle throat. The glass-phenolic had a specific gravity of 1.77 and a Barcol hardness of 70. JTA graphite made of 48% carbon, 35% zirconium, 8% boron, and 9% silicon. Hot processing converts this to a mixture of carbon, ZrB_2, and SiC. Parts of the battery case were made of rigid acrylonitrile-butadiene-styrene plastic. Electronic boxes were glass fiber reinforced epoxy laminates. Diallyphthalate was used for electronic connectors. Conformal coatings were a modified epoxy (Epon 828 cross-linked with versamide and menthanediamine). Polyurethane foam in densities from 2 to 10 lb/ft^3 was used in electronics packages for insulation and mechanical support. The Surveyor wiring harness was FEP-A Teflon and wiring insulation was Teflon with a coating of Surok polyimide.

Syncoms 1, 2, and 3. Spacecraft skin – 3-mil glass fabric with aliphatic amine curing epoxy (2 plies aft end, 3 plies forward and, and 1 ply on the cylindrical surface as a face sheet on the aluminum honeycomb.
Electrical terminal boards – copper-clad epoxy laminate with gold or silver plating.
Apogee motor nozzle – Raybestos-Manhattan Refrasil.
Potting in electronic boxes – CPR-23 polyurethane foam.
Conformal coatings on terminal boards – epoxy polyamide.

Syncom 2. Hookup wiring insulation – 6-mil-thick Teflon FEP with a coating of 0.5- to 1-mil modified polyimide resin.

Telstars 1 and 2. Teflon inserts for shielding; Rexolite (polystyrene); Tellite (irradiated polyethylene) as dielectric; Rexolite in connections; irradiated polyethylene boards filled with glass fiber; nylon lacing Dacron fibers; fiberglass spacers; polyurethane foam (encasing assemblies); epoxy glass h-f circuit boards.

Tiros. Epoxy fiberglass boards; Potting compounds: Epon 815, (modified), Epon 828 (A) and Epon 828 (B) – Shell Chemical Corp.; Eccofoam FP and Stycast 1090 – Emerson and Cuming, Inc.; Silastic RTV-881 – Dow Corning Corp.; PR 1201 Q – Products Research Co.; RTV-60 and RTV-40 – General Electric Co.; Hysol PC-12-006.

Low resolution infrared radiometer – Two highly aluminized truncated Mylar cones mounted on a 3-in. diameter, gold-plated, aluminum plate. At the base of each cone is mounted a thermistor detector fastened to the Mylar base by a grid of fibers of low thermal conductivity.

Transit. Fiberglass reinforced epoxy honeycomb material for shell; fiberglass epoxy laminate tubes forming central structure; 181 glass cloth epoxy bonded; nylon lacing supports for aluminum instrument tray.

Vanguard 1. Kel-F instrument support pieces plated with gold, Kel-F spacers; Teflon inserts; Eccofoam FP, potting of batteries and transmitters.

Vanguard 3. Eccofoam potting of electronics and batteries; Spiralloy monofilament wound fiberglass epoxy material for hemispheres; Spiralloy equatorial channel ring; fiberglass cylinder shaft.

Vela. End closures for apogee motor support tube – Epon 828 reinforced with 181 glass cloth.

Alouette 1. The sounding antenna system consists of crossed dipoles, one 150 ft tip to tip, the other 75 ft. The antennas are made of thin flat strips of heat-annealed spring steel, 0.004-in. thick and 4-in. wide, wound tightly on 3-in. long spools. After the satellite was inserted into orbit, the spools unwound with the flat strips curling as they passed through a set of guides to form tubular antennas.

Telemetry antennas were four whip antennas.

Alouette 2. Two sets of dipole antennas, one 75-ft long and the second 240-ft long-Be-Cu alloy strip formed into tubes in orbit.

Anna 1B. Silver paint in logarithmic spiral on outside of shell.

Apollo. High gain antennas – Rene 41 in open cell construction.

Ariel 1 and 2. Thin wall aluminum tubing whip antennas (four) which unfold to 21-3/4 in. long in orbit.

ATS. Beryllium rod, gold and copper-plated.

ERS (Environmental Research Satellite). 0.5-in. wide ribbon measuring tape steel stiffened by concave forming and gold plated, later Mylar coated.

Explorer. Early vehicles of this series used the stainless steel satellite skin as antenna. Some had whip antennas of 6061 aluminum alloy tubing.

Explorers 7 and 8. Four antenna wires, twisted fiberglass core, silver-plated/copper-braided jacket with wall of extruded Teflon.

Explorer 20. Beryllium-copper 2-mil thick forming a tube 1/2-in. in diameter when unfurled.

Explorers 29 and 36. Sprial antenna painted on hemispherical underside of spacecraft with silver-loaded epoxy C-93 (J. G. Motson Co.).

Explorer 33. Solar cell paddle facings – Epon 828 with No. 108 glass cloth laminate.

French D1-A. Four brass tubes 0.2-mm thick.

Mariner 2. Aluminum alloy 5052 screening on Al 2024-T4 angle and strip (high-gain antenna structure).

Mariners 3 and 4. High-gain antennas – aluminum honeycomb with 4-mil aluminum foil facings and honeycomb core of 1/4-in. cells fabricated from 0.7-mil foil.

Mercury. Aluminum alloy 2024-T4.

Nimbus 1. S-band antenna – a fiberglass cone containing on its surface two logarithmic spirals of copper.
Quadraloop antennas – dielectric was Fuorosint Teflon-based material; conductor, a special treatment for magnesium, DOW 23 or MD-678, consisting of a coating of magnesium stannate and tin on the magnesium surface.

OGO. Deployable antennas – tubular spring bronze and inflatable metallized Mylar ring.

Oscar 3. Measuring tape steel with silver plating.

OV3. Silver plated music wire.

Pioneer 4. 0.016-in. laminated epoxy-glass cloth formed into a conical section; cone flashed with Ag, then plated with Au; quarter-wavelength aluminum probe on top of cone.

Rangers 1–5. Aluminum alloy 5052 screening on 2024-T4 angle and strip (high-gain antenna structure).

Ranger 6 through 9. High-gain antenna – a circular dish-shaped structure constructed of fabricated sheet aluminum-alloy (2024) ribs emanating radially from the center and supported at midpoint and the outer diameter by sheet metal rings. The dish surface is covered by a black anodized aluminum alloy (5052) mesh, held in conformation by the radial ribs and the mid and outer rings.

Telstars 1 and 2. Mg belly band antenna.
VHF helix antenna: gold-plated beryllium wire; exterior sprayed with plasma-jet aluminum oxide coating.

Vanguard. 6061-T6 aluminum alloy; 12-in. long tubes, 5/16-in. OD with 0.02-in. wall.

Table 17-14

ELECTRONIC MATERIALS

Alouette. Solar cells – 6480 p-on-n type.
Batteries – nickel-cadmium, hermetically sealed.
Transistors – all silicon type.
Wiring insulation – Teflon.
Heat sink – BeO washers.

Alouette 2. 6580 n-on-p type solar cells, batteries – nickel-cadmium.

Anna 1B. n-on-p silicon solar cells; p-on-n silicon, and gallium arsenide solar cells with various covers on test panel; Ni-Cd batteries charged by solar cells; xenon flash tubes.

Apollo. Batteries in Command Module – six silver oxide-zinc batteries with capacity of 40 A-hr to provide entry, post landing, and pyrotechnic energy; batteries in Service Module – three 40 A-hr batteries.
Wiring insulation – 0.006-in. Teflon.

Ariel 1. Solar cells – silicon p-on-n type.
Wiring insulation – Teflon.
Batteries – Ni-Cd.

Ariel 2. Solar cells – 5376 silicon n-on-p type gridded cells 1 cm by 2 cm qualified to withstand 10^{16} electrons/cm^2 of 1 MeV.
Batteries – Ni-Cd.
Wiring insulation – Teflon.

Ariel 3. Batteries – Ni-Cd.
Solar cells – 10-ohm n-on-p type
Transistors – 2N930 planar npn devices and 2N2412 planar pnp devices.

ATS. Solar cells – 1 × 2 cm silicon n-on-p cells, 10 ohm-cm.
Batteries – Ni-Cd.
Wiring insulation – Teflon with polyimide coating.

BIOS. Batteries – silver-zinc.
Encapsulants – PR 1538 polyurethane and Scotchcast 8, 9, and 10.

Courier 1B. Solar cells – 19,152 Hoffman Type 120 C silicon cells 1 cm by 2 cm, cover 64% of surface; batteries – nickel-cadmium.

Early Bird. Solar cells – n-on-p type, 45-W array.
Batteries – Ni-Cd.

Echo 1. Ni-Cd batteries charged by 70 solar cells to power beacon for tracking.

ERS (Environmental Research Satellite). Solar cells – n-on-p cells, Heliotek.

Explorer. Batteries – Mercury type used on Explorer vehicles 1, 4, 7, 8, and 16; silver-zinc batteries used on Explorers 10 and 17; silver-cadmium type used on Explorers 12, 14, 15, 18, 21, 26 and 28; nickel-cadmium type used on Explorers 6, 7, 11, 13, 16, 22, and 29.

Solar cells – silicon cells of the p-on-n type used on earlier vehicles; later flights made use of n-on-p type for more resistance to space radiation.

Explorer 3. A detailed list of electronic components used is given in Ref. 17-1).

Explorer 6. No. 40 copper wire with iron-nickel alloy core as search-coil magnetometer; silicon solar cells, unshielded as test panel.

Explorer 8. Electric field meter: Servo Tek SA-640A-22 dc motor with modifications, Tachometer: Alnico V, magnet core.

Explorer 13. Enameled copper wire on melamine laminate card (sensors); CdS cells in aluminized Lucite glass covered with Mylar and aluminum.

Explorer 14. CdS scintillation counter.

Explorer 16. Pressurized beryllium (Berylco No. 25) copper cells filled with helium; copper wire on Melamine card (sensor); CdS cells in aluminum glass covered with Mylar and aluminum.

Impact detector: Brass dome, insulator; lead zirconate titanate, quartz transfer disk; plastic positioning ring.

Explorer 23. Solar cells – n-on-p type.
Capacitor type detectors for electron accumulation – sandwich of Mylar layer between copper and stainless steel electrodes.

Explorer 32. Solar cells – 2064, bonded directly to spacecraft shell; batteries – a silver oxide-zinc (Yardney) of 10.5 kW-hr capacity.

Explorer 33. Solar cells – n-on-p gridded cells, 0.0125-in. thick.
Battery – Silver-cadmium.

FR-1A (French). Batteries – silver-cadmium.

Gemini. Vehicles 3, 4, and 6 – silver-zinc batteries; Vehicles 5, 7, and subsequent ones – fuel cell system.
Connectors – cadmium plated (but kept out of line of sight with horizon scanners)

Lunar Orbiter. All wiring insulation was Teflon; electronic encapsulation was done with either Stycast 1090 or a silicone material; conformal coatings were Solithane 113. Spacecraft batteries were Ni-Cd of 12 A-hr capacity. Solar cells (10,856) were the n-on-p type, and yielded about 375 W.

Mariner 3 and 4. Earth sensor detector – S-11 photocathode Dumont photomultiplier tube.
Sun sensor detector – cadmium sulfide.
Solar cells – 28,244 silicon p-on-n cells.
Batteries – silver-zinc with 1200 W-hr rating.
Insulation between solar panel structure and solar cells – epoxy fiberglass sheet.

Mariner 4. Magnetometer detector – lead sulfide; cosmic ray telescope detectors – gold silicon surface barrier detectors; wire and cable insulation – Teflon fluorocarbon.

Mercury. Voice cable insulation – Teflon, electronic connectors – cadmium plated.

Nimbus 1. Solar cells – Approximately 11,000 2 cm by 2 cm silicon cells connected by means of beryllium-copper interconnecting strips.
Batteries – hermetically sealed nickel-cadmium type.
Radiometer detector – lead selenide operating in 3.4- to 4.2-μ range.
Sun sensors – silicon p-on-n cells.

OAO. Batteries – nickel-cadmium.

OGO. Batteries – OGO 1 had nickel-cadmium but OGO 2 and subsequent vehicles used silver-cadmium. Electronic wiring – nonmagnetic Alloy 180 (23% Ni, 77% Cu); wire insulation – irradiated polyolefin; electronics containers – A356 precision-cast aluminum alloy.

Solar cells – 32,256 gridded p-n silicon, 1.9 cm^2, 10.5% efficiency.
Sun sensors – p-on-n silicon cells.

Oscar 3. Solar cells – n-on-p silicon cells.

OSO-1. Solar cells – Hoffman p-on-n silicon cells.
Circuit boards – use gold plating.
Batteries – nickel-cadmium.

OSO-2. Solar cells – Heliotek n-on-p solar cells.
Circuit boards – use gold plating.

OSO. Encapsulating materials – RTV-60; shrinkable tubing – Rayclad Thermofit RNF 100, Type 2 polyolefin; circuit boards were gold plated on OSO 1 and OSO 2 but will not be in future; electrical connectors – diallyphthalate; wire insulation – Teflon; insulating spacers – nylon.

OV3. Wire insulation – polyolefin.

Pegasus 1 and 2. Hookup wiring to detector panels – Methode Plioduct ribbon cable
Solar cells – 1 cm by 2 cm n-on-p silicon cells (Hoffman and Texas Instruments).

Pegasus 1. Batteries – nickel-cadmium.
Earth sensor detector – thermocouples.

Pioneers 6 and 7. Solar cells – 10,368 n-on-p type; battery – silver-zinc; sun sensors – silicon rectifiers; electronic wiring – Alloy 180, 23% Ni-77% Cu (non-magnetic); capacitors – special non-magnetic solid tantalum; electronics containers – A 356 precision-cast aluminum alloy.

Rangers 6 through 9. Batteries – two silver-zinc batteries with capacity of 84 A-hr
Solar cells – p-on-n type silicon cells, 4,896 used on Ranger 7.

Relay. Aluminum wire No. 32 used in attitude control device; nickel-cadmium batteries charged by solar cells; p-n boron doped silicon cells with face grids.

Transistors used: 2N174A, 2N1485, 2N2015, 2N1016B, 2N665, 2N1905, and 2N1405.

Silicon and gallium arsenide solar cells, shielded, and unshielded on a test panel.

Relay 2. Solar cells – n-on-p cells.

Secor. Wiring insulation Teflon; shrink tubing – polyolefin.

Surveyor. Solar cells were Heliotek silicon chip type. An array of 3960 of these cells supplied up to 89 W to the spacecraft. Batteries of the silver-zinc type with the main bank supplying 3800 W-hr capacity and an auxiliary set of nonrechargeable batteries amounted to an additional 800 – 1000 W-hr.

Syncom 1 and 2. Solar cells – p-on-n type, 3,840 in number.
Batteries – nickel-cadmium.

Syncom 3. Solar cells – n-on-p silicon cells of 10 Ω-cm resistivity.
Batteries – Nickel-cadmium.

Telstar. Sealed Ni-Cd batteries; nickel cans with ceramic seals.

Capacitors: Tantalum, ceramic, glass, foil Mylar, glass and quartz tubular trimmers; Ag deposited on Mg for r-f circuits; Mg waveguides.

Insulation: Polyolefin by Raychem, Tellite (irradiated polyethylene), ceramic.

Resistors: Carbon, wire-wound vitreous enamel, metal film pyrolytic carbon.

Transistors: Germanium, silicon alloy-diffused germanium power transistor for switching.

Solar cells: n-p silicon solar cells – Western Electric Co.; titanium-silver contact; silicon monoxide anti-reflection coating; sapphire cover plates; n-p type silicon detector diodes.

Inductors: Nonmagnetic core, nonmagnetic slug, Permalloy dust core toroid, ferrite core.

Transformers: Nonmagnetic core, magnetic core toroid, closed ferrite core, ferrite cup core, laminated magnetic core, magnetic tape core toroid, Permalloy dust core toroid.

Coaxial cables: Copper wire encased in irradiated polyethylene dielectric.

Tiros. Attitude control coil – aluminum wire (250-turn coil) which when energized interacts with Earth's magnetic field to control the attitude of the satellite.

Sealed Ni-Cd batteries – Sonotone Corp.; 9260 boron-doped p-on-n silicon solar cells – International Rectifier Corp.; Teflon electrical insulation on wiring.

Tiros 9. Solar cells – n-on-p type instead of p-on-n type used in previous Tiros.

Transit. p-n silicon solar cells; Ni-Cd batteries (oscillators); ultra stable oscillators in Dewar flasks.

Vanguard 1. Mallory mercury batteries; printed circuits plated with solder; p-on-n silicon solar cells, six groups on spherical surface.

Vela. Encapsulating materials – Scotchcast 8 and 10; connector encapsulating – RTV-60; conformal coatings – polyurethane Solithane 113 with 300 hardener; solar cells – 13,000 p-on-n type with total 90 W output; x-ray and gamma-ray detectors – CsI crystals; neutron detector – polyethylene moderator; electronics containers – A356 precision-cast aluminum alloy.

Alouette. Load bearing – aluminum. The basic structure consists of seven parts. A central load-bearing column or thrust tube supports two payload platforms. A spun aluminum half shell is attached to the periphery of each platform. Finally, a radiation shield is attached to the top of each shell.
Electronic packages – aluminum.
Battery packages – aluminum castings.
Screw fasteners – stainless steel.

Anna 1B. Ti-6Al-4V fasteners; aluminum sheet metal for internal structures; aluminum alloy 2024-T4 for instrument trays.

Apollo. Launch Escape Tower – annealed 6Al-4V titanium alloy tubing; Command Module crew compartment pressure vessel – 2014-T6 face sheets on 5052 aluminum alloy core honeycomb; Command Module outer skin was brazed PH 14-8Mo stainless steel honeycomb. Rings and longerons for load carrying were forged 2014-T6 aluminum alloy. Service Module had radial beams of 7075-T6 aluminum alloy. Skin panels were aluminum honeycomb with 7178-T6 aluminum alloy face panels adhesively bonded to 5052-H39 core. Pressure vessels for fluids in the Command and Service Modules were 6Al-4V titanium alloy except for liquid oxygen service which used Inconel 718 and for liquid hydrogen which used 5Al-2.5 Sn titanium alloy. Propulsion system plumbing – 304L stainless steel tubing with all brazed joints; electrical power system – 6061-T6 aluminum alloy; environmental control system plumbing – 304 stainless steel tubing; fasteners – A286 stainless steel; valve and gear parts – 440C stainless steel
Lunar Excursion Module – descent stage was an eight-sided configuration of 7075 aluminum alloy sheet. Ascent stage and crew compartment was a stiffened cylindrical pressure vessel of preforged, rolled, and stretch-formed 2219 aluminum alloy plate. Landing gear was a tubular framework of 7079 and 7178 aluminum alloys. Both landing pads and energy absorption section of legs were 5052 aluminum alloy honeycomb. Propellant and pressurant tanks were forged and welded 6Al-4V titanium alloy; storage vessel for liquid helium was double-wall tank of 5Al-2.5Sn titanium. Ascent rocket engine nozzle skirt was of columbium-10 hafnium alloy C103.

Ariel 1. 6061-T6 aluminum alloy disk on upper dome assembly; stainless steel fasteners for hinges; aluminum alloy for fasteners of shell; gold-plated aluminum screws; 7075-T6 and 6061-T6 aluminum alloy used for electronic shelf, base, and struts; 7075-T6 aluminum alloy, for solar panel arms; steel spring despin mechanism; high-strength steel screws used to fasten solar panels to hinged spar; stainless steel detents on booms.

Ariel. End flanges for fiberglass midsection of spacecraft – aluminum alloy 6061-T6.
Instrument shelf and base assembly – aluminum alloys 7075-T6 and 6061-T6 plates, bars, and billets.
Paddle arms – 7075-T6 aluminum alloy channel.
Fasteners – gold-plated aluminum machine screws.
Battery case – stainless steel.

Ariel 2. Main structural member – magnesium cylinder.

Ariel 3. Main structure – aluminum alloy sheet, tube, and bar materials.
Pins, shafts, gears – stainless steel.

ATS. Hydrogen peroxide tank – 1060-H-14 aluminum alloy, 740 in.^{3}.
Main structure – 6061 and 2024 aluminum alloys.
Apogee motor case – Ti-6Al-4V alloy.
Gravity gradient booms – 2-mil Be-Cu alloy, silver plated.

BIOS. Main structure – pressure vessel of 6061 aluminum alloy, spun and welded.
Oxygen tank – 20-in. diameter Inconel sphere.
Hydrogen tank – 23-in. diameter titanium sphere.

Courier 1B. Basic frame of the satellite – aluminum alloy tubing assembled in the shape of an octahedron.
Central band to which fiberglass hemispheres are attached – magnesium; this band also carries the four vhf whip antennas.
Transmitter cases – magnesium, hermetically sealed by welding.
Sealed box for recorder-reproducer – aluminum alloy 6061-T6 sheet.

Echo 1. 26.5-in. diameter evacuated magnesium sphere, 24 lb; magnesium sheet, plate, and extrusions; AZ31 hemispherical spun shells; magnesium AZ31 flange, used to contain furled plastic balloon.

ERS (Environmental Research Satellite). Structure – aluminum 6061-T6 sheet and tubing.

ERS 16 and 17. Contacting surfaces in coldwelding experiment – 440C stainless steel, 17-4PH stainless steel, tungsten carbide, 2014-0 aluminum alloy, and OFHC copper in various combinations; spacecraft mostly aluminum alloy (6061) frame and 2014 or 2024 sheet.

Explorers 1, 3, and 4. Stainless steel shells, Explorer 3 used cast magnesium instrument housing.

Explorers 6, 7, 8, 11, and 14. Various aluminum (typically 2014 alloy) shapes used for basic structure.

Explorer 10. Magnesium ZK-60A as structural material, 10-in. diameter drum; aluminum foil between layers of fiberglass, a Faraday shield.

Explorer 12. Aluminum battery case.

Explorers 13, 16, 23. Forward shell of spacecraft – Type 410 stainless steel, 31-mil thick.

Heat-transfer band – aluminum alloy 1100-H14, 0.1-in. thick and 5-in. wide.
Telemetry canisters – aluminum alloy 2024-T4, machined from bar stock.
Telemetry cases – machined from mild steel and inside surfaces silver plated to prevent rusting.
Detector mounting structure – forward and aft rings were machined from AZ31B magnesium alloy; rings were riveted to an aluminum alloy 2024-T3 cylinder of 16-mil thick material.
Meteoroid detectors – stainless steel targets of both 3-mil and 6-mil thickness; gold grid detectors bonded to rear of steel by means of an intermediary layer of 1/2-mil thick Mylar.

Explorer 16 also exposed stainless steel meteoroid targets of thickness 1-mil in addition to the 3-mil and 6-mil ones. Pressurized cells of beryllium-copper were also included in 1-mil, 2-mil, and 5-mil thicknesses.

Explorer 9. Inflation bottle – AISI 4340 steel normalized after welding.
Sliding piston of the ejection bellows – aluminum.

Explorers 17 and 32. These spacecraft are completely sealed spheres of 321 stainless steel 25-mil thick and 35-in. diameter.

Explorers 12, 14, 15, 26. All have the same basic configuration of an octagonal box atop a truncated cone. Four solar cell paddles are attached to the base of the cone and a flux-gate magnetometer stands off from the box on a long tube. Running along the symmetry axis of the spacecraft is the main structural element, a tube of ZK60A-T5 magnesium alloy. Forming the top cover of the box is an aluminum core honeycomb sheet with an outer skin of 3-mil and an inner skin of 8-mil aluminum bonded with Bondmaster M-690 adhesive. The magnetometer support is a tube of 6061-T6 aluminum alloy. This tube was 14-mil except in Explorer 15, in which it was made 22-mil thick in order to provide a better conductive path to the magnetometer which was expected to be more shadowed and thus run colder. The lower surface of the spacecraft, covering the conical portion, is 6061-T6 aluminum alloy 20-mil sheet. Other metallic elements include the separation spring seat and the antenna cover support which are ZK60A magnesium, the damping springs on the solar paddles which are Elgiloy (nonmagnetic), and a beryllium copper actuator for turning on experiments after launch. Helicoil beryllium copper thread inserts were used in magnesium parts. Stainless steel fasteners were used in the smaller sizes and aluminum for larger ones.

Explorers 18, 21, 28, and 32. A ZK60A-T5 magnesium alloy center tube, 7075-T6 aluminum alloy struts, and a bottom shelf and cover of aluminum honeycomb constitute the basic structure. In IMP a rubidium vapor magnetometer is carried on a telescoping tube, one element of which is 40-mil thick aluminum and the other is fiberglass laminate.

Explorer 22. Side and end panels – honeycomb sheet metal sandwiches with inserts for local strengthening and fastener support.
Solar cell panels – corrugated core laminate assembly.

Explorer 29. Main frame was 2024T4 aluminum alloy fabrication spot welded or fastened with A286 steel or 6Al-4V titanium alloy bolts. Sides, top, and part of bottom surfaces were closed with aluminum alloy honeycomb made with 3003 alloy face sheets and 5052 core. Gravity gradient stabilization boom – 2% Be-Cu alloy strip 2-in. wide and 2-mil thick was deployed by the same method used on the Alouette satellite antennas to form a tube 0.5 in. in diameter.

Explorer 33. Retromotor case – 6Al-4V titanium alloy forged in two hemispheres then TIG-welded.

FR-1A (French). Most of structure was of magnesium alloys.

D1-A (French). All materials in spacecraft were divided as follows: aluminum alloys 50%, magnesium alloys 39%, titanium alloys 2%, steel 2%, and rubber and plastic 5%. The structure included 52% honeycomb materials; nuts and bolts were of titanium alloy. The central tube of the structure was magnesium alloy designated XT-1. The support plate was an aluminum alloy designated AU 4 G.

Gemini. Substructure of spacecraft – commercially pure unannealed titanium, Ti8Mn, Ti-5Al-2.5Sn, and Ti-6Al-4V alloys; the pure titanium was used for welded and severely formed parts.
Exterior covering – beryllium and René 41 shingles (beryllium shingles cover the rendezvous and recovery section and the reentry control section).
Crew compartment items, ejection, instrument panels, electrical consoles, and storage compartments – aluminum alloys 2024-T4, 2024-T6, and 7075-T6.
Adapter section skin – magnesium alloy HK31A.
Spacecraft attitude and trajectory control system pressure vessels – Ti-6Al-4V.
Spacecraft attitude and trajectory control system piping – 304L stainless steel.
Retrorocket case – Ti-6Al-4V forging.
Fuel cell tubing – 304 stainless steel.
Tubing other than fuel cell and control system – 5052 aluminum alloy.
Flare tubing nuts – 7075-T73.

LCS (Lincoln Calibration Sphere). This satellite consisted of a hollow aluminum sphere made by first spinning two hemispheres from 6061-0 aluminum alloy, then joining them with 440 aluminum screws. The resulting sphere was then machined to an exact sphere having an optical cross section of 1 m^2.

LES (Lincoln Experimental Satellite). Frame is a tubular aluminum structure in the shape of a rhombocuboctahedron. Tubing is dip-brazed into cast aluminum corner hubs.

Lunar Orbiter. The basic structure of the spacecraft was mostly aluminum alloys. The equipment mounting base plate was made of 7075 aluminum alloy while the base plate ring was of ZK60A magnesium alloy. Aluminum alloy 2219 tubing formed the side structural bracing and the upper structural module, which supports the rocket engine, was made of Mo-0.5Ti-0.8Zr alloy (TZM) while the engine bell was HS 25, also known as L605, a Co-base superalloy. The engine gimbals and actuating rods

were HK31A magnesium alloy. Just back of the rocket nozzle was a heat shield built up of five layers of aluminum sheet plus four layers of 321 stainless steel sheet (on the outside). Each layer was separated by spacers of epoxy-stabilized commercially pure titanium screen made of 10-mil diameter wire. The spacecraft contained two fuel tanks, two oxidizer tanks, and a nitrogen gas tank all constructed of Ti-6Al-4V alloy.

The solar panels were a honeycomb structure using 5052 aluminum alloy core and skin. The photographic system containers, which was pressurized to 1 psi, was made of 6061 aluminum alloy. The camera lens door had a frame of AZ31B magnesium alloy with a foil cover.

All bolts used on the spacecraft were Ti-6Al-4V alloy and nuts were A286 stainless steel. The plumbing system for the fuel, oxidizer, and nitrogen gas systems used 321 or 347 stainless steel tubing with 304 stainless steel fittings.

Other metallic parts of the spacecraft included beryllium used for the frame of the Inertial Reference Unit, Be-Cu windows of 1-mil thickness in the meteoroid detectors (20 detectors with a total area of 3 ft^2), and magnesium alloy with a beryllium nose-cap for the spacecraft ascent fairing shroud supplied by Lockheed with the Agena second-stage vehicle.

Launch protective shroud was beryllium and magnesium alloys.

Mariner 2. Aluminum alloy A-356 coating impregnated with diallylphthalate resin (antenna drive gear and motor housing); 2024-T4 and 6061-T6 aluminum alloy tubing; Mg alloy AZ-31B treated with Dow 7 for electronic component containers; aluminum truscor panels for solar cell arrays; aluminum alloy 2024-T6 sheet metal frame; magnesium alloy ZK-60 forgings for couplings and legs.

Mariner 3 and 4. High-gain antenna – aluminum honeycomb with 4-mil aluminum foil facings and honeycomb core of 1/4-in. cells fabricated from 0.7-mil foil.
Pressure vessels for nitrogen gas for attitude control system – titanium 6Al-4V alloy in the stabilized annealed condition.

Solar panels – truss-core construction with 5-mil 3003 H14 aluminum alloy facings and 3.5-mil 5052L aluminum alloy core.
Top and bottom octagonal plates and longerons in bus – ZK60-T5 magnesium alloy forgings.
Platforms for scientific experiments – 6061-T6 aluminum alloy, fasteners of 6Al-4V titanium and of A286.
Electronic module containers – ZK60 magnesium.
Mast for supporting instruments and waveguide – 6061-T6 aluminum, 25-mil thick, 6-ft long, 6-in. diameter.
Solar sail frame – 6061-T6 aluminum tubing.
Solar sail deployment mechanism – Be-Cu springs.
Support for Be mirrors in television system – Be-Cu alloy.

Mercury. Commercially pure titanium skin (pressure shell); titanium alloy 5Al-2.5Sn (ribs and channels); Ti-Al-V alloy (framing rings around cabin); high-strength aluminum alloys, magnesium and alloy steel (brackets and frames); titanium sidewalls with an aluminum ring (adapter between Mercury and Atlas); normalized 4130 steel (escape tower); aluminum honeycomb core (astronaut couch); glass fiber reinforced plastic faces on aluminum honeycomb core.

Nimbus 1. Sensor ring – ring is a 57-in. toroid, 40-in. diameter, 13-in. tall, and 8-in. deep, fabricated of magnesium alloy AZ31B-H24. The outboard webs in the sensory ring are also magnesium and the V-shaped separators are castings of magnesium alloy ZH62A.
Infrared Sensor housing – ZK60A-T5 magnesium.
Coarse sun sensor structure – aluminum alloys 6061-T6 and 5052-0.
Command antenna – sheet and tubing of aluminum alloys 5052-0, 6061-T6, and 2024-0.
Thermal control shutter – aluminum 2024-T3.
Sensory subsystem structure – magnesium AZ31B-H13 – ZK60A-T5 and aluminum 7075-T6-2024-T3.
Upper torus structure – magnesium AZ31B-H24-ZH62A-T5 and aluminum 2014-0.
Separator casting supporting the solar platform support – magnesium casting ZH62A-T5.
Pneumatic subsystem nitrogen gas storage tank – titanium 6Al-4V.
Solar array panel – aluminum alloy 3003 honeycomb material with 1-mil core and 3-mil skin.
Electronic equipment containers – magnesium ZH62A-T5 castings.
Tubing to attitude control jets – aluminum alloy 6061.

OAO. Structural frame was mostly channel and sheet 2024-T4 aluminum alloy.

OGO. Horizon scanner housing – K1A magnesium alloy; telescope tube – Carpenter 36FM Invar steel; electronic boxes – AZ31B wrought magnesium alloy sheet; kick-off springs – chrome silicon steel wire; solar cell substrates – beryllium. On OGO 2 and subsequent vehicles, boom hinge springs were Be-Cu.

OGO. A double-walled corrugated all aluminum structure was used for the box. On two sides (experiment door), the box wall consists of three sheets (two panels and core) of 0.016-in. 2014-T6 aluminum alloy. On the remaining sides, there are 0.016-in. outer sheets and cores and 0.020-in. inner sheets.
Experiment platform – 2024 aluminum fittings and sheet metal parts.
Hing Joints – standardized Elgiloy latching spring.
Fasteners – A286 in some special nuts, others from aluminum or 6Al-4V titanium alloy.
Solar panels – Substrate 0.04-in. cross-rolled sheet beryllium under solar cell modules; 2024 aluminum alloy channel reinforcing members vary from 0.020 to 0.032 in.

Louvers for thermal control are made of two thin hydroformed sections of 1145-H19 aluminum alloy that are spot-welded together. Louver operated by bimetallic spring.

Main spar of solar panel – extruded square tube of 2024-T42 aluminum alloy
Booms – 6061-T6 aluminum alloy 0.020-in. wall thickness; four short, single-element booms 1.25-in. O.D.; two long, 3-element booms 1.50-in. O.D. The OPEP booms machined in I-beam form from 2024-T351 aluminum alloy.

Oscar 3. Shell – magnesium-lithium alloy.

OSO-1. Panels, cover plates, and other sheet applications – 2024, 5051, 5052, 6061, and 7075 aluminum alloys, mostly in T3 condition.
Castings – 356 aluminum alloys.
Hinge pins – chrome-plated steel.
Fasteners (electronic assemblies) – A286 stainless steel (for lower magnetic permeability).
Solar cell panel substrate – AVCO aluminum honeycomb panel.
Hydraulic system – Type 18-8 stainless steel tubing with type 416 piston and type 302 for balance of system.

OSO-2. Same as OSO-1 except 7075 aluminum alloy replaced by 5051 aluminum alloy.
Pneumatic tubing – silver brazed.
Gas bottle (attitude control system) – titanium alloy 6Al-4V.

OV3. Main structure – 6061-T6 aluminum alloy.

Pegasus 1 and 2. Structural frame, wings – tubing of 6061-T6 aluminum alloy connection fittings of 2024-T4 aluminum alloy.
Center section – extruded 2024-T3 aluminum alloy.
Deployment gear train housing – A356 aluminum casting with zinc chromate coating
Lightly loaded gears – 4340 steel, black oxidized.
Drive – 302 stainless steel.
Heavily loaded gears – 9312 steel, black oxidized.
Meteoroid detecting surfaces – sandwich consisting of an aluminum alloy outer layer in various thicknesses up to 16 mil, a layer of Mylar, and a layer of HC copper (~25μin.) on the back of the Mylar:
1-1/2-mil sheets are 1100-0 aluminum and cover 80 ft^2.
8-mil sheets are 2024-T3 aluminum and cover 160 ft^2.
16-mil sheets are 2024-T3 aluminum and cover 1700 ft^2.
Solar panels – 0.75-in. thick aluminum honeycomb sandwich, 41 in. by 63.5 in.

Pioneer 4. Gold-plated outer surface; titanium alloy (6Al-4V) shell for fourth-stage motor case which was part of satellite (~60-in. long and 8-in. in diameter); counterweights of nichrome wires on despin mechanism reduced speed of spin from 420 to 11 rpm.

Pioneer 6 and 7. Main structure stiffener rings – 2014-T6 aluminum alloy; solar panel substrate honeycomb core – 3003 aluminum alloy; electronic equipment support shelf – honeycomb plate with 5052 aluminum alloy core and 2014-T6 aluminum alloy face sheets; electronic boxes – A356-T6 aluminum alloy precision

castings; thermal control louvers – A1100 aluminum foil; interstage ring support – magnesium alloy; control gas container – 6Al-4V titanium alloy, forged and welded hemispheres.

Ranger 1 to 5. 2024-T4 and 6061-T6 aluminum alloy tubing; magnesium alloy AZ-31B treated with Dow 7 for electronic containers; open sandwich Truscor aluminum solar panels; aluminum alloy 2024-T6 sheet metal frame; magnesium alloy ZK-60 (couplings and legs); aluminum alloy 356 casting impregnated with diallylphthalate resin (antenna drive, gear and motor housing); hexagonal base 10-ft diameter, 17 ft across solar panels, superstructure 10-ft 3 in. high.

Ranger 6 through 9. Solar panel substrates – corrugated 5052-H38 foil core aluminum alloy truss core in the longitudinal direction and by cross bracing in the transverse direction.
TV tower shroud – aluminum sheet 2024-T4 braced with aluminum ring support T-sections and rivets.
Main spacecraft bus – (mostly same as Ranger 1 through 5); however, the support legs which were gold-plated magnesium in Ranger 1 through 6 were changed in Ranger 7 and up to 6061-T6 aluminum alloy.
Gas tank for attitude control subsystem – titanium 6Al-4V alloy.
Plumbing for attitude control subsystem – all welded stainless steel.
Vidicon camera structure – right cone made from 2024 T4 aluminum alloy sheet 1/32-in. thick with T-sections for rings and longerons.
Brackets for base – machined from 2024-T3 bar stock.
Camera support ring – aluminum alloy 356-T6 casting.
Fasteners – A286 steel Longlock screws in Davis nuts.
Containers for power supplies and other electronic circuitry – 2024-T4 aluminum alloy sheet and bar stock.
Wire cable clamps – stainless steel.

Relay 1. Aluminum alloys; Al 2024-T3, sheet and machined elements; aluminum honeycomb, epoxy bonded solar cell panels; satellite shape, octagon 29 in. in diameter at base, 32 in. high.
Dry-friction damper – polished phenolic fiberglass rod sliding in a stainless steel tube.

Secor. Main structure – 6061 aluminum alloy; fasteners-stainless steel; magnetic despin rods – AEM 4750 (50% Ni – 50% Fe)

Soviet Spacecraft (Sputnik 2). Animal cabin and spherical container – AMT's AM sheet aluminum 2-mm thick (~0.080 in.). Surface was polished and subjected to special processing for thermal control purposes.
Sanitary tank – sheet aluminum alloy.

Surveyor. The landing leg framework of the Surveyor spacecraft was 7075-T6 aluminum alloy sheet and tubing riveted and spot-welded; the spacecraft frame was made of 7079-T6 aluminum alloy. No magnesium was used in the vehicle except in the battery case where AZ31B alloy was used. The case of the main retro motor was D-6A steel for the first three vehicles and after that will be 6Al-4V titanium alloy. The nozzle cone for this motor was made of molybdenum-0.5% titanium alloy. The vernier propulsion engine system thrust chamber case was made of titanium 6Al-4V. The solar panels were made of aluminum honeycomb with 2-mil thick titanium face sheets. The planar array antenna was thin gauge aluminum and glass fiber reinforced honeycomb. Aluminum honeycomb was also used in the crushable pads used in the landing system. The landing system hydraulic shock absorbers were made of 6Al-4V titanium alloy. Some fasteners, including the landing structure hinge pins, were A286 steel. Shock absorber tubes were B120VCA titanium alloy (13V, 11Cr, 3Al). Electronic boxes were fabricated of 6061-T6 aluminum alloy sheet and framework. Soil sampler device is constructed of both 7075-T6 and 2024-T4 aluminum alloys. Its scoop shell is 6061-0 aluminum alloy, scoop door is 6Al-4V titanium alloy, and blade is 250 grade maraging steel.

Syncom 1, 2, and 3. Basic structure – cylindrical forging of ZK60 magnesium alloy
Bulkheads – 6061-T6 aluminum alloy.
Electronics packages – 6061 aluminum alloy.
Electronics packages – 6061 aluminum alloy with a zincate pretreatment plated with electroless nickel, then copper flashed and silver plated.
Skin of cylindrical surface – 1/4-in. aluminum honeycomb with glass fabric facing
Apogee motor case – 410 stainless steel.
Attitude control gas tank – titanium-7Al-4Mo on Syncom 1 and 2, and 1060-H12 aluminum alloy on Syncom 3.

Telstars 1 and 2. 52% Ni-Fe alloy tabulation at positive terminal of nickel battery can; for corrosion protection and seal; Mg ZK21A for framework of 34.5-in. diameter sphere; aluminum skin on Mg frame, 18-mil thick beryllium oxide boards; aluminum caps as a shield; beryllium copper tabs on solar cell module; platinum frame for solar cell; aluminum ceramic plate for solar cells; silver for expansion joints of solar panels; Ivar – mica (expansion material); Mg-AZ31B-H24 (end rings of cage); Mg-AZ31B-H24 (machined plate welded on frame); Nilvar, soldered between silver and silicon solar cells; aluminum alloy 6061-T6 for solar cell panels; gold-plated aluminum cover and chasis of h-f circuits; AISI 302 bolts and fasteners.

Tiros. Al2024-T4 (sheet and formed parts); Al 7075-T6 (extrusions); stainless steel and aluminum framework; 18-sided polyhedron covered with solar cells 42-in. diameter, 22.5-in. high drum shaped satellite.

Transit 2B, 2A. 6061 aluminum rings and plates welded to form band between hemispheres; SAE 302 stainless steel fasteners; titanium alloy fasteners; 2024-T4 aluminum alloy for instrument tray.

Transit 4A and 4B. 3003 aluminum honeycomb, epoxy bonded; 2024-T4 aluminum alloy sheet metal (drum and support panels); 2117 aluminum alloy fasteners ; 6061 aluminum alloy for instrument trays; 2024-T4 aluminum alloy sheet metal for framework; drum shaped satellite 43-in. in diameter, 31-in. high.

Vanguard. Aluminum sphere 6.5 in. coated with film of silicon monoxide; 5052 aluminum alloy (hemispheric sections); aluminum antenna cups and caps; inner electronics package made of aluminum alloy 5052S, plated with zinc, copper, cadmium, silver.

Vela. Frame – 6061-T6 aluminum alloy; side panels – honeycomb with 2024-T4 aluminum alloy face sheets and 3003 aluminum alloy core; fasteners – A286 stainless steel or aluminum; apogee motor support tube – HM21A-T8 magnesium alloy.

Equipment platform – aluminum honeycomb sandwich
Injection engine housing – chem milled magnesium sheet.

17.2.4 Ariel

The Ariel satellite program, which so far has seen three vehicles launched, is the first international cooperative space program. The shells of the first two of these vehicles were designed and built by NASA-Goddard; the vehicles carried various scientific experiments which were planned and instrumented by British scientists, and the third Ariel was entirely British designed and built. Ariel 1 measured cosmic rays, solar radiation, and the structure of the ionosphere. Ariel 2 carried instruments to measure ozone concentrations in the upper atmosphere, micrometeoroid impacts, and galactic radio noise. Ariel 3 was intended to supplement and extend the investigations into the atmosphere and ionosphere carried out by the two previous satellites.

After launch on 26 April 1962, Ariel 1 performed successfully all its functions with the exception of a Lyman-alpha ultraviolet detector that was evidently damaged during launch. On 12 July 1962 just 3 days after the Starfish high-altitude nuclear tests of 9 July, Ariel began to malfunction. Periods of nontransmission and transmission only of the unmodulated carrier signal alternated with periods of good transmission of data. It was deduced that the undervoltage cutout system was in operation, pointing to a reduced power output from the solar cells (Ref. 18). The correlation between this performance and radiation damage to the solar cells by Starfish fission electrons trapped in the Earth's radiation belts seems clear. There is reasonable agreement between the observed performance of the power supply on Ariel 1 and the predicted degradation of 20% in output based on characteristics of the radiation and of the p-on-n type solar cells carried by Ariel 1 as protected by 12-mil glass covers (Ref. 18). The two later Ariel spacecraft carried the more radiation resistant n-on-p type cells.

The second Ariel vehicle was redesigned to increase its radiation tolerance and was launched 27 March 1964 into a slightly higher orbit than Ariel 1. These precautions have resulted in a successful performance of the spacecraft mission. The more radiation-resistant n-on-p solar cell complement of Ariel 2 was qualified to withstand the radiation environment expected at its orbital altitude by experiencing a degradation of 0.15 to 0.23% per day in its power output for the first 150 days. The actual performance of the satellite in orbit showed a degradation of 0.14% per day for the first 148 days (Ref. 19). It appears, therefore, that the solar cell array output current decreased due to anticipated causes, i.e., discoloration, radiation damage, and micrometeorite erosion leading to an observed correlation between simulation and space-gathered data that is reasonably close.

17.2.5 ATS

The Application Technology Satellite (ATS) series is intended to yield a wide range of data in the fields of meteorology, communications, navigation, Earth resources management, and spacecraft technology. The first three ATS vehicles were launched on 7 December 1966, 6 April 1967, and 5 November 1967. ATS-1 and ATS-3 achieved their planned synchronous orbits of 22,300 sm altitude but the ATS-2 went into a highly elliptical tumbling orbit instead of its planned 6900 sm orbit, making it useless for its primary mission of stabilizing on the Earth with a gravity gradient control system. Some useful communications, meteorological and scientific data was returned but the spacecraft has since been turned off.

The ATS-1, in its synchronous orbit, has been successful in performing its major planned experiments. It has transmitted high quality color television to stations ranging from North Carolina to Australia including simultaneous transmissions. The spacecraft has been used to make two-way voice communications by means of VHF between aircraft and ground stations for the first time. Its color meteorological and time-lapse motion pictures have made new contributions to the world weather picture. In a Weather Facsimile Experiment, good quality weather facsimile pictures, maps, and charts are being transmitted daily from ATS and received by stations in the United States, Canada, and Pacific areas (Ref. 20).

A solar cell radiation damage experiment was carried aloft by the ATS-1. Early results from this experiment are described in some detail in Chapter 14 of this volume (Ref. 21). After 120 days in orbit had suffered losses of power by amounts ranging from 4.5 to 11% (Ref. 22).

The mission of the ATS-3 has been similar to that of ATS-1. The ATS-3 was positioned initially over the South Atlantic Ocean, but has been moved twice, once farther north during the hurricane season and once over Ecuador to assist in a mapping project. The first full color picture of the Earth's entire disk was sent back by the ATS-3.

An interesting materials experiment carried by ATS-3 is that to measure mirror deterioriation in orbit (Ref. 20). The experiment will carry a number of reflective surfaces including electroformed nickel, beryllium, aluminum, Mylar, and other polymer compositions with reflective coatings (Ref. 23). One surface of each type is exposed to the space environment and another identical protected surface is included as a control. A spacecraft carried reflectometer will periodically measure reflectance from both the shielded and unshielded surfaces.

17.2.6 BIOS

The Biosatellite (BIOS) program after some initial delays and work stretchouts has recently resulted in the launch of two of the planned six vehicles. Both BIOS 1, launched 14 December 1966 and BIOS 2, launched 7 September 1967, were successfully orbited and performed effectively in orbit (Ref. 24). However, the first BIOS was not recovered due to failure of the retrorocket to fire and thus the data was lost. BIOS 2, on the other hand, was recovered after nearly 45 hours of weightless flight carrying 13 different experiments to test the effect of weightlessness and radiation in space on a variety of living organisms.

17.2.7 Courier

Representing one of the earliest of the communications satellites, Courier was launched 4 October 1960 and performed real-time communications tests for 17 days. Its beacon transmitter, powered by a solar-cell power supply, functioned until 16 September 1962 with no degradation in receiving signal strength until it stopped completely on that date, apparently because of loss of solar charging capability or failure of the acquisition transmitter (Ref. 25).

The passive temperature control performed well within design limits and, indeed, within a few degrees of the estimated values. Temperatures after 17 days in orbit were reported in Ref. 1.

17.2.8 Early Bird

The Early Bird satellite, although not the first privately developed spacecraft since that designation must go to Telstar, may truly be characterized as the first commercial satellite since it was the first to have available communications channels for rent. Launched on 6 April 1965 by NASA for the Communications Satellite Corp., Early Bird was successfully maneuvered into a synchronous orbit and, as of 27 June 1965, was approved for commercial operations. One of its earliest jobs was the transmission across the Atlantic of Tiros 10 weather maps at significantly improved resolution and speed.

In general, materials selection for Early Bird may be presumed to have followed rather closely that used for the Syncom series of satellites since several components such as the hydrogen peroxide attitude control system and the Jet Propulsion Laboratory solid-propellant apogee motor are the same as for Syncom. Early Bird carries 6000 n-on-p solar cells to provide a maximum power of 45 W. Since its communications operations will require only about 27 W, the extra margin should contribute to long life for this satellite.

The successors of Early Bird designated Intelsat have been similarly successful. Although the Intelsat 2A did not achieve synchronous orbit, Intelsat 2B was successfully placed over the Pacific Ocean on 11 January 1967. It is also called Pacific 1 satellite. The Intelsat 2C (Atlantic 2) was launched 22 March 1967 and another Pacific Ocean satellite on 27 September 1967.

17.2.9 Echo

The performance of Echo 1 has continued to surprise space scientists. Originally designed for a useful life of about 2 weeks, the satellite, a 100-ft diameter aluminized Mylar balloon, only recently reentered the Earth's atmosphere on 24 May 1968 and provided a great amount of long-term data on solar pressure and air drag effects on its orbit as well as on the effects of the space environment on its construction materials.

The long-term orbital behavior of Echo 1 and its rocket casing was particularly watched because Echo 1 was the first satellite to be appreciably influenced by solar pressure. The rocket casing also in orbit was relatively unaffected and furnished a "control" orbit.

In a study of the light reflected from Echo 1 and reported in Ref. 26, some interesting correlations were drawn between exposure of materials to the space environment and the expected degradation of them. This study showed, by means of visual, photographic, and photoelectric observation of the satellite, that its original property of specular reflectivity had been degraded very little by the effects of space environment. In 1963,

when the data were taken, the satellite was almost 4 yr in orbit and still showed approximately 96% specular reflection. In addition the study showed that the mean radius of curvature of the sphere had remained near the design value, although locally varying, and that its total reflection coefficient was near the value at the time of launch. These results were interpreted to indicate that the space environment had not appreciably removed or modified the reflectivity of the vapor-deposited aluminum coating of Echo 1 and that therefore the space environment does not degrade aluminized Mylar as rapidly as originally postulated. Also the orbital forces such as solar and meteoroid pressure, have not appreciably affected the satellite's overall geometry.

The environment, to which Echo is subjected, is near the maximum of dosage from the trapped radiation belts, since its orbit is roughly circular and at an altitude of 900 to 1000 sm. (Initial parameters were perigee – 941 sm, apogee – 1052 sm, and the inclination to the equator was 47.2 deg.)

The Echo 2 satellite differed from Echo 1 in several important respects. Echo 1 was primarily planned as a passive communications satellite and was deployed simply by blowing up a balloon in space with enough gas to hold it in shape for ~2 weeks during which measurements would be made. A rather unexpected result was that even after the inflation gas had presumable leaked out, the satellite still held its shape reasonably well. For Echo 2, a sufficient quantity of subliming material was included so that the resultant gas would stress the inflated balloon past its yield point and effect rigidization. The primary purpose of the Echo 2 was to serve as a test of this concept of deployment of rigid inflatable structures in space, although it too could and did serve as a passive communications satellite also. Echo 2 was launched on 25 January 1964 and successfully placed into an orbit of 816-sm apogee and 642-sm perigee.

17.2.10 Environmental Research Satellites

Variously known as TRS (Tetrahedral Research Satellite) and ORS (Octahedral Research Satellite) these vehicles, now generically termed ERS (Environmental Research Satellite), have been used to investigate the radiation environment of space, the effect of high vacuum on materials, and other space environmental effects. These small (up to 2-lb weight) satellites are sponsored by the Air Force Rocket Propulsion Laboratory (AFRPL) and have been launched as a subsidiary payload to other Air Force satellites.

The most significant experiment of the earlier versions of the ERS was measurement of solar cell degradation in the space environment. Through appropriate analysis the rate of deterioration can yield a comparison between types of cells, a comparison between the effectiveness of various solar cell cover materials, damage done to various adhesives used to fasten the covers, and conclusions regarding the intensity of space radiation environment. Some of these results as obtained from three ERS spacecraft are reported in Ref. 27.

ERS 13 was launched 17 July 1964 by the same booster which put the second Vela pair of satellites into orbit while ERS 17 similarly accompanied the third Vela launch on 20 July 1965 and ERS 18 was launched together with the fourth Vela launch on 28 August 1967. All these ERS vehicles were instrumented to measure the electron and proton densities in space.

Of more direct interest in the materials field were the satellites ERS 16 launched 10 June 1966 and ERS 15 launched 19 August 1966. These spacecraft carried flight experiments to measure the probability of coldwelding between materials contacting in the space environment. Each satellite was instrumented with four solenoid valves whose seating surfaces consisted of various pairs of the following materials: 440C stainless steel, 17-4PH stainless steel, tungsten carbide, 2014-0 aluminum alloy, and OFHC copper. In addition eight supplemental contactors tested as many other pairs of materials in a configuration simulating electrical contactors in aerospace mechanisms. The valves were periodically opened and closed so as to achieve 50,000 cycles in 6-months operation while the supplemental contactors were arranged to be cycled 400,000 times.

The actual in-flight status of the coldwelding experiments has thus far been only briefly reported (Ref. 28) since the materials data have unfortunately been kept under military classification. Since the subject of coldwelding in the space environment is a matter of general concern to many aerospace designers, this need indicates the desirability of the widest possible dissemination of the data consistent with the demands of national security.

17.2.11 ESSA

The Environmental Survey Satellite (ESSA) series of spacecraft are part of the follow-on to the Tiros weather satellite program called Tiros Operational System (TOS). This consists of a series of Tiros-type satellites of the "wheel" configuration with cameras pointing out through the sides of a cylindrical satellite body which will be launched so that two are always in orbit simultaneously. The first two were launched on 2 February 1966 and 28 February 1966. When one of ESSA 1's cameras failed in July, a successor satellite, ESSA 3 was launched on 2 October 1966. The currently operating pair of satellites are ESSA 5, launched 20 April 1967 and ESSA 6, launched 19 November 1967.

The operational version of Tiros has been engineered to optimize reliability in orbit, incorporating not only the use of materials proved by usage in previous flights, but also such features as completely redundant series of components with a switching system to replace in orbit from ground command any component with its stand-by counterpart (Ref. 29).

17.2.12 Explorer

Satellites carrying the designation of Explorer include a variety of vehicles of diverse shapes and weights and many different missions. In general, the name has been applied to scientific data gathering satellites developed and built by one of the NASA Space Flight Centers and which have as their mission the determination of more information about the space environment.

The first successfully orbited U.S. satellite was Explorer 1 on 31 January 1958; the latest of the series, Explorer 37 was orbited 5 March 1968. Most of the Explorers launched are still in orbit. Tables 17-7 through 17-15 include materials information on these spacecraft.

Explorer 1 was a relatively simple system when compared with more sophisticated satellites and space probes being launched today. The Explorer satellites 1 through 4 were the spent fourth-stage solid-propellant motor case of AISI 410 stainless steel. The electronics for transmitter, telemetry, and scientific instruments were mounted in the forward third of the cylindrical shell. Explorer 1 transmitted data on the first measurements of the trapped (Van Allen) radiation belts until May 1958 (~4 months).

Explorer 6 launched 7 August 1959 was the first USA satellite with erectable solar panels. Its basic structure was two hemispheres of 2014 aluminum alloy fastened together to form a sphere. Inside the satellite the electronic equipment was mounted on an epoxy-fiberglass nylon core honeycomb tray which was attached to the 2014 aluminum tubing internal supporting structure.

Explorers 10 and 12 presented a difficult problem in spacecraft materials selection because of the magnetometers on board. The total contribution of the spacecraft materials to the background magnetic field was kept to a minimum by the use of aluminum and magnesium alloys and glass-reinforced plastic filament-wound structures in their construction.

The more recent members of the Explorer series may be broadly grouped into several categories as follows:

- Meteoroid detection satellites including Explorers 13, 16, and 23
- Atmospheric Density Explorers or small ballon satellites including Explorers 9, 19, and 24
- Atmospheric Structure Explorers or sealed steel sphere satellites including Explorers 17 and 32
- Energetic Particles Explorers including Explorers 12, 14, 15, and 26
- Interplanetary Monitoring Platform (IMP) series, closely related to the EPE vehicles and including Explorers 18, 21, 28, 33, 34, and 35
- Ionospheric and geodetic satellites including ionospheric Explorers 20 and 31, Beacon Explorers 22 and 27 and the GEOS-A and B, Explorers 29 and 36
- The NRL Solar Radiation Explorers including Explorers 30 and 37

Several other satellite programs are closely related to Explorer. The Pegasus meteoroid detector satellites are the successors to Explorers 13, 16, and 23 in purpose and technology. The Canadian Alouette satellites and the British Ariel as well as the Italian San Marco also belong to this tradition.

17.2.12.1 Meteoroid Detection Explorers

This series of Explorer spacecraft includes Explorers 13, 16, and 23. The type meteoroid detectors used in this group of satellites has evolved from the resistance measuring card type through one-shot puncture cans to the more versatile capacitor type detectors which have now been applied to large areas on the Pegasus vehicles.

Explorer 13 was launched 25 August 1961 but due to an error caused by the Scout launch vehicle it achieved a very low perigee and thus remained in orbit only for 2.5 days instead of the designed 1 yr. The spacecraft carried six types of meteoroid detectors. The primary sensors were pressurized cells of beryllium-copper (typically alloy 25). The design of these cells limited detection by the loss of pressurization to only one meteoroid hit per cell. A total of 160 of these cells were carried in thickness of 1-mil, 1.5-mil, 2-mil, 2.5-mil, and 5-mil. Other sensors included two types of resistance detectors, two types of piezoelectric impact detectors, and cadmium-sulfide detectors for very small particles (Ref. 30).

Explorer 16 was launched 16 December 1962 carrying the same complement of meteoroid detectors as did Explorer 13; it stopped transmitting data 22 July 1963 and is still in orbit. The basis of this failure has not been determined; however, the telemetry data indicate that the power supply system was working properly up to the time of failure and that the failure cannot be attributed to the command receivers, the solar cells, the nickel-cadmium batteries, or the transmitters (Ref. 31).

The effect of the space meteoroid environment on the detector materials has been summarized in a series of progress reports on Explorer 16 (Refs. 31 through 34).

Explorer 23, the next of this series of spacecraft, was launched successfully on 6 November 1964. It was similar in configuration to the previous members of the series but with some changes in the meteoroid detectors. This spacecraft carried stainless steel sealed meteoroid-detecting cans instead of the beryllium-copper used on Explorer 16. Laboratory tests have shown that the resistance of both these materials to meteoroid puncture is very nearly the same. The space experience showed that the puncture rate as measured on the two satellites was closely similar to within 95% confidence level (Ref. 35).

The spacecraft also carried two of the capacitor-type detectors. Meteoroid strikes on these capacitor detectors were registered when the particle ionized the material forming the dielectric of the capacitor sheet thus allowing it to discharge and form an electrical pulse in the telemetered signal.

Capacitor detectors are not quickly used up as are the pressurized cell type detectors, but do have the disadvantage that the capacitors tend to accumulate electrons when exposed to high radiation levels and these electrons can cause capacitor shorts and millisecond current pulses.

17.2.12.2 Atmospheric Density Explorers

Satellites of this series were inflatable balloon structures of 12-ft diameter constructed of a four layer laminate of two 1/2-mil layers of vapor-deposited aluminum and two 1/2-mil layers of Mylar cemented together with GT-201 adhesive (Schjeldahl Co.). Use of Mylar for these satellites is based on its successful use in the Echo satellites as well as its low rate of degradation in the space environment as shown by laboratory testing (Ref. 36).

These satellites are constructed as two hemispheres with a dielectric gap between them. On Explorer 9 this gap ($\sim$1 in.) was also of Mylar, but on Explorers 19 and 24 it was changed to H-film because of a discharge phenomena noted in Mylar due to ionizing radiation (Ref. 37).

Explorer 9 was successfully tracked by optical observation to correlate upper atmosphere density with solar activity. It was originally estimated to have a lifetime of $\sim$1 yr but decayed after $\sim$3 yr. The other two small balloon satellites, Explorers 19 and 24, are still in orbit.

A detailed comparison has been made of ground tests and orbital launch results for the Explorers 9 and 19. The two flight tests have demonstrated that, in general, the in-flight operation of the ejection and inflation system was similar to that experienced during environmental tests and that a lightweight delicate structure can be erected in space after withstanding the severe conditions imposed by an orbiting spin-stabilized launch vehicle (Ref. 38).

17.2.12.3 Atmospheric Structure Explorers

Since Explorers of this series were designed to measure the physical parameters and chemistry of the atmosphere prevailing at a few hundred miles altitude, the entire spacecraft were carefully sealed to prevent contamination of the local region by materials evolved from the vehicle. For this reason, not many space environmental effects on materials are expected to be of interest here. The spacecraft was constructed as a sphere of AISI 321 stainless steel sealed with OFHC copper gaskets. The mass spectrometers, vacuum gages, and electrostatic probes of the scientific payload were likewise sealed with copper, gold, or glass-to-metal seals. The power supply for Explorer 17, the first of this series, was a primary battery system inside the sphere; solar cells were not used because of their unknown gas evolution characteristics.

Data on the structure of the atmosphere were successfully telemetered back with no failures in the spacecraft during the 100 days prior to the loss of reception due to the anticipated exhaustion of the battery (Ref. 39).

Explorer 32, launched 25 May 1966, represents the second in this series of Explorer spacecraft. Its structure was almost identical to that of Explorer 17 except that Explorer 32 carried solar cells on its external surface to supplement the power from its internal batteries. Like the earlier vehicle, the spacecraft was completely sealed

so as to contribute no contaminants to the tenuous atmosphere which it was designed to measure. An interesting problem which had to be solved in these completely sealed satellites was the disposal of gases arising inside the vehicle due to operation of the batteries. Explorer 17 carried palladium monoxide as a recombination material to keep its internal pressure down; the Explorer 32 made use of a fuel cell to absorb the hydrogen and/or oxygen which was evolved from the batteries (Ref. 40).

After its first four months in orbit, Explorer 32 has achieved most of its objectives. Its tape recorder malfunctioned after 430 activations, but the real time data capability was unaffected. One experiment, the neutral particle mass spectrometer, had failed after 100 activations thus providing some useful data before failure. All other experiments were still working (Ref. 41).

17.2.12.4 Energetic Particles Explorers

This series includes Explorers 12, 14, 15, and 26, all of which carried instrumentation to measure concentrations, energies, and directions of electrons, protons, and ions in the regions of space between a few hundred and several thousand miles above Earth. These spacecraft also measured magnetic fields and carried solar cell damage experiments.

Explorer 12, launched 15 August 1961, carried p-on-n-type solar cells, both bare and with various thicknesses covers. During the first 3 days in orbit, the bare cells were degraded 50% in power output; no degradation was observed for cells covered with 3-mil or with 20-mil glass covers (Ref. 42). Explorer 14 also carried a solar cell experiment which after about 8 days in orbit showed 70% degradation of unshielded p-on-n cells and 40% degradation of unshielded n-on-p cells. Cells of both types protected by a 3-mil thick glass cover degraded by 10% (Ref. 43).

Explorer 15 was launched 27 October 1962 to investigate the enhanced radiation situation following the Starfish nuclear explosion. Its orbit of 194 sm perigee and 10,760 sm apogee placed the satellite in the heart of the newly created radiation belt. Radiation damage to a component in the electronic system of the satellite caused failure of telemetry after 95 days in orbit (Ref. 29). This deduction is based on simulated environmental tests of electronic components exposed to radiation during which a number of parts that were used in Explorer 15 failed (Ref. 44).

Explorer 26, launched 21 December 1964, also carried a solar-cell experiment the objective of which was to compare solar cells of varying base resistivities to correlate space data with laboratory data which had indicated that cells of higher base resistivity were more resistant to degradation by space radiation. Solar cells of both 1 and 10 Ω-cm were orbited on this spacecraft and they were protected by either 6- or 60-mil thick cover glasses. After the first 500 orbits (about 160 days) degradation in power output was observed as follows (Ref. 45):

Cover	Base Resistivity (Ω-cm)	Power Loss (%)
6-mil glass (Corning 0211)	1	46
	10	30
60-mil quartz (Corning 794D)	1	16
	10	9

These results indicate that the higher base resistivity cells are relatively more resistant both to the high energy particles which penetrate the 60-mil covers and the wider range of energetic particles penetrating the 6-mil covers. Furthermore, use of the higher base resistivity cell provides a significant fraction of the radiation protection afforded by the heavy 60-mil cover glasses but at no cost in weight.

17.2.12.5 Interplanetary Monitoring Platforms

The IMP series of spacecraft are designed to make measurements of cosmic radiation, magnetic fields, and solar wind out to distances of 100,000 to 200,000 sm from Earth. The IMPs are closely related to the EPE spacecraft and share with them the same basic octagonal shape of the main spacecraft body.

The first IMP, Explorer 18, was launched 26 November 1963 and all electronic and mechanical systems in the spacecraft operated in a near perfect condition through the early part of 1964 (Ref. 44), but about June 1964 its signal became too weak to be picked up by NASA tracking stations. However, beginning 17 Sept 1964, the spacecraft again started up again and continued transmitting some useful data to 10 May 1965, 531 days after launch.

The second IMP spacecraft, Explorer 21, was launched successfully on 3 October 1964 but was labeled a mission failure because it did not reach the high apogee orbit planned for it. The spacecraft did return some useful data from the lower orbit attained but, like the IMP 1, developed battery problems. Partly because of the low orbit with its consequent longer shadow periods imposing a strain on the battery and partly due to overheating degradation, the battery failed after 63 days in orbit. After this time the spacecraft operated only during periods of favorable incident sun angles. In all, about 5 months of useful data were recorded. As of mid-1965, the spacecraft was operating intermittently with essentially no useful data being obtained (Ref. 46).

The third vehicle of the IMP series of Explorers, Explorer 28, was successfully launched 29 May 1965 into a planned high apogee orbit, and successfully completed its first year in orbit as planned (Ref. 47). A general heating trend of the spacecraft during this time has been attributed to an increase in absorptivity of the white paint coatings. Problems occurred in three experiments during launch but during its first 13-1/2 months in orbit no detectable failures occurred in any spacecraft instrument including the telemetry, data handling, power, programming, optical aspect, and performance parameter systems.

The fourth IMP or IMP-D spacecraft, launched 1 July 1966 as Explorer 33, was intended to be placed into lunar orbit but failed to reach this objective, going instead into a high Earth orbit of 296,000 sm apogee. Since higher temperatures were expected at the planned orbit of this vehicle, aluminized Mylar insulation was replaced with aluminized H-film (Ref. 48). Recent work at LMSC has established that the TiO_2 pigmented methyl silicone elastomer paint designated Q90-090 (Lockheed Thermatrol 2A-100) may be degraded much more than had been previously thought, due to a newly discovered discrepancy between UV degradation data taken in situ and those measured by conventional means. See Chapter 7. The Explorer 33 was accordingly designed to take account of this degradation in its use of Q90-090. The structure of this spacecraft was essentially the same as the previous IMP's except for a retrorocket motor replacing the rubidium vapor magnetometer at the top of the spacecraft. An insulating blanket of aluminized H-film layers interspersed with alternate layers of glass fiber paper was also added to protect the spacecraft experiments from heat produced from the retrorocket.

Explorer 33 was declared a mission success after passing its sixth month of life and, after ten months in orbit, still had all its systems operational except one radiation measuring experiment and the spacecraft battery (Ref. 49). The battery failed after a little over 5-1/2 months in orbit and it is thought this was due to storage at too high a temperature in the spacecraft, a condition to which silver-cadmium batteries of the type used on Explorer 33 are quite sensitive. Temperatures aboard the spacecraft were higher than predicted, ranging from 0° F to 63° F as opposed to the predicted limits of -52° F to 27° F. These temperatures while high were satisfactory for operation of all parts except the battery. Since failure of its battery, the spacecraft continued to operate on solar cells alone; due to its elongated orbit, eclipse periods are relatively brief.

The next two vehicles in the IMP series, Explorers 34 and 35 were launched on 24 May 1967 and on 19 July 1967, respectively. The Explorer 34 is in an elongated Earth orbit while Explorer 35 was successfully injected into a lunar orbit of the type originally planned for Explorer 33. Both vehicles are measuring interplanetary fields and particles and in addition Explorer 35 is investigating magnetic fields and the behavior of the solar wind in the vicinity of the Moon. Preliminary data (Ref. 50) indicate that the Moon has practically no magnetic field associated with it.

17.2.12.6 Ionospheric and Geodetic Explorers

The Explorer 20 spacecraft is closely related in mission to the Canadian Alouette satellite, since it is designed to probe the ionosphere by radiofrequency pulses reflected back to the satellite. Explorer 20 used a set of fixed frequencies for this purpose whereas Alouette used a continuously variable frequency probe.

Explorers 22 and 27, also called Beacon Explorers, are intended to provide data on the ionosphere by transmitting signals through it to a network of ground stations in 32 countries. A second purpose of these spacecraft was to conduct laser and Doppler-shift geodetic tracking experiments.

To accomplish this purpose, a passive optical laser reflector was mounted on the forward face of the satellite. This reflector was a mosaic built up of forty corner cube prisms of fused silica. A ground-based laser source tracking the satellite transmitted pulses of light to it which were reflected from the corner cube prisms back to a deflector near the source. Laser tracking was first accomplished 11 October 1964 on Explorer 22, two days after its launch on 9 October, although the returned signal was weaker than expected.

The Explorer 29 satellite, also known as the GEOS A for geodetic satellite, was orbited 6 November 1965 with the objectives of contributing to more accurate mapping of the Earth's surface and of measuring its irregular gravitational field. To stabilize the spacecraft pointing toward the Earth, use was first made of weighted cables for initial despinning; high magnetic permeability rods of 50-50 iron-nickel alloy, Allegheny 4750, were used to remove residual spins. Final stabilization in the Earth's gravitational field was accomplished by deploying from the top of the spacecraft a 60-ft long boom of a nominally 2% beryllium-copper alloy strip.

Initially the boom was deployed with the spacecraft facing away from the Earth. The boom was retracted and again deployed with the result that the spacecraft was turned to face Earth. Evidently the boom deployment mechanism worked satisfactorily twice in the space environment (vacuum greater than 10^{-9} Torr) of 692 sm perigee and 1414 sm apogee.

A possible materials selection problem that may have arisen in operation of the optical beacon system aboard the Explorer 29 is reported in Ref. 50. The xenon lamps of the beacon have varied in intensity and have generated noise during lamp flashes. After the spacecraft was orbited and before gravity-gradient capture the beacon lamps may have been exposed to direct sunlight for a period up to 10 hr. During this period, the rays from the Sun were focused on the base that supports the xenon tube rather than on the tube itself because the specified beam shape approximates a hollow cone. This base material, which was epoxy, may have been degraded as an insulator and formed a carbon path between parts of the tube sufficient to cause the observed problems. Reference 51 suggests the replacement of base material by beryllium oxide (BeO).

Explorer 31 satellite was another in the series of ionospheric measuring Explorers and was launched 28 November 1965 along with the Canadian satellite Alouette 2. The spin rate and attitude of this spacecraft, like Explorer 29, was also controlled initially by expendable weighted cables, then by magnetic rods and the deployable gravity gradient boom.

The second or GEOS-B spacecraft was orbited 11 January 1968 as Explorer 36. Its general configuration as well as its massion are similar to the first GEOS, Explorer 29.

17.2.13 French Satellites

Five French satellites have been launched to date, with four of them being orbited by a French-developed booster; France was the third nation to develop its own complete satellite system.

The A-1 satellite launched 23 November 1965 served as little more than a test payload for the French Diamant booster. The spacecraft transmitted fairly poor telemetry signals for only 2 days after launch; its design lifetime was 15 days.

The next French satellite, the FR-1A, was launched 6 December 1965 by a Scout vehicle under a cooperative agreement with NASA. Its mission was to study the ionosphere and specifically its characteristics in transmitting very low frequency radio wave propagation. The FR-1A might be considered functionally as a part of the ionospheric investigations program which has included the Canadian Alouette satellites and the ionospheric Explorers.

The D1 series of satellites began with the D1-A launched 17 February 1966 by a French Diamant booster system. It was a fully operational spacecraft instrumented to return geodetic data including an array of silica reflectors for interrogation by Earth-based laser beams similar to the Beacon Explorers. D1-A also carried a solar cell degradation test panel.

The D1-C, launched 8 February 1967, and the D1-D, launched 15 February 1967, continued in the same tradition as laser reflecting geodetic satellites.

Very little information is available on materials used in the French satellites but what has been released indicates that mostly conventional proven space construction materials have been used (Ref. 52).

17.2.14 Gemini and Mercury

Spacecraft in the current Gemini series and its immediate predecessor, the Mercury program, constitute one class of that rare group of objects recovered from space and available for examination. Thus far, however, little information has been published on results of examination of the materials orbited in these vehicles.

Electrical wiring insulation on the Mercury vehicle was irradiated polyolefin, while the Gemini was wired with Teflon insulated wire. This change was the result of tests in 5-psia O_2 atmosphere in which polyolefin burned vigorously when ignited while Teflon would burn but was self-extinguishing (Ref. 53). The Gemini continues to use polyolefin in areas outside the manned cabin.

The heat shield of the Gemini spacecraft has been tested in the actual space environment and found to perform well. This shield is a composite system consisting of a layer of Refrasil phenolic honeycomb plus another layer of the same honeycomb filled with Dow-Corning DC-325 ablative material. The two layers are bonded with HT-424 adhesive made by Ruberoid Co. and bonded with the same adhesive to a titanium backup plate. An edge ring around the shield is made of silica-cloth phenolic resin. The successful trial in space of this shield was on the GT-2 suborbital unmanned launch of 19 January 1965; no cracks were formed in the material and an even regression of the char line into the shield was noted. Charred material as formed was held in place by the honeycomb (Ref. 54).

One of the areas in which materials environmental testing has been extensively carried out for the Mercury and Gemini programs has been that of screening for toxicity of materials to be used in the manned cabin. Although only indirectly related to the space environment, this aspect of materials selection is obviously of great importance to the success of the spacecraft mission. Certain materials of obvious toxicity are easily spotted and eliminated. Many others have been tested by a simple odor test after material was subjected to simulated environmental conditions of the space capsule.

The Gemini program was brought to a successful close with the completion of the Gemini 12 mission of 15 November 1966 after a 11 November launch. The mission, which included the longest time to date devoted to extravehicular activity, a total of 5 hr and 37 min, went far toward clearing up doubts which had arisen in earlier flights as to man's ability to work in space.

The materials used in the Gemini have changed very little during the successive missions. They are reported in Tables 17-7 through 17-15. One interesting materials problem that now seems solved is the clouding of spacecraft windows which had appeared on several previous missions. This window fogging had earlier been blamed on gases from the launch vehicle engines and/or on dirt and moisture in the air during the boost phase. However, protective covers to shield the windows through powered flight had failed to eliminate the problem. It now appears (Ref. 55) that the prime reason for the problem was the outgassing of the silicone sealer used to seal the window panes in their mountings. As the silicone cured, the gas was emitted and collected on the surface of the windows. A new process of curing the material under vacuum was successful in solving the problem in the Gemini 12.

17.2.15 LES (Lincoln Experimental Satellite)

This spacecraft series, which has so far seen the launch of five spacecraft, is sponsored by the U.S. Air Force to develop and evaluate advanced devices and techniques for military communication satellites. LES-1 was launched 11 February 1965 but, due to the failure of an attached rocket package to operate as planned, did not go into elliptical orbit. The nature of signals received indicate that the satellite with the injection package still attached is tumbling as well as spinning about its axis. The second LES satellite was successfully injected into an elliptical orbit on 6 May 1965. LES-3 and -4, which were launched together on 21 December 1965, were planned for a high circular orbit; but, due to a Titan IIIC transtage malfunction, were placed instead into an elliptical orbit of apogee about 21,000 nm and perigee about 100 nm. The LES-3, which is essentially a UHF beacon, is operating successfully but the operation of LES-4 is expected to be compromised because of the elliptical orbit (Ref. 56).

The fifth satellite of this series, LES-5, was launched on 1 July 1967 as part of a multiple spacecraft launch. Like it predecessors LES-5 is also to conduct experimental UHF communications experiments.

In an allied program two satellites, designated LCS's (Lincoln Calibration Sphere) consisting of hollow aluminum spheres 1/8-in. thick, have been launched. LCS-1 was orbited 6 May 1965 and LCS-2 on 15 October 1965. These spheres were carefully machined to a precision surface of radius 22.232 ± 0.004 rms in. The satellites are intended to provide a high-quality reflecting surface for testing radio and radar systems.

17.2.16 Lunar Orbiter

The first vehicle in a series of five essentially identical Lunar-Orbiter spacecraft was launched on 10 August 1966. After performing a midcourse correction maneuver on 11 August and a de-boost maneuver near the Moon 14 August, the spacecraft was placed into lunar orbit with an apolune of 1159 nm and perilune of 117 nm. Some difficulty was experienced with the performance of the Canopus sensor during flight. However, once the spacecraft was in lunar orbit, it was found that the sensor could be used with no trouble when the spacecraft was in the shadow of the Moon. This suggested that the trouble might have been caused by reflection of sunlight into the sensor from the nearby low-gain antenna boom. In subsequent vehicles this boom was painted black in an attempt to alleviate this difficulty.

Photographs of the Moon's surface were taken from the initial spacecraft orbit with both the medium- and high-resolution cameras, with the results from the high-resolution system being degraded, evidently due to movement of the film during exposure. In spite of this problem the spacecraft was transferred on 21 August to a lower orbit of initial apolune 1148 nm and perilune 36 nm. From perilune altitudes of about 26 to 36 nm the spacecraft took most of its planned pictures and successfully completed the photographic part of its mission on 30 August. Film used in the lunar camera was S0243 (Kodak aerial film) which was selected as a highly radiation resistant film. Data on the radiation experiments and meteoroid detectors were transmitted until mission termination.

During the photographic mission of the Lunar Orbiter, the interior of the spacecraft tended to reach temperatures higher than its design limits of 35 to 100° F. No functional failures followed from this situation because it was possible to turn the spacecraft slightly away from the Sun to allow it to cool down. However, as a remedy the bottom of the equipment base plate on subsequent spacecraft was overcoated with S113G, a coating developed at IIT Research Institute, to keep internal temperatures from getting too high (Refs. 57, 58).

The mission of Lunar Orbiter 1 was terminated by commanding it to crack into the back side of the Moon on 29 October 1966 so that its continued operation would not jeopardize the success of future Orbiter missions. At the time the Lunar Orbiter 1 was commanded to inpact the moon, 79 days, 17 hours had elapsed since launch. This was the longest known period during which a bipropellant propulsion system had been exposed to a deep-space environment before reuse (Ref. 59).

Four more Lunar Orbiter spacecraft were launched approximately every three months with the Lunar Orbiter 5 vehicle, the last of the series, entering lunar orbit on 5 August 1967. This series of highly successful spacecraft transmitted back to Earth a large number of detailed pictures of the Moon's surface to be used in support of the Apollo program and also for scientific study of selenography. On 31 January 1968 the Orbiter 5 was commanded to crash on the Moon, as were all the Lunar Orbiters except Orbiter 4, in order to clear their transmitting frequency for future use by other spacecraft. Lunar Orbiter 4 decayed through natural causes and crashed on the Moon after it went out of contact with Earth control (Ref. 60).

In little more than a year, the orbiting cameras photographed more than 99% of the lunar surface at resolutions 10 times better than those possible with telescopes on Earth. One of the vehicles, Lunar Orbiter 3, flew over the landing site of the Moon-lander Surveyor 1 and made a series of pictures showing a man-made artifact standing on the lunar surface for the first time.

17.2.17 Mariner

The Mariner series of interplanetary spacecraft has so far shown a somewhat better record of success than the closely related Ranger program. Although Mariner 1 had to be destroyed when the guidance of the launch vehicle malfunctioned, Mariner 2 was launched the following month to achieve a spectacular success in its return of scientific data about the planet Venus. Similarly, Mariner 3 failed to achieve its planned orbit, while the closely following Mariner 4 has successfully completes its mission of photographing Mars.

The change in materials made to overcome the problem encountered with Mariner 3 shows an interesting correlation between laboratory and flight data. Mariner 3 apparently failed due to its failure to properly jettison the fiberglass fairing shroud and its consequent inability to deploy solar panels and acquire the Sun and Canopus. A laboratory test of a similar shroud showed that the inner facing of the laminated structure separated under combined stresses of aerodynamic heating and rapid pressure drop, simulating the launch environmental conditions. This delamination is thought to have occurred because the honeycomb cells of the composite structure were unvented (Ref. 61). On the basis of this evidence, the shroud material was changed back to the magnesium shroud previously used and separation occurred as planned on Mariner 4.

Mariner 4 was launched on its Mars encounter mission on 28 November 1964 and successfully carried out its midcourse correction maneuver and the reacquisition of Canopus reference on 5 December. The spacecraft fix on the star Canopus, essential to the operation of Mariner 4 in the later stages of its mission but not in the early part, was temporarily lost on December 7. It has been guessed that a small particle of dust reflected enough sunlight into the Canopus sensor to give a temporary false indication. In an attempt to shake loose any dust particles that might be causing this problem, the camera lens cover was removed by ground command on 11 February 1965 in advance of the normal sequence of removal during Mars encounter.

Mariner passed through both the Gemini and Ursid meteoroid streams on its was to Mars with no damage done to the spacecraft. Leaving Earth, Mariner experienced about one impact of interplanetary dust every 4 days. In the vicinity of the Martian orbit, this increased to about four impacts a day and the number of small-sized particles decreased.

On 14 July 1965 the months-long Mariner 4 mission came to a brilliant conclusion with the successful pass to within 5600 sm of Mars and the acquisition and return to Earth by telemetry of the most detailed pictures of the Martian surface yet obtained. The twenty-one pictures obtained were transmitted back to Earth-based tracking stations twice before Mariner traveled out of radio contact.

On once again coming near Earth in its solar orbit, Mariner was reacquired and responded to a series of commands during the latter part of 1967. However, on 20 December 1967, the spacecraft encountered an unexpected meteoroid shower of a density higher than any so far reported in space between Earth and Mars resulting in ending transmission from the long-lived spacecraft (Ref. 62).

The next spacecraft of this series, Mariner 5, was launched 14 June 1967 on a scientific mission to investigate the magnetic fields, radiation levels, and charged particles and gasses in the upper atmosphere of the planet Venus. It successfully executed a mid-course maneuver on 19 June 1967 and completed its data-gathering flyby within 2480 miles of Venus on 19 October 1967 (Ref. 4).

17.2.18 Nimbus

The Nimbus satellite is a relatively large and complex spacecraft. It represents the next generation of weather satellites following the successful Tiros program. Nimbus is Earth-stabilized in a polar orbit. The first satellite in this program was successfully orbited on 28 August 1964 and transmitted a number of excellent photographs of weather patterns before it ceased operating on 23 September 1964 because the solar panels failed to orient toward the sun with consequent catastrophic discharge of the spacecraft batteries.

The drive mechanism which oriented the solar panels to present the maximum surface to the Sun operated satisfactorily for 21 days, built up friction for 1 to 2 days, and then stalled completely. This behavior was attributed to a bearing failure resulting from degradation of the G-300 grease (F-50 oil in a lithium soap base) because of local high temperature (estimated 250 to 300°F or higher) at the drive motor bearings.

The solution to this problem was to change from the Kearfoot Size 8 gear-head drive motor, two phase, 400 cps, 28 V, 550 rpm, with a 0.2 in.-lb torque used in Nimbus 1 to a Size 11 motor having 0.4 in.-lb torque and similar electrical characteristics for the Nimbus 2 launched 15 May 1966. The heat conduction paths around the motor were changed so that at full load the temperature at the bearing, lubricated with the G-300 grease, would not be above 100 to 160°F.

The data obtained from a design analysis study undertaken at GE (Ref. 63) corroborated the supposition that the Nimbus 1 failed due to overheating of the bearing lubricant in the solar array drive and also indicated that no difficulty should be encountered in the Nimbus 2 because of the same problem. This prognosis was borne out by the successful operation of the Nimbus 2 from launch until 2 September 1966 when a tape recorder for the advanced vidicon camera system stopped recording TV pictures. However, the satellite is still operating as of this writing and transmitting real time weather pictures from the high resolution camera.

The solar panel orientation drive mechanism used in Nimbus 1 had a Berylco 10 (copper-based beryllium alloy) output shaft pinion mating with a Micro Mach 416 (a modified Type 301 austenitic stainless steel) nitrided gear with G-300 grease lubricant mounted on an aluminum alloy 2014-T3 tubular shaft which was connected to a backlash clutch mechanism and to the solar panels. The bearings were AISI 440 C stainless steel balls and races with crown retainers. Tests in vacuum reported in Ref. 4 have shown that lifetime of bearings with crown retainers are less than those with ribbon retainers and considerably less than those with paper base phenolic retainers.

For Nimbus 2 the output shaft pinion was changed to an AISI 4340 alloy steel hardened to 46 to 50 Rockwell C. The pinion mates with a hard anodized 2014-T4 aluminum alloy gear on the tubular aluminum shaft.

The external ring gears are now nitrided nitralloy No. 135, a nitriding-type steel, instead of the Micro Mach 416 previously used. The R4 shaft bearings and the R2 motor bearings are AISI 440 C stainless steel races and balls with paper-base phenolic retainers; a 25% pack of G-300 grease is in the bearings and the same lubricant is used for the gears.

17.2.19 OAO (Orbiting Astronomical Observatory)

The first spacecraft of this series was launched 8 April 1966 into a near circular orbit of ~500-nm altitude. At a weight of 3900 lb, the OAO represents the heaviest and most complex spacecraft yet built for the U.S. scientific series. The launch of OAO 1 was nominal in all parameters, but on its second day in orbit the primary batteries overheated and malfunctioned, rendering the spacecraft inoperative. One possible mechanism advanced to explain this failure is that a power distribution switch acted like a voltage regulator and switched solar cell power away from the battery which failed due to overloading by the entire spacecraft power requirements (Ref. 64).

17.2.20 OGO (Orbiting Geophysical Observatory)

The first OGO spacecraft, launched 4 September 1964, was successfully orbited but failed to deploy all its booms. One of the partially deployed booms obscured the Earth sensor so that the spacecraft could not be Earth-oriented. However, some useful data was initially returned from all twenty experiments, and some experiments still continue to operate 3 years later. On failure of the satellite to orient to the Earth, it was sent into an alternate spin-stabilized mode.

An extensive investigation into the causes for nondeployment of the OGO booms (Ref. 65) concluded that the latch spring on one of the solar array paddles failed to actuate properly and the paddle rebounded to a position where the spring torque was balanced by the electrical harness torque. Insufficient spring torque was also indicated as the cause for partial deployment of one of the two 22-ft booms and one of the four 6-ft booms.

As a result of the OGO 1 experience the following design modifications were made to the OGO 2 spacecraft which was orbited 14 October 1965 into a relatively near Earth polar orbit:

- The horizon scanner and some booms were relocated to assure a clear field of view for the scanner.
- A new type deployment spring was used and a separate boom "kick-off" spring added.
- The omnidirectional antenna was relocated.

The OGO 2 successfully deployed all its twelve appendages in orbit and achieved three axis stabilization. However, during stabilized flight an anomalous response of the infrared horizon scanners to the presence of high-altitude cold clouds in the tropic regions resulted in depletion of attitude control gas during the first 10 days of the mission. Subsequently the satellite went into a spin stabilized mode similar to that of OGO 1 but at a slower spin rate. As was the case with OGO 1, much useful scientific data have been obtained from the OGO 2 experiments up to the time it was turned off on 1 November 1967.

The third vehicle, OGO 3, in this series of spacecraft was launched 7 June 1966 into an eccentric orbit similar to that of OGO 1. This spacecraft avoided both the problems that arose on the earlier vehicles and operated in a fully stabilized mode for 46 days. It is now operating in a secondary spin stabilized mode.

The OGO 4 spacecraft was launched 28 July 1967 into a polar orbit and successfully deployed all its experimental booms and achieved a three axis mode of stabilization despite an unexpected oscillation in a 60-ft boom. The spacecraft carried sufficient control gas to remain stabilized for 50 days, but due to the boom oscillations would have exhausted its supply in about 2 weeks. However, by foregoing automatic operation and taking over control by ground commands its lifetime in the three-axis mode has been extended to more than six months now with more than half the gas supply remaining (Ref. 66). The boom oscillations are believed to be caused by the differential solar heating of the boom; they are not present when the satellite is in eclipse.

The fifth launch in a planned series of six for OGO spacecraft was accomplished 4 March 1968 when OGO 5 was put into an eccentric orbit of 168 sm perigee and 92,078 sm apogee.

The basic structure of the OGO spacecraft has remained unchanged throughout the series except for a few materials changes. The supplementary "kick-off" springs for the booms were constructed of chrome-plated silicon steel wire. The hinge springs have been changed to Be-Cu coil door-spring design 1 in. in diameter and 10-in. long wound from 1/8-in. diameter wire. The silicate bonded MoS_2 lubricant used on the springs in OGO 1 has been eliminated since it was suspected of inhibiting free movement of the springs. The electrical cabling connecting experimental instruments on the booms to telemetry and power supplies in the spacecraft proper were also re-routed around the boom hinges in such a manner that they could not hinder boom deployment. One of the factors that was believed to have contributed to the boom deployment malfunction on OGO 1 was that the hinge springs may have had to operate to manipulate the cable bundles as well as the booms. Thus, an extra deployment load could have been forced upon the springs which they were not designed to handle. For these reasons, the springs were redesigned, their materials changed, and the cable bundles re-routed. Performance of the later OGOs indicates that these changes resulted in a successful solution of the boom deployment problem.

17.2.21 OSO (Orbiting Solar Observatory)

The OSO program has resulted in the successful launch of four satellites designed to measure electromagnetic radiation from the sun in the ultraviolet, x-ray, and γ-ray regions of the spectrum and to study time variations of the emissions. OSO-1 was put into orbit 7 March 1962 and transmitted data until 6 August 1963, being still in orbit but silent; its design lifetime was only from 3 to 6 months.

The OSO spacecraft are designed to spin for stabilization purposes while at the same time keep sensors pointed steadily toward the sun. These requirements make necessary a continuously operating bearing between the stationary and spinning parts of the satellite. On OSO 1 this connection was made through an aluminum alloy shaft supported by AISI 52100 ball bearings with retainers of a reinforced fluorocarbon compound, the bearings being lubricated with a molybdenum disulfide slurry. This bearing was highly successful in operating in the space environment through the unexpectedly long lifetime of the satellite

For the second OSO satellite, launched 3 February 1965, this bearing used a lubricating fluid (Ball Bros, proprietary material) impregnated into a main bearing retainer, which is not sealed from the space environment. This change was made due to manufacturing problems, not as a result of space environmental degradation.

Another change made between OSO-1 and -2 was the replacement of the filament-wound glass fiber reinforced gas bottles of the attitude control system of OSO-1 with titanium alloy 6Al-4V bottles on OSO-2. This change was made because of manufacturing difficulties that developed in the filament-winding for these relatively small pressure vessels.

The most significant experiments carried aboard the first two OSO's from a materials application standpoint were those on thermal control materials stability. Samples of six materials which had been proposed as coatings for spacecraft were flown on OSO 1 along with a reference blackbody and suitable instrumentation to monitor the solar absorptance and infrared emittance of the materials over a long period. These data are reported and compared with laboratory simulation testing in Ref. 67, furnishing an exceedingly valuable example of correlation between flight and simulation data.

The OSO 2 thermal control materials experiment (Ref. 68) included eight coatings to evaluate possible thermal control materials for Apollo spacecraft radiators. Two additional coatings were flown which were the same as investigated during the so-called "round-robin" study of uv radiation of spacecraft thermal control coatings in progress since 1962 (Ref. 69). One of these latter two coatings, titanium dioxide in epoxy, was also the same as flown on the OSO 1, affording a unique opportunity to compare laboratory data with flight data from the two spacecraft.

The OSO 2 was turned off on 6 November 1964 after exceeding its six month life expectancy by 50%, then turned back on for five days on 1 June 1966 to gain some additional engineering data on instrumentation lifetimes.

Launch of a third OSO satellite was attempted on 25 August 1965 but, due to a premature ignition of the third stage, it failed to achieve orbit. A successful orbiting of another vehicle as OSO 3 came on 8 March 1967, and that of OSO 4 on 18 October 1967. The latter two spacecraft are intended to study the sun during its two year increase from minimum to maximum solar activity.

17.2.22 OV (Orbiting Vehicle)

The Orbiting Vehicle series of spacecraft has been developed under Air Force sponsorship by various aerospace contractors to fly as secondary scientific payloads either to accompany military satellite launches or to be orbited as a secondary objective to rocket booster developmental flights. The guidelines for developing these satellites generally require minimum expenditures of time and money. Since the OV's are secondary to the main purpose of each launch on which they are carried, a fairly large number of failures have been recorded because of malfunctions of developmental boosters. However, the successful launches have returned a considerable amount of scientific and engineering information

17.2.23 PAGEOS

The PAGEOS satellite, for Passive Geodetic Satellite, was launched 24 June 1966 into a circular orbit of ~2600 nm altitude to serve as a reflecting beacon to be tracked in making studies of the Earth's shape and gravitational field. Its construction is very simple, being a 100-ft balloon made of 1/2-mil thick Mylar covered with 2200 Å of vapor-deposited aluminum, and represents almost a repeat of the Echo 1 satellite except that PAGEOS did not carry the radio beacon package which Echo did, instead depending entirely on optical tracking. A lifetime of 5 yr has been postulated for the spacecraft.

17.2.24 Pegasus

Successful launches utilizing the Saturn I booster have put into orbit three large meteoroid detection satellites, designated as Pegasus. Launched on 16 February, 25 May, and 30 June, 1965, these three spacecraft are almost identical, their most distinguishing feature being the large "wings" which, when unfolded in orbit, expose more than 2000 ft^2 of detector surface to the near-Earth meteoroid flux.

Results obtained from the Pegasus meteoroid measurements have been of considerable importance in determining our current picture of this space environment. This data is discussed in Chapter 6.

The meteoroid detectors of Pegasus are the capacitor sandwiches first used on Explorer 23 and are described above. The materials of the Pegasus detector panels are listed in Tables 17-12 and 17-15. One problem of these detectors is that the Mylar tends to build up a concentration of electrons which may discharge and cause spurious pulses to be identified as meteoroid hits. Special discriminator circuitry has been built into the system to help differentiate between the two types of pulses. Also ten of the panels are left without their bias voltage of 40 V; any pulses coming from these panels would be immediately recognized as spurious.

The large surface area of the sensory panels of Pegasus is covered with an adaptation of the aluminum and chromium phosphate coating used on Echo 2. The version developed by Fairchild-Hiller Corp for Pegasus is designated MTL-3 and was developed with advice from NASA-Langley scientists. This phosphate coating aims at an α/ϵ of ~ 1.0. Flight results indicate that it has been very successful in controlling temperatures within design limits (Ref. 70). Table 17-16 compares design and actual temperatures in various locations for the three Pegasus spacecraft (Ref. 70).

Table 17-16

RANGE OF PEGASUS TEMPERATURES

Location	Design Range (° F)	Actual Range (° F)
Radiation Detector	-60 to 239	-45 to 117
Batteries	30 to 120	63 to 106
Other Electrical Component	12 to 139	36 to 135
Solar Panels	-110 to 151	-81 to 153
Meteoroid Detector Panels	-159 to 250	-54 to 234

17.2.25 Pioneer

The pioneer series of spacecraft are deep space probes and are divided chronologically into two subseries. The first Pioneers were launched early in the space age, 1958–60. The first four of the Pioneer series were intended to be lunar probes. Pioneer 3 reached an altitude of 63,580 sm and transmitted data on the outer Van Allen radiation belts, but reentered on the same day it was launched. Pioneer 4 passed within 37,300 sm of the moon and is now in solar orbit but silent. Pioneer 4 consisted of the spent fourth-stage solid-propellant motor case of titanium alloy 6Al-4V with a cone of laminated epoxy-fiberglass on the forward end to contain the telemetry, transmitter, power supply, and other electronic instrumentation.

The first of the more recent group of Pioneers, Pioneer 6, was successfully launched 16 December 1965 into a solar orbit somewhat nearer the Sun than that of the Earth while Pioneer 7 was launched 17 August 1966 into a solar orbit of larger diameter than that of the orbit of the Earth. Pioneer 8 was launched 13 December 1967 also into an orbit of larger diameter than the Earth's orbit. At the time of its launching both Pioneers 6 and 7 were still actively returning useful data on fields and particles in interplanetary space, having both outlived their design lifetime of 6 months.

One of the principal objectives in this series of spacecraft was to achieve very low self-generated magnetic fields so as to allow a sensitive measurement of the interplanetary magnetic fields. This objective of a field of 1/2 gamma or less at 80 in. from the center of the spacecraft was achieved by carefully eliminating all magnetic materials from the vehicle (or by compensating for the fields of those materials, such as the traveling wave tube magnets, which could not be dispensed with). For example, no colored epoxy resins were used in the spacecraft so as to avoid magnetic coloring pigments, special nonmagnetic hookup wiring was selected, and sawing of structural plastics was avoided because of contamination with iron from the saw blades.

Another design decision of interest in the Pioneer vehicles was the elimination of battery-assisted operation. Pioneers carry a small battery principally for use during launch but depend solely on solar cell power when in orbit (Ref. 71). Elimination of battery operation was intended to contribute to spacecraft longevity since experience has shown that batteries have often been the first item to fail on long missions.

17.2.26 Ranger

The Ranger spacecraft and the closely related Mariner discussed in Sec. 17.2.17 above were, at the time of their launching, relatively sophisticated systems when compared with the Earth-orbiting satellites which had, up to then, constituted most space research instruments. The necessity for midcourse trajectory correction coupled with relatively long-life requirements for all components constitute stringent limitations on the design of these spacecraft.

Rangers 1 and 2 were intended to be engineering spacecraft to test several functions prior to the Ranger 3 to 5 missions to impact instruments on the lunar surface. Because of second-stage malfunctions, Rangers 1 and 2 did not achieve the highly elliptical orbits intended. Ranger 2 reentered the same day of launch, 18 November 1961. Ranger 1, launched 23 August 1961, achieved a low earth orbit for $\sim$1 week and some data about the operational characteristics of the spacecraft instrumentation were obtained.

The Ranger program has been plagued with perhaps more than its share of failures in the early stages with Rangers 3 through 6 failing to reach their objective of landing instruments on the Moon and/or returning pictures. The Ranger spacecraft 7, 8, and 9 have performed as planned in transmitting high-quality television pictures of the lunar surface.

An extensive design review of the Ranger program was made immediately following the failure of operation of the TV system in Ranger 6. Both design changes and materials changes resulted from this review.

The most likely candidate for the cause of failure of the Ranger 6 television was its premature activation during the first few minutes of flight of the launch vehicle. It was this brief unscheduled operation that is believed to have caused arcing between terminals in the relatively high-pressure atmosphere prevailing at that time. The circuitry was redesigned to prevent such premature operation and in addition all exposed terminals were conformal coated with a layer of Solithane 113 (an isocyanate liquid polymer). Those terminals which had already been coated had thicker coatings installed. These changes followed from correlation with laboratory findings (Ref. 61) that corona discharge occurred at a pressure of 5×10^{-2} Torr with a 5-in. electrode spacing at 2000 V, 60 cps. In a further attack on this problem, junction connectors were filled with silicone rubber to cut down arcing.

17.2.27 Relay

The two successfully launched Relay communications satellites of 13 December 1962 and 21 January 1964 have significantly advanced satellite communications technology. The most interesting materials information from this program is the solar cell degradation data obtained on both Relay 1 and 2. The satellites also measured radiation effects to support future satellite design (Ref. 72). Experiments were continued with the Relay 1 until February 1965 and with Relay 2 until 26 September 1965.

17.2.28 Secor

The Secor satellite is a small Army-sponsored spacecraft used to establish with high accuracy distances between survey points on the ground for the benefit of the Army Map Service. It receives signals from ground stations and rebroadcasts with a given time delay which is used to determine station-to-satellite distances and, finally, station-to-station distances.

One interesting problem that arose during development of Secor was voltage breakdown in a diplexer assembly during thermal-vacuum testing at 300 to 500 volts (Ref. 23). In an effort to eliminate this problem which was resulting in the deposition of a black powder in the cavity, Teflon insulating blocks were first removed with no success. The solution was to remove silver plating on conductors and replace it with gold plating.

17.2.29 Surveyor

The first launch of a Surveyor spacecraft achieved remarkable success in the performance of its objectives. Launched on 30 May 1966, the spacecraft performed a midcourse maneuver of 30 May and touched down on the surface of the Moon with a velocity of approximately 10 ft/sec on 2 June. During its first lunar "day" up to about 14 June, the vehicle had transmitted back to Earth about 10,000 pictures of the Moon's surface and of various parts of the spacecraft itself. During its initial period of picture-taking, temperatures within electronics Compartment A had reached 99° to 116° F and in Compartment B 87° to 94° F. Just before the lunar "night" began Compartment A was at 35° F while Compartment B showed 0° F.

Contrary to general expectation, the spacecraft survived the dark period and was returned to operation on considerable reduced battery power by 6 July and transmitted another 1000 pictures to Earth by the close of its second sunlit period on the Moon. These pictures indicated that one out of the sixty glass radiators which dissipate heat from the electronics had been shattered during the dark period. In addition, the batteries, on being charged after the "night" period showed a severe overheating tendency after reaching about one-third full charge.

The spacecraft had transmitted a total of 11,150 photographs up to 13 July. Signals were again received from the spacecraft on 9 October and an attempt was made to take a few more pictures.

The major result following from the Surveyor flight (Ref. 74) was the discovery that the lunar surface was the consistency of ordinary soil rather than solid rock or deep dust. At least in the vicinity investigated by Surveyor, it appears that the Moon can support landing by the Apollo Lunar Excursion Module.

The Surveyor 2 spacecraft was launched 20 September 1966, but one of the three vernier engines failed to fire, setting the vehicle tumbling, and the probe finally crashed southeast of the crater Copernicus. A similar fate overtook the Surveyor 4 spacecraft launched the following year when communications were lost 2-1/2 minutes before landing.

However, three other Surveyor spacecraft landed successfully on the Moon during 1967 followed by the Surveyor 7 in 1968 to send back a great quantity of information regarding the moon's composition and properties. The successful operation of both the soil mechanics sampler mechanism and the alpha scattering chemical analysis experiment

added much to our knowledge of the Moon. Surveyor 6 became the first vehicle to be launched from the Moon when it was lifted about 14 feet and moved 8 feet away in an experiment to test the effect of the use of rocket motors on dust on the surface. It was found that very little dust was stirred up by this experiment.

17.2.30 Syncom

The first Syncom communications satellite was successfully orbited 14 February 1963 but all contact with the spacecraft was lost within 20 sec of firing of the apogee motor and attempts to re-establish communications were unsuccessful. Optical tracking has indicated that the satellite did go into the nominal 22,000-sm circular synchronous orbit which had been planned; however, the lack of communication made it useless.

Syncom 2 was successfully orbited 26 July 1963 and Syncom 3 on 19 August 1964. Both these vehicles have been used to carry on long distance communications experiments including television of the Tokyo Olympic Games.

17.2.31 Tiros

The Tiros series of weather satellites has included ten launches from 1960 through 1965 and has been highly successful in returning useful data to assist meteorologists in interpreting and predicting weather patterns. The last four Tiros satellites, Tiros 7 launched 19 June 1963, Tiros 8 launched 21 December 1963, Tiros 9 launched 22 January 1965, and Tiros 10 launched 2 July 1965 are still active and transmitting data as of 31 December 1967. The materials used in Tiros are reported in Tables 17-7 through 17-15.

The follow-on to the Tiros program is called the TOS for Tiros Operational System and consists of a series of Tiros-type satellites of the "wheel" configuration (cameras pointing out through the sides of the cylindrical satellite body) called ESSA (see Section 17.2.11.).

17.2.32 Vela

The mission of the Vela satellite program is to detect nuclear explosions at extreme ranges in space. The spacecraft are launched in pairs with the two vehicles of each launch being maneuvered so as to be 180 deg apart while orbiting at about 17 Earth radii altitude (near-circular radii achieved by all Velas launched). Each spacecraft is an icosahedron with eighteen of its twenty sides covered with solar cell panels. The remaining two sides accommodate a central cylinder which houses the apogee motor for circularizing the orbit of each satellite after separation. The basic structure of Vela is mostly aluminum and magnesium alloys. Details of the materials used are given in Tables 17-7 through 17-15.

In order to perform its mission of detection of x-ray, gamma-ray, and neutron emanations from nuclear explosions, the Vela spacecraft are instrumented with appropriate

detectors to measure these radiations as well as with instruments to measure the background radiations of space.

At the present time, a total of eight Vela satellites are in orbit. The satellite's contractually required lifetime is now 18 months instead of the 6 months of the earlier spacecraft (Ref. 75).

17.3 REFERENCES

17.3.1 Cited References

1. C. G. Goetzel, J. B. Rittenhouse, and J. B. Singletary, Space Materials Handbook, ML-TDR-64-40, [AD-640399] [X65-14878], Air Force Materials Laboratory, Wright-Patterson Air Force Base, Ohio, January 1965 [also published in a slightly abridged version by Addison-Wesley Publishing Co., Reading, Mass., 1965]

2. J. B. Rittenhouse and J. B. Singletary, Space Materials Handbook, Supplement 1 to the Second Edition, NASA SP-3025, ML-TDR-64-40, Supp. 1 (AD-629 720), Lockheed Palo Alto Research Laboratory, Palo Alto, Calif, 1966

3. J. B. Rittenhouse and J. B. Singletary, Space Materials Handbook, Supplement 2 to the 2nd Edition, AFML-TR-64-40, Supp. 2, Lockheed Palo Research Laboratory, Palo Alto, Calif., 1968

4. TRW Space Log 7, No. 4, Winter 1967–68

5. Satellite Situation Report., 8, No. 8, Goddard Space Flight Center, Greenbelt, Md., 30 April 1968

6. C. D. Florida, "Alouette's Successors," 131st Annual Meeting, AAAS, Montreal, Canada, 26–31 December 1964

7. R. L. Samuels, "The Extension, Profile, and Stability of Very Long Booms in Spacecraft Experimentation," Record of the International Space Electronics Symposium, 6–4 October 1964, Las Vegas, Nev., Institute of Electrical and Electronics Engineers, 1964

8. I. Paghis, C. A. Franklin, and J. Mar, Alouette I. The First Three Years in Orbit, DRTE-1159 (AD 822 875) (N68-10704), Defense Research Telecommunications Establishment, Ottawa, Canada, April 1967

9. The Environmental Test Program and System Evaluation of the Canadian S-27 (Topside Sounder) Spacecraft, S. A. Mills ed., NASA-TM-X-50 194, [X63-14249] Goddard Space Flight Center, Greenbelt, Md., 30 April 1963

10. G. L. Nelms, et al., "The Alouette 2 Satellite," Can. J. Phys. 44, 1419, 1966

11. C. A. Franklin and M. A. Maclean, The Alouette 2 Topside Ionospheric Sounder, DRTE 1189 (AD 824 215) (N68-12129), Defence Research Telecommunications Establishment, Ottawa, Canada, November 1967

12. S. J. de Amicis, Status Report APL Geodetic Satellite Project (ANNA) April-June 1967, TG 880-5 (AD 826-621), The John Hopkins University, Applied Physics Laboratory, Silver Spring, Maryland, December 1967

13. J. Dassoulas, "Transit ANNA Flight-Test Operations," Astronautics and Aerospace Engineering 1, No. 6, July 1963

14. M. E. Alper, "Space Vehicle Structures – Does Man's Presence Make Any Difference," SAE Paper 660673, Aeronautic & Space Engineering and Manufacturing Meeting, Los Angeles, Calif., 3–7 October 1966

15. K. Mori, A. Takamura, and T. Shimose, "Stress Corrosion Cracking of Ti and Zr in HC1-Methanol Solutions," Corrosion 22, No. 2, February 1966

16. R. L. Johnston, R. E. Johnson, G. M. Ecord, and W. L. Castner, Stress-Corrosion Cracking of Ti-6A1-4V Alloy in Methanol, NASA TN-D-3868, NASA Manned Space Flight Center, Houston, Texas, 1968

17. C. F. Tiffany and J. N. Masters, Investigation of the Flaw Growth Characteristics of 6A1-4V Titanium Used in Apollo Spacecraft Pressure Vessels, NASA CR-65586, The Boeing Company, Seattle, Washington, March 1967

18. M. O. Robins, "The Ariel 1 Satellite Project and Some Scientific Results," 9th Anglo-American Conference American Institute of Aeronautics and Astronautics, Canadian Aeronautics and Space Institute, and Royal Aeronautical Society, Cambridge, Mass., 16–18 October and Montreal, 21–24 October 1963

19. Ariel II Engineering Data Analysis, Phase III, NASA-CR-74494 (N66-23750), Westinghouse Electric Corp., Baltimore, Md., November 1965

20. "Project ATS-C," NASA News Release No. 67-276, 31 October 1967

21. R. C. Waddel, Early Results from the Solar Cell Radiation Damage Experiment on ATS-1, NASA-TM-X55772 (N67-26568), NASA Goddard Space Flight Center, Greenbelt, Md., April 1967

22. R. C. Waddel, ATS-1 Solar Cell Radiation Damage Experiment, First 120 days, NASA-TM-X-55908 (N67-335934), NASA Goddard Space Flight Center, Greenbelt, Md., August 1967

23. "ATS-C Satellite to Carry Device to Measure Mirror Deterioration," Space Tech. Intern. 10, No. 50, April 1967

24. "2nd Biosatellite to Study Biology of Space Flight," NASA News Release No. 67-217, 21 August 1967

25. Courier Satellite: Final Report, WDL-TR-1399 (AD-403881), Philco Corp., Western Development Labs., Palo Alto, Calif., January 1963

26. Richard H. Emmons, Photometric Measurements of Surface Characteristics of Echo I Satellite, NASA-CR-58240: GER-11648 (N64-29572), Goodyear Aerospace Corp., Akron, Ohio, June 1964

27. Final Flight Report, Tetrahedral Research Satellite 1963-14B, 1963-14C, 1963-30B, Vol. I, II, Report 8685-6006-RU-000, TRW Space Technology Laboratories, Redondo Beach, Calif., February 1964

28. J. H. Smith, "AFRPL In-Space Propellant Subsystems Experiments," Research and Technology Briefs 4, No. 10, November 1966

29. N. Sclater, "Weather Satellites Go Operational," Electronics Design, 14, No. 10, pp. 17, 18, 20, and 28, 26 April 1966

30. C. T. D'Aiutolo, The Micrometeoroid Satellite Explorer XIII (1961 Chi), NASA-TN-D-2468), Langley Research Center, Hampton, Va., November 1964

31. E. C. Hastings, Jr., The Explorer XVI Micrometeoroid Satellite. Supplement III, Preliminary Results for the Period May 27, 1963 Through July 22, 1963, NASA-TM-X-949 (N64-16692), NASA Langley Research Center, Hampton, Va., March 1964

32. E. C. Hastings, Jr., The Explorer XVI Micrometeoroid Satellite – Description and Preliminary Results for the Period December 16, 1962 Through January 13, 1963, NASA-TM-X-810, NASA Langley Research Center, Hampton, Va., 1963

33. E. C. Hastings, Jr., The Explorer XVI Micrometeoroid Satellite, Supplement II, Preliminary Results for the Period March 3, 1963 Through May 26, 1963, NASA-TM-X-899 (N63-20334), NASA Research Center, Hampton, Va., September 1963

34. E. H. Davison and P. C. Winslow, Jr., Micrometeoroid Satellite (Explorer XVI) Stainless-Steel Penetration Rate Experiment, NASA-TN-D-2445 (N64-27204), NASA Lewis Research Center, Cleveland, Ohio, August 1964

35. The Explorer XXIII Micrometeoroid Satellite: Description and Preliminary Results, November 6, 1964 – February 15, 1965, ed. R. L. D'Neal, NASA-TM-X-1123, (N65-31142), NASA Langley Research Center, August 1965

36. C. W. Coffee, Jr., W. E. Bressette, and G. M. Keating, Design of the NASA Lightweight Inflatable Satellites for the Determination of Atmospheric Density at Extreme Altitudes, NASA-TN-D-1243, NASA Langley Research Center, Hampton, Va., April 1962

37. H. L. Price, NASA Langley Research Center, Hampton, Va., personal communication, 20 May 1965

38. C. V. Woerner and C. W. Coffee, Jr., Comparison of Ground Tests and Orbital Launch Results for the Explorer IX and Explorer XIX Satellites, NASA-TN-D-24066 (N64-28233), NASA Langley Research Center, Hampton, Va., September 1964

39. P. C. Donnelly and C. F. Palondati, Silver Zinc Batteries Power Supply for the Atmosphere Structure Satellite Explorer XVII, NASA-TM-X-51150 (N64-10905), NASA Goddard Space Flight Center, Greenbelt, Md., October 1963

40. P. C. Donnelly and C. F. Palondati, Silver Zinc Batteries Power Supply for the Atmosphere Explorer-B Spacecraft (AE-B), NASA-TM-X-55383 (N66-17256), NASA Goddard Space Flight Center, Greenbelt, Md., October 1965

41. W. D. Hoggard, Environmental Test Program for the Atmosphere Explorer-B Spacecraft, Final Report. NASA-TM-X-55626 (N67-13166), NASA Goddard Space Flight Center, Greenbelt, Md., September 1966

42. A. H. Smith, "Power Sources," Space Programs Summary No. 37-17, Vol. IV, pp. 103–115, Jet Propulsion Laboratory, Pasadena, Calif., October 1962

43. TRW Space Log 3, No. 1, p. 28, Spring 1963

44. E. Ehrlich, "NASA Particles and Fields Spacecraft," presented at 1st Annual Meeting, American Institute of Aeronautics and Astronautics, Washington, D. C., 29 June – 2 July 1964

45. L. W. Slifer, Jr., and S. G. McCarron, Preliminary Results of the Explorer XXVI Solar Cell Experiment, NASA-TM-X-55385 (N66-17258), NASA Goddard Space Flight Center, Greenbelt, Md., October 1965

46. F. A. Carr, Flight Report: Interplanetary Monitoring Platform IMP II – Explorer XXI, NASA-TN-D-3353 (N66-26552), NASA Goddard Space Flight Center, Greenbelt, Md., June 1966

47. F. A. Carr, Interplanetary Monitoring Platform IMP 3 – Explorer 28,Interim Flight Report No. 2, NASA TM X-55561 (N66-37411), NASA Goddard Space Flight Center, Greenbelt, Md., July 1966

48. W. Logan, Goddard Space Flight Center, Greenbelt, Md., personal communication, 9 May 1966

49. J. J. Madden, Second Interim Flight Report AIMP-I Explorer 33, NASA-TM-X-55838 (N67-32307), NASA Goddard Space Flight Center, Greenbelt, Md., May 1967

50. "Explorer 35 Moon Findings," NASA News Release No. 67-295, 7 December 1967

51. J. R. Fischel, Explorer XXIX (GEOSA) Postlaunch Performance Evaluation, NASA-CR-75069 (N66-26701), System Sciences Corp., Falls Church, Va., March 1966

52. M. Quetard, "Structure of the D-1 Satellite," Air et Cosmos, No. 114, pp. 14, 15, and 46, 17 July 1965

53. E. C. McCandlish, McDonnell Aircraft Co., St. Louis, Mo., personal communication, 12 February 1965

54. E. K. Welhart, McDonnell Aircraft Co., St. Louis, Mo., personal communication, 12 February 1965

55. J. C. Blome and B. E. Upton, "Gemini Window Contamination Due to Outgassing of Silicones," presented to 11th National Symposium, Society of Aerospace Materials and Process Engineers, St. Louis, Mo., 19–21 April 1967

56. G. P. Dinneen, Space Communications, Division 6, Quarterly Technical Summary, 1 December 1965 – 28 February 1966, ESD-TDR-66-156 (AD-480 755), Lincoln Laboratory, Massachusetts Institute of Technology, Lexington, Mass., April 1966

57. John T. Stacey, Boeing Co., Seattle, Wash., personal communication, October 1966

58. P. M. Blair, Jr., G. F. Pezdirtz, and R. A. Jewell, "Ultraviolet Stability of Some White Thermal Control Coatings Characterized in Vacuum" presented to AIAA Thermophysics Specialist Conference, New Orleans, La., 17–20 April 1967

59. Lunar Orbiter 1. Extended-Mission Spacecraft Subsystem Performance, NASA-CR-870 (N67-35740), Boeing Co., Seattle, Washington, September 1967

60. Fifth and Final Lunar Orbiter Launch Planned, NASA News Release No. 67-192 (N67-31712), 27 July 1967

61. R. A. Boundy, "Non-Metallic Materials for Unmanned Spacecraft," 11th National Symposium Society of Aerospace Materials and Process Engineers, St. Louis, Missouri, 19–21 April 1967

62. "Micrometeorite Shower Disables Mariner 4," Aviation Week and Space Technology, p. 22, 1 January 1968

63. T. Neville, Nimbus Meteorological Satellite, Integration and Testing Materials Report No. 8, G. E. Report No. 65SD4410, General Electric Company, Valley Forge, Pa, July 1965

64. R. Micich, Grumman Aircraft Corporation, Bethpage, N. Y., personal communication, 21 July 1966

65. Final Report, Investigation of OGO-A Malfunctions, Report 2311-6094-SU-000, Space Technology Laboratories, Redondo Beach, Calif., December 1964

66. "OGO-E Launch Scheduled," NASA News Release No. 68-38, 26 February 1968

67. C. B. Neel, Research on the Stability of Thermal-Control Coatings for Spacecraft, Ames Research Center, Moffett Field, Calif., NASA-TM-X-51196 (X64-10410), 1963

68. B. D. Pearson, Jr., "Preliminary Results From the Ames Emissivity Experiment on OSO 2," AIAA Paper 65-651, AIAA Thermophysics Specialist Conference, Monterey, Calif., 13–15 September 1965

69. J. C. Arvesen, C. B. Neel, and C. C. Shaw, "Preliminary Results From a Round-Robin Study of Ultraviolet Degradation of Spacecraft Thermal-Control Coatings," pp. 443–452 in Symposium on Thermal Radiation of Solids, NASA-SP-55 (1965)

70. T. C. Bannister and R. J. Eby, Pegasus Thermal Design, NASA-TN-D-3625, NASA Marshall Space Flight Center, Huntsville, Alabama, November 1966

71. A. B. Mickelwait, "The Pioneer 6 Spacecraft," Raumfahrtforschung 10, pp. 138–144, July–September 1966

72. J. D. Kiesling, "The NASA Relay 1 Experimental Communication Satellite, RCA Review 25, 232–261, 1964

73. G. Sharman, Cubic Corporation, San Diego, Calif., personal communication, 11 January 1968

74. Surveyor I, A Preliminary Report, National Aeronautics and Space Administration, Wash., D. C., NASA SP-126, June 1966

75. G. S. Hunter, "USAF to Orbit 2 Advanced Velas in April," Aviation Week and Space Technology, pp. 71, 73, and 77, 13 February 1967

17.3.2 References Used in Preparing Tables 17-7 through 17-15

AIMP (IMP-D) Technical Summary Description, NASA-TM-X-55770 (N67-26592), NASA Goddard Space Flight Center, Greenbelt, Md., March 1967

Applications Technology Satellite, Quarterly Progress Report No. 8, NASA-CR-76643 (X66-20620), Hughes Aircraft Co., El Segundo, Calif., June 1966

Applications Technology Satellite Technical Data Report, Vol. I NASA-TM-X-60062 (N67-31864), NASA Goddard Space Flight Center, Greenbelt, Md., July 1967

"Ariel 3 the First All-British Satellite," Industrial Electronics 5, 297-300, July 1967

Becker, R. A., "Optical Material Problems of Interplanetary Space," Applied Optics 6, 955–962, May 1967

Blonstein, J. L., "The Structure of UK3,"/(N66-21183) C.N.E.S. Symposium on the Structure of Satellites, Paris, France, June 1965

Caltabiano, S., and T. E. Shaw, "Thermodynamic System Design of the Biosatellite," pp. 235–248 in Spacecraft Systems, Proceedings of the XVIth International Astronautical Congress, Athens, 1965

Carroll, W., G. G. Coyle, and H. Von Delden, Mariners Mars 1964 Temperature Control Hardware Design and Development, NASA-CR-84293 (N67-26581), June 1967

Charp, S. and S. Drabek, "Flight-Proven Mechanisms on the Nimbus Weather Satellite," First Aerospace Mechanisms Symposium, Santa Clara, Calif., 19–20 May 1966

DeLiberato, V. C., "Design of the Biosatellite Spacecraft," the Fourth Space Congress of the Canaveral Council of Technical Societies, Cocoa Beach, Fla., April 1967

Ebersole, R., L. Pochettino, and W. Kugler, "BIOSATELLITE Environmental Control and Life Support System Design," Aeronautic & Space Engineering and Manufacturing Meeting, Los Angeles, Calif., 2–6 October 1967

Flom, D. G., and A. J. Haltner, Lubricants for the Space Environment, R68SD6, General Electric Co., Missile and Space Division, March 1968

Freeman, R., Jet Propulsion Laboratory, Pasadena, Calif., personal communication, 9 January 1968

Gatzek, L., North American Aviation Corp., Downey, California, personal communication, 27 October 1967

Holmes, P. J. and I. C. Jennings, "Failure Analysis of Planar Transistors Used in the UK3 Satellite Programme," Microelectronics and Reliability 7, 37–44, February 1968

Korb, L. J., "Spacecraft Plumbing Systems," Metal Progress 91, 65–70 February 1967

Langston, M. E., "Materials in Atlas-Agena Shroud," Metal Progress 91, 125–128, February 1967

Luedke, E. E., Systems Group of TRW, Inc., Redondo Beach, Calif., personal communication, 19 March 1968

Lyman, P. T., "Mariner-IV Structural Dampers," First Aerospace Mechanisms Symposium, Santa Clara, Calif., 19–20 May 1966

Mueller, G. E., "Apollo Actions in Preparation for Next Manned Flight," Astro. and Aeronautics 5, 28–33, August 1967

Notthoff, A. P. "Apollo Antenna Fastens on the Beam to the Moon," Electronics 40, 80–86, May 1967

OSO Spacecraft Manual, NASA-TM-X-55616 (N67-11395), NASA Goddard Space Flight Center, Greenbelt, Md., July 1966

Paghis, I., C. A. Franklin and J. Mar, Alouette I. The First Three Years in Orbit, DRTE-1159 (AD 822 875) (N68-10704), Defense Research Telecommunications Establishment, Ottawa, Canada, April 1967

Paulkovich, J., Solar Array Regulation of Explorer Satellites 12, 14, 15, 18, 21, 26, 28, and Ariel 1, NASA-TN-D-3983 (N67-30026), NASA Goddard Space Flight Center, Greenbelt, Md., July 1967

Prentice, H. A. J., and J. Porter, Thermal Control Surfaces for the U. K. 3 Satellite, RAE-TR-66121 (AD 487813 (N67-13240), Royal Aircraft Establishment, Farnborough, England, April 1966

"2nd Biosatellite to Study Biology of Space Flight," NASA News Release No. 67-217, August 1967

Semple, E. C., "Thermal Design and Thermal Testing of the UK-3 Spacecraft," Radio and Elec. Eng. 35, 41–48, January 1968

Sharman, G., Cubic Corporation, San Diego, Calif., personal communication, 11 January 1968

Shipley, D. M. and R. J. Barra, Jr., "The Ariel II (UK-2), International Satellite Environmental Test Program," Proceedings of the Third Space Congress, Canaveral Council of Technical Societies, Cocoa Beach, Fla., March 1966

Space Programs Summary No. 37-48, Vol. 1, NASA-CR-91775 (N68-15004), November 1967

"Surface Treatments for the U.K. 3 Satellite," Metal Finishing J., 213–214, June 1967

Treble, F. C., Field Tests on UK3 Solar Cell Assemblies, RAE-TR-66112 (N66-35666), Royal Aircraft Establishment, Farnborough, England, April 1966

Warren, F., Space General Corporation, El Monte, Calif., personal communication, 10 January 1968

Chapter 18

SELECTION OF MATERIALS FOR OPTIMUM PERFORMANCE

J. B. Rittenhouse
J. B. Singletary

This chapter discusses selection of materials for spacecraft construction as influenced by the various space environments. Although this chapter summarizes information contained in earlier chapters of this handbook, it must not be regarded as a substitute for the detailed presentation of space effects given there. Selection of particular material for spacecraft application can be made only tentatively from the information in this chapter; the final decision must rely on the data of Chapters 9 through 16 and the literature referenced in them. The designer must satisfy himself that the material he selects is suitable for his intended application.

Materials are recommended for the performance of several hypothetical space missions. The space environments upon which these recommendations are based vary with the various mission parameters. Atmospheric pressure is a simple function of altitude, at least to the accuracy desired here; pressures vary with altitude as shown in Tables 3-2 and 3-3. The micrometeoroid flux is also weakly dependent upon the altitude. The radiation environments are more complicated. A treatment of nonpenetrating radiation from the solar, albedo, and earth emission sources requires that one consider not only altitude and orbit but also vehicle geometry to arrive at expected vehicle temperature values. The specialized calculations will not be presented here. On the other hand, the very important penetrating radiation environment permits a somewhat more generalized treatment.

An orbiting vehicle will experience cumulative effects from penetrating radiations which can be conveniently categorized by their distribution within several spatial zones. For example, at a 500-nm (576-sm) altitude, a polar orbiting vehicle will traverse the inner trapped radiation zone twice and the auroral zones four times per orbit, while a vehicle in an equatorial orbit at the same altitude will not pass through the auroral region at all. Solar flare activity occurs sporadically, but over reasonably long periods of exposure the dose received by a vehicle from this source can be specified by a statistical distribution of dose versus the probability that this dose will be exceeded. Since the earth's magnetic field deflects a charged-particle radiations such as solar flare protons and therefore provides a high degree of shielding at low latitudes, a polar orbiting vehicle will be exposed to these radiations primarily in the polar regions and a low-altitude equatorial orbiting vehicle will experience relatively little solar flare radiation. (See Tables 18-1 and 18-2.)

Primary cosmic rays, although they are somewhat affected by the earth's magnetic field, generally have such high energies that their spatial distribution is more uniform than the other radiations to which an orbiting vehicle is exposed. The contributions from the principal known radiation fields in space for a vehicle in various orbits near

Table 18-1

ANNUAL INTEGRATED RADIATION DOSES RECEIVED IN VARIOUS ORBITS

Sources of Radiation	Radiation Dose[a] (R)											
	90-deg Inclination Orbits (Polar)								30-deg Inclination Orbits			
	200 nm (230 sm)		500 nm (576 sm)		1000 nm (1152 sm)		2000 nm (2304 sm)		200 nm (230 sm)		500 nm (576 sm)	
	Surface	Internal	Surface	Internal	Surface	Internal	Surface	Internal	Surface	Internal	Surface	Internal
Cosmic Primary Protons	4	4	4	4	5	5	7	7	(b)	(b)	(b)	(b)
Trapped Protons	9×10^{2}	2×10^{2}	1.4×10^{4}	4×10^{3}	1.7×10^{5}	4×10^{4}	2×10^{5}	7×10^{4}	3×10^{2}	2×10^{4}	3×10^{3}	2×10^{3}
Trapped Electrons[c]	5×10^{4}	7×10^{2}	1.4×10^{6}	6×10^{3}	5×10^{7}	5×10^{4}	1×10^{8}	1.4×10^{5}	1×10^{5}	2.4×10^{1}	2×10^{6}	5×10^{2}
Auroral Protons[d]	2×10^{8}	0	2×10^{8}	0	2×10^{8}	0	2×10^{8}	0	(b)	(b)	(b)	(b)
Auroral Electrons[e]	1.5×10^{8}	(e)	1.5×10^{8}	(e)	1.5×10^{8}	(e)	1.5×10^{8}	(e)	(b)	(b)	(b)	(b)
Solar Flare[f] Protons	5×10^{2}	10^{2}	5×10^{2}	10^{2}	5×10^{2}	10^{2}	5×10^{2}	10^{2}	(b)	(b)	(b)	(b)

(a) Determined for vehicle surfaces and interiors (through 0.1-in. Al skin).

(b) These radiation sources have smaller intensities than those due to trapped electrons and will therefore not appreciably affect the total dose. When compared to doses for polar orbits, those for 30-deg inclination would be smaller approximately by a factor of 2 for cosmic rays, a factor of 10 for solar flares, and would be essentially zero for auroral protons and electrons.

(c) Calculated for December 1968 from data of Refs. 1 and 2. The doses for 90-deg inclination orbits will not change greatly up until this date, but the 30-deg inclination internal cases should be multiplied by a factor of ~ 3 for each year before December 1968 to account for the time variation of the artificial electron belt.

(d) Based on very limited data.

(e) This contribution arises from secondary processes in the vehicle skin and is small in comparison to the trapped particle doses.

(f) A "most probable" dose, defined as the dose which has a probability of being exceeded of $1/e = 0.37$. Fluxes are from data of Ref. 3.

Table 18-2

MAXIMUM RADIATION DOSE RATES RECEIVED IN VARIOUS ORBITS

Sources of Radiation	Radiation Dose Rate[a] (R/hr)											
	90-deg Inclination Orbits (Polar)								30-deg Inclination Orbits			
	200 nm (230 sm)		500 nm (576 sm)		1000 nm (1152 sm)		2000 nm (2304 sm)		200 nm (230 sm)		500 nm (576 sm)	
	Surface	Internal	Surface	Internal	Surface	Internal	Surface	Internal	Surface	Internal	Surface	Internal
Cosmic Primary Protons	4×10^{-4}	4×10^{-4}	4×10^{-4}	4×10^{-4}	5×10^{-4}	5×10^{-4}	7×10^{-4}	7×10^{-4}	(b)	(b)	(b)	(b)
Trapped Protons	10	3	50	14	160	40	200	60	2	1.4	12	8
Trapped Electrons[c]	140	12	450	40	1.8×10^{3}	150	3×10^{3}	200	1.8	6×10^{-1}	20	7
Auroral Protons[d]	3×10^{8}	0	3×10^{8}	0	3×10^{8}	0	3×10^{8}	0	(b)	(b)	(b)	(b)
Auroral Electrons[e]	2×10^{8}	(e)	2×10^{8}	(e)	2×10^{8}	(e)	2×10^{8}	(e)	(b)	(b)	(b)	(b)
Solar Flare Protons[f]	100	20	100	20	100	20	100	20	(b)	(b)	(b)	(b)

(a) Determined for vehicle surfaces and interiors (through 0.1-in. Al skin).

(b) These radiation sources have smaller intensities than those due to trapped electrons and will therefore not appreciably affect the total dose. When compared to doses for polar orbits, those for 30-deg inclination would be smaller approximately by a factor of 2 for cosmic rays, a factor of 10 for solar flares, and would be essentially zero for auroral protons and electrons.

(c) Calculated for December 1968 from data of Refs.1 and 2. The doses for 90-deg inclination orbits will not change greatly up until this date, but the 30-deg inclination internal cases should be multiplied by a factor of ~3 for each year before December 1968 to account for the time variation of the artificial electron belt.

(d) Based on very limited data.

(e) This rate is based on a maximum observed, but has a low frequency of occurrence. The internal dose rate arises from secondary processes in 0.1-in. aluminum and is small compared to the rate from solar flare protons.

(f) Peak observed in maximum activity period of the last solar cycle (Ref. 4).

earth are tabulated in Table 18-1. The corresponding maximum dose rates are given in Table 18-2. The accuracy to which these contributions are known and the time variations of the various radiation fields vary widely. Primary cosmic ray fluxes and their variation within the solar cycle are known quite accurately. Proton fluxes in the inner trapped (Van Allen) zone are known rather well, but their variation (particularly at low altitudes) with the solar cycle is less certain. Trapped electrons in this region include fluxes artificially injected from high-altitude nuclear explosions in 1962 which have been diminishing since that time and those injected from natural sources which were not well measured before the artificially injected electron belt was formed. Thus, there are uncertainties in specifying these fluxes which will be reduced only when the artificially injected component has diminished below the natural environment and this can then be measured. The dose contributions from outer zone electrons, auroral particles, and solar flare particles have the largest uncertainties associated with them. The specification of these doses relies on statistical models constructed from long-time averages of measurements (Refs. 1 and 2).

The radiation dose is given in roentgens (R), which is a measure of the ionization produced by a given amount of energy. Conversion of these units to equivalent fluxes of penetrating particles is inexact because interactions of particles with matter vary with the particle energy, mass, and flux. Nevertheless, the following statements may be used to give a rough estimation of the relationship between the dose and fluxes of penetrating particles:

1 rad = 100 erg/gm
1 rad = 10^6 protons/cm^2 (This may be inaccurate by a factor of 4; i.e., it may be 4×10^6 or 2.5×10^5 protons/cm^2
1 rad = 3×10^7 electrons/cm^2 (This may be inaccurate by a factor of 2; i.e., it may be 6×10^7 or 1.5×10^7 electrons/cm^2.)

18.1 THERMAL CONTROL MATERIALS*

Choice of a thermal control system for any given space vehicle will depend on a variety of factors. The initial choice which must be made is between an active or passive system or a combination of the two. An active system has many advantages if the additional weight and power requirements can be tolerated. Such a system can be designed to correct automatically for varying energy inputs to the vehicle, either from the space environment or from internal energy loading. In addition, accurate knowledge of the environment is not needed as is the case for passive systems. Active systems can be designed for a much greater range and more precise degree of temperature control. Active devices have been employed on most manned flights. On the other hand, an active system is subject to decreasing reliability with duration of flight, primarily due to the presence of moving parts, switches, and valves. Power requirement is another vital consideration; if power is subtracted to operate a temperature control device, this severely limits the power available to the spacecraft mission.

---

*Based on Chapter 7 by M. E. Sibert.

Passive systems have been employed for essentially all unmanned flights. These have high reliability despite some problems with radiation-induced change in the solar absorption of the materials. The total weight of thermal control materials employed is only a fraction of that for an active thermal control system.

Thus, the choice of basic system will depend on spacecraft size, mission duration, power available, degree of thermal control required, weight criticality, whether the mission is a near-earth one or interplanetary, and whether the spacecraft is manned or unmanned. Extensive consideration has not been given to choice of specific active systems, since this very strongly depends on the specific thermal design requirements for any given space vehicle. In the case of passive systems, a number of generalizations can be made. An ideal thermal control material should possess the following properties:

- It should exhibit reproducible values of solar absorptance and infrared emittance.
- It should be applicable to a variety of metallic and nonmetallic substrates with good adhesion, and should resist chipping, cracking, and abrasion while requiring only standard techniques of application.
- It should withstand the prelaunch environment with negligible property change.
- The surface should be susceptible to cleaning by standard techniques to remove any accidental soilage.
- The surface should be repairable at the launch site.
- Supplied material should not require elevated-temperature cure.
- The surface should withstand the ascent environment with no large changes in absorptance or emittance properties; it should not offgas during ascent or in the space environment.
- The material properties should not undergo large changes under the influence of ultraviolet, protons, electrons, alpha particles, solar wind protons, or any combination of these environments.

Obviously, materials do not exist that meet these ideals in all respects. Thus, compromises have to be made, depending on such factors as the following:

- Orbit or trajectory of the space vehicle
- Mission duration
- Magnitude of permissible temperature range
- Temperature criticality
- Ascent considerations
- Time of alunch
- Prelaunch environment
- Vehicle materials of construction and geometry

The data given on specific properties of currently available passive thermal control in Table 18-3 are provided to assist the design engineer in making an intelligent choice of materials for specific vehicle requirements. These data are listed in order of increasing solar absorptance/emittance ratio (or in approximate order), solar reflectors, flat absorbers, flat reflectors, and solar absorbers. The following remarks pertain to the data listed in Table 18-3.

Table 18-3

SELECTION OF THERMAL CONTROL SURFACES

No.	Material	α_s/ϵ	α_s	ϵ	Supplier or Developer	Substrate	Max. Ascent Temp. (°F)	Thermal Cycling		UV Stability		Proton Stability		Electron Stability		Flight Data[a]	
								Min./Max. Temp. (°F)	Cycles/ Minute	Equivalent Sun-Hours	$\Delta\alpha_s$	keV/ protons/cm^2	$\Delta\alpha_s$	keV/ electrons/cm^2	$\Delta\alpha_s$	Flight/ Equivalent Sun-Hours	$\Delta\alpha_s$
1C-1	Optical Solar Reflector (Ag-SiO_2)	0.06	0.05	0.80	LMSC	Any, with proper adhesive	Not qualified	-150/200		2,000 1,100	0 +	9R7/5 × 10^{15} 2/8 × 10^{15}	0 0	500/10^{16}	0		
1A-8	Synthetic ZrO_2-SiO_2-K_2SiO_3	0.08	0.07	0.85	LMSC	Any cleaned surface	>700			500 45	0.04 +	100/2 × 10^{15} 100/2 × 10^{15}	0.01 0.02[b]				
1A-16	ZrO_2-K_2SiO_3	(0.08)	0.07		LMSC	Any cleaned surface				300 300	0.04 +	1.4/5 × 10^{16} 1.4/5 × 10^{16}	0.03 0.06	100/1.3 × 10^{15}	0.02		
1C-2	Optical Solar Reflecter (Al-SiO_2)	0.12	0.10	0.80	LMSC	Any, with proper adhesive	Not qualified			2,000	0[b]						
1A-7	$ZrSiO_4$-K_2SiO_3 (Ultrox)	0.13	0.12	0.89	LMSC	Any cleaned surface	>700			800	0.09					300[1]	0.04
1A-10	Synthetic $LiAlSiO_4$-K_2SiO_3	0.13	0.12	0.90	LMSC	Any cleaned surface	>700			600	0.04			800/1 × 10^{15}	0.16		
1C-3	Mirror-Al on Vycor	0.14	0.11	0.79	Hughes	Any, with proper adhesive	Not qualified									(2)	
1A-9	$LiAlSiO_4$ (Ultrafrax)-K_2SiO_3	0.15	0.13	0.85	LMSC	Any cleaned surface	600	-240/70		600	0.04			800/1 × 10^{15}	0.15		
1A-18	Al Anodize (H_2SO_4)	0.17	0.15	0.90	AFML; Boeing	Al 1100	Structural Limits Only			500 500	0.03 +	10/1 × 10^{15} 10/1 × 10^{9}	<0.01 0.03			350[3]	0.05
1A-2	Plasmo clay-K_2SiO_3	0.18	0.17	0.93	Hughes	Cleaned surfaces				500	0.05					600[4]	0.06
1A-1	ZnO-K_2SiO_3 (Z-93)	0.19	0.17	0.90	IITRI, Douglas (MD-22)	Cleaned surfaces	>700	-80/200		500	0.01[b]	20/1 × 10^{16} 2/5 × 10^{16} 1/4 × 10^{17}	0.13 0.26[b] 0.35[c]	2/1 × 10^{16}	0.03	3800[5] 300[1]	0.11 <0.01
1B-8	Thermatrol 6A-100 TiO_2-Siloxane	0.19	0.17	0.88	LMSC/Dow Corning	Any Rigid substrate	700			1,330 190	0.15[b] +	10/5 × 10^{16} 10/5 × 10^{16} 2/5 × 10^{16}	0.42 0.48 0.11[b]	800/1 × 10^{15}	0.01		
1B-2	ZnO-Methyl Silicone, sweated pigment (S-13G)	~0.2	0.21		IITRI	Clean metal surfaces	650			800	0.01						
1B-3	ZnO-Silicone SC/5	~0.2	0.18		Boeing	Clean metal surfaces	650									700[6]	0.11
1B-6	Anatase-TiO_2-Silicone	0.22	0.19	0.86	GSFC	Any rigid substrate	650									700[8]	0.32 $\Delta\alpha_s/\epsilon$
1B-1	ZnO-Methyl Silicone (S-13)	0.24	0.21	0.87	IITRI	Clean metal surfaces (primer required)	650	-240/200		800 1,330	0.08[b] 0.10[b]	2/5 × 10^{16} 1/1.7 × 10^{16}	0.16[b] 0.07[c]			<50[7] 1300[8]	0.3 0.29 $\Delta\alpha_s/\epsilon$
1B-14	TiO_2-Silicone-Acrylic (C-2-A)	~0.22	0.19	~0.86	G.E.	Any rigid substrate				300	0.23[b]	4.5 × 10^{14}	0.11[b]				
1B-7	Thermatrol 2A-100 TiO_2-Silicone	0.24	0.20	0.85	LMSC/Dow Corning	Any rigid substrate	650	-80/200		1,000	0.05						
1B-15	White Velvet	0.24	0.21	0.86	3M	Any rigid substrate				400	0.17[b]						
1A-21	Aluminized Teflon (2 mil) FEP Type A	0.24	0.16	0.66	Hughes					100	0						
1B-19	Methacrylate-Epoxy-TiO_2	~0.24	0.20		Am. Cyanamid	Al and alloys				2,530	0.10						
1B-18	PV Butyral-Melamine-TiO_2	~0.25	0.21		Am. Cyanamid	Al and alloys				2,530	0.07						
1B-17	Epoxy-TiO_2-Skyspar	0.25	0.22	0.89	A. Brown Paint	Any rigid surface	450	-240/70		1,000	0.25	1/8.4 × 10^{17} 1/2.1 × 10^{18}	0.04[c] 0.12[c]	800/1 × 10^{15}	0.03		
1B-9	TiO_2-Silicone-Alkyd	0.27	0.24	0.88	Vita-Var Paint	Any rigid surface				500	+	10/1 × 10^{15}	0.05			- (3)	0.10
1B-11	TiO_2-Phenyl-Methyl Silicone	~0.27	0.23		MSFC							1/2.1 × 10^{16} 1/1.9 × 10^{18}	0.15[c] 0.48[c]				
1B-10	TiO_2-Methyl Silicone	~0.30	~0.23	~0.77	IITRI											1800[7]	0.27 $\Delta\alpha_s/\epsilon$
1B-13	TiO_2-Acrylic, Kemacryl	0.31	0.27	0.86	Sherwin-Williams	Any clean, rigid surface, needs primer	450; blisters at 200	-240/70	0.08	1,000 500	0.24 +	10/1 × 10^{15} 10/1 × 10^{15}	<0.01 0.06	800/1 × 10^{15}	0.02		
1A-3	$SrMoO_4$-K_2SiO_3	~0.3	0.24		AFML					500 500	0.03 +	10/1 × 10^{15} 10/1 × 10^{15}	<0.01 <0.01				
1B-12	TiO_2-Silicone-Alkyd	0.32	0.26	0.81	W. P. Fuller	Dow 17-coated Mg and alloys; Al, Ti alloys; stainless	450	-240/70	0.08	1,000	0.17			800/1 × 10^{15}	<0.01		
1A-17	Barrier Anodize	~0.34	0.12	~0.35	Boeing	Al and alloys				3,000	0.01					350[3]	0.15
1A-19	Al_2O_3-Flame Sprayed, Rokide A	0.36	0.27	0.75	Norton Co.	Any metallic substrate	>1000										
1A-15	SnO_2-$AlPO_4$ (Al93)	0.38	0.35	0.91	Atomics Intl.		700	70/770	0.43	3,000	0.10	150/1 × 10^{16}	0.15				
1A-11	Evaporated SiO_2 (1.5 μ) over evap. opaque Al	0.48	0.15	0.30	GSFC	Any clean surface										300[8]	0.07 $\Delta\alpha_s/\epsilon$
1A-20	Evaporated Al_2O_3 (1.1 μ) over opaque evap. Al	0.57	0.15	0.25	Ft. Belvoir	Any clean surface										1300[8]	0.08 $\Delta\alpha_s/\epsilon$
3-7	SiO_2-Ag-Polished Al	0.74	0.06	0.085	LMSC					2,000	0.02						
4-10	Alodine 401-41 (values depend on thickness)	0.8 to 7.1	0.33 to 0.41	0.04 to 0.51	Amchem Products	Al											
4-14	Stainless steel, sandblasted	0.88	0.75	0.85		AISI 410	>1200										

See footnotes at end of table.

Table 18-3 (cont.)

No.	Material	α_s/ϵ	α_s	ϵ	Supplier or Developer	Substrate	Max. Ascent Temp. (°F)	Thermal Cycling: Min./Max. Temp. (°F)	Thermal Cycling: Cycles/ Minute	UV Stability: Equivalent Sun Hours	UV Stability: $\Delta\alpha_s$	Proton Stability: keV/ protons/cm^2	Proton Stability: $\Delta\alpha_s$	Electron Stability: keV/ electrons/cm^2	Electron Stability: $\Delta\alpha_s$	Flight Data[a]: Flight/ Equivalent Sun-Hours	Flight Data[a]: $\Delta\alpha_s$
3-3	Al-Silicone Paint, 172-A-1, Leafing Al	0.89	0.25	0.28	W. P. Fuller	Any clean, rigid surface	800	-210/70	0.06	600	0.09						
3-1	Al-Acrylic Paint, non-leafing	0.90	0.15	0.50	Sherwin-Williams	Any clean, rigid surface	650	-150/70	0.06	1,600 (also decreases to 0.39)	0.07[b]						
4-15	Clear Teflon (2 mil) Mil-P-22241	0.91	0.80	0.88	DuPont											100[4]	0.04
3-4	Al-Silicone Paint, 171-A-152 Leafing Al	0.92	0.22	0.24	W. P. Fuller	Any clean, rigid surface	880	-240/70	0.06	600	0.09						
3-5	Al-Silicone Paint	0.93	0.26	0.28	JPL	Any clean, rigid surface										3800[5]	0.02
3-6	Al Paint, Cat-A-Lac	1.0	0.25	0.25	Finch Paint	Any clean, rigid surface											
3-2	Leafing Al Paint, D4D	1.0	0.26	0.25	GE	Any clean, rigid surface											
4-7	Conductive Black Paint	~1.0	>0.9	>0.8	Appl. Phys. Lab.												
4-12	85% Cr_2O_3 Flame-Sprayed, Rokide C	1.06	0.90	0.85	Norton Co.	2 mil nichrome-coated Rene' 41	>1660	70/1660	0.2	600	0						
4-9	Black Acrylic Paint, M49BC12	1.06	0.93	0.88	Sherwin Williams	Any clean, rigid substrate; primer required	>450	-150/70	0.06	600	<0.05						
4-8	Silicone-Carbon Paint	~1.1	0.96	~0.85	LMSC	Any clean, rigid surface				420	<0.01						
4-3	Cat-A-Lac Black Paint	1.10	0.96	0.85	Finch Paint											3800[5]	<0.01
4-5	Black Micabond Paint (L6X962)	1.11	0.93	0.84	Midland Ind. Finishes	Any metal surface											
4-11	Dow 17	1.11	0.78	0.70	Dow Chem-Co.	HM21 Mg	>500			600	0						
4-13	Pt Black Coating	1.11	0.94	0.85	LMSC	QMV Be	>1200			600	0						
4-1	Black Paint	1.14	0.97	0.85	3M Co.					600	0						
4-4	Silicone Black, 517 B-2	1.15	0.89	0.77	W. P. Fuller	Same as 1012	>1070	-240/70	0.06	600	<0.05						
2-19	Al_2O_3 over Ag on Mill Finish Al	1.26	0.07	0.06	LMSC					2,000	<0.01						
2-8	Sandblasted Al	2.0	0.42	0.21	LMSC	Al 2024	Structural limits only				0						
2-7	Al Foil, plain, annealed	2.4	0.12	0.05		–	Structural limits only				0						
2-1	Al, vapor Deposited	2.5	0.10	0.04		Any clean surface					0						
2-3	Al, Chem. Cleaned	2.7	0.16	0.06		Al 6061 as rolled	Structural limits only				0						
2-18	Ag, Electroplated	3.0	0.15	0.05	GE	Be-Cu										1300[8]	1.10 $\Delta\alpha_s/\epsilon$
2-4	Al, Chem. Cleaned	3.2	0.29	0.26		Al 2024	Structural limits only				0						
2-10	Inconel Foil, Quilted TPS 0101B	3.2	0.38	0.12	H. I. Thompson	–	2200										
2-5	Al, Chem. Cleaned, non clad,	3.3	0.20	0.06		Al 2024 as rolled, hand sanded	Structural limits only				0						
2-6	Al, Chem. Cleaned, Clad	3.7	0.22	0.06		Al 2024 as rolled	Structural limits only				0						
2-12	Be, Chem. Polished	5.0	0.50	0.10		QMV Be	>1700				0						
2-2	Polished Al	5.25	0.21	0.04		–	Structural limits only				0					3800[5]	0.04
2-15	Hanovia Gold 6518	6.0	0.53	0.09		Rene' 41	900				0						
2-11	Inconel X Foil	6.6	0.66	0.10			1500				0						
2-14	Gold Plate, Mil-G-45204	7.0	0.28	0.04							0						
2-17	Lockspray Gold, Epoxy Coated	7.3 to 4.8	0.22 to 0.24	0.30 to 0.05	LMSC	Anodized Mg or Al alloys				2,000	<0.01						
2-13	CoO_2/Mo/MgF_2	7.7	0.85	0.11	Honeywell					500 500	0.01 4	10/1 - 10^{15}	<0.01				
2-9	Alodine, 1200S, MTL-3	8.6 to 5.2	0.40 to 0.49	0.05 to 0.10	Amchem Products; MSFC	Al and alloys										1800[7]	~0.09 $\Delta\alpha_s/\epsilon$
2-16	High Purity Gold, Temper ex HD	9.0	0.27	0.03		Al 6061		-320/100			0		0		0		

(a) Flight data for:
(1) Orbiting Solar Observatory 2
(2) Surveyor
(3) OV1-10
(4) Surveyor 1
(5) Mariner 4
(6) Lunar Orbiter 2
(7) Pegasus
(8) Applications Technology Satellite 1

(b) In situ test.

(c) Solar wind protons.

18.1.1 Environmental Stability Data

Data are shown in Table 18-3 for stability in terms of ascent and thermal cycling conditions and for ultrviolet, proton, and electron radiation stability. In addition, flight test data are listed where available. Nuclear radiation test data are not included, since resistance to this environment has rarely been a requirement for thermal control materials. This information was given where available in Chapter 7.

18.1.1.1 Thermal Stability

Definition of the ascent environment is required for the structural and aerodynamic design of any particular vehicle. This environment was discussed in Chapter 7. Materials are evaluated under simulated ascent conditions, and materials are selected that satisfactorily withstand the particular behicle requirements. The maximum ascent temperatures given are the maximum short time (1 to 2 min) values which have been determined experimentally to result in no appreciable changes in properties of a particular thermal control material. In general, the longer the peak temperature is maintained, the more severe the property changes the materials will suffer. For many materials, no ascent test data are available; in other cases, values have been estimated on the basis of a generic class of materials. As a rule, inorganic materials possess appreciably greater thermal stabilities than organic-based materials. However, consideration has to be given to compatibility of the thermal control material with the substrate. Within the temperature limits shown, the behavior of the material as a thermal control surface is not affected. The minimum temperature limit for paints is often the temperature below which coating failure due to differential thermal contraction of coating and substrate occurs; in such cases, this limit must be related to a specific combination of coating and substrate.

Thermal cycling data shown are given as the maximum and minimum temperatures at which a material was tested without major changes in properties.

Other materials present on a space vehicle such as potting compounds, sealants, or wire insulations may react adversely with the ascent environment through liberation of gaseous products that can then condense and contaminate nearby thermal control surfaces. The possibilities must be examined closely and precautions taken to avoid this source of contamination.

In unmanned spacecraft, a nose fairing or shroud usually protects the spacecraft during the ascent phase of the mission. Temperatures on and under the shroud can become quite high. For example, simulation tests of the Mariner 3 shroud material showed a peak temperature at the surface of $\sim 675^\circ$F after about 120 sec, and $\sim 250^\circ$F at the back face of the shroud. Therefore, the thermal control coatings used should be able to withstand fairly high temperatures (at least short-time stability to 500°F) and thermal cycling in vacuum (should withstand more than three hundred 15-min cycles from -150°F to 70°F). Certain portions of the spacecraft will experience low temperatures (-250° to -350°F); therefore, the thermal control materials should be stable at low temperatures also.

18.1.1.2 Radiation Stability

Radiation stability data for ultraviolet, proton, and electron radiation are given as the maximum exposure (duration-intensity) available. The data show the increase in solar absorptance of the material, since emittance changes are negligible or nonexistent in most cases. Test data are listed where the changes in properties of the material were in situ and are denoted by asterisks. The equivalent sun hour (ESH) listed under ultraviolet stability corresponds to simulated extraterrestrial radiation of normal incidence at the earth's distance from the sun for 1 hr. These changes in properties are minimal for metallic, black, and optical solar reflector surfaces; they can be quite large for highly reflecting surfaces.

Proton and electron radiation data are limited. Proton radiation data corresponding to solar wind protons are designated by (s).

Combined radiation effects are also listed wherever available (i.e., UV/proton, UV/electron, or proton/electron). As in the case of UV effects, tabulated data are for tests of maximum duration-intensity. The flight test data are tabulated according to flight, coded by number according to the list at the end of the table. These data are also listed according to total equivalent sun hour exposure, and the resultant changes in material properties are indicated by an increase in solar absorptance.

Simulated environmental tests have served mainly to screen potential materials, rather than to ascertain their reliability. A limited, and by no means sufficient, number of materials have been tentatively accepted as suitable thermal control materials. Among these are organic paints, in spite of their inferiority to inorganic materials. The chief reasons for using them are their immediate availability, ease of application, and low cost. Similarly, other materials have been tentatively approved because superior materials are still in research, development, and testing stages.

18.1.2 Thermal Control Considerations for the Moon and Planets

A lunar satellite such as the Lunar Orbiter or Apollo Command and Service Module which orbits the moon is subjected to both solar radiation and lunar infrared radiation of $\sim$ 1100 W/m^2 at the equatorial lunar noon. Thus, the temperature control system and the spacecraft orientation have to be designed to consider both conditions (Ref. 5). During the lunar night the value drops to 12 W/m^2. The earth's radiation varies from $\sim$ 320 to 140 W/m^2; its albedo is 0.35 ± 0.03 (Ref. 15). The albedo of the moon is ~ 0.07. Thus, the thermal control problem for lunar-orbiting vehicles is somewhat more complex than that for earth-orbiting vehicles.

The instrument compartment of Lunar Orbiter was covered with an insulation blanket of multilayers of aluminized Mylar and Dacron. The outer aluminized surface was coated with SiO_x and clear RTV 608 (an epoxy resin) to arrive at an α/ϵ of 0.3. The inside design temperature was 35° to 100° F. The success of the Lunar Orbiters in their photographic missions around the moon attests to the selection of these materials for thermal control purposes.

The passive thermal control material for the Apollo Command Module in lunar orbit will be textured aluminum foil with a semitransparent outer coat to produce a mean value of $\alpha_s/\epsilon = 0.31$. The Apollo also will use active thermal control systems to remove large amounts of internal heat.

18.1.3 Summary

The thermal design of a specific spacecraft begins with information on the operating temperature limits and power dissipation levels of its components, together with a definition of the vehicle and trajectory geometries. From such information, the thermal design parameters required to obtain the necessary temperature environment are determined. The predominant parameters are the α_s/ϵ ratio of the external surfaces and the emittance of internal surfaces.

In the general, the thermal control materials used in successful satellites and space probes have performed reasonably close to the design limits expected of them. The few exceptions to this behavior have been discussed (Refs. 6, 7, and 8). An example of the selection of a passive thermal control material using the data given in Chapters 7 and 18 is presented in Chapter 7.

18.2 OPTICAL MATERIALS*

Optical materials for spacecraft are selected on the same basis as for ground applications where the optical design parameters with respect to transmittance and reflectance for a specified spectral range of electromagnetic radiation govern the choice. In general, the optical design has to be strong enough to withstand flight qualification tests in shock, vibration, and the like. Protection of precision parts and surfaces must be provided to prevent damage during ground handling of optical components during systems tests. Temperature stability of materials and the minimizing of temperature gradients with the spacecraft structure and the optical structure are prime requirements.

In most cases, since a shroud protects the spacecraft during the ascent phase of the mission, it is not necessary to protect the optics from direct contact with the ascent heating environment. However, measures must be taken to ensure stability of the construction materials for the shroud and the spacecraft so that materials such as paints and polymers do not volatilize under ascent heating conditions. The volatile constituents of the less stable materials can condense on sensitive surfaces of optical materials and cause undesirable changes in surface properties. When a shroud is not used, a cover that can be actuated for removal in space after completion of the ascent phase will protect sensitive optical components.

Flint glass or other optical glasses such as cerium-stabilized glass or fused quartz can be used for lens systems. Absorption of radiation causes a decrease in transmission by the formation of color centers. Ordinary glass is most susceptible to damage, fused silica and synthetic quartz are next, and crystalline quartz and sapphire as the least sensitive.

---

*Based on Chapter 8 by J. B. Singletary.

The effects of charged-particle radiation on optical grade glass (Aluminosilicate Corning Type 1723, Chemcor Corning Code 0311), fused silica (Corning Type 7940), and ultraviolet transmission grade (GE101 quartz) in vacuum (10^{-6} Torr) were determined (Ref. 9). It was found that the Corning 1723 glass was subject to surface pitting and cracking from dielectric breakdown at electron fluxes of 10^{13} e/cm^2 and change in transmittance from 95.3% before exposure to 53.3% after. Proton (30 MeV) irradiation did not cause pitting or cracking as did electrons but the transmittance of the specimens was reduced from 87.8 to 12%. The medium-energy proton irradiation was 10^3 p/cm^2 at a rate of 1.3×10^9 p/cm^2-sec. The darkening of the Corning Code 0311 glass was less than the 1723 material and this glass did not crack. Under irradiation by electrons at 1.85 MeV and 10^{13} e/cm^2, values of transmittance were as follows: 95.3 (pre) and 77.5 (post) for Code 0311; 93.4 (pre) and 70.0 (post) for Type 1723.

The GE 101 quartz specimens exposed to the medium-energy protons were darkened to 28% transmittance after exposure compared with 93% transmittance prior to exposure.

The Corning 7940 quartz material was irradiated by high-energy protons (60 MeV, 2.5×10^9 p/cm^2; 100 MeV, 7×10^8 p/cm^2; 160 MeV, 1.5×10^8 p/cm^2) as the front element (exposed directly to radiation) of a composite window with two rear elements of the aluminosilicate Corning 1723 glass (each surface coated with one layer of magnesium fluoride). Although the quartz element did exhibit a small change, from 93 to 92%, in transmittance after exposure, it offered some protection for the second 1723 glass element which changed from 88.3 to 77.8%, while the third element of the window showed very little change, from 88.6 to 87.7% transmittance.

The Gemini spacecraft used a double window with Vycor quartz as the outside pane and magnesium fluoride coated aluminio-silicate glass as the inner.

Synthetic sapphire is the most radiation-resistant solar cell cover sheet material. Simulation tests have shown no detectable change in transmittance after 500 hr in 5 times the sun intensity in simulated solar ultraviolet radiation. A thickness of 0.04 in. of sapphire showed no detectable change when irradiated with 3×10^{12} p/cm^2 at 19 MeV. A thickness of 0.030 in. of sapphire has a stopping power of 18 MeV for protons.

Fused silica, Corning 7940, is recommended for most satellite solar cell cover sheet applications. The thicknesses recommended are 0.006 in. for low orbits and 0.020 in. for higher orbits where electron and proton radiation damage is expected. The adhesive is either General Electric Silicone LTV 602 or Dow-Corning Sylgard 182; the magnesium fluoride antireflectance coating and the OCL 207 (Optical Coatings Laboratory, Inc.) blue filter are also recommended (Ref 10).

Tests at LMSC of 20-mil thick Corning 7940 quartz in a vacuum of 10^{-7} Torr showed a decrease in transmittance of about 1.3% (from 93.3 to 92.0%) after exposure to 700 ESH of simulated solar ultraviolet radiation (A-H6 lamp). For 7940 quartz with one layer of magnesium fluoride and coating of the Optical Coatings Laboratories proprietary interference filter No. 207, a blue mixture of metallic oxides, the decrease in transmittance after exposure 735 ESH was 1.2% (93 to 91.8%).

The data of Tables 8-5 and 8-6 furnish a guide for the selection of infrared transmitting materials.

18.3 MATERIALS FOR LUBRICATED SYSTEMS*

Lubricant recommendations for equipment exposed to the space environment are summarized in Table 18-4. Recommendations are made separately for different applications, since no one type of lubricant is best for all applications. The discussion amplifies the information in the table.

Design factors that influence the choice of lubricant of self-lubricating material include:

- Definition of lifetime
  Based on torque. Gyro bearings must operate with a very low and constant torque; a slight increase in the viscosity of the lubricant and the bearing torque means failure of the gyro to operate properly. Bearings for gears and motors can operate until actual freezing of the bearings.
  Based on wear. The lifetime may be limited by the accumulation of wear debris or by the actual consumption of the material, as in the operation of motor brushes or ball bearings with special plastic retainers, thin-film lubricants, self-lubricating materials, or laminar solids.
  Based on noise level. The lifetime of electrical contacts is limited by the electrical noise generated.

- Environment
  Vacuum
  Radiation
  Reactive materials

- Operating conditions
  Speed
  Load
  Temperature: (1) high-temperature operation, (2) low-temperature operation, and (3) operation over an extended temperature range
  Duty cycle (continuous or intermittent)
  Type of motion (sliding, reciprocating, rotating, oscillating, make-and-break contact)
  Current density (with electrical contacts)
  Brush force (with electrical contacts)

- Parts
  Geometry and type of part (e.g., bearing, gear, cam, and brush)
  Materials and material combinations
  Hardness

---

*Based on Chapter 9 by H. I. Silversher.

Surface finish
Tolerances
Effect on other parts (e.g., condensation of oil on nearby optical surfaces)

- Installation and handling variables
  Alignment
  Balancing
  Mounting rigidity
  Run-in
  Cleanliness
  Sealing and protection against corrosion and contamination

- Lubrication (other than type of lubricant)
  Amount of lubricant
  Manner of application
  Replenishment

The recommendations made in Table 18-4 should serve as guides in determining the types of lubrication that may be most suitable. They are based on limited space simulation tests mostly in vacuum, some with cobalt-60 radiation in vacuum, and experience with satellites and space probes launched to date. Equipment qualification tests should confirm the usefulness of the lubricant or self-lubricating material selected by the designer and establish their lifetime and reliability for specific applications.

The radiation stability of the lubricants recommended in the following sections should not be a limiting factor for lifetimes up to 1 year for all the altitudes considered here. Based on information now available, the problems of vacuum operation would not result in different recommendations at different altitudes from 115 to 2650 sm (100 to 2300 nm).

18.3.1 Small Lightly Loaded Ball Bearings

18.3.1.1 Operating Characteristics

Typical examples of small, lightly loaded ball bearings are those in drive motors for servomechanisms. These are generally fractional horsepower motors operating at speeds up to 24,000 rpm, with 8000 rpm being an everage speed for induction motors. The shaft bearings in gear trains of the drive motors range from high to very low speeds. Bearings used in cam followers will generally operate as much slower speeds than than the motor bearings. The loads on these bearings are small. There are no gravitational loads once the device is placed in orbit (although there may be heavy loads during the launch pahses). The principal loads in orbit are the equivalent radial loads due to the transmission of power (on the order of several ounces to several pounds in typical cases). Dynamic loads arise from centrifugal forces in the bearings and from unbalance or misalignment. The latter forces should be kept small by proper design and fabrication.

Table 18-4

RECOMMENDED LUBRICANTS

Application	Conditions	Recommendation	Specification	Notes
Small ball bearings (3/4-in. bore. 2-in. OD or less)	Temperature: -65 to 225°F Speed: to 8000 rpm Pressure: ambient to 10^{-9} Torr Operating life: 1 yr continuous operation Radiation: 1×10^6 rad	Versilube G-300 grease, EG 509, EG 429, Supermil No. 31052, MLG 61-92, MLG 62-142		Use double metal shields on bearing; use at 200,000 DN[a] or below. Thermal-vacuum tests and flight experience of Nimbus 1 solar array orientation mechanism demonstrated that the lifetime of this material in vacuum is drastically reduced when the bearing operating temperature is above 300°F. See also Chapter 9 for lifetime data of R3 ball bearings lubricated with G-300 grease.
		Aeroshell 15 grease	MIL-G-25013D	Use double metal shields on bearing; use at 200,000 DN or below.
	Same as above with additional requirement of low starting torque at low temperature (-30°F or lower)	Versilube F-50 oil, FS 1265. XRM 141C. MLO 61-97, FPPN-10802-77		Vacuum impregnate into linen or paper-reinforced phenolic retainer; use double metal shields.
	Temperature: -65 to 400°F Speed: to 8000 rpm Pressure: 10^{-9} Torr Operating life: limited Can be used when nearby surfaces such as camera windows are sensitive to clouding by volatiles from oil lubricants Radiation: 1×10^8 rad	Hi-T-Lube dry-film lubricant, Everlube 811 dry-film lubricant		Dry film lubricant. Apply to races, retainers, and balls; use unshielded bearings; limited to 8×10^6 revolutions bidirectionally, based on R3 size bearing; bearing should be run in at low speed and excess lubricant removed by blowing out with clean, dry gas.
	Same as immediately above except: Radiation: 1×10^6 rad Temperature: -65 to 300°F	Unlubricated bearing with retainer of Rulon C		Use unshielded bearing; good to 3×10^7 revolutions, based on R3 size bearing.
	Temperature: -65 to 400°F Speed: to 8000 rpm Pressure: 10^{-9} Torr Operating life: limited Radiation: 1×10^9 rad Can be used when required to carry electric current	Bearing with full complement (i.e., no retainer) of silver-plated balls of tool steel (e.g., M-2, M-50) and races of 52100 steel		Limited to 1×10^7 revolutions, based on R3 size bearing.
All bearings at atmospheric pressure (760 Torr) in a sealed unit	-65 to 250°F continuous with peak temperature to 300°F	MIL-G-23827	MIL-G-23827	Synthetic oil based grease, best for general application, corrosion inhibited; good to 400,000 DN.

	-20 to 300°F	MIL-G-3545	MIL-G-3545B	Sodium soap thickened petroleum oil base, good high-speed performance; good to 500,000 DN.
	-100 to 450°F	MIL-G-25013	MIL-G-25013D	Synthetic oil based grease, wide temperature range; good to 200,000 DN.
	-65 to 250°F	MIL-L-6085A	MIL-L-6085A Amendment 2	Synthetic oil, corrosion inhibited, good general-purpose oil.
	-65 to 350°F	MIL-L-7808	MIL-L-7808E	Synthetic oil, wide temperature range; for high-temperature use should be supplied by spray or oil mist.
Gyroscope bearings	Sealed unit Temperature: -45 to 165°F Require lubricant with minimum change in viscosity in operating temperature range	KG-80		Oil should be vacuum impregnated into linen- or paper-based phenolic retainer, bearing double shielded. Life test in vacuum discontinued at about 6000 hr. See Chapter 9.
Larger, low-speed bearings	Temperature: -65 to 150°F Speed: to 1800 rpm Pressure: 10^{-9} Torr Radiation: 1×10^6 rad	Unlubricated bearings with retainers of Rulon C or Duroid 5813 (Reinforced Teflon)[b]		Tests with Rulon in vacuum to 10^{-8} Torr are given in Chapter 9.
	Temperature: -65 to 400°F Speed: to 1800 rpm Pressure: 10^{-9} Torr Radiation: 1×10^8 rad	Unlubricated bearings with retainers of metal composites such as Sinitex or Westinghouse silver or copper matrix based material		Limited lifetime in vacuum with retainers of these materials.
All bearings	Exposure to the temperatures of cryogenic liquids Radiation: 1×10^6 rad	Unlubricated bearings with retainers of Rulon C		Races of 440C are preferred over 52100 for corrosion resistance.
	Exposure to strong oxidizers (liquid oxygen, nitrogen tetroxide) Radiation: 1×10^6 rad	Unlubricated bearings with retainers of Rulon C		Races of 440C are preferred over 52100 for corrosion resistance.
Lightly loaded sliding surface	Exposed to vacuum Temperature: -65 to 165°F	Dry lubricant such as MoS_2 or Teflon on hard metal surfaces; plastics such as nylon phenolic laminates, and Delrin; porous metals impregnated with oil and/or MoS_2		Radiation effects on plastics should be considered before they are used. Otherwise satisfactory for 1-yr orbit intermittent operation.

Table 18-4 (cont.)

Application	Conditions	Recommendation	Specification	Notes
Heavily loaded sliding surfaces	Exposed to vacuum Temperature: -65 to 1200°F	For lower temperatures, bonded solid film lubricant which is compatible with a grease or oil and a low volatility grease or oil; for example, Electrofilm 4856 and 4896, with Versilube F50 or Aeroshell 15; bonded solid film lubricant selected for use with hard metals and high loads such as Electrofilm 77-S; dispersion of MoS_2 in grease such as Molykote Type G; for higher temperatures, sodium silicate or ceramic bonded MoS_2 or CaF_2		Satisfactory for 1-yr orbit, intermittent operation. Microseal: a silica bonded molybdenum sulfide solid film lubricant was used on the A286 austenitic steel hinge pins of the Surveyor 1 landing structure which successfully landed on the moon 2 June 1966.
Fine-pitch gears	Sealed unit Temperature: -65 to 250°F Radiation: 1×10^7 rad	Aeroshell 15, G-300, EG 509, Supermil 31052, MLG 61-92, MLG 62-142, greases on Nitrided Nitralloy 135, heat-treated AISI 4340 (46-50RC), hard anodized aluminum alloy 2024T3, 7075T6, heat-treated Berylco 25, beryllium-copper alloy, stainless steel AISI 303, 416, 440C, carburized low-carbon low-alloy steels	MIL-G-25013D MIL-G-23824 MIL-L-7808	Best practice to have dissimilar metal or alloy pairs mating in gear train. Avoid running unlubricated hard anodized aluminum alloy gears in air. Wear rate greater in air than in vacuum for these materials.

Fine-pitch gears	Exposed to vacuum Temperature: -65 to 250°F	Metallic gears as discussed above with solid film lubricants; gears of composite materials such as Sinitex and sintered materials such as the Westinghouse copper and silver base compositions		Lube Co 905 a proprietary inorganic-resin bonded, high pigment content, solid film lubricant probably based on MoS_2. This material can only be applied to passivated stainless steels and anodized aluminum alloys processed according to MIL-A-8625, MIL-F-14672, and AMS 2469. This material was used on the movable parts of the Surveyor 1 camera equipment. Worked 2-14 June 1966, restarted after lunar night on 6 July to produce 1,000 more pictures. Service tests required to establish lifetime and reliability. Avoid mating similar pairs. Avoid operating hard anodized aluminum alloy gears in air unlubricated.
	Temperature: -45 to 165°F	Plastic gears such as Teflon, polyformaldehyde or polyamide, or acetal resins		Service tests required to establish lifetime and reliability. Load limits, speed ratings, and radiation resistance of plastic gears lower than for metallic.
High-speed, moderate heavily loaded gears	Sealed unit Temperature: -45 to 250°F Speed: to 30,000 rpm		MIL-L-7808E MIL-G-25336	MIL-G-25336 is modification of MIL-L-7808 and should be used for heavy loads.
Fittings on oxidizer or oxidizer pressurization lines		Non-adhesive backed Teflon tape Permacel 412 or Kel-F tape; inert highly halogenated lubricant such as Fluorolube oils and greases		Some tests have shown that Kel-F[(c)] may lose its lubricity in vacuum. Kel-F lubricant may have pyrophoric reactions with nonoxidized aluminum alloy surfaces in an oxygen-rich environment.

(a) DN equals bearing bore diameter (mm) times speed (rpm).
(b) Teflon is E. I. Dupont trade name for polytetrafluorethylene.
(c) Kel-F is Minnesota Mining and Manufacturing Co., trade name for polytrifluorethylene.

The passive temperature control techniques should maintain the temperatures of the mechanisms in which the bearings are used within a range from -45° to 165° F. Higher temperatures (200° to 300° F) are reached on motor bearings owing to power losses within the motor windings. For small sealed gear motor ball bearings lubricated with grease or oils, experience has indicated that careful thermal control design considerations are required to keep the bearing temperature below 300° F. Temperatures of motor windings and bearings can be significantly higher under vacuum conditions than in air because of the absence of convection cooling; and this factor should be considered in designing proper conductive paths for dissipation of the heat to obviate regions of high temperature. High temperatures promote evaporation of oils and greases, under vacuum conditions, and lead to early lubrication failures. Low temperatures, on the other hand, increase the viscosity of the lubricant and can result in stalling drive motors if the temperature becomes very low and the lubricant becomes very viscous.

The operation of the ball bearings may be continuous or intermittent, depending upon the duty cycle required. Bearing rotation can be unidirectional, bidirectional, or oscillating back and forth through small angles. Bidirectional or oscillating motion can reduce the lifetime, particularly with bonded films of MoS_2 or special retainer materials.

18.3.1.2 Recommended Lubricants

Small, lightly loaded ball bearings should preferably be lubricated with a low volatility grease, except where special considerations (see below) make oil or MoS_2 films more desirable. Based on information available on the performance of ball bearings lubricated with greases and operated under vacuum conditions: the following greases are recommended for general applications and for most orbital conditions: GE Versilube G-300, Aeroshell 15, Marlin-Rockwell EG 509, and Supermil ASU No. 31052 (American Oil Co.). Three other greases, MLG 61-92 and MLG 62-142 (developed for the U.S. Air Force Aeronautical Systems Division of Wright-Patterson Air Force Base, Ohio), and Marlin-Rockwell EG 429, have exhibited long operating times in vacuum.

Where the ball bearings are required to operate at low temperatures (e.g., below -30° F), a low volatility oil is preferable to grease. Based on information available on the performance of ball bearings lubricated with oils and operated under vacuum conditions, FS 1265, XR M141C, ML061-97, and F 50 oils are recommended for such applications and for most orbital conditions. The oil should be vacuum impregnated into a linen- or paper-reinforced phenolic retainer. These oils have exhibited operation times of greater than 20,000 hr in vacuum. Two Dow-Corning fluorosilicone oils of different viscosities have given long lifetimes in simulated space environment (vacuum): FS-1265, 250 centistrokes, 48,586 hr, and an oil of the same designation but at 1000 centistokes, 17,492 hr in vacuum. This behavior indicated a small dependence of oil lubricant lifetime on viscosity. This relationship is not clear, but in general low-viscosity oils, ~ 30 centistokes, and the higher viscosity oils, ~ 1000 centistokes, have lower lifetimes than those with viscosities in the 50 to 250 centistokes region. (See Chapter 9.)

A high phenyl content silicone oil, MLO 61-97, supplied by the U.S. Air Force Aeronautical Systems Division, gave a lifetime in excess of 2 years. This behavior follows a trend that indicates longer lifetimes in vacuum for the halogenated and high phenyl content silicone oils because of their higher polarity compounds. The relatively symmetrical compounds of dimethyl, phenylmethyl, or low phenyl content silicone oils have shorter lifetimes – as much as a factor of 4 to an order of magnitude lower lifetimes in ball bearings in vacuum.

A trifluoromethyl phenoxy phosphonitrile, FPPN-10802-77 of E.I. du Pont, had lifetimes in vacuum of the order of 1 year. In one test, failure occurred at 9640 hr in an ion-pumped system and more than 30,000 hr in a diffusion-pumped system.

Where the ball bearings are required to operate in vacuum at high temperatures (e.g., above 225° F), some means of relubrication (see below) or MoS_2 films should be considered. The use of MoS_2 films should be restricted to speeds below 8000 rpm and for lifetimes below 4×10^9 revolutions of unidirectional operation or 6×10^8 cycles of start-stop-reverse operation. Based on information available on the performance of ball bearings lubricated with MoS_2 films and operated under vacuum conditions, Hi-T-Lube and Ever Lube 811 are recommended for applications where MoS_2 appears suitable.

Where nearby or adjacent parts are best lubricated with oil (e.g., gears in a partially enclosed gear train, where grease lubrication would create excessive torque and cause stalling), the ball bearings can also be lubricated with the same oil as used for the other parts.

Where nearby or adjacent parts are sensitive to the condensation of oil films (e.g., a horizon sensor can be affected by infrared absorption by condensed oil films on its optical surfaces), bonded films of MoS_2 can be used.

Where the operation of the device requires that there be no outgassing from the lubricant (e.g., evacuated and sealed electronic tubes with rotating parts), films of MoS_2 such as Hi-T-Lube or Ever Lube 811, or thin films of silver or gold are recommended. The use of thin films of silver or gold requires special bearing design, handling, processing, and care in installation; their lifetime and reliability are limited. This behavior has been shown by service tests conducted on some typical applications.

Where the ball bearings must be able to conduct an electrical current through them (from inner rings to outer rings), thin films of silver are recommended

18.3.1.3 Additional Comments

Periodic relubrication of ball bearings with fresh lubricant will, of course, prolong the lifetimes of the ball bearings indefinitely. Conventional relubrication from oil and grease reservoirs is often impractical with these bearings on spacecraft mechanisms. The use of porous ball retainer rings impregnated with the oil or a porous reservoir impregnated with oil placed near the bearings permits the replacement of oil that evaporates from the bearing itself, and this procedure can extend operating lifetimes.

Bearings lubricated with grease or oil should be double shielded (both to reduce lubricant evaporation and to minimize contamination). Machined linen- or paper-based phenolic (e.g., Synthane) retainers are preferred for operation at high speeds with oil lubricants. Ribbon-like retainers have been less satisfactory than porous retainers with oil lubrication. The oil should be vacuum impregnated into the retainer; if a grease is used, a retainer that is vacuum impregnated with the same oil that is used in the grease may be used. For example, if G-300 silicone grease is used, the retainer may be impregnated with F-50 oil, since the G-300 grease is a combination of the F 50 oil in a lithium-base soap.

On ball bearings lubricated with grease or oil, the running torque may decrease slightly at first owing to channeling of the grease or removal of excess oil. This is followed by a nearly constant or slightly rising torque for perhaps 90% of the lubrication lifetime. During this time, the torque should be well within the operating specifications. Following this period, the torque increases at an accelerating rate, and lubrication failure finally results in excessive wear and rapid seizure of the high-speed ball bearings themselves. Ball bearings lubricated with bonded MoS_2 films retain a more nearly constant torque during operation (following an initial reduction in torque due to wear in), and the final increase in torque loading to failure is much more rapid than with oil and grease lubrication.

Ball bearings lubricated with bonded films of MoS_2 should be carefully run-in and blown free of loosened debris before operation. Excess MoS_2 in powdered or slurry form should also be removed by run-in and careful blasting with dry air.

18.3.2 Fine-Pitch Gears and Gear Trains for Servomechanisms

18.3.2.1 Operating Characteristics

Speeds of gear trains vary from a high of about 24,000 rpm down to several revolutions per day. The loads due to the transmission of torque are generally small, increasing as the speed is reduced. Temperatures in typical applications cover a range of -45° to 165° F. The primary consideration in sealed gear trains lubricated with oil is the effect of temperature on oil viscosity and lubricating qualities. At low temperatures, excessive oil viscosity can result in large increases in torque and cause the device to stall, whereas at high temperatures excessive thinning of the oil can occur with resultant poor lubricity. The operation of the gears may be continuous or intermittent; gear rotation can be unidirectional, bidirectional, or oscillating back and forth through small angles.

18.3.2.2 Recommended Lubricants

Very little information is available on which to base recommendations for attaining a specified lifetime for gears operating under specified conditions. Where the gear trains are sealed by labyrinth or rubbing seals so that there is some protection against the vacuum environment, oils, and greases such as those covered by MIL-L-7808,

MIL-G-23827, or Versilube F-50 oil or G-300 grease, appear most useful. The gear material itself is also important. Where metal gears are used, hard anodized aluminum 2024-T3 or 7075-T6 appears satisfactory and has the advantage of lighter weight as compared with stainless steel gears. Aluminum alloy gears should be lubricated with grease or oil if they are to be run in air, since wear rates are higher on anodized aluminum gears in air than in vacuum. Low-alloy, high-strength steel gears and pinions of AISI 4340 heat treated to Rockwell C 46 to 50 have been successfully used in Ranger and Mariner 2 sealed antenna actuators. Carburized and heat-treated low-alloy, low-carbon gears have also been used. Worm gears and pinions of Be-Cu (Berylco alloy 25) or AISI 303 stainless steel with worms lubricated with Electrofilm 4396, a proprietary MoS_2 dryfilm lubricant, operated successfully on Rangers 6–9 and Mariner 2. Other stainless steels such as AISI 416 and 440C can also be used for corrosion-resistant applications. Sintered D-10S (oil-impregnated bronze plus MoS_2) has given good results. Plastic gears, especially sintered nylon (e.g., Nylasint 64 and Nylasint 66), molded nylon polyamid (e.g., Zytel), phenolic laminates, Delrin (acetal plastic), and Lexan could also be considered. Plastic gears are suitable only for lightly loaded applications and should be initially lubricated and run-in with oil or grease.

18.3.3 Large Low-Speed Support Bearings

18.3.3.1 Operating Characteristics

Typical examples of large, low-speed support bearings are those used for rotating satellite payloads and other devices. These may be either ball or roller bearings that vary in size up to several feet in diameter. Speeds are generally low, below ~ 100 rpm. These bearings may be subjected to heavy shock and vibration loads during the launch phases. Once in orbit, loads are low. The principal loads are the equivalent radial loads due to the transmission of power and may be on the order of several pounds. Temperatures in typical applications cover a range from -45° to 165°F. The operation of these bearings can be continuous or intermittent; rotation can be unidirectional, bidirectional, or oscillating back and forth through small angles. In some cases it is difficult or impractical to enclose these bearings, so that they are required to operate under high vacuum conditions.

18.3.3.2 Recommended Materials

Experience with OSO and other satellites indicates that conventional bearings can be used. If design analysis indicates a problem that arises from shock or vibration, the load may be supported by blocking which is removed after launch. The large bearings in OSO-1 which permitted the "sail" to remain fixed while the "wheel" rotated for spin stabilization were SAE 52100 steel with a reinforced fluorocarbon retainer lubricated with a MoS_2 slurry. The bearing material has been changed to 440C stainless steel in subsequent OSO spacecraft.

18.3.4 High-Speed Gears and Bearings Transmitting Moderate Heavy Loads

18.3.4.1 Operating Characteristics

Typical examples of high-speed gears and bearings transmitting moderate to heavy loads are those used on turbine drive units for liquid propellant pumps. Speeds on such units vary upward from 10,000 rpm; 30,000 rpm is typical. The gears and bearings are subjected to loads that arise from transmitting several hundred horsepower. Ambient temperatures in typical applications cover a range from -45° to 165° F. In typical applications, the gears and bearings are enclosed and sealed from the vacuum environment of space by labyrinth seals.

The total running time of these gears and bearings is generally limited to less than a few hours. This running time may be intermittent in engines that have restart capability and spread over several much shorter operating periods separated by several months in deep space planetary missions.

18.3.4.2 Recommended Lubricants

The use of a low-volatility oil and labyrinth seals minimizes evaporation. Under the usual conditions, the main emphasis should be placed on gear lubrication rather than the space environment. Metal gears and bearings are needed because of the speeds and loads. The recommended lubricants are those that are presently used, namely, MIL L-7808 type oils and, for higher loads, MIL-G-25336. Radiation stability should be satisfactory for a 2-year orbit at all altitudes.

18.3.5 Lightly Loaded Sliding Surfaces

18.3.5.1 Operating Characteristics

There are many applications, such as cam-operated switches and other mechanisms, reset and positioning mechanisms, and guides that involve sliding contact between two surfaces that are lightly loaded and that move at relatively slow speeds. Such parts may be difficult to enclose and seal, so that they are often required to operate while exposed to the hard vacuum of space. Temperatures are in an operating range from -65° to 165° F. Operation is continuous or intermittent and may also be unidirectional or bidirectional. Sometimes such a device is required to operate only once.

18.3.5.2 Recommended Lubricants

The following materials and lubricants are useful in such applications:

- Surface coatings of solid lubricants, such as MoS_2 and Teflon, on hard metal substrates · Burnishing MoS_2 onto the surface is adequate in some cases; in more severe applications, a bonded film should be used.

- Plastics such as phenolic laminates, nylon, and Delrin. These have sufficient strength and wear resistance for many applications in this category. They have less weight than similar parts of steel or other metals, and they eliminate the need for lubrication.

- Powder metallurgy composites with MoS_2 or porous metal composites impregnated with oil.

18.3.5.3 Additional Comments

Contacting pressures should be kept to a minimum for least frictional drag and wear. Where contacting pressures are high, hardened materials should be used. Contact between similar metals should be avoided, and wherever possible dissimilar metal pairs should be used. Austentitic stainless steel rubbing against austenitic stainless steel is a poor choice, as are titanium alloys rubbing against titanium alloys. Some form of lubrication should be provided.

With surface coatings, the base metal should be pretreated before applying the coating (e.g., anodizing for aluminum alloys, passivating for stainless steels), and the coatings should be run-in after application.

18.3.6 Heavily Loaded Sliding Surfaces

18.3.6.1 Operating Characteristics

Applications that involve sliding surfaces under heavy loads include such mechanisms as the gimbal sleeve bearings and actuator rod spherical bearings in propulsion systems. Such applications may also involve heavy shock and vibration loads during the launch phase.

The normal operating conditions may call for long idle periods interrupted by short-time operation, with the parts oscillating back and forth through small angles rather than through complete revolutions. Temperatures are within the range -65° to 200° F. Excessive wear and galling can cause the parts to "freeze" and become inoperable. The geometry of the parts usually prevents the sliding surfaces from being directly exposed to the vacuum of space.

18.3.6.2 Recommended Lubricants

For such applications, the following lubricants should be satisfactory and adequate for all orbital conditions considered:

- Bonded solid film lubricant used in conjunction with and compatible with the oil or grease. Electrofilm 4856 plus MIL-G-23827 grease is an acceptable combination; for temperatures below -30° F, an oil conforming to MIL-G-25336 may be preferable to the grease.

- Bonded solid film lubricant, selected for use at high loads and with hard metals, such as Electrofilm 77-S (MoS_2 plus graphite in a thermosetting resin).

- Dispersion of MoS_2 in grease, such as Molykote Type G (MoS_2 in a mineral oil plus lithium soap base grease).

18.3.7 Gyroscope Bearings

18.3.7.1 Operating Characteristics

Gyroscope bearings must operate with the lowest possible torque and with a minimum change in torque with temperature. Very small increases in torque, due to wear, lubricant breakdown, or any other cause, result in large errors in the operation of the gyroscope and are considered as failures. Consequently, lubrication is more critical than in most other applications.

Gyroscope bearings usually operate in a hermetically sealed unit that is often filled with an inert gas such as helium. As a result, the bearings are not exposed either to the hard vacuum of space or to a reactive atmosphere.

Gyroscope bearings are usually oil-lubricated ball bearings or the self-acting gas bearing. Speeds are upward of 10,000 rpm, continuous and unidirectional. Loads are small. Sizes vary up to perhaps 1 in. in diameter. Temperatures are usually within the range -45° to 165°F.

18.3.7.2 Recommended Lubricants (for Ball Bearings)

Because gyroscope bearings are protected against exposure to vacuum and possibly to reactive atmospheric constituents, the choice of lubricant is based primarily upon the service conditions of load, speed, and lifetime. The lubricating oils normally selected for this service have sufficient radiation resistance for 1-year service in the orbits considered.

Lubricants generally used are highly refined mineral or synthetic oils such as KG 80 of the Kendall Refining Company. These are vacuum impregnated into the retainer, which is made of a porous material such as Synthane (a paper-base phenolic laminate).

18.3.8 Lubricants in Oxidizers

18.3.8.1 Operating Conditions

Liquid rocket engines employ strong oxidizers such as liquid oxygen. Materials in contact with these must be inert to prevent explosions.

18.3.8.2 Recommended Materials

Fittings on oxidizer and oxidizer pressurization lines may be lubricated with highly halogenated materials such as nonadhesive-backed Teflon and Kel-F tape, or Fluorolube oils and greases.

18.3.9 Slip-Ring Assemblies

18.3.9.1 Operating Characteristics

Slip-ring assemblies are used for transmitting power and signals in spacecraft devices. Lifetimes are limited by wear rates and excessive electrical noise, which interferes with the transmission of intelligible signals. Metal-to-metal contact is desirable from the standpoint of reducing noise but, on the other hand, results in more rapid wear than if lubricant films are used and eventually results in excessive noise.

18.3.9.2 Recommended Materials

Metal contacts impregnated with molybdenum disulfide should be considered for slip rings or brushes operating in vacuum. Graphite and metals impregnated with graphite should not be used unless the assembly can be pressurized with air and hermetically sealed. For miniature slip ring assemblies with brushes and rings of precious metals, low noise and wear can be achieved by providing a partial pressure on the order of 10^{-6} Torr of silicone oil; a porous material impregnated with the oil and mounted adjacent to the slip ring assembly provides a suitable reservoir for maintaining an oil vapor atmosphere, even if the unit is not sealed tightly. Studies have shown that the slip-ring mechanism average peak electrical noise was significantly reduced when a low partial pressure of the nonhalogenated silicone oil DC 704 was introduced into the vacuum test chamber. Graphite brushes impregnated with molybdenum disulfide should be considered for dc motors that must operate in vacuum.

18.3.10 Metal-Metal Adhesion (Cold Welding)

Unlubricated metal pairs in contact under load can adhere in air or in vacuum. This results because the unit load on the surface asperities (high points) may exceed the yield strength of the softer metal, and it is possible for metal transfer to occur because of plastic deformation during relative motion of the contacting pair. The temperature at the points of loading can be quite high so that the possibility of the welding of junctions is increased.

There has been much space simulation testing of the tendency of metal pairs to adhere. In some work to evaluate the metal-metal adhesion tendencies in vacuum of metals and alloys for the Apollo program, the ranking shown in Table 18-5 was developed.

The specimens were of controlled surface finish and flatness. They were at 200° C (392° F) in a vacuum of 5×10^{-9} Torr under a contact pressure of 1000 psi; the rotational velocity was 0.4 in/sec (Ref. 11). The tendency for metals to adhere depends

upon the condition of their surfaces, the presence of surface compounds (oxides, nitrides or sulfides), their relative velocities, and their yield strengths. Table 18-5 gives a complete realignment of the ranking under dynamic conditions as compared with static conditions. Thus, unless the complete history of the surfaces of the materials, their relative motion, their mechanical properties, and their metallurical pedigree are known, it is difficult to evaluate the cold-welding tendency of a given metal pair. Effective hydrodynamic or boundary lubrication can substantially minimize the tendency of a metal pair to adhere.

Table 18-5

RANKING OF TENDENCY FOR METALS TO COLDWELD IN ULTRAHIGH VACUUM

Static Breakaway After 300-hr in Vacuum[a]	Average Coefficient of Friction	Dynamic Coefficient, Maximum Value[a]	Average Coefficient of Friction
Ti-6Al-4V	0.46	Cobalt	1.43
Beryllium-copper	0.81	Ti-6Al-4V	1.59
321 Stainless steel	0.86	Beryllium-copper	2.36
René 41	0.86	2014-T6 aluminum	2.52
Cobalt	0.89	321 Stainless steel	2.53
Coin silver	0.92	E52100 steel	2.86
Copper	1.03	Coin silver	3.40
E52100 steel	1.06	René 41	3.63
2014-T6 aluminum	1.21	Copper	3.80

(a) Average values from metal combinations of specified metal with itself and the eight other metals.

18.4 POLYMERIC MATERIALS FOR ADHESIVES, SEALS, AND STRUCTURAL APPLICATIONS*

The principal environmental effects that must be considered in selecting optimum polymeric materials for adhesive, seal, structural, and related applications have been discussed in Chapters 10, 11, and 12. This section will present relative ratings of these materials for space use based on environmental effects. (See Tables 18-6 to 18-16.)

Explanation of the rating system for each of the classes of materials is given in Tables 18-6, 18-9, 18-10, and 18-14. Tables 18-7, 18-11, and 18-15 are materials selectors covering several typical spacecraft missions. Except for a few metallic seal materials required for the more severe applications, all the materials presented

*Based on Chapters 10 and 12 by R. E. Mauri and Chapter 11 by R. F. Betts.

are polymers. These materials are rated on the basis of their suitability to perform a given function and on their stability to the environments encountered in spacecraft service. The recommended materials belonging to the several rated categories along with summarized information on space environmental effects bearing on their selection are listed in Tables 18-8, 18-12, 18-13, and 18-16.

Only representative commercially available materials widely used by the aerospace industry are rated. No attempt has been made to rate all possible commercial materials or those that are considered experimental. Most polymeric materials are identified by their generic chemical names. However, adhesives, because of their complex formulations and proprietary natures are identified by tradenames. It is therefore necessary to rate examples of a specific manufacturer's product. It should not be construed that endorsement is given to a given product or its manufacturer. Other comparable and competitive formulations having properties similar to those recommended may be equally suited for the intended application, but are not referred to in order to keep the volume of the information at a manageable level and because of the lack of supporting test data in the literature.

The relative ratings presented were made for materials applications on space vehicles for mission durations of 0.1 and 1 year. Each orbital altitude and mission duration establish the natural environment associated with materials service. In particular, the total incident dose of penetrating radiation varies greatly with these parameters and also with the degree of shielding afforded a material by the vehicle skin or component housing.

The use of the tables may be illustrated by randomly selecting a specific material application such as high-energy propellant seal for use in a vehicle to orbit at, say, an altitude of 1152 sm. If the seal is required to perform reliably for 1 year in such an environment, reference to Table 18-11 shows that materials of relative rating A or A* are recommended. Table 18-9 gives the relative ratings and Table 18-12 identifies the materials. Since the application was that of a seal for propellant service, the choice is limited to A and A* materials. Further qualifications and limitations regarding the use of the materials are given under "Remarks." Note that there may be some limitations on the use of some A materials, although considered satisfactory for propellant seal service from the compatibility standpoint, because of the high internal radiation dose encountered even with the shielding afforded by a 0.01-in.-thick aluminum alloy skin (or equivalent). This dose approaches the limiting radiation dose for retention of useful properties of Teflon. Incorporation of additional shielding, however, such as the use of a sufficiently thick seal housing, would permit the use of A-rated materials for this mission. Notice that although Teflon could be the choice for this application, consideration must be given to the selection of nitroso rubber if the application is for sealing of N_2O_4 or IRFNA systems. The limitations on this choice are, of course, a current lack of radiation effects data and the incompatability of the material with hydrazine and Freon.

As another example of the use of these tables, consider an application involving the use of a polymer film for wrapping electrical cable harnesses on the external portions

Table 18-6

RELATIVE RATING OF ADHESIVE MATERIALS

Relative Rating	Description
I	Recommended structural adhesives for high-strength metal-to-metal bonding applications
II	For moderate elevated and reduced temperature, high-strength, general purpose, metal-to-metal bonding applications
III	For general and specific non-structural bonding applications at moderate temperature and radiation
IV	For general and specific non-structural bonding applications at moderate temperature and low radiation

Table 18-7

MATERIALS SELECTOR FOR ADHESIVES IN SPACE MISSIONS

Mission Duration (yr)	Application	Materials Rating[a]			
		230-sm orbit	576-sm orbit	1152-sm orbit	2304-sm orbit
0.1	Surface	I, II, III	I, II, III	I, II, III	I, II, III
	Internal	I, II, III, IV	I, II, III, IV	I, II, III	I, II, III
1	Surface	I, II, III	I, II, III	I	I, II
	Internal	I, II, III, IV	I, II, III	I, II, III	I, II, III

(a) Relative ratings are given in Table 18-6 and lists of adhesives in Tables 18-8.

Table 18-8

RECOMMENDED ADHESIVES FOR SPACECRAFT BONDING APPLICATIONS

Relative Material Rating	Chemical Types	Radiation Dose Limit (rad)	Temperature (°F)		
			Maximum		Minimum
			Short Time (1/2 hr)	Continuous	
I	Epoxy-phenolic	10^9	600	500	-300
	Vinyl-phenolic	10^8	180	180	-67
II	Nitrile-phenolic	5×10^8	300	250	-65
	Epoxy (filled)	5×10^8	250	200	-300
	Modified epoxy	3×10^8	400	300	-423
	Polyimide	—	1000	600	-423
	Polybenzimadazole				
III	Nylon-epoxy	10^8	200	180	-423
	Neoprene-phenolic	10^8	200	180	-100
	Nylon-phenolic	10^9	250	200	-100
	Modified phenolic		600	450	-100
	Polyurethane	5×10^8	150	120	-423
IV	Silicones	5×10^6	650	500	-65
	General Purpose Thermoplastic and Elastomeric Non-structural (low-strength) Adhesives	5×10^6	225	180	-40

Table 18-9

RELATIVE RATINGS OF MATERIALS FOR PROPELLANT, HYDRAULIC, AND PNEUMATIC SEALING APPLICATIONS

Relative Rating	Applications and Qualifications
A	Preferred material for most applications. Suitable for long-term operation under the most severe environmental and service conditions.
A*	Preferred metallic seal materials but use should be restricted to those applications where the most severe environmental and service conditions are encountered and where operational requirements cannot be met with conventional elastomeric seals.
B	Satisfactory. Use wherever processing or design considerations do not permit use of A-rated material or when environmental or service conditions are less severe.
C	Not recommended. Use only in specialized, limited service applications.
D	Not to be used as seals under these conditions.

Table 18-10

RELATIVE RATINGS OF MATERIALS FOR VACUUM SEALING APPLICATIONS

Relative Rating	Applications and Qualifications
S	Preferred material for vacuum seals.
S*	Limited to vacuum applications whose seal will not be broken.
M	Marginal for vacuum seals, more permeable to gases than S-rated materials.
U	Not generally recommended for vacuum sealing operations.
N	Radiation dose in these orbits exceeds limit of resistance of available elastomeric or plastic sealing materials.

Table 18-11

MATERIALS SELECTOR FOR SEALS IN SPECIFIC SPACE MISSIONS

Mission Duration (yr)	Materials Rating[a]									
	Service			Vacuum Sealing		Service			Vacuum Sealing	
	Propellant	Hydraulic	Pneumatic	External	Internal	Propellant	Hydraulic	Pneumatic	External	Internal
	230-sm Orbit					576-sm Orbit				
0.1	AA*BC	AA*BC	AA*BC	SS*M	SS*MU	AA*BC	AA*BC	AA*BC	SS*M	SS*MU
1	AA*BC	AA*BC	AA*BC	SS*M	SS*M	AA*	AA*	AA*	N	SS*M
	1152-sm Orbit					2304-sm Orbit				
0.1	AA*BC	AA*	AA*	N	SS*M	AA*BC	AA*BC	AA*BC	N	SS*M
1	AA*	AA*	AA*	N	SS*	AA*	AA*	AA*	N	SS*

(a) Relative ratings are given in Table 18-9 and materials in Table 18-12; relative ratings for materials for vacuum seals are given in Table 18-10 and materials for vacuum seals are given in Table 18-13. When more than one rating symbol appears for a given mission, materials in all of the indicated rating categories are considered suitable for that mission.

Table 18-12

SEAL MATERIALS FOR PROPELLANT, HYDRAULIC, AND PNEUMATIC APPLICATIONS

Material	Application	Continuous Operating Temperature Range (°F)	Penetrating Radiation Damage (rad)	Relative Ratings			Remarks
				Propellant Service	Hydraulic	Pneumatic Service	
Metal Seals							
Aluminum (1100)	Static crush and wedge type seals (primarily for long-term service under severe environmental usage)	-300 to 700	$> 10^{12}$ (Not a limitation for spacecraft)	A*	A*	A*	Preferred seal materials for long-term service with high-energy fuels and oxidizers (e.g., N_2O_4, IRFNA, UDMH, hydrazine). Avoid dynamic applications (e.g., reciprocating and rotating shaft seals). Limited use in hydraulic and pneumatic seal applications where extreme environmental resistance is required.
Stainless Steel (301)		-300 to 1500		A*	A*	A*	
Nickel (Inconel)		-300 to 1800		A*	A*	A*	
Copper		-300 to 700		D	A*	A*	Same as above except unsatisfactory for oxidizer and fuel service. May be used for hydraulic and pneumatic seal applications where conditions warrant.
Carbon Steel		-300 to 1500		D	A*	A*	
Elastomeric Seals							
Butadiene-Acrylonitrile Rubber (Buna-N)	Static and dynamic seals (e.g., O-rings gaskets, boots) for applications such as access doors, air locks, pneumatic, hydraulic, and propellant seals for tanks, lines, and valves	-40 to 250		D	A (Except silicate and phosphate esters)	A	Preferred seal material for hydraulic and pneumatic service under static and dynamic conditions. Do not use with MIL-L-7808 diester oils, phosphate, and silicate esters. Depending on type and nitrile content, fair to good resistance to hydrocarbon fuels, oils, alkalis, and acids. Fair heat resistance with low permeability to gases.

Table 18-12 (cont'd)

Material	Application	Continuous Operating Temperature Range (°F)	Penetrating Radiation Damage (rad)	Relative Ratings			Remarks
				Propellant Service	Hydraulic	Pneumatic Service	
Neoprene		-65 to 250	10^7 to 2×10^8	D	D (Except silicate esters)	B	Recommended for pneumatic service under static and dynamic conditions. Similar to Buna-N in radiation and temperature resistance. Wide range of mechanical properties depending on formulation type. Not recommended for propellant or hydraulic service. Good resistance to non-aromatic fuels, solvents, and fatty oils; good water and alkali resistance.
Natural Rubber		-40 to 225	10^6 to 3×10^8	D	D	B	Not to be used for propellant or hydraulic seal service but can be used for low pressure pneumatic seals. Poor weathering and aging resistance. Stress cracks in ozone and ultraviolet. Highest radiation resistance in absence of O_2. Fair gas permeability. Resistance to water, acids, and alkalis. Poor aromatic and aliphatic fuel, oil, and solvent resistance.
Ethylene-Propylene Rubber		-65 to 300		A			Recommended for propellant service in contact with hydrazine.

Butyl Rubber		-65 to 225	10^6 to 10^7	C (Except oxidizers)	D	A	Preferred seal material for pneumatic service under static and dynamic conditions. Limited service to hydrazine type fuels for short periods. Not compatible with oxidizers (e.g., N_2O_4, IRFNA) except for momentary (splash) contact. Good water and alkali resistance. Poor resistance to oils, aromatic and aliphatic gasolines, and all but oxygenated solvents. Least radiation-resistant elastomer. Gradually softens and at 6×10^7 rad becomes useless tarry fluid. Extremely low permeability to gases.
Nitroso Rubber	N_2O_4 or IRFNA propellant seals	-40 to 375	Not known	B (Except hydrazine)	C	C	Has best long-term resistance to N_2O_4 or IRFNA of all elastomeric sealing materials. Avoid use with hydrazine-type fuels and highly fluorinated materials such as Freon.
Fluoro-silicone Rubber		-100 to 400	10^6	D	D	C	Not to be used for propellant or hydraulic seal service but can be used for low pressure pneumatic seals. Static sealing applications only.
Styrene-Butadiene Rubber (Buna-S, GRS, SBR)	Static and dynamic seals (e.g., O-rings, gaskets, boots) for applications such as access doors, air locks, pneumatic,hydraulic, and propellant seals for tanks, lines, and valves	-40 to 250	5×10^6 to 6×10^8	D	D	B	Not recommended for propellant or hydraulic service although compatible for short period with hydrazine type fuels. May be used for low-pressure pneumatic seals. Poor resistance to aromatic and aliphatic gasolines, oils, and solvents. Fair to good resistance to water, acids, and alkalis.

Table 18-12 (cont'd)

Material	Application	Continuous Operating Temperature Range (°F)	Penetrating Radiation Damage (rad)	Relative Ratings			Remarks
				Propellant Service	Hydraulic	Pneumatic Service	
Buna-S (Cont)							Better weathering and ultraviolet resistance than natural rubber, which it otherwise closely resembles in properties.
Silicone Rubber		-70 to 480	5×10^6 to 5×10^7	D	D (Except phosphate esters)	B	Not recommended for propellant or hydraulic service. Satisfactory for high temperature pneumatic seals but has highest gas permeability of any elastomer. Among highest heat resistance of all elastomers (smokes at 550°F). Fair water resistance poor resistance to oils, gasoline, and solvents. Poor radiation stability. Becomes brittle and crumbly at 5×10^8 rad.
Viton (Fluororubber)		-65 to 450	5×10^6 to 5×10^7	C (Short term only)	A (Except phosphate esters)	A	Preferred seal material for pneumatic and hydraulic applications for high temperature, high pressure operation. Extremely low permeability to gases, and outstanding temperature resistance. May be used for limited short-term service with UDMH, but incompatible with oxidizers for more than momentary (splash) contact. Poor radiation stability, especially when irradiated in air at temperatures above 250°F. Can be used at high temperature with many types of fuels, lubricants, hydraulic fluids, and solvents, and is highly resistant to ozone and weathering. Good mechanical properties.

Elastomeric Sealants							
Polysulfide Rubber (RTV)	Sealant applied as a trowelable caulking to adherend surfaces. Intended for fluid pressure sealing of non-removable doors, bulkheads, windows, etc., to structure.	-65 to 180	5×10^5 to 5×10^6	D	C	C	Very good water resistance. Good alkali resistance. Fair acid resistance. Excellent hydrocarbon fuel and oil resistance. Used as fuel tank sealant. Poor vacuum and temperature resistance. Low radiation stability. Gradually softens to tarry material. Satisfactory for pneumatic and hydraulic sealing at low pressures (except silicate and phosphate esters). Fair to poor gas permeability. Poor mechanical properties. Room temperature curing.
Silicone Rubber (RTV or LTV)		-70 to 480	5×10^6 to 5×10^7	D	D (Except phosphate esters)	C	Room temperature vulcanizing Smokes at 210° F. See silicone rubber. Good vacuum stability but high permeability to gases. Incompatible with propellants and hydraulic fluids (except phosphate types). Limited use for sealing pneumatic lines. Poor adhesion to substrates – requires metal priming. Poor radiation stability. Excellent thermal resistance.
Thread Sealant	Thread sealant and retainer (nuts and bolts)	-75 to 250	10^8 est.	C	B	A	"Loctite A," Class 10 smokes at 450° F. Backup thread seal for low order pressure differential.

Table 18-12 (concl'd)

Material	Application	Continuous Operating Temperature Range (°F)	Penetrating Radiation Damage (rad)	Relative Ratings			Remarks
				Propellant Service	Hydraulic	Pneumatic Service	
Plastic Seals and Retainers							
Nylon (Hexamethylene-diamine Adipimide)	Back-up rings and low pressure moving seals and gaskets	-100 to 300	5×10^7 to 10^9	C	B	B	Recommended seal or retainer material for UDMH service only. Not for use with hydrazine or oxidizers. May be used for hydraulic or pneumatic seals, gaskets, and retainers. Good radiation and temperature resistance.
Teflon (TFE) Unfilled and filled with inorganic fibers (Polytetrafluoro-ethylene)		-400 to 500	10^5 to 10^6	A	C	C	Preferred seal or retainer material for propellant service for all but the longest exposures. Inert to practically all materials but lacks resiliency and subject to "cold-flow" under compressive stress. Very poor radiation resistance, particularly in air. At 10^7 rad it becomes a useless crumbly solid. In vacuum or inert atmosphere, radiation resistance is up to two orders of magnitude higher. Most heat-resistant polymer for seal use. Fillers improve radiation resistance slightly but lower chemical inertness. Filled Teflons hold seal better than solids.

Teflon (FEP) (Fluorinated-ethylene-propylene) (Filled and unfilled)		-400 to 450	10^5 to 10^6	A	C	C	Similar properties to TFE except more limited temperature range. Slightly higher radiation resistance. Preferred for seal service with propellants under all but longest exposures. Limited use in hydraulic, pneumatic seal application.
Kel-F (Polytrifluoro-chloroethylene)		-400 to 350	10^6 to 10^7	B	C	C	Similar properties to Teflon. Slightly more permeable to N_2O_4. Radiation stability slightly better than Teflon, above 10^8 rads becomes very brittle.
Kynar (Polyvinylidene fluoride)		-80 to 300	10^7	C	C	C	More abrasion resistant than Teflon.
Polyethylene		-100 to 180	2×10^7	D	B	D	Resists most solvents.
Polyvinyl chloride		-100 to 200	2×10^7	D	A	D	Good compressibility and resiliency.

Table 18-13

MATERIALS FOR VACUUM SEALING

Material	Air Permeability at 75° F (10^{-7} cm^3/sec-cm^2-cm-atm STP)(a)	Penetrating Radiation Damage (rad)	Continuous Operating Temperature Range (° F)	Relative Rating	Application and Remarks
Metal Seals					
Aluminum	3.1×10^{-21}	$>10^{12}$	-300 to 700	S*	Crush and wedge seal one time application only
Copper		$>10^{12}$	-300 to 700	S*	Crush and wedge seal one time application only
Elastomeric Seals					
Viton (Fluororubber)		5×10^6 to 5×10^7	-65 to 450	S	Low permeability to gases, good vacuum stability, good temperature resistance, moderate radiation stability
Butyl Rubber	0.02	10^6 to 10^7	-65 to 225	S	Low permeability to gases, good vacuum stability, temperature resistance moderate, least radiation resistant elastomer, softens at 6×10^7 rad and becomes tarry liquid
Buna-N (Butadiene-Acrylonitrile Rubber)	0.13	10^7 to 10^8	-40 to 250	M	More permeable to gases than S-rated materials. Moderate temperature resistance, moderate radiation resistance
Neoprene	0.09	10^7 to 2×10^8	-65 to 250	M	Properties similar to Buna-N
Styrene-Butadiene Rubber (Buna-S) (SBR)	0.25	5×10^6 to 6×10^8	-40 to 250	M	Properties similar to Buna-N
Silicone Rubber	22	5×10^6 to 5×10^7	-70 to 480	U	Used because of high temperature stability, moderate radiation resistance; limited by gas permeability

Fluorosilicone		10^6	-100 to 400	U	Not generally recommended for internal or external vacuum seals. Has limited application because of high temperature stability, has high gas permeability and low radiation resistance.
Plastic Seals Teflon (TFE) (Polytetrafluoro-ethylene) Filled and Unfilled		10^5 to 10^6	-400 to 500	M	Has low resiliency and subject to cold flow under compressive stress. Has poor radiation resistance in air, in vacuum or inert atmosphere radiation resistance is two orders of magnitude higher. Has good temperature stability. Has higher permeability to gases than viton or butyl elastomers.
Plastic Seals Teflon (FEP) (Fluorinated ethylene-propylene) Filled or Unfilled		10^5 to 10^6	-400 to 500	M	Properties similar to Teflon (TFE)
Kel-F (Polytrifluoro-chloroethylene		10^6 to 10^7	-400 to 350	M	Slightly better radiation resistance than Teflon; slightly less temperature resistant than Teflon, otherwise properties similar to Teflon
Nylon (Hexamethylene-diamine Adipimide)		5×10^7 to 10^9	-100 to 300	U	Not generally recommended for internal or external vacuum seal applications; better radiation resistance than Teflon or Kel-F; lower temperature resistance; more permeable to gases and retains moisture which can outgas in vacuum.

(a) For helium.

Table 18-14

RELATIVE RATING OF STRUCTURAL PLASTICS

Relative Rating	Application
A	Recommended for general use in interior and external structural applications, particularly involving high energy penetrating radiation and elevated temperatures.
B	Not preferred for primary structural use but may be used in place of A-rated materials if electrical or processing requirements dictate. Recommended for internal or external secondary structure and electrical or thermal applications.
C	Not recommended for high-load structural applications but satisfactory for all internal and external low-load or nonstructural uses and where electrical requirements dictate.
D	For structural and non-structural sandwich construction, internal insulation or electrical harness lacing applications.

Table 18-15

MATERIALS SELECTOR FOR POLYMERS FOR STRUCTURAL AND RELATED APPLICATIONS

Mission Duration (yr)	Application	Materials Rating[(a)]							
		230-sm Orbit		576-sm Orbit		1152-sm Orbit		2304-sm Orbit	
		Reinforced Plastics – Laminates & Moldings	Polymer Films, Foams & Fibers	Reinforced Plastics – Laminates & Moldings	Polymer Films, Foams & Fibers	Reinforced Plastics – Laminates & Moldings	Polymer Films, Foams & Fibers	Reinforced Plastics – Laminates & Moldings	Polymer Films, Foams & Fibers
0.1	Surface	ABC	BC	ABC	BC	ABC	BC	ABC	BC
	Internal	ABCD	BCD	ABCD	BCD	ABCD	BCD	ABCD	BCD
1	Surface	AB	BC	AB	BC	AB	B	AB	B
	Internal	ABCD	BCD	ABCD	BCD	ABCD	BCD	ABCD	BCD

(a) Relative ratings are listed in Table 18-14 and Materials in Table 18-16.

Table 18-16

STRUCTURAL PLASTICS

Material	Continuous Material Temperature Range (°F)	Radiation Damage Threshold (rad)	Ultraviolet and Vacuum Stability	Relative Rating	Design Remarks
Phenolic Resin, Glass Fabric Laminate	-300 to 500	8×10^8 to 8×10^9	Good	A	Preferred structural plastic. Thermosetting. Excellent resistance to temperatures > 1000°F for short periods. Combined heat (to 900° F) and irradiation at doses up to 10^{10} rad produce no more degradation than does high temperature alone. Excellent mechanical properties throughout operating temperature range if properly postcured.
Epoxy Resin, Glass Fabric Laminate (Low Pressure) and Sheet (High Pressure)	-300 to 250	2×10^9 to 5×10^9	Good	A	Preferred structural plastic. Thermosetting. Undamaged in significant mechanical and electrical properties at dose of 10^9 rad, except impact strength which decreases approximately 30%. Best mechanical properties of any reinforced plastic at ambient temperatures but strength decreases rapidly at elevated temperatures.
Silicone Resin, Low Pressure Glass Fabric Laminate and Low Pressure Pre-Preg Glass Fabric Laminate	-300 to 500	10^9 to 5×10^9	Good	B	Excellent elevated temperature electrical properties. Good mechanical properties at temperatures of 750° F for short exposures.

Table 18-16 (cont.)

Material	Continuous Material Temperature Range (°F)	Radiation Damage Threshold (rad)	Ultraviolet and Vacuum Stability	Relative Rating	Design Remarks
Polyimide Polybenzimidazole Glass Fabric Laminates	-423 to 600	Not known	Not known	B	Both resins are comparatively new materials and are difficult to process as reinforced resin-glass composites. High-temperature strength retention warrants consideration for applications where this property governs selection.
Polyester Resin, Glass Fiber Laminate, Low Pressure	-100 to 200 -100 to 300	2×10^9 to 5×10^9 8×10^8 to 2×10^9	Good	B	Thermosetting. Laminate has good electrical and structural properties. General purpose structural laminate.
Phenolic Resin, Glass Fiber Molding	-300 to 450	8×10^8 to 8×10^9	Good	C	General purpose moldings. Good strength and temperature resistance. Not for primary structural applications.
Silicone Resin, Glass Fiber Molding	-300 to 500	10^9 to 5×10^9	Good	C	Not for primary structural applications.
Polyester Resin, Glass Fiber Molding	-100 to 180	2×10^9 to 5×10^9	Good	C	Not for primary structural applications. General purpose nonstructural moldings. Thermosetting. Good physical and electrical properties.
Melamine Resin, Glass Giber Molding	-65 to 350	10^8 to 10^9	Good	C	Not for primary structural applications. Excellent electrical properties, moderate temperature resistance. Thermosetting.

Modified Epoxy, Phenolic-Glass Fiber (heat resistant epoxy)	-300 to 500	5×10^9	Good	B	For general use in interior and exterior structural applications particularly where moderate to high temperatures and radiation exposures are encountered; excellent mechanical strength properties and good stability to vacuum and UV radiation
Films					
Polyimide (H-Film)(Kapton) Polyvinylfluoride (Tedlar)	-423 to 600	5×10^8	Good	B	Preferred materials for internal and external semi-structural and related applications (e.g., inflatable space structures, blanket insulation) particularly where long-term resistance to UV radiation is required and moderate temperatures and radiation doses are encountered; good vacuum stability and mechanical strength properties. Polymer films are generally aluminized on one side in most spacecraft applications.
Polyester Film (Mylar)	-100 to 300 (Low load applications)	5×10^7 to 1×10^8	Fair to poor UV stability unless metallized. Good in vacuum.	C	Inflatable semistructural film. Thermosetting type. For spacecraft, antennas, blanket insulation, etc. Low vapor permeability. Can be rigidized in space with foam-in-place materials and techniques. Aluminizing surface improves UV stability in space.
Polyethylene (High Density)	-320 to 225	10^8	Poor	D	Not preferred for long-term exposures to UV radiation unless surface is metallized but may be used for shorter missions internally or externally at low to moderate exposures and moderate temperatures; good vacuum stability. Note that radiation resistance of Teflon (FEP and TFE) is improved about two orders of magnitude in vacuum or inert atmosphere.
Polypropylene	-423 to 275	10^8	Fair	D	
Kel-F	-423 tp 350	10^6	Good	C	
Teflon (TFE)	-423 to 500		Good	C	
Teflon (FEP)	-423 to 450	5×10^5	Good	C	

Table 18-16 (cont.)

Material	Continuous Material Temperature Range (°F)	Radiation Damage Threshold (rad)	Ultraviolet and Vacuum Stability	Relative Rating	Design Remarks
Polyethylene (Low Density	-320 to 180	10^8	Poor	D	Not recommended for external applications because of UV radiation susceptibility; may be used internally in applications where low-to-moderate temperatures are encountered.
Polyvinyl Chloride (PVC)	-100 to 165	10^8	Poor	D	
Foams, Thermoplastic					
Polyurethane, Rigid Foam (Polyether)	-300 to 350	10^8 to 10^9	Good	D	Foamed sandwiches do not degrade in flexure and compression up to 10^9 rad. Vibration damping. Good electrical properties. Density range: 2 to 20 lb/cu ft (closed cell).
Polystyrene, Rigid Foam	-100 to 165	8×10^8 to 4×10^9	Good	D	Thermal insulation. Sandwich construction for low load applications. Density range: 2 to 6 lb/cu ft.
Foams (Closed Cell, Rigid Thermoset Types)					
Phenolic	-423 to 450	10^9	Not applicable; protected by sandwich skin	D	General purpose foamed sandwich and honeycomb materials for internal spacecraft applications.
Epoxy	-423 to 250	10^9			
Silicone	-423 to 500	10^9			
Fibers					
HT 1 (Nomex)	-423 to 600	5×10^8	Good	D	General purpose use for electrical harness lacing and other nonstructural applications. Dacron has slightly better thermal-vacuum stability than nylon.
Dacron (Polyester)	-423 to 300	10^8	Good	D	
Nylon	-320 to 300	5×10^7	Fair	D	

of an unmanned instrumented spacecraft. The purpose of the material is for thermal control, and analysis has shown that an aluminized polymer film will provide the required thermal properties. The orbit is beyond 2000 sm; the duration is 1 year.

Table 18-15 shows that B-rated materials are the only ones suitable for this orbit or duration. Table 18-14 shows that B-rated materials are recommended for external electrical or thermal applications. Table 18-15 shows two B-rated films, a polyimide (H-film) or a polyvinylfluoride (Tedlar). Since the application does not require the wide range of temperature stability of H-film (-423 to 600 °F), the choice for this application will be Tedlar.

In this application, the film is wrapped around the cable harness bundle and secured with a pressure-sensitive adhesive aluminzed tape. In the process of wrapping, many creases are developed in the film. These creases may crack the aluminized layer, allowing passage of unfiltered solar ultraviolet radiation to the substrate polymeric film. If the film were subject to embrittlement by ultraviolet degradation, the creases and cracks could cause flaking off of the aluminized layer. Vacuum-ultraviolet simulation tests of aluminized Mylar (polyester film) has indicated that this was indeed the case but that aluminized polyvinylfluoride did not flake. It has been found by space flight experience in the Mariner program that aluminized polyvinylfluoride films are more stable than the aluminized Mylar. One condition that must be considered is the loss of strength of these materials in ethylene oxide decontaminant (see Chap. 22).

There are many examples of the successful application of structural plastics for external and internal primary and secondary structure in successfully orbited spacecraft. Many other polymeric materials such as seals and adhesives have been successfully used in many exacting applications. Proper selection of these materials by designers and engineers for the correct application have resulted from examination of these materials properties where advantageous weight savings would be achieved through tradeoffs for higher density materials.

It should not be inferred that all the materials having the same relative rating will perform equally well for a given application. The best material for one design is not necessarily the best for another, and the designer must make the final selection based on his particular requirements. This section is intended only as a general guide to the designer and is a broad generalization of the material properties and environmental effects presented in detail in Chapters 10, 11, and 12 and the experience with materials related in Chapter 17.

18.5 MATERIALS FOR SPACECRAFT ANTENNAS*

The most frequently used metals for spacecraft antennas are aluminum and magnesium. The several alloys of these metals have good physical characteristics, are lightweight, and have good stability in the space environment. Titanium also has excellent properties for lightweight structural applications. Other lightweight structural metals are beryllium and beryllium-aluminum alloy. Table 18-17 lists metals recommended for

*Based on Chapter 13 by A. S. Dunbar.

Table 18-17

RECOMMENDED METALS FOR SPACECRAFT ANTENNAS

	Sheet Metal	Castings	Extrusions	Tubes	Weldments	Foil	Wire and Screen	Plating	Remarks
Aluminum Alloys	●	●	●	●	●	●	●		Used extensively, readily available, easily machined
Magnesium Alloys	●	●	●	●	●				Frequently used, readily available, easily machined
Titanium	●	●	●	●	●	●	●		Not commonly used
Steel	●	●		●	●		●		Used in structural applications where greater strength is required or high temperatures prevail
Stainless Steel	●	●		●	●	●	●		
Copper				●		●	●	●	Used for waveguides, transmission lines, and plating
Beryllium Copper	●			●		●	●		Fatigue resistant; excellent spring-forming qualities
Invar	●			●		●	●		Extremely low thermal expansion of both metals may be used to advantage in structures requiring thermal stability
Kovar	●			●		●	●		
Silver				●			●	●	Used principally for high microwave frequency waveguides
Gold								●	Excellent plating material
Rhodium								●	Used as flash over silver; does not oxide

● Recommended for use

spacecraft antennas. The selection of various metals will be based upon the required mechanical properties consistent with reliable fabrication processes, good engineering practice, and overall economic considerations.

Examples of the use of metals in spacecraft antennas include: beryllium copper tape for the Alouette 2 dipole antennas; aluminum honeycomb with aluminum foil skins for the Mariner Mars high gain antenna; aluminum honeycomb with titanium face sheets for the ATS-4 reflector antennas; and steel tape with Mylar coating for the Environmental Research Satellites. Surveyor used a planar array of thin aluminum face sheets on a glass fiber reinforced honeycomb core.

Table 18-18 lists recommended dielectric materials for spacecraft antennas. In all these materials, the dissipation factors are low and the physical properties are stable in the space environment except where noted. Polystyrene is one of the most stable in penetrating radiation. Teflon, polyurethane, and Kel-F are susceptible to radiation damage and should not be used in exposed situations where the radiation dose may exceed 7×10^6 rad. Micalex may be used for antenna windows where good structural strength is required and for dielectric structural components. Beryllium oxide has good dielectric properties and its thermal conductivity is similar to many metals, so so it can be used where heat flow is important. Boron nitride has also been used as a heat sink material in spacecraft electronic applications. Fiberglass laminates have been utilized with epoxy, phenolic, and silicone resins for structures as well as for good dielectric properties. High strength with low weight and good thermal properties in these materials make them useful for many antenna applications. Windows have been painted with metallic paint or laminated with metal foil to form complicated slot apertures and printed rf circuits. The foamed dielectrics, polystyrene and polyurethane, are used to load or pressurize cavities and to strengthen cantilevered components.

Table 18-19 lists materials used for inflatable and/or pressure-erected antenna designs. An inflatable Mylar ring antenna was deployed in space and operated satisfactorily on the OGO spacecraft.

All vehicle environments must be considered in the selection of cable insulation for spacecraft application. The vehicle environment will differ from the external space environment owing to temperature at the skin, temperature gradients, and the internal equipment rack environment. Table 18-20 summarizes the comparative temperature and rf attenuation characteristics of the Teflon, polyethylene, and polyolefin cable materials. The polyimide (H-film), polyvinylidene fluoride, polyvinylfluoride and FEP Teflon films are now finding considerable use as cable insulation.

Modified irradiated polyethylene has good radiation resistance but a low softening point. It cannot be used where the temperature will exceed 185° F. Modified polyolefin insulation has been used in some applications. Polytetrafluoroethylene polymers in cable is a good compromise insulation. Small-diameter Teflon insulated cables show severe radiation damage at high radiation dose rates (in excess of 5×10^6 R). One problem with thin Teflon insulation is the tendency to cold flow. A small amount of pressure between wires in contact can produce a short circuit.

Table 18-18

RECOMMENDED DIELECTRIC MATERIALS FOR SPACECRAFT ANTENNAS

	Molded Forms	Machined Forms	Structural Components	Radomes &/or Windows	Foam	Film	Fabric	Cable Core Material	Remarks
Polystyrene	●	●			●				
Polyurethane	●	●			●			●	Flexible Foam
Mylar						●			Highly resistant to ultraviolet
Teflon	●	●						●	Subject to radiation damage; should not be used in thin films
Kel-F	●	●							Subject to radiation damage
Rexolite	●	●							
Delrin	●	●	●						Harder than nylon, better machining than Teflon
Nylon	●	●	●				●		
Dacron							●		Fabric plated with copper, silver or gold used for reflectors
Aluminum Oxide	●			●					
Beryllium Oxide				●					Lower dielectric constant, higher temperature than Aluminum Oxide
Boron Nitride	●			●					Hot-pressed Boron Nitride more readily available, easier to work than isotropic pyrolytic material
Fused Silica	●			●	●				Slip-cast fused silica frequently used
Epoxy-glass laminates	●		●	●					
Polyester-glass laminates	●		●	●					
Silicone-glass laminates	●		●	●					Good high temperature material
Lockheat		●	●	●					A glass-inorganic composite material for high temperature radomes

● Recommended for use

Table 18-19

RECOMMENDED MATERIALS FOR PRESSURE-ERECTED ANTENNAS

Recommended Material	Remarks
Mylar-Aluminum Foil Laminates	Mylar-foil-Mylar laminates are flexible, have good thermal properties, are resistant to radiation, and possess adequate strength. They are the predominant materials used for inflatable and pressure-erected antenna designs
H-Film-Aluminum Foil Laminates	H-Film (Kapton) more resistant to ultraviolet radiation
Fiberglass Fabric Dacron Fabric Nylon Fabric	Plated with gold or copper, woven fiber materials make excellent flexible reflecting surfaces when held in tension by erected frame structures
Polyurethane Foam	An excellent flexible foam
Epoxy Cements	Strong, stable cements used to "iron-on" Mylar foil laminates

Table 18-20

TEMPERATURE AND r-f ATTENUATION CHARACTERISTICS OF CABLE MATERIALS

	Teflon	Polyethylene	Polyolefin
Maximum temperature	420° F	185° F	224° F
Minimum temperature	-120° F	-65° F	-65° F
Attenuation	least	acceptable	acceptable

An advantage of the H-film (polyimide) insulated cable, usually combined with fluorinated ethylene polymer (FEP) interlayers, is that it does not burn in a 5-psia oxygen atmosphere. The polyvinylidene fluoride and polyvinylfluoride continues to burn in this atmosphere, whereas the polytetrafluorethylene extinguishes when the source of heat is removed (Ref. 12). Semiflex outer conductor cables are the preferred engineering material for spacecraft application. Type TNC connectors are recommended for frequencies below 2 Gc and Type N or Type SC above 2 Gc. Above 4 Gc, waveguide is recommended where possible.

Gold plating is recommended for all contact surfaces.

Active rf components such as diodes, varactors, and ferrites should be used in a protected environment. The selection of component types and materials will be based on the application and the complete physical environment. Additional information on materials for antennas is given in Chapter 13.

18.6 ELECTRONIC AND MISCELLANEOUS COMPONENTS AND MATERIALS*

The space environment of overriding importance to the performance of electronic components is penetrating radiation. Except for the case of solar cell arrays, most electronic equipment is usually located within the interior of a vehicle so as to be shielded by the structure from ultra violet radiation and meteoroid bombardment; individual components are sealed against the vacuum environment where necessary.

Recommended components and materials for orbits of 230, 576, 1115, and 2304 sm are given in Tables 18-21 and 18-22.

At doses of penetrating radiation above 10^{12} n/cm^2 (fast), 10^{12} p/cm^2, 10^{13} e/cm^2, or 10^6 R of gamma radiation, this environment becomes a dominant factor in the choice of electronic materials and the design of electronic circuits. Semiconductor devices are among the electronic components most sensitive to radiation. To ensure successful operation in the radiation environment, the degradation of the electronic components should be known, and the design should take it into account.

Tunnel diodes, zener diodes, and high-speed thin-base switching diodes are relatively radiation resistant. Silicon-controlled rectifiers, unijunction transistors, and low-speed transistors are easily destroyed by radiation and should be used with caution. High-speed and field effect transistors are moderately resistant to radiation and may be used if their degradation is taken into account. Thin-base transistors are more radiation resistant than thick-base ones. High-frequency transistors are more resistant than low-frequency ones, and n-p-n silicon transistors are better than p-n-p ones of similar characteristics.

*Based on Chapter 14 by P. S. Castro, R. A. Glass, J. C. Lee, P. V. Phung, and F. F. Stucki.

Table 18-21

RECOMMENDED ELECTRONIC COMPONENTS FOR 1-YR CIRCULAR ORBIT SPACE MISSIONS

Component	90-deg Inclination Orbit (Polar)								30-deg Inclination Orbit			
	230 sm		576 sm		1152 sm		2304 sm		230 sm		576 sm	
	E[a]	I	E	I	E	I	E	I	E	I	E	I
Capacitors												
Paper and paper/plastic	U[b]	S	U	S	U	S	U	S	S	S	S	S
All others	S	S	S	S	S	S	S	S	S	S	S	S
Resistors												
Precision wire wound and film potentiometers	U	S	U	S	U	S	U	S	S	S	S	S
Other types	S	S	S	S	S	S	S	S	S	S	S	S
Electron Tubes												
Photomultipliers	U	M	U	M	U	M	U	M	M	M	U	M
Traveling wave tubes	U	S	U	S	U	M	U	M	M	S	U	M
Camera tubes	U	S	U	S	U	M	M	M	M	M	U	M
Infrared Detector Cells	S	S	U	S	U	S	U	S	S	S	U	S
Silicon Charged Particle Detectors	U	S	U	S	U	S	U	S	S	S	S	S
Semiconductor Devices												
P-N Junction Diodes	U	S	U	S	U	S	U	S	S	S	S	S
Tunnel Diodes	S	S	S	S	S	S	M	S	S	S	S	S
Bipolar Transistors	U	S	U	S	U	S	U	S	S	S	M	S
Junction Field Effect Transistors	U	S	U	S	U	S	U	S	S	S	S	S
MOS Field Effect Transistors	U	S	U	S	U	M	U	M	M	S	U	S
Unijunction Transistors	U	S	U	S	U	S	U	S	S	S	S	S
Silicon Controlled Devices	U	S	U	S	U	U	U	U	U	M	U	S
Miscellaneous												
Quartz crystals	S	S	S	S	S	S	S	S	S	S	S	S
Differential transformers	S	S	S	S	S	S	S	S	S	S	S	S
Magnetic cores	S	S	S	S	S	S	S	S	S	S	S	S

(a) E, external; I, internal (refer to components located outside, or inside, the shielding of a satellite skin of at least 0.1-in. Al alloy or equivalent.

(b) S, satisfactory for use; U, unsatisfactory; M, marginal value—more information needed.

Table 18-22

RECOMMENDED MISCELLANEOUS MATERIALS FOR
1-YEAR CIRCULAR ORBIT SPACE MISSIONS

Component	90-deg Inclination Orbit (Polar)								30-deg Inclination Orbit			
	230 sm		576 sm		1152 sm		2304 sm		220 sm		576 sm	
	E[a]	I	E	I	E	I	E	I	E	I	E	I
Refrigerants												
Freon	U[b]	S	U	U	U	U	U	U	U	S	U	U
Carbon dioxide	S	S	S	S	S	S	S	S	S	S	S	S
Explosives and Propellants												
RDX	M	S	U	S	U	U	U	M	M	S	U	M
TNT	S	S	S	S	S	S	S	S	S	S	S	S
Tetryl	S	S	S	S	S	S	S	S	S	S	S	S
Lead Styphnate	S	S	S	S	S	S	S	S	S	S	S	S

(a) E, external; I, internal (refer to components located outside, or inside, the shielding of a satellite skin of at least 0.1-in. Al alloy or equivalent).
(b) S, satisfactory for use; U, unsatisfactory; M, marginal value, more information needed.

Table 18-23 shows some of the materials used for insulation and dielectric applications. Most of these materials will be used in internal locations in the spacecraft so that some shielding of the space-penetrating radiation and most if not all of the unfiltered ultra violet radiation is effected by the spacecraft skin or structure. In most instances, electronic equipment is housed in some sort of a metallic container of either aluminum or magnesium alloys. (See Chapter 17.)

The relative ratings of these insulation and dielectric materials are as follows:

- A – Preferred materials for insulation and dielectric applications with stable properties in severe environments
- B – Satisfactory material with application limited by initial properties or property degradation in radiation, or thermal environments
- C – Use of such material limited to specific application unless shielded by protection of vehicle skin or container or some loss of certain properties can be tolerated

Encapsulating materials are listed in Table 18-24. The basis for selection of the best material for each application depends on the properties required and processing methods.

The list of acceptable materials has been reduced to epoxy and polyurethanes, with some use of silicone rubber and polysulfides to keep the list of materials to a manageable level. Ultraviolet radiation stability of these materials is applicable only when they are used external to the spacecraft structure.

Encapsulants for electronic devices should be selected on the basis of analysis of the electrical, mechanical, and thermal requirements of the particular design. Encapsulating resins have considerably higher coefficients of thermal expansion than embedded component materials such as metals, ceramics, and glass. These differences in coefficient of thermal expansion may cause severe internal stresses in electronic packages during thermal cycling and may cause cracking of the encapsulant or voids which can be sources of short circuits or high-voltage breakdown or arcing.

The recommendations listed in Tables 18-21 through 18-24 must be regarded as guideposts rather than as firm specifications because of uncertainties regarding the space environment, the statistical accuracy of tolerance data, and the exact applicability of the tolerance data. Within any single category, specific items may be better or worse than the tables indicate. More details on the behavior of electronic components are to be found in Chapter 14.

It is expected that new product developments and improvements will add rapidly to the list of preferred parts since the technology of radiation resistance is being accelerated in many areas. It is also noted that there is no strong discrimination between preferences for 230- and 576-sm orbits. This occurs because the altitude dependence of radiation fields is probably no stronger than their normal variations during a specific mission lifetime.

18.7 STRUCTURAL MATERIALS – INORGANIC*

Spacecraft usually are designed for specific mission requirements. Unmanned spacecraft are generally instrumented vehicles and require structure and housings for the support of guidance, telemetry, command, control, and power systems with mechanisms and actuators for solar panel arrays, horizon scanners, TV cameras, antennas, and instrument deployment booms. Manned spacecraft require structural materials for life support systems, cabin pressurization, communications, guidance, and attitude control. All spacecraft need surfaces for passive temperature control and mechanisms for active thermal control. Thus, the primary factors governing selection of inorganic structural materials are based upon optimum strength-to-weight ratios and required mechanical properties that are consistent with reliable manufacturing processes. In general, the effects of the space environment related to a specific orbit or trajectory do not govern the selection of spacecraft inorganic structural materials.

The inorganic structural materials that have proved successful in aircraft construction are readily applicable to spacecraft. Therefore, the aluminum alloys (A356, 2014, 2024, 2219, 5052, 5456, 6061, 7075, 7079, and 7178), the magnesium alloys (HM21A, HM31A, HK31A, AZ31B, ZH62A, and ZK60A), titanium alloys (commercially pure,

*Based on Chapter 15 by R. W. Parcel.

Table 18-23

ELECTRICAL INSULATION AND DIELECTRIC MATERIALS

Material	Continuous Material Temperature Range (°F)	Radiation Damage Threshold (rads)	Stability-Space UV and Vacuum[a]	Relative Rating[b]	Remarks
Electrical Insulation					
Polyethylene Expanded Tubing, Heat Shrinkable Types 1, 2, and 3	to 215	2×10^7 to 10^8	Fair	A	Type 1 – Heat shrinkable jacket insulation for equipment wiring. Type 2 – Material for repair of jacket defects Type 3 – Dual-wall shrinkable material for embedding parts (~75%) Excellent electrical properties for wire connector insulation and membrane insulation
Modified Neoprene Rubber Tubing Heat Shrinkable, Flexible	-65 to 250	3×10^6 to 3×10^8	Fair	C	For repair of jackets where oil resistance is needed; softens in benzene group solvents and in ketones
Polytetrafluoroethylene Coated Tape, Glass Braid Lacing	to 500	10^6	Good	B	Teflon coating limits radiation resistance, excellent electrical properties at elevated temperature
Vinyl Coated Tape, Glass Braid Lacing and Tying	to 215	2×10^7 to 5×10^8	Fair	C	Excellent electrical properties

(a) A 1 yr mission is considered here.

(b) A – Preferred materials for insulation and dielectric applications with stable properties in severe environments; B – Satisfactory material with application limited by initial properties or property degradation in radiation, or thermal environments; C – Use of such material limited to specific application unless shielded by protection of vehicle skin or container or some loss of certain properties can be tolerated.

Table 18-23 (cont'd)

Material	Continuous Material Temperature Range (°F)	Radiation Damage Threshold (rads)	Stability-Space UV and Vacuum	Relative Rating	Remarks
Irradiated polyalkene insulation with irradiated polyvinylidene fluoride jacket (Kynar)	-65 to 275	2×10^9	Good	A	Preferred cable insulation for all flight items. Is generally used in preference to polyolefin insulation, shielded cable will have irradiated polyvinylidene fluoride jacket
Irradiated Modified Polyolefin, Insulation for Vehicle Wiring	-65 to 275	5×10^8	Fair	A	Used for vehicle wiring and all flight items, thermally stabilized, and irradiated modified polyolefin insulated wire
Polyamide (Nylon)	-65 to 300	5×10^6 to 10^8	Good	C	Electrical insulation
Polyester (Mylar), Glass Filled	-70 to 300	2×10^9 to 5×10^9	Good	B	Electrical insulation
Polytetrafluoroethylene (Teflon TFE)	to 500	10^4 (air) to 5×10^6 (vacuum)	Good	B	Special applications requiring unique electrical properties or heat resistance, where radiation total dose is low
Natural Rubber (Anti-Rad Type)	-40 to 225	2×10^7 to 2×10^8	Poor	B	Elastomer for vibration damping; wire insulation and sheathing
Polychloroprene Rubber (Neoprene)	-65 to 250	3×10^6 to 2×10^8	Fair	C	Elastomeric cable sheathing, molded parts, bumpers, and shock absorbers, jacketing and sheathing only, not insulation

Synthetic Rubber (Buna-N)	-40 to 250	10^7	Fair	C	Cable jacket and tubing material; wire insulation
Neoprene Sheath, Buna-N insulated	-40 to 250	6×10^6 to 3×10^7	Fair	C	Cable sheath; wire insulation
Butyl Rubber	-65 to 250	10^6 to 10^7	Good	C	Elastomer for vibration damping; wire insulation or sheathing
Polyvinyl Formal (Formvar)	-75 to 325	2×10^7 to 3×10^8	Good	B	Magnet wire insulation; solar array application
Polyvinylidene fluoride (Kynar)	-65 to 275	2×10^7	Good	A	Preferred insulation material because of high resistance to UV radiation
Polyethylene	-70 to 250	2×10^7 to 2×10^8	Fair	A	Embrittled in UV radiation
Polyester (Mylar)	-100 to 300	5×10^7 to 5×10^8	Fair in UV unless metallized Good in vacuum	B	Electrical insulation in manufacture of cables. Thermosetting
Polyvinyl Chloride	-40 to 180	2×10^7 to 2×10^8	Poor	C	Electrical insulation and vibration protection. Plasticized types outgas and embrittle above 10^8 rad. Liberates HCl above 10^7 rad. Thermal decomposition may also liberate HCl.
Polyvinyl Fluoride (Tedlar)	-100 to 250	10^8	Good	A	Electrical insulations in manufacture of wire and cables. Has better UV stability than Mylar. Absorbs ethylene oxide and loses strength.

Table 18-23 (concl'd)

Material	Continuous Material Temperature Range (°F)	Radiation Damage Threshold (rads)	Stability-Space UV and Vacuum	Relative Rating	Remarks
Polyimide (H-Film, Pyre ML)	-423 to 600	10^8	Good	A	Electrical insulation in manufacture of wire and cables. Has better stability than Mylar. Absorbs ethylene oxide and loses strength. Can withstand thermal sterilization cycling.
Kel-F (Monochlorotrifluorethylene) AMS 3650	-80 to 300	3×10^6 to 2×10^7	Fair	C	Electrical insulation, thermoplastic elastomer; embrittled in UV radiation; may evolve corrosive gases
Tetrafluorethylene (Teflon TFE)	-150 to 500	10^5 air to 10^6 (vacuum)	Good	B	Electrical insulation, thermoplastic; low radiation resistance, releasing corrosive fluoride gases at higher doses
Polymethyl Methacrylates	-80 to 190	1×10^7	Good in vacuum; fair in UV	C	Magnet wire insulation; thin coating
Circuit Boards and Other Electrical Laminates					
Copper-Clad Epoxy, Glass Laminate	-65 to 300	5×10^9	Good	A	Printed circuit board
Epoxy-Glass Laminate	-65 to 300	5×10^9	Good	A	Material in thickness of 7 mils up to 0.25 in.
Epoxy-Glass Laminate	-65 to 250	5×10^9	Good	A	Satisfactory where used within temperature limits; antenna window and related uses

Phenolic Glass Laminate	-65 to 450	8×10^9	Excellent	A	Elevated temperature resistance to 700°F for short time less than 10 min; brackets, insulating blocks, and strips
Silicone Glass Laminated Sheet	-65 to 500	3×10^8	Fair	A	Use only where continuous temperature is over 300°F
Silicone Glass Laminate	-65 to 500	3×10^8	Fair	A	Good electrical properties and temperature resistance; antenna application
Diallyl Phthalate	-100 to 400	10^8		B	Used for molded potting containers; specify type and size
Copper-Clad Teflon Glass Laminate	-65 to 400	10^5 (air) 10^6 (vacuum)	Good	C	Restricted Use: Do not use in general applications; use only for VHF or UHF where other material is not satisfactory or a very precise or low dielectric constant is required. Specify laminate and copper thickness

Table 18-24

ELECTRICAL ENCAPSULANT MATERIALS

Material	Application	Continuous Material Temperature Range (°F)	Radiation Damage Threshold (rads)	Remarks
Polyurethane Encapsulants				
Eccofoam FP (Class A, B, and C) Emerson and Cuming, Inc.; Hitco R (Class A, B, and C) H. I. Thompson Co. Cond. I	Foam-in-place Cond. I	-65 to 165	10^8	Rigid foam encapsulant for mechanical shock and vibration damping; type is determined by maximum temperature of use, class is determined by density: Class A – 2 lb/ft^2, Class B – 10 lb/ft^2, Class C – 20 lb/ft^3
Eccofoam FP (Class A, B, and C) Emerson and Cuming, Inc.; Hitco MT (Class A, B, and C) H. I. Thompson Co. Cond. I	Foam-in-place Cond. I	-65 to 250	10^9	Type I: 165°F Type II: 250°F Type III: 350°F
Eccofoam FPH (Class A and B) Emerson and Cuming, Inc.; Hitco HT (Class B and C) H. I. Thompson	Foam-in-place Cond. I	-65 to 350	10^9	Vacuum and UV stability: Good. Discolors in UV
PE-102 American Latex Co.	Foam-in-place Cond. I Foamed slab Cond. II	-65 to 165		Flexible foam packing material; specify density and softness; not to be used for structural applications. Vacuum and UV stability: Good. Discolors in UV

Silicone Rubber				
Dow-Corning Corporation Class 1 Q-9-0031-1/2 Class 2 Q-9-3003-1/2 Class 3 Q-9-0006-1/2 Class 4 RTV-503 Products Research Company Class 1 PR-1930-1/2 Class 2 PR-1920-1/2 Class 3 PR-1910-1/2	Potting	-85 to 500	5×10^6	Requires rigid mold for mechanical shock and vibration, class determined by viscosity; should not be used at 400−500°F unless given a progressive cure in 100° steps to 500°F; use for elevated temperature where limited to room temperature to cure. Vacuum and UV stability: Good
Silicone Rubber Primer				
General Electric Co. SS-4004 Products Research Company 1902	Primer to RTV rubber	-85 to 500	5×10^6	Primer used silicone rubber; 1-hr cure at room temperature
Polysulfide				
3C-737, Class A 3C-747T Class B Churchill Chemical Co.	Potting	-70 to 300	10^6	Use for cable connectors; not for general purpose potting or embedding of electric modules. Vacuum and UV stability: Poor, may be used for ground based equipment

Table 18-24 (concl'd)

Material	Application	Continuous Material Temperature Range (°F)	Radiation Damage Threshold (rads)	Remarks
Epoxy Encapsulants				
Insulating Lacquer 1162 Dennis Chemical Company	Moisture resistant coating (thin)	-65 to 200	10^7	Spray or dip coat (< 0.005 in.); printed wiring board coating and pre-encapsulation check for non-welds in welded modules.
Coating, IRFNA and UDMH Resistant Furane Plastics, Inc., H2C-101	Coating, missile fuel and acid	-65 to 200	10^7	Packaged in aerospray bomb; acid and missile-fuel-resistant overspray coating.
Epocast H2E-011 Furane Plastics, Inc. Scotchcast No. 3 Minnesota Mining & Mfg. Co.	Impregnating	-65 to 300	5×10^8	Low-viscosity coil impregnant for inductors; not recommended for welded modules; rigid, unfilled epoxy.
Epocast H2E-012 Furane Plastics, Inc.	Potting	-65 to 300	5×10^8	Rigid, filled epoxy.
Hysol 4238/3475 Class A Hysol 4239/3487 Class B Eccobond 70C Class C	Conformal coating	-65 to 250		Electrically conductive; r-f interference applications, silver filled
Stycast 2762/Cat 17 Emerson and Cuming, Inc.	Potting and embedding	-65 to 500		Require elevated temperature cure for 500°F use

Epoxy Encapsulants				
Epocast 202/9615, Class A and B Epocast 202/9647, Class C and D Epocast 202-11/9615A, Class E Furane Plastics, Inc.	Potting, embedding, conformal coating	-65 to 200	10^7	Preferred material in its type for radiation protected applications in electronic enclosures in vehicles; clear amber-liquid resin; class is determined by hardness; hardener/resin ratio can be varied to produce Shore D hardness from 3 to 95; low Shore D will have decreased resistance to radiation and vacuum; shore D range of 50−85 is recommended for encapsulation of soldered and welded modules.
Epocast H2E-037 Furane Plastics, Inc.	Embedding	-65 to 250	10^8	Filled opaque compound for electrical insulation; semirigid, good thermal shock resistance. Vacuum and UV stability of epoxy encapsulants: Good.

Ti-6Al-4V, and Ti-5Al-2.5Sn), some stainless steels (AISI 302, 304, 410, 440C) and some low-alloy, high-strength steels (AISI 4340) in sheet, plate, structural shapes, extrusions, forgings, and some castings have been applied in spacecraft construction. Some of the high-alloy, high-strength steels have been used in special applications. For specialized applications such as rocket engines and rocket motor combustion chambers and nozzles, the refractory metals and alloys such as high-alloy stainless steels, nickel-based alloys (Rene 41), molybdenum, tantalum, and tungsten are being used where resistance to high-temperature, erosive exhaust gases may be encountered.

No appreciable effects on any of the inorganic structural materials are expected from the space environmental factors of vacuum, temperature, and radiation in earth satellite orbits or space probe trajectories. Vacuum sublimation of inorganic materials for lifetimes on the order of a year or more will not affect the structural properties of inorganic materials (i.e., metals and alloys, refractory metals, or ceramic materials). Erosion damage by sputtering of ions or solar plasma will be negligible for all structural inorganic materials.

Penetration and spalling of spacecraft skins by meteoroids is a potential problem. The probability of hits and penetration of spacecraft skins by meteoroids of a certain mass was discussed in Chapter 6. Explorer and Pegasus satellites and the Mariner 2 and 4 space probes have returned data on meteoroid encounters which were discussed in Chapter 6. From these data and the known properties of materials, survival probabilities can be estimated and material selection can be based upon structural requirements which will permit the calculation of required skin thicknesses.

In some of the more recent spacecraft such as Surveyor and the forthcoming Lunar Excursion Module (LEM), aluminum alloy honeycomb was used as an energy-absorbing material for the lunar landing. The recently published photographs from the Surveyor 1 mission showed that these crushable pad materials had successfully met their requirements.

Recent spacecraft have had onboard midcourse correction, vernier propulsion systems, and retrorockets. Refractory and high-strength materials have been used for the motor case, fuel and oxidizer tankage, and nozzle inserts and cones of these systems. The motor case of the Surveyor retrorocket was D-6A low-alloy, high-strength steel originally developed as a hot working die material but now finding aerospace applications. Fuel and oxidizer tankage, pressure vessels, and cryogenic tankage of stainless steel alloys and titanium alloys have also been used. Titanium alloy 6Al-4V in forged and welded hemispheres has been used for pressure vessels in such spacecraft as Apollo, Lunar Orbiter, Pioneer, and Surveyor. Interesting developments in the compatibility of this material with the hypergolic oxidizer N_2O_4 have been reported. A tendency for stress-corrosion cracking with water concentrations of below 0.6% in the N_2O_4 is possible. This tendency can be inhibited by the addition of up to 10% NO to the N_2O_4.

Stress corrosion cracking of welded titanium alloy tankage in aqueous solutions of methanol has also been reported. Methanol solutions were used to simulate the hydrazine fuel for qualification pressure testing of the tankage. The obvious solution to this problem is not to use methanol or chloride containing solutions for pressure testing titanium tankage (Refs. 13, 14, and 15).

To avoid possible compatibility problems of titanium alloys with liquid oxygen, the Apollo system will use forged and electron beam welded tanks of Inconel 718 alloys. Because of its excellent toughness at -423° F, the Ti-5Al-2.5Sn alloy will be used for liquid hydrogen and supercritical helium storage in this spacecraft system. One interesting metallurgical and design consideration with this material is the room-temperature creep with the low interstitial content specified for the application. In order to decrease the stress level, it was necessary to increase the design thickness of the vessel to take this behavior into account.

The refractory materials used recently were the graphite nozzle inserts in the Surveyor retro rocket motor and the silicon carbide nozzle inserts for the hypergolic liquid propellant vernier engines. The nozzle cones of the vernier engines were molybedenum-0.5% titanium alloy. For the LEM ascent engine, the nozzle skirt will be the columbium-10 hafnium alloy C103.

Some conflicting results of the effects of vacuum upon the mechanical properties of inorganic materials have been reported. Most of the experimental work has been done on aluminum and magnesium alloys. One investigator has reported decreasing fatigue life for polycrystalline aluminum with decreasing vacuum pressure in the 10^{-2} to 10^{-6} Torr region. Another investigator reports the opposite effect. For magnesium single crystals, it was reported that the stress required for a given strain decreased with decreasing pressure in the 10^{-6} to 10^{-8} Torr region and that the effect was more pronounced with higher strain rates.

For single crystal aluminum, a decrease in the work hardening coefficient was reported at low strain rates (4×10^{-6}/sec) in vacuum as compared with the value in air. In creep testing, a decrease in the activation energy of 500 cal/mole was found at shear strains of less than 2% and the change in activation energy decreased with increasing strain in the 10^{-4} to 10^{-7} Torr region.

The tensile behavior of polycrystalline aluminum, copper, and stainless steel did not change in vacuum. There was a 16.5% increase in the activation volume for creep in polycrystalline aluminum when tested in vacuum of 10^{-5} Torr; this effect did not appear to be strain-rate dependent (Refs. 16, 17, and 18).

These investigations seem to indicate that the plastic flow characteristics of metals and alloys may change in vacuum. These effects may be strain-rate dependent. It is postulated that changes in surface stress distribution in vacuum may be responsible for the reported changes in mechanical properties.

In summary, the selection of inorganic structural materials for spacecraft is not usually determined by the effects of the space environment on them. The selection and design can be based upon strength-to-weight ratios and the required mechanical properties consistent with reliable manufacturing processes. The base metals or alloys of aluminum, beryllium, magnesium, titanium, and high-strength steels and refractory metals are all candidate materials.

In presenting the behavior of materials in actual space environment or simulated environments, there is no implication that materials reported or not reported are either superior or inferior. The designer must satisfy himself that the materials selected are satisfactory for their intended use.

18.8 REFERENCES

1. E. E. Gaines et al., Satellite Encountered Radiation Doses From Trapped Particles, LMSC 6-75-65-3, Lockheed Missiles & Space Company, Sunnyvale, Calif., January 1965

2. J. I. Vette et al., Models of the Trapped Radiation Environment, NASA SP-3024, Aerospace Corp., El Segundo, Calif., 1966

3. J. L. Modisette et al., Model Solar Proton Environments for Manned Spacecraft Design, NASA TN-D-2746, April 1965

4. W. R. Webber, An Evaluation of the Radiation Hazard Due to Solar-Particle Events, BOAC D2-90469, December 1963

5. Robert M. Van Vliet, Passive Temperature Control in the Space Environment, The Macmillan Co., New York, 1965

6. C. G. Goetzel, J. B. Rittenhouse, and J. B. Singletary, Space Materials Handbook, 2nd ed., ML-TDR-64-40 (AD-646399) (X65-14878), Lockheed Missiles & Space Co., Sunnyvale, Calif., January 1965

7. J. B. Rittenhouse and J. B. Singletary, Space Materials Handbook, Supplement 1 to Second Edition, ML-TDR-64-40 Supp. 1, NASA SP-3025 (AD 629 720), March 1966

8. J. B. Rittenhouse and J. B. Singletary, Space Materials Handbook, Supplement 2 to Second Edition, AFML-TR-64-40, Supp. 2, 1968

9. J. L. Chinn, N. M. Ewbank, and G. Gigos, "Charged Particle Radiation Effects on Selected Transparent Materials in Aerospace Enclosures," in Transparent Materials in Aerospace Enclosures, AFMC-TR-65-212, Robert E. Williams, ed., September 1965

10. Program 461 Spacecraft Materials Handbook, LMSC-A327227, Lockheed Missiles & Space Company, Sunnyvale, Calif., August 1965

11. C. E. Moeller, J. Bossert, and M. Noland, Cold Molecular Welding Study in Ultra-High Vacuum, MRI Project 2817-E, Mid-West Research Institute, Kansas City, Mo., 8 October 1964 – 17 December 1965

12. L. J. Frisco and K. N. Mathes, Evaluation of Thin Wall Spacecraft Electrical Wiring, General Electric Company, Schenectady, N. Y., Report for Manned Spacecraft Center, Houston, Texas, 28 September 1965

13. J. D. Jackson, W. K. Boyd, and R. W. Stachle, Stress Corrosion of Ti-6Al-4V in Liquid Nitrogen Tetroxide, Defense Metals Information Center, Columbus, Ohio, DMIC Tech. Note, 11 April 1966

14. W. E. Berry, E. L. White, and J. J. English, Review of Recent Developments, Corrosion and Compatibility, DMIC, 30 November 1966

15. K. Mori, A. Takomura, and T. Shimose, "Stress Corrosion Cracking of Ti and Zr in HCl-Methanol Solutions," Corrosion 22 (2), 29 – 31, February 1966

16. R. H. Christensen and R. J. Bellenfonte, Some Considerations in the Fatigue of Launch and Spacecraft Structures, NASA CR-242, Douglas Aircraft Co., Santa Monica, Calif., June 1965

17. I. R. Kramer, H. Shea, and S. E. Podleseck, Effect of Vacuum on the Mechanical Behavior of Metals, AFOSR 64-2509, The Martin Co., Baltimore, Md., October 1964

18. D. P. Williams and H. G. Nelson, Effects of Vacuum on the Tensile Properties of Magnesium Single Crystals, Trans. AIME 233, 1339 – 1344, July 1965

PART 4

BIOLOGICAL INTERACTION WITH SPACECRAFT MATERIALS

Chapter 19

MATERIALS FOR MANNED SYSTEMS

M. Honma
G. B. McCauley

The design and construction of closed ecological systems, particularly for outer-space manned probes, lunar stations, orbiting space platforms, or other manned space centers require very careful consideration of materials behavior and characteristics. Because of great differences in the operating parameters in space, on the moon, or on other planets, materials that are usable in the ordinary earth environment must be thoroughly investigated in regard to their reaction to these new environmental conditions. Atmosphere contamination and fire hazards, among the many problems anticipated in this new manned venture, can become most serious or even lethal; thus, careful selections of materials become necessary. Recent symposia on toxicity and contamination in manned orbital flights such as Mercury and Gemini (Refs. 1, 2, 3) and in simulator studies (Refs. 4, 5) have pointed out problems with material associated with the closed system. Thus, in this new environment it is extremely important for the astronauts to reside compatibly with equipment and machinery within the confines of the living volume since the interdependence and relationships have achieved a new significance and the failure of either can result in compromise of the mission. In this sense, the newly expanded concepts of toxicity and environmental hazards cover not only the resident human within the closed system but also the multifold interaction with equipment and machinery. Hence, it is quite obvious that judicious selection of all materials, equipment, and parts, particularly those within the confines of the living volume, is necessary. In this respect, the "preventive" approach is preferable to the "removal" or "cure" approach. The preventive concept selects materials which will contribute minimally or not at all to contamination of the environment and hazards to the occupants, whereas the second approach relies on environmental control systems for the attenuation of the hazard and toxicity potential. At present, it seems likely that a compromise between the two approaches will be necessary.

19.1 SELECTION OF MATERIALS

The significance of proper selection and qualification of materials for use within a closed system has been amply demonstrated by both spacecraft successes and failures. The role played by materials in equipment performance and reliability is illustrated by partial failures attributed to materials. Usually it is not until a functional failure has occurred that a material is identified as the source and proper attention is focused on material selection. Even carefully selected materials for particular performance and design may show incomplete total engineering and the material performance may be unsatisfactory. Thus, for the selection of materials and their qualifications, the

specific requirements, their functions, relationships to other equipment, total mission objectives, and environmental parameters must be thoroughly evaluated. W. A. Symonds (Ref. 6) has shown schematically the order, process, and interaction involved in material selection, which narrows down to the following essential steps:

- Identification of requirements
- Selection of candidate materials
- Analysis of environmental capability of the material
- Qualification of the material

Figure 19-1 amplifies the material selection process. Identification of material requirements requires consideration of design, mission or system, and environment. The primary consideration is the function for which it is intended, i.e., electrical, optical, mechanical, or thermal. In addition, the mission or system requirement further includes functional period, reliability, weight, cost, and scheduling. The environmental requirements take into consideration materials use environment and such parameters as atmospheric pressure, radiation field, and thermal fluxes, as well as interactions with other functions. In this case, the interaction phenomena achieve an added significance because man with his multifold function further complicates the material requirements. The selection of candidate materials is based on the foregoing requirements applicable to the manned system and must include alternates and tradeoff considerations. Considered in the tradeoff are competing requirements based on mission objectives and include functional property retention, weight limitations, costing, and secondary material characteristic constraints. Selection techniques and acceptability limits for materials usage in the manned system are discussed in the next section.

In the analysis of material capability in the particular environment, detailed analysis of the effects of environment on specific engineering and material properties is required. The data required for this evaluation can be obtained from existing flight performances or laboratory tests that show the questionable functional property during exposure to a specific selected environment. For environmental parameters not specifically applicable, it may be possible to interpolate conditions such that the data generated are on an equivalent basis. For example, off-gassing of plastics and flammability of combustibles are affected by zero-gravity, which cannot be readily simulated on earth, but by judicious application of other parameters some equivalence can be obtained. Practical limitations are also imposed on material evaluations, especially in the exposure rate. Since equivalent space conditions are required for space simulation, the time factor becomes prohibitive and accelerated conditions become necessary. Generally one wishes to compress the time factor; accordingly other environmental parameters such as pressure, temperature, and composition of the atmosphere must be modified.

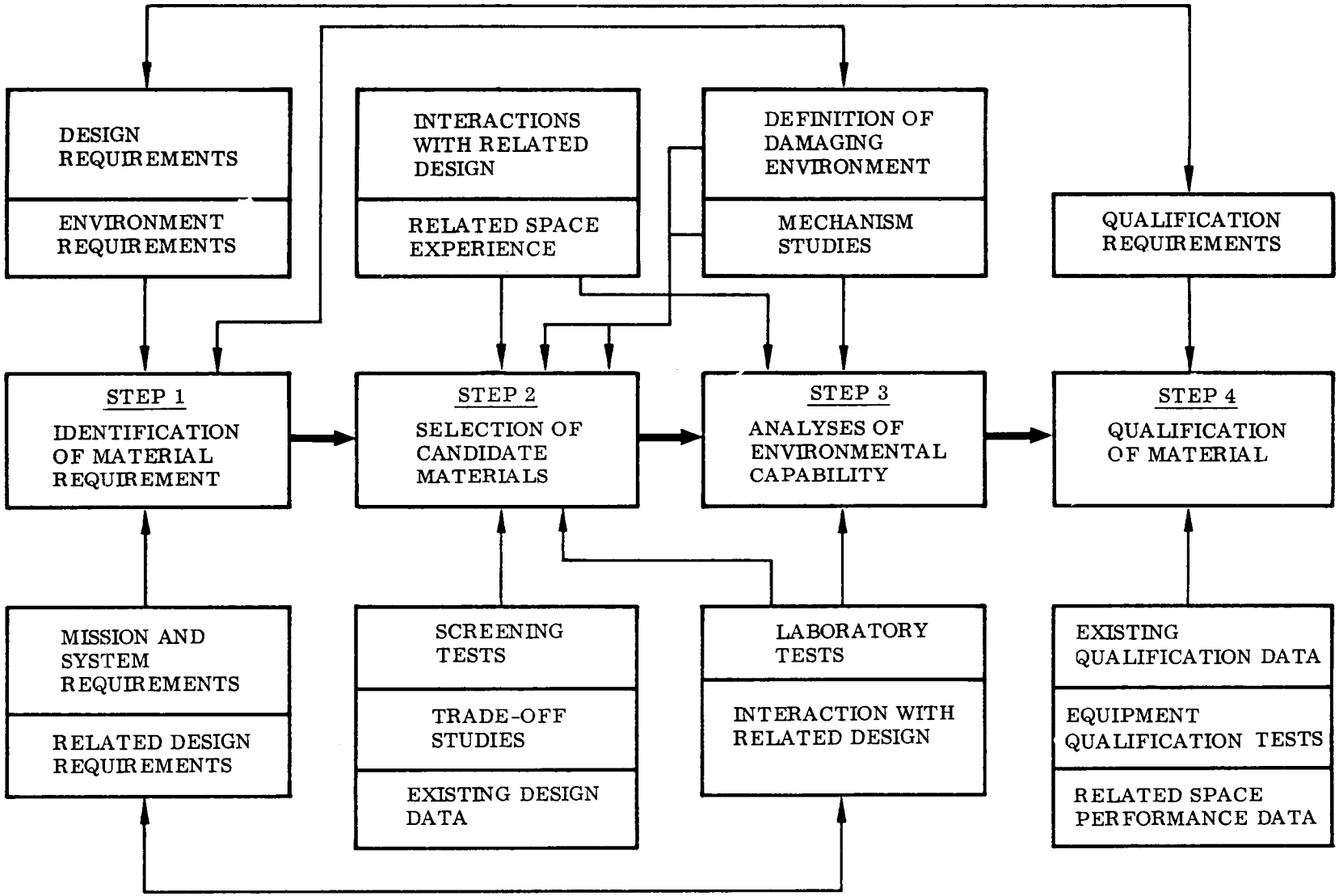

Fig. 19-1 Material Selection Process (Ref. 6)

The material or component must be qualified to the specific design, mission, and environment associated with the particular manned space program. The qualification is performed by the maximum utilization of previously developed data, which includes not only tradeoffs and screening tests but also data obtained from previous manned ventures, simulator statistics, and related studies. The qualification requirements are fulfilled from data and information obtained from specification and design data, materials qualification tests, equipment qualification tests, or related manned space qualifications resulting from relevant manned space missions.

19.2 ACCEPTABILITY LIMITS OF MATERIALS

The evaluation of acceptability limits here will include only factors that will ensure a safe, habitable atmosphere for the crew, although such factors constitute only part of the overall materials selection requirements. The selected limits are based at present on sustaining man so that he can adequately perform the tasks included in the mission objectives.

At present, NASA's Manned Spacecraft Center is concerned with the Apollo Command Module and the Lunar Excursion Module, while the Air Force is involved in the MOL program. Experience has shown that toxicity of materials, primarily inhalation hazards, noxious substances, and fire hazards, are of chief concern during manned occupancy of a closed system (Refs. 4, 7, 8). It has become necessary to control atmosphere contamination in the closed environment arising from the materials used within the spacecraft, in addition to contamination caused by man himself. Materials off-gassing is primarily of organic origin, such as plastics, surface coatings, adhesives, elastomers, and trace quantities of volatiles from these materials which gradually accumulate in the closed system producing hazards to both man and equipment. Fires in a closed system are extremely hazardous, and oxygen-enriched atmospheres have resulted in numerous explosions and unextinguishable fires. The recent Apollo 204 accident further emphasizes this hazard (Ref. 9).

The acceptability limits used and the testing methods employed to ensure a safe habitable atmosphere differ with each space program and with each manufacturer. Thus, some differences can be attributed to differing requirements for a particular spacecraft and its mission and others are simply due to idiosyncrasies of individual investigators and manufacturers upon which costs and urgency factors are superimposed. However, all present efforts are directed at toxicity and flammability hazards.

In earlier space programs, the manufacturers of Gemini determined the acceptability of nonmetallic materials based only on odor threshold where the material was tested in a simulated environment of 3 to 24 hr of continuous usage in 100% 5-psia oxygen at anticipated maximum-use temperature. Toxicity and temperature limits, although not based on actual tests, were extrapolated from basic physicochemical knowledge and odor tests. The later Apollo program requirements are much more stringent, and detailed testings are performed in both problem areas.

Boeing (Ref. 10), Lockheed (Ref. 12), Minneapolis-Honeywell (Ref. 13), NASA's Manned Spacecraft Center (Ref. 11), North American Aviation (Ref. 14), and others (Refs. 1, 2, 15, 16, and 17) have developed specialized techniques for assessment of materials for manned closed-environment use. Review of the data presented and the methods used point out the apparent need for standardization of testing procedures and material selection processes. In this respect, E. S. Harris of NASA-MSC has started a computerized parts and materials data retrieval program for nonmetallic materials based originally on toxic hazards but now including flammability data (Refs. 1 and 2). This Parts and Materials Master-File, at present composed of over 1,900 entries, is the most comprehensive to date. Available nonmetallic materials data may be obtained from the Non-Metallic Materials Information Center, Houston, Texas. The data, however, are a listing of pertinent properties, and the acceptability is left to the discretion of the user.

Acceptability limits for materials must be based on usage parameters and materials characteristics, much in the same manner as designated in the Apollo program (Ref. 18) where the selected categories are as follows:

- Extensively used materials exposed to crew bay
- Special applications and minor exposed materials in crew bay
- Materials in suit loop – low pressure to 19 psia
- Materials in high-pressure oxygen system
- Materials in hermetically sealed containers
- Materials in vented containers
- Materials in nonflight equipment
- Materials in uninhabited portions of the spacecraft

Each category of materials requires conformance to selected standard acceptance tests before approval for particular usage. Eleven acceptance tests and seven optional tests are indicated, and each category of materials must pass a designated set of these tests. Selection of nonmetallic materials is based on the following acceptability limits:

- Odor. The material after heating must have an odor of less than 1.5 based on olfactory test. The odor scale is 0 – not detectable, 1 – detectable, 2 – objectionable, 3 – irritating.
- Carbon Monoxide. 22 ppm (μg/g) or less based on sample weight.
- Total Organics. 100 ppm (μg/g) or less based on sample weight.

- Combustion Rate. 0.5 in./sec or less in 260 Torr of pure O_2.
- Flash Point. 400°F or greater.
- Fire Point. 400°F or greater.

19.3 TECHNIQUES FOR EVALUATION OF NONMETALLIC MATERIALS

19.3.1 Odor Test

Ten grams of bulk material are sealed in a glass chamber with 5 psia of pure oxygen. The chamber is heated at 200°F for 48 hr. (NASA-MSC prefers 155°F for 72 hr.) At the end of this time a known volume of the sample atmosphere is extracted and tested by a panel of selected evaluators using olfactometers (a mask made of odorless flexible material that is worn over the evaluator's face). The odor is evaluated according to the aforementioned scale and the rating of the panelists is placed on a common denominator.

19.3.2 Carbon Monoxide

Carbon monoxide is evaluated in conjunction with the odor test or as a separate test. In the separate test, carbon monoxide and total organic contents are obtained from a single test setup. In this respect, NASA-MSC (Ref. 22) has a well-defined test procedure.) The test equipment consists of a test chamber, heating source, vacuum pump, and analysis equipment. The test chamber, 2-liter minimum with the gas handling system, is constructed of stainless steel or lined with stainless steel, and other parts are certified nonvolatile under test conditions. The chamber is designed to prevent condensation or trapping of gaseous products except in the room-temperature condenser. The test chamber is provided with a thermometer or thermocouple and a pressure gage. Furthermore, the test chamber is connected to a series of traps, and inlet tubes – for evacuation, pressure reading, oxygen introduction, helium flow, and sample withdrawal for quantification of off-gassed products. The test chamber may be connected to a gas chromatograph and/or a mass spectrometer. The heating source is an oven capable of maintaining a constant temperature to ±5°F. The vacuum pump must be capable of vacuum of less than 1 Torr with little or no system contaminants. The analysis equipment is a calibrated gas chromatographic system equipped with suitable gas sampling devices.

Prior to sample evaluation, the test equipment is checked out with 5.0-psi oxygen and heated at 200°F for 24 hr, and the oxygen is analyzed for total organics and carbon monoxide. It is certified for use if the total organics are below 10 ppm by volume. If not, the container is heated and purged with clean air or nitrogen, then loaded with 5.0-psi oxygen and rechecked as described above.

The test system is also checked for leaks. At reduced pressure, 1 Torr for a period of 1 hr is the maximum allowable leakage.

Test specimens are classified in four categories, based on surface, volume, weight, or special items.

- Surface – films, coatings, finishes, fabrics, primers, tapes, adhesives, insulation, and the like; 300 ± 15 cm^2/liter of test container is used as the test sample. For materials having two surfaces exposed (e.g., fabrics, films) when in use, the total surface area is counted.

- Volume – materials having volume but also large surface areas – matting, foams, felts; 50 ± 5 cm^2 of total surface area per liter of test container is used.

- Weight – definite bulk (e.g., potting compounds, thick plastics, solid wires, molded compounds); 5 ± 0.25 g/liter of test container is used. Liquids are placed in a 2.25 ± 0.25 in. diameter aluminum dish weighed to the above specifications.

- Special Items – usually nonhomogeneous materials that do not fit the above classifications. The sample size, preparation, and testing are specified at the discretion of the test engineer and are completely documented.

The test procedure consists of the following steps:

- The test chamber is purged with MIL-0-27240 type 1 oxygen until the minimum oxygen concentration is 95% as determined with the gas chromatograph.

- The chamber is heated to 155° ± 5°F and the oxygen pressure adjusted to 5.0 ± 0.1 psia, then allowed to remain pressurized for leak checking.

- After 24 hr, the oxygen is checked for contaminants using gas chromatography. If the contamination level is below 10 ppm, sample exposure is initiated.

- A clean specimen prepared according to the above category is placed in the test chamber. The test chamber is then evacuated through a liquid nitrogen trap below 1 Torr.

- The test chamber is then closed off, heat is applied, and filtered oxygen (through Molecular Sieve 5X) is bled into the chamber. The exposure conditions are:

  T = 155°F ± 5°F
  p = 5.0 ± 0.1 psia 95% pure oxygen
  t = 72 hr

- At the end of the exposure time, the chamber is brought to room temperature and the gas analyzed for total organics and carbon monoxide. After final gas samples are taken, the test specimen is removed from the test chamber and weighed.

19.3.3 Total Organics

The organic off-gassing products are also determined with the odor test or performed separately. The separate determination of organic offgassing products is performed, together with the carbon monoxide determination. The NASA-MSC method (Ref. 22) is amply described in the preceding paragraph. A gas chromatograph with appropriate column and flame ionization detector (or equivalent), the Beckman Total Hydrocarbon Analyzer, or an equivalent instrumentation is used for the analysis.

19.3.4 Flash Point

For nonmetallic materials used in manned spacecraft exposed to pure oxygen environment, the flash point is defined as the lowest temperature at which a material will give off, at or near its surface, a flammable vapor which, when mixed with oxygen in the environment and exposed to an ignition source, will provide a non-self-sustaining flash or flame. This test is performed on a programmed temperature heated specimen in a special container that is sparked at 1-min intervals using a high voltage dc power supply.

19.3.5 Fire Point

Similar to the flash point, in the present concept the fire point is the lowest temperature at which a mixture of vapors from the surface of a material and oxygen continues to burn after ignition. A self-sustaining, self-propagating glow is considered to be equivalent to flaming combustion. The test is performed on the same apparatus as used for the flash point evaluation and constitutes a continuation of the flash point test.

19.3.6 Combustion Rate

Two types of tests are used to screen materials that could promote rapid spread of fire: propagation rate upward, and propagation rate downward. The upward burning test qualifies materials in sensitive areas such as crew bay, suit loop, and high-pressure oxygen area. The downward burning rate test qualifies minor exposed materials in the crew bay. A special test apparatus is used and the prepared sample is flame ignited at the bottom in the upward burning test and at the top in the downward burning test.

Many other test procedures for screening out potential toxicity and fire hazards have been designed. NASA-MSC (Ref. 18) has devised many methods for determining potential sources of fire. Listed below are tests and the failure modes leading to fire.

• Electrical wire insulation and accessory flammability	Combustion of insulation due to electrical overload
• Electrical potting and coatings flammability	Fire due to short-circuit and dielectric breakdown
• Materials in vented containers	Rupture and scattering of flame

• Electrical overload of hermetically sealed containers	Rupture and scattered fire and debris
• Simulated panel and assembly flammability	Electrical overload, short-circuit, or flame propagation from adjacent burning material
• Simulated crew bay configuration flammability	Hot wire ignition source fire in mockup vehicle
• Combined thermogravimetric analysis and spark ignition	Electrical fire combined with weight loss of material

Other supplementary tests for fire hazards are as follows (Ref. 18):

- Differential scanning calorimeter spark ignition: Fire and flash point of materials
- Electrochemical initiation of wire insulation fire: Fire caused by ignition of coolant fluid
- Autogenous ignition point determination: Lowest ignition temperature where mixing vapors will continue to burn after ignition
- Friction and impact ignition: Fire due to sensitivity of material
- Gap propagation: Effect of gap in preventing fire propagation
- Combustion test characteristics: Measure of amount of heat during combustion

Some of the experimental methods used in evaluation of toxicity potential are as follows:

- Vacuum stability: Volatiles weight loss, analysis of off-gas products
- Thermogravimetric analysis: Off-gassing as function of temperature
- Kinetics of off-gassing: Rate of contaminant evolution
- Analysis of off-gassing: Chemical species and their concentrations

When reliable spacecraft maximum allowable concentrations (SMAC) have been determined, together with the kinetics and off-gassing analysis, the acceptability of materials can be determined. Furthermore, in the not too distant future

the incorporation of a computer program with addition of considerable data and essential relevant parameters may permit prediction of the following:

- Rate of specific contaminant buildup
- Peak value and time of particular contaminant
- Time and value of eventual equilibrium

19.4 ACCEPTABLE MATERIALS FOR MANNED SPACECRAFT

The list of acceptable nonmetallic materials that may be candidates for manned spacecraft applications given in Table 19-1 and that will meet the specified acceptability limits with a few reservations has been obtained from several sources (Refs. 10, 13, 14, 15, 19, 20, 21). The selection of a particular material is dependent on its specific usage which more closely dictates material requirements. For example, materials used in suit loops should not burn at all in 19-psia oxygen, and hence the combustion rate value should be essentially zero. The table lists the functional category of the material (e.g., adhesive, molding compound), the chemical description (e.g., epoxy, silicone), the manufacturer's designation, and the manufacturer. The parameters for acceptability are based on the following toxicity and fire hazard potentials:

Toxicity Potential	Criterion
Odor	1.5
Carbon Monoxide	22 ppm
Total Organics	100 ppm

Fire and Flame Potential	Criterion
Combustion Rate	0.5 in./sec
Flash Point	400°F
Fire Point	400°F

Except for the last column in Table 19-1, a dash indicates that the material has not been tested but has been established as acceptable based on similarity or application. In the last column, which shows the pure oxygen pressure used during material testing, a dash indicates that the sample atmosphere is unknown.

Table 19-2 presents a list of acceptable metals and their alloys and their maximum use temperatures. The sublimation property of the metal is the principal property evaluated.

Over 2,000 materials have been evaluated by these test methods, and most of them were found to be unacceptable.

Table 19-1

ACCEPTABLE NONMETALLIC MATERIALS FOR SPACECRAFT

Polymer	Manufacturer	Combustion Rate (in./sec)	Odor Rating	CO (ppm)	Total Organics (ppm)	Flash Point (°F)	Fire Point (°F)	O_2 (psia)
ADHESIVE								
Epoxy A-2 Activator "E"	Armstrong Products	0.000	1.5	22	100	400	400	16.5
Epoxy-Polyamide FM-123-2	Am. Cyanamid	–	1.5	0.91	2.61	400	400	5.0
Epoxy-Phenolic HT-424	Am. Cyanamid	0.077	1.5	0.02	0.01	400	400	5.0
Heat Activated PS-9	Avery Adhesive	–	1.5	22	100	–	–	–
Silver Paste, Air Dry B + V A-23942	Bradley & Vroonan	–	1.5	22	100	400	400	–
Epoxy, Conapoxy 1610, Ca + 039	Conap, Inc.	–	1.5	1.6	0.23	400	400	5.0
Epoxy, Conapoxy, 1241 (+0568)	Conap, Inc.	0.109	1.5	22	100	–	–	16.5
Silicone, DC-140	Dow Corning	0.397	1.5	0.00	0.00	420	420	16.5
Silicone, DC-140	Dow Corning	–	1.5	0.07	0.04	400	400	5.0
Rubber, Silicone, Q30079	Dow Corning	–	1.5	22	100	400	400	–
Rubber, Silicone, 3C-121	Dow Corning	–	1.5	–	–	400	400	–
Polyurethane, Adiprene L-100	DuPont	–	1.5	22	100	400	400	–
Epoxy, Eccobond 51, Cat. 9	Emerson & Cuming	–	–	22	100	400	400	–
Rubber, Silicone, RTV108	General Electric	–	–	22	100	400	400	–
Rubber, Silicone, RTV112	General Electric	0.388	–	–	–	400	400	16.5
Rubber, Silicone, RTV112	General Electric	–	–	–	5.9	–	–	5.0
Velcro No. 40	Hartwell Co.	0.5	1.5	–	–	400	400	–
Epoxy, 6020A	Minn. Honeywell	–	1.5	22	100	–	–	–
Epoxy, 6293C	Minn. Honeywell	–	1.5	22	100	400	400	–
Epoxy, 6293P	Minn. Honeywell	–	1.5	22	100	–	–	–
Epoxy, 6293N	Minn. Honeywell	–	1.5	22	100	–	–	–
AF-126	3M Corp.	–	1.0	0.57	3.41	–	–	5.0
Epoxy, XD-126	3M Corp.	–	1.0	1.25	2.50	–	–	5.0
Rubber, EC-870	3M Corp.	0.5	1.5	22	100	400	400	–
Neoprene M-1A(6-1015)	Organo-Ceram	–	1.5	22	100	–	–	–
Bondmaster M-611, APCO 320	Pittsburgh Plate Gl.	–	1.5	22	100	400	400	–
Epoxy, Epon 828, CAT DETA	Shell Chemical	0.5	1.5	22	100	–	–	–
Epoxy, Epon 954	Shell Chemical	0.04	1.5	22	100	–	–	5.0
Epoxy, Epon 954	Shell Chemical	0.125	1.5	22	100	–	–	16.5
BEARING RETAINER								
Fabroid	Micromatic Hone	–	1.5	22	100	400	400	–
CABLE INSULATION								
Coax, Polyole Fin, Foam-filled	Rayclad Tubes	–	1.5	22	100	–	–	–
Coax, 60-116	Rayclad Tubes	–	1.5	22	100	–	–	–
Triaxial, 62-366	Raychem.	–	1.5	0	1.25	400	400	–
COATING								
Polyurethane, Clear ABOBO-007	Applied Plastics	–	1.5	–	–	400	400	–
Humiseal-Acrylic 1-B-12	Columbia Technical	–	1.5	22	100	400	400	–
Humiseal, 2A-58	Columbia Technical	–	1.5	–	100	400	400	
Lucite, Water Base	DuPont	–	1.5	22	100	–	–	–
Casting, Impregnation Dapon 2575	Food Mach. Corp.	–	1.5	22	100	–	–	–
Alum/Silicone 101A174	Grimes Mfg.	–	1.5	22	100	–	–	–
Polyurethane, Insulube 448	Inter. Latex	–	1.5	1.59	2.04	–	–	–
Polyester, Velvet, White 401-A10	3M Corp.	0.5	1.5	22	0.13	400	400	5.0
Polyester, Velvet, Grey, 401-B2	3M Corp.	0.00	1.5	0.01	0.19	400	400	5.0
Polyester, Velvet, Black, 401-C10	3M Corp.	0.5	–	0.01	0.25	400	400	–
Polyester, Velvet, Yellow-Tan 401-F2	3M Corp.	0.5	–	–	–	–	–	–
Polyester, Velvet, Blue 401-H2	3M Corp.	–	–	–	–	–	–	–
Polyester, Velvet, Tan 401-51	3M Corp.	–	–	–	–	–	–	–
Polyester, Velvet, Tan 401-52	3M Corp.	–	–	–	–	–	–	–
Optical, 11-002A	Opt. Coating Lab.	–	1.5	22	100	–	–	–
Polyurethane, PR-1538	Products Research	0.5	1.5	22	100	470	470	14.7
Enamel, Black, Q36K802	Rinshed-Mason	–	1.5	22	100	–	–	–
CONNECTOR								
PTO GE-10-6S (SR)	Bendix	–	1.5	22	100	–	–	–
DSO 7, 37-S-5039-DM 5623-37PP	Deutsch	–	1.5	22	100	–	–	–
Insert, DS07-19-2PW-1-5030	Deutsch	–	1.5	0.00	0.11	–	–	5.0
Insert, DS07-19-2SW-5030	Deutsch	–	1.0	0.00	0.23	–	–	5.0
CA310-6E-14S-6S-A95-A105-C22	ITT-Cannon	–	1.5	22	100	–	–	–
CA310-6E-10SL-4S-A29-A95-C22	ITT-Cannon	–	1.5	22	100	–	–	–
KPT 2P16-26-P25-6428-7/64D/S7ASA	ITT-Cannon	–	1.5	22	100	–	–	–
MC414-0164, SM3500 Silicone/Epiall 1459	ITT-Cannon	–	1.5	22	100	–	–	–
DESSICANT								
Silicagel, SC-14618	E. H. Sargent	–	0.00	0.00	0.00	–	–	5.0

Table 19-1 (cont.)

Polymer	Manufacturer	Combustion Rate (in./sec)	Odor Rating	CO (ppm)	Total Organics (ppm)	Flash Point (°F)	Fire Point (°F)	O_2 (psia)
FABRIC								
Viton/Glass, Fairprime 85-001	Dupont	0.2	1.5	22	100	–	–	14.7
Silicone Rubber/Glass/Al, SS1533	Hitco	–	1.5	2.50	2.38	–	–	5.0
Silicone Rubber/Glass, Class H, RMS	3M Corp.	–	1.0	0.00	0.34	–	–	5.0
FILM								
Polyethylene	Union Carbide	0.5	–	22	100	400	400	–
INSULATOR								
Teflon,FEP, Foamed	ITT-Wire & Cable	–	1.5	22	100	–	–	–
T.C. 15,000	HITCO	–	1.5	22	100	400	400	–
KNOB								
Acrylic V-1001, Epoxy Coated, 473-1	Rohm & Haas/Finch	–	1.5	22	100	400	400	–
LAMINATE								
Silicone, F130-40	Coast Mfg. Co.	–	1.5	–	–	400	400	–
Silicone/Glass, Textolite, 11617 G-7	General Electric	–	1.0	0.00	0.45	400	400	–
Epoxy, Cu Clad, EG 758-T Type GE	Mica Corp.	–	1.5	22	100	–	–	–
Glass/Epoxy, Scotchply 1002	3M Corp.	–	1.5	22	100	–	–	–
Epoxy, Narmco-S10	Narmco	–	–	–	–	400	400	–
Epoxy/Glass EM 7022	U.S. Polymeric	–	1.2	0.25	0.02	–	–	–
LUBRICANT								
Silicone, DC 340	Dow-Corning	0.027	.7	0.00	0.03	400	400	5.0
Silicone, DC 340	Dow-Corning	0.000	1.5	22	100	320	320	16.5
Silicone, DC 510	Dow-Corning	–	1.5	22	100	500	500	6.2
Fluorosilicone, Inrelco 33F	DriLube	0.430	1.5	22	100	400	400	16.5
Fluorocarbon, Krytox DR-240AC	DuPont	0.000	1.5	0.00	0.00	420	420	16.5
Fluorocarbon, Krytox 143-AB	DuPont	–	–	22	100	400	400	–
Dry Film, 905	Lubeco	–	1.5	22	100	–	–	–
Dry Film, 905-S	Lubeco	–	1.5	22	100	–	–	–
Dryfilm, N-350A	Lubeco	0.000	1.5	0.03	100	–	–	5.0
MOLDING COMPOUND								
Epoxy, ECM-90-B-1	Am. Marietta	–	1.5	22	100	–	–	–
Chevron Polyester 5461	Chevron, Ebonite Div.	–	1.5	22	100	400	400	–
Nylon, Zytel 101	DuPont	0.212	1.5	22	100	400	400	16.5
Butyrate, Tenite, 218A15 MoH	Eastman. Chem.	–	1.5	0.00	3.41	–	–	–
Polycarbonate, Clear LEXAN 103	General Electric	0.060	1.0	0.00	0.00	400	400	5.0
Polypropylene 6523	Hercules Powder	–	1.0	0.00	3.06	400	400	–
Epoxy, CPI-4267	Hysol	–	1.5	22	100	–	–	–
Epoxy, C-39	Hysol	–	1.5	22	100	–	–	–
Diallylphthalate FS-4	Mesa Plastics	–	1.5	22	100	–	–	–
Diallylphthalate FS-10	Mesa Plastics	–	1.5	22	100	400	400	–
Diallylphthalate, Diall FS-80	Mesa Plastics	–	1.5	22	100	400	400	–
Epoxy, Epiall 14S9	Mesa Plastics	–	1.5	22	100	–	–	–
Epiall 1908	Mesa Plastics	–	1.5	22	100	400	400	–
Diallylphthalate 52-70-70	Mesa Plastics	–	1.5	22	100	–	–	–
Terminal Strip, Silicone/Glass MAS-1064	Olympic Plastics	–	1.5	22	100	–	–	–
Diallylphthalate RX-B60T	Rogers Corp.	–	1.5	22	100	–	–	–
Diallylphthalate RX-B60T, Green	Rogers Corp.	–	1.5	22	100	–	–	–
Acrylic V-100	Rohm & Haas	–	1.5	22	100	450	450	–
Polypropylene, 5224-1000	Shell Chem.	–	1.5	22	100	–	–	–
Phenolic, BKS2600	Union Carbide	–	1.0	0.00	8.97	–	–	5.0
PLASTIC								
Kel-F	Carmer Ind.	0.000	–	22	100	400	400	5.0
Butyrate, Epoxy Coated Tenite 293-A-44813H4	Collins Radio	–	1.5	22	100	–	–	–
Teflon, Fluorogreen, 25% Glass Filled	Dore, John L.	–	–	–	–	400	400	–
Epoxy Resin, Dow 332	Dow Chem.	–	1.5	22	100	420	420	–
Epoxy Novalac Dow 438	Dow Chem.	–	1.5	22	100	–	–	–
Nylon Rod, Zytel 101	DuPont	–	1.5	22	100	400	400	–
Teflon	DuPont	0.000	1.5	0.91	1.14	400	400	16.5
Vinyl, Ag Filled, Eccoshield SV	Emerson & Cuming	–	1.5	22	100	400	400	–
Teflon, FEP, RBO130-007	Gulton Ind.	–	–	–	–	400	400	–
Polycarbonate, Merlon M40, 1510 Black	Mobay Chem.	–	1.0	0.00	1.14	–	–	–
Teflon Rod, 6008	Polymer Corp.	–	1.5	22	100	–	–	–
Nylon Rod, Molysulfide Filled	Polymer Corp.	–	1.5	22	100	400	400	–

Table 19-1 (cont.)

Polymer	Manufacturer	Combustion Rate (in./sec)	Odor Rating	CO (ppm)	Total Organics (ppm)	Flash Point (°F)	Fire Point (°F)	O_2 (psia)
PLASTIC (Cont.)								
Acrylic, Plexiglass II, UVA	Rohm & Haas	0.085	1.5	0.01	0.01	400	400	5.0
Acrylic, SW 350	Swedlow	–	–	–	–	400	400	–
Acrylic, SW 320	Swedlow	–	1.5	22	100	–	–	–
ABS, PR-55	U.S. Rubber	–	1.5	22	100	400	400	–
Nylon, Slide Fastener	Walles-Hakinoor	–	1.5	22	100	–	–	–
Teflon, Glass Filled, RP-125-MM	Western Felt Works	–	1.5	22	100	–	–	–
POTTING COMPOUND								
Rubber, Silicone, RTV-503	Dow Corning	–	1.5	22	100	–	–	–
Rubber, Silicone, RTV-521	Dow Corning	–	1.5	22	100	400	400	–
Rubber, Silicone, Sylgard 182	Dow Corning	–	1.5	22	100	–	–	–
Rubber, Silicone, Sylgard 183	Dow Corning	–	1.0	0.00	0.11	400	400	5.0
Epoxy, TC 245	Elect. Products & Dev. Corp.	0.147	1.5	22	100	400	400	16.5
Epoxy, Stycast 1090 CAT9	Emerson & Cuming	–	1.5	22	100	400	400	–
Epoxy, Stycast 2651 CAT11	Emerson & Cuming	0.038	.9	0.01	0.01	–	–	5.0
Stycast No. 2762	Emerson & Cuming	–	1.5	0.03	0.39	–	–	5.0
Epoxy, Epocast 226/951	Furane Plastics	–	1.5	22	100	420	420	16.5
Epoxy, Epocast II	Furane Plastics	–	1.5	22	100	–	–	–
Polyurethane, Uralane 5712	Furane Plastics	–	1.5	0.68	6.13	–	–	5.0
Silicone, RTV 60	General Electric	0.5	–	–	–	400	400	–
Rubber, Silicone, RTV-560	General Electric	0.091	1.5	22	100	420	420	16.5
Rubber, Silicone, RTV-560/RTV-577 82.5/17.5	General Electric	0.088	–	–	–	–	–	14.7
Epoxy, 70836	Minn. Honeywell	–	1.5	22	100	400	400	–
Epoxy, XC8F-H316	Hysol	–	1.0	1.32	0.24	400	400	5.0
Alkyd Polyester, 466	Mesa Plastics	–	1.5	22	100	–	–	–
Polyurethane, Scotchcast XR 5095	3M Corp.	–	1.5	22	100	–	–	–
Polyurethane, PR 1542	Products Research	–	1.5	22	100	–	–	–
RUBBER								
Silicone, Black EMS-323	AiResearch	–	1.5	22	100	–	–	–
Silicone, EMS-342	AiResearch	–	1.5	22	100	–	–	–
Silicone, EMS-345	AiResearch	–	1.5	22	100	–	–	–
Hypalon, EMS-352	AiResearch	–	1.5	22	100	–	–	–
Ethylene-Propylene EMS-364	AiResearch	–	1.5	22	100	–	–	–
Neoprene, 3-430-1	AiResearch	–	1.5	22	100	–	–	–
Silicone, SR 25140	Arrowhead Prod.	–	–	–	–	400	400	–
CHO-1212	Chomerics, Inc.	–	1.5	22	100	–	–	–
Silicone, CHR 506	Conn. Hard Rubber	–	1.5	22	100	–	–	–
Rubber/Fabric, Silicone/Glass CHR-3320	Conn. Hard Rubber	–	1.5	22	100	–	–	–
Silicone Sponge CHR-10470	Conn. Hard Rubber	–	1.5	22	100	400	400	–
Silicone (Hadbar) DC-50	Dow-Corning	–	1.5	22	100	400	400	–
Silicone, DC 651	Dow-Corning	–	1.5	22	100	–	–	–
Silicone, (ADEL 7010) DC 960	Dow-Corning	0.5	1.5	22	100	–	–	–
Silicone, S-2007	Dow-Corning	–	1.5	22	100	400	400	–
Silicone, XR-6-3501	Dow-Corning	–	1.0	0.00	4.09	–	–	5.0
Nitrile, Fairprene, N-5580-HA	DuPont	–	1.5	22	100	400	400	
Silicone, SE-565	General Electric	–	1.5	22	100	–	–	–
Silicone, SE-4511	General Electric	–	1.5	22	100	–	–	–
Neoprene Latex LN-2500A	Golden State Rubber & Latex	–	1.0	0.00	3.30	–	–	5.0
Silicone, 6000-40	Hadbar	0.5	1.5	22	100	–	–	–
Silicone, N1030	Hexseal, APM	–	1.5	22	100	–	–	–
Silicone, N-9050	Hexseal, APM	0.5	1.5	22	100	400	400	–
Neoprene, Closed Cell Sponge Tube	Inter Chem.	–	1.5	22	100	–	–	–
Silicone, CR-541E	ITT-Cannon	–	1.0	0.00	3.86	–	–	5.0
Silicone, (ME193-0001-2020), G2204	L.A. Std. Rubber	–	1.5	22	100	–	–	–
Silicone, 5000 Medium	L.A. Std. Rubber	0.5	1.5	22	100	400	400	–
Silicone Sponge, 5000 Firm	L.A. Std. Rubber	–	1.0	0.00	2.72	–	–	5.0
Silicone (Thomas Assoc. HE91) 5521	L.A. Std. Rubber	–	1.5	22	100	400	400	–
Silicone, DB 53750-2	Liberty Electronics	–	1.5	22	100	–	–	–
Nitrile, O-Ring MS-28775	Miller Sales	–	–	22	100	–	–	–
Silicone, S493-5	Parker Seal	–	1.0	0.00	0.23	400	400	5.0
Silicone, S563-5	Parker Seal	–	1.0	0.00	0.23	–	–	5.0
Silicone, Metalastic (ME5) 40-8520	(Metex Corp.) Perlmuth Elec.	–	1.0	0.00	0.00	–	–	–
Silicone/Glass, Heater No. 2027	Permacel	–	1.5	22	100	–	–	–

Table 19-1 (cont.)

Polymer	Manufacturer	Combustion Rate (in./sec)	Odor Rating	CO (ppm)	Total Organics (ppm)	Flash Point (°F)	Fire Point (°F)	O_2 (psia)
RUBBER (Cont.)								
Butyl, SR630-70	Stillman Rubber	–	–	22	100	400	400	–
Silicone, TH 1028	Stillman Rubber	–	1.5	22	100	–	–	–
Silicone, Clamp Pad 7A93	Thomas Assoc.	–	1.0	0.00	2.84	–	–	5.0
Silicone, K-1203	Union Carbide	–	1.0	0.00	1.14	–	–	5.0
SEALANT								
Rubber Silicone, DCQ-2-0078	Dow Corning	–	1.0	0.68	0.11	–	–	5.0
Rubber Silicone, EC 1663	3M Corp.	–	1.5	0.23	6.70	–	–	5.0
SLEEVING								
Silicone/Glass, 1151	Bentley-Harris	0.159	1.5	22	100	400	400	16.5
Teflon, FEP	ITT-Wire & Cable	–	1.5	22	100	–	–	–
SWITCH								
No. X32167	Honeywell	–	1.5	22	100	–	–	–
TAPE								
Tefglass, 90L0 F-13A	Western Filament	–	1.5	22	100	–	–	–
WIRE INSULATION								
FEP-ML Insulated, 19/36 Wires	Am. Super Temp.	–	1.5	22	100	–	–	–
Polyimide/TFE, 35-00271, Green	Haveg	0.000	1.3	0.00	0.01	–	–	5.0
Polyimide/TFE, 35-00291, White	Haveg	0.000	1.3	0.00	0.01	–	–	5.0
Polyimide/TFE, 35-00273, Black	Haveg	0.000	1.3	0.00	0.01	–	–	5.0
Polyimide/TFE, 35-00268, Red	Haveg	0.000	1.3	0.00	0.01	–	–	5.0
Polyimide/TFE, 35-00269, Yellow	Haveg	0.000	1.3	0.00	0.01	–	–	5.0
Magnet #24	Hi Temp. Wire & Cable	–	1.5	22	100	400	400	–
Magnet, Bondese #26	Phelps Dodge	–	1.5	22	100	400	400	–
Polyolefin, Coaxin, RF	Ray Chem.	–	1.5	22	100	–	–	–
Al-Clad Cable, 12-162A	Ray Chem.	–	1.5	22	100	–	–	–
Cable, Triax 62-366	Ray Chem.	–	1.5	0.00	1.25	–	–	–
Teflon, Leadwire, #22	Suprenant	–	1.5	22	100	400	400	–

Table 19-2

ACCEPTABLE METALS FOR MANNED SPACECRAFT APPLICATIONS

Metal[a]	Maximum Use Temperature (°F)
Molybdenum	1000
Chromium	1000
Titanium	1000
Iron (steel)	1000
Cobalt	1000
Nickel	1000
Silicon	1000
Beryllium	1000
Copper (except brasses)	1000
Gold	1000
Germanium	1000
Aluminum	930
Silver	900
Tin	450[b]
Lead	440
Bismuth	390
Indium	310[b]
Lithium	200[c]
Magnesium	200
Brass (exterior)	350
Brass (interior)	250

(a) Rejected metals or alloys: zinc, cadmium, and mercury.
(b) Melting point.
(c) Approved for Ag/Li braze in PH 15-7 Mo and Ph 14-8 Mo.

19.5 REFERENCES

1. Proceedings of the Conference on Atmospheric Contamination in Confined Spaces, AMRL TR-65-230, December 1965

2. Proceedings of the Second Annual Conference on Atmospheric Contamination in Confined Spaces, AMRL TR-66-120, December 1966

3. M. Honma and H. J. Crosby, eds., A Symposium on Toxicity in the Closed Environmental System, Lockheed Missiles & Space Company, Palo Alto, Calif., July 1963

4. Manned Environmental System Assessment, NASA CR-134, Boeing Company, November 1964

5. J. P. Conkle, Contaminant Studies in Closed Ecological System at the USAF School of Aerospace Medicine, AMRL TR 66-120, August 1966

6. W. A. Symonds, "Design, Mission, and Environmental Considerations in Selection of Materials for Space," pp.43–65 in The Effects of Space Environment on Materials, Vol. 11, Society of Aerospace Material and Process Engineers, North Hollywood, Calif., 1967

7. E. M. Roth, "Fire and Blast Hazard," Part II of Space-Cabin Atmospheres, NASA SP-48, 1964

8. The Present Status of Chemical Research in Atmosphere Purification and Control on Nuclear-Powered Submarine, Report No. 5814, Naval Research Laboratory, August 1962

9. "Report of Apollo 204 Review Board to the Administrator, NASA," 5 April 1967

10. Investigation of Toxic Properties of Materials Used in Space Vehicles, AMRL TDR 63-99, December 1963

11. Characteristics of Materials (COMAT), NM-116, Non-Metallic Materials Information Center, NASA-MSC, Houston, Tex., 30 August 1967

12. R. J. Jaffe, Non-Metallic Materials for Manned Closed Atmosphere Systems, LMSC-670476, November 1966

13. T. L. Willard, "Evaluation and Selection of Materials for Compatibility With Manned Spacecraft Environment, pp.171–180 in The Effects of Space Environment on Materials, Vol. 11, Society of Aerospace Material and Process Engineers, North Hollywood, Calif., 1967

14. C. Kurtz and R. Lewis, Approved Materials for Use in Apollo Spacecraft, MC 999-0058, Rev. B, North American Aviation, 1 March 1965

15. R. Holden, "Space Cabin Materials," NASA N66-34130, Adhesive Bonding Conference, 15 March 1966

16. J. V. Pustinger and F. N. Hodgson, Identification of Volatile Contaminants of Space Cabin Materials, AMRL TR 67-58, June 1967

17. J. F. March, E. B. Nicholas, and J. G. Demaree, Flammability and Smoke Characteristics of Aircraft Interior Materials, ADS-3, Federal Aviation Agency, January 1964

18. A. F. Ringwood, Procedures and Requirements for the Evaluation of Spacecraft Non-Metallic Materials, NASA-MSC-A-D-66-3, Rev. A, 5 June 1967

19. F. F. Clark, Approved Materials for Use in the Apollo Spacecraft, MC 999-0058, Rev. F, North American Aviation, 8 May 1967

20. Polymers for Spacecraft Applications, Project ASD 5046, Final Report, JPL Control No. 950745, Stanford Research Institute, Menlo Park, Calif., 15 September 1967

21. M. Honma et al., Thermal Degradation of Polymeric Materials. III. Thermal Outgassing of Some Plastics, 65-75-66-1, Lockheed Missiles & Space Company, Palo Alto, Calif., January 1966

22. J. W. Craig, Apollo Spacecraft, Nonmetallic Materials Requirements, NASA-MSC-PA-D-67-13, 9 February 1968

Chapter 20

EFFECTS OF MATERIALS DEGRADATION PRODUCTS ON MAN

J. T. Wilson, Jr.
R. J. Jaffe

Degradation products of materials may produce spacecraft atmospheric contamination and a wide range of responses in the inhabitants. When subjected to heat and reduced pressure, candidate nonmetallic spacecraft materials often produce carbon monoxide as well as many different organic substances. (See Chapter 19.) The human response to inhalation of atmospheric contaminants varies with the nature of the contaminant and its concentration in the atmosphere.

In a generalized way, A. A. Thomas has characterized the response of the organism as follows (Ref. 1):

- Equilibrium (intake equals excretion)

  The total organism appears to maintain its equilibrium, since the excretion of the contaminant equals the intake or input. There is no apparent biochemical reaction.

- Adaptation, desensitization, cross-tolerance

  Here there may be chemical reactions but these are countered by an adaptation of the organism to the contaminant exposure.

- Cumulative damage (summation of interest)

  In this instance, the adsorbed contaminant damages one or more internal organs, with concomitant biochemical derangement and probably physiological dysfunction.

- "None or All" (Carcinogens, sensitizers, irritants)

  The response may be immediate, as with irritant substances, or delayed, as with sensitizing substances. Some materials may be involved in cancer production.

20.1 EFFECTS OF MATERIALS DEGRADATION PRODUCTS ON MAN

Most of the degradation products will enter man's system through absorption from the lungs. Before this, however, they may be noticed as odorous or irritant substances. In many instances, neither of these qualities is present. Irritation of the mucus membranes may become so intense as to produce large amounts of secretion in the nose and lungs, sometimes leading to coughing or respiratory embarrassment. Some substances

cause readily detectable derangements of blood chemistry (carbon monoxide) along with effects on the central nervous system. Poor performance or reduced activity may be most notable early after exposure to certain other substances. Finally, the exposure may produce damage to one or more internal body organs.

It should be stressed that different organic substances produce a variety of functional effects and similarly their toxic effects also vary. Thus, while the substances may be grouped by the type or response produced,or the organs affected, chemical analogs will often produce dissimilar effects and the active amounts of these substances may differ greatly. Therefore, to appraise the toxicity of each contaminant, animal or human exposure data must be obtained by experimentation or experience. Low-level continuous exposures provide the most relevant data for setting provisional limit values for spacecraft atmospheric contaminants.

20.2 DERIVATION OF LIMITS

The National Academy of Sciences has recently considered the question of atmospheric contamination in spacecraft and published a report on this question. On the question of criteria for trace contaminant control, the Academy has stated the following (Ref. 2):

> "On the basis of the characteristics and objectives of man's spaceflights of 90 to 1,000 days duration, the committee has derived the following criteria for trace contaminant control in manned spacecraft:
>
> 1. Contaminants must not produce significant adverse changes in the physiological, biochemical or mental ability of the crew.
>
> 2. The spacecraft environment must not contribute to a performance decrement of the crew that will endanger mission objectives.
>
> 3. The spacecraft environment must not interfere with physical or biological experiments nor with medical monitoring.
>
> This rigorous approach is also consistent with scientific requirements. The NASA Space Medicine Advisory Group and the Respiratory Physiology Group of the Space Science Board's 1966 Summer Study have reaffirmed the principle that engineering exigencies should not dictate the environment:
>
> The environment must be supplied to provide the best medium for the experimental effort and one might also add, the best medium for the mission profile. Thus, if one of the goals of prolonged manned spaceflight is to ascertain man's adaptability and response to the weightless environment, it is necessary to design manned spacecraft in such a fashion that the earth atmosphere or a reasonable facsimile thereof be provided in order not

to prejudice the study of the one facet of spaceflight that cannot be duplicated on earth – weightlessness. We have therefore developed conservative air quality standards for prolonged manned missions on the following premises:

1. Any contamination of the spacecraft atmosphere may be detrimental,

2. Zero contamination of the spacecraft atmosphere is impossible,

3. Data does not exist that will permit one to predict with certainty the maximum contaminant concentration that will not cause degradation of the mission,

4. Provisional limit values can be established for some contaminants to serve as guidelines in design, development and testing of future space systems,

5. These provisional limits can perhaps ultimately be transformed into limit values if sufficient data about the effects of continuous exposure to a single compound and to multiple compounds can be obtained.

The uncertainties in establishing even provisional limits for prolonged manned missions are many and range from engineering, to environmental, to toxicological considerations. Since the materials to be used in future spacecraft construction and the type of regenerative environmental control systems to be employed have not been determined, there are major uncertainties regarding the kind and amount of air contaminants that will be present. There is also a major uncertainty as to how reduced pressures may alter the toxicity of contaminants.

The uncertainties are relatively minor, however, in comparison with those due to inadequate or incomplete toxicological information. Industrial threshold limit values have not been established for many of the compounds identified in spacecraft tests and very few contaminants have documented 90-day values. Data relative to continuous exposure are few and information on continuous exposure to multiple compounds is virtually non-existent. The importance of this latter point is not clear, however, since significant toxicological interactions may not occur at the low contaminant levels recommended in this report for prolonged spaceflight.

A further consideration is the fact that most of the available data have been obtained on subjects in a "normal" physiological state. The effect of stress, prolonged confinement, weightlessness, and other factors that might tend to alter man's normal physiology,

and thus change his response to any given compound cannot be accurately predicted at this time. For all of these reasons, the limits recommended in this report are provisional and subject to revision."

In the recommendations for atmospheric contaminantion in spacecraft, the NAS committee introduced a new unit for designating contaminants. The limits are expressed in millimoles of contaminant per 25 m^3. This unit was selected because it gives a numerical value which at 1-atm pressure and at 25°C is the equivalent of parts per million by volume (the unit used for submarine standards and by the American Conference of Governmental Industrial Hygienists). At the same time, it expresses the molar concentration per unit of space volume and is therefore equivalent to partial pressure of the contaminant. Hence, this unit is independent of the partial pressures of the surrounding gases and requires no mathematical correction for different total atmospheric pressures. This unit is used in the listing of the provisional limits taken from the NAS document.

20.3 PROVISIONAL LIMITS FOR SPACECRAFT ATMOSPHERES

To assist design engineers and other persons concerned with personnel subsystem design, Table 20-1 has been prepared, which compares the recommended limits for 90-day spaceflights and the reported occurrences of contaminants in manned spaceflights, spacecraft simulator studies, and offgassing studies. It is apparent that limits have not been established for all the observed contaminants. Where no limits have been established or recommended, designers should seek advice from qualified toxicologists or the National Academy of Sciences.

20.4 CONTROL OF SPACECRAFT ATMOSPHERIC CONTAMINATION

Generally speaking, it is best to prevent spacecraft atmospheric contamination whenever possible. Proper material selection thus favors materials having a high degree of stability, i.e., little or no outgassing. Since man and various system components also provide some atmospheric contaminants, other measures are necessary. The Handbook of Instructions for Aerospace Personnel Subsystem Design (HIAPSD) (Ref. 3) provides a good basis for developing these additional measures.

20.5 REFERENCES

1. Man's Tolerance to Trace Contaminants, AMRL-TR-67-146, A. A. Thomas, Aerospace Medical Research Laboratories, Wright-Patterson Air Force Base, Ohio, January 1968

2. Atmospheric Contaminants in Spacecraft, Report of the Panel on Air Standards for Manned Space Flight of the Space Science Board, National Academy of Sciences—National Research Council, Washington, D.C., June 1968, revised November 1968

3. Handbook of Instructions for Aerospace Personnel Subsystem Design (HIAPSD). AFSC Manual 80-3

Table 20-1

TRACE CONTAMINANTS IN CLOSED ATMOSPHERE SYSTEMS

Compound	Provisional Limits		Recommended Limits		Industrial Limits	Reported Occurrences	
	Spacecraft 90 Days	Spacecraft 1-hr Emergency	Submarine 90 Days	Submarine 24-hr Emergency	Threshold Limit Value[a]	Manned Systems[b]	Materials Screening[c]
Acetaldehyde					200	XX	†
Acetic Acid					10	XX	†
Acetone			300	2,000	1,000	XX	†
Acrylonitrile[d]					20	X	
Allene[d]			(e)			X	
Allyl Alcohol					2	XX	†
Ammonia			25	50	50	XX	†
Amyl Acetate					100	XX	
Amyl Alcohol					100	X	
Benzene			1	100	25	XX	†
Benzyl Ether						X	
1,3-Butadiene			(e)		1,000	XX	†
n-Butane			(e)			XX	†
iso-Butane			(e)			X	†
2-Butanone[d]	20	100			200	XX	†
1-Butene			(e)			XX	†
2-Butene (cis-, trans-)			(e)			XX	
Butyl Acetate					150	X	
n-Butyl Alcohol	10				100	XX	†
iso-Butyl Alcohol						XX	†
sec-Butyl Acrylate						X	
n-Butyl Benzene			(e)			X	
tert-Butyl Benzene			(e)			X	
iso-Butylene			(e)			XX	
Butyraldehyde						XX	
Butyric Acid						X	
Butyrolactone							†
Carbon Dioxide			5,000	10,000	5,000	XX	†
Carbon Disulfide					20	XX	†
Carbon Monoxide	15		25	200	50	XX	†
Carbon Tetrachloride					10	XX	†
Carbonyl Fluoride		25				(f)	
Carbonyl Sulfide						X	†
Chlorine			0.1	1	1	X	
Chlorobenzene					75	XX	
1-Chlorobutane						X	
Chlorofluorobromomethane						X	
Chlorofluoroethylene						X	
Chloroform	5				50	XX	†
Chloromethane					100	XX	
Chloropropane[d]						X	
Cyclohexane			(e)		300	XX	
Cyclohexene			(e)		300	X	
Cyclopentane			(e)			XX	
Cyclopentene			(e)			X	
Cyclopropane			(e)			X	†
Decaline (various isomers)						X	
Decane			(e)			X	
Dichloroacetylene						X	
o-Dichlorobenzene					50		†
p-Dichlorobenzene					75		†
1,2-Dichloroethane					50	XX	
1,1-Dichloroethylene[d]			25	2		XX	
1,2-Dichloroethylene					200	X	
Dichloromethane[d]	25				500	XX	
1,2 Dichloropropane					75	X	

See Footnotes on p. 658.

Table 20-1 (Cont.)

Compound	Provisional Limits		Recommended Limits		Industrial Limits	Reported Occurrences	
	Spacecraft 90 Days	Spacecraft 1-hr Emergency	Submarine 90 Days	Submarine 24-hr Emergency	Threshold Limit Value(a)	Manned Systems(b)	Materials Screening(c)
1,3 Dichloropropane						X	
Diethylbenzene			(e)			X	
1,4 Dimethoxybenzene						X	
Dimethylamine					10	X	
2,2 Dimethylbutane			(e)			XX	
2,3 Dimethylbutane			(e)			X	
Dimethylcyclohexane			(e)			XX	
Dimethylcyclopentane			(e)			X	
1,3 Dimethyl, 5-Ethylbenzene			(e)			X	
Dimethyl Furane						X	
Dimethyl Naphthalene			(e)			X	
2,4 Dimethyl Pentane			(e)			X	
Dimethyl Propane			(e)			X	
Dimethyl Sulfide						X	
Dimetnyl Thiophene						X	
1,4 Dioxane	10				100	XX	
Dioxene						XX	
Ethane			(e)			XX	†
Ethanethiol(d)					10	XX	
2-Ethoxyethanol					200	X	
2-Ethoxyethyl Acetate					100	X	
Ethyl Acetate	40				400	XX	†
Ethyl Acetylene						X	
Ethyl Acrylate					25	X	
Ethyl Alcohol			100	500	1,000	XX	†
Ethyl Benzene			(e)		100	XX	†
Ethyl Chloride					1,000	X	†
Ethyl Cyclohexane						X	
Ethyl Ether					400	XX	
Ethyl Formate					100	XX	
Ethyl Mercaptan(d)					10	XX	
p-Ethyl Toluene(d)			(e)			X	†
Ethylamine					10		†
Ethylene			(e)			XX	†
Ethylene Glycol		100				(g)	
Ethylene Oxide					50		†
Fluoroethane						X	
2-Fluoropropene						X	
Formaldehyde	0.1				5	XX	†
R-11 Fluorotrichloromethane			5(h)	20(h)	1,000	XX	†
R-12 Dichlorodifluoromethane			200(h)	1,000(h)	1,000	XX	
R-22 Chlorodifluoromethane						XX	
R-23 Trifluoromethane						X	
R-113 FCl_2C-$CClF_2$(d)	200	20			1,000	XX	
R-114 F_2ClC-$CClF_2$			200(h)	1,000(h)	1,000	XX	
R-125 F_2HC-CF_3(d)						XX	
Furan						XX	
Furfural					5	X	
Furfural Alcohol					50	X	
n-Heptane			(e)		500	XX	†
Heptene			(e)			X	
Hexafluorobenzene						X	
Hexamethylcyclotrisiloxane						X	
n-Hexane			(e)		500	XX	†
Hexene			(e)			X	
Hexene-1			(e)			X	

See Footnotes on p. 658.

Table 20-1 (Cont.)

Compound	Provisional Limits		Recommended Limits		Industrial Limits	Reported Occurrences	
	Spacecraft 90 Days	Spacecraft 1-hr Emergency	Submarine 90 Days	Submarine 24-hr Emergency	Threshold Limit Value[a]	Manned Systems[b]	Materials Screening[c]
Hydrogen			10,000	10,000		XX	
Hydrogen Chloride			1	4	5	X	
Hydrogen Fluoride			0.1	1	3	X	
Hydrogen Sulfide					10	XX	
Indene						XX	
Indole						X	
Isoprene						XX	†
Mesitylene[d]			(e)			XX	
Methane			5,000	5,000		XX	†
Methanethiol[d]					10	XX	
Methyl Acetate					200	X	
Methyl Acetylene[d]					1,000	X	
Methyl Alcohol			10	200	200	XX	
Methyl isoButyl Ketone[d]					100	XX	†
Methyl Butyrate						X	
Methyl Chloride					100	XX	
Methyl Chloroform			2.5	10	350	XX	
Methyl Cyclohexane			(e)		500	XX	
Methyl Cyclohexene			(e)			X	
Methyl Cyclopentane			(e)			X	
Methyl Ethyl Benzene[d]			(e)			X	†
Methyl Ethyl Ketone[d]	20	100			200	XX	†
Methyl Ethyl Thiophene						X	
Methyl Formate					100	X	
Methyl Furan						X	
Methyl Mercaptan[d]					10	X	
Methyl Methacrylate					100	X	†
Methyl Naphthalene			(e)			X	
2-Methyl Pentane			(e)			X	†
3-Methyl Pentane			(e)			X	
4-Methyl, 2-Pentanone[d]					100	XX	†
Methyl iso-Propyl Ketone[d]	20	100				XX	†
Methyl Thiophene						X	
Methylamine					10	X	
2-Methylbutanone-3[d]	20	100				XX	†
Methylene Chloride					500	XX	
Methylsiloxane Polymers						XX	
Monochloroacetylene						X	
Monoethanolamine			0.5	3	3	X	
Naphthalene			(e)		10	X	
Nitric Oxide						X	
Nitrogen Dioxide			0.5	1.0	5	X	
Nitrous Oxide						X	
n-Nonane			(e)			X	
Octane			(e)		500	X	
iso-Octane			(e)			X	
Ozone			0.02	0.1	0.1	X	
Pentafluoroethane[d]						XX	
Pentane			(e)		1,000	XX	
iso-Pentane			(e)			XX	
1-Pentene			(e)			X	
Perchloroethylene[d]					100	XX	
Phenol					5		†
Phosgene			0.05	0.1	0.1	X	
Propane			(e)		1,000	XX	

See Footnotes on p. 658.

Table 20-1 (Cont.)

Compound	Provisional Limits		Recommended Limits		Industrial Limits	Reported Occurrences	
	Spacecraft 90 Days	Spacecraft 1-hr Emergency	Submarine 90 Days	Submarine 24-hr Emergency	Threshold Limit Value(a)	Manned Systems(b)	Materials Screening(c)
Propene			(e)			X	
Propenenitrile(d)					20	X	
Proprionaldehyde							†
Propionic Acid						XX	
Propyl Acetate					200	X	
n-Propyl Alcohol					200	XX	†
iso-Propyl Alcohol					400	XX	†
iso-Propyl Benzene			(e)		50	X	†
n-Propyl Benzene			(e)			X	
Propyl Chloride(d)						X	
Propyl Mercaptan(d)						X	
Propylene			(e)			XX	
iso-Propyl Ether					500	X	
Propanethiol(d)						X	
iso-Propanethiol(d)						X	
Propyne(d)			(e)		1,000	X	†
Pseudocumene			(e)			X	
Silicone Oil							†
Skatole						X	
Styrene			(e)		100	X	
Sulfur Dioxide			1.0	5.0	5	XX	
1,2,4,5-Tetrachlorobenzene							†
Tetrachloroethane					100	XX	
Tetrachloroethylene(d)						X	
Tetrafluorobenzene						X	
Tetrafluoroethylene						X	
Tetrahydrofurane					200	X	
Tetramethylbenzene			(e)			X	
Toluene			(e)	100	200	XX	†
1,1,1-Trichloroethane(d)			2.5	10	350	XX	
Trichloroethylene	10				100	XX	†
1,1,2-Trichloro, 1,2,2-Trifluoroethane(d)	200	20			1,000	XX	
Trifluorobenzene						X	
Trifluorochloroethane						X	
1,3,5-Trimethyl Benzene(d)			(e)			XX	
Trimethyl Hexane			(e)			XX	
Trimethyl Pentane(d)			(e)			XX	
Trimethyl Silanol							†
Valeric Acid						X	
Vinyl Chloride					500	XX	
Vinylidene Chloride(d)			2	10		XX	
Xylene (Various Isomers)			(e)	100	100	XX	†

(a) These values have been established by the American Conference of Governmental Industrial Hygienists (1967) as the Threshold Limit Values which "represent conditions under which it is believed that nearly all workers may be repeatedly exposed, day after day, without adverse effect." They refer to normal industrial workday duration practices and are not intended for use in estimating the toxic potential of continuous uninterrupted exposures. The values are given here for reference purposes only.

(b) An X indicates that the compound has been identified in atmospheric analysis of a closed manned system or an environmental system designed for manned occupancy. An XX indicates that a compound is reported for 3 or more of the 16 systems studied.

(c) A † indicates that the compound has been observed as an offgas product from a material being studied for use in a manned system.

(d) The compound is listed under two synonyms.

(e) The recommended 90-day submarine level is 60 mg/m^3 for aliphatic hydrocarbons, 10 mg/m^3 for aromatic hydrocarbons (other than benzene), and 3 mg/m^3 for benzene.

(f) Carbonyl fluoride is a possible degradation product of fluorinated hydrocarbons.

(g) Ethylene glycol may be present in spacecraft temperature control system coolant loops.

(h) Submarine limit based on formation of pyrolysis products by submarine air purification equipment.

Chapter 21

EFFECTS OF MANNED OCCUPANCY ON SPACECRAFT MATERIALS

L. L. Reed

The presence of man in a space vehicle causes potential problems related to the compatibility of spacecraft structural materials with the biological products related to or of man. These products, which are either the excretions and secretions of normal metabolic activity or materials of biological origin that are associated with the presence of man, include urine, feces, sweat, tears, vomit, sebum, flatus, respiratory products, hair and skin debris shed by the body, and microorganisms. The effect of such products on spacecraft materials may be direct due to the physical and chemical composition and characteristics of the product of may be indirect as a result of subsequent microbial activity or interaction with other materials.

The reported physical characteristics and chemical composition of the various excretions and secretions of man have been compiled and published (Refs. 1 and 2). These compilations show that the biological products are complex mixtures of various physical structures and chemical compounds of varying amounts. The number of reported chemical constituents in many of the products is astounding. For example, 190 chemical entities, excluding hormones, are reported in one table on urine composition. The composition of other body excretions and secretions is equally formidable. Information on the effects of these products on spacecraft materials is incomplete or totally lacking, especially regarding storage of the products for extended periods of time. Therefore, reported constituents and their concentrations in these various products are presented and potential problem areas are discussed.

21.1 URINE

The volume of urine normally excreted by man in a 24-hr period is reported to range from 750 to 2000 ml with an average of 1500 ml (Ref. 3). However, the volume may vary considerably, depending upon individuals and conditions. This is illustrated in Fig. 21-1 (Ref. 2). Volume variability during the 14-day Gemini VII mission is shown in Fig. 21-2 (Ref. 4). Because of the volume generated and the need to recover water for long-term flights, the storage of total urine volume appears impractical except for relatively short time periods. Storage of small samples for medical analyses may be required.

Reported chemical constituents of urine and their concentrations are shown in Table 21-1. In addition to the constituents listed in the table, urine also contains small quantities of vitamins and hormones. If urine is to be stored for periods of time longer than 12 hr, it should be treated or processed to prevent microbial decomposition, which generally produces ammonia and possibly hydrogen sulfide. Other degradation products may also be produced that are toxic or induce corrosion. Normally, urine is slightly acidic,having an average pH of 6.0, although the pH may range from 4.8 to 8.0. Urine also contains several electrolytes, notably chlorides which may give rise to electrolytic reactions with metals. Metals such as aluminum, magnesium, copper, and titanium will react in this way with urine. Soft plastics may react with the ammonia in solution

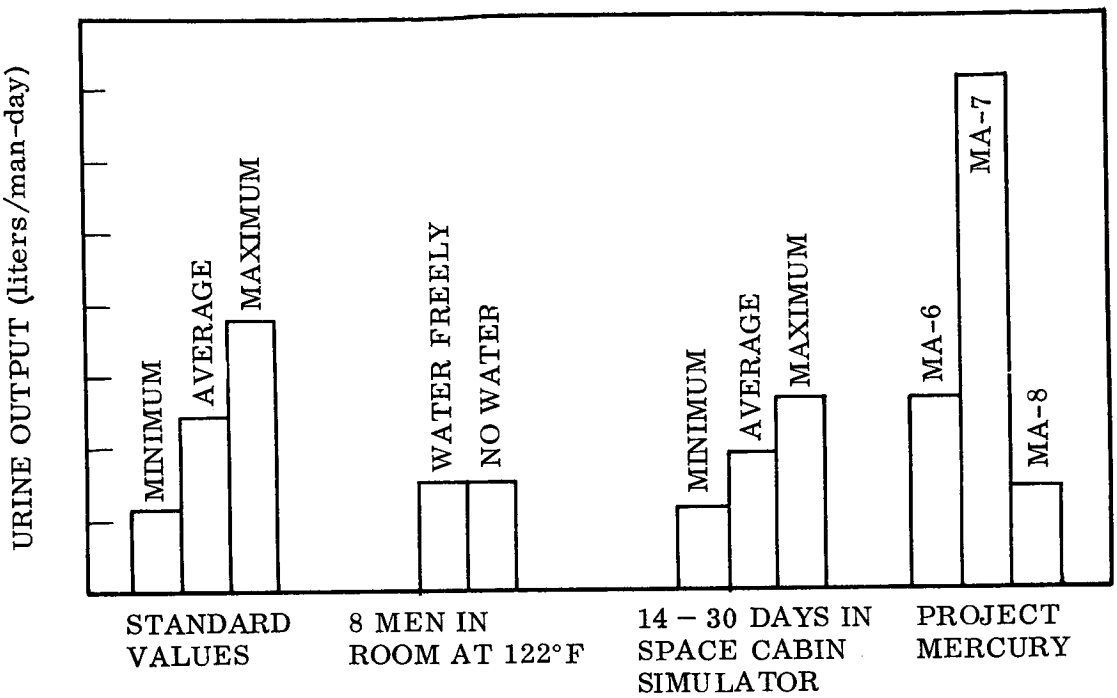

Fig. 21-1 Examples of Variability in Urine Production (Ref. 2)

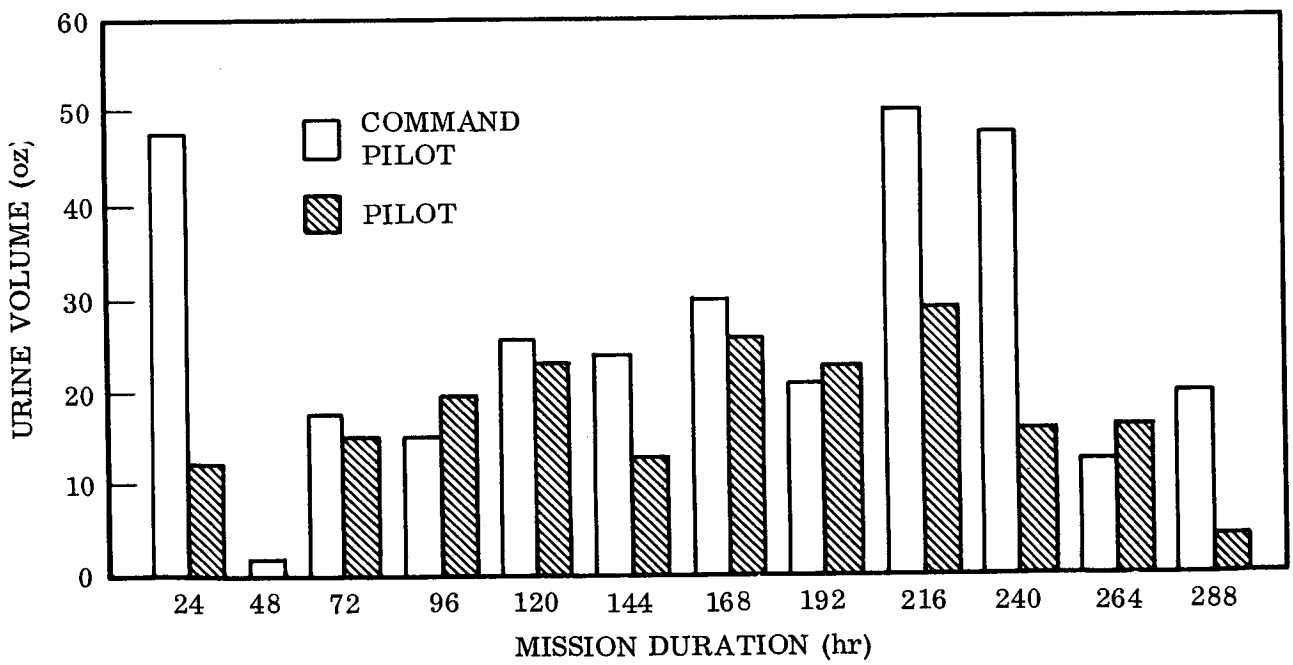

Fig. 21-2 Urine Volume of Gemini VII Crew (Ref. 4)

Table 21-1

COMPOSITION OF URINE

(The solid contents are recorded as mg/ 24 hr.)

Component	Mean			Range
	Ref. 1	Ref. 5	Ref. 6	Ref. 2
pH				4.6 to 8.0
Solids				55,000 – 70,000
Electrolytes				
Aluminum	0.077	0.078	–	0.049 – 0.112
Arsenic	0.0231	–	–	0 – 0.091
Bicarbonate	140.0	–	–	35 – 840
Bromine	–	2.1	–	0.840 – 7.70
Calcium	231.0	–	–	43.0 – 581.0
Chloride (as NaCl)	12,000	–	7,638	7,600 – 15,000
Chlorine	7,000	–	–	2,800 – 12,600
Copper	0.035	–	0.018	0 – 0.049
Fluorine	1.540	–	–	0.30 – 7.0
Iodine	–	–	–	0.007 – 0.490
Iron	0.490	–	0.045	0.02 – 1.1
Lead	0.028	0.035	–	0.004 – 0.15
Magnesium	94.5	–	103	29.4 – 307
Manganese	–	–	–	0.007 – 0.098
Nickel	–	0.15	–	0.140 – 0.280
Phosphorus (as P)	–	–	1,100	700 – 1,600
Inorganic	840	–	–	700 – 1,300
Organic	9.17	–	–	6.23 – 13.09
Potassium	2,380	–	2,740	1,120 – 3,920
Selenium	0.035	–	–	0 – 0.140
Silicon	9.10	–	–	420 – 14.0
Sodium	4,200	–	4,615	1,750 – 6,580
Sulfur, total	1,120	–	–	357 – 3,400
Inorganic	777	–	–	245 – 2,700
Ethereal	66.5	–	–	40 – 300
Natural	133	–	–	73 – 400
Conjugated	–	–	–	80 – 300
Tin	–	–	–	0.0091 – 0.0175
Zinc	0.364	–	0.457	0.110 – 0.500
Nitrogen compounds				
Adenine	1.40	1.4	–	1.1 – 1.7
Allantoin	11.9	–	–	2.8 – 40
Amino Acids, Total	–	–	–	1,100 – 2,800
Free	–	–	–	500 – 1,400
Alanine, Total	38.5	46.0	–	21 – 71
Amino-adipic acid	–	10.0	–	8 – 11
Amino-butyric acid	–	10.0	–	Traces-10
Amino-isobutyric acid	–	20.0	–	4 – 180
Anserine	–	–	–	5 – 7
Arginine, Total	31.5	10.0	47.0	10 – 56.8
Asparagine	–	54.0	–	34 – 99
Aspartic acid, Total	119.0	10.0	113.4	10 – 258.8
Carnosine	–	–	–	2 – 3
Citrulline	63.0	10.0	–	0 – 196.0
Crystine, Total	119.0	10.0	87.7	10 – 200
Glutamic acid, Total	–	10.0	249.9	10 – 484.7
Glutamine	–	100.0	–	–
Glycine, Total	455.0	132.0	405.0	132 – 670.6
Histidine, Total	189.0	216.0	284.0	65.4 – 498.8
Hydroxylysine	–	<10.0	–	<10
Hydroxproline, Total	1.40	0.51	23.05	0.26 – 1.4
Isoleucine, Total	14.0	18.0	11.3	6.5 – 33.4
Leucine, Total	21.0	14.0	27.9	11.9 – 40.0
Lysine, Total	56.0	19.0	102.0	7 – 166.0
Methionine, Total	9.8	10.0	6.6	3.8 – 15.0
1-methylhistidine	–	180.0	–	47 – 384
3-methylhistidine	–	50.0	–	–
Ornithine	10.5	10.0	–	10 – 10.5
Phenylalanine, Total	21.0	18.0	28.7	9 – 45.4
Proline, Total	42.7	10.0	13.3	10 – 63.0
Sarcosine	–	10.0	–	10
Serine, Total	42.0	43.0	–	27 – 73
Taurine	–	156.0	156.0	7.7 – 294
Threonine, Total	35.0	28.0	83.2	14.8 – 182.0
Tryptophan, Total	28.0	–	22.9	8 – 86.1

Table 21-1 (cont.)

Component	Mean		Range
	Ref. 1	Ref. 5	Ref. 6	Ref. 2
Tyrosine, Total	49.0	35.0	55.5	15 – 103.3
Valine, Total	21.0	10.0	30.1	10 – 44.7
Ammonia	–	700.0	–	300 – 1.100
Bilirubin	49.0	–	5.0	5 – 49.0
Coproporphyrin I & III	–	–	–	0.0168 – 0.280
Creatine	56.0	–	–	0 – 800
Creatinine	1,610.0	–	2,145.0	1,000 – 3,219
Ethanolamine	–	12.2	–	4.8 – 22.9
Glycocyamine	–	–	–	21 – 67
Guanidine	–	–	–	10 – 20
Guanidinoacetic acid	–	–	30.0	14.0 – 35.0
Guanine	0.42	1.6	–	0.21 – 2.0
8-Hydroxy-7-methyl	1.40	1.6	–	1.1 – 2.0
7-Methyl	6.30	6.5	–	5.5 – 7.8
N^2-Methyl	0.490	0.5	–	0.4 – 0.6
Hippuric acid	–	–	700.0	70 – 2,500
Histamine	–	–	–	0.014 – 0.070
Hypoxanthine	9.80	9.7	–	5.6 – 13.3
I-Methyl	0.42	0.4	–	0.2 – 0.7
Imidazole derivatives	–	–	286.1	140.0 – 300.0
Indoxylsulfuric acid	70.0	100.0	–	5 – 160.0
Lipoproteins	–	23.5	–	–
Methionine sulfoxide	–	–	–	0 – 21.70
Nitrogen				
Total N	–	–	15,300	1,000 – 21,000
Amino Acid N	–	–	349.0	100 – 431
Ammonia N	–	–	–	210 – 1,000
Protein	–	–	50.0	2.10 – 80
Albumin				10 – 100
Purine bases	–	–	–	0.01 – 70.0
6-Succinopurine	0.980	–	–	–
Urea	–	22,000	–	14,000 – 35,000
Uric acid	140.0	567.0	528.0	56 – 1,000
Urobilin	–	–	–	10 – 130
Urobilinogen	–	–	–	0 – 25.0
Uropepsin (as tryrosine)	–	–	417.0	98 – 835
Xanthine	6.30	6.1	–	4.90 – 8.6
Acids				
Acetoacetic acid	2.80	–	–	2.10 – 4.20
Carbolic (phenol) Total	–	–	–	14.0 – 42.0
Free	–	–	–	0 – 3.50
Carbonic acid	189.0	–	–	147.0 – 231.0
Citric acid	–	–	678.0	128 – 1,400
Formic acid	56.0	–	–	28.0 – 140.0
Glucuronic acid	–	–	–	100 – 1,325
m-Hydroxybenzoic acid	–	–	–	10 – 16
m-Hydroxyhippuric acid	–	4.0–6.0	–	2 – 150
p-Hydroxyphenyl-hydrocrylic acid	–	10.0	–	2 – 150
Lactic acid	210.0	73.0	–	50 – 600.0
Oxalic acid	35.0	22.0	–	1 – 49.0
Oxoglutaric acid	–	22.0	–	20 – 40
Pyruvic acid	–	–	100.0	2.5 – 100
Misc. organic compounds				
Acetone bodies, Total	14.0	–	19.4	2.10 – 23.5
Amylase (Somogyi)	–	–	–	260 – 950 units
Cholesterol	–	–	–	0 – 4.998
Glucose (true)	–	–	72.0	50 – 300
Ketones (total)	–	–	50.5	19.8 – 81.2
Phenols	–	–	437.0	200 – 636
Reducing substances	–	–	–	490 – 1,500
Glucose	–	4.3	–	1 – 12
Fructose	–	5.0	–	0 – 5
Arabinose (mgm per 100 ml)	–	1.5	–	0 – 3
Ribose	–	18.7	–	–
Xylose	–	1.0	–	0 – 3
Lactose	–	7.0	–	0 – 10
Sucrose	–	5.0	–	0 – 5

or as a gas, and are not desirable for the storage of urine. Epoxy plastics and stainless steel alloys are sufficiently low in reactivity with urine components and urine decomposition products to be acceptable. Fluorocarbons are more desirable for use than neoprene and other rubbers. Resistant materials must also be used in any urine treatment equipment (e.g., urine stills, or evaporators), since undesirable reactions or reactive products may result from concentrated constituents and elevated temperatures.

21.2 FECES

In general, the average amount of feces excreted by man is 100 to 200 gm/day (Ref. 3). However, the actual amount is dependent upon the kind and quantity of food ingested. Table 21-2 illustrates the effect of diet on the generation of feces.

Table 21-2

GENERATION OF FECES

Type of Diet	Wet Weight		Dry Weight (gm/day)	Reference
	Mean (gm/day)	Range (gm/day)		
Mixed	–	60 – 250	–	6
Mixed	150	–	61	8
Mixed	–	110 – 170	25 – 45	9
Vegetable	370	–	–	6
Vegetable	350	–	75	9
Meat	–	54 – 64	–	6
Fasting man	–	7 – 8	–	9

A normal stool consists of 65 to 85% liquid and 15 to 35% dry solids, depending upon type of diet. It is estimated that approximately one third of the dry solids weight is composed of bacteria (Ref. 7). The chemical constituents and their concentrations that have been reported are presented in Table 21-3.

Feces are normally neutral in reaction, with pH values ranging from 6.9 to 7.5, although acid or alkaline reactions may result from certain diets. Acid reactions are generally due to lactic and butyric acids. Organic materials are principally cellulose, proteins, and fats. Important products that are derived primarily from bacterial action in the intestine are indole, skatole, paracrisol, phenol, p-oxyphenylpropionic acid, p-oxyphenylacetic acid, hydrogen sulfide, methane, methylmercaptan, carbon dioxide, ammonia, and protein derivatives (Ref. 3). Both saturated and unsaturated fatty acids are found in feces and are composed of carbon chains varying from 10 to 20 carbon atoms. The obnoxious odors of fecal material are due principally to indole and skatole.

Contact of spacecraft materials with feces will be necessary in storage and treatment equipment. Storage up to a few weeks would be possible in chemically compatible plastics such as polyethylene or polyvinylidine chloride. Polyvinylchloride is also compatible but is undesirable in biological systems because of objectionable plasticizers. If plastics are used in storage units, it is mandatory that a film of sufficient thickness or density be used to prevent permeation of toxic or undesirable gases (e.g., H_2S, CH_4, NH_3, CH_3S_4) in quantities that would lead to toxic concentrations in the spacecraft atmospheres.

Table 21-3

COMPOSITION OF FECES

(Values in mg/ 24 hr unless otherwise noted.)

Component	Mean Values			Range
	Ref. 1	Ref. 6	Ref. 8	Ref. 2
Bulk	–	–	150,000	50,000 – 350,000
Dry matter	–	–	27,000	23,500 – 35,000
Electrolytes				
Aluminum	0.0428	–	–	0.0428 – 2.9
Arsenic	2.353	–	–	0.071 – 8.27
Calcium	534.0	640.0	1,180	100.0 – 1,180
Chloride	–	90.0	–	14.97 – 35.65
Cobalt	0.0005	–	1.400	0.0001 – 1.400
Copper	1.925	–	1.020	1.020 – 2.638
Iron	8.556	–	28.80	4.6 – 100.0
Lead	0.299	–	–	0 – 400
Lithium	–	–	2.600	–
Magnesium	178.2	200.0	252.0	107 – 252
Manganese	–	–	3.430	1.283 – 8.556
Mercury	0.001	–	–	–
Molybdenum	–			2 – 4
Nickel	–	–	2.900	0.0856 – 10.0
Phosphorus	703.0	510.0	–	506.2 – 1700
Potassium	470.0	470.0	291.0	291 – 1037
Silver	0.0570	–	–	–
Sodium	121.2	120.0	116.0	116 – 122
Strontium	–	–	0.590	–
Sulfur, total	142.7	130.0	–	–
Tin	–	–	–	0.5 – 32.09
Zinc	7.130	–	–	4.135 – 10.27
Nitrogen compounds				
Arginine	–	–	–	1200 – 2100
Bile pigments	–	–	150.0	–
Histidine	–	–	–	600 – 800
Indole	90.0	–	–	60 – 100
Isoleucine	–	–	–	1400 – 2300
Leucine	–	–	–	1800 – 2900
Lysine	–	–	–	1900 – 2900
Methionine	–	–	–	500 – 800
Nitrogen, total	–	–	1500.0	700 – 2100
Threonine	–	–	–	1400 – 2200
Urobilinogen	–	10.0	101.0	10 – 280
Valine	–	–	–	1500 – 2600
Misc. organic compounds				
Fiber[a]	–	–	–	10 – 30
Fats & derivatives:				
Total fat	–	–	4500	1000 – 7000
Vitamins				
Vitamin A	–	–	–	0.17 – 0.33
p-Aminobenzoic acid	–	–	0.246	–
B vitamins	–	–	15.0	–
Vitamin B_2 (uroflavin)	1.029	–	–	0.823 – 1.313
Vitamin B_6	–	–	–	0.5 – 0.8
Biotin	–	–	0.133	0.1 – 0.2
B-carotene	–	–	–	1.7 – 3.3
Vitamin E	21.0	–	–	–
Folic acid	–	–	0.304	–
Pantothenic acid	–	–	2.20	1.8 – 3.8
Pyridoxin	–	–	0.38	0.1 – 0.5
4-pyridoxic acid	–	–	–	0.5 – 0.6
Nicotinic acid	–	–	3.63	3.5 – 5.5
Thiamine	–	–	0.548	0.2 – 0.8
Riboflavin	–	–	1.020	0.4 – 1.20

[a]Percent of dry weight.

For long trips, storage of untreated feces is impractical, and feces must be dried, decomposed, or treated with biocidal agents, in which case the effect of the agent upon materials must be considered. Probable treatment methods are vacuum drying without elevation of temperature or complete heat decomposition of organic compounds and ventilation of gases to the outside. Under both conditions, feces would react with aluminum, copper, unalloyed steel, magnesium, and titanium. Vacuum drying below 500°F can be handled in phenolic or epoxy moldings. If higher temperatures (500° to 1500°F) are necessary to decompose feces, stainless steels would be required.

The bulk of the material will volatilize rapidly, leaving behind a solid residue of higher acids, fatty acid salts, proteins, and minerals. The exhausts from either vacuum drying or heat decomposition units must be adequately separated from solar cell panels and temperature control surfaces to avoid impingement and possible contamination or otherwise changing of the optical properties of the surfaces. Since traces of volatile fecal substances may leak into the spacecraft atmosphere and may be removed only after passage of the atmosphere through a scrubber or absorber, consideration should be given to reaction of fecal gases in low concentration with structural materials of the cabin. Greases used as lubricants or on seals or gaskets in flanges and fittings may concentrate the gases and may reach concentrations that could alter their properties and possibly off-gas into the cabin atmosphere to add to the load of the environmental control system purification train.

21.3 FLATUS

The volume of flatus emitted by man each day is largely dependent upon types and quantities of food ingested and the bacterial flora of the intestinal tract. The range of volumes expelled varies considerably as shown in Table 21-4.

Table 21-4

FLATUS EMISSION

Specimen	Volume		Refs.
	Mean (ml/day)	Range (ml/day)	
Estimated average volume of discharged gas	1000	–	10 and 11
Average volume of discharged gas	2000	–	14
Discharged gas; 47 normal individuals on ordinary (cabbage-free) diet	825	100 – 2800	12
Five male medical students		300 – 655	13
Five men changing to a pork and beans or dried lima bean diet (25 – 50% of calorie intake) for 2 weeks		240 – 4872	13

The principal chemical components of flatus are carbon dioxide, oxygen, methane, hydrogen, nitrogen, and hydrogen sulfide. Trace amounts of other gases, e.g., ammonia, oxides of nitrogen, and organic volatiles, may be present, depending upon diet. The concentrations of the principal flatus gases are shown in Table 21-5.

Table 21-5

CHEMICAL CONSTITUENTS OF FLATUS (Ref. 12)

Constituent	Cabbage-Free Diet		Cabbage-Milk-Free Diet	
	Mean (%)	Range (%)	Mean (%)	Range (%)
Carbon Dioxide	9.0	1.2 – 15.0	9.7	0.7 – 24.7
Oxygen	3.9	0.0 – 15.7	5.5	0.5 – 20.0
Methane	7.2	0.0 – 30.3	3.1	0.0 – 21.4
Hydrogen	20.9	3.1 – 34.0	12.0	0.4 – 36.5
Nitrogen	59.0	39.7 – 88.2	70.0	24.7 – 87.7
Hydrogen Sulfide	0.0003	0.0 – 0.0017	0.0002	0.0 – 0.0003

Of these gases, hydrogen sulfide might be expected to cause the most problems relative to spacecraft materials. It affects many metals (e.g., aluminum and copper) and possibly some lubricants. Flatus gases (and the rest of the cabin atmosphere) will probably be treated in a catalytic burner. In this, H_2S goes to SO_2 which, on contact with water, is converted to H_2SO_3. About 2 gm of sulfurous acid may be produced per man per day. This will have to be absorbed by the environmental control system or it could cause some corrosion of such materials as aluminum and magnesium alloys. The oxides of nitrogen may also cause an unusual demand on the environmental control system and in water or a humid atmosphere could have corrosive reactions with aluminum and magnesium alloys. The other gases would not be expected to cause any particular materials problem.

21.4 SWEAT

Sweat is a weak solution of sodium chloride in water, the sodium chloride concentration of which varies from 0.2 to 0.5%; muscular exercise increases the salt concentration (Ref. 7). The production and composition of sweat depend very much on temperature, relative humidity, work load, clothing, and acclimatization. Production can vary from very small amounts to more than 12 liters per day. Table 21-6 illustrates the variation in the generation of sweat.

Table 21-6

GENERATION OF SWEAT

Subject and Condition	Volume (ml/hr)		
	Mean	Range	Ref.
Normal adult	–	33–50	15
70-kg man	20.8	–	6
Heat and exercise	783	–	16
Maximum-rate exercise	1000		7
Strenuous exercise for extended periods	–	500–2500	10
Strenuous exercise for short periods	3900	–	10

The solids content of sweat is small – less than 2% – and is composed of inorganic electrolytes and several organic compounds. The composition of sweat is shown in Table 21-7.

The hydrogen ion activity of sweat varies in pH from 4.2 to 7.5, with acidic values due primarily to the presence of lactic acid. The salt concentrations and free acids may react with certain materials. Although wide dissemination of sweat would not be expected, sweat from the hands can change the optical properties of materials that are frequently touched or handled. The sweat solids would generally be found in clothing, washing materials, and wash water. Without microbiological controls, microbial decomposition of the organic solids can produce ammonia and hydrogen sulfide in addition to obnoxious odors. The primary problem produced by sweating is the water load introduced into the cabin atmosphere which must be handled by the life support system. The solid residues left as a result of evaporation of sweat can be corrosive to aluminum, magnesium alloys, and low-alloy steels.

21.5 SEBUM

Approximately 4 gm of sebum are secreted per man per day. The total amount is dependent upon the individual and his size. The generation of sebum on the forehead has been reported at mean values of 2.82 mg/cm^2 to 3.38 mg/cm^2 at saturated levels (Ref. 17). A production level for the chest, back, and shoulders has been reported as 54 mg/hr (Ref. 2). The main components of skin secretions are shown in Table 21-8.

None of the sebaceous secretions in the prevailing amounts is especially reactive. However, accumulations of the organic acids over long periods of time may create corrosive reactions with materials that are touched by the hands or the uncovered heads of the astronauts. Deterioration of the organic constituents by microorganisms may produce ordorous byproducts. On long trips, the skin secretions will appear in the wash water, which will be processed for water recovery. Accumulations of secretions in the processing equipment may react and affect the purification efficiency of the equipment, resulting in impure water, which could affect the health of the astronauts and jeopardize the length of the mission.

21.6 EXHALED AIR

Water and carbon dioxide are the principal waste products in exhaled air, and the amount of each expired per man per day is approximately 550 gm and 1000 gm, respectively. In Table 21-9, inspired air and expired air are compared at a pressure of 1 atm. The values given are general figures, and considerable variation can occur between individuals and under different conditions. Argon, neon, helium, and other rare gases occur in the atmosphere. They are considered inert and are usually included in values given for nitrogen. The water vapor of expired air may present problems from the standpoint of forming moist films upon condensation which could cause short circuits in open electrical contacts such as switches, relays, and circuit breakers. It can also form favorable conditions for microbial growth. The presence of carbon dioxide would not cause any undue materials problems, since it will be constantly removed from the atmosphere in the environmental control system.

Table 21-7

COMPOSITION OF SWEAT (Ref. 2)

(Values in mg/100 ml unless otherwise noted.)

Component	Mean	Range
Water	–	99.0 – 99.5%
Solids, total	–	1.174 – 1.597%
Electrolytes		
Calcium	2.1	1 – 8
Chloride	–	30 – 468
Copper	0.006	0.006 – 7.5
Iodine	0.0009	0.0005 – 0.0012
Iron	0.027	0.022 – 0.2
Magnesium	0.2	0.004 – 4.5
Manganese	0.006	0.002 – 7.4
Phosphorus	0.5	0.003 – 2.0
Potassium	–	21 – 126
Sodium	–	24 – 312
Sulfur	–	0.7 – 7.4
Nitrogen Compounds		
Amino Acids		
Arginine	13.6	5.8 – 21.4
Histidine	8.0	4.25 – 14.00
Isoleucine	2.27	1.0 – 3.73
Leucine	2.69	1.2 – 4.2
Lysine	2.26	1.4 – 3.38
Phenylalanine	2.19	1.0 – 3.5
Threonine	5.38	1.7 – 9.1
Tryptophan	1.12	0.4 – 1.85
Tyrosine	3.15	1.2 – 5.45
Valine	2.96	1.5 – 4.5
Creatinine		0.1 – 1.3
Urea		1.2 – 5.7
Uric Acid	0.16	0 – 2.5
Nitrogen		
Total N	33.2	27 – 64
Non-protein N	31.0	27 – 64
Amino acid N	2.8	1.1 – 10.2
Ammonia N	–	2.5 – 35.0
Urea N	–	5 – 39
Misc. organic compounds		
Ascorbic acid	–	0 – 0.002
Carbolic acid (phenol)	–	2 – 8
Lactic acid	–	45 – 452
Corticoids	–	0.004 – 0.008
Sugar (as glucose)	–	0.1 – 40
Vitamins	–	0.0195 – 0.082

Table 21-8

MAJOR COMPONENTS OF SKIN SECRETIONS (Ref. 2)

(Values in gm/100 gm)

Component	Mean	Range
Water	31.7	–
Epithelial cells and protein	61.75	–
Fat	4.16	–
Butyric, Valeric, and Caproic Acid	1.21	–
Ash	1.18	–
Fatty Acids combined	34.6 (Fa)	27.5 – 41.0 (Fa)
	28.0 (S)	21.0 – 39.0 (S)
Monoglycerides	3.7	1.8 – 7.1
Diglycerides	10.1	–
Triglycerides	32.5 (Fa)	14.8 – 44.0
	44.0 (Fh)	–
	16.0 (S)	16.0 – 24.8
Waxes (cholesterol esters)	23.7	–
Fatty Acids (free)	28.3 (Fa)	2.3 – 38.3
	38.0 (Fh)	–
	33.0 (S)	–
Unsaponifiable matter (total)	30.1 (Fa)	25.1 – 35.9 (Fa)
	34.0 (S)	29.0 – 40.0 (S)
Aliphatic alcohols (total)	9.0 (S)	–
Straight chain	2.4 (Fa)	–
Branched chain	3.8 (Fa)	–
	0.9 (S)	–
Cholesterol	4.1 (Fa)	1.2 – 9.5
	3.5 (Fh)	–
Dihydrocholesterol	0.1 (Fa)	–
Hydrocarbons	8.1 (Fa)	5.0 – 20.0
	9.0 (S)	–
Paraffins	1.5	1.2 – 1.9
Phosphatides	0.9 (Fh)	–
Squalene	5.5 (Fa)	5.5 – 17.3
	7.0 (S)	

Fa: forearm
Fh: forehead
S: scalp

Table 21-9

COMPOSITION OF RESPIRED AIR (Ref. 7)

Barometer 760 mm Hg Gas	Partial Pressure	
	Inspired Air (mm Hg)	Expired Air (mm Hg)
Oxygen	158.25	116
Carbon dioxide	0.30	28
Nitrogen, argon, etc.	596.45	569
Aqueous vapor	5.00	47
Total	760.00	760

21.7 VOMIT

The presence of vomit in a space cabin environment is not a usual condition, but vomiting may occur under some circumstances and must therefore be given consideration. Vomit consists of gastric secretions and, perhaps, ingested water and food or both. The gastric secretions are acid in reaction and contain hydrochloric acid in concentrations of 0.1 to 0.5% in addition to water, mineral salts, acid phosphates, and the enzymes pepsin and renin (Ref. 3). Food particles, if present, may be in various stages of digestion. Partially digested food may release certain components that may be reactive with materials. The primary problem would be the corrosiveness of the free hydrochloric acid of the gastric secretion on such materials as aluminum and magnesium alloys and low-alloy steels. Most plastics and stainless steels would be suitable for waste containers.

21.8 FUNGI AND BACTERIA

Various microorganisms are usually present in environments that are the same as man's environment. The most common ones, fungi and bacteria, can grow on a wide variety of organic materials and under a wide range of environmental conditions. Almost any material containing organic compounds, even in trace amounts, can support growth of some microorganism (Refs. 18, 19, and 20). Microbiological deterioration has been found in a wide variety of plastics, hydrocarbons, rubbers, paraffins, and lubricants. Growth of these microorganisms on structural materials can lead to physical breakdown and malfunction.

Microorganisms can also grow in organic compounds such as lactic acid and ammonia which have dissolved in water films. Under suitable conditions, microbial growth can produce corrosion and etching of metal parts and optical components. The growth of microorganisms in biological wastes and organic compounds may also produce toxic and obnoxious gaseous materials, such as hydrogen sulfide, ammonia, oxides of nitrogen, and sulfur.

A number of physical and chemical treatments are available to control the growth of microorganisms (Ref. 21). The method selected is dependent upon the application and the type of material requiring treatment. The control technique must be compatible with the materials of the system.

Growth of microorganisms, unless controlled, can be extensive enough to plug flow systems. It has been reported that growth of microorganisms in jet fuels was extensive enough to block fuel injection jets (Ref. 22).

21.9 REFERENCES

1. Philip L. Altman and Dorothy S. Dittmer, eds., Biology Data Book, AMRL-TR-64-100, Aerospace Medical Division, Wright-Patterson Air Force Base, Ohio, October 1964

2. Paul Webb, ed., Bioastronautics Data Book, NASA SP-3006, Scientific and Technical Information Division, National Aeronautics and Space Adminstration, Washington, D.C., 1964

3. S. Frankel and S. Reitman, eds., Gradwohl's Clinical Laboratory Methods and Diagnosis, Vol. 2, 6th ed., C. V. Mosby Co., St. Louis, Mo., 1963

4. Charles A. Berry, "Man's Response to Long-Duration Flight in the Gemini Spacecraft," pp. 235 – 261 in Gemini Midprogram Conference, NASA SP-121, National Aeronautics and Space Administration, Washington, D.C., 1966

5. C. Long, Biochemists Handbook, D. Van Nostrand Co., New York, N. Y., 1961

6. Konrad Diem, ed., Documentia Geigy Scientific Tables, 6th ed., Geigy Pharmaceuticals, Ardsley, N. Y., 1962

7. Charles H. Best and Norman B. Taylor, ed., The Physiological Basis of Medical Practice, The Williams and Wilkins Co., Baltimore, Md., 1961

8. S. A. Goldblith and E. L. Wick, "Analysis of Human Fecal Components and Study of Methods for Their Recovery in Space Systems," ASD TR 61-419, Aerospace Medical Laboratory, Wright-Patterson Air Force Base, Ohio, August 1961

9. P. B. Hawk and O. Bergheim, Practical Physiological Chemistry, Blakiston Co., Philadelphia, Pa., 1954

10. Carl J. Clemedson, "Toxicological Aspects of the Sealed Cabin Atmosphere of Space Vehicles," Astronautik 1, 133 – 158, 1959

11. J. A. Fries, "Intestinal Gases of Man," Am. J. Physiol. 16, 468 – 474, 1906

12. E. Kirk, "Quantitative Determinations of the Skin Lipid Secretion in Middle-Aged and Old Individuals," J. Gerontol. 3, 251 – 266, 1948

13. H. W. Davenport, Physiology of the Digestive Tract, Year Book Medical Publishers, Inc., Chicago, Ill., 1961

14. R. H. Mattoni and G. H. Sullivan, Sanitation and Personal Hygiene During Aerospace Missions, MRL-TDR 62-68, Aerospace Medical Research Laboratories, Wright-Patterson Air Force Base, Ohio, June 1962

15. F. W. Sunderman and F. Boerner, Normal Values in Clinical Medicine, W. B. Saunders Co., Philadelphia, Pa., 1950

16. D. B. Dill, Life, Heat and Altitude, Harvard University Press, Cambridge, Mass., 1938

17. S. Rothman, Physiology and Biochemistry of the Skin, The University of Chicago Press, Chicago, Ill., 1950

18. C. J. Wessel, "Effects of Contaminants: Harmful Effects on Materials and Equipment," Navy-Lockheed Symposium on Toxicity in the Closed Ecological System, 29 – 31 July 1963

19. L. Irvine, "Microbiological Contamination and Its Effects in the Closed Ecological System," Navy-Lockheed Symposium on Toxicity in the Closed Ecological System, 29 – 31 July 1963

20. N. M. Butler and H. O. W. Eggins, "Microbiological Deterioration," New Scientist 26, No. 439, 154 – 186, 1965

21. G. F. Reddish, ed., Antiseptics, Disinfectants, Fungicides, and Chemical and Physical Sterilization, Lea and Febiger, Philadelphia, Pa., 1961

22. A. E. Prince, "Microbiological Sludge in Jet Aircraft Fuel," pp. 197 – 203 in Developments in Industrial Microbiology, Vol. 2., Plenum Press, New York, 1961

Chapter 22

EFFECTS OF STERILIZATION PROCEDURES ON SPACECRAFT MATERIALS

J. B. Rittenhouse
W. G. Jurevic

One of the goals of the unmanned space programs is to ascertain the existence of extraterrestrial life. Because of the absence of an atmosphere, the consequent wide temperature extremes at the surface, and exposure to unfiltered solar radiation, the probability of viable life on the Moon is low. The temperature of the Moon to a considerable depth into the surface is below the freezing point of water. Therefore, viable organisms transported to the Moon from Earth may not propagate. Nevertheless, it is desirable to minimize the number of organisms transported there. This has been accomplished by using sterilization procedures on Rangers 3 to 5 and clean room fabrication on Rangers 6 to 9, the Surveyors, and the Lunar Orbiters so that the total number of organisms transported was kept below 10^{10} per flight. Thus, with a possible 40 missions the transported biological loading should be kept in the region of 10^{11}. Since the surface area of the Moon is 4×10^{17} cm^2, biological loading would amount to one earth organism for 10^{-6} cm^2 of surface (Ref. 1).

The near planets Venus and Mars have some atmosphere. The surface temperature of Venus is thought to be too high for growth of Earth organisms. There are regions in the atmosphere of Venus having low enough temperature for organisms to survive. However, Earth microorganisms do not multiply in the Earth's atmosphere and presumably would not do so in the atmosphere of Venus. Therefore, the assurance against releasing viable Earth organisms in the atmosphere of Venus can be about 10^{-1} (Ref. 1).

There is no question that the placing of Earth organisms on Mars should be avoided. Tests of the growth of Earth organisms in simulated Martian conditions have shown that the chance for their propagation is unity (Ref. 1). Therefore, the chance of accidental release of Earth organisms during unmanned exploration of the planet should be kept below a small probability of about 10^{-5}. It is estimated that a single microorganism transported to Mars with a replication time of 30 days could in 8 years equal the total population of bacterial life on Earth. These organisms would compete with any Martian life; would make the detection of Martian life, if it exists, almost impossible; and would alter the geochemical and atmospheric characteristics of the planet (Ref. 2).

One way to avoid contamination of a nearby planet is not to land on it, but it is doubtful if much could be learned about the existence of extraterrestrial life unless an unmanned lander equipped to make biological measurements were used. The other method of avoiding contamination of the planet is to place a low probability of impact, 3×10^{-5}, on a planetary fly-by trajectory. This technique – a variation of the technique of not landing – was used in the Mariner 4 flight. This sort of probability would have to be assured for unsterilized boosters or other unsterilized components that would assist

the lander mission. Another method is to decontaminate and sterilize the spacecraft. NASA calls the last two methods Planetary Quarantine (Ref. 3). The sterilization requirement imposes many engineering and materials selection problems on the spacecraft designer and the materials and process engineer.

22.1 STERILIZATION AND DECONTAMINATION

The requirement of NASA to assure the landing of a sterile spacecraft on Mars is for terminal sterilization prior to launch. This procedure requires that the biological loading prior to sterilization of the assembled spacecraft is less than 10^7 viable organisms, which can be accomplished by heat sterilizing of parts and clean assembly throughout; by heat decontamination of parts and clean assembly; or by heat contamination at the subsystem level and clean final assembly. Each of these techniques would be followed by terminal sterilization. The requirements are subject to periodic changes as more is learned by the research and development programs in progress to develop heat sterilizable equipment, clean room assembly techniques, and biological barriers to protect subsystems during assembly and transportation as well as the assembled spacecraft through assembly. Protection must be provided for the spacecraft after terminal sterilization through launch and to some safe point in the trajectory where contamination from nonsterile components of the vehicle will not recontaminate.

Sterility is an absolute quantity. A component cannot be termed "slightly sterile." Either it is sterile or it is not. The quantity that is specified is some low probability such as 10^{-4} that no viable organism is present. This can best be assured for the solid internal components of spacecraft such as plastics or solid propellants by dry heat sterilization. The present requirement is for three complete cycles of 36 hr each at 135°C (276°F) in dry nitrogen.

Decontamination can be used at certain stages of manufacturing and assembly to lower the biological loading to some level below 10^7 organisms prior to terminal sterilization. The term decontamination is often misused; it means the reduction of the quantity of living material to a low level but not to zero (Ref. 3).

To a great extent, it has been established that the space environment itself cannot be depended upon to kill any earth microorganisms. The conditions in space of deep cold and vacuum are those used on earth to preserve microbial life. Although ultraviolet radiation will kill organisms over a long period of time, it reaches only exposed surfaces. Shorter wavelength radiation, such as x-rays, cannot be expected to penetrate further than inches within the spacecraft and thus also must be ruled out as a ready means of sterilization.

The actual sterilization goal established for a Mars lander is a probability of less than 1 in 10,000 (10^{-4}) that a single organism will be onboard. Laboratory studies on the kinetics of heat kill of resistant organisms show that at 135°F (276°F) the number of organisms can be reduced one logarithm or (90% of those remaining) for every 2 hr of exposure. Assuming 10^6 organisms on the spacecraft and a factor of safety of 10^2, a total of 12 logarithms of reduction in count has been accepted as a safe value. It is proposed that this can be achieved by a heat treatment of 135°C for 24 hr.

Control of the quantity of biological loading on the spacecraft is necessary for the success of sterilization, since the greater the number of organisms on the spacecraft, the longer the heat must be applied or the higher must be the temperature. Therefore, periodic biological load reduction will be required during fabrication and assembly.

Surface decontamination of spacecraft can be done using ethylene oxide. The vapor consists of 12% ETO and 88% Freon 12. The specifications call for an exposure to 300 mg of ETO per liter of space in an enclosure. The temperature should be 70°F for 4 hr. Prior to the ETO exposure, the surface to be treated should be exposed to more than 35% relative humidity for more than 72 hr (Ref. 3). The ethylene oxide treatment cannot be used for internal decontamination and or for sterilization of planetary spacecraft.

22.2 EFFECTS ON METALS AND ALLOYS

Most of the structural aluminum alloys can withstand the thermal sterilization cycles. The only exceptions to this behavior are the 1100, 3003, and 7075 alloys. The 1100 alloy should not be used for load-bearing structures; the 3003 alloy is rated as not sterilizable; and the 7075 alloy loses strength by overaging during the long heat cycles.

The main concern is for structural elements under load during the heat cycle. For example, a container pressurized at 14.7 psi will show an increase in pressure to 21 psi. Thus, a container not designed as a pressure vessel actually becomes one during the long sterilization cycles and could burst or bulge. However, the material may lose as much as 20% of its room-temperature strength at the nearly 300°F temperature of heat sterilization. These effects have to be taken into account in the design. The main concern is prevention of buckling of structural elements under load, and thickness may have to be increased with a consequent increase in weight. Such devices as preloaded clamps can undergo creep or relaxation which can cause leakage at the joint, and thermal stresses that are superposed on the clamping stresses can cause either an increase in weight of the ring or a loss in clamping force.

Only magnesium alloys AZ91C and HK31A are rated able to withstand the heat sterilizing temperature. The application of magnesium alloys to heat-sterilizable spacecraft is restricted because of their high creep rates at low stresses and their loss of room-temperature strength after exposure to elevated temperatures.

The use of beryllium and beryllium-aluminum alloy will not be restricted by the thermal sterilization requirement for planetary landing spacecraft. The governing factor will be the limitation imposed by the low ductility and difficult fabrication procedures required. The beryllium-aluminum alloy has better ductility and can be joined by welding, and its slightly lower strength than that of the unalloyed metal will not limit its use. The low coefficient of thermal expansion and the high modulus of elasticity compared with those of aluminum and magnesium alloys can result in high thermal stresses in parts that are attached to aluminum or magnesium members.

The effect of the sterilization temperature on the structural properties of titanium alloys is small. However, since titanium alloys are used for pressure vessels, the slight loss in properties at the sterilization temperature should be taken into consideration in design if the pressure vessel must carry its design load during sterilization.

These considerations also should be applied to piping that might be under pressure during the sterilization cycles. Tank and tubing thicknesses might have to be increased, which could add weight. Another design factor to be considered is the low thermal conductivity of titanium alloys. This property lengthens the transient heating and cooling times of titanium alloy structures relative to those of parts of the spacecraft made of aluminum alloys which will heat and cool faster, thereby imposing an interface thermal load upon adjacent components.

The effect of the heat sterilization cycles on the steel alloys generally used in spacecraft construction will be no problem. The steel alloys have strength properties at the sterilization temperature in excess of those required for structural purposes. The maximum temperature of heat sterilization is well below that used in the heat treatment of most steel alloys. However, hard-drawn steel springs and music wire should not be used for springs above 250°F. Stainless steel AISI 316 can be used for this application because it retains properties from subzero to 550°F and is nonmagnetic. For electrical conducting springs, 2.5% Be-Cu alloys would be preferred to spring brass.

Most of the special-purpose alloys will withstand the sterilization cycles. The exceptions are Ni-Span-C, the constant-modulus alloy, for precision springs that will not withstand the sterilization cycles. The zinc-4 copper, zinc-1 copper, zinc-1 aluminum, and zinc-4 aluminum-1 copper alloys have high creep rates and undergo rapid recrystallization at sterilization temperatures.

The tensile strength of lead-tin solders drops by a factor of 5 at the sterilization temperature, so that stressed solder joints will fail. Tests have shown that the 90-deg peel strength of 60/40 solder joints between nickel and copper ribbons was reduced to near zero at 150°C (300°F).

Most of the magnetic alloys will withstand the temperature cycles of sterilization.

The low melting metals gallium and indium sometimes used for seals or lubrication in propellant systems are not compatible with the thermal sterilization cycles.

Most of the metals and alloys will be compatible with the ethylene oxide-Freon 12 mixture used for surface decontamination. The exceptions to this behavior are copper and copper-based alloys such as brass and bronze, anodized aluminum, magnesium alloys treated with chemical conversion coatings, silver, phosphate-coated steel, and mercury and its alloys. Two reactions are possible: the materials can catalyze the polymerization of the ETO, or in the case of copper or mercury they can cause an explosive reaction if acetylene is present. The carbon steels and the 400 series of stainless steels should also be free of rust because the ETO reacts with iron oxide. To keep a nonstainless steel free of rust in the 35% relative humidity atmosphere for 72 hr prior to ETO, decontamination can be a problem.

The solution to the problems of incompatibility of these metals and alloys with the ETO is to refrain from using these materials externally, since the ETO is used as an external decontaminant. This procedure may cause a difficult but not insurmountable design problem (Ref. 4).

22.3 EFFECTS ON PLASTICS

The effects of high temperature on the properties of organic materials used for adhesive, sealing, encapsulating, and structural applications are discussed in Chapters 10, 11, and 12. The mechanical properties of most plastics drop to lower levels at lower temperatures than those of most metals and alloys. The plastics to be used on sterilized spacecraft must be chosen carefully; some candidate materials have fairly good long-term strength retention at the sterilization temperature. A great deal of attention will have to be given to creep for materials that may have to withstand some load during the sterilization cycles.

Consideration must also be given to the amount and kind of offgassing products that are developed during the heat cycles. It should be recognized that the sterilization temperature of 275° F is near or above the post-cure temperatures used in the fabrication of some plastics. This circumstance may be favorable for some plastics as far as stability is concerned. Several polymeric materials have been tested for their compatibility with the dry heat sterilization environment. In one program, more than 150 different materials among adhesives, encapsulants, elastomers, coatings, reinforced plastics, moldings, films, oils and greases, and tapes were tested, and 20 to 25% were found to be marginal or incompatible. Of these, enough materials of a given class were capable of withstanding the sterilization cycles so that suitable substitututions for the marginal and incompatible materials could be made (Ref. 5).

The epoxy, epoxy-nylon, and polyurethane adhesives cannot be used in applications that require heat in sterilization. The phenolic-nitrile, silicone, modified epoxy, and epoxy-phenolic adhesives can be used to temperatures approaching 500° F and will withstand the sterilization cycles. The polyimide and polybenzimidazole adhesives are also useful to these high temperatures.

Of the encapsulants, the only materials not affected by the heat sterilization temperature cycles are the RTV silicones. The Buna-N, Viton, neoprene, nylon, and polyurethane encapsulating materials cannot withstand the heat sterilization temperature. High thermal expansion causes high thermal stresses which may fracture thick sections or damage encapsulated parts. Low thermal conductivity causes large thermal gradients because of long thermal transient time.

The stability of the elastomers for sealing applications in the thermal sterilization environment depends mainly on the formulation and cure. However, with few exceptions most of the silicone, fluorosilicone, and fluorocarbon elastomeric materials are heat stable. The butyl, neoprene, and nitrile elastomers are either marginal or not compatible with the thermal sterilization cycling.

The reinforced plastic laminates used for primary and secondary structural applications and for circuit boards in electronic modules can withstand the thermal sterilization cycling in most cases. Such laminates as diallyl phthatate-glass, epoxy-glass, epoxy-glass-copper, and phenolic-glass are compatible with the thermal cycling. The phenolic-linen and the phenolic-nylon laminates are either marginal or not compatible with the thermal cycling treatment. Most of these materials that can be heat sterilized should be treated in an inert atmosphere. This procedure also should be applied to Teflon-impregnated glass fabric and to glass tissue used for thermal insulation.

The basis for determining whether a material is marginal is a loss in mechanical or electrical properties of less than 20% or a weight loss of less than 1.0%. If changes in properties are greater than these amounts, the materials are considered incompatible with the thermal cycling treatment.

The results of the thermal cycling testing of the polymeric film materials has to be coupled with the effects of exposure to the ETO decontamination gas because although the H-film and Tedlar materials are compatible with the heat cycles, they absorb the ETO gas and lose strength, part of which is regained in the heat cycling. Only the Mylar HS material and the 3-mil-thick Mylar D film are compatible with both the ETO and the thermal cycles. The Mylar films must be preshrunk prior to exposure (Refs. 5, 6, and 7).

The fabric materials for parachutes and biological barriers that can witstand the heat cycles are Dacron and Nomex. Nylon and silk cannot withstand the thermal cycling.

The thermal control materials undergo changes in their reflectance properties and in some cases suffer a loss of adhesion during the thermal sterilization heat cycles. The epoxy-amine and the polyurethane materials with white, black, or aluminum powder pigments become brittle or lose adhesion after heat exposure. The white pigments become yellow, which indicates an increase in absorptance. Such materials as Cat-A-Lac 443-1 gloss white, Cat-A-Lac 463-1 flat white, and CAT-A-Lac 463-1B flat black all are embrittled and the white yellows. The aluminum silicone 171-A-28 (Fuller Paint Co.) and Laminar X500 (Magna Coatings) polyurethane lose adhesion during the heat cycling.

The silicone-alkyd aluminum pigmented D4D and the TiO_2 pigmented Vitavar PV100 can withstand the thermal cycles in an inert atmosphere. Such silicone-based materials as gloss white (Fuller 517 W-1), flat black (Fuller 517-B-2), and the aluminum pigmented (Fuller 172-A-1 and 171-A-152) as well as the dull black vinyl-phenolic Microbond L6 X 962 can withstand the thermal cycling. This is also true of the zinc-oxide-silicate material MSD105 produced by the General Electric Co., Missiles and Space Division (Refs. 4, 6, and 7).

Irradiated polyethylene, polyvinyl chloride, and silicone wire insulations are subject to loss of resistance at the heat sterilization temperature. The FEP and TFE Teflons and the polyimide insulations are compatible with the heat sterilization treatment. Wires insulated with H-film or Pyre-ML (polyimides) will be satisfactory in the heat sterilization environment but will be incompatible with the ETO external decontamination treatement. The fluorocarbons will have limited compatibility with the ETO external decontamination treatment. External cable harness insulations will have to be carefully chosen to assure compatibility with both the decontamination and the heat sterilization requirements.

Lubricants that have long lifetimes in space such as oils and greases may not be compatible with the thermal sterilization requirement because of volatilization and possible recondensation on optical surfaces or electrical contacts. Petroleum-based lubricants are not compatible with the ETO decontaminant gas. The solid film lubricants such as MoS_2 and gold films or glass-reinforced Teflon-MoS_2 composites may be satisfactory in both media but the lifetime in vacuum of these lubricating materials is considerably shorter than that of the oils and greases (Ref. 4).

Tapes with epoxy or rubber adhesives cannot withstand the heat sterilization cycles. The glass fabric-silicone adhesive tape is marginal. The only satisfactory tape is the aluminized-glass fabric-silicone adhesive material (Ref. 6).

22.4 EFFECTS ON MATERIALS USED IN ELECTRONIC COMPONENTS

It is desirable to keep the biological load on electronic parts or components at a low level by decontamination and clean room manufacturing and assembly in order to keep the time at elevated temperature to a minimum in terminal sterilization. Indications are that the biological loading of electronic parts is low, and also that the manufacturing and assembly processes are quite destructive to microorganisms, which will keep the biological loading low.

The effects of the heat sterilization cycles, as well as the effects of acceleration, shock, vibration, and high vacuum, on the reliability of electronic parts and integrated circuits for use in sterilizable spacecraft have been evaluated. About 73,000 parts of 577 types for a total of 650 million part hours of testing has been accumulated in one program (Refs. 8 and 9).

The solid tantalum fixed capacitors are affected by the heat cycles, with a decrease in resistance resulting in capastrophic failures. The nonhermetic Mylar capacitors become unstable in the heat sterilization environment.

Radio-frequency choke coils show permanent shifts in properties resulting from temperature effects on the core material. Temperature effects on the epoxy insulation also have caused short circuits. Transformers are similarly affected where short or open circuits result from the thermal cycling.

The carbon resistors have significant resistance drift after heat sterilization. The most stable are the carbon film resistors. A ranking of resistor types for performance after heat sterilization would be (1) carbon film, (2) precision power wire wound, (3) metal film, (4) precision wire wound, and (5) carbon. The trimming resistors are ranked (1) wire wound, (2) carbon, and (3) metal film.

The silicon varactor diodes experience an increase in leakage current and decrease in capacitance. In other types of diodes, the purchase specifications require capability to 150°C or higher. Most of these devices will withstand the sterilization cycles. The one exception to this behavior is the gallium arsenide tunnel diode, which cannot withstand the 150°C temperature cycling.

The transistors usually fail because of mechanical deficiencies or contamination during fabrication rather than because of the effects of heat sterilization. The silicon transistor devices are specified to withstand storage at 200°C. The germanium devices cannot tolerate the 150°C temperature cycling. Oscillators using germanium devices will have to be designed to use silicon devices to withstand the thermal cycles. Timer devices using silicon semiconductors can drift due to the temperature cycles.

Most of the failures of integrated circuits result from mechanical and workmanship deficiencies which are revealed during the thermal cycling. The thermal cycling itself should not affect these components, since specifications require storage capability at 150°C or higher.

Quartz crystals may drift in frequency, and the Curie point of some ferrites can be exceeded at 150°C

Heat treatment reduces the power-to-weight ratio of batteries by about 40 to 10 kw/lb. This behavior is the result of degradation of the separators. Sealed secondary silver-zinc cells may be heat sterilized without excessive degradation of electrical characteristics. Nickel-cadmium batteries, although quite low in watt-hours per pound efficiency, have proved capable of surviving the thermal sterilization environment. In general, a significant loss in energy of temperature-soaked cells can be expected; therefore, extensive testing in the heat sterilization environment of cells and batteries to assure their reliability will be required. Special designs and sealing techniques can produce batteries that will be heat sterilizable.

22.5 MISCELLANEOUS MATERIALS

The thermal sterilization cycles do not affect the performance of the solid propellant rocket motors that would be used for orbit injection or for retro maneuvers of the planetary lander. Thus, terminal sterilization would be required to assure that no viable organisms remained on them. Both the orbit injection rockets and the retro rockets could crash land on the planet even though jettisoned from the lander capsule itself.

Biological loading can be maintained at a low level during fabrication of the rocket motor, but terminal sterilization will be required if the motors are a part of the planetary spacecraft. Careful handling of the loaded rocket motors during the thermal cycling, systems test, checkout and transportation to launch sites will be necessary (Refs. 4 and 10).

The materials associated with the solid rocket motor such as the motor case, the insulating liner, O-rings, and nozzle and exit cone materials will have to be chosen to withstand the heat cycling. Most of these materials are chosen to withstand the short-duration high temperature of the rocket firing. However, unless the three 36-hr heating cycles at nearly 300°F are taken into account, some of these materials can suffer changes in properties that could affect the performance of the rocket motor.

Most planetary spacecraft will contain a number of explosively activated devices. The Mariner 4 spacecraft had about 30 of these. Heat sterilization of these devices can affect such materials of construction as metal-to-ceramic seals because of differential thermal expansion between the mating materials. Tolerances of close-fitting members in pin pullers may bind after thermal sterilization. The shear characteristics of safety-locking screws, safety wire, and frangible links may be altered so as to render the device unsafe, or to cause premature firing or failure to fire. The entire actuation device including the explosive squib should be qualified as a unit to the thermal sterilization specification (Ref. 4).

Honeycomb structures of metal or reinforced plastic will not be affected by the thermal sterilization cycles. Brazing alloys are available for metal honeycomb panels that can withstand the heat treatment. The thermal expansion and conduction characteristics of materials of construction will have to be chosen carefully to avoid mismatching. For example, reinforced plastic core with metal face sheets can present a problem both of thermal expansion and of conduction from one metal face to the other during heat-up

or cool-down portions of the heat cycle. The 3003 aluminum alloy face sheets or core could not be used because this alloy cannot withstand the heat cycling. Adhesives for bonding both metal and reinforced plastic honeycomb are available that can withstand the elevated temperature cycling. (See Chapter 10).

The thermal expansion and conductivity of joints and fasteners of dissimilar materials must also be carefully considered in the selection of materials of construction for sterilizable spacecraft Steel bolts and rivets may be required in several sections where aluminum alloys are presently used. Some A286 steel bolts have been used in unmanned spacecraft such as Ranger and Surveyor that have been qualitifed to sterilization specifications. However, the weight penalty of using the heavier bolting or fastening material will have to be carefully assessed. Self-locking nuts with nylon pellets have a maximum use temperature of 250°F and will not withstand heat sterilization. Materials with a maximum use temperature of 300°F should be chosen

Generally, materials and design techniques are available to construct unmanned planetary spacecraft to qualify to the thermal sterilization requirement. The biological loading can be kept low by heat decontamination and clean room manufacturing and assembly. Surface decontamination of an assembled spacecraft can reduce the biological loading to a low enough level to assure reliable terminal heat sterilization. The selection of materials, design, manufacturing, and assembly techniques to assure a reliable sterilized spacecraft will require the critical attention of designers and materials and process engineers. Heating of equipment to produce sterility has a degrading effect on the reliability of the spacecraft, its subsystems, and its components (Ref. 11).

22.6 REFERENCES

1. L. D. Jaffe, "Sterilizing Unmanned Spacecraft," Astronautics and Aerospace Engineering, p. 22–29, August 1963

2. H. E. Newell, "The Role and Responsibility of NASA in Relation to Spacecraft Sterilization," pp. 11–18 in Spacecraft Sterilization Technology, NASA SP-108, 1966

3. L. B. Hall, "NASA Requirements for the Sterilization of Spacecraft," pp. 25–36 in Spacecraft Sterilization Technology, NASA-SP-108, 1966

4. Procedure Manual for Planetary Spacecraft To Be Sterilized by Heating, Vol. I, "Design Guidelines," NASA CR 87131(X67-19474), General Electric Co., Missiles and Space Division, Philadelphia, Pa., 31 July 1965

5. D. P. Kohorst and H. Harvey, "Polymers for Use in Sterilized Spacecraft," pp. 327–342, Spacecraft Sterilization Technology, NASA SP-108, 1966

6. S. H. Kalfayan and B. A. Campbell, Effects of the Thermal Sterilization Procedure on Polymeric Products, TR-32-973, Jet Propulsion Laboratory, 15 November 1966.

7. R. F. Rydelek and A. L. Landis, Study of the Effects of Ethylene Oxide-Freon 12 Upon Properties of Polymers and Metallic Surfaces, Rept. No. P66-96, Hughes Aircraft Company, 1 June 1966

8. J. Visser, "Current Results of the Electron Part Sterilization Program at the Jet Propulsion Laboratory," pp. 312–322, in Proc. of 1967 Annual Symposium on Reliability, Washington, D. C., 10–12 January 1967

9. A. G. Fitak, L. M. Michel, and R. F. Hotlze, "Sterilizable Electronic Packaging, Connectors, Wires, and Cabling Accessories," pp. 343–360, in Spacecraft Sterilization Technology, NASA SP-108, 1966

10. W. Ginn, "Heat Sterilization of Pyrotechnics and Onboard Propulsion Subsystems," pp. 443–453, in Spacecraft Sterilization Technology, 1966

11. G. B. Kautz and P. Tarver, "Plan for Sterilization of Voyager Capsule," NASA SP-108, pp. 559–567, in Spacecraft Sterilization Technology, 1966

GLOSSARY

GENERAL TERMS

Ablation – The removal of surface material from a body by vaporization, melting, or other process, due to aerodynamic effects while moving at high speed through a planetary atmosphere

Absorptance – The ratio of quantity of absorbed radiation to the quantity incident upon it

Absorption – Assimilation of molecules of gases or liquids into the body of a solid material

Absorptivity – The absorptance of an opaque, optically smooth, clean portion of material

Adhesion – Attraction exerted between the surfaces of unlike bodies in contact

Adsorption – Adhesion of molecules of gases or liquids on the surface of a solid material

Aerodynamic heating – Surface heating of a body caused by air friction and compression processes on passage of air or other gases over the body; significant chiefly at high speeds

Aeronomy – Study of the upper regions of the atmosphere where physical and chemical reactions due to solar radiation take place

Albedo – The reflecting power expressed as the ratio of light reflected from an object to the total amount falling on it

Ambient – Condition of the environment surrounding an aircraft or other body in motion, but undisturbed or unaffected by it, as in "ambient air," or "ambient temperature"

Aphelion – That point in the orbit of a planet or comet which is farthest from the Sun

Apogee – That point in the orbit of an earth satellite which is farthest from the Earth

Apolune – That point in the orbit of a lunar satellite which is farthest from the Moon

Apsides (sing. Apsis) – Points in the orbit of a satellite or planet nearest to or farthest from the center of attraction

Asphyxia – The consequence of interference with respiration, whether by mechanical means or by the inhalation of gases containing insufficient oxygen

Astronomical unit, A. U. – The mean distance from the Earth to the Sun

Balanced circulation – System of winds resulting when the horizontal pressure gradient force is just balanced by the Coriolis and centrifugal forces associated with the circulation

Ballistic trajectory – The trajectory followed by a body under the action of gravitational forces and the resistance of the medium through which it passes. (A rocket vehicle without lifting surfaces will describe a ballistic trajectory after its engines are shut off)

Biconical antenna – An antenna consisting of two conical conducting surfaces, excited at the vertices of the cones

Blackbody – The blackbody or ideal radiator absorbs all incident radiant energy and radiates energy at the maximum rate possible per unit area at each wavelength for any given temperature

Blackout – A fadeout of radio communications due to environmental factors such as ionosphere disturbances or a plasma sheath surrounding a reentry vehicle

Bremsstrahlung – Radiation due to acceleration of fast charged particles by nuclei

Canopus – A star used as a fixed reference point in space during certain space probe missions

Chain scission – Cleavage of primary skeletal bonds in a polymer chain causing degradation to form low molecular weight fragments: see depolymerization

Cohesion – Force of attraction between the molecules or atoms within a single phase

Coldwelding – Solid-phase welding in which pressure, without added heat, is sufficient to create a welded joint

Coriolis force – A deflecting force due to the Earth's rotation, diverting moving objects to the right in the northern hemisphere, and to the left in the southern hemisphere

COSPAR – Acronym for Committee on Space Research, international council of scientific unions for coordinating space data of international significance

Covalent linkage – Chemical bond formed by the sharing of electrons between elements; electron pairing is the most common type of chemical linkage existing in organic materials (i.e., compounds of carbon) in contrast to the electrostatic or Van der Waal forces encountered in the ionic bond of inorganic compounds

Cross-linking – Mechanism whereby adjacent molecular chains of certain high polymers are interlocked by means of a bridge, thus forming a three-dimensional network; polymers undergoing cross-linking are converted from soft, thermoplastic to hard, thermosetting types

Cryogenics – The science of producing and maintaining very low temperatures; for example, from -50°F to absolute zero

Cyanosis – An effect of asphyxia, among other causes, in which there occurs an abnormally large amount of un-oxygenated blood, resulting in a blue color of the skin and mucous membranes

Depolymerization – Process whereby high molecular weight polymers are degraded into low molecular weight fragments or monomers; depolymerization involves cleavage of the primary skeletal bonds in the polymer chain

Discone antenna – An antenna consisting of a conical conducting surface and a concentric circular image plane, excited at the apex of the cone, usually by a coaxial transmission line through the circular image plane

Dissipation factor – A quantity derived from the complex inductive capacity of a dielectric material that specifies the relative attenuation of an electromagnetic wave in the dielectric; often expressed as $\tan \delta$, where δ is the phase angle of the total current density J with respect to the applied electric field strength

Diurnal – Happening each day

Doppler effect – An apparent change in wavelength of the radiation emitted by a source when there is relative motion between source and observer

Dose (Dosage) – The radiation delivered to a specified area or to the whole body. Units of dose specification are roentgens for x or γ rays, reps for beta rays and protons, and alternatively rads for all types of radiation

Dose rate – Radiation dose delivered per unit time

Ecliptic – The plane of the Earth's orbit around the Sun, inclined to the Earth's equator by about 23 deg 27 min

Ecology – The biological science dealing with the relations of organisms and their environment, including relations with other organisms

Elastomer – Type of rubbery high polymer having elastic properties manifested by a high degree of elongation and compressibility

Electron volt, eV – The kinetic energy acquired by a particle of electronic charge when the particle has fallen through a potential drop of 1 volt, V; 1.602×10^{-12} erg, 1.602×10^{-19} joule, J, 1.52×10^{-22} Btu

Emissivity – The emittance of a specimen of material with an optically smooth, clean surface, and sufficient thickness to be opaque

Emittance – The ratio of the radiant flux intensity from a given body to that of a blackbody, at the same temperature

Ephemeris – A table or listing showing the location of a celestial body for regular intervals

Faying surfaces – The adherend surfaces in contact with each other in a bonding operation or bonded structure

Flux – The rate of flow of energy through a surface

Gamma – A magnetic field intensity unit equal to 10^{-5} gauss

Gamma ray, γ-ray – Penetrating short wavelength electromagnetic radiation of nuclear origin

Gauss – A unit of magnetic field intensity in the cgs (centimeter-gram-second) system of units

Gyro – A device utilizing the angular momentum of a spinning rotor to sense angular motion of its base about one or two axes at right angles to the spin axis. Also called "gyroscope"

Heat shield – A material system providing protection of a spacecraft or reentry vehicle from the effects of high temperature. It may operate by absorbing the heat (a heat sink), by reradiating it to space (a radiative shield), or by a combination of these processes plus phase changes (an ablator)

Heat sink – A material capable of absorbing heat; a device utilizing such material for the thermal protection of a spacecraft or reentry vehicle

Hertz – A unit of frequency equal to 1 cycle per second

Hohlraum – An apparatus for determining infrared reflectance in which a sample forms a part of one wall of a uniformly heated cavity

Honeycomb material – Composite material laminate consisting of a central core layer made up of open cells (usually hexagonal, hence the name) and outside facing layers of thin solid material

IMP – Acronym for Interplanetary Monitoring Platform, an Explorer series satellite measuring fields prevailing in space

Injection – The process of putting an artificial satellite into orbit. Also the time of such action

Ionization – The process or the result of any process by which a neutral atom or molecule acquires either a positive or a negative charge

Ionizing radiation – Any electromagnetic or particulate radiation capable of producing ions, directly or indirectly, in its passage through matter

Laser – From Light Amplification by Stimulated Emission of Radiation

Maser – From Microwave Amplification by Stimulated Emission of Radiation

Meteor – The light flash resulting from the entrance of a meteoric particle into the Earth's atmosphere at high speed

Meteoric particle – An intra-solar-system body or particle of any size smaller than a planet and generally of cometary or asteroidal origin

Meteorite – A meteoric particle reaching the Earth's surface with a mass greater than 10^{-4} gm

Meteoroid – A meteoric particle in space of any size greater than 10^{-4} gm

Micrometeorite – A meteoric particle reaching the Earth's surface with a mass equal to or less than 10^{-4} gm

Micrometeoroid – A meteoric particle in space of mass equal to or less than 10^{-4} gm

Monocoque – A construction technique, extensively used in the aircraft industry, wherein the vehicle skin is designed as the load bearing member

Monopole – Usually a quarter-wavelength long radiator perpendicular to a conducting image plane, excited by means of a coaxial transmission line through the image plane

Micron, μ – 10^{-6} meter, m; 10^{4} angstroms, Å; 10^{-4} cm; 3.94×10^{-5} in.

NaK – An alloy of sodium and potassium used as a reactor coolant

Nodal regression – The slow westward motion of the nodes (those points at which the orbit passes through the plane of the ecliptic) of the Moon's orbit, a cycle being completed in about 18.6 yr; this effect is caused by solar attraction

n-on-p solar cells – Photovoltaic energy conversion cells in which a base of p-type silicon (having fixed electrons in a silicon lattice and positive holes which are free to move) is overlaid with a surface layer of n-type silicon (having fixed positive holes in a silicon lattice with electrons which are free to move)

OAO – Acronym for Orbiting Astronomical Observatory

OGO – Acronym for Orbiting Geophysical Observatory

OSO – Acronym for Orbiting Solar Observatory, a satellite designed to make measurements of solar parameters

Ozone – The triatomic form of oxygen. A blue gas with a characteristic pungent odor and of high toxicity

Perigee – That point in the orbit of an earth satellite which is nearest to the Earth

Perihelion – That point of the orbit of a planet or comet at which it is nearest to the Sun

Perilune – That point in the orbit of a lunar satellite at which it is nearest to the Moon

Photon – According to the quantum theory of radiation, the elementary quantity or quantum of radiant energy

Polymer – High molecular weight resinous composition consisting of a repeating chemical unit

p-on-n solar cells – Photovoltaic energy conversion cells in which a base of n-type silicon (having fixed positive holes in a silicon lattice and electrons which are free to move) is overlaid with a surface layer of p-type silicon (having fixed electrons in a silicon lattice and positive holes which are free to move)

Rad – An absorbed radiation unit equivalent to 100 ergs/gm of absorber

Radome – Housing for an antenna, essentially transparent to radio frequency radiation

Rayleigh scattering – The law, discovered by Lord Rayleigh, which related the scattering of light to the fourth power of its wavelength

Reflectance – The fraction of radiation incident on an object which is reflected

Reflectivity – The reflectance of an opaque, optically smooth, clean portion of material

Restrahlen bands – Spectral regions (usually in the infrared region) in which certain materials exhibit extraordinarily high reflectivity

Roentgen, R – The quantity of x- or γ-radiation, the associated corpuscular emission of which, per 0.001293 gm of air, produces, in air, ions carrying 1 electrostatic unit of electricity of either sign

Satellites – Devices, manned or unmanned, that are designed to be placed into an orbit around the Earth, the Moon, or any other body

Scale height – A measure of the altitude variation between density and/or temperature in an atmosphere

Solar constant – The rate at which solar radiation is received in a surface perpendicular to the incident radiation and at the Earth's mean distance from the Sun, but outside the Earth's atmosphere. G = 442 Btu/hr-ft^2 or 1.94 cal/min-cm^2

Solar cycle – Sunspot cycle of approximately 11-yr duration

Solar flare – A sudden disturbance on the surface of the Sun in the course of which high-energy particles are emitted

Spallation – A type of nuclear reaction in which several particles are ejected from the nucleus. Also the ejection of secondary material from the rear surface of a sheet of material bombarded by a meteoric particle

Spectral irradiance – Radiation falling on unit area of a body and having wavelengths lying in some range between λ and $\lambda + \Delta\lambda$

Spacecraft – Devices, manned and unmanned, that are designed to be placed into an orbit about the Earth or into a trajectory to another celestial body

Synchronous satellite – A satellite orbiting the Earth at periods equal to, or multiples of, the Earth's rotational period; i.e., making one, two, three, etc., orbits in a 24-hr period

Tabor black – A type of thermal control surface having a high absorptance at wavelengths shorter than 2 μ and a low absorptance at longer wavelengths

Telemetry – The science of measuring a quantity or quantities, transmitting the measured value to a distant station, and there interpreting, indicating, or recording the quantities measured.

Terminator – The line dividing the illuminated and the dark parts of the disk of a satellite or planet

Thermistor – A resistance element made of a semiconducting material which exhibits a high negative temperature coefficient of resistivity

Torr – A pressure unit equivalent to that required to support a column of mercury 1 mm high

Total hemispherical emittance – This is generally taken to be equivalent to the unmodified term, emittance. Total indicates that emitted energy of all wavelengths is accounted for; hemispherical means that all energy emitted into the hemispherical space above the surface element of interest is accounted for

Transmittance – The fraction of radiation incident on an object which is transmitted through the object

TRS – Acronym for Tetrahedral Research Satellite

Twilight orbit – An orbit in which the satellite orbital plane is perpendicular to the earth-sun line; the satellite always passes over those parts of the earth experiencing twilight conditions

Type N connector, Type TNC connector, Type SC connector – Units for joining coaxial radio frequency cables and transmission lines, fabricated according to standardized military specifications

Ullage – The amount that a container lacks of being full

Whip antenna – A monopole antenna consisting of a thin conductor, such as wire or a metal rod, usually flexible

X rays – Penetrating electromagnetic radiations having wavelengths shorter than the ultraviolet. It is customary to refer to photons originating as a result of some nuclear change as γ rays and to reserve the term x rays to those photons originating as a result of a change in only the extranuclear part of the atom

Yagi – An antenna array consisting of a driven element and one or more subsidiary elements which radiate due to currents induced in them by the primary field of the driven element

Zodiacal light – Light bands extending on either side of the sun approximately in the plane of the ecliptic, and believed to be part of its outer atmosphere

POLYMER TERMS

Generic or Trade Name	Chemical Name or Composition	Commercial Products Referred to in This Handbook
PLASTICS		
Epoxy, Epon	Epoxide, Epoxy	Epon 828, Epon 1001, Epon 815, Epon 8, Epon VIII
Phenolic	Phenol-formaldehyde	Conolon 506, Trevarno F-130, CTL-91LD
Silicone	Siloxane	DC 2104, DC 2106
Kel-F	Monochlorotrifluoroethylene	Kel-F-K25, -300, -500, -81
Teflon (TFE)	Polytetrafluoroethylene	
Teflon (FEP)	Fluorinated ethylene propylene	
Tenite	Cellulose acetate butyrate	Tenite II
Marlex, Hi-Fax	Polyethylene (linear or high density)	Marlex-50
Geon, PVC, Tygon	Polyvinyl chloride	Geon 2046, 8630, 8640
Teslar, Tedlar, PVF	Polyvinyl fluoride	
Kynar	Polyvinylidene fluoride	
Acrylic, Plexiglass, Lucite	Polymethyl methacrylate	Plexiglass II
Lexan	Polycarbonate	
Irrathene	Irradiated polyethylene	
Saran	Polyvinylidene chloride polyvinyl chloride (copolymers)	
Mylar	Polyethylene terephthalate	
Dacron fiber	Polyethylene terephthalate	
Orlon fiber, Acrilan	Polyacrylonitrile	Acrilan 16
Nylon (6, 6)	Hexamethylene adipamide	Zytel 101

Generic or Trade Name	Chemical Name or Composition	Commercial Products Referred to in This Handbook
Nomex, H-Film, HT-1 Fiber, PI	Polyimide	
Delrin	Polyacetal	Delrin 500, 507
TAC	Triallylcyanurate	Vibrin 135, Laminac 4232
DAP	Diallylphthalate	
PBI	Polybenzamidazole	
ELASTOMERS		
Thiokol	Polysulfide	
Nitrile, Buna-N	Polybutadiene-acrylonitrile	Hycar OR-15, Hycar OS-10
Neoprene	Polychloroprene	Neoprene W, Neoprene GN
Natural rubber	Polyisoprene	
Viton	Hexafluoropropylene and vinylidene fluoride (copolymers)	Viton A, Viton B
Butyl	Polyisobutylene-isoprene	
Buna-S, SBR, GR-S	Polybutadiene-styrene	
Philprene	Polyisoprene (synthetic)	
PFBA	Polyperfluorobutyl acrylate	IF4
Fluorosilicone	Fluorosilicone	LS-53, LS-55
Hypalon	Chlorosulfonated polyethylene	
Kel-F	Monochlorotrifluoroethylene	Kel-F-3700, Kel-F-550
Silastic, Silicone	Siloxane, methyl	Silastic 7-170, RTV
Adiprene	Polyurethane (isocyanate)	Adiprene C
Acrylic, Acrylate	Polyethylacrylate	Vyram

CONVERSION FACTORS

LENGTH

1 angstrom, Å	$= 10^{-8}$ cm
1 micron, μ	$= 10^{-4}$ cm
1 mil	= 0.001 in.
1 cm	= 0.3937 in.
1 meter, m	= 3.281 ft
1 kilometer, km	= 0.5396 sm
1 statute mile, sm	= 1.609 km
1 nautical mile, nm	= 1.853 km = 1.1516 sm
1 Earth radius	= 3963 sm = 3440 nm
1 astronomical unit, AU	$= 9.29 \times 10^{7}$ sm $= 1.495 \times 10^{8}$ km

MASS

1 gram, gm $= 2.205 \times 10^{-3}$ lb
1 pound, lb = 453.6 gm

PRESSURE

1 Torr = 1 mm of Hg $= 1.934 \times 10^{-2}$ psi = 133.3 Newton/m^2
1 psi = 51.71 mm of Hg $= 6.805 \times 10^{-2}$ atm $= 6.895 \times 10^{3}$ Newton/m^2
1 atm = 14.696 psi

TEMPERATURE

To obtain °F from °C, multiply by 9/5 and add 32
To obtain °K from °C, add 273.16
To obtain °R from °K, multiply by 9/5
To obtain °R from °F, add 459.69

ENERGY

1 electron volt, eV	$= 1.602 \times 10^{-12}$ erg $= 1.52 \times 10^{-22}$ Btu
1 calorie, cal	$= 4.184 \times 10^{7}$ erg $= 3.968 \times 10^{-3}$ Btu
1 British thermal unit, Btu	$= 1.0549 \times 10^{10}$ erg
1 kilowatt-hour, kW-hr	= 3413 Btu

Temperature corresponding to 1 eV = 11606 °K
1 Ton (nuclear equivalent of TNT) $= 4.20 \times 10^{16}$ ergs $= 3.98 \times 10^{6}$ BTU

POWER

1 watt, W	=	10^7 erg/sec = 1.341×10^{-3} hp
1 horsepower, hp	=	745.65 W = 0.70696 Btu/sec
1 British thermal unit per second, Btu/sec	=	1.0549 kW = 1.4145 hp

RADIATION

1 rad	=	100 ergs/gm
1 roentgen, R	=	87.7 ergs/gm (approximately)
1 rad	=	10^6 protons/cm^2 (to within factor of 4)
1 rad	=	3×10^7 electrons/cm^2 (to within factor of 2)

MISCELLANEOUS

1 cal/cm^2-sec-° C/cm	=	0.8062 Btu/ft^2-sec-° F/in.
	=	241.8 Btu/ft^2-hr-° F/ft
1 mean solar year, yr	=	8766 hours, hr = 3.16×10^7 sec

PREFIXES TO METRIC UNITS

Prefix	Symbol	Exponential Equivalent to Prefix
giga	G	10^{+9}
mega	M	10^{+6}
kilo	k	10^{+3}
deci	d	10^{-1}
centi	c	10^{-2}
milli	m	10^{-3}
micro	μ	10^{-6}
nano	n	10^{-9}
pico	p	10^{-12}
femto	f	10^{-15}

INDEX

-A-

A-2/A adhesive, use in Ranger spacecraft 503
A 286 stainless steel, use in spacecraft 524–528
A 4000 adhesive, use in Nimbus spacecraft 502
Able spacecraft, active thermal control of 83
Absorptance of materials 77, 79, 83, 85, 93, 97, 100, 119–132, 489, 570, 571
Absorptance to emittance ratio, effect of simulated space environment on 101, 119–132, 570, 571
Absorptance to emittance ratio, effect of space environment on 97, 119–132, 570, 571
Absorptance to emittance ratio of materials 77, 85, 92, 93, 97, 100, 119–132, 485, 488, 491, 570, 571
Absorptance to emittance ratio of solar reflectors 86, 97, 119–127, 570
Absorptance to emittance ratio of spacecraft surfaces 93, 95–97, 100, 119–132, 139, 485, 488, 491, 569, 570, 571
Acceleration 7–9
Accelerator, electrostatic, as meteoroid simulator 68
Accelerator, exploding foil, as meteoroid simulator 67, 68
Acceptability limits of nonmetallic materials 636, 642
Acceptability of materials for manned systems 636–649
Acceptability of meterials for manned systems, odor test 636, 642
Acoustic excitation 7, 8, 10
Acrylate elastomer, compatibility with reactive fluids 317
Acrylic, effect of space radiation on 181
Acrylic binders, effect of simulated space environment on 104, 110, 125, 126, 130, 131, 139
Acrylic binders, use in solar reflectors 86, 104, 125, 570, 571
Acrylic binders, use in spacecraft thermal control materials 485, 486
Acrylic elastomer, effect of temperature on permeability 313
Acrylonitrile butadiene styrene plastic, use in spacecraft 510
Active thermal control, use in spacecraft 83–85, 93, 485, 486, 488, 489, 491, 492, 568
Adhesion, coefficient of, definition 203
Adhesion metal to metal in vacuum 589, 590
Adhesion of metals 202
Adhesion to substrate of solid lubricants 216
Adhesives (see specific generic or trade name of adhesive sought)
Adhesives, design and manufacturing considerations to selection 241
Adhesives, effect of heat sterilization on 677
Adhesives, effect of high temperature on 246–267
Adhesives, effect of low temperature on 268–274
Adhesives, effect of radiation on 275–290
Adhesives, effect of temperature on 245–274
Adhesives, flammability characteristics of 643
Adhesives, materials selector table 592
Adhesives, odor rating of 643
Adhesives, recommendations for various spacecraft missions 593
Adhesives, relative rating table 592
Adhesives, solar cell cover bonding 283, 285–290
Adhesives, spacecraft applications 242
Adhesives, use in spacecraft 501–503
Adhesives classes 242
Adhesives for optical elements; effects of vacuum environment 174
Adiabatic wall temperature 4
Aerodynamic considerations in antenna design 383
Aerodynamic heating 3, 4, 7
Aerodynamic shear 3
Aeroshell 7 grease, use in Ranger spacecraft 500
Aeroshell 15 grease, effect of simulated space environment on 230
Aeroshell 15 grease, recommended applications 578, 580, 582
AF 300 adhesive, use in Surveyor and Syncom spacecraft 503
Agena (Gemini target) spacecraft, launch and orbital data 473, 474
AISI 440C ball bearings, use in spacecraft 84
Air density, 4
Air density, upper atmosphere 13, 14, 19–21
Albedo, earth 82, 92, 93, 573
Albedo, Mars 82
Albedo, Mercury 82
Albedo, moon 82, 573
Albedo, planetary 80, 81, 82, 91, 92, 573

Albedo, Venus 82
Albedo of planets or moon (see also Reflected radiation) 25, 26, 29, 30, 31, 32, 34
Alloys, effect of heat sterilization on 675, 696
Allyl carbonate, effect of radiation on 178, 179
Alodine coating, use in spacecraft 485, 486, 571
Alodine 401-41, coating, effect of simulated space environment on 131, 571
Alouette spacecraft, launch and orbital data 463, 467
Alouette spacecraft, materials used for 482, 485. 494, 497, 505, 512, 514, 519
Alouette spacecraft, performance in space 481–483
Alpha particles, effect on thermal control materials 149
Alpha particles, trapped 45
Alpha particles, solar flare origin 52
Al-SiO-Ge films, use in spacecraft thermal control 490
Aluminate glass, effect of radiation on 178–180
Aluminized Dacron, use in spacecraft thermal control 488
Aluminized Kapton, use in spacecraft thermal control 490
Aluminized Mylar, use in spacecraft 505–509, 511
Aluminized Mylar, use in spacecraft thermal control 485, 486, 488–493
Aluminized polyvinylfluoride, use in spacecraft thermal control 488
Aluminized tape, use in spacecraft thermal control 485–487
Aluminized Teflon, use in spacecraft thermal control 488, 490
Aluminized Teflon-FEP, effect of simulated space environment on 122, 571
Aluminized Teflon-FEP, use as solar reflector 122, 571
Aluminum, anodized, effect of simulated space environment on 112, 122, 131, 139, 141, 570, 571
Aluminum, effect of sputtering on 176
Aluminum-acrylic paint, effect of simulated space environment on 110, 130, 571
Aluminum alloy, sandblasted, effect of simulated space environment on 128, 571
Aluminum alloy, sandblasted, use as solar absorber 128, 571
Aluminum alloy, use in antennas 384
Aluminum alloy A356, use in spacecraft 523, 525, 526
Aluminum alloy 1060, use in spacecraft 520, 527
Aluminum alloy 1080, use in spacecraft 505
Aluminum alloy 1100, effect of heat sterilization on 701
Aluminum alloy 1100, effect of simulated ascent heating on 106, 570
Aluminum alloy 1100, use in spacecraft 521, 525, 526
Aluminum alloy 1100, use in spacecraft thermal control 491
Aluminum alloy 1145, use in spacecraft 524
Aluminum alloy 2014, use for gears in Nimbus spacecraft 498
Aluminum alloy 2014, use in spacecraft 519, 520, 524, 525
Aluminum alloy 2117, use in spacecraft 528
Aluminum alloy 2024, perforation by meteoroids 68, 69, 71
Aluminum alloy 2024, recommended applications for gears 585
Aluminum alloy 2024, use for antennas on various spacecraft 512, 513
Aluminum alloy 2024, use for gears on various spacecraft 497, 499
Aluminum alloy 2024, use in spacecraft 519–528
Aluminum alloy 2024, use in thermal control 128, 485
Aluminum alloy 2219, use in spacecraft 522
Aluminum alloy 3003, effect of sterilization on 675, 681
Aluminum alloy 3003, use in spacecraft 523–525, 528
Aluminum alloy 5051, use in spacecraft 525
Aluminum alloy 5052, use for antennas on Mariner and Ranger spacecraft 512, 513
Aluminum alloy 5052, use in spacecraft 493, 519, 522–528
Aluminum alloy 6061, use for Vanguard spacecraft antennas 513
Aluminum alloy 6061, use in spacecraft 519–528
Aluminum alloy 6061, use in thermal control 108, 128, 129, 488
Aluminum alloy 7075, effect of heat sterilization on 675
Aluminum alloy 7075, recommended application for gears 585
Aluminum alloy 7075, wear of gears made of 237, 238
Aluminum alloy 7079, use in spacecraft 519, 521, 522, 524, 525, 527
Aluminum alloys, recommended antenna applications 610
Aluminum alloys, selection of 618, 628, 629

Aluminum alloys, use for antennas on various spacecraft 512, 513
Aluminum alloys, use in spacecraft 433, 519–528
Aluminum castings, use in spacecraft 520, 522, 523, 525, 526
Aluminum coated glass, use as thermal control material 102, 103, 127, 570
Aluminum coated quartz, use as solar reflector 86, 127, 570
Aluminum foil, use in spacecraft 84, 116, 128, 141, 489, 491, 493, 574
Aluminum foil, use in unfurlable antennas 394
Aluminum foil, 3M FP2, effect of simulated space environment on 116
Aluminum foil-Teflon composite, use in spacecraft 507
Aluminum honeycomb, use in spacecraft 521–528
Aluminum oxide, effect of ultraviolet radiation on 101, 120, 122, 128, 570, 571
Aluminum oxide, polycrystalline, single crystal, properties of 435, 440
Aluminum oxide, recommended antenna applications 612
Aluminum oxide, Rokide A, use as thermal control material 101, 122, 570
Aluminum oxide, use in spacecraft thermal control 485, 486, 492
Aluminum oxide, use in Telstar 101, 492
Aluminum paint, effect of simulated space environment on 110, 130, 150, 571
Aluminum paint, use as flat reflector 87, 89, 93, 110, 130, 571
Aluminum paint, use as thermal control materials 87, 89, 93, 110, 130, 154, 487–491, 571
Aluminum-silicone paint, effect of simulated space environment on 114, 130, 571
Aluminum-silicone paint, use in spacecraft thermal control 130, 154, 488–491, 571
Aluminum tapes, effect of simulated space environment on 105, 116
Alzak coating, use in spacecraft thermal control 485, 490
Andok C grease, effect of simulated space environment on 230
ANNA spacecraft, launch and orbital data 463
ANNA spacecraft, materials used for 485, 494, 501, 505, 512, 514, 519
ANNA spacecraft, performance in space 483
Annual variation of albedo 32
Anodized aluminum, effect of simulated space environment on 112, 122, 131, 139, 141, 570, 571
Anodized coatings, effect of ethylene oxide on 676
Anodized coatings, effect of simulated space environment on 112, 122, 131, 139, 141, 570, 571
Anodized coatings, use in thermal control 99, 102, 109, 112, 115, 122, 485, 489, 493, 570, 571
Antenna aperture 386, 387
Antenna design considerations 386
Antenna erection devices 396
Antenna gain 387
Antenna geometry, effect on breakdown 389
Antenna irregularities, effect on radiation pattern 395
Antenna materials, effect of environment on, general considerations 391
Antenna radiation pattern as affected by reflector tolerances 395
Antenna reflector, effect of sectioning on 396
Antenna types, use on spacecraft 384
Antennas, applications 383
Antennas, directional 387
Antennas, effect on spacecraft stability 393
Antennas, effect of temperature gradients on 391, 396, 398, 399
Antennas, lubrication of 388
Antennas, millimeter-wave 398
Antennas, optimum locations on spacecraft 392
Antennas, spacecraft, frequencies used for 392
Antennas, steerable 386, 387, 399
Antennas, stowage of aboard spacecraft 398
Antennas, structural requirements 394
Antennas, types used for spacecraft 383
Antennas, unfurling considerations 394
Antennas, use on Topside Sounder satellite 396
Antennas, voltage breakdown at low pressures 388
Antennas used on Alouette spacecraft 482
Antimony trioxide-potassium silicate, effect of simulated space environment on 121
Antimony trioxide-potassium silicate, use as solar reflector 121
Apiezon C oil, use in OSO spacecraft 499
Apiezon J lubricant, effect of simulated space environment on 229
Apiezon K lubricant, effect of simulated space environment on 229
Apiezon K lubricant, use in OGO spacecraft 498

Apiezon L lubricant, use in OSO spacecraft 499
Apogee and inclination of various spacecraft 478–480
Apollo spacecraft, materials used for 484, 485, 497, 501, 504, 505, 512, 514, 519
Apollo spacecraft, meteoroid calculations for 73
Apollo spacecraft, performance in space 483, 484
Apollo spacecraft antenna 384
Apollo spacecraft materials, screening by metal-metal adhesion tendencies 203, 204, 589, 590
Apollo spacecraft window materials, effect of space radiation on 178, 181
Araldite 951 adhesive, use in Ariel spacecraft 501
ARF-2 white, zinc oxide-silicate white, use in spacecraft thermal control 154
Ariel spacecraft, launch and orbital data 462, 464, 471
Ariel spacecraft, materials used for 485, 494, 497, 501, 505, 512, 514, 519, 520
Ariel spacecraft, performance in space 529
Ariel spacecraft antenna 384
Armstrong C-7 encapsulant, use in spacecraft 508
Arsenic trisulfide, effect of gamma ray irradiation on infrared transmission 187, 188
Ascent (see also Acceleration) 11
Ascent environment 3
Ascent environment, actual and simulated 104–117, 570–572
Ascent environment, effect on antennas 389
Ascent environment, effect on lubricant performance 206
Ascent heat transfer 4, 7
Ascent heating, effect on optical materials selection 574
Ascent heating, effect on thermal control materials 104–117, 485, 570–572
Ascent heating, temperature of 97, 104–116
Atlantic spacecraft, launch and orbital data 470
Atmosphere, spacecraft, allowable contamination 654–658
Atmosphere composition, effect of altitude 13, 18–22
Atmosphere concentration, effect of altitude 13, 18, 20–22
Atmospheric contaminants, human response to 651
Atmospheric contaminants, limits for 652
Atmospheric properties, effect of altitude 20–22
Atomic argon, effect of altitude 18, 20
Atomic helium, effect of altitude 15, 18–21
Atomic hydrogen, effect of altitude 18–22
Atomic nitrogen, effect of altitude 19–21
Atomic oxygen, effect of altitude 15, 18–22
Atomic oxygen, effect on metals 436
Atoms, neutral, concentrations in space 55
ATS spacecraft, launch and orbital data 469, 470, 472
ATS spacecraft, materials used for 486, 494, 501, 512, 514, 520
ATS spacecraft, performance in space 529, 530
ATS spacecraft, results from solar cell experiment 416
ATS spacecraft antennas 384
Aurora spacecraft, launch and orbital data 471
Auroral protons and electrons, dose and dose rates from 566, 567
Auroral radiation 52

B

B, L coordinates for trapped radiation 38
B 1056 thermal control material, effect of simulated space environment on 123
B 1056 thermal control material, use in spacecraft 123, 158, 488
Bakelite C-11, use in spacecraft 507
Bakelite microballoons, use in spacecraft 509
Ball bearings, use in spacecraft 84
Barium fluoride, effect of electron irradiation on 183, 186
Barometric law, upper atmosphere 16
BarTemp bearings, use in various spacecraft 498
Batteries, effect of heat sterilization on 680
Batteries, spacecraft, characteristics of 426
Batteries, use in various spacecraft 514–517
Battery failure on OAO spacecraft 546
Bearing retainer, flammability characteristics of 643
Bearing retainer, odor rating of 643
Bearing retainer materials, self-lubricating 233
Bearings, antifriction, types of 208
Bearings, ball, recommended lubricants for small lightly loaded applications 577, 582–584

Bearings, conclusions from space simulation testing 233, 236
Bearings, gyroscope, lubrication recommendations 588
Bearings, large low-speed, lubrication recommendations 585
Bellows, use in spacecraft 84, 489, 492
Beryllium, use for antenna on ATS spacecraft 512
Beryllium, use in spacecraft 489
Beryllium alloys, effect of heat sterilization on 675
Beryllium alloys, use in spacecraft 433, 520, 522, 524
Beryllium-copper alloy, effect of simulated space environment on 129
Beryllium-copper alloy, recommended antenna applications 610
Beryllium-copper alloy, use as solar absorber 129
Beryllium-copper alloy, use for antennas 396, 512
Beryllium-copper alloy, use for gears in space environment 497–499, 585
Beryllium-copper alloy, use in spacecraft 129, 520–524
Beryllium mirror, use in Mariner and Surveyor spacecraft 494, 496
Beryllium oxide, heat sink, use in spacecraft 490
Beryllium oxide, properties of 435, 440
Beryllium oxide, recommended antenna applications 612
Beryllium oxide, use in Alouette spacecraft 514
Beryllium-platinum black, effect of simulated space environment on 115, 132, 571
Beryllium QMV, effect of simulated space environment on 115, 128, 132, 571
Beryllium QMV, use as solar absorber 128, 571
Bimetallic thermal switch, use in spacecraft 84, 491
Binders, acrylic, effect of simulated space environment on 104, 110, 125, 126, 130, 131, 139
Binders, acrylic, use in solar reflectors 86, 104, 125, 570, 571
Binders, acrylic, use in spacecraft thermal control materials 485, 486
Biological loading, limitations on 673, 675, 676, 681
BIOS spacecraft launch and orbital data 469, 472
BIOS spacecraft, materials used for 486, 505, 514, 520
BIOS spacecraft, performance in space 530
Black epoxy paint, use in spacecraft 492, 493
Black glyceryl phthalate paint, effect of simulated space environment on 131
Black glyceryl phthalate paint, use in spacecraft 489
Black paint, effect of radiation on 89, 131, 571
Black paint, effect of simulated space environment on 104, 115, 131, 571
Black paint, use as flat absorber 87, 89, 97, 115, 131, 571
Black paint, use as thermal control material 87, 89, 97, 115, 131, 485, 486, 489–493, 571
Black paint, use in spacecraft 485, 486, 488–493, 571
Black paint, use in thermal control 84, 87, 89, 93, 97, 115, 131, 485, 486, 489–493, 571
Bondmaster M648, use in Tiros spacecraft 504
Bondmaster 688, encapsulant, use in spacecraft 510
Booms, use on spacecraft 384, 396
Boron nitride, recommended antenna applications 612
Boron nitride, use as heat sink 486
Borosilicate glass, use in OSO spacecraft 495
Boundary friction, definition of 201
Boundary lubrication, definition of 205
Brass, use for antennas on French spacecraft 512
Brass, use in spacecraft 84, 492
Breakdown, high-voltage of electronic components in vacuum 428
Breakdown field, antenna, minimum 389
Bremsstrahlung x-rays in space 55
Bronze, spring, use for OGO spacecraft, antennas 513
Bronze bearing composites, friction and wear 224
Brushes, electrical, silver-MoS_2 composites for 224, 225
Bumper concept for meteoroid protection 70, 72–74
Buna-N elastomer, compatibility with reactive fluids 317
Buna-N elastomer, description of 296, 297
Buna-N elastomer, effect of low temperature on stiffness 331–333
Buna-N elastomer, effect of reactor gamma radiation 342, 343
Buna-N elastomer, effects of thermal vacuum testing on 335
Buna-N elastomer, recommended space applications 595, 602
Buna-N elastomer, swelling, effect on properties 315
Buna-N elastomer, use in Nimbus spacecraft 504
Buna-N insulation, recommended space applications 621
Buna-S, effect of temperature on permeability 313
Buna-S elastomer, compatibility with reactive fluids 317

Butadiene elastomer, effects of thermal vacuum testing on 335
Butadiene elastomer, effect of ultraviolet radiation on 350
Butadiene elastomer, recommended space applications 497, 602
Butyl elastomer, air leakage rates 312, 314
Butyl elastomer, compatibility with reactive fluids 317
Butyl elastomer, description of 297, 298
Butyl elastomer, effect of elevated temperature on stress-strain properties 324
Butyl elastomers, effect of high temperature on mechanical properties 325–328
Butyl elastomer, effect of hydrazine fuels on 318
Butyl elastomer, effect of low temperature on stiffness 332, 333
Butyl elastomer, effect of nitrogen tetroxide on 319
Butyl elastomer, effect of reactor gamma radiation 343, 347, 349
Butyl elastomer, effect of temperature on permeability 313
Butyl elastomer, effect of thermal vacuum testing on 335, 337, 338
Butyl elastomer, effect of ultraviolet radiation on 350
Butyl elastomer, recommended space applications 597, 602
Butyl elastomer, use in various spacecraft 504
Butyl insulation, recommended space applications 621
Butyral-phenolic adhesives, description of 243, 245

-C-

C-93 paint, use on spacecraft 384
Cabins, spacecraft, sealing materials for 294
Cable insulation, flammability characteristics of 643
Cable insulation, odor rating of 643
Cables, dielectric breakdown 389
Cadmium, evaporation in space 388
Cadmium plating, use in spacecraft 528
Cadmium sulfide detectors, use on Explorer and Mariner spacecraft 515, 516
Calcium fluoride, effect of electron irradiation on 186
Capacitors, effect of heat sterilization on 679
Capacitors, radiation effects on 421, 423, 424
Capacitors, recommended space applications 616
Carbon black, use in spacecraft thermal control 485, 486, 488, 489, 491
Carbon monoxide, acceptability limits for 637, 638–642
Carbon monoxide, test procedures for 638, 639
Carbon resistors, effects of radiation on 422
Carboxy elastomer, effect of temperature on permeability 313
Carboxy nitroso elastomer, description of 297, 303
Cat-a-lac black paint, effect of simulated space environment on 131, 571
Cat-a-lac black paint, use in spacecraft 84, 97, 131, 154, 486–489, 491, 493, 571
Cellulose acetate propellant, effect of radiation on 455
Ceramic capacitors, effect of neutrons on 424
Ceramic materials, effect of space environment on 433–445
Ceramic materials, use for bearings 210
Ceramic materials, use in spacecraft 433
Ceramic materials for electronics, effects of irradiation on 404
Cerium, inhibiting effect on radiation coloring of glass 177–178
Cerium glass, use in OSO spacecraft 495
Cerium oxide-magnesium fluoride, effect of simulated space environment on 129, 571
Cerium oxide, magnesium fluoride coating, use as solar absorber 129, 571
Cermet materials, use for bearings 210
Charged particles, solar origin 49
Charged particles, trapped, calculation of combined fluxes 45
Charged particles in space 37
Chemically cleaned metals, use as thermal control materials 128, 571
Chemically polished metals, use as thermal control materials 128, 571
Chrome-silicon steel springs, use in spacecraft 524
Chromium aluminum phosphate, use in spacecraft thermal control 486, 491
Chromium-nickel spinel, effect of simulated space environment on 111, 121
Chromium-nickel spinel, use as solar reflector 111, 121
Chromium oxide, Rokide-C, effect of space environment on 115, 131, 571

Chromium oxide, Rokide-C, use as thermal control material 101, 115, 131, 488, 571
Ciba 502 adhesive, use in Tiros spacecraft 503
Cine Positive 5302 film, sensitivity to simulated space radiation 452
Circuit boards, effects of radiation on 406
Circuits, integrated, effects of radiation on 417, 418
Circulation effects in the atmosphere 15
Clay-silicate material, use in spacecraft 153, 570
CLD 5940 dry film lubricant, use in various spacecraft 497, 498
Closed ecological system, materials for 633
Coatings, anodized, effect of ethylene oxide on 676
Coatings, anodized, effect of simulated space environment on 112, 122, 131, 139, 141, 570, 571
Coatings, anodized, use in thermal control 99, 102, 109, 112, 115, 122, 485, 489, 493, 570, 571
Coatings, flammability characteristics of 643
Coatings, odor rating of 643
Cobalt base alloy, L605, use in spacecraft 522
Coefficient of adhesion, definition of 203
Coefficient of friction, definition 200
Cold welding, effect of simulated space environment on 441
Cold welding experiments carried by ERS spacecraft 533
Cold welding in space environment 441
Cold welding in vacuum 589, 590
Cold welding of A286 alloy 441
Cold welding of aluminum alloys 441
Cold welding of copper 441
Cold welding of metals 202, 441
Cold welding of René 41 nickel alloy 441
Cold welding of stainless steels 441
Cold welding of steels 441
Cold welding of titanium alloys 441
Coloration of glass by radiation 177, 178
Columbium, use in spacecraft 433, 519
Communication, spacecraft, general considerations 392
Compatibility of metals with chlorine trifluoride 444
Compatibility of metals with hydrazine 444
Compatibility of metals with hydrogen peroxide 444
Compatibility of metals with liquids 443, 444, 628, 629
Compatibility of metals with nitrogen tetroxide 444, 628
Compatibility of metals with perchloryl fluoride 444
Compatibility of metals with propellants 15–23, 443–445, 628, 629
Compatibility of titanium alloy with liquid oxygen 444, 629
Composite materials 355–382, 505–511, 603–609
Condensation of volatiles in vacuum, effect on lubricant performance 207
Conductivity, thermal, effect of low values in vacuum on lubricant performance 207, 208
Connector, odor rating of 643
Connectors, cable, dielectric breakdown 389
Contact area for friction phenomena 200
Contacts, electrical, silver-MoS_2 composites for 224, 225
Contaminants in the atmosphere, human response to 651
Convection coefficient 3, 4
Conversion coatings, chemical and electrochemical, use in thermal control 99, 131, 490, 493, 570, 571
Copper, recommended antenna applications 610
Copper based alloys, effect of ethylene oxide on 676
Copper-clad fiberglass reinforced epoxy 506, 510, 511
Copper plating, use in spacecraft 525, 528
Copper seals, use in Explorer spacecraft 504
Cork, use in spacecraft thermal control 485
Cork insulation, use in spacecraft 505
Corning microsheet, use in various spacecraft 494–496
Corning 0160 glass, effect of gamma-ray irradiation on infrared transmission 187
Corning 0211 glass, effect of electron irradiation on 182
Corning 0211 glass, effect of space environment on as solar cell cover 189
Corning 0311 glass, effect of high temperature on modulus 192
Corning 1723 glass, effect of electron irradiation on 185
Corning 1723 glass, effect of space radiation on 181
Corning 1865 glass, effect of electron irradiation on 182, 183
Corning 7740 quartz, effect of gamma-ray irradiation on infrared transmission 187

Corning 7940 quartz, effect of electron irradiation on 182
Corning 7940 quartz, effect of space radiation on 181
Corning 7940 quartz, use as solar cell cover sheet 191
Corning 7940 quartz, use for solar cell covers in various spacecraft 494–496
Corning 8362 lead glass, effect of electron irradiation on 182
Corning 8363 lead glass, effect of electron irradiation on 182
Cosmic ray particles, dose and dose rates from 566, 567
Cosmic ray radiation, energies and fluxes 54
Cosmos spacecraft 460
Courier spacecraft, launch and orbital data 462
Courier spacecraft, materials used for 486, 494, 497, 501, 505, 514, 520
Courier spacecraft, performance in space 530, 531
Covers, solar cell, materials used for 189
Cross-linking as radiation effects mechanism on adhesives 275
Crystallization of elastomers at low temperature 329
Crystals, recommended space applications 616
Cure of encapsulants, factor in space stability 407
Current leakage, increase due to radiation effects 406

- D -

D4D aluminum paint, effect of simulated space environment on 130
D4D aluminum paint, use in spacecraft 489
D-6A steel, use in spacecraft 527
Dacron, aluminized, use in spacecraft thermal control 488
Dacron, recommended antenna applications 612, 613
Dacron, use in spacecraft antenna 386
Dacron cloth, use in spacecraft 507–509
Dacron fiber, effect of radiation on 608
Dacron fiber, effect of temperature on 608
Dacron fiber, effect of vacuum on 608
DATS spacecraft, launch and orbital data 471
DC Q 92-090, Q 92-009 white paints, effects of simulated space environment on 124
DC Q 92-090 white paint, use in spacecraft thermal control 124, 156, 487
DC-4 grease, use in cable connectors 389
DC-4 silicone grease, use in Nimbus spacecraft 498
DC-40 grease, effect of simulated space environment on 230
DC-55 silicone grease, use in Nimbus spacecraft 498
DC-704 silicone oil, recommended applications 589
Debris, space, origin of 64
Decontamination procedures 674, 675
Deformations in antennas, allowable amount 395
Degassing of adhesives 257, 259–267
Degradation, principal modes in integrated circuits due to radiation 417
Degradation products from materials, effects on man 651, 652
Delrin, recommended antenna applications 612
Delrin, recommended gear applications 585
Delrin, recommended lubrication applications 579, 587
Density, air 4
Density gradient, in atmosphere 15, 19–21
Density of meteoroids 64
Deployment of antennas after orbiting 387
Design considerations, antennas 383, 386, 387
Detection, meteoroids, methods for 63
Diallylphthalate, effect of temperature on 376
Diallylphthalate, use on OSO spacecraft 516
Diallylphthalate circuit boards, recommended space applications 623
Diallylphthalate molding compound, use in spacecraft 507, 510
Diallylphthalate plastic, effect of reactor gamma radiation on 349
Diazodinitrophenol, effect of gamma radiation on 453
Dielectric constant, changes in due to radiation 408
Dielectric materials, effects of radiation on 406
Dielectric materials, effects of vacuum on 388
Dielectric materials, recommended antenna applications 611–614
Dielectric materials, relative ratings for space usage 619–623
Diester oils, use in various spacecraft 497
Diffusion effects in upper atmosphere 13, 14, 17–19
Diodes, pn junction, effects of charged particles on 410, 412
Diodes, semiconductor, effects of radiation on 405

Diodes, tunnel, effects of charged particles on 410, 412
Diphenyl-oxide-E glass laminates, mechanical properties of 369
Diphenyl-oxide-glass laminates, effect of temperature on 367, 369
Dissipation factor for insulators, changes in due to radiation 408
Dissociation effects in atmosphere 13, 18
Diurnal effect in atmosphere 14, 18, 22
Diurnal variation of albedo 32
DODGE spacecraft, launch and orbital data 471
Dow Corning 200, effect of gamma radiation on 451
Dow Corning 703, effect of gamma radiation on 451
Dow Corning 710, effect of gamma radiation on 451
Dow 7, use in spacecraft 488, 491, 523, 526
Dow 17 anodized coating, effect of simulated space environment on 115, 131, 571
Dow 17 anodized coating, use in thermal control 102, 108, 115, 131, 488, 492, 571
Drag, effect of atmosphere 14
Duroid 5183 modified Teflon, effect of simulated space environment on 235
Duroid 5813 retainers, recommended applications 579
Dynasil fused silica, effect of electron irradiation on 182

-E-

Early Bird spacecraft, launch and orbital data 466
Early Bird spacecraft, materials used for 514, 531
Early Bird spacecraft, performance in space 531
Earth albedo 82, 91, 93, 573
Earth's atmosphere (see also Upper atmosphere) 13, 14, 19–21
Eastman 910 adhesive, use in Nimbus spacecraft 502
EC 1469 adhesive, use in OGO spacecraft 502
EC 2216 adhesive, use in Secor spacecraft 503
Eccobond 55 adhesive, use in Tiros spacecraft 503
Eccobond 57C, adhesive, use in Nimbus spacecraft 502
Eccofoam FP encapsulant, use in spacecraft 505–507, 511
Echo spacecraft, launch and orbital data 462, 464
Echo spacecraft, materials used for 486, 501, 505, 506, 514, 520, 531
Echo spacecraft, performance in space 531, 532
Echo 1 spacecraft, effects of meteoroids 390
Effective temperature, upper atmosphere 17–21
EG 429 lubricant, effect of simulated space environment on 230
EG 429 lubricant, recommended applications 578, 582
EG 509 lubricant, effect of simulated space environment on 230
EG 509 lubricant, recommended applications 578, 582
EGRS spacecraft, launch and orbital data 464
Elastomeric sealing materials, effect of thermal vacuum testing on 335, 337, 338
Elastomers, effect of heat sterilization on 703
Elastomers, effect of high vacuum on 330, 334–341
Elastomers, effect of low temperatures on 329–333
Elastomers, effect of temperature on permeability 313
Electrofilm 77-S lubricant, recommended applications 580, 588
Electrofilm 4396 lubricant, use in various spacecraft 497, 499
Electrofilm 4856 lubricant, recommended applications 580, 587
Electrolytic capacitors, effect of neutrons on 424
Electromagnetic radiation (see also Solar radiation, Nonpenetrating radiation) 25–34
Electron bombardment, effect on optical materials 178, 182, 183
Electron collision frequency, relation to antenna breakdown 388
Electron tubes, effect of radiation on 418–420
Electron tubes, space applications 616
Electronic components, effect of heat sterilization on 679, 680
Electronic materials and components, effects of space environment on 403–431
Electronics housings, sealing materials for 295
Electrons, auroral origin 52
Electrons, effect on photographic emulsions 452
Electrons, effect on semiconductor devices 410
Electrons, effect on solar cells 415
Electrons, solar flare origin 49
Electrons, trapped, calculation of fluxes in specific orbits 45, 48

Electrons, trapped, originating from nuclear explosions 44, 56, 57
Electrons, trapped, spatial intensity distribution 44, 46
Electrons, trapped, spectral energy distribution 44, 47
Electrons in space, dose and dose rates from 566, 567
Elgiloy spring, use in spacecraft 521, 524
Emission, planetary 80, 81, 94, 573
Emissivity of solar cell covers 90
Emissivity of solar cells 90
Emittance of materials 77, 85, 91, 97, 100, 102, 119–132, 489, 570, 571
Emittance of spacecraft 81, 83, 97
Emitted radiation, from planet or spacecraft 25, 34
Emulsions, photographic, sensitivity to simulated space radiation 450, 452
Encapsulants, effect of heat sterilization on 677
Encapsulants, electronic, effects of radiation on 407
EP DX 74 adhesive, use in OGO spacecraft 502
Epibond 123 adhesive, use in Nimbus spacecraft 502
Epiphen 825A adhesive, use in Syncom spacecraft 503
Epon 6, use in spacecraft 502, 509
Epon 8, use in spacecraft 509
Epon 8 adhesive, use in OGO spacecraft 502
Epon 815 adhesive, use in Nimbus and Surveyor spacecraft 502, 503
Epon 815 encapsulant, use in spacecraft 511
Epon 826 – TETA cure, impregnated with aluminum, use in spacecraft 508
Epon 828 adhesive, use in various spacecraft 501–503, 505–507
Epon 828 encapsulant, use in spacecraft 510, 511
Epon 828 laminate, use for spacecraft antenna on Explorer 512
Epon 828-181 glass cloth laminate, use in spacecraft 506–509, 511
Epon 834 encapsulant, use in spacecraft 506
Epon 901 adhesive, use in Ariel and Pioneer spacecraft 501, 503
Epon 913 adhesive, use in Mariner spacecraft 502
Epon 934 adhesive, use in Apollo spacecraft 501
Epoxy, effect of radiation on 406, 488
Epoxy, effect of simulated space environment on 104, 126, 129, 131, 141, 570, 571, 573
Epoxy adhesives, degassing in vacuum 260, 262–267
Epoxy adhesives, effect of high temperature on 250, 253, 256, 258, 260
Epoxy adhesives, effect of low temperature on 270
Epoxy adhesives, effect of penetrating radiation on 277, 280, 281
Epoxy adhesives, effect of UV on transmittance 285–287
Epoxy adhesives, recommended applications for specific spacecraft missions 593
Epoxy adhesives, use for bonding solar cells to substrate 288, 290
Epoxy adhesives, use in various spacecraft 501
Epoxy-amine adhesives, effect of thermal sterilization on 256
Epoxy-amine adhesives, weight loss in vacuum 267
Epoxy binders, use in flat absorbers 97, 131, 570, 571
Epoxy binders, use in solar reflectors 86, 570
Epoxy binders, use in spacecraft thermal control 153, 484–489, 491, 570, 571
Epoxy closed cell foam, effect of simulated space environment on 608
Epoxy encapsulant, RCA 688, use in spacecraft 510
Epoxy encapsulants, recommended space applications 626, 627
Epoxy encapsulating materials, effect of thermal vacuum testing on 339
Epoxy-fiberglass honeycomb, use in spacecraft 505, 507, 511
Epoxy-glass, recommended antenna applications 612
Epoxy-glass cloth, use in spacecraft 509, 511
Epoxy-glass fiber laminates, effect of radiation on 355–357, 359–361, 363, 605
Epoxy-glass fiber laminates, effect of vacuum on 356, 357, 359–361, 363, 367, 370, 372–376, 378, 379, 605
Epoxy-glass laminate, use in spacecraft 505, 506, 508, 510, 511
Epoxy-glass laminate circuit boards, recommended space applications 622
Epoxy (modified) adhesives, description of 243, 244
Epoxy (modified) adhesives, effect of high temperature on 247, 250, 252, 256
Epoxy (modified) adhesives, effect of low temperature on 269, 273
Epoxy (modified) adhesives, effect of penetrating radiation on 277, 280, 282

Epoxy (modified) adhesives, recommended applications for specific spacecraft missions 593
Epoxy-nylon laminates, use in spacecraft 506
Epoxy-phenolic adhesives, description of 243, 245
Epoxy-phenolic adhesives, effect of high temperature on 247, 254–256, 258
Epoxy-phenolic adhesives, effect of low temperature on 269–271, 273
Epoxy-phenolic adhesives, effect of penetrating radiation on 277–282
Epoxy-phenolic adhesives, recommended applications for specific spacecraft missions 593
Epoxy-phenolic adhesives, use in OAO spacecraft 502
Epoxy-phenolic-143 glass cloth, use in spacecraft 509
Epoxy plastic, effect of reactor gamma radiation on 349
Epoxy-polyamide adhesives, description of 243, 245
Epoxy-polyamide adhesives, effect of low temperature on 270–273
Epoxy-polyamide adhesives, effect of penetrating radiation on 277, 280, 282
Epoxy-polyamide adhesives, effect of thermal sterilization on 256
Epoxy-polyamide conformal coatings, use in spacecraft 510
Epoxy-polyamine adhesives, effect of low temperature on 270, 271
Epoxy sealing material, use in various spacecraft 504
Epoxy 828/A, effect of radiation on 357, 363
Epoxy 828/A, effect of temperature on 357, 374–376, 563
Epoxy 828/A, effect of vacuum on 357, 372, 374–376
Epoxy 828/A, mechanical properties of 357, 363
Erection of antennas, mechanisms for 396
Erection of antennas, pressure methods 397
Erection of antennas, self-erection techniques 398
Erosion of optical materials by meteoroids 175, 177
ERS (Environmental Research Satellites) antenna 384
ERS spacecraft, launch and orbital data 463, 464, 466, 468–470
ERS spacecraft, materials used for 486, 494, 506, 512, 514, 520
ERS spacecraft, performance in space 532, 533
ES-10 adhesive, use in OSO and Surveyor spacecraft 502, 503
ESSA spacecraft, launch and orbital data 467–470, 472
ESSA spacecraft, performance in space 53
Esters, dibasic-acid, silicate and phosphate, lubricating properties of 212
Ethers, polyglycol and polyphenyl, lubricating properties of 212
Ethylene oxide, use in decontamination procedures 675–677
Ethylene oxide decontaminant, effect on materials 676, 678
Ethylene propylene elastomer, effects of hydrazine fuels on 318
Ethylene propylene elastomer, effects of thermal vacuum testing on 337, 338
Ethylene propylene elastomer, recommended space applications 596
Ethylene propylene rubber, description of 297, 300
Evaluation of thermal control materials in vacuum 79, 98, 101, 119–132, 570, 571
Evaluation of thermal control materials on spacecraft 78, 98, 119–132, 570, 571
Evaporated aluminum, use in spacecraft 509
Evaporated aluminum, use in spacecraft thermal control 486
Evaporated aluminum oxide, effect of space environment on 122, 129, 570
Evaporated aluminum oxide, use as solar absorber 129, 570
Evaporated aluminum oxide, use as solar reflector 122, 570
Evaporated aluminum oxide, use in spacecraft thermal control 153, 155, 570
Evaporated gold, use in spacecraft thermal control 405, 486
Evaporation, effect on inorganic structural materials 437, 438, 441
Evaporation, effect on metal surface films 436, 437, 440, 441
Evaporation, effect on refractory metals 438
Evaporation, effect on steel alloys 438
Evaporation of ceramics 438, 440
Evaporation of metal alloys 437, 438, 441
Evaporation of metals 437, 438, 441
Evaporation of spacecraft materials 387
Evaporation rate, effect of temperature on 438
Evaporation rate of aluminum 437, 438
Evaporation rate of aluminum oxide 440
Evaporation rate of beryllium 437, 438

Evaporation rate of beryllium oxide 438, 440
Evaporation rate of cadmium 437, 438
Evaporation rate of magnesium 437, 438
Evaporation rate of magnesium oxide 438, 440
Evaporation rate of molybdenum 437, 438
Evaporation rate of silicon dioxide 440
Evaporation rate of silicon oxide 440
Evaporation rate of tantalum 438
Evaporation rate of thoria 440
Evaporation rate of thorium dioxide 440
Evaporation rate of tin 437, 438
Evaporation rate of titanium 438
Evaporation rate of tungsten 437, 438
Evaporation rate of zinc 437
Evaporation rate of zirconia 440
Evaporation rate of zirconium dioxide 438, 440
Evaporation rates of some metals 437, 438
Everlube 811 dry film lubricant, recommended applications 578, 583
Everlube 811 dry film lubricant, use in various spacecraft 498, 499
Everlube 811 molybdenum disulfide film, effect of simulated space environment on 234
Excitation, acoustic 7, 8, 10
Exhaled air, composition and effects on materials 667, 670
Exosphere 13, 16, 22
Explorer 3, damage due to meteoroids 390
Explorer spacecraft, launch and orbital data 461–469, 471, 472
Explorer spacecraft, materials used for 486, 487, 494, 497, 501, 504, 506, 507, 512, 515, 520–522, 534–537, 539, 540
Explorer spacecraft, meteoroid data from 65
Explorer spacecraft, performance in space 533–540
Explorer spacecraft antenna 384
Explosive devices, effect of heat sterilization on 680
Explosive shaped charges as meteoroid simulator 67
Explosives, effect of simulated space environment 450, 453, 454
Explosives, radiation degradation modes 454
Explosives and propellants, recommended space applications 617

- F -

F 50 oil, effect of simulated space environment on 229
F 50 oil, recommended applications 578, 580, 582, 585
F 50 oil, use in various spacecraft 84, 497–499
F 100 adhesive, use in Nimbus spacecraft 502
Fabric, flammability characteristics of 644
Fabric, odor rating of 644
Fasteners, effect of heat sterilization on 681
Fatigue behavior of adhesives at low temperature 273
Fatigue properties, effects of vacuum and radiation on 440–442
Feces, composition and effects on materials 663–665
Ferrite cores, effects of radiation on 425–427
Ferrites, effect of heat sterilization on 680
Feurex glass, effect of electron irradiation on 182, 184
Film, flammability characteristics of 644
Film lubricants, bonded, effect of simulated space environment on 233–235
Films, polymeric, effect of ethylene oxide on 678
Films, polymeric, effect of heat sterilization on 678
Films, polymeric, selection of 603, 607, 609
Filters, various types, effect of high-intensity thermal radiation on 194
Fire point of nonmetallic materials 638, 642–646
Fish-Summer perforation equation for meteoroids 68, 69
Flammability characteristics of nonmetallic materials 634, 636, 643–646
Flammability of liquid lubricants 215
Flash point of nonmetallic materials 638, 642–646
Flat absorber 85, 87, 89, 97, 104, 115, 118, 131, 132, 570, 571
Flat absorbers, absorptance to emittance ratio for 89, 97, 131, 132, 570, 571
Flat absorbers, effect of radiation on 89, 131, 132, 570, 571
Flat absorbers, effect of simulated space environment on 104, 115, 131, 132, 570, 571
Flat absorbers, effect of space environment on 89, 131, 132, 570, 571
Flat absorbers, use as thermal control materials 89, 97, 115, 131, 132, 570
Flat absorbers, use in Mariner 4 and 5 89, 131

Flat absorbers, use of anodic coatings for 89, 99, 102, 103, 115, 131, 570, 571
Flat absorbers, use of black paint for 87, 89, 97, 104, 115, 131, 571
Flat absorbers, use of sand-blasted metals for 89, 115, 132, 570
Flat reflector 85, 87–89, 104, 114, 118, 130, 571
Flat reflector, use of aluminum paint for 87–89, 104, 114, 130, 571
Flat reflectors, use in Mariner 4 130
Flat reflectors, use of metal pigments for 89, 104, 114, 130, 571
Flat reflectors, use of polished metals for 89, 114, 130, 571
Flat reflectors, use of polished silver for 88, 130, 571
Flatus, composition and effects on materials 665, 666
Flexibility of elastomers, effect of low temperature on 329, 330
Fluid systems, sealing materials for 294, 295
Fluids, organic, effects of simulated space environment on 449–451
Fluids, reactive, compatibility with sealing materials 311–320
Fluorinated ethylene-propylene plastic, description of 305, 306
Fluorinated silicone elastomer, effects of thermal vacuum testing on 335, 337
Fluorine-containing oxidizers, effect on sealing materials 316, 320
Fluorocarbon elastomers, effect of high temperature on mechanical properties 325–328
Fluorocarbon elastomers, effect of low temperature on stiffness 331–333
Fluorocarbon lubricants, use in various spacecraft 497
Fluorocarbon rubber, description of 297, 301
Fluorochemical FC-43, effect of gamma radiation on 451
Fluorosilicone elastomers, description of 297, 299
Fluorosilicone elastomers, effects of hydrazine fuels on 318
Fluorosilicone elastomers, recommended space applications 597, 603
Fluorosint bearings, use in Pegasus spacecraft 499
FM 86 adhesive, use in Vela spacecraft 503
FM 97 adhesive, use in Tiros spacecraft 503
FM 123-2 adhesive, use in Apollo spacecraft 501
FM 1000 adhesive, use in antennas 384
FM 1000 adhesive, use in various spacecraft 501–503
Foam-in-place unfurling of antennas 394
Foams, polymeric, selection of 608
FPPN-10802-77 lubricant, recommended applications 578, 583
FPPN-10802-77 trifluoro-methylphenoxy phos-phonitrile lubricant, effect of simulated space environment on 229
French spacecraft, launch and orbital data 467, 468, 470
French spacecraft, materials used for 494, 507, 512, 515, 522
French spacecraft, performance in space 540, 541
Freon 11, Freon 114, use in spacecraft thermal control 489
Frequency, radio, antenna applications 383, 386
Fretting, definition of 201
Friction, boundary type, definition of 201
Friction, hydrodynamic type, definition of 201
Friction, rolling type, definition of 202
Friction, stick-slip type, definition of 201
Friction, welded junction theory of 200
Friction mechanisms 199–203
FS 1265 fluoro-silicone oil, effect of simulated space environment on 229
FS 1265 lubricant, recommended applications 578, 582
FS 1290 grease, effect of simulated space environment on 230
FS 1290 lubricant, use in Apollo spacecraft 497
Fuller Gloss White, effect of simulated space environment on 108, 111, 112, 125, 149, 150, 570
Fuller Gloss White, use as solar reflector 112, 570
Fuller leafing aluminum, effect of simulated space environment on 114, 130, 571
Fuller silicone, effect of simulated space environment on 112, 125, 130, 131, 570, 571
Fuller silicone black, effect of simulated space environment on 115, 131, 571

Fuller silicone black, use as flat absorber 115, 131, 571
Fungi and bacteria, effect on materials 670, 671
Furane 15E adhesive, use in OSO spacecraft 502
Fused silica, use as solar cell covers 90

-G-

G-300 grease, effect of simulated space environment on 229, 230
G-300 grease, recommended applications 578, 580, 582, 585
G-300 grease, use in various spacecraft 497, 498
Gallium arsenide solar cells, effect of charged particles on 415
Gallium arsenide solar cells, use on ANNA and Relay spacecraft 514
Gamma radiation, effect on metals 442
Gamma radiation, effect on thermal control materials 150
Gas gun as meteoroid simulator 67
GE 104, 105, and 106 fused quartz, effect of electron irradiation on 182
Gears, fine-pitch, lubrication recommendations 580, 581, 584, 585
Gears, high-speed, moderate load, lubrication recommendations 586
Gears, lubrication methods used on 236
Gears, materials used for in spacecraft 236–238
Gears, self-lubricating materials used for 236
Gemini spacecraft, launch and orbital data 473, 474
Gemini spacecraft, materials used for 487, 494, 497, 501, 504, 507, 515, 522, 541
Gemini spacecraft, meteoroid data from 65
Gemini spacecraft, performance in space 541, 542
Gemini spacecraft windows, effect of meteoroids on 175
Gemini space windows, effect of vacuum environment on 174
Geomagnetically trapped radiation 37
Geophysical Research spacecraft, launch and orbital data 463
Geopotential, effect on atmosphere diffusion 17
Germanium, effect of gamma-ray irradiation on infrared transmission 187, 188
Germanium, effect of sputtering on 177
Germanium, optical use in Nimbus and Tiros spacecraft 495, 496
GGSE spacecraft, launch and orbital data 464, 465, 471
GGTS spacecraft, launch and orbital data 468
Glass, aluminum coated, use as spacecraft thermal control material 102, 103, 127, 570
Glass, effects of high temperature on mechanical properties 191–193
Glass, use as solar cell covers 90
Glass, use in second surface mirrors 99, 102, 103, 127, 570
Glass, various types, effects of electron irradiation on 182–185
Glass capacitors, effects of neutrons on 424
Glass fiber paper, use in spacecraft 489, 492, 493
Glass fiber reinforcements, use in structural plastics 355–382, 505–511, 605–609
Glass solar cell covers, use in various spacecraft 494–496
Glasses, recommendations for space applications 574, 575
Glasses for electronics, effects of radiation on 404
Gold, recommended antenna applications 610
Gold, vacuum deposited, use as spacecraft thermal control material 486
Gold O-rings, use in Explorer spacecraft 504
Gold plate, use in spacecraft 519, 525, 526
Gold plating, effect of simulated space environment on 129, 571
Gold plating, lubrication uses in space environment 497–500
Gold plating, use as solar absorber 129, 571
Gold plating, use in spacecraft 129, 485, 486, 488, 491–493, 571
Graphite, lubricating properties for space usage 220
Gravity, zero, effects on electronic devices 428
Grease lubricants, space simulation testing of 229–231
Greb spacecraft, launch and orbital data 461–465
Ground activities, effect on lubricant performance 205
Ground-plane antennas, use on spacecraft 384
GT 301 adhesive, use in spacecraft 501, 506

GTS A-29 and A-49 adhesives, use in Pegasus spacecraft 502
Gyro fluids, categories of 449

-H-

H-film, effect of ethylene oxide on 304
H-film, effect of radiation on 607
H-film, effect of temperature on 607
H-film, effect of vacuum on 607
H-film, use in antennas 391
H-film, use in spacecraft 506
H-film, use in spacecraft thermal control 485, 487, 488
H-10 clay-silicone based paint, use in spacecraft 153
H-10 thermal control material, effect of simulated space environment on 119
Halocarbon lubricants, properties of 212
Halocarbon 4-1 fluid, effect of gamma radiation on 450, 451
Halocarbon 208, effect of gamma radiation on 451
Hardening of electronic assemblies to radiation 409
Heat shield temperature 7
Heat sterilization (see also Thermal sterilization) 673–682
Heat transfer to satellites 79, 80, 97, 98
Heat transfer to spacecraft 79, 80, 82, 92, 97, 98
Heat transfer to space probes 80
Heating, aerodynamic 3, 4, 7
Helium atoms, effect on Echo satellite 20
Heterosphere 13
Hitchhiker spacecraft, launch and orbital data 463
Hi-T-Lube, dry film lubricant, recommended applications 578, 583
Hi-T-Lube, molybdenum disulfide film, effect of simulated space environment on 234
Homosil fused quartz, effect of electron irradiation on 182
Homosphere 13
Honeycomb aluminum, use for antenna 386
Honeycomb structures, effect of heat sterilization on 680
Honeycomb structures, use in antennas 384
HT-1 fiber, effect of radiation on 608
HT-1 fiber, effect of temperature on 608
HT-1 fiber, effect of vacuum on 608
HT-424 adhesive, use in Apollo and Gemini spacecraft 501
HT-424 adhesive, use in spacecraft 505, 507
Humidity, effects on electronic equipment 428
Hydraulic systems, sealing materials for 295
Hydrazine fuels, effect on sealing materials 316, 318
Hydrazine propellant, effect of radiation on 453
Hydrocarbon elastomers, effect of nitrogen tetroxide on 319
Hydrocarbon fluids, effect on elastomeric sealing materials 312, 315–317
Hydrocarbon propellant, effect of radiation on 455
Hydrodynamic friction, definition of 201
Hydrodynamic lubrication, definition of 204
Hydrogen ions, effect of altitude 18
Hydrogen ions, effect on gold plating 436
Hydrogen ions, effect on metals 436
Hydrolytic stability of liquid lubricants 215
Hydrostatic equation, for atmosphere 15, 19
Hypalon elastomer, compatibility with reactive fluids 317
Hypalon elastomer, effect of high temperature on mechanical properties 325–328
Hypalon elastomer, effect of nitrogen tetroxide on 319
Hypalon elastomer, effect of temperature on permeability 313
Hypalon elastomer, effect of thermal vacuum testing on 335
Hypalon elastomer, effect of ultraviolet radiation on 350
Hysol adhesives, use in Tiros spacecraft 503

-I-

IDCSP spacecraft, launch and orbital data 468–471
Image converter tubes, effect of high-intensity thermal radiation on 195
Inclination and apogee of various spacecraft 478–480
Inconel, effect of simulated space environment on 127, 128, 571
Inconel, use in spacecraft 489
Inconel 718, use in spacecraft 519
Indium foil, use ir spacecraft thermal control 488
Inductors, coils, transformers, effect of heat sterilization on 679
Inductors, effects of radiation on 423, 427
Inductors, types used in Telstar spacecraft 518

Infrared detectors, recommended space applications 616
Infrared emittance of spacecraft 80, 101
Infrared emittance of thermal control materials 102
Infrared radiation of earth 25, 32, 33
Infrared transmitting materials, effect of gamma-ray irradiation on 183, 187
Infrared transmitting materials, effect of high-intensity thermal radiation on 195
Infrasil fused quartz, effect of electron irradiation 182
Injun spacecraft, launch and orbital data 462, 463
Inorganic structural materials 433–445, 519–528, 618, 628–632
Inorganic structural materials, effect of space environment on 433–445
Inspired air, composition of 670
Insulating materials, effects of radiation on 407
Insulation, wire, effect of heat sterilization on 678
Insulation materials, relative ratings for space usage 617
Insulator, flammability characteristics of 644
Insulator, odor rating of 644
Integrated circuits, effect of heat sterilization on 679
Integrated circuits, effect of radiation on 417, 418
Intelsat spacecraft, launch and orbital data 469
Internal power dissipation of spacecraft 93, 96, 97
Invar, use in spacecraft 524, 527
Invar alloy, recommended antenna applications 610
Irradiated polyolefin, use in spacecraft 507–509, 511
Iridite coating, use in spacecraft 493
Iron oxide pigmented black paint, use in spacecraft 485
IRTRAN 4 windows, use in OGO spacecraft 495

- J -

JTA graphite, use in Surveyor 510

- K -

Kapton, aluminized, use in spacecraft thermal control 490
Kapton, effect of simulated space environment on 607
Kapton, recommended antenna applications 613
Kel-F, compatibility with fuels and oxidizers 321
Kel-F, effect of gamma-ray irradiation on infrared transmission 187
Kel-F, effect of simulated space environment on 607
Kel-F, recommended antenna applications 612
Kel-F, recommended lubrication applications 589
Kel-F elastomer, compatibility with reactive fluids 317
Kel-F elastomer, description of 297
Kel-F elastomer, effect of hydrazine fuels on 318
Kel-F elastomer, effect of nitrogen tetroxide on 319
Kel-F elastomer, effect of temperature on permeability 313
Kel-F elastomer, effect of thermal vacuum testing on 335
Kel-F insulation, recommended space applications 622
Kel-F lubricant, use in spacecraft 497, 500, 510
Kel-F plastic, description of 305, 306
Kel-F plastic, effect of reactor gamma radiation 345, 347–349
Kel-F plastic, use in spacecraft 511
Kel-F plastic sealing material, recommended space applications 601, 603
Kemacryl, use as flat absorber 115, 131, 571
Kemacryl black, effect of simulated space environment on 107, 111, 113–115, 131, 571
Kemacryl on aluminum, effect of simulated space environment on 114, 571
Kemacryl white, effect of simulated space environment on 107, 112, 113, 125, 149, 570
Kemacryl white, use as solar reflector 86, 111–113, 125, 570
KG-80 lubricant, effect of simulated space environment on 229
KG-80 lubricant, recommended applications 579, 588
Kinetic temperature, effect of altitude on 17, 20, 21
Kinetic temperature, effect of heat capacity 17
Kinetic temperature, effect of thermal conductivity 17
Kinetic temperature, upper atmosphere 17, 20, 21
Kodak 80-20, effect of gamma-ray irradiation on infrared transmission 187
Kodak films, sensitivity to simulated space radiation 452
Kovar alloy, recommended antenna applications 610

Kynar, effect of radiation on 408
Kynar insulation, recommended space applications 621
Kynar plastic, description of 305, 307

-L-

Laminar X500 black paint, use in spacecraft thermal control 488
Laminates, flammability characteristics of 644
Laminates, odor rating of 644
Latitudinal effect in atmosphere 14, 20
Launch and orbital data for various spacecraft 460–481
Launch heating profiles 4–6
LCS spacecraft, launch and orbital data 466
LCS spacecraft, materials used for 522
LCS spacecraft, performance in space 543
Lead styphnate, effect of gamma radiation on 453
Lead sulfide detectors, effect of high-intensity thermal radiation on 195
Leakage of sealing materials 310–314
LES spacecraft, launch and orbital data 465–467, 471
LES spacecraft, materials used for 488, 522
LES spacecraft, performance in space 542
Lexan, recommended applications for gears of 585
Lexan, use in spacecraft 509
Lifetime of unmanned spacecraft 457–459
Limits for spacecraft atmospheric contamination 654–658
Lithafrax, lithium aluminum silicate-sodium silicate, effect of simulated space environment on 111, 120, 139, 140, 149, 570
Lithafrax, lithium aluminum silicate-sodium silicate, use as solar reflector 111, 120, 139, 140, 570
Lithium aluminum silicate, effect of simulated space environment on 106, 111, 120, 121, 139, 140, 144, 149, 150, 570
Lithium aluminum silicate, use as solar reflector 86, 88, 111, 120, 121, 139, 140, 570
Lithium fluoride, effect of electron irradiation on 183, 186
Lockheat, recommended antenna applications 612
Lockspray gold, effect of simulated space environment on 129, 571
Lockspray gold, use in spacecraft thermal control 487
Loctite sealant, recommended space applications 599
Loctite sealant, use in Nimbus spacecraft 504
Lofti spacecraft, launch and orbital data 463
Louvers, use in active thermal control 84, 488–491
LS-53 elastomer, compatibility with reactive fluids 317
LS-53 elastomer, effect of low temperature on stiffness 331, 332
LTV 502, use in spacecraft 500
LTV 602 adhesive, use in Syncom spacecraft 503
LubeCo 905, use in Surveyor spacecraft 500
Lubricant lifetime, definition of 576
Lubricants, design factors influencing choice of 567, 577
Lubricants, dry film, use in various spacecraft 497–499
Lubricants, effect of ethylene oxide on 678
Lubricants, effect of heat sterilization on 678
Lubricants, flammability characteristics of 644
Lubricants, liquid, properties of 212
Lubricants, liquid, use for spacecraft 211–215
Lubricants, odor rating of 642
Lubricants, recommended for spacecraft applications 578–581
Lubricants, solid, effect of simulated space environment on 234
Lubricants, solid, use for spacecraft 216–226
Lubricants, space simulation testing of 227–236
Lubricants, types used on spacecraft 211–226
Lubrication, antennas 388
Lubrication, boundary, definition of 205
Lubrication, definition of 204, 205
Lubrication, hydrodynamic, definition of 204
Lubrication requirements 199
Lunar Excursion Module, meteoroid calculations for 73
Lunar Orbiter spacecraft, launch and orbital data 469–471
Lunar Orbiter spacecraft, materials used for 488, 494, 502, 507, 516, 522, 523, 543
Lunar Orbiter spacecraft, performance in space 543, 544
Lunar Orbiter spacecraft antenna 384

- M -

Magnesium, evaporation in space 388
Magnesium alloy, cast, use in spacecraft 520, 524
Magnesium alloy AZ 31, use in spacecraft 491, 520–524, 526, 527
Magnesium alloy HM 21A, use in spacecraft 97, 102, 108, 109, 131
Magnesium alloy K1A, use in spacecraft 524
Magnesium alloy ZH62, use in spacecraft 524
Magnesium alloy ZK21, use in spacecraft 527, 528
Magnesium alloy ZK21A, use in spacecraft 84
Magnesium alloy ZK60, use in spacecraft 520–524, 526, 527
Magnesium alloys, effect of heat sterilization on 675
Magnesium alloys, recommended antenna applications 610
Magnesium alloys, selection of 618, 629
Magnesium alloys, use as spacecraft structural materials 84, 433, 513, 519, 520, 523
Magnesium fluoride, effect of electron irradiation on 186
Magnesium fluoride, effect of gamma-ray irradiation on infrared transmission 187, 188
Magnesium fluoride coating, effect of space environment on 129, 571
Magnesium fluoride coating, use as solar absorber 90, 129, 571
Magnesium fluoride coating, use in spacecraft 492, 493
Magnesium-lithium alloy, use in spacecraft 525
Magnesium oxide, effect of gamma-ray irradiation on infrared transmission 187
Magnesium oxide, properties of 435
Magnetic cores, recommended space applications 616
Magnetic fields, effects on electronic components 429
Magnetic materials, effects of radiation on 425–427
Magnetic storms, effect on atmosphere 15
Magnetic trapping of charged particles 37
Magnetosphere, effect on trapped radiation 37
Mariner spacecraft, active thermal control 84, 488
Mariner spacecraft, antenna 305, 384, 386
Mariner spacecraft, launch and orbital data 463, 465, 471
Mariner spacecraft, materials used for 488, 494, 497, 502, 504, 507, 512, 516, 523, 544
Mariner spacecraft, performance in space 544, 545
Mariner 4 spacecraft, meteoroids detected by 175
Martin Hard coat, use in spacecraft 493
Materials degradation products, effects on man 651, 652
Materials for manned systems 633–649
Materials for manned systems, acceptance tests for 637, 643–646
Materials for manned systems, flammability of 634, 636, 643–646
Materials for manned systems, qualification of 634–636
Materials for manned systems, selection of 633–636
Materials for manned systems, toxicity of 636, 637, 642
Materials for spacecraft antennas, requirements 383
Materials recommended for spacecraft applications (see also specific material desired) 565–631
Materials used in orbited spacecraft (see also specific materials and spacecraft desired) 457–563
Mean free path 4
Mean molecular mass, effect of altitude 19
Measurement of absorptance and emittance 77, 79, 98–100, 103
Melamine resin, glass fiber molding, effect of radiation on 606
Melamine resin, glass fiber molding, effect of temperature on 606
Melamine resin, glass fiber molding, effect of vacuum on 606
Mercury batteries, use on Explorer and Vanguard spacecraft 515
Mercury spacecraft, launch and orbital data 473
Mercury spacecraft, materials used for 489, 495, 497, 498, 504, 507, 512, 516, 524, 541
Meridional density of atmosphere 14
Metal film resistors, effects of radiation on 422
Metal-metal adhesion processes, relation to friction 202
Metal sealing materials, description of 308–310
Metal seals, recommended space applications 595, 602
Metal seals, use in Telstar spacecraft 504

Metal whiskers 442, 443
Metal whiskers, in electrical circuits 443
Metal whiskers, of cadmium 443
Metal whiskers, of solder 443
Metal whiskers, of tin 443
Metal whiskers, of zinc 443
Metallic films, electro-plated, use in thermal control 102, 103, 129, 490, 571
Metallic paints, use in thermal control 93, 571
Metals, acceptability limits for 647
Metals, effect of heat sterilization on 675, 676
Metals, effect of temperature on 434
Metals, recommended antenna applications 610
Metals, soft, use as thin film solid lubricants 226, 227
Metals, types used for bearings 208, 209
Metals and alloys, effect of ethylene oxide decontamination on 676
Metals for electronics, effect of radiation on 404
Metals for manned spacecraft applications 647
Meteor, definition of 64
Meteor showers, periodicity of 65
Meteorite, definition of 64
Meteoroid, definition of 64
Meteoroid bumper concept 70, 72–74
Meteoroid flux, relation to mass 65, 66
Meteoroid impingement on spacecraft 65
Meteoroid penetration (see also Chapter 6) 445, 628
Meteoroids, detection methods for 63
Meteoroids, effect on antennas 390
Meteoroids, effect on electronic components 428
Meteoroids, effect on Explorer 3 transmitters 390
Meteoroids, effect on Mariner 4 spacecraft 390
Meteoroids, effect on optical materials 175, 177
Meteoroids, origin of 64
Methacrylate, cross-linked, effect of space radiation on 181
Methacrylate elastomer, effect of temperature on permeability 313
Methane, photodissociation of 18
Metlbond 406 adhesive, use in Mariner spacecraft 502
Mica, effect of radiation on 406
Mica, use in Mariner spacecraft 494
Mica capacitors, effects of neutrons on 424
Micabond black, effect of simulated space environment on 115, 131, 571
Micabond black, use as flat absorber 115, 131, 571
Micarta, use in spacecraft 505
Micro Mach 416 gears, use in Nimbus spacecraft 498
Microcircuits, effects of radiation on 417, 418
Microfile film, sensitivity to simulated space radiation 452
Micrometeoroid, definition of 64
Micrometeoroids, dimensions and masses 63
Microseal dry film lubricant, use in Surveyor spacecraft 500
MIL-G-3545 lubricant, recommended applications 579
MIL-G-23827 lubricant, recommended applications 578, 585, 587
MIL-G-25013 lubricant, recommended applications 579
MIL-G-25336 lubricant, recommended applications 586, 587
MIL-L-6085A lubricant, recommended applications 579
MIL-L-7808 lubricant, recommended applications 579, 584, 586
Millimeter-wave antennas 386, 398
Millimeter-wave communications, use in spacecraft 392
MIL-O-5605 hydraulic fluid, effect of gamma radiation on 451
Min-K insulation, use in spacecraft 487
MLG-61-92 grease, effect of simulated space environment on 230
MLG-61-92 grease, recommended applications 578, 580, 582
MLG-62-142 grease, effect of simulated space environment on 230
MLO-61-97 oil, effect of simulated space environment on 229
MLO-61-97 lubricant, recommended applications 578, 582, 583
Model atmosphere, altitude profile 19, 22
Modified epoxy-glass fiber, effect of radiation on 607
Modified epoxy-glass fiber, effect of temperature on 607
Modified epoxy-glass fiber, effect of vacuum on 607
Molding compounds, flammability characteristics of 644
Molding compounds, odor rating of 644
Molding materials, acceptable for manned systems 662
Molding materials, offgassing products of 657
Molecular collisions 4
Molecular nitrogen, effect on metals 436
Molecular nitrogen, in atmosphere 18, 20–22

Molecular oxygen, effect on metals 436
Molecular oxygen, in atmosphere 18, 20–22
Molecular weight, upper atmosphere 20–22
Molybdenum, use in spacecraft 433, 522, 527
Molybdenum disulfide, lubricating properties for space usage 220–223
Molybdenum disulfide, use in spacecraft 84, 497, 499, 500, 585
Molybdenum disulfide composites for lubrication applications 223, 224
Molybdenum disulfide lubricant, recommended applications 579–581, 583, 586, 589
Molycote X-15 lubricant, use in Pegasus spacecraft 499
Molykote Type G lubrication, recommended applications 580, 588
Monochlorotrifluoroethylene, effect of radiation on 408
Mylar, aluminized, use in spacecraft 505–509, 511
Mylar, aluminized, use in spacecraft thermal control 485, 486, 488–493
Mylar, effect of radiation on 406, 607
Mylar, effect of reactor gamma radiation on 349
Mylar, effect of temperature on 607
Mylar, effect of thermal vacuum testing on 336
Mylar, effect of ultraviolet radiation on 350
Mylar, effect of vacuum on 607
Mylar, recommended antenna applications 612, 613
Mylar, use in antennas 386, 391, 394
Mylar, use on spacecraft 397, 512, 513, 515
Mylar insulation, recommended space applications 620, 621
Mystik 7455, aluminum tape, effect of simulated space environment on 116
Mystik tape, use in spacecraft thermal control 490

-N-

N-on-p solar cells, effect of charged particles on 415
N-on-p solar cells, use in various spacecraft 514–518
National Academy of Sciences recommendations 652
Neoprene adhesives, effect of thermal sterilization on 256
Neoprene elastomer, air leakage rates 312, 314
Neoprene elastomer, compatibility with reactive fluids 317
Neoprene elastomer, description of 296, 297
Neoprene elastomer, effect of high temperature on mechanical properties 325–328
Neoprene elastomer, effect of low temperature on stiffness 333
Neoprene elastomer, effect of reactor gamma radiation 342, 343, 347, 349
Neoprene elastomer, effect of temperature on permeability 313
Neoprene elastomer, effect of thermal vacuum testing on 335, 337
Neoprene elastomer, effect of ultraviolet radiation on 350
Neoprene elastomer, recommended space applications 596, 602
Neoprene insulation, recommended space applications 619–621
Neoprene-phenolic adhesives, description of 243, 245
Neoprene-phenolic adhesives, recommended space applications 593
Neutral hydrogen, density in upper atmosphere 17
Neutrons, effect on metals 442
Neutrons in space, galactic origin 55
Neutrons in space, solar origin 54
Nickel-cadmium batteries, use on various spacecraft 514–518
Nilvar, use in spacecraft 527
Nimbus spacecraft, launch and orbital data 465, 468
Nimbus spacecraft, materials used for 489, 495, 498, 502, 504, 507, 513, 516, 524, 545, 546
Nimbus spacecraft, performance in space 545, 546
Nitralloy, nitrided, wear of gears made of 237, 238
Nitralloy gears, use in Nimbus spacecraft 498
Nitric oxide in upper atmosphere 18
Nitrile elastomer, description of 296, 297
Nitrile elastomer, effect of high temperature on mechanical properties 325–328
Nitrile elastomer, effect of hydrazine fuels on 318
Nitrile elastomer, effect of nitrogen tetroxide on 319
Nitrile elastomer, effect of temperature on permeability 313
Nitrile elastomer, effect of ultraviolet radiation on 350
Nitrile-phenolic adhesives, effect of penetrating radiation on 277, 281
Nitrile-phenolic adhesives, recommended applications for specific spacecraft missions 593
Nitrile rubber, effect of reactor gamma radiation on 347, 349

Nitrogen tetroxide, effect on sealing materials 316, 319
Nitroglycerin, effect of gamma radiation on 453
Nitroso elastomer, description of 297, 303
Nitroso elastomer, effect of nitrogen tetroxide on 319
Nitroso elastomer, recommended space applications 597
Noise, random 7
Nomex fiber, effect of radiation on 608
Nomex fiber, effect of temperature on 608
Nomex fiber, effect of vacuum on 608
Nomex (HT-1) cloth, use in spacecraft 505
Nonmetallic materials, acceptability of 636, 643–646
Nonmetallic materials, accepted for manned systems 660–663
Nonmetallic materials, combustion rates of 638, 642–646
Nonmetallic materials, fire point of 638, 642–646
Nonmetallic materials, flash point of 638, 642–646
Nonpenetrating radiation (see also Solar radiation) 25–34
Nose cone stagnation temperature 5, 6
NRL silicone white paint, use in spacecraft thermal control 487
Nuclear radiation, effect on thermal control materials 150
Nylasint, use in spacecraft 508
Nylon, effect of reactor gamma radiation 345, 349
Nylon, recommended antenna applications 612
Nylon, recommended applications for gears of 585
Nylon, recommended lubrication applications 579, 581, 587
Nylon, sintered, use for lubrication applications 224
Nylon, use in spacecraft antenna 386
Nylon, use in Tiros spacecraft 500
Nylon-epoxy adhesives, description of 242, 243
Nylon-epoxy adhesives, effect of low temperature on 269–274
Nylon-epoxy adhesives, effect of temperature on 252, 258
Nylon-epoxy adhesives, recommended applications for specific spacecraft missions 593
Nylon-epoxy adhesives, weight loss in vacuum 267
Nylon fiber, effect of simulated space environment on 608
Nylon honeycomb, use in spacecraft 506, 507
Nylon insulation, recommended space applications 620
Nylon lacing cord, use in spacefraft 505, 507, 509, 511
Nylon nut caps, use in spacecraft 508, 510
Nylon-phenolic adhesive, recommended applications for specific spacecraft missions 593
Nylon-phenolic fiberglass reinforced plastic, use in spacecraft 505
Nylon plastic, compatibility with fuels and oxidizers 321
Nylon plastic, effect of ultraviolet radiation on 350
Nylon plastic sealing material, recommended space applications 600, 603
Nylotron bushings, use in Mariner spacecraft 497

·O·

OAO spacecraft, launch and orbital data 468
OAO spacecraft, materials used for 490, 498, 502, 507, 516, 524
OAO spacecraft, performance in space 546
Octoil S oil, use in Pioneer spacecraft 499
Odor, acceptability limits for 637, 638, 642
Odor rating of nonmetallic materials 643–646
Odor test for materials 636, 637
Offgassing of nonmetallic materials 655–658
Offgassing of sealing materials in vacuum 330
Offgassing products, of nonmetallic materials 636–638, 655–658
OGO spacecraft, launch and orbital data 465, 467, 468, 471, 472
OGO spacecraft, materials used for 490, 495, 498, 499, 502, 507, 513, 516, 524, 525, 547, 548
OGO spacecraft, performance in space 546–548
Oil lubricants, space simulation testing of 228–232
Omnidirectional antennas 393
Optical materials, applications in spacecraft 173
Optical materials, effect of high-intensity thermal radiation on 194
Optical materials, effect of high temperatures on 191–195
Optical materials, effect of proton and ultraviolet bombardment on 178, 181
Optical materials, effect of radiation 177–191

Optical materials, effect of space environment 174
Optical materials, effect of sputtering 175–177
Optical materials, effect of vacuum environment 174
Optical materials, recommendations for space applications 574, 575
Optical solar reflector, effect of simulated space environment on 113, 127, 149, 570, 573
Optical solar reflector, mirror, use in spacecraft 127, 153, 570
Orbital decay, effect of upper atmosphere 14
Orbits, data for various spacecraft 460–481
Orbits, spacecraft arranged by apogee and inclination 460, 478–481
Orbits of meteoroids 64, 65
Organic fluids, effects of simulated space environment on 449–451
Organic materials for structural applications (see also Structural plastics, Reinforced plastics, Composite materials) 355–382, 505–511, 603–609
Organic structural materials, selection of 603–609
Organic structural materials, use in spacecraft 505–511
Organics, total, acceptability limits for 636, 637, 643–646
Organics, total, in nonmetallic materials 637, 643–646
Organics in nonmetallic materials, test procedures for 638, 639
Oscar spacecraft, launch and orbital data 462, 466, 467
Oscar spacecraft, materials used for 490, 495, 507, 513, 516, 525
OSO spacecraft, launch and orbital data 462, 465, 470, 472
OSO spacecraft, materials used for 490, 495, 499, 502, 504, 507, 516, 525, 548, 549
OSO spacecraft, performance in space 548, 549
OSO 1 spacecraft, effect of sputtering on surfaces 177
OV spacecraft, launch and orbital data 467–472
OV spacecraft, materials used for 490, 502, 513, 517, 525
OV spacecraft, performance in space 549
Owens-Illinois Inorganic Polymer 100, effect of space radiation on 181
Owens-Illinois Inorganic Polymer 650, effect of space radiation on 181
Oxidation stability of liquid lubricants 215
Oxide film resistors, effect of radiation on 422
Oxide films, effect on friction 203
Oxides for electronics applications, effects of radiation on 404, 405
Oxidizers, compatibility of lubricants with 588
Oxygen enriched atmospheres, materials in 636, 637

P

Pacific spacecraft, launch and orbital data 469, 472
PAGEOS spacecraft, launch and orbital data 468
PAGEOS spacecraft, materials used for 509, 549
PAGEOS spacecraft, performance in space 549
Paper capacitors, effects of neutrons on 424
Paper phenolic honeycomb core, use in spacecraft 493
Paraboloidal antennas, manufacturing techniques 398
Particle concentration, upper atmosphere 16
Particle detectors, effect of electron irradiation on 411
Particle detectors, recommended space applications 616
Passive thermal control of spacecraft 83, 85–91, 485, 488, 489, 568, 569
PD-454 adhesive, use in Nimbus spacecraft 502
Peel strength of adhesives, effect of low temperature on 271
Pegasus spacecraft, launch and orbital data 465, 466
Pegasus spacecraft, materials used for 491, 495, 499, 502, 503, 509, 517, 525, 550
Pegasus spacecraft, meteoroid data from 65
Pegasus spacecraft, performance in space 550
Penetrating radiation, effect on reinforced plastics 355–363, 605–607
Penetrating radiation, effect on sealing materials 334, 342–346
Penetrating radiation in space 565–568
Penetration equation for meteoroids 68
Penetration equation for meteoroids, plot of results 69

Penetration of spacecraft by meteoroids 65, 67
Pentane, use in spacecraft 84, 492
Perfluorobutyl acrylate elastomer, compatibility with reactive fluids 317
Perforation equation for meteoroids 68
Perforation equation for meteoroids, plot of results 69
Perforation of materials by projectiles 67
Permacell EE6100, aluminum tape, effect of simulated space environment on 116
Permacell P-112 aluminum tape, effect of simulated space environment on 116
Phenolic-asbestos felt, effect of radiation and vacuum on 359, 362
Phenolic-asbestos felt, effect of radiation on 359
Phenolic-asbestos felt, effect of vacuum on 359, 362
Phenolic butyral adhesive, effect of temperature on 252
Phenolic-chopped glass fibers, effect of radiation and vacuum on 359, 362
Phenolic-chopped glass fibers, effect of radiation on 359, 362
Phenolic-chopped glass fibers, effect of vacuum on 359, 362
Phenolic-chopped graphite, effect of radiation and vacuum on 359, 362
Phenolic-chopped graphite, effect of radiation on 359, 362
Phenolic-chopped graphite, effect of vacuum on 359, 368
Phenolic closed cell foam, effect of radiation on 608
Phenolic closed cell foam, effect of temperature on 608
Phenolic closed cell foam, effect of vacuum on 608
Phenolic Conolon 506, effect of radiation on 356–358
Phenolic Conolon 506, effect of temperature on 356–358
Phenolic Conolon 506, effect of vacuum on 357
Phenolic Conolon 506, mechanical properties of 356–358
Phenolic-fiberglass laminate, use in spacecraft 510
Phenolic-fiberglass reinforced honeycomb, use in spacecraft 508
Phenolic-glass fiber laminate circuit boards, recommended space applications 623
Phenolic-glass fiber laminates, effect of radiation on 355–361, 363, 605
Phenolic-glass fiber laminates, effect of temperature on 356–358, 360–364, 367, 370, 372–374, 376–380, 605
Phenolic-glass fiber laminates, effect of vacuum on 355–357, 359–364, 367, 370, 372–374, 376–380, 605
Phenolic-graphite fabric, effect of radiation on 359, 362
Phenolic-graphite fabric, effect of vacuum on 359, 362
Phenolic laminates, recommended lubrication applications 587
Phenolic Mobiloy 81-AH7, effect of radiation on 356, 357, 363
Phenolic Mobiloy 81-AH7, effect of temperature on 357, 363
Phenolic Mobiloy 81-AH7, effect of vacuum on 357
Phenolic Mobiloy 81-AH7, mechanical properties of 357, 363
Phenolic (modified) adhesive, recommended space applications 593
Phenolic nitrile adhesives, description of 242, 243
Phenolic nitrile adhesives, effect of low temperature on 269–271
Phenolic nitrile adhesives, effect of temperature on 252, 258
Phenolic resin, glass fiber molding, effect of radiation on 606
Phenolic resin, glass fiber molding, effect of temperature on 606
Phenolic resin, glass fiber molding, effect of vacuum on 606
Phenolic-silica fabric, effect of radiation and vacuum on 359
Phenolic-silica fabric, effect of radiation on 359
Phenolic-silica fabric, effect of vacuum on 359
Phenolic 91 LD, effect of radiation on 356, 357
Phenolic 91 LD, effect of temperature on 357, 372, 374, 376, 377
Phenolic 91 LD, effect of vacuum on 357, 372, 374, 376, 377
Phenolic 91 LD, glass reinforced honeycomb, use in spacecraft 505
Phenolic 91 LD, mechanical properties of 356, 357, 379, 380
Phenyl silane-glass fiber laminates, effect of radiation on 359
Phenyl silane-glass fiber laminates, effect of temperature on 378–380
Phenyl silane-glass fiber laminates, effect of vacuum on 359, 378–380

Photographic emulsions, sensitivity to simulated space radiation 450, 452
Photo-sensitive tubes, effect of radiation on 419
Physical impact, effect on thermal control materials 153, 160, 485
Pioneer spacecraft, active thermal control 84, 491
Pioneer spacecraft, launch and orbital data 461, 467, 469, 472
Pioneer spacecraft, materials used for 491, 495, 499, 503, 509, 513, 517, 525, 526
Pioneer spacecraft, performance in space 551
Planetary emission 80–82, 91, 573
Plasmo clay, effect of space environment on 119, 570
Plasmo clay, use as solar reflector 86, 88, 119, 570
Plasmo clay, use in spacecraft 119, 153, 154, 570
Platinum, use in spacecraft 527
Plexiglass, effect of radiation on 178, 179
Plexiglass, effect of space radiation on 181
Pliobond adhesive, use in Explorer spacecraft 501
Plastic, odor rating of 644, 645
Plastic capacitors, effect of neutrons on 424
Plastics, effect of heat sterilization on 677–679
Plastics, flammability characteristics of 644, 645
Plastics, types used for bearings and lubricants 209, 210
Plastics, use as solid thin film lubricants 225
Pneumatic systems, sealing materials for 295
Poisson distribution applied to meteoroid penetration 70, 71
Polaroid film, sensitivity to simulated space radiation 452
Polished aluminum, effect of simulated space environment on 128, 571
Polished aluminum, use as solar absorber 87, 128, 571
Polished aluminum, use as thermal control material 87, 128, 153, 485, 488, 491, 492, 571
Polished aluminum, use in spacecraft thermal control 128, 153, 154, 485, 486, 490, 491, 571
Polished metals, use in thermal control 87, 93, 101, 102, 128, 153, 485, 570–571
Polyacrylic elastomer, effect of high temperature on mechanical properties 325–328
Polyacrylic elastomer, effect of thermal vacuum testing on 335, 337, 338
Polyacrylic rubber, effect of reactor gamma radiation on 347, 349
Polyacrylonitrile propellant, effect of radiation on 455
Polyalkene insulation, recommended space applications 620
Polyaromatic adhesives, description of 243, 244
Polybenzimidazole adhesives, effect of high temperature on 246–249
Polybenzimidazole adhesives, recommended applications for specific spacecraft missions 593
Polybenzimidazole-glass fabric, effect of temperature on 365, 366, 606
Polybenzimidazole-glass fabric, mechanical properties of 366
Polybenzimidazole plastic, use in spacecraft 505
Polybutadiene elastomer, effect of hydrazine fuels on 318
Polybutadiene elastomer, effect of low temperature on stiffness 331, 332
Polycarbonate plastic, compatibility with fuels and oxidizers 321
Polycarbonate plastic, effect of reactor gamma radiation on 349
Polychloroprene elastomer, effect of hydrazine fuels on 318
Polychloroprene elastomer, effect of nitrogen tetroxide on 319
Polyester, Paraplex P-43, effect of radiation on 356–358
Polyester, Paraplex P-43, effect of temperature on 356–358, 372
Polyester, Paraplex P-43, effect of vacuum on 357, 372
Polyester, Paraplex P-43, mechanical properties of 356–358
Polyester, Selectron 5003, effect of radiation on 357, 363
Polyester, Selectron 5003, effect of temperature on 357, 363, 372
Polyester, Selectron 5003, effect of vacuum on 357, 372
Polyester, Selectron 5003, mechanical properties of 357, 363
Polyester adhesives, effect of thermal sterilization on 256
Polyester elastomer, effect of temperature on permeability 313
Polyester encapsulating materials, effect of thermal vacuum testing on 339
Polyester film, effect of radiation on 607
Polyester film, effect of temperature on 607
Polyester film, effect of vacuum on 607

Polyester-glass, recommended antenna applications 612
Polyester-glass fabric laminates, effect of radiation on 355–358, 360, 361, 363, 606
Polyester-glass fabric laminates, effect of vacuum on 356, 357, 360, 361, 363, 367, 372, 378, 379, 606
Polyester-glass laminates, effect of temperature on 356–358, 360, 363, 367, 372, 378, 379, 606
Polyester resin, glass fiber molding, effect of radiation on 606
Polyester resin, glass fiber molding, effect of temperature on 606
Polyester resin, glass fiber molding, effect of vacuum on 606
Polyethylacrylate propellant, effect of radiation on 455
Polyethylene, effect of radiation on 406, 607, 608
Polyethylene, effect of reactor gamma radiation 345, 347, 348
Polyethylene, effect of temperature on 607, 608
Polyethylene, effect of thermal vacuum testing on 336
Polyethylene, effect of vacuum on 607
Polyethylene, recommended antenna applications 614
Polyethylene, use in cables 391
Polyethylene elastomer, effect of high temperature aging on 326, 327
Polyethylene encapsulating materials, effect of thermal vacuum testing on 339
Polyethylene insulation, recommended space applications 619, 621
Polyethylene plastic, compatibility with fuels and oxidizers 321
Polyethylene plastic, description of 305, 307
Polyethylene plastic, effect of ultraviolet radiation on 350
Polyethylene plastic sealing material, recommended space applications 601
Polyethylene terephthlate (see Mylar) 391
Polyethylene terephthlate, use in spacecraft 505
Polyimide, effect of reactor gamma radiation on 345, 348
Polyimide, effect of thermal vacuum testing on 336
Polyimide adhesives, effect of high temperature on 250, 251
Polyimide adhesives, recommended applications for specific spacecraft missions 593
Polyimide-E glass laminates, mechanical properties of 368
Polyimide film, effect of ethylene oxide on 704
Polyimide film, effect of radiation on 607
Polyimide film, effect of temperature on 607
Polyimide film, effect of vacuum on 607
Polyimide film, HT-1, effect of thermal vacuum testing on 336
Polyimide-glass fiber laminates, effect of temperature on 365–368, 606
Polyimide insulation, recommended space applications 622
Polyimide insulation, use in spacecraft 510, 511
Polyimide plastic, effect of ultraviolet radiation on 350
Polyisoprene elastomer, compatibility with reactive fluids 317
Polymer films and foams, selection of 604, 607–609
Polymer films, fibers and foams, effect of radiation on 607, 608
Polymer films, fibers and foams, effect of temperature on 607, 608
Polymer films, fibers and foams, effect of vacuum on 607, 608
Polymethyl methacrylate insulation, recommended space applications 622
Polymethyl methacrylate plastic, effect of ultraviolet radiation on 350
Polyolefin, recommended antenna applications 614
Polyolefin, use in cables 391
Polyolefin insulation, recommended space applications 620
Polyolefin insulation, use on various spacecraft 516, 517
Polyolefin shrinkable sleeving, use in spacecraft 508
Polypropylene, effect of radiation on 607
Polypropylene, effect of temperature on 607
Polypropylene, effect of vacuum on 607
Polypropylene plastic, effect of ultraviolet radiation on 350
Polystyrene, effect of radiation on 178, 179, 406
Polystyrene, recommended antenna applications 612

Polystyrene, use in antennas 391
Polystyrene plastic, effect of ultraviolet radiation on 350
Polystyrene rigid foam, effect of radiation on 608
Polystyrene rigid foam, effect of temperature on 608
Polystyrene rigid foam, effect of vacuum on 608
Polysulfide adhesives, effect of thermal sterilization on 256
Polysulfide elastomer, compatibility with reactive fluids 317
Polysulfide elastomer, effect of high temperature on mechanical properties 325–328
Polysulfide elastomer, effect of radiation on 408
Polysulfide elastomer, effect of reactor gamma radiation 344, 347, 349
Polysulfide elastomer, effect of temperature on permeability 313
Polysulfide elastomer, effect of thermal vacuum testing on 335
Polysulfide elastomer, recommended space applications 599
Polysulfide encapsulants, recommended space applications 625
Polysulfide propellant, effect of radiation on 455
Polysulfide rubber, description of 297, 301
Polytetrafluoroethylene, effect of radiation on 406, 408
Polytetrafluoroethylene insulation, recommended space applications 619, 620, 622
Polytetrafluoroethylene plastic, compatibility with fuels and oxidizers 321
Polytetrafluoroethylene plastic, description of 304, 305
Polytetrafluoroethylene (see also Teflon)
Polytrifluorochloroethylene (see also Kel-F)
Polytrifluorochloroethylene plastic, compatibility with fuels and oxidizers 321
Polytrifluorochloroethylene plastic, description of 305, 306
Polyurethane, effect of radiation on 408
Polyurethane, recommended antenna applications 612, 613
Polyurethane adhesive, description of 243, 245
Polyurethane adhesive, effect of low temperatures on 269–274
Polyurethane adhesive, effect of penetrating radiation on 277, 280, 282
Polyurethane adhesive, recommended applications for specific spacecraft missions 593
Polyurethane binder, use in spacecraft thermal control 485, 488, 492
Polyurethane elastomer, description of 297, 302
Polyurethane elastomer, effect of high temperature on mechanical properties 325–328
Polyurethane elastomer, effect of reactor gamma radiation 343, 347, 349
Polyurethane elastomer, effect of temperature on permeability 313
Polyurethane elastomer, effect of thermal vacuum testing on 335
Polyurethane encapsulants, recommended space applications 624
Polyurethane encapsulating materials, effect of thermal vacuum testing on 340
Polyurethane foam, use in spacecraft 505–510
Polyurethane propellant, effect of radiation on 455
Polyurethane rigid foam, effect of radiation on 608
Polyurethane rigid foam, effect of temperature on 608
Polyurethane rigid foam, effect of vacuum on 608
Polyurethane 113 conformal coating, use on Lunar Orbiter and Vela spacecraft 516
Polyvinyl alcohol, use in Mariner spacecraft 494
Polyvinyl chloride, effect of reactor gamma radiation on 345, 348, 349
Polyvinyl chloride film, effect of thermal vacuum testing on 336
Polyvinyl chloride insulation, recommended space applications 621
Polyvinyl chloride plastic, compatibility with fuels and oxidizers 321
Polyvinyl chloride plastic, effect of ultraviolet radiation on 350
Polyvinyl chloride plastic sealing material, recommended space applications 601
Polyvinyl fluoride, aluminized, use in spacecraft thermal control 488
Polyvinyl fluoride, effect of radiation on 607
Polyvinyl fluoride, effect of temperature on 607
Polyvinyl fluoride, effect of vacuum on 607
Polyvinyl fluoride insulation, recommended space applications 621
Polyvinyl fluoride plastic, compatibility with fuels and oxidizers 321
Polyvinyl fluoride plastic, effect of reactor gamma radiation on 349

Polyvinyl formal insulation, recommended space applications 621
Polyvinyl sleeving, use in spacecraft 508
Polyvinylidene chloride plastic, effect of reactor gamma radiation on 348
Polyvinylidene fluoride, effect of reactor gamma radiation 345, 349
Polyvinylidene fluoride, use in spacecraft 505, 509
Polyvinylidene fluoride plastic, description of 305, 307
Polyvinylidene fluoride plastic sealing materials, recommended space applications 601
P-on-n solar cells, effect of charged particles on 415
P-on-n solar cells, use in various spacecraft 514, 516–518
Potassium silicate, effect of simulated space environment on 111, 119–121, 141, 144, 147, 570
Potassium silicate, use in solar reflector materials 86, 88, 111, 119–121, 570
Potassium silicate, use in spacecraft thermal control 154, 485, 490, 491, 570
Potting compounds, encapsulants, flammability characteristics of 645
Potting compounds, encapsulants, odor rating of 645
PR 1538 polyurethane encapsulant, use on BIOS spacecraft 514
Pressure, upper atmosphere 20–22
Pressure, erection of antennas 398
Pressure scale height, upper atmosphere 16
Pressurized components, effect of heat sterilization on 675, 682
Probability for meteoroid penetration 70, 71
Propellants, effect of simulated space environment on 450, 453, 455
Propellants, effect on elastomeric sealing materials 316, 318, 319
Properties of ceramic materials 435
Propulsion systems, sealing materials for 295
Propulsion tanks for Apollo spacecraft, stress corrosion cracking of 484
Proton bombardment, effect on optical materials 178, 181
Protons, auroral origin 54
Protons, effect on aluminum 436
Protons, effect on metals 15–20, 436, 442
Protons, effect on optical surfaces 436
Protons, effect on photographic emulsions 452
Protons, effect on semiconductor devices 410
Protons, effect on solar cells 415
Protons, solar flare origin 49, 51–53
Protons, trapped, calculation of fluxes in specific orbits 49, 50
Protons, trapped, energy spectra for 38, 42, 43
Protons, trapped, spatial intensity distribution 38–41
Protons in space, dose and dose rates from 566, 567
Puncture of spacecraft by meteoroids 65, 67
PV 100 white paint, use in spacecraft thermal control 488, 489, 491
Pyrochrome green, use in spacecraft 492

·Q·

QMV-Beryllium-platinum black, effect of simulated space environment on 115, 132, 571
Quartz, fused, effect of electron irradiation on 182, 183
Quartz, natural crystal, effect of electron irradiation on 182
Quartz, recommendations for space applications 574, 575
Quartz crystals, effect of heat sterilization on 680
Quartz microballoons, use in spacecraft 509
Quartz solar cell covers, use in various spacecraft 494–496

·R·

Radiation, charged particle, solar wind 52
Radiation, cosmic ray, energies and fluxes 54
Radiation, effect of protons on thermal control materials 79, 98, 119–122, 124–126, 129, 138, 141–147, 150, 570, 571, 573
Radiation, effect of solar wind on thermal control materials 79, 119, 123, 124, 126, 570
Radiation, effect of ultraviolet on thermal control materials 77, 79, 98, 119–132, 133–140, 142, 150, 570, 571, 573
Radiation, effect on adhesives 275–290
Radiation, effect on black paint 89, 131, 154, 571, 573

Radiation, effect on ceramic material 442
Radiation, effect on electronic materials and components 403–426
Radiation, effect on flat absorbers 89, 131, 571
Radiation, effect on flexural strength of reinforced plastics 359, 360
Radiation, effect on magnesium 442
Radiation, effect on mechanical properties of reinforced plastics 355–363
Radiation, effect on metals 442
Radiation, effect on optical materials 177–191
Radiation, effect on polymer films, fibers, and foams 607, 608
Radiation, effect on reinforced plastics 355–368, 605–607
Radiation, effect on solar absorbers 98, 128, 129, 570
Radiation, effect on solar reflectors 88, 119–127, 570
Radiation, effect on tensile strength of reinforced plastics 356–358, 361–363
Radiation, effect on thermal control materials 118–153, 570, 571, 573
Radiation, electrons, effect on thermal control materials 98, 119–121, 125–127, 129, 130, 147, 148, 150, 570, 571, 573
Radiation, penetrating, dose rates received in various orbits 567
Radiation, penetrating, effect on lubricant performance 206
Radiation, penetrating, integrated doses received in various orbits 566
Radiation, satellite-borne reactors 55, 59
Radiation damage to materials, mechanisms for 58
Radiation damage to tissue, calculations 58
Radiation dose units 568
Radiation due to nuclear device detonation 55, 56
Radiation-elevated temperature, effect on reinforced plastics 356, 357
Radiation environment, internal to spacecraft 57
Radiation environment, natural 37
Radiation in space 565–568
Radiation-low temperatures, effect on reinforced plastics 356, 358, 360–363
Radiation pressure, effect on meteoroids 64, 65
Radiation shielding, calculations for 57, 58
Radiation stability of liquid lubricants 214
Radiation tolerance of devices, limitations of concept 409
Radiation-vacuum, effect on reinforced plastics 356, 357, 359–362
Radio astronomy antennas 386
Radio Astronomy Explorer satellite, antennas for 396
Radio frequencies, antenna applications 383
Random noise 7
Ranger spacecraft, launch and orbital data 462–466
Ranger spacecraft, materials used for 491, 495, 499, 500, 503, 504, 509, 510, 513, 517, 526, 552
Ranger spacecraft, performance in space 551, 552
Rayolin N, wire insulation, use in spacecraft 510
Recombination, effects in atmosphere 18
Reflectance of aluminum coated glass 103
Reflected radiation (see also Albedo) 25, 26, 29–31
Reflector, antenna, effect of sectioning on 396
Refractory metals, effect of space environment on 433–445
Refractory metals, selection of 628, 629
Refractory metals, use in propulsion systems 433, 522, 527
Refractory metals, use in spacecraft 433, 522, 527
Refrasil-phenolic honeycomb, use in spacecraft 507, 510
Refrigerants, recommended space applications 617
Refrigerants, use in spacecraft 84, 89
Reinforced plastics 355–382, 505–511, 603–609
Reinforced plastics, effect of heat sterilization on 677
Reinforced plastics, effect of radiation on 355–363, 605–607
Reinforced plastics, selection of 603–609
Relative biological effectiveness of radiation 58
Relay spacecraft, launch and orbital data 463, 464
Relay spacecraft, materials used for 492, 495, 510, 517, 526
Relay spacecraft, performance in space 552
Relays, effect of radiation on 423, 424
Reliability increase of unmanned spacecraft 457–459
René 41, nickel alloy, use in spacecraft 131, 489, 522
René 41, use for antennas on Apollo spacecraft 512
René 41 alloy, use in antennas 384
Resistive electronic components, effect of radiation on 420–422

Resistive electronic components, failure modes 421
Resistivity of dielectrics, effect of radiation on 406
Resistivity of insulators, change due to radiation 408
Resistivity of metals, change due to irradiation 404
Resistivity of solar cells, effect on charged particle sensitivity 415
Resistors, effect of heat sterilization on 679
Resistors, recommended space applications 616
Resistors, types used in Telstar spacecraft 517
Respired air, composition of 670
Rexolite, recommended antenna applications 612
Rexolite insulation, use in spacecraft 509, 511
Rhodium, recommended antenna applications 610
Rocket exhaust, effect on thermal control materials 160, 485
Rokide-A, effect of simulated space environment on 112, 122, 570
Rokide-A, use as thermal control material 101, 112, 122, 486, 570
Rokide-C, effect of simulated space environment on 115, 131, 571
Rokide-C, use as thermal control material 101, 115, 131, 571
Rokide-C, use in spacecraft 131, 571
Rolling friction, definition of 202
RTV-11 adhesive, use in Surveyor spacecraft 503
RTV-11 silicone, use in spacecraft 506
RTV-40 adhesive, use in various spacecraft 501–503
RTV-40 encapsulant, use in spacecraft 511
RTV-60 adhesive, use in various spacecraft 501–503
RTV-60 encapsulating material, use on OSO and Vela spacecraft 516, 518
RTV-60 silicone rubber, use in spacecraft 505–509, 511
RTV-90, use in Mercury spacecraft 504
RTV-102 adhesive, use in Nimbus and Pegasus spacecraft 502
RTV-560 adhesive, use in Lunar Orbiter spacecraft 502
RTV-560 elastomer, use on Apollo spacecraft 504
RTV-571 adhesive, use in Vela spacecraft 503
RTV-577 adhesive, use in Pegasus spacecraft 502
RTV-580 adhesive, use in Lunar Orbiter spacecraft 502
RTV-602 adhesive, use in various spacecraft 501, 503
RTV-612 adhesive, use in Mariner spacecraft 502
RTV-731 adhesive, use in Nimbus and Syncom spacecraft 502, 503
RTV-732 adhesive, use in OV spacecraft 502
RTV-881 encapsulant, use in spacecraft 511
Rubber, flammability characteristics of 645, 646
Rubber, natural, compatibility with reactive fluids 317
Rubber, natural, effect of elevated temperature on stress-strain properties 323
Rubber, natural, effect of high temperature on mechanical properties 325–328
Rubber, natural, effect of low temperature on stiffness 331–333
Rubber, natural, effect of reactor gamma radiation 342, 344, 347
Rubber, natural, effect of temperature on permeability 313
Rubber, natural, effect of thermal vacuum testing on 335
Rubber, natural, recommended space applications 596, 620
Rubber, odor rating of 645, 646
Rubber-epoxy-phenolic adhesives, effect of low temperature on 270
Rubber-phenolic adhesives, description of 243, 244
Rubber resin adhesive, effect of low temperature on 270, 271
Rulon bearings, use in OAO spacecraft 498
Rulon C modified Teflon, effect of simulated space environment on 234, 235
Rulon C retainers, recommended applications 578, 579
Rulon C retainers, use in Pegasus spacecraft 499
Run-in procedure for solid lubricant films 223

-S-

S-13 material, effect of ultraviolet radiation on 88, 123, 134, 136, 137, 139, 140, 570
S-13 zinc oxide-silicone paint, effect of simulated space environment on 112, 123, 134, 136–140, 142, 143, 157, 570
S-13 zinc-oxide-silicone paint, use as a solar reflector 86, 111, 123

S-13 zinc oxide-silicone paint, use in spacecraft 123, 153, 157, 491, 493, 570
S-13G zinc oxide pigmented paint, effect of simulated space environment on 123, 137, 158, 570
S-13G zinc oxide pigmented paint, use in spacecraft 123, 153, 158, 491, 493, 570
San Marco spacecraft, launch and orbital data 465, 470
Sapphire, effect of electron irradiation 182, 183
Sapphire, effect of gamma-ray irradiation on infrared transmission 187
Sapphire, recommendations for space applications 574, 575
Sapphire, shielding efficiency as solar cell cover sheet 191
Sapphire, use as solar cell covers 90
Sapphire solar cell covers, use in Telstar spacecraft 496
Satellite temperatures 91
Saureisen No. 31 adhesive, use in ATS spacecraft 501
Scale height, upper atmosphere 20, 21
Scattered radiation, from atmosphere 30–32, 34
Score spacecraft, launch and orbital data 461
Scotchcast encapsulants, use on BIOS and Vela spacecraft 514, 518
Scotchcast epoxy encapsulant, use in spacecraft 508
Sealant, odor rating for 646
Sealing materials, applications 294, 295
Sealing materials, compatibility with reactive fluids 311–320
Sealing materials, effect of elevated temperatures on 320–328
Sealing materials, effect of penetrating radiation on 334, 342–346
Sealing materials, effect of ultraviolet radiation on 350
Sealing materials, elastomers, description of 296–304
Sealing materials, leakage of 310–314
Sealing materials, materials selector table 594
Sealing materials, plastics, description of 304–308
Sealing materials, relative rating tables 593, 594
Seals for dynamic applications 310
Seals for optical elements, effect of vacuum environment 174
Seasonal effect on atmosphere 14
Sebum, composition and effect on materials 667
Second surface mirrors, effect of space environment on 127, 570
Second surface mirrors, use as solar reflector 86, 88, 99, 127
Secor spacecraft, launch and orbital data 466–469, 471
Secor spacecraft, materials used for 495, 503, 517, 526, 553
Secor spacecraft, performance in space 552, 553
Semiconductor devices, radiation effects on 407–418
Semiconductor devices, recommended space applications 616
Semiconductor materials, effect of radiation on 405
Semiconductors, effect of heat sterilization on 679, 680
Shear, aerodynamic 3
Shielding, radiation, calculations for 57
Shock 7, 8
Shroud, materials used for on Mariner spacecraft 544
Shroud ejection 5–7
Shroud temperature 7
Silane lubricants, properties of 212
Silastic 140 adhesive, use in OSO spacecraft 502
Silcoloid 201 adhesive, use in Ariel spacecraft 501
Silica, fused, effect of space environment on 127, 570
Silica, fused, recommendations for space applications 574
Silica, fused, recommended antenna applications 612
Silica, fused, shielding efficiency as solar cell cover sheet 189
Silica, fused, solar cell covers, use in various spacecraft 494–496
Silica, synthetic fused, effect of electron bombardment on 178, 182
Silica cloth-phenolic, use in spacecraft 507
Silicate binders, use in solar reflectors 86, 88, 119–121
Silicate binders, use in spacecraft thermal control 153, 485, 487, 490, 570
Silicate-nitrile, coating use in spacecraft thermal control 153
Silicates, effect of simulated space environment on 79, 88, 104–106, 119–121, 141–143, 570
Silicon, effect of gamma-ray irradiation on infrared transmission 187, 188
Silicon, effect of neutron irradiation on infrared transmission 189, 190
Silicon carbide, properties of 435

Silicon charged particle detectors, effect of electron irradiation on 411
Silicon controlled devices, effect of charged particles on 410, 412
Silicon dioxide, effect of simulated space environment on 79, 88, 130, 570
Silicon dioxide, properties of 435, 550
Silicon monoxide, effect of simulated space environment on 121, 127, 141, 570, 573
Silicon monoxide, infrared emittance of 90
Silicon monoxide, solar absorptance of 90, 121, 127, 570
Silicon monoxide, use as solar reflector 121, 127
Silicon monoxide, use as thermal control material 90, 121, 127, 485, 487, 488, 490, 493, 570, 573
Silicon oxide, properties of 440
Silicone adhesives, effect of charged particles on transmittance 288, 289
Silicone adhesives, effect of thermal sterilization on 256
Silicone adhesives, effect of ultraviolet on transmittance 285–287
Silicone adhesives, recommended applications for specific spacecraft missions 593
Silicone adhesives, use for bonding solar cells to substrate 288, 290
Silicone binders, effect of simulated space environment on 108, 112, 113, 123–125, 130, 131, 134–143, 148, 150, 570
Silicone binders, use in flat reflectors 130, 131
Silicone binders, use in solar reflectors 86, 88, 97, 113, 123–125
Silicone binders, use in spacecraft thermal control 153, 485–489, 570
Silicone closed cell foam, effect of radiation on 608
Silicone closed cell foam, effect of temperature on 608
Silicone closed cell foam, effect of vacuum on 608
Silicone DC 2104, effect of radiation on 357, 363
Silicone DC 2104, effect of temperature on 357, 363
Silicone DC 2104, effect of vacuum on 357, 372
Silicone DC 2104, mechanical properties of 357, 363
Silicone DC 2106, effect of temperature on 372
Silicone DC 2106, effect of vacuum on 372
Silicone elastomer, air leak rates 312, 314
Silicone elastomer, compatibility with reactive fluids 317
Silicone elastomer, description of 297, 299
Silicone elastomer, effect of high temperature on mechanical properties 325–328
Silicone elastomer, effect of hydrazine fuels on 318
Silicone elastomer, effect of low temperature on stiffness 331–333
Silicone elastomer, effect of nitrogen tetroxide on 319
Silicone elastomer, effect of radiation on 408
Silicone elastomer, effect of reactor gamma radiation 343, 347, 349
Silicone elastomer, effect of temperature on permeability 313
Silicone elastomer, effect of thermal vacuum testing on 335, 337, 338
Silicone elastomer, effect of ultraviolet radiation on 350
Silicone elastomer, recommended space applications 598, 599, 602
Silicone elastomer, use in various spacecraft 504
Silicone encapsulants, recommended space applications 625
Silicone encapsulating material, effect of thermal vacuum testing on 340, 341
Silicone foam, use in spacecraft 508
Silicone-glass, recommended antenna applications 612
Silicone-glass fabric laminates, effect of radiation on 355–357, 359–361, 363, 605
Silicone-glass fabric laminates, effect of vacuum on 355–357, 359–361, 363, 372–374, 605
Silicone-glass fiber laminates, effect of temperature on 605
Silicone-glass laminate circuit boards, recommended space applications 623
Silicone lubricants, properties of 212
Silicone lubricants, use in various spacecraft 498–500
Silicone oils, effect of composition on bearing lifetime 232
Silicone oil, use in spacecraft 84
Silicone plastic, effect of reactor gamma radiation on 349
Silicone resin, glass fiber molding, effect of radiation on 606
Silicone resin, glass fiber molding, effect of temperature on 606
Silicone resin, glass fiber molding, effect of vacuum on 606

Silicone rubber, effect on Gemini spacecraft windows 174
Silicone rubber, use in spacecraft 506–510
Silicone rubber impregnated fiberglass, insulation use in spacecraft 508
Silicone R-65, effect of temperature on 374, 377
Silicone R-65, effect of vacuum on 374
Silicone-TiO_2 tape, effect of simulated space environment on 113, 125
Silicone-TiO_2 tape, use as solar reflector 113, 125
Silver, effect of sputtering on 176
Silver, recommended antenna applications 610
Silver, use in spacecraft 527, 528
Silver-cadmium batteries, use on various spacecraft 515, 516
Silver chloride, effect of gamma-ray irradiation on infrared transmission 187
Silver-coated quartz, or silica second surface mirror, use as solar reflector 86, 127, 571
Silver paint, use for antenna on ANNA spacecraft 512
Silver plate, use in spacecraft 487, 492, 493
Silver-plated balls for bearings, recommended applications 578
Silver-zinc batteries, use on various spacecraft 514–518
Simulated ultraviolet radiation 77, 88, 119–132, 133–138, 570, 571
Simulated ultraviolet radiation, measurement of in vacuum 77, 79, 88, 119–132, 133–138, 570, 571
Simulation of n.eteoroid impact 67
Simulation of meteoroid velocity and mass (see also Chapter 6) 445
Sinitex retainers, recommended applications 579, 581
Skin secretions, composition of 669
Skyspar, titanium dioxide-epoxy white paint, use in spacecraft 153, 159, 570
Skyspar, use as solar reflector 86, 109, 113, 126
Skyspar, white paint, effect of simulated space environment on 109, 113, 126, 138, 149, 570
Sleeving, wire insulation, flammability characteristics of 646
Sleeving, wire insulation, odor rating of 646
Sliding surfaces, heavily loaded, lubrication recommendations 587
Sliding surfaces, lightly loaded, lubrication recommendations 586
Slip-ring assemblies, electrical, silver composites for 225
Slip-ring assemblies, lubrication recommendations 589
Slip-ring assembly, silver-MoS_2, use in various spacecraft 498, 499
Slot antennas, use on spacecraft 383
Snapshot spacecraft, launch and orbital data 466
Sodium silicate, effect of simulated space environment on 106, 111, 120, 121, 570
Sodium silicate, use as solar reflector 120, 121
Solar absorbers, absorbtance to emittance ratio 88, 128, 129, 570
Solar absorbers, effect of silver on emittance 88, 129, 570
Solar absorbers, effect of simulated space environment on 106, 128, 129
Solar absorbers, use in spacecraft 88, 118, 128, 129, 570
Solar absorbers, use of metal oxides for 88, 129, 570
Solar absorbers, use of polished aluminum for 87, 128, 570, 571
Solar absorbers, use of polished metals for 87, 88, 128, 570, 571
Solar absorptance, of solar absorbers 88, 128, 129, 570
Solar absorptance, of spacecraft 80, 98
Solar activity, effect on upper atmosphere 19–22
Solar arrays, thermal control of 84
Solar cell cover adhesives 283, 285–290
Solar cell covers, meterials used for 189
Solar cell damage from ANNA spacecraft 483
Solar cell degradation experiments on Explorer spacecraft 537
Solar cells, conversion efficiency of 90
Solar cells, emittance 90
Solar cells, effect of radiation on 405, 412, 415
Solar cells, effect of space radiation on 413, 416
Solar cells, radiation damage experiment on ATS spacecraft 530
Solar cells, silicon, effect of high-intensity thermal radiation on 195
Solar cells, solar absorptance 90
Solar cells, spectral response 90
Solar cells, thermal control of 90
Solar cells, use in various spacecraft 514–517
Solar cells, use on Alouette spacecraft 482
Solar constant, value of 26

Solar cycle, effect on solar radiation 26
Solar flare protons, dose and dose rates from 566, 567
Solar flare radiation, types of particles 49
Solar heating, effect of atmosphere 14, 19
Solar intensity 80–82
Solar radiation 25–34, 91
Solar radiation, effect on atmosphere 13, 14, 17–20
Solar radiation, effect on materials 34
Solar radiation, in solar system 82
Solar radiation, in thermal control 80
Solar reflectors 118–127, 570
Solar reflectors, as white paints 86, 87, 97, 119–126, 570
Solar reflectors, effect of simulated space environment on 86, 87, 104, 111–113, 119–127, 138, 570
Solar reflectors, use in spacecraft 86, 97, 119, 122, 123, 570
Solar spectrum 25–27
Solar wind, effect on metals 436
Solar wind, effect on meteoroids 65
Solar wind, effect on thermal control materials 119, 123, 126, 127, 138, 141, 142, 570
Solar wind particles, fluxes, and energies 52
Solder, effect of heat sterilization on 676
Solex glass, effect of electron irradiation on 182
Solid lubricants, advantages of usage in spacecraft 218
Solid lubricants, disadvantages of usage in spacecraft 219
Solid lubricants, use in antenna mechanisms 388
Solid propellants, effect of heat sterilization on 680
Solithane 113 conformal coating, use in various spacecraft 502, 503
Solithane 113 polyurethane, conformal coating, use in spacecraft 508, 510
Soviet spacecraft, launch and orbital data 475–477
Soviet spacecraft, materials used for 496, 526
Space environment, effect on antenna design 387
Space radiation, effect on metals 442
Space radiation, solar x-rays 54
Space radiation, stellar x-rays 55
Spacecraft, materials used in (see also specific material and spacecraft desired) 457–563
Spacecraft, various, launch and orbital data 460–481
Spacecraft atmosphere, allowable contamination 654–658
Spacecraft components, thermal control of 92, 97
Spacecraft decontamination, requirement for 674–676, 678, 681
Spacecraft radiation 84
Spacecraft sterilization, effect on reliability 679–681
Spacecraft sterilization, requirements for 673–682
Spacecraft temperatures 91, 92, 97
Spalling by meteoroids 70, 72
Specifications, structural adhesives 284
Spectral absorptance 87
Spectral distribution, albedo 82
Spectral distribution, solar radiation 82
Spectrosil fused quartz, effect of electron irradiation on 182
Spinel, effect of gamma-ray irradiation on infrared transmission 187
Spodumene, effect of simulated space environment on 111, 121
Spodumene, use as solar reflector 121
Sporadic meteoroids, definition of 64
Springs, effect of heat sterilization on 676
Sputtering, effect on metals 436
Sputtering, effect on surfaces 436
Sputtering on optical materials in space 175–177
SRM 141-C oil, effect of simulated space environment on 229
Stability, spacecraft, effect of antenna location 387, 393
Stafoam 110, use in Nimbus spacecraft 504
Stainless steel, recommended antenna applications 610
Stainless steel, recommended applications for gears of 585
Stainless steel, SAE 302, use in Transit spacecraft 500
Stainless steel, use in spacecraft 84, 132, 433, 487–489, 492, 519–521, 525, 526
Stainless steel bushings, use on Alouette spacecraft 497
Stainless steel 303, use for gears in Mariner spacecraft 497
Stainless steel 440C, use in space environment 497–499, 585
Stainless steel 440C, wear of gears made of 237, 238

Stannic oxide-aluminum phosphate, effect of simulated space environment on 111, 113, 121, 570
Stannic oxide-aluminum phosphate, use as solar reflector 86, 111, 113, 121, 570
Starfish nuclear burst, trapped electrons from 57
Steel, AISI 4130, use in spacecraft 524
Steel, AISI 4340, use for gears in space environment 585
Steel, AISI 4340, use in spacecraft 521, 525
Steel, AISI 9312, use in spacecraft 525
Steel, carburized AISI C1020, wear of gears made of 237, 238
Steel, maraging, 250 grade, use in spacecraft 527
Steel, recommended antenna applications 610
Steel, SAE 52100, use in space environment 499, 500, 585
Steel, stainless, sand blasted, effect of simulated space environment on 115, 132, 570
Steel, stainless, PH 14-8 Mo, use in spacecraft 519
Steel, stainless, 17-4 PH, use in spacecraft 520
Steel, use for antennas in various spacecraft 512, 513
Steel, 302 stainless, use in spacecraft 525, 527
Steel, 304 stainless, use in spacecraft 519, 522, 523
Steel, 321 stainless, use in spacecraft 521, 523
Steel, 347 stainless, use in spacecraft 523
Steel, 410 stainless, use in spacecraft 520, 527
Steel, 416 stainless, use in spacecraft 525
Steel, 440C stainless, use in spacecraft 519, 520
Steel alloys, effect of ethylene oxide on 676
Steel alloys, effect of heat sterilization on 676
Steel alloys, selection of 628
Steel tape, use as antenna 384
Steering of antennas 386, 387, 399
Sterilization, thermal, effect on adhesives 254, 256
Sterilization procedures 674
Sterilization requirements, for Lunar missions 673
Sterilization requirements, Mars missions 673–675
Sterilization requirements, Venus missions 673
Stick-slip friction, definition of 201
Stress corrosion, of metals 444, 445, 628
Stress corrosion, of steels 444
Stress corrosion, of titanium alloys 444, 628
Stress corrosion, of titanium alloys, in chlorides 444
Stress corrosion, of titanium alloys, in methanol 444, 628
Stretch forming, use in antenna construction 398
Strontium molybdate, effect of space environment on 119, 570
Strontium molybdate, use as solar reflector 119, 570
Structural adhesives specifications 284
Structural materials, effect of meteoroids on (see also Chapter 6) 445, 628
Structural materials, inorganic, selection of 618, 628–631
Structural materials, organic, use in spacecraft 505–511
Structural plastics 355–382, 505–511, 603–609
Structural plastics, effect of radiation on 355–363, 604–609
Structural plastics, relative ratings for use in space environment 604–609
Structural plastics, selection of 603, 609
Structural requirements for antennas 394
Stycast 1090 encapsulant, use on Lunar Orbiter spacecraft 516
Stycast 1090 modified epoxy encapsulant, use in spacecraft 507, 508, 510, 511
Stycast 1095 adhesive, use in Tiros spacecraft 503
Styrene, copolymer, effect of space radiation on 181
Styrene-butadiene elastomer, effect of hydrazine fuels on 318
Sublimation, effect on inorganic structural materials 437, 438, 628
Sublimation of cadmium 439
Sublimation of ceramics 439
Sublimation of metals 437–439
Sublimation of refractory metals 438, 439
Sublimation of spacecraft materials 387, 388
Sublimation of tungsten 438
Sublimation of zinc 439
Substrate hardness, influence on solid lubricant wear life 222
Substrate preparation for solid lubricants 217
Sunspot cycle, effect on upper atmosphere 14, 17–22
Supermil No. 31052 lubricant, recommended applications 578, 580, 582
Suprasil fused silica, effect of electron irradiation on 182

Surcal spacecraft, launch and orbital data 466, 467, 471
Surface erosion by meteoroids 390
Surface radiation characteristics, of planets, of spacecraft or satellites 25, 29–32, 34
Surfaces, smooth, microscopic description of 200
Surveyor spacecraft, active thermal control of 83, 492
Surveyor spacecraft, antennas 384
Surveyor spacecraft, launch and orbital data 468–472
Surveyor spacecraft, materials used for 492, 496, 500, 503, 504, 510, 517, 527
Surveyor spacecraft, performance in space 553, 554
Sweat, composition and effects on materials 666–668
Swelling of elastomers due to reactive fluid contact 312, 315
Switches, effect of radiation on 423, 424
Sylgard adhesives, use in various spacecraft 501, 502
Syncom spacecraft, launch and orbital data 463, 464
Syncom spacecraft, materials used for 492, 496, 503, 510, 511, 517, 527
Syncom spacecraft, performance in space 554
Synthane ball bearing retainers, use in spacecraft 84
Synthane L retainer, use in OGO spacecraft 498

-T-

Tantalum, use in spacecraft 433
Tape, aluminized, use in spacecraft thermal control 485–487
Tape, odor rating of 646
Tedlar, compatibility with fuels and oxidizers 321
Tedlar, effect of ethylene oxide on 678
Tedlar, effect of radiation on 607
Tedlar, effect of temperature on 607
Tedlar, effect of vacuum on 607
Teflon, aluminized, use in spacecraft thermal control 488, 490
Teflon, clear, effect of simulated space environment on 132, 571
Teflon, clear, use as flat absorber 132, 571
Teflon, compatibility with fuels and oxidizers 321
Teflon, effect of air on radiation effects 276
Teflon, effect of radiation on 406, 408
Teflon, effect of reactor gamma radiation 345, 348, 349
Teflon, effect of temperature on 376, 607
Teflon, recommended antenna applications 612, 614
Teflon, recommended lubrication applications 579, 581, 586, 589
Teflon, use in antennas 391, 512, 513
Teflon, use in cables 391
Teflon, use in space environment 497–500
Teflon, use in various spacecraft 507, 508, 511, 514, 516–518
Teflon, wire insulation use in spacecraft 508, 510
Teflon FEP, aluminized, effect of simulated space environment on 122, 571
Teflon FEP, aluminized, use as solar reflector 122, 571
Teflon FEP, effect of radiation on 607
Teflon FEP, effect of temperature on 607
Teflon FEP, effect of vacuum on 607
Teflon FEP, use in spacecraft 510, 511
Teflon-glass laminate circuit boards, recommended space applications 623
Teflon impregnated glass cloth, use in spacecraft 489, 505
Teflon insulation, recommended space applications 622
Teflon plastic, effect of ultraviolet radiation on 350
Teflon plastic sealing material, description of 304–306
Teflon plastic sealing material, recommended space applications 601, 603
Teflon reinforced, aluminized Mylar sheet, use in spacecraft thermal control 491
Teflon sealing materials, use in Mariner spacecraft 504
Teflon TFE, effect of radiation on 607
Teflon TFE, effect of temperature on 607
Teflon TFE, effect of thermal vacuum testing on 336
Teflon TFE, effect of vacuum on 607
Teflon TFE, use in spacecraft 508
Telemetry antennas, types used for spacecraft 383
Telstar satellites, use of active thermal control 84, 492
Telstar spacecraft, launch and orbital data 462, 463
Telstar spacecraft, materials used for 492, 496, 500, 504, 511, 513, 517, 518, 527

Temperature, effect on electronic components 429
Temperature, effect on leakage rates of seals 311
Temperature, effect on thermal control materials 104–117, 161, 570–572
Temperature, elevated, effect on sealing materials 320, 328
Temperature, upper atmosphere 17–22
Temperature control of satellites 80, 83, 93–95, 150, 153
Temperature control of spacecraft 77, 80, 83, 93–95, 150, 153
Temperature control of spacecraft components 77, 78, 91
Temperature extremes, effect on lubricant performance 206, 207
Tensile-shear strength of adhesives, effect of low temperature on 269, 270
Tensile-shear strength of adhesives, effect of radiation on 277–279, 281, 282
Thermal conductivity, effect on thermal control 92, 97, 98
Thermal control (see also Active thermal control and Passive thermal control) 77–172, 485–493, 568–574
Thermal control, spacecraft components 77, 78, 91
Thermal control coatings experiment on OSO spacecraft 549
Thermal control considerations for the moon and planets 573
Thermal control materials 77–172, 485–493, 568–574
Thermal control materials, effect of ascent environment on 104–117
Thermal control materials, effect of heat sterilization on 678
Thermal control materials, effect of prelaunch environment on 99, 101–103
Thermal control materials, effect of processing variables on 99, 101–103
Thermal control materials, effect of simulated space environment on 104–162, 570–574
Thermal control materials, effect of space environment on 104–162, 570–574
Thermal control materials, selection of 91, 93, 97–99, 119–132, 568–574
Thermal control materials, use in spacecraft 485–493
Thermal cycling, effect on thermal control materials 105, 111–117, 570–572
Thermal deflection of antennas 386
Thermal degradation of nonmetallic materials 614
Thermal emission of earth 25, 32, 34
Thermal environment in space 79, 82
Thermal expansion, effect on thermal stress 434
Thermal expansion of ceramics 434, 435
Thermal expansion of structural adhesives at low temperatures 272
Thermal radiation, effect on thermal control 92, 98, 102
Thermal radiation from nuclear explosions 56
Thermal radiation of earth 32, 33
Thermal stability of liquid lubricants 214, 215
Thermal stability of solid lubricants 216, 219, 220
Thermal sterilization (see also Heat sterilization) 673–682
Thermal stress, effect of temperature on 434
Thermal switch, use in spacecraft thermal control 84, 85, 492
Thermatrol, use as solar reflector 86, 97, 112, 124
Thermatrol 2A100 and 6A100, effect of simulated space environment on 112, 124, 135, 138–143, 146–150, 570
Thermatrol 2A100, use in spacecraft thermal control 487
Thermatrol 6A100, effect of proton and ultraviolet radiation on 151, 153, 570
Thermistors, effect of radiation on 404
Thermofit CRN sleeving, use in spacecraft 510
Thermophysical properties of thermal control materials 99, 100–102, 119–132, 570, 571
Thermoplastic foams, selection of 608
Thermosetting foams, selection of 608
Thermosphere 13, 16
Thermostatically controlled heaters 83
Thorium oxide, properties of 435, 440
Threshold of failure for electronic components, limitations of concept 417
Threshold limit values of toxic materials 655–658
TIMMS units, effect of radiation on 419, 420
TiO_2 (see Titanium dioxide)
Tiros spacecraft, launch and orbital data 461–466
Tiros spacecraft, materials used for 496, 500, 503, 504, 511, 518, 527

Tiros spacecraft, performance in space 554
Titanium, commercially pure, use in spacecraft 524
Titanium, 5 aluminum, 2.5 tin, use in spacecraft 519, 522, 524
Titanium, 6 aluminum, 4 vanadium alloy, use in spacecraft 519, 522–527
Titanium, 7 aluminum, 4 molybdenum, alloy, use in spacecraft 527
Titanium, 13 vanadium, 11 chromium, 3 aluminum, alloy, B120VCA, use in spacecraft 527
Titanium alloys, compatibility with propellants 628, 629
Titanium alloys, effect of heat sterilization on 675, 676
Titanium alloys, recommended antenna applications 610
Titanium alloys, selection of 618, 628, 629
Titanium alloys, use in spacecraft 433, 519, 522–527
Titanium dioxide, effect of simulated space environment on 79, 104, 119, 120, 123–126, 135, 138–140, 142, 147, 570
Titanium dioxide-acrylic, use as solar reflector 86, 125
Titanium dioxide-epoxy, skyspar, use in spacecraft 153, 159, 490, 570
Titanium dioxide-epoxy paint, use as solar reflector 86, 126
Titanium dioxide pigmented paints, effect of simulated space environment on 119, 120, 123–126, 135, 138–140, 147, 570
Titanium dioxide pigmented paints, use in spacecraft thermal control 79, 104, 119, 120, 123–126, 135, 138–140, 142, 147, 485–487, 490–492, 570
Titanium dioxide pigmented S7094-3 and S7094-4, effect of simulated space environment on 126, 139, 140, 570
Titanium dioxide pigmented S7094-3 and S7094-4, use as solar reflectors 126
Titanium dioxide-silicone paint, effect of simulated space environment on 123–125, 135, 139–141, 143, 156, 570
Titanium dioxide-silicone paint, use as solar reflector 86, 97, 123–125
Titanium dioxide-silicone paint, use in spacecraft 153, 156, 488, 490, 570
TNT, effect of gamma radiation on 453
Total solar irradiance 77
Toxicity of materials 636, 637, 652, 653
Transformers, effect of radiation on 423, 427
Transformers, recommended space applications 616
Transformers, types used in Telstar spacecraft 518
Transistors, bipolar, effect of charged particles on 410, 412
Transistors, effect of space radiation on 413, 414
Transistors, field effect, effect of charged particles on 410, 412
Transistors, types used in various spacecraft 514, 517, 518
Transistors, unijunction, effect of charged particles on 410, 412
Transit spacecraft, launch and orbital data 461–463
Transit spacecraft, materials used for 493, 496, 500, 511, 518, 527, 528
Transmittance of solar cell cover adhesives 285
Transparent epoxy encapsulants, use in spacecraft 508
Transparent polyurethane encapsulant, use in spacecraft 508
Transparent silicone RTV60 encapsulant, use in spacecraft 508
Transport processes, in atmosphere 18
Trapped electrons, zone model for 44
Trapped particles, calculations of combined fluxes 45
Trapped protons, variation with solar cycle 44
Trapped protons, zone model for 38
Trapped protons and electrons, dose and dose rates from 566, 567
Trapped radiation 37
Trapped radiation, loss mechanism 38
Trapped radiation, spatial distribution 38
Trapping centers in semiconductors, formation by radiation 405
TRS (see ERS) 384
TRS spacecraft, launch and orbital data 464
Tubes, electron, effect of radiation on 418–420
Tubes, electron, recommended space applications 616
Tubes, gas-filled, failure modes under irradiation 419

Tubes, vacuum, failure modes under irradiation 419
Tungsten, use in spacecraft 433
Tungsten disulfide, use as solid lubricant 225
TZM, molybdenum alloy, use in spacecraft 522, 527

- U -

UDMH propellant, effect of radiation on 453
Ultrasil fused quartz, effect of electron irradiation on 182
Ultraviolet radiation, effect on electronic components 429
Ultraviolet radiation, effect on reinforced plastics 363, 605–607
Ultraviolet radiation, effect on sealing materials 346, 350
Ultraviolet transmitting materials, effect of electron irradiation on 183, 186
Ultraviolet transmitting materials, effect of proton irradiation on 183
Ultrox, zirconium silicate-potassium silicate, effect of simulated space environment on 120, 139, 140, 150, 570
Ultrox, zirconium silicate-potassium silicate, use as solar reflector 120
Upper atmosphere 13–23
Upper atmosphere, density (see also Air density, Density) 13, 14, 19–22
Upper atmosphere, effect on materials 23
Upper atmospheric pressure 16, 19–22
Urethane foam, use in antennas 398
Urine, composition and effect on materials 659–663
U.S. Standard Atmosphere 13

- V -

Vac-Kote lubricant, use in OAO spacecraft 498
Vacuum, effect on anodized coatings 439
Vacuum, effect on antenna materials 387
Vacuum, effect on ceramic materials 440
Vacuum, effect on diffusion in metals 440
Vacuum, effect on electronic components 428
Vacuum, effect on fatigue life of aluminum 440, 629
Vacuum, effect on fatigue life of metals 440, 441, 629
Vacuum, effect on lubricant performance 207
Vacuum, effect on mechanical properties of metals 440, 441, 628, 629
Vacuum, effect on metal surfaces 441, 628, 629
Vacuum, effect on metals 436, 439–441, 628, 629
Vacuum, effect on optical surfaces 439
Vacuum, effect on protective coatings of metals 439
Vacuum, effect on refractory metal coatings 439
Vacuum, effect on reinforced plastics 356, 357, 359–362, 370, 372–380, 605–607
Vacuum, effect on thermal control materials 79, 98, 101, 119–132, 133–138, 139–142, 145–150, 151–153, 160
Vacuum Condensible Materials (VCM) determinations for adhesives 261, 267
Vacuum deposited aluminum, use in spacecraft thermal control 48, 487, 490, 492, 493
Vacuum environment, effect on optical materials 174
Vacuum-temperature, effect on reinforced plastics 355, 370, 372–380, 605–607
Van Allen radiation 37
Vanguard spacecraft, launch and orbital data 461
Vanguard spacecraft, materials used for 493, 496, 511, 513, 518, 528
Vapor deposited metals, use as thermal control materials 127–130, 485, 486, 492, 570
Vapor pressure, of metals 437
Variable external radiation characteristics 83, 91
Variable resistors, effect of radiation on 420, 422
Vela spacecraft, launch and orbital data 464, 466, 470
Vela spacecraft, materials used for 493, 503, 511, 518, 528, 554
Vela spacecraft, performance in space 554, 555
Velcro tape, use in spacecraft 507
Velocity distributions, upper atmosphere 17
Velocity of meteoroids 64, 65
Velocity of simulated meteoroids 67

Velvet paint, 3M black, effect of simulated space environment on 131, 571
Velvet paint, 3M black, use in spacecraft 490
Velvet paint, 3M white, effect of simulated space environment on 125, 570
Velvet paint, 3M white, use in spacecraft 490, 492
Versamid adhesive, use in Ariel spacecraft 501
Versamid adhesives, use in various spacecraft 502, 503
Vibration 7–9
Vibration response of Alouette spacecraft 483
Vinyl adhesives, effect of thermal sterilization on 256
Vinyl-epoxy-nylon adhesive, effect of high temperature in vacuum 258
Vinyl-epoxy-nylon adhesive, effect of penetrating radiation on 277
Vinylidene fluoride elastomer, effect of high temperature aging on 326, 327
Vinyl insulation, recommended space applications 619
Vinyl-phenolic adhesives, description of 243, 244
Vinyl-phenolic adhesives, effect of low temperature on 270
Vinyl-phenolic adhesives, effect of high temperature in vacuum on 258
Vinyl-phenolic adhesives, effect of penetrating radiation on 277, 281
Vinyl-phenolic adhesives, recommended applications for specific spacecraft missions 593
Vinyl plastic sealing materials, description of 305, 308
Viscosity of liquid lubricants 215
Vita Var PV 100, effect of proton and ultraviolet radiation on 152, 153, 570
Vita Var PV 100, effect of simulated space environment on 124, 145, 153, 570
Vita Var PV 100, use in spacecraft thermal control 124, 384, 487, 489, 492
Viton A elastomer, air leakage rates 312, 314
Viton A elastomer, compatibility with reactive fluids 317
Viton A elastomer, effect of hydrazine fuels on 318
Viton A elastomer, effect of nitrogen tetroxide on 319
Viton A elastomer, effect of reactor gamma radiation 343, 347, 349
Viton A elastomer, effect of temperature on permeability 313
Viton A elastomer, effect of thermal vacuum testing on 335, 337, 338
Viton A elastomer, effect of ultraviolet radiation on 350
Viton A elastomer, recommended space applications 598, 602
Viton A elastomer, use in various spacecraft 504
Viton B elastomer, effect of reactor gamma radiation 342, 343
Viton B elastomer, effect of thermal vacuum testing on 335
Volatility of liquid lubricants 213, 214
Volatilization in vacuum, effect on lubricant performance 207
Voltage breakdown, antennas 388
Vomit, composition and effect on materials 696
Vycor, aluminized, effect of simulated space environment on 127, 570
Vycor, aluminized, use as solar reflector 127
Vycor, aluminized, use in spacecraft 127, 492, 570
Vycor, silver plated, use in spacecraft 492
Vycor, use for windows in Mercury and Gemini spacecraft 494, 495
Vycor fused quartz, effect of electron irradiation on 182, 183
Vyram elastomer, compatibility with reactive fluids 317
Vyram elastomer, effect of temperature on permeability 313

- W -

Water vapor, photodissociation of 18
Waveguides, dielectric breakdown in 389
Wear life of molybdenum disulfide 221, 222
Wear of gears in vacuum environment 237, 238
Weight loss of reinforced plastics 372, 374–378
Weightlessness, effect on lubricant performance 206
Welded junction theory of friction 200
Whisker growth, of oxides or sulfides 443

White paint, effect of simulated space environment on 101, 107–109, 119–126, 134, 135, 147, 570

White paint, use as solar reflectors 86, 87, 97, 119–126

White paint, use as spacecraft thermal control material 86, 87, 97, 99, 119–126, 147, 153–157, 485–492, 570

Winsor Lube, use in various spacecraft 497, 498, 500

Wire insulation, effect of heat sterilization on 678

Wire insulation, effect of radiation on 407

Wire insulation, flammability characteristics of 646

Wire insulation, odor rating of 646

Wirewound resistors, effect of radiation on 420, 422

Wiring insulation, types used in various spacecraft 514–518

WRESAT, first Australian spacecraft 457, 472

-X-

X-rays, effect on ceramics 442

X-rays, effect on metals 442

X-rays from nuclear explosions 56

X-rays in space, solar origin 54

X-rays in space, stellar origin 55

XR 63-489 adhesive, use in Secor spacecraft 503

XRM 128C oil, effect of simulated space environment on 229

XRM 141C lubricant, recommended applications 578, 582

-Z-

Z-93, zinc oxide-potassium silicate, effect of simulated space environment on 111, 119, 138–143, 570

Z-93, zinc oxide-potassium silicate, use as solar reflector 86, 88, 111, 119

Z-93, zinc oxide-potassium silicate, use in spacecraft thermal control 119, 153, 154, 485, 570

Z-93 material, effect of ultraviolet radiation on 88, 119, 138, 570

Zero gravity, effect on lubricant performance 206

Zinc, evaporation in space 388

Zinc alloys, effect of heat sterilization on 676

Zinc oxide, effect of simulated space environment on 79, 88, 104, 123, 134, 136, 137, 141–143, 570

Zinc oxide-silicone paint, use as solar reflectors 86, 88, 123

Zinc oxide-silicone paint, use in spacecraft 84, 123, 153, 157, 485, 486, 488, 491, 570

Zinc plating, use in spacecraft 528

Zirconia-silicate, use as solar reflector 86, 88, 111, 120, 121

Zirconium dioxide, effect of simulated space environment on 79, 88, 111, 120, 121, 147, 149, 570

Zirconium dioxide, use in spacecraft thermal control 486, 487, 490, 491

Zirconium dioxide-silicate paint, use in spacecraft thermal control 487, 490, 491

Zirconium oxide, properties of 435, 440

Zirconium silicate, effect of simulated space environment on 111, 120, 570